Y 3. At 7 : 16/19-21

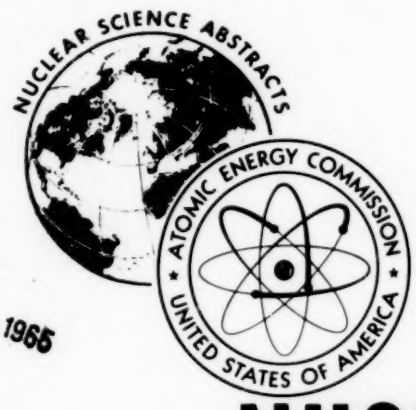

DEC 6 1965

NUCLEAR SCIENCE ABSTRACTS

Volume 19 Number 21

Abstracts 40303–42228

November 15, 1965

MIAMI UNIVERSITY LIBRARY

UNITED STATES ATOMIC ENERGY COMMISSION
Division of Technical Information

USAEC DEPOSITORY LIBRARIES

Collections of USAEC reports are maintained in the libraries of the organizations listed below for reference use by the general public. Facilities for making photocopies are available. The USAEC also makes available through these libraries atomic energy reports of countries other than the U. S. that are abstracted in *Nuclear Science Abstracts*.

ALABAMA
Auburn, Auburn University
ARIZONA
Tucson, University of Arizona
ARKANSAS
Fayetteville, University of Arkansas
CALIFORNIA
Berkeley, University of California
Davis, University of California
Los Angeles, University of California
San Diego, Public Library
Stanford, Stanford University
COLORADO
Boulder, University of Colorado
Denver, Public Library
CONNECTICUT
New Haven, Yale University
DELAWARE
Newark, University of Delaware
DISTRICT OF COLUMBIA
Washington, Library of Congress
FLORIDA
Coral Gables, University of Miami
Gainesville, University of Florida
GEORGIA
Atlanta, Georgia Institute of Technology
HAWAII
Honolulu, University of Hawaii
ILLINOIS
Chicago, John Crerar Library
Chicago, University of Chicago
Evanston, Northwestern University
Urbana, University of Illinois
INDIANA
Bloomington, Indiana University
Lafayette, Purdue University
IOWA
Ames, Iowa State University
KANSAS
Manhattan, Kansas State University
KENTUCKY
Lexington, University of Kentucky
Louisville, University of Louisville
LOUISIANA
Baton Rouge, Louisiana State University
New Orleans, Tulane University
MARYLAND
Baltimore, Johns Hopkins University
College Park, University of Maryland
MASSACHUSETTS
Cambridge, Harvard University
Cambridge, Massachusetts Institute of Technology
MICHIGAN
Ann Arbor, University of Michigan
Detroit, Public Library
East Lansing, Michigan State University
MINNESOTA
Minneapolis, University of Minnesota
MISSISSIPPI
State College, Mississippi State University
MISSOURI
Kansas City, Linda Hall Library
Rolla, University of Missouri School of Mines and Metallurgy
St. Louis, Washington University
MONTANA
Bozeman, Montana State College
NEVADA
Las Vegas, Nevada Southern University
Reno, University of Nevada
NEW JERSEY
Princeton, Princeton University
Teaneck, Fairleigh Dickinson University
NEW MEXICO
Albuquerque, University of New Mexico
NEW YORK
Albany, The University of the State of New York
Buffalo, State University of New York at Buffalo
Ithaca, Cornell University
New York, Atomic Industrial Forum, Inc.
New York, Columbia University
New York, New York University
Rochester, University of Rochester
Schenectady, Union College
Syracuse, Syracuse University
Troy, Rensselaer Polytechnic Institute
NORTH CAROLINA
Charlotte, Public Library of Charlotte and Mecklenburg County
Durham, Duke University
Raleigh, North Carolina State College
NORTH DAKOTA
Grand Forks, University of North Dakota
OHIO
Cincinnati, University of Cincinnati
Cleveland, Public Library
OHIO (CONT.)
Columbus, Ohio State University
Toledo, University of Toledo
Youngstown, Youngstown University
OKLAHOMA
Norman, University of Oklahoma
Stillwater, Oklahoma State University
OREGON
Corvallis, Oregon State University
Portland, Reed College
PENNSYLVANIA
Philadelphia, University of Pennsylvania
Pittsburgh, Carnegie Library
University Park, Pennsylvania State University
PUERTO RICO
Rio Piedras, University of Puerto Rico
RHODE ISLAND
Providence, Brown University
SOUTH CAROLINA
Columbia, University of South Carolina
TENNESSEE
Knoxville, University of Tennessee
Memphis, Public Library
Nashville, Joint University Libraries
Oak Ridge, Oak Ridge Institute of Nuclear Studies
TEXAS
Austin, University of Texas
College Station, Texas A & M University
Dallas, Southern Methodist University
Houston, Rice University
Lubbock, Texas Technological College
San Antonio, Public Library
UTAH
Salt Lake City, University of Utah
VIRGINIA
Blacksburg, Virginia Polytechnic Institute
Charlottesville, University of Virginia
Norfolk, Old Dominion College
WASHINGTON
Pullman, Washington State University
Seattle, University of Washington
WEST VIRGINIA
Morgantown, West Virginia University
WISCONSIN
Madison, University of Wisconsin
Milwaukee, Public Library
WYOMING
Laramie, University of Wyoming

Volume 19, Number 21, November 15, 1965

NUCLEAR SCIENCE ABSTRACTS

A semimonthly publication of the USAEC Division of Technical Information, Edward J. Brunenkant, Director. Published by the USAEC Division of Technical Information Extension, Robert L. Shannon, Extension Manager.

Nuclear Science Abstracts covers the international literature on nuclear science and technology and provides the only comprehensive abstracting and indexing of this body of information. Published twice each month since 1947, *NSA* covers technical reports of the U. S. Atomic Energy Commission and its contractors, technical reports of U. S. Government agencies and other governments, universities, industrial and research organizations, as well as patents, books, and journal literature on a world-wide basis. Nearly 300,000 abstracts have appeared in *NSA* through Volume 18. The subject matter covered in *NSA* is described in issue Number 1 and in TID-4552, *Subject Scope of Nuclear Science Abstracts*, available free from the U. S. Atomic Energy Commission, Division of Technical Information Extension, P. O. Box 62, Oak Ridge, Tennessee 37831.

Abstracts are arranged according to a number of subject categories and subcategories. Definitions of categories appear in issues Number 1 and 13. If the language of the original item is not English, the language will be indicated. Translations are not abstracted where an abstract of the original item has appeared in *NSA*.

INDEXES TO NSA

Corporate author, personal author, subject, and report number indexes appear in each issue and are cumulated quarterly, semiannually, and annually. At the end of Volume 19, report number indexes will be cumulated in two separate publications. Indexes for Vols. 1–15 will be reissued with the latest public availability known at that time. This index will not be reissued. Indexes for Vols. 16–19 will be cumulated as a separate issuance and will be reissued annually to include all volumes beginning with Volume 16.

AVAILABILITY OF PUBLICATIONS ABSTRACTED

The public availability of all U. S. Atomic Energy Commission reports is indicated in the report number indexes. The availability of other reports, when known, is also indicated. The availability of some unnumbered reports is given in the abstract.

Dissertations abstracted in *Dissertation Abstracts* and included in *NSA* are available from University Microfilms, Inc., 315 N. First Street, Ann Arbor, Michigan.

Most of the published literature abstracted in *NSA* is on deposit at the Oak Ridge Institute of Nuclear Studies Library, Oak Ridge, Tennessee, (a USAEC depository library) and is available through interlibrary loan. When requesting papers from this source, it is important that *NSA* volume and abstract number be cited.

HOW TO OBTAIN NUCLEAR SCIENCE ABSTRACTS

NSA is available on an exchange basis to universities, research institutions, industrial firms, and publishers of scientific information. Inquiries should be directed to the U. S. Atomic Energy Commission, Division of Technical Information Extension, P. O. Box 62, Oak Ridge, Tennessee 37831.

Government agencies may obtain *NSA* free of charge.

NSA is available to the general public on a subscription basis from the Superintendent of Documents, U. S. Government Printing Office, Washington, D. C. 20402, as follows:

For the 24 regular issues, $30.00 domestic, $37.00 foreign. A single issue costs $1.75, plus 25 per cent for foreign mailing. Domestic rates apply to the United States, Canada, Mexico, and Central and South American countries except Argentina, Brazil, British and French Guiana, Surinam, and British Honduras. Foreign rates apply to the countries excepted above and to all other countries throughout the world.

For the quarterly, semiannual, and annual indexes, $22.00 domestic, $25.00 foreign.

Multivolume subject and author indexes are available as follows:

Vols. 1–4 (1948–1950) Johnson Reprint Corporation, 111 Fifth Avenue, New York, N. Y. 10003, $30.00.

Vols. 5–10 (1951–1956) Superintendent of Documents, U. S. Government Printing Office, Washington, D. C. 20402, $5.25.

Vols. 11–15, Subjects, Superintendent of Documents, U. S. Government Printing Office, Washington, D. C. 20402, $19.00.

Vols. 11–15, Personal Authors, Superintendent of Documents, U. S. Government Printing Office, Washington, D. C. 20402, $14.25.

Vols. 11–15, Corporate Authors, Superintendent of Documents, U. S. Government Printing Office, Washington, D. C. 20402, $2.50.

Cumulative Report Number Index, Vols. 1–18, is available from the Superintendent of Documents, U. S. Government Printing Office, Washington, D. C. 20402, $5.75.

Annual Indexes are available separately from the U. S. Government Printing Office as follows:

Vol. 16, Subject and Authors, $9.75.
Vol. 17, Subject and Authors, $12.25.
Vol. 18, Subject and Authors, $12.50.

ACKNOWLEDGMENTS

Agreements between the United States Atomic Energy Commission and the following organizations with regard to providing continuing services and specific literature coverage for *Nuclear Science Abstracts* are gratefully acknowledged:

American Institute of Physics; Atomic Energy of Canada Limited; Atomic Energy Research Establishment, United Kingdom; European Atomic Energy Community (EURATOM); Gmelin Institute; International Atomic Energy Agency; Japan Atomic Energy Bureau — Japan Atomic Energy Research Institute; Netherlands Patent Office; Reactor Centrum Nederland.

TABLE OF CONTENTS

Volume 19, Number 21, November 15, 1965

Category	Page
BIOLOGY AND MEDICINE	5023
General	5023
Ecology	5023
Metabolism, Tissue Distribution, and Toxicology	5024
Radiation Effects	5031
Radiation Effects Therapy and Countermeasures	5035
Radiotherapy and Radiodiagnosis	5036
CHEMISTRY	5038
General	5038
Analytical Procedures	5038
Inorganic and Physical Chemistry	5045
Organic Chemistry	5055
Radiation Chemistry	5056
Radiochemistry	5070
Separation Processes and Procedures	5071
ENGINEERING	5078
General	5078
Applications of Nuclear Explosions	5079
Facilities and Equipment	5080
Heat Transfer and Fluid Flow	5082
Materials Testing	5085
Protective Structures	5085
Space Propulsion	5085
Vacuum Engineering	5087
GEOLOGY AND MINERALOGY	5089
General	5089
Natural Radioactivity and Fallout	5089
Techniques and Equipment	5091
Thorium and Uranium Minerals	5092
HEALTH AND SAFETY	5093
INSTRUMENTATION	5098
General	5098
Radiation Detection	5100
Radiation Effects	5107
ISOTOPE TECHNOLOGY	5109
Industrial Applications	5109
Separation and Production	5109
MATHEMATICS AND COMPUTERS	5110
METALS, CERAMICS, AND OTHER MATERIALS	5111
General	5111
Corrosion	5113
Fabrication	5115
Properties and Structure	5117
Radiation Effects	5128
METEOROLOGY	5132
PHYSICS	5133
General	5133
Accelerators	5139
Astrophysics and Cosmology	5143
Atomic Physics	5149
Cosmic Radiation	5154
Direct Energy Conversion	5158
Elementary Particles and Radiations	5159
Field Theory and Quantum Mechanics	5181
Geophysics	5185
Low Temperature Physics	5190
Neutron Physics	5194
Nuclear Properties and Reactions	5196
Plasma Physics and Thermonuclear Processes	5220
Shielding	5233
Solid State Physics	5235
REACTOR TECHNOLOGY	5241
General	5241
Auxiliaries and Components	5242
Criticality Studies	5244
Design and Feasibility	5247
Fuels	5248
Power and Power-Breeder Reactors	5249
Process Heat Reactors	5254
Production Reactors	5254
Propulsion and Space	5255
Research and Test Reactors	5256
WASTE DISPOSAL AND PROCESSING	5261
GENERAL AND MISCELLANEOUS	5263
CORPORATE AUTHOR INDEX	INDEX-1
PERSONAL AUTHOR INDEX	INDEX-10
SUBJECT INDEX	INDEX-51
REPORT NUMBER INDEX	INDEX-130

STAFF OF NUCLEAR SCIENCE ABSTRACTS

MANAGING EDITOR

John W. Norris

ASSISTANT MANAGING EDITOR

Donald D. Davis

ASSOCIATE EDITORS

Lawrence T. Whitehead
David E. Bost
Robert C. Kelly
Lee M. Thompson

SUBJECT INDEX EDITOR

Everett J. Hoffman

EVALUATORS

William D. Matheny
John H. Mitchell
Mary H. Newman

ABSTRACTORS

F. S. Armstrong (AECL)
Jane G. Buchanan
D. Lamar Cason
Helen G. Donald
James R. Dulaney
Wells L. Green
Bernard O. Griggs
Mary Catherine Grissom
Fernando J. Hamilton
Phyllis C. Hansen
Thomas F. Heagerty
Carolyn D. Houston
Rose V. Jermain
Betty L. McDowell
Jean F. Peckham
Mona H. Raridon
Julia Redford
Lila B. Smith
Charles E. Stuber
Martha J. Thomas
Anne G. Ward
David C. West
Milton O. Whitson

SUBJECT HEADING SPECIALIST

Robert E. Upchurch

CORPORATE AUTHOR SPECIALIST

Clara L. Fox

DESCRIPTIVE CATALOGING SPECIALIST

J. Paul Meredith

SCHEDULING AND PUBLISHING COORDINATOR

Brainard L. Patton

Communication concerning the editorial policy and content of *NSA* should be addressed to the Managing Editor, *Nuclear Science Abstracts*, AEC Division of Technical Information Extension, P. O. Box 62, Oak Ridge, Tennessee 37831.

Use of funds for printing this publication approved by the Director of the Bureau of the Budget, May 20, 1963

Volume 19, Number 21 November 15, 1965

NUCLEAR SCIENCE ABSTRACTS

BIOLOGY AND MEDICINE

General

40303 (FTD-TT-65-48) TENTH CONGRESS OF THE ALL-UNION PAVLOV PHYSIOLOGICAL SOCIETY AT EREVAN, 1964. VOLUME II, NO. 2. SUBJECTS OF SCIENTIFIC PAPERS. Translation of p.1-440 from X Sezd Vsesoyuznogo Fiziologicheskogo Obshchestva imeni I. P. Pavlova, Erevan-1964. Tom II Tezisy Nauchnykh Soobshchenly, Vypusk 2., Izdatel'stvo Nauka. 701p. CFSTI.

Separate abstracts were prepared on 10 papers presented at this congress. Other papers report the results of physiological studies in man and a variety of experimental animals. (C.H.)

For abstracts of individual papers see: 40353–40360, 40385, and 40386.

40304 A LIGHT-TIGHT, DUST-FREE DRYING BOX FOR AUTORADIOGRAPHY. Hillemann, Howard H.; Ritschard, Ronald L. (Oregon State Univ., Corvallis). Stain Technol, 39: 327-8(Sept. 1964).

Specifications are given for a portable dark-box with a built-in ventilating system. A reinforced metal box, measuring about 18 × 16 × 14 in., is sprayed inside with black paint. Black rubber sponge tape is applied to the lid along the inside margins to prevent light leaks. Noncorrosive rods (brass welding rods) were used to support slide clips or paper clips, suspended from the rods by snap rings. Air circulation is provided by an electric blower (squirrel cage type) connected with black plastic fittings to the box. The intake end of the tubing is covered with an air filter, the air being forced into the box through the T system of plastic fittings from which it is dispersed through vents in each arm of the tee. After flowing across wet slides, it passes out through the left wall. Right-angle turns provide a light-trap. The opaque plastic fittings used were of the type made for low-pressure fluids, and readily obtainable. All joints were wrapped with black plastic tape as further assurance against light leakage. (BBB)

40305 MOESSBAUER EFFECT IN HEMOGLOBIN AND SOME IRON-CONTAINING BIOLOGICAL COMPOUNDS. Gonser, U; Grant, R. W. (North American Aviation Science Center, Thousand Oaks, Calif.). 56p. (CONF-650317-2). Gmelin, AED-CONF-65-039-22.

From American Physical Society Meeting, Kansas City, Mo.

The feasibility of Mössbauer spectroscopy for biological investigations is discussed in general terms. ^{57}Fe was used to study the Mössbauer effect in hemoglobin (within red cells) and some related compounds. The temperature dependence of the quadrupole splitting and relative recoil-free fractions for hemoglobin with different ligands was studied and the recoil-free fraction in O_2-hemoglobin at 5°K was determined. An asymmetry in the quadrupole splitting observed in hemoglobin was interpreted in terms of a directional dependence of the recoil-free fraction and established that the lowest lying d orbital of the Fe atoms in this molecule is |xy⟩. (auth)

40306 APPLICATION OF THE MOESSBAUER EFFECT TO BIOLOGICAL SYSTEMS. Gonser, U.; Grant, R. W. (North American Aviation Science Center, Thousand Oaks, Calif.). 39p. (CONF-650101-6). Gmelin, AED-CONF-65-006-6.

From Moessbauer Symposium, New York.

The usefulness and limitations of the Mössbauer effect for biological studies are pointed out, and appropriate samples of measurements that have been made on biological materials are given. As yet only the isotope ^{57}Fe has been used for Mössbauer studies of a biological nature. It was concluded that the Mössbauer effect should offer a new and interesting tool for biological research dispite the many limitations that restrict its usefulness. (P.C.H.)

Ecology

40307 (BNL-9253) ECOLOGICAL CHANGES IN THE INSECT COMMUNITY OF A PITCH PINE-OAK FOREST SUBJECTED TO CHRONIC GAMMA IRRADIATION (thesis). Brower, John H. (Brookhaven National Lab., Upton, N. Y.). May 28, 1965. Contract AT-30-2-GEN-16. 184p. Dep. mn; CFSTI, $5.00 cy, $1.00 mn.

Submitted to Massachusetts Univ., Amherst.

A project was established in 1961 to study the effects of chronic gamma radiation on the insect fauna of a natural forest community. The area of pitch pine-oak-blueberry was irradiated for 20 hours each day with a 9,500 curie Cesium-137 source. A sweep sampling technique was employed to give reliable samples of shrub insects. A numerical survey was made to determine the density and distribution pattern of an aphid on white oak leaves along a decreasing radiation gradient. Pines were checked monthly to determine the intensity of bark beetle infestation. Later, squares of the bark were removed and the developmental success was determined by estimating the per cent of cambial surface utilized. Trap logs were also used to provide populations at very high radiation intensities. Radiation had extensive effects on the vegetation of the experimental forest. Pitch pines were the most sensitive and died within 75 meters of the source. White oaks were more resistant and died to about 60 meters while the ericaceous shrubs were killed entirely at 33 meters. The abundance of the shrub insects was greatly depleted near the radiation source in the area of severe shrub damage. Omitting Psocoptera, insect abundance was 5% of normal at 10m. Normal abundance for most species was reached at about 60m. Near the source the leaf feeding species and their parasites and predators were mostly absent; the insects present were fungivorous or forms with ample vagility to move through the area. The fungivorous Psocoptera were normal or above normal in abundance in the area of complete shrub mortality. In 1963 a species of aphid, Myzocallis discolor, was observed on the radiation damaged white oaks. This aphid was not found in the unaffected forest but increased in abundance on the debilitated oaks to over 25 winged aphids per leaf. This increase

amounted to as much as 350,000 aphids per square meter of forest floor area. A possible increase in the soluble amino acid content in damaged leaves was a likely causal factor for the aphid increase. Bark beetles attacked dead and dying trees and the area of infestation increased as pines further from the source died. Trees at high radiation levels were attacked by Ips where the exposure level proved lethal. Several zones of effect on Ips developmental success were recognized at different intensities of exposure. Developmental success was greater on the self-shielded side than on the exposed side of trees. Trap logs were used for studies of developmental success at high radiation intensities. In 1962 development in them was subnormal reaching about 60%. In 1963 total utilization at low radiation intensities approached 100%. The zones of effect were comparable to those in the standing trees. The per cent of cambial surface utilized by Ips increased from 9% at 2,300r/day to about 80% at 300r/day. The difference between sides of the same log was as great as 30% because of the shielding factor. Ants are the only insects reported to have a radiation avoidance response. The habits of a colony of Formica integra changed so that ants were no longer exposed to high radiation levels. The ants constructed a 12.5 meter sunken runway from the nest away from the radiation source and they no longer appeared on the exposed nest snag. The insect community in the irradiated area was divided into two parts on the basis of food requirements, one ecologically sensitive and the other ecologically resistant. The former was composed of herbivorous populations and their parasites and predators while the latter contained fungivorous, xylophagous, and saprophagous populations, insects favoring debilitated plants, and the parasites and predators of these groups. (auth)

Metabolism, Tissue Distribution, and Toxicology

40308 (BNL-8379) STUDIES WITH DL-ALANINE-2-^{14}C OF INTERACTION OF ETHANOL METABOLISM WITH PATHWAYS OF HEPATIC GLUCONEOGENESIS IN THE RAT. Joubert, S. M.; Shreeve, W. W. (Brookhaven National Lab., Upton, N. Y.). [Aug. 12, 1964]. Contract AT(30-2)-Gen-16. 14p. Dep. mn; CFSTI, $1.00 cy, $0.50 mn.

It was postulated that metabolism of ethanol loads would change the distribution of ^{14}C in hepatic glutamic acid labeled from DL-alanine-2-^{14}C if changes in redox potential of the NAD$^+$/NADH system, occasioned by ethanol load, inhibit the oxidation of malic acid and thus decrease activity of the gluconeogenic pathway via dicarboxylic acids. However, ethanol metabolism enhanced rather than decreased the labeling of C-2 and C-3 of glutamate (indicative of CO_2 fixation with pyruvate) relative to the labeling of C-5 (oxidative decarboxylation of pyruvate to acetyl CoA), thus suggesting that oxidation of malate was uninhibited relative to oxidative decarboxylation of pyruvate. (auth)

40309 (NP-15180) DISTRIBUTION STUDIES OF COMMON AND RADIOACTIVE CESIUM IN NATURE AND IN MAN. Progress Report. Yamagata, Noboru (Institute of Public Health, Tokyo (Japan). Dept. of Radiological Health). Sept. 7, 1964. IAEA Contract 140/R2/RB. 17p. Dep. mn.

Progress is reported on: assessment of the whole-body burden of ^{137}Cs by blood analysis; analysis of stable Sr in biological materials using spectrography; and evaluation of marine contamination with radioisotopes with long half lives. Results indicate a general increase in the whole-body burden of ^{137}Cs and in the whole-body ^{137}Cs : K ratio during February to July 1964. Stable Sr was determined in human rib-bone. The Sr/Ca ratio in 20 samples was 3.3×10^{-4}, and the median value for Sr on a ppm-ash basis was 10^5. Maximum permissible levels of radioisotopes in sea food or in sea-water would be easily calculated for Japanese on the basis of the average estimated concentration factor or the equivalent daily intake of sea-water. The dietary composition of sea food differed by population and even by segments of a population. Therefore, the average concentration factor from sea-water to sea food as a whole was obtained for the Japanese population, and was not always usable for others. (H.G.D.)

40310 THE EFFECT OF POTASSIUM PHOSPHATE AND CALCIUM HYDROXIDE ON THE ACCUMULATION OF STRONTIUM-90 IN PLANTS AND ITS DEPENDENCE ON THE STABLE STRONTIUM CONTENT OF THE SOIL. Skadchenko, N. M. Vestn. Mosk. Univ., Ser. VI: Biol., Pochvoved., No. 5, 57-62(1964). (In Russian).

As a result of radioactive fallout, long half-life radioactive isotopes, among which ^{90}Sr is potentially the most dangerous one, are introduced into the human organism, mostly by the intermediary of agricultural products. The accumulation of these radioisotopes was investigated in tests carried out in podzolic soils, attempting to determine the effect of $Ca(OH)_2$ and K_3PO_4 additions to the soil on the ^{90}Sr content of oats as a function of the stable Sr content of the soil. The fertilizer additions included 0.285 g of NH_4NO_3, 0.5 g of superphosphates, and 0/17 g of K salts per kg of soil; the ^{90}Sr was introduced at a rate of 30 μcurie/kg of soil, while the stable Sr content of soil was 219.4 mg. The results indicated that if no stable Sr is added to the soil, the addition of large amounts of K_3PO_4 reduces markedly the amount of ^{90}Sr introduced into the plant; liming exerted an even stronger inhibiting effect on the accumulation of ^{90}Sr. The presence of increasing amounts of stable Sr in the soil resulted in an increase of ^{90}Sr in the grains and leaves. The effectiveness of the separate or simultaneous addition of K_3PO_4 and $Ca(OH)_2$ for reducing the accumulation of radiostrontium in the plant was reduced by adding increasing amounts of stable Sr to the soil. (TTT)

40311 RASPREDELENIE, BIOLOGICHESKOE DEISTVIE, USKORENIE VYVEDENIYA RADIOAKTIVNYKH IZOTOPOV. (Distribution, Biological Effects, and Rapid Excretion of Radioactive Isotopes). Moskalev, Yu. I. (ed). Moscow, Meditsina, 1964. 375p.

A single abstract was previously prepared for this collection of papers and appears in NSA as 19: 3884. Separate abstracts have now been prepared for the 45 papers included. (D.E.B.)

For abstracts of individual papers see: 40312–40348 and 40377–40384.

40312 DISTRIBUTION OF STRONTIUM-90 IN RATS AFTER INTRATRACHEAL ADMINISTRATION. Korolev, G. K. pp 9-14 of Raspredelenie, Biologicheskoe Deistvie, Uskorenie Vyvedeniya Radioaktivnykh Izotopov. Moscow, Meditsina, 1964. (In Russian).

Strontium-90 was rapidly absorbed from the lungs after intratracheal administration. Judging by the amount of strontium accumulating in the bones, the intratracheal route is very similar to the intravenous and intraperitoneal routes (the rat skeleton contained 76% after the first route was used and 81% after the second and third). Elimination of strontium from the skeleton may be characterized by two exponents. The first exponent for 14.27% of the content of the element in relation to the amount administered covered the first to third days, while the second exponent for 61.9% covered the third to sixtieth days. Regression analysis of the ^{90}Sr content of various organs and tissues showed that there was a correlation between the amount of ^{90}Sr in the blood, the total amount in the soft tissues and blood, the amount in the skeleton, and the time from administration of the substance during the period of maximum growth of the isotope in the skeleton. (ATD)

40313 DISTRIBUTION OF CERIUM-144 IN RATS AFTER INTRATRACHEAL ADMINISTRATION. Korolev, G. K. pp 15-22 of Raspredelenie, Biologicheskoe Deistvie, Uskorenie Vyvedeniya Radioaktivnykh Izotopov. Moscow, Meditsina, 1964. (In Russian).

Cerium-144 was absorbed from the lungs slowly. Half of the element administered was eliminated within 24 hours.

The maximum amount of absorbed activity was 41% (sixth day). The isotope was deposited mostly in the liver (27 ± 2.4%) and skeleton (15 ± 0.79%). Radiocerium was absorbed from the lungs exponentially. Intratracheal administration of 0.4 $\mu c/g$ of ^{144}Ce produced foci of catarrhal serous-hemorrhagic pneumonia in the lungs within 24 hours. The symptoms were most pronounced by the tenth day. Signs of emphysema and destruction became dominant after 6 months. Histoautograms of the lungs revealed that ^{144}Ce accumulated in the alveoli and interalveolar septa the first few days after administration. During the next 30 days it concentrated mainly in the interalveolar septa. (ATD)

40314 DISTRIBUTION OF YTTRIUM-91, ZIRCONIUM-95, AND NIOBIUM-95 IN RATS AFTER INHALATION. Moskalev, Yu. I.; Semenov, D. I.; Buldakov, L. A. pp 23-8 of Raspredelenie, Biologicheskoe Deistvie, Uskorenie Vyvedeniya Radioaktivnykh Izotopov. Moscow, Meditsina, 1964. (In Russian)

From 15 minutes to 6 hours after inhalation of ^{95}Nb, ^{91}Y, or ^{95}Zr, most of the activity in rats is found in the head, gastrointestinal tract, skin, and lungs. The lungs retained about 13% of the inhaled ^{91}Y, ^{95}Zr, and ^{95}Nb. A comparison of the distribution of the radioisotopes in relation to the route of entry showed that after inhalation the portion of yttrium resorbed from the lungs was distributed the same way as when it was injected intravenously. Soon after inhalation, more zirconium was found in the skeleton and less in the liver than after intravenous injection. The amount of niobium deposited in the skeleton, kidneys, and muscles was greater after inhalation than after intravenous injection, but less was deposited in the liver and blood. These differences in distribution were obliterated by the 16th day of the experiment. (ATD)

40315 DISTRIBUTION OF THE RADIUM ISOTOPE THORIUM-X. Moskalev, Yu. I. pp 29-34 of Raspredelenie, Biologicheskoe Deistvie, Uskorenie Vyvedeniya Radioaktivnykh Izotopov. Moscow, Meditsina, 1964. (In Russian).

When ThX (^{224}Ra) is injected intravenously in rats, the amount of radium concentrating in the bones, kidneys, salivary glands, thyroid, and gastric and intestinal mucosa is higher than in other tissues. The diaphysis contains less radium than does the epiphysis. The distribution of ThX varies with the age of the animal. More ThX is deposited in the bones of young rats than in the bones of old rats. On the other hand, less ThX accumulates in the soft tissues of old animals than in the tissues of young animals. Adult rats excrete more ThX with urine than do young rats. ThX is rapidly absorbed from muscular tissue, more than 60% within an hour and about 95% within 24 hours. The absorption of ThX proceeds more slowly in adult rats than it does in young, rapidly growing animals. There seems to be a connection between the excretory functions of the gastrointestinal tract and the kidneys. For example, one of the experimental rats that excreted 3.6% more radium with feces than did another animal excreted the same amount less (by 3.23%) with urine. (ATD)

40316 BEHAVIOR OF A CITRATE COMPLEX OF PLUTONIUM-239 IN RATS AFTER INHALATION. Lyubchanskii, E. R. pp 35-41 of Raspredelenie, Biologicheskoe Deistvie, Uskorenie Vyvedeniya Radioaktivnykh Izotopov. Moscow, Meditsina, 1964. (In Russian).

Immediately after a citrate complex of ^{239}Pu was inhaled by rats, 50, 18.7, 28.8, and 2.6% of the activity in the organism was found in the gastrointestinal tract, head, lungs, and viscera, respectively. The amount of ^{239}Pu in the gastrointestinal tract decreased 100-fold in 8 days, 1,000-fold in 32 days. The radioisotope was removed from the lungs during four periods differing in time and portion of the isotope removed: about 9% with a half-life of a few minutes; about 56% with a biological half-life of 19 hours; 65% of the activity noted after 24 hours was removed with a half-life of 7.4 days; and 35% with a half-life of 137 days. After 64 days the amount resorbed was 35 to 40% of the original content in the lungs. The amount deposited in the skeleton and liver did not exceed 25% and 6%, respectively, of the original content in the lungs. Clearance from the liver, starting the 32nd day, proceeded with a biological half-life of 119 days. Most of the resorbed ^{239}Pu was deposited in the skeleton from the first day. The concentration of the radioisotope in the lungs exceeded that in the skeleton throughout the investigation. (ATD)

40317 CONTENT AND MICRODISTRIBUTION OF PLUTONIUM-239 IN RAT LUNG AND LIVER AND MORPHOLOGICAL CHANGES IN THESE ORGANS AFTER INTRATRACHEAL ADMINISTRATION OF THE ISOTOPE. Erokhin, R. A.; Koshurnikova, N. A.; Lyubchanskii, E. R.; Nifatov, A. P.; Reshetov, G. N. pp 42-61 of Raspredelenie, Biologicheskoe Deistvie, Uskorenie Vyvedeniya Radioaktivnykh Izotopov. Moscow, Meditsina, 1964. (In Russian).

The behavior of ^{239}Pu in the lung of rats following intratracheal administration of various salts is determined largely by the physicochemical form of the compound used. The plutonium content of the lungs after administration of the nitrate was 5 to 10 times higher than after administration of sodium plutonyl triacetate. The clearance of plutonium administered in the form of these two salts obeys the exponential law, but it was more rapid in the case of the second salt. A large quantity of plutonium was transported from the lungs by macrophages into the regional lymph nodes. Plutonium accumulated in the liver during the early phase (20 minutes to 24 hours) more slowly after administration of the nitrate than it did after administration of sodium plutonyl triacetate. During the later phases (4 to 6 months) the rate of deposition in the liver was about the same after administration of either form of plutonium, 0.90 to 0.56 and 0.95 to 0.57% of the dose administered. The microdistribution of plutonium in rat liver after intratracheal administration of the two plutonium salts was quite diffuse. Histological changes in the lung varied with the nature of the microdistribution of the element and they arose mainly in the places where the isotope concentrated. The severity of the pathological changes and the time when they developed were related to the ionization dose that accumulated. Among the earliest changes were degeneration, desquamation of bronchial and alveolar epithelium, and perivascular edema. These were followed by chronic inflammation, chiefly productive in character. The pathological process developed into pneumosclerosis as a result of the proliferation of connective-tissue cellular elements with the formation of fibrous structures. No significant morphological changes were noted in the liver after intratracheal administration of 7 $\mu c/kg$ of plutonium nitrate or sodium plutonyl triacetate. (ATD)

40318 DISTRIBUTION OF ANTIMONY-124 AND TELLURIUM-127. Moskalev, Yu. I. pp 62-70 of Raspredelenie, Biologicheskoe Deistvie, Uskorenie Vyvedeniya Radioaktivnykh Izotopov. Moscow, Meditsina, 1964. (In Russian).

About 75% of the ^{124}Sb injected into rats intravenously (in the form of antimonyl potassium tartrate) was excreted with urine during the first 24 hours of the experiment. Comparatively little of the isotope was retained in the organs: 10.7% in the liver, 2.2% in the skeleton, 0.91% in the blood, and 0.73% in the muscles. After oral administration, most of the ^{124}Sb was excreted with feces (about 94% during the 3 days of the experiment). The amount of ^{124}Sb absorbed from the gastrointestinal tract was about 3%. After intravenous injection, ^{127}Te was distributed comparatively uniformly in the various organs of rats. It was slowly cleared from the blood, kidneys, lungs, and skin. Most of the tellurium was deposited in the blood (18.6%), muscles (11.9%), liver (9.7%), skeleton (8.6%), and kidneys (2.5%). After oral administration, 10 to 25% of the ^{127}Te was absorbed. The ^{127}Te absorbed from the gastrointestinal tract was deposited, as in the case of intravenous injection, mainly in the blood (1.95%), muscles (1.19%), liver (0.41%), skeleton (0.39%), and kidneys (0.22%). (ATD)

40319 COMPARISON OF THE DISTRIBUTION OF MOLYBDENUM-99 AND PHOSPHORUS-32 IN ANIMALS. Borisov, V. P. pp 71-7 of Raspredelenie, Biologicheskoe

Deistvie, Uskorenie Vyvedeniya Radioaktivnykh Izotopov. Moscow, Meditsina, 1964. (In Russian).

The absorption and subsequent deposition of ^{99}Mo in rats is virtually the same whether the isotope is in the form of molybdenum oxide or molybdate. Molybdenum-99 metabolism differs considerably from ^{32}P metabolism. Specifically, ^{99}Mo does not concentrate in bone as does ^{32}P. With respect to distribution (in the early phase), ^{99}Mo may be classified with the isotopes that are distributed uniformly. It is also absorbed at a high rate (about 90%) from the digestive tract and is rapidly excreted (usually within 24 hours); chiefly through the kidneys. If the young products of uranium fission (up to 1 to 2 weeks old) enter the body, ^{99}Mo may constitute a substantial part of the resorbed radioisotopes. The role of ^{99}Mo is particularly significant during the first few hours after intoxication in the total radioactivity of the blood, skin, liver, kidneys, and urine. (ATD)

40320 DISTRIBUTION OF TIN-113. Moskalev, Yu. I. pp 78-82 of Raspredelenie, Biologicheskoe Deistvie, Uskorenie Vyvedeniya Radioaktivnykh Izotopov. Moscow, Meditsina, 1964. (In Russian).

The distribution of various ^{113}Sn compounds was studied in rats in relation to the method of administering the isotope. After parenteral injection, the concentration of tin was highest in the liver, spleen, bone marrow, skeleton, and kidneys. It was lowest in the brain (0.07%) and testes (0.06%). The pattern of distribution and method of excretion of the isotope varied with the pH and compound used (simple salt, complex compound). About 20% of ^{113}Sn was absorbed after oral administration. The nature of the distribution was the same as after parenteral injection. (ATD)

40321 DISTRIBUTION OF A MIXTURE OF CERIUM-144 AND STRONTIUM-89, -90. Moskalev, Yu. I. pp 83-93 of Raspredelenie, Biologicheskoe Deistvie, Uskorenie Vyvedeniya Radioaktivnykh Izotopov. Moscow, Meditsina, 1964. (In Russian).

After intravenous injection of a mixture of ^{144}Ce, ^{89}Sr, and ^{90}Sr to rats most of the activity was concentrated in the skeleton (46.6%) and liver (26%). The lowest concentration of activity was noted in the brain, testes, and muscles. The mixture was excreted chiefly with the feces. After oral administration, the resorbed radioactive substances were deposited almost exclusively in the skeleton (about 18.6%). When introduced into the stomach, the mixture of radioactive strontium and cerium left the stomach and small intestine during the first 6 hours of the experiment. The small intestine was the principal site of absorption and excretion of the radioactive mixture. The experiments clearly showed that when the two isotopes were administered simultaneously, each followed its own distribution pattern independently of the other. (ATD)

40322 ON THE CHANGE OF ISOTOPIC RATIO IN A MIXTURE OF URANIUM FISSION PRODUCTS AFTER ABSORPTION FROM THE INTESTINAL TRACT. Borisov, V. P. pp 94-7 of Raspredelenie, Biologicheskoe Deistvie, Uskorenie Vyvedeniya Radioaktivnykh Izotopov. Moscow, Meditsina, 1964. (In Russian).

The isotopic ratio of uranium fission products absorbed from the intestinal tract of rats was studied using a 2-yr-old solution containing 91% ^{144}Ce, 5.1% ^{89}Sr, 1.7% ^{90}Sr, 1.7% ^{90}Y, and 0.2% ^{95}Zn. After oral administration of the solution, at a dose of 75 μc/kg body weight, the concentrations of Sr and Y increased in the rats while the concentrations of the rare earth elements decreased. Strontium, Y, and Zr concentrated in bone tissues and cerium concentrated in the skin. (R.V.J.)

40323 STRONTIUM-90 CONTENT IN RATS AFTER CHRONIC ORAL ADMINISTRATION OF THE ISOTOPE. Buldakov, L. A.; Erokhin, R. A. pp 98-105 of Raspredelenie, Biologicheskoe Deistvie, Uskorenie Vyvedeniya Radioaktivnykh Izotopov. Moscow, Meditsina, 1964. (In Russian).

After chronic oral administration of ^{90}Sr to rats, most of the activity was found in bones. The specific activity of the soft tissues was 50 to 100 times greater than that of the bones. A relative balance between the daily excretion and deposition of the isotope developed in the skeleton between the 16th and 20th weeks of the experiment. At this time the accumulation multiplicity factor for strontium in the skeleton was 9.68 to 9.78 in mature and old rats and 13.3 in young rats. At later periods there was no significant increase in the accumulation multiplicity factor in the old rats, but it was 17.45 ± 3.51 in the young animals by the 52nd week. The removal of ^{90}Sr from bone was not related to the daily dose of the emitter or duration of the exposure. After 600 days of oral administration of strontium, 35.5% of the activity deposited in the skeleton was removed with an effective period of 5.6 days and 64.5% with T_{eff} = 599 days. After termination of the experiment, which ran for a year, 41.8% of the strontium was excreted from the skeleton with T_{eff} = 25.6 days and 58.2% with T_{eff} = 533 days. The empirical values of the maximum accumulation multiplicity factor for ^{90}Sr in the rat skeleton were 7 to 8 times smaller than the theoretical values. (ATD)

40324 DISTRIBUTION OF STRONTIUM-90 IN THE SKELETON OF DOGS AFTER CHRONIC EXPOSURE TO THE ISOTOPE. Yartsev, E. I.; Burykina, L. N. pp 106-11 of Raspredelenie, Biologicheskoe Deistvie, Uskorenie Vyvedeniya Radioaktivnykh Izotopov. Moscow, Meditsina, 1964. (In Russian).

After daily ingestion of ^{90}Sr with food for periods ranging from 1 to 17 months, higher levels of accumulation of the isotope were observed in cancellous bones than in compact bones. The redistribution of the isotope in the skeleton varied with the duration of exposure (the rate of deposition was higher in the skull than in the sternum). The longer the period of uptake of the isotope, the more uniformly was it distributed in different parts of the skeleton. The rate of ^{90}Sr accumulation in the skeleton kept rising as the time of chronic administration of the isotope was increased. A distinct relationship was observed between the accumulation of ^{90}Sr and the age of the animal. The highest levels were found in young growing animals. The mean value of the differential accumulation factor was 750 for the skeleton of young dogs, 266 for that of mature dogs, and 140 for that of old dogs. Compared with ^{90}Sr distribution in old dogs, young dogs had a much higher content of the isotope in the skull, teeth, and growing long bones, but a lower content in the sternum. (ATD)

40325 ACCUMULATION OF STRONTIUM-90 IN THE SKELETON OF DOGS AFTER CHRONIC ADMINISTRATION OF THE ISOTOPE. Kushneva, V. S. pp 112-16 of Raspredelenie, Biologicheskoe Deistvie, Uskorenie Vyvedeniya Radioaktivnykh Izotopov. Moscow, Meditsina, 1964. (In Russian).

The dynamics and extent of ^{90}Sr accumulation in vivo and the doses absorbed in dogs after prolonged chronic uptake of the isotope with food were studied. After 3 years of ingesting ^{90}Sr (at first 11.2 μc/kg, then 35 days later 1 μc/kg was regularly added every 2 weeks), the experimental animals differed very little from the control in outward appearance, but several of the bodily systems were impaired, especially the hematopoietic organs. Radiometry of tail vertebrae amputated 2, 6, 19, 24, 30, and 36 months after the start of the experiment revealed the presence of strontium in the bones. The rate of deposition seemed to be constant. But the concentration of the isotope was not the same in different parts of the skeleton. The differential accumulation factor ranged from 40 to 5. The correlations established between the concentrations of activity in the tail vertebrae and in other parts of the skeleton can be used for in vivo evaluation of tissue doses of radiation in various parts of the skeleton of animals chronically exposed to ^{90}Sr. They are also of value in determining the average amount of strontium throughout the body. (ATD)

40326 BEHAVIOR OF PLUTONIUM-239 CITRATE IN RATS AFTER SINGLE AND REPEATED INTRAPERITO-

NEAL INJECTION OF THE ISOTOPE. Lyubchanskii, E. R. pp 117-23 of Raspredelenie, Biologicheskoe Deistvie, Uskorenie Vyvedeniya Radioaktivnykh Izotopov. Moscow, Meditsina, 1964. (In Russian).

Five days after a single intraperitoneal injection of ^{239}Pu citrate in rats, the animals were found to contain 13.8 ± 0.84% of the administered dose in the liver, 3.72 ± 0.16% in the femur, 0.81 ± 0.05% in the scapula, and 2.11 ± 0.16% in the muscles. Eighty-five percent of the isotope was excreted from the liver with a biological half-life of 7 days, and 15% with a biological half-life of 125 days; 35% was excreted from the spleen with a biological half-life of 31 days and 65% with a biological half-life of 600 days. Plutonium-239 was excreted from the femur, scapula, and muscles with a biological half-life of 840, 700, and 108 days, respectively. The age of the rats affected the rate of deposition and excretion of ^{239}Pu. In the femur and scapula of old rats (18 months), 5 days after injection of the isotope, 25 and 20% less was deposited than in young animals (3 months). The rate of excretion was twice as high in the old animals. The behavior of ^{239}Pu after repeated injection differed from its behavior after a single injection in that it was followed by a gradual decrease in deposition of the isotope in the femur and scapula along with an increase in excretion with feces. The deposition of ^{239}Pu in the liver and muscles was wavelike in character. (ATD)

40327 PASSAGE OF STRONTIUM-90 FROM MOTHER TO OFFSPRING IN DOGS UNDER CONDITIONS OF CHRONIC UPTAKE. Burykina, L. N.; Parfenov, Yu. D. pp 124-30 of Raspredelenie, Biologicheskoe Deistvie, Uskorenie Vyvedeniya Radioaktivnykh Izotopov. Moscow, Meditsina, 1964. (In Russian).

Seven mature female dogs received 0.002 μc/kg, 0.2 μc/kg, or 0.2 μc/kg of ^{90}Sr daily with food over a long period. At various times during the experiment they were mated, and 19 to 41 months after they began to receive the isotope, they produced offspring. Administration of the isotope continued throughout pregnancy and lactation. The amount of ^{90}Sr accumulating in the mother's skeleton reached a maximum 11 to 17 months after the start of the experiment and remained constant thereafter. Thus, the puppies were born at a time when the level of radioactivity in their mothers' skeletons remained unchanged. The ^{90}Sr concentration was found to be twice as high in the skeleton of the puppy as in that of the mother. The maximum concentration during postembryonal development was 4 times higher than in the fetus. The results of the experiment show that puppies produced and suckled by mothers who regularly received ^{90}Sr with food accumulated disturbingly large amounts of radioactivity. Data are summarized from earlier investigations on rats and rabbits. (ATD)

40328 ACCUMULATION AND DISTRIBUTION OF STRONTIUM-90 IN SWINE AFTER PROLONGED ADMINISTRATION OF RADIOSTRONTIUM. Annenkov, B. N.; Chukhin, S. G.; Bakhareva, Z. A. pp 131-5 of Raspredelenie, Biologicheskoe Deistvie, Uskorenie Vyvedeniya Radioaktivnykh Izotopov. Moscow, Meditsina, 1964. (In Russian).

Swine received ^{90}Sr with their rations. About 4% of the isotope ingested was deposited in different parts of the body and in varying amounts: 93.3 to 96.9% in the skeleton, the rest in the soft tissues and organs. Of the two alkaline earth elements (calcium and ^{90}Sr), Ca was favored by the swine. The factor of discrimination between ^{90}Sr and calcium in the food-bone link was 0.17 to 0.33. As soon as the administration of radiostrontium was halted, the amount of the isotope in the body decreased rapidly. The effective half-life of ^{90}Sr was 112 ± 26 days. (ATD)

40329 ACCUMULATION OF STRONTIUM IN THE SKELETON OF CALVES. Buldakov, L. A.; Burov, N. I. pp 136-41 of Raspredelenie, Biologicheskoe Deistvie, Uskorenie Vyvedeniya Radioaktivnykh Izotopov. Moscow, Meditsina, 1964. (In Russian).

The distribution of ^{90}Sr in the skeleton of calves from birth to 9 months of age varied from bone to bone. The difference between the maximum and minimum concentrations of strontium in the different bones ranged from 3.5 to 10. The differences did not exceed 3 in 1½ year old calves. The amount of strontium retained in the skeleton of the fetus during the last 120 days of pregnancy was not related to the quantity of the isotope entering the stomach of the cow. It ranged from 0.52 to 2.25, averaging 1.41. In growing calves the amount of strontium deposited in the skeleton decreased with age from 67.5% during the first month of life to 12.85% after 18 months. Between 9 and 18 months of age, 3.64% of the strontium entering the stomach was deposited in the skeleton. The accumulation multiplicity factor for ^{90}Sr in the skeleton of newborn calves averaged 1.69, with fluctuations from 0.63 to 2.71. The maximum value of the accumulation multiplicity factor (100.5 to 121.0) was found during the 9th month of life of the calf, after which this value decreased to 70 to 73.2 by the 18th month. The factor of discrimination between strontium and calcium in the mother food-fetus skeleton system was 0.259 during the second half of pregnancy. During the first 9 months the discrimination between strontium and calcium in the food-skeleton system fluctuated from 0.83 to 1.05. From 9 to 18 months of age it dropped to 0.204. (ATD)

40330 ACCUMULATION OF STRONTIUM-90 IN CATTLE DURING THE EMBRYONAL AND POSTEMBRYONAL PERIODS OF DEVELOPMENT. Annenkov, B. N.; Bakhareva, Z. A. pp 142-6 of Raspredelenie, Biologicheskoe Deistvie, Uskorenie Vyvedeniya Radioaktivnykh Izotopov. Moscow, Meditsina, 1964. (In Russian).

Following the addition of ^{90}Sr to the food of cows during the last few months of pregnancy, 0.50 to 1.24% of the radiostrontium passed into the fetus. The amount of the isotope deposited in the calves came to about 60% by the 2nd to 3rd month of life, dropping to 30 to 40% between the 4th and 6th months. Some 0.9 to 1.6% of the ^{90}Sr ingested with hay was retained by the cows. The addition of a mineral supplement to the food of the cattle to ensure an excess of calcium reduced the amount of radiostrontium deposited in the fetus. The distribution of ^{90}Sr in the various age groups of the cattle was the same. Most of it (92 to 99%) was retained in the skeleton; only 1 to 8% of the total amount found in the organism accumulated in the soft tissues and organs. A comparison of the data on ^{90}Sr concentration in the bones of animals of different age groups showed that it decreases with age. The explanation may be that, first, the amount of ^{90}Sr deposited decreases and, second, the radiostrontium taken up is distributed over a larger skeleton since the skeleton of adult cows weighs 7 to 10 times more than that of newborn calves. (ATD)

40331 PENETRATION OF STRONTIUM-90 THROUGH THE PLACENTAL BARRIER OF SHEEP. Burov, N. I.; Buldakov, L. A. pp 147-53 of Raspredelenie, Biologicheskoe Deistvie, Uskorenie Vyvedeniya Radioaktivnykh Izotopov. Moscow, Meditsina, 1964. (In Russian).

The amount of ^{90}Sr passing from the mother to the fetus of sheep varied with the time of pregnancy and method of administering the isotope. Some 10 to 12 times more strontium was deposited in the newborn lamb after intravenous injection of the isotope than after oral administration. After 30, 90, 120, 136, and 152 days of pregnancy, 0.207, 1.23, 6.72, 9.41, and 12.13%, respectively, of the strontium injected into the blood of the mother was deposited in the skeleton of the fetus. After a single oral administration 500 to 510 and 50 to 100 days before pregnancy and on the 120th, 136th, and 152nd days of pregnancy, 0.0144 ± 0.0029%, 0.082 ± 0.003%, 0.876%, 1.10%, and 0.509% of the dose was deposited in the skeleton. The amount of ^{90}Sr passing from the mother to the fetus during the entire period of pregnancy in the case of chronic administration of the isotope varied with the length of the experiment. The longer the animal received strontium before the next pregnancy, the greater the amount of the isotope that entered the fetus. Strontium was distributed unevenly in the skeleton of the baby lamb, and it too varied with the time of pregnancy. After chronic uptake of the

isotope and when it was administered before or early in pregnancy, the highest concentrations were found in the skull bones, mandible, and diaphysis, and when administered later, in the metaphysis. (ATD)

40332 MIGRATION OF RADIOACTIVE STRONTIUM THROUGH THE FODDER-COW-MILK CHAIN. Annenkov, B. N. pp 154-60 of Raspredelenie, Biologicheskoe Deistvie, Uskorenie Vyvedeniya Radioaktivnykh Izotopov. Moscow, Meditsina, 1964. (In Russian).

A study was made to determine in extended experiments on cows the amount of ^{90}Sr entering milk, to determine the amount of ^{90}Sr entering milk from different kinds of hay, to obtain data concerning the effect of the calcium nutrition level on the secretion of ^{90}Sr by the mammary gland, to find the factor of ^{90}Sr discrimination in relation to calcium as the isotope passed from fodder into milk, and to observe the excretion of ^{90}Sr with milk after administration of the radioisotope to cows was halted. After chronic administration of radiostrontium to cows with the ration, 1 liter of milk was found to contain 0.10 to 2.20% (average of 0.142%) of the daily intake of ^{90}Sr. The mammary gland secreted in 24 hours 0.204 to 4.70% of the ^{90}Sr ingested with the ration during this time. The total amount of strontium excreted with the yield of milk varied with the level of mammary gland secretion. If 400 g of $CaCO_3$ was added to the ration, or leguminous hay was substituted for herbaceous hay in the ration, the amount of ^{90}Sr entering the milk was reduced 20 to 35%. The ^{90}Sr discrimination factor in the milk-fodder link ranged between 0.093 and 0.251. The value of the discrimination factor was largely determined by the amount of stable calcium ingested with the ration. When the administration of radiostrontium to the cows was halted, the isotope concentration in the milk decreased rapidly at first ($T_{eff} \sim 3$ days), but more slowly thereafter ($T_{eff} \approx 100$ days). (ATD)

40333 DISTRIBUTION OF LEAD (THORIUM B) AFTER INTRA-ARTERIAL AND INTRAVENOUS INJECTION. Moskalev, Yu. I. pp 161-4 of Raspredelenie, Biologicheskoe Deistvie, Uskorenie Vyvedeniya Radioaktivnykh Izotopov. Moscow, Meditsina, 1964. (In Russian).

The results of experiments performed on 11 rabbits showed that the distribution of ^{212}Pb(ThB) varies with the method of administration of the isotope. Relatively more of it was found in the kidneys, liver, spleen, and blood after intravenous injection than after subcutaneous or intra-arterial injection. After intravenous injection it was most abundant in the kidneys, and after intra-arterial injection in the kidneys and bone marrow on the side of the injection site. After intra-arterial injection, bone, bone marrow, and muscular tissue on the side of the injection site contained 10 to 18 times more activity than after intravenous or subcutaneous injection. The liver, kidneys, lungs, and spleen contained almost half as much ThB after subcutaneous injection as after intravenous or intra-arterial injection, showing that absorption of the isotope from subcutaneous tissue was comparatively slow and incomplete. The results of experiments on 15 rats show that the distribution of ThB differs markedly, depending on whether it is injected into the mesenteric or tail vein. A day after injection into the mesenteric vein, the liver contained 3.3 times more ThB than after injection into the tail vein. The author considers his findings of significance not only for what they indicate about the nature of isotope distribution in relation to the route of entry into the body, but for the light they may throw on several problems in physiology pertaining to the mechanism of action of stimulants following intravenous and intra-arterial injection. (ATD)

40334 METABOLISM AND BIOLOGICAL EFFECTS OF CESIUM-137 IN SHEEP. Buldakov, L. A. pp 167-82 of Raspredelenie, Biologicheskoe Deistvie, Uskorenie Vyvedeniya Radioaktivnykh Izotopov. Moscow, Meditsina, 1964. (In Russian).

Cesium-137 administered orally to sheep (2.2 μc/24 hours) for 105 days was distributed uniformly in the viscera. Somewhat higher concentrations of the isotope were noted in muscle tissue and skin; lowest concentrations, in bones and bone marrow. The maximum ^{137}Cs accumulation multiplicity factor by the 105th day of the experiment was 2.55, 0.89, 0.25, 1.83, and 4.54 for the muscles, liver, kidneys, skin, and viscera plus skin, respectively. The isotope was excreted with feces, 11.04%, with urine, 9.16%, and with milk, 2.02% of the daily dose per kg of body weight. When administration of the isotope was halted, the activity of the excrement dropped between the 10th and 45th days to 1.83 to 3.51% (urine and feces) and to 0.251 to 0.68% (milk) of the daily dose. The rate of excretion followed the exponential law. The biological half-life of ^{137}Cs from all the soft tissues was 10.4 days for 70%, and 68 days for 30% of the amount retained in the organism. In growing animals, the half-life of ^{137}Cs from all the soft tissues was 24.4 days for 36%, and 49.5 days for 64% of the initial content of the isotope in the organism. Cesium was transmitted from the mother mainly during the first month of life of the baby lamb. During the period of intrauterine development, the concentration of cesium in the fetal tissues was almost 10 times lower than that in the mother's tissues. Oral administration of ^{137}Cs (230 μc over 105 days, 2,000 μc over 10 days, and 2,000 μc at one time) failed to produce significant changes in the peripheral blood cells of the adult animals and their offspring. Very slight changes in the hemoglobin concentration (decrease from 64 to 39.4 to 46%) and in the leukocyte count (from 9,300 to 6,350 and from 7,820 to 6,060 in 1 mm^3) were noted in the sheep that received 2,000 μc of the isotope either at one time or over 10 days. (ATD)

40335 BIOLOGICAL EFFECTS OF STRONTIUM-90, CESIUM-137, AND PROMETHIUM-147 AFTER CHRONIC ORAL ADMINISTRATION OF LOW DOSES OF THE ISOTOPES. Nifatov, A. P.; Buldakov, L. A. pp 183-91 of Raspredelenie, Biologicheskoe Deistvie, Uskorenie Vyvedeniya Radioaktivnykh Izotopov. Moscow, Meditsina, 1964. (In Russian).

Oral administration of 0.00051 and 0.012 μc/24 hours of ^{90}Sr, 0.00124 μc/24 hours of ^{137}Cs, or 0.0027 μc/24 hours of ^{147}Pm to rats for almost two years had no significant effect on the average survival time, weight, peripheral blood, or rate of tumor formation in the rats. Although the overall number of tumors was the same in both the experimental animals and the controls, the spectrum of neoplasms was different. The experimental animals had more tumors of the adrenal cortex, testes, gastrointestinal tract, and generalized leukemias, a phenomenon not explained by the authors. Since the greater frequency of glandular tumors was not related to the dose or to local irradiation, the authors doubt that these neoplasms were the result of direct radiation injury or that they were the determining factor in the death of the animals. The main causes of death seemed to be various inflammatory processes in the lungs and gastrointestinal tract, periarteritis nodosa, cirrhosis of the liver, and nephrosclerosis. These diseases were equally common in the experimental and control animals. (ATD)

40336 BIOLOGICAL EFFECTS OF STRONTIUM-90 IN RELATION TO THE DURATION AND FREQUENCY OF UPTAKE OF THE ISOTOPE. Moskalev, Yu. I.; Strel'tsova, V. N.; Teplinskaya, G. N. pp 192-201 of Raspredelenie, Biologicheskoe Deistvie, Uskorenie Vyvedeniya Radioaktivnykh Izotopov. Moscow, Meditsina, 1964. (In Russian).

The results of experiments on 699 white rats showed that the rate of administration of strontium-90, as well as the dose, markedly contributed to the biological effects of the isotope. For example, shortening of the survival time, lag in weight increase, decrease of leukopenia and thrombocytopenia, and frequency of osteosarcomas were greatest after a single administration of strontium-90. On the other hand, the development of anemia and leukemia was not related to the frequency of uptake of the isotope, which indicates that after ^{90}Sr lesions the processes of summation and regeneration in different tissues took place at different rates. This was also true of the erythrocyte series. The

values of $LD_{50/240}$ after a single administration of ^{90}Sr were 224 and 126 μc per rat; with daily administration for 100 days, they were 776 and 209 μc per rat, respectively. (ATD)

40337 TOXICITY OF TRITIUM UNDER EXPERIMENTAL CONDITIONS. Zhuravlev, V. F. pp 202-8 of Raspredelenie, Biologicheskoe Deistvie, Uskorenie Vyvedeniya Radioaktivnykh Izotopov. Moscow, Meditsina, 1964. (In Russian).

Tritium oxide introduced into the stomach of rabbits (by means of a syringe) caused radiation sickness, the severity varying directly with the dose: 0.3 c/kg induced the mild form; 0.4 c/kg the severe form; and 0.5 c/kg the extremely severe form. The 0.3 c/kg dose was followed by gradual regeneration of the blood and disappearance of clinical symptoms. The symptoms of the acute form of the sickness induced by tritium oxide are scarcely distinguishable from those resulting from external irradiation. The differences are a shorter latent period and earlier manifestation of the clinical symptoms. A feature of tritium oxide behavior is that it is more uniformly distributed in the body compared with many other radioactive substances. It was found that the development of radiation sickness and the time when the experimental animals died varied both with the dose of the isotope used and with the distribution of the tissue dose. (ATD)

40338 EFFECT OF ADDITIONAL PATHOLOGICAL AGENTS ON THE PERIPHERAL BLOOD OF RATS EXPOSED TO PLUTONIUM-239. Kudasheva, N. P.; Koshurnikova, N. A. pp 217-24 of Raspredelenie, Biologicheskoe Deistvie, Uskorenie Vyvedeniya Radioaktivnykh Izotopov. Moscow, Meditsina, 1964. (In Russian).

Additional stresses (repeated bleeding and aseptic inflammation produced by turpentine) placed on rats that had received ^{239}Pu in a low dose (0.63 μc/kg) known to have little effect on the peripheral blood failed to produce significant changes in the number of erythrocytes and reticulocytes or the hemoglobin concentration, nor were there appreciable effects on the white blood cells. The gradual decrease noted in the total number of leukocytes and lymphocytes and the increase in the neutrophils were probably age-related because they were found in both experimental and control animals at more or less the same intervals. (ATD)

40339 EVALUATION OF SOME DRUGS FOR EMERGENCY USE IN CASE OF INJURY BY RADIOACTIVE SUBSTANCES. Borisov, V. P.; Krivchenkova, R. S. pp 291-8 of Raspredelenie, Biologicheskoe Deistvie, Uskorenie Vyvedeniya Radioaktivnykh Izotopov. Moscow, Meditsina, 1964. (In Russian).

When radioactive substances pass into the stomach, the effectiveness of therapeutic preparations varies with the method of use. The simultaneous entry of ^{238}U and sodium bicarbonate, ^{238}U and the antidote for metals, or ^{144}Ce and complexing agents into the gastrointestinal tract of rats accelerated deposition of the radioactive substances in the tissues and organs. Activated charcoal failed to prevent absorption of the isotopes. The complexing agents trisodium–calcium salt of diethylenetriaminopenta-acetic acid ($Na_3CaDTPA$), proved to be less effective after entry of ^{144}Ce into the digestive tract than after intraperitoneal injection. The use of complexing agents to wash the stomach or decontaminate the buccal cavity is contraindicated because the entry of these substances into the stomach after oral poisoning by ^{144}Ce was found to elevate the level of deposition of the isotope in the liver and bones. Phosphates were useful in reducing deposition of the isotope in the liver of animals poisoned by ^{238}U. The antidote for metals and dry hydrogen sulfide (hydroquinoline hydrosulfide) were effective against polonium in the stomach; barium sulfate against ^{90}Sr poisoning; fluorexon (N,N-di-carboxymethyl aminomethylfluorescein) was effective against ^{144}Ce, reducing deposition of the isotope in the skeleton and liver at the same time. (ATD)

40340 EXPERIMENTAL THERAPY OF RABBITS POISONED BY TRITIUM OXIDE. Zhuravlev, V. F. pp 299-310 of Raspredelenie, Biologicheskoe Deistvie, Uskorenie Vyvedeniya Radioaktivnykh Izotopov. Moscow, Meditsina, 1964. (In Russian).

Tritium has adverse effects on various systems of the body, hematopoiesis, vascular permeability, nerves, etc. Thus, combined therapy is indicated for poisoning by this isotope. Rabbits given 0.4 c/kg of tritium oxide developed severe radiation sickness. Diuretin and water accelerated the excretion of the isotope. The preparation KO-2 (cobalt and nicotinic acid) was used to stimulate hematopoiesis. The combined therapy enabled most of the animals (17 out of 20) to survive. The three treated animals that died lived twice as long as the controls. The clinical symptoms of radiation sickness were much less pronounced in the treated animals and restoration started sooner in the various organs and systems. (ATD)

40341 EFFECT OF FOOD CALCIUM ON METABOLISM OF STRONTIUM-90 IN THE FODDER-MILK LINK IN COWS. Buldakov, L. A.; Burov, N. I.; Ukhanova, V. A. pp 311-15 of Raspredelenie, Biologicheskoe Deistvie, Uskorenie Vyvedeniya Radioaktivnykh Izotopov. Moscow, Meditsina, 1964. (In Russian).

During the summer the amount of ^{90}Sr penetrating into milk from green fodder varies with the calcium in the ration and the extent of daily milking. With equal daily milking of cows kept on a diet with a low calcium content (oats, 30 g of calcium daily) and with a high calcium content (vetch, 70 g of calcium daily), 0.27 and 1.12% of the dose of strontium was excreted with one liter of milk, and 2.78 and 1.16% with the daily yield of milk. When the milking was considerably different, the excretion of ^{90}Sr with one liter was somewhat higher in the low milkers (0.12 to 0.27%) than in the high milkers (0.10 to 0.23% of the daily dose). In terms of the daily yield, the excretion of ^{90}Sr with milk was much higher in the good milkers (1.96 to 4.95%) than in the poor milkers (1.164 to 2.78%). The ^{90}Sr discrimination factor in the fodder-milk link during the summer was 0.080 and 0.088 and it was not related to the extent of daily milking or to the amount of calcium in the fodder. (ATD)

40342 EFFECT OF SOME CONSTITUENTS OF FOOD PRODUCTS (CALCIUM, MAGNESIUM, PROTEIN, FAT) ON ACCUMULATION OF STRONTIUM-90 IN ANIMALS. Annenkov, B. N. pp 316-28 of Raspredelenie, Biologicheskoe Deistvie, Uskorenie Vyvedeniya Radioaktivnykh Izotopov. Moscow, Meditsina, 1964. (In Russian).

Increasing the amount of calcium to the rations of rats and rabbits from 0.25 to 1.5% decreased the deposition of ^{90}Sr in the skeleton of young rats 2.8 to 3 times; in that of adult rats, 1.9 to 2 times. In growing chicks and mature hens, increasing the amount of calcium from 0.35 to 3.35% reduced the deposition of ^{90}Sr in the skeleton 1.36 and 1.8 times respectively. This occurred when calcium was added to rations containing various amounts of phosphorus, magnesium, fat, and protein. The protective effect of calcium was evident only when the diet had a low (0.25 to 0.3%) content of this element, but when added to rations with a normal (1.2 to 1.25%) content, calcium had little or no effect. The protective effect of calcium compounds depends not only on the calcium ion, but on the anion with which it is bound. The compounds may be arranged in the following order of decreasing effectiveness: $Ca_3(PO_4)_2 \rightarrow CaO$, $Ca(COO)_2 \rightarrow CaCO_3 \rightarrow Ca(C_5H_9O_2)_2$. Among the magnesium compounds tested (MgO, $MgCl_2$, $MgCO_3$, $MgSO_4$), the first two proved to be the most effective against the deposition of ^{90}Sr; 250 to 400 mg/kg of magnesium introduced into the gastrointestinal tract of rats, rabbits, and dogs reduced the amount of ^{90}Sr deposited in the skeleton by one third. The effect of fats on ^{90}Sr metabolism depends on the kind of fat used. Vegetable oil increased the amount of the radioisotope deposited in the skeleton 1.4 to 2.1-fold, whereas fats of animal origin did so 1.2 to 1.4-fold. Increasing the protein concentration of the ration (from 20 to 30%) or decreasing it (from 20 to 11%)

reduced the amount of ^{90}Sr deposited in the skeleton of young and adult rats 1.4 to 1.5-fold and 1.2 to 2-fold, respectively. Changes in the deposition of ^{90}Sr in the skeleton of animals following changes in the amount of calcium, phosphorus, magnesium, fat, or protein included in the ration were due mainly to changes in the amount of the radioisotope absorbed in the gastrointestinal tract. (ATD)

40343 EFFECT OF HYPOCALCEMIA AND SUBCUTANEOUS INFLAMMATORY FOCI ON THE LEVEL OF RADIOACTIVE STRONTIUM IN THE SKELETON. Razumovskii, N. O.; Torchinskaya, O. L. pp 329-33 of Raspredelenie, Biologicheskoe Deistvie, Uskorenie Vyvedeniya Radioaktivnykh Izotopov. Moscow, Meditsina, 1964. (In Russian).

Hypocalcemia induced by NaEDTA (sodium ethylenediaminetetraacetate) soon after the injection of ^{90}Sr in rabbits increased the deposition of the isotope in bone, possibly due to the fact that the loss of calcium was partly compensated by the strontium. But 14 days later the amount of strontium in the bones of the experimental animals decreased by about 20%. However, the situation was quite different after subcutaneous droplet injections of NaEDTA, for the amount of ^{90}Sr deposited in the bones did not increase; in fact, it tended to decrease. Extensive foci of inflammation, edema, and hemorrhage developed at the injection sites. After the necrotic masses sloughed off, the injection sites became scarred and covered with fur. This suggests that after subcutaneous injection of NaEDTA, the decrease in the radiostrontium content of bony tissue was caused by inflammation. The authors tested their hypothesis by subcutaneously injecting rabbits with turpentine after they had been given ^{90}Sr. The turpentine inflammation likewise resulted in a decrease in the amount of strontium deposited in the bones. (ATD)

40344 EFFECT OF COMPLEXING AGENTS ON THE AMOUNT OF RADIOACTIVE STRONTIUM DEPOSITED IN BONES. Razumovskii, N. O.; Torchinskaya, O. L. pp 334-7 of Raspredelenie, Biologicheskoe Deistvie, Uskorenie Vyvedeniya Radioaktivnykh Izotopov. Moscow, Meditsina, 1964. (In Russian).

Two complexing agents, DTPA (diethylenetriaminopentaacetic acid) and DEETA (ethyl-ester-diaminetetra-acetic acid) and several 8-hydroxyquinoline derivatives were tested as means of reducing the amount of radioactive strontium deposited in the body. DTPA had no effect on deposition of the isotope in the bones of rats. DEETA, when simultaneously injected with ^{89}Sr reduced the amount of the latter deposited in the animals' bones by an average of 25%. However, when used an hour before or one-half hour after intraperitoneal injection of ^{89}Sr, the amount of activity in the femur of the experimental animals was virtually indistinguishable from that in the controls. The 8-hydroxyquinoline derivatives were used both simultaneously with radiostrontium, and prophylactically, one hour before injection of the isotope. In all cases the experimental animals had a higher content of ^{89}Sr in the femur than did the controls. (ATD)

40345 ORAL ADMINISTRATION OF SOME COMPLEXING AGENTS TO REMOVE PLUTONIUM FROM RATS. Belyaev, Yu. A. pp 338-42 of Raspredelenie, Biologicheskoe Deistvie, Uskorenie Vyvedeniya Radioaktivnykh Izotopov. Moscow, Meditsina, 1964. (In Russian).

Experiments were performed on male rats given 0.66 to 1.01 μc/ of ^{239}Pu intraperitoneally. The complexing agents were administered orally through a stomach tube at various intervals after the injection of plutonium. EDTA (ethylenediaminetetra-acetic acid) and DCTA (1.2-diaminecyclohexanetetra-acetic acid) proved to be wholly ineffective in removing plutonium from the skeleton or liver. EDPA (ethylenediaminebis-acetic-bimethylphosphinic acid) was effective only when used 2 or 6 hours after the injection of plutonium. The repeated use of EEDTA (ethylesterdiaminetetra-acetic acid) within 24 hours reduced the amount of plutonium both in the liver (1.6-fold) and in the skeleton (65% of the control). But when used after 30 days, it affected mainly the plutonium content of the liver (reduced it by half). DTPA (diethylenetriaminepenta-acetic acid) was the most effective of the agents, for it reduced the amount of plutonium in the liver and skeleton regardless of when it was used. Administered 30 days after the injection of plutonium, it reduced the amount of the isotope in the liver 4.5 times, in the skeleton 1.6 times (61% of the control). (ATD)

40346 EFFECTIVENESS OF DIETHYLENETRIAMINEPENTA-ACETIC ACID (DTPA) AFTER INTRATRACHEAL ADMINISTRATION OF PLUTONIUM TO RATS. Belyaev, Yu. A.; Lemberg, V. K. pp 343-7 of Raspredelenie, Biologicheskoe Deistvie, Uskorenie Vyvedeniya Radioaktivnykh Izotopov. Moscow, Meditsina, 1964. (In Russian).

Following the intratracheal administration of ^{239}Pu in the nitrate form or carbonate complex, diethylenetriaminepentaacetic acid (DTPA) proved to be effective in removing the isotope from the lungs of rats even when applied soon afterward. Intraperitoneal injection of DTPA was somewhat more effective than intratracheal. Eighty per cent of the ammonium plutonium pentacarbonate injected intravenously was retained in the liver. The average amount of ^{239}Pu excreted with urine was 0.1% with feces, 1% (from the 1st to 7th days). A single intraperitoneal injection of DTPA (24 hours after intravenous injection of the carbonate complex of plutonium) reduced the amount of ^{239}Pu in the liver by 23% of that in the control. The author concludes that it is much more difficult at present to remove plutonium from the lungs than from the skeleton. (ATD)

40347 ORAL ADMINISTRATION OF COMPLEXING AGENTS TO REMOVE RARE-EARTH ELEMENTS (CERIUM-144) FROM RATS. Torchinskaya, O. L.; Razumovskii, N. O. pp 348-55 of Raspredelenie, Biologicheskoe Deistvie, Uskorenie Vyvedeniya Radioaktivnykh Izotopov. Moscow, Meditsina, 1964. (In Russian).

Complexing agents can be used orally if the stability of the complex that it forms with the element under study, routes by which the radioisotope enters the organism, and the time since administration of the isotope are taken into account. Diethylenetriaminepenta-acetic acid (DTPA) forms a highly stable complex with cerium and it may be used after oral or parental administration of the radioisotope. This can be done early, when ^{144}Ce is in the gastrointestinal tract or is circulating in the blood, or later, when the isotope is already deposited in the tissues. Ethylenediaminetetraacetic acid (EDTA) should not be used too soon after oral administration of ^{144}Ce, when the isotope is in the gastrointestinal tract, because the complexing agent increases the rate of ^{144}Ce deposition in the organs. However, it can be administered orally 24 hours or more after oral use of the isotope. If the latter is injected parenterally, the oral administration of EDTA is effective regardless of when the isotope is used. (ATD)

40348 EFFECT OF N,N,N',N'-TETRA-ACETIC ACID 2,2'-DIAMINODIETHYLSULFIDE (DDSTA) ON THE EXCRETION OF URANYL NITRATE AND COURSE OF URANIUM POISONING IN RATS. Ivannikov, A. T.; Razbitnaya, L. M.; Smolin, D. D. pp 356-60 of Raspredelenie, Biologicheskoe Deistvie, Uskorenie Vyvedeniya Radioaktivnykh Izotopov. Moscow, Meditsina, 1964. (In Russian).

DDSTA proved to be an effective complexing agent for uranyl nitrate. It intensified the excretion of uranium from the body whether administered immediately after uranium poisoning or much later when deposition in the tissues and skeleton had already taken place. The complex compound of uranium with DDSTA was excreted with urine. The residual uranium found in the rats was indicative of a marked decrease in uranium deposition in the treated animals, especially in the skeleton (the main depot). The rapid excretion of uranium under the influence of DDSTA had a favorable effect on the course of uranium poisoning. The symptoms of kidney involvement were less distinct in the experimental animals than in the controls and there were no tremors or convulsions. In addition, treatment with DDSTA increased the survival rate of the animals. The authors consider this compound a promising agent for the treatment of uranium poisoning. (ATD)

Radiation Effects

40349 (BNL–9345) PATHOGENESIS OF RADIOLESIONS IN THE MATURE CENTRAL NERVOUS SYSTEM. Zeman, Wolfgang (Brookhaven National Lab., Upton, N. Y.). [1965]. Contract AT-30-2-GEN-16. 14p. (CONF-650807–1). Dep. mn; CFSTI, $1.00 cy, $0.50 mn.

From 5th International Congress of Neuropathology, Zurich.

Responses of the nervous system to ionizing radiations span a wide range, from minimal physiologic effects to immediate tissue death. That narrow segment of the spectrum designated as radiation necrosis is discussed. Such morphologic alterations may develop acutely or after a latent period. Acute radionecrosis has been the domain of experimental pathologists, whereas delayed radionecrosis figures importantly in human pathology as an occasional complication of radiotherapy. Only recently, with the introduction of topical irradiation by radionuclides and by beams of accelerated heavy particles, has acute radionecrosis been observed in human nervous tissue. A review of recent literature indicates that acute radionecrosis invariably follows the focal absorption of large amounts of energy, about 10,000 rads or more, given within minutes to hours. In this reaction the physical characteristics of the radiation other than dose, especially the temporal and spatial distribution of absorption events in the tissue, are of little importance. The irradiated tissue undergoes non-selective, complete necrosis which evolves within hours to days. Because most of the irradiated cells are more or less synchronously and also similarly affected, the pathogenesis of acute radiation necrosis is easily studied. Cell death stems from a poisoning of the energy producing and synthesizing cellular organelles by radiochemically produced toxic compounds and from a disturbance of certain cellular and subcellular membranes, presumably due to electron and exciton migration and to other phenomena of charge transfer. These events terminate in cellular autolysis by acid hydrolases. The most important practical aspect of this response is the fact that the acute death of the exposed cells precludes the development of delayed damage. It is therefore possible to utilize acute radionecrosis as a means for the production of sharply delimited ablations of brain tissue, practically unencumbered by scar formation, provided that the geometry of the radiation field was precisely defined. The absorption of a single dose of a few thousand rads by the central nervous tissues results in a necrosis, which becomes manifest after a latent period, the duration of which is dose-dependent, at least under experimental conditions. That this relationship holds also for fractionated irradiation, such as employed in human radiotherapy, has been demonstrated on the rabbit spinal cord. In contrast to acute radionecrosis, the delayed type usually displays selectivity. Often, damage to blood vessels predominates, but white matter lesions and selective destruction of certain brain stem griseae are also observed. With the exception of an initial acute necrosis of a few scattered cells, the exposed nervous tissue appears morphologically and functionally normal until delayed damage develops. (16 references.) (C.H.)

40350 (HW-SA-3723) CORRELATION OF ROSE BENGAL CLEARANCE AND HISTOPATHOLOGICAL CHANGE OF SHEEP LIVERS DAMAGED BY NEPTUNIUM-237. Wood, D. H.; Murray, J. L.; Palotay, J. L. (General Electric Co., Richland, Wash. Hanford Atomic Products Operation). [Sept. 18, 1964]. Contract AT(45-1)-1350. 8p. Dep. mn; CFSTI, $1.00 cy, $0.50 mn.

There was a close correlation between ^{131}I-rose bengal liver function tests and the histopathologic changes found in serial liver biopsies from sheep following the intravenous administration of the hepatotoxic agent, neptunium-237. The most severe cellular damage and the slowest blood clearance of the dye occurred the fourth day post-injection. Cellular repair was evident by the sixth day and was almost complete by the tenth day. (auth)

40351 (NYO–1913-1) EFFECTS OF IRRADIATION ON THE CALCIFYING MECHANISM OF EPIPHYSEAL CARTILAGE. Final Report. Hirschman, Albert (State Univ. of New York, Brooklyn. Downstate Medical Center). Feb. 14, 1962. Contract AT(30-1)-1913. 10p. Dep. mn; CFSTI, $1.00 cy, $0.50 mn.

Results are reported from studies on the effects of x radiation on the calcifying mechanism of epiphyseal cartilage in normal and rachitic rats. Data are included from studies on the effects of radiation on calcification in sections of fresh tibial epiphyseal cartilage; morphological and histochemical studies of mucopolysaccharides and mucoproteins of epiphyseal cartilage irradiated in vivo; the development of staining techniques for use in morphological studies; and the effects of x radiation on the growth of the tibial epiphysis in normal and rachitic rats in which ^{35}Sr, administered as Na_2SO_4, was used as a tracer. (C.H.)

40352 (WASH–1059) LATE IRRADIATION EFFECTS CONFERENCE. INVENTORY OF CAPABILITY. Summary of Proceedings, December 4-6, 1963, Germantown, Maryland. Henshaw, Paul S. (ed.) (Division of Biology and Medicine (AEC), Washington, D. C.). May 1965. 348p. (CONF-631203). Dep. mn; CFSTI, $7.00 cy, $1.50 mn.

The criteria used to define late irradiation effects; the characteristics of natural and radioinduced degenerative changes in living systems; and the future direction of research in the field were discussed. Topics discussed in detail include the effects of radiation on the life span, on reproduction, on resistance to disease, on learning ability, on the nervous system, and on the incidence of neoplasia in mammals; manifestation of late radiation effects in tissues; manifestations of late radiation effects in micröorganisms; manifestations of late radiation effects in cells; manifestations of late radiation effects at subcellular levels; the similarity of late irradiation effects and signs of aging; the effects of irradiation on the rate of degenerative changes; and the effects of prenatal irradiation on late life vigor. (C.H.)

40353 (FTD-TT-65–48, pp 16-17) CHANGES IN MAMMARY-GLAND ACTIVITY AFTER IRRADIATION. Lebedeva, K. A. (Translation).

Biochemical, histological, and physiological methods were used for studies on the effects of various doses of γ and x radiation on mammary gland activity in goats, mice, and rabbits. Data were compared with results of studies of lactation during radiation sickness. It was concluded that irradiation of the mammary gland at an early age causes an arrest in its growth and that the response of the mammary gland to local irradiation during lactation is an initial retention of milk in the alveolar portion, apparently as a result of a decrease in tonus, followed by a rapid decrease in alveolar capacity caused by proliferation of connective tissue and a gradual change in milk quality as a result of impoverishment in basic biochemical components. It is postulated that radiation affects the mammary gland by altering the nerves innervating it. (C.H.)

40354 (FTD-TT-65–48, pp 38-9) COMBINED ACTION OF WHOLE-BODY VIBRATION AND IONIZING RADIATIONS ON CERTAIN FUNCTIONS OF THE CENTRAL NERVOUS SYSTEM. Livshits, N. N.; Apanasenko, Z. I.; Kuznetsova, M. A.; Luk'yanova, L. D.; Meyzerov, E. S. (Translation).

The combined effects of 15-min whole-body vibration and subsequent exposure to γ or x radiation on respiration and nervous responses were evaluated in rats and guinea pigs. Results showed that the state of stress induced by vibration altered reactions to irradiation. Possible physiological factors involved are discussed. (C.H.)

40355 (FTD-TT-65–48, pp 111-12) INFLUENCE OF IONIZING RADIATION ON THE SPONTANEOUS IMPULSE ACTIVITY OF INDIVIDUAL NEURONS OF THE RABBIT CORTEX. Melekhova, A. M. (Translation).

The effects of 1200 R whole-body x radiation on the activity of neurons of the sensomotor region of the rabbit cortex were studied. The impulse activity was recorded and cortical excitability was determined from the threshold

motor reactions of a hind paw to isolated electrical stimulation of the cortex using microelectrodes. Results indicated there was a relation between the number of active neurons and the changes in threshold stimulating current both under normal conditions and after exposure to x radiation and the number of active neurons increased when the threshold decreased. Irradiation caused a reduction in the number of spontaneously active neurons and resulted in a depression of cortical excitability. Despite an acceleration of impulsation, specific activity was reduced at all times after irradiation except the 2nd and 13th and subsequent days, when it exceeded the value calculated for the animal's normal condition. It was concluded that radiation exposure produces rapid and severe disruptions of normal cortical-neuron activity. (C.H.)

40356 (FTD-TT-65-48, pp 469-70) EFFECT OF SMALL DOSES OF RADIOACTIVE PHOSPHORUS (P^{32}) ON THE HIGHER NERVOUS ACTIVITY OF DOGS OF DIFFERENT AGES ON CHRONIC INTERNAL IRRADIATION. Tekutov, P. F.; Chervinskaya, A. F.; Varukha, E. A. (Translation).

The effects of chronic internal irradiation with very small doses on higher nervous activity were studied in dogs of various ages after the injection of 5 μC/kg body weight of ^{32}P during early postnatal development or in mature animals. Parallel hematological and cardiographic examinations were also conducted for one year after injection of ^{32}P. Irradiation at an early age caused changes in higher nervous activity as demonstrated by the attenuation of excitability and a disruption of cortical linking function. Histological studies revealed structural changes in the neurons of the cortex and in the synaptic structures. No material changes in higher nervous activity were noted in irradiated mature dogs. Electrocardiographic studies of mature dogs showed that the regulatory function of the nervous system and the cardiac conductivity system was altered briefly after each irradiation but no chronic effects were observed. (C.H.)

40357 (FTD-TT-65-48, pp 552-3) DISRUPTIONS OF CARDIAC METABOLISM IN RADIATION INJURIES. Fomichenki, K. V. (Translation).

The effect of radiation injury on cardiac metabolism in mammals was studied. Tissue respiration and oxidative phosphorylation were disrupted in the myocardium by irradiation. Marked changes in protein metabolism were demonstrated by a reduction in the content of ribonucleic acid and desoxyribonucleic acid and phase-like changes in the content of phosphoprotein. Chronic irradiation led to a decrease in the content of lipoprotein. (C.H.)

40358 (FTD-TT-65-48, pp 577-8) FUNCTIONAL AND SUBMICROSCOPIC CHANGES IN THE INSULAR APPARATUS OF THE PANCREAS AFTER ADMINISTRATION OF RADIOACTIVE STRONTIUM. Khomutovskii, O. A. (Translation).

Strontium-89 and ^{90}Sr were injected at doses of 0.32 μC/gm into the abdominal cavity of rats and guinea pigs. Microscopic studies were made of the pancreas and the effect on blood sugar content was followed for 200 days. Microscopic changes were detected in the cell nuclei, mitochondria, arcoplasmic membranes, ribonucleoproteins, and capillary membranes. A test involving double sugar stress showed that the pancreatic insular apparatus was affected. The disruptions of pancreatic structure and function depended on the quantity of radiation absorbed during the first few days after administration of the isotopes and the disruptions persisted for an extended time. (C.H.)

40359 (FTD-TT-65-48, pp 590-1) REACTIONS OF THE RETINA TO IONIZING RADIATION. Tsypin, A. B.; Trunova, N. M. (Translation).

The effects of ^{60}Co γ radiation on retinal function were studied in frogs and rabbits using electrical reaction of the retina as the criteria. Results showed that the animal retina responds to γ radiation with a physiological reaction very similar to the response to photostimulation. The threshold γ dose necessary to cause an electrical response of the retina was found to be 0.01 to 0.001 R/sec, as measured by an electroretinogram (ERG). Retinal function was found to be disrupted at doses of 1000 to 3000 R, based on ERG data. The amplitude of retinal biopotentials produced in response to photostimulation was found to decrease at these doses. (C.H.)

40360 (FTD-TT-65-48, pp 666) REACTION OF THE ENDOCRINE ORGANS TO FRACTIONAL IRRADIATION WITH SMALL DOSES OF X-RAYS. Yankovskaya, Ts. L.; Konstantinova, M. S. (Translation).

The reaction of blood pressure was used as the index of the reaction of the endocrine glands of rats to fractionated doses of x radiation. A similarity in reactions of blood pressure to pain stimulation, adrenaline injections, and fractional irradiation with small doses of x radiation was found in rats. This similarity was manifested by two-phase changes in blood pressure. The second phase of the blood pressure reaction disappeared in all the animals after irradiation, after adrenaline denervation, and after transection of the base of the hypophysis. Microscopic studies, showed degenerative changes in the adrenal glands after irradiation. (C.H.)

40361 (ORNL-tr-437) MEDICAL DEFENSE AGAINST NUCLEAR WEAPONS. Kovalenko, V. Ya; Rybasov, V. A. Translated by C. D. Stout (Oak Ridge National Lab., Tenn.), from Chapter I of Okazanie Meditsinskoi Pomoshchi Postradavshim ot Yadernogo Oruzhiya (a publication of Atomizdat, 1964, Moscow). 22p. Dep. mn; CFSTI, $1.00 cy, $0.50 mn; JCL, $2.60 fs, $0.86 mf.

The biological effects of thermonuclear explosions are reviewed. The basic principles of radiological defense are discussed with emphasis on medical assistance to inhabitants of cities subjected to a thermonuclear attack. The hazards of shock waves, thermal radiation, x radiation, neutrons, and fallout are considered. Data on injuries sustained by the populations of Hiroshima and Nagasaki as a result of atomic bomb explosions in 1945 are cited as examples. (C.H.)

40362 EARLY INDUCTION BY X RAYS OF DISCOLORATION OF FOLIAR SPOTS IN MARANTA LEUCONEURA. Gillet, C.; Ramaut, J. Bull. Classe Sci., Acad. Roy. Belg. (5), 50: 1061-6(1964). (In French).

X rays induce early destruction of the cyanidine pigment in the spots of Maranta leuconeura leaves. This discoloration requires a minimum dose of more than 300 Kr to be complete; its speed increases with the doses. (auth)

40363 PLASMA PEPSINOGEN AFTER WHOLE-BODY IRRADIATION OF RAT. Shauer, P.; Klemenc-Sebek, S. Bull. Sci., Conseil Acad. RPF Yougoslavie, 10: 7(Jan. 1965). (In Slovenian).

Male Wistar rats were exposed to 600 and 1200 R from a ^{60}Co source. Blood samples were taken from the vena cava the 1st, 24th, and 48th hour after 600 R exposure and also on the 11th, 16, and 18th day after 1200 R exposure. The concentration of pepsinogen was determined and the results are tabulated. In the 600-R irradiated rats, there is a continuing decrease, reaching 59% at 48 hrs. after irradiation. In the rats exposed to 1200 R, the minimum quantity of pepsinogen is found on the 11th day; there is then progressive increase of the pepsinogen. (J.S.R.)

40364 INFLUENCE OF REPEATED ^{60}Co GAMMA IRRADIATION ON URINARY EXCRETION OF TAURINE IN RATS. Jovanovic, M. M. Bull. Boris Kidrich Inst. Nucl. Sci., 16: 49-54(Jan. 1965).

X irradiation of rats led to an increase in the urinary excretion of taurine. The effect is, up to a certain limit, a function of the radiation dose. The influence of repeated ^{60}Co gamma irradiation on the urinary excretion of taurine in rats was studied. (auth)

40365 CHANGES IN THE GROWTH OF PROGENY OF MALE RATS EXPOSED TO LOW X-RAY DOSES IN THE INFANTILE PERIOD. Savkovic, N.; Hajdukovic, S. Bull. Boris Kidrich Inst. Nucl. Sci., 16: 55-62(Jan. 1965).

Malformations of the F_1-generation progeny of male rats whole-body x irradiated with doses of 50, 100, 200, 300,

and 400 R at the age of 8 days were investigated. The results showed that the growth of the progeny was delayed compared with that of normal animals. (auth)

40366 VARIATIONS OF THE REGENERATING CAPACITY OF IRRADIATED PLANARIA (DUGESIA SUBTENTACULATA) AS A FUNCTION OF THE X-RAY DOSE. Chandebois, Rosine (Faculte des Sciences, Marseille). Compt. Rend., 260: 4834-7(May 3, 1965). (In French)

The total inhibition of the regeneration can be obtained in Dugesia subtentaculata at doses above 500 R. The cross sectioning should be made after a delay, with the lower doses requiring a longer delay. Above 700 R, the D. subtentaculata become necrose in about two or three weeks. Below this dose, a delayed recovery occurs. The minimum dose to obtain the destruction of all the cells in mitosis is about 500 R. (tr-auth)

40367 COMPARATIVE STUDIES OF RADIOACTIVELY LABELED PRECURSORS IN THE RNA OF X-IRRADIATED NON-DIPLOID YEAST. Robev, S.; Decev, G.; Marinova, Ts. (Inst. of Radiology and Radiation Protection, Sofia). Compt. Rend. Acad. Bulgare Sci., 18: 133-6(1965). (In Russian).

Studies were made of the effects of labeled phosphates and some precursors of RNA, uracil-2 ^{14}C, adenine-2 ^{14}C, and orotic acid-^{14}C, as inclusions on the synthesis of RNA in non-diploid x-irradiated yeast in suspensions. The curves for doses of 52, 78, and 104 r with 5, 10, 15, 20, 30, and 40 min incubation periods showed a certain inhibiting influence of labeled inclusions only at a dose of 104 r and at the longer incubation periods. A table of nucleotide composition of newly synthesized RNA in intact and irradiated suspension, investigated by means of ^{32}P-phosphate showed that nucleotide content remained unchanged. The inclusion of ^{32}P was inhibited about 40% while ^{14}C precursors in irradiated yeast RNA were not inhibited at the same incubation period. It was postulated that phosphate inhibition took place before inclusion into nucleoside phosphates (the RNA precursors). The fact that the inhibition of phosphate does not indirectly inhibit adenine, uracil, and orotic acid indicated that the cell must have sufficient phosphate resources for the synthesis. An experiment with 30-min inclusion of adenine-^{14}C into the yeast with and without phosphate, showed again that the absence of phosphate does not inhibit adenine inclusion. (R.V.J.)

40368 CONTRACTILITY, HEART RATE, AND RESPONSE TO NOREPINEPHRINE OF ISOLATED RAT MYOCARDIUM FOLLOWING ^{131}I-INDUCED HYPOTHYROIDISM. Benforado, Joseph M.; Wiggins, L. L. (State Univ. of New York, Buffalo). J. Pharmacol. Exptl. Therap., 147: 70-5 (Jan. 1965).

Basal metabolic rate (BMR) and other parameters were investigated in Sprague-Dawley rats given a dose of ^{131}I that was shown previously to destroy the thyroid gland. A single intraperitoneal injection of 300 μC of ^{131}I into 100-g rats produced a severe hypothyroidism as evidence by loss of body weight, bradycardia, and a 35% reduction in the BMR. The bradycardia persists under in vitro conditions and is therefore not entirely vagal in origin. Right ventricle strips of hypothyroid animals are less resistant to stretch than controls but are able to increase the active tension developed with stretch over a greater range than controls. In such an in vitro system it seems probable that the effect is not due to a greater efficiency of hypothyroid myocardium but that it is a consequence of decreased oxygen needs in the face of a limited oxygen supply imposed by problems of diffusion. No difference in the frequency-tension relation was observed. The hypothyroid strips were not significantly less sensitive to the automaticity-producing or chronotropic effects of norepinephrine. The hypothyroid hearts were smaller than controls and thinner walled. The water contents of the hearts per 100 g wet weight were about the same but the (heart weight)/(body weight) ratios were significantly smaller than the controls. The in vitro studies indicating that acute hypothyroidism is not necessarily associated with cardiac muscle weakness, are compatible with the observation that myxedema heart occurs late during chronic hypothyroidism. The improved performance of the hypothyroid strips suggests that efficiency of oxidative phosphorylation might be enhanced in such preparations and that the larger energy supply required for the increase in developed tension with stretch might be more easily attained. (BBB)

40369 THE IMPORTANCE OF THE QUANTITATIVE ALTERATIONS OF THE EXTRACELLULAR SPACE IN THE WATER-IMBALANCES OF THE EXPERIMENTAL INTESTINAL X-RAY DEATH. Szeboek, Zoltan; Petranyi, Gyoezoe. Magy Radiol., [No. 1], 1-8[(1964)].

The importance of the gastrointestinal x-ray syndrome was examined in rats, using the inulin method combined with the ligation of the hilum of the kidney. Giving 1300 R, after 24, 48, and 72 hours the alterations of the active extracellular space of the whole organism and the single organs and those of the inulin permeability of the gastrointestinal tract were examined. Two phases of the reaction are distinguished in the disturbance of the water equilibrium, concomitant with the gastrointestinal x-ray syndrome. In the first phase, the extracellular space of the organs increases, except the cerebral and the muscle tissues. In the second phase, considerable diminution of the extracellular space of the whole organism and the examined organs was found, persisting until the animal's death, except the spleen. In the small intestine, however, the diminution of the water space was only of lesser degree and was observed in the late phase. On the basis of the data of the literature, the results of the experiments are discussed. (tr-auth)

40370 INVESTIGATION OF RADIATION CHEMICAL PROCESSES WITH CRYOSCOPIC METHOD. Kosa Somogyi, Istvan. Magy. Tud. Akad. Kozp. Fiz. Kut. Int. Kozlemen., 13: 185-94(1965). (In Hungarian).

A measuring device was built for recording the cooling curves and for determining the melting points of small volume (~1 cm^3) samples in order to characterize the radiation behavior of organic materials by the decrease in their freezing point after irradiation. This device was used in the determination of the G-values of condensed radiolytic products in benzene and diphenyl-methane, irradiated in the vertical channels of the WWR-S type reactor. The mechanism of polymer production is discussed in the terms of a comparison of the measured data with results in the literature. (auth)

40371 ASCORBIC ACID AND ASCORBIC ACID OXIDASE OF γ-IRRADIATED MOMORDICA CHARANTIA. Vyas, D. N.; Thanki, R. J.; Patel, K. C.; Patel, R. D. (Sardar Vallabhbhai Vidyapeeth Univ., Vallabh-Vidyanagar, India). Naturwissenschaften, 52: 345-6(1965).

The ascorbic acid (AA) and ascorbic acid oxidase (AAO) content of γ-irradiated seeds of a special variety (Surati Karela) of Momordica charantia was determined. The γ irradiation dose was from 10 to 120 kr. The seeds were germinated and the AA and AAO content was determined after 0, 1, 3, 9, 15, and 20 days. The results indicated that the seeds possess AA even in dormant conditions. There was an increase in AA after γ irradiation, with the dose level of 10 kr being more effective. The AA content decreased with the period of germination for irradiated seeds. Very little AAO was found in dormant seeds and there was no apparent increase up to the third day of germination. There was then a sudden increase in AAO. (J.S.R.)

40372 CALCULATED TISSUE CURRENT-TO-DOSE CONVERSION FACTORS FOR NUCLEONS BELOW 400 Mev. Zerby, C. D.; Kinney, W. E. (Oak Ridge National Lab., Tenn.). Nucl. Instr. Methods, 36: 125-40(Sept. 1965). (ORNL-P-1126).

To assist in the evaluation of the hazard associated with exposure to high-energy neutrons or protons, a series of Monte Carlo computer programs were used to calculate the energy deposition that results from high-energy incident nucleons as a function of depth in a slab of tissue. The programs included nonelastic and elastic interactions,

as well as evaporation processes and nuclear recoils. A 30-cm-thick infinite slab of tissue was treated and cases of normal and isotropic incidence of 400-, 300-, 200-, 100-, and 60-Mev protons and neutrons were computed. From these data current-to-dose conversion factors were extracted for the average-whole-body, the 5 cm depth, the surface, and the maximum doses. A set of quality factors (QF's) was adopted for transforming rad dose to Rem dose, but detailed energy-deposition data are also presented so that any preferred set of QF's can be used to obtain estimates of the Rem dose. (auth)

40373 CATECHOLAMINE CONTENT IN MACACO TISSUES IMMEDIATELY AFTER WHOLE-BODY γ IRRADIATION. Kulinskii, V. I.; Semenov, L. F. (Inst. for Medical Graduate Work, Khar'kov and Inst. of Experimental Pathology and Therapy, Sukhumi, USSR). Radiobiologiya, 5: 494-500(1965). (In Russian).

Studies made by the trihydroxyindole method showed changes in catecholeamine metabolism in Macacus monkeys after whole-body ^{60}Co γ irradiation at a dose of 666 R. The noradrenalin content of the hypothalamus and the adrenalin content of the superenals decreased the first day but returned to normal after 3 days. The noradrenalin contents of the medulla oblongata, pons variolii, midbrain, caudate nucleus, and the spleen increased after 4 to 12 hr, returned to normal after 1 to 2 days, and increased again (except in the caudate nucleus) after 3 days. No significant changes were found in the noradrenalin contents of the heart or liver or in the frequency of the appearance of adrenalin in the organs. Changes in the catecholeamine metabolism are interpreted as indicating malfunction of the various branches of the sympatico-adrenalin system. The possible role of activation of this system in the development of neurophysiological reactions is considered. (tr-auth)

40374 CHANGE OF THYROID GLAND ACTIVITY AFTER WHOLE-BODY X IRRADIATION. Kalina, V. K. (Inst. for Medical Graduate Work, Kiev). Radiobiologiya, 5: 525-7(1965). (In Russian).

Studies on thyroid secretion, made with ^{131}I, showed that the first action of x irradiation is disturbance of the hormone output. There was no direct correlation between the accumulation of radioactive iodine in the thyroid of the irradiated animal and hormone formation, which must be considered in using ^{131}I for diagnostic studies in patients who have been subjected to irradiation. (tr-auth)

40375 X-RADIATION INDUCED CYTOCHEMICAL CHANGES IN RABBITS. Volovik, M. P. Uch. Zap., Khar'kovsk. Gos. Univ., Tr. Biol. Fak., 36: 19-24(1963). (In Russian).

The effects of various doses of x radiation on the testes and liver cells of rabbits were investigated, in order to determine the cytological and cytochemical changes in the cells of animals subjected to whole-body irradiation. The 4 to 6 months old animals were irradiated at the rate of 18.1 R/min. for total doses from 600 to 900 R. The spermatogonia and spermatocytes were found to be most radiation-sensitive, while the spermatids and the mature spermia possessed a marked radiation resistance. The radiation caused a fatty degeneration of the tissue. Within 2 days after exposure to 700 R, vacuolation of the plasma and injury to the cells was observed. Regeneration of the liver cells was slow and was completed only 30 to 40 days after exposure. The isoelectric point of the albumins of the karyoplasm of the testes and the liver shifted toward the side of alkaline pH values, indicating a decreased physico-chemical activity of the protoplasma albumins as the result of the radiation. The change in the isoelectric point of the cytoplasma was less noticeable, indicating a lower degree of injury. The exposure also caused changes in the synthesis of the nucleoproteins in the testes and liver cell nuclei, as indicated by the sharp reduction of the chromatin content in the nuclei of the irradiated cells. The DNA synthesis was slowed down but the RNA content of the cytoplasm was increased by the irradiation. (TTT)

40376 STUDIES ON GUAR-CYAMOPSIS TETRAGONOLOBA (L.) TAUB (thesis). Hymowitz, Theodore. Stillwater, Okla., Oklahoma State Univ., 1963. 124p.

A study was made on the history of guar in the United States, the genetic diversity in the plant introductions of the genus Cyamopsis, competition studies in guar, investigations on seedcoat color, the branching habit of Texsel guar, and the critical point for x-ray dosage of dormant seed of guar. Groehler and Texsel varieties of guar and all of the available plant introductions of Cyamopsis were used as experimental materials in extensive agronomic studies. Plant competition studies indicated that, regardless of competition, Texsel had the tallest plants, and except for per cent mature pods and threshing percentage, had significantly lower values when compared to Groehler and P.I. 164801 in each of the other characters studied. The correlation values among the individual plant characters of weight of pod, weight of seed in pod, pod length, and number of seed in pod were positive and highly significant. Evidence was found to support the position that unbranched and branched plants of Texsel are directly related to plant competition rather than ellelic heterozygosity. A lethal dosage of 42% was obtained when guar seed were irradiated at 40,000 R. (Dissertation Abstr.)

40377 CHANGES IN THE BLOOD SYSTEM OF DOGS INTRAVENOUSLY INJECTED WITH YTTRIUM-91. Petrovich, I. K.; Shchelkonogova, M. I. pp 209-12 of Raspredelenie, Biologicheskoe Deistvie, Uskorenie Vyvedeniya Radioaktivnykh Izotopov. Moscow, Meditsina, 1964. (In Russian).

Yttrium-91 injected intravenously once in a dose of 0.1 to 0.2 μc/kg produced marked changes in the composition of the peripheral blood and hematopoietic organs of dogs. The acute phase of radiation sickness caused by injection of 0.1 μc/kg of ^{91}Y was characterized by leukopenia for 3 to 5 weeks due to a decrease in the number of neutrophils, a decrease in the number of erythrocytes (by 30%) for 4 to 7 weeks, and a decrease in the number of thrombocytes for 2 to 3 weeks after injection. In the animals that survived the acute phase, erythrocytopoiesis was restored after the second month, but leukocytopoiesis remained 50% below the original level for 14 months after injection of the isotope. (ATD)

40378 CHANGES IN THE BLOOD CONTENT OF PREGNANT ANIMALS AFTER ADMINISTRATION OF STRONTIUM-90. Petrovich, I. K. pp 213-16 of Raspredelenie, Biologicheskoe Deistvie, Uskorenie Vyvedeniya Radioaktivnykh Izotopov. Moscow, Meditsina, 1964. (In Russian).

Intravenous injection of 0.2 μc/kg body weight induced acute radiation sickness in dogs. The acute stage was followed by a period of restoration of hematopoiesis in males and non-pregnant females while in pregnant females the restoration process was interrupted during the second half of pregnancy. This was manifest by a decrease in the number of erythrocytes, thrombocytes, and leukocytes in the blood. This was attributed to the effects of ^{90}Sr on metabolism and the transmission of Ca salts to the skeleton of the fetus. (R.V.J.)

40379 HEMATOPOIESIS IN DOGS DURING SUBACUTE INTOXICATION INDUCED BY PLUTONIUM-239. Baisogolov, G. D.; Podgorodetskaya, V. N. pp 225-9 of Raspredelenie, Biologicheskoe Deistvie, Uskorenie Vyvedeniya Radioaktivnykh Izotopov. Moscow, Meditsina, 1964. (In Russian).

Eight stock-bred dogs received a single intravenous injection of 2 μc/kg of the nitrate form of ^{239}Pu. A moderate wavelike decrease was noted throughout the experiment (one year) in the number of erythrocytes; it was most pronounced between the 10th and 14th weeks (averaging 22%) and after 8 months (15%). The hemoglobin concentration remained unaffected until the last three months when it rose by 12% on the average. The reticulocyte count decreased sharply from the first few days and remained at a low level for 22 weeks, when restoration occurred in some of the dogs. A

few oxyphilic erythroblasts and Golgi bodies appeared the 4th week. The changes in the number of leukocytes were more pronounced. After a slight increase during the first 3 days, they gradually decreased to 40% below the original count and thereafter remained more or less at this depressed level. The first examination of bone marrow (7th day) revealed a decrease in the absolute number of nucleated cells, which reached a minimum (about 25% of the original level) by the 4th week. Eventually the number of myelokaryocytes increased slightly (to 30%). This decrease in the total number of nucleated cells was caused by a reduction in both the erythrocytes and, even more, the leukocytes. Thus, the findings indicate that intravenous injection of 2 μc/kg of ^{239}Pu rapidly produces destructive changes in the bone marrow of dogs which affect the composition of the peripheral blood. (ATD)

40380 OXYGEN SATURATION OF BLOOD OF RATS AFTER INHALATION OF PLUTONIUM-239. Kalmykova, Z. I. pp 230-6 of Raspredelenie, Biologicheskoe Deistvie, Uskorenie Vyvedeniya Radioaktivnykh Izotopov. Moscow, Meditsina, 1964. (In Russian).

Oxygen saturation of the blood became impaired in rats after they inhaled ^{239}Pu citrate. Normalization then set in. The degree and duration of the impairment varied with the amount of the alpha emitter deposited in the lungs. The bigger the dose of the isotope, the more pronounced the changes. They were most distinctly revealed by a functional test involving temporary suffocation. No significant quantitative changes were noted in the hematological indices after 8 months' observations. (ATD)

40381 LONG-TERM EFFECTS OF ASEPTIC INFLAMMATION IN RATS EXPOSED TO PLUTONIUM-239. Koshurnikova, N. A.; Lemberg, V. K. pp 237-42 of Raspredelenie, Biologicheskoe Deistvie, Uskorenie Vyvedeniya Radioaktivnykh Izotopov. Moscow, Meditsina, 1964. (In Russian).

Aseptic inflammation was induced in rats by subcutaneous administration of 0.1 ml of turpentine once every 2 weeks for 3 months. Turpentine is not a carcinogen; it results in inflammation with an acute leukocyte reaction. The turpentine combined with low doses of ^{239}Pu (0.63 μc/kg) shortened the survival time of the experimental female rats. Aseptic inflammation reduced the number of bone and blood tumors in the animals of both sexes. However, repeated injections of turpentine, the administration of small amounts of ^{239}Pu, and a combination of the two factors caused some increase in the number of glandular tumors in the experimental rats. The tumors were often multiple, e.g., in the females, tumors of the hypophysis were often combined with mammary and ovarian tumors. The authors ascribe the lack of osteosarcomas to the inhibitory effect of turpentine on the development of neoplasms in bony tissue. (ATD)

40382 BONE TUMORS IN DOGS EXPOSED TO PLUTONIUM-239. Lemberg, V. K. pp 243-50 of Raspredelenie, Biologicheskoe Deistvie, Uskorenie Vyvedeniya Radioaktivnykh Izotopov. Moscow, Meditsina, 1964. (In Russian).

Anatomical and histological investigation were made of the skeleton of 10 dogs that died, or were sacrificed, at various times after receiving four intravenous injections of ^{239}Pu nitrate in a total dose of 0.2 μc/kg. Six of the eight animals that survived more than 2 years were found to have malignant bone tumors. The latent period of the osteosarcomas averaged 1421 days, or 32.5% of the mean life expectancy. Of the seven osteosarcomas described in the article, four arose in the epiphyseal-metaphyseal regions of the long bones (femur, humerus, and tibia), two in the vertebrae, and one in the scapula. In histological structure, six of the osteosarcomas were of the osteoplastic type, and one, of the osteoiytic type. Tumor-free portions of the skeleton showed signs of impairment of normal reconstruction of bony tissue and a slight increase in the number of obliterated Haversian canals. The author stresses, however, that obliteration of Haversian canals and degenerative changes in cartilage are also signs of normal age-related changes. Thus, the intensification of such changes in chronic plutonium-induced injury may also be regarded as an indication of premature aging. (ATD)

40383 PATHOLOGICAL ANATOMY OF RADIATION INJURY INDUCED BY PROMETHIUM-147. Strel'tsova, V. N. pp 251-72 of Raspredelenie, Biologicheskoe Deistvie, Uskorenie Vyvedeniya Radioaktivnykh Izotopov. Moscow, Meditsina, 1964. (In Russian).

Pathological changes are described that developed in rats after acute, subacute, and chronic injury induced by parenteral injection of ^{147}Pm. Acute injury was characterized by aplastic changes in the hematopoietic tissue of bone marrow and the spleen, disturbances of the capillary circulation of the liver with atonia and persistent dilatation of the capillaries and small veins, degenerative changes in the liver and kidneys (albuminous and fatty degeneration, necrosis), and changes in the intestinal mucosa typical of ulcerative enterocolitis. Subacute injury was in the form of specific parenchymatous hepatitis with a shifting relationship between the degenerative, proliferative, reparative, and sclerotic processes and the formation of cirrhosis developing against a background of atrophic changes in the hematopoietic organs accompanied by lympho-, leuko-, and erythropenia. Chronic injury reflected the polymorphism of the pathological processes. The predominant features were tumors in various sites (osteosarcomas, malignant and benign tumors of soft tissues) or liver pathology (chronic hepatitis and cirrhosis), hyperplastic tumors of the hematopoietic organs (leukemia), and panangitis. (ATD)

40384 PATHOLOGICAL ANATOMY OF RADIATION INJURY INDUCED BY NIOBIUM-95. Strel'tsova, V. N. pp 273-88 of Raspredelenie, Biologicheskoe Deistvie, Uskorenie Vyvedeniya Radioaktivnykh Izotopov. Moscow, Meditsina, 1964. (In Russian).

The pathological changes are described that developed in 3-month-old rats after acute, subacute, and chronic parenteral injection of ^{95}Nb. Acute injury induced by 9 to 18 μc/g was characterized by initial suppression of bone marrow hematopoiesis followed by restoration in 14 to 16 days and rapid normalization of the ratio of immature to mature cell forms; predominance of degenerative necrobiotic changes in the parenchymatous organs with very severe kidney damage; early suppression of spermatogenesis and disappearance of germinal cells. Subacute injury induced by 1.1, 4.5, or 9 μc/g involved the coexistence of atrophic, degenerative, and regenerative processes in the parenchymatous organs. The hematopoietic tissue of bone marrow exhibited a predominance of the restorative processes while lymphoid tissue at this time reflected the processes of death and new formation of lymphoid cells, the former predominating. Spermatogenesis had ceased and degenerative changes noted in renal parenchyma included granular degeneration and necrosis of the epithelium of the convoluted tubules. Inflammatory processes of bacterial origin could be seen in all the animals. The chronic stage of radiation injury induced by 1.1, 2.25, 4.5, and 6.3 μc/g was characterized by the formation of benign and malignant tumors of the mammary glands, small intestine, subcutaneous hematopoietic organs (reticuloendotheliosis) in 25% of the rats that survived more than 200 days, or in 17% of all the experimental animals (half the tumors developed after intraperitoneal injection of 6.3 μc/g; abnormally high hyperplasia of the reticuloendothelial elements of bone marrow, spleen, and liver; occasional cases of reticulosarcomatosis; and suppression of spermatogenesis. (ATD)

Radiation Effects Therapy and Countermeasures

40385 (FTD-TT-65-48, pp 134-5) SERUM PROTEIN FRACTIONS OF THE BLOOD OF IRRADIATED ANIMALS

DURING MARROW TRANSFUSION. Minasyan, S. M. (Translation).

The effects of bone marrow therapy on blood serum protein metabolism, hematopoiesis, and survival were evaluated in 8 dogs exposed to lethal doses of radiation. Five of the dogs survived and exhibited complete clinical recovery, three died, and all irradiated controls died. Changes in blood serum protein fractions observed soon after irradiation included a decrease in albumin content and a simultaneous increase in globulin content. These changes were less pronounced in animals treated with marrow transfusions and the restoration of hematopoiesis was more pronounced in animals treated with marrow. The animals that received marrow transfusions exhibited a gradual increase in albumin content of the blood serum beginning about the 15th to 20th day after irradiation and the albumin-globulin ratio approximated normal levels during the recovery period. (C.H.)

40386 (FTD-TT-65-48, pp 661-2) INFLUENCE OF UNITOL ON CERTAIN BIOCHEMICAL INDICES OF WHITE RAT TISSUE AFTER X-IRRADIATION. Yakubovskaya, V. I.; Mokhir, Yu. M. (Translation).

Results are reported from a study of the effects of unitol, a drug used to prevent radiation sickness, on the total lipid and cholesterol content of the blood and liver of irradiated rats. Unitol was administered at a dose of 30 mg/kg body weight 20 min before exposure to 1000 R x radiation. The rate of cholesterol synthesis in the liver was measured using ^{14}C-acetate as a tracer. Measurements made 48 hr after irradiation showed a substantial decrease in total lipid content of the liver in irradiated rats and irradiated rats treated with unitol. The rate of cholesterol synthesis in the liver increased by a factor of 4.5 after irradiation and by a factor of 2.5 after unitol treatment before irradiation. Unitol alone did not cause any marked changes in cholesterol synthesis rate. It is suggested that hepatic cholesterol synthesis rate can be used as a test to evaluate the effectiveness of radioprotective compounds. Data are included on the effects of unitol on hepatic glycogen content and blood serum lipoprotein content in irradiated rats. (C.H.)

40387 COMBINED TREATMENT OF ACUTE RADIATION SICKNESS (BK-8, VITAMIN B_{12}, BATYLIC ALCOHOL, BICILLIN-3). Chebotaryov, E. E. (Bogomoletz Inst. of Physiology, Kiev). Fiziol. Zh., Akad. Nauk Ukr. RSR, 11: 385-92(May-June 1965). (In Ukrainian).

The combined action of the protein blood substitute, BK-8, batylic alcohol, vitamin B_{12}, and bicillin-3 on the course of acute radiation sickness in dogs irradiated with x rays in doses of 600 R was studied. The efficacy of the therapeutic complex was assayed on the basis of the clinical picture of radiation sickness, the alteration on the morphological composition of the peripheral blood, and the fractional composition of the blood serum proteins. The research showed that application of combined treatment alleviates radiation sickness and increases survival of the dogs (2 out of 22 control dogs and 6 out of 10 treated dogs survived). When studying the morphological composition of the peripheral blood and the fractional composition of the serum proteins, it was noted that dysproteinemia is less pronounced, and the fractional composition was sooner restored in treated dogs; leukopoesis was depressed to a lesser extent than in the control group. The total quantity of leukocytes and the absolute number of lymphocytes and, partly, neutrophils, were sooner restored in the treated dogs than in the controls. All this indicates the efficacy of the tested combined treatment. (tr-auth)

40388 THE RADIOPROTECTION EFFECTIVENESS OF SEROTONIN IN RATS. Ladner, H.-A.; Wollschlaeger, G.; Schneider, J. (Universitaet, Freiburg i. B.). Naturwissenschaften, 52: 393(1965). (In German).

The prophylactic radiation protective effect of serotonin was investigated in rats. The serotonin was injected before irradiation with doses from 810 to 1450 R. The effects of tryptophan on the survival of rats receiving serotonin was also studied. The results showed that serotonin gave a protective effect to the rats. The survival rates of the rats exposed to 1250 and 1450 R were improved by the supplementary injection of tryptophan. (J.S.R.)

40389 THE PROPHYLACTIC EFFECT OF HISTAMINE IN WHOLE-BODY IRRADIATED RATS. Ladner, H.-A.; von Duesterlho, R. (Universitaet, Freiburg i. B.). Naturwissenschaften, 52: 393-4(1965). (In German).

The prophylactic radiation protective effectiveness of histamine on Wistar rats was tested. Male rats were injected 10 minutes before whole-body irradiation with 690, 810, 955, 1050, and 1250 R. The results showed that the prophylactic injection of histamine dihydrochloride caused an increase of the survival rate. The results with histamine diphosphate were not as significant, although some increase in the survival rate was noted. (J.S.R.)

Radiotherapy and Radiodiagnosis

Refer also to abstracts 40910 and 40913.

40390 (BNL-9384) A DATA PROCESSING METHOD FOR A MULTIDETECTOR POSITRON SCANNER. Bozzo, S. R.; Robertson, J. S. (Brookhaven National Lab., Upton, N. Y.). [nd]. Contract AT(30-2)-Gen-16. 26p. (CONF-650544-1). Dep. mn; CFSTI, $2.00 cy, $0.50 mn.

From Symposium on Fundamental Problems in Scanning, Chicago.

The neutron-deficient radionuclides generally decay by the emission of a positron, or β^+ particle, a form of antimatter. At the end of its track, the positron and an electron disappear in an annihilation reaction, producing two 0.511 Mev gamma rays that travel in opposite directions. This unique feature of positron emission has been exploited in scanning by coincidence-counting methods, particularly in clinical procedures for locating brain tumors. Two principles are involved here. One is that if the initial positron track is short, so that annihilation occurs near the point of emission, simultaneous detection of the two gamma rays, one by each of a pair of detections, indicates that the source is within the volume defined by the straight lines that connect the sensitive volumes of the two detectors. The second principle is that there are a large number of substances that enter certain brain tumors more rapidly than they do normal brain tissue, so a form of selective uptake is achieved, at least transiently. Labeling of any of these substances with a positron emitter provides the necessary vehicle for getting the positron source into the lesion. In particular, ^{74}As and ^{64}Cu DTPA (diethylenetriaminepentaacetic acid) have proved useful. In the standard positron counting procedure two detectors placed on opposite sides of the head are moved synchronously, giving an orthographic projection-type of mapping of the distribution of the radionuclide used. The singles counting rate is also useful in this procedure in that the detector on the same side of the head as the lesion will have the higher counting rate, and this information can be used to indicate the side of the lesion. A numerical method is described that was developed to process the data obtained from a 32-detector positron scanner. The procedure involves an iterative scheme to generate a linear combination of known spectra to obtain the best fit to the data. Also the possibility of a straight matrix inversion method is mentioned. Experimental and clinical results show good positional accuracy as well as a good activity level discrimination. At the present, total activity levels of approximately 3 μc in the total field with a counting time of 5 minutes can be analyzed with good statistical accuracy. Further development in the coincidence circuitry of the instrument theoretically will enable the machine to reduce the counting time to below 1 minute per scan. This shortened acquisition time will allow for the possibility of conducting uptake studies at selected points within the body. (C.H.)

40391 (NP-14921) ERGAENZENDES GUTACHTEN UEBER DIE BEHANDLUNG MIT THORIUM-X. (Supplementary Opinions on Treatment With Thorium-X). Seelen-

tag, W.; Schmier, H.; Kessel, F. (Bundesgesundheitsamt, Berlin (West Germany). Institut fuer Wasser-, Boden- und Lufthygiene). Feb. 1964. 64p. Dep. mn.

The opinion that external treatment with ThX (^{224}Ra) is justified only very seldom and that special knowledge and facilities are necessary to control the possible secondary effects and injuries resulting from its use was re-evaluated on the basis of new studies. The contamination of ^{224}Ra with radiothorium, determination of the dose output, effect of emanations on dose output, relation between activity and dose administration, the deep-dose received, and radiation contamination of environment were experimentally investigated. The results confirmed the previous evaluations. (J.S.R.)

40392 (NYO-3364-6) INDUCED RADIOACTIVITY CAUSED BY THERAPEUTIC USE OF HIGH ENERGY RADIATION. Stroemme, Aksel (Norsk Radiumhospital, Oslo). [nd]. Contract AT(30-1)-3364. 9p. Dep. mn; CFSTI, $1.00 cy, $0.50 mn.

Measurements of patients in a whole-body counter after therapeutic irradiation indicated induced radioactivity of the order of 350 microcuries. The therapeutic betatron beam used contained, besides γ rays, a certain unknown neutron flux. The counting equipment used allowed the detection of only those isotopes giving rise to γ radiation in excess of 25 kev energy and with half-lives in excess of about 20 sec. The isotopes detected and identified by measurements of their half life and energy spectrum included ^{11}C, ^{13}N, ^{15}O, ^{30}P, ^{34}Cl, ^{38}K, and iodine. These were created by (γ,2n) or (n,γ) reactions. The amounts of isotopes created per gramatom during an 11 min irradiation, the equivalent of 200 R, were calculated. (C.H.)

40393 THE USE OF ^{131}I PEANUT OIL IN ASSESSING LIPID METABOLISM IN CORONARY ATHEROSCLEROSIS. Lou, Fu-ching; Chen, Ko-yun; Pao, Chin-liang; Chien, Chien-hua (Chekiang Medical Coll., Hangchow, China). Chinese Med. J., 84: 262-7(Apr. 1965).

The use of ^{131}I-peanut oil, instead of the usual ^{131}I-triolin, in the assessment of lipid metabolism in 75 cases is reported. Preparation of ^{131}I-peanut oil is described. Peanut oil is an unsaturated fatty acid which can be combined with iodine under certain conditions. Its iodine value is 88 to 98%. Iodine was combined first with chlorine into the trichloride of iodine for the process of iodination. This derivative was more active and easily reacted with the double bonds of the fatty acids. By acidification ^{131}I was combined with chlorine into iodine trichloride of high sp act. Peanut oil in ether was added, mixed well, and left standing for 6 hr until completely labeled. Alkaline sodium thiosulfate was then added and the unlabeled free iodine discarded. The mixture was washed repeatedly with potassium iodide solution until the supernatant fluid showed no radioactivity. The ether solution containing ^{131}I-peanut oil was evaporated in a water bath and ^{131}I-peanut oil was obtained. Tween 20 was added to give an emulsified solution. This process ensured an emulsion of ^{131}I-peanut oil in which the isotopic labeling was generally between 40 and 75%. The evening before the study the patients were given 10 drops of Lugol's solution to prevent the uptake of ^{131}I by the thyroid gland. After a 12-hr overnight fast they were given a dose of 300 μC of ^{131}I-peanut oil (1–2 ml of peanut oil in 50 ml of emulsified solution). Venous blood samples (2 ml each) were drawn at one to 24 hr after administration of the test dose. Urine and feces were also assayed for radioactivity. In 50 cases of coronary atherosclerosis, the peak uptake levels of whole blood, blood esters and the uptake level of 24 hr whole blood were 24.6 ± 11.8%, 9.5 ± 8.9%, and 5.3 ± 3.9%. In 10 cases of aortic atherosclerosis the corresponding figures were 16.6 ± 7.9%, 6.3 ± 3.2%, and 2.3 ± 2.6%; while those in 15 cases of hypercholesteremia were 21.7 ± 9.0%, 10.5 ± 6.5%, and 3.9 ± 2.8% respectively. In 48 cases out of 50 with coronary atherosclerosis abnormal results in the ^{131}I-labeled lipid metabolism test were seen (96.0%). It is concluded that the ^{131}I-labeled lipid metabolism test is more sensitive than the chemical estimations of blood lipids in reflecting the state of lipid metabolism. (BBB)

40394 TISSUE TOLERANCE AND SYSTEMIC TOXICITY OF 5-FLUOROURACIL, EXTERNAL RADIATION, AND DRUG-RADIATION COMBINATION IN RABBITS. Diethrich, Edward B.; Campbell, Darrell A.; Korst, Donald R. (St. Joseph Mercy Hospital, Ann Arbor, Mich.). Surgery, 57: 868-75(June 1965).

The controversy concerning the true nature of atypical cells circulating in the blood-stream in patients undergoing operations for malignancy and the current status of Thio-TEPA as an adjuvant to radical mastectomy in the cure of breast carcinoma are discussed. The hypothesis that 5-fluorouracil sensitizes the skin in the radical mastectomy site to subsequent external x radiation was tested in the rabbit and subsequently observed in 17 patients with carcinoma of the breast. Both the laboratory and clinical material suggest that the antitumor agent has no effect on the skin when administered prior to external radiation and that there is no apparent contraindication to the use of a combined cancer chemotherapy-radiation program in the treatment of breast carcinoma. The clinical results of this combined program are being studied on a long-term basis. (auth)

40395 A FEASIBILITY STUDY OF THE THERAPEUTIC POSSIBILITIES OF π^- MESONS. Aceto, Henry Jr. Austin, Tex., Univ. of Texas, 1964. 123p.

The feasibility of extending the arsenal of heavy particles available in radiotherapy to include mesons (π^-) produced in the Berkeley 184-inch synchrocyclotron was investigated by employing several dosimetric techniques. On the basis of the data obtained, a preliminary assessment of the use of mesons (π^-) is discussed. The results are indicative of many possible advantages, both in improving radiotherapeutic techniques and in offering new areas for basic radiobiologic investigation. (Dissertation Abstr.)

CHEMISTRY

General

40396 (HMI-B-39) JAHRESBERICHT 1964. (Annual Report 1964 of the Hahn-Meitner-Institut fur Kernforschung, Berlin). (Hahn-Meitner-Institut fur Kernforschung, Berlin (West Germany)). May 1965. 124p. Dep. mn.

The 1964 Annual Report of the Hahn-Meitner-Institut für Kernforschung is presented, and it includes the work done in nuclear chemistry, mathematics, nuclear physics, radiochemistry, electronics, reactor physics, and radiophysics. Publications by the various sections are listed, and abstracts of some of them are given. The work in progress is indicated. Backgrounds of new studies initiated during the year are reviewed. Training sessions and symposia held by the different sections are tabulated. (J.S.R.)

40397 (ORNL-TM-1134) IODINE TRANSPORT AND DEPOSITION IN A HIGH-TEMPERATURE, HELIUM LOOP. FIRST TEST SERIES. Neill, F. H.; Eissenberg, D. M.; Gray, D. L. (Oak Ridge National Lab., Tenn.). Aug. 1965. Contract W-7405-eng-26. 42p. Dep. mn; CFSTI, $2.00 cy, $0.50 mn.

The results of an investigation of the transport and deposition of trace amounts of iodine in a high-temperature flowing helium stream are reported. All tests were conducted in the turbulent flow range with the deposition surface in the temperature range of 300 to 600°F. Four surface materials were studied—copper, silver, carbon steel, and stainless steel. Small-diameter silver wires were arranged in arrays perpendicular to the coolant stream to study the applicability of the heat-mass analogy to fission-product deposition studies. The investigation indicated that the amount of iodine deposited per unit amount injected varied with different materials. A silver-plated surface had the highest deposition and the stainless steel surface had the lowest amount deposited. Desorption, under similar test conditions, was greater on the silver-plated surface than on the stainless steel surface. However, other tests indicated that desorption may not be uniform from a stainless steel surface maintained at isothermal conditions. The silver wire tests indicated that the heat-mass analogy gave reasonable correlations with experimental results when calculating the ratio of deposition for various diameter wires. (auth)

40398 (UCRL-16047) GAS ABSORPTION BY DROPS TRAVELLING ON A VERTICAL WIRE (thesis). Rajan, S. M. (Lawrence Radiation Lab., Univ. of California, Berkeley). June 1965. Contract W-7405-eng-48. 68p. Dep. mn; CFSTI $3.00 cy, $0.75 mn.

Liquid phase-controlling mass transfer was studied for a gas–oil system. Pure CO_2 is absorbed in white oil travelling on a wire in the form of drops interconnected by a thin film. Circulating tori within the drops moving down with the wave velocity were observed. The effects of drop size, flow rate, diffusivity, and column length on the mass transfer were examined. The results were plotted by a method suggested in the literature for mass transfer to circulating spherical drops. A model is presented to get a handle on a correlation to coalesce all the obtained data. The results indicate that there are three stages of mass transfer. First, the gas is transferred to the film and the drop; next the gas in the film is transferred to the circulating tori; finally, the tori carry the dissolved gas out of the column. Any correlation would have to include all three of these contributions. The proposed model coalesces the obtained results to within experimental accuracy. (auth)

40399 PROGRESS IN THE SCIENCE AND TECHNOLOGY OF THE RARE EARTHS. VOLUME 1. Eyring, LeRoy. A Pergamon Press Book. Progr. Sci. Tech. Rare Earths, 1: 1-532(1964). New York, The Macmillan Company, 1964.

This book is the first of a series of annual surveys of progress by a group of specialists. This volume covers the years 1955 to 1961. Separate abstracts were prepared for 14 of the 16 chapters; for abstracts of the other two chapters, see NSA 18: 6835 and 32203. (D.L.C.)

For abstracts of individual chapters see: 40400, 40401, 40448, 40449, 40531–40535, 40690–40693, and 40793.

40400 INORGANIC AND ORGANIC COMPOUNDS. Gaume-Mahn, F. (Universite, Lyon). pp 259-309 of Progress in the Science and Technology of the Rare Earths. Vol. I. New York, The Macmillan Co., 1964. (In French).

A survey is presented of the chemical and physical properties of certain classes of inorganic and organic compounds and complexes of the rare earths. 244 references. (T.F.H.)

40401 USES AND APPLICATIONS. Mandle, Richard M.; Mandle, H. H. (W. R. Grace and Co., Pompton Plains, N. J.). pp 416-500 of Progress in the Science and Technology of the Rare Earths. Vol. I. New York, The Macmillan Co., 1964.

A review is presented on the technical, industrial, and commercial applications disclosed in scientific and patent literature during the past five years. An extensive bibliography with descriptive subheadings is included. (D.L.C.)

Analytical Procedures

See also Separation Processes and Procedures.

40402 (BMI-X-10137) THE DEVELOPMENT OF AN IMPROVED METHOD OF SAMPLING AND ANALYSIS FOR ATMOSPHERIC IODINE. Sunderman, D. N.; Howes, J. E.; Rosenberg, H. S. (Battelle Memorial Inst., Columbus, Ohio). July 22, 1965. Contract W-7405-eng-92. 20p. Dep. mn; CFSTI $1.00 cy, $0.50 mn.

A new iodine sampler was developed which comprises a column of sodium bisulfite on a solid matrix coated with a viscous organic solvent. A glass-fiber filter precedes the column to remove particulate iodine; the elemental iodine will react with the solid to form the iodide, while the organic iodide will remain dissolved in the organic film. A survey of gas-liquid chromatographic studies was made, and experiments were conducted on the reactions between the various forms of iodine and the organic phase (dodecane) and on the reactions between the organic-soluble forms of iodine and a reducing phase ($NaHSO_3$). The results demonstrate the feasibility of the new sampling technique. (D.L.C.)

40403 (BNWL-SA-166) AUTOMATED PROCEDURE FOR ZIRCONIUM ANALYSIS IN WATER. Demmitt, T. F. (Battelle-Northwest, Richland, Wash. Pacific Northwest Lab.). Aug. 2, 1965. Contract AT(45-1)-1830. 11p. Dep. mn; CFSTI, $1.00 cy, $0.50 mn.

A simple and effective technique for automating differential fluorescence analysis procedures was developed. The technique was used to adapt an existing manual procedure for zirconium analysis in water for continuous operation. Although the procedure has not been optimized and the ultimate sensitivity and reproducibility have not been determined yet, it is apparent that it can be used to monitor zirconium concentrations in the ppb range. The procedure may eventually be suitable for detecting accelerated corrosion of zirconium and zirconium alloys in water environments. (auth)

40404 (BNWL-SA-167) AUTOMATED PROCEDURE FOR H_3BO_3 ANALYSIS IN WATER. Demmitt, T. F. (Battelle-Northwest, Richland, Wash. Pacific Northwest Lab.). Aug. 2, 1965. Contract AT(45-1)-1830. 12p. Dep. mn; CFSTI $1.00 cy, $0.50 mn.

An original inverse colorimetric analysis procedure was developed, and an automated sample handling system was designed, to permit continuous measurement of trace concentrations of H_3BO_3 in water. The integrated system has been used for on-line monitoring of H_3BO_3 in the Plutonium Recycle Test Reactor moderator under actual process conditions. The results obtained confirmed the suitability of the sample handling and analysis techniques employed. It is felt that this system has significant response time and safety advantages over other published procedures for this application. (auth)

40405 (CONF-650919-1) AUTOMATED PROCEDURES FOR LITHIUM, COBALT, AND THORIUM AND THEIR APPLICATIONS IN NUCLEAR PROCESSES. Gaddy, R. H. (Du Pont de Nemours (E. I.) and Co., Aiken, S. C. Savannah River Lab.). Aug. 4, 1965. Contract AT(07-2)-1. 27p. Dep. mn; CFSTI, $2.00 cy, $0.50 mn.

From Technicon Analytical Symposium, New York.

The following applications of the AutoAnalyzer are described: lithium in Tramex process (flame photometry), cobalt in Al–Co neutron flux monitor wires (colorimetry), and thorium in Thorex process (colorimetry). Reagents and procedures are given. (D.L.C.)

40406 (CONF-650919-2) AUTOMATED ANALYSES FOR THE CHARACTERIZATION OF HEAVY WATER MODERATOR. Gaddy, R. H. (Du Pont de Nemours (E. I.) and Co., Aiken, S. C. Savannah River Lab.). Aug. 3, 1965. Contract AT(07-2)-1. 25p. Dep. mn; CFSTI, $1.00 cy, $0.50 mn.

From Technicon Analytical Symposium, New York.

Methods are needed for the analysis of in-reactor heavy water for trace impurities at the ppb level. Automatic colorimetric procedures are given for the determination of peroxide, ammonia, nitrate, nitrite, iron, phosphate, chromium, chloride, and fluoride. (D.L.C.)

40407 (KY-485) A CHROMATOGRAPH FOR THE ANALYSIS OF HIGHLY REACTIVE AND CORROSIVE COMPOUNDS. Williamson, E. L.; Johnson, C. M.; Mayo, T. J.; Rossmassler, W. R. (Paducah Gaseous Diffusion Plant, Ky.). July 8, 1965. Contract W-7405-eng-26. 21p. Dep. mn; CFSTI $1.00 cy, $0.50 mn.

A chromatograph for the analysis of corrosive gases was designed, built, and tested. The instrument features a unique sample valve and a bleed to the carrier system to improve the analysis for hydrofluoric acid. Data on several individual and mixed gases are tabulated. (auth)

40408 (LA-3333) THE X-RAY FLUORESCENCE SPECTROMETRIC DETERMINATION OF PLUTONIUM IN URANIUM–PLUTONIUM–MANGANESE ALLOYS. Hakkila, E. A.; Hurley, R. G.; Waterbury, G. R. (Los Alamos Scientific Lab., Univ. of California, N. Mex.). Mar. 1, 1965. Contract W-7405-eng-36. 15p. Dep. mn; CFSTI, $1.00 cy, $0.50 mn.

Plutonium in uranium–plutonium–manganese alloys is determined without chemical separation using an x-ray fluorescence spectrographic method. The ternary alloy is dissolved in hydrochloric acid, thorium is added to serve as the internal standard, and the solution is irradiated using a tungsten target x-ray tube. The ratios of the intensities of the $L\alpha_1$ x-ray lines for thorium and plutonium are measured. The method is applicable to the determination of 10 to 50% of plutonium with a relative standard deviation of approximately 1.3% for samples containing no greater than 50% of uranium. Greater uranium concentrations result in selective enhancement of the thorium internal standard line, requiring separate calibration curves for samples containing greater than 50% of uranium. Sulfuric acid is added to samples and standards to minimize absorption effects. (auth)

40409 (MSAR-65-95) DEVELOPMENT OF TECHNIQUES FOR MEASUREMENT OF IMPURITIES IN SODIUM. Quarterly Progress Report, April–June 1965. (MSA Research Corp., Callery, Pa.). July 30, 1965. Contract AT(11-1)-765. 46p. Dep. mn; CFSTI $2.00 cy, $0.50 mn.

Laboratory and instream techniques are in the testing stage. Apparatus were obtained or built, and test data are being collected and evaluated. The initial data verify that the parameters being studied are related to some degree to the Na impurities of interest. Further testing and evaluations will be required to assert to what degree the methods under study are practical. Surface tension measurements of clean and contaminated K were made. K was used initially because the surface tension apparatus had been previously filled with this metal. The results showed a measurable increase in surface tension between pure K and O_2-contaminated K. The tests will be repeated using Na. Encapsulated samples of clean Na, air-contaminated Na, and C-contaminated Na were affected to different degrees in magnetic fields. The magnetic properties of Na impurities were shown to be diamagnetic in nature for both C and Na. Results of one completed run on pure Na indicated an analysis of 80 ppm O_2. The initial run is believed to be reasonable since contamination of the sample after charging was observed. Modifications in both apparatus and procedure are being made. Further evaluation of this procedure is planned. (J.R.D.)

40410 (ORNL-P-494) RADIO-RELEASE METHODS FOR THE EVALUATION OF ATMOSPHERIC POLLUTION. SULFUR DIOXIDE. Ross, H. H.; Lyon, W. S. (Oak Ridge National Lab., Tenn.). [1964]. Contract W-7405-eng-26. 13p. Dep. mn; CFSTI, $1.00 cy, $0.50 mn.

A radio-reagent method is presented for the sensitive determination of sulfur dioxide in the atmosphere. The system exhibits a number of advantages when compared with existing methods. Foremost of these advantages is the extreme sensitivity and dynamic range of the method. Without changing any operational step or reagent, sulfur dioxide can be determined from 8×10^{-4} to 0.2 ppm in a 100 liter gas sample. This range is not fixed, however, since the specific activity of the reagent can be varied over wide limits both up and down. Flow rates can be suited to the particular application; no error was observed at any flow rate up to 4 liter/minute. The method does not require the judgment of a skilled operator making possible a completely automatic remote monitoring station. Although the radio-reagent was synthesized with ^{131}I, which requires a day-to-day decay correction, the reagent can also be made with longer half life ^{125}I to extend the useful life. There are essentially no important variables in the method, and the only significant interference is hydrogen sulfide. However, this is not a real problem since hydrogen sulfide levels are typically lower than those of sulfur dioxide by more than two orders of magnitude. The method should be generally adaptable to any gas system without modification of the basic system. (auth)

40411 (RT/CHI(65)2) DETERMINAZIONE DIRETTA DI ALCUNI PRODOTTI DI FISSIONE IN MISCELA MEDIANTE SPETTROMETRIA GAMMA. (Direct Determination of Some Fission Products in Mixtures by Gamma Spectrometry). Pompei, V. (Comitato Nazionale per l'Energia Nucleare, Rome (Italy)). Feb. 1965. 28p. Dep. mn.

A rapid method for the direct determination of fission products by gamma-ray spectrometry is described. The method is suitable for irradiated power reactor fuels after at least 120 days cooling time. The standard deviation for each determination is ≤6%. (auth)

40412 (TIM-924) THE ELECTRON MICROPROBE AND LIGHT ELEMENT ANALYSIS. Manzione, A. V.; Fornwalt, D. E. (Pratt and Whitney Aircraft, Middletown, Conn. Connecticut Advanced Nuclear Engineering Lab.). July 15, 1965. Contract AT(30-1)-2789. 15p. (CONF-650634-1). Dep. mn; CFSTI, $1.00 cy, $0.50 mn.

From 16th Annual Mid-America Symposium on Spectroscopy, Chicago.

Factors affecting the detection, identification, and determination of the light elements carbon (Z = 6) through fluorine (Z = 9) by electron microprobe were investigated. Comparison of resolution among several lead stearate decanoate crystals is shown. Variations in the intensities

of carbon K alpha x rays are related to absorption edges associated with the metal components of carbides studied. Calibration curves for the determination of carbon in the uranium–carbon system and the titanium–niobium–carbon system are reported. Carbon diffusion into UN to form a U(CN) type compound is discussed. Practical applications of the electron microprobe to the detection and identification of nitrides and complex oxy-fluorides are presented. (auth)

40413 (TIM-948) A COMPACT 1900F RESISTANCE-WOUND COMBUSTION FURNACE FOR REMOTE OPERATION. Farmelo, D. R. (Pratt and Whitney Aircraft, Middletown, Conn. Connecticut Advanced Nuclear Engineering Lab.). July 23, 1965. Contract AT(30-1)-2789. 7p. Dep. mn; CFSTI, $1.00 cy, $0.50 mn.

A compact resistance-wound furnace was developed for the combustion of refractory metals for carbon or sulfur analysis. Over 200 hours operating time in the chemistry hot cell has been accrued in the 1900–1950°F temperature range. The coefficient of variation on 200 and 100 μg quantities of carbon was ±6% and ±11%, respectively. (auth)

40414 (UCRL-7967) THE SPECTROPHOTOMETRIC DETERMINATION OF TRACE AMOUNTS OF TANTALUM. Hill, John H. (Lawrence Radiation Lab., Univ. of California, Livermore). Aug. 28, 1964. Contract W-7405-eng-48. 9p. Dep. mn; CFSTI, $1.00 cy, $0.50 mn.

A spectrophotometric method was developed for the determination of 2 to 50 μg of tantalum. The tantalum is separated from most interfering elements by extracting with methyl isobutyl ketone from HCl–HF solution. It is then back-extracted into buffered ethylenedinitrilo-tetraacetate solution and $AlCl_3$ is added to complex excess fluoride ions. 2,6,7-Trihydroxy-9-phenylisoxanthene-3-one (phenylfluorone) is used to form the colored complex with tantalum. The coefficient of variation of the method ranges from 2.7% for the determination of 50 μg of tantalum to 7.2% for 2.5 μg. The interference of 33 foreign ions was investigated. Only Mo(VI), Nb(V), and Sn(II) interfered with the determination of 10 μg of tantalum. Up to 100 μg of Mo(VI) or Sn(II), or 50 μg of Nb(V) can be tolerated. (auth)

40415 (CEA-tr-R-1839) DOSAGE DES GAZ PERMANENTS PAR LA METHODE DELA CHROMATOGRAPHIE GAZEUSE AVEC LE DETECTEUR A IONISATION-BETA. (Determination of Permanent Gases by the Method of Gaseous Chromatography with the Aid of a Beta-Ionization Detector). Gnauck, G. Translated into French by B. de Trezvinsky from p.68-72 of Gazovaya Khromatografiya, Moscow, 1961. 10p. Dep. mn.

The preliminary results obtained on the determination of H_2, O_2, N_2, and CH_4 by the method of gaseous chromatography using a β ionization chamber with ^{90}Sr as the radioactive source are reported. The results showed that the sensitivity of the determination with neon as the gas carrier is much larger than the sensitivity when argon is used. Quantities of gas of the order of 10^{-7} to 5×10^{-8} could be determined. Techniques for increasing the sensitivity of the determination are indicated. (J.S.R.)

40416 CHARACTERIZATION OF THE VOLTAGE FLUCTUATION IN THE DIRECT CURRENT ARC FOR SPECTROCHEMICAL ANALYSIS. Millichamp, James W. (Army Electronics Command, Fort Monmouth, N. J.). Anal. Chem., 37: 1211-16(Sept. 1965).

Recordings of voltage fluctuation in the d-c arc give direct evidence of events that take place and can be used for the development of analytical procedures. Recordings showed sample consumption time, arc stability, reproducibility, and irregularities that are not readily discernible from spectrograms alone. The voltage fluctuation for different materials, including 67 elements in the elemental state, was studied to correlate the recorded voltage patterns with the properties of the material. The patterns were found to be a function of both the analytical conditions under which they are made, (e.g., arc current electrode design, arc gap, etc.), and the properties of the sample material such as boiling point, density, ionization potential, and reactivity with the electrode material or the surrounding atmosphere. Under standardized analytical conditions, voltage fluctuation patterns are different for each material and are characteristic of that material. (auth)

40417 A CONSTRICTION RESPONSE ANALYZER AND ITS APPLICATION TO CONTINUOUS URANIUM HEXAFLUORIDE DETERMINATION. Weber, C. W.; Pappas, W. S. (Oak Ridge Gaseous Diffusion Plant, Tenn.). Anal. Chem., 37: 1221-5(Sept. 1965). (K-L-6038).

A continuous nondestructive analyzer, which responds pneumatically to changes in density and viscosity of the fluid passing sequentially through an orifice and a capillary was developed. It provides a pneumatic signal directly applicable to stream analysis and to feedback control systems. Good agreement with chemical analyses was obtained where applied to the determination of uranium hexafluoride in complex, corrosive, gas mixtures. A sensitivity of 0.03 mole % uranium hexafluoride in nitrogen was achieved, with a standard deviation of ±0.03 mole %. Little maintenance was required during a field application period exceeding three years. (auth)

40418 LIQUID SCINTILLATION COUNTING OF ^{14}C IN AQUEOUS DIGESTS OF WHOLE TISSUES. Tye, Russell; Engel, J. David (Univ. of Cincinnati). Anal. Chem., 37: 1225-7(Sept. 1965).

The accuracy and precision of a method for determination of ^{14}C in animal tissues and excreta were evaluated. This method has the merit of being very general in applicability to different tissues and to different β emitters and is relatively simple in execution. Animal tissues may be digested to near homogeneity in aqueous sodium hydroxide. Such digests are suitable for the determination of ^{14}C by liquid scintillation counting. Dispersions of the digests are stabilized by suspension on Cab-O-Sil, in a scintillation medium consisting of dioxane, naphthalene, toluene, the scintillators 2,5-diphenyloxazole and 1,4-bis-2-(5-phenyloxazolyl)-benzene, and a compound to prevent freezing. In this medium urine may be dissolved and its radioactivity counted without a gelling agent, but larger amounts may be handled as a second phase, suspended on Cab-O-Sil. ^{14}C in feces may be determined by partial digestion in aqueous hydrochloric acid, mechanical homogenization, neutralization, and counting in suspension. Labeled compounds of widely differing polarities and characteristics of solubility were used to show that the counting efficiency of the system is adequately independent of phase distribution or other phenomena affected by such differences. (auth)

40419 ACTIVATION ANALYSIS FOR ^{18}O ISOTOPE ABUNDANCE UTILIZING RECOIL PROTONS. Hunt, Larry H.; Miller, Warren W. (Pennsylvania State Univ., University Park). Anal. Chem., 37: 1269-72(Sept. 1965).

The use of protons recoiling from collisions with fission-bred neutrons as a method for the determination of ^{18}O abundances in water samples is discussed. The ^{18}O in the water undergoes the reaction $(p,n)^{18}F$, and the radiations from the decay of 110-min ^{18}F are measured. The recoil proton flux induced in a water sample is a complex function of the fast-neutron energy spectrum, the energy-dependent neutron-proton scattering cross section, the energy distribution of the scattered protons from a given neutron energy, the stopping power of the medium for protons, and the protium content of the sample. To avoid the errors caused by variations in the recoil proton flux, a method for monitoring the proton flux within the sample was developed and is described. (F.J.H.)

40420 MICRODETERMINATION OF FLUORIDE USING AN IMPROVED DISTILLATION PROCEDURE. Wade, Marven A.; Yamamura, Stanley S. (Phillips Petroleum Co., Idaho Falls, Idaho). Anal. Chem., 37: 1276-8(Sept. 1965).

A versatile microdistillation procedure that is applicable to the separation of microgram levels of fluoride from anions and cations that interfere in colorimetric procedures is described. The distillation was carried out from a phos-

phoric acid medium with a micro still. The fluoride in the distillate is determinable by a number of colorimetric methods. (F.J.H.)

40421 ESTIMATION OF VANADIUM IN BIOLOGICAL MATERIAL BY NEUTRON ACTIVATION ANALYSIS. Livingston, H. D.; Smith, Hamilton (Univ. of Glasgow). Anal. Chem., 37: 1285-7(Sept. 1965).

Activation analysis of vanadium in biological materials is a rapid and sensitive technique. Naturally occurring vanadium is 99.76% ^{51}V, which on irradiation with thermal neutrons produces ^{52}V. The cross section for thermal neutrons is 4.5 barns and the ^{52}V half life is 3.8 minutes. Both β and γ radiations are emitted, but detection by Geiger counting is preferred because of comparatively low background of this type of counter. The application of activation analysis to vanadium microestimations allows amounts of the order of 10^{-9} gram to be measured. (F.J.H.)

40422 SYSTEMATIC ANALYSIS OF COPPER OF VERY HIGH PURITY AFTER IRRADIATION BY THERMAL NEUTRONS. Cuypers, Marc (Centre d'Etudes de Chimie Metallurgique, Vitry-sur-Seine, France). Ann. Chim. (Paris)(13), 9: 509-40(Sept.-Oct. 1964). (In French).

A method for systematic analysis after thermal neutron irradiation was developed. It permits the determination of 45 elements on a copper sample of the order of 1 gram. For simplicity the analysis is made in two steps. In one step the elements whose isotopes have long half lives are separated after decay of the copper radioactivity. In a second the elements whose radioisotopes have short periods are separated immediately after irradiation. The causes of error of a nuclear origin that can distort the determinations of Ni, Zn, and Co were studied in order to define with precision the limits of determination under the irradiation conditions. A new scheme for separation of the elements, precipitating them as sulfides in diluted acid medium, was developed. The scheme is based on the separations by electrolysis and ion exchange. Conditions for the determination of sulfur from the nuclear reaction $^{34}S(N,\gamma)^{35}S^{*}$ were defined exactly. The new technique for the systematic analysis was applied to the study of industrial electrolytic copper after its treatment by the fused zone technique. After complete decay of the copper radioactivity, it is shown that it is possible to determine some elements by γ spectrometry without further chemical treatment if the sample is sufficiently pure. (tr-auth)

40423 EXTRACTION OF COPPER AND URANIUM WITH 2-METHYL-HEPTANE-4,6-DIONE AND HEXANE-2,4-DIONE. Stevancevic, D. B.; Antonijevic, V. G. Bull. Boris Kidrich Inst. Nucl. Sci., 16: 11-21(Jan. 1965).

Two-phase dissociation constants of 6-methyl-2,4-heptanedione (IVA) and 2,4-hexanedione (PA) were determined in the chloroform-water system. The values of (pK_a + log P_R) are 10.97 (PA) and 12.24 (IVA), and the distribution coefficients of the diketones have the following values: log P_R = 1.75 (PA) and log P_R = 2.97 (IVA). The extraction of copper and uranium using these diketones was investigated. The two-phase stability constants for copper are log K_NP = 18.2 (PA) and 20.96 (IVA), and for uranium 17.9 (PA) and 22.37 (IVA). The pH's for 50% extraction of copper with a concentration of 0.1 M diketone are 2.85 (PA) and 2.76 (IVA), and of uranium 4.40 (PA) and 4.04 (IVA). (auth)

40424 SUBSTOICHIOMETRIC DETERMINATION OF NON-ISOTOPIC RADIOACTIVE ADMIXTURES AND THE CONTENT OF ISOTOPIC CARRIER IN RADIOACTIVE PREPARATIONS. Ruzicka, J. (Czech Technical Univ., Prague). Collection Czech. Chem. Commun., 30: 1808-12(June 1965).

Substoichiometric separation, which was used in the assay of various materials by activation analysis and isotopic dilution, can be used as well in analysis of other mixtures of radioisotopes, such as e.g., radioactive preparations supplied for all sorts of applications. A method for the determination of the content of radioactive admixtures present in the solution of the analyzed radioisotope and isolated from this by a substoichiometric quantity of the reagent is described. The content of the isotopic carrier was determined by inverse isotopic dilution with substoichiometric separation, making it possible to attain a high sensitivity, which is important especially in the analysis of carrier-free preparations. Since the separation carried out with substoichiometric quantities of the reagent is more selective than separation with excess reagent this new method can be expected to considerably simplify the techniques employed to the present in analysis of radioactive materials as well. (auth)

40425 PREPARATION OF SAMPLES OF BIOLOGICAL MATERIAL FOR LIQUID SCINTILLATION MEASUREMENT OF LOW-ENERGY β-EMITTERS. Vavrejn, B.; Franc, Z.; Svobodova, J.; Turek, S.; Lipovska, M.; Francova, V.; Hondlik, J. (Research Inst. for Pharmacy and Biochemistry, Prague). Collection Czech. Chem. Commun., 30: 2084-90(June 1965).

The determination of ^{14}C, ^{35}S, ^{32}P, ^{131}I, and ^{3}H in biological material is described. The samples were dissolved in a mixture of formamide with a primary or secondary amine and transferred into a toluene scintillator with the aid of ethanol. The required quantity of the sample is 20 to 200 mg depending on radioactivity. (auth)

40426 CERTAIN NEW ARSENAZO III ANALOGS AND THEIR ANALYTICAL PROPERTIES. Budesinsky, B.; Haas, K.; Vrzalova, D. (Inst. for Nuclear Research, Czechoslovak Academy of Sciences, Rez). Collection Czech. Chem. Commun., 30: 2373-81(July 1965). (In German).

The following derivatives of 1,8-dihydroxynaphthalin-3,5-disulfonic acid were prepared: 2-(2′-arsono-5′-methylphenylazo)-7-(2′′-arsonophenylazo)-chromotropic acid (I), 2,7-bis(2-arsono-5′-methylphenylazo)chromotropic acid (II), 2-(2′-arsono-5-propylphenylazo)-7-(2′′ arsonophenylazo)chromotropic acid (III), 2-(2′-arsono-5-cholorophenylazo)-7-(2′′-arsonophenylazo)chromotropic acid (IV), 2-(2′-arsono-5′-carboxyphenylazo)-7-(2′′-arsonophenylazo) chromotropic acid (V), 2,7-bis(2′-arsono-5′-carboxyphenylazo)chromotropic acid (VI), 2-(2′-arsononaphthylazo)-7-(2′′-arsonophenylazo)chromotropic acid (VII), 2-(2′-phosphono-4-chlorophenylazo)-7-(2′′-arsonophenylazo)chromotropic acid (VIII), and 2-[2′-bis(carboxymethyl)-aminomethylphenylazo]-7-(2′′-arsonophenylazo)chromotropic acid (IX). The reactions of these materials with the ions Sc^{3+}, Zr^{4+}, Hf^{4+}, Th^{4+}, U^{4+}, UO_2^{2+}, La^{3+}, Lu^{3+}, and Y^{3+} were investigated by spectrophotometric methods. (tr-auth)

40427 ELECTROCHEMICAL BEHAVIOUR OF CADMIUM IN THE H_2O–D_2O SYSTEM. I. POLAROGRAPHIC STUDY. Alonso-Lopez, J. (Junta de Energia Nuclear, Madrid). Electrochim. Acta, 10: 803-8(Aug. 1965).

The diffusion current of Cd^{2+} in a H_2O–D_2O system with a supporting electrolyte of 0.1M KCl + 0.01M HCl was studied as a function of parameters such as time, height of the mercury reservoir, and electrolyte temperature. The characteristics of the process are those of a reversible diffusion-controlled process. In the H_2O–D_2O system, the values of the diffusion current were smaller than the corresponding ones in H_2O, at 25°C. The decrease was proportional to D_2O concentration when this was greater than 35%. This fact may be used as an analytical means of determining D_2O in H_2O mixtures. (auth)

40428 PHOTOCOLORIMETRIC DETERMINATION OF URANIUM(VI) WITH ARSENAZO III IN PRESENCE OF FLUORIDE. Opalovskii, A. A.; Kuznetsova, Z. M. (Inst. of Inorganic Chemistry, Novosibirsk, USSR). Izv. Sibirsk. Otd. Akad. Nauk SSSR, No. 3, Ser. Khim. Nauk, No. 1, 130-3 (1965). (In Russian).

The effect of fluoride on the extraction photometric determination of uranium(VI) using Arsenazo III was investigated and it was shown that the hundredth part of a milligram in 1 ml of the solution inhibits the determination. The dependence of the effects of the fluoride on the optical density of the solution of uranium(VI) with Arsenazo III was established, and this made it possible to determine U in the presence of fluoride. (tr-auth)

40429 THE IN SITU IDENTIFICATION OF PHOSPHATE SPECIES IN MULTISPOT CHROMATOGRAMS BY NEUTRON ACTIVATION ANALYSIS. Rommel, Marjorie A.; Keller, Roy A. (Univ. of Arizona, Tucson). J. Chromatog., 18: 349-58(May 1965).

The solute zones obtained on paper chromatography of phosphates were analyzed for the sodium to phosphorus ratio by neutron activation analysis. Where double spots were formed, the analysis indicated different phosphate species in the two zones. The work also indicated that the sodium in the paper plays an active role in the phenomenon, probably through some ion exchange mechanism. (auth)

40430 SEPARATION OF IODINE ANIONS BY GLASS FIBRE PAPER CHROMATOGRAPHY. Naeumann, R. (Technical Univ. of Norway, Oslo). J. Chromatog., 18: 385-9(May 1965).

The separation of iodide, iodate, and periodate by chromatography on glass fiber paper with different eluants was investigated. Cellulose papers were unsatisfactory for trace-scale separations of periodate because the bulk of the periodate was reduced, probably to iodate. (auth)

40431 SULPHUR^{35}: ITS RADIOCHEMICAL ESTIMATION IN SEA WATER. Basu, D. K. (Atomic Energy Establishment, Trombay, India). J. Indian Chem. Soc., 42: 263-6(Apr. 1965).

A method suitable for routine estimation of ^{35}S in sea water is described. The method was checked, using radiotracers for estimation of 0.005 $\mu\mu$C/ml of ^{35}S in sea water. (auth)

40432 A TRIAL METHOD OF DETERMINING URANIUM AND THORIUM CONTENT IN ROCKS BY MEANS OF AN ALPHA-RAY SCINTILLATION COUNTER AND A RADIOSCOPE. Hatuda, Zin'itiro; Nishimura, Susumu (Kyoto Univ.). Mem. Coll. Sci. Univ. Kyoto, Ser. B., 31: 215-26(Feb. 1965).

An α scintillation counter, suitable for measurement of radioactivity of pulverized rocks, is described. The total number of α particles emitted from the unit surface area of the sample per unit time can be calculated from the observed counting rate. The absorption of α rays, in the sample itself, the air intervening between the scintillator and the sample, and the thin aluminum foil which serves as a cover protecting the scintillator against contamination, are taken into consideration. It was found that by combining the results obtained by this scintillation counter and the radioscope, the uranium and thorium content of a rock sample can be obtained (on the assumption that the contribution of potassium to the ionization in the radioscope is negligible as compared with that due to thorium and uranium). Some α-ray counts were carried out with pulverized borax glass containing chemically pure U_3O_8, 7.53×10^{-9} g/g, used as a thick source. The results of the pulse-height analyses with the uranium and thorium standards and pulverized borax glass fused with allanite containing 6.05×10^{-4} g Th/g are described. Formulas were derived for use in determining U and Th content of geologic samples from combined α scintillation counter and radioscope measurements. (TCO)

40433 RADIOMETRIC SENSING OF ATOMIC HYDROGEN IN TRACE QUANTITIES. Bersin, Richard L. (Tracerlab, Richmond, Calif.). Nucl. Sci. Eng., 23: 21-7(Sept. 1965).

This study was undertaken to evaluate radiometric techniques for sensing atomic hydrogen in trace quantities at low pressure, for possible application to satellite measurements. A reaction utilizing radioactive ^{74}As metallic surfaces demonstrated quantitative evolution of $^{74}AsH_3$ vapor in linear relation with the impingent flux of atomic hydrogen. Equivalent partial pressures of atomic hydrogen below 10^{-6} torr were quantitatively measured. (auth)

40434 SPECTRAL ANALYTICAL TRACE DETERMINATION IN UO_2 NUCLEAR FUEL ELEMENTS USING RADIOCHEMICAL CONTROLLED STANDARD PROBES. Golling, E.; Neeb, K. H. (Siemens-Schuckertwerke AG, Erlangen, Ger.). Nukleonik, 7: 217-20(May 1965). (In German).

For the preparation of standards for trace determination in UO_2 fuel elements, the impurity was added, generally, to pure UO_2 powder using aqueous solutions. The impurity was fixed on the surface of the powder by drying and glowing. In the to-be-analyzed samples, the trace elements, however, are built in the crystal lattice. In order to deter systematic errors conditioned by the type of introduction of the trace elements, radiochemically controlled standards with definite contents of Cd, Co, Cr, Cu, Fe, Pb, and Zn in the UO_2 lattice were prepared. The spectral comparison of the standard series thus prepared gave significant differences in the sensitivity factors. Standards prepared using aqueous solutions of the traces can falsify an analytical result by a factor of 10. (tr-auth)

40435 ANALYSIS OF THE CONCENTRATIONS OF Cr, Ag, Fe, Co, Pt, AND Rb IN NORMAL HUMAN DENTINE. Soeremark, Rune; Lundberg, Max (Univ. of Umea, Sweden). Odontol. Revy, 15: 285-9(1964).

Additional studies are reported on a continuing program of elemental analysis of constituents of human teeth by neutron-activation and γ-ray spectrometric analysis. Earlier studies were done with a thermal neutron flux of about 1.7×10^{12} n cm^{-2} sec^{-1}. A similar experimental procedure was used in the present investigation but a higher thermal neutron flux (6.0×10^{13} n cm^{-2} sec^{-1}) was available. This made it possible to investigate the concentrations of elements that have lower excitation cross sections and longer half lives. Fifteen intact first bicuspids from humans, between 14 and 16 yr old, were used. An Al can containing the sample and standards was irradiated in a thermal neutron beam for six days. After irradiation the samples were dissolved in N HCl, and 0.3% H_2O_2 was added. Chemical group separation was based on a system of ion exchange columns for separation of elements as a pretreatment for γ-ray spectrometric analysis. After the radioactive elements had been collected in the various ion exchange columns the resins were homogenized and transferred to polyethylene tubes for counting. The results, on the basis of ppM dry weight, for human dentine were: Rb, 5.6; Cr, 0.0049; Ag, 0.0051; Fe, 110; Co, 0.00034; and Pt, 0.0. No significant difference with respect to sex was found, nor were any differences found between the teeth from upper and lower jaws. The possible biological significances of some micro elements and the chemistry of the mineral phase in the hard tissues of human teeth are briefly discussed. The layer of dentine adjacent to the pulp has a greater accumulation of some micro elements than does the main body of the dentine. There is probably a continuous interchange of micro elements between the hard tissues of the tooth and their environment. Thus, the inorganic composition will be reflected by such factors as age, food, and water intake, and various local and general changes in the physiological conditions. The exchangeable fraction of the element is located partly in the water phase and partly on the surface of the crystals. This surface area is enormous because of the infinitesimal size of the individual hydroxyapatite crystals in the dentine. There are, consequently, many factors which together may explain the high deviation observed in concentrations of micro elements in dentine. (BBB)

40436 LIQUID SCINTILLATION COUNTING OF NONVOLATILE WATER-SOLUBLE COMPOUNDS. Slot, C. (Glostrup Hospital, Copenhagen). Scand. J. Clin. Lab. Invest., 17: 182-4(1965).

The liquid scintillation counting of water-soluble β emitters involves a problem due to the fact that the most efficient scintillators are completely immiscible with water. The best way of solving the problem is to evaporate the water before the scintillator is added; if this is done directly in the counting vial, however, a great reduction in counting efficiency results. So evaporation of water must be carried out in a vehicle which can afterwards be soaked with scintillator in order to secure a good contact. In testing a method for counting creatinine-1-^{14}C, it was discov-

ered that different filter papers yielded different counting efficiencies and that glass fiber gave the highest counting efficiency of all the vehicles examined. Thus, a counting method was developed using glass fiber as vehicle for the compound to be counted. Results of comparing different vehicles show that different filter papers count with efficiencies from 27 to 57%. The glass fiber invariably counted carrier-free activity with an efficiency of about 75%. The counting of ^{14}C-labeled creatinine in serum was performed with an efficiency of about 60% with glass fiber. The high counting efficiency for the glass fiber is ascribed to the fact that the indices of refraction for the glass fiber and the scintillator are nearly equal, a dry glass fiber disk becoming almost invisible when the scintillator is added. The glass fiber should never be stored in cellophane, as this will make the fiber less absorbent and thus less suited for the purpose. Counting can be performed directly on serum and urine samples by use of glass fiber disks with polyethylene mesh used as support for the disks. It has a sharp edged outer surface, which gives a very small area of contact between the mesh and the disk. As the mesh is water repellent, too, the sample will remain on the disk during the evaporation. (BBB)

40437 SUBSTOICHIOMETRIC DETERMINATION OF TRACES OF GOLD BY NEUTRON-ACTIVATION ANALYSIS. Beardsley, D. A.; Briscoe, G. B.; Ruzicka, J.; Williams, M. (Coll. of Advanced Tech., Birmingham, Eng.). Talanta, 12: 829-39(Sept. 1965).

A highly selective, rapid, one-step radiochemical separation procedure for gold was developed. It is based on the solvent extraction of gold diethyldithiocarbamate from a 0.01 to 10N sulfuric or hydrochloric acid medium using a substoichiometric amount of copper diethyldithiocarbamate in chloroform. The separation was applied to the determination of traces of gold by neutron-activation analysis in high-purity lead, the rock W-1, gold-doped semiconductor-grade silicon and a biological material (kale). Amounts of gold down to 2×10^{-10} g were determined. (auth)

40438 DETERMINATION OF NITROGEN IN URANIUM–PLUTONIUM DIOXIDES. Sinclair, V. M.; Davies, W.; Melhuish, K. R. (Dounreay Experimental Reactor Establishment, Thurso, Caithness, Scotland, U. K.). Talanta, 12: 841-5(Sept. 1965).

Both mass spectrometric and chemical procedures were used to determine nitrogen in uranium–plutonium dioxides. An improved chemical procedure, involving dissolution of the oxide in sulfuric-phosphoric acid mixtures, distillation of the ammonia in the presence of Devarda's alloy, and spectrophotometric determination of the distilled ammonia, was developed. (auth)

40439 ON THE SEPARATION OF THORIUM FROM URANIUM AND THE USUAL ACCOMPANYING ELEMENTS AND ON ITS GRAVIMETRIC DETERMINATION. Spacu, Petru; Popea, Florica (Sectia de Chimie Anorganica, Academia R.P.R., Bucharest). Z. Anal. Chem., 195: 251-4(1963). (In German).

Thorium was estimated in the presence of U by extraction of U with ethyl acetate, followed by precipitation of Th with alizarin yellow GG (Na m-nitrobenzeneazosalicylate) and combustion to ThO_2. Separation of rare earths by usual techniques (mesityl oxide in saturated $Al(NO_3)_3 \cdot 9H_2O$ or $LiNO_3$ solution; tributyl phosphate) was attempted; traces of retained solvent or salt gave errors in results in these cases. A recommended procedure is given. Uranium is extracted from at least 60 ml of HNO_3 solution containing 19 g NH_4NO_3 and 0.0020-0.0950 g ThO_2 by two extractions with 10 ml ethyl acetate for 3 min each. The remaining aqueous solution is buffered dilute (1:4) acetic acid and (1:9) ammonia to pH 4.5-5. Aqueous reagent (0.5%) is added with continuous agitation until precipitation is complete as judged by KIO_3 or thorone. After 5 min the precipitate settles and further addition of reagent causes no more precipitate. Excess reagent may cause precipitation of the carboxylic acid, which does not affect results but which does not settle within 24 hr. The precipitate is collected on medium filter paper and washed with room temperature water until no more color indicates removal of all reagent. Two or three washings suffice. The precipitate is dried in a porcelain or quartz crucible and ashed to constant weight as ThO_2. (BBB)

40440 INVESTIGATIONS WITH AN APPARATUS FOR X-RAY FLUORESCENCE SPECTRAL ANALYSIS IN MICRO AMOUNTS. II. DETERMINATION OF SMALL AMOUNTS. Grothe, Karl Heinz (Technische Hochschule, Hanover). Z. Anal. Chem., 211: 401-6(1965). (In German).

Investigations were carried out in order to determine low concentrations of yttrium and neodymium in mixed oxides of rare earths using the internal standards technique with a special x-ray fluorescence equipment, which consisted of a spectrometer of advantageous resolution combined with an x-ray tube that permits a strong fluorescence excitation of a few milligrams of substance within the tube. It was not necessary to measure the background. The intensity ratios of the total intensities yielded linear calibration curves within the concentration range from 0.1 to 1% of oxide. The detection limit was 0.1% for the oxides of yttrium and neodymium. (auth)

40441 NEW REAGENTS FOR ZIRCONIUM. Cherkesov, A. I.; Pushinov, Yu. V. (Saratov State Pedagogical Inst., USSR). Zh. Analit. Khim., 20: 665-70(1965). (In Russian).

Two new reagents for zirconium–stilbazogall I and stilbazogall II were synthesized. Stilbazogall II is satisfactorily selective and can be used for spectrophotometric determination of zirconium in strong acid media (1–2 N HCl). Stilbazogall I interacts with zirconium in a molar ratio of 1 : 1 (at pH 1.5); stilbazogall II interacts in a molar ratio of Me : R = 1 : 1 (at pH 1.5) and in a molar ratio of 1 : 2 (at pH 0.1). Conditional unstability constants of compounds formed were calculated. The sensitivity of the reactions for zirconium was estimated by the values of oscillating charges of coloured complexes f: f is 0.700 for stilbazogall I, it is 0.290 and 0.300 for stilbazogall II (in the units of the electron charge). (auth)

40442 NEW PHOTOMETRIC METHODS FOR DETERMINING NIOBIUM AND TANTALUM IN METALS AND ALLOYS. COMMUNICATION 4. A STUDY OF NIOBIUM COMPLEX WITH 1-(2-PYRIDYLAZO)-RESORCINOL IN THE PRESENCE OF OXALATE, TARTRATE IONS AND OTHER ADDENDA. Elinson, S. V.; Pobedina, L. I.; Rezova, A. T. Zh. Analit. Khim., 20: 676-82(1965). (In Russian).

A study was made of the interaction between niobium and I-(2-pyridylazo)-resorcinol (PAR) in the presence of oxalate, tartrate, fluoride and other addenda. The best results for niobium determination using PAR are obtained in the presence of oxalate and tartrate ions. The complex solution exhibits maximum absorption in an oxalate medium at 540 mμ (pH 5.5), in a tartrate medium–at 520 mμ (pH 5.5–7.0). When acidity is increased from 0.2 to 0.75 N HCl in the presence of tartrate ions the optical density increases; thus niobium can be determined under conditions when the most of other ions do not form colored complexes. The molar extinction coefficient is 23,300 in the oxalate solution and 28,000 in the tartrate one. It was established by the isomolar series method that in oxalate and tartrate solutions niobium reacts with PAR in the proportion of 1:1. The complexes have maximum optical density at the content of oxalate ions up to 30 mg and that of tartrate ions up to 100 mg (in 50 ml); the optical density in 0.75 N HCl does not change on the increase of the tartrate ions concentration up to 0.1M. Methods were developed for determining niobium in alloys based on U, Mo, W and Zr in the presence of oxalate ions at pH 5.5 and in a tartrate solution in 0.75N HCl for alloys containing Mo, W, Ti, Al, Fe, Co and Ni. (auth)

40443 ON CATALYTIC WAVES OF THE REDUCTION OF A PEROXIDE NIOBIUM COMPLEX IN SULPHURIC ACID. Sharipov, R. K.; Songina, O. A. (Kirov Kazakh State Univ., Alma-Ata, USSR). Zh. Analit. Khim., 20: 683-7(1965). (In Russian).

Catalytic currents of hydrogen peroxide on a dropping mercury electrode observed in sulphuric acid solutions of niobium (V) were studied. A sensitive polarographic method for niobium determination was suggested. (auth)

40444 DETERMINATION OF NITROGEN IN METALS BY AN ISOTOPE-DILUTION METHOD. Orlova, K. B.; Vitol, E. N. Zh. Analit. Khim., 20: 694-9(1965). (In Russian).

An isotope-dilution method was applied to the determination of nitrogen in Nb, W, Mo, La, Ce, Re, Fe, Cr and Ni. The relative sensitivity of the method is 1×10^{-4}%. (auth)

40445 DETERMINATION OF SAMARIUM, GADOLINIUM, DYSPROSIUM, ERBIUM AND SCANDIUM (0.01-0.6 PERCENT) IN STEELS AND ALLOYS BY A CHEMICO-SPECTROGRAPHIC METHOD. Fedorov, A. A.; Sorokina, N. N. (Bardin Central Scientific-Research Inst. of Ferrous Metallurgy, Moscow). Zh. Analit. Khim., 20: 745-7(1965). (In Russian).

A chemico-spectrographic method was developed for determining 0.01-0.6% of samarium in chromium-nickel steels and alloys based on nickel, and for determining gadolinium, dysprosium, erbium, and scandium (0.01-0.6%) in alloys of iron metal with rare earth elements or scandium and in medium alloyed steels. The experimental errors when 1×10^{-2}-2×10^{-2}; 2×10^{-2}-5×10^{-2}; 5×10^{-2}-1×10^{-1}; 1×10^{-1}-2.5×10^{-1}; 2.5×10^{-1}-6×10^{-1}% of a rare earth element (or scandium) is determined are correspondingly 3×10^{-3}; 5×10^{-3}; 9×10^{-3}; 1.5×10^{-2} and 3×10^{-2}% absolute. (auth)

40446 ADVANCES IN ANALYTICAL CHEMISTRY AND INSTRUMENTATION. VOLUME 4. Reilley, Charles N. (ed.). New York, Interscience Publishers, 1965. 519p.

Information is included on: recent advances in precipitation from homogeneous solution; differential dialysis; oxygen-flask method; phase-solubility techniques; electrochemistry of cation-sensitive glass electrodes; advances in time-of-flight mass spectrometry; and organic analysis with uv absorption spectroscopy. Separate author, subject, and Vols. 1 to 4 cumulative indexes are included. (P.C.H.)

40447 ION EXCHANGE SEPARATIONS IN AMMONIUM THIOCYANATE-ORGANIC SOLVENT-WATER SYSTEMS (thesis). Kiser, Donald Lee. Iowa City, Iowa, Univ. of Iowa, 1964. 110p.

The distribution coefficients of many metals were measured on both anion and cation resins in ammonium thiocyanate-organic solvent-water systems. The effects of the concentration of ammonium thiocyanate, the nature of the organic solvent to water ratio were evaluated. On anion resin, Dowex 1-X8, the distribution coefficients of Th were higher in all systems studied than are those of the rare earth members and Y. The distribution values of the rare earths increased in a given system with increase in atomic number. Using distribution data, procedures were developed for the separation of rare earth members and Y from Th. On the cation resin, Dowex 50-X8, in methanol the distribution coefficients of Zn, Cd, Fe^{3+}, and Co^{2+} decreased as the concentration of ammonium thiocyanate was increased from 0.01 to about 0.1 M, then increased at higher concentrations. Column characteristics suggest that at least in the case of Co^{2+} and Fe^{2+}, the increase may be due to the formation and entrapment of a large complex inside the resin pores. Quantitative elution of Co^{2+} can be made with an eluant of 0.1 M ammonium thiocyanate in 90 per cent methanol, but not with 0.1 M ammonium thiocyanate in 100 per cent methanol. Sorbed Fe^{3+} cannot be removed with either of these eluants. The distribution coefficient for Th in methanol-thiocyanate solutions with air-dried Dowex 50-X8 was dependent on the degree of resin loading at low concentrations of Th. The lower the loading, the greater was the ratio of Th on the resin to Th in solution. This is attributed to the influence of partitioning of a Th species with the residual water of the resin. Several successful separations on Dowex 50-X8 verified the utility of the distribution data. Separations were performed on the cation resin by either changing the methanol-water ratio at fixed ammonium thiocyanate concentration or by changing the ammonium thiocyanate concentration in 100 per cent methanol. (Dissertation Abstr.)

40448 ANALYTICAL CHEMISTRY OF RARE EARTHS. Loriers, Jean (Centre National de la Recherche Scientifique, Bellevue, France). pp 351-98 of Progress in the Science and Technology of the Rare Earths. Vol. I. New York, The Macmillan Co., 1964. (In French)

A survey is presented of the analytical properties and analytical separations of rare earths. Techniques for measurement and control of purity of rare earths are also surveyed. 228 references. (T.F.H.)

40449 SOVIET RESEARCH ON ANALYTICAL CHEMISTRY OF THE RARE EARTHS. Ryabchikov, D. I.; Ryabukhin, V. A. (Academy of Sciences, Moscow). pp 399-415 of Progress in the Science and Technology of the Rare Earths. Vol. I. New York, The Macmillan Co., 1964.

A review is presented of studies on the development of methods for the determination of the individual rare earths in their mixtures and in the presence of other elements. Qualitative reactions, separations, polarography, volumetric methods, colorimetric and spectral methods, and nuclear methods are discussed. (D.L.C.)

40450 ACTIVATION ANALYSIS PROGRAM AND FACILITIES AT THE NATIONAL BUREAU OF STANDARDS. DeVoe, James R.; Smith, Gilbert W. (National Bureau of Standards, Washington, D. C.). 21p. (CONF-650405-8). Gmelin, AED-CONF-65-040-21.

From International Conference on Modern Trends in Activation Analysis, College Station, Tex.

In order to meet the requirements of the Standard Reference Materials Program, it was necessary that activation analysis techniques be developed to provide maximum accuracy and precision. The concepts and plans for meeting these requirements are discussed. The facilities of the National Bureau of Standards for activation analysis are described. (M.C.G.)

40451 COMPUTER PROGRAMS TO OPTIMIZE TIMES OF IRRADIATION AND DECAY IN MULTIELEMENT ACTIVATION ANALYSIS. Isenhour, T. L.; Evans, C. A. Jr.; Morrison, G. H. (Cornell Univ., Ithaca, N. Y.). 17p. (CONF-650405-14). Gmelin, AED-CONF-65-040-12.

From International Conference on Modern Trends in Activation Analysis, College Station, Tex.

Computer programs were developed for the computation of irradiation and decay in multielement activation analysis. The computer program; program MULTIOPT computes the irradiation time that allows a group of elements to be analyzed to a specific minimum selectivity. The program OPTIMIZE determines the optimum irradiation and decay times for any single element in any mixture regardless of its complexity. The OPTIPLOT program graphically presents the results of considering various irradiation times with optimized decay times. All three programs were combined into a single system controlled by the master program AARDVARK. This system permits a rapid evaluation of the feasibility of applying either single element or multielement activation analysis to any problem. Examples are presented for evaluation of the program. (F.J.H.)

40452 SIMULTANEOUS DETERMINATION OF COPPER AND ZINC IN HUMAN LUNG TISSUE BY NEUTRON ACTIVATION ANALYSIS. Keenan, Robert G.; Marcus, Judith H.; DeVoe, James R. (National Bureau of Standards, Washington, D. C.). 17p. (CONF-650405-9). Gmelin, AED-CONF-65-040-20.

From International Conference on Modern Trends in Activation Analysis, College Station, Tex.

Certain trace elements, including copper and zinc, are constituents of numerous enzymes and function as essential catalysts in biosyntheses. The expanded interest in these substances has supplied a demand for micro-analytical

techniques of increased sensitivity, accuracy, and precision. Good precision may be realized in the activation analysis of complex biological specimens with only a few, one-step chemical separations. The nuclear reactions ^{63}Cu (n,γ) ^{64}Cu (12.8hr) and ^{68}Zn (n,γ) ^{69m}Zn (13.8hr) were used for the analysis. The samples were irradiated in a thermal neutron flux of 10^{13} n cm^{-2} s^{-1}. The copper was extracted as the acetylacetonate into chloroform from an acetate system buffered at a pH of 4.75. The remaining aqueous phase was extracted with chloroform to remove most of the acetylacetone dissolved in the aqueous phase. The zinc was extracted as the dithizonate into chloroform, and is back-extracted into 1% HCl for counting. Careful internal standardization was used for correction of results for variation in chemical yields. Application of the method to the simultaneous determination of copper and zinc in lung samples provided values of the same order of magnitude as those reported by Tipton and Cook for U.S. adults using emission spectrographic procedures, which were between 7 and 10 ppm for copper and 40 and 70 ppm for zinc. Comparison of the precision of this method with that of emission spectroscopy indicated that this activation technique had at least three times better precision. (auth)

40453 THE MEASUREMENT OF SURFACE CONTAMINATION OF HIGH PURITY BERYLLIUM SAMPLES. Blake, K. R. (Texas Nuclear Corp., Austin); Martin, T. C.; Morgan, I. L.; Houston, C. R. 25p. (CONF-650405-7). Gmelin, AED-CONF-65-040-16.

From International Conference on Modern Trends in Activation Analysis, College Station, Tex.

The oxygen, nitrogen, and carbon surface contamination of a group of high-purity beryllium samples was measured. Also surface photographic studies were made to observe changes after repeated, controlled chemical etches. The surface oxygen contamination was calculated from total oxygen content measurements made by fast neutron activation analysis using a 15-Mev neutron generator. The carbon and nitrogen surface contamination was measured by using deuterons from a Van de Graaff accelerator. The total oxygen content of these high-purity beryllium samples was found in general to decrease slightly after controlled chemical etchings. However, inconsistent results were obtained with those samples having observable cracks and fissures. At times a higher oxygen content was detected after a chemical etch indicating that oxygen was apparently retained in these surface irregularities. Deuteron bombardment of the surfaces of high-purity beryllium samples revealed in general that most of the carbon and nitrogen was contained within surface layers. A high surface contamination of carbon was expected in beryllium samples from a long extruded rod cut with a carborundum cutting disc. Surface photographs of unetched surfaces showed striations, which undoubtedly were caused by the cutting disc and which provided contaminant traps. Even after several chemical etches in which several thousandths of an inch of material was removed, there were still several contaminant sites per field of view. These results indicated that a significant percentage of the total carbon and nitrogen content of high-purity beryllium samples is contained in surface layers. Also these results indicated that in general it would be advisable to chemically etch the surfaces of beryllium samples to remove any surface oxides present prior to oxygen measurements by fast neutron activation analysis. (auth)

40454 IMPROVEMENTS RELATING TO MEASURING APPARATUS. Allenden, Dennis; Boddy, Keith; Freck, David Vernon; Hunt, Stanley Ernest (to Associated Electrical Industries Ltd.). British Patent 999,434. July 28, 1965. Filed July 7, 1961.

A measuring apparatus for measuring the relative relationship of one quantity to another includes means for generating electronic pulses having a recurrence rate dependent upon the first quantity and means for generating a second set of pulses of a recurrence rate dependent upon the second quantity. A first pulse counter counts the first set of pulses positively (commencing at zero), and a second counter counts the second set of pulses negatively (commencing at the maximum count and reducing). The readings are indicated and recorded when they reach a predetermined relationship. The apparatus is particularly adapted for the analysis of radioactive materials in which the output of a solid state radiation detector(s) is passed to analyzing apparatus producing outputs at recurrence frequencies representative of the amounts of constituents in the mixture, and the pulse outputs are fed to the counters. The maximum count, i.e. the starting figure, of the negatively going counter in the apparatus may be so chosen that when the two counts are equal the first counter will give a direct reading of the proportion of the first constituent. (B.L.M.)

Inorganic and Physical Chemistry

Refer also to abstracts 40833 and 41073.

40455 (BNL-9297) SLOW NEUTRON STUDIES OF MOLECULAR MOTIONS IN CONDENSED MATTER. Palevsky, Harry (Brookhaven National Lab., Upton, N. Y.). June 1965. Contract AT-30-2-GEN-16. 37p. (CONF-650630-2). Dep. mn; CFSTI, $2.00 cy, $0.50 mn.

From Society of Physical Chemistry, 15th Annual Meeting, Paris.

A survey of how neutrons are used to probe the microscopic motions of condensed matter is presented. (M.O.W.)

40456 (IAE-713) TEKHNOLOGIYA PEREVODA SIL'NOOSNOVNYKH ANIONITOV (TIPA AB-17 I AM) IZ KHOLRIDNOI V GIDROKSIL'NUYU FORMU METODOM DVUKHSTADIINOI REGENERATSII. (Technique of Conversion of Highly-Basic Anion-Exchange Resins (Type AV-17 and AM) from the Chloride to the Hydroxyl Form by the Method of Two-Stage Regeneration). Chernorotov, E. S. (Institut Atomnoi Energii, Gosudarstvennyi Komitet po Ispol'zovaniyu Atomnoi Energii SSSR, Moscow). 1964. 13p. Dep. mn.

A new technology is given for converting strongly basic anionites from the chloride into the hydroxyl form, by successively treating the anionite with a solution of ammonium carbonate and caustic soda. The anionites in hydroxyl form are needed for the purification of water used in nuclear reactors. The requirements that must be satisfied by the anionite are listed in tabular form and the chemical conversion procedure is listed step by step. The proposed technology was verified experimentally at the IAE im. I. V. Kurchatova (Institute of Atomic Energy) and turned out to be much cheaper and to yield a product of higher purity, with respect to chlorine, than the technology based on processing with a solution of caustic soda only. (ATD)

40457 (IS-1156) A TABULATION OF THE SPECIFIC HEAT CONTRIBUTION DUE TO THERMAL EXCITATION (SCHOTTKY EFFECT) OF THE 4F ELECTRONS OF SOME DI- AND TRI-VALENT LANTHANIDE ELEMENTS. Dennison, David H.; Gschneidner, Karl A. Jr. (Ames Lab., Iowa State Univ. of Science and Tech.). May 1965. Contract W-7405-eng-82. 40p. Dep. mn; CFSTI $2.00 cy, $0.50 mn.

The 4f electronic specific heat contribution for divalent samarium and for the trivalent lanthanide elements Ce, Pr, Nd, Pm, Sm, Eu, Tb, Dy, Ho, Er, Tm, and Yb were calculated and is tabulated at 25°K intervals from 50 to 200°K, at 50°K intervals from 200 to 400°K, and at 100°K intervals from 400 to 2000°K. (auth)

40458 (JINR-P-2224) IZUCHENIE KOMPLEKSOOBRASOVANIYA Am, Cm, Cf, I Fm S MOLOCHNOI KISLOTOI. (The Investigation of Complexes of Am, Cm, Cf and Fm With Lactic Acid). Ermakov, V. A.; Stary, I. (Joint Inst. for Nuclear Research, Dubna (USSR). Lab. of Nuclear Reactions). 1965. 9p. Dep. mn.

The extraction constants of Am(log K_{ex} = −7.97), Cm (log K_{ex} = −7.84), Cf(log K_{ex} = −7.11), and Fm(log K_{ex} = −6.80) with thenoyltrifluoracetone in benzene were determined. Further, the composition and stability constants of complexes of Am(log β_3 = 5.71), Cm(log β_3 = 5.76), Cf(log

β_3 = 6.09), and Fm(log β_3 = 6.36) with lactic acid were determined using extraction method. With the aid of an ion-exchange method the following values of stability constants were obtained: log β_3 = 5.78 for Cm, log β_3 = 6.08 for Cf, and log β_3 = 6.27 for Fm. (auth)

40459 (NP-15324) A SUMMARY OF THE SOVIET PAPERS ON THE HIGH PRESSURE EQUATION OF STATE OF METALS. Poulter Laboratories Technical Report 003-65. Anderson, Gordon D. (Stanford Research Inst., Menlo Park, Calif.). June 15, 1965. 52p.

The experimental methods, handling of the data, and the equations of state models used to describe the behavior of metals at high pressures and temperatures as reported in Soviet papers during 1958 to 1962 are presented. The numerical information presented in the papers was collected and is presented in two appendices. The experimental data such as measured shock velocities and flying plate velocities and quantities computed directly from the data by the Rankine-Hugoniot jump conditions are present in the first appendix. On the basis of particular equation of state models suggested by the experimental data, thermodynamic quantities such as 0°K isotherms, Gruneisen functions, and shock temperatures were calculated and are presented in the second appendix. (W.L.G.)

40460 (NYO-3462-1) STABLE ISOTOPE STUDIES, Annual Progress Report, September 15, 1964-July 15, 1965. Hughes, T.; Kander, Lois Nash; Monse, E. U.; Spindel, W. (Belfer Graduate School of Science, Yeshiva Univ., New York). July 15, 1965. Contract AT(30-1)-3462. 36p. Dep. mn; CFSTI, $2.00 cy, $0.50 mn.

Isotopic exchange equilibria and partition function ratios were calculated with a high speed digital computer. Molecules studied include NO, NO_2, NO_2^+, NOF, NOCl, NOBr, NO_2F, NO_2Cl, NO_3^-, HNO_3, and cis and trans nitrous acids. In the course of the calculations, force fields were calculated for several species from recent spectroscopic data, and in several cases force fields still unpublished were used to calculate vibrational frequency shifts on isotopic substitution. Where sufficient spectroscopic data were available, isotopic partition function ratios were calculated from both fundamental and zero-order frequencies, to permit an evaluation of anharmonicity on the ratios. Many of these calculations are still in progress. (auth)

40461 (ORNL-P-491) SOME FLUORINE COMPOUNDS OF RHENIUM AND TECHNETIUM. LaValle, D. E.; Steele, R. M.; Smith, Wm. T. Jr. (Oak Ridge National Lab., Tenn. and Tennessee Univ., Knoxville. Dept. of Chemistry). [1963]. Contract W-7405-eng-26. 27p. Dep. mn; CFSTI, $2.00 cy, $0.50 mn.

The compound potassium hexafluororhenate(IV), K_2ReF_6, previously reported to exist in several forms, was prepared in its pure state and was characterized. The corresponding technetium compound, K_2TcF_6, was also prepared. The new compound rhenium nitrogen fluoride, ReNF, and also a possible technetium analog were obtained. A method was developed for the preparation of previously known but not well characterized rhenium tetrafluoride, ReF_4; some properties of the compound were determined. (auth)

40462 (SC-TM-65-183) THE KINETICS OF THE REACTIONS OF KO_2 AND KOH WITH WATER. Cuthrell, R. E. (Sandia Corp., Albuquerque, N. Mex.). Apr. 1965. Contract AT(29-1)-789. 14p. Dep. mn; CFSTI $1.00 cy, $0.50 mn.

Results are given of a kinetic study of the reactions of potassium hydroxide and potassium superoxide with water vapor and carbon dioxide. The equipment used and the mathematics required for calculating time dependent concentrations are described. (auth)

40463 (SRIA-425-5) SORPTION OF GASES ON METAL SURFACES IN ULTRAHIGH VACUUM. Quarterly Progress Report No. 10, February 15-May 15, 1965. Bergsnov-Hansen, B.; Endow, N.; Pasternak, R. A. (Stanford Research Inst., Menlo Park, Calif.). May 21, 1965. Contract AT(04-3)-425. 12p. Dep. mn; CFSTI, $1.00 cy, $0.50 mn.

The sorptive behaviqr of two molybdenum films deposited at 60°C and -196°C was examined, and their physical properties were investigated by electron diffraction and microscopy. The hydrogen-deuterium exchange reaction was investigated further, particularly, the room temperature isotherms of hydrogen, deuterium, and their mixtures on molybdenum. Finally, a detailed study of the interaction of oxygen with niobium was pursued further. (D.L.C.)

40464 (UCRL-11816(Rev.)) PHYSICAL CHEMISTRY OF GLASS-METAL INTERFACES. Pask, Joseph A.; Borom, Marcus P. (Lawrence Radiation Lab., Univ. of California, Berkeley). May 7, 1965. Contract W-7405-eng-48. 37p. (CONF-650640-1). Dep. mn; CFSTI $2.00 cy, $0.50 mn.

From 7th International Glass Congress, Brussels.

The phase equilibria of glass-metal heterogeneous systems are discussed; thermodynamic equilibrium is established in the presence of oxygen when the molten silicate becomes saturated with the low valence oxide of the metal. When the glass contains transition metal oxides whose metals have a lower oxidation potential than the base metal and form alloys with the base metal, reactions occur that result in adjustments of the compositions of the alloy and glass at the interface in a drive to achieve and maintain equilibrium. Presence of multivalent cations in the glass also assists in this drive by providing a transport mechanism for atmospheric oxidation of the base metal. If glass and metal are not at equilibrium and oxygen is not readily available, reactions of a redox type occur. Maintenance of equilibrium compositions at the interface while the whole system moves toward thermodynamic equilibrium is dependent upon the kinetics of the various reactions. It is theorized that when thermodynamic equilibrium is present in heterogeneous systems, chemical bonding can occur between the phases providing there are no complications of a physical nature. This condition then corresponds to an equal attraction between the atoms at the interface leading to a balance of bond energies and a continuity of the electronic structure. This hypothesis is applied to glass-metal systems. Furthermore, with the development of a chemical bond the surface energy of the metal is lowered by an amount approximately equivalent to the surface energy of the molten glass; this condition corresponds to a zero contact angle in a sessile drop experiment. (auth)

40465 (UCRL-16175) ELECTRON SPIN RESONANCE STUDIES OF TRANSITION METAL ION COMPLEXES (thesis). Spencer, John Brockett (Lawrence Radiation Lab., Univ. of California, Berkeley). Aug. 1965. Contract W-7405-eng-48. 127p. Dep. mn; CFSTI $4.00 cy, $0.75 mn.

The spectrum of $Cr(CN)_5NO^{-3}$ was examined in solution and in a glass using enriched $^{13}CN^-$. The isotropic hyperfine coupling constants were determined to be $A(^{53}Cr)$ = 18.39 gauss, $A(^{14}N)$ = 5.27 gauss for the NO ligand, $A(^{13}C_a)$ = 8.80 gauss, and $A(^{13}C_e)$ = 12.64 gauss for the axial and equatorial CN ligands. The anisotropic magnetic parameters determined were $A_\perp(^{53}Cr) = 11.6 \times 10^{-4}$ cm^{-1}, $A_\parallel(^{53}Cr) = 30.9 \times 10^{-4}$ cm^{-1}, $A_\perp(^{14}N) = 6.3 \times 10^{-4}$ cm^{-1}, $A_\perp(^{13}C_a) = 9.2 \times 10^{-4}$ cm^{-1}, $A_\perp(^{13}C_e) = 11.0 \times 10^{-4}$ cm^{-1}, $g_\perp$ = 2.006, and $g_\parallel$ = 1.973. The rate of exchange of $^{13}CN^-$ with $Cr(CN)_5NO^{-3}$ was determined in the temperature range 60-100°C from changes in the ESR spectrum. The results obtained were $k_a = 6 \times 10^{-5}$ sec^{-1} at 75°C with $\Delta H_a^\ddagger$ = 33.5 kcal/mole and $\Delta S_a^\ddagger$ = +18 eu for axial exchange; and $k_e = 6 \times 10^{-6}$ sec^{-1} with $\Delta H_e^\ddagger$ = 30.5 kcal/mole and $\Delta S_e^\ddagger$ = +5 eu for equatorial exchange. Implications for bonding in this complex are discussed. Solution and glass spectra for cupric ion in water and in ammonia were investigated. The magnetic parameters determined were $g_\parallel$ = 2.379, $g_\perp$ = 2.066, $A_\parallel = 155 \times 10^{-4}$ cm^{-1}, and g = 2.199 in water; and $g_\parallel$ = 2.228, $g_\perp$ = 2.055, $A_\parallel = 192 \times 10^{-4}$ cm^{-1}, g = 2.124, and $A = 69 \times 10^{-4}$ cm^{-1} in ammonia. Line widths for cupric ion in water were measured from -40 to +200°C and in liquid ammonia from -80 to +20°C. The line widths were corrected for unresolved hyperfine structure. Two contributions to the line width were distinguished. One con-

tribution increases with increasing temperature and is the same for all four hyperfine components. The second increases with decreasing temperature and varies with the hyperfine component. A transition region was observed for cupric ion in ammonia between −80 and −100°C. In this region the sample was frozen but an isotropic spectrum was obtained. These results are discussed with regard to several theories of electron spin relaxation. Glass spectra for ferric chloride in concentrated HCl and concentrated $HClO_4$ were examined. A sharp resonance at g = 4.24 was observed and assigned to the species $FeCl_4^-$. The theory for high g-value resonances in ferric complexes is reviewed and applied to $FeCl_4^-$. Glass spectra for the chromic complexes $CrCl(H_2O)_5^{+2}$, cis- and trans-$CrCl_2(H_2O)_4^+$ were examined and compared with the spectrum for $Cr(H_2O)_6^{+3}$. The spectra for the chloro complexes extend from g = 6 to g = 2. The results are discussed in terms of zero field energies and symmetries of the complexes. (auth)

40466 (UJV-1209/65) GENERAL ACIDOBASICITY. III. AN EXPLANATION OF THE AUTHOR'S CONCEPTION. Baran, V. (Ustav Jaderneho Vyzkumu, Ceskoslovenska Akademie Ved, Rez). 1965. 18p. Dep. mn.

General acidobasicity is considered to be an objective property of solutions of ionized solvents. The essence of its specificity is determined by mechanism of permanent interruption and recombination of bonds. For this viewpoint the general acidobasicity appears as an interference with the autodissociation mechanism and the chemical classification of acidobasic reactions may then be deduced: Any interference corresponds to the concept of acidobasic reactions, merely a chemical interference to the solvolytic reactions in general sense, the chemical interference based on ionic reactions to solvolysis in narrower sense, which as a special as well as a specific case contains dissolution of acids and bases. (auth)

40467 (ORNL-tr-578) EQUILIBRIUM BETWEEN CERIUM AND ITS DI- AND TRIVALENT IONS IN A MOLTEN EUTECTIC MIXTURE OF LITHIUM AND POTASSIUM CHLORIDES. Smirnov, M. V.; Sokolovskii, Yu. S.; Krasnov, Yu. N. Translated by Martha Gerrard (Oak Ridge National Lab., Tenn.) from Tr. Inst. Elektrokhim., Akad. Nauk SSSR, Uralsk. Filial, 5: 7-16(1964). 13p. Dep. mn; CFSTI $1.00 cy, $0.50 mn; JCL $1.60 fs, $0.80 mf.

The equilibrium potentials of Ce in molten eutectic LiCl–KCl containing 0.84, 1.65, and 5.62 wt % Ce at 400 to 700°C were measured. The average valence of Ce in the melt is less than 3. The standard electrode potentials were determined to be: $E^0_{Ce/Ce^{3+}} = -3.61 + 7.4 \times 10^{-4}T \pm 0.01$ volt and $E^0_{Ce/Ce^{3+}} = -3.36 + 5.8 \times 10^{-4}T \pm 0.02$ volt. The equilibrium constant of the reaction 2 Ce^{3+}(molten) + Ce(solid) → 3 Ce^{2+}(molten) is $\log[Ce^{2+}]^3/[Ce^{3+}]^2 = 4.84 - 7560/T$. The thermodynamics of $CeCl_2$ was investigated; it was found that liquid $CeCl_2$ cannot exist in the free state. (auth)

40468 (SC-T-65-721) THE TEMPERATURE DEPENDENCE OF DIELECTRIC POLARIZATION IN SOME BENZENE DERIVATIVES. Bretscher, Egon. Translated by Marcel I. Weinreich (Sandia Corp., Albuquerque, N. Mex.) from Physik. Z., 32: 765-73(1931). 20p. Dep. mn; JCL, $1.60 fs, $0.80 mf.

The temperature dependence of dielectric polarization of molecules in dilute solutions and deviations from the 1/T law are discussed. The requirements for accurate measurements of polarization are considered, and the experimental apparatus and methods are described. Measurements are reported for diethyl phthalate in decalin and tetrachloroethylene, decalin, p-cymene, tetrachloroethylene, benzyl benzoate in decalin, and the diethyl ester of pyrocatechin in decalin. The causes of the observed anomalies are discussed. (D.L.C.)

40469 REFRACTOMETRIC STUDY OF THE FORMATION OF COMPLEX PRASEODYMIUM HALIDES IN AQUEOUS SOLUTION. Spacu, P.; Albescu, Ileana; Dragomir, Eugenia (Centrulde Cercetari Chimice, Academia R.P.R., Bucharest). Acad. Rep. Populare Romine Studii Cercetari Chim., 11: 269-76(1963). (In Rumanian).

Data for the refractive index vs molarity of aqueous $PrCl_3$ are presented in tabular and graphical form. Tabular and graphical data are also given for mixtures of $PrCl_3$ with NaCl, KCl, and CsCl in which the total molarity of the solution remains approximately constant at about 1M. Deviations from ideal behavior indicate the existence of $Na(PrCl_4)$, $K(PrCl_4)$, $Cs(PrCl_4)$, $Cs_2(PrCl_5)$, and $Cs_3(PrCl_6)$. Experimental data for the refractive index vs molarity of aqueous $PrBr_3$ are likewise presented in tabular and graphical form. Mixtures of $PrBr_3$ with NaBr and KBr were studied; data are given for solutions in which the sum of the molarities equals 0.5M. In the latter cases no compound formation could be detected. This supports the suppositions about the greater complexing ability of Cl as opposed to Br. (BBB)

40470 ISOTOPIC EFFECT ON THE INFRA-RED SPECTRUM AND MOLECULAR STRUCTURE OF TRIMETHYL BORATE ESTER. Barcelo, Jose R. (Instituto de Optica Daza de Valdes, Madrid). Anales Real Soc. Espan. Fis. Quim. (Madrid), Ser. B., 60: 763-70(Dec. 1964). (In Spanish).

The infrared spectrum of trimethyl borate ester was registered for samples with different isotopic composition of boron. The trimethyl borate is a liquid highly volatile and it is possible to scan the spectrum in vapor phase. With the present data and the Raman data of the literature it was possible to classify the frequencies of this molecule and study the isotopic shifts. (auth)

40471 NITRYL NITRATO COMPLEXES OF INDIUM AND THORIUM. Schmeisser, M.; Koehler, G. (Technische Hochschule, Aachen). Angew. Chem., 4: 436(May 1965).

The synthesis of anhydrous nitrates using chlorine nitrate and chlorides or bromides was applied to indium halides. On treatment of $InBr_3$ with excess $ClNO_3$ at 20°C, a quantitative yield of nitryl tetranitratoindate, $NO_2[In(NO_3)_4]$, was obtained. In a vacuum at 135°C this compound partially decomposed to indium oxide nitrate. Analogous thorium compounds were prepared from $ThCl_4$. Infrared spectra of the compounds were obtained. (M.C.G.)

40472 SYNTHESIS AND PROPERTIES OF RED TANTALUM NITRIDE Ta_3N_5. Brauer, G.; Weidlein, J. R. (Universitaet, Freiburg i. B.). Angew. Chem. Intern. Ed. Engl., 4: 241-2(Mar. 1965).

Ta_3N_5 was produced from pure tantalum pentoxide and extremely pure ammonia at 860 to 920°C. Titanium turnings were used to act as getter for the oxygen. The Ta_3N_5 is stable up to about 950°C under ammonia at normal pressure. It has a tetrazonal crystal lattice with A = 10.265 and C = 3.898Å. (M.C.G.)

40473 A PULSE METHOD FOR THE INVESTIGATION OF THE TIME BEHAVIOR OF THE DYNAMIC PROTON POLARIZATION. Werner, K. (Karl-Marx Universitaet, Leipzig). Ann. Physik (7), 14: 125-8(1964). (In German)

A method was described by which the increase of the nuclear polarization up to the maximum value and the decrease to equilibrium could be measured directly. Results for the Overhauser effect on radical solution were reported and compared with theoretical considerations. (tr-auth)

40474 INTERACTIONS OF METAL IONS WITH POLYNUCLEOTIDES AND RELATED COMPOUNDS. III. DEGRADATION OF POLYRIBONUCLEOTIDES BY LANTHANUM IONS. Eichhorn, Gunther L.; Butzow, James J. (National Heart Inst., Bethesda, Md.). Biopolymers, 3: 79-94(1965).

The polyribonucleotides of adenylic, cytidylic, and uridylic acids (poly A, C, U) were degraded in a 2-hr period at 64°C into low molecular weight oligonucleotides and mononucleotides by La(III) or other trivalent inner transition metal ions. Polyinosonic acid (poly I) was degraded more slowly. Cleavage of the polynucleotide chains occurs at the 5′-phosphate linkages. The reaction between La(III) and the polynucleotide involves one metal ion for every three nucleotide residues, with each metal ion apparently chelated to a 2′-hydroxyl and a phosphate group and bound to only one polynucleotide chain. Removal of protons from

the coordinated water molecules around the La ion occurs between pH 7.5 and 8.5 and requires 3 moles of base per mole of La. The data are in accord with the picture of each La bound to one phosphate. When the course of the degradation of poly A and poly U by Ce and of poly U by Lu was determined under conditions identical to those for La, the degradation of both poly A and poly U was accomplished more rapidly by Ce than by La. Lutetium, on the other hand, produced a slower reaction. It was concluded that the rare earth ions vary little in their influence upon the degradation of polynucleotides, and that the observed variabilities are complicated by solubility relations. (T.C.O.)

40475 THE OXYSULFIDES AND SESQUISULFIDES OF TERBIUM, HOLMIUM, THULIUM, AND LUTETIUM. Collin, Gaston; Loriers, Jean (C.N.R.S., Bellevue, France). Compt. Rend., 260: 5043-6(May 10, 1965). (In French)

The oxysulfides of Tb, Ho, Tm, and Lu were prepared by the reaction of hydrogen on the sulfates or of hydrogen sulfide on the oxides. They are compounds with hexagonal structure whose crystalline parameters decrease regularly with the radius of the rare earth ion. The sesquisulfides of Tb, Ho, Tm, and Lu were prepared by the action of hydrogen sulfide on the oxides at high temperature. According to the ratio of the radius of the sulfur ions to the rare earth ions, they have three different crystalline forms: cubic Th_3P_4 type for Tb_2S_3, monoclinic for Ho_2S_3 and Tm_2S_3, and rhombohedric for Lu_2S_3. These results are in good agreement with those given for the same compounds of the elements with even atomic number of the rare earths near Tb, Ho, Tm, and Lu. (tr-auth)

40476 CRYSTAL STRUCTURE OF $LaTe_2$. Eliseev, A. A.; Kuznetsov, V. G. (Kurnakov Inst. of General and Inorganic Chemistry, USSR). Izv. Akad. Nauk SSSR, Neorgan. Materialy, 1: 692-7(May 1965). (In Russian).

X-ray structure investigations of single crystals of $LaTe_2$ were carried out and the structure type Cu_2Sb was established. By the method of projection of interatomic vectors and electron densities it was established that atoms of La and Te have the double multiple positions (c) and (a) with the parameters $Z_{La} = 0.275$, $Z_{Te_{II}} = 0.638$, and $Z_{Te_I} = 0$. The coordinate number of the atoms and the coordination polyhedron of La and Te in the structure were determined. The structure $LaTe_2$ has a laminar character with alternating layers, parallel to the coordinate plane xy according to the type: $Te_I - La - Te_{II} - Te_{II} - La - Te_I$. (tr-auth)

40477 CRYSTALLINE STRUCTURE OF La_5Si_3, Ce_5Si_3, Pr_5Si_3, Nd_5Si_3, Sm_5Si_3. Gladyshevskii, E. I.; Kripyakevich, P. I. (L'vov State Univ.). Izv. Akad. Nauk SSSR, Neorgan. Materialy, 1: 702-5(May 1965). (In Russian).

By x-ray structural analysis of monocrystals and powders it was established that the compounds M_5Si_3, where M = La, Ce, Pr, Nd, and Sm, have the structure type Cr_5Be_3. However, some samples of Nd_5Si_3 and the compound Sm_5Si_3 (probably containing oxygen) have the structure type Mn_5Si_3. The values of the lattice constants are tabulated. (tr-auth)

40478 CRYSTALLINE STRUCTURE OF La_3Si_2, Ce_3Si_2, AND Pr_3Si_2 COMPOUNDS. Gladyshevskii, E. I. (L'vov State Univ.). Izv. Akad. Nauk SSSR, Neorgan. Materialy, 1: 706-10(May 1965). (In Russian).

The existance of the silicides La_3Si_2, Ce_3Si_2, and Pr_3Si_2 was established by x-ray structure studies. All the compounds belong to the structure type U_3Si_2 (space group $P_4/mbm - D_{4h}^5$) and the lattice parameters are tabulated. A comparison of the dimensions of the elementary cell indicated that cerium in the compound Ce_3Si_2 is present principally in the form of Ce^{4+} ions. (tr-auth)

40479 SCANDIUM MONSILICIDE AND ITS CRYSTAL STRUCTURE. Dvorina, L. A.; Protasov, V. S.; Gladyshevskii, E. N. (L'vov State Univ. and Inst. of Problems in Studies of Materials, Academy of Sciences, Ukrainian SSR). Izv. Akad. Nauk SSSR, Neorgan. Materialy, 1: 711-4(May 1965). (In Russian).

The existence of the compound ScSi, with structure type CrB, was established. Its crystal paramenters are a = 3.99, b = 9.86, and c = 3.65 Å, the space group is Cmcm – D_{2h}^{17}; $4ScN_4(C_I)$ with y = 0.140 and $4SiN_4(C_{II})$ with y = 0.420. (tr-auth)

40480 SOME QUESTIONS CONCERNING RADICAL-LUMINESCENCE OF CRYSTALS. Gorban, A. N. (Zaporozhe Machine-Building Inst., USSR). Izv. Akad. Nauk SSSR, Ser. Fiz., 29: 519-20(Mar. 1965). (In Russian).

Experimental data from the literature are cited to verify a mechanism, involving the formation of electron-hole pairs, for the transfer of energy released by the recombination of radicals on the surface of a crystal phosphor to the luminescence centers within it. Discussions are given of the appearance of absorption bands characteristic of the H – O and H – Zn bonds when hydrogen is adsorbed on ZnO, the increase of the afterglow intensity of ZnS : CdS : Cu phosphors by adsorption of hydrogen, the effect of an electric field (which displaces the Fermi surface) on the intensity of radical-luminescence, and the low yield of radical-luminescence. (ATD)

40481 PHASE TRANSITIONS OF URANIUM TETRAFLUORIDE AND TETRACHLORIDE. Khripin, L. A.; Gagarinskii, Yu. V.; Luk'yanova, L. A. (Inst. of Inorganic Chemistry, Novosibirsk, USSR). Izv. Sibirsk. Otd. Akad. Nauk SSSR, No. 3, Ser. Khim. Nauk, No. 1, 13-19(1965). (In Russian).

Differential thermal analysis methods were used to determine that the melting points of uranium tetrafluoride and uranium tetrachloride are 1003 ± 2 and 564 ± 1°C, respectively. The polymorphous transition described earlier at the temperature of 837 ± 3°C for uranium tetrafluoride was not found. The heat of transformation has a value of the order of 3.4 to 3.8 kcal/mole. In uranium tetrachloride one polymorphous transformation was detected, occurring at 587 ± 3°C. The heat of this transformation was approximately 2.7 kcal/mole. (tr-auth)

40482 REACTIONS OF URANYL NITRATE SOLUTION WITH SODIUM MALONATE SOLUTION. Nikolaeva, N. M. (Inst. of Inorganic Chemistry, Novosibirsk USSR). Izv. Sibirsk. Otd. Akad. Nauk SSSR, No. 3, Ser. Khim. Nauk, No. 1, 60-7(1965). (In Russian).

The composition and the range of stability of uranyl malonate complexes in solution were determined. It was determined that the composition of the complex does not vary with time. The step and total constants of the dimalonate complexes were determined by ion exchange. From spectrophotometric data the step constants of some $k_{3.2}$ trimalonate complexes were calculated. (tr-auth)

40483 THERMAL RELAXATION IN OXYGEN WITH H_2O, HDO, AND D_2O VAPORS AS IMPURITIES. Henderson, Malcolm C.; Clark, Anna Vincent; Lintz, Paul R. (Catholic Univ. of America, Washington, D. C.). J. Acoust. Soc. Am., 37: 457-63(Mar. 1965).

Using the 100% relative-humidity technique for controlling the mole fraction of water vapor, the Napier (relaxation) frequency of oxygen was measured as a function of the mole fraction of various water vapors, consisting of pure H_2O, pure D_2O, and three mixtures thereof. Pure H_2O gave a quadratic in H, the mole fraction; pure D_2O gave a linear relation down to 0.7×10^{-3}. The mixtures showed a linear relation above 1.5×10^{-3} and a curvilinear approach to zero below that. Calculation indicated that the heterogeneous molecule HDO is far more effective as a thermal equilibrator for oxygen than either of its homogeneous parents. Quantitatively, with $(f/p)_m$ in cps per atm and h in mole fraction $\times 10^3$, the results are: for 100% H_2O, $(f/p)_m = 7 + 183h + 132h^2$; for 50% D_2O, $(f/p)_m = -664 + 1100h$; for 80% D_2O, $(f/p)_m = -490 + 908h$; for 92% D_2O, $(f/p)_m = -250 + 585h$ (above h = 1.3); for 92% D_2O, $(f/p)_m = 7 + 275h + 100h^2$ (below h = 1.3); and for 99.8% D_2O, $(f/p)_m = -85 + 385h$. (auth)

40484 HYDROGEN ADSORPTION ON ZIRCONIUM BORATE AND DIOXIDE. Khundkar, M. H.; Khan, A. S.; Das, P. K. (Dacca Univ., East Pakistan). J. Indian Chem. Soc., 42: 301-6(May 1965).

Zirconium borate is formed by dehydration of the trihydrate, $ZrO_2 \cdot B_2O_3 \cdot 3H_2O$, at 400°C, or above. The compound $ZrO_2 \cdot B_2O_3$ decomposes only slightly (2 to 3%) at 500 to 600°C. Neither $ZrO_2 \cdot B_2O_3$ nor ZrO_2 is reduced by hydrogen up to 600°C, but some amount of the gas is adsorbed. The extent of adsorption has a negative temperature coefficient (physical adsorption in the crystal lattice). The extent of adsorption is relatively small with respect to chromium or manganese borate. (auth)

40485 THERMODYNAMIC PROPERTIES OF NONSTOICHIOMETRIC THORIUM MONOCARBIDE. Aronson, S.; Sadofsky, J. (Brookhaven National Lab., Upton, N. Y.). J. Inorg. Nucl. Chem., 27: 1769-78(Aug. 1965). (BNL-8269).

Thermodynamic information on nonstoichiometric thorium monocarbide was obtained from measurements on solid electrochemical cells. The cells were of the type Th, $ThF_4|CaF_2|ThF_4$, ThC_{1-x}. Measurements were made at temperatures of 800 to 950°C. Partial molar free energies of thorium and carbon were calculated from the data. The monocarbide phase was found to be stable from a composition of $ThC_{0.88}$ to $ThC_{0.96}$ from measurements of the variation of lattice parameter with composition. The results are discussed in connection with theories of chemical bonding, which were proposed for transition metal and actinide metal carbides. A qualitative picture of the bonding in nonstoichiometric thorium carbide is presented in which it is assumed that thorium and carbon form covalent bonds that increase in strength when some of the carbon is removed from the lattice. (auth)

40486 THE STABILITY OF SOME LANTHANIDE COMPLEXES WITH ISOBUTYLMETHYLGLYCOLATE, ISOPROPYLMETHYLGLYCOLATE, DIETHYLGLYCOLATE AND DIPROPYLGLYCOLATE. Thun, H. (Rijksuniversiteit, Ghent); Verbeek, F.; Vanderleen, W. J. Inorg. Nucl. Chem., 27: 1813-24(Aug. 1965).

The successive formation constants were determined for the isobutylmethyl-, isopropylmethyl-, diethyl-, and dipropylglycolate complexes of several lanthanide elements by potentiometric titration. The formation constants increased as a function of the atomic numbers for each ligand system with some irregularity in the trend in the Eu–Gd region. For a given lanthanide the order of complex stability was isobutylmethylglycolate > dipropylglycolate > isopropylmethylglycolate > diethylglycolate. The average ligand number per metal ion exceeding a value of three, indicated the formation of a uninegative tetraligand complex. The acid dissociation constant for each of the four ligands was also calculated. (auth)

40487 LANTHANIDE COMPLEXES. III. COMPLEXES OF 2,2′-DIPYRIDYL WITH LANTHANIDE CHLORIDES, THIOCYANATES, ACETATES AND NITRATES. Hart, F. A.; Laming, F. P. (London Univ.). J. Inorg. Nucl. Chem., 27: 1825-9(Aug. 1965).

Well-crystallized complexes of the types $MCl_3(dipy)H_2O$, $M(CH_3COO)_3(dipy)$, $MCl_3(dipy)_2$, $MCl_3(dipy)_2EtOH$, and $M(CNS)_3(dipy)_3$ are reported and described (M = a lanthanide and dipy = 2,2′-dipyridyl). Further data are presented concerning the complexes $M(NO_3)_3(dipy)_2$, and all the complexes were compared with the corresponding 1:10-phenanthroline compounds with respect to possible structures and relative stability. (auth)

40488 PREPARATION AND PROPERTIES OF TRICAESIUM PLUTONIUM(III) HEXACHLORIDE DIHYDRATE. Stevens, R. E. (Dow Chemical Co., Golden, Colo.). J. Inorg. Nucl. Chem., 27: 1873-6(Aug. 1965).

Addition of excess solid CsCl to concentrated $PuCl_3$ in 6N HCl yielded a deep green crystalline solid, occurring as well-formed rectangular tablets. Chemical and thermogravimetric data verified the composition of the salt as $Cs_3PuCl_6 \cdot 2H_2O$. X-ray and optical data are presented. (M.C.G.)

40489 ON THE THERMAL DECOMPOSITION OF THE CHLOROHYDRATES OF THE RARE EARTH ELEMENTS. Haeseler, Guenther; Matthes, Franz (Technische Hochschule fuer Chemie Carl Schorlemmer, Leuna-Merseburg, Ger.). J. Less-Common Metals, 9: 133-51(Aug. 1965). (In German).

The thermal decomposition of hydrates of rare earth chlorides was investigated under various conditions using an automatic thermal balance. The application of very slow heating velocities made it possible to determine the hydrate decomposition and the formation of the oxide compounds in a very accurate form. The thermal decomposition of the hydrated chlorides of La, Pr, and Nd in an air current made it possible to detect the formation of different hydrates and anhydrous chlorides. The end products of the thermal decomposition, at temperatures up to 500°C, are the oxychlorides, MeOCl; cerium forms CeO_2 under these conditions. For the elements from Sm to Lu, the preparation of anhydrous chlorides in an air current was no longer possible even with extremely low heating. The decomposition of the monohydrates always gave oxide compounds. During decomposition in air and hydrogen chloride the following hydrates were found: $MeCl_3 \cdot 6H_2O$, $3.5H_2O$, $3H_2O$, $2.5H_2O$, $2H_2O$, and H_2O. In the formation of the oxychloride from the monohydrates (Sm to Lu) in an air stream, steps in relation to heating velocity, were recorded for which the following compounds could be assumed: $Me(OH)Cl_2$, $MeOCl \cdot H_2O$, and $MeOCl \cdot MeCl_3 \cdot 2H_2O$. The compound $MeOCl \cdot H_2O(Me(OH)_2Cl)$ was prepared by hydration in the gaseous phase and thermal decomposition of the hydration product. For each element the formation of the water-free trihalogenide from the oxychloride or the oxides was investigated in hydrogen chloride atmosphere. (tr-auth)

40490 GAS-METAL REACTIONS DURING ANNEALING AND MELTING OF NIOBIUM AND TANTALUM. Fromm, E.; Jehn, H. (Max-Planck-Institut fuer Metallforschung, Stuttgart). Metall, 19: 747-52(July 1965). (In German).

The reactions of nitrogen, oxygen, and water vapor with Nb and Ta at high temperatures and low pressures are reviewed. The quantitative relations obtained between pressure, temperature, and concentration made possible calculations of the degassing obtainable through vacuum glowing. By fusion studies in an electron beam furnace, the relationship between degassing reactions in the solid and the liquid state was determined. Extrapolation of the relations valid for the solid state up to the melting point gave a residual gas content that agrees with the values found by gas analysis. (tr-auth)

40491 CHEMISTRY OF THE RARE EARTH METALS. VIII. TARTRATE COMPLEXES OF LANTHANUM. Brezina, Frantisek (Palacky Univ., Olomouc, Czechoslovakia); Rosicky, Jaroslav. Monatsh. Chem., 96: 1025-9 (1965). (In German).

A systematic investigation of the system in the acidic range was performed, and the compounds $La_2(H_2T)_3 \cdot 9\ H_2O$ and $H[La(H_2T)_2] \cdot 3\ H_2O$ (where $H_4T = C_4H_6O_6$) were isolated. X-ray powder diagrams were taken, and thermal analysis carried out. The infrared absorption bands were assigned, and the dissociation constants, based on pH measurements determined. (auth)

40492 CHOICE OF COLLIMATORS FOR NEUTRON POWDER DIFFRACTOMETRY. Popovici, M. (Inst. of Atomic Physics, Bucharest). Nucl. Instr. Methods, 36: 179-80(Sept. 1965).

The angular divergences of collimators, assuring the maximum of luminosity for a given resolution for a crystal spectrometer for neutron powder diffraction, are determined. (auth)

40493 CHEMICAL POTENTIALS BY DIRECT SUMMATION OF FERMI-DIRAC FUNCTIONS. Gold, L. (Stevens Inst. of Tech., Hoboken, N. J.). Nuovo Cimento (10), 38: 1519-30(Aug. 16, 1965).

A method of evaluating Fermi levels from Fermi-Dirac (F-D) functions is developed, founded upon the central aspect of suitably bifurcating the requisite sums around turning points associated with a change in sign of the exponentials. This technique allows identification of the principal contributions of the summations in the neighbor-

hood where the F-D function changes most rapidly. By this means the Fermi energy can be computed in one, two, and three dimensions and, in principle, the calculation may be carried out to any desired accuracy. Comparison with the values deduced by Sommerfeld's classic approach requires elaboration to lowest order where, in fact, the replacement of sums by integrals becomes valid. The latter cannot be instituted with impunity in general as it implies a sufficiently high electron density to warrant representation by a continuum. Anisotropic modification of the chemical potential is also dealt with to allow for possible mass tensor effects. (auth)

40494 THE FLUORESCENCE OF RARE EARTHS. II. EMISSION SPECTRA OF BORATE PHOSPHORS ACTIVATED BY CERIUM AND SAMARIUM. Mueller-Bushbaum, G.; Vitsman, G. (Griefswald Universitaet, Ger.). Opt. Spectry. (USSR)(English Transl.), 18: 354-6(Apr. 1965).

Translated from Optika i Spektroskopiya, 18: 622-7 (Apr. 1965).

The redistribution of energy in the spectrum of samarium, resulting from coactivation by cerium, was investigated by studying borate phosphors activated by cerium and samarium. (auth)

40495 PHOTON MULTIPLICATION IN CRYSTALS. II. THE MECHANISM OF PHOTON MULTIPLICATION. Ilmas, E. R.; Lildya, G. G.; Lushchik, Ch. B. Opt. Spectry. (USSR)(English Transl.), 18: 359-61(Apr. 1965).

Translated from Optika i Spektroskopiya, 18: 631-6 (Apr. 1965).

The excitation spectra of the instantaneous components of the steady-state luminescence and the excitation spectra of the photostimulated luminescence of alkali iodides activated with indium and thallium were investigated in the region of 4 to 21 ev. The conclusion was drawn, on the basis of the analysis of the experimental results, that there exist at least two mechanisms of photon multiplication – exciton and electron-hole. It was discovered that in the region of photo multiplication the dependence of the luminescence yield on the intensity of excitation has properties connected with a discontinuous increase in the volume density of the excitation. (auth)

40496 $EuGd_2S_4$, A NEW FERROMAGNETIC SEMICONDUCTOR. Hulliger, F. (Cyanamid European Research Inst., Geneva); Vogt, O. Phys. Letters, 17: 238-9(July 15, 1965).

Investigations were made in which $EuGd_2S_4$ was found to be a nonmetallic Th_3P_4-type ferromagnet with a Curie point of 6°K. Preliminary measurements of the saturation magnetization at 1.5°K on a sintered sample gave a magnetic moment of 18.6 Bohr magnetons per formula unit. Above 10°K the magnetic susceptibility obeys a Curie-Weiss law with $13.5\mu_{Bohr}$/formula compared to a theoretical value of $13.75\mu_{Bohr}$. The structure of the compound, which is a representative of a family of related compounds within which by mixed-crystal formation the magnetic and electric properties may be widely varied, is discussed. (L.B.S.)

40497 DIFFERENTIAL DYNAMIC POLARIZATION OF FLUORINE AND HYDROGEN NUCLEI. Thompson, Don D. (California Research Corp., La Habra); Poindexter, Edward H. Phys. Rev. Letters, 15: 281-2(Aug. 16, 1965).

Some samples are studied in which hydrogen and fluorine are differentially polarized, and other samples in which they are almost identically polarized. While the fluorine-hydrogen coupling can be demonstrated, observations suggest that the chemical situation of the fluorine nuclei on the solvent molecule may sometimes exert a commanding influence on the dynamic polarization. Several samples were prepared, and all were de-oxygenated and sealed in glass. Dynamic polarization was observed and the results are summarized. The data suggest that the polarization of fluorine nuclei depends on their location in the solvent molecule, with a particular difference between aromatic and aliphatic positions. It is expected that the methyl F nuclei should experience less scalar interaction than the ring nuclei, and this effect seems to be observed. (J.F.P.)

40498 PARAMAGNETIC RESONANCE OF DIVALENT EUROPIUM IN LEAD CHLORIDE. Vrehen, Q. H. F.; Volger, J. (Rijksuniversiteit, Utrecht). Physica, 31: 845-65 (June 1965).

Paramagnetic resonance spectra of Eu^{2+} ions at Pb^{2+} sites in $PbCl_2$ were measured at room temperature and 3 cm wavelength. The point group symmetry at a Pb^{2+} site is monoclinic. Apart from a reflection, all sites in the unit cell are magnetically equivalent. Analysis yielded the following values for the dominant parameters in the spin hamiltonian: $g = 1.993 \pm 0.003$ isotropic; $b_2^0 = (+107 \pm 1) \times 10^{-4}\ cm^{-1}$; $b_4^3 = (-527 \pm 2) \times 10^{-4}\ cm^{-1}$. The z-axis is along the crystallographic a axis, x and y axes 23.5° from the crystallographic b and c axis respectively. In order to obtain a fit with the measured hyperfine structure for ^{151}Eu terms $\Sigma_i A_i' S_i^3 I_i$ are added to the spin hamiltonian. The values for the HFS parameters are (in units $10^{-4}\ cm^{-1}$): $^{151}A_x = -31 \pm 1$; $^{151}A_y = -33.0 \pm 0.5$; $^{151}A_z = -33.6 \pm 0.5$; $^{153}Q_1 = +0.33 \pm 0.06$; $|^{153}Q_2| = +3.8 \pm 0.1$; $^{151}A_x' = -0.10 \pm 0.02$; $^{151}A_y' = +0.10 \pm 0.02$; $^{151}A_z' = +0.11 \pm 0.02$. The results are interpreted in terms of crystal field theory. Evidence is presented indicating that the second degree crystal field splittings found are mainly linear in the field strength. Under the assumption that a perturbation mechanism, linear in field strength and cubic in spin-orbit coupling, is mainly responsible for the second degree crystal field splittings, a value is derived for the electronic shielding coefficients γ_∞ and γ_2. The result is $(1 - \gamma_\infty)/(1 - \gamma_2) = +169$, in reasonable agreement with present theoretical estimates. (auth)

40499 NUCLEAR MAGNETIC RELAXATION. Hennel, Jacek W. (Inst. of Nuclear Physics, Krakow). Postepy Fiz., 16: 41-9(1965). (In Polish)

A brief outline of the theory of nuclear magnetic relaxation is given for spin-½ particles (protons) in liquids, and it is shown by what methods of research with magnetic relaxation one can obtain information about the statistical properties of Brownian motion which induces changes in the orientation of particles. The treatment considers only those cases in which the time constant T_1 for relaxation along a magnetic field is equal to the time constant T_2 for relaxation along any axis perpendicular to the magnetic field. These cases are for relaxation in low-viscosity liquids such as water, alcohol, and condensed gases. A number of comparisons of theoretical and experimental relaxation times are given. (TTT)

40500 THERMODYNAMIC CHARACTERISTICS OF ELECTRODE PROCESSES WITH PARTICIPATING RARE EARTH AND ACTINIDE ELEMENTS. Krestov, G. A. Radiokhimiya, 7: 68-78(1965). (In Russian).

On the basis of the introduction of enthalpic and entropic components of normal electrode potentials (π_H^0 and π_S^0), complete thermodynamic characteristics of a series of electrode processes with participating rare earth and actinide elements were obtained. By the use of numerical values and signs of normal electrode potentials and their components, the classification of the electrode processes under examination was obtained. Some singularities of their pattern were determined. (tr-auth)

40501 BROMINATION OF MICROQUANTITIES OF PROTACTINIUM-233 IN CARRIERS. Lapitskii, A. V.; Berdonosov, S. S. Radiokhimiya, 7: 118-19(1965). (In Russian).

Studies of the bromination of microquantities of ^{233}Pa on different carriers (HfO_2 and Ta_2O_5) showed that the reaction of ^{233}Pa with Br begins at a very high temperature (1000°C). The possibility of the complete separation of Pa from $HfBr_4$ and $TaBr_5$ by volatilization was shown. (tr-auth)

40502 INELASTIC SCATTERING OF ELECTRONS BY ALKALI-HALIDE COMPOUNDS. Gomoyunova, M. V.; Letunov, N. A. (Ioffe Inst. of Physics and Tech., Leningrad). Soviet Phys.-Solid State (English Transl.), 7: 311-15(Aug. 1965).

Translated from Fiz. Tverd. Tela, 7: 387-93(Feb. 1965).

A formula is obtained for the inelastic electron scattering coefficient for compounds, and the concept of the equivalent element is justified. The method developed earlier by Everhart for elements is used in the calculations. An experimental study of the inelastic scattering of electrons by all alkali-halide compounds was carried out in the primary electron energy range 0.2-4 kev. The results of the experiments are in satisfactory agreement with the calculated data. (auth)

40503 SECONDARY ELECTRON EMISSION OF ALKALI-HALIDE COMPOUNDS. Gomoyunova, M. V.; Letunov, N. A. (Ioffe Inst. of Physics and Tech., Leningrad). Soviet Phys.-Solid State (English Transl.), 7: 316-20(Aug. 1965).

Translated from Fiz. Tverd. Tela, 7: 394-9(Feb. 1965).

The secondary electron emission (s.e.e.) coefficients of all the alkali-halide compounds in the primary electron energy interval from 0.2 to 4 kev were measured using the single-pulse method. The investigated specimens consisted of film emitters. The results show good correlation between the dependences of the s.e.e. coefficient and the density of the alkali-halides on the effective atomic number. (auth)

40504 TRANSFER OF TRIPLET STATE ENERGY FROM ACETOPHENONE TO RARE EARTH IONS. Ballard, R. E.; Edwards, J. W. (United Kingdom Atomic Energy Authority, Harwell, Berks, Eng.). Spectrochim. Acta, 21: 1353-60(Aug. 1965).

The bright line emission of certain rare earth ions, energized by intermolecular transfer from triplet acetophenone, was studied and the intensity was found to be dependent on rare earth ion concentration according to a modified Stern-Volmer equation. Self-quenching of rare earth ions was observed. (auth)

40505 CERTAIN REGULARITIES IN ISOTOPIC EXCHANGE EQUILIBRIUM. Knyazev, D. A.; Bantysh, A. N. (Mendeleev Inst. of Chemical Engineering, Moscow). Zh. Fiz. Khim., 39: 1068-74(May 1965). (In Russian).

An attempt was made to establish certain regular characteristics of various groups in order to find optimum systems for comparing the sum ratio according to the isotopic molecular state in series formed by similar molecules. The magnitude of the sum ratio was not correlated with group number and atomic period of the molecule components. It was found that at certain ratios between the frequencies and mass in the atoms there existed the same bonding. The curves of the relation of the sums for diatomic halides, $^{36}Cl-^{35}Cl$, $^{80}Br-^{79}Br$, and $^{128}I-^{127}I$, and for $^{11}B-^{10}B$ and $^{14}C-^{13}C$ were analyzed. (R.V.J.)

40506 ISOTOPIC EXCHANGE OF OXYGEN IN GAS-MELT SYSTEMS AT 700 TO 955°C. Finikov, V. G. (Inst. of Physical Chemistry, Academy of Sciences, USSR). Zh. Fiz. Khim., 39: 1105-7(May 1965). (In Russian).

Isotopic exchange of oxygen in a gas-melt system was observed on the surface and in the liquid volume. The rate of oxygen isotopic exchange in Na_2SO_4, Na_2MoO_4, and Na_2WO_4 melts was found and the isotopic exchange activation energy on the surface and in the melt volume was calculated. Further studies of the activation energy as a function of ^{18}O concentration are suggested. (R.V.J.)

40507 ON THE AMMONIATED Be, Mg, Ca, Al, Sc, AND Y ACETATES. Grigor'ev, A. I.; Pogodilova, E. G.; Novosilova, A. V. (Moscow State Univ.). Zh. Neorgan. Khim., 10: 772-9(Apr. 1965).

Reactions of anhydrous normal Al, Sc, Y, Mg, and Ca acetates with liquid ammonia in ampuls at room temperature, followed by evaporation of excess ammonia, produced $Mg(OCOCH_3)_2 \cdot 2NH_3$, $2Ca(OCOCH_3)_2 \cdot 2NH_3$, $Al(OCOCH_3)_3 \cdot 3NH_3$, $2Sc(OCO \cdot CH_3)_3 \cdot 3NH_3$, and $Y(OCOCH_3)_3 \cdot 3NH_3$ compounds. The compounds $2Ca(OCOCH_3)_2 \cdot 2NH_3$ and $2Sc(OCOCH_3)_3 \cdot 3NH_3$ were quite soluble in liquid ammonia while $2Ca(OCOCH_3)_2 \cdot 2NH_3$ and $2Sc(OCOCH_3)_3 \cdot 3NH_3$ were only slightly soluble. The compounds contain only one ammonia molecule per one acetate group, or per two acetate groups in the case of the slightly soluble Ca, and Sc compounds. The thermographical analyses and infrared absorption spectra of Be, Mg, Ca, Al, Sc, and Y acetates are discussed in detail and models of molecular structure and chemical bonds of the compounds are illustrated and analyzed. (R.V.J.)

40508 ACID DISSOCIATION CONSTANTS OF RARE EARTH GLUCONATES. Kostromina, N. A. Zh. Neorgan. Khim., 10: 1369-73(June 1965). (In Russian).

Potentiometric alkali titration of $MCl_3-HGH_4-H_2O$ (where M = La, Pr, Nd, Sm, Eu, Gd, Tb, Dy, Ho, Er, Yb, Lu, and Y and HGH_4 is gluconic acid) was carried out at 5×10^{-3} mole/l MCl_3 and HGH_4, 0.2 and ~0.025 ion forces, and 25°C. Equilibrium constants for MGH_2^{2+} complex formation were calculated at ion forces of 0.2 and ~0.025. The constants obtained were recalculated at zero ion force, and the results showed that the constants at zero force and at the various other ion forces are the same. (R.V.J.)

40509 RARE EARTH PERCHLORATES. Bel'kova, M. M.; Alekseenko, L. A. (Tomsk State Univ., USSR). Zh. Neorgan. Khim., 10: 1374-8(June 1965). (In Russian).

The thermal stability of rare earth perchlorates was studied in order to find the relation between the cation radius and the crystalline lattice. A stage dehydration of La, Nd, Dy, Yb, and Lu perchlorate crystal hydrates was observed and it was found that MeOCl oxychlorides (Me is rare earth except CeOCl, which decomposes into dioxide) formed the precipitate from decomposed perchlorates at 500°C. The reduced temperature of the initial La, Nd, Sm, Dy, Ho, Er, Yb, and Lu decomposition was the result of increased cation polarization effect related to its diminished radius. The higher decomposition temperature for aged La, Nd, and Sm perchlorates was due to the ordering of the crystalline lattice. (R.V.J.)

40510 COMPLEX COMPOUNDS OF CERIUM(III) AND EUROPIUM(III) WITH TARTARIC ACID. Stepanov, A. V.; Shvedov, V. P.; Rozhnov, A. P. Zh. Neorgan. Khim., 10: 1379-87(June 1965). (In Russian).

Electromigration and potentiometric studies showed that the composition of Ce(III) and Eu(III) complexes in tartaric acid solutions depends not only on the concentration of the additive but also on the general concentration of the metal in the solution. It was also shown that with the concentration of one of the rare earth metals $> 10^{-6}$ mole both cerium and europium are capable of forming mixed binuclear complexes, which prevent electrophoretic separation of these metals. (R.V.J.)

40511 THERMAL PROPERTIES OF BINARY SODIUM SULFATES OF CERTAIN CERIUM SUB-GROUP RARE EARTHS. Zaitseva, L. L.; Konarev, M. I.; Kruglov, A. A.; Cherstvenkova, E. P.; Yaroshinskii, V. I. Zh. Neorgan. Khim., 10: 1441-8(June 1965). (In Russian).

Thermographic, thermogravimetric, and x-ray diffraction analyses of binary La, Ce, Pr, Nd, Sm, and Gd sodium sulfates were carried out at 20 to 1100°C. It was observed that dehydration processes for binary lanthanum and cerium sodium sulfates passed through intermediate phases while binary Pr, Nd, Sm, and Gd sodium sulfates did not form any intermediate phases. Anhydrous lanthanum sodium sulfate is isostructural with anhydrous cerium sodium sulfate. Data are given on the x-ray characteristics of the anhydrous salts: $Pr_2(SO_4)_3 \cdot Na_2SO_4$; $Nd_2(SO_4)_3 \cdot Na_2SO_4$; $Sm_2(SO_4)_3 \cdot Na_2SO_4$; $Gd_2(SO_4)_3 \cdot Na_2SO_4$; $La_2(SO_4)_3 \cdot Na_2SO_4$; and $Ce_2(SO_4)_3 \cdot Na_2SO_4$. The disintegration temperature of anhydrous binary cerium sodium sulfate was found at 750 to 1100°C and that of the rest of the rare earth sodium sulfates at 1100°C. Stability constants were found for crystal hydrates and anhydrous binary sodium sulfates of the cerium subgroup rare earths. (R.V.J.)

40512 SYSTEMS OF FLUORIDES OF SODIUM, POTASSIUM, AND SCANDIUM. Babaeva, E. P.; Bukhalova, G. A. (Rostov Construction Inst., USSR). Zh. Neorgan. Khim., 10: 1455-8(June 1965). (In Russian).

Investigations of $NaF-ScF_3$ and $KF-ScF_3$ systems revealed the existence of sodium and potassium hexafluoroscandiates with a maximum on the melt diagram of 894°C for Na_3ScF_6 and 1170°C for K_3ScF_6. The ternery $NaF-KF-ScF_3$ system has four crystallization fields corresponding to the components and the solid solution of the sodium and potassium hexafluroscandiates. The triple eutectics correspond to 5% ScF_3, 35% NaF, and 60% KF at 674°C. (R.V.J.)

40513 RARE EARTH COMPLEXES WITH SULFOSALICYLIC ACID IN AQUEOUS SOLUTIONS. Poluektov, N. S.; Meshkova, S. B. (Inst. of General and Inorganic Chemistry, Academy of Sciences, Ukrainian SSR). Zh. Neorgan. Khim., 10: 1588-92(July 1965). (In Russian).

Spectrophotometric measurements of complexes of the rare earth elements with sulfosalicylic acid were made. It was established that in the pH range from 5.6 to 10 complex compounds were formed with a ratio of metal to addend of 1:1. From calculations of the results of potentiometric titrations of mixtures of rare earth salts and sulfosalicylic acid it could be assumed that the formula of the complex anion was $[Me(OH)SSal]^-$. The apparent formation constants increased with increasing atomic number of the elements. (tr-auth)

40514 COMPLEX COMPOUNDS OF RARE EARTHS WITH 1,10-PHENANTHROLINE. Lobanov, N. I.; Smirnova, V. A. Zh. Neorgan. Khim., 10: 1593-7(July 1965). (In Russian).

A series of previously unknown complex compounds of 1,10-phenanthroline with chlorides of the rare earth elements was prepared. The compounds prepared were: $LaCl_3 \cdot 2phen \cdot H_2O$, $CeCl_3 \cdot 2phen \cdot 2phen \cdot 2.5H_2O$, $CeCl_3 \cdot 2phen \cdot 6H_2O$, $PrCl_3 \cdot 2phen \cdot 2H_2O$, $NdCl_3 \cdot 2phen \cdot 6.5H_2O$, $NdCl_3 \cdot 2phen \cdot 2H_2O$, $SmCl_3 \cdot 2phen \cdot 4H_2O$, $EuCl_3 \cdot 2.5H_2O$, $GdCl_3 \cdot 2phen \cdot 3H_2O$, $TbCl_3 \cdot 2phen \cdot 4.5H_2O$, $DyCl_3 \cdot 2phen \cdot 4.5H_2O$, $HoCl_3 \cdot 2phen \cdot 5H_2O$, $ErCl_3 \cdot 2phen \cdot 6H_2O$, $TuCl_3 \cdot 2phen \cdot 5H_2O$, $YbCl_3 \cdot 2phen \cdot 6H_2O$, and $LuCl_3 \cdot 2phen \cdot 6H_2O$, where phen = 1,10-phenanthroline. Measurements of the electron conductivity indicated the presence in the solution of tetravalent ions. The absorption spectra in the ultraviolet and visible region were measured and indicated the formation of complex compounds. (tr-auth)

40515 REACTIONS OF LANTHANUM AND YTTRIUM OXIDES WITH FERRIC OXIDE. Rubinchik, Ya. S.; Pavlyuchenko, M. M.; Tsybul'ko, I. A.; Leitsina, V. G. (Inst. of General and Inorganic Chemistry, Academy of Sciences, Belorussian SSR). Zh. Neorgan. Khim., 10: 1663-7(July 1965). (In Russian).

The reactions of yttrium and La oxides with Fe_2O_3 were investigated in the temperature interval from 700 to 1400°C using x-ray, chemical, and magnetic analyses and measurement of the absorption spectra. The phase diagram of the reaction products was established in the temperature and time interval studied. A kinetic analysis of the experimental data of the reaction is reported. (tr-auth)

40516 VAPOR PHASE COMPLEXING OF ERBIUM TRICHLORIDE–POTASSIUM CHLORIDE. Novikov, G. I.; Gavryuchenkov, F. G. Zh. Neorgan. Khim., 10: 1668-74 (July 1965). (In Russian).

Data on the volatilization and vapor stability of complex forms of $KErCl_4$ in the $KCl-ErCl_3$ system were produced in the temperature interval from 800 to 1200°C. From the experimental data the thermodynamic characteristics of the equilibrium $KErCl_4 \rightleftharpoons KCl + ErCl_3$ with $\Delta F_T^0 = 59{,}000 - T \times 32$ and of the hypothetical sublimation process $KErCl_4 \rightleftharpoons KErCl_4$ with $\Delta F_T^0 = 57{,}000 - T \times 41$ was calculated. On the basis of the present and previous experimental data, it was concluded that in the systems $KCl-LnCl_3$ (where Ln = the rare earth elements) the formation of stable complex compounds could be observed. The compound $KLnCl_4$ did not exist in crystal state and evaporates from its melts, during which its volume in the vapor increased in the series La–Lu. (tr-auth)

40517 SYSTEM $SmCl_3$–NaCl–KCl. Korshunov, B. G.; Drobot, D. V.; Petrov, K. I.; Bukhtyarov, V. V.; Rubtsov, M. V. (Moscow Inst. of Fine Chemical Tech.). Zh. Neorgan. Khim., 10: 1675-80(July 1965). (In Russian).

The fusion diagram of the system was constructed and the conversion below the liquidus surface was noted. The boundary limits of the crystal phase were determined. The formation of the γ phase, the composition of which can be indicated by the formula $KNa_3Sm_2Cl_{10}$, was observed in the system. The fusion temperature of the γ phase was 478°C. The electron absorption spectra of $SmCl_3$, of the γ phase, and of the phase generated in the two systems $SmCl_3-NaCl$ and $SmCl_3-KCl$ were obtained. The comparison of the spectra established the individuality of the γ phase. X-ray analysis of the individual chlorides and chemical compounds produced in the systems studied was used for the purpose of identification of the phase. Assumptions on the possibilities for formation of phases were made on the basis of three components in systems formed by other rare earth chlorides (such as Sm) with chlorides of sodium and polonium. (tr-auth)

40518 SYNTHESIS OF LANTHANUM SILICATES FROM AQUEOUS SOLUTIONS. Permyakova, T. V.; Lileev, I. S. Zh. Neorgan. Khim., 10: 1695-1700(July 1965). (In Russian).

The reaction between solutions of La sulfate and solutions of the metasilicate, disilicate, and orthosilicate of sodium was investigated by methods of solubility, potentiometric titration, pH measurement, solution equilibrium, and volume of the precipitate. It was shown that in all of the systems exchange reactions occurred with the formation of La silicates, containing in their lattice silicate anions corresponding to the introduction of the sodium silicate. In all three systems up to the ratio $Si^{4+}:La^{3+}$, La hydroxide is precipitated. The greatest quantity of La hydroxide appeared during the reaction with sodium orthosilicate as the most alkali of the compounds and the least amount during reactions with sodium disilicate. The thermal stability of the La silicates formed decreased in the series: orthosilicate > metasilicate > disilicate. La disilicate was formed only in an amorphous gel form; on crystallization it immediately decomposed. La metasilicate in the crystalline form of the compound existed only in the narrow temperature interval from 850 to 950°C. La orthosilicate appeared to be a stable compound. (tr-auth)

40519 SOLUBILITY IN THE $Ce(NO_3)_3-LiNO_3-H_2O$ SYSTEM AT 10, 20, AND 30 deg C. Bogdanovskaya, R. L.; Sheveleva, A. D.; Zhuravlev, E. F. (Perm State Univ., USSR). Zh. Neorgan. Khim., 10: 1713-15(July 1965). (In Russian).

The solubility in the system $Ce(NO_3)_3-LiNO_3-H_2O$ was investigated at temperatures of 10, 20, and 30°C. It was established that the system $Ce(NO_3)_3-LiNO_3-H_2O$ in the temperature interval investigated corresponds to a simple eutonic type. (tr-auth)

40520 SOLUBILITY OF SCANDIUM CHLORIDE IN HYDROCHLORIC ACID AT 25 deg C. Samodelov, A. P. Zh. Neorgan. Khim., 10: 1735-7(July 1965). (In Russian).

The solubility of scandium chloride in solutions of hydrochloric acid was investigated at 25°C for various concentrations of scandium chloride and hydrochloric acid. The results are tabulated. (J.S.R.)

40521 ENTHALPY OF THE γ-UO_3 REACTION WITH HYDROFLUORIC ACID AND ENTHALPY OF FORMATION OF γ-UO_3. Vidavskii, L. M.; Byakhova, N. I.; Ippolitova, E. A. (Moscow State Univ.). Zh. Neorgan. Khim., 10: 1746-7(July 1965). (In Russian).

The enthalpy of the reaction of γ-UO_3 with hydrofluoric acid solutions was measured as $\Delta H_{298} = -24.56 \pm 0.11$ kcal/mol. The normal enthalpy of formation of γ-UO_3 at 298.15°K was calculated as $\Delta H_f^0 = -295.80 \pm 0.45$ kcal/mol. (tr-auth)

40522 THEORETICAL INVESTIGATION OF THE STEREOCHEMISTRY OF COMPLEX COMPOUNDS WITH F-ELECTRONS. II. ANALYSIS OF THE MOST STABLE CONFIGURATION OF $Th(NCS)_8^{4-}$ ION BY METHOD OF

MAXIMUM OVERLAPPING. Volkov, V. M.; Dyatkina, M. E. (Kurnakov Inst. of General and Inorganic Chemistry, Academy of Sciences, USSR). Zh. Strukt. Khim., 5: 611-19(July-Aug. 1964). (In Russian).

A stable configuration of a complex $Th(NCS)_8^{4-}$ ion in π-bond approximation of Th–N was found using a method of maximum overlapping. The tetragonal antiprism (a twisted cube of D_{4d} symmetry) proved to be the most stable among the examined cube, tetragonal antiprism, and dodecahedronal configurations. (tr-auth)

40523 VOLUME-TEMPERATURE RELATIONSHIPS OF SOME RARE-EARTH CHLORIDE SOLUTIONS (thesis). Gildseth, Wayne Merlyn. Ames, Iowa, Iowa State Univ., 1964. 187p.

A dilatometric apparatus was constructed which was capable of measuring the change in density of a liquid or solution with an accuracy of about two parts per million over the temperature range of 20 to 80° C. The variations of the volumes of the dilatometers with temperature were determined using mercury as a standard. Densities of water and aqueous lanthanum chloride and neodymium chloride solutions were determined at five degree temperature intervals from 20 to 80° C. Twelve lanthanum chloride solutions ranging in concentration from 0.6362 to 3.3907 molal and eleven neodymium chloride solutions ranging in concentration from 0.1050 to 3.4160 molal were investigated. These data were used to calculate coefficients of thermal expansion of water and the rare-earth chloride solutions. Apparent and partial molal volumes of the salt, apparent and partial molal expansibilities of the salt, and partial molal volumes and expansibilities of water in these rare-earth chloride solutions were also calculated. Empirical least square equations were computed with the use of an IBM-7074 computer to represent the above properties versus temperature and versus concentration. From a study of the values of the above properties, it was concluded that the water molecules in the neighborhood of a neodymium ion were more tightly bound than those about a lanthanum ion. In addition, the results obtained were in agreement with the formation of a pseudo salt-like lattice of the ions in the most concentrated solutions. (Dissertation Abstr.)

40524 RARE EARTH BORIDES: THE SAMARIUM–BORON SYSTEM (thesis). Sturgeon, George Dennis. East Lansing, Mich., Michigan State Univ., 1964. 97p.

New preparations of rare earth borides reported include thulium diboride and pure samarium tetraboride. However, attempts to obtain hexaborides of erbium, thulium, lutetium and scandium, all of which have been reported elsewhere, were unsuccessful. On the basis of x-ray data which had been erroneously interpreted, it was concluded that the reports of the above-mentioned hexaborides are unreliable. The existence of a minimum boron-boron single bond distance of 1.69 Å in borides is proposed. No boron compound with similar bonding is known to have a smaller boron-boron distance. The fashioning of a molybdenum Knudsen effusion cell containing a zirconium diboride cup supported on tungsten pins allowed the measurement of the free energy change for the reaction $3SmB_{6(s)} \rightarrow 2SmB_{8(s)} + Sm_{(g)}$ by determining the equilibrium vapor pressure of samarium above the two solid phases. The pressures measured fell between 10^{-10} and 10^{-5} atmospheres. The trace amounts of samarium collected from the effusate of the cell orifice were quantitatively analyzed using neutron activation analysis. An effectively negligible heat capacity change for the reaction above made it possible to determine the standard enthalpy and entropy for the reaction from the slope and intercept of the least squares plot of the logarithm of pressure versus reciprocal temperature. The value for the standard enthalpy change calculated by the Third Law method essentially corroborates the value obtained by the Second Law method: $\Delta H^\circ_{298} = 91.32 \pm 3.32$ kilocalories (Second Law), $\Delta H^\circ_{298} = 93.93 \pm 2.0$ kilocalories (Third Law), and $S^\circ_{298} = 24.62 \pm 1.95$ calories (Second Law). (Dissertation Abstr.)

40525 SOME NEW TERNARY OXIDES OF RHENIUM (thesis). Longo, John M. Storrs, Conn., Univ. of Connecticut, 1964. 136p.

Many new ternary oxides of rhenium were prepared and characterized. Preparation was by high temperature solid state reactions in air or under vacuum conditions. Characterization was by x-ray diffraction, chemical analysis, and density measurements. Most of the new compounds prepared had structures which are based on the close packing of AO_3 layers (A = Ba, Sr, Ca) with the octahedral holes between the layers being filled by rhenium or lower valent cations. In some cases, a fraction of the available octahedral positions are left vacant. Many of the compounds prepared have the ordered perovskite structure with the following general formula: A_2BReO_6. When B is divalent, rhenium is +6; when B is trivalent, rhenium is +5. The compounds with B = Fe, Mn, or Cr were magnetic. Another series of compounds had the general formula $A_4Re_2BO_{12}$ (A = Ba or Sr; B = divalent cation). The unit cell repeated in twelve close packed AO_3 layers with the following sequence: hhcchhcchhcc. A cubic layer is represented by c while an h represents an hexagonal layer. One-quarter of the octahedral positions are left vacant. A series of compounds having the same general formula, $A_4Re_2BO_{12}$, was also prepared. In this series the B position contained a divalent cation with an ionic radius of one angstrom or larger. The structure of this series appeared to be related to an eight-layer close packed unit cell. The sequence of layers was ccchcccch. Single crystals could be prepared. Two compounds, $Ba_3Fe_2ReO_9$ and $Ba_3Cr_2ReO_9$, were prepared and found to have the hexagonal $BaTiO_3$ structure. The compound $Cd_2Re_2O_7$ was prepared and found to have the pyrochlore structure. An oxide of lanthanum and rhenium was also prepared. In both cases, single crystals could be prepared. (Dissertation Abstr.)

40526 THE ATOMIC ABSORPTION SPECTRA OF THE LANTHANIDE ELEMENTS (thesis). Mossotti, Victor Giovoni. Ames, Iowa, Iowa State Univ., 1964. 140p.

It is shown that the fuel-rich oxygen-acetylene flame provides a favorable environment for the existence of free atoms in lanthanide elements. Through this expedient more than 1000 rare earth absorption lines were observed, and their wavelengths and relative strengths estimated. These wavelengths provide a convenient starting point in the analysis of atomic spectral structure. Inquiry was made into the nature of the flame environment. A reasonable mechanistic scheme was proposed to account for the observed enhancements in atomic emission and absorption spectra of those elements that have a strong predilection to form stable monoxide molecules in stoichiometric flames. This mechanism was judged in the light of existing data on hydrocarbon flames. A double-beam atomic absorption spectrometer was assembled from the electronic and optical components of an infrared spectrophotometer. This instrument was used to evaluate the analytical potentialities of the atomic absorption spectra of the lanthanide elements and to assess the usefulness of a spectral continuum as a spectroscopic light source for atomic absorption. The continuous source in conjunction with low dispersion and photoelectric detection have furnished analytically useful atomic absorption spectra of many of the lanthanides and a host of common elements. (Dissertation Abstr.)

40527 I. THE ABSOLUTE DIELECTRIC CONSTANTS OF LIGHT AND HEAVY WATER BETWEEN 0 AND 40 deg C. II. THE TRANSFERENCE NUMBERS OF LITHIUM CHLORIDE AND CADMIUM CHLORIDE IN ANHYDROUS METHANOL AT 25 deg C (thesis). Vidulich, George Anthony. Providence, Brown Univ., 1964. 115p.

I. An all glass and platinum cell for the absolute measurement of dielectric constants was designed and constructed. The cell is completely shielded and equipped with a guard electrode. The cell can be constructed with cell constants ranging from 2 to 26 pf or possibly higher. The absolute dielectric constants of H_2O and D_2O at various temperatures are reported and compared to various previous investigations. The use of the cell for the measure-

ment of conductances of electrolytes in benzene and for determining dipole moments is also described. II. The transference numbers and equivalent conductance for LiCl and $CdCl_2$ in anhydrous methanol are reported at 25°C. The moving boundary method was used to measure the transference numbers and the boundary movement was followed by means of the probe detector developed in this laboratory. Conductances were carried out in a conductance cell fitted with guarded electrodes. Transference numbers for $CdCl_2$ were obtained by using the Kohlrausch regulating function and the concentration of the following $CdCl_2$ solutions obtained by means of probe electrodes. The transference numbers of $CdCl_2$ were influenced to a considerable extent by the amount of complexing present. It is shown that in the measurable range above 5×10^{-4}N very little if any Cd^{2+} is present. Approximate limiting transference numbers for Cd^{2+} and $CdCl^{+}$ were found to be 0.41 and 0.38, respectively. The electrophoretic contribution to conductance was calculated from the concentration dependence of the transference numbers for LiCl in methanol. The electrophoretic effect was found to agree with the Fuoss-Onsager second approximation. It was concluded that the Fuoss-Onsager conductance theory was applicable to solutions of dielectric constant 30 or higher. (Dissertation Abstr.)

40528 ELECTRONIC SHIELDING BY CLOSED SHELLS IN THULIUM COMPOUNDS (thesis). Poindexter, John Marlan. Pasadena, Calif., California Inst. of Tech., 1964. 128p.

The Moessbauer effect was used to investigate electronic shielding by closed electron shells in salts of trivalent thulium, by measuring the temperature dependence of the nuclear quadrupole splitting of the 8.42 kev gamma transition in ^{169}Tm. The nuclear quadrupole interaction was studied for Tm^{3+} ions in thulium ethyl sulfate, thulium oxide, and thulium trifluoride within a temperature range from 0.6 to 1970°K. Interpretation of the experimental data in terms of the contributions of distorted closed electron shells to the quadrupole interaction yields values for electronic shielding factors. The results lead to amounts of 10% or less for the atomic Sternheimer factor R_Q. The experiments also revealed substantial shielding of the 4f electrons from the crystal electric field, expressed by the shielding factor σ_2. Values of 250 and 128 were obtained for the ratio $(1 - \gamma_\infty)/(1 - \sigma_2)$ for thulium ethyl sulfate and thulium oxide respectively, where γ_∞ is the lattice Sternheimer factor. (Dissertation Abstr.)

40529 KINETICS OF HYDROFLUORINATION OF ZIRCONIUM OXIDE IN A FLUIDIZED BED (thesis). Slotnick, Herbert. Storrs, Conn., Univ. of Connecticut, 1964. 108p.

The kinetics of the hydrofluorination of coarse granular zirconium oxide in a fluidized bed were correlated with a rate equation based on a theoretical reaction model. It is assumed that, as the surface layers of the reacting particles become converted to oxyfluoride and fluoride, gaseous hydrogen fluoride diffuses through the porous product to maintain a first order reaction at the interior fluoride-oxide interface. Reaction rate depends upon area of transmission, concentration of hydrogen fluoride, and two resistances in series,—chemical and diffusional. Tests were conducted in a batch fluidized bed at a flow rate of 1.4 standard liters per minute. Nitrogen was used as an inert carrier gas and contained 41% hydrogen fluoride in tests made at 650°C (1200°F) and 64% or 79% hydrogen fluoride at 627°C (1160°F). (Dissertation Abstr.)

40530 PHYSICAL METHODS FOR DETERMINING MOLECULAR GEOMETRY. Brey, Wallace S. Jr. Selected Topics in Modern Chemistry. New York, Reinhold Publishing Corp., 1965. 124p. $1.95.

Physical methods available for establishing qualitatively and quantitatively the geometry of molecules are presented. These include: electromagnetic radiation; diffraction methods; electrical polarization in molecules; quantum theory, wave mechanics, and the Boltzmann distribution; rotational spectra of molecules; and molecular vibrations. (P.C.H.)

40531 SOLUTION CHEMISTRY. Krumholz, P. (Orquima S.A., Sao Paulo, Brazil). pp 110-38 of Progress in the Science and Technology of the Rare Earths. Vol. I. New York, The Macmillan Co., 1964.

In a review of the solution chemistry of rare earths, attention is paid to the causes of the small differences in the properties of the individual rare earth tripositive ions. Structural features of the ions and their compounds are considered. Solubilities, coordination chemistry, valency changes, and catalytic properties are also discussed. (D.L.C.)

40532 RECENT SOVIET RESEARCH ON THE CHEMISTRY OF RARE EARTH COMPLEXES. Ryabchikov, D. I.; Terentyeva, E. A. (Academy of Science, Moscow). pp 139-51 of Progress in the Science and Technology of the Rare Earths. Vol. I. New York, The Macmillan Co., 1964.

A review is presented of Soviet work on the complexes of rare earths with organic and inorganic addenda. It is concluded that the most stable rare earth complexes, are those with organic addenda; in these complexes, the rare earth element is bonded through the oxygen atom of carboxyl, carbonyl, and hydroxyl groups. (D.L.C.)

40533 CRYSTAL CHEMISTRY OF RARE EARTH OXIDES. Brauer, G. (Universitat, Freiburg i. B.). pp 152-66 of Progress in the Science and Technology of the Rare Earths. Vol. I. New York, The Macmillan Co., 1964. (In German).

A review is presented of the structure and structure-related properties (stability, heat of formation, phase relations, etc.) of sesquioxides, higher oxides, and lower oxides of the rare earths. (D.L.C.)

40534 PHASE EQUILIBRIA STUDIES IN MIXED SYSTEMS OF RARE EARTH AND OTHER OXIDES. Roth, R. S. (National Bureau of Standards, Washington, D. C.). pp 167-202 of Progress in the Science and Technology of the Rare Earths. Vol. I. New York, The Macmillan Co., 1964.

A summary is presented of the work done on mixtures of rare earth oxides with other oxides, and the areas where data are still lacking are pointed out. The problem of accurate measurement of high melting temperatures is considered. (D.L.C.)

40535 CRYSTAL CHEMISTRY OF RARE EARTH SESQUIOXIDES, ALUMINATES AND SILICATES. Warshaw, Israel; Roy, Rustum (National Science Foundation, Washington, D. C. and Pennsylvania State Univ., University Park). pp 203-21 of Progress in the Science and Technology of the Rare Earths. Vol. I. New York, The Macmillan Co., 1964.

A review is presented of the crystal chemistry of rare earth sesquioxides, aluminates, and silicates from the viewpoint of the effects of small changes in the cation radius. It is concluded that the rare earths should be divided into three groups: the large rare earths (La, Ce, Pr, and Nd), the small rare earths (Er, Tm, Yb, and Lu), and the intermediate rare earths exhibiting variable behavior (Sm, Eu, Gd, Tb, Dy, Y, and Ho). (D.L.C.)

40536 THE ROLE OF GRAIN BOUNDARIES IN THE PLASTIC DEFORMATION OF CALCIUM FLUORIDE. Pratt, P. L.; Roy, C.; Evans, A. G. (Imperial Coll. of Science and Tech., London). 18p. (CONF-641116-8). Gmelin, AED-CONF-64-224-11.

From Conference on the Role of Grain Boundaries and Surfaces in Ceramics, Raleigh, N. C.

Experimental evidence on the plastic deformation of single crystals of calcium fluoride was used to predict the behavior of polycrystalline calcium fluoride. The predictions are compared with experiment, and the role of grain boundaries in determining the brittleness at low temperatures is emphasized. (auth)

40537 ISOTOPIC EXCHANGE REACTIONS OF DIFLUORAMINE WITH DEUTERIUM OXIDE AND TRIFLU-

OROACETIC ACID. Becker, Warren E.; Impastato, Fred J. (Ethyl Corp., Baton Rouge, La.). 17p. (CONF-650401-12). Gmelin, AED-CONF-65-041-19.

From American Chemical Society, Detroit.

The isotopic exchange reactions of HNF_2 with D_2O and with CF_3COOD were investigated in tetrahydrofuran-d8 solution at low temperatures using NMR techniques. The former exchange is first order with respect to HNF_2 and zero order with respect to D_2O. The latter exchange proceeds by this same path plus a second order path. Both exchange reactions were studied at several temperatures and the activation energies were determined. (auth)

40538 LIQUIDS: STRUCTURE, PROPERTIES, SOLID INTERACTIONS. Proceedings of the Symposium, General Motors Research Laboratories, Warren, Michigan, 1963. Hughel, Thomas J. (ed.). New York, Elsevier Publishing Company, 1965. 393p. $20.00. (CONF-366).

A collection of papers and discussions are presented from a symposium on the structure, properties and solid interactions of liquids. Included in the topics discussed are a volume model, structural geometry and molecular theory of liquids. Also considered are transport properties and processes, x-ray and neutron diffraction studies, neutron scattering, proton magnetic resonance studies of compounds, pre-freezing phenomena, surface tension of metals and oxide melts, dynamic nucleation, eutectic solidification, and the fusion curve. (J.F.P.)

40539 IMPROVEMENTS IN OR RELATING TO THE PURIFICATION OF GASEOUS HELIUM. Marsh, William Robert; Sach, Roger Stuart (to United Kingdom Atomic Energy Authority). British Patent 998,771. July 21, 1965. Filed June 20, 1962.

A method and apparatus are provided for the purification of gaseous He that includes the following steps: (1) the catalytic combination of gaseous O_2 and H_2, (2) passing the gas through a first molecular sieve apparatus, (3) oxidizing residual H_2 and CO to water vapor and CO_2 respectively, and (4) passing the gas through a second molecular sieve and gettering stage. The preferred process of gettering is to pass the gas into contact with lithium vapor and subsequently cooling the gas to remove traces of Li vapor. Helium gas purified by this process is suitable for gas chromatography application. (B.L.M.)

Organic Chemistry

40540 (RT/CHI(64)16) SINTESI DI ALCUNE ALCHIL BENZIL AMMINE AD ALTO PESO MOLECOLARE DEL TIPO C_6H_5–CH_2–$NH(R_1)(R_2)$. (Synthesis of Some Alkyl Benzylamines of High Molecular Weight of the Type C_6H_5–CH_2–$NH(R_1)(R_2)$). Grossi, G.; Jagodic, V. (Comitato Nazionale per l'Energia Nucleare, Rome (Italy)). July 1964. 11p. Dep. mn.

The synthesis of new high molecular weight secondary amines of the type: $C_6H_5-CH_2-NH-CH(R_1)(R_2)$ with R_1, R_2 straight chain alkyl radicals is described. Amines of this type have an interesting potential in the solvent extraction of actinides from sulfuric acid solutions. The compounds were prepared by a reductive amination of a n-alkylketone according to Leuckart. The resulting primary amine reacts with benzaldehyde yielding, after hydrogenation, the desired compound. This method is suitable up to the di-n-undecylketone. For higher ketones the Leuckart reaction has unacceptably low yields. In these cases the primary amines were prepared by reduction of the oximic compounds. The following substances were prepared and characterized: 9-n-heptadecylamine, N-benzal-9-n-heptadecylimine, N-benzyl-9-n-heptadecylamine, 10-n-nonadecylamine, N-benzal-10-n-nonadecylimine, N-benzyl-10-n-nonadecylamine, 11-n-heneicosylamine, N-benzal-11-n-heneicosylimine, and N-benzyl-11-n-heneicosylamine. (auth)

40541 ISOTOPE EFFECTS IN ELECTRON SPIN RESONANCE: THE NEGATIVE ION OF CYCLO-OCTATETRAENE-1-d. Carrington, A.; Longuet-Higgins, H. C.; Moss, R. E.; Todd, P. F. (Cambridge Univ., Eng.). Mol. Phys., 9: 187-90(1965).

Replacement of one hydrogen atom by deuterium in the negative ion of cyclo-octatetraene, makes no significant difference to the electron spin densities at the hydrogen nuclei. This result contrasts with a recent observation that mono-deuteration produces a measurable change in the spin distribution in the benzene negative ion. The difference between the two systems is interpreted in terms of the Jahn–Teller effect. (auth)

40542 MOESSBAUER STUDIES OF INEQUIVALENT FERROUS ION SITES IN FERROUS FORMATE. Hoy, Gilbert R.; de S. Barros, F. (Carnegie Inst. of Tech., Pittsburgh). Phys. Rev., 139: 929-34(Aug. 2, 1965).

The iron ions in ferrous formate, $Fe(HCOO)_2 \cdot 2H_2O$, are located at two sites with different environments. The nearest-neighbor symmetry of the type-1 site is nearly octahedral, while the type-2 site has lower symmetry. Mössbauer experiments with a powder absorber of ferrous formate show a spectrum composed of four lines resulting from the inequality of the effective electric-field gradients at the two sites. The lines are grouped in two pairs having the same center of gravity located at the usual ferrous-ion isomer shift. The quadrupole splittings at the two sites are 2.97 mm/sec (type 2) and 0.59 mm/sec (type 1) at room temperature, and 3.36 mm/sec (type 2) and 1.48 mm/sec (type 1) at 6°K. The larger splitting was naturally assigned to the more asymmetrical site (type 2). Calculations based on the temperature dependence of the quadrupole splittings indicate that the energy separation between the ground and first excited ion orbital states corresponds to 850°K (type 2) and 250°K (type 1). The method used for the calculations is based on known properties of spherical harmonics. (auth)

40543 CHEMICAL ENHANCEMENT OF SUPERCONDUCTIVITY. McConnell, H. M.; Hoffman, B. M.; Thomas, D. D.; Gamble, F. R. (John Stauffer Lab. for Physical Chemistry, Stanford, Calif.). Proc. Natl. Acad. Sci. U. S., 54: 371-4(Aug. 1965).

Studies were made on the enhancement of superconductivity by conjugation of the free electron system of the metal with the electron system of the molecule which leads to finite amplitudes for the conduction electron eigenfunctions throughout the molecules. An experiment demonstrating the enhancement of the superconductivity of a thin vanadium film by 3,4,7,8-tetramethyl-10-phenanthroline (I) is described. (I) caused the critical current to increase from 2.2 to 2.8 ma. The critical temperature of the film was increased by 0.09°K, as defined by the increase in temperature of the helium bath necessary to reduce the critical current to its original value for the pure film. The critical temperature for the sandwich was determined to be 2.50°K. (P.C.H.)

40544 KINETIC DEUTERIUM ISOTOPE EFFECT IN THE REACTION OF 2,4-DINITROPHENYL PHENYL ETHER WITH PIPERIDINE IN BENZENE. Pietra, Francesco (Universita, Pisa, Italy). Tetrahedron Letters, No. 28, 2405-10(July 1965).

In the reactions of primary or secondary amines with nitro-activated aryl fluorides or chlorides, the change from H to D at the amino nitrogen does not affect the rate. This lack of a significant isotope effect was investigated in reactions of 2,4-dinitrophenyl phenyl ether with piperidine or N-d-piperidine in benzene, in the presence or absence of pyridine. Results for the reaction of piperidine showed that the second-order rate coefficient increases linearly with increasing amine concentration and extrapolates to zero at zero amine concentration. The rate data are fitted by a third-order equation. This kinetic order behavior does not arise from a general medium effect; thus, the reaction of the ether in benzene is piperidine catalyzed. The change from piperidine to N-d-piperidine (about 90% deuterated) slowed down the rate of reaction by a factor of 1.27, without changing the pattern of the kinetic orders. This small isotope effect was interpreted as a primary one as far as deuteration at the amino nitrogen appears to increase the

nucleophilicity of amines. The results are interpreted on the basis of the intermediate complex mechanism proposed by Bunnett. The findings refute the elaborations, whereby an intermediate (I) decomposes by a fast proton transfer to a base (B) to give a second intermediate which then loses the leaving group in a slow, uncatalyzed, step. Such a mechanism could not provide a primary isotope effect. Moreover, the isotope effect appears to arise from a rate-limiting proton transfer from the intermediate I to a base B. Thus the addition of minute amounts of methanol decreased the rate of reaction of 2,4-dinitrophenyl phenyl ether with piperidine in benzene. (TCO)

40545 THE POLAROGRAPHY AND ANALYTICAL APPLICATIONS OF 8-SUBSTITUTED QUINALDINES AND QUINALDINIC ACIDS (thesis). Turner, W. Richard. Storrs, Conn., Univ. of Connecticut, 1964. 193p.

The polarographic behavior of the following compounds was investigated: 8-hydroxyquinaldine, 8-aminoquinaldine, 8-methoxyquinaldine, 8-methylquinaldine, quinaldine, 8-chloroquinaldine, 8-nitroquinaldine, 8-hydroxyquinaldinic acid, 8-methoxyquinaldinic acid, 8-methylquinaldinic acid, and 8-nitroquinaldinic acid. In solutions of pH 7.5 to 12.0, the substituted quinaldines produced a single wave which corresponded to a single electron reduction of the quinoline ring. The half-wave potentials were pH dependent. The quinaldinic acids were reducible over the entire pH range of 2 to 12. Two principal waves were observed which were both two electron processes. One wave was found to be due to the reduction of the undissociated acid and the other due to the reduction of the anion. The half-wave potentials of the undissociated acid increased linearly with pH. The anion waves for 8-methyl- and 8-methoxyquinaldinic acid had half-wave potentials which were independent of pH. The current – pH relationship for these two compounds was logarithmic. A linear relationship was found between the Hammett sigma constants and the half-wave potentials for the 8 substituted quinaldines at pH values of 8, 9, 10, and 11; and for the 8 substituted quinaldinic acids at pH 12. All of the quinaldinic acids were screened to ascertain their ability to react with metal ions. The 8-hydroxy-derivative was found to react with a number of metal ions, among them were uranyl and thorium ions. Amperometric titrations were carried out for these two ions. The titration of thorium ions over the concentration range of 5×10^{-4} to 3×10^{-3} molar gave results that were reasonably accurate and precise. (Dissertation Abstr.)

40546 THE SYNTHESIS AND EVALUATION OF SOME 2-ARYLINDENES AND 2-ARYL-3H-BENZ[e]INDENES AS LIQUID SCINTILLATION SOLUTES (thesis). Schornick, James Leslie. Albuquerque, N. Mex., Univ. of New Mexico, 1964. 134p.

Some 2-arylindenes and 2-aryl-3H-benz[e]indenes were prepared and evaluated as liquid scintillation solutes. Treatment of the Grignard reagent of the appropriate aryl halide with 2-indanone followed by dehydration of the alcohol with 99% formic acid gave the following 2-arylindenes: 2-phenylindene, 2-p-tolylindene, 2-(1-naphthyl)-indene, 2-(2-naphthyl)indene, 2-(4-biphenylyl)indene, and 2-(p-methoxyphenyl)indene in overall yields of 25, 38, 17, 31, 16, and 4%, respectively. In the last case, p-methoxyphenyl lithium was used. Alkylation of the appropriate arylacetonitrile with 2-(chloromethyl)naphthalene using sodium amide in benzene gave: α-phenyl-2-naphthalenepropionitrile (83%); α-(1-naphthyl)-2-naphthalenepropionitrile (89%); 2,3-di(2-naphthyl)propionitrile (59%); and α-(4-biphenylyl)-2-naphthalenepropionitrile (92%). These nitriles were hydrolyzed with sulfuric acid and the acids obtained were: α-phenyl-2-naphthalenepropionic acid (75%); α-(1-naphthyl)-2-naphthalenepropionic acid (65%); 2,3-di(2-naphthyl)-propionic acid (76%); and α-(2-biphenylyl)-2-naphthalenepropionic acid (99%). These acids were converted to the acid chlorides and cyclized by treatment with aluminum chloride in benzene and the following ketones were obtained: 2,3-dihydro-2-phenyl-1H-benz[e]-inden-1-one (75%); 2,3-dihydro-2-(1-naphthyl)-1H-benz[e]-inden-1-one (84%); 2,3-dihydro-2-(2-naphthyl)-1H-benz[e]-inden-1-one (65%); and 2-(4-biphenylyl)-1H-benz[e]inden-1-one (74%). These ketones were reduced with lithium aluminum hydride in near quantitative yields to the 2-aryl-2,3-dihydro-1H-benz[e]inden-1-ols, which were subsequently dehydrated to the 2-aryl-3H-benz[e]indenes in good yield. The 2-arylindenes and the 2-aryl-3H-benz[e]indenes were evaluated as liquid scintillation solutes and were found to be good to excellent scintillators. Ultraviolet and fluorescence spectral measurements were taken of these compounds. (Dissertation Abstr.)

Radiation Chemistry

See also BIOLOGY AND MEDICINE — Radiation Effects.

Refer also to abstract 40916.

40547 (AGN-8137(Vol.I)) FISSIOCHEMICAL PROCESS DEVELOPMENT PROGRAM. VOLUME I. APPLIED RESEARCH. Final Report, March 1965. Kahn, S.; Standerfer, F. R. (Division of Reactor Development and Technology (AEC), Washington, D. C.). Contract AT(04-3)-368. 143p. Dep. mn; CFSTI, $4.00 cy, $1.00 mn.

Results of theoretical and experimental studies to develop broader knowledge of basic fissiochemical relationships are reported. In fissiochemistry processes, fission product energy is deposited along recoil tracks, splitting reactant molecules into highly energetic ions and radicals which recombine to form new products. The goals of the program described were to improve means of measuring and predicting the amount of energy per fission deposited in the reactant, to determine effect of significant variables on yield, and to undertake preliminary determination of the economic potentials of various systems. Energy spectra from fission products escaping from fully enriched UO_2 thin films were measured. A reasonably accurate predictive computer code was developed which, with the introduction of geometry alteration terms in the predictive equation, should allow prediction of energy deposition from sources of any configuration. Effects of variables on hydrazine yield from liquid ammonia reactant were studied. Hydrazine yield was found to vary with temperature and hydrazine concentration and to be directly related to fission fragment-to-gamma deposited energy ratio. Gas overpressure was found to have a second order effect on yield. Preliminary evaluation of the economic potential of two systems, hydrogen peroxide and fluorine, indicate that the former is not competitive but that the latter may merit further study. (auth)

40548 (BNWL-82) THE FORMATION OF CHEMICALS BY REACTOR IRRADIATION OF OXYGENATED WATER AND AMMONIATED WATER. Winegardner, W. K. (Battelle-Northwest, Richland, Wash. Pacific Northwest Lab.). July 1965. Contract AT(45-1)-1830. 19p. Dep. mn; CFSTI $2.00 cy, $0.50 mn.

Tests were conducted with two experimental facilities in the Hanford production reactors to gain insight into the formation of chemicals by reactor radiation. The tests consisted of the exposure of flowing dilute aqueous solutions to reactor radiation, primarily gamma rays and fast neutrons. The formations of hydrazine in ammoniated water and hydrogen peroxide in oxygenated water were studied. The maximum hydrazine concentration observed, 450 ppb, was associated with an 850 ppm ammonia concentration, the highest reactant stream concentration used. The maximum concentration of hydrogen peroxide observed, 300 ppm, resulted from the addition of oxygen to demineralized water. (auth)

40549 (COO-1032-1) RECOMBINATION OF HYDROGEN AND OXYGEN IN THE PRESENCE OF WATER VAPOR UNDER THE INFLUENCE OF RADIATION. Final Report. Benjamin, B. M.; Isbin, H. S. (Minnesota Univ., Minneapolis Dept. of Chemical Engineering). July 1965. Contract AT(11-1)-1032. 36p. Dep. mn; CFSTI, $2.00 cy, $0.50 mn.

The gamma-ray-induced recombination of H_2 and O_2 in the presence of H_2O vapor was carried out using a cesium-137 source at water vapor pressures around atmospheric and high temperatures up to 400°F. The initial yields $G^0(H_2O)$ range from 3.0 to 6.0, and two empirical rate expressions were derived. The recombination rate was found to be first order in the H_2 concentration, increases with O_2 concentration but at a decreasing rate, and is linear with H_2O vapor concentration up to 0.3 g/l (above it, the rate becomes almost constant). The rate increases with radiation intensity but at a decreasing rate. The rate is independent of temperature up to 280°F, but increases at the higher temperatures. (D.L.C.)

40550 (IS-T-27) DEACTIVATION OF REACTION COMPLEXES IN THE RECOIL CHEMISTRY OF ^{11}C (thesis). Mesich, Frank Gerald (Ames Lab., Iowa State Univ. of Science and Tech.). July 1965. Contract W-7405-eng-82. 96p. Dep. mn; CFSTI, $3.00 cy, $0.75 mn.

The nature and yields of products resulting from the reactions of recoil carbon-11 atoms in liquid hydrocarbons were studied. Compounds irradiated include n-pentane, isopentane, 1-pentene, cyclopentane, cyclopentene, and benzene. Analyses were carried out using high temperature, high flow rate radio-gas chromatography. The effects of radiation dose on the yields of products containing more than two carbon atoms were studied. It was found that the contributions to the yields from radiation damage were minimal. The total product yields determined in three systems, n-pentane, isopentane, and 1-pentene, approached 100%. Lower recoveries in the three cyclic systems indicate that appreciable amounts of the activity, up to 75%, are present in the form of products containing two or more carbon atoms than the parent. The product distributions are discussed in terms of the reactions of ^{11}C, ^{11}CH, and $^{11}CH_2$ radicals. The primary reaction mechanism involves the insertion of a ^{11}C, ^{11}CH, or $^{11}CH_2$ radical into a carbon-hydrogen bond or a carbon-carbon double bond forming an excited reaction complex. The final carbon-11 containing product is determined by the nature and the energy of the inserting radical. If sufficient energy is present, the reaction complex will fragment, forming a number of different radicals which then lead to the formation of products containing fewer carbon atoms than the parent. Insertion at a lower energy may lead to stabilization of the reaction complex forming products with one more carbon atom than the parent. Examination of the nature of the products formed indicates that the ^{11}C and ^{11}CH radicals probably occur at energies above the thermal range. The products found which are due to the reactions of the $^{11}CH_2$ radicals are indistinguishable from similar products formed from the reactions of low energy methylene radicals. The product distributions are discussed in the light of reaction cross sections for the ^{11}C, ^{11}CH, and $^{11}CH_2$ radicals. (auth)

40551 (KFK-293) SOLVATISIERTE ELEKTRONEN IN γ-BESTRAHLTEN, EINGEFRORENEN LOESUNGEN. (Solvated Electrons in γ-Irradiated, Frozen Solutions). Eiben, Klaus (Kernforschungszentrum, Karlsruhe (West Germany). Laboratorium fuer Strahlenchemie). Dec. 1964. 81p. Dep. mn.

The direct detection of the occurrence of hydrated electrons in the γ radiolysis of water and aqueous solutions was studied and the optical and paramagnetic properties of these reducing radical species were investigated. Alkali solutions frozen to 77°K were colored blue by γ irradiation. Simultaneously with the occurrence of the blue color, an ESR singlet signal was also detected. The place of the absorption maximum and the form of the ESR signals are dependent on the alkali hydroxide used. The concentration in paramagnetic centers and the color intensity per absorbed dose are directly proportional to the irradiation dose, but both are dependent upon the hydroxide concentration. The site of the absorption maximum is dependent on the solution medium in alkali solutions of heavy water and alcohols. It is displaced with respect to light water. At higher temperatures, both the light absorption and the ESR singlet decrease more from the melting point of the stabilizing matrix. The time pattern of this process corresponds to a pseudomonomolecular reaction. The addition of electron acceptors in high concentrations reduces the occurrence of the blue color in alkali ice. With the addition of electron acceptors at low concentrations, the blue coloration occurs in γ radiolysis. The simultaneous occurrence of a blue color and an ESR singlet signal was observed also in condensates of alkali metal vapors and water or alcohols at 77°K. From the experimental results, it was concluded that solvated electrons are formed in the γ radiolysis of frozen solutions. The hydrated electrons produced by radiation chemistry are chemically held in the solid solutions at low temperature in an arrangement of water molecules which does not vary from that postulated for liquid water by Platzman. (J.S.R.)

40552 (NP-15287) ASYMPTOTIC THEORY OF A PHOTOIONIZATION CHAMBER. [PART] I. Cohen, Ira M. (Brown Univ., Providence, R. I. Div. of Engineering). Apr. 1965. Contract Nonr 562(35). 40p.

A photoionization chamber consists of two parallel plates between which a test gas is photoionized. The charged particles thus produced then diffuse to the plates where they recombine. This process is analyzed in detail when the fraction of ionization is very low and the mean free path for charged-neutral encounters is very small compared to the chamber width. Particular attention is paid to the physically important limit of sufficiently large charged particle densities to make the Debye length small compared with any macroscopic dimension. In this limit the plasma is quasineutral in the body of the chamber. Near the walls, however, quasineutrality breaks down and a new scaling of the variables is necessary to account for the changed orders of magnitude of the properties in the sheaths. The sheath equations are reduced to one previously solved (in connection with a spherical electrostatic probe problem). The sheath solution and quasineutral plasma solution are asymptotically matched in their region of common validity. Thus charged particle and electric field distributions are found and typical curves are given. From the tabulated data, current-voltage characteristics of the photoionization chamber may be constructed. Three sample characteristics are given with a little discussion of their interpretation. (auth)

40553 (NYO-2978-34) EVALUATION OF BETA RADIATION AS A HYDROGENATION CATALYST. Interim Technical Status Report, March 1, 1962–October 31, 1963. Yavorsky, P. M.; Gorin, E. (Consolidation Coal Co., Library, Pa. Research Div.). Sept. 11, 1964. Contract AT(30-1)-2978. 78p. Dep. mn; CFSTI, $3.00 cy; $0.75 mn.

The concept of using high intensity beta radiation from an isotopic source, ^{90}Sr, inside a high temperature, high pressure chemical reactor was developed for potential radiation chemical processes. Distinct advantages include high utilizable intensity from a relatively small source with a minimum of shielding against external radiation. The first internal source used was of 90 Curies of radiating microspheres, encapsulated in hollow-steel needles, stacked in the reactor. Thirty-four percent of all the radiation energy was available for processing at 0.98 megarad/hour. Source integrity was satisfactory for several months of operations, and then slight leakage required development of an improved source. A new source design was developed, consisting of a long thin metal tube swaged over a hard compaction of strontium titanate. The resultant practically solid 0.077-in. rod can be bent to any irradiator form. Coils of it were proven to not deform and remain leakproof in tests to 5000 psi at 500°C. A 500 Curie source of this style is being made for further studies of radiation processes. Radiation processing studies at elevated temperatures and pressure showed that radiation does not significantly promote hydrogenation in the form of hydrogen addition to the aromatic structure of coal extract nor aromatic model compounds. Radiation does cause a marginal increase in the rate of hydrocracking of coal extract at 429°C, but not sufficient for exploitation. The ultimate extent of hydrocracking was the same as for the purely thermal reaction. Radiation was found to pro-

mote hydrofining, the removal of nitrogen and sulfur from distillate oils derived from hydrogenated coal extract. (auth)

40554 (AEC-tr-6565) ANNUAL REPORT OF THE JAPANESE ASSOCIATION FOR RADIATION RESEARCH ON POLYMERS, VOLUME 5, 1963–1964. Translation of "Nippon Hoshasen Kobunshi Kenkyu Kyokai Nempo, Vol. 5, 1963–1964," (a publication of the Japanese Association for Radiation Research on Polymers). 324p. Dep. mn; CFSTI, $7.00 cy, $1.50 mn.

Research work at Osaka laboratory is presented in 29 papers. An abstract is prepared for one paper; 28 abstracts appeared previously in NSA as 19: 15620, 15621, 26375, 26418, 26419, 26420, 26421, 26422, 26423, 26424, 26425, 26426, 26427, 26428, 26429, 26430, 26431, 26432, 26433, 26434, 26495, 28397, 28398, 28399, 28400, 28401, 28969, and 29442. (M.O.W.)

For an abstract of the individual paper see: 40555.

40555 (AEC-tr-6565, pp 1-7) SUMMARY RESEARCH REPORT: OSAKA LABORATORY. Sakurada, Ichiro. Translated from Nippon Hoshasen Kobunshi Kenkyu Kyokai Nempo, 5: 1-5(1963-64).

The Osaka experimental plant consists of five laboratories in which research is conducted. An outline of the work carried out in each of the laboratories through 1963 and in the first half of 1964 is presented. (M.O.W.)

40556 DETERMINATION OF VINYL ACETATE IN ETHYLENE VINYL ACETATE COPOLYMERS BASED ON HIGH ENERGY RADIOLYSIS. Kamath, P. M.; Barlow, Anthony (U. S. Industrial Chemicals Co., Cincinnati). Anal. Chem., 37: 1266-7(Sept. 1965).

A series of samples of pure polyethylene and ethylene vinyl acetate copolymers of differing vinyl acetate content was subjected to radiolysis by a measured dose of gamma radiation from a ^{60}Co source. The products of radiolysis consisted mainly of low-molecular-weight hydrocarbons, carbon monoxide, carbon dioxide, and hydrogen. They were analyzed by gas chromatography to determine the carbon monoxide content and its G value. As the vinyl acetate content increased, the amount of carbon monoxide product increased. (F.J.H.)

40557 SENSITIVITY OF PYRIMIDINES AND PURINES TOWARDS NEUTRON IRRADIATION. Wacker, A.; Chandra, P. (Universitaet, Frankfurt am Main). Angew. Chem., 4: 434(May 1965).

When aqueous solutions of pyrimidines and pur'nes were irradiated with thermal neutrons, they decomposed to an extent directly proportional to their nitrogen content. It was concluded that the destructive action is probably due to the nuclear reaction $^{14}N(n,p)^{14}C$. If the pyrimidines and purines were part of a nucleic acid they were more resistant to neutrons. (M.C.G.)

40558 ELECTRON SPIN RESONANCE DETERMINATION OF THE RADIOLYTIC YIELDS OF TRAPPED ELECTRONS AND OTHER SPECIES IN AN ORGANIC GLASS. Smith, D. R.; Pieroni, J. J. (Atomic Energy of Canada Ltd., Chalk River, Ont.). Can. J. Chem., 43: 2141-7(Aug. 1965). (AECL-2304).

The radiolytic yields, at liquid nitrogen temperature, of trapped electrons and radicals or radical-ions in 2-methyltetrahydrofuran and the yields of these species plus the biphenyl anion in solutions containing biphenyl were determined by ESR. These measurements were also carried out after photolysis of the trapped electrons. The combined results are interpreted in terms of the identity of the intermediates and the reactions which they undergo. Dual ESR cavity techniques enabled greater accuracy and precision than in normally obtained when concentrations of paramagnetic species are determined by ESR. (auth)

40559 PROMOTION OF CHEMICAL PROCESSES WITH REACTOR RADIATION. Dondes, S.; Harteck, P.; Neil, D. E.; Steinhouser, H. (Rensselaer Polytechnic Inst., Troy, N. Y.). Chem. Eng. Progr., 60: Symp. Ser., No. 51, 150-60(1964).

Promotion of chemical processes with reactor radiation is technically feasible but economically only approaches feasibility. Mechanisms by which nuclear reactors synthesize chemicals; fuel element requirements; conceptual reactor designs to fix nitrogen; applicable chemical systems; loop operations; and problems to be overcome are discussed. (auth)

40560 FABRICATION AND UTILIZATION OF LARGE BETA RADIATION SOURCES. Weinstock, Jacques J. (Radiation Applications Inc., Long Island City, N. Y.). Chem. Eng. Progr., 60: Symp. Ser. No. 53, 62-7(1964).

An extensive research and development program has produced vitreous enamel formulations suitable for the fabrication of large planar beta radiation sources using promethium-147, cerium-144, or strontium-90 as the active component. The physical and chemical properties of these enamels have been characterized, and actual source dosimetry patterns have been established for promethium-147 and cerium-144 sources. (auth)

40561 STRUCTURAL MODIFICATIONS IN IRRADIATED 1,4 TRANS POLYBUTADIENE. Baccaredda, M.; Butta, E.; Frosini, V.; Magagnini, P. L. (Universita, Pisa, Italy). Chim. Ind. (Milan), 47: 249-56(Mar. 1965). (In Italian).

The Young's modulus and damping factor were determined between −180 and +280°C, at frequencies of some kHz, in samples of 1,4-trans-polybutadiene submitted to pile irradiation, at doses from 200 to 4000 Mrads. Young's modulus, at any temperature below the crystal melting point exhibited a minimum as function of dose at 400 to 600 Mrads; at temperatures above the melting point, it increased with increasing dose. The glass transition temperature was practically independent of radiation dose, while the main maximum damping was shifted towards higher temperatures with increasing dose. In the irradiated samples a γ transition, absent in the unirradiated material, was found at about −100°C. It is attributed to motions of long polymethylene sequences formed during irradiation through saturation of some C=C bonds of the main chain. The effects of the radiochemical vulcanization are compared with those provoked by the conventional (sulfur) vulcanization, and it is shown that in the former case, at least for low degrees of crosslinking, an increase instead of a decrease of segmental mobility occurs. (auth)

40562 THERMAL DECOMPOSITION OF EXPLOSIVES EXPOSED TO GAMMA RAYS. Piazzi, Marcello (Istituto di Chimica dell'Accademia Navale, Livorno, Italy). Chim. Ind. (Milan), 47: 276-81(Mar. 1965). (In Italian).

Thermal decomposition of explosives, propellants, and high explosives, before and after exposure to ^{60}Co γ rays is discussed. Decomposition was studied by DTA (differential thermal analysis) at constant temperature by pressure changes of decomposition products, and also at various temperatures. Effects of irradiation on explosives were also examined after extended storage. (auth)

40563 THERMOLUMINESCENCE OF MOLECULAR SOLIDS IRRADIATED BY γ RAYS AT 77 deg K. EVIDENCE OF T → S AND S → S EMISSIONS. Bullot, Jacques; Kieffer, Fernand (Faculte des Sciences, Orsay, France). Compt. Rend., 260: 4721-4(May 3, 1965). (In French).

After γ irradiation at 77°K, a sample of crystalline biphenyl containing traces of naphthalene emits, during reheating, a luminescence corresponding to the phosphorescence of naphthalene and to the fluorescence of biphenyl. The forced purification of biphenyl causes the naphthalene-induced luminescence. The fluorescence of the biphenyl alone remains, but is descreased in intensity. (tr-auth)

40564 DETERMINATION OF THE THRESHOLDS OF SENSITIVITY FOR THE RECORDING OF DIFFERENT IONIZING PARTICLES IN SOLID-STATE POLYMERS. Debeauvais, Monique; Monnin, Michel (Centre de Recherches Nucleaires, Strasbourg and Faculte des Sciences, Clermont, France). Compt. Rend., 260: 4728-30(May 3, 1965). (In French).

The thresholds for the registration of different solid-

state polymers were determined with respect to the ionizing particles. The results were explained by supposing that the particle during its passage across the detector loses its energy in two different ways: along the trajectory as the energy given up was very great, all the chemical bonds are broken. In the immediate vicinity of the trajectory, the bonds between the monomer units, which are the most fragile, alone are broken. The most important faults would then be obtained when the number of intermonomeric bonds was the lowest possible per unit length. This was verified experimentally. (tr-auth)

40565 RECOMBINATION PROCESSES IN CdS DURING EXCITATIONS BY α PARTICLES. Kirov, K.; Bandamalieva, E.; Mladenov, I. (Inst. of Physics at the Bulgarian Academy of Sciences). Comp. Rend. Acad. Bulgare Sci., 18: 97-100(1965). (In Russian).

The pulse factor in irradiation of monocrystals by α particles was studied in order to determine the ratio of electron recombinations. Select CdS crystals prepared by the Frerix method, with electrodes on both plane sides were irradiated by ^{210}Po α particles, which penetrated the whole crystal forming a conducting channel with high current concentration. The pulses were observed and photographed using a 0- to 7-MH_z frequency oscillograph. (R.V.J.)

40566 INFLUENCE OF ULTRAVIOLET RADIATION ON THERMIONIC CONVERTER. Tomkova, E.; Faenhrich, J. (Charles Univ., Prague). Czech. J. Phys., 15: 526-8(1965).

The influence of ultraviolet radiation on the magnitude of the converter current was measured in the system of the converter and the impregnated cathode, which by itself is not a sufficient source of positive ions. Cesium vapor was used as the auxiliary ion source. The change in current from that of the unlighted converter to that of the lighted converter was studied for various values of the incident radiation and for three different values of the cesium vapor temperature. The magnitude of the current maximum depends on the pressure and lighting. The applied lighting was varied at the most in the ratio of 1 : 4. Upon making the simplified assumption that the values of currents relating to the maxima of the measured curves are in the same ratio a shift is expected at about 70°K at a cathode temperature of T ~ 1000°K; but such a shift was not observed. Although the light source was not intense enough, it was seen that photo-ionization is an effective means for obtaining positive cesium ions. (J.F.P.)

40567 SOME DATA ON THE LUMINESCENT PROPERTIES OF EUROPIUM ACTIVATED SODIUM CHLORIDE AND POTASSIUM CHLORIDE PHOSPHORS. Parfianovich, I. A.; Shuraleva, E. I.; Dobrzhanskii, G. F.; Magaril, I. G.; Kazintseva, M. D. (Irkutsk State Univ., USSR). Izv. Akad. Nauk SSSR, Ser. Fiz., 29: 409-11(Mar. 1965). (In Russian).

NaCl : Eu and KCl : Eu crystals were grown from melts containing from 0.1 to 3 mole % europium and their luminescence properties were investigated. Excitation spectra, emission spectra, and glow curves were recorded and the effects on these of various heat treatments and irradiation with 50 kev x rays and F-band light were investigated. The excitation bands of NaCl : Eu at 245 and 335 mμ appeared to be due to a single type of luminescence center, but a band of 265 mμ, distinguished by its behavior under heat treatment, appeared to be due to a second type of center. Centers of this second type did not occur in KCl : Eu. Irradiation with x rays greatly reduced the luminescence of both materials; this effect was fully reversible in KCl : Eu, the luminescence being restored by a 300°C anneal, but only partly reversible in NaCl : Eu. Irradiation with x rays also led to the formation of F centers; the F band in NaCl : Eu was much wider than in pure NaCl. The light sum stored in NaCl : Eu was reduced by x irradiation, and the structure of its glow curve was somewhat altered. (ATD)

40568 INVESTIGATION OF THE ROENTGENOLUMINESCENCE AND THERMOLUMINESCENCE OF THALLIUM ACTIVATED SODIUM IODIDE CRYSTAL PHOSPHORS. Lyskovich, A. B.; Chornii, Z. P.; Guseva, N. K. (L'vov State Univ.). Izv. Akad. Nauk SSSR, Ser. Fiz., 29: 423-6(Mar. 1965). (In Russian).

Results of work on the roentgenoluminescence of NaI : Tl crystals with a high (>2 mole %) thallium content are reported. Roentgenoluminescence spectra excited by 40 kev x rays were recorded at temperatures from 100 to 650°K, glow curves were recorded, and the spectral composition of the low-temperature thermostimulated emission was examined. These results are presented graphically and discussed. In addition to the principal roentgenoluminescence emission band near 420 mμ, a weak band was clearly observable at 330 mμ even at the lowest temperature. This band increased in intensity with increasing temperature up to 450°K, and decreased in intensity with further increase of temperature. The peak of the principal emission band shifted toward the shorter wavelengths with increasing temperature, from about 430 mμ at 100°K to 400 mμ at 520°K. The roentgenoluminescence yield decreased rapidly with decreasing temperature in the region from 150 to 100°K; this is ascribed to self-trapping of holes. The yield decreased with increasing temperature above 400°K, owing to thermoquenching. Five peaks were observed in the glow curve; these occurred at 120, 140, 160, 220, and 295°K. Only radiation of the thallium luminescence band with a peak at 420 mμ contributed to the two lowest temperature peaks of the glow curve. Of the three low temperature glow curve peaks, only one appeared in crystals grown in an inert gas atmosphere. From the effect of low-temperature x irradiation on the behavior of the 295°K glow curve peak, it is concluded that the trapping centers that are responsible for this radiation, and thus adversely affect the scintillation properties of the phosphor, may be due to radiation damage to the crystal. (ATD)

40569 RADIOPHOTOLUMINESCENCE OF POLYCRYSTALLINE PELLETS OF SILVER-ACTIVATED SODIUM CHLORIDE. Druskina, L. S. (Inst. of Physics and Tech., Academy of Sciences, USSR). Izv. Akad. Nauk SSSR, Ser. Fiz., 29: 434-7(Mar. 1965). (In Russian).

The radiophotoluminescence of silver-activated alkali earth-doped polycrystalline sodium chloride pellets was investigated because of the possible use of such pellets as sensitive integrating detectors of soft x rays. The pellets were made by fusing NaCl with the appropriate quantities of activator and dopant ($SrCl_2$, $CaCl_2$, or $BaCl_2$), grinding the cooled melt to a powder, heating in vacuum at 120–140°C for 2–3 days, and forming in a hot press. The silver content was varied from 0.1 to 5 mole %, and the alkali earth content from 0 to 2 mole %. The fluorescence yield of the pellets was found to be greater than that of single crystals of the same composition by a factor 15. When the pellets were irradiated with x rays they developed a stable green emission band, the position of which was independent of the silver concentration. The intensity of the x-ray induced emission increased gradually after irradiation, or more rapidly if the pellet was heated to 200–250°C, indicating the participation of slow ionic processes. After heating, the emission intensity was stable. The material was found to be suitable for detecting soft x rays with energies as low as 10–15 kev. (ATD)

40570 AFTEREFFECTS OF F BAND ILLUMINATION OF X-RAY-IRRADIATED ALKALI HALIDE PHOSPHORS. Maksimova, N. D.; Kosikhin, V. F. Izv. Akad. Nauk SSSR, Ser. Fiz., 29: 460-2(Mar. 1965). (In Russian).

The effect of pulsed illumination with F band radiation on the x-ray excited phosphorescence of a number of alkali halide phosphors was investigated. In KCl : Tl, NaCl : Tl, KCl : Ag, NaCl : Ag, KBr : Ag, and NaBr : Ag, illumination with a flash of F band radiation increased the intensity of the phosphorescence. In KCl : Tl the intensity of this secondary phosphorescence decreased as the primary phosphorescence decayed, i.e., the weaker the primary phosphorescence at the time of illumination with F band radiation, the weaker the secondary phosphorescence; in NaCl : Tl it did not. In KBr : Tl and KBr : In, the F band radiation quenched the phosphorescence. In NaBr : Tl and NaBr : In, the F band radiation flash temporarily quenched

the phosphorescence, i.e., the intensity of the primary phosphorescence decreased sharply and subsequently returned to its normal value. Possible explanations of all these effects are discussed briefly. (ATD)

40571 ON THE MEMORY EFFECT IN THE ACTION OF AN ELECTRIC FIELD ON THE LUMINESCENCE OF ALKALI HALIDE PHOSPHORS. Parfianovich, I. A.; Pologrudov, V. V. (Irkutsk State Univ., USSR). Izv. Akad. Nauk SSSR, Ser. Fiz., 29: 490-2(Mar. 1965). (In Russian).

The effect of pre-exposure to an electric field on the roentgenoluminescence of KBr : In and NaCl : Ni phosphors was investigated. The crystal phosphors were subjected to a $1-5 \times 10^5$ v/cm electric field between electrodes with which they were not in contact and were subsequently excited by 20-kev x rays. In the case of the KBr : In phosphors the duration of exposure to the electric field was varied from a few seconds to several minutes. Five seconds after the field was removed the exciting x rays were applied, and the time variation of the resulting luminescence was followed. The initial intensity of the luminescence was much greater than without previous exposure to an electric field. This luminescence decayed rapidly at first but subsequently increased and reached a maximum one or two minutes after the beginning of the excitation. As a function of duration of exposure to the electric field, the initial intensity of the fluorescence increased rapidly, reached a maximum for an exposure of the order of a few seconds, and decreased with further increase of the exposure. The luminescence intensity at the subsequent maximum increased monotonically with duration of exposure to the electric field. The NaCl : Ni phosphors were exposed to the electric field for 6 min and subsequently excited to luminescence by x-ray pulses of 2 sec duration. The intensity of the luminescence flashes was greater when the phosphor was previously exposed to the electric field than when it was not. The maximum intensity of the luminescence flashes was reached approximately one minute after exposure to the field. (ATD)

40572 INFLUENCE OF AN ELECTRIC FIELD ON THE LUMINESCENCE OF ALKALI HALIDE COMPOUNDS. Andrianov, A. S.; Kats, M. L.; Kirillov, L. A.; Fomichev, V. V. Izv. Akad. Nauk SSSR, Ser. Fiz., 29: 493-6(Mar. 1965). (In Russian).

The electroroentgenoluminescence of NaCl, KCl, KBr, KI, CsCl, CsBr, and CsI was investigated. A powder of the salt under investigation was incorporated into the dielectric of a capacitor and excited to fluorescence by x rays. The x-ray tube was powered by a half-wave rectifier from the 50 cps mains, and a 10^5 v/cm alternating electric field of the same frequency was applied to the capacitor. The ratio, r, of the luminescence intensity with the field to the intensity without the field ranged from 0.92 for CsI to 1.5 for KBr. Further experiments were performed with KCl. The material was irradiated with continuous x rays and a 1 millisecond square pulse was applied to the capacitor. An oscillogram of the resulting fluorescence suggests a time constant for the build-up and decay of the order of a millisecond. The ratio r was found to decrease when the material was either heated or cooled from room temperature, and thermal hysteresis was observed. At about −100°C, r was unity. The thermostimulated phosphorescence light sum was the same whether the preliminary activation by x rays was performed in the presence or the absence of the electric field, but the presence of the field during the thermostimulation itself increased the light sum. The interpretation of the results is discussed briefly; it is concluded that release of trapped electrons is not involved, but that both electron and hole processes participate in the electroroentgenoluminescence. (ATD)

40573 INVESTIGATION OF THE PROCESSES OCCURRING IN EXCITED THALLIUM ACTIVATED POTASSIUM IODIDE PHOSPHORS UPON APPLICATION OF AN ELECTRIC FIELD. Pologrudov, V. V.; Penzina, E. E. Izv. Akad. Nauk SSSR, Ser. Fiz., 29: 497-9(Mar. 1965). (In Russian).

The influence of a 5×10^4 v/cm 50 cps electric field on the roentgenoluminescence and photoluminescence of KI : Tl phosphors was studied. The electric field had both a quenching and a stimulating effect on the roentgenoluminescence. When the activator concentration was large and the stimulating x-ray intensity was low, the quenching effect was predominant. Under some conditions both effects could be observed; the fluorescence intensity decreased immediately when the field was applied and subsequently increased beyond its initial value. There are two bands in the photoluminescence spectrum. Thermal quenching was observed in both bands, and most strongly in the shorter wavelength band; when the temperature was increased from room temperature the photoluminescence intensity decreased and the peaks of both excitation bands shifted toward the longer wavelengths. The thermal quenching was observed as soon as the temperature was raised above room temperature. This is in contradiction with the finding of Shvarts. It is suggested that this discrepancy may be due to Shvarts' failure to take account of the shift in the positions of the excitation bands. The results are discussed briefly. The most likely mechanism for the stimulation of the luminescence by an electric field is considered to be the reduction by the action of the field of the number of nonradiative recombinations outside the luminescence centers. (ATD)

40574 ON INFLUENCE OF FINE SPLITTING OF LOWER LEVEL Cr^{+3} IN A RUBY UPON SOME CHARACTERISTICS OF COHERENT RADIATION. Freidman, G. I. (Gor'kii State Univ., USSR). Izv. Vysshikh Uchebn. Zavedenii, Radiofiz., 8: 272-84(1965). (In Russian).

The equations for coherent radiation of Cr^{3+} ions in ruby placed in a traveling-wave resonator are obtained taking into account the fine splitting of the lower level of the Cr^{3+} ions. This splitting is shown to yield the deviation of the mean frequency in the transient regime. (D.C.W.)

40575 DIRECT CHARGE TRANSFER BY X IRRADIATION IN THE SYSTEM CaF_2 : Eu, Tm. Welber, Benjamin (IBM Watson Research Center, Yorktown Heights, N. Y.). J. Appl. Phys., 36: 2744-5(Sept. 1965).

Starting with CaF_2 containing Eu^{2+} and Tm^{3+} ions, optical techniques were used to observe the decrease in valence of the Tm ion under x irradiation. It is found that the number of Tm^{2+} ions produced corresponds closely to the number of Eu^{2+} ions which disappear, and it is suggested that the underlying mechanism is a direct transfer of an electron between the two types of ions. (auth)

40576 THERMAL ANNEALING PHENOMENA IN SOME NEUTRON-IRRADIATED LIQUID ORGANIC BROMIDES. Katsanos, N. A.; Varvoglis, A. G. (Nuclear Research Centre Democritus, Athens). J. Chem. Soc., Suppl. II, 5935-42(1964).

Post-irradiation thermal annealing phenomena in liquid organic bromides were recognized and studied. Four compounds, viz, n-propyl bromide, bromobenzene, 4-bromo-o-xylene, and benzyl bromide were neutron irradiated and then thermally annealed, at 40.0°C, in the absence and in the presence of elemental bromine, added after irradiation. A pronounced increase in retention of ^{82}Br with time of heating was observed in all compounds, when no elemental bromine was added. The maximum obtainable retention ranged from 69 to 99%, depending on the compound irradiated, the method of its purification and the conditions of the irradiation. Initial retentions, on the other hand, were not influenced by the latter two factors. Reproducible results were obtained in all cases, provided that the delay between the end of irradiation and the beginning of the treatment of the samples was always the same. The addition of elemental bromine to irradiated 4-bromo-o-oxylene resulted in an increase of both the initial and the maximum obtainable retentions. In n-propyl bromide the opposite effect was observed; both initial and maximum retentions were lowered by the addition of bromine. In bromobenzene the reaction of annealing was completely suppressed by bromine. The increase of total retention in n-propyl bromide was found to be due almost exclusively to an increase

in the amount of the parent compound when bromine was absent, and, in its presence, to formation of other products. In bromobenzene the increase of total retention was due to both parent and other products in the absence of bromine. The reaction was found to be second-order with respect to inorganic radiobromine. Some possible mechanisms of the reaction are discussed. (auth)

40577 OXIDATION OF CO ON NiO AND ZnO; EFFECT OF A PRELIMINARY IRRADIATION WITH ^{60}Co γ RAYS. Peers, Arthur Mackenzie; Dran, Jean-Claude; Ohno, Shinichi (Universite, Paris). J. Chim. Phys., 62: 711-17 (July-Aug. 1965). (In French).

The catalytic oxidation of CO was studied on NiO at 25°C and on ZnO at 270°C. The kinetics followed an Elovich equation $\frac{dq}{dt} = a \exp(-bq)$, for which the a and b parameters were evaluated. The catalysts were exposed to a preliminary irradiation with ^{60}Co γ rays, under vacuum or in a gaseous atmosphere (CO or O_2). No effect on the oxidation kinetics could be detected. In the case of NiO, the effects of different factors on the values of the Elovich parameters were determined. The initial velocity a of the reaction was very sensitive to the effectiveness of the CO_2 condensation; this factor affected relatively little the b parameter. An increase of the initial pressure P_0 of the stoichiometric reaction mixture provoked a very rapid decrease in b, whereas a passed through a minimum in the pressure region studied. A preliminary adsorption of CO lowered the initial velocity and could lead to kinetics of the first order. It was shown that the Elovich kinetics are distinguished with difficulty from first-order kinetics for certain values of b. (tr-auth)

40578 ADSORPTION OF CO AND O_2 ON ZnO AND NiO: EFFECTS OF IRRADIATION WITH RADIOCOBALT GAMMA RAYS. Peers, Arthur M.; Dran, Jean-Claude (Universite, Paris). J. Chim. Phys., 62: 718-27(July-Aug. 1965). (In French).

The adsorption of CO on ZnO and of CO and O_2 on NiO was studied at room temperature. The effects of the irradiation of these oxides under vacuum by ^{60}Co rays were investigated by examining the modifications to the isotherms and also, in the case of the CO–NiO system, to the adsorption kinetics. Irradiation appeared always to increase the adsorption energy of the gases. The effect of irradiation seemed bound to the presence of water traces on ZnO and an excess of oxygen on NiO. The results were interpreted by assuming, in the first case, a radiolytic decomposition of the chemisorbed water and by admitting, in the second case, the capture under irradiation of a positive hole by the O^{2-} ion in excess. (tr-auth)

40579 STUDY BY ELECTRON PARAMAGNETIC RESONANCE OF THE FREE RADICALS FORMED BY γ IRRADIATION OF NITROMETHANE AT 77°K. Chachaty, Claude (CEN, Gif-sur-Yvette, France). J. Chim. Phys., 62: 728-31(July-Aug. 1965). (In French).

The EPR spectrum obtained after γ irradiation of nitromethane at 77°K indicated the presence of $CH_3^{\cdot}$ and $^{\cdot}NO_2$ radicals. After disappearance of $CH_3^{\cdot}$, it was established that the central band of the triplet corresponding to $^{\cdot}NO_2$ is superposed on a 9-ray spectrum that can be attributed to the nitromethyl radical. The mean deviation of the rays gives $|a|_H = 20 \pm 1$ and $|a|_N = 6 \pm 1$ gauss for this radical. The evolution of the spectrum as a function of temperature was studied between 77 and 195°K. The interpretations were confirmed by calculating the spectrum of $^{\cdot}NO_2$ and $^{\cdot}CH_2NO_2$, taking into consideration the anisotropy of the g factor and the hyperfine interaction. This calculation was made on an electronic calculator using the Lefebvre and Maruani method. (tr-auth)

40580 REACTIONS OF RADICALS FORMED BY γ IRRADIATION OF SOLID MIXTURES OF METHYL METHACRYLATE WITH PARAFFIN OIL. Marx, Rose (Universite de Paris, Orsay). J. Chim. Phys., 62: 767-74 (July-Aug. 1965). (In French).

The free radicals formed during the radiolysis of solid mixtures containing methyl methacrylate (MMA) and paraffin oil (PO) in variable proportions were studied by EPR spectroscopy. Analysis of the spectra at –185°C after irradiation at –196°C showed that increases in the radiochemical yields MMA radicals, in the concentration region where the polymer yields also increased, came from secondary chemical reactions and not from a sensitization of the methacrylate with respect to radiation. It was a question of addition, on the double vinyl bond, of $H^{\cdot}$ radicals produced in large number by the radiolysis of PO. The evolution of the form of the spectra, during an increase in temperature after irradiation, showed that the radicals from the paraffin can also be added to MMA to give crossed chain radicals. The curves of the decay of the number of radicals as a function of the temperature indicated the existence of important molecular movements in the regions of temperature and composition of mixtures where polymerization is also important. In the hypothesis of radical polymerization, these results showed directly the role of paraffin in the chain-initiation process. They made it possible to believe that the competition between chain propagation and termination reactions is connected to molecular movements favored by the presence of paraffin. (tr-auth)

40581 ISOTOPIC EFFECTS IN THE DISSOCIATION OF TRIATOMIC MOLECULES BY ELECTRON COLLISION. III. FORMATION OF O^+ IN H_2O, HOD, AND D_2O. Fiquet-Fayard, Florence; Guyon, Paul-Marie (Universite de Paris, Orsay). J. Chim. Phys., 62: 817-20(July-Aug. 1965). (In French).

The abundance of O^+ ions in various mixtures of light heavy water was studied by mass spectrometry. The abundance in H_2O was 1.38 ± 0.03 times higher than the abundance in D_2O; the abundances in HOD and D_2O were identical. The isotopic effect did not vary as a function of the energy of the incident electrons from 60 to 140v. The dissymmetric effect could not be explained by direct ionization, and self-ionization or predissociation is suggested. (tr-auth)

40582 RECTIFICATION ON THE APPARENT EFFECT OF AN ELECTRIC FIELD ON THE RADIOCHEMICAL POLYMERIZATION OF SOLID ACRYLONITRILE. Chapiro, Adolphe; Inoue, Miyako (CNRS, Bellevue, France). J. Chim. Phys., 62: 835-7(July-Aug. 1965). (In French).

Experiments showed that the modification of the kinetic characters of the polymerization of solid acrylonitrile observed previously when the irradiation cell was bound electrically to earth was in reality due to an increase in the temperature of the sample. The presence of the electric wire under the cell introduced a layer of air that insulated the cryostat cell and caused an increase in the temperature of the monomer above –140°C, the temperature at which acrylonitrile undergoes a structure transformation. It was this that was responsible for the modification of the polymerization characters. (tr-auth)

40583 SELF-DECOMPOSITION AND RADIOLYSIS, AT LOW TEMPERATURE, OF TRITIATED THYMIDINE IN AQUEOUS SOLUTION. Apelgot, Sonia; Ekert, Bernard (Universite, Paris). J. Chim. Phys., 62: 845-52(July-Aug. 1965). (In French).

It is shown that at low temperature the speed of the self-decomposition of the tritiated thymidine does not decrease with temperature from 0 to –75°C. The tritiated thymidine decomposes only under the action of the β rays of its own ^3H atoms. The heterogeneity of the frozen solutions make it possible to take into account the ensemble of the phenomena observed. (tr-auth)

40584 POLYMERIZATION BY X RAYS OF MIXTURES OF VINYL CHLORIDE AND NOBLE GASES. Herman, Jan. A.; Hupin, Pierre M. (Universite Laval, Quebec). J. Chim. Phys., 62: 863-6(July-Aug. 1965). (In French).

The speed of polymerization by x rays of vinyl chloride mixed with Ar, Kr, or Xe increased proportionally with the noble gas content and with its absorption of the ionizing radiation. The regime velocity of the low-pressure poly-

merization (< 30 cm) was more affected by the presence of noble gases than the initial speed of polymerization. (tr-auth)

40585 CHEMICAL RESULTS OF NUCLEAR PROCESSES IN MIXED CRYSTALS. I. CHEMICAL RESULTS OF THE $^{185}Re(n,\gamma)^{186}Re$ NUCLEAR PROCESSES IN K_2ReBr_6–K_2SnCl_6 MIXED CRYSTALS. Mueller, Horst (Universitaet, Freiburg i. B.). J. Inorg. Nucl. Chem., 27: 1745-59(Aug. 1965). (In German).

The chemical effects of the nuclear reaction $^{185}Re(n,\gamma)^{186}Re$ were investigated for K_2ReBr_6–K_2SnCl_6 mixed crystals in the range from 1 to 28 mol-% K_2ReBr_6 to distinguish between the different retention theories. The formation of all mixed hexa(chlorobromo)-rhenates $ReCl_nBr_{6-n}^{2-}$ ($0 \le n \le 6$) seemed to prove the hot-spot model; the billiard-ball model must be disregarded. Primary retention by conservation of the original bonds did not exceed 10%. The reaction probability of rhenium recoil atoms with chloride and bromide in the solid was nearly the same, which was shown by comparison with the recoil products in irradiated K_2ReCl_6–K_2SnBr_6 mixed crystals. The ligands originally co-ordinated to the rhenium were enriched to 35% in the recoil reaction products, even in the most dilute mixed crystals; this allowed the calculation of 5 Å as the radius of the reaction zone and 20 atoms as its content. The hot-spot theory predicted values larger by one order of magnitude and could not account for the individual yield of the mixed chlorobromorhenates. A model is proposed, the "disorder model", to explain the chemical effects of (n,γ) transformations. In this model the recoil atom generates around its starting point only small changes in the lattice arrangement without producing a melt, and the final fate of the recoil atom is determined by the structure of the immediate environment it has reached after having lost its kinetic energy. In the most dilute K_2ReBr_6–K_2SnCl_6 mixed crystals, bromine-containing complexes are produced if the recoil atom still remains near the octahedron of bromine ligands; farther moved atoms preferentially form $^{186}ReCl_6^{2-}$. The radius of the reaction zone is also a representation of the recoil range. (auth)

40586 HYDROLYSIS OF NEUTRON-IRRADIATED URANIUM AND URANIUM–PLUTONIUM MONOCARBIDES. Evered, S.; Moreton-Smith, M. J.; Sowden, R. G. (Atomic Energy Research Establishment, Harwell, Berks, Eng.). J. Inorg. Nucl. Chem., 27: 1867-8(Aug. 1965).

The hydrolysis of neutron-irradiated UC and (U,Pu)C was studied. Two years elapsed between removal of the specimens from the reactor and the hydrolysis experiments. A specimen of UC irradiated to 0.4% burnup was hydrolyzed only slowly in excess water at 80°C. Specimens irradiated to 0.8 and 1.0% burnup were completely inert to boiling water. None of the irradiated samples of (U, Pu) C tested was attacked by water. It was concluded that the observed changes in chemical reactivity were brought about by structural changes. (M.C.G.)

40587 RADIATION QUENCHING OF RADIO- AND RADIOTHERMO-LUMINESCENCE OF ZnS PHOSPHORS. I. LUMINESCENT PROCESS UNDER EXCITATION. Huzimura, Ryoitiro (Government Industrial Research Inst., Nagoya, Japan). J. Phys. Soc. Japan, 20: 1146-55 (July 1965).

Spectra and buildup-decay curves of the luminescence of ZnS : Cu : Cl phosphors under excitation by 5.5-Mev electrons from a linear accelerator or β rays of $^{90}Sr-^{90}Y$ were compared with those by near uv light. It was found that the ratio of the blue intensity to green one in the spectra of radioluminescence is markedly reduced from that of uv-luminescence. The intensity of uv-luminescence increases with the concentration of Cu up to 0.1% while that of β-luminescence begins to decrease at concentrations more than 0.02%. The normalized deficiency area of buildup curves of β-luminescence is greater than that of uv-luminescence for several phosphors but inverse for others. The results are interpreted as radiation quenching by assuming the production and migration of energetic energy carriers to cause the quenching. A localized transport process in a region along the path of incident electron was proposed to be probable. (auth)

40588 POLARIZATION OF RADIO-PHOTOLUMINESCENCE OF FLUORO-DOSIMETER GLASS. Kishii, Toru; Sakurai, Junji (Tokyo Shibaura Electric Co., Kawasaki, Japan). J. Phys. Soc. Japan, 20: 1271(July 1965).

Polarization of radio-photoluminescence of a fluoro-dosimeter glass was observed. This was excited by polarized ultra-violet light. The composition of the glass was $Al(PO_3)_3$ 50, $LiPO_3$ 50, and $AgPO_3$ 7 in weight ratio. Prisms of the glass with polished surfaces were irradiated by ^{60}Co gamma rays for 2, 10, 30, 60, 120, 480, and 1440 minutes respectively with a dose rate of $1.4(10)^5$ r/hr. The intensity ratio was plotted vs the irradiation time by gamma rays. (J.F.P.)

40589 REACTION OF ETHYLENE WITH PHOSGENE INDUCED BY GAMMA RADIATION. Takehisa, Masaaki; Yasumoto, Masahiko; Hosaka, Yoshinobu (Government Chemical Industrial Research Inst., Tokyo). Kogyo Kagaku Zasshi, 68: 495-9(Mar. 1965). (In Japanese).

The ^{60}Co γ-radiation initiated reaction of ethylene with phosgene was carried out in the liquid phase under pressures of 10 to 56 kg cm^2. The main products were a series of 1-chloroalkanes and a series of α, ω-dichloroalkanes. G values of ~1 were obtained for each product in the series of chloroalkanes, indicating that the chain length was rather short. Valeric acid, enanthic acid, peralgonic acid, chloropropionic acid, chlorovaleric acid, chloroenanthic acid, and chloroperalgonic acid were identified by gas chromatography in aqueous $NaHCO_3$ extracts of the reaction products. The ir absorption spectra of a high-boiling fraction showed that a considerable amount of olefinic compounds and ketones are formed as byproducts. These results indicate that the reaction takes place according to a free-radical mechanism. The product distribution of the chloroacids, however, suggests that the chain transfer to phosgene to produce a new •COCl radical is improbable in the temperature range of –78 to 80°C. Step-wise reactions of free radicals and monomer units are offered in postulation of a reaction mechanism. (BBB)

40590 REACTION OF ETHYLENE WITH 1,2-DICHLOROETHANE INDUCED BY GAMMA RADIATION. Takehisa, Masaaki; Urano, Yokichi; Yasumoto, Masahiko (Government Chemical Industrial Research Inst., Tokyo). Kogyo Kagaku Zasshi, 68: 499-503(Mar. 1965). (In Japanese)

G values are given for a series of 1,2-dichloroalkanes and a series of 1-chloroalkanes obtained by the γ-ray induced reaction of ethylene with 1,2-dichloroethane in the pressure range of 10 to 46 kg/cm^2 and the temperature range of –10 to 80°C. The results are consistent with a free-radical telomerization mechanism which includes the following steps: $C_2H_4Cl_2$ (γ ray) $\rightarrow Cl\cdot + C_2H_4Cl\cdot$; $Cl\cdot + C_2H_4 \rightarrow C_2H_4Cl\cdot$; $C_2H_4Cl\cdot + \underline{n}(C_2H_4) \rightarrow Cl(C_2H_4)_{n+1}\cdot$; $Cl(C_2H_4)_{n+1}\cdot + C_2H_4Cl_2 \rightarrow Cl(C_2H_4)_{n+1}H + C_2H_3Cl_2\cdot$; $C_2H_3Cl_2\cdot + \underline{n}(C_2H_4) \rightarrow C_2H_3Cl_2(C_2H_4)_n\cdot$; $C_2H_3Cl_2(C_2H_4)_n\cdot + C_2H_4Cl_2 \rightarrow C_2H_3Cl_2(C_2H_4)_nH + C_2H_3Cl_2\cdot$. Besides these main products, 1,4-dichlorobutane, 1,2,4-trichlorobutane, and 1,2,3,4-tetrachlorobutane were found as the radical recombination products. The molecular weights of the high boiling telomers were found to be 250 to 1000 by means of elution chromatography. About 1.5 atoms of chlorine per molecule were found in these fractions regardless with molecular weight, suggesting the same telomer composition (about 1 to 1 mixtures of 1-chloroalkane and 1,2-dichloroalkane) in the whole molecular weight range. $G(-C_2H_4)$ was 100 to 400 under the experimental conditions used. (BBB)

40591 THE EFFECT OF THE TYPE OF RADIATION ON THE RADICLYSIS OF DIPHENYL-METHANE. Kules, Inna; Opauszky, Istvan; Kosa Somogyi, Istvan; Schiller, Robert. Magy. Tud. Akad. Kozp. Fiz. Kut. Int. Kozlemen., 13: 137-47(1965). (In Hungarian).

The radiolysis of in-pile and ^{60}Co γ-irradiated diphenylmethane was studied by evaluating the total gas and polymer yields as well as the composition of the former. Under

the two different radiations essentially the same gases are produced, but in different proportions. The greatest difference is observed in the hydrogen to acetylene ratio. This can be attributed to the competitive deactivation and recombination reactions between excited molecules taking place in spurs. The polymer production is thought to proceed by successive reactions of radicals and excited molecules which are not accompanied by gas evolution consisting actually in double-bond rupture and saturation. (auth)

40592 ELECTRON SPIN RESONANCE SPECTRA OF GAMMA-IRRADIATED POLYCRYSTALLINE GLYCOLLIC ACID. Hawke, J. G.; Rawson, B. J. (Univ. of Sydney). Nature, 207: 293-4(July 17, 1965).

Polycrystalline glycolic acid was irradiated at 77°K, and the changes in the ESR spectrum as the crystals were warmed to room temperature were observed. Purified samples were irradiated to 10^5-10^6 rads using a ^{60}Co gamma source. Three separate signals were observed with increasing temperature; various reactions of the radicals in the samples are postulated to explain the changes. Evidence to support the postulated reactions was found from an examination of the room-temperature radiolysis products of glycolic acid. (M.J.T.)

40593 MEASUREMENT OF THE ABSOLUTE YIELD OF ALKALI-HALIDE CRYSTALS IN CASE OF γ LUMINESCENCE. Pertsev, A. N.; Pisarevskii, A. N.; Soshin, L. D. Opt. Spectry. (USSR)(English Transl.), 18: 366-7 (Apr. 1965).

Absolute yields of the scintillators NaI(Tl), CsI(Tl), KI(Tl) upon excitation by γ rays from a ^{137}Cs source at room temperature were measured by comparing the scintillation amplitude with the amplitude of single-electron pulses at the PM (photomultiplier) output and taking into account the necessary parameters. The following data were obtained: $\kappa = (15.3 \pm 1.0)\%$ for NaI(Tl), $\kappa = (6.0 \pm 0.4)\%$ for CsI(Tl), $\kappa = (3.1 \pm 0.3)\%$ for KI(Tl). (auth)

40594 ON THE PLASTIC FLOW INDUCED BY PARTIAL X-RAY IRRADIATION OF NaCl. Alvarez Rivas, J. L.; Agullo-Lopez, F. (Junta de Energia Nuclear, Madrid). Phil. Mag. (8), 12: 205-8(July 1965).

The possibility of plastic flow induced by the expansion of the irradiated part was investigated in partly x-irradiated (120 kv, 13 mamp) NaCl single crystals. No bulk plastic flow was found at variance with results recently published. (auth)

40595 X-RAY STUDIES OF POLYAMIDE FILMS CAST FROM IRRADIATED SOLUTIONS. Afanas'ev, A. M.; Pavlov, S. A.; Karpov, V. L.; Zverev, B. I. Plasticheskie Massy, No. 4, 52-5(1965).

The structures of mixed polyamide films after ^{60}Co gamma irradiation were investigated. The samples were irradiated in an atmosphere of limited air at 20°C. After irradiating the solutions with integral doses of 0 to 500 mrd, the concentration was reduced to 10% (dilution, warming, and shaking). The film was poured from the remaining solution at 60°C on a glass base also at 60°C. The film was then heated to 75°C, and x-ray studies were made. Radiation doses of 50 to 100 mrd was accompanied by increased ordering of the macromolecules in the film, but further increase in radiation dose to 500 mrd caused decrease in the crystalline phase. (CFSTI)

40596 UNIT FOR GAS-PHASE RADIATION-INDUCED GRAFT POLYMERIZATION. Bessonov, A. I.; Vitushkin, N. I.; Glazunov, P. Ya.; Karapetyan, Sh. A.; Parfanovich, B. N.; Ryabchikova, G. G.; Yakubovich, A. A. Plasticheskie Massy, No. 5, 3-4(1965).

A pilot-plant unit was built for producing graft polymerization products by gas-phase radiation-induced graft polymerization in quantities sufficient for technical testing. The unit is suitable for grafting polymer molecules to the surface of mineral powders and synthetic and mineral fibers, fabrics, and films by irradiating them with fast electrons in an atmosphere of gaseous monomer and inert gas. The unit is designed to operate either with monomers whose boiling point is above room temperature or with monomers which are normally gaseous. (CFSTI)

40597 ON THE INFLUENCE OF THE LENGTH OF α-PARTICLE TRACK IN NUCLEAR PHOTOEMULSION IN RELATION TO THE pH OF THE IMPREGNATING SOLUTION. Zaborenko, K. B.; Korobkov, V. I. Radiokhimiya, 7: 126-8(1965). (In Russian).

The marked effect of the pH of the impregnating solutions, containing α-emitting radio isotopes, on the length of α particle tracks in photoemulsions is connected with the amphoteric character of the gelatin and the variable pH of the developer. (tr-auth)

40598 PAIRS OF CdS CRYSTALS WITH MATCHED PHOTORESPONSES. Snyder, Donald D. (Andrews Univ., Berrien Springs, Mich.). Rev. Sci. Instr., 36: 767(June 1965).

A study is undertaken to ascertain the feasibility of developing identically photoresponsive CdS crystals for x-ray monitoring applications. Of the crystals studied, nearly half could be matched into pairs with very nearly identical photoresponse to changes in visible and x-ray (30 kv) irradiation intensity. (auth)

40599 CHEMICAL REACTION BY IONIZING RADIATION. III. ON RESTRAINT ACTION OF PHENOL COMPOUNDS. Ishikawa, Sumio (Inst. of Physical and Chemical Research, Tokyo). Rika Gaku Kenkyusho Hokoku, 36, 325-7(1960). (In Japanese).

In studies on the method of γ dosimetry using the after-effect of a chromogenic polymer, the restraining action of phenol compounds on the after-effect was studied. When phenol compounds were added to chromogenic polymer, o-cresol and p-cresol showed an accelerating action, while resorcinol, catechol, and hydroquinone were observed to have a restraining action. (BBB)

40600 OPTICAL PROPERTIES OF CaF_2–Dy^{3+} CRYSTALS. Voron'ko, Yu. K.; Osiko, V. V.; Udovenchik, V. T.; Fursikov, M. M. (Lebedev Inst. of Physics, Moscow). Soviet Phys.-Solid State (English Transl.), 7: 204-9(July 1965).

Translated from Fiz. Tverd. Tela, 7: 267-73(Jan. 1965).

Results of an investigation of absorption, luminescence, and excitation spectra of various types of CaF_2-Dy^{3+} crystals differing in chemical composition and crystal structure are presented. (auth)

40601 PHOTOCONDUCTIVITY IN IRRADIATED AROMATIC COMPOUNDS. Tochin, V. A. (Inst. of Chemistry and Physics, Moscow). Soviet Phys.-Solid State (English Transl.), 7: 232-3(July 1965).

Translated from Fiz. Tverd. Tela, 7: 293-5(Jan. 1965).

Frozen samples of benzene, biphenyl, and n-terphenyl were irradiated in darkness by a 1.6-Mev fast electron beam at 77°K. Photoconductivity was measured under illumination by light of various wavelengths. The results indicate the presence of various traps in the irradiated samples and confirm earlier data on the charge accumulation by low-temperature radiolysis in organic compounds. (A.G.W.)

40602 ELECTRON PARAMAGNETIC RESONANCE OF IRRADIATED SINGLE CRYSTALS OF FLUORITE CONTAINING A NEODYMIUM ADDITION. Kask, N. E.; Kornienko, L. S.; Rybaltovskii, A. O. (Moscow State Univ.). Soviet Phys.-Solid State (English Transl.), 7: 532-3(Aug. 1965).

Translated from Fiz. Tverd. Tela, 7: 663-5(Feb. 1965).

Single crystals of fluorite containing Nd^{3+} ions were irradiated with 1.2-Mev γ quanta. Investigation of the electron paramagnetic resonance (EPR) spectra before irradiation showed that the Nd^{3+} ions are located in crystal fields having tetragonal and rhombic symmetry. After irradiation, the optical absorption spectra showed new bands belonging to the Nd^{2+} ion, but no EPR spectrum ascribable to this ion was found. The EPR spectrum of the ions located in a tetragonal environment did not change, but the intensity of the EPR spectra of the ions located in the rhombic environment did change. A new EPR spectrum of the Nd^{3+} ion showed up. When the irradiated crystals were heated to 150-200°C, the new

EPR spectrum disappeared and the intensity of the rhombic spectrum was restored. Possible explanations of the observed changes are discussed. (A.G.W.)

40603 EFFECT OF NUCLEAR RADIATION ON THE THERMAL CONDUCTIVITY OF POLYETHYLENE. Tomlinson, J. N. (Pennsylvania State Univ., University Park); Kline, D. E.; Sauer, J. A. SPE (Soc. Plastics Engrs.) Trans., 5: No. 1, 44-8(Jan. 1965).

Polyethylene samples were tested from 0°C to the softening point where loss of form stability prevented further testing. By use of low dose irradiation, samples were lightly crosslinked to obtain form stability, and thermal conductivity tests were then conducted over the 0 to 170°C temperature range to obtain an estimate of the conductivity through the crystalline melting point and beyond. Subsequently, samples were also irradiated to successively higher radiation doses to determine the effects of large-scale radioinduced changes on the thermal conductivity. As the temperature increased from 0°C there appeared to be a small rise in conductivity, which was somewhat more pronounced for the irradiated samples, to a slight maximum near 50°C. From 50 to 100°C, values for all samples decreased with increasing temperature. Above 100°C conductivity values for the irradiated samples approached a value of about 4.5×10^{-4} cal/cm-sec-°C and became essentially independent of temperature. At room temperature thermal conductivity decreased with increased irradiation, while above 100°C there was an increase in conductivity with increasing dose. (M.C.G.)

40604 ON THE PROBLEM OF UTILIZATION OF HEAVY NUCLEI FISSION ENERGY FOR IONIZING THE AIR. Dmitriev, M. T. Tr. Nauchn.-Issled. Inst. Gidrometeorol. Priborostr., 12: 161-4(1964). (In Russian)

The possibility of using radioinduced oxidation of atmospheric nitrogen for the industrial production of nitric acid, employing fission fragments as the radiation source, is examined. Tests carried out in a very broad range of pressures (from 0.1 mm of Hg to 150 atm) and at temperatures from 5 to 200°C indicated that the NO_2 yield amounts at most to only 6 molecules per 100 ev of absorbed radiation energy; the N_2O yield is lower by a factor of 2 to 3. The type of radiation (slow and fast neutrons or gamma rays) did not seem to affect the yield. On the basis of the information available in the literature, it is concluded that it is feasible to design an industrial plant operating in connection with a reactor for the production of bound nitrogen, yielding HNO_3 and radioactive C as end-products. Consideration should be given to the production of NH_4NO_3 by the irradiation of natural waters from rivers, lakes, or irrigation canals containing dissolved air. This irradiation would increase the fish production and would add bound N to the soil. Irradiation of the soil with its contained water would achieve the enrichment in N compounds directly, while simultaneously destroying weeds. The large-scale application of such a process promises to be one of the most effective methods for influencing the climate. (TTT)

40605 RADIOCHEMISTRY OF CARBONS. III. EFFECTS OF γ RADIATION ON THE AQUEOUS SOLUTIONS OF α-METHYL-D-GLUCOSIDE. Kochetov, N. K.; Kudryashov, L. I.; Chlenov, M. A. (Inst. of Chemistry of Natural Compounds, Academy of Sciences, USSR). Zh. Obshch. Khim., 35: 897-900(May 1965). (In Russian).

A method for the quantitative determination of α-methyl-D-glucoside using densimetric paper chromatograms was developed with a precision of 4 to 5%. The decomposition yield of α-methyl-D-glucoside in weak solutions at concentrations of 10^{-2}M under the effects of γ radiation was determined. It was shown that during radiolysis of dilute solutions of α-methyl-D-glucoside hydrolysis does not appear to be the principal process and, as a result of the radiolysis, complex mixtures consisting of reducible sugars, lower oxyaldehydes, and acids, are produced. (tr-auth)

40606 SEPARATION OF RADIOPHOSPHINE FROM MIXED KCl–$CaCl_2$ CRYSTALS IRRADIATED WITH HIGH-ENERGY PROTONS. Bogdanov, R. V.; Murin, A. N. (Inst. of Organic Chemistry, Academy of Sciences, Ukrainian SSR and Inst. of Physical Chemistry, Academy of Sciences, Ukrainian SSR). Zh. Obshch. Khim., 35: 916-23 (May 1965). (In Russian).

A method for the production of radioactive phosphine by irradiation of mixed crystals of KCl–$CaCl_2$ with high energy protons using calcium phosphide in carrier concentration is described. It was found that the quantity of radiophosphine, separated from the irradiated crystals, depends on the quantity of added Ca_3P_2 carrier and the acidity of the medium in which the active crystals are dissolved. The acidity dependence occurred in proportion to the percentage of radioactive phosphorus, resulting in solutions in the form of hydroxy acids, to an extreme degree in the pH interval from 0.5 to 5. The character of the dependence found indicated that a significant part of the radioactive phosphorus in the irradiated crystals does not occur in the structure of either carrier, but is capable of assuming a given chemical form under the effects of conditions accompanying the transition of phosphorus from solid targets into solution. (tr-auth)

40607 ON THE RADICALS FORMED IN RADIOLYSIS OF CERTAIN BENZENE DERIVATIVES. Chkheidze, I. I.; Trofimov, V. I.; Buben, N. Ya. (Inst. of Chemical Physics, Academy of Sciences, USSR). Zh. Strukt. Khim., 5: 624-7 (July-Aug. 1964). (In Russian).

Electron paramagnetic resonance studies were made of the radicals formed in low-temperature radiolysis of benzene derivatives. The EPR spectra of irradiated benzene, alkyl-substituted benzenes, thiophenol, aniline, and anisole showed triplet spectra distrubited between the components $\Delta H \approx 45$ to 50 e with the central component intensity higher than that anticipated from the binominal law of distribution of intensities. An analysis of EPR spectra of irradiated benzene at 143°K, toluene at 110°K, butylbenzene at 113°K mesidine at 211°K, 1-phenyl-1 cyclohexyldodecane at 143°K, chlorobenzene at 143°K, anisole at 123°K, and aniline at 140°K showed a varying contribution of cyclohexadiene radicals in various compounds, which did not exceed 30 to 40%. In the EPR spectra for other benzene derivatives, phenol at 143°K, resorcinol at 138°K aminophenol at 123°K, benzyl alcohol at 138°K, benzoic acid at 143°K, azobenzene at 153°K, nitrobenzene at 128°K, benzylchloride at 143°K, and benzaldehyde at 123°K, the contribution of cyclohexadienyl radicals was small (<10%) and in some compounds this radical was completely absent indicating that the secondary reactions in radiolysis of the second group followed a different scheme than the first group due to the selectivity of hydrogen reactions of polar molecules in the crystal. (R.V.J.)

40608 ON CERTAIN TRANSFORMATIONS IN EPR SPECTRA OF IRRADIATED POLYISOBUTYLENE. Teleshov, E. N.; Sharpatyi, V. A.; Pravednikov, A. N.; Medvedev, S. S. (Karpov Inst. of Physics and Chemistry, Academy of Sciences, USSR). Zh. Strukt. Khim., 5: 627-9(July-Aug. 1964). (In Russian).

An accumulation of free radicals with the EPR spectrum expressed as an ~22 e split doublet, $\sim C(CH_3)_2-CH-C(CH_3)_2$, was previously observed during irradiation of polyisobutylene (PIB) at liquid nitrogen temperature. Additional data on the origin and properties of radical products showed that heating of samples irradiated at −180°C by accelerated 1.6-Mev electrons to a dose $\sim 10^{22}$ ev/g, resulted in disappearance of the initially observed radicals and in irreversible changes in the EPR spectra. The EPR spectrum of a PIB mixture with isobutylene (38%) irradiated at −196°C to a dose of 9.6×10^{20} ev/g and the EPR spectrum of PIB irradiated at −60°C by accelerated electrons to a dose of 3.6×10^{22} ev/g were analyzed. (R.V.J.)

40609 GAMMA RADIATION INDUCED DECOMPOSITION OF ALKALI NITRATE CRYSTALS (thesis). Di Martini, Raymond G. Hoboken, N. J., Stevens Inst. of Tech., 1964. 134p.

Gamma radiolysis of alkali nitrates was studied using a variety of physico-chemical techniques, including x-ray diffraction, infrared spectrophotometry, ultraviolet spec-

trophotometry, and optical microscopy. The basic reaction that takes place is decomposition of nitrate ion to nitrite ion with oxygen molecules formed and trapped in the lattice. Data gathered indicate, that for a given material, decomposition products are not just a function of dose. Single crystal material and powder material were used to show that factors such as impurity content, crystal perfection, crystal size, crystal surface treatment, and crystal geometry are effective in producing variations in the amount of nitrate decomposition obtained at a given dose. Controlled impurity content experiments were extensively investigated for the substance KNO_3. Radiation produces defect sites that are effective in trapping electrons in s type or p type orbitals. Charge compensation and extension partially limit the number of traps that can be formed. An injection of vacancies into the crystal leads to a dislocation density decrease, which in turn, results in nucleation and interface movement controlling topochemical decomposition. (Dissertation Abstr.)

40610 THE RADIOLYSIS OF ALKALI METAL SULFATES, HYDRATED TRANSITION METAL SULFATES, AND HYDRATED ALKALINE EARTH METAL SULFATES (thesis). Huang, Suei-rong. Hoboken, N. J., Stevens Inst. of Tech., 1964. 103p.

The gamma radiolysis of alkali metal sulfates, and hydrated transition metal sulfates was investigated at room temperature, −78°C, and −195°C. Alkali sulfates, in general, are very stable toward the oxidation-reduction reactions induced by gamma rays. The hydrated transition metal sulfates undergo different reaction mechanisms upon irradiation. The decomposition products of irradiated $MnSO_4 \cdot H_2O$ are Mn^{4+} ion and H_2 gas in equivalent amounts. The irradiation of $NiSO_4 \cdot 6H_2O$ yields Ni^{3+} ion, H_2 gas, and SO_3^- ion as decomposition products in the ratio of 2 : 1 : 1, respectively. This ratio is observed up to the dose of 4×10^{21} ev/g. At doses higher than 4×10^{21} ev/g, the observed ratio is 3 : 2 : 1, respectively. The decomposition products of irradiated $ZnSO_4 \cdot 6H_2O$, $CoSO_4 \cdot 7H_2O$, $CuSO_4 \cdot 5H_2O$, $MgSO_4 \cdot 7H_2O$, and $Cr_2(SO_4)_3 \cdot aq$ are H_2 gas and O_2 gas in the ratio of 2 to 1, respectively. It is obvious from these results, the water molecules within the crystal undergo radioinduced decomposition. The decomposition product yield shows a temperature dependence as indicated by a 5 to 6% decrease at −78°C, and 8 to 15% at −195°C. In all cases except $MgSO_4 \cdot 7H_2O$, saturation effects are exhibited at higher doses. Ligand field theory and solubilities of sulfate compounds were used to account for the results observed. Similarly, an attempt was made to establish a relation between crystal structure and the nature, and extent of a gamma decomposition. (Dissertation Abstr.)

40611 FISSION FRAGMENT INDUCED OXIDATION OF LIGHT HYDROCARBONS (thesis). Maa, Jer Ru. University Park, Penna., Pennsylvania State Univ., 1964. 229p.

A fairly rigorous analysis was made and resulted in a very practical calculation procedure for determining the quantity of fission fragment energy which is deposited in a reacting-fluid mixture. The importance of free radical diffusion and dose rate on G-values and product distribution was examined theoretically and by experiment. Calculations for reaction and diffusion in the wake of an ionizing particle showed that diffusion is so rapid relative to reaction in gaseous media that the system can be treated as a homogeneous mixture of radicals and molecules. Further, relatively simple calculations were sufficient to establish that an extremely high dose rate would be required before radical concentrations would be high enough to make radical-radical combinations very probable. Hence, the conclusion that the high linear energy transfer of fission fragments relative to gamma rays should have little effect on a gaseous reaction; and also that dose rate should be unimportant over the range used. Mixtures of methane–oxygen, ethane–oxygen, propane–oxygen, and ethylene–oxygen were placed in one of the cells containing a cylinder coated with enriched uranium oxide. The cell was exposed to neutrons from the nuclear reactor which cause some of the uranium to fission and release fission fragments to the surrounding gas mixture. The effects of the variables: temperature, pressure, oxygen content, total dose, and dose rate were observed and the results were interpreted in relation to the current understanding of oxidation mechanisms and radiation-chemical processes. Total hydrocarbon reacted seldom exceeded ten mole percent. Oxygenated hydrocarbons produced in significant quantities included: methanol from methane–oxygen mixtures; methanol, ethanol, and acetaldehyde from ethane–oxygen mixtures; isopropanol, acetone, and acetaldehyde from propane–oxygen mixtures; and acetaldehyde, ethanol, and isopropanol from ethylene–oxygen mixtures. A cell constructed for use in exposing gas mixtures to gamma rays was used for irradiating propane–oxygen mixtures. These data, when compared with the fission-fragment irradiation results, showed almost the same product distribution and propane G-values. If the same kind and distribution of molecular species is assumed in the gamma and fission-fragment tracks, then this similarity in experimental results supports the postulate that the reacting system can be considered homogeneous and that there is no effect of dose rate or linear energy transfer (LET) over this relatively large range. (Dissertation Abstr.)

40612 SZILARD-CHALMERS (n,γ) RECOIL REACTIONS IN METALLOPORPHINES (thesis). Rosenberg, Henry Ernest. Worcester, Mass., Clark Univ., 1964. 182p.

The Szilard-Chalmers (n,γ) recoil reaction in the Co, Ni, Cu, Zn, Pd, Ag, and Pt metal complexes of α, β, γ, δ–tetraphenylporphines (TPP) were investigated in the solid state and interpreted on the basis of the Seitz and Koehler model. The percent retentions in the parent molecule determined by the chromatographic procedure (R_c) were: ^{65}Ni, 4.1; ^{64}Cu, 13.4; ^{65}Zn, 6.6; ^{69m}Zn, 13.8; ^{103}Pd, 14; ^{109}Pd, 19.8; ^{191}Pt, 10.8; and ^{197}Pt, 5.0. The percent of recoil atoms bound in a mixture of parent molecules and various species other than parent molecules were obtained by extracting a benzene solution of the porphines with 0.1 and 8N HCl. The percent retentions for the 0.1N HCl extractions ($R_{0.1N}$) were: ^{65}Ni, 9.6; ^{64}Cu, 24.4; ^{65}Zn, 8.8; ^{69m}Zn, 18.3; ^{103}Pd, 25; ^{109}Pd, 31.7; ^{110m}Ag, 66; ^{191}Pt, 30.4, and ^{197}Pt, 21. The percent retentions for the 8N HCl extractions (R_{8N}) were: ^{65}Ni, 8.1; ^{64}Cu, 17.2; ^{103}Pd, 18; ^{109}Pd, 27; ^{191}Pt, 27.5; and ^{197}Pt, 20. For CoTPP two sets of results were obtained which were not in agreement. The first batch of CoTPP gave lower results (R_c, 5.3; $R_{0.1N}$, 10.3; R_{8N}, 7.5) than the other batches (R_c, 24.8; $R_{0.1N}$, 21.0; R_{8N}, 29.4), some of which were prepared in the same manner as the first. While there are no satisfactory explanations at present, possible reasons are discussed. No such problems occurred with the other compounds. The Co, Ni, and Pd isotopes did not respond to isothermal annealing. The ^{65}Zn and ^{191,197}Pt isotopes responded very slightly, while the ^{69}Zn and ^{64}Cu exhibited a more pronounced effect. Retention in the parent molecules of the light transition metals is attributed to two processes: a hot process in which the recoil atom forms an excited collision complex, making exchange which would not occur under ordinary circumstances a distinct possibility; and a process which may occur either during the lifetime of the hot zone or thereafter in which the recoil atom diffuses back to and recombines with the parent molecule. (Dissertation Abstr.)

40613 ELECTRON SPIN RESONANCE IN GAMMA-IRRADIATED SINGLE CRYSTALS OF HYDROXYLATED ORGANIC COMPOUNDS. Rao, Medicharla Jagannadha. Worcester, Mass., Clark Univ., 1964. 139p.

Radicals trapped in irradiated single crystals of the following hydroxylated organic compounds were studied: Monoammonium l-malate ($HOOCCH_2CHOHCOONH_4$), monoammonium l-malate monohydrate ($HOOCCH_2CHOHCOONH_4 \ H_2O$), ammonium dl-tartrate ($NH_4OOCCHOHCHOHCOONH_4$), and potassium d-tartrate ($KOOCCHOHCHOHCOOK \ \frac{1}{2}H_2O$). In both monoammonium malate and its monohydrate the trapped radicals, $HOOCCH_2\dot{C}OHCOONH_4$, thus formed were found to be very stable at room temperature. In these

radicals the two methylene protons were found to be chemically distinct. The hyperfine splittings due to the two methylene protons were almost isotropic, one of them having principal values of 34.0, 34.0, 35.0 gauss and the other 7.8, 11.0, 7.8 gauss in monoammonium malate. These values in the monohydrate are 32.5, 33.4, 36.3, and 13.2, 13.8, 17.2 gauss, respectively. The two methylene protons, instead of being located symmetrically with respect to the radical plane, which would have made them equivalent, were found to be situated in such a way that the methylene H−C−H group was twisted through an angle of 30° in monoammonium malate and through 20° in the monohydrate. The hydroxyl proton coupling in the monohydrate has principal values of 6.0, 1.0, 0.0 gauss, and is believed to have similar values in monoammonium malate. The radicals, $NH_4OOCCHOH\dot{C}OHCOONH_4$ in ammonium tartrate and $KOOCCHOH\dot{C}OHCOOK$ in potassium tartrate, were found to be similar. In potassium tartrate, in addition to the stable radical, there was an unidentified, less stable radical which showed a complex spectral pattern of weaker intensity. The isotropic part of the C−H proton hyperfine coupling in the stable radical of both the compounds was found to be only 2.1 gauss. This small value of the isotropic coupling indicates that the C−H proton lies very close to the nodal plane of the π-orbital of the unpaired electron (C−H bond making an angle of 77° with the π-orbital). The hydroxyl protons in both these compounds contributed only a small line broadening. In all four molecules, the formation of the trapped radicals was the result of the splitting of a C−H bond adjacent to both the hydroxyl and carboxyl groups. This indicates that in molecules containing the hydroxyl and carboxyl groups, the most probable bond to be broken by high energy radiation, is the C−H bond adjacent to both these groups. (Dissertation Abstr.)

40614 CHEMICAL EFFECTS OF NUCLEAR TRANSFORMATIONS. VOL. I. Proceedings Series. Proceedings of the Symposium Held in Vienna, 7-11 December 1964. (International Atomic Energy Agency, Vienna). Apr. 1965. 448p. (STI/PUB/91(Vol. I.); CONF-773 (Vol. I)). IAEA $9.00; S 189.-; £2.14.0; F.Fr. 36.-; DM 31,50 cy.

Twenty-eight articles and the abstract of one paper are included; separate abstracts were prepared for 15. Thirteen articles were previously abstracted in NSA as 19: 430, 2370, 4173, 9165, 9225, 13484, 13485, 13490, 13491, 13494, 13495, 13496, and 17957. The single abstract on chemical effects of the nuclear isomeric transition of ^{80m}Br in glassy and polycrystalline alkyl bromides was not included in NSA. (P.C.H.)

For abstracts of individual papers see: 40615—40629.

40615 KINETIC ISOTOPE EFFECTS IN RECOIL TRITIUM REACTIONS THROUGH MEASUREMENT OF ISOTOPIC MOLECULE YIELDS. Lee, E. K. C.; Root, J. W.; Rowland, F. S. (Univ. of Kansas, Lawrence; Univ. of California, Irvine). pp 55-69 of STI/PUB/91(Vol.I).

The intermolecular kinetic isotope effect in atom displacement reactions $T^* + CH_4 \rightarrow CH_3T + H$ and $T^* + CD_4 \rightarrow CD_3T + D$ has been shown to be 1.33 ± 0.04 for the ratio $(CH_3T/CH_4)/(CD_3T/CD_4)$ in experiments carried out in CH_4− CD_4 mixtures. The intramolecular kinetic isotope effect in the replacement of an alkyl group by an energetic tritium atom was found to be 1.25 ± 0.04 for the ratio CH_2T/CD_2T from CH_2CD_2. The four isotopic isomer molecules of propylene-t were separated into $CH_2TCH = CH_2$ and a combined olefinic-t group by gas chromatography. A similar separation has been carried out for $(CH_3)_2C = CHT$ and other tritiated butenes. Application of this analytical method to the olefinic radioactive products from recoil tritium reactions with gaseous propane, isobutane, n-butane, and neo-pentane has provided information about the origin of these products. The propylene-t formed from reactions of tritium with propane is about half $CH_2TCH = CH_2$, indicating that the primary mechanism of its formation is by secondary decomposition of an excited molecule, rather than by a simultaneous double displacement of 2H atoms. The separation of the products C_2H_3T, C_2H_2DT, C_2HD_2T, and C_2D_3T from recoil tritium reactions with CH_3CD_3 has shown the major yields to be only of the two molecules, C_2H_2DT and C_2HD_2T. The ratio of C_2HD_2T/C_2H_3DT is about 1.6. Taken with the other experiments concerning the origin of tritiated olefins from alkanes, these results show an isotope effect in the elimination of HD from $CH_2TDC_2^*$ versus CH_3CD_2T. The probable explanation for this effect is related to the energy deposition in the replacement of H versus D in very high energy reactions. (P.C.H.)

40616 QUANTITATIVE STUDIES OF THE REACTIONS OF HOT TRITIUM ATOMS WITH HYDROCARBONS AND HYDROCARBON MIXTURES. Urch, D. S.; Welch, M. J. (London Univ.). pp 71-85 of STI/PUB/91(Vol.I).

The kinetic theory of hot-atom reactions was expanded to cover the general system of two reactive species and an inert moderator. From results with a single-reactant and moderator, two reactants without moderator, and two reactants with moderator, values of, or ratios of, the reactivity integral I and the average logarithmic energy loss per collision α can be calculated. New results are presented from the reaction of hot tritium produced by the $^3He(n,p)^3H$ reaction with the following systems (all contain oxygen scavenger): ethane with helium moderator; butane with helium moderator; neopentane with helium moderator; ethane and butane with and without helium moderator; and ethane and neopentane with and without helium moderator. Values of α and I for the three reactants were calculated from the three types of system and the agreement between the results is discussed in the terms of the accuracy of the model. The results obtained from the different systems agree to within the limits of the experimental error, and this shows that the kinetic theory model can be applied to hot-atom systems with some certainty and that the assumptions made when considering mixtures are reasonable ones. The ratios of the reactivity of the hydrocarbons in mixtures with regard to substitution reactions are not the same as the ratios of the number of hydrogen atoms in the hydrocarbons. The values obtained for these ratios are explained in terms of the values of I and S (the collision cross-section) for the hydrocarbons. (auth)

40617 THE EFFECT OF KINETIC ENERGY ON THE REACTIONS OF NUCLEOGENIC CARBON ATOMS WITH HYDROCARBONS. Dubrin, J. (Yale Univ., New Haven); Rosenberg, H.; Wolfgang, R.; MacKay, C. pp 133-47 of STI/PUB/91(Vol. I).

New results on product yields in two systems neon-ethylene and neon-ethane, are presented, and the relation of these results to other work involving degradative studies and double tracer experiments is discussed. The discussion of the neon-ethylene results is in terms of the two previously postulated insertion mechanisms, insertion of the C atom into the C=C and into the C—H bonds to give $C\text{-}C_2H_4$ adducts. As neon concentration is increased no product is eliminated, but the relative yields of products are altered markedly. Those products such as acetylene and vinyl acetylene which can be formed from the initial $C\text{-}C_2H_4$ adducts via processes with a high energy requirement decrease in importance, and the yields of products formed in low energy processes, such as C_5 compounds, increase. The ethane pattern is similar. Degradative studies have already shown that the intramolecular ^{11}C distribution in allene and methylacetylene formed from ethylene is affected by neon moderation. These results imply both participation of the C=C and C—H bonds in formation of these products, and a dependence of the ratio of attack at the two bond types on the kinetic energy of the reacting C atom. Other work involving double tracer studies on acetylene formation from single molecules such as CH_2CD_2, CH_3CH_2D, CD_3CDH_2 and from various mixtures of other labeled alkanes and alkenes indicate that the removal of kinetic energy from the C atom has little effect on the relative rate of attack at various types of C—H bonds. (P.C.H.)

40618 GAS-PHASE REACTIONS OF (n,γ) AND ISOMERIC TRANSITION-ACTIVATED ^{80}Br WITH ALKANES

AND HALOALKANES. Spicer, L. D.; Gordus, A. A. (Univ. of Michigan, Ann Arbor). pp 185-93 of STI/PUB/91 (Vol. I).

Experimental data are presented on the gas-phase reactions of alkanes and haloalkanes with bromine atoms and ions activated by nuclear transformations. The target molecules include CH_4, CD_4, C_2H_6, C_2D_6, CH_3Cl, CH_2Cl_2, $CHCl_3$, CCl_4, CH_2F_2, CHF_3, CF_4, C_2F_6, CF_3Br, and CH_3Br. The nuclear reactions and transformations used in producing the energetic recoil atoms and ions were ^{80m}Br (isomeric transition, ^{80}Br, and $^{79}Br(n,\gamma)^{80}Br$. The percentage of radioactivity found in organic combination (the organic yield, O.Y.) was determined as a function of the concentration of the target molecule in the mole-fraction range of about 0.95 to 1.00. Elemental Br_2 served both as a source of hot atoms and as a scavenger. Usually 20-50 separate samples of each reaction system were examined and the data of O. Y. as a function of the concentration of scavenger were plotted and extrapolated to unit mole fraction of target molecule. In all cases, the O. Y. decreased with increasing halogen concentration. Data on the (n,γ) activated reactions of ^{80}Br with isotropic alkanes suggest a comparable extrapolated O. Y. for C_2H_6 and C_2D_6, but an O. Y. for CD_4 about half of the O. Y. with CH_4. Gas chromatographic analysis of the organic products indicates that about 90% of the O. Y. in CH_4 is caused by CH_3Br and 10% by CH_2Br_2. For CD_4 as the target the distribution of organic activity is approximately 75% CD_3Br and 25% CD_2Br_2. These various data are discussed in terms of possible mechanisms involving hot halogen atoms and ions. (auth)

40619 DEVELOPMENT OF METHODS FOR THE HOT SYNTHESIS OF ^{35}S-LABELLED BIOLOGICALLY ACTIVE SUBSTANCES. Dzantiev, B. G.; Shishkov, A. V. (Inst. of Chemical Physics, Moscow). pp 209-17 of STI/PUB/91 (Vol.I). (In Russian).

It was found in investigations with model systems that sulfur-35 recoil atoms are capable of entering atom and atom-group substitution reactions through interactions with cyclic and heterocyclic compounds, as well as by way of the C—C bond. Therefore the specific properties of hot sulfur atoms were used for the synthesis of labeled biologically active compounds. 4-methyl-5β-hydroxyethyl thiazole (an intermediate product of vitamin B^1 synthesis), triethylenimine thiophosphoramide, and amino acids(methionine, norvaline, and norleucine) were selected for investigation. Binary systems containing the compounds enumerated above, as well as CCl_4 or HCl (donors of hot ^{35}S atoms) were also investigated. Irradiation was carried out in an IRT-1000 reactor channel at a thermal neutron flux of 10^{11}-10^{12} n/cm^2·s. The ^{35}S recoil atoms, formed by the reaction $^{35}Cl(n,p)^{35}S$ with a recoil energy of 16 kev, interact with the thiazole giving thiazole-^{35}S. The yield of labeled product was highly dependent on the composition of the system, reaching a maximum of 20-25%. The addition of benzene (acceptor of the excitation energy) increases the yield of product, the maximum yield being reached when the ratio of CCl_4, thiazole and benzene is 1:1:1. When the mixture of triethylenimine thiophosphoramide and CCl_4 was irradiated, an initial product labeled with ^{35}S and ^{32}P was obtained, the ^{32}P being formed by the reactions $^{35}Cl(n,\alpha)^{32}P$, $^{32}S(n,p)^{32}P$, and $^{31}P(n,\gamma)^{32}P$. Methionine-^{35}S was obtained by irradiating methionine and HCl in an aqueous solution. The labeled product formed was usually diluted by a carrier, although it was possible to obtain compounds without a carrier by selecting the initial compounds appropriately. Thus, by irradiating systems of norvaline-HCl and norleucine-HCl, methionine-^{35}S was obtained without a carrier due to the entry of ^{35}S by way of the C—C bond into the norvaline molecule or the substitution of the CH_2 group in the norleucine. In both cases the yield of methionine-^{35}S amounted to 7-12%. The products in question were separated and identified both chemically and by paper chromatography. In the case of triethylenimine thiophosphoramide biological tests were carried out on the labeled products. The hot synthesis method thus enables complex, biologically active compounds to be obtained by means of a single-stage process, in many cases without a carrier. (auth)

40620 CHEMICAL EFFECTS OF NUCLEAR TRANSFORMATIONS AND ENERGY TRANSFER PROCESSES. Nesmeyanov, An. N.; Filatov, Z. S. (Moscow State Univ.). pp 239-54 of STI/PUB/91(Vol.I). (In Russian)

As a result of the interaction of hot atoms with molecules, excited molecules containing a hot atom are formed The molecules become stabilized through a dissipation of energy resulting from a transfer of energy from the site of the collision of the hot atom with the molecule, either intramolecularly or intermolecularly. In certain cases the excited molecule enters into chemical reactions with surrounding molecules. Radiation chemical transformations have shown the possibility of the dissipation of excitation energy in binary mixtures. Excitation-energy transfer phenomena of this kind were found in a number of binary systems of organic compounds, on the example of the reactions of recoil atoms of tritium and bromine. The problem of an unambiguous interpretation of the results obtained is discussed in the light of the lack of knowledge concerning any of the parameters for the process of interaction of hot atoms with molecules in a binary mixture that has different reaction cross-sections for the components, the probability values for impact reactions, the change in the logarithmic decrement of extinction, and the energy of the liquid cage in response to a change in the composition of the system. The intramolecular transfer of excitation energy in the reactions of tritium recoil atoms with a number of organic compounds is also discussed. (auth)

40621 REACTIONS OF TRITIUM RECOIL ATOMS IN LIQUID ORGANIC MIXTURES. Sokolowska, A. (Inst. of Nuclear Research, Warsaw). pp 255-64 of STI/PUB/91 (Vol.I).

Studies on reactions of recoil tritium atoms in organic liquids were carried out in the mixtures of cyclohexane and benzene. It was observed that the activities found in the form of tritiated benzene and cyclohexane are linearly proportional to their mole fraction in the mixture. It was concluded that the reactions of T for H substitution in cyclohexane and benzene molecules in the studied system do not depend on the composition of a mixture. (auth)

40622 REACTIONS OF HOT TRITIUM ATOMS WITH ALCOHOLS AND WITH SOME OF THEIR BINARY HYDROCARBON MIXTURES. Filatov, E. S.; Nesmeyanov, An. N.; Chiang, Tai-wang (Moscow State Univ.). pp 277-99 of STI/PUB/91(Vol.I). (In Russian).

The reaction yields of hot tritium atoms were studied with the aim of investigating the influence exerted by processes of intramolecular and intermolecular energy transfer in reactions of hot tritium atoms with, firstly, aliphatic alcohols, and secondly, in binary mixtures of alcohols with benzene and cyclohexane, as a function of concentration of components, and length of the alcohol molecule. Mixtures of lithium carbonate and the experimental substances were irradiated in a reactor at fluxes varying between 10^{11} and 10^{13} n/cm^2·s, over periods of between 15 and 6 hr. Analysis was carried out on a chromatographic unit with interchangeable columns (molecular sieves, tricresylphosphate and liquid petrolatum on kieselguhr, and cotton wool treated with methyl alcohol). The data obtained are explained in terms of the existence of a mechanism for the effective intramolecular energy transfer from the collision site of the hot atom along the hydrocarbon chain of the alcohol molecules to the OH group capable of dissipating it. The influence of the intermolecular energy transfer process was not unequivocally established. It is possible that a considerable part is played in this process by the difference in microscopic cross-section of the primary event in the interaction of the hot atom with the molecule, and by the change in the moderating atom spectrum with the increase in concentration of one of the components. (auth)

40623 REACTIONS OF HOT ^{38}Cl ATOMS IN MIXTURES OF CARBON TETRACHLORIDE WITH ALIPHATIC ALCOHOLS. Vasaros, L. (Central Research Inst. for Physics, Budapest). pp 301-9 of STI/PUB/91(Vol.I).

Chemical processes induced by hot ^{38}Cl from the nuclear reaction $^{37}Cl(n,\gamma)^{38}Cl$ were investigated in mixtures of CCl_4-ROH (where R = CH_3-, C_2H_5-, C_3H_7- and $(CH_3)_2CH$-). The irradiations were performed in the thermal column of the 2 Mw VVRS reactor using rather short exposure times to keep the radiation chemical effects at negligible level. The organic fractions were separated from the inorganic ones by extraction and the former were analyzed by gas chromatography. Total retention and the yield of the complete set of organic chlorine compounds were determined in terms of alcohol concentration. Some interesting results were that the yield of reaction products in which the OH radical of aliphatic alcohol was replaced by ^{38}Cl increased with increasing alcohol concentration with a simultaneous decrease in the labeled CCl_4 yield and that, in addition to the monochlorine derivates with less carbon atoms than the alcohol molecule, a considerable amount of chloroform was formed with maximum yield at a given alcohol concentration. The relative contributions of the hot and the epithermal stabilization processes of energetic ^{38}Cl and the mechanism of the various reactions are discussed. (P.C.H.)

40624 CHEMICAL EFFECTS OF NUCLEAR RECOIL IN ORGANIC HALIDE SYSTEMS: A NEW THEORETICAL TREATMENT AND EXPERIMENTAL VERIFICATION OF THE THEORY. Kontis, S. S.; Sanitwongs, P.; Weston, M. (Univ. of Durham, Eng.). pp 311-31 of STI/PUB/91(Vol.I).

Methods were developed for calculating the organic retention of radiohalogen to be expected following neutron activation of mixtures of two organic halides and the corresponding free halogen. The methods are based on the concepts of the Libby billiard-ball process of hot-atom labeling and retentions are expressed in terms of two types of parameters: the fractional chance that collision of a hot radiohalogen atom with a particular molecule will lead to retention of the hot atom in that molecule: the upper and lower energy limits for what is termed a hot bromine atom. It is shown how the former type of parameter may be derived from experiments with binary mixtures of an organic halide and the corresponding free halogen: the second type of parameter must be deduced from nuclear and chemical data. These methods were tested by studies on the systems C_2H_5Br-CCl_4-Br_2 and C_2H_5Br-C_6H_5Br-Br_2. The calculated retentions (using parameters derived from studies of the systems C_2H_5Br-Br_2, CCl_4-Br_2, and C_6H_5Br-Br_2) are in good agreement with those found experimentally in mixtures with a bromine mole-fraction greater than about 0.1. It is therefore considered that the Libby mechanism is adequate to explain the observed organic retentions in such mixtures. As the bromine mole-fraction is reduced below 0.1 the observed retentions become progressively higher than calculated values. This is attributed to there being additional modes of hot-atom labeling which become operative when the bromine concentration is not high enough to give adequate radical scavenging. (auth)

40625 THE STEREOCHEMISTRY OF THE REACTIONS OF (n,γ) HALOGEN ATOMS WITH ALKYL HALIDES IN THE LIQUID PHASE. Rowland, F. S.; Wai, C. M.; Ting, C. T.; Miller, G. (Univ. of Kansas, Manhattan; Univ. of California, Irvine). pp 333-48 of STI/PUB/91 (Vol. I).

The reactions of $(n,\gamma)^{38}Cl$ atoms with meso- and dl-2, 3-dichlorobutane were investigated under a variety of experimental conditions, using radio gas chromatography for product analysis. In the liquid phase at 20°C, the ratio of the two radioactive diastereomers formed in this reaction is 5:2 favoring the irradiated molecule, for irradiations of either the meso or the dl forms. In the gas phase, the amounts of each are reduced by a factor of >10 for both products. The results indicate that the $CH_3CHClCH^{38}ClCH_3$ molecules found in the liquid phase are formed primarily by combination reactions on a time scale comparable to the racemization of $CH_3CHCHClCH_3$ radicals, i.e. in cage-like processes. Irradiations in the liquid phase at lower temperatures or in the solid phase show that the two diastereomers are formed in more nearly equal amounts than in the liquid at room temperature. The reactions of $(n,\gamma)^{38}Cl$ with either cis- or trans- 1,2-dichloroethylene in the liquid phase produced radioactive forms of each in both cases, with the yield of the labeled parent molecule strongly predominating over the opposite isomer in each case. These reactions again illustrate a substitution reaction occurring on a time scale comparable to that required for the racemization of radicals. The replacment of Cl by ^{80m}Br was much more stereospecific than the corresponding ^{38}Cl reactions, but again radioactive forms of both of the dl pairs of $CH_3CHBrCHClCH_3$ were observed. The substitution of ^{38}Cl for H was studied in detail with CH_3Cl, and with both 1-chlorobutane and 2-chlorobutane. Radioactive 1, 1-, 1,2-, 1,3-, and 1,4-dichlorobutane and 1,3-dichloropropane were observed from 1-chlorobutane; radioactive 1,3-, 2,2-, 2,3-, and 2,4-dichlorobutane, and 1,1- and 1,2-dichloropropane were found in 2-chlorobutane; the yields of the remaining dichloropropanes and dichlorobutanes were negligible in each case. These reactions are therefore highly specific and result from the replacement without rearrangement of the H atoms or CH_3 groups of the original molecule. The yields of all products were roughly comparable with the number of groups whose displacement leads to their formation, but show some chemical selectivity in addition, e.g. the yields of meso and dl-2, 3-dichlorobutane are not equal from 2-chlorobutane. (auth)

40626 EFFECTS OF TEMPERATURE AND PRESSURE ON HOT-ATOM REACTIONS IN BROMOETHANE. Cole, A. J.; Mia, M. D.; Miller, G. E.; Shaw, P. F. D. (Oxford Univ.). pp 351-72 of STI/PUB/91(Vol.I).

A study was made of the yields of compounds containing ^{80m}Br produced by irradiation of bromethane-bromine mixtures with 14 Mev neutrons at 18, −80, and −115°C, and at atmospheric pressure, and also at 18°C at pressures up to 10^4 atm. In addition to compounds previously reported in this system, small quantities of bromoethene, 1:2 dibromoethene, mono- and dibromopropanes, and mono-, di-, tri-, and tetra-bromobutanes were found. There was also indirect evidence for the production of bromobutenes. The diffusion-dependent reactions are complex, and can be explained by assuming that pyrolysis of the liquid occurs in the vicinity of the hot atom to give bromoethyl radicals and ethylene. Addition of radicals to the latter then accounts for the formation of bromides containing more than two carbon atoms and for their diffusion-dependent yields. Reduction in temperature or increase in pressure generally causes an increase in yield attributable to a decreased rate of diffusion. The effect was most marked upon the yield of 1:2 dibromoethane, which was largely produced by the diffusive reaction of bromoethyl radicals and which increased fourfold by the application of 10^4 atm because of the suppression of the dissociation $CH_2-CH_2Br \rightarrow CH_2=CH_2 + Br$ under the influence of the hot-spike. By contrast, dissociation of the radical (CH_3-CHBr) into bromoethene and a hydrogen atom is energetically forbidden, and the yield of 1:1 dibromoethane is roughly independent of pressure. The variation with temperature and pressure of the yield of bromoethane at large bromine concentrations was close to that predicted previously. (auth)

40627 THE INTERACTION OF ^{14}C RECOIL ATOMS IN BINARY MIXTURES. Firsova, L. P.; Barakat, M. F.; Forys, M.; Nesmeyanov, An. N. (Moscow State Univ.). pp 373-83 of STI/PUB/91(Vol.I). (In Russian).

A study was made of the intermolecular distribution of activity in ^{14}C-labeled products, formed as a result of the interaction of ^{14}C atoms with components of binary liquid mixtures containing heterocyclic compounds. Particular attention was paid to the systems indole-aniline, indole-pyridine, α-picoline-toluene, α-picoline-aniline, etc. Data were obtained on the relation between the radiochemical yields of labeled products and the concentration of compo-

nents in dilute solutions and in comparable concentrations of substances in mixtures. Analysis of the experimental results for an additive system enabled the deviations to be determined from the additivity principle. The deviations observed were interpreted as the result of the participation of the second component of the system in the primary and secondary reactions accompanying nuclear transformations. In considering the role of the second component, the variations in its predominant reaction mechanisms in various concentration ranges were considered. Special attention was paid to the possibility of an intermolecular transfer of the energy of a radiation shield, and also of the mechanism of the corresponding processes. (auth)

40628 THE FORMATION OF POLYMERIC PRODUCTS IN REACTIONS OF POLYVALENT RECOIL ATOMS. Dzantiev, B. G.; Stukan, R. A.; Shvedchikov, A. P.; Shishkov, A. V. (Inst. of Chemical Physics, Moscow). pp 399-409 of STI/PUB/91(Vol.I). (In Russian).

Studies were made on the behavior of recoil atoms of sulfur-35 and carbon-14, obtained in the nuclear reactions $^{35}Cl(n,p)^{35}S$ and $^{14}N(n,p)^{14}C$ in gas and liquid phases. It can be assumed that in the stabilization process hot carbon atoms form methylene biradicals, whose behavior, by reason of their reaction capacity, greatly resembles that of atomic sulfur. The investigations were conducted like those for paraffins (CH_4, C_2H_6), and for cyclic hydrocarbons (cyclohexane, cyclohexene, benzene). The binary systems comprising hydrocarbons on the one hand and ^{35}S and ^{14}C hot-atom donors on the other were subjected to irradiation. Compounds of CCl_4, HCl, and ammonia were used as the donors. Irradiation was carried out on a reactor type IRT-1000 with a thermal neutron flux of 10^{11}-10^{12} n/cm^2·s. It is shown that for various compounds in the liquid phase, up to 60-90% of the sulfur-35 becomes stabilized in the form of a polymer, the yield of which is highly dependent on the composition, passing through the maximum at a nearly equimolecular ratio of components. In the gas phase the polymer yield amounts to 30-40% of the total activity. By means of paper radiochromatography it was established that labeled polymer products have a complex structure and are, at the least, a mixture of compounds of two qualitatively different types whose yield changes in various ways depending upon the ratio of the components. An increase in irradiation time leads to an increase in the labeled polymer yield. In the case of the liquid phase system C_6H_{12}–CCl_4, the molecular weight of the polymer was determined by capillary diffusion and found to be 5000 for the polymer of one type and 500-1000 for the other. The formation of a labeled product with a high boiling point was also observed when pure CCl_4 was irradiated. Analogous experiments were carried out in an ethylene-ammonia system in the gas phase, at high pressure. It is shown that in this case, when pure anhydrous ammonia is irradiated the basic labeled product is $^{14}CH_4$. However, when even small additions of ethylene are made, a considerable proportion (up to 80%) of ^{14}C becomes stabilized in the form of a polymer, whose yield also varies extremely with the growth in the proportion of ethylene in the system, attaining a maximum when there is 10-15% of C_2H_4. It is shown that if ^{14}C polymer yield is plotted against composition, the shape of the curve does not change when dose rate and flux are increased. (auth)

40629 REACTIONS OF HOT TRITIUM ATOMS WITH AMINO ACIDS. Simonov, E. F.; Nesmeyanov, An. N. (Moscow State Univ.). pp 411-19 of STI/PUB/91(Vol.I). (In Russian).

A study was made of the yields from the reaction of hot tritium atoms: with amino acids having lengthened chains, and with amino acids having a carbon chain of constant length, but with various functional substitutes. For this purpose mixtures of lithium carbonate and the acids under study were irradiated for 15 min with a slow neutron flux of 0.87×10^{13} cm^2/s. Analysis was carried out on a gas chromatography unit with interchangeable columns (molecular sieves, and liquid petrolatum on kieselguhr) and with paper chromatography. Although the data obtained for the radiation survival capacity of amino acids as a function of carbon chain length were at variance with a basic tenet of radiation chemistry according to which the conservation of molecules increases in proportion to the length of their chains, the data can be explained in terms of an intramolecular transfer of energy along the carbon chain from the collision site of the hot atom to the hydroxyl group, and subsequent de-excitation; on the other hand, although the energy of tritium recoil atoms is greater than that of the chemical bond, the latter nevertheless exerts an influence on the radiation conservation of molecules with a carbon chain of constant length but with various substitutes. (P.C.H.)

40630 RELATIVE ROLES OF PYROLYSIS AND RADIOLYSIS IN THE DEGRADATION OF TERPHENYLS. Mason, Edward A.; Terrien, Jean-Francois; Timmins, Tom H. (Massachusetts Inst. of Tech., Cambridge). 4p. (CONF-654-90). Gmelin, AED-CONF-64-219-113.

From American Nuclear Society Meeting, San Francisco, Nov.-Dec. 1964.

The effects of radiation on terphenyl coolants for nuclear reactors were studied at 425 and 610°F. It was previously proposed that the rate of pyrolysis of irradiated coolant is considerably greater than that of unirradiated coolant and that coolant degradation could be considered to be due to the combined, but independent, effects of pyrolysis and radiolysis. The pyrolysis constants obtained for irradiated Santowax WR were greater than those for unirradiated coolant. Degradation yields reported for irradiations of encapsulated samples of terphenyls by electrons, gamma rays, and mixed reactor radiations produced values ranging from unity to a high of about 2.4. (F.J.H.)

40631 THERMOLUMINESCENT FORMATION OF Cr^{2+} IN MAGNESIUM OXIDE. Wertz, John E.; Coffman, Robert E. (Univ. of Minnesota, Minneapolis). 13p. (CONF-641210-20). Gmelin, AED-CONF-64-236-33.

From American Physical Society Meeting, Berkeley, Calif.

In undoped crystals of MgO, x irradiation converted a large fraction of Cr^{3+} in octahedral symmetry to Cr^{2+}. Heating such crystals until a blue thermoluminescence was observed caused further reduction. Usually 95% or more of the Cr^{3+} was converted by the combined treatments. However, in Cr-doped MgO only a small fraction of the octahedral chromium could be reduced to Cr^{2+}. The Cr^{2+} was reconverted to Cr^{3+} by heating. ESR measurements showed that in the same temperature interval nearly all of the Fe^{1+} formed on x irradiation disappeared. The source of electrons acquired by Cr^{3+} thus appeared to be the Fe^{1+} ions. The thermoluminescence is ascribed to the Cr^{3+}-electron interaction, as suggested by Hansler and Segelken. (auth)

40632 FINE STRUCTURE OF OPTICAL ABSORPTION BANDS IN NEUTRON IRRADIATED MgO. Tanton, George A.; Shatas, Romas A.; Coulter, C. Alton (Army Missile Command, Redstone Arsenal, Ala.). 58p. (CONF-641114-7). Gmelin, AED-CONF-64-194-16.

From American Physical Society, Southeastern Section, Chattanooga.

The fine structure of optical absorption bands in neutron-irradiated MgO was observed at liquid He temperatures. Samples that received a total integrated epi-cadmium neutron flux of 10^{16} neutrons/cm^2 were studied and compared to samples that received a total dosage of 10^{17} and 10^{18} neutrons/cm^2. An interpretation of the fine structure in terms of phonon creation and annihilation, based on earlier theories for broad band absorption, was attempted with emphasis on the 0-phonon line. In 10^{18} neutrons/cm^2 MgO, the 0-phonon line of the 4.4-ev absorption band (α_{max} ~200 cm^{-1}, width at half maximum ~0.5 ev at 77°K) appeared as a sharp peak on the low energy shoulder at 3.425 ev (α_{max} >5 cm^{-1}, width at half maximum $< 2 \cdot 10^{-3}$ ev) at 77°K and 3.428 (α_{max} >9 cm^{-1}, width $< 2 \cdot 10^{-3}$ ev) at 4°K. Only the height of the 0-phonon transition depended on the irradiation dose. The mirror symmetry of the absorption and the luminescence band was also found. At

77°K, the luminescence band caused by 4.4-ev excitation was in the region of 2.4 ev. Above 100°K, the luminescence band as well as the 0-phonon transition was quenched. At 4°K, the fine structure on the shoulder of the absorption band, caused by the first few phonon transitions, yielded information concerning the vibrational spectrum of the lattice. The Huang-Rhys factor was compared to values given by other authors for alkali halides. Essential agreement was found between values calculated from the theory and values found from the investigations of others for a given compound. Discrepancies existed in results obtained from calculating the Huang-Rhys factor in different ways. (auth)

40633 PROCESS FOR PREPARING RADIATION STABILIZED POLYETHYLENE AND FOOD PACKAGE UTILIZING SAME. Schlein, Herbert N.; La Liberte, Bernard R. (to U. S. Army). U. S. Patent 3,194,668. July 13, 1965. Filed Apr. 8, 1963.

The addition of 0.1 to 5.0 wt % of 2,2'-methylene-bis-(4-methyl-6-t-butyl-phenol) prevents odor formation when polyethylene film is exposed to high energy ionizing radiation. After exposure to a dose of ionizing radiation sufficient for food-sterilization, the modified polyethylene is suitable for the use as an envelope for containing food that is being sterilized by high energy ionizing radiation without danger of offensive odor formation that would render the food unusable. (B.L.M.)

Radiochemistry

See also Separation Processes and Procedures.

Refer also to abstract 41657.

40634 (BNL-8405) A NOVEL SYNTHESIS OF CARRIER-FREE ^{106}Ru-LABELED RUTHENOCENE. Zahn, Ursel; Harbottle, Garman (Brookhaven National Lab., Upton, N. Y.). [1961]. Contract AT(30-2)-Gen-16. 9p. Dep. mn; CFSTI, $1.00 cy, $0.50 mn.

A simple synthesis of ^{106}Ru-labeled ruthenocene is reported which consists of the direct reaction of carrier-free $^{106}RuCl_3$ with liquid cyclopentadiene at room temperature, and the separation of the synthesized ruthenocene with ferrocene carrier. Yields were about 2% owing to the termination of the reaction by dimerization of cyclopentadiene. Gamma rays and light had little or no effect on the yields, while the addition of base slightly improved the yields. (D.L.C.)

40635 (NUS-217) CALCULATIONAL MODELS FOR BETA DOSE FROM SPHERICAL PARTICLES. Anno, George H. (Nuclear Utility Services, Inc., Washington, D. C.). Feb. 26, 1965. 83p. Dep. mn; CFSTI, $3.00 cy, $0.75 mn.

A means of calculating the beta ray dose in tissue from a mixed radionuclide source particle of arbitrary size is considered for possible inclusion in the ROVER Flight Safety evaluation or NURSE programs. For the present case, the source particle is a high-Z material ($Z \simeq 84$) and contains a mixed beta ray spectra, while dose distribution in tissue, a low-Z material ($Z \simeq 7$), is desired; a situation for which appropriate data are lacking. An investigation of the presently available techniques and data was carried out in order to (1) prescribe a method of computing the beta dose from a fuel particle for present use and also to (2) determine alternate methods to accomplish this task more accurately, perhaps by more detailed methods, if necessary in the future. A current calculational model based on experimental dose attenuation of more monoenergetic beta ray sources was developed for which the equations can readily be translated to FORTRAN. Some hand calculations have been made in order to compare results with experimental data and results obtained by other methods. These comparisons indicate good agreement with measured data for the particle surface leakage dose, and only approximate agreement for deeper penetration. (auth)

40636 (WAPD-TM-516) MO608—A FORTRAN PROGRAM TO EVALUATE RADIOCHEMICAL DATA. Rider, J. L. (Bettis Atomic Power Lab., Pittsburgh, Pa.). July 1965. Contract AT-11-1-GEN-14. 32p. Dep. mn; CFSTI $2.00 cy, $0.50 mn.

MO608, a program to evaluate experimental radiochemical data, modifies basic sample counting data to correct for background radiation, counter efficiency, fraction of carrier recovered, decay of the sample, and fraction of the total sample which is counted. Provisions are incorporated to permit correlation of the basic data with material deposition and release, energy deposition, etc. The program also provides the probable percentage error of the net average counting rates of the sample. (auth)

40637 (ORNL-tr-625) THE USE OF ETHANOL IN ISOLATING ^{22}Na FROM CYCLOTRON TARGETS. Zhukovskaya, A. S. Translated by S. J. Rimshaw and J. J. Pinajian (Oak Ridge National Lab., Tenn.), from Radiokhimiya, 7: 125-6(1965). 6p. Dep. mn; CFSTI, $1.00 cy, $0.50 mn; JCL, $1.10 fs, $0.80 mf.

Sodium-22 is separated from a cyclotron target of magnesium metal by first leaching the sodium with ethyl alcohol from magnesium sulfate, followed by purification of the solution on an ion exchange column. The yield of ^{22}Na is 97%, the time necessary for the procedure is 6-8 hr starting with dissolution of the target. (auth)

40638 RADIOACTIVE HYDROGEN. White, G. R. (Univ. of Auckland, N. Z.). J. New Zealand Inst. Chem., 29: 14-20(Feb. 1965).

Properties of tritium are discussed. Methods of detecting beta particles from tritium decay are considered. Uses of tritium and methods of preparing tritium-labeled compounds are outlined. (M.C.G.)

40639 ASEPTIC PRODUCTION OF STERILE PYROGEN-FREE HUMAN ALBUMIN, LABELED WITH ^{131}I. Elekes, Istvan; Koritsanszky, Denes (MTA Orvosradiologiai Kutatocsoport, Budapest). Magy. Radiol., 17: 166-9 (June 1965). (In Hungarian).

Improvements on the McFarlane method of producing pyrogen-free, ^{131}I-labeled serum albumin are described in detail. The new method lends itself for use in small hospitals with less complete lab facilities. The method involves the following six steps: preparation of radioiodine solution, preparation of the albumin solution, iodine labeling, removal of inorganic iodine, filtering, and packaging. Cleaning and sterilization of all vessels, filters, and surrounding area is described. The resulting solution has a specific activity of 1 mC/ml, the albumin-bound ^{131}I activity is 45 to 52% of that theoretically possible, and the protein content is 6 to 7%. It was noted that the inorganic iodine content was about 0.5% after ion-exchange resin treatment, and this percentage increased during storage and reached 5% after 10 days. The inorganic iodine content should be checked before use. (TCO)

40640 DETERMINATION OF THE NUMBER OF FISSIONS IN NATURAL URANIUM MIXTURE IRRADIATED BY NEUTRONS. Belov, S. V.; Anikin, V. S. Radiokhimiya, 7: 120-4(1965). (In Russian).

Descriptions are given of a method for determining the number of fissions in irradiated specimens using a gamma-scintillation spectrometer with a 30-mm dia, 15-mm thick NaI(Tl) crystal and an FEU-C photomultiplier. The method was based on determining the activity of ^{140}Ba in relation to the γ emission of ^{140}La at 1.59 Mev. The order of error did not exceed 5%. The tabulated data from radiochemical analysis of ^{140}Ba in irradiated uranium products was in agreement with the data obtained by means of the gamma scintillation spectrometer. (R.V.J.)

40641 THE BIOSYNTHESIS OF RADIOACTIVE UBIQUINONE-50 (thesis). Black, Wayne Edward. St. Louis, St. Louis Univ., 1964. 158p.

Experiments were devised in an attempt to prepare chemically synthetic derivatives of ubiquinone by an alkoxide exchange reaction. This reaction involved the ex-

change of alkoxyl groups with the methoxyl groups present on the quinone ring under basic conditions. Routinely 5 mg of ubiquinone-50 was reacted with 23 mg of ethanol and 2-3 mg of sodium under a nitrogen atmosphere. Numerous attempts to obtain evidence for one of the ethoxy derivatives were unsuccessful. Studies on the biosynthesis of ubiquinone-50 in Rhodospirillum rubrum were initiated. Ubiquinone-50 was isolated from the bacteria after addition of several substrates to the culture media were sodium acetate, shikimic acid, p-aminobenzoic acid, acetate-1-^{14}C, acetate-2-^{14}C, tritiated acetate, DL-mevalonic acid-2-T-lactone, and uniformly labelled phenylalanine-^{14}C. Addition of 200 mg of sodium acetate to cultures containing acetate-1-^{14}C, acetate-2-^{14}C and tritium labelled acetate resulted in a 2-3 fold increase in the specific activity of ubiquinone-50 compared to control cultures. Tritium labeled mevalonic acid was not incorporated into the bacteria since almost 100% of the radioactivity was found in the culture medium after the bacteria was removed by centrifugation. When uniformly labeled phenylalanine-^{14}C was added to a culture medium, some activity was found in ubiquinone. Since the amount of activity was low, this is probably a reflection of phenylalanine metabolism rather than incorporation of the phenyl ring into the nucleus of the quinone. The addition of p-aminobenzoic acid to a culture medium in the presence of tritiate acetate and 200 mg of unlabeled acetate resulted in a 50% decrease of incorporation of radioactivity into the quinone as compared to a control culture without p-aminobenzoic acid present. When a similar experiment was performed with shikimic acid added, approximately a 15% increase in radioactivity in the quinone was observed. Relatively high specific activity (2.6×10^9 dpm/mmole) ubiquinone-50 was obtained biosynthetically from the bacteria R. rubrum by the addition of high specific activity tritiated acetate (100 mc/mmole) to culture media. (Dissertation Abstr.)

Separation Processes and Procedures

See also Analytical Procedures
ISOTOPE TECHNOLOGY — Separation and Production

Refer also to abstracts 40719, 40720, and 40807.

40642 (AERE-R-4969) THE EXTRACTION OF ZINC BY DITHIZONE RETAINED ON CELLULOSE ACETATE. Pierce, T. B.; Peck, P. F. (Atomic Energy Research Establishment, Harwell (England)). July 1965. 7p. Dep. mn; BIS $0.30; HMSO 1s. 9d.

Zinc was extracted from aqueous solution by dithizone (diphenyl thiocarbazone) on cellulose acetate and the uptake of the element compared with the dithizone content of the solid. The distribution of zinc varied as the second power of the hydrogen ion concentration of the aqueous phase, and the rate of extraction of zinc depended on the amount of organic solvent added to the carrier. (auth)

40643 (BNWL-57) RECOVERY OF PLUTONIUM AND URANIUM FROM REACTOR FUEL METALLURGICAL SCRAP. Schulz, W. W. (Battelle-Northwest, Richland, Wash. Pacific Northwest Lab.). June 1965. Contract AT(45-1)-1830. 30p. Dep. mn; CFSTI $2.00 cy, $0.50 mn.

Two flowsheets for the solvent extraction separation of plutonium from uranium and thorium are presented and discussed. In both, uranium and thorium are coextracted (partition column) into a TBP–CCl_4 solvent from an aqueous feed solution derived from various kinds of metallurgical scrap. Plutonium is rejected to the aqueous phase as plutonium(III) in both flowsheets. Finally, in both flowsheets, uranium and thorium are stripped from the organic phase into dilute HNO_3. However, in one flowsheet, a modified version of one proposed earlier by Bruns, a small volume of HNO_3 is used to concentrate the uranium and thorium; the bulk of this concentrate is recycled to the partition column as a reflux stream. Uranium and thorium are stripped into a larger volume of HNO_3 in the other flowsheet and concentration and reflux features are not involved. The reflux flowsheet was tested extensively in mixer-settler runs as well as on a batch scale. Satisfactorily low losses of thorium and uranium to the aqueous phase in the partition column were achieved at the expense of extraction of 0.1 to 0.2% of the plutonium. The nonreflux flowsheet appears capable of giving a cleaner separation of plutonium from uranium and thorium but involves handling large volumes of solution. The possibility of using a static bed of 30% DBBP–CCl_4 to separate plutonium(III) and thorium (after prior extraction of uranium into a TBP–CCl_4 solution) was scouted briefly. This approach does not appear feasible. Finally, extraction of thorium by mixed TBP–DBBP extractants was studied under the condition that the total concentration of both extractants was held constant at 20 vol%. In one set of experiments an unexpected and unexplained, but apparently real, minimum thorium distribution ratio occurred at about 19.5% TBP–0.5% DBBP. (auth)

40644 (BNWL-78) HOT-CELL STUDIES ON THE SEPARATION OF PROTACTINIUM-233 FROM IRRADIATED THORIA BY COPRECIPITATION WITH MANGANESE DIOXIDE. Humphreys, L. L. (Battelle-Northwest, Richland, Wash. Pacific Northwest Lab.). July 1965. Contract AT(45-1)-1830. 12p. Dep. mn; CFSTI $1.00 cy, $0.50 mn.

The most important results were that 97% of the protactinium could be recovered by coprecipitation with manganese dioxide (3.5 g/l) at a loading of 10 mg ^{233}Pa per gram MnO_2, and that after standing for 20 hours with the feed solution (1 M $Th(NO_3)_4$, 1 M HNO_3, 0.01 M HF, 0.1 M NH_2SO_3H, and 35 mg/l ^{233}Pa) 85% of the protactinium was still recovered. This ^{233}Pa concentration results in 1.33 watts per liter of solution. The use of either sulfamic acid or urea, to destroy nitrites, gave very good precipitate stability in this high radiation. Attempts to scavenge protactinium from an 0.1 M acid deficient 1 M $Th(NO_3)_4$ solution using both coformed and preformed MnO_2 and PbO_2 gave low recovery of protactinium and introduced problems with colloid formation. High salt concentration (thorium, aluminum, and sodium nitrates) and fluoride were found to interfere with the scavenging efficiency. Little effect was observed by increasing the amount of scavenging agent over 0.05 moles of coformed MnO_2 precipitated per liter of feed. At this concentration, precipitate volume was found to be about 9% of solution volume. (auth)

40645 (CONF-650918-1) BEHAVIOR OF ACTINIDES AND FISSION PRODUCTS IN TRI-n-BUTYL PHOSPHATE AND IN DI-2-AMYL 2-BUTYLPHOSPHONATE SOLVENT EXTRACTION PROCESSES USING SHORT-RESIDENCE CONTACTORS. Schlea, C. S.; Jennings, A. S. (Du Pont de Nemours (E. I.) and Co., Aiken, S. C. Savannah River Lab.). Sept. 1965. Contract AT(07-2)-1. 34p. Dep. mn; CFSTI, $2.00 cy, $0.50 mn.

From International Conference on the Chemistry of the Solvent Extraction of Metals, Harwell, Berks, Eng.

The behavior of U(VI), Pu(IV)-Pu(III), Np(V)-Np(VI), Zr-Nb, and Ru in recovery of natural and enriched uranium with 2.5 and 30% tri-n-butyl phosphate and 30% di-2-amyl 2-butylphosphonate in short-residence contactors (4 sec/stage) is described and interpreted in terms of mass transfer and chemical kinetic rate constants that have been measured for normal contact times. The observed behavior at short contact times indicates that the particular rate constants used in the interpretation are applicable, and that short-residence-time contactors will perform satisfactorily in conventional radiochemical separations processes. In this comparison and interpretation, the over-all process variables—contact time, radiolysis, and extractant—were varied while the nature of the feed material was maintained constant. Anomalous behavior of Zr–Nb, which was similar in all systems studied, indicates that the nature of the zirconium species in the irradiated fuel before and after dissolution may be a variable affecting its behavior. (auth)

40646 (CONF-650918-2) SELECTION, COST, AND PERFORMANCE OF n-PARAFFIN DILUENTS. Marston, A. L.; West, D. L.; Wilhite, R. N. (Du Pont de Nemours (E. I.) and Co., Aiken, S. C. Savannah River Lab.). July 29, 1965. Contract AT(07-2)-1. 32p. Dep. mn; CFSTI $2.00 cy, $0.50 mn.

From International Conference on the Chemistry of the Solvent Extraction of Metals, Harwell, Berks, Eng.

Commercial normal paraffins have performed well as diluent for tributyl phosphate in the first cycle of the Purex process at the Savannah River Plant since 1961. A variety of chemical and instrumental measurements that have been performed to monitor performance of the solvent are summarized. Normal paraffins were chosen (for the first cycle solvent) as a result of a laboratory study of a wide variety of pure hydrocarbons and of different compound types that were separated from kerosene by molecular sieves. Test procedures used in these studies are described; the tests included chemical and radiolytic degradation, and tendency to form fission product-complexing ligands. Sources of supply and purity of n-paraffins are reviewed, and the current laboratory program to find and evaluate less expensive diluents is described. (auth)

40647 (COO-499-1) SEPARATION OF AMINES BY LIGAND EXCHANGE. PART II. Latterell, J. J.; Walton, H. F. (Colorado Univ., Boulder). [1962]. Contract AT(11-1)-499. 22p. Dep. mn; CFSTI, $1.00 cy, $0.50 mn.

Mixtures of amines were separated by elution chromatography on cation-exchange resins loaded with nickel ions or other cations capable of forming amine complexes. The cations are complexed with ammonia beforehand, and amine molecules exchange with ammonia molecules as ligands. Aqueous ammonia is used as the eluant. The method has proved particularly effective for separating diamines. (auth)

40648 (COO-499-2) SEPARATION OF AMINES BY LIGAND EXCHANGE. PART III. A COMPARISON OF DIFFERENT CATION EXCHANGERS. Hill, Ann Gertrude; Sedgley, Robert; Walton, Harold F. (Colorado Univ., Boulder). [1962]. Contract AT(11-1)-499. 16p. Dep. mn; CFSTI, $1.00 cy, $0.50 mn.

The elution behavior of four amines, ethanolamine, diethanolamine, dimethylamine, and n-butylamine, was studied on four cation-exchange resins and zirconium phosphate, all loaded with nickel ions. Aqueous ammonia was used for elution. Different selectivity orders were found with exchangers of different types. The carboxylic cation-exchange resin gave the sharpest bands, but 2% crosslinked sulfonic resin gave the best separation of these amines. (auth)

40649 (DP-982) SEMIWORKS EVALUATION OF THE MANGANESE DIOXIDE HEAD-END STEP IN THE THOREX PROCESS. Kishbaugh, Albert A. (Du Pont de Nemours (E. I.) and Co., Aiken, S. C. Savannah River Lab.). July 1965. Contract AT(07-2)-1. 11p. Dep. mn; CFSTI $1.00 cy, $0.50 mn.

The standard Savannah River Plant procedure for precipitating MnO_2 as a head-end step in the Purex process is satisfactory for sorption of protactinium in the dilute Thorex process at rates of ~4000 lb Th/day with the following modifications: (1) sulfamic acid is added to the dissolver solution to decompose nitrous acid, which would otherwise dissolve some of the MnO_2, (2) residual liquid skimmed from the centrifuge is recycled, and (3) the volume of dilute acid used in each of the five washes of the MnO_2 precipitate is doubled to 50 gallons. (auth)

40650 (HW-77805) DEVELOPMENT IN CONTINUOUS ION EXCHANGE CONTACTORS—A PROGRESS REPORT. Brandt, H. L. (General Electric Co., Richland, Wash. Hanford Atomic Products Operation). June 7, 1963. Contract AT(45-1)-1350. 18p. Dep. mn; CFSTI $1.00 cy, $0.50 mn.

A pump was developed for moving resin in a differential continuous countercurrent apparatus. Results are reported on the possibility of using this resin pump in a continuously operating unit. The adaption to semi-continuous operation is discussed. (D.L.C.)

40651 (IDO-14657) DECONTAMINATION OF RADIOACTIVE EFFLUENT WITH CLINOPTILOLITE. Rhodes, D. W.; Wilding, M. W. (Phillips Petroleum Co., Idaho Falls, Idaho. Atomic Energy Div.). July 1965. Contract AT(10-1)-205. 14p. Dep. mn; CFSTI $1.00 cy, $0.50 mn.

The removal of strontium-90 and cesium-137 from fuel storage basin effluent by ion exchange using the mineral clinoptilolite as the exchanger is described. The concentration of cesium-137 in the effluent after decontamination was less than its drinking water tolerance, and the concentration of strontium-90 was approximately equal to its tolerance. (auth)

40652 (NAA-SR-11340) PYROCHEMICAL REPROCESSING OF URANIUM CARBIDE. Summary Report. Murbach, E. W.; Brand, G. E. (Atomics International, Canoga Park, Calif.). Aug. 31, 1965. Contract AT(11-1)-Gen-8. 38p. Dep. mn; CFSTI, $2.00 cy, $0.50 mn.

A program was carried out to investigate low decontamination reprocessing of uranium carbide reactor fuel. Three processes were investigated: 1) the CARBOX process which is based on oxidation-carbothermic reduction; 2) a nitride-carbide cycle in which UC is converted to a nitride and then reconverted to the carbide; and 3) a fused-salt electrolysis process in which UC is anodized in a KCl-LiCl salt bath and the uranium cathode deposit converted to UC by reaction with propane in mercury at 350 to 600°C. Decontamination by all three processes was studied with lightly irradiated UC (nvt ~10^{17}). The CARBOX and nitride processes remove about 75% of the fission products, but plutonium losses are high. The electrolysis process removes most fission products except zirconium. Reaction kinetics were studied for a number of the processes. Rates for the reactions between UC and air, oxygen, carbon dioxide, and nitrogen are dependent on the chemical reactivity of the UC. Cost studies on the CARBOX process indicate a potential savings of 0.1 to 0.2 mills/kwh when compared to conventional solvent extraction. (auth)

40653 (NAA-SR-11389) PYROCHEMICAL REPROCESSING OF UO_2 BY AIROX. Summary Report. Brand, G. E.; Murbach, E. W. (Atomics International, Canoga Park, Calif.). Aug. 31, 1965. Contract AT(11-1)-Gen-8. 65p. Dep. mn; CFSTI, $3.00 cy, $0.75 mn.

The AIROX process is based on the oxidation of UO_2 to U_3O_8 and reconversion to UO_2 by reduction with hydrogen. Repeated oxidation-reduction effectively pulverizes the UO_2. Three-foot sections of stainless steel-clad UO_2 were effectively declad by piercing the cladding at 1-in. intervals and exposing to oxygen at ~400°C. Uranium oxide carried through three oxidation-reduction cycles was pressed and sintered at 1700°C. Pellets of over 98% theoretical density were produced. Kilogram scale experiments, using oxides of stable isotopes of representative fission products simulating burnups up to 100,000 Mwd/MTU, showed no significant physical or chemical effect of these elements on the process. A multicycle experiment, using remote methods, demonstrated this process on the 100-g scale with irradiated fuel. Material irradiated to 21,000 Mwd/MTU was declad, oxidized, and reduced through three cycles, pressed into pellets, sintered at 1700°C, re-irradiated to an additional 10,000 Mwd/MTU, and the process repeated. Final pellet densities were from 94 to 96% theoretical. Cesium, rare gases, and iodine were virtually completely removed. Tellurium was partially removed and ruthenium could be removed by carrying out one oxidation step above 725°C. No removal of rare earths was detected. Fuel cycle cost studies on UO_2 fuel, carried out for a 1000 Mw(e) complex (three BWR's), indicate an economic advantage for AIROX, as compared to aqueous reprocessing. The ^{235}U inventory and burnup requirements are higher than for aqueous reprocessing, but the resultant savings from a simpler process more than offset the higher burnup costs. (auth)

40654 (ORNL-3613) THE JOINT NATIONAL INSTITUTES OF HEALTH-ATOMIC ENERGY COMMISSION ZONAL CENTRIFUGATION PROJECT. I. THE DEVEL-

OPMENT OF LOW-SPEED ZONAL ROTORS. Anderson, N. G.; Barringer, H. P.; Nunley, C. E.; Canning, R. E.; Babelay, E. F.; Burger, C. L.; Rankin, C. T. (Oak Ridge National Lab., Tenn.). Oct. 1964. Contract W-7405-eng-26. 18p. Dep. mn; CFSTI $1.00 cy, $0.50 mn.

Two low-speed zonal centrifuge rotors (designated A-V and A-VI) were developed to test the feasibility of zonal separation of particles in the micron size range. Based on these studies rotor A-IX was designed. It has a capacity of 1300 ml, a maximal design speed of 6000 rpm, and suitable seals to allow the gradient and sample layer introduction as well as gradient and zone recovery during rotation. The applicability of this rotor to the problem of isolating subcellular particles is demonstrated. (auth)

40655 (RT/CHI(65)-1) DISSOLUZIONE DEI RIVESTIMENTI IN ALLUMINIO ED IN S.A.P. DI ELEMENTI DI COMBUSTIBILE IN UN DISSOLUTORE A RICIRCOLAZIONE. (Dissolution Experiments of Aluminum and S.A.P. Cladding Material in a Laboratory Recirculation Dissolver). Beone, G. (Comitato Nazionale per l'Energia Nucleare, Rome (Italy)). Jan. 1965. 43p. Dep. mn.

Experiments on the sulfuric acid dissolution of aluminum tubes catalyzed by mercuric sulfate, and on the caustic attack of S.A.P. are reported. A glass recirculation dissolver was used, and the dissolution rates were evaluated under different experimental conditions. The dissolution times and the composition of the resulting solutions are quite acceptable on the bases of applicability to an industrial process. Settling rates of suspended alumina in the caustic dissolution of S.A.P. are favorable. A tentative head end flowsheet for decladding S.A.P. or aluminum-clad fuels is outlined. (auth)

40656 (CEA-tr-X-609) DOSAGE DES IODURES DANS LES PREPARATIONS DE ROSE BENGALE-131I, DE TRIOLEINE-131I, DE GLOBULINE 131I ET DE IODALBUMINE 131I, ET SEPARATION PREALABLE PAR CHROMATOGRAPHIE SUR COUCHE MINCE. (Determination of Iodides in the Preparations of ^{131}I-Rose Bengal, ^{131}I-Triolein, ^{131}I-Globulin, and ^{131}I-Iodoalbumin and Preliminary Separation by Thin Layer Chromatography). Mitta, E. A.; Camin, L. Fraga, H. Translated into French from report CNEA-Inf. No. 110. 1962. 7p. Dep. mn; JCL, $1.10 fs, $0.80 mf.

Thin layer chromatography for the separation of inorganic iodides from labelled organic compounds was evaluated. The experimental technique used is briefly indicated and the results are tabulated for rose bengal, triolein, globulin, and iodoalbumin. (J.S.R.)

40657 LIQUID-LIQUID EXTRACTION OF METAL IONS FROM AQUEOUS SOLUTIONS OF ORGANIC ACIDS WITH HIGH-MOLECULAR-WEIGHT AMINES. THE TRIVALENT ACTINIDE–LANTHANIDE ELEMENTS. Moore, Fletcher L. (Oak Ridge National Lab., Tenn.). Anal. Chem., 37: 1235-9(Sept. 1965). (ORNL-P-1298).

Liquid-liquid extraction systems for trivalent actinide and lanthanide elements are described. High-molecular-weight amines are excellent extractants for anionic complexes of these elements from aqueous solutions of most organic acids. Liquid-liquid extraction behavior is described for the acid systems, citric, tartaric, oxalic, (ethylenedinitrilo)tetraacetic (EDTA), α-hydroxyisobutyric, and acetic, with various primary, secondary, tertiary, and quaternary amines. The high extractability of the anionic EDTA complexes of trivalent actinide, lanthanide, and other metal ions from both acid or alkaline solution is of considerable practical importance. In the actinide–lanthanide series the order of decreasing extractability is americium, curium, californium > europium > samarium > promethium > cerium > yttrium > thulium. Several potential applications in separations are discussed. (auth)

40658 CATION EXCHANGE SEPARATION OF MOLYBDENUM, TUNGSTEN, NIOBIUM, AND TANTALUM FROM OTHER METAL IONS. Fritz, James S.; Dahmer, Lionel H. (Ames Lab., Ames, Iowa). Anal. Chem., 37: 1272-4(Sept. 1965).

The separation of molybdenum, niobium, tantalum, and tungsten from other metal ions by cation exchange is discussed and the procedure described. Analysis of alloys using this method is considered. (F.J.H.)

40659 RARE EARTHS SEPARATION BY ANION EXCHANGE CHROMATOGRAPHY IN SALT SOLUTION. Hamaguchi, Hiroshi; Ishida, Koji; Hikawa, Ikuko; Kuroda, Rokuro (Tokyo Kyoiku Univ.). Anal. Chem., 37: 1283-5 (Sept. 1965).

A stock solution of each rare earth was prepared by dissolving the oxide (99.9% purity) in 3M HNO_3, evaporating to dryness, and diluting with 0.1M HNO_3 to a definite volume. The solutions were standardized by titration with .001M EDTA solution using xylenol orange as indicator. Radioactive tracers, ^{140}La, ^{143}Pr, and ^{159}Gd were produced by irradiating the respective oxide of spectral purity with neutrons. Magnesium nitrate was used as eluent in rare earth separation by anion exchange chromatography. The adsorption of rare earths from the magnesium nitrate solution depended to some extent on free acid concentration. Examples of typical separations are shown. (F.J.H.)

40660 DETERMINATION OF MASS TRANSFER COEFFICIENTS FOR THE LIQUID FILM IN THE SYSTEM UO_2SO_4–ANION EXCHANGE RESINS. Estrada, J.; Jodra, L. G. (Junta de Energia Nuclear, Madrid). Anales Real Soc. Espan. Fis. Quim. (Madrid), Ser. B, 61: 777-82(May 1965). (In Spanish).

Mass transfer coefficients for the liquid film in the process of uranium adsorption from sulfuric acid solutions by anion exchange resins were determined. The concentrations studied varied from 0.1 to 0.5 g U_3O_8/l for resin particle sizes between –20 +48 mesh (Tyler). The data were correlated as a function of the particle size and the solution mass rate. The numerical values of the mass transfer coefficients obtained ranged between 0.140 and 0.565 mg U/(sec) (g of resin) (mg U/ml). (auth)

40661 COMMENTS ON THE ECONOMICS OF FUEL PROCESSING. Thayer, V. R.; Colven, T. J. (E. I. du Pont de Nemours and Co., Inc., Wilmington, Del.). Chem. Eng. Progr., 60: Symp. Ser., No. 51, 95-9(1964).

The unit cost for chemical processing of irradiated nuclear fuel is sharply dependent upon the processing rate. Attainment of acceptable costs depends primarily upon demand sufficient to justify the initial investment, which is large regardless of capacity. Capital and operating costs are shown for rates of one and ten tons per day. (auth)

40662 STUDIES ON THE EFFECT OF SOME POLYHYDRIC ALCOHOLS ON ION-EXCHANGE AND SEPARATION OF RARE EARTHS WITH THE AID OF α-HYDROXYBUTYRIC ACID. Vojtech, O.; Beranova, H. (Inst. of Nuclear Research, Czechoslovak Academy of Sciences, Rez). Collection Czech. Chem. Commun., 30: 1799-1807 (June 1965).

The effects of some compounds from the group of glycols mixed with water on the sorption of tracer quantities of ^{152,154}Eu and ^{90}Y on the cation exchanger S-katex-X8 were investigated. The distribution ratios of the radioisotopes were measured in all these systems in the presence and absence of the complexing agent α-hydroxyisobutyric acid. On the basis of these data separation coefficients were calculated, which indicated the possibility of the application of these compounds for improvement of the chromatographic separation of the rare earths. The possibility of improving the separation of the rare earths by elution chromatography by using, instead of an aqueous solution, an aqueous mixture of solvents with a low dielectric constant, a high dipole moment, and suitable structure is discussed. (auth)

40663 ION EXCHANGE CHROMATOGRAPHY OF RARE EARTHS IN AQUEOUS ORGANIC MEDIA. I. EFFECT OF SOME MIXED MEDIA ON THE SEPARATION OF A MIXTURE OF EUROPIUM WITH YTTRIUM AND PROMETHIUM. Alexa, J. (Inst. of Nuclear Research, Czechoslovak

Academy of Sciences, Rez). Collection Czech. Chem. Commun., 30: 2344-9(July 1965).

Results of the chromatographic separation of a mixture of europium with yttrium and promethium in the presence of α-hydroxyisobutyric acid in media containing various concentrations of acetone, ethylene glycol, dimethyl cellosolve, glycerol, methanol, ethanol, propanol, isopropanol, and tert-butanol are presented. (auth)

40664 ION EXCHANGE CHROMATOGRAPHY OF RARE EARTHS IN AQUEOUS ORGANIC MEDIA. II. EFFECTS OF AQUEOUS ALCOHOL SOLUTIONS ON SORPTION IN NON-COMPLEXING MEDIA. Alexa, J. (Inst. of Nuclear Research, Czechoslovak Academy of Sciences, Rez). Collection Czech. Chem. Commun., 30: 2351-60(July 1965).

The results of measurements of the sorption of europium and yttrium by a strongly acidic cation exchanger in 0.2N sodium perchlorate medium and various concentrations of five alcohols are presented and their theoretical explanation is given. (auth)

40665 ION EXCHANGE CHROMATOGRAPHY OF RARE EARTHS IN AQUEOUS ORGANIC MEDIA. III. EFFECT OF AQUEOUS ALCOHOL SOLUTIONS ON SORPTION FROM COMPLEXING MEDIA. Alexa, J. (Inst. of Nuclear Research, Czechoslovak Academy of Sciences, Rez). Collection Czech. Chem. Commun., 30: 2361-7(July 1965).

The results of studies on the distribution functions of europium and yttrium in media containing α-hydroxyisobutyric acid and various concentrations of five alcohols are reported. (auth)

40666 ION EXCHANGE CHROMATOGRAPHY OF RARE EARTHS IN AQUEOUS ORGANIC MEDIA. IV. EFFECT OF AQUEOUS ALCOHOL SOLUTIONS ON THE SEPARATION FACTOR. Alexa, J. (Inst. of Nuclear Research, Czechoslovak Academy of Sciences, Rez). Collection Czech. Chem. Commun., 30: 2368-72(July 1965).

The results of measurements of the separation factor of a mixture of europium and yttrium in aqueous alcohol solution in the presence of α-hydroxyisobutyric acid are presented. The results showed that the separation factor increased with the decreasing dielectric constant of the medium and decreased with the rising concentration of the nonaqueous component. (auth)

40667 CHEMICAL TREATMENT OF IRRADIATED NUCLEAR FUELS. Faugeras, P. Energie Nucl., 7: 214-27(June 1965). (In French).

The chemical treatment of irradiated fuels is necessary either to recycle the incompletely burned-up fuel in power reactors or, in the case of reactors producing synthetic elements, to isolate these elements. The procedures based on solvent extraction in nitric acid medium have the disadvantage of immobilizing the fuel (by decrease of the activity) and producing large quantities of waste. Several dry method procedures are described, some of which lead to total decontamination and others to partial decontamination. Two promising cycles are emphasized: the procedure based on the volatilization of fluorides for which a pilot installation was constructed at Fontenay-aux-Roses and the pyrometallurgical cycle associated with the American EBR-II reactor. (tr-auth)

40668 PHOSPHO-ORGANIC COMPLEXING RESINS. Nikolaev, A. V.; Gribanova, I. N.; Yakovleva, N. I.; Krylova, L. F. (Inst. of Inorganic Chemistry, Novosibirsk, USSR). Izv. Sibirsk. Otd. Akad. Nauk SSSR, No. 3, Ser. Khim. Nauk, No. 1, 77-81(1965). (In Russian).

The sorption and adsorption rate of uranyl nitrate was studied in order to determine the sorptive properties of five resin polymers: triallylphosphates, diallylmethyl-, diallylbutyl-, and diallylphosphonates and diallylisoamylphosphonate. Complete uranyl nitrate desorption by an aqueous alcoholic ammonium carbonate solution was achieved by treating the resins with the ammonium carbonate solution followed by water elution. Polymer selectivity was illustrated using $UO_2(NO_3)_2$, $La(NO_3)_2$, $Nd(NO_3)_2$, and $FeCl_3$ sorption by butylphosphonate from aqueous and aqueous alcoholic solutions acidified with 2N nitric acid. (R.V.J.)

40669 ON THE ENTHALPY VARIATIONS DURING EXTRACTION ACCORDING TO STANDARD ENTHALPY OF FORMATION. Nikolaev, A. V.; Afanas'ev, Yu. A.; Kuznetsov, F. A. Izv. Sibirsk. Otd. Akad. Nauk SSSR, No. 3, Ser. Khim. Nauk, No. 1, 115-17(1965). (In Russian).

Enthalpy variations during uranyl and thorium nitrate extraction were determined using known magnitudes of standard enthalpy of formation for the anhydrous salts, their hydrates, and water. Data on enthalpy variations for uranyl and thorium nitrates are tabulated and compared with previously published data. (R.V.J.)

40670 ON THE SOLUBILITY OF LANTHANUM FLUORIDE IN BERYLLIUM NITRATE SOLUTIONS. Doronina, V. P.; Batsanova, L. R. (Inst. of Inorganic Chemistry, Novosibirsk, USSR). Izv. Sibirsk. Otd. Akad. Nauk SSSR, No. 3, Ser. Khim. Nauk, No. 1, 128-30(1965). (In Russian).

The solubility of lanthanum fluoride was determined colorimetrically using Arsenazo I. Comparisons of lanthanum, neodymium, and samarium fluorides showed close solubility values, which were 2.5×10^{-4}, 3×10^{-4}, and 3×10^{-4}%, respectively. Lanthanum fluoride began dissolving in dilute beryllium nitrate solutions and with increasing concentration of the latter the content of LaF_3 also increased. The content of LaF_3 in 55% $Be(NO_3)_2$ solution increased about 10000 times in comparison to the content in water. (R.V.J.)

40671 ELECTROPHORESIS OF LANTHANIDES, Sc, Th, U AND Zr IN GLYCOLIC ACID. Guedes de Carvalho, R. A. (Centro de Estudos de Quimica Nuclear, Porto, Portugal). J. Chromatog., 18: 381-4 (May 1965).

The influence of the concentration of glycolic acid and glycolate ion in the electrophoresis of lanthanides was studied. The mobilities of all the lanthanides, and also of Sc, Zr, Th, and U were determined using 1.0M glycolic acid as electrolyte. The best conditions for lanthanide separation were with 1.0M glycolic acid without neutralization. The sign of the predominant ionic species depended on the concentration of glycolate ion. Above 0.3M glycolate all the lanthanides were anionic. (auth)

40672 GAS CHROMATOGRAPHIC SEPARATION OF DEUTERATED METHANES. Bruner, F.; Cartoni, G. P. (Universita, Naples). J. Chromatog., 18: 390-1(May 1965).

Separation of deuterated methanes by gas-solid chromatography with an adsorption glass capillary column is described. A chromatogram of CH_4, CH_3D, CH_2D_2, and CD_4 resolved at low temperature (188°C) is shown. (F.J.H.)

40673 CATION-EXCHANGE SEPARATION OF PROTACTINIUM-233 FROM IRRADIATED THORIUM. Kuroda, Rokuro; Ishida, Koji (Tokyo Kyoiku Univ.). J. Chromatog., 18: 428-40(May 1965).

An ion exchange chromatographic method for separating carrier-free protactinium from neutron-irradiated thorium with a strong acid cation exchanger in thiocyanate–hydrochloric acid solution is described. Protactinium has a tendency to form a stable complex with thiocyanate ions. Protactinium-233 was eluted with 1M NH_4SCN–0.5M HCl, and was recovered in the first 100 ml of the effluent. Thorium removal was completed by elution with approximately 55 ml of 2M NH_4SCN–0.5M HCl solution. (F.J.H.)

40674 CHELATING RESINS. VI. PYRIDINE-2,6-DICARBOXYLIC ACID RESINS FOR THE SEPARATION OF Ca^{2+}/Sr^{2+}. Blasius, E.; Brozio, B. (Universitaet, Berlin and Universitaet des Saarlandes, Saarbruecken, Ger.). J. Chromatog., 18: 572-80(June 1965). (In German).

Three chelating resins were produced by reaction of polyaminostyrene, polyethyleneimine, and poly(ethylenediaminomethyl)-styrene with 4-chloropyridine-2,6-dicarboxylic acid. The structures of the exchanging units of these resins approximate the structures of 4-(N-phenyl)-amino-, 4-dimethylamino-, and 4-methylamino-pyridine-2,6-dicarboxylic acid. A fourth resin was prepared by

mixed condensation of pyridine-2,6-dicarboxylic acid dihydrazide, resorcinol, and formaldehyde. With one exception [matrix poly-(ethylenediaminomethyl)-styrene] the chelating resins described are of good mechanical and chemical stability and possess high capacity. Chromatographic separations were performed in columns containing pyridine-2,6-dicarboxylic acid resins with the matrices polyaminostyrene and polyethyleneimine, respectively. The polyethyleneimine resin was found to be especially well suited for the chromatographic separation of Ca^{2+}/Sr^{2+}. Its Ca^{2+}-capacity was remarkably high (4.2 mequiv/g), so that it could be used for the separation of fairly large quantities. (auth)

40675 A SEQUENTIAL ANALYTICAL SCHEME FOR THE CARRIER-FREE SEPARATION OF MICROGRAM QUANTITIES OF INDIVIDUAL FISSION PRODUCT AND ACTINIDE ELEMENTS FROM HIGHLY BURNT-UP FUELS. de Wet, W. J.; Crouch, E. A. C. (Atomic Energy Research Establishment, Harwell, Berks, Eng.). J. Inorg. Nucl. Chem., 27: 1735-44(Aug. 1965).

An analytical scheme is described which allows for the sequential separation of the elements remaining after large neutron doses are absorbed in 1-mg of a fissile element. The products isolated were in a form amenable to the determination of isotopic abundances by solid source mass-spectrometric methods; solvent extraction, ion exchange, partition chromatography, and precipitation were used to achieve this end. (auth)

40676 DISSOCIATION CONSTANTS OF THE TRANSPLUTONIUM ELEMENT CHELATES OF DIETHYLENETRIAMINEPENTAACETIC ACID (DTPA) AND THE APPLICATION OF DTPA CHELATES TO SOLVENT EXTRACTION SEPARATIONS OF TRANSPLUTONIUM ELEMENTS FROM THE LANTHANIDE ELEMENTS. Baybarz, R. D. (Oak Ridge National Lab., Tenn.) J. Inorg. Nucl. Chem., 27: 1831-9(Aug. 1965). (ORNL-P-1016).

The dissociation constants of the DTPA complexes with Am, Cm, Bk, Cf, Es, and Fm were determined by an ion exchange technique, and the values obtained are: americium $10^{-22.92}$, curium $10^{-22.99}$, berkelium $10^{-22.79}$, californium $10^{-22.57}$, einsteinium $10^{-22.62}$, and fermium $10^{-22.70}$. A solvent extraction system was developed to completely separate the transplutonium elements from the lanthanide fission products by extracting the lanthanide elements into an organophosphonate solution from a carboxylic acid-buffered solution of DTPA. The separation factor between americium and the lanthanide elements was about fifty. (auth)

40677 THE PARTITION COEFFICIENTS OF NITRATONITROSYLRUTHENIUM COMPLEXES BETWEEN NITRIC ACID AND TBP PHASES. Fletcher, J. M.; Lyon, C. E.; Wain, A. G. (Atomic Energy Research Establishment, Harwell Berks, Eng.). J. Inorg. Nucl. Chem., 27: 1841-51(Aug. 1965).

Both the non-ionic trinitrato complex and the tetranitrato acid of nitrosylruthenium (III) have relatively high partition coefficients at 0°C in TBP–diluent–HNO_3 systems. That of the tetranitrato acid was slightly the higher for > 10% TBP. The acid also formed a second organic phase more rapidly. The partition coefficients indicated that it is only the free TBP, i.e. that not present as TBP-HNO_3, that is available for the extraction of these complexes. For the trinitrato complex, both its extraction behavior and the infrared spectrum of a saturated TBP phase indicated that TBP groups are attached by hydrogen bonding. The partition coefficients were consistent with the attachment of four TBP groups to the hydrogen atoms of the two aquo groups; the formation constant, calculated for this tetra-solvated complex was $\sim 2 \times 10^4$ over the range 5 to 30% TBP and 0.5 to 5M aqueous nitric acid. The partition coefficients for the tetranitrato acid were also consistent with there being only hydrogen-bonded TBP groups in the organic phase with the cation of the ion-pair as $[(TBP{\cdot}H)_3O]^+$. (auth)

40678 THE EXTRACTION OF URANIUM(VI) FROM HYDROCHLORIC ACID SOLUTIONS BY DI-(2-ETHYLHEXYL)-PHOSPHORIC ACID. Sato, Taichi (Government Chemical Industrial Research Inst., Tokyo). J. Inorg. Nucl. Chem., 27: 1853-60(Aug. 1965).

The partition of uranium (VI) between hydrochloric acid solutions and solutions of di-(2-ethylhexyl)-phosphoric acid (DEHPA) in kerosene was investigated, and the effects of organic solvent and of the addition of tri-n-butyl phosphate (TBP) on this extraction system were examined. The mechanism of the extraction is discussed. (auth)

40679 THE SORPTION OF Sr, Ce, Ru AND Zr ON TUNGSTEN FERROCYANIDE. Krtil, J. (Inst. of Nuclear Research, Czechoslovak Academy of Sciences, Rez). J. Inorg. Nucl. Chem., 27: 1862-4(Aug. 1965).

Static sorption of Sr, Ce, Ru, and Zr on tungsten ferrocyanide was studied by tracer techniques. Distribution and selectivity coefficients were determined. (M.C.G.)

40680 INVESTIGATION OF THE ION EXCHANGE SEPARATION OF THE RARE EARTH METALS. III. A REVERSAL OF THE ORDER OF ELUTION OF EUROPIUM AND YTTRIUM IN THEIR ELUTION FROM DOWEX 50W x 8 WITH AMMONIUM ACETATE. Mikler, J. (Universitaet, Vienna). Monatsh. Chem., 96: 1007-13 (1965). (In German).

The elution sequence of yttrium and europium from Dowex 50 W × 8 with ammonium acetate is dependent on the concentration of the eluant. Using 0.73M $(NH_4)_{0.94}H_{0.06}OCOCH_3$ europium and yttrium showed the same behavior on elution. With lower concentrations but constant composition of the eluant, europium was eluted before yttrium; with higher concentrations the situation was reversed. Comparison with another study showed that different crosslinked resins at otherwise identical conditions also give inverse elution positions of the two elements. (auth)

40681 THE POLAROGRAPHIC BEHAVIOUR OF THE LANTHANOIDS IN DIMETHYLSULPHOXIDE AND DIMETHYLFORMAMIDE. Gritzner, G.; Gutmann, V.; Schoeber, G. (Technische Hochschule, Vienna). Monatsh. Chem., 96: 1056-64(1965). (In German).

The half wave potentials of chlorides of lanthanides were measured in dimethylsulfoxide and in dimethylformamide vs an aqueous saturated calomel electrode. La, Ce, Pr, Nd, Gd, Tb, Dy, Ho, and Er give one wave and Sm, Eu, and Yb two waves all with limiting currents due to diffusion without maxima. The differences in half wave potentials of the cerium group and the yttrium group in dimethylformamide allow their polarographic separation. The influence of traces of water was negligibly small. (auth)

40682 EXTRACTION OF URANYL SALTS BY THENOYLTRIFLUOROACETONE IN CARBON TETRACHLORIDE. Awwal, M. A. (Pakistan Atomic Energy Commission, Karachi). Pakistan J. Sci. Ind. Res., 8: 70-2(Apr. 1965).

The extraction of uranyl chlorides, nitrates, and sulfates with equal volume of thenoyltrifluoroacetone in carbon tetrachloride is described. Data are presented in tables. (F.J.H.)

40683 SEPARATION COEFFICIENTS FOR RADIOACTIVE FISSION ELEMENTS IN THE DIRECTIONAL PROCESS OF SODIUM NITRATE CRYSTALLIZATION. Kirgintsev, A. N.; Avvakumov, E. G.; Kuleshov, I. M. Radiokhimiya, 7: 1-7(1965). (In Russian).

The distribution of some radioactive fission fragments in the process of directional crystallization of sodium nitrate was investigated. Their separation coefficients were determined. It was found that for microquantities of nonisomorphous admixtures the equation $\lambda = 1-(-bf)$ is suitable. From the data obtained it was concluded that the capture of radioactive elements during the crystallization of sodium nitrate from melts increases with the increasing charge of ionic admixtures. (tr-auth)

40684 URANIUM EXTRACTION FROM HF–HNO_3 BY THE TERNARY AMINES IN BENZENE. Vdovenko, V. M.;

Koval'skaya, M. P.; Smirnova, E. A. Radiokhimiya, 7: 7-14(1965). (In Russian).

During the extraction of HNO_3 and HF from their mixtures, the presence of HNO_3 in HF solution strongly reduces the HF concentration in the organic phase. In the extraction of uranium from aqueous solutions containing constant concentrations of uranyl fluoride and hydrofluoric acid and variable concentrations of nitric acid, the curves of the dependence of the distribution coefficients of uranium on the concentration of HNO_3 passes through a minimum. On the basis of spectrophotometric measurement it was shown that during extraction of uranium from HF – HNO_3 mixtures with increased concentration of nitric acid in aqueous solution, the fraction of uranium fluoride complexes decreased in the organic phase and the fraction of nitrate complexes increased. For constant concentrations of nitric acid and variable concentrations of hydrofluoric acid, the extraction of uranium from acid mixtures strongly depended on the ratio of concentrations of nitric acid in amines. When $C_{HNO_3} < C_{amine}$, the distribution coefficient of uranium at first increased sharply with increased concentration of HF in the aqueous phase and then gradually decreased. If $C_{HNO_3} > C_{amine}$, the addition of HF to the aqueous solution led to a decrease of the distribution coefficient of uranium. (tr-auth)

40685 MICROCHROMATOGRAPHIC COLUMN WITH REMOTE CONTROL. Lebedev, N. A.; Tolstoi, N. S.; Khalkin, V. A. Radiokhimiya, 7: 115-17(1965). (In Russian).

Descriptions are given of the design and operation of a remotely controlled microchromotographic column used for separating radioactive elements. Over-all dimensions of the installation are $0.23 \times 0.33 \times 0.70$ M^3 and a weight of 15 kg. It can be easily installed in a specially designed shielded cupboard or behind a temporary shielding made of lead bricks with TF-5 type glass. (R.V.J.)

40686 USE OF ETHANOL IN SEPARATION OF SODIUM-22 FROM CYCLOTRON TARGET. Zhukovskaya, A. S. Radiokhimiya, 7: 125-6(1965). (In Russian).

A method for the separation of ^{22}Na from Mg cyclotron targets including a preliminary leaching of Na with ethyl alcohol from magnesium sulfate and subsequent purification of the solution in ion exchange columns was proposed. The yield of ^{22}Na was 97%. The time necessary for the separation beginning with the disolution of the target is 6 to 8 hrs. (tr-auth)

40687 SEPARATION OF TRACES OF METALS FROM URANIUM BY CHROMATOGRAPHY ON CELLULOSE COLUMN. Muzzarelli, R. A. A.; Bate, L. C. (Oak Ridge National Lab., Tenn.). Talanta, 12: 823-7(Sept. 1965). (ORNL-P-964).

Submicrogram amounts of thirteen metals were separated from 50 g of uranyl nitrate by adsorption chromatography on cellulose column. The adsorbed metals were eluted by solutions of potassium thiocyanate and hydrochloric acid in organic solvents. The quantitative recovery of metals was verified by using radioisotopes and gamma spectrometry. (auth)

40688 REACTION OF $U(SO_4)_2 \cdot 4H_2O$ WITH TRI-n-OCTYLAMINE SULFATES AND BISULFATES. Nazarov, A. S.; Sergievskii, V. V.; Gromov, B. V. (Mendeleev Inst. of Chemical Tech., Moscow). Zh. Neorgan. Khim., 10: 1500-1(June 1965). (In Russian).

The crystal hydrate of $U(SO_4)_2 \cdot 4H_2O$ is soluble in TOA (tri-n-octylamine) sulfate solutions and it is not soluble in the similar TOA bisulfate solutions. A saturation method showed that the soluble crystal hydrate in the organic phase formed $(R_3NH)_6\ U(SO_4)_5 \cdot 5H_2O$. (R.V.J.)

40689 SORPTION AND EXTRACTION OF SCANDIUM BY PHOSPHOORGANIC COMPOUNDS. Samodelov, A. P. Zh. Neorgan. Khim., 10: 1723-30(July 1965). (In Russian).

The sorption of scandium from aqueous solution of nitric, sulfuric, hydrochloric, and perchloric acids with phosphoric acid ionites and phosphate cellulose was investigated as a function of the acidity of the aqueous solutions. During the absorption of scandium the extraction minimum was observed in the range from 1 to 2N HCl, which is related to the modification of the sorption mechanism. The cation exchange absorption with increase acidity was altered with respect to the solvation character of the interaction of scandium with ionite. The extraction of scandium using alkyl phosphoric acids from solutions of nitric, sulfuric, hydrochloric, and perchloric acids was studied as a function of the concentration of these acids in the aqueous phase. It was shown that the dialkyl phosphates, forming very stable compounds with scandium, effectively extract it in a wide acid range from aqueous solutions. The mechanism for the extraction of scandium mono- and dialkyl phosphates was established. In the region of small concentrations of the extraction, scandium was extracted in the organic phase in the form of common salts, where the dialkyl phosphate appeared with the anion. In the area of high concentration of the extractant, supplementary solvations, which produced common salts with three molecules of the extractant, were observed. (tr-auth)

40690 MASS EXTRACTION AND SEPARATION. Bril, K. J. (Orquima S.A., Sao Paulo, Brazil). pp 30-61 of Progress in the Science and Technology of the Rare Earths. Vol. I. New York, The Macmillan Co., 1964.

A review is presented of the recovery of rare earths from raw materials. Dressing of rare earth minerals, isolation of the rare earth group, group separations, and separation of some individual rare earth elements are discussed. Both rare earth minerals and non-rare-earth minerals are considered, and the separation methods include valency changes, crystallization, and precipitation. (D.L.C.)

40691 THE SEPARATION OF RARE EARTHS BY ION EXCHANGE. Powell, Jack E. (Iowa State Univ., Ames). pp 62-84 of Progress in the Science and Technology of the Rare Earths. Vol. I. New York, The Macmillan Co., 1964.

A review is presented of recent progress in the separation of rare earths by ion exchange. The state of development and the theory of ion exchange separations are discussed as well as their application to rare earth separation. Elution and displacement chromatography are discussed. (D.L.C.)

40692 LIQUID-LIQUID EXTRACTION OF THE RARE EARTHS (EXCLUDING THE USE OF PHOSPHORUS BASED EXTRACTANTS). Weaver, Boyd (Oak Ridge National Lab., Tenn.). pp 85-8 of Progress in the Science and Technology of the Rare Earths. Vol. I. New York, The Macmillan Co., 1964.

A brief review is presented of developments on the extraction of rare earths by reagents other than phosphorus compounds. Unpublished work on the extraction of transplutonium elements by tertiary amines from concentrated LiCl solutions is discussed. (D.L.C.)

40693 FRACTIONATION OF RARE EARTHS BY LIQUID-LIQUID EXTRACTION USING PHOSPHORUS-BASED EXTRACTANTS. Peppard, D. F. (Argonne National Lab., Ill.). pp 89-109 of Progress in the Science and Technology of the Rare Earths. Vol. I. New York, The Macmillan Co., 1964.

The various organophosphorus compounds are arranged into four classes, and the separation of rare earths using these classified extractants is reviewed. It is concluded that the TBP vs HNO_3 system is workable, although the separation factors are marginal, and that the use of monoacidic phosphates and phosphonates is complicated by gelation. (D.L.C.)

40694 RECOVERY OF THORIUM FROM URANIUM PROCESS SOLUTIONS. Vermeulen, L. W. (Rio Tinto Dow Ltd., Elliot Lake, Ont.). 18p. (CONF-650203-10). Gmelin, AED-CONF-65-005-9.

From National American Inst. of Mechanical Engineers Meeting, Chicago.

The process used at Elliot Lake, Ontario, for thorium recovery from uranium ore leach solutions, after removal of the uranium by ion exchange, is described. It is a solvent extraction process and the thorium is recovered as thorium sulfate by stripping the loaded solvent with moderately strong sulfuric acid. The product, recovered by filtration, is directly shippable, but could also be easily converted into other thorium compounds. (auth)

40695 KRYPTON–XENON SEPARATION FROM A GAS MIXTURE. Dennis, Wolcott (to Air Reduction Co., Inc.). U. S. Patent 3,191,393. June 29, 1965. Filed Dec. 30, 1959.

A method and apparatus are provided for recovering Kr and Xe from gaseous mixtures such as atmospheric air or process streams containing the desired elements. The apparatus includes a primary rectification column, a concentrating column, and means for transferring an enriched liquid fraction from the primary column to the concentrating column. Condensing means connected at the top of the concentrating column receive the enriched liquid fraction from the primary column where the fraction is vaporized by heat transfer from the condensing means to form an enriched evaporated fraction, forming reflux in the concentrating column by condensation of vapor. Hydrocarbons are removed from the enriched fraction by catalyzing means, and the purified fraction is then fed into the concentrating column as feed. The reboiling means in the concentrating column is heated by the low boiling effluent from the primary column so that the Kr–Xe rich liquid accumulates in the concentrating column and is then transferred to a simple batch still for fractional distillation to separate the two. The reboiled vapor from the concentrating column is returned to the primary column. The batch still has a top condenser refrigerated by low boiling effluent from the primary column and a reboiler heated by warmed up low boiling effluent from the primary column. The fractionally distilled product is withdrawn from the top of the condenser in accord with the temperature at the top. (B.L.M.)

40696 PROCESS FOR SEPARATING THE RARE EARTH ELEMENTS BY MEANS OF SOLVENT EXTRACTION. Rice, Andrew C. (to Dept. of Interior). U. S. Patent 3,192,012. June 29, 1965. Filed Aug. 9, 1962.

A process is described for the separation of the rare earths, elements having atomic numbers from 57 to 71, inclusive, and Yt, from aqueous sulfate solutions containing the rare earths in concentrations of about 0.005 to 0.05 mole/l by extraction with amine solutions in organic, water-immiscible inert solvents. The extraction is enhanced by the addition of a complexing agent selected from the group consisting of ethylenediamine tetraacetic acid, diethylenetriamine pentaacetic acid, nitrilotriacetic acid, 1,2-diaminocyclohexane tetraacetic acid, N-hydroxyethylenediamine triacetic acid, and α-isobutyrate. The inert solvents used were either kerosene or hexane. Commercially available amine mixtures, Primene 81-R and Primene JM-T, or N-benzylheptadecylamine in the inert solvent in a concentration of 0.1 to 0.5 mole/l were used as extractants. (B.L.M.)

40697 RADIOACTIVE DECONTAMINATION OF MILK. Higgins, Irwin R. (to Chemical Separations Corp.). U. S. patent 3,194,663. July 13, 1965. Filed Apr. 1, 1963.

A process is described for removing Sr-90 and I-131 from milk by contacting the milk first with a cation ion exchanger and then an anion exchanger in moving bed ion exchange columns. The milk is slightly acidified, pH 5.2–5.4, with HCl to release the Sr-90 bound with the proteins prior to contacting successive portions of the milk with successive portions of a strong acid sulfonated polystyrene cation exchange resin. Subsequent to the cation exchange treatment, the milk is restored to its original pH level and is contacted with a moving bed anion exchange resin that has been preconditioned with a mixture of chloride, phosphate, and citrate that will leave these components on the resin in the same ratio as they occur in the milk. The process also includes regeneration stages to prepare the resins for reuse. (B.L.M.)

ENGINEERING

General

40698 (ACF-9) FILAMENT WOUND SPHERE WITH POLAR OPENING. ROVER PROGRAM. Ney, L. A. (ACF Industries, Inc., Albuquerque, N. Mex.). Jan. 4, 1965. Contract AT(29-1)-1352. 11p. (ACF-SA-706). Dep. mn; CFSTI $1.00 cy, $0.50 mn.

A filament-wound sphere with a polar opening under internal pressure was analyzed with a view to optimization of the wrap pattern on a 2-in. dia sphere with 0.5-in. polar opening and a 20,000-psi burst pressure. Computer calculations were made for pole radii of 0 to 0.40 in. (D.L.C.)

40699 (ORNL-TM-826) A COMPARISON OF MULTI-STAGE FLASH AND LONG-TUBE VERTICAL MULTIPLE-EFFECT EVAPORATORS UNDER IDENTICAL CONDITIONS. Van Winkle, R. (Oak Ridge National Lab., Tenn.). Jan. 30, 1964. Contract W-7405-eng-26. 12p. Dep. mn; CFSTI, $1.00 cy, $0.50 mn.

Detailed cost estimates of a multi-stage flash evaporator (MSF), and long-tube vertical multiple-effect evaporator (LTV) were used as a basis for comparing these two types of evaporators. Although the cost estimates were both for one billion gpd plants, the steam temperatures and maximum brine temperatures specified for the two plants were different (mainly because the specifications were written at two different points in time). Hence it was necessary to modify the MSF flowsheet to the steam, maximum brine and sea water temperature conditions of the LTV to permit making a normalized cost estimate for the MSF. Comparison of the systems was made for evaporators using 246°F steam, 230° maximum brine temperature, and 80°F sea water; the LTV had six effects, and the MSF had 42 stages. For the assumptions of this study, the principal findings are: (1.) Although the LTV requires about one-third more heat transfer surface than the MSF, its total construction cost was less--247 million vs 269 million dollars for the MSF. (2.) The LTV, having a larger fraction of its total capital cost in aluminum brass tubing which might have to be replaced once during the 30 or 35 year lifetime of the whole plant, requires a higher fixed charge rate for interim replacement--about 1 to 1.2% vs about 0.8 to 0.9% for the MSF. (3.) The cost of water produced in the LTV of performance ratio 5 lb product/1000 Btu is about 2¢/1000 gal cheaper than that of the MSF; this margin is obtained primarily as the result of lower pumping and chemical treatment costs. This difference is small relative to the accuracy of the two estimates; use of higher performance ratios would improve the MSF economics relative to those of the LTV. (auth)

40700 (ORNL-TM-1187) THE DEVELOPMENT OF A PULSE HEATING CALORIMETRIC TECHNIQUE FOR MEASURING THE SPECIFIC HEAT OF ELECTRICAL CONDUCTORS AND ITS APPLICATION TO PURE IRON FROM 100 TO 1400 DEGREES C. Kollie, Thomas Gilman (Oak Ridge National Lab., Tenn.). Aug. 1965. Contract W-7405-eng-26. 259p. Dep. mn; CFSTI $6.00 cy, $1.25 mn.

Thesis submitted to Univ. of Tennessee, Knoxville.

A pulse heating calorimetric technique for measuring the specific heat of electrical conductors over a wide temperature range was developed and tested on iron between 100 and 1400°C. This technique employed a direct current to self-heat an instrumented, rod-type specimen suspended in a constant-temperature, blackbody vacuum chamber. Total hemispherical emittance and electrical resistivity measurements were obtained with the specimen at a constant temperature. To determine the specific heat, the current flowing through the specimen was increased in a stepwise manner. A digital voltmeter capable of recording 300 readings per second was employed to measure the time dependence of the temperature change and power dissipation in a known length of the specimen. Each specific heat determination required about eight seconds, and due to the wealth of data collected in this time interval, a high-speed digital computer was employed to calculate the specific heat. An error analysis of the technique predicted an accuracy of ±1.0 per cent from 100 to 800°C. Specific heat measurements on a sample of pure iron were reproducible to ±0.5 per cent to 820°C and were in agreement with several literature sources to ±1.0 per cent from 100 to 450°C and to ±2.2 per cent from 450 to 720°C. From 720 to 890°C, the agreement of all sources was poor due to the presence of the Curie transformation at 770°C. The specific heat values from 910 to 1400°C are within 5 per cent of several investigators. At 772.8°C, the specific heat of iron was found to change in a discontinuous manner from a value of 0.3457 to 0.2672 calories per gram per degrees Celsius. Consequently, the Curie phenomenon was adjudged to be a second-order transformation caused by a change in the rate of decoupling of aligned atoms at the ferromagnetic to paramagnetic transition. (auth)

40701 (TID-22007) NMPO BLOWER SHAFT SEAL-TEST REPORT. Stein Seal Project No. 2166. (Stein Seal Co., Philadelphia, Pa.). [1963]. Contract AT(40-1)-2847; Subcontract NMPO-201. 17p. Dep. mn; CFSTI, $1.00 cy, $0.50 mn.

For General Electric Co., Cincinnati, Ohio. [Nuclear Materials and Propulsion Operation].

Results are reported of a 50-hour duration test with the NMPO blower shaft seal under conditions of 12,516 rpm shaft speed and seal inlet pressure of 375 to 400 psig. The test demonstrated the feasibility of a non-rubbing face seal for operation at 400 psi and 320 ft/sec. (D.L.C.)

40702 (TIM-914) WATER TESTS OF HIGH SPEED CENTRIFUGAL DYNAMIC SHAFT SEALS. Noell, G. L. (Pratt and Whitney Aircraft, Middletown, Conn. Connecticut Advanced Nuclear Engineering Lab.). June 23, 1965. Contract AT(30-1)-2789. 40p. Dep. mn; CFSTI $2.00 cy, $0.50 mn.

Current higher speed liquid metal pumps under development require smaller diameter seals with minimum power consumption. Four models were tested in water at shaft speeds up to 13,000 rpm. A 36 vane dynamic seal, designated DS-11, with a vane height of 0.200 inch, an axial vane clearance of 0.010 inch, and two circumferential tang slots exhibited the most stable liquid-to-gas interface at high speeds and provided optimum values of vane and torque coefficients. (auth)

40703 (TIM-916) SINGLE FILM JOURNAL BEARING TESTS IN WATER. Weinberg, B. (Pratt and Whitney Aircraft, Middletown, Conn. Connecticut Advanced Nuclear Engineering Lab.). July 1965. Contract AT(30-1)-2789. 28p. Dep. mn; CFSTI, $2.00 cy, $0.50 mn.

A description is given of a series of tests conducted with fluid-film bearings as part of a program for developing a shaft-bearing system for liquid metal pumps to be used in the SNAP-50/SPUR powerplant. Hydrodynamic, hydrostatic, and hybrid type bearings were tested using water to simulate the low kinematic viscosity condition of lithium. The test unit, which was basically a shaft supported by a conventional single deep-groove ball bearing at one end and the test bearing at the other, was also operated to simulate the dynamic conditions of a similar test unit which was operated with lithium at 600°F. (auth)

40704 (Y-KA-9) PROVIDING REAL-TIME INFORMATION ON PRODUCTION SCHEDULES AND COSTS. Christman, A. M. (Union Carbide Corp., Oak Ridge, Tenn. Y-12 Plant). June 25, 1965. Contract W-7405-eng-26. 21p. (CONF-650915-1). Dep. mn; CFSTI $1.00 cy, $0.50 mn.

From Systems Engineering Conference, Chicago.

The Oak Ridge Y-12 Plant has developed a middle-of-the-road system to provide real-time information on production schedules and costs. The system utilizes transacter data collection to provide immediate feedback of selected information from the shop floor to specific control areas. Portions of the system are unique to the Y-12 Plant. Since this approach offers a number of the advantages of more sophisticated real-time systems at a fraction of their cost, it has provided Y-12 with initial entry into a field that has proved to be very satisfactory. (auth)

40705 JOINTS BETWEEN TUBULAR MEMBERS. White, William Paul; Bromidge, Noel Arthur Clifford (to United Kingdom Atomic Energy Authority). British Patent 997,765. July 7, 1965. Filed July 2, 1963.

A method is described for making a substantially leak-tight joint up to 600°C between two tubular members. Each member has an annular sealing face with a series of concentric grooves of specific geometrical form. The members are assembled with a soft metal gasket between the faces, and a loose locating ring encircles the gasket and compresses it by controlled external clamping with clamping rings to effect a seal between the faces. The outer wall of each of the tubular members tapers inwardly in a longitudinally direction away from external flanges on the members on which the clamping rings seat. (B.L.M.)

Applications of Nuclear Explosions

40706 (ORNL-TM-1191) CHEMICAL APPLICATIONS OF NUCLEAR EXPLOSIONS (CANE). Progress Report for January 1–June 30, 1965. Brown, K. B.; Blake, C. A. Jr. (comps.) (Oak Ridge National Lab., Tenn.). July 20, 1965. Contract W-7405-eng-26. 17p. Dep. mn; CFSTI, $1.00 cy, $0.50 mn.

Studies were started on the possible behavior of radionuclides that will be present in copper recovery processes as a result of using nuclear explosives for breaking the ore. In preliminary calculations and laboratory tests, consideration was given to the possible movement of radionuclides in the environment, a guesstimate as to the level of build-up of radioactive materials in the leach liquor, and possible contamination of the copper product. A laboratory study of the kinetics of exchange of tritium for hydrogen in water and methane was initiated since this exchange requires consideration in the feasibility study of the stimulation of gas production from wells by nuclear explosives. Tests are nearly complete of a jet sampler method for recovering specimens irradiated near a nuclear detonation. An experimental program was started to investigate the thermal stability of various actinide compounds. A literature survey was started to determine whether the Plowshare program could assist the minerals industry of the Appalachian region. Literature surveys have also been started to assess the possible chemical and chemical engineering problems associated with the use of nuclear explosives to (1) aid in recovery of oil from shales and (2) exploit geothermal heat through steam generation. (auth)

40707 (PNE-502F) CRATER MEASUREMENTS. Final Report, Project Pre-SCHOONER. Sprulll, Joseph L.; Paul, Roger A. (Army Engineer Nuclear Cratering Group, Livermore, Calif.). Mar. 1965. 128p. Dep. mn; CFSTI $1.40 cy, $1.00 mn.

In Project Pre-Schooner, four 40,000-pound spherical nitromethane charges were detonated at depths of burst of 42, 50, 58, and 66 feet in the basalt of Buckboard Mesa at the Nevada Test Site in February 1964. Based upon the results of Project Pre-Schooner, new cratering curves for basalt were developed. The depth of burst for maximum apparent crater radius and depth are 160 and 135 $ft/kt^{1/4}$, respectively. The deepest detonation Charlie, produced a mound of broken rock and earth that had a crater-like depression in its center entirely above the preshot ground surface. Average cross sections of the apparent craters showed them to be hyperbolic rather than parabolic, with the average inclination from horizontal of the upper, approximately straight, slopes about 31°. A curve was also developed for apparent crater volume for basalt. Apparent crater volumes for craters in hard rock at depths of burst near optimum for radius may be predicted as $V_a = 0.4\ R_a^3 D_a$. Prediction curves were developed for apparent lip crest height and radius. For depths of burst near optimum for crater radius, lip crest heights and radii averaged $H_{al} = 0.2\ R_a$ and $R_{al} = 1.4\ R_a$. Around the circumference of a single crater, lip crest height varied by about ±50 percent from the average. Outer edges of crater lips at depths of burst near optimum averaged between 4 and 5 apparent crater radii. The extreme range of rock missiles decreased very rapidly with increasing depth of burst. A curve showing the variation of extreme rock missile range with depth of burst was developed. At near optimum depths of burst, the extreme missile range was about 20 apparent crater radii. The weights of rock missiles thrown to maximum ranges appeared to vary inversely with charge depth. For the shallower shots (at 129 and 155 $ft/kt^{1/4}$), the number of large missiles at maximum ranges indicated that a significant safety hazard exists. (auth)

40708 (PNE-503F) BASE SURGE AND CLOUD FORMATION. Final Report, Project Pre-SCHOONER. Rohrer, Robert (Lawrence Radiation Lab., Univ. of California, Livermore). Feb. 1964. Contract W-7405-eng-48. 10p. Dep. mn; CFSTI $0.45 cy; $0.50 mn.

A summary is presented of the base surge cloud histories for the Pre-Schooner series of high explosive shots. An analysis of the data results in a correlation of the maximum base surge radius in a neutral atmosphere as a function of the scaled depth of the explosive in a basalt medium. The maximum base surge radius for explosions in basalt appears to be significantly less than those for comparable explosions in alluvium. (auth)

40709 (PNE-5003) INVESTIGATION OF MANUFACTURE OF AGGREGATE AND RIPRAP BY NUCLEAR MEANS. Polatty, J. M.; Houston, B. J.; Stone, R. L.; Banks, D. C. (Army Engineer Waterways Experiment Station, Vicksburg, Miss.). Feb. 1965. Contract AT(29-2)-752. 78p. Dep. mn; CFSTI $0.75 cy, $0.75 mn.

The objectives of the work reported were to investigate the feasibility of producing aggregate and riprap by nuclear means and to verify and supplement size distribution data obtained by a photogrid method. This was accomplished by determining the size distribution, density, absorption, abrasion resistance, shape characteristic, rock types, and degrees of new fractures of material from 16 piles of ejecta from a trench excavated into the lip of the DANNY BOY crater. Particle sizes were estimated by comparisons with the 1-foot grid spacing. Results of tests indicate that approximately 10 percent of the ejecta could be used for concrete aggregate after proper separation without secondary crushing. Physical tests and geologic examinations confirm that this ejecta would be acceptable as concrete aggregate. Thirteen percent of the ejecta was in the size range needed for riprap. Fracturing of the ejecta was minor, and the dense particles would make good riprap. All ejecta could be used with moderate sizing for jetty stone. The photogrid method indicated that the material was coarser than shown by mechanical separation, though a direct comparison may not be valid in this case since different areas of the deposit may have been analyzed. However, because of the speed and low cost of the photogrid method, further study is warranted. (auth)

40710 (SC-DC-65-1485) NUCLEAR EXPLOSIVES—A NEW TOOL FOR THE ENGINEER. Vortman, L. J. (Sandia Corp., Albuquerque, N. Mex.). May 1965. Contract AT(29-1)-789. 29p. (CONF-650712-1). Dep. mn; CFSTI $2.00 cy, $0.50 mn.

From National Society of Professional Engineers, Albuquerque, N. Mex.

The principal characteristics of nuclear explosives and

of contained explosives are outlined. Excavation costs using nuclear and conventional methods are compared. Scientific and engineering non-military uses of nuclear explosives are considered, and the engineering uses are discussed in detail: water resources, power production, mining, chemistry, and excavation. (D.L.C.)

40711 (SC-RR-65-220) COMPILATION OF CRATER DATA. Dietz, John P.; Hayes, Dennis B. (Sandia Corp., Albuquerque, N. Mex.). July 1965. Contract AT(29-1)-789. 160p. Dep. mn; CFSTI $5.00 cy, $1.00 mn.

A compilation of crater dimensions, resulting from high explosive and nuclear cratering experiments in desert alluvium, Albuquerque alluvium, playa, wet clay and basalt, is presented in both tabular and graphical form. Both scaled and unscaled crater dimensions are included. In this presentation, crater dimensions are scaled by $W^{\frac{1}{3}}$, $W^{\frac{1}{3.4}}$, and $W^{\frac{1}{4}}$. A scheme of scaling which takes into account the overburden of material is also presented. (auth)

40712 (SC-RR-65-277) DIMENSIONS OF A CRATER FROM A 500-TON TNT HEMISPHERE DETONATED ON ROCK. Vortman, L. J. (Sandia Corp., Albuquerque, N. Mex.). July 1965. Contract AT(29-1)-789. 25p. Dep. mn; CFSTI $1.00 cy, $0.50 mn.

A hemispherically shaped 500-ton charge of TNT was detonated on discontinuous basalt rock at Kahoolawe Island, Hawaii, as a part of Operation Sailor Hat. The crater dimensions were: radius -78.6 feet, depth, 39.18 feet, and volume -2.87×10^5 cubic feet. The crater depth was greater than that in an earlier identical charge detonated on soil, and radius and volume were smaller. The usually quoted ratio (8/10) of linear dimensions of craters in rock to those in soil is not supported. (auth)

40713 (VUF-2401) SHOCK SPECTRUM MEASUREMENTS. Galbraith, Frank W.; Barton, M. V. (TRW Space Technology Labs., Thompson Ramo Woolridge Inc., Redondo Beach, Calif.). May 21, 1965. Project 1.7 of VELA UNIFORM— PLOWSHARE PROGRAM, PROJECT GNOME. 36p. Dep. mn; CFSTI, $2.00 cy, $0.50 mn.

A total of twelve reed gages were installed to measure displacement shock spectra resulting from the Project Gnome underground nuclear explosion. Seven of the gages were installed on the ground surface at four locations out to a distance of 3000 feet from surface zero. All of these gages yielded usable records. Four of the gages were installed in the floor of the Gnome tunnel at two locations. Those at the 1033-foot range gave valid records; those at the 900-foot range were not recovered after the test. The one gage located underground at the International Minerals and Chemical Corporation (IMCC) mine, some nine miles distant, did not record any motion. The plotted displacement spectra showed the expected results in that displacements and peak accelerations decreased with increasing slant range for the surface gages. The vertical spectra were higher than the corresponding horizontal radial spectra for the surface gages. For the gages in the Gnome tunnel, the horizontal radial spectrum was higher than the vertical spectrum. (auth)

Facilities and Equipment

Refer also to abstracts 41186, 42173, and 42174.

40714 (EUR-2421.d) MULTIPLEX-MESSEINRICHTUNG ZUR ERFASSUNG MEHRERER MESSDATEN UBER EIN EINZIGES KABEL (z.B. EINADRIGES KOAXKABEL) BEI VERWENDUNG NUR PASSIVER BAUELEMENTE (R, L, C) ZUR MESSWERTWANDLUNG AUF DER EINGANGSSEITE DES KABELS. (Multiplex Measuring Set-Up for Registering Several Measuring Data Via a Single Cable (e.g. One-Wire Coaxial Cable) by Utilizing Only Passive Components (R, L, C) for Measurand Conversion on the Intake Side of the Cable). Becker, W. (European Atomic Energy Community, Ispra (Italy). Joint Nuclear Research Center). May 1965. 22p. Dep. mn.

It is shown that the principle of a measurement set-up allows the conversion of several slowly changing quantities (e.g., temperatures and mechanical deformations) by a transducer system in such a way that they can be transferred as electrical oscillations of certain frequencies, by means of a common high-frequency cable (e.g., coaxial cable) from the measurement to the evaluation room. Because of the nuclear radiations, the measurement area should only contain passive elements. The proposed set-up, therefore, mainly consists of an amplifier with positive feedback on the evaluation side, furnished with switchable frequency passbands. The definite oscillation frequency of this system is always determined by the resonant circuit in the measurement area tuned to a frequency inside the chosen passband. The resonant frequency of each of the resonant circuits in the measurement area is influenced by one of the quantities to be measured. It is necessary to reduce the means of transfer to one simple cable because difficulties arise as to hermetic sealing in leading several cables through the wall of the measurement container. The assembly is explained by some examples. (auth)

40715 (NAA-SR-Memo-7438) EQUIPMENT FOR FABRICATION AND ENCAPSULATION OF IRRADIATED UO_2 PELLETS. Bodine, J. E.; Guon, J.; Sullivan, R. J.; Stanwood, D. E.; Gandolfo, F. W. (Atomics International, Canoga Park, Calif.). May 22, 1962. Contract AT(11-1)-Gen-8. 36p. Dep. mn; CFSTI $2.00 cy, $0.50 mn.

A lower isolation box was constructed and equipped for remotely fabricating UO_2 pellets and assembling irradiation capsules. One hundred gram quantities of highly irradiated UO_2 powder can be processed. Equipment consists of a blender, powder dispenser, pellet press, sintering furnace, balance, gas pycnometer, dimensional gage, capsule rack and welder-leak check chamber. The equipment complex was tested using 100 gram quantities of unirradiated UO_2 powder. Pellets with densities greater than 95% of theoretical were fabricated. Helium leak tight irradiation capsules were prepared by remote welding. (auth)

40716 (NP-15280) RESEARCH IN THE FIELD OF LIQUID-METAL-LUBRICATED BEARINGS. QUARTERLY PROGRESS REPORT FOR PERIOD ENDING JUNE 15, 1965. (Rocketdyne, Canoga Park, Calif.). June 25, 1965. Contract AF33(657)-10553. 52p.

Investigation of K-lubricated bearings is reported. Performance tests of special hybrid bearings in the simulated system test rig using water were concluded and data were reduced. Analyses were performed to predict bearing performance. Correlation between analysis and test data is excellent and typical results are presented. Preparations are now under way for K-lubricated simulated system tests at temperatures up to 1200°F. (auth)

40717 (RISO-98) FACILITIES FOR MECHANICAL TESTING OF IRRADIATED REACTOR MATERIALS AT RISOE. Winther, A. C. (Atomenergikommissionen, Risoe (Denmark). Forsoegsinstitut). May 1965. 15p. Dep. mn.

A β, γ lead-shielded facility for mechanical testing of irradiated reactor structural materials has been established and operated for a year and a half in the Risö Hot-Cell Laboratory. The facility is described, and the operational experiences so far obtained are summarized. (auth)

40718 (TIM-909) SUMMARY OF SHAFT FACE SEAL DEVELOPMENT PROGRAM. Manfredi, D. V. (Pratt and Whitney Aircraft, Middletown, Conn. Connecticut Advanced Nuclear Engineering Lab.). June 30, 1965. Contract AT(30-1)-2789. 78p. Dep. mn; CFSTI, $3.00 cy, $0.75 mn.

A program for the development of a sealing system with a minimum operating life of 10,000 hours for shafts of pumps used to circulate Li, K, or NaK at 1600°F is described. The shafts, supported by oil-lubricated ball bearings, were to operate up to speeds of 8500 rpm. The purity requirements of the cover gas above the liquid metal were 2 ppm or less of O_2 or moisture. The sealing system consisted of two oil cermet face seals, one dry gas cermet face seal, a centrifugal dynamic seal, and two sweep gas systems. Seal manufacturing techniques, performance data,

and experimental techniques evolved in the program are reported. A total of over 150,000 hours of testing was accumulated in the overall program. (auth)

40719 (UCRL-7844-T) AN OPERATING TRANSCURIUM ELEMENT RADIOCHEMISTRY FACILITY. Coops, M. S.; Scribner, V. E.; Hanson, C. L. (Lawrence Radiation Lab., Univ. of California, Livermore). July 31, 1964. Contract W-7405-eng-48. 12p. Dep. mn; CFSTI, $1.00 cy, $0.50 mn.

The Livermore neutron cave facility was modified to accept extended-reach master-slave manipulators. Two additional process boxes that are fully interchangeable with the original enclosure were constructed to accommodate specialized equipment necessary to remotely perform transcurium element chemistry. Some of the items included in these enclosures are: high geometry fast-neutron detectors for the determination of spontaneous fission content of process solutions, electromechanical devices to count and collect a predetermined number of drops of ion-exchange eluate per tube, built-in console-operated chemical process system, and an ultramicro remote pipetting system for the radioanalysis of very alpha active solutions. (auth)

40720 (UCRL-7845-T) REMOTELY-OPERATED TRANS-PLUTONIUM CHEMICAL PROCESS CELLS. Coops, M. S.; Hanson, C. L.; Hawk, R. W.; Scribner, V. E. (Lawrence Radiation Lab., Univ. of California, Livermore). July 29, 1964. Contract W-7405-eng-48. 28p. Dep. mn; CFSTI, $2.00 cy, $0.50 mn.

Twenty-eight radioactive pile slugs containing gram quantities of plutonium, americium, and curium have been successfully processed in a heavily shielded, remotely operated chemical facility utilizing push button flow process control techniques. The chemical process, which is designed for trans-plutonium element processing, utilizes filtration, distillation, and ion-exchange techniques to separate the gamma active actinide elements from the gross quantities of fission products produced during irradiation. The equipment operates at kilocurie alpha activity levels in the presence of corrosive chemical reagents, is exposed to high beta and gamma radiation levels, and yet allows total confinement of the hazardous contaminants to the primary enclosures. Ventilation equipment includes refrigerated caustic scrubbers and multiple high-efficiency filters. (auth)

40721 (UCRL-11454) A CONCRETE LOW-BACKGROUND COUNTING ENCLOSURE. Wollenberg, Harold A.; Smith, Alan R. (Lawrence Radiation Lab., Univ. of California, Berkeley). June 15, 1964. Contract W-7405-eng-48. 21p. Dep. mn; CFSTI, $1.00 cy, $0.50 mn.

A massive concrete low-background γ-ray counting enclosure was recently constructed. Walls and roof are 4 to 5 ft thick; inside dimensions are $23.5 \times 11.5 \times 11.5$ ft. A substantial effort was made to secure materials adequately low in radioactivity for the concrete. Of primary concern were the concentrations of potassium, uranium, and thorium in possible low-radioactivity sources of aggregate and cement materials. Geologic considerations indicated that ultramafic igneous rocks are the lowest in these radioisotopes. An examination was conducted of possible sources of low-radioactivity aggregate material; samples were analyzed for radioactivity on a 100-channel γ-ray spectrometer. Evaluation of the spectrometer analyses and economic considerations resulted in the choice of serpentinized ultramafic rock from a deposit in the foothills of the Sierra Nevada as the source of low-background aggregate. Raw materials from 12 Portland cement plants in California, and finished products from 114 plants in the United States and Canada, were also examined for radioactivity by γ-ray spectrographic analysis. Cement from a producer on Vancouver Island, British Columbia, was chosen as the lowest-radioactivity cement product commercially available. The completed enclosure furnishes a nearly twofold reduction in background in comparison with the previous counting arrangement. Equally important, the thick concrete shield with its included water of hydration keeps the present level of radioactivity nonfluctuating, whereas the background in the previous counting arrangement varied in proportion to the external fast-neutron flux produced by nearby accelerators. Future installation of a 1-ft-thick ultra-low-background liner and (or) an approximately $\frac{1}{8}$-in.-thick lead membrane on the inside surface of the enclosure should significantly reduce the present background. A comparison of costs indicates that to shield a similar-sized counting space with steel of equivalent attenuation and low-background characteristics would cost (in place) about four times as much as the existing concrete structure. (auth)

40722 RADIOGRAPHIC EXAMINATION USING COLD NEUTRONS. Barton, J. P. (Univ. of Birmingham, Eng.). Brit. J. Appl. Phys., 16: 1051(July 1965).

Radiography may be conveniently performed using beams of cold neutrons. The advantages of this method include high sensitivity to many light elements and a small scattering effect in iron. (auth)

40723 FREQUENCY MODULATION OF LARGE CAVITIES. Rajangam, K. B.; Hai, F.; MacKenzie, K. R. (Univ. of California, Los Angeles). Rev. Sci. Instr., 36: 794-6 (June 1965).

A model study is described in which a rotating capacitor is coupled to a large re-entrant cavity. The size and capacitive loading (~500 pf) are such as to make modulation by ferrites or broadband amplifiers difficult and expensive. A nominal frequency range of 3 to 1 is achieved with a single-plate six-bladed rotor. On a possible full-scale cavity with a range of approximately 9 to 3 Mc, the data are scaled to a voltage of 5 kv peak for r-f power requirements of 1 to 4.4 kw. (auth)

40724 LINEAR ELECTROMAGNETIC BRAKE. Deutsch, F. (Hebrew Univ., Jerusalem). Rev. Sci. Instr., 36: 849(June 1965).

The purpose of the brake is to halt a tubular, highly electrically conducting projectile, whose motion is parallel to its axis. The brake consists of a tube that is larger in diameter than the projectile tube. Around the brake tube is wound a succession of coils, equally spaced and coaxial with the brake tube. The currents in these coils flow in opposite directions in successive coils. The magnetic fields induced by the entry of the projectile into the brake produce a linear decrease in projectile velocity. With 20 amp in the coils, a 450-g projectile with a velocity of 45 m/sec can be stopped in 90 cm. (T.F.H.)

40725 CATAPHORETIC COATING LANTHANUM BORIDE ON RHENIUM FILAMENTS. Favreau, Louis J. (General Electric Research Lab., Schenectady, N. Y.). Rev. Sci. Instr., 36: 856-7(June 1965).

LaB_6 is deposited from a suspension of finely divided LaB_6 in alcohol onto a Re wire. A drop of HCl is added to the suspension as an electrolyte. A Ta electrode and the Re wire to be coated are then immersed in the suspension, and a voltage of about 90 v is applied between the two electrodes. The depth of LaB_6 coating on the Re is dependent on the duration of the cataphoresis. The coating is sintered by flashing the filament in vacuum for 10 min at 1600 to 1700°C. Either straight or helical Re wires can be used. (T.F.H.)

40726 STABLE LINEAR PULSE-SUMMING CIRCUIT. Rogers, P. C.; Crawford, R. L.; Toevs, J. W. (Los Alamos Scientific Lab., N. Mex.). Rev. Sci. Instr., 36: 857-8(June 1965).

A circuit is developed to sum positive pulses. The circuit provides an extremely linear non-inverted, low-impedance output, suitable for driving a transmission line. The circuit consists of two separate sections, an adder stage and an output amplifier-driver stage. (T.F.H.)

40727 EXPERIMENTAL LIQUID-METAL GALLIUM LOOP FOR MAGNETOHYDRODYNAMIC INVESTIGATIONS. Kovner, D. S.; Krasil'nikov, E. Yu.; Mironov, O. M. Teplofiz. Vysokikh Temp., 3: 315-17(1965).

To eliminate various problems associated with the use of mercury and alkali metals as working media in magnetohydrodynamic investigations (e.g., the high toxicity of mercury vapors, and the high temperature and danger of fire and explosion connected with the use of alkali metals) an experimental unit with a liquid-metal loop was developed in which technically pure gallium is being used as a working substance. The unit is designed for testing electromagnetic pumps and various types of electromagnetic flowmeters, and for conducting magnetohydrodynamic research. The gallium temperature in the loop is maintained at ~50 to 70°C. A special technique was developed for measuring the gallium flow rate in the loop. The unit operated continuously for 6 hr with a maximum metal flow rate of 0.8 m^3/hr. The development of the unit constitutes the first step in a program of magnetohydrodynamic investigations. (ATD)

40728 IMPROVEMENTS IN OR RELATING TO CONCRETE PRESSURE VESSELS. Bell, Robert (to United Kingdom Atomic Energy Authority). British Patent 997,882. July 14, 1965. Filed Apr. 26, 1963.

A prestressed concrete pressure vessel has a generally cylindrical portion with one closed end with both the cylindrical portion and the closed end being prestressed. The other end of the cylindrical portion is shaped to give a flared opening and is closed by an end cap with stressing means passing through the end cap. The stressing means are so arranged that the end cap can be unstressed and separated from the cylindrical portion and subsequently replaced and restressed. (B.L.M.)

40729 IMPROVEMENTS IN OR RELATING TO CONVEYOR SYSTEMS. Williams, Kenneth John; Ralph, John Charles; Langridge, Eric Graham (to United Kingdom Atomic Energy Authority). British Patent 999,621. July 28, 1965. Filed May 11, 1961.

A dispatch system includes a container for the article to be dispatched and a carrier to convey the container. The container has a tubular body portion, retaining members at each end of the body, and resilient means by which the members are urged to a container retaining position. Sending and receiving points are provided for the container, and two stations are located between the two points with means at each station for automatically inserting or removing the container relative to the carrier. Each station is provided with retractive means including a tubular projecting member enterable into the carrier to abut and retract the retaining members to permit insertion and removal of the container. Energy absorbing means at each station include a piston and spring damping means for the piston. The tubular projecting member may be associated with the piston. Each station may be provided with a number of permanent magnets arranged in a ring in an end face of the piston to attract a ring of ferromagnetic material provided in the end of each carrier. (B.L.M.)

40730 MECHANICAL MANIPULATORS FOR THE DISPLACEMENT OF OBJECTS LOCATED IN A RADIOACTIVE MEDIUM. Rene Le Guenec and Pierre Pesenti (to Commissariat a l'Energie Atomique). Canadian Patent 696,293. Oct. 20, 1964. Priority date Feb. 20, 1960, France.

Remote handling equipment is described, which uses an "articulated parallelogram" to communicate the movement of the pilot member (operator) to the controlled member. A pair of concentric tubes together with cables and pulleys assist in transferring movement through the shielding wall to the hot cell. It is claimed that a much more effective seal against escape of radioactivity is possible with this device. (F.S.A.)

Heat Transfer and Fluid Flow

See also PHYSICS — General.

Refer also to abstract 42073.

40731 (AD-609969) ANALYSIS OF RADIATORS FOR SPACE NUCLEAR POWER SYSTEMS. Blanton, Roy W. Jr. (Brown Engineering Co., Inc., Huntsville, Ala. Research Labs.). Dec. 1964. Contract NAS 8-5289. 48p. (R-125). CFSTI $2.00 cy, $0.50 mn.

A theoretical analysis is presented for designing heat radiators for space nuclear power systems. The analysis is for two configurations: conical, single-surface radiators and flat, tapered plate radiators. Both condensing and noncondensing fluid conditions are considered. A FORTRAN IV program is included. (auth)

40732 (CEND-3336-237) DEVELOPMENT AND TESTING OF A TEMPERATURE TRANSIENT METHOD FOR PERFORMING IN-PILE THERMAL CONDUCTANCE TESTING. Progress Report, January 1–March 31, 1965. Burdg, C. E. (Combustion Engineering, Inc., Windsor, Conn. Nuclear Div.). Apr. 1965. Contract AT(30-1)-3336. 20p. (EURAEC-1371). Dep. mn; CFSTI $1.00 cy, $0.50 mn.

Work Performed Under United States–Euratom Joint Research and Development Program.

The concept investigated is one whereby measurement of the transient temperature response at the surface of an operating fuel element, following a reactor power change, will yield thermal conductance values. This two-phase investigation consists first of out-of-pile demonstrations of feasibility, followed by in-pile confirmation of the method. Concurrent mathematical analyses of the thermal model will provide the bases for data interpretation, as well as guides for the design of the experimental portions of the program. Completion of the computer studies of both the out-of-pile case and the in-pile case has led to the conclusion that the clad response to cyclically varying input may yield both effective conductivity and fuel-clad conductance values. With the aid of these analyses of the thermal models, out-of-pile experimental tests were designed to permit verification of the predicted performance. These tests will include introduction of sinusoidal variations of power input in the frequency range from 0.1 to 1 radians per second, testing of both UO_2 and ZrO_2 pellets, and testing of elements with various pellet-clad assembly clearances. (auth)

40733 (GEAP-4863) TWO-PHASE FLOW AND HEAT TRANSFER IN MULTIROD GEOMETRIES. Quarterly Progress Report No. 2, January 26–April 25, 1965. (General Electric Co., San Jose, Calif. Atomic Power Equipment Dept.). May 1965. Contract AT(04-3)-189. 15p. Dep. mn; CFSTI, $1.00 cy, $0.50 mn.

An annular test section apparatus for air–water flow structure measurements is in operation. Single-phase and two-phase pressure drop data, operating both as a simple round tube and as a concentric annulus, agree with well-known correlations. The inlet mixing device appears to provide fully developed two-phase flow in the test section. Thus, this apparatus is suitable for meaningful detailed flow structure measurements. Instrumentation development continues. Difficulty in obtaining true isokinetic flow sampling was encountered. Five probe designs were tested. A direct wall shear measurement instrument model was designed and tested. (auth)

40734 (NP-15331) HYDROGEN HEAT TRANSFER DATA COMPILATION. McCarthy, J. R.; Miller, W. S.; Okuda, A. S.; Seader, J. D. (Rocketdyne, Canoga Park, Calif.). June 26, 1964. 162p. (R-5752).

A compilation of experimental hydrogen heat transfer data for turbulent flow inside electrically heated tubes is presented. In all cases the tubes were straight and had a circular cross section. A total of 276 experiments are reported. (auth)

40735 (NYO-2404-5) EFFECTS OF ELECTRICAL FIELDS ON BOILING HEAT TRANSFER. Quarterly Progress Report, May 26–September 30, 1964. Nichols, Charles R.; Spurlock, Jack M.; Markels, Michael Jr. (Atlantic Research Nuclear Corp., Alexandria, Va.). Contract AT(30-1)-2404. 25p. Dep. mn; CFSTI, $1.00 cy, $0.50 mn.

The test section and its improvements are described. A series of runs was conducted on water at 250-300 psi

and mass velocities of 5, 1.0, and 2.0×10^6 lb/hr-ft^2. A-c electric fields of up to 2200 volts were used. Plots of heat flux vs temperature difference, burnout heat flux vs exit steam energy flow, and pressure drop vs exit steam energy flow are given. The results show that the maximum nucleate boiling heat flux is significantly increased by a high voltage field, and that the increase in burnout heat flux is approximately proportional to the field. (D.L.C.)

40736 (NYO-2512-1) DESIGN GUIDE FOR GAS-LUBRICATED TILTING-PAD JOURNAL AND THRUST BEARINGS WITH SPECIAL REFERENCE TO HIGH-SPEED ROTORS. Gunter, Edgar J. Jr.; Hinkle, James G.; Fuller, Dudley D. (Franklin Inst. Research Labs., Philadelphia, Pa.). Nov. 1964. Contract AT(30-1)-2512. 230p. (I-A2392-3-1). Dep. mn; CFSTI $6.00 cy, $1.25 mn.

The geometrical considerations and relationships for single and multiple pad journal bearings are derived, and the basic equations of hydrodynamic lubrication are reviewed. Design field maps are given for tilting-pad journal bearings, and the step-wise procedure for the design of a tilting pad journal bearing for a high speed rotor is outlined in detail. The theory of rotor critical speeds is considered. Sample calculations are given for a typical rotor journal bearing. The design of thrust bearings is next considered. Finally, physical design and material considerations are developed. (D.L.C.)

40737 (NYO-3114-6) TWO-PHASE FLOW AND BOILING HEAT TRANSFER. THE SEPARATE-CYLINDERS MODEL OF TWO-PHASE FLOW. Interim Report. Turner, J. M.; Wallis, G. B. (Thayer School of Engineering, Dartmouth Coll., Hanover, N. H.). May 1965. Contract AT(30-1)-3114. 69p. (EURAEC-1415). Dep. mn; CFSTI $3.00 cy, $0.75 mn.

Work Performed Under United States–Euratom Joint Research and Development Program.

This report is concerned with two-phase flow in pipes. General equations are developed applicable to laminar or turbulent, vertical or horizontal flow. The general equations describe two-phase pipe flow in terms of seven dimensionless parameters. Several of the same groups have previously been used intuitively by Wallis and other workers. The present work provides a rationale for their use. The Separate-Cylinders Model of two-phase flow is described. This simple "lumped-flow" model provides a theoretical basis for Martinelli's correlation of horizontal two-phase flow when used in conjunction with the general equations. Simple equations are presented which closely approximate Martinelli's empirical curves for void fraction and pressure drop. The Separate-Cylinders Model also predicts the flooding point in counter-current vertical flow by equations very similar to Wallis' empirical equations. (auth)

40738 (NYO-3114-7) TWO-PHASE FLOW AND BOILING HEAT TRANSFER. Quarterly Progress Report, January–March 1965. Wallis, G. B.; Turner, J. M.; Meyer, P.; Runge, D. (Thayer School of Engineering, Dartmouth Coll., Hanover, N. H.). Apr. 1965. Contract AT(30-1)-3114. 21p. (EURAEC-1414). Dep. mn; CFSTI, $1.00 cy, $0.50 mn.

Work Performed under United States–Euratom Joint Research and Development Program.

Work on the annular flow regime has continued. General equations were derived relating shear stress and velocity profiles in both horizontal and vertical flow. A simple model was developed which gives a pressure drop correlation very close to Martinelli's prediction and also predicts countercurrent flow flooding in vertical pipes. Comparison of various analytical techniques for studying drop-annular flow seems to show that as long as there is any noticeable entrainment the homogeneous flow model gives good correlation of experimental data. Various fluids and tube sizes were used to measure the rise velocity of slug flow bubbles in inclined tubes. (auth)

40739 (OTR-112) FLUID AMPLIFICATION. (National Bureau of Standards, Washington, D. C.). May 1965. 30p. CFSTI $0.50 cy, $0.50 mn.

Significant reports covering the period since 1960 were selected for this study with reference to earlier works. Recent Government-sponsored research has shown that fluid amplification is a feasible technique that shows promise, particularly for operation in extreme environments such as high radiation flux, high temperatures, and shock vibrations. Devices based on this concept possess high potential reliability. Fluid amplifiers will most likely be seen first in military applications where the potential advantages outweigh the development costs. To date, some computer devices have been developed based on the Coanda effect and some systems have been devised by combining these devices. (auth)

40740 (RT/ING(64)16) MODELLI ANALOGICI PER ELEMENTI DI COMBUSTIBILE NUCLEARE A BARRE CILINDRICHE. (Analog Model for Cylindrical Nuclear Fuel Rods). Giordano, P.; Mathis, A.; Petrarca, S. (Comitato Nazionale per l'Energia Nucleare, Rome (Italy)). Nov. 1964. 61p. Dep. mn.

Four simplified mathematical models are presented, describing the thermal behavior of cylindrical fuel rods; corresponding analogic circuits are also discussed. One of these models is based on exact transfer functions and is taken, therefore, as a reference to compare the precision of the responses. Complexity of calculations and number of computing elements needed for each model are also taken into account. In some particularly interesting cases the responses are jointly recorded on a common base to facilitate comparison. (auth)

40741 (SAN-409-23) HIGH ACCELERATION FIELD HEAT TRANSFER FOR AUXILIARY SPACE NUCLEAR POWER SYSTEMS. Quarterly Technical Report, December 1, 1964–February 28, 1965. Poppendiek, H. F.; Greene, N. D.; Sabin, C. M.; Feigenbutz, L. V.; Livett, R. K.; Schwartz, P. E.; Connelly, D. J. (Geoscience Ltd., Solana Beach, Calif.). Contract AT(04-3)-409. 17p. Dep. mn; CFSTI $1.00 cy, $0.50 mn.

Research is being conducted on high acceleration field boiling liquid metal heat transfer. Additional helical, forced flow boiling potassium measurements are presented and the results compared to boiling mercury data obtained previously; comparisons to theory are also made. A review of the heating method used in the current forced convection boiling potassium experiments is made. The information is presented which demonstrates where the power added to the directly heated tube is dissipated in a liquid metal boiling system. The high boiling liquid metal heat transfer conductances obtained by the General Electric Company are interpreted on the basis of annular, superheated, liquid metal films at the wall. (auth)

40742 (TID-22002) BASIC STUDIES IN GAS-SOLID SUSPENSION. Quarterly Report No. 65-2, March–May 1965. (Rutgers–The State Univ. of New Jersey, New Brunswick. Bureau of Engineering Research). June 11, 1965. Contract AT(30-1)-2930. 16p. Dep. mn; CFSTI, $1.00 cy, $0.50 mn.

Theoretical and experimental studies are being conducted on the basic fluid mechanics and heat transfer processes of gas-solid suspensions in turbulent flow. The studies include heat transfer and cooling, mass transfer, supersonic gas particle flows, pressure pulsation, solids density profiles, turbulence generation, particle-gas momentum interchange, statistics of solid motion in gases, and Eulerian-Lagrangian turbulence. (D.L.C.)

40743 (TIM-929) DIRECT CURRENT ELECTROMAGNETIC PUMP ANALYSIS. McConville, J. H. (Pratt and Whitney Aircraft, Middletown, Conn. Connecticut Advanced Nuclear Engineering Lab.). July 8, 1965. Contract AT(30-1)-2789. 31p. Dep. mn; CFSTI, $2.00 cy, $0.50 mn.

This report is a twofold endeavor to evaluate the two-pass Direct Current Electromagnetic Pump. The first section is concerned with analyzing the classical rectangular channel EM pump. The second section utilizes this analysis to develop a computer program which can be used to aid in design of the pump. None of the results of this anal-

ysis have been experimentally verified; thus some refinement and modification would be expected. (auth)

40744 (UCRL-14264) THERMAL RESISTANCE OF CONTACTING SURFACES: HEAT TRANSFER BIBLIOGRAPHY. Vidoni, Carlotta M. (Lawrence Radiation Lab., Univ. of California, Livermore). June 1965. Contract W-7405-eng-48. 17p. Dep. mn; CFSTI $1.00 cy, $0.50 mn.

A bibliography of approximately 100 references is presented on interface contact resistance and related subjects such as surface heat flux and temperature measurements. The bibliography covers the period 1938 to May 1965 and is arranged alphabetically. (D.L.C.)

40745 MEASUREMENT OF THE VOID FRACTION IN TWO-PHASE FLOW BY X-RAY ATTENUATION. Pike, R. W.; Wilkins, Bert Jr.; Ward, H. C. (Georgia Inst. of Tech., Atlanta). A.I.Ch.E. (Am. Inst. Chem. Engrs.) J., 11: 794-800(Sept. 1965).

The use of an x-ray tube that emits a spectrum of energy was found to be an effective source of monoenergetic radiation for the measurement of the void fraction in two-phase, steam-water flow with the proper selection of the tube wall thickness, x-ray tube operating conditions, collimation, and traverse time. Assuming monoenergetic radiation, equations were derived for the local and average void fraction and the statistical error associated with the measurement, and were confirmed to be applicable by using the mock-up technique. This consisted of simulating the two-phase, steam-water flow patterns of the experimental system with mock-ups of Lucite and air. Experimental data are presented to show that confidence could be placed in the measurements to within the probable statistical error, as all deviations of the measured values of the void fraction from the actual values were less than the probable error. Local and average void fractions for steam-water, two-phase flow are given. Application to other systems can be inferred from these results. (auth)

40746 FORCED CONVECTION MASS TRANSFER. PART II. EFFECT OF WIRES LOCATED NEAR THE EDGE OF THE LAMINAR BOUNDARY LAYER ON THE RATE OF FORCED CONVECTION FROM A FLAT PLATE. Thomas, David G. (Oak Ridge National Lab., Tenn.). A.I.Ch.E. (Am. Inst. Chem. Engrs.) J., 11: 848-52(Sept. 1965). (ORNL-P-917).

The local and average rates of forced convection through laminar boundary layers on a flat plate were found to be markedly increased by locating small cylinders near the outer edge of the boundary layer. The local rate of forced convection was strongly peaked directly beneath each cylinder; the magnitude of the effect depended upon the free stream velocity, the spacing between cylinders, and the gap between the cylinders and the plate. Under optimum conditions, local values of the rate of forced convection were increased as much as 340%, while the average values were increased by over 190%. (auth)

40747 HEAT TRANSFER THROUGH A VERTICAL ANNULAR GAS LAYER. Novakovic, M.; Jovic, V.; Pislar, V. Bull. Boris Kidrich Inst. Nucl. Sci., 16: 1-10 (Jan. 1965).

The determination of heat transfer through a vertical annular gas layer is discussed. A correlation was found experimentally allowing determination of the equivalent gas convection coefficient, i.e., of the heat transferred through the gas layer, for a given pressure, temperature, and thickness of the layer. (auth)

40748 HEAT TRANSFER OF A REACTOR FUEL ELEMENT MODEL WITH POLYZONAL-SPIRAL FINNING AT LOW GAS FLOW RATES (Re < 15,000). Becirspahic, S.; Vehauc, A.; Kulundzic, P. Bull. Boris Kidrich Inst. Nucl. Sci., 16: 33-47(Jan. 1965).

Heat transfer of a reactor fuel element model with polyzonal-spiral finning was investigated in the Re-number range 1500 to 15,000. The distribution of the St-number over the length and perimeter of the fuel element and its dependence on the flow-rate was determined. The minimum and mean St-numbers were plotted against the Re-number. The flow pattern and heat transfer were found to be considerably different from those at higher gas-flow rates. (auth)

40749 LAMINAR DUCT FLOW OF A PARTIALLY IONIZED GAS (thesis). Bahadori, Mehdi Nejad. Urbana, Ill., Univ. of Illinois, 1964. 128p.

The transport properties of partially ionized argon, the relaxation of electron temperature, and the electronic recombination coefficient were determined semi-experimentally by solving the momentum and energy integral equations. The equations of change, being non-linear, second-order partial differential equations, were transformed to first-order, non-linear differential equations by application of the integral method. The integral equations of momentum, energy and diffusion are, due to variable transport properties and presence of recombination terms in the energy equation, inter-dependent. An order of magnitude approximation shows that heat transfer to the walls due to electron-ion recombination is small compared to the heat transfer by conduction. The energy equation thus becomes separated from the diffusion equation. The heat loss by radiation and aerodynamic heating are also negligible. The momentum and energy integral equations are solved simultaneously by the iteration method, by assuming simple velocity and temperature profiles. The electron-ion recombination coefficient is evaluated for the range of $5500 < T_e < 8500°K$; $10^{18} < n_e < 10^{21}$ m^{-3}; and p = 250 and 750 mm Hg; and compared with the data obtained by others. The data show that the recombination coefficient increases as pressure, electron temperature and concentration decrease. The study of the interaction of a partially ionized gas with cooled walls shows that non-equilibrium states and properties due to electron relaxation have to be considered. When applied to the problem of re-entry, substantial electrical and thermal conductivities, not too much lower than those of ionized gas behind the shock wave, exist at a cooled wall, although the gas temperature decreases significantly toward the wall. (Dissertation Abstr.)

40750 RADIATIVE TRANSFER STUDIES AND OPACITY CALCULATIONS FOR HEATED GASES. Penner, S. S.; Patch, R. W. (California Inst. of Tech., Pasadena). p.211-38 of "High Temperatures in Aeronautics." New York, Pergamon Press and Milan, Tamburini Editore, 1964.

Representative radiative transfer studies and recent developments in opacity calculations for heated gases are outlined. The spectroscopy of gases forms the basis for a quantitative understanding of radiative transfer problems. The following topics are treated: the formulation of radiative transfer problems; the definition of opacities and radiation free paths for the important limiting cases of a transparent gas and an opaque gas; the reformulation of the conservation equations with proper allowance for radiative energy transport; selected calculations of spectral absorption coefficients in molecular systems; and continuum radiation in plasmas containing polyelectronic, partially or completely ionized atoms. (auth)

40751 CAVITATION IN REAL LIQUIDS. Proceedings of the Symposium, General Motors Research Laboratories, Warren, Michigan, 1962. Davies, Robert (ed.). New York, Elsevier Publishing Company, 1964. 193p. $10.00. (CONF-620906).

The proceedings contain the papers presented in a symposium on the theory of cavitation in real liquids. Included topics are bubble dynamics, the growth and decay of bubbles, flow around a bubble rising in a tube, measurements of bubble growth during mass transfer, supercavitating flows and practical applications, and cavitation in hydrodynamic lubrication. Also considered are free boundary problems for viscous flows in channels, cavities between moving parallel plates, cavitation in lubricating oil films, the molecular theory of surface tension, and surface effects in non-spherical motions of small cavities. (J.F.P.)

40752 IMPROVEMENTS IN AND RELATING TO TUBULAR HEAT EXCHANGERS. Lindley, Bryan Charles (to C. A. Parsons and Co. Ltd.). British Patent 998,315. July 14, 1965. Filed Feb. 28, 1962.

A heat exchanger, particularly applicable to use with magnetohydrodynamic or magneto-plasma-dynamic apparatus, consists of an exchanger in which a gas containing a metal vapor is cooled. The gas flows through a casing and a bank of cooling tubes are arranged in concentric coils within the casing. Each coil includes one or more tubes extending from one end of the heat exchanger to the other in helical fashion with respect to the axis of the exchanger. A condensing region is provided adjacent to the outlet end of the exchanger in which the gas velocity is reduced to permit condensation of the metal vapors from the gas. This cooled region has an enlarged flow area to reduce the velocity of the gas and incorporates a metal screen surrounding the ends of the tubes and condensing the vapor. (B.L.M.)

Materials Testing

40753 (EURAEC-1378) NON-DESTRUCTIVE WELDING TESTS. Quarterly Report No. 14, October 1–December 31, 1964. (Roentgen Technische Dienst N. V., Rotterdam (Netherlands)). Apr. 29, 1965. Contract 045-61-5 RDH. 24p. (EUR-2339). Dep. mn; CFSTI, $1.00 cy, $0.50 mn.

Work Performed under United States–Euratom Joint Research and Development Program.

Radiographs were made of defects in steel test blocks and the image quality evaluated for a 5 Mev linear accelerator, a 17 Mev betatron, and a 31 Mev betatron. Other variables evaluated included the testblock thickness, film type, and thickness and position of lead or tantalum screens. (W.L.G.)

40754 PROCEEDINGS OF THE FOURTH INTERNATIONAL CONFERENCE ON NON-DESTRUCTIVE TESTING HELD IN LONDON ON 9th–13th SEPTEMBER, 1963. London, Butterworths, 1964. 375p. $39.00. (CONF-630905).

Proceedings of the Fourth International Conference on Non-Destructive Testing are presented. Topics covered include: practical considerations on non-destructive testing, radiography, ultrasonics, non-destructive testing of pressure parts, and other non-destructive testing techniques and practices. Separate abstracts were prepared for 8 papers. Two papers were previously abstracted for NSA and appeared as 19: 13263 and 13603. (M.C.G.)

For abstracts of individual papers see: 40755–40757, 41201, 42024, 42025, 42071, and 42146.

40755 AN IMPROVED TECHNIQUE FOR THE MEASUREMENT OF DENSITY OF CONCRETE AND SOILS WITH GAMMA RADIATION. Preiss, K.; Newman, K. pp 135-41 of Non-Destructive Testing. London, Butterworths, 1964.

An instrument and testing technique were developed for measuring the density of concretes or soils in situ, which are negligibly dependent on the proportions of the constituent elements in the material. Sources of gamma energy, nuclear cross sections, nuclear reactions, and the detection system are discussed. A sodium iodide scintillation counter was used to detect photons scattered by the material. Calibration curves and source-detector geometry are discussed. The effectively infinite volume and acceptable calibration curve are given. Improvements to the calibration curve are considered. (M.C.G.)

40756 ULTRASONIC DETECTION OF NON-BOND IN CLAD STRUCTURES. McClung, R. W.; Cook, K. V. pp 267-71 of Non-Destructive Testing. London, Butterworths, 1964.

The ultrasonic methods described for non-bond evaluation in clad structures may be divided into two categories: the transmission method, in which the sonic energy transmitted through the bond region is monitored, and the reflection method, in which the energy reflected from the bond region is evaluated. Uses for inspection of clad fuel plates are described. (M.C.G.)

40757 RECENT EDDY-CURRENT DEVELOPMENT AT THE OAK RIDGE NATIONAL LABORATORY. Dodd, C. V. pp 304-7 of Non-Destructive Testing. London, Butterworths, 1964.

Developments in eddy-current testing are reviewed. Analytical calculations and empirical measurements were made for various eddy-current probe-coil designs pertaining to both coil impedance and magnetic field distribution. Amplitude-sensitive devices in eddy-current testing are used for coating thickness measurements, flaw detection, and dimensional gaging. Errors in amplitude-sensitive measurements due to coil-to-specimen spacing were studied and improvements made in equipment and techniques to reduce these errors. Phase measurements were used. A transistorized instrument was developed, which employs a driving coil to furnish the magnetic field and a pick-up coil for measuring the transmitted field. These measurements can be made either by through transmission or from one side. Reactor components fabricated from aluminum, stainless steel, and graphite were measured by these phase-sensitive techniques. (M.C.G.)

Protective Structures

40758 (AD-426249) STUDY OF GROUND-MOTION EFFECTS ON THE CONTENTS OF BURIED STRUCTURES. Beck, E. J. (Naval Civil Engineering Lab., Port Hueneme, Calif.). Oct. 30, 1963. 40p. CFSTI $3.60 cy, $0.50 mn.

Many facets of ground-motion damage to the contents, both animate and inanimate, of buried shelters used for protection against nuclear weapons are considered. A discussion is given of possible shock-mitigation and evasion schemes. An extended experimental program based on design accelerations, velocities, and transient displacements as measured in weapons tests is outlined. The economics of various isolation systems are discussed, major design and test areas are delineated, and priorities for work in the experimental program are suggested. (auth)

40759 (ORNL-TM-1183) ENGINEERING AND COST CONSIDERATIONS FOR TUNNEL GRID BLAST SHELTER CONCEPT. Narver, David L. Jr.; Robbins, Donald T. (Holmes and Narver, Inc., Los Angeles, Calif.). Aug. 1965. Contract W-7405-eng-26. 130p. Dep. mn; CFSTI $4.00 cy, $1.00 mn.

For Oak Ridge National Lab., Tenn.

From the data developed, it is possible to establish the areas of most cost as well as the areas having the greatest potential of cost savings. For example, about half of the cost of the assumed design is in the entrance complex, so additional thought will now be given with regard to making the arrangement compatible with prefabricated mass production construction methods. This might entail using more circular sections or going to an arch section in lieu of the rectangular section used. The type of entrance door will be more fully explored because of the problems inherent with moving large numbers of people through an entrance that has any form of barrier in the way. The mechanical and electrical systems can be refined. Even though the use of this system as a shelter is for only 30 days, it may be that some of the cost can be offset by using portions of the system for everyday uses, such as selling refrigeration capacity to adjacent buildings, leasing small amounts of tunnel space to power or telephone companies, or using the tunnel as a pedestrian walkway. (auth)

Space Propulsion

See *also* REACTOR TECHNOLOGY — Propulsion and Space.

40760 (N64-25008) SUMMARY REPORT ON ELECTRON BOMBARDMENT ION ENGINE DEVELOPMENT. Final Report. Eckert, A. C.; Bond, A. F.; Coerdt, R. J.; Mueller, M. W. (TRW Electromechanical Div., Thompson

Ramo Wooldridge Inc., Cleveland, Ohio). Feb. 1964. Contract NAS 3-2522 134p. (NASA-CR-54082; TRW-ER-5805). CFSTI $10.50 cy, $1.00 mn.

Experimental and analytical efforts to develop an electron bombardment ion engine having a slit aperture geometry and using permanent magnets are described. Data on engine performances of several accel-decel extraction system geometries are presented, and the dependence of the source performance on the source geometry is discussed. A cathode development program is described and evidence for the occurrence of cathode sputtering is indicated. The results of extended testing of the developed ion engine system are presented. Extraction system lifetime is predicted. (auth)

40761 (N64-30604) CONTINUOUS MICROWAVE MAGNETIC ACCELERATOR. Summary Report, August 8, 1963-August 7, 1964. Miller, David B. (General Electric Co., Philadelphia, Pa. Missile and Space Div.). Contract NAS 3-3567. 109p. (NASA-CR-54134). CFSTI $4.00 cy, $0.75 mn.

A cyclotron-resonance accelerator (8.35 gc) was tested up to 4,150 watts, and was shown under proper conditions to convert over 50% of the incident r-f power into directed motion of the accelerated exhaust stream. Continuous operating times at these several kilowatt power levels were typically 1 to 4 minutes. Total and sampling collectors were used to measure power and ion-flux density within the accelerated plasma stream. Calorimetry in the thrustor walls, shielded antenna probes, bare-electrode probes, and a microwave reflectometer yielded additional thrustor characteristics. (auth)

40762 (N64-31010) MAGNETIC INDUCTION PLASMA ENGINE. Summary Report. Heflinger, Lee; Schaffer, Allan (General Technology Corp., Torrance, Calif.). June 10, 1964. Contract NAS 3-3566. 53p. (NASA-CR-54063). CFSTI $3.00 cy, $0.50 mn.

Experimental performance of an induction plasma engine shows a strong accelerative coupling between magnetic field and high-density plasma. The engine consists of a constant phase velocity 450-G magnetic field oriented perpendicular to the axis of a 4.6-cm-diam propulsion tube and powered by a megawatt-level 480 kc oscillator. The engine runs at a steady state without preionization during 1.25 msec runs. About 200 kw of power have been transferred to a helium plasma. Thrust exerted on the drive coils and the propellant flow rate reveal that approximately half of the 200 kw is supplied to the plasma as directed kinetic energy, the other half as disordered energy. This performance approaches one theoretical limit for a constant phase velocity accelerator. However, at present approximately half of the power and thrust supplied to the plasma are in turn lost to the tube walls. A program to alleviate plasma wall interactions is suggested. (auth)

40763 (N64-31453) PERFORMANCE STUDY OF A REPETITIVELY PULSED TWO-STAGE PLASMA PROPULSION ENGINE. Summary Report. Gorowitz, B.; Gloersen, P., Ruess, A.; Kenney, J. (General Electric Co., Philadelphia, Pa. Missile and Space Div.). Aug. 17, 1964. Contract NAS 3-3570. 123p. (NASA-CR-54064). CFSTI $4.00 cy, $1.00 mn.

The major fraction of the program was devoted to increasing the energy term representing work done on the plasma, $\int_0^t i^2 L\,dt$, with respect to the loss term, $\int_0^t i^2 R\,dt$, or, in other words, by increasing L with respect to R. Several possible means for increasing L were explored, i.e., by altering engine geometry, altering propellant distribution in the engine, and increasing peak currents (since, under certain conditions, L was found to be proportional to i) by increasing circuit capacitance and decreasing initial circuit inductance. The energy efficiency trends were monitored by means of exhaust stream calorimetry. Of the above variations explored, propellant distribution and engine geometry proved by far to be the most fruitful. (auth)

40764 (N65-27691) CYCLOTRON RESONANCE PROPULSION SYSTEM. Semiannual Report. Miller, David B.; Bethke, George W. (General Electric Co., Philadelphia, Pa. Missile and Space Div.). May 17, 1965. Contract NAS 3-6266. 72p. (NASA-CR-54213).

Two cyclotron-resonance plasma accelerators were built. Both are of the longitudinal-interaction type, and each has a 1.152 inch inside diameter. One features axial injection of the propellant through a hole in the waveguide window. Peripheral injection is employed in the other. A total calorimeter, an array of diode probes, an energy analyzer, and potential probes were employed to study the exhaust stream. The axial injection accelerator was shown to have relatively low power efficiency (a maximum of 42% of the r-f power was observed in the exhaust stream) and the window design is not structurally adequate. Preliminary diode probe array studies of the peripheral injection accelerator indicate that the efficiency may be better. The energy analyzer probe shows that the ions have mean energies of 57-197 ev with spreads of ±15-35%. (auth)

40765 (NP-15309) ION ROCKET ENGINE DEVELOPMENT. Quarterly Progress Report No. 2, January 1, 1965-March 31, 1965. Zimmerman, R. L.; Garvin, H. L.; Thompson, S. A.; Kami, S.; Killgrove, T.; Hammond, J. M.; Couvillion, J.; Smith, J.; McKee, W. (Hughes Research Labs., Malibu, Calif.). June 18, 1965. Contract NAS 3-6271. 139p.

Efforts during the report period were directed toward evaluation of a 20-strip cold focus electrode ion engine. A 44-hr test of a four-strip integral focus ion engine was completed, and another four-strip engine is being assembled along with a 13-strip integral focus system. Research on a decelerating collector structure for ions is summarized. Techniques for joining W inserts to porous W ionizers were continued. A system designed to permit ionizer evaluation at high current density without contamination by sputtered material from beam deflecting plates was completed. In other work, a correlation was established between the permeability and time decay messurements on ionizer material. Development of improved high-temperature solenoid valves used in engine tests is reported. (J.R.D.)

40766 PHYSICAL ELECTRONIC PHENOMENA IN ION PROPULSION ENGINES. Brewer, George R. (Hughes Research Labs., Malibu, Calif.). IEEE (Inst. Elec. Electron. Engrs.), Spectrum, 2: 65-79(Aug. 1965).

The development and special problems and effects of ion propulsion engines are discussed. There are two classes of electrostatic or ion engines currently under development, differing principally in the method of creation of the ions. In the electron bombardment engine the ions are created by electron impact in a Penning-type discharge and are extracted from the resulting plasma by means of a set of accelerating grids placed at one end of the discharge chamber. In the contact ion engine, ions are created by contact ionization of the propellant (cesium) with a hot ionizer electrode and are accelerated in a geometry of electrodes roughly similar to conventional electron guns used in traveling-wave tubes. These ion engines are discussed in detail. The topics considered are ionization and emission phenomena, the cesium and plasma ion sources, charge-exchange effects, electron emission, focus-electrode emission, ion-beam neutralization, and environmental effects. The engine development is currently in a phase of long-duration reliability testing. (J.F.P.)

40767 HIGH TEMPERATURES IN AERONAUTICS. Proceedings of the Symposium Held in Turin 10-12 September, 1962. Ferrari, Carlo (ed.). International Series of Monographs in Aeronautics and Astronautics. Division IX: Symposia, Volume 15. New York, Pergamon Press and Milan, Tamburini Editore, 1964. 467p. (CONF-620904).

Separate abstracts were prepared for six of the eighteen papers included. The remaining papers deal with rocket propulsion and materials problems. (W.L.G.)

For abstracts of individual papers see: 40750, 40768, 41081, 41154, 41935, and 41936.

40768 EXPERIMENTS OF ELECTRIC PROPULSION BY THERMOELECTRIC MOTORS. Robotti, A. C.; Oggero, M. (Politecnico, Turin). p.299-313 of "High Temperatures in Aeronautics." New York, Pergamon Press and Milan, Tamburini Editore, 1964. (In Italian).

Some research on electric propulsion for space flight is discussed. Several types of arc jets with magnetic stabilization were developed. Tests of these devices (operating with nitrogen) at a power level of the order of 30 kw for periods for several hours are summarized. (D.C.W.)

40769 SURFACE IONIZATION ENGINE DEVELOPMENT. Ernstene, M. P.; Forrester, A. T.; James, E. L.; Purmal, G. W.; Worlock, R. M. (Electro-Optical Systems, Inc., Pasadena, Calif.). New York, American Institute of Aeronautics and Astronautics, 1965, Preprint No. AIAA 65-375, 22p, $1.00. (CONF-650711-3). ORINS.

From AIAA 2nd Annual Meeting and Technical Demonstration, San Francisco.

Several surface ionization engines of a nominal 10 mlb size have been tested for efficiency and lifetime. All of these are characterized by sastrugi contoured porous emitters, but with different geometric details and slightly different overall dimensions. The first high performance engine operated at a power/thrust ratio of 200 kw/lb. Performance was improved on subsequent engines, first to 175 and then to 160 kw/lb. Decreased ionizer cell size and better ionizer materials have led to these improvements. Endurance tests as long as 750 hours have been made. Zero-g cesium feed systems are generally used. Attempts to operate neutralizers for long duration have disclosed difficulty in positioning a conventional emitter so that it is both well coupled to the beam and safe from sputtering damage. A new form of neutralizer has been developed to solve this difficulty. It uses the plasma from a small cesium discharge to couple electrons into the ion beam. Electron emission efficiency above 50 mA/watt, beam potentials below 10 volts, and unlimited neutralizer life appear possible with this device. (auth)

40770 CESIUM ELECTRON BOMBARDMENT ION ENGINES. Speiser, R. C.; Reid, G.; Sohl, G. (Electro-Optical Systems, Inc., Pasadena, Calif.). New York, American Institute of Aeronautics and Astronautics, 1965, Preprint No. AIAA 65-373, 31p, $1.00. (CONF-650711-5). ORINS.

From AIAA 2nd Annual Meeting and Technical Demonstration, San Francisco.

Both electromagnet and permanent magnet versions of the electron bombardment cesium ion engine have been developed. The two types of engines are similar in performance. Mass utilization efficiencies over 90% are obtained at discharge energy expenditures of 350 to 400 ev/ion. Overall engine efficiencies range from 55% at 3000 seconds specific impulse to efficiencies of 87% at 9000 seconds. In three consecutive tests an engine system was operated for a total thrusting time of 2610 hours at the nominal design point of 7000 seconds I_{sp}, 10 mlb thrust, and 182 kw/lb. Each of the three runs was terminated by exhaustion of the cesium supply. In each case over 99% of the initial cesium load in the zero-g feed system was extracted. As a result of these tests lifetimes in excess of 10,000 hours can be extrapolated for electron bombardment cesium ion engines. (auth)

40771 ELECTRIC PROPULSION GROUND TESTING. Worlock, Robert; Moore, Robert A. (Electro-Optical Systems, Inc., Pasadena, Calif.). New York, American Institute of Aeronautics and Astronautics, 1965, Preprint No. AIAA 65-478, 22p, $1.00. (CONF-650711-4). ORINS.

From AIAA 2nd Annual Meeting and Technical Demonstration, San Francisco.

Continuing development of electric propulsion devices has increased the need for testing techniques and facilities. Current testing programs include qualification testing of flight hardware, developmental testing for achieving improved thrustor performance, and reliability testing for achieving useful operating lifetime. Two types of electric propulsion devices, plasma thrustors and ion engines, appear most promising at this time and are receiving the majority of the effort. Ground testing requirements and measurement techniques for the two are quite different. The plasma thrustors require only modest vacuum; a tentative criterion for chamber pressure allows background gas flow into the accelerating region of 1 to 10 per cent of the propellant flow. This corresponds to chamber pressures of about 10^{-4} torr. Ion engines require high vacuum; typical pressures are in the 10^{-6} torr range. Gas analysis studies are under way to determine the constituents of the residual gas and the effects of these constituents on engine performance. Ion beam collection techniques are being studied; improvements promise to decrease sputtering erosion of the facility and to decrease propellant and collector material returned to the vicinity of the engine, an important consideration in the simulation of space operation. (auth)

Vacuum Engineering

40772 (ORNL-P-1465) AN UNCONVENTIONAL ULTRA-HIGH VACUUM FACILITY. Barnett, C. F.; Ray, J. A. (Oak Ridge National Lab., Tenn.). [nd]. Contract W-7405-eng-26. 7p. (CONF-650512-5). Dep. mn; CFSTI $1.00 cy, $0.50 mn.

From Symposium on Engineering Problems of Controlled Thermonuclear Research, Livermore, Calif.

A vacuum system was developed which is capable of maintaing a pressure of 10^{-10} torr in the interaction region during measurements of atomic collision cross sections. The performance of two pumps is compared. The compartmentalized vessel is described, and the procedure for obtaining the required vacuum is given. Typical mass scans are given. (D.L.C.)

40773 VACUUM TECHNOLOGY. Nucl. Eng., 10: 295-300(Aug. 1965).

Developments in subsidiary techniques in vacuum technology are reviewed. Pumps, pumping methods, low-pressure measurement techniques, and leakage and leak testing procedures are considered. Uses of vacuum systems are reviewed. (M.C.G.)

40774 A NEW SINGLE-WALLED UHV EVAPORATOR WITH VERY LOW CYCLING TIMES. Schuetze, H. J.; Hennings, K. E. (Telefunken AG, Ulm, Ger.). Vakuum-Tech., 14: 117-25(June 1965). (In German).

A vacuum evaporator is described, which permits deposition of thin films in ultrahigh vacuum at very low cycling times. In this two-chamber plant, the stainless steel deposition chamber is separated from the evaporation chamber by a plane separation wall. A small aperture is provided for the transfer of the evaporating material from the source to the substrate. The aperture can be closed, hence allowing for a separate degassing of the evaporation source and of materials, completely shielded from operations in the deposition chamber. The total arrangement is differentially pumped, and pressures in the 10^{-9} torr range are obtained within a total cycling time of two hours. The vacuum evaporator is characterized by a simple and reliable operation. Results on the pumpdown performance under various conditions are presented. (auth)

40775 UHV-HIGH TEMPERATURE VALVES WITH GOLD-WIRE SEALING. Bueltemann, H.-J.; Ewers, J.; Meyer, W. (ATLAS Mess- und Analysentechnik GmbH, Bremen). Vakuum-Tech., 14: 132-7(June 1965). (In German).

Ultrahigh vacuum valves, which can be baked out in a closed condition and which can be operated at 350°C without causing early corrosion of the sealing are described. Method and results of the test of durability and of the measurement of conductivity are discussed. (auth)

40776 DESIGN AND FUNCTION OF A HYDRAULICALLY ACTUATED ULTRA VACUUM THROUGH-WAY VALVE. Hauff, A.; Kienel, G.; Wamser, A. (W. C. Heraeus GmbH, Hanau, Ger.). Vakuum-Tech., 14: 139-41(June 1965). (In German).

A hydraulically actuated ultra vacuum through-way valve with a valve disk of 160 mm dia is described. In open as well as in closed positions the valve can be heated up to 300°C. The conductance in open position amounts to 250 $l \cdot s^{-1}$, the total leakage in the closed position is less than 10^{-10} Torr $\cdot l \cdot s^{-1}$. Based on the same construction principle it is possible to fabricate still larger ultra vacuum valves. (auth)

40777 USE OF A MASS SPECTROMETER DURING OUTPUT MEASUREMENTS OF SPUTTERING PUMPS. Robinson, N. W. (Mullard Research Lab., Redhill, Eng.). Vide, 20: 186-93(May-June 1965). (In French and English).

A small r-f mass spectrometer was used to observe peculiarities in the behavior of a sputter ion pump during speed measurements. The selective pumping and desorption of nitrogen, and argon was demonstrated under various conditions of pumping. (auth)

GEOLOGY AND MINERALOGY

General

40778 (COO-689-50) CORRELATION AND CHRONOLOGY OF ORE DEPOSITS AND VOLCANIC ROCKS. Annual Progress Report. Damon, Paul E. (Arizona Univ., Tucson. Geochemical Section). Aug. 1, 1965. Contract AT(11-1)-689. 157p. Dep. mn; CFSTI $5.00 cy, $1.00 mn.

The chief interest in the research was on Cenozoic magmatism and ore deposition within the Basin and Range Province of Arizona. Developments in analysis of argon, potassium, rubidium, and strontium are discussed. Areal and topical studies were conducted on the Tucson Mts., Roskruge Mts., post-Paleozoic igneous activity in the Dos Cabezas Mts., rock ages in Sierrita Mts., initial $^{87}Sr/^{86}Sr$ ratios of Laramide igneous rocks at Silver Bell, Arizona, ^{40}Ar in feldspar from rocks, K-Ar dates for volcanism adjacent to Colorado River, granites from Kabaing Batholithic complex, and Mesozoic-Cenozoic pulses. Some trace element research was conducted on the "Turkey Track" andesite problem, the behavior of Cu, Zn, and fourth period divalent transition elements during magmatic crystallization, and genesis of copper porphyry deposits. Papers on the individual topics are included as appendices. (D.L.C.)

40779 TRAVEL TIMES FROM CENTRAL PACIFIC NUCLEAR EXPLOSIONS AND INFERRED MANTLE STRUCTURE. Carder, Dean S. (Coast and Geodetic Survey, Washington, D. C.). Bull. Seismol. Soc. Am., 54: 2271-94(Dec. 1964).

Travel time data were compiled from widely recorded nuclear detonations in the Eniwetok and Bikini atolls of the central Pacific. These data were taken from several sources, including: seismograph records in the files of the Coast and Geodetic Survey; readings supplied by Australian and Indian seismologists; and readings made from stations under the control of the the U.S.S.R. and subsequently published. Although a number of stations recorded ten or more events from each atoll, the resulting data were considered as from a single point source, precisely known in time and place. Composite P-wave travel times are presented in a graphical form and, in the distance range from 3 to 102°, are shown as eight nearly straight-line segments. P-wave speeds in the top of the mantle averaged about 8.2 km/sec to distances beyond 17°, and a sharp discontinuity at 19.5° was indicated. There was no evidence for or against a low-speed layer in the upper mantle nor for a regional shadow zone. A mantle model consisting of discrete spherical shells was constructed. A core depth of 2870 km, 30 km short of the accepted value, was calculated from PcP arrival times at Matsushiro and College outposts, which were 2.5 and 3.5 sec earlier than indicated in the Jeffreys-Bullen (J-B) tables. These travel time data and inferred mantle structure apply to the Pacific basin and portions of the bordering continents, but similar data from high energy sources in the Nevada test site (NTS) and Sahara in the distance range from 23° to 70° pointed to somewhat the same conditions, with allowances for regional variations and station corrections. Regional corrections could account for the apparency of the three straight line segments beyond 70° since most of the stations in this range were located in western North America. In comparison with the J-B times, travel times to the western cordillera (70 to 85°) were relatively late, and to the central plains, 85° to 97°, they were relatively early. The same tendency was indicated when travel was from the opposite direction, from Sahara sources, except that the order of distances was reversed. P-wave travel time and amplitude data from large explosions in the NTS are under investigation and are being combined with the Pacific data presented to obtain an average travel time curve compatible with source and station corrections indicated by application of standard statistical methods to the body of existing data. A computer program, which will provide continuous updating of the curve and corrections as new data become available, is being formulated. (BBB)

Natural Radioactivity and Fallout

See also HEALTH AND SAFETY.

Refer also to abstract 40835.

40780 (BNWL-SA-242) FALLOUT RADIONUCLIDES IN ALASKAN FOOD CHAINS. Hanson, W. C. (Battelle-Northwest, Richland, Wash. Pacific Northwest Lab.). July 13, 1965. Contract AT(45-1)-1350. 25p. (CONF-650713-1). Dep. mn; CFSTI, $1.00 cy, $0.50 mn.

From American Veterinary Assn., 102nd Annual Meeting, Portland, Oreg.

Results of radioecological research in northern Alaskan ecosystems during the period 1959 to 1965 showed that ^{90}Sr, ^{131}I, and ^{137}Cs were the most important fallout radionuclides from a public health standpoint. Iodine-131 concentrations in caribou thyroids usually obtained maximum values about two months following a major series of atmospheric nuclear weapons tests. Total radiation dosages received by the animal thyroids were much less than those at which damage might occur. Strontium-90 and ^{137}Cs concentrations in Alaskan Arctic biota increased gradually from 1959 through 1962, and then increased rapidly. The lichen-caribou-man food web maintained radionuclide levels greater than in most other ecosystem components. Strontium-90 concentrations in caribou bone samples from northwestern Alaska increased from about 10 to 20 picocuries per gram dry weight during 1960 and 1961 to about 50 pCi/g in 1964. Concentrations in caribou bone were about 3 to 4 times those in lichens and about 1,000 times those in caribou flesh. Strontium-90 ingestion rates of Anaktuvuk Pass Eskimos from caribou meat were within recommended radiation protection guides. Cesium-137 concentrations in lichens doubled during the period 1962 to 1964. Greater than average precipitation may have been a major cause of the increase. Cesium-137 concentrations in lichens were about seven times those of ^{90}Sr; among caribou flesh samples the $^{137}Cs:^{90}Sr$ ratio was about 800. Caribou flesh ^{137}Cs concentrations changed greatly with season. Minima occurred during summer periods when caribou are eating much green forage and maxima occurred during winter when lichens form a major part of the diet. There were no major differences in radionuclide burdens of caribou and reindeer samples collected from the same region. A tenfold difference between concentrations in caribou and moose flesh collected from the same location at the same time is ascribed to very different food habits. Cesium-137 body burdens in various ethnic groups of Alaskan natives during the summers of 1962 to 1964 were directly proportional to caribou or reindeer consumption. Maximum amounts in native residents occurred in Anaktuvuk Pass Eskimos, river village and coastal Eskimos contained intermediate amounts, and Little Diomede Eskimos and Fort Yukon Indians contained the least. Periodic whole-body counting of Anaktuvuk Pass Eskimos demonstrated a seasonal cycle of ^{137}Cs body burdens. Lowest values occurred in January and maxima during July. This resulted from the Eskimo practice of utilizing caribou killed during spring and fall seasons. Spring-killed animals contained greater ^{137}Cs concentrations than did fall-killed animals because of the utilization of lichens during winter periods. Cesium-137 body burdens of Alaskan natives during the summer of 1963 were about 50 per cent greater than during 1962 and during 1964 were twice those of 1963. It is concluded that ^{131}I is of transitory

importance in Alaskan ecosystems while ^{90}Sr and ^{137}Cs are fallout radionuclides of long-range importance. The higher levels of ^{90}Sr and ^{137}Cs concentrations in the Alaskan lichen-caribou-man food web during the summer of 1964 resulted from the ability of lichens to retain fallout radionuclides for considerable time; the greater utilization of lichens for food, especially in winter, by caribou as compared to other animals; and the dependence upon caribou or reindeer for food by certain native populations. Although there appeared to be some difference between radionuclide concentrations in plants and animals from various locations in Arctic Alaska, the statistical significance of such differences was not demonstrated. (C.H.)

40781 (NP-15179) DISTRIBUTION STUDIES OF COMMON AND RADIOACTIVE CESIUM IN NATURE AND IN MAN. Final Report, April 1, 1962–March 31, 1965. Yamagata, Noboru (Institute of Public Health, Tokyo (Japan). Dept. of Radiological Health). 18p. Dep. mn.

The relation between the content of stable Cs and ^{137}Cs in blood and the whole-body was determined by parallel measurements of Cs and ^{137}Cs in whole-body and blood made on human subjects at monthly intervals. Cesium was determined in whole blood after neutron activation. Relatively small monthly fluctuations were found in whole-body values but blood values showed considerable monthly fluctuations. Results suggested the validity of employing a factor of 6 in relating whole-body to blood concentrations in a quasi-equilibrium state between the diet and whole-body content of ^{137}Cs. Comparison of data with measurements of ^{137}Cs content in blood samples obtained from blood banks throughout Japan indicated there may be a slight geographical variation. The data also indicated that women have less Cs in their blood than men have. On the assumption of the Japanese standard man having a body weight of 56 kg, of which one-third by weight is total blood, the whole-body blood Cs content was calculated as 9 μg. The whole-body content of Cs was calculated to be 1.1 mg. Thus 0.8% of the whole-body Cs is in blood. This finding can be applied in the assessment of the whole-body content of ^{137}Cs by analysis of blood. It is concluded that whole-blood analysis for ^{137}Cs may be valuable where whole-body counters are not available. Twenty samples of human rib bone were analyzed for stable Sr and Ca content. The results showed 124 ppm of Sr and 37.3 of Ca on the average, based on ash weight. The Sr/Ca ratio was found to be 3.3×10^{-4}. Rice samples collected throughout Japan were analyzed for Sr and Ca content. The results showed a considerably higher Sr content in polished rice than in unpolished brown rice. The discrimination ratio of Sr/Ca from polished rice to human bone was calculated as 0.13 and from brown rice to human bone as 0.22. The discrimination factor from diet to bone in Japan is 0.17. Mechanisms of the distribution of ^{137}Cs and stable Cs in nature and the role of food chains in the incorporation of ^{137}Cs in man are discussed. Standard diets in Japan and in the U. S. are compared as to content of stable Cs, Mn, and Fe. It is concluded that the radiological protection of a population should be planned on the basis of dietary differences. (C.H.)

40782 (NP-15325) THEORETICAL ASPECTS ON THE FORMATION OF NUCLEAR WEAPON DEBRIS. Edvarson, K. (Forsvarets Forskiningsanstalt, Stockholm (Sweden)). Apr. 1965. 41p. Dep. mn.

The processes which lead to the formation of radioactive debris after a nuclear explosion in the air are discussed. It is assumed, that the material in the explosion cloud is completely vaporized in the first moments after the explosion, and that the debris is produced by nucleation in the gas phase and in later stages by condensation on the particles already formed. Under the conditions prevailing in explosion clouds at moderate altitudes, the coagulation process that occurs after the formation of the primary debris particles, determines the final particle size distribution. The effect of the coagulation process on the distribution of the radioactive material on particles of different sizes was studied. In an appendix a more general study of the particle size distributions resulting from coagulation processes of different types is presented. (auth)

40783 (NP-15327) OBSERVATIONS ON THE PARTICLE PROPERTIES OF NUCLEAR DEBRIS IN THE UPPER ATMOSPHERE. Edvarson, K.; Sisefsky, J. (Forsvarets Forskiningsanstalt, Stockholm (Sweden)). Apr. 1965. 18p. Dep. mn.

By means of an autoradiographic method, the number concentration of nuclear debris particles of different radioactivity content was studied. The material consisted of air-filter samples taken at an altitude of 8-12 km in 1961-1963. In the periods studied, the concentration of particles with diameters larger than about 0.5 μm was of the order 10-100 kg^{-1} in the lower stratosphere and decreased slowly with time. It was found, that the content of such particles relative to the total radioactivity decreases fairly rapidly. It was also observed, that the relative concentration of larger particles is higher in the tropospheric samples than in the stratospheric. (auth)

40784 (RME-129(Rev.)) AIRBORNE RADIOMETRIC SURVEYING — OFFICE AND FIELD TECHNIQUES. Boyle, Thomas L. (Grand Junction Office (AEC), Colo. Production Evaluation Div.). July 1963. 32p. Dep. mn; CFSTI, $2.00 cy, $0.50 mn.

In the method of airborne radiometric surveying, commercially available scintillation counters are installed in light aircraft that are flown about 80 miles per hour at elevations of 25 to 100 feet. Ground crews examine all the anomalies detected and evaluate the discoveries. In the three-year AEC program, 81,000 square miles were aerially surveyed in 14 western states, and 1140 anomalies were located. These anomalies included uranium discoveries in the Colorado Plateau, the Black Hills, Wyoming, New Mexico and Arizona. (auth)

40785 (TID-21224) FISSION PRODUCTS IN THE ATMOSPHERE AND IN RAIN. Kuroda, P. K.; Kauranen, Pentti; Palmer, B. D.; Menon, K. K.; Fry, L. M. (Arkansas Univ., Fayetteville. Dept. of Chemistry). [1964]. Contract AT(40-1)-3235. 21p. Dep. mn; CFSTI $1.00 cy, $0.50 mn.

The concentrations of ^{89}Sr, ^{90}Sr, ^{140}Ba, ^{141}Ce, and ^{144}Ce in individual samples of rain and snow have been measured radiochemically at Fayetteville, Arkansas, for the past several years. Certain features of the isotopes ratio data may be explained as due to atmospheric fractionation of nuclear debris taking place on a global scale. High concentrations of ^{54}Mn, ^{124}Sb, and ^{125}Sb were observed in air filter samples collected in connection with the Project Star Dust in 1962 and 1963. The $^{125}Sb/^{90}Sr$ ratio in 1963 samples was found to correspond to values reported for the production ratio in thermonuclear explosions, but some samples collected at high northern altitudes in 1962 showed an excess of ^{125}Sb. It appears that ^{125}Sb was partly produced through second order neutron capture in ^{124}Sb. A sudden increase of ^{54}Mn concentration was observed in April 1963 at an altitude of 30,000 to 35,000 feet. (auth)

40786 (JPRS-30500) DETERMINATION OF THE FRACTIONATION COEFFICIENTS AND THE BIOLOGICAL AVAILABILITY OF THE PRODUCTS OF NUCLEAR EXPLOSIONS IN RADIOACTIVE FALLOUT. Izrael', Yu. A. Translated from Dokl. Akad. Nauk SSSR, 161: 343-6(1965). 9p. (TT-65-31211). CFSTI $1.00 cy.

Radioactive products bound, within the nuclear fission cloud, to particles produced within the high-temperature fission zone comprise the main part of radioactive fallout. The present paper investigates the distribution of radioactive products on large spherical particles (diameter larger than 10 to 20μ) produced in large quantities during ground level explosions (basically as a result of the melting of ground particles). The results of these theoretical studies are used for an illustrative calculation of fractionation coefficients and biological accessibility of ^{90}Sr and ^{140}Ba. The author points out that, in the case of high-altitude explosions, during which particle formation is the result of condensation of the evaporated bomb substance and the subsequent coagulation of the submicron

particles, many of the assumptions of the present work require further refinement. (A.T.D.)

40787 THE MOBILITY SPECTRUM OF THE SMALL RADIOACTIVE IONS OF THE AIR. Bricard, Jean; Girod, Paul; Pradel, Jacques (CEA, Gif-sur-Yvette, France). Compt. Rend., 260: 6587-90(June 21, 1965). (In French).

The mobility spectrum of small radioactive ions of the air, derived from radon and thoron, is obtained by using an Erickson spectrograph in which the collecting electrode is replaced by a nuclear photographic plate made conducting by coating with metal. The existence of two categories of ions is shown. The more numerous constitutes a mobility band between 0.3 and 1.1 $cm^2v^{-1}sec^{-1}$. The other is a narrow band centered on the mobility 2.1 $cm^2v^{-1}sec^{-1}$. (tr-auth)

40788 THE RADIOACTIVITY OF THE GRANES METEORITE (FALLEN NOVEMBER 13, 1964), MEASURED BY γ SPECTROMETRY. Nordemann, Daniel; Tobailem, Jacques; Schneizer, Michele (CEN, Saclay, France; CNRS, Gif-sur-Yvette, France). Compt. Rend., 260: 6664-6(June 21, 1965). (In French).

The activities of γ emitters in a 1.186-kg sample of the Granes (Aude) stone meteorite were determined by quantitative γ spectrometry with low self-movement. (tr-auth)

40789 RESULTS OF MEASUREMENTS AND ANALYSES OF NUCLEAR FALLOUT UP TO THE BEGINNING OF 1965. (Charles Univ., Hradec Kralove Czechoslovakia). Czech. J. Phys., 15: 506-12(1965).

In consequence of the Moscow Agreement on the cessation of nuclear tests in the atmosphere there was a further decrease in the activity of dry fallout and rainout, as well as in ground level air, in 1964. The daily activities decreased in order to tenths of mc/km^2. From April to August an increase in the activity was again seen, which was caused by the fall of radioactive dust from the stratosphere to the troposphere in consequence of meteorological factors. Seasonal variation was not so pronounced in 1964 as in the previous year, when the activity increased in May and June 6 to 7 times that of February and March. In 1964 the activity increased approximately 3 times. The conception of the existence of a stratospheric reservoir of artificial radioactivity, formed as a result of nuclear tests, was thus confirmed once again and so was the existence of a certain residence time of radioactive dust in the stratosphere because in 1963 nuclear explosions were no longer performed. The mean residence time was calculated from the decrease of strontium-90, separated by radiochemical analysis. The mean value of the residence time is 1.6 of a year, which indicates a reservoir in the higher stratosphere. (auth)

40790 AIRBORNE OBSERVATIONS OF NATURAL RADIOACTIVITY IN THE ATMOSPHERE. Warburton, J. A. (Commonwealth Scientific and Industrial Research Organization, Sydney); Fookes, R. A.; Watt, J. S. Nature, 207: 181(July 10, 1965).

Measurements of background counting rates at altitudes up to 3.6 km were made using a scintillation detector. Counting-rate values at intervals of 150 m altitude for six aircraft flights are plotted against altitude. Effects of humidity are discussed. Probably mainly radon and its decay products were the sources of the detected activity, with ^{214}Pb and ^{214}Bi the principal gamma sources. The day-to-day variations in count rate were surprisingly large and were found to occur largely in the atmosphere between the ground and temperature inversion layers. The variations are due mostly to changes in concentration of natural radioactivity. (M.J.T.)

40791 STRONTIUM ISOTOPE COMPOSITION AND POTASSIUM-RUBIDIUM RATIOS IN SOME ROCKS FROM REUNION AND RODRIGUEZ, INDIAN OCEAN. McDougal, Ian; Compston, W. (Australian National University, Canberra). Nature, 207: 252-3(July 17, 1965).

Results on the isotopic composition of Sr and the K/Rb ratio obtained on a series of rocks covering a wide range of composition from the volcanic island of Reunion, Indian Ocean, are presented. Two samples also were analyzed from Rodriguez, an island about 800 km east of Reunion. The work was performed to examine the geographic homogeneity of the Sr isotopic composition and the K/Rb ratio in rocks derived from the upper mantle and to see whether there is a correlation between these values and the bulk chemical composition of the rocks. (M.J.T.)

40792 BULLETIN OF THE ATMOSPHERIC RADIOACTIVITY, NO. 38, JULY-SEPTEMBER, 1964. Tokyo, The Japan Meteorological Agency, 1964. 67p. (In English and Japanese).

The results of measurements of a temporary standard sample (U_3O_8) at several stations and of radioactivity in rain, airborne dusts, and sea water are tabulated. (D.C.W.)

40793 ASPECTS OF THE GEOCHEMISTRY OF THE RARE EARTHS. Ahrens, L. H. (Univ. of Cape Town). pp 1-29 of Progress in the Science and Technology of the Rare Earths. Vol. I. New York, The Macmillan Co., 1964.

A review is presented of the geochemistry of the lanthanons and yttrium. Abundances and abundance relationships in meteorites, rocks, and sediments are discussed in detail. The geochemical coherence of the rare earths is compared with that of other groups of elements. (D.L.C.)

Techniques and Equipment

Refer also to abstract 40920.

40794 (AEC-tr-6577) MODERNIZATION OF RADIOACTIVITY LOGGING APPARATUS. Kukharenko, N. K.; Basin, Ya. N. Translation of pp 19-26 from Yadernaya Geofizika, Gostoptekhizdat, Moscow, 1961. 12p. Dep. mn; CFSTI $1.00 cy, $0.50 mn; JCL $1.60 fs, $0.80 mf.

The limitations of available gamma-logging and neutron-gamma-logging (NGK) instruments are discussed. A method was developed for modernizing existing NGGK-55 and NGGK-57 instruments, and an improved NGK probe was also developed. With the modernized instruments, the porosity of a carbonate section in wells of diameter 20–30 cm can be determined with an accuracy of 20%. The individual elements of the modernized instruments are described. (D.L.C.)

40795 AGE MEASUREMENTS USING THE CARBON-14 METHOD. Delibrias, G.; Guillier, M.-T.; Labeyrie, J. Bull. Inform. Sci. Tech. (Paris), No. 89, 3-22(Jan. 1965). (In French)

Some examples of dating in archeology and geology performed by the Service d'Electronique Physique using the carbon-14 method are summarized. Some of these measurements proved that the Sahara had a wet climate not so very long ago. It was shown that the carbon-14 method can be successfully applied to the dating of mortars. (tr-auth)

40796 RADIOMETRIC AGE OF THE SERRA GERAL FORMATION. Creer, K. M. (Univ. of Newcastle upon Tyne); Miller, J. A.; Smith, A. Gilbert. Nature, 207: 282-3(July 17, 1965).

Rock samples from the Serra Geral formation, a mass of lava flows in Uruguay and Brazil, were dated by the whole-rock potassium-argon method. The petrographic composition of the samples is given, and results of the age determination are tabulated. (M.J.T.)

40797 THE UTILIZATION OF RADIOCARBON ^{14}C IN THE INVESTIGATION OF ATMOSPHERIC MOVEMENTS. Moscicki, Wlodzimierz (Gdansk Polytechnic Inst., Poland). Postepy Fiz., 16: 159-74(1965). (In Polish).

Carbon age estimation techniques are described, along with their application to the inverse problem, which is the determination of the relative amount of ^{14}C in the atmosphere throughout a period of several millennia. The past values were compared with recent measurements that span

the period of thermonuclear explosions. These explosions inject a quantity of ^{14}C that is localized both in position and time. The worldwide efforts at mapping ^{14}C concentrations as a function of time and geographic location are outlined. ^{14}C diffusion by motions of air masses were analyzed. A model of vertical-turbulence diffusion is presented that can be studied with an electric circuit analog. It includes as primary or secondary diffusion sources the stratosphere, troposphere, biosphere, water and soil surfaces, deep water, and a sub-soil sink. The motion of ^{14}C via the atmosphere is treated in terms of a turbulence-diffusion constant of about five months. (TTT)

Thorium and Uranium Minerals

40798 (RME-4571(Rev.)) RECONNAISSANCE FOR URANIUM IN THE COLIMAPU FORMATION OF CENTRAL CHILE. Bowes, William A.; Knowles, Paul H.; Moraga B., Aldo; Klohn H., Erik; Serrano C., Mario (Division of Raw Materials (AEC), Washington, D. C. and Instituto de Investigaciones Geologicas, Santiago (Chile)). Oct. 1962. 20p. Dep. mn; CFSTI, $1.00 cy, $0.50 mn.

Laboratory and field studies showed that the geologic history and environment of the Colimapu formation of central Chile differed considerably from those of the uranium-bearing Diamantiano formation of Argentina with which the Upper Colimapu has been correlated. However, the Lower and Middle Colimapu correlate with the Huitriniano formation in Argentina. (auth)

40799 MCKELVEYITE, A NEW HYDROUS SODIUM BARIUM RARE-EARTH URANIUM CARBONATE MINERAL FROM THE GREEN RIVER FORMATION, WYOMING. Milton, Charles; Ingram, Blanche; Clark, Joan R.; Dwornik, Edward J. (Geological Survey, Washington, D. C.). Am. Mineralogist, 50: 593-612(May-June 1965).

A mineral of composition $Na^{1+}_{1.3}Ba^{2+}_{1.0}Ca^{2+}_{1.1}Sr^{2+}_{0.2}RE^{3+}_{1.5}U^{4+}_{0.3}(CO_3)^{2-}_{8} \cdot 5H_2O$ was found in 4 subsurface localities some 20 miles apart in Sweetwater County, Wyoming. It was the first known mineral with considerable uranium (4.6% as UO_2) from the Green River Formation. Two types are known, one in apple green crystals and simple morphology and a more abundant type, dark green or black, massive and in crystal aggregates, both of which were analyzed. The massive material contained 20.7% insoluble (organic 8.7%, acmite 3.5%, biotite 7.5%, and quartz 1.0%); and the crystal aggregates contained 18% insoluble (organic 3.0%, acmite 2.45%, biotite 9.4%, and quartz 3.0%). This was the first authigenic biotite recognized in the Green River Formation. All these insoluble constituents are presumably syngenetic with mckelveyite. The composition of mckelveyite (crystal aggregates) recalculated for these impurities, is BaO 40.6, CaO 4.0, SrO 1.7, Y_2O_3 7.7, La_2O_3 0.09, Ce_2O_3 0.16, Pr_2O_3 0.05, Nd_2O_3 0.26, Sm_2O_3 0.34, Eu_2O_3 0.19, Gd_2O_3 1.18, Tb_2O_3 0.38, Dy_2O_3 1.00, Ho_2O_3 0.28, Er_2O_3 0.95, Tm_2O_3 0.12, Yb_2O_3 0.61, Lu_2O_3 0.08, UO_2 4.6, ThO_2 0.1, Na_2O 3.9, K_2O 0.1, CO_2 25.7, and H_2O 6.1% for a sum of 100.2%. The crystals are trigonal, space group P3, a 9.174 ± 0.002, c 19.154 ± 0.007 Å and cell volume 1396.1 ± 0.7 Å^3; the three strongest observed x-ray powder lines are 2.942 (100), 4.47 (85), and 6.40 Å (35). The density calculated for two formula units per cell is 3.62 g cm^{-3}; the measured density of the massive aggregate is 2.87 gm cm^{-3}, of the crystals 3.14 gm cm^{-3}; corrected for impurities, the density of mckelveyite in the massive aggregate is 3.58 gm cm^{-3}, in the crystals 3.47 gm cm^{-3}. There is no good cleavage, but fractures are approximately paralleled to (0001) and (11$\bar{2}$1). Piezoelectric tests are negative. Forms observed: c {0001}, r {10$\bar{1}$1}, e {01$\bar{1}$2}, m {10$\bar{1}$1}, and −m {01$\bar{1}$0}. Mckelveyite is uniaxial, negative, $\epsilon = 1.57$, $\omega = 1.66$, pleochroic, green, and $\omega > \epsilon$. Mckelveyite with essentially yttria rare earths occurred together with burbankite, a cerium rare earth mineral. The mineral was named in honor of Vincent E. McKelvey, geologist of the U. S. Geological Survey. (auth)

HEALTH AND SAFETY

See also BIOLOGY AND MEDICINE — Radiation Hazards and Protection
GEOLOGY AND MINERALOGY — Natural Radioactivity and Fallout

Refer also to abstracts 40361, 40402, 40410, 40881, 40911, 40940, and 41171.

40800 (AERE-PR/HPM-7) HEALTH PHYSICS AND MEDICAL DIVISION PROGRESS REPORT, JANUARY-DECEMBER 1964. (Atomic Energy Research Establishment, Harwell (England)). Mar. 1965. 38p. Dep.; BIS, $1.60; HMSO, 8s.

Progress is reported in studies of the properties of radioactive aerosols and their behavior in the atmosphere and deposition on surfaces. Polystyrene aerosols labeled with ^{51}Cr were prepared and methods used in size measurements are discussed. Results are reported from studies of the physical chemistry of iodine compounds formed when elemental I at low concentrations is released in air or carbon dioxide as under the conditions of release during an accident involving a gas-cooled reactor. Progress is reported in the development of neutron dosimeters employing nuclear emulsions; the development of an instrument for measuring the dose-equivalent rate from neutrons in the range 0.025 ev to 10 Mev; the dosimetry of criticality accidents; studies of the biological effects of neutrons using somatic mutations induced in Tradescantia occidentalis as the test object; the neutron activation analysis of man in vivo; and the development of a new film dosimeter, automatic densitometer, and automatic proton recoil counting and data handling procedures. Improved facilities for whole-body counting of radioactivity in man are reported. Results are reported from preliminary studies of the retention and metabolism of inhaled radioactive particles and aerosols. Data are presented on the activity of the thyroid resulting from the inhalation of ^{132}I-methyl iodide. A list is included of 66 publications during the period covered by this report. (C.H.)

40801 (ANL-6991) RADIATION SAFETY TECHNICIAN TRAINING COURSE. PART I. Moe, H. J.; Lasuk, S. R. (Argonne National Lab., Ill.). Dec. 1964. Contract W-31-109-eng-38. 151p. Dep. mn; CFSTI, $5.00 cy, $1.00 mn.

This manual presents information on the basic principles of radiation; natural radioactivity; the properties of α, β, γ, x radiations and neutrons; wave properties; electromagnetic waves; the interactions of γ and x radiations and neutrons with matter; radiation units and dose determinations; shielding; biological effects of radiation; background radiation; radiation protection standards; and internal dose calculations. (149 references). (C.H.)

40802 (CONF-650616-5) DEVELOPMENT OF SAFETY PERFORMANCE CRITERIA AND TESTS STANDARD FOR RADIOISOTOPE SEALED SOURCES AND DEVICES. Hitch, James W. (Division of Isotopes Development (AEC), Washington, D. C.). [1963]. 12p. Dep. mn; CFSTI $1.00 cy, $0.50 mn.

From Health Physics Society, Annual Meeting, Los Angeles.

The Atomic Energy Commission, in recognizing the ever-increasing use of radioisotopes, also recognizes the increased possibility of the accidental release of radioactive materials to the environment through fires, collisions, etc. Accordingly, a safety testing program has been initiated to develop a technical basis for safety performance standards. The program is aimed at preventing mishaps during the many types of applications and associated handling procedures for radioactive materials and/or isotopic devices. The tests are designed to provide information for more accurate assessment of the engineering safeguards for control of the risks involved in permitting wider beneficial usage. This information should assist the manufacturer in designing more reliable equipment and assist regulatory groups in establishing safe, yet reasonable, safety standards. Equally important, the public will be more assured that isotope equipment is built to meet carefully developed safety standards. The classification of sources within a performance rating system, together with a companion system for classification according to application, is described. The development of specially designed radioactive materials for selected applications, and the type of tests necessary to assure that these desired standards are met, are also briefly described. (auth)

40803 (NAA-SR-Memo-9719) SODIUM FIRES AND THE RELEASE CHARACTERISTICS OF PARTICULATES AND FISSION PRODUCTS. Lauben, G. N.; Koontz, R. L.; Jarrett, A. A. (Atomics International, Canoga Park, Calif.). Apr. 12, 1965. Contract AT-11-1-GEN-8. 23p. Dep. mn; CFSTI $1.00 cy, $0.50 mn.

Physical and chemical characteristics of sodium fires are described briefly. The modeling of large sodium fires is considered. Laboratory experiments and field experiments on large fires are described. The results show that most of the iodine remained trapped in the oxide phase in the burnpot. (D.L.C.)

40804 (NP-14925) STRAHLEN-ALARMES. (Alarm Plan). Seelentag, Walter; Schmier, Herbert (Bundesgesundheitsamt, Berlin (West Germany). Institut fuer Wasser-, Boden- und Lufthygiene). Nov. 6, 1961. 24p. Dep. mn.

The factors that should be considered in the drawing up of an alarm system in the event of local or wide-spread contamination or radiation danger are outlined in order to serve as the basis of discussions on the drawing up and implementation of a national radiation alarm system. The factors indicated are establishment of the maximum permissible limit as assumption for the "alarm level," proposal for the alarm system, proposal for composition of the Radiation Commission, precautions in danger and alarm cases, classification of the necessary precautions, and formulation of the precautions to be taken. (J.S.R.)

40805 (NRS-30) ENVIRONMENTAL RADIOACTIVITY IN NEW SOUTH WALES. Pallister, E. T.; Green, J. H. (New South Wales Univ., Kensington (Australia). Dept. of Nuclear and Radiation Chemistry). 1965. 26p. Dep. mn.

The inhalation and ingestion of the natural alpha-emitting nuclides of uranium, thorium, polonium, and radium, the natural beta-emitter, potassium-40, and the artificial beta-emitters, cesium-137 and strontium-90 are discussed. Emphasis is put on the somatic effects in lungs and bone of the presence of these radionuclides. Difficulties in the assessment of the tissue dose levels arising from the inhalation of radioactive aerosols and in understanding the precise nature of the aerosol are noted. The natural water contents of ^{226}Ra, ^{222}Rn, and daughters in water from Australia, United Kingdom, and the U. S. A. are compared. The attempt to measure body burdens of ^{226}Ra by the analysis of teeth in the Illinois area is considered. Fallout of natural nuclides arising from ^{222}Rn is reviewed and the significance of coal combustion in adding to the fallout is treated in a general account of mining hazards. It is possible that these are contributing factors in the production of lung carcinoma in mining. The discovery of minute amounts of alpha-emitters in tobacco in Australia and England has led to the confirmation of the presence of ^{210}Po, a daughter of ^{226}Ra, in tobacco smoke and the human lung and to an estimate of tissue dose rates. It is suggested that the ^{210}Po content is in excess of that required for equilibrium with ^{226}Ra, and that the excess could arise from natural fallout and subsequent absorption from the ground. High values of the ^{90}Sr content of tea consumed in Australia suggest a plant specificity for this nuclide.

Levels of ^{90}Sr and ^{137}Cs in rainfall at Sydney and Milford Haven (U.K.) are compared for 1963. (auth)

40806 (RL-SA-37) INDUSTRIAL NOISE CONTROL IS PRACTICAL. Hutton, P. H. (General Electric Co., Richland, Wash. Hanford Atomic Products Operation). May 21, 1965. Contract AT(45-1)-1350. 12p (CONF-650808-1). Dep. mn; CFSTI, $1.00 cy, $0.50 mn.

From American Industrial Hygiene Assn., Seattle.

An extensive program of noise control has been conducted at the various process sites within the Hanford Atomic Plant. At the outset, criteria were developed to provide a basis for judging the severity of noise conditions and the high noise level areas were surveyed and categorized on the basis of these criteria. This program demonstrated that effective control of industrial noise does not require sophisticated, expensive techniques. This statement is supported by a number of specific examples where glass fiber blanket material, acoustical baffles, mufflers, and simple system modifications were utilized to good effect in combating problems of high noise level. (auth)

40807 (RL-SEP-389(Rev.)) CRITICALITY SAFETY OF FISSILE MATERIALS IN THE CHEMICAL PROCESSING DEPARTMENT. Warren, J. H. (General Electric Co., Richland, Wash. Hanford Atomic Products Operation). July 28, 1965. Contract AT(45-1)-1350. 11p. Dep. mn; CFSTI $1.00 cy, $0.50 mn.

Four procedures are given for applying criticality safety controls to the shipping and receiving of fissile materials in the Chemical Processing Dept. These procedures are for the off-site shipment of fissile materials, for receiving fissile materials from off-site, for posting and labeling fissile materials, and for transfer of fissile materials between the Chemical Processing Dept. and other Hanford components. (D.L.C.)

40808 (SC-RR-65-98) PROCEEDINGS OF THE INTERNATIONAL SYMPOSIUM FOR PACKAGING AND TRANSPORTATION OF RADIOACTIVE MATERIALS, HELD AT ALBUQUERQUE, NEW MEXICO, JANUARY 12–15, 1965. (Sandia Corp., Albuquerque, N. Mex.). June 1965. Contract AT(29-1)-789. 743p. (CONF-650103). Dep. mn; CFSTI, $10.58 cy, $3.00 mn.

Participants in the symposium included representatives, from AEC, major contractors, laboratories and universities, IAEA, traffic authorities, Bureau of Explosives, licensees, shipping cask manufacturers, and foreign countries. The technical papers covered recent developments in regulations, standards, proof-testing, and research and development on containers. Safety factors in handling and transport are considered. Separate abstracts were prepared for 24 of the papers; for abstracts of 19 other papers, see NSA 18: 6972, 39528, and 40211; 19: 7650, 13557, 13666, 15697, 15790, 15942, 18193, 20196, 20239, 24814, 24815, 24816, 24817, 26571, 26572, and 30436. (D.L.C.)

For abstracts of individual papers see: 40809–40832.

40809 (SC-RR-65-98, pp 17-31) A SURVEY OF RESEARCH IN THE TRANSPORTATION OF RADIOACTIVE MATERIALS. Thompson, J. Trueman; Morgan, James M. Jr.

An extensive survey was conducted during the first quarter of 1964. The purpose of the review was (1) to ascertain what work has been completed, what is in progress, what lies ahead, and (2) to judge if duplication is present, if gaps exist, or if needed areas of research are being neglected. From the observations and opinions obtained, the strengths and weaknesses of the program were evaluated and are presented with some final comments. (auth)

40810 (SC-RR-65-98, pp 32-44) PACKAGING STANDARDS. Appleton, G. J.; Servant, J. Y.

The two standards of packaging, Type A and B, are discussed. A review is given of the research conducted to make the standards for Type A and B packaging more objective. After a consideration of normal and accident conditions in the transport environment, mechanical and physical tests for prototype packages of Type A and B are discussed. It is pointed out that the revised IAEA regulations no longer contain reference to normal transport or maximum credible accidents, but instead define Type A and B packages in relation to tests. (D.L.C.)

40811 (SC-RR-65-98, pp 45-54) REGULATORY PACKAGING STANDARDS. Barker, Robert F.; Hopkins, Donald R.

A discussion is presented of the transport regulations recommended by IAEA and of these proposed for use within U. S. The principles involved in the proposed AEC regulations are defined. The transport of fissile materials is considered in some detail. (D.L.C.)

40812 (SC-RR-65-98, pp 74-8) ASPECTS OF TRANSPORTATION OF RADIOACTIVE MATERIALS. George, T. C.

An informal discussion is presented of various aspects such as avoidance of accidents, accident experience, regulations, and hysteria following accidents. The Bureau of Explosives and its activities are described briefly. (D.L.C.)

40813 (SC-RR-65-98, pp 107-13) RESISTANCE TO FIRE OF LEAD LINED CASKS. Aupetit, A.

The problem of the fire resistance of lead-lined containers and the time required to reach the melting point of the lead was studied using theoretical methods. The calculated heating flux of ~4 w/cm^2 is higher than the real fluxes reached in fire tests (~3 w/cm^2). A small scale model testing method is proposed. (D.L.C.)

40814 (SC-RR-65-98, pp 114-18) FIRE TESTS OF PACKAGINGS FOR RADIOACTIVE MATERIALS. Sousselier, Yves.

Fire-test methods are considered. Two open-air fire tests were conducted on two shielded packagings: "Cendrillon" type for radioactive solutions and GT-200-type for radioactive sources. The temperatures, winds, and lead melting are discussed for each test. An oven test was also conducted on the "Cendrillon" packaging. It is concluded that open-air and oven tests produce comparable results. (D.L.C.)

40815 (SC-RR-65-98, pp 133-40) CAN WE MODEL A FIRE TEST? Wachtell, George Peter.

The internal temperature distribution at time t_p in a prototype shipping container will be modeled at time t_m in a scale model, if the same construction materials are used, $t_m = s^2 t_p$, and the net flux per unit area is $F_m = (1/s) F_p$. Here s is the scale factor. Stress and strain distributions will then also be modeled. These conclusions are only approximate if natural convection of molten lead occurs, but the approximation is very good if the convection is rapid. By repeating a model test several times, one should be able to observe the variability of thermal stress damage. Since net flux per unit area is practically independent of object size in a fire, it is not sufficient to place the model in a fire. Instead, another source of flux must be used. (auth)

40816 (SC-RR-65-98, pp 141-86) NEW DEVELOPMENTS IN ACCIDENT RESISTANT SHIPPING CONTAINERS FOR RADIOACTIVE MATERIALS. Sisler, J. A.

A shipping container was developed which can withstand the fire and drop tests given in the proposed regulations. The container comprises a laminated plywood shell with a 4-inch minimum wall thickness. Results of drop and fire tests of the container are reported. (D.L.C.)

40817 (SC-RR-65-98, pp 243-60) AN ANALYTICAL APPROACH TO STUDY VEHICLE COLLISIONS. Doshi, K. D.

An analytical procedure is presented for studying the structural response of vehicle-container-tiedown systems during longitudinal collisions. After a definition of the problem, the approach to its analytical study is described. A mathematical model is given for a tractor-semitrailer-type vehicle. Equations of motion are presented, and recommendations are given for obtaining numerical results. (D.L.C.)

40818 (SC-RR-65-98, pp 261-82) EXPERIMENTAL STUDIES OF CASK IMPACT RESISTANCE. Clarke, H. G. Jr.

Methods are being developed for assessing the response of casks to impacts that could occur in vehicular or handling accidents. Penetrating and crushing impact tests were made on small scale models of casks for irradiated fuels, and the results are described. (D.L.C.)

40819 (SC-RR-65-98, pp 330-56) PROGRESS REPORT ON A CLASS II CONTAINER FOR LOW ASSAY URANIUM COMPOUNDS. Gutman, Thomas.

A simple and inexpensive container was designed to provide a practical means of shipping uranium having a ^{235}U assay of 5 percent or less. The container has a tare weight of approximately 150 pounds, and provides a payload of 37.8 liters. The determination of a safe array is based on the absence of an internal moderator subsequent to immersing the container under 3 feet of water after having been (1) dropped 30 feet onto an unyielding surface; (2) dropped 40 inches onto a 6-inch diameter target; and (3) exposed to a temperature of 1475°F for ½ hour. Since unmoderated low assay (< 5% ^{235}U) uranium cannot achieve criticality, the consideration of optimum interspersed moderation limits the size of the array to approximately 900 containers, as determined using a proposed calculational technique. When subjected to the above conditions, dryness of the payload was essentially but not completely maintained. The presence of minute amounts of water indicates that the incorporation of minor modifications will provide a satisfactory means of shipping dry low assay uranium compounds. (auth)

40820 (SC-RR-65-98, pp 357-76) TESTING SHIPPING CONTAINERS FOR SLIGHTLY ENRICHED URANIUM BILLETS, INGOTS, AND FUEL CORES. Dunaway, D. L.

A series of tests was conducted to evaluate the ability of wide steel-banded wooden boxes to retain their loadings under simulated vehicular accident conditions. These boxes are shipping containers for slightly enriched uranium fuel cores and other metallic pieces. The tests included a box drop test, a tumble test, and a fire test. The tests demonstrated that a wooden box with sufficiently wide steel banding provides a package capable of withstanding considerable impact. This capability is of particular significance when the integrity of the package is a factor in criticality control. (auth)

40821 (SC-RR-65-98, pp 423-41) DESCRIPTION AND EVALUATION OF FOUR $Pu(NO_3)_4$ SHIPPING CONTAINERS. Delnay, R. L.

Structural integrity tests were conducted on 3-liter and 10-liter packages for Class I and II shipments of plutonium nitrate solutions. Results are described for these tests and for shipment tests. Costs of these packages are listed. (D.L.C.)

40822 (SC-RR-65-98, pp 442-9) THE PROBLEM OF CONTAINER INTERCHANGEABILITY. Patterson, D. E.

The special approval system used by the ICC and AEC in shipping radioactive materials is discussed. It is stated that an updated ICC regulation with standardized rules is needed. The advantages of specification containers and their development in the future are considered. (D.L.C.)

40823 (SC-RR-65-98, pp 450-72) DESIGN OF CONTAINERS FOR SHIPMENT OF RADIOACTIVE MATERIALS. Peterson, Reuben W.

A review is presented of design requirements and special features required in containers for shipping radioactive material. The engineer's approach to container design is discussed, and the characteristics of different types of casks in service are examined. (D.L.C.)

40824 (SC-RR-65-98, pp 580-608) TESTING OF 10-TON CAPACITY URANIUM HEXAFLUORIDE SHIPPING CONTAINERS. Myers, J. L.; Pedigo, W. R.; Hamer, W. J.; Smith, V. A.; Bernstein, S.

Drop tests were performed on two types of 10-ton containers: a thin-wall (5/16 in. thick) cylinder used only for storage of UF_6, and a heavy-wall (5/8 in. thick) cylinder used for both storage and interplant transport of UF_6. Horizontal and vertical impact tests were made at heights up to 20 feet. None of the four thin-wall cylinders showed any indication of failure; the only failure that occurred was with the heavy-wall cylinder. The thin-wall cylinders will be used for interplant shipments of UF_6. A 15-min film illustrating the test results was shown. (D.L.C.)

40825 (SC-RR-65-98, pp 609-19) DESIGN OF PLUTONIUM OXIDE AND PLUTONIUM NITRATE SHIPPING CONTAINERS. Adcock, F. E.

The design, construction, and testing of PuO_2 packages for both Class I and II shipments are discussed. A review is made of existing $Pu(NO_3)_4$ container designs to reduce size, weight, and cost. (D.L.C.)

40826 (SC-RR-65-98, pp 625-9) SPECIAL PROBLEMS IN PACKAGING AND TRANSPORTATION OF RADIOACTIVE MATERIALS. Edlow, Samuel.

The subject of packaging and transportation problems is discussed from the viewpoint of traffic management. It is stated that there are no, or only a few, special problems now. The regulatory functions of the various agencies are discussed. The experience gathered on the first movement of irradiated reactor fuel from Sweden to U. S. is described briefly. The turnover in personnel working on packaging and transportation is criticized. (D.L.C.)

40827 (SC-RR-65-98, pp 631-50) FIRE TEST OF 15-TON SHIPPING CONTAINER. Wachtell, George Peter.

Instrumentation and preliminary test results are described for the fire test of the 15-ton shipping container, performed during the symposium. A previous test of various test objects, including a finned box having a similar external configuration but one-third the size, is also described. In the present test, lead leakage occurred, mostly from the lid, starting about half an hour after the start of the test. Leakage appears to have occurred where modifications were made for instrumentation purposes. Chrome-plated and unplated surfaces of auxiliary test objects absorbed heat at the same rate, indicating that soot formed on cool surfaces. This conclusion is uncertain, however, because it is not known how long the chrome-plated surfaces survived. Leaking lead destroyed the stainless-steel sheathed thermocouples wherever it made contact. (auth)

40828 (SC-RR-65-98, pp 679-90) CRITICALITY SAFETY EVALUATION OF PACKAGES FOR THE TRANSPORT OF FISSILE MATERIAL. Smith, David R.

The critical behavior of individual units of fissile material and the interrelationship between density and dimension are discussed. The behavior of arrays of fissile units is next considered, and the reflector effect is shown to be equivalent to a number of units in a critical array. The ratio bare/reflected critical mass is tabulated for several materials. The use of a density analog technique in the evaluation of reflected arrays in transportation problems is described with examples. The degree of conservatism in the calculations is considered. (D.L.C.)

40829 (SC-RR-65-98, pp 711-18) THE TRANSPORT CONTAINER FOR IRRADIATED FUEL FROM CIVIL POWER STATIONS IN THE UK. Johnston, K. W. H.

The container is a fabricated steel flask designed with a limit of 50 tons/load; fuel elements are randomly packed in a skip and cooled by water and fins on the flask. The gas relief filter which prevents water loss is described. Thermal tests with external solar radiation and internal heat sources up to 15 kw show that transport regulations will not be violated. Difficulties encountered in operation are described. (D.L.C.)

40830 (SC-RR-65-98, pp 719-22) DISPERSION OF RADIOISOTOPES CAUSED BY TRANSPORT FIRES. Moriya, T.; Jin, T.

Measurements were carried out on the dispersion ratio of radioisotopes caused by a fire, i.e., the ratio of airborne activity to the activity remaining in the burned materials. The measurements were made burning $^{24}NaCl$

and $NH_4{}^{82}Br$ solutions with various combustible materials at temperatures up to 800°C in a propane fire. The measured dispersion rates are tabulated. (D.L.C.)

40831 (SC-RR-65-98, pp 723-31) STUDIES ON FIRE RESISTIVITIES OF RADIOISOTOPE CONTAINERS. Moriya, T.; Jin, T.

Experimental studies and theoretical calculations were made of the fire resistance of lead-shielded containers of various sizes. Fire tests were also performed on packages used for mailing radioisotopes, and the leakage of $^{24}NaCl$ and $NH_4{}^{82}Br$ solutions from the packages was measured. (D.L.C.)

40832 (SC-RR-65-98, pp 732-5) APPROXIMATE CALCULATIVE ASSESSMENT MADE RELATING TO WALL TEMPERATURES AND BEHAVIOUR OF CASK IN FIRE TESTS. Teague, H. J.; Brook, A. J.

A rough estimate was made of the likely outcome of the fire test, using the assumptions used in the IAEA thermal test (flame temperature, 800°C; flask wall emissivity, 0.8; and convection neglected). Lead begins to melt at 21 min, and is completely molten at 52 min. (D.L.C.)

40833 (UCRL-14116) INDEX TO HAZARDS CONTROL QUARTERLY REPORTS, NOS. 1 THROUGH 19. Block, Seymour; Kathren, Ronald; Kusian, Ross; Lindeken, Carl; Schimmelfennig, Victor (comps.) (Lawrence Radiation Lab., Univ. of California, Livermore). May 23, 1965. Contract W-7405-eng-48. 42p. Dep. mn; CFSTI, $2.00 cy, $0.50 mn.

Subject and author indexes are given for the first 19 quarterly reports (through December 1964) of the Hazards Control Department of Lawrence Radiation Laboratory, Livermore. The subject index is cross-referenced to serve the interests of workers in various disciplines within the field of Health and Safety. A total of 275 articles are indexed. (auth)

40834 (UCRL-14151) HAZARDS CONTROL QUARTERLY REPORT NO. 20, JANUARY–MARCH 1965. (Lawrence Radiation Lab., Univ. of California, Livermore). Contract W-7405-eng-48. 63p. Dep. mn; CFSTI $3.00 cy, $0.75 mn.

K-fluorescent x-ray sources were found to provide clean and uniform monoenergetic spectra with variable intensity. An automatic sampler-changer was constructed which will count up to 100 4-in. × 9-in. air filter papers. Simultaneous counting of alpha and beta radiations is completed by printout of the data on paper tape for each filter. The design of a large-area gas-flow proportional detector for use either in an automatic sample changer or as a manual probe was undertaken for its desirable efficiency and stability. A shield was constructed that provides a low background environment for low-level gamma pulse-height analysis, and minimizes effects of transient gamma and neutron fields. A trailer was equipped for continuous air monitoring of fission product gases. It can be used to measure and record concentrations of 10^{-5} Ci/m^3 or greater. Thermoluminescent dosimeters were used to measure the gamma-ray dose rates in the LPTR thermal columns, irradiation facilities, and core. Improvements in analysis of natural airborne background using solid state detectors are discussed. Universal personalized respirator kits were assembled and issued for use in emergency conditions or for monitoring hazardous operations. A modification of the standard quick-disconnect coupling was developed which prevents inadvertent release of air-line respiratory hose. Investigation results indicate that fiberglass ladders can provide good safe service if an inspection and maintenance program is enforced. (J.R.D.)

40835 GEOCHEMISTRY AND RADIOACTIVITY OF WATERS IN LOURDES, SAN LUIS POTOSI, MEXICO. Stretta, E. J. P.; del Arenal, R. Anales Inst. Geofis. UNAM, Mex., 9: 69-84(1963). (In Spanish).

Geological and chemical studies of the curative waters in Lourdes, Mexico confirmed the presence of low radioactivity in the buildings and the bathing waters of the spa. The presence of low doses of radioactivity are considered to have beneficial therapeutic effects on human organisms. (R.V.J.)

40836 INTERVENTION-DECONTAMINATION BUILDING. CENTRE D'ETUDES NUCLEAIRES DE FONTENAY-AUX-ROSES. Cerre, P.; Mestre, E.; Winter, J. Bull. Inform. Sci. Tech. (Paris), No. 89, 39-51(Jan. 1965). (In French)

A pre-decontamination installation at the Centre d'Etudes Nucleaires is described. All of the techniques used are among the most classic, with no attempt made to attain a fine decontamination. The essential purpose of the installation is to transport safely partially decontaminated and packaged materials. All the regulations on safety were respected in the design of the installation. (tr-auth)

40837 SHIPPING AND STORING POWER FUELS PRIOR TO REPROCESSING. Smiley, S. D.; Langhaar, J. W.; Maher, R. (E. I. du Pont de Nemours and Co., Inc., Aiken, S. C.). Chem. Eng. Progr., 60: Symp. Ser., No. 51, 65-73(1964).

Conditions and regulations for storing and processing spent fuels and blanket materials from nuclear reactors are discussed. Designs of casks for shipping irradiated fuels are reviewed for hazards to the public. Technical design considerations of facilities at the Savannah River Plant for receipt and storage of certain assigned fuels are discussed. Physical layout, services offered, and plant operation are described. (auth)

40838 THE UTILIZATION OF A MAGNETIC INDUCTION FIELD IN THE EXPOSURE MEASUREMENTS OF X AND γ RAYS. Allisy, Andre; Boutillon, Mireille (Bureau International des Poids et Mesures, Sevres, France). Compt. Rend., 260: 6576-9(June 21, 1965). (In French).

The values of the magnetic induction fields necessary to maintain in a cylinder of given radius the paths of electrons produced in air along a beam of photons with energy $\leq$1.3 Mev are given. A simple expression for the radial distribution of the mass ionization around the beam is deduced. (tr-auth)

40839 ON THE CONTROL OF URANIUM IN URINE FOR THE PREVENTION OF PROFESSIONAL INTOXICATION: A STATISTIC CONTRIBUTION. Strambi, E.; Testa, C. (Universita, Rome and Centro di Studi Nucleari, Casaccia, Italy). Energia Nucl. (Milan), 12: 378-82(1965). (In Italian).

The urinary concentration of natural uranium in 77 workers of a nuclear center was determined for a two year period; the workers were subdivided in three groups according to professional exposure, and 1,127 analyses were carried out on a weekly, monthly, and quarterly basis. Because of the low specific activity of natural uranium a fluorimetric determination was used, which allows detection of 1×10^{-6} grams of uranium in 0.2 ml of urine. The experimental results showed a concentration lower than 5 μg/liter in 73% of the cases, from 5 to 25 μg/liter in 26%, and greater than 25 μg/liter in less than 1%. Such results confirmed that the safety provisions in use at the Center were sufficiently adequate. (auth)

40840 SAFETY IN HANDLING FISSIONABLE MATERIALS. Callihan, Dixon (Oak Ridge National Lab., Tenn.); Johnson, E. B. Mag. Std., 36: 81-4(Mar. 1965).

Prevention of nuclear chain reactions in handling, storing, processing, transporting, and treating fissionable nuclides outside reactors is the purpose of a new safety standard. The standard presents generalized criteria on which to base design of equipment and processes for handling fissionable materials. It also references literature that provides solutions to specific problems. Prevention of unintentional chain reactions is important because the energy released in the reaction, principally as heat and radiation, might be lethal to nearby personnel, cause property damage, or interrupt process schedules. (Public Health Eng. Abstr., 45: No. 6, (June 1965).

40841 MONITORING OF COSMIC RADIATION LEVEL DURING THE FLIGHT OF SATELLITES VOSTOK-3, VOS-

TOK-4, VOSTOK-5, AND VOSTOK-6. Savenko, I. A.; Pisarenko, N. F.; Shavrin, P. I.; Nesterov, V. E. (Scientific Research Inst. of Nuclear Physics, USSR). Vestn. Mosk. Univ., Ser. III: Fiz. Astron., No. 2, 40-3(Mar.-Apr. 1965). (In Russian).

The various radiation hazards in space—cosmic charged particles and gamma rays, bremsstrahlung and protons from the radiation belts, solar flares—and their contribution to the total exposure in a space ship are described. The hazard created by the United States' high-altitude nuclear test on Johnston Island in 1962 is discussed. The monitoring, telemetry, and personal dosimetry apparatus used on the Vostok and Kosmos series of satellites is described briefly. The total biological doses to the various Soviet cosmonauts are given. Graphs are presented of the accumulation of absorbed dose inside Vostok-3 and -4 and of dosimetric readings on Vostok-5 and -6. (M.J.T.)

40842 THE IONIZING RADIATIONS IN SUPERSONIC TRANSPORT FLIGHTS. Foelsche, Trutz. (Langley Research Center, Hampton, Va.). 20p. (CONF-720-30). Gmelin, AED-CONF-64-190-35.

From 2nd Symposium on Protection Against Radiation Hazards in Space, Gatlinburg, Tenn., Oct. 1964.

Commercial supersonic transport planes are envisioned to cruise at altitudes up to 23 km or 75,000 feet. The exposure to crew and passengers from galactic and solar cosmic rays at these altitudes on polar routes is estimated and compared with the maximum permissible dose rates (MPD) cited in the guide lines of the Federal Radiation Council or the International Commission for Radiation Protection. (L.B.S.)

INSTRUMENTATION

General

Refer also to abstracts 40409, 40940, 41163, and 41638.

40843 (CEAL–1021) AN ACCURATE CURRENT INTEGRATOR IN THE RANGE OF 10^{-5} TO 10^{-9} AMPERES. Law, Lewis Arthur; Weinstein, Joel (Cambridge Electron Accelerator, Mass. and Harvard Univ., Cambridge, Mass.). May 14, 1965. Contract AT(30-1)-2076. 23p. Dep. mn; CFSTI $1.00 cy, $0.50 mn.

A current integrator is constructed having accuracy 0.3% or better over the range from 4×10^{-5} amperes to less than 10^{-9} amperes, with leakage current less than 5×10^{-14} amps. Positive or negative input currents can be integrated with a duty cycle as low as 0.25%. The unit has a temperature coefficient of 0.03%/°C and is relatively insensitive to external shunt capacity at the input. (auth)

40844 (MATT-341) A HIGH VOLTAGE RADIO FREQUENCY VARIABLE CAPACITOR USING A LIQUID DIELECTRIC. Deitz, Allan (Princeton Univ., N. J. Plasma Physics Lab.). July 1965. Contract AT(30-1)-1238. 27p. (CONF-650512-6). Dep. mn; CFSTI $2.00 cy, $0.50 mn.

From Symposium on Engineering Problems of Controlled Thermonuclear Research, Livermore, Calif.

The theory and construction are described for a compact, high-voltage, high-current, radio-frequency capacitor having a Q in excess of 2000. Four capacitors are utilized in a matching network for a 6-Mw, 25 Mc, pulsed r-f generator, where they are subjected to voltages of 100 kV and currents of 1 kA. The capacitors utilize a liquid dielectric and have operated for 1000 hours. (auth)

40845 (N64–33676) MAGNETORESISTANCE, SUPERCONDUCTIVITY AND THE HALL EFFECT FOR INVERTER APPLICATIONS. Annual Report, June 1963–June 1964. Bechtel, Richard; Pak, Sang So; Grannemann, W. W. (New Mexico Univ., Albuquerque. Engineering Experiment Station). Aug. 1964. 49p. (NASA-CR-59188; EE-115). CFSTI, $2.00 cy, $0.50 mn.

Several Dewar superconductivity measurements were obtained on various magnetoresistor configurations at liquid-nitrogen temperature in relatively low magnetic fields. Two tests were made, but the results were not conclusive. Magnetoresistance samples of ultrahigh-purity carbon were discarded as unusable; but one superconductor wire sample of a 6-foot piece of 20-mil niobium wire, with an insulating copper coil as a field coil, was developed for further testing. A mathematical solution was obtained for a multiterminal Hall generator, and a general equivalent circuit for the N output terminal was developed. The experimental values were found to be accurate within 10%. This multiterminal Hall generator may be used as a dc-to-ac converter by application of an alternating magnetic field. (auth)

40846 (NP-15209) NEKOTORYE VOPROSY TEORII SHIROKODIAPAZONNYKH GENERATOROV. (Certain Theoretical Problems of Wide-Band Oscillators). Vodop'yanov, F. A. (Akademiya Nauk SSSR, Moscow. Radiotekhnicheskii Institut). 1964. 150p. Dep. mn.

Expressions are obtained for the quantitative estimation of the nonlinear frequency correction, the influence of nonlinear and parametric effects on the reactive elements, parametric and Schottky frequency fluctuations, the dependence of frequency on the rate of modulation of parameters, and the filtering properties of the auto-oscillator. The analysis is carried out by the method of integral equations and statistical treatment of the reactions of the auto-oscillator on a delta pulse of the anode current. (64 references.) (tr-auth)

40847 (NYO–2910-11) APPLICATIONS OF ULTRASONIC ENERGY: ULTRASONIC INSTRUMENTATION FOR NUCLEAR APPLICATIONS. Bimonthly Progress Report No. 23 Covering Period From June 1, 1965–July 31, 1965. (Aeroprojects, Inc., West Chester, Pa.). Aug. 1965. Contract AT(30-1)-2910. 10p. Dep. mn; CFSTI, $1.00 cy, $0.50 mn.

An instrument for the determination of proximity to boiling was constructed in accordance with specifications set up by Oak Ridge National Laboratory. Preliminary tests were conducted prior to installation in a pool-boiling capsule. (J.R.D.)

40848 (SC-R-65-935) COMPUTER AIDED CIRCUIT RELIABILITY ANALYSIS. Allen, B. O.; Blazek, D. R.; Purdue, C. H. (Sandia Corp., Albuquerque, N. Mex.). July 1965. Contract AT(29-1)-789. 13p. (CONF-650115-1). Dep. mn; CFSTI, $1.00 cy, $0.50 mn.

From 11th National Symposium on Reliability and Quality Control, Miami Beach, Fla.

A brief review of the Reliability Program is presented. It was found that considerable analysis and design time savings can be achieved by using computers and programs such as the general purpose circuit analysis program, NET-1. Schematic diagrams of two circuits analyzed by the NET-1 program are presented. The necessary input data and plots of the observed and NET-1 predicted output waveforms are also included. Some of the limitations and problems in using the NET-1 program are discussed. Plans in process are presented which upon completion will make the NET-1 program even more useful and universal. (M.O.W.)

40849 (TID–22061) EFFICIENCY OF HIGH PRESSURE ELECTRIC SHOCK TUBES (thesis). Mayes, Terrill Wayne (Vanderbilt Univ., Nashville, Tenn.). Aug. 1965. Contract AT(40-1)-1087. 51p. Dep. mn; CFSTI, $3.00 cy, $0.50 mn.

An experiment was conducted to better understand the operation of electric shock tubes so that a shock tube could be assembled which would produce a shock velocity of about Mach 25 at a pressure of a few hundred torr. The performance of three types of electric shock tubes, each of which is operated at gas pressures between 200 and 760 torr, is studied. (M.O.W.)

40850 (ORNL-tr-588) A DEVICE FOR THE MEASUREMENT OF LIBERATED ENERGY IN EXPLOSION. Sander, Howard H.; Gowen, Maynard Jr.; White, Stuart C. Translated for Oak Ridge National Lab., Tenn., from Japanese Patent 410,184. May 27, 1963. 19p. Dep. mn; JCL, $1.60 fs, $0.80 mf.

The invention of a device for measuring the energy liberated in nuclear or other explosions is reported. The various functions carried out by each section of the device are explained in detail. Diagrams show the actual wiring for the measuring device and a cross-sectional view of the pressure sensing device in the measuring device. (M.O.W.)

40851 SENSITIVITY AND ADMISSIBLE FIELD INHOMOGENEITY OF A NUCLEAR MAGNETOMETER. De Martini, F. (Politecnico di Milan); Lucchini, A. Alta Freq., 33: 746-52(Nov. 1964).

Sensitivity and noise considerations are given for the marginal oscillator in order to obtain an expression for the maximum admissible field inhomogeneity for an autodyne nuclear magnetometer. An experimental nuclear magnetometer is also described, and experimental results for the maximum field gradient that allows a field measurement is compared to the corresponding calculated value. (auth)

40852 LOW-TEMPERATURE CHAMBER FOR NEUTRON-DIFFRACTION STUDIES. Weiss, L. (Zentralinstitut fuer Kernphysik, Rossendorf, Ger.); Kleinstueck, K. Exptl. Tech. Physik, 13: 111-17(1965). (In German).

Cryostats suitable for neutron-diffraction studies are described. Whereas in one chamber (TTK 2) the sample temperature can be varied from 63 to 300°K by draining

of the coolant surface (nitrogen) or by heat resistance, the other chamber (TTK 3) is suitable for sample temperatures of 20°K (hydrogen as coolant) or 27°K (neon as coolant). The construction characteristics and the operational properties are described and discussed. (tr-auth)

40853 MULTICHANNEL ANALYZER OF PULSES FOR IONIZATION CALORIMETER AT CAPACITY MEMORY CELLS AND THE SYSTEM OF INFORMATION OUTPUT. Garibashvili, D. I.; Grigolashvili, T. S.; Kakhidze, G. P.; Chikovani, G. E.; Shrabshtein, S. A. Fiz. Chastits Vysokikh Energii, Akad. Nauk Gruz. SSR, Inst. Fiz., 1: 105-9(1965). (In Russian).

The description of a multichannel system is given. The system is designed to store information obtained from an ionization calorimeter and for the output of the data in the form of figureprint. Data storage is realized at the capacity elements of memory. The operation range of the stored pulses is 0.5 to 100 volts. (auth)

40854 MULTICHANNEL SYSTEM FOR THE ANALYSIS OF PULSES FROM IONIZATION CALORIMETERS. Berger, A. R.; Garibashvili, D. I.; Kakhidze, G. M.; Kakauridze, D. B.; Chikovani, G. E. Fiz. Chastits Vysokikh Energii, Akad. Nauk Gruz. SSR, Inst. Fiz., 1: 111-16(1965). (In Russian).

The description of a multichannel system is given. The system is designed to store and analyze information obtained from an ionization calorimeter. Storage is realized by permalloy cores in the form of their different magnetizations depending on the amplitude of the stored signal. (auth)

40855 INVESTIGATION OF AN RF-ION SOURCE. Gombos, Peter; Kakuk, Janos; Roosz, Jozsef; Valyi, Laszlo. Magy. Tud. Akad. Kozp. Fiz. Kut. Int. Kozlemen., 13: 127-35(1965). (In Hungarian).

An r-f source delivering pulsed ion currents is described. The mass composition and energy distribution of the ion beam for ion-current pulses of 2 to 200 μsec duration at frequencies from 10 to 10000 Hz were measured. The mass spectrum of the ion beam is found to agree with that obtained for a continuous ion current; the energy distribution, however, is a function of the length and shape of the ion-current pulse. (auth)

40856 OPERATION OF A TRANSISTOR IN SATURATION STATE AND A LINEAR GATE. Papadopoulos, L. (Nuclear Research Center Democritus, Athens). Nucl. Instr. Methods, 36: 122-4(Sept. 1965).

When the collector-base junction of a transistor is biased at a low forward voltage (saturation region), every signal to the base appears at the collector without being amplified or reversed. The transistor therefore behaves like a resistor whose value depends on the external network. This principle is used for the design of a linear gate. (auth)

40857 PROTON MAGNETOMETER AND STABLE OSCILLATOR FOR REMOTE MEASUREMENT OF STRONG MAGNETIC FIELDS. Garwin, R. L.; Patlach, A. M. (Columbia Univ., New York). Rev. Sci. Instr., 36: 741-2 (June 1965).

A simple apparatus for proton-resonance magnetic-field measurement permits remote location of the r-f source and indicator. A high-stability variable-frequency oscillator is also described. (auth)

40858 PRECISION (0.1°C) VACUUM CRYOSTAT AND FURNACE FOR MOESSBAUER EXPERIMENTS. van der Woude, F.; Boom, G. (State Univ., Groningen, Netherlands). Rev. Sci. Instr., 36: 800-2(June 1965).

The design of a small vacuum cryostat and furnace for a Moessbauer spectrometer is described. A regulating system for a 0.1°C temperature stability for periods of several days is given. (auth)

40859 INSTABILITY OF REFRACTORY METAL THERMOCOUPLES. Walker, B. E. Jr.; Ewing, C. T.; Miller, R. R. (Naval Research Lab., Washington, D. C.). Rev. Sci. Instr., 36: 816-25(June 1965).

Thermoelectric instabilities of some refractory metal thermocouples have been studied in the temperature range 1000 to 2000°C under vacuum and neutral atmospheres. The sources of instability were found to be complex, involving contamination from ceramic protection tubes and furnace environments, preferential volatilization, and various thermal anomalies such as recrystallization and phase changes in the refractory thermoelements. Refractory thermocouples and thermoelements were studied under a variety of conditions, and emf changes associated with each are reported. Recommendations are presented for the selection and application of these thermocouples to attain maximum thermoelectric stability. (auth)

40860 INVESTIGATION OF PLASMA FREQUENCY MULTIPLIER. Brandt, A. A.; Kaminskii, V. N.; Tyagunov, A. V. Vestn. Mosk. Univ., Ser. III: Fiz. Astron., No. 1, 82-4(Jan.-Feb. 1965). (In Russian).

The efficiency of a plasma microwave multiplier was investigated experimentally at frequencies low enough for the plasma deionization time to be much shorter than, or at least comparable with, the period of the exciting-field oscillations. The multiplier circuit is shown. The nonlinear element was the plasma in an MN-6 neon lamp. The tank circuits were tuned to harmonic frequencies. In view of the dependence of the results on the bias voltage, optimal bias was used in all tests. The results show a marked decrease in the multiplication efficiency (ratio of the harmonic to fundamental power output) with increasing harmonic. This decrease, which can also be derived theoretically, is shown to be due to the gradual linearization of the voltage-current characteristic of the neon lamp with increasing frequency. It is noted that plasma deionization is hindered in neon, and that the use of another gas, say hydrogen, would increase the threshold of efficient frequency conversion by a factor of several times. (ATD)

40861 IONIZATION CHARACTERISTICS OF AN ELECTROMAGNETIC ION SOURCE. Su, Shih-chun; Fu, Chi-hsi. Yuan Tzu Neng, No. 1, 8-17(1965).

The production and distribution of ions were measured in an ionization chamber, and the physical phenomenon was studied by measuring the concentration of n^+ ions and the electron gas temperature. The ionization chamber used in the experiment was a Nielsen type (Nucl. Instru., 1: 287 (1957)). The length was 60 mm. A stainless steel cylinder 52 mm in length and 26 mm in diameter was used as the anode. The cathode was a tungsten filament with a diameter of 0.75 mm. The ionization chamber was placed with its axis in the same direction as the longitudinal magnetic field having a maximum strength of 350 gauss. The magnetic field was not uniform in the chamber. The chamber was filled with argon at a pressure of 0.8 to 5×10^{-3} mm Hg and ionized. The ionization current was found to depend on the gas pressure, arc voltage, and magnetic field. Experimental results showed that volt-ampere curves can be obtained by varying the ionization conditions. The dI_a/dE_a value was found to be low in the absence of a magnetic field with a correspondingly low ion production. The dI_a/dE_a value becomes larger in a magnetic field. Positive ions tend to migrate to the filament where ion concentration is the heaviest. Calculation results showed that the positive ion ratio in an ionization chamber decreases with the increasing voltage and increases with the increasing magnetic field. The distribution of ionic current density diminishes as the ionic radius is increased in a magnetic field. The ionization current density reaches a maximum value near the filament in the absence of a magnetic field. Curves were also obtained for a probe. All electrons are repelled and only positive ions are attracted when the probe potential is greater than the equivalent ionization potential. The output of ions can be increased by using a well designed filament. Moreover, the combined effect of an electric field and magnetic field should be considered. The voltage for argon is about 100 v, and the magnetic field is 150 to 250 gauss. The pressure must be also regulated for stable ionization. The electron gas temperature increases with the increasing arc voltage but diminishes as the pressure and magnetic field are increased. (ATD)

40862 ELECTROMAGNETIC THEORY AND ANTENNAS. Proceedings of a Symposium held at Copenhagen, Denmark, June [25-30], 1962. Parts 1 and 2. Jordan, E. C. (ed.). A Pergamon Press Book. International Series of Monographs on Electromagnetic Waves. Volume 6. New York, The Macmillan Company, 1963. 1360p. $30.00. (CONF-620601(Pts. 1 and 2).

Papers (126) dealing with (Pt. 1) scattering and diffraction theory; anisotropic and stratified media; (Pt. 2) random media and partial coherence; surface waves, leaky waves, and mode propagation; antenna theory and radiating elements; and antenna arrays and data processing are included. Many of the papers are in summary form. (D.C.W.)

40863 INSTRUMENTATION FOR MOESSBAUER-EFFECT EXPERIMENTS AT LOW TEMPERATURES. Murray, B. W. 5p. (CONF-640406-4). Gmelin, AED-CONF-64-198-6.

From American Physical Society, Ohio Section, Spring Meeting, Cleveland.

Experimental apparatus consisting of a cryostat, speaker drive and counting system is described for studying the effect of low temperatures (1 to 100°K) on the fraction of Moessbauer gamma rays from crystalline sources, and also for studying the effects of electric quadrupole splitting of nuclear states in nuclei and magnetic ordering in solids. (L.B.S.)

40864 6600/OCTOPUS INTERFACE CONTROL (Engineering Materials). (Lawrence Radiation Lab., Univ. of California, Livermore). (CAPE-1246).

26 drawings.

A system was designed to permit control of teletypes from the Control Data Corporation's 6600 Computer. Among the specially constructed modules are the 6600/DEC pulse stretcher, 6600/teletype driver card, and resistor card. The pulse stretcher takes the standard 6600 pulse and converts it to a standard Digital Equipment Corporation (DEC) negative-going pulse. The teletype driver card takes standard DEC levels and converts them to the levels required for driving the teletype line. In addition, there is a line current sensing circuit, which converts the line current to standard DEC levels. A 68 ohm resistor, mounted on the resistor card, is used to attenuate the 2.5-v pulse to the amplitude needed. The unit, housed in a double-bay rack 46 in. long, 33 in. wide, and 72 in. high, weighs ~200 lb. The input is 3 amps, 117 v, and 60 cycles. For details, see TID-4100. (M.C.G.)

40865 HIGH PRESSURE X-RAY CAMERA, 12 TON (Engineering Materials). (Lawrence Radiation Lab., Univ. of California, Livermore). (CAPE-1245).

59 drawings.

The apparatus described is used to obtain Debye-Sherrer x-ray-diffraction patterns on polycrystalline substances that are subjected to pressure. In this apparatus, the x rays are collimated so that the beam traverses a compressed wafer normal to its axis. Pressure in an oil chamber is measured with a gage so that an estimate may be made of the nominal pressure at the wafer. The nominal pressure, which is the force on the platen face, is calculated by the usual rules of hydraulics, neglecting friction. For details, see TID-4100. (M.C.G.)

Radiation Detection

Refer also to abstracts 40390, 40432, 40722, 40834, 41301, and 41678.

40866 (AECL-2217) A SOLID-STATE MULTIPLEXER FOR USE WITH SELF-POWERED NEUTRON FLUX DETECTORS. Morin, K. R.; Lennox, C. G. (Atomic Energy of Canada Ltd., Chalk River (Ontario)). Apr. 1965. 26p. Dep.; AECL $1.00 cy.

A 128-input low-current-level, high input impedance solid-state analog multiplexer is described. This multiplexer was designed and built to connect the signals from about 80 self-powered neutron flux detectors to the PDP-5 computer at NRU. The multiplexer consists of a double-banked switching arrangement (eight groups of 16 shunt switches, followed by a second bank of eight series switches). The switches are followed by a common amplifier which produces an output of 0.8 volts full scale for a signal input of one microampere. A seven-bit address register determines the selected input. The source impedance can be neglected if greater than 10^8 ohms. The overall accuracy of the multiplexer is one percent. (auth)

40867 (BNWL-64) BORON-11 NEUTRON FLUX MONITORS — INTERIM REPORT. Bunch, W. L.; Wood, M. R. (Battelle-Northwest, Richland, Wash. Pacific Northwest Lab.). Apr. 1965. Contract AT(45-1)-1830. 16p. Dep. mn; CFSTI, $1.00 cy, $0.50 mn.

The performance of ^{11}B neutron-activation flux monitors is discussed from the viewpoints of response speed, radiation stability, temperature coefficients of response, dynamic range, and physical dimensions. The operation of the detectors is dependent on the beta emission by ^{12}B (half life = 20 μsec) formed by neutron absorption by ^{11}B. (T.F.H.)

40868 (BNWL-SA-23) THERMOLUMINESCENT DOSIMETRY STUDIES AT HANFORD. Endres, G. W. R. (Batelle-Northwest, Richland, Wash. Pacific Northwest Lab.). June 7, 1965. Contract AT(45-1)-1830. 14p. (CONF-650637-1). Dep. mn; CFSTI $1.00 cy, $0.50 mn.

From International Conference on Luminescent Dosimetry, Palo Alto, Calif.

Many substances exhibit the property of thermoluminescence and several were studied and used for dosimetry applications, but the phosphor lithium fluoride appears to be most favorable for use as a neutron gamma dosimeter. Lithium fluoride has good sensitivity to ionizing radiation and retains the radiation damage well for long periods of time. Several different batches of phosphor supplied by two different manufacturers were used to study the energy and dose response, damage storage properties, and parameters of the readout system. The neutron dosimeter system requires two capsules of lithium fluoride, one filled with phosphor only for gamma dose measurement, the other filled with the phosphor plus alcohol (or other hydrogenous material) for gamma plus neutron dose measurement. Results of the two measurements are subtracted to obtain the neutron dose. Extensive tests of the characteristics of the gamma-only dosimeter were conducted. The dose response was quite linear over the dose range studied. A number of neutron exposures were made to monoenergetic neutrons and to a spectrum of neutrons from isotopic sources (PuF_4 and PuBe). (auth)

40869 (CONF-650510-14) INNOVATIONS IN BUBBLE CHAMBER DEVICES. Pewitt, E. G. (Argonne National Lab., Ill. and Carnegie Inst. of Tech., Pittsburgh, Pa.). June 1965. Contract W-31-109-eng-38. 47p. Dep. mn; CFSTI $2.00 cy, $0.50 mn.

From Purdue Conference on Instrumentation for High Energy Physics, Lafayette, Ind.

Outstanding recent developments which make a new generation of bubble chambers economically and technically feasible are discussed. The performance of Scotchlite, a retrodirector for use in bright field bubble chamber photography, is discussed. The status of six large bubble chambers is briefly reviewed. The use of superconducting magnets and a hydrogen-neon mixture in large bubble chambers is considered. (M.O.W.)

40870 (IAE-695) METOD STABILIZATSII TRAKTA USILENIYA STSINTILLYATSINNOGO SCHETCHIKA. (Method of Stabilizing the Amplification Channel of a Scintillation Counter). Sotnikov, S. K.; Efimov, B. V.; Tsitovich, A. P. (Institut Atomnoi Energii, Gosudarstvennyi Komitet po Ispol'zovaniyu Atomnoi Energii SSSR, Moscow). 1964. 16p. Dep. mn.

A method for stabilization of the amplification channel of a scintillation counter using a reference light pulse is considered. The outstanding difference of the method is the use in the comparison circuit of a current pulse proportional to the intensity of the light flash of the counter. A control

circuit governs the amplification factor of the linear amplifier connected to the photomultiplier load. The introduction of this circuit into a gamma spectrometer improved the stability of the position of the spectral lines from 3 to 5% to 0.3 to 0.4%. (tr-auth)

40871 (JINR-P-2179) VOSSTANOVLENIE PROSTRANSTVENNOI KARTINY SOBYTIYA V KSENONOVOI PUZYR'KOVOI KAMERE. (A Reconstruction of the Spatial Picture of an Event in the Xenon Bubble Chamber). Kanarek, T.; Okhrimenko, L. (Joint Inst. for Nuclear Research, Dubna (USSR). Lab. of High Energy). 1965. 14p. Dep. mn.

The processing technique for the xenon bubble chamber photographs is described: 1. The photography parameters are determined whose account is necessary to exclude the distortions of the track images when simulating their spatial picture in the xenon chamber. 2. The application of the methods is described for simulating events by measuring respective and non-respective points in the xenon chamber. (auth)

40872 (JINR-P-2203) PRIMENENIE UPRAVLYAEMOGO FOTOUMNOZHITELYA V KACHESTVE ELEMENTA OTBORA SOVPADENII NANOSEKUNDNOGO DIAPAZONA. (Application of Controlled Photo-Multiplier as a Separating Element in the Nanosecond Coincidence Circuit). Vysochanskii, M.; Nad, L.; Ondrish, L. (Joint Inst. for Nuclear Research, Dubna (USSR). Lab. of High Energy). 1965. 12p. Dep. mn.

The results are presented of investigation of special controlled photomultipliers at a frequency of 150 MHz. When the light source with a duration of light flashes of about 1 ns is used the resolving time is obtained to be 0.7 ns. (auth)

40873 (JINR-P-2215) OPTIMAL'NOE OPREDELENIE EFFEKTIVNOSTI PEGISTRATSII (VESA) SOBYTIYA. (Optimal Determination of the Detecting Efficiency (Weight) of an Event). Vishnevskii, V. F.; Moroz, V. I.; Shakhbazyan, B. A.; Yen, Wu-kuang (Joint Inst. for Nuclear Research, Dubna (USSR). Lab. of High Energy). 1965. 9p. Dep. mn.

The problem of the optimal determination of the detecting efficiency (weight) of events was considered. It is shown that the averaging of the detecting efficiency treated previously increases the accuracy of the final result regardless of the number of detected events. A formula is suggested which shows how the dispersion of the experimental results can be decreased if an improvement is made in the processing procedure. (auth)

40874 (JUL-227-CA) DER GEOMETRISCHE FEHLER BEI DER ABSOLUTZAHLUNG MIT DER β-γ-KOINZIDENZMETHODE. (The Geometry Error in Absolute Counting with the β-γ Coincidence Method). DER STATISTISCHE FEHLER BEI DER ABSOLUTZAHLUNG MIT DER B-γ-KOINZIDENZMETHODE. (The Statistical Error in Absolute Counting With the β-γ Coincidence Method). Erdtmann, Gerhard (Kernforschungsanlage, Julich (West Germany)). Feb. 1965. 17p. Dep. mn.

In the β-γ coincidence measurement of decay rates of radioactive nuclides an error occurs in the use of counters with large volumes (as for instance in liquid scintillators) since the counting yield is site dependent for β and γ rays. This error was calculated for cylindrical detectors. In an approximately cylindrical arrangement of the detectors it is negligently small. A general formula valid for the calculation of the statistical error in absolute counting with β-γ coincidence detectors was derived. (J.S.R.)

40875 (NP-15254) STABIL'NOST SPEKTROMETRICHESKIKH ZHARAKTERISTIK USTANOVKI LSU-5K I POVYSHENIE TOCHNOSTI RADIOMETRICHESKOGO ANALIZA PRIRODNYKH RADIOAKTIVNYKH ELEMENTOV. (Stability of the Spectrometric Characteristics of the LSU-5k Apparatus and Increase in the Accuracy of Radiometric Analysis of Natural Radioactive Elements). Report No. 87. Babichenko, S. I.; Krynov, L. N.; Raikov, V. S.; Utekhin, A. P. (Gosudarstvennyi Komitet po Ispol'zovaniyu Atomnoi Energii SSSR, Moscow. Institut Teoreticheksoi i Eksperimental'noi Fiziki). [1965]. 8p. Dep. mn.

On the basis of analysis of the gamma spectra $N = f(E)$ of U, Ra, Th, and K, the requirements leading to stability of a gamma spectrometer are calculated. The principle of construction of a high-stability amplitude pulse analyzer with several differential channels is considered, and one of the methods for stabilizing a gamma scintillation counter is described. Basic characteristics of the spectroscopic apparatus LSU-5k are presented. The method and physical bases of multicomponent radiometric analysis of weakly radioactive samples using the apparatus LSU-5k were discussed previously. (tr-auth)

40876 (NVO-162-5(Rev.)) REMOTE RADIATION MONITORING AT THE NEVADA TEST SITE. Hill, R. W.; Brown, B. L.; Milligan, V. M. (Reynolds Electrical and Engineering Co., Inc., Mercury, Nev. Radiological Sciences Dept.). Apr. 1965. Contract AT(29-2)-162. 10p. (CONF-279-3). Dep. mn; CFSTI $1.00 cy, $0.50 mn.

From 7th Annual Western Industrial Health Conference, San Francisco, Sept. 1963.

A telemetry system was developed for monitoring areas in close proximity to underground and surface nuclear explosion sites. The basis of the system is a Victoreen Radector which uses an ionization chamber; its adaption is described. The circuit makes it possible to calibrate all the equipment by adjusting each telemetry channel to a uniform loop resistance. The accuracy, applications, and weaknesses of the system are discussed. (D.L.C.)

40877 (RISO-101) THERMOLUMINESCENCE READ-OUT INSTRUMENT FOR MEASUREMENT OF SMALL DOSES. Lippert, J.; Mejdahl, V. (Atomenergikommissionen, Risoe (Denmark). Forsoegsinstitut). May 1965. 16p. Dep. mn.

A thermoluminescence read-out instrument based on modulation of the light emitted by the luminophor during heating was designed and constructed. After amplification, the alternating signal from the PM tube is rectified by a phase-sensitive detector. By this method an effective reduction of the noise caused by the PM dark current was obtained. The performance of the instrument was tested with LiF (Harshaw, TLD 100) and $CaSO_4$: Mn luminophors. With $CaSO_4$: Mn an exposure of 5 μR of Co-60 gamma radiation could be measured with a standard deviation of 10%. The lower limit for LiF was approximately 1 mR. Various properties of the luminophors, including response characteristics, sensitivity to light and decay of stored energy, were investigated. (auth)

40878 (UCRL-9672(Rev.)) SENSITIVE DIFFERENTIAL PRESSURE SYSTEM FOR MEASURING DEPTHS OF CRYOGENIC LIQUIDS. Pope, William L.; McLaughlin, Edwin F. (Lawrence Radiation Lab., Univ. of California, Berkeley). Aug. 26, 1964. Contract W-7405-eng-48. 8p. Dep. mn; CFSTI, $1.00 cy, $0.50 mn.

A system for measuring depths of cryogenic liquids is described. The indicating device is a commercial differential-pressure gage; the level-sensing probes are of various types, either permanent or removable. The heat leak to the cryogenic liquids may be made negligibly small. (auth)

40879 (UCRL-12371) THE SULFIDES OF STRONTIUM, CALCIUM AND MAGNESIUM IN INFRARED STIMULATED LUMINESCENCE DOSIMETRY. Sanborn, E. N.; Beard, E. L. (Lawrence Radiation Lab., Univ. of California, Livermore). June 9, 1965. Contract W-7405-eng-48. 17p. (CONF-650637-2). Dep. mn; CFSTI $1.00 cy, $0.50 mn.

From International Conference on Luminescent Dosimetry, Palo Alto, Calif.

A study was made of Ca, Mg, and Sr sulfides doped with Eu and Sm for gamma dosimetry using infrared-stimulated luminescence. The sulfides were prepared by reduction of the sulfates, and the optimum Eu and Sm concentration was found to be 3.17×10^{-4} mole fraction of each. The optimum infrared wavelength and the luminescence spectrum were determined for each sulfide. Emission decay, energy out-

put, and shelf life were studied. It is concluded that MgS is the best material, but that its packaging is still a major problem. (D.L.C.)

40880 (UCRL-16035) THE USE OF SEMICONDUCTOR DETECTORS FOR INTERNAL-CONVERSION COEFFICIENT MEASUREMENTS. Hollander, J. M. (Lawrence Radiation Lab., Univ. of California, Berkeley). May 1965. Contract W-7405-eng-48. 9p. (CONF-650525-8). Dep. mn; CFSTI $1.00 cy, $0.50 mn.

From International Conference on the Internal Conversion Process, Nashville.

The application of silicon and germanium detectors for measurement of internal-conversion coefficients is discussed. Data taken by the semiconductor method are used to point out the capabilities of this new method. Some advantages over previous methods are discussed. (M.O.W.)

40881 (UR-667) THE EFFECT OF WIDE X-RAY BEAM AND FINITE PHANTOM THICKNESS ON 1000 KVP X-RAY DEPTH DOSE. Maillie, H. D.; Mermagen, H. (Rochester Univ., N. Y. Atomic Energy Project). May 24, 1965. Contract W-7401-eng-49. 21p. Dep. mn; CFSTI, $1.00 cy, $0.50 mn.

An industrial x-ray machine operating at 1000 kvp and 3 ma with no additional filtration was used in a study of the effect of wide x-ray beam and finite phantom thickness on 1000 kvp x-ray depth doses. This unit, operating under the above conditions, has a half-value layer of 3.0 mm Pb. The target to surface distance was 100 cm. Dose measurements were made with a Victoreen Model 154 R ionization chamber. Depth measurements were made using a presswood phantom constructed of sheet masonite 12 × 12 inches in area and 0.25 inch thick. Surface dose measurements were made with a specially constructed sheet of masonite with a cut-out just sufficient to contain one-half of the R chamber with a minimum of surrounding air space. Measurements were made within the phantom using a solid slab of masonite 1.25 inches thick containing a hole into which a 1-inch diameter lucite rod could be inserted. A lucite rod specially machined to contain the R chamber with a minimum of surrounding air space was used for in depth measurements. Two types of phantom measurements made included long phantom measurements, in which the presswood phantom was backed up by a lucite tank filled with water, and finite phantom measurements, in which the phantom was used for depth dose measurements in phantoms less than 20 cm thick. Results indicate that errors of as much as 30% may be incurred if center-beam depth doses are derived from published depth dose tables. It is concluded that dosimetric evaluation of an irradiation procedure must involve measurements that are unique to the situation. (C.H.)

40882 (USNRDL-TR-839) CALORIMETERS AND RADIOMETERS FOR THE MEASUREMENT OF LARGE THERMAL IRRADIANCES. Jenkins, R. J. (Naval Radiological Defense Lab., San Francisco). Apr. 6, 1965. 67p. (DASA-1592).

Information is compiled on field-type radiometers and calorimeters developed to measure the total thermal energy and the radiant thermal power from nuclear detonations. Equations for deriving the sensitivities and time constants from physical parameters are presented and methods of construction and calibration are described. Information is also presented on laboratory sources for simulating thermal radiation from a nuclear weapon. Examples of data reduction from both field and laboratory sources are included. (auth)

40883 THE CHARACTERISTICS OF THE MOELLENSTEDT VELOCITY ANALYSER. Metherell, A. J. F.; Whelan, M. J. (Cambridge Univ., Eng.). Brit. J. Appl. Phys., 16: 1038-40(July 1965).

The performance of the Möllenstedt electron velocity analyzer is investigated by numerical trajectory tracing using a digital computer. A model of the analyzer consisting of two parallel cylinders midway between earthed plates is employed. The relevant design factors, such as the dispersion of the instrument and the effects of slit width and angular divergence of the electron beam on resolution, are investigated. (auth)

40884 EFFECTS OF CORRECTIVE SUBSTANCES ON THE TREATMENT OF NUCLEAR EMULSIONS WITH ULTRASONIC OSCILLATIONS. Akopova, A. B. Dokl. Akad. Nauk Arm. SSR, 40: 151-3(1965). (In Russian).

Aluminum-potassium alum and sodium sulfate in quantities of 10 and 5 g/l respectively were added at the fixing and the washing stages of development of nuclear emulsions to significantly lessen the degree of swelling. Measurements of swelling for corrective additions at the two different stages and of the degree of spurious scattering for cell thicknesses of 250, 500, and 1000 μ were made for emulsions with and without addition of corrective substances. (M.J.T.)

40885 COUNTING OF EVENTS FROM PULSED SOURCES. De Lotto, I. (CNR-CISE, Milan); Ghirardi, A.; Manfredi, P. F. Energia Nucl. (Milan), 12: 365-71 (July 1965).

The statistical problems of counting systems with pulsed sources were studied. Counters with constant non-paralyzable or constant paralyzable dead-time, counters with variable non-paralyzable dead-time and buffers with constant non-paralyzable writing time were examined. The equations that give the exact expressions of the mean number and the variance of the registered events are discussed and asymptotic approximations examined. Several experimental results are presented to check the developed theoretical analysis. (auth)

40886 A SPARK CHAMBER WITH A BIG DISCHARGE GAP. Mikhailov, V. A.; Roinishvili, V. N., Chikovani, G. E. Fiz. Chastits Vysokikh Energii, Akad. Nauk Gruz. SSR, Inst. Fiz., 1: 85-9(1965). (In Russian).

The construction of a spark chamber with a big discharge gap is described. The main characteristics are given. The chamber operates in the track regime with neon filling and operating volume of 26 liters. The estimation of the accuracy of determination of the direction of the motion of a particle is given; for the chamber with the gap of 5 cm it is 2.5×10^{-3} rad. (auth)

40887 340-LITERS EXPANSION-CONDENSING CHAMBERS USED TO STUDY NUCLEAR INTERACTIONS OF HIGH ENERGY PARTICLES. Gogitidze, O. A.; Manzhavidze, Z. Sh., Shtaerman, A. Yu.; Tserelov, A. A.; Rusishvili, N. S. Fiz. Chastits Vysokikh Energii, Akad. Nauk Gruz. SSR, Inst. Fiz., 1: 91-6(1965). (In Russian).

An expansion-condensing chamber with the sensitive volume of 349 liters is a part of a device designed to study interactions of high energy particles. The chamber is placed in the magnetic field with the strength of 6800 Oe generated by an 80-ton electromagnet. One of the peculiarities of the construction is the introduction of a simple and compact hinged mechanism and of a braking arrangement into the expansion assembly. The system provides unperturbed plane-parallel motion of the piston with a smooth decrease of the velocity at the end of the track according to the graph given beforehand. Due to this improvement the most optimum aerodynamic and thermodynamic regimes of the chamber operation are obtained for precise measurements. (auth)

40888 SEMI-AUTOMATIC DEVICE FOR TREATMENT OF TRACK PHOTOS IN A CLOUD CHAMBER. Chikovani, G. E.; Shrabshtein, S. A. Fiz. Chastits Vysokikh Energii, Akad. Nauk Gruz. SSR, Inst. Fiz., 1: 97-103(1965). (In Russian).

The description is given of a semiautomatic device for a microscope to obtain data on the position of the microscope table in the form of a perforated tape. The accuracy of measurement is 5 microns. Telegraphic apparatus of the type ST-2M is used to obtain data. (auth)

40889 THEORETICAL AND TECHNICAL ASPECTS OF PHOTOGRAPHIC DOSIMETRY. Soudain, Georges (CEN Fontenay-aux-Roses, France). Ind. At., 9: 75-82 (1965). (In French).

The fundamental principles of dosimetry of direct radi-

ation and indirect ionization by photographic means are explained. Definitions and the different magnitudes used in dosimetry are given. The essential characteristics of the photographic emulsion are discussed. These include the film, the latent image, fading of the image, sensitivity variation, the transfer of energy between charged particles and the emulsion, its sensitivity to x rays and gamma rays. Characteristic curves showing the relation between the optical density after development and the energy received by the emulsion are also discussed. (J.F.P.)

40890 ENERGY RESPONSE OF BF_3 COUNTER USING PARAFFIN MODERATORS. Tatsuta, Hatsumi; Katoh, Kazuaki; Yoshida, Yoshikazu (Japan Atomic Energy Research Inst., Tokyo). Japan. J. Appl. Phys., 4: 321-5 (May 1965).

The neutron energy response of a BF_3 counter using paraffin moderator was obtained in the energy range from 2 ev to 1 kev. Neutron energy was determined by the time-of-flight method. The counter was covered with a cadmium sheath to eliminate the thermal neutron diffusion from the moderator. The results for BF_3 counters with a thinner moderator were consistent with Fräki's calculation, while those with thicker moderators were not. This inconsistency may be due to the fact that the mean energy of neutrons passing through the cadmium sheath decreases in the case of a thicker moderator and that the counting efficiency of the counter varies according to the 1/v law of the $^{10}B(n,\alpha)$ reaction. (auth)

40891 PROMPT CASCADE GAMMA PEAK EFFICIENCIES OF WELL-TYPE NaI FOR FISSION PRODUCTS. Aoki, Ryozo; Aoki, Rei (Hitachi Ltd., Tokyo). Japan. J. Appl. Phys., 4: 348-52(May 1965).

Gamma spectrum peak efficiencies of well-type NaI(Tl) are calculated for prompt cascade gamma disintegration nuclei ^{138}Cs, ^{101}Mo, ^{131}Te, ^{92}Y, ^{93}Y, ^{91}Sr, ^{133}I, ^{88}Rb, ^{88}Kr, ^{99}Mo, ^{132}I, ^{140}Ba, ^{140}La, ^{131}I, ^{147}Nd, ^{144}Ce, ^{144}Pr, ^{106}Rh, and ^{149}Nd, using probability principles and mono-photon gamma peak efficiencies. Measured peak intensities for ^{106}Rh are compared with the calculated results; better agreement is obtained at the main peaks than with the mono-photon approximation result. (auth)

40892 ON THE PULSE-HEIGHT DEFECTS IN SEMICONDUCTOR DETECTORS FOR FISSION FRAGMENTS. Shirato, Shoji (St. Paul's Univ., Tokyo). Japan. J. Appl. Phys., 4: 380(May 1965).

A revised explanation of pulse-height defects in semiconductor detectors for fission fragments is summarized. (D.C.W.)

40893 ACTIVITY MEASUREMENT ON THE BASIS OF THE GAMMA SPECTRUM. Voedroes, Daniel. Magy Radiol., [No. 2], 106-9[(1963]).

A simple method of activity measurement is described. By means of this method, activities between 50 and 0.005 microcurie are easily determined with instruments available in most laboratories. In order to facilitate the right choice of the parameters, the shape of the photo-peak was determined as a function of the high voltage, amplification, and channel width. Hints are given for their optimal synchronization. (tr-auth)

40894 ON ANGULAR CORRELATION MEASUREMENTS BETWEEN FAST NEUTRONS. Adam, Andras; Kozma, Gyula; Quittner, Pal. Magy. Tud. Akad. Kozp. Fiz. Kut. Int. Kozlemen., 13: 99-108(1965). (In Hungarian).

The principle and electronics of a measuring assembly developed for the investigation by the time-of-flight technique of angular and energy correlations between two neutrons produced simultaneously are described. Counts due to events caused by the two neutron detectors responding to one and the same neutron are suppressed by the electronics, only coincidences from two different neutrons are counted. The assembly has been tested with the 14.7-Mev neutrons from the D-T reaction. A slight change in counting efficiency which is sensitive both to neutron energy and detector geometry can be accounted for by calculation. (auth)

40895 IMPROVEMENT OF RESOLUTION IN LARGE AREA PHOTOMULTIPLIERS. Mead, J. B.; Martin, J. P. (Martin Co., Baltimore). Nucl. Instr. Methods, 36: 13-22 (Sept. 1965).

The factors that influence pulse height resolution of photomultiplier detectors are discussed. One of these factors, the apparent photocathode nonuniformity becomes rather serious for large-area photomultipliers. A technique is described to measure and reduce this nonuniformity by optically trimming the external photocathode surface. This method has been used successfully on a 16″ phototube to reduce the line width of the photocathode response function from 40% to less than 10% while reducing the peak of the pulse height distribution by only 20%. Experimental pulse height distributions for relativistic μ-mesons are compared to the results of convolution calculations involving the energy loss distribution, statistical effects and an approximation to the photocathode response function. Pulse height resolutions using μ-mesons were compared as a function of electrode voltage for several 16″ photomultipliers. Collection efficiency for the dynode structure was found to be between 16 and 21 percent. (auth)

40896 TREATMENT OF CAPTURE GAMMA RAY SPECTRA OBTAINED WITH THE AID OF A CENTRAL CRYSTAL IN ASSOCIATION WITH AN ANNULAR CRYSTAL. Huynh, V. D.; Meinadier, J. P.; De Barros, S.; Julien, J.; Le Poittevin, G.; Morgenstern, J.; Netter, F.; Samour, C. (C.E.N., Saclay, France). Nucl. Instr. Methods, 36: 29-39(Sept. 1965). (In French).

The knowledge of the detector response is the main difficulty in analyzing experimental data. A simple response shape is obtained with an annular crystal operating in coincidence or anticoincidence with a central crystal 4″ × 6″. Merits of this detector are discussed and results are presented. A program is described to find intensities of different gamma lines in complex spectra. This analysis is checked by fitting many thermal-neutron-capture gamma spectra. (auth)

40897 EFFECT OF DESIGN PARAMETERS ON THE CHARACTERISTICS OF CERENKOV'S SHOWER GAMMA-SPECTROMETERS. Grushin, V. F.; Latypova, R. A.; Leikin, E. M. (Academy of Sciences, Moscow). Nucl. Instr. Methods, 36: 40-4(Sept. 1965).

Results are given of a calculation of the main characteristics of the Cherenkov shower gamma spectrometers with lead-glass radiators having different transparancies and thicknesses for gamma energies of 50 to 1000 Mev. (auth)

40898 THE BEHAVIOR OF SPARK DISCHARGE CHAMBERS BY TRIGGERING BY THE PRIMARY IONIZATION AND THE AVALANCHE. Allkofer, O. C.; Kraft, E. (Universitaet, Kiel). Nucl. Instr. Methods, 36: 45-51(Sept. 1965). (In German).

A comparison is given between two different triggering modes of spark chambers filled with argon–acetone, with special regard to efficiency and accuracy of track location. In the case when the chamber is triggered with primary ionization, the mean deviation of the spark from the point where the particle passed the chamber is $\sigma \approx 0.52$ mm and in the case of avalanche $\sigma \approx 0.30$ mm. Examination of the relation between the incident angle of the particle and the point of localization of the spark shows in both cases that the deterioration of σ gets larger with increasing incident angle. When the triggering pulse is delayed up to 1.6 μsec the value of σ increases in primary ionization whereas it remains constant in the avalanche. The efficiency increases rapidly with increasing amplitude of the high-voltage trigger pulse, and the plateau reaches an efficiency of 95%. In the case of delayed triggering the efficiency decreases more slowly in avalanche than in the primary ionization method. (auth)

40899 ANALYSIS OF SOME CIRCUITS USED IN AMPLIFIERS FOR SEMICONDUCTOR NUCLEAR PARTICLE DETECTORS. Poenaru, D. N.; Vilcov, N. (Inst. of Atomic Physics, Bucharest). Nucl. Instr. Methods, 36: 52-8(Sept. 1965).

Three circuit configurations used in preamplifiers for semiconductor nuclear particle detectors are analyzed. These vacuum-tube circuits are: amplifier with bootstrapped plate load; cascode stage; and cascode with bootstrapped load. For each of the three circuits, formulas of the gain, output impedance and transient response both in the initial (edge response) and final part (flat-top response) are presented. The relationships for the gain and output impedance in the case of amplifier with bootstrapped load are given both in analytical and graphical forms. Two important practical cases are considered: pentode in the first stage and triode in the second one; and double triode. (auth)

40900 FINITE SOLID ANGLE ATTENUATION FACTORS IN ANGULAR CORRELATION FUNCTIONS. Rao, B. N. Subba (Tata Inst. of Fundamental Research, Bombay). Nucl. Instr. Methods, 36: 59-60(Sept. 1965).

Exact expressions for the attenuation factors in the P_2 and P_4 terms of the angular correlation function are deduced and presented as functions of τx (x = detector thickness, τ = interaction cross section) and the semivertical angle only. These are also given in the limit of low energies for which $\tau x > 15$. These expressions are useful for any radiation energy, detector, and source-detector geometry. (auth)

40901 RESPONSE OF SEMICONDUCTOR SURFACE BARRIER DETECTORS TO FISSION FRAGMENTS. Konecny, E.; Hetwer, K. (Universitaet, Gieben, Ger. and Technischen Hochschule, Muenchen). Nucl. Instr. Methods, 36: 61-72(Sept. 1965).

The pulse-height defect for fission fragments of surface-barrier detectors from the firms ORTEC (Oak Ridge) and NUCLETRON (Munich) is investigated, dependent on mass kinetic energy of the fission particles. An exact determination of these quantities was possible by means of the Mattauch-Herzog-type fission-particle mass spectrometer at FRM, Munich. For constant kinetic energy of the detected particles, the variation of pulse height with mass proved to be about 100 kev/amu. Losses in the dead layer measured by tilting the detector respective to the direction of the particle beam proved to be somewhat larger for fission fragments than for α particles. For fission particles these losses increase considerably when bias is decreased, and therefore very probably are caused by recombination effects. Furthermore, energy resolution respective to fission fragments is given for several detectors. Unexpectedly, some counters showed a very poor resolution, though possessing the same resistivity and even better α resolution than others showing good resolution, suggesting that the region very close to the surface layer plays an important role in forming the fission-fragment response pulses. (auth)

40902 THERMAL-VACUUM BEHAVIOR OF LITHIUM-DRIFTED SILICON DETECTORS. Tuzzolino, A. J.; Kristoff, J.; Perkins, M. A. (Univ. of Chicago). Nucl. Instr. Methods, 36: 73-87(Sept. 1965).

The potential advantage of lithium-drifted silicon detectors compared with conventional silicon surface-barrier detectors under conditions of a thermal-vacuum environment are discussed. Both surface-barrier and n-i-p lithium-drifted detectors have been fabricated that can operate at elevated temperatures and high vacuum for extended periods of time with no evidence of noise instability. The operating characteristics of several lithium-drifted silicon detectors have been studied before, during, and after environmental testing, to investigate the effects of such testing on detector properties. (auth)

40903 A VERSATILE TWO-ELEMENT LOW-BACKGROUND FLOW-TYPE BETA-COUNTER. Rajagopalan, G.; Lal, D. (Tata Inst. of Fundamental Research, Bombay). Nucl. Instr. Methods, 36: 105-11(Sept. 1965).

The use of a simple two-element Geiger counter for sensitive measurement of beta activity of solid sources is discussed. The counter provides information simultaneously on the number of beta particles absorbed in traversing a given thickness of absorber, as well as those which have sufficient energy to emerge through the absorber. These counting rates suffice to determine the maximum energy of the beta-particle if the source contains a pure beta-emitting radionuclide. If the source contains a mixture of two known beta-emitting radionuclides of significantly different E_{max}-values, this information also suffices to determine the individual disintegration rates of the two nuclides. (auth)

40904 A NEW DOUBLE FOCUSING BETA SPECTROMETER. II. Bartlett, A. A.; Keith, J. (Univ. of Colorado, Boulder). Nucl. Instr. Methods, 36: 119-21 (Sept. 1965). (COO-535-542).

The results of four sets of measurements of the performance of a high-aperture double-focusing spectrometer are presented. The high-aperture double-focusing spectrometer of the University of Colorado has been described, and a detailed discussion of the empirical method of optimizing its performance is given. (auth)

40905 PERFORMANCE AND PROPERTIES OF A PROTON POLARIMETER. Drigo, L.; Manduchi, C.; Nardelli, G. C.; Russo-Manduchi, M. T.; Tornielli, G.; Zannoni, G. (Universita, Padua). Nucl. Instr. Methods, 36: 153-60(Sept. 1965).

The performance of an experimental device employed to measure proton polarization is studied. The polarimeter is designed so that data may be taken simultaneously in the entire angular range (from 20 to 160°) seen by the asymmetry detectors. The method of performing the measurements is illustrated by measuring the spin polarization of protons elastically scattered by ^{4}He and ^{16}O. A critical examination is made of the properties of the polarimeter. (auth)

40906 OPTIMUM PROCESSING OF SPECTROMETRIC INFORMATION BY NUMERICAL ADAPTED FILTERS. Escudie, B.; Carriere, M.; Chery, R. (Inst. de Physique Nucleaire, Lyon, France). Nucl. Instr. Methods, 36: 161-7(Sept. 1965). (In French).

Signal processing often uses sampling and quantitizing methods to increase the usefulness of the circuits they use. The use of these two methods brings up the problem of the order in which the process should be set. Hence, the problem of "commutation properties" is important. The random signal processing implies the study of the stationarity of sampled quantized signals. (auth)

40907 A SCATTERING CHAMBER FOR CHARGED PARTICLE WORK. Zurmuehle, R. W. (University of Pennsylvania, Philadelphia). Nucl. Instr. Methods, 36: 168-72(Sept. 1965).

This scattering chamber has been designed for experiments using primarily solid state detectors. It offers a great flexibility in the arrangement of counters. Two concentric turntables are mounted at the bottom of the chamber. A 3'' × 4'' NaI(Tl) crystal can be introduced into the chamber for coincidence work. Provisions are made for the use of chemically active targets. The use of a Vaclon pump greatly reduces the deposition of impurities onto targets during the experiment. (auth)

40908 X-RAY LUMINESCENCE OF THE NaI(Tl) PHOSPHOR. Shamovskii, L. M.; Dunina, A. A. Opt. Spectry. (USSR)(English Transl.), 18: 411-12(Apr. 1965). Translated from Optika i Spektroskoptya, 18: 728-9 (Apr. 1965).

The properties of an NaI(Tl) phosphor prepared under the best conditions were studies. The luminescence was excited by x rays through an aluminum foil. However, only a low-sluggish x-ray luminescence was formed. The brightness of the x-ray luminescence was practically constant from 293 to 473°K. The long-lasting component in the stationary luminescence constituted less than 1%. The crystals were slightly colored at large doses of intense excitation due to the evolution of iodine and the formation of V centers. Hole levels of a depth of 0.69 ev were formed. Pulse or stationary illumination in the region of the F band did not affect

the stationary brightness of the x-ray luminescence or the de-excitation process of the light sum. (P.C.H.)

40909 THE RESPONSE OF PHOTOGRAPHIC FILM DOSEMETERS TO HIGH ENERGY GAMMA RADIATION. Holt, P. D. (Atomic Energy Research Establishment, Harwell, Berks, Eng.). Phys. Med. Biol., 10: 345-54 (July 1965).

The calibration of dosimeters (mainly film dosimeters) for gamma energies above 3 Mev is described, with particular reference to the measurement of the 6 Mev gamma radiation from gas-cooled power reactors. The dosimeter responses were compared with the readings of condenser ionization chambers which had been calibrated against a standard radium source. The response of the film dosimeters, designed for energies up to about 3 Mev, varied at high energies depending whether or not secondary electron equilibrium exists. The relative sensitivity of the tin-lead filter area of the new plastic A.E.R.E./R.P.S. dosimeter containing Kodak Radiation Monitoring film increased with energy up to a value of 2.0 for 20 Mv x rays in equilibrium. (auth)

40910 CALORIMETRIC MEASUREMENT OF ABSORBED DOSE WITH 15 Mev ELECTRONS. Bradshaw, A. L. (St. Bartholomew's Hospital. London). Phys. Med. Biol., 10: 355-64(July 1965).

An absolute measurement of the ratio of absorbed dose in carbon to the air ionization density in a carbon ionization chamber exposed to 15 Mev electrons is described. A twin isothermal calorimeter was used, with thermistors as temperature sensitive elements. A sensitivity of about 5×10^{-5}C per cm was obtained with this arrangement. For carbon a value of 0.768 ± 0.014 rads for a cavity ionization density of 1.0 esu/cc was measured and this was calculated to be equivalent to an energy absorption in water of 0.872 ± 0.016 rads per esu/cc. This measured value is compared with a calculated value of 0.91 based on the assumption that the incident beam of electrons was monoenergetic. (auth)

40911 DOSE EQUIVALENT ESTIMATION IN HEALTH PHYSICS INSTRUMENTATION. Wheatley, B. M. (Berkeley Nuclear Labs., Berkeley, Glos., Eng.). Phys. Med. Biol., 10: 431-2(July 1965).

Advantages of using dose equivalent estimation in health physics dosimetry are discussed. It was concluded that instruments can be designed to have an energy response based on a calculated relation between dose equivalent and fluence. (P.C.H.)

40912 ERRORS IN ELECTROMAGNETIC CASCADE MEASUREMENTS DUE TO THE TRANSITION EFFECT. Pinkau, Klaus (Louisiana State Univ., Baton Rouge). Phys. Rev., 139: B1548-55(Sept. 20, 1965).

The transition of an electromagnetic cascade which passes from one material to another having a different critical energy is discussed using Rossi and Greisen's approximation B. It is shown that an infinitely rapid change in the total number of particles takes place at the boundary layer. This leads in certain geometries to a strong dependence of the signal measured on the transition effect. A few of these arrangements are discussed and it is shown that they cause difficulties if measurements are made on cascades in ionization spectrometers or air-shower arrays. As a result, it appears to be strongly advisable to have no appreciable change in the critical energy over dimensions of more than several times 10^{-3} radiation length prior to the depth at which the cascade is measured. (auth)

40913 A NEW NUCLEAR-MEDICAL MULTI-CHANNEL MEASURING DEVICE USED FOR THE DIAGNOSIS OF ONE-SIDED DEFICIENCY OF RENAL FUNCTION IN THE ISOTOPE NEPHROGRAM. Bettenhaeuser, K. (Radiologische Klinik und Poliklinik, Medizinische Akademie, Erfurt, Ger.). Radiol. Diagn., 6: 321-7(1965). (In German).

A new simultaneously recording multi-channel measuring device for nuclear medicine is described. The new device is movable, its recording part has a great range of variation and allows universal application in nuclear-medical investigations. The possibilities of application in isotope nephrography are discussed. The significance of the investigation is demonstrated on the basis of cases with one-sided deficiency of renal function. (auth)

40914 CALCULATION OF SPECTRAL DISTORTION DUE TO PILE-UP EFFECT. Gold, Raymond (Argonne National Lab., Ill.). Rev. Sci. Instr., 36: 784-94(June 1965).

The effect of pile-up distortion in the pulse height spectrum of a detector has been determined in the form of an integral representation. A number of important special cases, which arise in experimental applications, are treated. The integral representations for these cases have been evaluated in regions of experimental interest. Comparisons are given between the present numerical results and other estimates of pile-up distortion. (auth)

40915 IBM 1620 RECONSTRUCTION OF BUBBLE CHAMBER INTERACTIONS. Chin, S. H.; Vittitoe, C. N.; Munir, B. A. (Ohio Univ., Athens). Rev. Sci. Instr., 36: 846(June 1965).

The PARIS program is written in FORTRAN II for the IBM 1620 desk computer. PARIS reconstructs and analyzes particle tracks in bubble chamber photographs. Typical computing time for a two-prong event is 7 min. (T.F.H.)

40916 DETERMINATION OF P/B RATIO FOR PLASTIC SCINTILLATOR. Miller, T. G. (Army Missile Command, Redstone Arsenal, Ala.). Rev. Sci. Instr., 36: 847(June 1965).

The ratio of the responses of Pilot B plastic scintillator to 2.64-Mev protons and to 0.639-Mev electrons is measured to be 0.26. (T.F.H.)

40917 INVESTIGATION OF "SCOTCHLITE" AS A REFLECTIVE SURFACE IN A LIQUID HYDROGEN BUBBLE CHAMBER. Karageorge, G. K. (Massachusetts Inst. of Tech., Cambridge). Rev. Sci. Instr., 36: 852-3(June 1965).

The bonding characteristics of Scotchlite SPR704 reflective material to stainless steel are tested, to evaluate the feasibility of use of this material in hydrogen bubble chambers. The stainless steel (SS) samples are cleaned and bonded to Mylar using several adhesives. The Scotchlite is then bonded to the Mylar using the pressure-sensitive adhesive furnished on the Scotchlite backing. The effects of thermal cycling between liquid-nitrogen and room temperatures are evaluated. The samples are then immersed in a 12-in. liquid-hydrogen bubble chamber, and the chamber is expanded 400,000 times in a 58-hr period. The performances of the various bonding combinations are evaluated for use in the liquid hydrogen environment. (T.F.H.)

40918 STORED PROGRAM COMPUTER AS AN ASSOCIATIVE RADIATION ANALYZER. Soucek, Branko (Brookhaven National Lab., Upton, N. Y.). Rev. Sci. Instr., 36: 950-3(June 1965).

A system design based on the use of a stored-program on-line computer is presented here. The system is used as an associative radiation analyzer. The channel capacity of the system is 20 bits (one million channel analyzer). The data storage program is based on a threaded list (tree) algorithm. The number of different events which will be measured during a particular experiment can be assigned for each experiment. The count capacity is 4096 counts per channel, but can be extended. Two alternatives are discussed, depending on whether a fast or medium-speed computer is used. The mean input rates are 5000 or 1000 events per second respectively. In both cases the resolution between two events is determined mainly by the analog-to-digital converters used. There is a flicker-free display on the CRT. The display can be in map, isometric, or curve form. The display format (grid, unblanking, etc) as well as the experimental conditions are under typewriter control. (auth)

40919 REDUCTION OF CARRIER TRAPPING IN GERMANIUM LITHIUM-DRIFT γ RAY SPECTROMETERS. Tavendale, A. J. (Atomic Energy of Canada Ltd., Chalk River, Ont.). Rev. Sci. Instr., 36: 1275-6(Aug. 1965).

It was previously found that charge-carrier trapping led to low-energy tails on the full energy peaks of gamma spectra, impairing the energy resolution. An investigation of pairs of comparable lithium-drifted germanium diodes showed that a post-drift high-temperature cycle reduced the carrier trapping. (D.C.W.)

40920 STUDY ON RADIOCARBON DATING. I. CHARACTERISTICS OF THE CO_2-FILLED PROPORTIONAL COUNTER. Hamada, Tatsuji (Inst. of Physical and Chemical Research, Tokyo). Rika Gaku Kenkyusho Hokoku, 36: 635-9(1960). (In Japanese).

Radioactivity of natural radiocarbon was measured with a copper proportional counter which has an effective volume of about 1.8 l and was shielded by 17 cm iron. When filled with purified CO_2 up to about 1 atm and connected with a nonoverloading amplifier, the counter showed a good plateau, of more than 600 v at about 5.5-kv anode voltage. The background counting rate was found to vary linearly with filling pressure. It also decayed with an apparent half life of ten days which might be due to contamination with fallout fission products. (BBB)

40921 THE DESIGN CRITERIA OF A PHOSWICH TRANSDUCER (thesis). Crawford, Richard Lyle. Albuquerque, N. Mex., Univ. of New Mexico, 1964. 178p.

An experimental and theoretical treatise on the design criteria of a phoswich transducer is presented. The major emphasis is on the application in a gamma spectrometer. The conversion efficiency, gamma cross sections, response to charged particles, luminescence decay time, spectral response, and physical qualities are discussed, in considerable detail, in making the optimum choices for the inorganic crystal and the organic phosphor which will act as the charged particle anticoincident shield. The effect of the thickness of the anticoincident shield on resolution, the percentage of gamma rays absorbed, the percentage of gamma rays that are attenuated in energy, and the lower threshold for charged particle rejection was analyzed. The principle involved, which causes a difference in the gamma spectra when the anticoincident shield is operating, was determined experimentally. The signal limitations that influence the dynamic range of the phoswich transducer for the energy analysis of the gamma rays is discussed. The statistical factors that affect the resolution and the dynamic range were determined. The optimum choice of integrating time constants for both signal paths, the input to the analyzer, and the input to the anticoincident circuit were determined mathematically. The cause of the adverse effect of operating a phoswich transducer in a high flux of highly energized charged particles was determined experimentally. The best choice for an inorganic crystal is CsI(Tl). A new figure of 9.25% was obtained for the conversion efficiency by using a photomultiplier tube with a S-20 spectral response. The complete luminescence decay curve for CsI(Tl) is plotted. The long-term metastable phosphorescence decays to the noise level of the photomultiplier in 2.5 milliseconds. When the anticoincidence shield is operating, 62.5% of the difference in gamma spectra is due to a Compton scattered electron escaping from the crystal and interacting in the plastic anticoincidence shield, causing that event to be rejected from analysis. The theoretical maximum ratio of pulse heights from the fast and slow scintillators is degraded by the transit time spread of the photomultiplier and the integrating time constant of the output circuit. A mathematical treatment, to obtain the ratio of the pulse heights from general equations, is presented. The results of this analysis show that for a given phoswich transducer, there is an optimum integrating time constant. Graphs are included which show the relative pulse heights and the time spread between the fast and slow voltage pulses as a function of the integrating time constant. (Dissertation Abstr.)

40922 MEASUREMENTS BY SCATTERING TECHNIQUES. [PART] I. Major, J. K. 9p. (CONF-650101-5). Gmelin, AED-CONF-65-006-7.

From Moessbauer Symposium, New York.

Measurement techniques used in transmission and scattering experiments are discussed along with advantages and disadvantages in both. Particular attention is given to geometries. Various experiments previously performed on Moessbauer and Rayleigh scattering are noted. Mention is made of the use of resonant scattering in the design of a resonant detector which is selectively sensitive to recoil-free gamma rays. (L.B.S.)

40923 NEUTRON AND GAMMA SENSITIVE IONIZATION CHAMBER /Q-2289/ (Engineering Materials). (Oak Ridge National Lab., Tenn.). (CAPE-1273).

3 drawings.

An ionization chamber is described, which is used with a monitoring system located at the Tandem Van de Graaff installation of the High Voltage Laboratory. The chamber is housed in a shielded container of polyethylene. The chamber within the shield has the following sensitivities: Ra(γ) 2.65×10^{-13} amps/mR/hr; PoBe (neutrons) 2.65×10^{-13} amps/mR/hr, when the sides and bottom are covered with 0.003 in. thick Cd foil; and 1.4×12^{-12} amps/mR/hr without the foil. The effective chamber volume is ~1000 cm^3 and the gas volume is 1500 cm^3. The chamber is filled under pressure with 95% $^{10}BF_3$. For details, see TID-4100. (M.C.G.)

40924 MONITORING SYSTEM, H. V. LABORATORY /Q-2338/ (Engineering Materials). (Oak Ridge National Lab., Tenn.). (CAPE-1070).

14 drawings.

The monitoring system includes electrometer amplifiers, which are located in the shielded and unshielded target rooms, control room, low mass target room, and in the accelerator areas. Shielded ion chambers supply input for these amplifiers. Also included are signal interconnection and grounding relays, a preset timer and counter, a Lectrocounter integrator, and the door operated relays. For details, see TID-4100. (M.C.G.)

40925 ION CHAMBER MONITOR /Q-2202/ (Engineering Materials). (Oak Ridge National Lab., Tenn.). (CAPE-1230).

3 drawings.

The instrument described is used in monitoring isotopes packaged for shipment. The chamber, which consists of a linen phenolic tube, is attached to an aluminum tube. The probe is a stainless steel tube. For details, see TID-4100. (M.C.G.)

40926 BUILDING MONITOR /Q-2274/ (Engineering Materials). (Oak Ridge National Lab., Tenn.). (CAPE-1272).

2 drawings.

The portable monitor described measures dose rate and integrated dose in a γ field using an ionization chamber electrometer with a bridge circuit, which is powered by Ni–Cd batteries. The integrating ionization chamber is combined with a counting circuit. The chamber produces one pulse per 0.2 mR of dose counted by scaler glow tubes at preselected values of counts. The time period, during which the dose is integrated, can continue indefinitely or it can be set to integrate the dose for a desired period. Normally the dose is integrated for successive 8-hr periods. For details, see TID-4100. (M.C.G.)

40927 IMPROVEMENTS IN OR RELATING TO METHODS OF AN APPARATUS FOR DETECTING THE DIRECTION OF INCIDENCE OF A RADIOACTIVE EMISSION. (to Atomic Energy of Canada Ltd.). British Patent 997,328. July 7, 1965. Priority date May 23, 1963, Canada.

A method and apparatus are provided for determining the direction of incidence of radiation from gamma, beta, alpha, neutron, and other radioactive sources and for detecting the direction of reflection of such radiations from reflecting media. The radiation incident at the point of measurement is divided into two zones by means of a radiation reducing shield symmetrically disposed on a plane of symmetry, and at least one pair of radiation detectors are disposed symmetrically at each side of the plane with the shield between the detectors. The radiation count is de-

tected in each zone. Ratio means are connected to each detector and adapted to produce an output signal voltage that is zero when the counting rate of each of the detectors is substantially equal, to produce an output signal voltage having one polarity when one detector has the higher counting rate, and to produce an output signal having the opposite polarity when the other detector has the higher rate. Indicating means are responsive to the output signal and are adapted to indicate when the rotation of plane of symmetry disposes it in alignment with the source of radiation. (B.L.M.)

40928 NEUTRON ENERGY SPECTROMETERS. Aoki, Ryozo (to Hitachi Ltd.). British Patent 998,117. July 14, 1965. Filed Jan. 1, 1963.

A neutron energy spectrometer is patented that has an improved detecting efficiency and energy spectrum resolution. The spectrometer includes a detector section that is made up of a main scintillator formed of liquid ^{3}He and a photoelectric transducer connected to the main scintillator by way of a light-transmitting pipe. An output circuit including an anti-coincidence gate circuit is provided for analyzing the output of the detector section. (B.L.M.)

40929 RADIOISOTOPE IDENTIFIER. Tolmie, Ronald W. (to Atomic Energy of Canada Ltd.). Canadian Patent 711,364. June 8, 1965.

A portable device for measuring the energy of local radiation for identification of radioisotopes is described. The apparatus consists of a pair of radiation detectors of the pulse counting type, whose rate of counting depends on the radiation intercepted in a given time. There is also a shield for absorbing a proportion of the radiation falling on one detector. From the ratio of the counts on the shielded detector to the sum of the counts on both detectors a voltage is read which is a function of the local radiation energy. Routine checking of isotopes from a reactor, production line or on floors, walls, air filters or elsewhere is claimed as the use of the device. (F.S.A.)

40930 VARIABLE GUARD. Nicholls, Jack (to Minister of National Defence). Canadian Patent 712,677. June 29, 1965.

A radiation intensity measuring device is designed which consists of an ionization chamber and a triode electrometer; the tube and grid circuitry is enclosed in a conductive guard which is maintained at the same potential as the grid. The ionization chamber has a volume of about 100 cc and the guard 200 cc. The ionization chamber may be remote from the electrometer circuitry. (F.S.A.)

Radiation Effects

40931 (AD-609424) ELECTRON BOMBARDMENT OF SILICON SOLAR CELLS. Downing, R. G. (Space Technology Labs., Inc., Los Angeles, Calif.). Feb. 24, 1960. 52p. (STL/TR-60-0000-04057; EM-10-5). CFSTI $3.00 cy, $0.50 mn.

Silicon solar cells were irradiated with 500-kev electrons to determine the effect of electron radiation similar to that encountered in satellites on the efficiency of solar cells. The experiments show that an integrated flux of about 5×10^{13} e/sq cm reduces silicon solar cell efficiency by about 25 percent. Additional experiments using quartz and glass shielding for radiation protection show the suitability of reducing the radiation damage by this technique. Combining the experimental results with the simple theory, 0.065 in. of quartz or glass are indicated as necessary to provide protection from 800 kev electrons in the trapped radiation bands. Additional protection of shielded silicon solar cells will result from annealing of radiation induced defects at a low rate near room temperatures. No quantitative data on annealing were obtained from these experiments, but this effect should be regarded as a subject for further investigation in addition to detailed investigation of radiation damage in silicon solar cells. (auth)

40932 (CEA-R-2723) ETUDE DU PROCESSUS DE RECOMBINAISON DES PAIRES ELECTRON-TROU DANS LE GERMANIUM IRRADIE PAR LES RAYONS γ DU COBALT 60 A L'AIDE DE L'EFFET PHOTOVOLTAIQUE DANS LES JONCTIONS P-N. (Study of Recombination Processes for Electron-Hole Pairs in Germanium Irradiated by γ rays From ^{60}Co Using the Photovoltaic Effect in P-N Junctions). Zahedi-Moghadam, Ali-Asghar (Commissariat a l'Energie Atomique, Saclay (France). Centre d'Etudes Nucleaires). 1965. 76p. Dep. mn.

Thesis submitted to Universite, Paris.

Using the photo-voltaic effect in p-n junctions, the mechanism of the recombination of electron-hole pairs in the presence of structure defects was studied during bombardment. The structure defects were produced in n- and p-type germanium by γ rays from a ^{60}Co source. At 310°K the level of the recombination centers is located 0.25 ev above the conduction band and the capture cross sections of the holes and of the electrons have the respective values of: $\sigma_p = 4 \times 10^{-15}$ cm^2 and $\sigma_n = 3 \times 10^{-15}$ cm^2. The value of σ_n appears to be underestimated because the number of defects in p-type samples appears to be lower than that in n-type samples. These results lead to the conclusion that the interstitials are responsible for the recombination. (auth)

40933 (NP-15300) INVESTIGATION OF TRANSIENT RADIATION DAMAGE IN SEMICONDUCTOR MATERIALS. Quarterly Progress Report No. 7, August 1–October 31, 1964. Lichtenstein, Roland M. (Rensselaer Polytechnic Inst., Troy, N. Y.). Contract DA-36-039-AMC-02165(E). 26p. CFSTI.

A reliable single pulse light source, which can be used in the high radiation field of the LINAC target room, was developed. Significant permanent damage occurred in silicon from one electron burst; however, no transient radiation damage was observed 10 msec after the electron pulse. (auth)

40934 (NP-15301) INVESTIGATION OF TRANSIENT RADIATION DAMAGE IN SEMICONDUCTOR MATERIALS. Quarterly Progress Report No. 8, November 1, 1964–January 31, 1965. Lichtenstein, Roland M.; Willard, H. James Jr.; Corelli, John C. (Rensselaer Polytechnic Inst., Troy, N. Y.). Contract DA-36-039-AMC-02165(E). 25p. CFSTI.

Transient radiation damage effects in high purity p-type silicon due to 50 Mev electrons were observed. Roughly equal changes in magnitude and decay time of photoconductivity occurred; 30 to 60% of these changes annealed out within the first few minutes after the electron pulse. (auth)

40935 (SC-DC-65-1247) INTRODUCTION RATE OF ELECTRICALLY ACTIVE DEFECTS IN N-TYPE SILICON BY NUCLEAR RADIATION. Stein, H. J. (Sandia Corp., Albuquerque, N. Mex.). June 25, 1965. Contract AT(29-1)-789. 19p. (CONF-650707-5). Dep. mn; CFSTI $1.00 cy, $0.50 mn.

From IEEE Annual Conference on Nuclear and Space Radiation Effects, Ann Arbor, Mich.

Carrier removal rates in n-type silicon at 270°K for a resistivity range of 1.0 ohm cm to 50 ohm cm and for material prepared by widely different methods were investigated. Float zone (O_2 free, dislocation rich), crucible grown (O_2 containing with few dislocations), Lopex, and Dash (both materials O_2 free and dislocation free) materials were studied. Studies were performed both under 2 Mev electron and under fission spectrum neutron irradiations. Particular care was exercised to obtain results of good accuracy and reproducibility in order to find differences between materials from different sources. The reference material was phosphorus doped and zone refined, having a carrier concentration of 7×10^{14} cm^{-3}. The carrier removal rates observed for it are 0.88 cm^{-1} for electron irradiation and 5.0 cm^{-1} for neutron irradiation. For p-type material the carrier removal rate under electron irradiation is approximately a factor of ten smaller for the same irradiation conditions and carrier concentration, while for neutron irradiations in p-type material the carrier removal rate is 30% larger than for the corresponding n-type material. There is a significant dependence on crys-

tal growth method for material of equal carrier concentration under electron irradiation, while under neturon irradiation these effects are considerably smaller. (auth)

40936 (SC-R-65-912) A STUDY OF THE NEUTRON-INDUCED BASE CURRENT COMPONENT IN SILICON TRANSISTORS. Goben, C. A. (Sandia Corp., Albuquerque, N. Mex.). July 1965. Contract AT(29-1)-789. 15p. (CONF-650707-4). Dep. mn; CFSTI, $1.00 cy, $0.50 mn.

From IEEE Annual Conference on Nuclear and Space Radiation Effects, Ann Arbor, Mich.

In a previous paper a neutron-induced component of base current was reported that increases in proportion to integrated neutron flux and varies with base-to-emitter voltage, V_{BE}, as $\exp(q/nkT/V_{BE})$, n being approximately 1.5. A component of base current which varies similarly with base-to-emitter voltage has previously been reported to be of surface-perimeter origin. For this reason it is significant to unambiguously locate the origin of the neutron-induced component. For this, a detailed study of the current-voltage characteristics, an analysis of the deviation of the characteristics from an exponential caused by emission concentration for "ring-dot" structures, and an analysis for the transverse bias dependence of the base current components for a special "tetrode-type" test structure were performed. The results indicate that the small "1.5 component" of current initially present is indeed of surface-perimeter origin while the added "1.5 component" of current induced by neutron bombardment is of bulk space charge region origin. To determine whether this effect is universal, an investigation was made of many different types of silicon transistors, and all were found to exhibit a similar neutron-induced current component. The number n in the exponential term is found to be a function of temperature decreasing with increasing temperature. For example at –50°C, n = 1.6, and at +100°C, n = 1.3. Annealing studies reveal an apparent difference in annealing rates for the neutral bulk base region and the high-field region of the emitter-base junction. (auth)

40937 (UCRL-11958) ALPHA PARTICLE BOMBARDMENT OF Si AND GaAs DIODES; ENERGY CONVERSION AND RADIATION DAMAGE (thesis). Posey, Lawrence D. (Lawrence Radiation Lab., Univ. of California, Berkeley). June 1965. Contract W-7405-eng-48. 307p. Dep. mn; CFSTI, $7.00 cy, $1.50 mn.

The α-voltaic effect, associated with α-particle stopping in a semiconductor diode, was investigated in p-on-n and n-on-p Si solar cells and p-on-n GaAs solar cells at operating temperatures of 200 and 275°K. An initial maximum conversion efficiency of approximately 4%, well below theoretical predictions, was realized for all three cell types at 200°K, and in all cases at 275°K the efficiency was less than 1%. The discrepancy between theory and experiment was attributed to the substantial non-ideal contribution to the dark I-V characteristic present in all the cells employed. The dark I-V characteristics of p-on-n and n-on-p Si solar cells and p-on-n GaAs solar cells were measured for temperatures between 90 and 360°K. The ideal diffusion term was isolated for all the cells, but sheet resistance effects in the surface region were not discernible. The non-ideal current term was found to be more consistent with a junction tunneling current than with a junction recombination-generation current. The GaAs solar cells were found to be the most resistant to radiation damage from a device standpoint while the n-on-p and p-on-n Si cells exhibited decreasing radiation resistance in that order. The diffusion length degradation constants were also determined for both materials at 200 and 275°K. These values in order of decreasing radiation resistance are, for the p-type Si, $K_p(Si) \approx 3 \times 10^{-5} cm^{-2}\alpha^{-1}$ at 275°K and $5 \times 10^{-5} cm^{-2}\alpha^{-1}$ at 200°K, for the n-type Si, $K_n(Si) \approx 7 \times 10^{-5} cm^{-2}\alpha^{-1}$ at both temperatures, and for the n-type GaAs, $K_n(GaAs) \approx 4 \times 10^{-4} cm^{-2}\alpha^{-1}$. The dark I-V characteristics of the cells underwent substantial changes during exposure. The changes in the ideal current were consistent with a bombardment induced decrease in minority carrier lifetime. The changes in the non-ideal current term for all the cell types tested were not consistent with a junction recombination-generation current and in fact indicate that a substantial current contribution must be controlled by the surface state of the cells. (auth)

40938 TRANSIENT RADIATION ENVIRONMENT OF NUCLEAR WEAPON DETONATIONS. Boucher, R. J.; Pearson, J. B. (Hughes Aircraft Co., Culver City, Calif.). J. Appl. Phys., 36: 2722-30(Sept. 1965).

Mathematical models, including a generalized diffusion equation with time varying coefficients, are developed which approximate the propagation of both the initial neutron and the initial gamma radiation from nuclear weapon detonations. Typical plots of neutron and gamma pulse shapes obtained from these models are compared and show that for many cases the gamma spike, or unscattered components of gamma radiation, is predominant. Therefore, it is concluded that for most cases the simplified gamma spike formula commonly used in calculating the radiation environment is appropriate for use in predicting the effects of nuclear weapon detonations upon electronic equipment. (auth)

40939 5-Mc MAGNETIC TUNNEL-SEMICONDUCTOR LOGIC FOR NUCLEAR RADIATION ENVIRONMENTS. Briggs, G. R.; Ricci, R. C. (Radio Corp. of America, Princeton, N. J.). 24p. (CONF-650403-3). Gmelin, AED-CONF-65-038-3.

From International Conference on Non-Linear Magnetics, Washington, D. C.

The balanced core-tunnel semiconductor logic circuits are described which have demonstrated feasibility of the approach for nuclear-radiation resistant, 5-Mc logic. The logic is faster than all-magnetic logic and has a greater potential for reliability than all-vacuum tube logic. At present, however, information run-down exists and fan-in and fan-out are limited. (auth)

ISOTOPE TECHNOLOGY

Industrial Applications

Refer also to abstracts 40553 and 40560.

40940 (NP–14924) GUTACHTLICHE STELLUNGNAHME ZUR VERWENDUNG RADIOAKTIVER LEUCHTFARBEN IN NAVIGATIONSINSTRUMENTEN DER FLUGZEUGKANZEL. **(Expert Opinion on the Application of Radioactive Luminous Paints in Navigational Instruments of the Aircraft Cockpit). Seelentag (Bundesgesundheitsamt, Berlin (West Germany). Institut fuer Wasser-, Boden- und Lufthygiene). Apr. 13, 1962. 23p. Dep. mn.**

The utilization of radioactive luminous paints on the cockpit instrument of aircraft was investigated by measurement and evaluation of the radiation charge in the cockpit. The dangers to the general public from these instruments were also evaluated. The results showed that modern aircraft had only isolated instruments with radioactive luminous paints. Some circuits used luminous paints however. The total charge to the pilot varied from 0.01 to 0.1 mR/hr in the modern aircraft. (J.S.R.)

40941 (SB–403(Suppl.1)(Rev.)) FOOD PRESERVATION BY IRRADIATION. (Clearinghouse for Federal Scientific and Technical Information, Springfield, Va.). [1965]. 18p. CFSTI.

A list of 215 recent publications on the radiation processing of foods is presented. The list includes 24 translations. (C.H.)

Separation and Production

See also CHEMISTRY — Separation Processes and Procedures.

Refer also to abstract 41243.

40942 METHOD OF PRODUCING DEUTERIUM-ENRICHED OR HEAVY WATER. (to Friedrich Uhde GmbH). British Patent 999,618. July 28, 1965. Priority date Jan. 24, 1961, Germany.

In the first stage of a process for the production of deuterium-enriched or heavy water, the deuterium content of liquid NH_3 is increased by isotopic exchange with H_2. In an intermediate stage, the deuterium content of NH_3 is further increased by isotopic exchange with H_2. The NH_3 is converted to H_2O, and at least a part of the water is separated in a separating stage into a less highly deuterium-enriched part and a part that is either more highly enriched or is heavy water. The less highly deuterium-enriched part is converted to H_2 that exchanges with NH_3 in the intermediate stage to yield deuterium-impoverished H_2. The deuterium impoverished H_2 from the intermediate stage is combined with H_2 of substantially the same deuterium content, and the combination is introduced into the first stage of the process. Preferably, a part of the H_2O into which the NH_3 is converted is introduced into the separating stage, and the remainder is converted into H_2. The H_2 exchanges with NH_3 from the intermediate stage to reduce the deuterium content of the H_2 to a value substantially equal to that of the H_2 into which the less highly deuterium-enriched part of the H_2O has been converted. The H_2 into which the H_2O has been converted is combined with the H_2 that leaves a further stage, and the H_2 produced is introduced into the intermediate stage. (B.L.M.)

MATHEMATICS AND COMPUTERS

Refer also to abstract 40396.

40943 POLYNOMIAL APPROXIMATION TO THE FUNCTION $\psi(A, C; X)$. Nemeth, Geza. Magy. Tud. Akad. Kozp. Fiz. Kut. Int. Kozlemen., 13: 163-70(1965). (In Hungarian).

The polynomial approximation to the confluent hypergeometric function $\psi(a, c; x)$ by Chebyshev expansion is discussed. The Chebyshev expansion coefficients of the function $x^a\psi(a, c; x)$ for $x = \geq \lambda$ are evaluated from an integral constructed by means of a Stieltjes transform. The reproduction of the recursion formula of the coefficients from the new expression is shown. For the expansion coefficients an asymptotic formula is derived which has the form $\varphi_n = An^{b_1}(a+c-2)e^{-3\lambda^{1/3}n^{1/3}}\{1 + 0(n^{-1/3})\}$, $n \to \infty$. Finally, a simple method is presented by which it is possible to obtain from the polynomial approximation with fixed parameters a and c further approximations to other parameters as well. (auth)

40944 CHEBYSHEV EXPANSION OF INTEGRAL SINE AND INTEGRAL COSINE FUNCTIONS. Nemeth, Geza. Magy. Tud. Akad. Kozp. Fiz. Kut. Int. Kozlemen., 13: 171-8(1965). (In Hungarian).

The Chebyshev expansion of the functions Ci(x) and Si(x) is discussed. This type of expansion proves to be more useful in practice than the other types used in the literature due to its earlier convergence. The decrease in the Chebyshev expansion coefficients for $0 \leq x \leq a$ is higher by a factor of 4^{-n} as compared with that in Taylor expansion coefficients. In the case $x \geq a$, instead of the divergent asymptotic series, convergent Chebyshev series are given. The convergence of the series is of the order $e^{-2\sqrt{an}}\,0(n^{-1/4})$ $n \to \infty$. (auth)

40945 DIFFERENTIAL EQUATIONS AND THEIR APPLICATIONS. Proceedings of the Conference held in Prague in September 1962. Prague, Czechoslovak Academy of Sciences, 1963. 247p. (CONF-620907).

Three sections, which were ordinary differential equations, partial differential equations, and applications of differential equations are included. The three sections contained 104 papers. (J.F.P.)

METALS, CERAMICS, AND OTHER MATERIALS

General

40946 (AI-65-93) SOLUBILITY STUDIES OF ULTRA PURE TRANSITION ELEMENTS IN ULTRA PURE ALKALI METALS. Quarterly Report No. 7, January 3–April 1965. McKisson, R. L.; Eichelberger, R. L. (Atomics International, Canoga Park, Calif.). June 2, 1965. Contract NAS3-4163. 29p. (NASA-CR-54097).

Solubility testing is continuing, and data were obtained for the solution of high purity iron, niobium, and molybdenum in high purity potassium. The problem, previously noted, of the potassium retention within the crucible-collector sub-assembly was resolved by the use of a nickel braze which seals the joint. A modification of the quench apparatus was made, and the new water-cooled device is much more effective than the chill-blocks previously used. Cooling of the sample capsule to below the melting point of potassium is now achieved in less than 20 minutes. This tends to limit the time during which the dissolved solute may have the mobility required to deposit on, and to diffuse into, the collector walls. Tentative values for the solubility of very pure metals in potassium containing 14 wppm oxygen are: for iron at 1000°C, 80 wppm; for niobium at 1000°C, 15 wppm; and for molybdenum at 1000°C, 3 wppm. (auth)

40947 (EURAEC-1403) [MECHANICAL PROPERTIES OF STEELS]. Final Report No. 1. Chaudron, G. (Centre National de la Recherche Scientifique, Paris (France)). [1965]. Contract 085-62-7-RDF. 33p. (EUR-2362). Dep. mn; CFSTI $2.00 cy, $0.50 mn.

Work Performed under United States–Euratom Joint Research and Development Program.

The corrosion resistance and microstructure of 18-8 and 18-10 stainless steels made from high purity metals was investigated. The steels exhibited improved resistance to stress corrosion and intercrystalline corrosion by boiling nitric acid and potassium dichromate solutions. Both steels underwent a spontaneous martensitic transformation at room temperature. (W.L.G.)

40948 (IS-1195) THE APPLICATION OF VACUUM METALLURGY IN THE PURIFICATION OF RARE-EARTH METALS. Gschneidner, Karl A, Jr. (Ames Lab., Iowa State Univ. of Science and Tech.). Aug. 10, 1965. Contract W-7405-eng-42. 53p. (CONF-650617-3). Dep. mn; CFSTI, $3.00 cy, $0.50 mn.

From Vacuum Metallurgy Conference, New York.

In that the metal preparation step is the major source of impurities, a significant reduction in the amount of contamination can be achieved by improvement of the techniques applied in preparing the metals from their oxides. Two of the most important purification processes are vacuum melting and distillation. There is a wide variation in both the chemical and physical properties of the rare-earth metals and different reduction and purification techniques or combinations of both are required, i.e., no one technique is universally applicable to all of these metals. Special purification techniques, such as the $MgCl_2$ process, tungsten filtration, dehydrogenation, gettering by tantalum, electron beam melting, zone refining, electrorefining and solid-state electrolysis, are discussed. A summary of the techniques to remove or reduce a particular major impurity, such as oxygen, fluorine, calcium and tantalum, is given. The current best values of the lattice constants, metallic radii, densities, transformation temperatures, melting points, boiling points, heats of sublimation and vapor pressures are also included. (auth)

40949 (ISC-640) APPLICATION OF METAL COATINGS ON URANIUM. Summary Report. Chiotti, P.; Woerner, P. F.; Klepfer, H. H.; Gill, K. J.; Cutrell, R. E. (Ames Lab., Iowa State Univ. of Science and Tech.). Sept. 20, 1955. Contract W-7405-eng-82. 49p. Dep. mn; CFSTI $2.00 cy, $0.50 mn.

A number of procedures for applying metallic coatings to U was investigated. The coating materials were tested in boiling distilled water and in some cases were further tested in 178°C water. Coated U samples were tested in boiling distilled water. Hot-press bonding conditions for bonding Al to the coating materials and to coated U were studied. In a number of cases the temperature dependence of the interpenetration rate between the coating material and U as well as between the coating material and Al were measured. Coats of Zn, Zn–5 wt % Al, Cu–9.7 wt % Mg, and Mg were applied by the hot dip procedure. It was found that predipping the U for a few seconds in a fused salt bath consisting of KCl–LiCl eutectic composition to which 10 to 20 anhydrous $ZnCl_2$ is added promoted rapid and uniform wetting of the U by the molten metal bath. Smooth adherent coats one mil thick were obtained by centrifuging the hot coated specimens. Without centrifuging the coats varied in thickness from one to three mils. Mg coats were considered of questionable value due to the poor corrosion resistance of Mg and the extremely weak and brittle nature of the bond formed between Al and Mg. Zn has much better corrosion resistance than Mg in 178°C water and hot-press bonded Zn/Al couples show a tensile strength of as high as 7900 psi. However, diffusion of Zn along Al grain boundaries is rapid ($K = 4.2 \times 10^{-10}$ cm^2/sec at 200°C). Cu–9.7 wt % Mg serves as an effective diffusion barrier between U and Al. This alloy has excellent corrosion resistance to 178°C water. One mil coats of this material were found to give effective protection to U against boiling distilled water for periods up to 100 hours. The alloy is quite hard (Rockwell C 24-27) but still forms a relatively strong bond with Al. Al/Cu–Mg couples pressed at 480°C for 10 minutes and at pressures of 16,000 to 30,000 psi gave tensile strength values ranging from 4640 to 7450 psi. Diffusion coats of Ni, Si, and Zr were produced on U by heating the U in a Mg bath containing the desired metal in solution. Adhering bath material was removed with dilute acid and the alloy case formed was tested in boiling water. The Ni and Si diffusion coats were found to give a fair degree of corrosion protection to the U. Diffusion coats approximately 0.3 mil thick offer effective protection to U in boiling water for periods of about 100 hours. The Zr diffusion coats produced were found to be rapidly undercut by boiling water. All of the above coats as well as one mil electroplates of Cu, Ni, and Cr were found to be rapidly attacked by molten Al–Si eutectic composition. (auth)

40950 (LA-3338) THE SOLUBILITY OF SELECTED ELEMENTS IN LIQUID PLUTONIUM. V. REVISIONS TO THE TANTALUM STUDY. Bowersox, D. F.; Leary, J. A. (Los Alamos Scientific Lab., Univ. of California, N. Mex.). June 7, 1965. Contract W-7405-eng-36. 9p. Dep. mn; CFSTI, $1.00 cy, $0.50 mn.

The solubility of Ta in liquid Pu was redetermined over the temperature range 750 to 950°C. The solubility is given by the equation $\log N_{Ta} = 0.7690 - 3.938 \times 10^3 T^{-1}$, where N_{Ta} is the solubility of Ta expressed as atomic fraction, and T is the temperature in degrees Kelvin. The solubility increased from 644 ppm Ta (by weight) at 750°C to 2667 ppm Ta at 950°C. (auth)

40951 (NRL-6290) OPTICAL TECHNIQUES FOR ELECTRON PROBE ANALYSIS. Grosso, J. (Naval Research Lab., Washington, D. C.). Apr. 12, 1965. 13p. CFSTI $0.50 cy, $0.50 mn.

This study is concerned with two techniques in optical microscopy which exploit the principle of light interference to enhance optical contrast in metallurgical specimens. The first method achieves this through interference layers formed within the specimen by anodization in an electrolyte. A variety of experimental arrangements are suggested for carrying out the anodization. It is also noted that the optical effects of anodization can be adjusted by overlaying the

specimen with films of nitrocellulose. The second method produces optical contrast through interference layers formed by replicating the etched-out surface of the specimen. This latter technique has the advantage of being applicable to any specimen which can be etched, and it is not limited to anodizable species. Here too, the optical results of replication can be adjusted by exposing the replica to the vapors of its solvent. (auth)

40952 (ORNL-TM-1179) PROCUREMENT AND QUALITY EVALUATION OF Nb-1 PERCENT Zr STOCK FOR BOILING ALKALI METAL CORROSION STUDIES. Roche, T. K. (Oak Ridge National Lab., Tenn.). Aug. 1965. Contract W-7405-eng-26. 25p. Dep. mn; CFSTI, $1.00 cy, $0.50 mn.

Tubing, plate, and bar stock of Nb–1% Zr were procured for evaluation in boiling alkali metal systems. Costs for this material, together with the results of evaluating its quality upon receipt from the various vendors, are presented. (auth)

40953 (PWAC-441) UTILIZATION OF YTTRIUM IN GETTERING OXYGEN AND NITROGEN IN COLUMBIUM BASE MATERIALS. Carlson, C. E.; Delgrosso, E. J. (Pratt and Whitney Aircraft, Middletown, Conn. Connecticut Advanced Nuclear Engineering Lab.). June 24, 1965. Contract AT(30-1)-2789. 21p. Dep. mn; CFSTI $2.00 cy, $0.50 mn.

Yttrium additions were made to a series of non-consumably arc melted niobium base materials to ascertain the efficiency of yttrium as a scavenging agent for refractory interstitial elements. A relationship was derived for the loss of oxygen as a function of yttrium loss. The influence of yttrium on the hardness and grain size of these materials is described. (auth)

40954 PREPARATION OF URANIUM MONOCARBIDE ON A PILOT PLANT SCALE. McMurtry, Carl H. (Carborundum Co., Niagara Falls, N. Y.). Am. Ceram. Soc. Bull., 44: 612-15(Aug. 7, 1965).

Results are reported on the pilot plant preparation of high purity UC from UO_2 and carbon. An evaluation is made of the effect of UO_2 to carbon ratio, synthesis temperature, hold time at temperature, and the rate of CO removal from the reaction site. With UO_2 and carbon mixtures calculated to yield stoichiometric UC, a reaction product can be obtained routinely with less than 500 ppm oxygen and 100 ppm nitrogen. A sampling and analysis plan is presented for the determination of the oxygen content in UC, to a precision of ±20%. (auth)

40955 DISPLACEMENT OF HALOGENS FROM RARE EARTHS AND YTTRIUM BY MEANS OF MAGNESIUM. PREPARATION AND STUDY OF MAGNESIUM–YTTRIUM ALLOYS. Caro, Paul (Laboratoire de Energie Solaire, Citadelle de Montlouis, France). Ann. Chim. (Paris), 9: 481-507(Sept.-Oct. 1964). (In French).

The Trombe-Mahn method of preparing an Mg–Y alloy is discussed. Yttrium halides are reduced to metal in a magnesium salt bath at 800°C. The alloys produced by this method showed a lower content of Y than alloys produced by the same method using rare earths (1 to 2% for Y; 20 to 30% for Gd, for example). This result led to a study of the chemical equilibrium: $3\ Mg + 2\ LnX_3 \rightarrow 2\ Ln + 3\ MgX_2$ in terms of thermodynamic and electrochemical data. The preparation of alloys of low Y content was studied in particular. A method was perfected for distilling Mg without the use of pressure, that led to higher concentrations of Y and eventually to pure Y in both solid and liquid forms. These experiments led to several important findings: data on the structure of alloys manufactured by this method and on the possibilities of improving their mechanical qualities by refining the product by appropriate treatment; the measurement of the composition of Mg_3Y, Mg_2Y, and MgY; and the possibility of obtaining a spongy form of Y at low temperature. Some general remarks on these observations are made. The importance to industry of the economical production of Mg-rare earth alloys is emphasized, especially Mg–Y, and the preparation of the rare metals from these alloys. Also stressed are the study of fluoride baths and their use in exchanges with Mg. Finally, it is pointed out that Mg–Y alloys have different properties from other Mg–rare earth alloys and could form a new class of Mg alloys important for the aeronautics and space industry. (BBB)

40956 TWO-DIMENSIONAL SECOND VIRIAL COEFFICIENTS OF KRYPTON ON GRAPHIC CARBON. Sams, John R. (Univ. of British Columbia, Vancouver, Can.). Mol. Phys., 9: 195-6(1965).

Second and third gas-surface virial coefficients are calculated for krypton on graphitic carbon. The results are tabulated along with the two-dimensional (12, 6) potential parameters for krypton. Three-dimensional parameters are also given for comparison. (L.B.S.)

40957 REACTOR MATERIALS. Volume 8, Number 2. Dayton, R. W.; Simons, E. M. (Battelle Memorial Inst., Columbus, Ohio). Summer 1965. Contract W-7405-eng-92. 118p. GPO $0.70(domestic), $0.90(foreign).

One of the Technical Progress Reviews prepared quarterly for the Division of Technical Information, USAEC.

Recent developments in reactor materials are reviewed under the following topics: fuel and fuel materials, moderator materials, nuclear poisons, cladding and structural materials, and special fabrication techniques. Separate abstracts were prepared for each of the 5 topics. (W.L.G.)

For abstracts of individual sections see: 40958–40961, and 40989.

40958 FUEL AND FERTILE MATERIALS. Reactor Mater., 8: No. 2, 57-73(Summer 1965).

Recent research developments are reviewed for uranium and its alloys, plutonium and its alloys, thorium and its alloys, metal-ceramic fuels, coated-particle fuel materials, uranium oxides, uranium and thorium carbides, uranium and thorium nitrides, uranium corrosion, and radiation effects on uranium and uranium carbide. (69 references). (W.L.G.)

40959 MODERATOR MATERIALS. Reactor Mater., 8: No. 2, 74-82(Summer 1965).

Recent research developments are reviewed for graphite, beryllium and its alloys, beryllium oxide, beryllium intermetallic compounds, and solid hydrides. (20 references). (W.L.G.)

40960 NUCLEAR POISONS. Reactor Mater., 8: No. 2, 83-5(Summer 1965).

Research on metallic, dispersion, and nonmetallic poison materials is reviewed. (12 references). (W.L.G.)

40961 CLADDING AND STRUCTURAL MATERIALS. Reactor Mater., 8: No. 2, 86-104(Summer 1965).

Recent research developments are reviewed for corrosion, mechanical properties of cladding and structural materials, metallurgical aspects of cladding materials, diffusion, ceramic technology, and radiation effects in nonfuel materials. (78 references). (W.L.G.)

40962 THE USE OF SEMI-CONDUCTOR DETECTORS FOR SURFACE ANALYSIS BY ELASTIC SCATTERING OF ACCELERATED CHARGED PARTICLES. Peisach, Max; Poole, Darrell O. (Southern Universities Nuclear Inst., Faure, South Africa). 27p. (CONF-650405-11). Gmelin, AED-CONF-65-040-23.

From International Conference on Modern Trends in Activation Analysis, College Station, Tex.

Charged particles with energies of a few Mev, having a limited range in solid material, undergo their reactions within a short distance from the surface rather than in the depth of the target, and by so doing, enable the surface layers of the target to be studied. Such a method of surface analysis was investigated with protons. Elastically scattered protons have proved suitable for the determination of the chemical elements in the surface of solids. Targets were bombarded with a collimated beam of particles at constant energy from the 5.5 Mev Van de Graaff accelerator at SUNI. Scattered particles were analyzed 10cm from

the source at 90° to the incident beam. Other angles are currently under investigation. Elements such as carbon, aluminium, iron and gold were identified and measured on the surfaces of other metals with a sensitivity of the order of 10^{-6} g. per cm^2. The sensitivity of the method increases with increasing scattering angle and with the energy of the incident particle. By using surface barrier semiconductor detectors with a window of less than 0.05 microns thick, the energy of the measured particle is not altered within the resolution limits of the detector. The main advantages of these detectors are their compactness, stability and cheapness, which enables surface analyses to be carried out at a fraction of the cost with more usual methods using mass-spectrometry. Their disadvantage lies in the decreased resolution when compared with the more conventional method. Gold was measured on surfaces of aluminum, quartz, steel, brass and similar metals, and aluminium layers on heavy metals could readily be analyzed. However, the quantitative determination of aluminium on light metals presented difficulties owing to the resolution limits of the detectors. This problem is being investigated with heavier charged particles at comparable energies. (auth)

40963 A PROCESS FOR PREPARING FINE SPHERICAL PARTICLES OF THORIUM OXIDE. (to Nihon Genshiryoku Kenkyu Sho). British Patent 997,314. July 7, 1965. Priority date July 5, 1961, Japan.

A process for preparing fine spherical particles of ThO_2 includes coagulating colloidal particles in a colloidal solution of thorium hydroxide nearly saturated with ammonium nitrate by dispersing the solution in a mixture of a water-miscible and water-immiscible organic solvent by injection through a glass nozzle. The coagulated particles are separated from the liquid phase and washed free of organic solvent prior to calcining. The separated particles are calcined by first heating them to 600°C to convert the hydroxide to the oxide and then to above 1300°C to increase the specific gravity of the oxide particles. (B.L.M.)

40964 METALLOGRAPHIC SAMPLE CARRYING DEVICE. (to Groupement Atomique Alsacienne Atlantique). British Patent 999,934. July 28, 1965. Priority date Nov. 16, 1962, France.

A metallographic sample carrying device is provided for use in a polishing machine equipped with a guide member. The device includes a cylindrical body provided with a central bore and a number of recesses for samples arranged around the central bore. Each recess communicates with the central bore through a longitudinal slot. Two longitudinally threaded spindles are adapted to bite into the material of a sample located in each recess approximately symmetrically with regard to each other and the slot so as to extend into the recess. A chuck member is formed with a central bore to accommodate the guide member of the polishing machine and carries a number of longitudinal spring leaves adapted to apply pressure on the samples in the recesses through the slots and to locate the chuck against rotation when it is inserted into the central bore of the body. The locking mechanism may be provided by a locking ball that is urged by the spring bearing against the screw threaded into the body. A circular slot or groove is formed around the chuck as a detent to accomodate the ball. Loading and unloading devices may be provided with the sample carrying device. A plane table co-operating with the body during loading has recesses for locating the samples in the recesses until the chuck is inserted. A second plane table co-operating with the body has a central bore through which the chuck may be driven to release the samples. (B.L.M.)

Corrosion

40965 (BNWL-83) CORROSION IN SIMULATED PRTR FUEL ELEMENT SURFACE CREVICES. Winegardner, W. K. (Battelle-Northwest, Richland, Wash. Pacific Northwest Lab.). July 1965. Contract AT(45-1)-1830. 28p. Dep. mn; CFSTI $2.00 cy, $0.50 mn.

Two out-of-reactor tests were conducted to study corrosion of Zircaloy-2 in crevices with geometries similar to those existing on heat transfer surfaces of Plutonium Recycle Test Reactor fuel elements. The tests were conducted in high temperature (293°C), lithiated water at a pH of about 10 and used electrically heated, Zircaloy-2 clad test assemblies. Heat flux associated with heated crevices was about 1100 w/in^2. Examination after 70 days of loop exposure revealed test assembly cladding penetration, up to 0.007 in., in heated crevices. It is felt that the accelerated attack was the result of the concentration of lithium hydroxide by local boiling. (auth)

40966 (BNWL-92) ENVIRONMENTAL TESTS OF CANDIDATE MATERIALS FOR THE HIGH TEMPERATURE LATTICE TEST REACTOR. O'Keefe, D. P. (Battelle-Northwest, Richland, Wash. Pacific Northwest Lab.). July 1965. Contract AT(45-1)-1830. 26p. Dep. mn; CFSTI $2.00 cy, $0.50 mn.

A series of screening tests established that definite problems would exist with the use of some alloys, and permitted a selection of materials for later and more detailed testing. Candidate cladding, structural, control, and fuel materials were evaluated on the bases of weight gain, metallographic change, and room temperature mechanical properties. Test specimens were exposed in a simulated HTLTR environment for various periods up to 840 hr in a nitrogen-graphite environment at 1000 or 1200°C. The most pronounced effect on metallic specimens was carburization of alloys containing carbide formers. TD Nickel and Nickel 200 showed the least effects. Hastelloy B and Inconel 600 displayed limited serviceability, and were more stable than nickel when in contact with the refractory brick which will be used for insulation in the reactor. Embrittlement occurred in Hastelloy X, Inconel 625, molybdenum, and Hastelloy X with commercially applied coatings of aluminum and ceramic. Reactions between granulated B_4C and nickel and powdered UO_2 and nickel resulted in low melting alloys which melted during exposure. Massive B_4C and powdered UO_2 did not react with TD Nickel cladding in other tests. Aluminum nitride was found to be stable, but boron nitride decomposed in the simulated reactor environment. (auth)

40967 (COO-1319-27) A STUDY OF THE MECHANISM OF STRESS CORROSION CRACKING IN THE IRON-NICKEL-CHROMIUM ALLOY SYSTEM. Quarterly Report, March 17-June 16, 1965. Staehle, R. W.; Beck, F. H.; Fontana, M. G.; Hirth, J. P. (Ohio State Univ. Research Foundation, Columbus). July 9, 1965. Contract AT(11-1)-1319. 43p. Dep. mn; CFSTI $2.00 cy, $0.50 mn.

The addition of 17 different elements as fourth-components in the Cr-Fe-Ni alloy system caused stress-corrosion cracking in all cases. Tests in combinations of water, chloride, and oxygen at 600°F indicate that both chloride and oxygen are necessary for accelerated surface attack. Tensile properties were determined from room temperature to 1200°F for selected alloys. An increase in strength with increasing chromium content was noted. Electron micrographs of oxide films revealed a distinct difference between those on low- and high-nickel alloys. (W.L.G.)

40968 (EURAEC-1424) THE RELATIONSHIP OF NITROGEN CONTENT OF AUSTENITIC STAINLESS STEELS TO STRESS CORROSION. Quarterly Report No. 4. Ferry, B. N. (Virginia Polytechnic Inst., Blacksburg. Dept. of Metals and Ceramic Engineering). June 1965. Contract AT(40-1)-3208. 16p. Dep. mn; CFSTI $1.00 cy, $0.50 mn.

Work Performed under United States-Euratom Joint Research and Development Program.

The percentage of nitrogen dissolved in type 304 stainless steel was measured as a function of the nitriding time at 1000°F for different ammonia-hydrogen ratios. This information enables nitriding and diffusion anneal treatments to be combined. Two torsional pendulum experiments were performed and the relaxation spectrum obtained for unni-

trided type 304 stainless steel at 0.50 cps frequency. No internal friction peaks occurred between 80 and 423°F. The mean internal friction (logarithmic decrement) values were 0.0016 for the first and 0.0021 for the second experiments. (W.L.G.)

40969 (MSAR-65-96) EFFECT OF HIGH TEMPERATURE SODIUM ON AUSTENITIC AND FERRITIC STEELS. MECHANICAL PROPERTIES OF MATERIALS. Quarterly Progress Report, April-June 1965. (MSA Research Corp., Callery, Pa.). Aug. 6, 1965. Contract AT(11-1)-765. 66p. Dep. mn; CFSTI, $3.00 cy, $0.75 mn.

Specimens of type 316 stainless steel in high-carbon sodium formed carbide films that reduced the ductility, fatigue life, and impact strength and increased the creep-rupture strength. The degree of carburization of the loop piping appeared to be a function of the downstream distance from the carbon bed. Data from tests in high-oxygen sodium are more scattered and show little difference in the effects on rupture life and creep rates. The impact strength decreased, but not as great as in high-carbon environments. Fatigue tests show a differently shaped failure-versus-time curve than those in other environments. This is attributed to oxygen scaling. (W.L.G.)

40970 (NASA-CR-54390) STUDIES OF ALKALI METAL CORROSION ON MATERIALS FOR ADVANCED SPACE POWER SYSTEMS. Quarterly Progress Report No. 3, December 26, 1964-March 26, 1965. Harrison, R. W. (General Electric Co., Cincinnati, Ohio. Space Power and Propulsion Section). Contract NAS 3-6012. 31p.

A D-43 alloy reflux stress-corrosion capsule was fabricated, filled with purified potassium, sealed, and installed in the test facility. Assembly and instrumentation of the Task I test facility was completed and the system was evacuated to a pressure of 2×10^{-9} torr prior to the bakeout cycle. The initiation of the test is pending receipt of tungsten caps which are to be installed over the Al_2O_3 probes to prevent any possible reaction between the Al_2O_3 and the D-43 alloy. Two Type 321SS and two Type 316SS capsules, each containing two Nb-1Zr alloy test specimens, were tested isothermally at 1400°F for 1,000 hours without difficulty. Post-test evaluation of capsules has shown that Type 321SS has a significant advantage over Type 316SS in refractory metal-stainless steel-potassium systems in inhibiting mass transfer of the interstitial elements carbon and nitrogen from the stainless steel to the refractory metal. (auth)

40971 (RT/CHI(65)20) RICERCA BIBLIOGRAFICA SUL FOULING. (Bibliography on Fouling Research). Bordonali, C.; Biancifiori, M. A. (Comitato Nazionale per l'Energia Nucleare, Rome (Italy)). Apr. 1965. 19p. Dep. mn.

A literature survey was prepared on the mechanism of the formation of fouling films on the heat exchange surface of fuel elements in organic moderated reactors. These results were obtained mainly by researches carried out at the Atomics International and the Phillips Petroleum Co. This survey includes a description of the methods so far envisaged and tested for effecting the removal of the impurities which are connected to the formation of fouling films. (auth)

40972 HIGH TEMPERATURE METALLOGRAPHIC MICROSCOPE STUDIES OF INITIAL OXIDATION OF TANTALUM. Kofstad, P.; Krudtaa, O. J. (Central Inst. for Industrial Research, Oslo). Mem. Sci. Rev. Met., 62: 17-25(May 15, 1965).

High-temperature metallographic microscope studies of the initial oxidation of tantalum in the temperature range from 300 to 1300°C at oxygen pressures of 0.1, 0.01, and 0.001 torr were carried out. The results are presented as a consecutive series of photographs of the specimen surface during oxidation. In all cases an incubation period preceded the first visual observation of oxide formation. At any temperature the duration of this incubation period became longer the lower the oxygen pressure. During the incubation period oxygen dissolution in the metal was the predominant part-process. The initial oxide formation, as revealed by the metallographic microscope, never resulted in a continuous film or scale with an approximately even thickness, but always involves formation of individual oxide nuclei or crystallites and the subsequent growth of these. The results were correlated with previous studies of oxidation of tantalum. (auth)

40973 OXIDATION OF IRON SURFACES UNDER ION BOMBARDMENT. Haymann, P.; Waldburger, C.; Trillat, J. J. (Centre National de la Recherche Scientifique, Bellevue, France). Mem. Sci. Rev. Met., 62: 135-9(May 15, 1965). (In French).

As was shown by different experimenters, the oxidation kinetics of a metal is modified by the bombardment with low-energy ions of inert gases. Under the same conditions, the germination of the oxide layer is also modified. The ionic attack force section was investigated to determine the action of ions on metals at temperatures between -50 and 1200°C. In order to compare the results with those of Bardolle and Bernard, monocrystalline or multicrystalline electrolytically pure iron was used; the oxidation was produced either by Ar^+ and O^+ from an ionic source or by the impact of a very low oxygen current on the sample. The sample was also oxidized after bombardment by Ar^+ ions alone by using a controllable leak fed with O_2. During the bombardment and in an initial vacuum of 10^{-5} mm Hg, the oxidation of the sample at 600°C was very rapid and the epitaxic oxide FeO was attacked selectively. For a temperature close to 820°C, in addition to the selective attack on FeO, the formation of oxide crystallites on grain boundaries in multicrystalline samples was also observed; these crystallites have an orientation that depends on the orientation of the subjacent iron crystal. These results were still valid above the $\alpha \rightleftharpoons \gamma$ transformation point. Under the conditions of initial vacuum and without bombardment, no germination was established whatever the temperature of the sample. The mechanism of oxidation under bombardment was not fundamentally different from oxidation under conditions of thermodynamic equilibrium: only certain details are changed, in particular the speed of oxidation, the growth of crystallites, the aspect of the continuous layer of oxide between the crystallites, and the partial pressure of oxygen when an attempt is made to induce germination phenomenon on the surface of an iron crystal previously bombarded by Ar^+ ions. (tr-auth)

40974 SOME ASPECTS OF THE INITIAL STAGE OF OXIDATION OF NIOBIUM. Van Landuyt, J. (SCK-CEN, Mol, Belg.). Mem. Sci. Rev. Met., 62: 153-5(May 15, 1965). (In French).

Fused zones of Nb in foils 100-μ thick were used to study the initial stages of oxidation. The foils were annealed, polished electrolytically, and rinsed. They were then oxidized in a resistance furnace under reduced air pressure. Nucleation phenomena were observed on foils oxidized for 10 minutes at 600°C. The oxidation germs were composed of parallel platelets. The crystallographic orientation of the metal subjacent to the germination centers affected the oxidation germs. There was preferential nucleation at the dislocations of the grain sub-boundaries and at other dislocations in polygonized samples. An oxidation of 30 minutes at 600°C revealed oxidation germs that developed according to a crystallographic direction of the metal. The mechanism of oxidation was affected by the thickness of the foil. A striation was observed in the (110) direction of the metal or of the solid solution NbO. No suboxide or oxide phases were observed in the platelets and germs. (J.S.R.)

40975 REACTIONS OF GASES WITH GRAPHITE. Sella, C.; Trillat, J. J. (Centre National de la Recherche Scientifique, Bellevue, France). Mem. Sci. Rev. Met., 62: 187-96(May 15, 1965). (In French).

Microscopic and electron defraction studies of the oxidation of graphite monocrystals make it possible to define the mechanism of formation of corrosion patterns, which develop at the surface of crystals heated in air or in carbon dioxide. In effect, in thin films obtained by cleavage in air,

the basal dislocations are visible at great distances. This makes it possible to show that the oxidation occurs at the place where crystalline dislocations are the strongest (convergent zones of dislocations, points of emergence of dislocations on grain boundaries, etc.) and progresses from these points by giving birth to hexagonal corrosion patterns analogous to those observed at the surface of massive samples oxidized under the same conditions. (tr-auth)

40976 OXIDATION OF NIOBIUM–COPPER AND ZIRCONIUM–COPPER ALLOYS. Voitovich, R. F. (Inst. of Metallography, Academy of Sciences, USSR). Zh. Fiz. Khim., 39: 1112-15(May 1965). (In Russian).

Kinetics of Nb–Cu and Zr–Cu alloy oxidation at 500 to 900°C was studied. The equation for the temperature dependence of Zr–Cu alloy oxidation rate was developed. Alloying of niobium with copper, especially with copper concentration up to 30 to 50%, sharply reduced the corrosion resistance of this metal. Small (up to 10%) addition of copper to zirconium increased zirconium corrosion resistance at temperatures not exceeding 700°C. (R.V.J.)

40977 IMPROVEMENTS IN OR RELATING TO ZIRCONIUM ALLOYS. (to Siemens-Schuckertwerke Aktiengesellschaft). British Patent 999,367. July 21, 1965. Priority date Dec. 27, 1961, Germany.

A Zr alloy suitable for use as a reactor structural element or as sheath or can material for fuel elements in reactors includes 0.005 to 1 wt % Ca and one or more of the elements Nb, Sn, Fe, Cr, Ni, Mo, Cu, W, V, Ta, and Pd, each in a percentage by weight of from 0.05 to 5% of the total alloy. The alloy is at least a ternary system. One alloy is the ternary system consisting of 0.1 to 0.5 wt % Ca and 0.3 to 2.5 wt % Nb, and the rest of the alloy consisting of Zr with or without impurities. (B.L.M.)

Fabrication

Refer also to abstracts 41006, 42172, and 42175.

40978 (ANL–6955) DEVELOPMENT OF A PROCESS FOR MANUFACTURING ZPR-III U–Pu–Mo TEST FUEL ELEMENTS. Shuck, A. B.; Pilarski, E. M.; Hins, A. G.; Burton, G. Jr. (Argonne National Lab., Ill.). Mar. 1965. Contract W-31-109-eng-38. 41p. Dep. mn; CFSTI $2.00 cy, $0.50 mn.

Work performed to determine the design and fabrication processes to manufacture uranium-plutonium alloy fuel elements for ZPR-III critical experiments is described. These fuel elements consist of vacuum-cast uranium–plutonium–molybdenum alloy fuel plates sealed in stainless steel jackets. Four areas were investigated: fuel-plate casting, jacket design and fabrication, fuel-element-assembly techniques to produce fuel elements free from alpha contamination, and jacket seal welding and weld-casting of bearing shoes. Sample fuel elements were manufactured as described to test the feasibility of the process. (auth)

40979 (EURAEC–1351) STAINLESS STEEL CLADDING OF VERY THICK STEELS. Quarterly Report No. 3, January 1–March 31, 1965. (Soudometal, S. A., Brussels (Belgium)). Apr. 29, 1965. Contract 008-63-12 TEEB(RD). 34p. (EUR–2326). Dep. mn; CFSTI $2.00 cy, $0.50 mn.

Work Performed Under United States–Euratom Joint Research and Development Program.

The effects of the stainless steel tape size, deposition rate, and current density on the structure, ferrite content, chemical composition, and the as-welded and relaxed state bending properties of the deposit were evaluated. (W.L.G.)

40980 (LA–3302) FEASIBILITY OF BRAZED JOINTS BETWEEN Cb–1 Zr ALLOY AND ALUMINA CERAMICS. Kirby, R. S.; LaMotte, J. D. (Los Alamos Scientific Lab., Univ. of California, N. Mex.). Dec. 1, 1964. Contract W-7405-eng-36. 25p. Dep. mn; CFSTI $2.00 cy, $0.50 mn.

Two brazing systems were developed for ceramic-metal seals whose helium leak-rate was less than 1×10^{-9} cc/sec. Nickel plated Mo–Mn metallized Al_2O_3 ceramics were brazed to Nb–1 Zr metal components using a Cu–45 wt % Ni filler alloy. Unmetallized Al_2O_3–0.5 wt % Y_2O_3 ceramics were brazed to Nb–1 Zr metal components using a Ti–48 wt % Zr–4 wt % Be alloy. Both types of joints remained leak-tight during limited cycling tests at 1000°C but failed during the first 1100-1200°C cycle. Neither system was considered suitable for use above 1000°C as developed. (auth)

40981 (NUMEC–2389-6) SINTERING BEHAVIOR OF PLUTONIUM DIOXIDE. Houston, M. D. (Nuclear Materials and Equipment Corp., Apollo, Pa.). [1964]. Contract AT(30-1)-2389. 24p. Dep. mn; CFSTI $1.00 cy, $0.50 mn.

Compacts of PuO_2 were prepared and sintered to study the sinterability of PuO_2 powders prepared by various methods and to study the effect of controlled impurity additions. The PuO_2 was prepared by precipitation from nitrate solution of oxalate, hydroxide, and peroxide and subsequent conversion. Some powders were also prepared by direct oxidation of Pu metal and by direct denitration of plutonium nitrate solution. Sintering was performed at 1600°C in N_2–6% H_2 and O_2. Generally, higher densities resulted from compacts sintered in O_2 as sintering in a reducing atmosphere tends towards the formation of lower density suboxides. Sintered densities also tended to be higher for the oxalate derived material. Controlled additions primarily of Y_2O_3 and SrO were studied as sintering aids. The results indicate that SrO addition in the range of 0.4 to 1.0 mole % has a pronounced beneficial effect in increasing sintered density. (auth)

40982 (ORNL–3819) MOTION OF SPHERES IN SMOOTH ROTATING DRUMS AND APPLICATIONS TO THE COATING OF NUCLEAR FUEL PARTICLES. Pilloton, R. L.; Flamm, H. J. (Oak Ridge National Lab., Tenn.). Aug. 1965. Contract W-7405-eng-26. 47p. Dep. mn; CFSTI $2.00 cy, $0.50 mn.

A process that consists of coating spherical nuclear particles by blowing a coating gas over the charge placed in a heated cylindrical smooth drum that rotates around a horizontal axis is described. In such a technique, the control of the particle motion must be precisely adjusted to achieve uniform coating and to avoid the formation of irregular particle shapes or the agglomeration of particles during the coating step. The physical characteristics of nuclear fuel particles that affect particle motion were investigated. By observing the motion of these particles or of rheologically similar materials in plastic or glass models and the angles of slide of these particles on smooth graphite, glass, or steel, we have found that their friction coefficients (the tangents of the angles of slide) are small. Consequently the particles have a tendency to slip on rotating drum walls or even to remain motionless. The investigation showed that near-spherical nuclear fuel particles will not be properly agitated in horizontally rotating, smooth drums unless loading, rotational speed, and wall-surface characteristics are carefully selected. Furthermore, even when these variables are optimized, the particles remain motionless relative to one another and to the wall for an appreciable fraction of time. Thus, it is concluded that smooth drums are unsuitable for coating. (auth)

40983 (ANL-Trans–189) CHANGE IN THE WALL THICKNESS OF TUBES DURING DRAWING. Pocta, Bohumil. Translated for Argonne National Lab., Ill., from Hutnicke Listy, 10: 194-200(1955). 28p. Dep. mn; JCL. $2.60 fs, $1.04 mf.

Experimental measurements were made of the changes in wall thickness produced by tube sinking. The ratio of the wall thickness to the tube diameter had the greater effect. The change did not depend directly on the degree of deformation, but on the forming efficiency, which comprises the degree of deformation. Experiments indicate that when the ratio between the wall thickness and the diameter was about 17%, the wall thickness did not change during drawing. The wall thickness increased for smaller ratios and decreased for larger ratios. (W.L.G.)

40984 THE ELECTRON BEAM ZONE REFINING OF RUTHENIUM. Schriempf, J. T. (Naval Research Lab., Washington, D. C.). J. Less-Common Metals, 9: 35-9 (1965).

Single-crystal ruthenium specimens of nominally one-half cm diameter and up to eight cm long were prepared by electron-beam zone melting in a vacuum of about 1×10^{-6} torr. Purity profiles obtained by measuring RRR (the ratio of the electrical resistance at room temperature to that at 4.2°K) are shown for crystals grown from both 99.9% pure and 99.999% pure starting material. With the more pure substance a crystal with an RRR value of 1100 was obtained. (auth)

40985 ACTIVATION SINTERING OF TUNGSTEN. Toth, I. J.; Lockington, N. A.; Derry, L. W. (Battersea Coll. of Tech., London). J. Less-Common Metals, 9: 157-67(1965).

Tungsten powder compacts were sintered in hydrogen/bromine atmospheres at temperatures from 1200 to 1700°C, and the rates of densification compared with those of compacts sintered in hydrogen alone. The presence of bromine increased densification rates with the effect most marked at temperatures in the middle of the range. The densities achieved were not high, and the porous product broke in a brittle manner when tested by bending at room temperature; however, the load to fracture of a bromine-treated test-piece of a given density was greater than for a similar test-piece sintered in hydrogen alone. (auth)

40986 TUNGSTEN AND MOLYBDENUM COATED NONMETALLIC POWDER. Landsberg, A.; Campbell, T. T.; Block, F. E. (Bureau of Mines, Albany, Ore.). J. Metals, 17: 850-5(Aug. 1965).

Two methods were studied for applying coatings of W or Mo to the surface of powdered magnesia, alumina, zirconia, zirconium carbide, and zirconium boride. In both methods coatings were applied to particles while they were suspended in a fluidized bed. In one case coatings were applied by the vapor phase reduction of metal chlorides. In the other method a two step process was used in which a metal oxide was applied to the fluidized particles and the oxide reduced subsequently by hydrogen. The oxide process appeared more favorable from the standpoint of materials handling, reactor corrosion, and byproduct disposal. Also, coatings could be applied by the oxide process four times faster than by the chloride process. (P.C.H.)

40987 FREEZE-DRY TECHNIQUE FOR MAKING ULTRA-FINE METAL POWDER. Landsberg, A.; Campbell, T. T. (Bureau of Mines, Albany, Ore.). J. Metals, 17: 856-60(Aug. 1965).

The application of a freeze-drying method for preparing ultrafine materials which were subsequently reduced to form fine tungsten metal powder or tungsten-rhenium alloy powders was investigated. This method requires only a means of rapidly freezing solutions and commercially available vacuum equipment for the removal of water. The results showed that the method is feasible for preparation of ultra-fine particles from soluble materials. (P.C.H.)

40988 PRODUCTION AND APPLICATION OF NIOBIUM CARBIDE PARTS. Kolchin, O. P.; Berlin, I. K. Porosh. Met. Akad. Nauk Ukr. SSR, No. 4, 25-34(1965).

Experiments were conducted to develop the technology of making large NbC parts for use as heaters and shields for industrial high-temperature induction vacuum furnaces. Sound NbC specimens with a bend strength of 278.5 Mn/m^2, a compression strength of 288.3 Mn/m^2, and a room-temperature resistivity of 0.4×10^{-6} ohm/m were produced by vibrational compacting of dry carbide powders with a particle size of 5μ or less and subsequent sintering in a H_2 atmosphere at 2373°K. It was found that NbC heaters and other furnace parts can be used at 2773°K and above in vacuum furnaces and in furnaces with an atmosphere of gases nonreactive with the carbide. The technology of making NbC can, with some changes, be used for making parts from tantalum, zirconium, and hafnium carbides, and from double carbides. (CFSTI)

40989 SPECIAL FABRICATION TECHNIQUES. Reactor Mater., 8: No. 2, 105-18(Summer 1965).

Recent research developments are reviewed for melting, hot and cold working, cladding, explosive joining, welding, brazing, and nondestructive testing techniques. (57 references). (W.L.G.)

40990 HOLLOW METAL SINGLE CRYSTAL FOR NMR EXPERIMENTS. Schone, H. E.; Olson, P. W. (Boeing Scientific Research Labs., Seattle). Rev. Sci. Instr., 36: 843(June 1965).

A cylindrical graphite mold is used to prepare a hollow, cylindrical, ^{119}Sn-enriched Sn single crystal. The dimensions of the resulting Sn cylinder are: length, 2.5 cm; diameter, 7.6 mm; and wall thickness, 0.25 mm. The NMR spectra of the sample are shown. (T.F.H.)

40991 PREPARATION OF SINGLE CRYSTAL SPHERES OF REFRACTORY METALS AND ALLOYS. van Torne, L. I. (Martin Co., Orlando, Fla.); Thomas, G. Rev. Sci. Instr., 36: 859-60(June 1965).

A wide groove is cut around the circumference of a cylindrical single crystal of the refractory material under consideration, near the end of the cylinder. The short part of the cylinder, between the groove and the end, is then bombarded by an electron beam until its surface becomes fluid. The surface tension then causes the material to assume a roughly spherical form. The beam power is then reduced gradually, in order to allow the solid monocrystalline center of the sphere to act as a seed for the solidifying surface. The spheroidal body is then cut from the cylinder, polished, and finally electropolished to the final form. Results obtained with a Mo–19 at. % Ta single crystal produced by this method are shown on a Laue photograph. (T.F.H.)

40992 IMPROVEMENTS IN OR RELATING TO COATED ARTICLES. (to General Dynamics Corp.). British Patent 998,247. July 14, 1965. Priority date Apr. 11, 1963, United States.

A coated article is provided that has increased structural stability under conditions of thermal and/or radiation stress. The article includes a core, an exterior coating about the core, and a low density, spongy, shock absorbing coating capable of absorbing stresses interposed between the core and the exterior coating. The coated article may be a particular fissionable material or a poison, and the shock absorbing coating may be a low density, spongy, pyrolytic carbon. (B.L.M.)

40993 IMPROVEMENTS IN OR RELATING TO NUCLEAR REACTORS. Carlson, Walter Berndt (to Babcock and Wilcox Ltd.). British Patent 998,301. July 14, 1965. Filed Nov. 24, 1960.

A process is described for machining a finned fuel element can from a cylindrical can. An even number of fins extend both circumferentially and longitudinally around the can. The fins are arranged in adjacent sets of oppositely handed form. The outer parts of the fins at neighboring parts of each pair of adjacent sets are inclined in longitudinal axial section of the can relative to the axis of the can in the direction in which the neighboring parts of adjacent sets of fins converge. The inclination of outer parts of the fins gradually decreases in a direction away from the neighboring parts of adjacent sets until at intermediate locations in the length of the fins the fins extend radially. The peripheral edge of the fins follow respective helical paths of greater lead than the paths followed by the fin roots. (B.L.M.)

40994 IMPROVEMENTS IN OR RELATING TO NUCLEAR REACTOR FUEL ELEMENTS. Gittus, John Henry (to United Kingdom Atomic Energy Authority). British Patent 998,387. July 14, 1965. Filed June 5, 1962.

A reactor fuel element is composed of particles of nuclear fuel material aggregated together to form a composite structure with interconnecting pores to allow coolant to pass through the pores as well as over the surface of the element. The particles of the element may be spheroidal or rod-like in form and are coated with a cladding material

to prevent the escape into the coolant of fission products generated in the fuel element during irradiation in the reactor. The coating on the aggregated particles may be in the form of a metal, alloy, or ceramic and may be effected by deposition of the metal or alloy from the vapor phase; by deposition from emulsion, sol, suspension, or amalgam; by deposition by the thermal decomposition of the halide of suitable metals or alloys; or by deposition from aqueous or organic solutions of the salts of suitable metals or alloys. Ceramics may be deposited by first depositing a coating metal by an appropriate method and then converting the metal coating to ceramic by heating in an oxidizing, nitriding, or carbonizing atmosphere. Alternatively, the particles may first be coated with the cladding material and then sintered together into the required shape, or the coated particles may be held loosely together in a perforated container to allow the passage of cooling gas through the spaces between the particles. The element may comprise clad filaments of a U-Mo alloy extending the length of the element and joined together in a bundle by sintering between the coating of the filaments along the lines of contact. (B.L.M.)

40995 IMPROVEMENTS IN OR RELATING TO METAL OXIDE POWDER SINTERING. Bourrasse, Andre; Caillat, Roger; Delmas, Roger; Elston, Jean; Francois, Bernard; Morize, Pierre (to Commissariat a l'Energie Atomique). British Patent 999,463. July 28, 1965. Priority date June 2, 1961, France.

A process for sintering a metal oxide powder having a specific surface of at least 4 m^2/g includes initially compressing the powder to give a density equal to at least 45% of the theoretical density of the oxide. The compressed powder under a neutral or reducing atmosphere so as to subject it to a rapid increase in temperature to a temperature in the range of 1200 to 1800°C and to maintain it at such a temperature for a time sufficient to effect the desired sintering, and then cooling the sintered oxide. The total time for the heating must not exceed 3 hrs. The process is particularly applicable to the sintering of uranium dioxide, beryllium oxide, and aluminum oxide. (B.L.M.)

40996 METHOD OF MANUFACTURE OF URANIUM DIOXIDE HAVING A HIGH DENSITY. Bauschmann, Walter; Pascard, Roger (to Commissariat a l'Energie Atomique). Canadian Patent 712,078. June 22, 1965. Priority date Dec. 30, 1960, France.

Uranium dioxide powder, having poor sinterability is combined with a lubricant and an additive and compressed under about 10,000 kg/cm^2. The mixture is heated to remove the lubricant and the additive and then is sintered. Examples cited show densities as high as 98.4% of theoretical. (F.S.A.)

40997 REFRACTORIES AND METHODS OF MANUFACTURE THEREFOR. Davies, Ben; Smoot, Thomas W. (to Harbison-Walker Refractories Co.). U. S. Patent 3,192,058. June 29, 1965. Filed May 23, 1962.

A method is described of forming refractory shapes from size-graded, non-plastic, refractory aggregates that are either basic or non-basic, such as zirconia, alumina, and magnesia. The refractory aggregate is mixed with 1 to 15 wt % of a water-insoluble, finely divided, high purity Cr_2O_3 having a uniform particle size averaging less than 1 μ in diameter. The aggregate and the Cr_2O_3 are mixed with sufficient tempering agent to allow forming. (B.L.M.)

40998 METHOD OF FORMING MOLYBDENUM SILICIDE COATING ON MOLYBDENUM. Page, John P.; Moeller, Roger D.; Sneesby, George V. (to North American Aviation, Inc.). U. S. Patent 3,192,065. June 29, 1965. Filed June 1, 1962.

A process is described for providing an oxidation-resistant coating of molybdenum silicide on molybdenum. Other properties of molybdenum or its alloys, Mo–Ti and Mo–Ti–Zr, that are improved by the coating are hardness, ductility, resistance to thermal shock, surface appearance, erosion, abrasion resistance, and resistance to mechanical impact. The molybdenum is immersed in a molten alkali metal, preferably Na, bath at a temperature of 1000 to 2000°C under an inert gas atmosphere. Dissolved in the bath is approximately 10 wt % Si, 5 wt % Sn, and 1 wt % C. The molybdenum is maintained in the bath for a period of 3 to 5 hours to form the coating. The role of Sn and C in the process is not fully understood. (B.L.M.)

40999 PROCESS FOR MAKING WORKABLE RUTHENIUM AND PRODUCT THEREOF. Betteridge, Walter; Taylor, Brian (to The International Nickel Co., Inc.). U. S. Patent 3,194,657. July 13, 1965. Priority date Mar. 13, 1963, Great Britain.

A process for improving the workability of Ru metal includes permeating the molten Ru with a small amount of at least 0.005% of a permeating element in a non-oxidizing atmosphere. The permeating element is selected from the group consisting of up to about 5% Zn, Bi, or Cd; or up to about 0.25% Ba, Ge, Hf, Ti, Ce, Er, Gd, Ho, La, Pr, Sm, Yb, or Yt. The Ru is maintained in the molten state until it is quiescent and free from gas evolution and is then solidified. (B.L.M.)

Properties and Structure

Refer also to abstract 40722.

41000 (ACF–10) PHYSICAL PROPERTY STUDY OF POLYSTYRENE FOAM (210-050). McCandless, T. D. (ACF Industries, Inc., Albuquerque, N. Mex.). June 30, 1965. Contract AT(29-1)-1352. 32p. (ACF–412-248). Dep. mn; CFSTI $2.00 cy, $0.50 mn.

Polystyrene foam made by the expanded bead process and having 0.01, 0.05, and 0.10 specific gravities were studied. The following properties were measured: compressive strength and modulus, thermal conductivity, thermal coefficient of expansion, water absorption, humid aging, creep, and stability to thermal cycling. Equipment and test procedures are described. (D.L.C.)

41001 (AGN–8154) ALKALI METALS EVALUATION PROGRAM. Quarterly Progress Report, April 1–June 30, 1965. Achener, P. Y.; Parr, E. D.; Fisher, C. R. (Aerojet-General Nucleonics, San Ramon, Calif.). July 1965. Contract AT(04-3)-368. 25p. Dep. mn; CFSTI, $1.00 cy, $0.50 mn.

A research program is being conducted to determine the heat transfer, thermophysical, and transport properties of alkali metals. Methods for measuring liquid and vapor viscosity are being evaluated. Calorimeters which are to be used in the other measurements are described. (D.L.C.)

41002 (APS–5157-R) SNAP 50/SPUR PROGRAM MATERIALS INVESTIGATION—MECHANICAL PROPERTIES OF TZM. Salley, R. L.; Kovacevich, E. A. (Garrett Corp., Phoenix, Ariz. AiResearch Mfg. Div.). June 25, 1965. Contract AF33(615)-2289. 63p. (AFAPL-TR–65-51).

The effects of carbon content, ingot processing, and forging schedule on the fabrication and long-time high-temperature properties of TZM molybdenum alloy were investigated. (W.L.G.)

41003 (BAW–3376-3) IRRADIATION PERFORMANCE OF THORIA–URANIA FUEL MATERIALS. Quarterly Technical Report No. 3, January–March 1965. (Babcock and Wilcox Co., Lynchburg, Va.). Contract AT(30-1)-3376. 47p. Dep. mn; CFSTI $3.00 cy, $0.50 mn.

The permeability coefficient of compacted UO_2 was measured. The gas flow was identified as a combination of Knudsen and viscous flows. Thermal transpiration occurred at atmospheric pressure but decreased at higher pressures. Thoria–urania fuel was produced from pure thoria and normal uranium in an application of the sol-gel method. The sorbed gas release indicated that the gas content of the sol-gel thoria–urania is generally less than 0.1 cm^3/gm. Gas content tended to increase when the urania content was increased. (W.L.G.)

41004 (BMI–1735) CHARACTERIZATION OF PYROLYTIC-CARBON FUEL-PARTICLE COATINGS PREPARED

WITH ACETYLENE. Browning, Melvin F.; Vaughan, Dale A.; Dettore, Joseph F.; Blocher, John M. Jr. (Battelle Memorial Inst., Columbus, Ohio). July 19, 1965. Contract W-7405-eng-92. 43p. Dep. mn; CFSTI $1.00 cy, $0.50 mn.

The structure and properties of fuel particle coatings prepared by thermal decomposition of acetylene were studied as a function of preparation conditions. Comparisons were made with reference coatings prepared from methane. Three types of coatings were identified: dense laminar structures with a relatively high degree of anisotropy and a small crystallite size; low-density, relatively isotropic deposits with small crystallite size; and, dense granular (columnar) structures with a low degree of long-range anisotropy and a relatively large crystallite size. With minor exceptions, the boundaries between structures, though not distinct, appear to be shifted toward lower temperature in going from methane to acetylene. (auth)

41005 (CALT-221-11) A STUDY OF CsCl TYPE INTERMEDIATE PHASES INVOLVING RARE EARTH ELEMENTS. Report No. 36. Chao, C. C. (California Inst. of Tech., Pasadena. W. M. Keck Lab. of Engineering Materials). June 1965. Contract AT(04-3)-221. 88p. Dep. mn; CFSTI $3.00 cy, $0.75 mn.

Results are presented of a systematic study of CsCl type phases in binary alloys of rare earth elements with other metals. Thirty-nine new phases of this type were found. The linear variation of the lattice parameter of CsCl phases with the trivalent ionic radius of the rare earth metal previously established for a limited number of alloys, was extended to seventy-nine phases. This linear relationship leads to some interesting qualitative arguments on the ionic size of the non-rare earth element in these phases. The electrical resistivities of nineteen CsCl type phases of rare earths with copper, silver, and gold were measured between 4.2°K and about 250°K. With the exception of the yttrium–silver phase, all others exhibited an anomaly in the resistivity-temperature curve which is attributed to an antiferromagnetic transition. This conclusion is confirmed by previously published results of neutron diffraction experiments and magnetic susceptibility measurements. The electrical resistivity results are interpreted on the basis of an indirect interaction between two rare-earth ions. These two ions can be both magnetic or non-magnetic, or mixed. (auth)

41006 (CEND-3107-238) BURNABLE POISON ADDITIONS TO UO_2. Progress Report, January 1–March 31, 1965. Brayer, R. C.; Chernock, W. P. (Combustion Engineering, Inc., Windsor, Conn. Nuclear Div.). May 1965. Contract AT(30-1)-3107. 42p. (EURAEC-1438). Dep. mn; CFSTI $2.00 cy, $0.50 mn.

Work Performed under United States–Euratom Joint Research and Development Program.

Further analyses were performed on a UO_2-B_4C fuel element which was thermally tested under both radial and axial thermal gradients. A new sampling technique was employed which permitted the division of radial samples into smaller volumes of material than was previously used for boron analyses. With this technique, the boron losses, predicted for open systems, was observed, especially in that region of the fuel which was operating above 1350°C. No significant boron migration was detected in either the radial or axial directions in the fuel element, indicating that the boron losses were carried off in the flowing helium stream, verifying earlier results in open systems. A fabrication process for the irradiation test elements was finalized and four depleted UO_2 fuel elements were fabricated. These rods were evaluated and show the process to be satisfactory for the fabrication of fuel rods for irradiation testing in Saxton. A thorough evaluation was carried out on all materials, (304 stainless steel tubing, 6% enriched UO_2, 308L end plugs) obtained from the vendors to ensure that all Saxton specifications for quality were achieved. (auth)

41007 (EURAEC-1400) STUDY OF THE APPLICATION OF THE VERTICAL WELDING PROCESS UNDER ELECTRO-CONDUCTING SLAG ON THICK STEEL PLATES IN SHOP OR FIELD CONDITIONS. Special Report No. 6. (Chantiers de l'Atlantique Penhoet-Loire, Paris (France)). Nov. 20, 1962. Contract 054-61-12-RDF. 68p. (EUR-2359). Dep. mn; CFSTI $3.00 cy, $0.75 mn.

Work Performed under United States–Euratom Joint Research and Development Program.

The effects of heat treatments on the impact strength of thick steel plates were measured. Results showed that heat treatment should be limited to two successive temperings and that a 10 to 20° deviation from the optimum tempering temperature greatly affects the impact strength. The impact strength was relatively insensitive to the cooling rate. Transition temperature tests revealed that it would be difficult to enhance the properties of the welded joint by varying the filler metal and flux. (W.L.G.)

41008 (EURAEC-1407) STUDY OF THE BASE METAL INTENDED FOR RESEARCH ON THE BRITTLE FRACTURE OF LARGE WELDED ASSEMBLIES. Special Report No. 7, May 1, 1964–May 1, 1965. (Institut de Recherches de la Siderurgie, St. Germaine-en-Laye (France)). Contract 031-64-5 TEEF. 26p. (EUR-2366). Dep. mn; CFSTI $2.00 cy, $0.50 mn.

Work Performed under United States–Euratom Joint Research and Development Program.

Data on the general properties, brittle fracture strength, and structural transformations of specimens from the core and outer layers of Super-Elso Ni–Cr–Mo steel are presented. (W.L.G.)

41009 (GEMP-375) PROPERTIES OF SOME REFRACTORY METALS. III. THERMAL EXPANSION CHARACTERISTICS OF TUNGSTEN, RHENIUM, TANTALUM, MOLYBDENUM, NIOBIUM, W–25Re, Ta–10W, AND Mo–50Re. Conway, J. B. (General Electric Co., Cincinnati, Ohio. Nuclear Materials and Propulsion Operation). June 29, 1965. Contract AT(40-1)-2847. 33p. Dep. mn; CFSTI, $2.00 cy, $0.50 mn.

Previously published linear thermal expansion data for several refractory metals and refractory metal alloys are reviewed and compared. In addition, an optical technique is described which was employed to measure the expansion characteristics of several refractory metals and alloys to 2500°C. These most recent data are also compared to the existing data. A refraction error has been identified which is inherent in the optical measurement of thermal expansion for certain experimental conditions. Tests in helium have been shown to yield results that are noticeably lower than those obtained in vacuum. Correction factors have been obtained for use with the helium tests to obtain accurate expansion values. Linear thermal expansion data to 2500°C are reported for W, Re, Ta, Mo, Nb, W–25 Re, Ta–10 W, and Mo–50 Re. (auth)

41010 (IITRI-578P27-10) YIELD PHENOMENA AND FRACTURE OF HYDRIDED ZIRCONIUM. Quarterly Report, April 1, 1965–June 30, 1965. (IIT Research Inst., Chicago, Ill.). Aug. 6, 1965. Contract AT(11-1)-578. 33p. (EURAEC-1456). Dep. mn; CFSTI $2.00 cy, $0.50 mn.

Work Performed under United States–Euratom Joint Research and Development Program.

Results of studies of yield point phenomena in high-purity zirconium is reported. An abrupt yield point was found to exist during the tensile deformation of zirconium having grain diameters smaller than approximately 0.0065 mm. Yield point occurrence was favored by air-cooling from the recrystallization temperature as compared to water-quenching. Specimens cut transverse to the rolling direction showed greater yield drops, and the discontinuity persisted to larger grain sizes. Yield point appearance was favored at temperatures above –22°C, and disappearance of yield was noted at lower temperatures. On the basis of supplementary microstraining experiments and in consideration of other known deformation characteristics of zirconium, the occurrence of a yield point is explained by a dynamic dislocation model developed by Johnston and Hahn for bcc materials. (auth)

41011 (IS-T-15) SOLID SOLUBILITY OF MAGNESIUM IN THE CLOSE-PACKED MODIFICATIONS OF SOME RARE-EARTH METALS (thesis). Joseph, Robert Roderick (Ames Lab., Iowa State Univ. of Science and Tech.). May 1965. Contract W-7405-eng-82. 52p. Dep. mn; CFSTI $3.00 cy, $0.50 mn.

The maximum solubility of magnesium in the rare-earth metals was found to show an unusual behavior as a function of atomic number of the rare-earth metal. For the light rare-earth metals it was found to vary from 9.4 at. % for lanthanum to 8.2 at. % for neodymium and the jump up to 14.1 at. % for gadolinium. For the heavy rare-earth metals the solid solubility was found to decrease again in a regular fashion. However, when the solid solubility was compared at a homologous temperature, the solubility was found to increase in a smooth manner with decreasing size factor. It was found that the apparent atomic diameter of magnesium dissolved in the rare-earth metals was constant and could be best accounted for by combining the first and second order elasticity theories. (auth)

41012 (IS-T-16) SINGLE CRYSTAL ELASTIC CONSTANTS OF LEAD–THALLIUM ALLOYS (thesis). Shepard, Marion LaVerne (Ames Lab., Iowa State Univ. of Science and Tech.). May 1965. Contract W-7405-eng-82. 74p. Dep. mn; CFSTI $3.00 cy, $0.75 mn.

The adiabatic elastic constants of seven fcc lead–thallium alloy single crystals were measured by the ultrasonic pulse-echo method over the composition range 5 to 72 at. % thallium and over the temperature range 4.2 to 300°K. The room temperature values of the elastic constants C_{11}, $(C_{11} - C_{12})/2$, and C_{44} were combined with the room temperature values of the fcc indium–thallium elastic constants and the values for the interpolated constants for the metastable fcc allotrope of thallium are $C_{11} = 4.08 \times 10^{11}$dyn/cm^2, $C_{12} = 3.40 \times 10^{11}$dyn/cm^2, and $C_{44} = 1.11 \times 10^{11}$dyn/cm^2. These interpolated values have been converted to a trigonal representation and compared to the elastic constants of hcp thallium. The temperature variations of the Debye temperatures of the alloys were computed and the vibrational contributions to the entropies of formation of the alloys were determined from the Debye temperatures. A comparison of the vibrational entropies and the published values of the entropies of formation showed that ordering exists in the lead–thallium system. Additional analyses of the elastic constants of the alloys indicate that the ordered structure is probably $PbTl_3$. (auth)

41013 (IS-T-25) THERMODYNAMIC MEASUREMENTS ON CsCl-TYPE STRUCTURES IN RARE EARTH–MAGNESIUM SYSTEMS (thesis). Ogren, John Roger (Ames Lab., Iowa State Univ. of Science and Tech.). Feb. 1965. Contract W-7405-eng-82. 48p. Dep. mn; CFSTI, $2.00 cy, $0.50 mn.

The vapor pressure of magnesium over binary alloys of magnesium with samarium, gadolinium, terbium, holmium, erbium, thulium and lutetium was measured by the Knudsen effusion method in the temperature range 400–600°C. The vapor pressure data were used to determine the Gibbs free energy change in kcal/g-atom associated with the formation of CsCl-type compounds from the pure solid elements: $F^0(SmMg) = -0.9 \pm 0.8 - (2.3 \pm 1.0) \times 10^{-3}T$; $F^0(GdMg) = -1.7 \pm 0.4 - (0.9 \pm 0.6) \times 10^{13}T$; $F^0(TbMg) = -0.9 \pm 0.8 - (1.9 \pm 1.0) \times 10^{-3}T$; $F^0(DyMg) = -1.4 \pm 0.8 - (1.4 \pm 1.1) \times 10^{-3}T$; $F^0(HoMg) = -0.3 \pm 0.9 - (2.3 \pm 1.2) \times 10^{-3}T$; $F^0(ErMg) = -1.6 \pm 0.7 - (0.3 \pm 0.9) \times 10^{-3}T$; $F^0(TmMg) = -2.1 \pm 1.0 + (0.1 \pm 1.0) \times 10^{-3}T$; $F^0(LuMg) = -0.3 \pm 0.5 - (1.0 \pm 0.6) \times 10^{-3}T$. Because heat capacity data were not available, the ΔC_p values for the associated reactions were taken to be zero. A Raoult's law approximation was used to describe the activity of the lanthanons in the terminal solid solutions. The free energies of formation evaluated at the midpoint of the temperature range exhibit a trend showing decreasing magnitude with increasing atomic number. The magnitudes of the enthalpies of formation are consistent with the view that bonding in the CsCl-type structures is of a metallic nature. (auth)

41014 (LA-DC-6819) PHASE RELATIONSHIPS OF THE HIGH CARBON PORTION OF THE LANTHANIDE DICARBIDES. Krikorian, N. H.; Wallace, T. C.; Bowman, M. G. (Los Alamos Scientific Lab., Univ. of California, N. Mex.). [1964]. Contract W-7405-eng-36. 17p. (CONF-650913-1). Dep. mn; CFSTI, $1.00 cy, $0.50 mn.

From International Colloquium on Semi-Metallic Derivatives, Paris.

A study of the rare earth dicarbides as well as YC_2 and LaC_2 to determine the MC_2-C eutectic temperatures, and the tetragonal to cubic transformation temperatures by thermal analysis techniques is reported. Microhardness measurements of the dicarbides are also reported. Lattice parameters of the tetragonal dicarbides were measured as well as the parameters of the high temperature cubic form of some of the dicarbides. (auth)

41015 (MIL-TDR-64-282) APPLICATION OF THIN-FILM ELECTRON MICROSCOPY TO REFRACTORY METAL PROCESSING. Final Report. Jewett, R. P. (Rocketdyne, Canoga Park, Calif.). May 11, 1965. Contract No. 64-0299-d. 90p. (R-6142).

A comprehensive study was conducted to establish the progressive changes in dislocation morphology that occur during tensile elongation and during cold rolling of refractory metals. Commercially pure tantalum and molybdenum and one commercial alloy of each, tantalum–10% tungsten and TZM, were studied. It was established that three distinct stages exist that can describe the deformation process for each of these materials. The first stage is a random array of dislocations; the dislocation distribution during this stage may be homogeneous or heterogeneous. The second stage is one of dislocation cluster, or tangle, formation. The clusters in this stage are isolated and are not continuous. The third stage is one of cell formation. In this stage the clusters have developed into continuous networks, have high dislocation densities, and surround areas of a low dislocation density. The effect of alloying was to delay the onset of the cluster and cell formation stages. The effect of increasing strain rate in molybdenum was to delay the onset of cell formation, while in TZM the effect of increasing the strain rate was to accelerate cell formation. The arrays, clusters, and cells that form during deformation appear to be fundamental structures that will give a theoretical basis to the understanding of the properties of cold-worked metals and a guideline to their fabrication. (auth)

41016 (N64-30997) BEND TRANSITION TEMPERATURE OF ARC-CAST MOLYBDENUM AND MOLYBDENUM–0.5-PERCENT-TITANIUM SHEET IN WORKED, RECRYSTALLIZED, AND WELDED CONDITIONS. Sinclair, John H. (National Aeronautics and Space Administration, Cleveland, Ohio. Lewis Research Center). Oct. 1964. 18p. (NASA-TN-D-1869). CFSTI $0.50 cy, $0.50 mn.

Effects of recrystallization and welding on ductile-to-brittle transition temperatures of arc-cast, carbon-deoxidized molybdenum and molybdenum–0.5-percent-titanium alloy sheets were determined by guided bend tests (90° bend over a 4 T radius punch descending at a rate of ½ in./min). Both materials annealed at low temperatures (2000 to 2400°F) to yield structures having approximately 3500 grains/sq mm and ductile-to-brittle transition temperatures below ambient (0 to 40°F) but 35 to 130°F higher than in the as-worked condition. Welded specimens showed transition temperatures ranging from 140 to 350°F. Annealing at 3500°F gave grain sizes equivalent to those of fusion zones of welds and transition temperatures of 350°F and higher. (auth)

41017 (NAA-SR-10482) RAPID PULSE HEATING OF MODIFIED ZIRCONIUM–URANIUM HYDRIDES TO DESTRUCTION. Final Report. Finch, R. A. (Atomics International, Canoga Park, Calif.). July 25, 1965. Contract AT-11-1-GEN-8. 55p. Dep. mn; CFSTI $3.00 cy, $0.50 mn.

Twenty-one samples of modified zirconium–10 wt% uranium hydride were pulse heated to destruction. The experiments were conducted to study the behavioral characteristics of the fuel used in SNAP reactors when the reactors are subjected to severe temperature transients. Data on power input, electrical resistivity, temperature, hydrogen evolution, and thermal expansion during

pulses are presented. The duration of these pulses ranged from 28 to 450 msec. H/Zr ratios of the samples varied from 0.50 to 1.81. All of the samples heated uniformly. Initial heating rates were varied from 7000 to more than 100,000°C/sec. Phase changes were observed to take place in all of the samples. Theoretical predictions of sample failure mechanisms were verified. The gas temperatures after evolution from the samples were determined. (auth)

41018 (NAA-SR-10768) NONEQUILIBRIUM URANIUM CARBIDE PHASE RELATIONSHIPS. Ritchie, E. E. (Atomics International, Canoga Park, Calif.). Sept. 1, 1965. Contract AT(11-1)-Gen-8. 27p. Dep. mn; CFSTI $2.00 cy, $0.50 mn.

Because the solubility of uranium in uranium monocarbide, and the variation of this solubility with temperature, may have an influence on the high-temperature irradiation behavior of hypostoichiometric uranium carbide, a study of the uranium–carbon phase relationships was performed. As part of the study, effects of rapid cooling from high temperatures were investigated. Fuel specimens, in the composition range of 4.0 to 4.8 wt % C, were heat treated at 1300, 1600, and 1800°C, followed by rapid (75°C/sec), medium (20°C/sec), and slow (0.4°C/sec) cooling rates. Selected specimens were subsequently vacuum annealed at 650 and 1000°C for periods up to 500 hr. Microstructural observations indicated that the metastable distribution of phases is dependent on heat treatment, and that microstructural changes can occur at expected service temperatures. A two-phase grain boundary structure, observed in both as-cast and heat-treated fuel samples, was tentatively identified as α uranium containing small grains of $UC_{(1-x)}$. (auth)

41019 (NAA-SR-11323) STUDY OF INSTANTANEOUS COLLAPSE AND CREEP BUCKLING CHARACTERISTICS OF LARGE SGR PROCESS TUBES. Lemcoe, M. (Atomics International, Canoga Park, Calif.). July 25, 1965. Contract AT-11-1-GEN-8. 47p. Dep. mn; CFSTI $3.00 cy, $0.50 mn.

The instantaneous collapse (<0.2 hr) and creep buckling characteristics (up to 5000 hr) of Type 304 stainless steel tubes, under external radial pressure and varying axial load, were determined at temperatures up to 1200°F in an argon environment. The length of each tube was essentially infinite from a buckling standpoint. In addition, tubes in combination with fuel element bundles corresponding to those proposed for a Large Sodium Graphite Reactor were also investigated to determine the extent to which the fuel element bundle increased the resistance to collapse of the process tube. Ways of increasing the tube resistance to collapse, using stiffener rings, and existing creep buckling theories were also examined. The results of the study indicated: (1) stiffener rings or thicker walled tubes should not be necessary under normal reactor operating conditions; (2) stiffener rings or thicker walled tubes should not be necessary to provide for a possible malfunction (overpressure) in the calandria vessel pressurization system, if the pressure does not exceed 8 psi over the 1000-hr period of overpressure; (3) axial loads ranging from approximately 200 lb tension to 200 lb compression were found to have very little effect on instantaneous collapse pressure; (4) from the data obtained, accurate prediction of the instantaneous collapse pressures should be possible for temperatures and wall thicknesses other than those at which the tests were conducted; (5) considerable scatter in test results might occur in the determination of the time to collapse, during creep buckling tests, because of variations in the magnitude and distribution of the out-of-roundness and thickness parameters along the length of the tube; (6) resistance to collapse of a tube may be enhanced by a factor of 2½ by installing compact "slip-on" stiffener rings; and (7) analytical predictions for time to collapse are not reliable and may be inaccurate by one or more orders of magnitude. (auth)

41020 (NAA-SR-Memo-2987) THE THERMAL EXPANSION OF Al_2O_3. Rachal, Lawrence H. (Atomics International, Canoga Park, Calif.). Aug. 7, 1958. Contract AT(11-1)-Gen-β. 8p. Dep. mn; CFSTI, $1.00 cy, $0.50 mn.

The thermal expansion of two single Al_2O_3 crystals with known C axis orientations was measured at temperatures between 24 and 1100°C. Coefficients of thermal expansion parallel and normal to the C axis were calculated. (D.L.C.)

41021 (NMI-8002.1) STUDY OF DISPERSION-STRENGTHENED ALLOYS PRODUCED BY SLIS TECHNIQUES. Quarterly Letter Report, March–June 1965. Russell, R. B.; Muller, W. C. (Nuclear Metals, West Concord, Mass.). July 9, 1965. Contract NOw-65-0386-f. 18p.

A research program is being conducted to correlate the thermal stability of nickel-compound particles dispersed in a Ni matrix with the maximum solid solubility of the compound in the matrix and with the thermal stability of the compound itself. In the solid solubility study, dilute alloys of La, Gd, and Er in Ni were prepared by melting and examined. Preliminary metallographic studies and resistance ratio measurements are reported. In the compound stability study, splatcooled Ni–UNi_5 was produced, and preliminary work for the production of splatcooled Ni–$MgNi_2$ and Ni–Y_2Ni_{17} was carried out. (D.L.C.)

41022 (NP-15292) DEVELOPMENT OF IMPROVED STRENGTH AND OXIDATION RESISTANCE OF CHROMIUM COMPOSITES. Final Report, March 17, 1964–March 16, 1965. Farrington, Wayne A.; Watkins, Robert V. (Bendix Products Aerospace Div., Bendix Corp., South Bend, Ind.). Apr. 1965. Contract NOw 64-0321-c. 122p.

Efforts directed toward improvement of the atmospheric contamination resistance and high temperature strength of a ductile chromium composite material are described. Numerous results of high temperature continuous weight gain determinations and strength tests are presented. Improvements in the high temperature weight gain resistance, oxide scale adherence, and resistance to nitridation were attained through compositional variations. Minor additions of calcia or silica or a larger addition of magnesio-aluminate spinel to a basic chromium–3 weight percent magnesia composition were shown to improve resistance to contamination without large ductility penalties. Other additions including alumina were also beneficial to oxidation resistance but produced detrimental effects on low temperature ductility. A manganese alloy was produced which during a 100 hour exposure in air at 2200°F displayed a weight gain of approximately 9 mg/cm², did not suffer scale detachment during cooling, and did not display a nitride surface layer. Substantial increases in high temperature strength were associated with alloying additions including tantalum, niobium, and molybdenum, but these elements caused a loss of ductility at room temperature. The use of manganese as an alloying element produced a material with superior low temperature ductility and slightly higher elevated temperature strength. (auth)

41023 (NP-15334) IMPROVEMENT OF URANIUM–MOLYBDENUM ALLOYS FOR GYROSCOPE WHEEL RIMS BY AGING HEAT TREATMENTS. Schiesser, Robert J. (Massachusetts Inst. of Tech., Cambridge, Mass. Instrumentation Lab.). July 1964. Contract AF33(657)-7668. 64p. (R–460).

Gyro sensitivity can be improved by increasing the angular momentum of the wheel. Angular momentum can be increased by the use of a compound wheel composed of a Be hub and a U–8% Mo alloy rim. An aging heat treatment method was developed that provides a U–Mo alloy with physical properties desired in a gyro wheel rim material. A wheel design using a U–Mo rim for operation at 36,000 rpm was defined. (auth)

41024 (NUMEC-2389-5) MORPHOLOGICAL CHARACTERISTICS OF COPRECIPITATED (U,Pu)O_2 POWDERS BY ELECTRON MICROSCOPY. Roth, J.; Halteman, E. K. (Nuclear Materials and Equipment Corp., Apollo, Pa.). [1962]. Contract AT(30-1)-2389. 41p. Dep. mn; CFSTI $2.00 cy, $0.50 mn.

Electron microscopy was developed as a tool for study-

ing the characteristics of plutonium-bearing fuel materials. The development of replication techniques necessary to prevent contamination of the electron microscope are discussed herein as are the conclusions that may be drawn from examination of the electron micrographs. While multiple step replication techniques were investigated, a single-step technique was found to be most satisfactory because of the relative ease of preparation, the minimization of artifacts, and the general excellence of resolutions. Examination of $(U,Pu)O_2$ materials over the entire composition range and the precursors from ammonium diuranate–plutonium hydroxide coprecipitation from uranyl nitrate–plutonium nitrate solutions generally shows that the morphological characteristics of the powders are determined by the initial precipitation chemistry and thereafter are transferred from step to step throughout the oxide production process. (auth)

41025 (ORNL-TM-1144) PROPERTIES OF THORIUM, ITS ALLOYS, AND ITS COMPOUNDS. Peterson, Sigfred; Adams, R. E.; Douglas, D. A. Jr. (Oak Ridge National Lab., Tenn.). [1965]. Contract W-7405-eng-26. 29p. Dep. mn; CFSTI, $2.00 cy, $0.50 mn.

Physical and mechanical data pertinent to nuclear application were reviewed for thorium, its alloys, and its ceramic compounds. Thorium-base fuels are superior to uranium at elevated temperatures. Although thorium oxide is well characterized, the effect of incorporated uranium oxide on its properties is very poorly known. Data are incomplete on thorium carbides, but these compounds are being actively investigated along with their uranium substitution products. (auth)

41026 (UCRL-16024) ANALYSIS OF DISLOCATION LOOPS IN QUENCHED FCC METALS (thesis). Bell, Walter Lee (Lawrence Radiation Lab., Univ. of California, Berkeley). June 1965. Contract W-7405-eng-48. 75p. Dep. mn; CFSTI, $3.00 cy, $0.75 mn.

In electron micrographs of quenched fcc metals of intermediate or high stacking fault energies, large perfect prismatic loops often appear as double-arc images. Double-arc contrast is explained in terms of dipole relaxation of the dislocation strain fields at the intersections of the mixed screw and edge components of the loop, thereby reducing the diffraction contrast of the images near these regions. Strain contrast images of loops too small to be observed by diffraction contrast are used to evaluate the applicability of the Ashby-Brown strain contrast theory to planar vacancy aggregates. The double-arc loop model can be used to identify the Burger's vector of a large perfect prismatic loop on {111} by comparing its diffraction contrast image, or its strain contrast image, to the projections of ⟨110⟩ directions onto the plane of the foil. In most cases the double-arc image is characterized by being skewed in a projected ⟨112⟩ direction, and the habit plane can be uniquely identified by this skewness. The model is also valid for interstitial loops or loops in metals with crystal structures other than fcc. The Ashby-Brown theory is found to be reasonably valid for high-order dark-field images of small edge-on defects in thick foils. Differences and contradictions arise when the theory is applied to bright-field images, low-order reflections, thin foils, or defects which are large and not edge-on. In quenched copper it is found that Frank loops are stable below about 125 Å and perfect loops are the stable defect above this size. (auth)

41027 (WERL-0029-2) THE ULTRASONIC TESTING CHARACTERISTICS OF FORGED INCONEL. Clark, W. G. Jr. (Westinghouse Research Labs., Pittsburgh, Pa.). Feb. 1965. 56p.

For Bettis Atomic Power Lab., Pittsburgh, Pa.

The basic ultrasonic testing characteristics of forged Inconel were explored in order to optimize the ultrasonic test procedures currently being used on Inconel forgings for the determination of structural homogeneity and detection of flaws. Inconel test blocks of various grain structures containing a series of artificial flaws were examined ultrasonically at frequencies of 2.25 and 1 Mc. Distance-amplitude data as well as flaw size-response relationships were determined using both contact and immersion testing techniques. (auth)

41028 (BNWL-tr-4) EFFECT OF THERMAL CYCLING ON THE α-β TRANSFORMATION TEMPERATURE OF PLUTONIUM. Spriet, B. Translated by E. R. Appleby (Battelle-Northwest, Richland, Wash. Pacific Northwest Lab.), from J. Nucl. Mater., 13: 13-22(1964). 22p. Dep. mn; JCL, $2.60 fs, $0.86 mf.

The hysteresis of the alpha-beta transformation temperature during heating and cooling is attributed to internal stresses. Thermal cycling introduces stress of opposite sign, thus modifying the transformation kinetics. The stresses arise from two sources: one due to the large volume change; and the other due to a cold-hardening of the alpha matrix during the beta-to-alpha transformation. (W.L.G.)

41029 THERMAL CONDUCTIVITY OF HIGH CONDUCTIVITY MATERIALS. I. MEASUREMENT. Day, Ralph K. Am. Ceram. Soc. Bull., 44: 608-11(Aug. 7, 1965).

The cut bar in vacuum ATSM C-408-58 method was investigated and evaluated to measure the thermal conductivity of high conductivity materials such as BeO ceramics. Preliminary measurements indicated serious errors in results caused by inefficient bar-to-sample joints and resulting tilted equi-temperature planes. Apparatus changes were made which add measurement of thermal transfer efficiency at joints. Results of critical tests are reported. (auth)

41030 APPLICATION OF THE ZONE FUSION METHOD TO THE PURIFICATION OF ZIRCONIUM AND STUDY OF SOME PROPERTIES OF THIS METAL. Langeron, Jean-Paul (Centre National de la Recherche Scientifique, Vitry-sur-Seine, France). Ann. Chim. (Paris)(13), 9: 547-78 (Nov.-Dec. 1964). (In French).

The metallography of Zr was studied on metals of various origin and very different purities. The allotropic transformation, instability of structures obtained by transformation, preparation of large crystals, dilatometric study, and determination of the orientation of the precipitates of Zr hydride were investigated. These studies showed the marked effects of impurities. The purification of Zr by the vertical fusion zone technique was investigated. Under vacuum it was possible to superpose on the segregation of the impurities, a significant purification by preferential distillation of the more volatile impurities. For the elimination of O, N, and C it was necessary to operate under a static ultravacuum. The specific role of impurities on certain properties was determined in some respects. O and N cause an increase of the electrical resistivity at low temperature. The metallic impurities affect the recrystalization temperature of Zr. (J.S.R.)

41031 THE SYSTEMS TIN(IV)–OXYGEN–POTASSIUM AND ZIRCONIUM–OXYGEN–POTASSIUM. Tournoux, Michel (Faculte des Sciences, Bordeaux). Ann. Chim. (Paris)(13), 9: 579-600(Nov.-Dec. 1964). (In French).

The systems Sn(IV)–O–K and Zr–O–K were studied. The methods of preparation were perfected and the regions of existence of some potassium stannates and zirconates were determined. The use of potassium nitrate as an etching agent was very effective and made possible the elaboration of strongly basic compounds. Stannates with the composition K_4SnO_4, K_2SnO_3, $K_2Sn_2O_7$ and two hydrates of the metastannate $K_2SnO_3 \cdot H_2O$ and $3K_2SnO_3 \cdot 2H_2O$ were isolated. A tetrastannate $K_2Sn_4O_9$ was obtained by action of calcium dioxide on the orthostannate or the metastannate. The zirconates K_2ZrO_3, $K_2Zr_2O_5$, and $K_2Zr_3O_7$ were isolated. The thermal stability of all these compounds was determined. The existence of the dizirconate $K_2Zr_2O_5$ with two allotropic varieties was shown. It has a transformation point near 850°C and the transformation speed is very low. The symmetry elements were determined for the majority of the phases obtained. A monocrystal study was made for the orthostannate, metastannate, tristannate, and the β variety of the dizirconate.

The metastannate K_2SnO_3 has a structure of a new type. The Sn has a coordination number of 6. The O layers alternate with layers of K and Sn. The metazirconate is an isotope of the metastannate. The preparation of an ortho-type phase for K_4SnO_4 in the case of Sn is explained by the fact that SnO_2 is more acid than ZrO_2. Among the phases of the same formulation obtained in the two systems, only the meta compounds particularly rich in K have isostructures. (tr-auth)

41032 THE CRYSTAL DYNAMICS OF URANIUM DIOXIDE. Dolling, G.; Cowley, R. A.; Woods, A. D. B. (Atomic Energy of Canada Ltd., Chalk River, Ont.). Can. J. Phys., 43: 1397-1413(Aug. 1965). (AECL-2311).

The frequency/wave-vector dispersion relation for normal modes of vibration propagating along the [00ζ], [ζζ0], and [ζζζ] directions in uranium dioxide at 296°K was determined by studying the coherent one-phonon scattering of slow neutrons from a single-crystal specimen. Analysis of the results showed that a simple rigid-ion model of the crystal with axially symmetric forces between near-neighbor ions can provide qualitative agreement with experiment. A more complicated model, in which the ionic polarizabilities are taken into account, is needed to obtain quantitative agreement with the dispersion curves and with the known dielectric properties. Such a model provides an interpolation formula for computing the frequency distribution function and other related quantities, such as the Debye-Waller factors and lattice specific heat. Information concerning the anisotropy of the Debye-Waller factor for the oxygen ions and the configuration of the magnetic electrons in UO_2 was derived by comparing these calculations with the appropriate experimental data. The optic-mode frequencies and dielectric constants of UO_2 are shown to satisfy the Lyddane, Sachs, and Teller relation. The slopes of the acoustic-mode branches at small wave vectors are consistent with independently measured elastic constants. (auth)

41033 THE TRANSFORMATION IN ZIRCONIUM–NIOBIUM ALLOYS. McMullen, A. G.; Parr, J. Gordon (Univ. of Windsor [Can.]. Can. Met. Quart., 4: 117-28(Apr.-June 1965).

Transformation temperatures at cooling rates to 5,500°C/s were determined for zirconium alloys with 1.0, 2.5, 3.0, and 5.0 weight per cent niobium, and for pure zirconium at cooling rates to 35,000°C/s. On the basis of the surface-rumpling criterion, the transformation (at rates greater than critical) is martensitic in the alloys, and non-martensitic in pure zirconium. The suggestion is made that in pure zirconium the rumpling phenomenon is not an adequate criterion of martensite transformation. (auth)

41034 STRUCTURE AND RECRYSTALLIZATION OF COLD ROLLED AND ANNEALED ZIRCALOY-2. Bassi, A.; Camona, G.; Paganini, L. (Laboratori CISE, Milan; Universita, Pisa, Italy). Energia Nucl., 12: 471-83(Sept. 1965).

Samples of Zircaloy-2 were rolled at 70% and subsequently annealed at 550, 600, 650, and 750°C during times varying between 5 min and 2 hours. Results enabled determination of the temperature and time at which the recrystallization process begins in annealing. The recrystallization, mechanism and its effects on the technological use of the material were studied. (auth)

41035 INVESTIGATION OF THE TERNARY W–Mo–Zr PHASE DIAGRAM. Zakharov, A. M.; Savitskii, E. M. Izv. Akad. Nauk SSSR, Metal., No. 1, 151-9(1965).

A series of the W–Mo–Zr alloys were melted from 99.95%-pure W, 99.95%-pure Mo, and 99.7%-pure iodide Zr in an arc furnace with a nonconsumable W electrode, in a helium atmosphere, at a pressure of 200 mm Hg. The investigated binary W–Zr alloys contained from 3.36 to 18.40 wt % Zr, binary Mo–W alloys contained from 18.62 to 80.78 wt % Mo, and binary Mo–Zr alloys contained from 2.52 to 31.1 wt % Zr; the ternary W–Mo–Zr alloy contained W and Zr in the 4:1, 1:1, and 1:4 ratios. The results showed that the mutual solubility of W, Mo, and Zr in the solid state decreased with decreasing temperature. The alloys tested had a single- or two-phase structure. The single-phase alloys were ternary α- or β-solid solutions of Zr in W and Mo, or W and Mo in Zr, respectively. The two-phase alloys, in addition to the α- or β-solid solutions, contained solid solutions of the W_2Zr and Mo_2Zr compounds. The ternary peritectic and eutectic transformations, which occur in the ternary alloys at 2260 to 1890 and 1640 to 1570°C, respectively, can be described as $L + \alpha \rightarrow (W,Mo)_2Zr$ and $L \rightarrow \beta + (W,Mo)_2Zr$. (CFSTI)

41036 CONSTITUTION DIAGRAMS OF THE TERNARY SYSTEMS V–Ta–Nb AND V–Ta–Mo. Nefedov, A. P.; Sokolovskaya, E. M.; Grigor'ev, A. T.; Sokolova, I. G. (Moscow State Univ.). Izv. Akad. Nauk SSSR, Neorgan. Materialy, 1: 715-20(May 1965). (In Russian).

Alloys (in the cast, homogenized, annealed, and hardened state) of two ternary systems of V–Ta–Nb and V–Ta–Mo were investigated using physical-chemical analysis. Constitution diagrams of the two systems were constructed; the distribution of the phase range was established at various temperatures in these ternary systems. (tr-auth)

41037 STUDIES OF Nd_2O_3–ZrO_2. INVESTIGATIONS OF REGIONS RICH WITH ZIRCONIUM DIOXIDE. Davtyan, I. A.; Glushkova, V. B.; Kiler, E. K. (Grebenshchikov Inst. of Chemistry of Silicates, Academy of Sciences, USSR). Izv. Akad. Nauk SSSR, Neorgan. Materialy, 1: 743-50(May 1965). (In Russian).

The effect of the addition of neodymium oxide at the temperature of the monoclinic-tetragonal transformation of zirconium dioxide was investigated. It was found that the addition of Nd_2O_3 leads to the formation of solid solutions of neodymium oxide in zirconium dioxide and decreases the temperature of the polymorphous transformation. The parameters of the elementary cell of zirconium dioxide and of the solid solutions were calculated at various temperatures. The stability of the heavy solution was studied on the basis of the zirconium oxide. It was found that the cubic solid solution produced at high temperatures decomposes, during slow cooling or by annealing at very low temperatures, to a mixture of two solid solutions of the tetragonal (or monoclinic) and cubic pyrochlore types. The boundaries of the biphase region were determined. (tr-auth)

41038 SUBSOLIDUS STRUCTURE OF Li_2O–ZrO_2–SiO_2 AND ITS PROPERTIES. Polezhaev, Yu. M.; Chukhlantsev, V. G. (Kirov Ural Polytechnic Inst., USSR). Izv. Akad. Nauk SSSR, Neorgan. Materialy, 1: 784-7(May 1965). (In Russian).

The interaction in the solid phase between compounds of the system $Li_2O - ZrO_2 - SiO_2$ was investigated by chemical and x-ray analyses. The following lines of compatability were established: $Li_2Si_2O_5 - ZrSiO_4$; $Li_2Si_2O_5 - ZrO_2$; $Li_2SiO_3 - ZrO_2$; $Li_2SiO_3 - ZrO_2$; $Li_2SiO_3 - LiZrO_3$; and $Li_4SiO_4 - Li_2ZrO_3$. Ternary compounds were not discovered in the system. On the basis of the data obtained, triangulations of the system $Li_2O - ZrO_2 - SiO_2$ were made. It was established that Li_2O appears with the mineralization reaction for the formation of zirconium from ZrO_2 and SiO_2. (tr-auth)

41039 REPORT, SECOND ALL-UNION SYMPOSIUM ON PHYSICS OF THIN FERROMAGNETIC FILMS, IRKUTSK, USSR, JULY 10-15, 1964. Izv. Akad. Nauk SSSR, Ser. Fiz., 29: 538-712(Apr. 1965) (In Russian). (CONF-640709)

Papers (41) are included on the preparation, properties, and structure of thin ferromagnetic films. The effects of stresses are also considered, as well as experimental techniques. (D.C.W.)

41040 ATOMIC SIZE OF RARE EARTHS IN INTERMETALLIC COMPOUNDS. MX COMPOUNDS OF CsCl TYPE. Iandelli, A.; Palenzona, A. (Universita, Genoa). J. Less-Common Metals, 9: 1-6(1965).

The crystal structure of the intermetallic compounds of the rare earths with Cu, Mg, Zn, Cd, Hg, Tl, with MX formula, was studied. In the majority of cases this structure was of the CsCl type. Exceptional behavior was found for Eu and Yb compounds; this was connected with their valency of 2. The other compounds showed a regular change of the lattice constants with the ionic radii. (auth)

41041 RARE EARTH INTERMEDIATE PHASES. I. PHASES FORMED WITH TIN AND INDIUM. Harris, I. R.; Raynor, G. V. (Univ. of Birmingham, Eng.). J. Less-Common Metals, 9: 7-19(1965).

Room temperature lattice spacings were measured for twenty-one intermediate phases of the type $R.E.Sn_3$ and $R.E.In_3$, where R.E. = rare earth. Results indicated that in $CeSn_3$, the cerium atoms are in a valency state similar to that in γ-cerium (effective valency approximately 3.1). In $CeIn_3$, however, the cerium atoms are expanded, suggesting that in this case the effective valency is closer to 3. Thermal expansion curves from −186°C to room temperature were determined for $LaSn_3$, $CeSn_3$, $PrSn_3$, $CeIn_3$, and $PrIn_3$, and from room temperature to 500°C for $CeSn_3$, $CeIn_3$, $PrIn_3$, $GdIn_3$, and YIn_3. $CeSn_3$ was abnormal in that the coefficient of thermal expansion up to 140°C exceeded the typical value ($LaSn_3$, $PrSn_3$), and the effects were consistent with variable occupancy of the 4f levels of the cerium atom, such that conduction band → 4f transitions were encouraged by increases in temperature. Minor abnormalities occurred in the expansion curve of $CeIn_3$. (auth)

41042 THE STRAIN-AGEING AND QUENCH-AGEING OF TANTALUM. Formby, C. L.; Owen, W. S. (Univ. of Liverpool). J. Less-Common Metals, 9: 25-34(1965).

The quench-aging and strain-aging of tantalum containing oxygen, nitrogen, and carbon as the major impurities were studied and compared over a range of aging temperatures from 100 to 200°C. Measurement of the Petch parameters σ_i and k_y at room temperature as a function of aging time was used to follow the progress of aging. It is shown that the change in discontinuous yield with aging is dependent on the migration of oxygen, but not on the other impurities. No precipitation occurred during strain-aging, nor was the rate of strain-aging effected by extreme changes in the cooling rate from the annealing temperature prior to straining. The rate of quench-aging was slower than that of strain-aging at the same temperature but the maximum value of k_y developed by quench-aging was larger than that produced by strain-aging. (auth)

41043 LOSS OF UO_2 FROM MOLYBDENUM−UO_2 CERMETS BY HIGH-TEMPERATURE DIFFUSION. Wagner, Paul (Los Alamos Scientific Lab., N. Mex.). J. Less-Common Metals, 9: 40-7(1965). (LA-DC-6799).

The loss of UO_2 from Mo−UO_2 cermet on heating was investigated. Loss was measured as a function of temperature, time, and sample thickness. Despite the inhomogeneous nature of the solid, the results were treated by application of diffusion theory. The diffusion coefficient was found to vary with temperature as $D = 2.40 \times 10^{-9} \exp(-77500/RT)$. The technique for treating inhomogeneous systems is discussed. It was concluded that the escape of UO_2 occurs along the grain boundaries of the Mo. (auth)

41044 HEATS OF MIXING IN PRASEODYMIUM−NEODYMIUM SOLID SOLUTIONS. Lundin, C. E.; Pool, M. J. (Univ. of Denver). J. Less-Common Metals, 9: 48-53(1965).

The heats of solution in liquid tin of pure praseodymium, pure neodymium, and nine praseodymium−neodymium binary alloys were measured using liquid metal solution calorimetry. A plot of the measured heat effect for the alloys as a function of composition was linear with the terminal points the measured values for the pure components. This linear dependency indicated that the heat of mixing in the binary praseodymium−neodymium system is zero within experimental error, and therefore the binary alloys obey one of the criteria for an ideal solution. (auth)

41045 LATTICE PARAMETERS OF TANTALUM−OSMIUM ALLOYS. Rudman, P. S. (Battelle Memorial Inst., Columbus, Ohio). J. Less-Common Metals, 9: 77-9 (1965).

Crystal structures and lattice parameters of Ta−Os alloys were determined from x-ray diffraction films. (M.C.G.)

41046 DEFORMATION AND FRACTURE OF TUNGSTEN SINGLE CRYSTALS. Beardmore, P.; Hull, D. (Univ. of Liverpool). J. Less-Common Metals, 9: 168-80(1965).

The deformation behavior and fracture modes of tungsten single crystals were studied as a function of orientation. The orientation of the crystals was varied systematically around the edge of the unit stereographic triangle, and tensile tests were carried out at 77 and 295°K. The stress-strain curves showed considerable variation with orientation and only crystals of orientation close to [110] showed discontinuous yield behavior. Deformation occurred purely by slip but the proportional limit did not obey a critical resolved shear stress criterion. The tensile behavior was rationalized in terms of the number of operative slip vectors. Specimens of orientation [100] were tested over a temperature range from 20 to 465°K. The proportional limit increased rapidly at temperatures below 250°K. The specimens always necked before fracture, even at 20°K, indicating that tungsten single crystals are not inherently brittle. (auth)

41047 DETERMINATION OF THE STRUCTURE OF TANTALUM SUBOXIDES $TaO_2(TaO_2)$ WITH ELECTRON DIFFRACTION. Steeb, S.; Renner, J. (Max-Planck-Institut fuer Metallforschung, Stuttgart). J. Less-Common Metals, 9: 181-9(1965). (In German).

Thin monocrystalline films of tantalum, which were obtained by electropolishing, displayed superstructure diffraction diagrams when they were heated up to 300 to 450°C in an electron diffraction camera and then exposed to oxygen at 5×10^{-4} Torr pressure. These diagrams corresponded to the phase TaO_z. Interpretation of the diagrams showed that the phase TaO_z belongs to the cubic system (a = 6.68 Å) and revealed the composition Ta_2O. Every four oxygen atoms surround tetrahedrally a tantalum atom, the distance between oxygen and tantalum being $(a/8)\sqrt{3}$, between the midpoints of two tetraheders $(a/2)\sqrt{3}$, respectively. The structure of Ta_2O was similar to that of the C3-(Cu_2O)-type. (auth)

41048 THE CONSTITUTION DIAGRAM OF THE TUNGSTEN−MOLYBDENUM−OSMIUM SYSTEM. Taylor, A.; Doyle, N. J. (Westinghouse Electric Corp., Pittsburgh). J. Less-Common Metals, 9: 190-205(1965).

Using a combination of thermal, micrographic and x-ray diffraction techniques, tentative constitution diagrams of the ternary system W−Mo−Os were drawn for the temperatures of 1600, 2000, and 2375°C. No ternary intermediate phases of a structure different from those of the constituent binary systems were found. Above 2210°C, the system contained three single phase fields. A body-centered cubic primary solid solution extended along one edge of the ternary composition triangle from 100 at.% Mo to 100 at.% W and could take up to 16 at.% Os into solid solution along the Mo−Os edge and 10 at.% Os into solid solution along the W−Os edge at 2210°C. A wide tetragonal σ-phase formed peritectically at 2430°C and 37 at.% Os in the Mo−Os binary system and stretched across the composition triangle to the W−Os edge, where the phase formed peritectically at 2945°C and 22 at.% Os. A hexagonal close-packed terminal solid solution based on θ-Os was observed with the phase field roughly triangular in shape. The solid-solubility limit stretched from about 52 at.% Os on the Mo−Os edge to about 54 at.% Os on the W−Os edge at 2210°C. At 2210°C, a β-phase having the cubic β-W structure formed in the binary Mo−Os system at the composition Mo_3Os. This increased in size with added tungsten and falling temperature, stretching into the ternary system as a long, narrow phase field as far as 23.0 at.% W−54.5 at.% Mo−22.5 at.% Os at 1600°C. (auth)

41049 BINARY OXIDE SYSTEMS OF NIOBIUM PENTOXIDE WITH OXIDES OF COMMON NIOBIUM ALLOYING ELEMENTS. Felten, Edward J. (Pratt and Whitney Aircraft, North Haven, Conn.). J. Less-Common Metals, 9: 206-13(1965).

Work on binary oxide systems of Nb_2O_5 with Al_2O_3, Cr_2O_3, TiO_2, V_2O_5, Ta_2O_5, WO_3, and MoO_3 is reviewed. Some of the systems were characterized fairly completely. The mixed oxide phases in these systems can be identified with a good

degree of confidence. The binary systems containing WO_3 and MoO_3 present a different situation. (auth)

41050 SOLID SOLUBILITY LIMITS OF Y AND Sc IN THE ELEMENTS W, Ta, Mo, Nb, AND Cr. Taylor, A.; Hickam, W. M.; Doyle, N. J. (Westinghouse Electric Corp., Pittsburgh). J. Less-Common Metals, 9: 214-32 (1965).

Alloys and diffusion couples of yttrium and scandium with Nb, Ta, Cr, Mo, and W were examined by means of the optical microscopy, x-ray diffraction, and mass spectrometry. The results indicated that the solid solubility of Y and Sc in these elements is less than 1 ppm. This was in conformity with the Hume-Rothery Rule that only a very restricted range of solid solutions can be expected when the atomic diameter of solvent and solute differ by more than 14 to 15%. (auth)

41051 STRUCTURE OF NIOBIUM NITRIDES. Terao, Nobuzo (Union Carbide European Research Associates, Brussels). Japan. J. Appl. Phys., 4: 353-67(May 1965). (In French).

Crystal structure studies of niobium nitrides by electron and X-ray diffraction technique led to the identification of four phases: NbN (cubic, δ-phase), Nb_2N (hexagonal, β-phase), NbN (hexagonal, ϵ-phase) and Nb_4N_3 (tetragonal, γ-phase). Various methods were used to prepare thin films of Nb nitrides for electron diffraction studies. Firstly, three kinds of oxynitrides, Nb(N,O)I, Nb(N,O)II, and Nb(N,O)III were obtained by nitriding the evaporated thin films of Nb in an atmosphere of ammonia. NbN (cub) was formed on heating in vacuo of thin films of Nb(N,O)I, and it was further decomposed into Nb_2N(hex) at a higher temperature. Covering with Nb fine powders makes possible the nitriding of thin films of Nb into NbN (hex). Successive structure transformations NbN (hex) → NbN (cub) → Nb_4N_3 (tet) → Nb_2N (hex) were observed by heating in vacuo. Electron diffraction diagrams show the superlattice structures of Nb_2N (hex) and Nb_4N_3 (tet). The crystal structure of Nb_2N (hex) is the same type as that of Nb_2C. The structure of Nb_4N_3 (tet), however, is derived from the cubic NaCl type structure of NbN (cub) by the loss of one quarter of nitrogen atoms. (auth)

41052 THERMAL TREATMENT OF Ti–Al–Mo–Zr–Sn ALLOYS. Molchanova, E. K.; Konstantinov, V. A. Metalloved. i Term. Obrabotka Metal., No. 6, 38-9(June 1965). (In Russian).

The effects of various rates of cooling on the mechanical properties of annealed Ti–Al–Mo–Zr–Sn specimens heated at 800 to 1200°C and aged for 1, 5, and 25 hrs at 400 to 700°C were studied. The alloys exhibited high mechanical properties up to 500°C. Aging at 550 to 600°C formed β phase and lowered the stability of the alloy. (R.V.J.)

41053 INFLUENCE OF ZIRCONIUM ADDITIONS ON THE EPSILON PHASE OF THE TITANIUM–ALUMINUM SYSTEM. Spragins, S. V.; Myers, J. R.; Saxer, R. K. (Air Force Inst. of Tech., Wright-Patterson AFB, Ohio). Nature, 207: 183-4(July 10, 1965).

Causes of the brittleness and possible ways of increasing the ductility of the epsilon phase of the TiAl alloy system are discussed. A study was made to refine the 2325°F ϵ-phase boundary of the Al-Ti-Zr system and to determine the effect of Zr on the c/a ratio within the ϵ phase at this temperature; it is assumed that a reduction of the c/a ratio would improve the ductility. Eighteen experimental alloys were prepared from high-purity components. Samples were x-ray analyzed to determine the ϵ phase boundary as a function of alloy composition and examined metallographically to determine metallurgical structure; results of the analyses agree. The c/a ratios of samples in the ϵ single phase region were computed by the Myers and Davies graphical method; the c/a ratio did not approach unity with Zr additions but increased, contrary to predictions. (M.J.T.)

41054 PHASE EQUILIBRIA IN THE PLUTONIUM–CERIUM–COPPER SYSTEM. Wittenberg, L. J.; Etter, D. E.; Selle, J. E.; Tucker, P. A. (Monsanto Research Corp., Miamisburg, Ohio). Nucl. Sci. Eng., 23: 1-7 (Sept. 1965).

The quilibrium phase diagram of the plutonium–cerium–copper system is presented, based on data obtained by differential thermal analysis, metallography and electron-microprobe x-ray analysis. Liquid-solid phase transitions were found between 419 and 1083°C. Ten crystalline phases solidify as primary phases from molten plutonium–cerium–copper solutions. No ternary compounds occur in the system. The ternary system is divided into two subsystems by the quasibinary section, $CeCu_2$–$PuCu_2$. Continuous solid solubility occurs along this join with neither a maximum nor a minimum. Solid solubility also occurs between the congruent compound, $CeCu_6$, and the incongruent compound, Pu_2Cu_{11}. The ternary system is characterized by a single eutectic (4 at. % Pu-68 at. % Ce-28 at. % Cu at 419°C), four peritectics, and two inversion points. (auth)

41055 DETERMINATION OF THE SLIP SYSTEMS IN SINGLE CRYSTALS OF TUNGSTEN MONOCARBIDE. Takahashi, T.; Freise, E. J. (Northwestern Univ., Evanston, Ill.). Phil. Mag. (8), 12: 1-8(July 1965).

Slip in single crystals of tungsten monocarbide was observed around Vickers pyramid hardness indentations. The slip plane is $\{1\bar{1}00\}$ at room temperature and the slip directions are postulated to be the $\langle 0001\rangle$ and $\langle 11\bar{2}0\rangle$. The Vickers hardness value on a (0001) face is approximately twice the value determined for a $(1\bar{1}00)$ face. This is attributed to the ease of motion of dislocations with $\langle 11\bar{2}0\rangle$ Burgers vectors as opposed to the dislocations having $\langle 0001\rangle$ Burgers vectors since the former can dissociate into $\langle 11\bar{2}3\rangle$ partial dislocations. The occurrence of a $\{1\bar{1}00\}$ slip plane is explained on the basis of the fact that a minimum number of only two covalent tungsten–carbon bonds need be broken for a unit of slip on this plane. (auth)

41056 ON THE FORMATION OF INTERSTITIAL LOOPS IN B.C.C. METALS. Eyre, B. L.; Bullough, R. (U.K.A.E.A. Research Group, Harwell, Berks.). Phil. Mag. (8), 12: 31-9(July 1965). (AERE-R-4741).

Two types of interstitial loops with Burgers vector b = $a/2\langle 111\rangle$ and b = $a\langle 100\rangle$, respectively, were observed experimentally in irradiated bcc metals. A discussion of how these loops can form from a common loop nucleus consisting of a single platelet of interstitials on a $\{110\}$ plane is given. Such a loop contains a stacking fault which is removed by one of two shears described by the following dislocation reactions: $(a/2)[110] + (a/2)[00\bar{1}] \rightarrow (a/2)[11\bar{1}]$, $(a/2)[110] + (a/2)[\bar{1}10] \rightarrow a[010]$. It is suggested that the latter higher energy, $\langle 10\rangle$ shear, requires thermal energy to assist it and therefore only occurs at elevated temperatures. Consideration is given to the elastic energy of the loops with particular reference to their shape and orientation. The calculations predict that the loops are initially rectilinear and as they grow they should change to the circular form and rotate into a pure edge orientation. The crystallographic symmetry of the a $\langle 100\rangle$ loops and their growth mechanism probably explains the observed retention of the rectilinear form. (auth)

41057 THE MECHANISM OF CAVITATION IN MAGNESIUM DURING CREEP. Ratcliffe, R. T.; Greenwood, G. W. (Berkeley Nuclear Labs., Glasgow). Phil. Mag. (8), 12: 59-69(July 1965).

During the creep of magnesium, cavities form on some grain boundaries, limiting the ductility of the material and causing its density to decrease. It is shown that cavitation is eliminated if a hydrostatic pressure is superimposed which is equal to the creep stress. If the hydrostatic pressure is applied after cavities are already present in the material, continuing creep results in negligible density change and existing cavities do not continue to grow. When hydrostatic pressure is applied throughout the early stages of creep and is then removed, the subsequent cavitation develops at a rate which is unaffected by the prior deformation. The fractional change in density during creep is approximately proportional to the duration of creep to the power of 2.5 increasing to about 4 immediately prior to

fracture. This rate of change of density is greater than can be accounted for by the growth of a constant number of cavities by vacancy condensation and suggests a progressive creation of nuclei. The number of cavities is observed to increase with strain and the change in density during creep is interpreted in terms of a continuous formation of cavities which grow exclusively by condensation of vacancies which diffuse from grain boundaries approximately perpendicular to the applied stress. (auth)

41058 DEFORMATION AND FRACTURE OF THORIA. Gilbert, A. (Battelle Memorial Inst., Columbus, Ohio). Phil. Mag. (8), 12: 139-44(July 1965).

A transmission-electron microscope study was made of thoria platelets extracted from a thoriated tungsten alloy sheet. Trace analyses performed on electron diffraction patterns showed cleavage to occur primarily on {111}-type planes with occasional instances of {011} and {001} cleavage. A low-dislocation density within the platelets implies that they recrystallize during fabrication, possibly into single crystals of a preferred orientation. This, together with trace analyses on slip bands, suggests that slip occurs on {111} planes at high temperature. (auth)

41059 DETERMINATION OF THE CURIE POINT OF THE FERROELECTRICS $YMnO_3$ AND $YbMnO_3$. Ismailzade, I. G.; Kizhaev, S. A. (Inst. for Semiconductors, Leningrad). Soviet Phys.-Solid State (English Transl.), 7: 236-8(July 1965).

Translated from Fiz. Tverd. Tela, 7: 298-301(Jan. 1965).

The results of high-temperature x-ray-diffraction studies and the temperature dependence of the pyroelectric current of $YMnO_3$ indicate that the transition from the ferroelectric to the paraelectric state occurs near 660°C. X-ray-diffraction studies show that $YbMnO_3$ changes from the ferroelectric to the paraelectric state in the range 700–725°C. The phase transitions in both materials are apparently of the first kind. (A.G.W.)

41060 MAGNETIC SUSCEPTIBILITY OF SAMARIUM MONOSULFIDE. Adamyan, V. E.; Golubkov, A. V.; Loginov, G. M. (Inst. for Semiconductors, Leningrad). Soviet Phys.-Solid State (English Transl.), 7: 239-40(July 1965).

Translated from Fiz. Tverd. Tela, 7: 301-4(Jan. 1965).

The magnetic susceptibility of samarium monosulfide was measured by the Faraday method in the temperature range 290–1300°K. Results are compared with theoretical values, and possible reasons for discrepancies are discussed. (A.G.W.)

41061 DIRECT OBSERVATION OF THE REESTABLISHMENT OF CONTACTS BETWEEN FRAGMENTS OF A TUNGSTEN MICROCRYSTAL. Garber, R. I.; Dranova, Zh. I.; Mikhailovskii, I. M. (Inst. of Physics and Tech., Khar'kov). Soviet Phys.-Solid State (English Transl.), 7: 395-8(Aug. 1965).

Translated from Fiz. Tverd. Tela, 7: 496-501(Feb. 1965).

The formation of cracks under the action of quenching stresses and electric field forces is observed at liquid-nitrogen temperature in a tungsten microcrystal, using a field-ion microscope. The evolution of cracks that takes place when a small number of atomic layers are vaporized by the field is described in detail. A spontaneous formation of a bridge and a subsequent recrystallization, accompanied by the reestablishment of the continuity of the microcrystal, are observed. The results of observations are in complete agreement with the earlier hypothesis of the possible reestablishment of contacts between fragments of microblocks formed during plastic deformation of a solid and recrystallization at very low temperatures after low-temperature activating deformation. (auth)

41062 GOLD-RICH RARE-EARTH-GOLD SOLID SOLUTIONS. Rider, P. E.; Gschneidner, K. A. Jr.; McMasters, O. D. (Ames Lab., Ames, Iowa). Trans. Met. Soc. AIME, 233: 1488-96(Aug. 1965). (IS-1056).

The solid solubilities for thirteen rare earths in gold were determined using the x-ray parametric method. Solubilities ranged from 0.1 at. % for lanthanum in gold up to 8.8 at. % for scandium in gold. The solubilities from lanthanum to gadolinium were very small and essentially constant, but a sharp increase occurred from gadolinium to scandium. The large solubilities for the heavy rare earths were not expected because of the large size and electrochemical differences between rare earth atoms and the gold atom. Contributions from first- and second-order elasticity theory plus an electronic contribution were found to reasonably account for a more favorable size factor. Electron transfer from the rare earth metal to the gold is thought to occur such that the resultant rare earth and gold electronegativities are favorable for solid-solution formation. It was also found that this mutual adjustment of size and electronegativity does not occur if the pure-metal size factors are greater than a critical value of 25%. The eutectic temperatures for ten systems were determined and these remained fairly constant at approximately 809°C for the lighter lanthanide metal–gold systems until the Er–Au system was reached, at which point the eutectic temperature successively increased reaching a maximum of 1040°C in the Sc–Au system. This rise was correlated to the size factor becoming more favorable for solid-solution formation at erbium. The valence state of ytterbium was found to change from two in the pure metal to three when ytterbium is dissolved in the gold matrix. (auth)

41063 NUCLEATION OF CREEP CAVITIES IN MAGNESIUM. Harris, J. E. (Berkeley Nuclear Labs., Eng.). Trans. Met. Soc. AIME, 233: 1509-16(Aug. 1965).

By elimination of other possible nucleation processes, it was demonstrated, for commercially pure magnesium and a Mg–Al alloy, that at stresses less than that necessary for triple-point cracking creep cavities are most probably nucleated heterogeneously at second-phase particles. Evidence for the existence of such particles is presented and the role of grain boundary sliding in the nucleation process is examined quantitatively. (auth)

41064 DIFFUSION OF Nb-95 AND Ta-182 IN NIOBIUM (COLUMBIUM). Lundy, T. S.; Winslow, F. R.; Pawel, R. E.; McHargue, C. J. (Oak Ridge National Lab., Tenn.). Trans. Met. Soc. AIME, 233: 1533-9(Aug. 1965). (ORNL-P-962).

The volume-diffusion coefficients of ^{95}Nb and ^{182}Ta in niobium were measured over the temperature range 878 to 2400°C. High-temperature specimens ($T \geq 1500$°C) were sectioned by conventional lathe and grinding techniques while low-temperature specimens were sectioned by an anodizing and stripping technique previously described. Over a range of more than ten orders of magnitude in diffusivity, the self-diffusion data is well-represented by the equation: $D = (1.1 \pm 0.2) \exp[-(96{,}000 \pm 900)/RT]$ cm²/sec. Upward deviations from this line are explained by short-circuit diffusion in combination with the loss of resolution of the sectioning techniques. Oxygen contamination within the range 100 to 450 ppm was found to have little or no effect on the self-diffusivity of niobium. In a limited number of measurements, the diffusivity of ^{182}Ta in niobium was found to be about half that of ^{95}Nb in niobium. These data may be described by $D = (1.0^{+0.3}_{-0.2}) \exp[-(99{,}300 \pm 2400)/RT]$ cm²/sec. (auth)

41065 EQUILIBRIA OF NITROGEN WITH THE REFRACTORY METALS TITANIUM, ZIRCONIUM, COLUMBIUM, VANADIUM, AND TANTALUM IN LIQUID IRON. Evans, Donald B.; Pehlke, Robert D. (Univ. of Michigan, Ann Arbor). Trans. Met. Soc. AIME, 233: 1620-4(Aug. 1965).

The solubility of nitrogen in liquid binary alloys of iron with titanium, zirconium, niobium, vanadium, and tantalum was measured for alloy compositions up to the solubility limits of the alloy nitrides. All five alloying agents were found to decrease markedly the activity coefficient of nitrogen in liquid iron. The metal/nitrogen mole ratios in the alloy nitrides formed were generally found to be slightly greater than 1.0, but in no case greater than 1.5. From the experimental data, the standard free energies of formation of titanium and zirconium nitrides were calculated for the temperature range 1550 to 1750°C. The solubility products for niobium, tantalum, and vanadium nitrides are also reported. (auth)

41066 ON THE DEFORMATION OF TUNGSTEN SINGLE CRYSTALS BY ROLLING. Raymond, L.; Neumann, J. P. Trans. Met. Soc. AIME, 233: 1625-31 (Aug. 1965).

At temperatures near 1000°C, only the {112} ⟨111⟩ slip systems are operative in tungsten. Therefore, the substructure introduced into the billet on deforming a single crystal by rolling at 1000°C can be controlled by proper selection of processing variables. Using a reduction of 10% per pass, the (001) [110] and the (110) [001] crystals deform by duplex slip up to a 50% reduction in thickness. These rolled single-crystal sheets are characterized by anisotropic hardening, retention of ductility with warm working, lattice bending, which is related to the contact angle, and macroscopic dimensional changes in the length but not the width of the billet. When several slip systems become operative, a greater degree of work hardening is introduced into the crystal. This rolling condition is characterized by isotropic hardening, loss of ductility with warm working, complex lattice distortions, and macroscopic dimensional changes in both the length and width of the billet. (auth)

41067 THE INFLUENCE OF ADDITIONS ON THE PROPERTIES OF TANTALUM. Raub, Ernst; Roeschel, Erich (Forschungsinstitut fuer Edelmetalle und Metallchemie, Schwabisch Gmund, Ger.). Z. Metallk., 56: 339-45(June 1965). (In German).

The effect of metallic additions on the properties of tantalum is influenced by its gas content. As in pure tantalum the properties of the alloys depend on the method of melting. Electron beam melted samples show little change of their properties by the addition of up to 6 at. % vanadium and 6 at. % niobium. Arc-melted alloys show an increase in strength where the specific effect of vanadium is higher than that of niobium. Electron beam melted tungsten and molybdenum alloys of tantalum show a higher specific effect of the former, while alloys melted in a tungsten arc show the opposite behavior. Already small amounts of ruthenium have a considerable effect on strength at room and elevated temperatures. The effect also depends on the method of melting. Titanium shows a relatively small effect on the properties; that of zirconium is considerably larger. The effects of small additions of dysprosium and beryllium may be due to the desoxidation caused by these metals. (auth)

41068 ON THE POSSIBLE METHOD FOR STUDYING FERMI SURFACES. Sharvin, Yu. V. (Inst. of Problems in Physics, Academy of Sciences, USSR). Zh. Eksperim. i Teor. Fiz., 48: 984-5(Mar. 1965). (In Russian).

An idea is described for an experiment which produces inside a metal single crystal a configuration operating like a beta spectrograph with focusing of the electrons in a longitudinal magnetic field. The principle of the configuration is based on the fact that if there is an elliptic turning point on the Fermi surface for a given direction of the uniform magnetic field, then electrons located in the vicinity of this point of momentum space will be focused by the magnetic field in such a way that electrons emerging from some point inside the metal will collect again at a point lying on the same line of force at a distance L from the first point. The distance L is uniquely connected with the field strength H. In order to observe the focusing effect, it is proposed to measure the resistance of the sample between two contacts of very small size. Two possible physical arrangements are proposed. An estimate shows that for L = 0.05 cm, a contact diameter of 10^{-4} cm, and a measuring current of 10 mamp, the amplitude of the voltage can reach 10^{-7} v, which is fully measurable. One of the basic difficulties of the method is exact adjustment of the magnetic field direction. The effect described can yield information on the curvature of the Fermi surface and on the electron mean free path and its temperature dependence. (ATD)

41069 CRYSTALLINE STRUCTURE OF CERTAIN TERNARY COMPOUNDS IN Nb–Co–Si SYSTEM. Kuz'ma, Yu. B.; Gladyshevskii, E. I.; Byk, D. S. (L'vov State Univ.). Zh. Strukt. Khim., 5: 562-7(July-Aug. 1964). (In Russian).

Microstructure and x-ray structure analyses of the ternary Nb–Co–Si systems showed six ternary compounds. The crystal structure was determined for three of these compounds: Nb_3Co_2Si had a structure similar to Mn_3Ni_2Si ($a = 11.196 \pm 0.003$ Å); Nb_3Co_3Si was similar to Mg_2Cu_3Si ($a = 4.794 \pm 0.002$ Å, $c = 7.760 \pm 0.003$ Å, and $c/a = 1.619$), and $Nb_2Co_{16}Si_7$ was similar to the $Mg_6Cu_{16}Si_7$ ($a = 11.251 \pm 0.004$ Å). A compound containing ~60 at. % Nb in a binary Nb–Co alloy was found. (R.V.J.)

41070 ROENTGENOGRAPHIC STUDIES OF LANTHANUM TELLURIDES La_4Te_7. Eliseev, A. A.; Kuznetsov, V. G.; Yarembash, E. I.; Antonova, L. I. (Kurnakov Inst. of General and Inorganic Chemistry, Academy of Sciences, USSR). Zh. Strukt. Khim., 5: 640-1(July-Aug. 1964). (In Russian).

Debye crystallograms of lanthanum tellurides La_2Te_3, La_4Te_7, and $LaTe_2$ were analyzed. The tabulated indexes of x-ray pictures for La_4Te_7 and measured and calculated magnitudes of the intraplane distances showed that the crystal belongs to the Pmmn = D_{2h}^{13} group. The data obtained indicated a similarity between the $LaTe_2$ and $LaTd_7$ crystal structure. (R.V.J.)

41071 ROENTGENOGRAPHIC STUDIES OF LANTHANUM DITELLURIDE. Eliseev, A. A.; Kuznetsov, V. G.; Yarembash, E. I. (Kurnakov Inst. of General and Inorganic Chemistry, Academy of Sciences, USSR). Zh. Strukt. Khim., 5: 641-2(July-Aug. 1964). (In Russian).

The lanthanum telluride (0.05 mm) crystal prepared revealed a tetragonal lattice with spatial group p4/nmm and lattice parameters $a = 4.556 + 0.003$, $c = 9.176 \pm 0.006$ Å, and $c/a = 2.018$. The pycnometric density of the crystal was $d_{meas.} = 6.82$ g/cm³, which assigned to $LaTe_2$ two formula units per elementary cell $d_{calc.} = 6.80$ g/cm³. Atom coordinates of La and Te were determined. (R.V.J.)

41072 AN ATLAS OF MODELS OF CRYSTAL SURFACES. Nicholas, John F. Materials Science and Engineering Program. New York, Gordon and Breach Science Publishers, 1965. 256p. $27.50.

Models, positions of atoms in a unit cell of surface, coordination of the surface atoms, and construction of models are discussed. 162 pages of crystallographic formulas are appended. (P.C.H.)

41073 HIGH-TEMPERATURE COMPOUNDS OF RARE EARTH METALS WITH NONMETALS. Samsonov, Grigorii Valentinovich. New York, Consultants Bureau, 1965. 291p. $17.50.

Authorized translation from the Russian.

Detailed data are presented on the physicochemical properties, crystal structures, and electron structures of borides, carbides, nitrides, silicides, and sulfides of the rare earth metals. Methods of preparing the compounds and the solid state reactions on which most of these methods are based, as well as the structure of the compounds and their properties, are given. (P.C.H.)

41074 THERMAL RADIATIVE PROPERTIES. Wood, W. D.; Deem, H. W.; Lucks, C. F. Plenum Press Handbooks of High-Temperature Materials. No. 3. New York, Plenum Press, 1964. 475p. $17.50.

A compilation of data on thermal radiative properties is given. Also included is a brief discussion of the basic fundamentals of thermal radiation and of the methods of measuring these properties. Thermal radiative data are included for the following materials: Ti and its alloys; stainless steels; Fe, Ni, and Co base superalloys; refractory metals (Cr, Nb, Mo, Ta, and W) and their alloys; coated materials for elevated temperature service; ceramics; and graphite. (P.C.H.)

41075 ENERGETICS IN METALLURGICAL PHENOMENA. VOLUME I. Mueller, William M. (ed.). Materials Science and Engineering Program. New York, Gordon and Breach Science Publishers, 1965. 435p.

Information is included on: intermetallic diffusion; solid solutions; nucleating processes; transformations; metastable phases obtained by rapid solidification; annealing mechanisms in deformed metals; energetics in dislocation mechanics; and oxidation of metals. Separate author and subject indexes are given. (P.C.H.)

41076 DEFORMATION TWINNING. Proceedings of a Conference, Gainesville, Florida, March 21-22, 1963. Reed-Hill, R. E.; Hirth, J. P.; Rogers, H. C. (eds.). Metallurgical Society Conferences, Volume 25. New York, Gordon and Breach Science Publishers, 1964. 474p. $11.50 Paper; $25.00 Cloth. (CONF-276).

Twenty-five articles are included. Current theories of twin crystallography, nucleation and growth, and the role of twinning in plastic deformation and fracture are summarized and reviewed. Recent experimental results including twinning phenomena by transmission electron microscopy are also given. (P.C.H.)

41077 THE INFLUENCE OF HYDROSTATIC PRESSURE ON THE MAGNETIC TRANSITIONS IN TERBIUM AND DYSPROSIUM. Tan, Swie-In. Los Angeles, Univ. of California, 1965. 82p.

The effects of hydrostatic pressure on the magnetic transitions in terbium and dysprosium were investigated. The transformer method was used, in which the toroidal core of the miniature transformer is the rare earth metal itself. Results were obtained as curves of secondary voltage versus temperature. A cusp in the secondary voltage indicates the occurrence of a Néel temperature, at which a transformation takes place from a paramagnetic to an antiferromagnetic state, while a sharp rise in the secondary voltage indicates the passage through a Curie temperature, where a transformation from an antiferromagnetic to a ferromagnetic state occurs. The pressures, up to 25 kb, were obtained by the piston-cylinder technique, using silver chloride as the pressure transmitting medium. The temperature range was from 40°K to room temperature. This was achieved with the use of a new 4-wall cryogenic dewar and liquid helium as coolant. The pressure coefficient of the Néel temperature of terbium was found to be -1.0°K/kb. Under pressure, the atmospheric Curie temperature either disappeared or because of the narrowness of the antiferromagnetic region, was difficult to separate from the Néel temperature. The pressure coefficient of the Néel temperature for dysprosium is -0.4°K/kb. In the range of from zero to about 7 kb, the Curie temperature increased with increasing pressure; beyond 7 kb. the Curie temperature decreased with increasing pressure. In the low pressure range, the pressure coefficient of the Curie temperature is +1.4°K/kb and in the high pressure range -0.8°K/kb. A qualitative explanation for the behavior of the ferromagnetic and antiferromagnetic transitions under pressure is given by means of a ferromagnetic and an antiferromagnetic exchange curve, respectively. (Dissertation Abstr.)

41078 A STUDY OF THE EVAPORATION BEHAVIOR OF THE ZIRCONIUM BERYLLIDES (thesis). McMullen, William Dale. Denver, Univ. of Denver, 1964. 104p.

The evaporation rates of the zirconium beryllides: $ZrBe_{13}$, Zr_2Be_{17}, $ZrBe_5$, and $ZrBe_2$, were measured as function of temperature in the range 950 to 1343°C by the Langmuir and the Knudsen cell technique. The Langmuir technique gave equilibrium data for all compounds except Zr_2Be_{17}. Monatomic beryllium was assumed to be the primary evaporating species in all cases. Evaporation rates were converted to vapor pressures and van't Hoff plots were constructed. The standard enthalpies and entropies of evaporation were calculated from the slopes and intercepts of the van't Hoff plots. The results are: $ZrBe_{13}$, $\Delta H^0 = 94.77$ kcals; $\Delta S^0 = 40.34$ eu, Zr_2Be_{17}, $\Delta H^0 = 84.52$ kcals; $\Delta S^0 = 32.26$ eu, $ZrBe_5$, $\Delta H^0 = 91.66$ kcals; $\Delta S^0 = 36.58$ eu, $ZrBe_2$, $\Delta H^0 = 84.52$ kcals; $\Delta S^0 = 30.23$ eu, where all values are per g atom of beryllium. From these enthalpy values standard enthalpies of formation of the compounds from the solid elements were calculated, giving: $ZrBe_{13}$, $\Delta H_f^0 = -167.6$; Zr_2Be_{17}, $\Delta H_f^0 = -169.8$; $ZrBe_5$, $\Delta H_f^0 = 58.8$; $ZrBe_2$, $\Delta H_f^0 = -14.9$, all in kcal mole. From the measured entropies the standard entropies of the compounds were calculated, giving: $ZrBe_{13}$, $S^0 = 73.81$; Zr_2Be_{17}, $S^0 = 152.04$; $ZrBe_5$, $S^0 = 49.46$; $ZrBe_2$, $S^0 = 39.65$, all in eu/mole. From consideration of the intersections of the van't Hoff curves possible modifications of the zirconium–beryllium phase diagram are proposed. Crystallographic transitions from one intermetallic compound to another with the loss of beryllium are discussed. (Dissertation Abstr.)

41079 STRUCTURES AND TRANSFORMATION KINETICS OF PHASES IN THE URANIUM-RHENIUM ALLOY SYSTEM (thesis). Jackson, Ross Jones. Ames, Iowa, Iowa State Univ., 1964. 162p.

A study was made of the time-temperature-composition dependency of crystal structure and microstructure under nonequilibrium cooling conditions for uranium-rich alloys in the uranium–rhenium system. Sluggish solid-state reactions of the stable phases led to nonequilibrium quantities of the equilibrium α, β, γ, and δ phases. The principal causes for nonequilibrium quantities of stable phases were: the slow rate of formation of the peritectoidally formed $\delta(U_2Re)$ phase; and the ease with which the β and γ solid solutions were retained. The growth rate of the δ phase and the retention conditions for the β and γ phases were studied. The $\beta \rightarrow \alpha$ transformation was found to proceed via an isothermal martensitic reaction or by a sluggish nucleation and growth process. The γ phase under certain conditions was found to transform to α without passing through the intermediate β structure. Accompanying this transformation was a number of metastable transition states. The compositional limits within which the stable and metastable phases form, and the effect of cooling rate and temperature on producing alternative structures were determined. From this was deduced the sequence of phase changes. A crystallographic and microstructural model was developed to explain the observed crystal structures and microstructures and the effect of cooling rate and composition thereon. Finally, the relation between metastability in uranium–rhenium alloys and other systems in which metastable states are observed is discussed. (Dissertation Abstr.)

41080 STUDIES OF PHOTOEFFECTS OCCURRING WITH ANODIZED NIOBIUM ELECTRODES (thesis). Schell, Robert Aloysius. Philadelphia, Temple Univ., 1964. 122p.

Open-circuit photopotentials and short-circuit photocurrents were observed with anodized niobium electrodes of the form $Nb/Nb_2O_5/M$, where M is a thin evaporated metal film. The decay of the open-circuit photovoltage was found to follow the equation $V = -A \ln(t)$, where V is the photovoltage at time (t) and A is a constant. It was possible to correlate the slope of a voltage-ln(t) curve with theory and the constant A was equated to kT. The values of T were generally high compared to the experimental temperature and were termed partial or effective temperatures. As a result, the relaxation phenomena was interpreted in terms of a non-equilibrium effect by which the photoexcited carriers take a rather long time to reach thermal equilibrium with the oxide lattice. The short-circuit photocurrents exhibited a maximum when viewed as a function of the oxide film thickness. This was explained on the basis of optical anisotropy in the oxide film. The spectral response curves of the short-circuit photocurrent were very unusual. These curves exhibit structure in the intrinsic region of absorption. The measurements were performed as a function of wavelength of radiation, radiation intensity, and oxygen pressure. The fact that there was not correspondence between these curves and the absorption spectra was rather surprising. An explanation is given in terms of interband transitions. A trapping scheme is postulated to explain the unusual current-light curve characteristics. This is based on an exponential distribution of traps. A superlinearity in the current-light curves was sometimes observed. The superlinearity was interpreted in terms of a redistribution of these trapping states upon illumination. The observed decay times of the short-circuit photocurrent were of the order of seconds.

Judging from these values, the traps are probably deep-lying states. In addition to the short-circuit photocurrents, normal photocurrents were also observed. These photocurrents, in general, were linear in applied voltage. The shape of the spectral response curves were similar to those of the short-circuit photocurrent for the range of applied fields investigated. (Dissertation Abstr.).

41081 SILICON NITRIDE: A REVIEW OF ITS PROPERTIES AND ATTRACTIVENESS FOR USE AT ELEVATED TEMPERATURES. Oliver, D. A. p.377-84 of "High Temperatures in Aeronautics." New York, Pergamon Press and Milan, Tamburini Editore, 1964.

The manufacture of silicon nitride and its influence on the density of the product; the high thermal-shock resistance and its relation to the low coefficient of thermal expansion; the mechanical properties; and possible applications of silicon nitride are discussed. (W.L.G.)

41082 TEMPERATURE DEPENDENCE OF THE OPTICAL REFLECTIVITY OF CERIUM METAL. Millhouse, A. H.; Leinhardt, T. E. (Virginia Polytechnic Inst., Blacksburg). 9p. (CONF-650410-15). Gmelin, AED-CONF-65-073-19.

From American Physical Society, Washington, D. C.

Optical reflectivity measurements were made on annealed cerium at 300 and 80°K. The reflectivity in arbitrary units was obtained by forming the ratio of the intensity of monochromatic light reflected from the sample (incidence angle of 45°) to the intensity of the incident beam. There was found to be a decrease in the reflectivity at 80°K over that at 300°K varying from about 10% at 0.6μ to 25% at 0.4μ. Data also indicated an isothermal transition in reflectivity at 80°K, probably due to an isothermal transition of the crystal structure. Data are presented in tables and graphs. (M.C.G.)

41083 THE CRYSTAL STRUCTURE AND RESISTIVITY OF CERIUM AS DETERMINED BY TEMPERATURE. Major, R. W.; Leinhardt, T. E. (Virginia Polytechnic Inst., Blacksburg). 8p. (CONF-650410-16). Gmelin, AED-CONF-65-073-18.

From American Physical Society, Washington, D. C.

Previous investigations of the resistivity and allotropes of cerium were extended in an effort to correlate the relative amounts of each of the three crystallographic phases coexisting below 300°K, and the corresponding values of electric resistivity. Resistivity is shown as a function of temperature for 5 thermal cycles. Fifth cycle values showed an increase of 115 and 72% over the first cycle values at 20 and 85°K warming, respectively. The resistivity difference between 85°K cooling and 85°K warming was reduced by more than one-half in five cycles. (M.C.G.)

41084 MAGNETO-OPTIC MEASUREMENTS ON MAGNETIC RARE EARTH-COBALT ALLOY FILMS. Stoffel, A. M.; Strnat, K. (Air Force Materials Lab., Wright-Patterson AFB, Ohio). 13p. (CONF-650403-4). Gmelin, AED-CONF-65-038-4.

From International Conference on Non-Linear Magnetics, Washington, D. C.

The Kerr magneto-optic effect and the complex refractive index for pure cobalt and for four ferromagnetic rare earth-cobalt alloys of the composition RCo_5 were investigated. The thin film samples were prepared by vapor deposition in ultrahigh vacuum and measured in situ. The effect of atmospheric corrosion on the Kerr parameters was investigated; they were found to increase considerably after short exposure to air. The rare earth alloys had a refractive index similar to that of cobalt and Kerr parameters up to 1.5 times higher. Dispersion curves of n, k, Θ_K, ϵ_K, Q_o and q for wavelengths of 400 to 616 μ are presented. The vacuum evaporator and the polarimeter are described. (auth)

41085 MANGANESE-MOLYBDENUM DUCTILE STEEL. (to Ishikawajima-Harima Jukogyo Kabushiki Kaisha). British Patent 997,292. July 7, 1965. Priority date May 16, 1961, Japan.

An Mn-Mo steel with improved mechanical properties for use in boilers and reactor vessels contains an amount of precipitated aluminum nitride and metallic aluminum dissolved in solid solution. The steel has a composition of 0.25% C, 0.60% Si, 1.00 to 2.00% Mn, 0.30 to 1.00% Mo, <0.030% P, <0.040% S, 0.006 to 0.10% aluminum nitride, <0.15% aluminum dissolved in solid solution, optionally 1.00% Cr, and the balance Fe. The steel is heat treated by heating to a temperature above the A_3 transformation point and up to 1050°C and cooling rapidly in air, oil, or water. The cooling is followed by tempering at a temperature above 150°C and below the A_1 transformation point. (B.L.M.)

41086 ELECTROLYTIC DISSOLUTION OF URANIUM FUEL ELEMENTS. Raviv, Samuel; Levin, Iddo (to Ministry of Defence). Canadian Patent 713,034. July 6, 1965. Priority date May 6, 1963, Israel.

A process for the electrolytic dissolution of spent uranium fuel elements encased in aluminum is described. The anode is the fuel element and the cathode is of graphite, platinum, or steel. The dissolution of aluminum is accomplished by immersion in a 15% sodium or potassium hydroxide solution at low voltage until the current ceases. Replacement of the electrolyte by 3 to 5 molar nitric acid dissolves the uranium. The mild conditions make the process simpler, economical, and easily controlled compared with previous methods. (F.S.A.)

Radiation Effects

***See also* CHEMISTRY — Radiation Chemistry.**

41087 (AAEC/E-135) MICROHARDNESS MEASUREMENT OF UNIRRADIATED AND IRRADIATED BERYLLIUM OXIDE. Davis, P. J. (Australian Atomic Energy Commission Research Establishment, Lucas Heights). Apr. 1965. 19p. Dep. mn.

The measured Knoop hardness of beryllium oxide was found to depend on both the indenter load and the orientation of grains within the matrix. Single crystal measurements showed that both prism and basal planes exhibit hardness anisotropy, with a two- and six-fold symmetry respectively. All irradiated specimens except those of lowest density showed irradiation hardening. It is shown that density predominates over such properties as grain size, fabrication methods, and source of supply, in controlling the initial hardness of the material and the rate and extent of the irradiation hardening. No correlation was evident between the extent of irradiation hardening and observable microcracking. (auth)

41088 (GEAP-4572) FISSION GAS RELEASE FROM UO_2 FUEL RODS WITH GROSS CENTRAL MELTING. I. PELLET FUEL. Nelson, R. C.; Coplin, D. H.; Lyons, M. F.; Weidenbaum, B. (General Electric Co., San Jose, Calif. Atomic Power Equipment Dept.). July 24, 1964. Contract AT(04-3)-189. 58p. (EURAEC-1435). Dep. mn; CFSTI $3.00 cy, $0.75 mn.

Work Performed under United States-Euratom Joint Research and Development Program.

The fission gas release from fuel rods was correlated with the gas produced in the fuel volume, which exhibits fission product mobility as observed by autoradiography. In these fuel rods, the region of fission product mobility corresponds to that volume of fuel operating above 1650°C. Above this temperature, the UO_2 experiences microstructural changes. A fission gas release model was proposed which divides each fuel rod into four temperature regions: <1650, 1650 to 1900, 1900 to 2800, and >2800°C. These regions were based on the temperature distribution present in each rod just before reactor shutdown. The volume fraction of the fission gas produced in each of these regions was calculated. Then from statistical analysis, the fraction of the fission gas released from each temperature region was correlated with the measured release from each fuel rod. The results of this analysis show a release of all of the fission gas produced in that volume of UO_2 above 1900°C where columnar grain growth and melting occurred. In the

region of equiaxed grain growth, between 1650 and 1900°C, approximately 20% of the fission gas produced in this fuel volume was released. For UO_2 fuel rods operating under conditions of central melting, the fraction of fission gas released from the fuel volume below 1650°C is relatively small and may be neglected. (auth)

41089 (HW-56028) ULTRASONIC BOND TESTING OF IRRADIATED FUEL ELEMENTS. Bokish, K. P. (General Electric Co., Richland, Wash. Hanford Atomic Products Operation). May 9, 1958. Contract W-31-109-eng-52. 11p. Dep. mn; CFSTI $1.00 cy, $0.50 mn.

Ultrasonic bond test equipment, recently installed in the 105-C Metal Examination Facility, is described and results of tests are presented. This equipment has proven feasible in determining the extent of unbonded areas on irradiated cylindrical fuel elements to an accuracy of from 2 to 5 mils. (auth)

41090 (NAA-SR-11121) URANIUM–10 WT PERCENT Mo FUEL ELEMENT IRRADIATION IN SRE. Arnold, J. L.; Miller, K. J.; Peterson, R. M. (Atomics International, Canoga Park, Calif.). Aug. 31, 1965. Contract AT(11-1)-Gen-8. 34p. Dep. mn; CFSTI $2.00 cy, $0.50 mn.

The fuel element assembly was successfully irradiated in the SRE to a maximum burnup of 5300 Mwd/MtU, at a peak fission rate of approximately 1.5×10^{13} fissions/cm^3-sec and a maximum central temperature near 1200°F. The post-irradiation examination of the fuel rods showed a low fission gas release of 0.1% and fuel dimensional changes ranging from −0.2 to +2.2% with corresponding density decreases from 0.2 to 6.4%. The fuel slugs that had burnups less than 4,000 Mwd/MtU were in excellent condition with maximum dimensional changes of less than +0.6%. Fuel slugs with burnups greater than 4,000 Mwd/MtU had extensive surface cracking and greater fuel dimensional changes. Metallographic examination of the fuel showed that the slugs that had experienced the extensive surface cracking had most of their structure transformed to the $\alpha + \gamma'$ phase. The structure of the fuel that had no surface cracking and small dimensional changes was essentially in the γ phase. There was evidence that the fuel that operated at lower temperatures had been homogenized as a result of fission events, the mechanism being the radiation induced phase reversion. Metallographic examination of the cladding showed that there were no compatibility problems associated with this system, although there was some slight carburization as shown by chemical analysis. In predicting the limiting life of the HNPF Core I U–10 wt % Mo fuel elements, it appears that a lifetime limit below a maximum burnup of 4,000 Mwd/MtU is highly unlikely, and a maximum burnup in excess of 6,000 Mwd/MtU may be achieved. Because of uncertainties in application of the SU-9 data to Hallam, a more quantitative estimate is believed unwarranted. Periodic examination of the Core I U–10 wt % Mo fuel elements will be required to form the basis for a more exact estimate of allowable burnup. (auth)

41091 (SC-R-65-943) SOME PROPERTIES OF CONDUCTIVITY INDUCED IN POLYSTYRENE BY PULSED GAMMA RAYS. Coppage, F. N.; Peterson, F. C. (Sandia Corp., Albuquerque, N. Mex.). July 1965. Contract AT(29-1)-789. 9p. (CONF-650707-6). Dep. mn; CFSTI $1.00 cy, $0.50 mn.

From IEEE Annual Conference on Nuclear and Space Radiation Effects, Ann Arbor, Mich.

Pulsed techniques were used to determine the limits for some basic conductivity parameters in polystyrene irradiated by gamma ray pulses. It is concluded that: the drift mobility lies between 2×10^{-7} and 1.5×10^{-4} cm^2/v-sec, the energy required to create carriers is less than 3×10^4 ev per carrier, and the long-lived photocurrent component has an activation energy of 0.2 ± 0.03 ev and is attributed to a thermally activated drift mobility. (D.L.C.)

41092 (WAPD-TM-457) PROPERTIES OF A HAFNIUM CONTROL ROD AFTER EXPOSURE DURING THREE SEED LIVES IN PWR CORE 1. Salvaggio, G. J.; Weinberg, J. G.; Kass, S.; Longua, K. J. (Bettis Atomic Power Lab., Pittsburgh, Pa.). June 1965. Contract AT-11-1-GEN-14. 49p. Dep. mn; CFSTI $3.00 cy, $0.50 mn.

A PWR Core 1 control rod irradiated to as high as approximately 6×10^{21} nvt (>1 Mev) during three seed lives in the Shippingport Atomic Power Station was destructively tested to determine the effect of irradiation on the properties of hafnium and to further assess the consequences of abnormal corrosion of weld joints of Zircaloy-2 welded to hafnium. Tests performed included hardness, tensile, fatigue, post-irradiation corrosion, chemical analysis, and metallographic examination. Results indicate that the strength increases as the square root of the fast neutron exposure with saturation effects occurring at high exposures for the room temperature strength but not at 300 or 600°F. The adequacy of the control rods for continued use is demonstrated by the apparent saturation of ductility decrease and the lack of further major changes in properties resulting from the corroded weld joints. (auth)

41093 (FTD-TT-65-125) EFFECT OF NEUTRON RADIATION ON CERTAIN MECHANICAL AND STRUCTURAL PROPERTIES OF AUSTENITIC CHROME NICKEL STEEL. Cervasek, Jiri; Kutka, Jan. Translated from Jaderna Energie, 9: 342-6(1963). 13p. CFSTI.

The change of mechanical and structural properties of 13 kinds of stainless steels of Cr–Ni-type exposed to an integral dose of 1.6×10^{19} n/cm^2 (E > 1 Mev) was investigated. The dose was held at a constant value and the chemical composition varied in the Cr and Ni content. A strengthening effect was observed, i.e., yield point, strength, and hardness increased and plasticity decreased at the same time. Primarily, the rate of strengthening is independent of chemical composition, namely chrome and nickel content; however it depends on the physical condition of steel before the radiation. As long as the alloying elements do not influence the properties in initial condition of steel, they exercise no influence on the radiation stability. Ferromagnetic induction measurement indicated the decrease of corrosion resistance of austenitic steels by radiation to be negligible. Transient austenitic-ferritic structure steels only show a 0.43–0.72% increase of magnetic phase caused by $\gamma \rightarrow \alpha$ decay. (auth)

41094 (NP-tr-1235) IRRADIATIONS OF RODS FOR RAPSODIE. Translated for Atomic Power Development Associates, Inc., Detroit, Mich., from the French. [nd]. 12p. Dep.(mn); $1.60(fs), $0.80(mf) JCL.

A series of irradiation of fuel element rods of mixed UO_2-PuO_2 clad with 304 L stainless steel was carried out. The purpose of these irradiations was to test the rods under conditions as similar as possible to operations in the reactor. Results from the testing are presented. (M.O.W.)

41095 (ORNL-tr-667) IRRADIATION OF Cu-Co ALLOYS. Blaise, Alain (Commissariat a l'Energie Atomique, Grenoble (France). Centre d'Etudes Nucleaires). Translated by Gregory L. Boisvert (Oak Ridge National Lab., Tenn.). [1964]. 23p. Dep. mn; JCL, $2.60 fs, $0.89 mf.

The effects of fast neutrons on Cu–0.9% Co alloys at 42 to 210°C were measured by magnetic techniques. The radioinduced precipitation was much greater than that induced by annealing at the same temperatures. There was a distinct enhancement of the antiferromagnetic interactions in the matrix and a smaller particulate size distribution in the irradiated samples. (W.L.G.)

41096 ENERGY SPECTRUM OF DEFECTS APPEARING IN INDIUM ANTIMONIDE AT LOW-TEMPERATURE γ-IRRADIATION. Mashovets, T. V.; Khansevarov, R. Yu. Fiz. Tverd. Tela, 7: 2229-31(1965).

The energy spectrum of defects appearing in n-type indium antimonide irradiated with a dose of 2.4×10^{10} quanta/cm^{-2}/sec^{-1} of γ-rays from a ^{60}Co source at 77°K was investigated. The specific resistance, the concentration of current carriers, and the spectral dependences of impurity photoconductivity were measured on specimens before and after irradiation. The increased photoconductivity of the specimens in proportion to the irradiation was attributed to the rise in the concentration of radiation defect levels.

During irradiation the conductivity changed from n to p type when the specimens passed over the region of total compensation. After the change in conductivity, the hole concentration at first increased, when approached a limiting value. The rate of the electron concentration decrease was 3×10^{-3} e/cm^{-1}/photon^{-1}. Discontinuation of the rise of the radiation defect concentration levels was due to an equilibrium between the processes of the generation and annealing of the defects. (CSFTI)

41097 CONDUCTIVITY INDUCED BY ELECTRON BOMBARDMENT. Trodden, W. G.; Jenkins, R. O. (General Electric Co., Wembley, Eng.). G.E.C. J. Sci. Tech., 32: 85-91(1965).

The low electrical conductivity normally possessed by insulators in the dark can often be increased substantially by electron bombardment. A brief account of investigations into conductivity induced in this way is given and some applications of the effect are given. Some physical processes governing electrical conductivity are outlined. Finally, investigations on cadmium sulfide crystals are described. (auth)

41098 EFFECTS OF RADIATION ON YAKUTIAN DIAMONDS. Snytsyn, V. I.; Pirogova, G. N. (Inst. of Physical Chemistry, Moscow). Izv. Sibirsk. Otd. Akad. Nauk SSSR, No. 3, Ser. Khim. Nauk, No. 1, 40-7(1965). (In Russian).

The absorption spectrum in the ultraviolet, visible, and infrared region of yakutian diamonds irradiated with slow and fast neutrons, ^{60}Co γ rays, and fast electrons was investigated. Absorption in the ultraviolet and visible regions of the spectra increased after irradiation. In the infrared region changes were not observed. Annealing of the irradiated diamonds from 200 to 1100°C gradually produced a decrease of the absorption, but complete annealing was not detected. Slow neutrons (integral current of 2.5 to 17.5 $\times$ 10^{17} n/cm^2) colored the diamonds green. The presence in the current of 1% fast neutrons colored the diamonds black. Under the effect of fast electrons (at a dose of 0.5 to 6.0 $\times$ 10^{24} e/cm^2) the diamonds became blue, but ^{60}Co γ rays gave them a bluish-green color (at a dose of 9.3×10^8 R). The blue and green colors of the diamonds were stable at room temperature and at heating up to 400°C. Irradiation of the diamonds caused the appearance of paramagnetic centers. The character of the EPR spectra depended on the form and dose of radiation. Prolonged aging at room temperature and heating led to the disappearance of the EPR signals. The density of the diamonds was not altered after irradiation with slow neutrons (current of 3×10^{18} n/cm^2), fast electrons (dose of 6×10^{24} ev/cm^2), and ^{60}Co γ radiation (dose of 2×10^9 R). (tr-auth)

41099 THE EFFECTS OF PREIRRADIATION OF THE ACTIVITIES OF SOLID ACIDIC CATALYSTS. Mitsutani, Akio; Eguchi, Tamotsu; Hamamoto, Yoshito (Kurashiki Rayon Co., Ltd., Osaka). Kogyo Kagaku Zasshi, 68: 695-9(Apr. 1965). (In Japanese).

Silica-alumina, activated alumina, and solid phosphoric acid were preirradiated with γ rays of ^{60}Co or β rays, and changes of activities of these catalysts for various acid-catalyzed reactions were investigated. The activities of silica-alumina for the polymerization of propylene or the dehydration of alcohols were markedly increased by preirradiation of the catalyst in vacuo or in the presence of inert gases, and especially in steam. On the contrary, the activities of alumina for the dehydration of alcohols or the polymerization of acetaldehyde were lowered by the same treatment. Activity of solid phosphoric acid for polymerization of propylene was enhanced and that for catalytic decomposition of 4,4-dimethyl-metadioxane was slightly lowered by preirradiation of the catalyst. From their results, it was concluded that the effects of preirradiation of solid acid catalysts by ionizing radiation are complex. Differences between the effect of preirradiation on alumina and that on silica-alumina may be attributed to the difference in chemical structures of the structures adjacent to the active sites, in addition to the difference in acid strengths and Brönsted or Lewis acid properties of both catalysts. (BBB)

41100 BASAL PLANE CONTRACTION IN GRAPHITE DUE TO MONO-VACANCIES. Kelly, B. T. (United Kingdom Atomic Energy Authority, Culcheth, Lancs, Eng). Nature, 207: 257-9(July 17, 1965).

The causes of the observed contraction in the a-axis lattice parameter and the basal plane contraction ϵ_a in graphite crystals under fast-neutron irradiation are discussed. It is proposed that the major contribution to basal plane contraction is due to the modification of the interatomic linkages in the layer by the presence of a vacancy. Changes in the bond order of the layer due to the formation of a vacancy are estimated, using the molecular orbital method. The change in average bond length of the layer is computed and correlated with experimental results. (M.J.T.)

41101 INVESTIGATION OF THERMAL DE-EXCITATION PROCESSES IN X-RAYED ALKALI-HALIDE PHOSPHORS. Shamovskii, L. M.; Maksimova, N. D. Opt. Spectry. (USSR)(English Transl.), 18: 362-5(Apr. 1965).

Translated from Optika i Spektroskopiya, 18: 637-43 (Apr. 1965).

The thermal de-excitation and optical flash associated with pulse illumination in the F band in x-rayed alkali-halide crystal phosphors was investigated. The optical flash was found to grow without lag and to decay in two stages. The slowly decaying component—the secondary phosphorescence (P_F)—continues for up to 5 min. In KCl (Tl), P_F is weakened as the intensity of phosphorescence is decreased at room temperature. On subsequent heating it is strengthened and passes through a maximum at + 85°C. A new thermoluminescence peak, which is ascribed to V_2 centers, appears at this temperature. The described phenomena are explained on the basis of a hole system of luminescence recombination. It was noted that every thermoluminescence peak in the x-rayed crystal phosphors corresponds to the overlapping of two peaks, associated with the thermal dissociation of electron and hole centers. The limits of thermal dissociation of hole centers may be estimated from the secondary phosphorescence. (auth)

41102 RADIATION SATURATION AND DEFECT STRUCTURE IN SOLIDS. Balarin, M.; Hauser, O. (Zentralinstitut fuer Kernforschung, Deutsche Akademie der Wissenschaften, Rossendorf, Ger.). Phys. Status Solidi, 10: 475-80(Aug. 1, 1965). (In German).

A simple analytical possibility for the determination of the saturation concentration and the entry volume α for the spontaneous recombination was given on the basis of the work of Lueck and Sizmann on the saturation type growth of the defect concentration in the irradiation of solids. It was considered that according to the defect structure two cases can occur: in the case of the statistical production of isolated point defects, the entry volume is dependent on the defect concentration produced; in the case of defect cascades, a constant effective value for the entry volume is obtained. The entry volumes were calculated for some metals from different irradiation experiments. (tr-auth)

41103 INVESTIGATION OF THE INTERACTION OF OXYGEN WITH TUNGSTEN BY THE METHOD OF ELECTRON-STIMULATED DESORPTION. Zingerman, Ya. P.; Ishchuk, V. A. (Inst. of Physics, Kiev). Soviet Phys.-Solid State (English Transl.), 7: 173-80(July 1965).

Translated from Fiz. Tverd. Tela, 7: 227-37(Jan. 1965).

A method for the quantitative investigation of the kinetics of adsorption and injection of oxygen in tungsten is proposed which employs the phenomenon of oxygen desorption accompanying irradiation of the adsorbed film by a stream of slow electrons. A method of interpreting experimental data obtained by this method is suggested according to which at temperatures $\leq$1040°K injection of oxygen into the subsurface layer of the metal occurs only during the period of interaction between the oxygen molecules and the tungsten surface. The heat of adsorption liberated during this interaction acts as the source of energy required to overcome the activation barrier of the injection process. (auth)

41104 IRRADIATION OF n-TYPE Ge WITH FAST NEUTRONS. Starostin, K. L.; Tuturov, Yu. F.; Poretskii, L. B. Soviet Phys.-Solid State (English Transl.), 7: 522-3 (Aug. 1965).

Translated from Fiz. Tverd. Tela, 7: 654-5(Feb. 1965).

Germanium samples were irradiated at low temperatures with neutrons whose spectrum was such that the fraction of neutrons having energies higher than 0.6 Mev amounted to about 160%. The samples were then heated to about 250°K in 30 min, cooled, and heated again. Results of measurements of the Hall coefficient and electric conductivity during the first and second heating cycles and the temperature dependence of the Hall coefficient recorded after storage of the sample for 24 hr at room temperature are shown. Explanations of the observed changes are suggested. (A.G.W.)

41105 CURRENT OSCILLATIONS IN GERMANIUM CONTAINING RADIATION DEFECTS. Gerasimov, A. B.; Ryvkin, S. M. (Ioffe Inst. of Physics and Tech., Leningrad). Soviet Phys.-Solid State (English Transl.), 7: 526-7(Aug. 1965).

Translated from Fiz. Tverd. Tela, 7: 657-8(Feb. 1965).

Germanium samples were converted by irradiation from n- into p-type. Current oscillations appeared at the temperature of liquid nitrogen, in darkness, after the application of a certain constant voltage $V_c = 20-30$ v. The nature and frequency of the oscillations depended on the direction of flow of current through the sample. Effects of change in the applied field, illumination, and storage in darkness on the oscillations are noted. (A.G.W.)

41106 COMPUTED EFFECT OF NEUTRON IRRADIATION ON THE CONCENTRATION OF INTERSTITIALS AND VACANCIES IN NIOBIUM (thesis). Kristianson, Bryant Neil. Ames, Iowa, Iowa State Univ., 1964. 86p.

The development on a macroscopic scale of the equations describing the production and annealing of interstitial atoms and vacant lattice sites in niobium metal which is in the presence of a steady-state, energy-dependent neutron flux is presented. The equations are solved for the purpose of illustration using representative values. A method is devised which allows the steady-state, energy-dependent neutron flux arising from an infinite plane source of neutrons in the niobium to be described. This flux is used in the solutions of the equations. The rate of accumulation of neutron-induced interstitial atoms and vacant lattice sites in niobium metal is equal to the rate of production minus the rate of recovery. The recovery rate is composed of two terms—temperature annealing and radioinduced annealing. The production rate and radioinduced annealing rate are dependent upon the energy-dependent neutron flux, the defect concentration, neutron parameters, and metal parameters. The temperature annealing rate is dependent upon the temperature, type of defect, defect concentration, and metal parameters. (Dissertation Abstr.)

41107 IRRADIATION EFFECTS IN CLADDING AND STRUCTURAL MATERIALS. Bush, Spencer H. Monograph Series on Metallurgy in Nuclear Technology. New York, Rowman and Littlefield, Inc., 1965. 233p.

A general picture of the state of the art in the field of irradiation damage to nuclear reactor materials used as fuel cladding or as structural components is presented. This includes information on: mechanisms of irradiation damage; general description of irradiation; stainless steels; Al and Mg alloys; Be; Zr alloys; Ni base alloys; refractory metals and alloys; other metals for cladding or structures; and problems, programs, and future trends. (P.C.H.)

41108 PHONON INDUCED INFRA-RED ABSORPTION SPECTRUM IN IRRADIATED MgO. Stettler, John D.; Shatas, Romas A.; Tanton, George A. (Army Missile Command, Redstone Arsenal, Ala.). 16p. (CONF-641114-6). Gmelin, AED-CONF-64-194-17.

From American Physical Society, Southeastern Section, Chattanooga.

The phonon-induced absorption spectrum located to the high-energy side of the "Moessbauer pip" at 9572 cm^{-1} of IR color centers in 10^{18} n cm^{-2} irradiated MgO was analyzed in terms of the strain hamiltonian $C\epsilon$ (C is function of electronic coordinates and ϵ is effective strain). Observed peaks in the effective density of phonon states (310, 370, 430, and 500 cm^{-1}) agreed closely with recent Raman infrared measurements and roughly with Sturge's transition metal ion data except for the reversal of the relative intensities of the various peaks. Assuming that the Condon approximation holds and that only one state $|E\rangle$ is stress-affected, a value of $\langle E|C|E\rangle \approx 6 \cdot 10^{-12}$ erg was calculated from the ratio of the integrated absorption coefficients of the 1-phonon band to the 0-phonon pip. Within experimental error this value was also obtained using uniaxial stress data. (auth)

41109 METHOD OF TESTING GRAPHITE. Brocklehurst, James Ernest (to United Kingdom Atomic Energy Authority). British Patent 998,153. July 14, 1965. Filed July 26, 1962.

A method of testing polycrystalline graphite for its dimension-determining properties under irradiation by neutrons consists of exposing a sample of the graphite to bromine vapor so that the bromine is absorbed progressively into the sample, performing measurements on the sample to ascertain bulk dimensional change as a function of the amount of bromine absorbed, and deducing from such change the extent to which changes in the graphite crystal dimensions are reflected in the bulk material. The amount of bromine absorbed is adjusted to make allowance for non-expansive surface absorption of the bromine. Such measurements are necessary to ascertain if the bulk material of polycrystalline graphite is suitable for use in reactors where the graphite is subjected to neutron irradiation. (B.L.M.)

METEOROLOGY

See also GEOLOGY AND MINERALOGY — Site Survey and Selection.

41110 (BNWL-74) MIDAS COMPUTATION OF WATERDROP EVAPORATION. Engelmann, R. J. (Battelle-Northwest, Richland, Wash. Pacific Northwest Lab.). July 1965. Contract AT(45-1)-1830. 35p. Dep. mn; CFSTI $2.00 cy, $0.50 mn.

An explanation is given of the MIDAS program for IBM 7090 machine computation of evaporation of waterdrops falling through varying temperature and humidity profiles. Because of its simplicity, MIDAS programming (similar to analog programming) can be quickly learned. (auth)

41111 (EUR-2296.e) CLIMATIC CHARTS SHOWING THE AVERAGE ANNUAL PRECIPITATION AND PRECIPITATION FREQUENCY FOR THE EUROPEAN COMMUNITY, THE UNITED KINGDOM, DENMARK AND THE ALPS DURING THE PERIOD 1921-1950. (SCALE 1:5,000,000). PART I. AVERAGE ANNUAL PRECIPITATION (MM). PART II. AVERAGE ANNUAL NUMBER OF DAYS WITH 1.0 MM OR MORE OF PRECIPITATION. Schirmer, H.; Manig, M. (Deutscher Wetterdienst, Offenbach am Main (West Germany). ABT. Klima). 1965. 13p. Dep. mn.

In the study of problems concerning radioactive contamination of the biosphere, detailed information on the rainfall pattern is indispensable. Data are presented on annual precipitation and precipitation frequency for Europe from 1921 to 1950. (C.H.)

41112 (SC-DC-65-1312) CIRCULATION PROCESSES AND MIXING MECHANISMS IN THE UPPER ATMOSPHERE ABOVE 30 KM. Final Report on SEDIMENTATION AND DISPERSION OF PARTICULATE CLOUDS IN THE UPPER ATMOSPHERE. Cote, Owen (GCA Technology Div., GCA Corp., Bedford, Mass.). Mar. 1965. Contracts AT(29-1)-789 and P.O. 82-6256. 129p. (GCA-TR-65-4-G). Dep. mn; CFSTI, $4.00 cy, $1.00 mn.

For Sandia Corp., Albuquerque, N. Mex.

The factors affecting the fall speed and relative dispersion of small particles—1 to 100 micron diameter and 5 g/cm^3 density—are considered in this study. Terminal fall speeds, corrected for slip flow, and the total gravitational settling time from 70 to 30 km are computed using atmospheric parameters taken from the ARDC model atmosphere (1959). The influences of particle shape and orientation, of photophoresis, and of hydrodynamical interaction between the particles in a cloud on fall speed are reviewed and shown to be significant. Transport and dispersion processes affecting the cloud are assumed to be independent. The total gravitational settling time to 100,000 feet is taken to represent the time available for atmospheric dispersion. The relative dispersion of the particle cloud is calculated assuming a Gaussian cloud distribution having a variance or relative dispersion $\sigma^2 = 2K_e t$. The magnitude of the effective eddy diffusion coefficient, K_e, is based upon both observed radioactive debris dispersion and theoretical studies of atmospheric dispersion. Maximum particle concentrations to be expected at 100,000 feet are equated to particle concentrations at the center of the model cloud. The surface concentration is discussed in terms of the present model and recommendations are made for refining the method of concentration calculation. (auth)

41113 COSMIC DUSTS. RECENT C.E.A. STUDIES. Grjebine, T. Bull. Inform. Sci. Tech. (Paris), No. 89, 23-37(Jan. 1965). (In French)

Cosmic dust studies at the C.E.A. are conducted in three fields: monitoring of atmospheric fallout, marine sediments, and polar ice. These studies have made it possible to establish that cosmic dust differs from terrestrial dust in form and chemical composition. The probable origin of this dust is cometary or meteoric. (tr-auth)

PHYSICS

General

Refer also to abstracts 40396 and 40862.

41114 (AD-617258) SINGULAR-PERTURBATION METHODS APPLIED TO MAGNETO-GASDYNAMICS AND PLASMA PROBLEMS. Final Report. Chang, I-Dee (Stanford Univ., Calif. Dept. of Aeronautics and Astronautics). June 24, 1965. 7p. (AROD-4284:3).

The magnetic effect in a conducting fluid upon boundary layer separation over a circular cylinder was studied based on a linear model. Conclusions are presented. The statistical theory of homogeneous hydromagnetic turbulence is discussed. The slow motion of a sphere in a compressible viscous fluid is discussed. Conclusions are presented. (M.O.W.)

41115 (ANL-6967) A STUDY OF CONVECTIVE MAGNETOHYDRODYNAMIC CHANNEL FLOW. Singer, Ralph M. (Argonne National Lab., Ill.). Mar. 1965. Contract W-31-109-eng-38. 45p. Dep. mn; CFSTI, $2.00 cy, $0.50 mn.

The steady, combined, free and forced convective flow of an electrically conducting fluid through a vertical channel in the presence of a horizontal magnetic field was studied. Three distinct physical situations were investigated: parallel-plate channel with walls of arbitrary electrical conductivity, rectangular channel containing a fluid with a very small magnetic Prandtl number, and rectangular channel with nonconducting walls. Numerical results were presented for only the first two cases. (auth)

41116 (IAE-668) O KOMPENSATSII VOZMUSHCHENII VINTOVOGO MAGNITNOGO POLYA. (Compensation of Helical Magnetic Field Disturbances). Karmanov, F. V.; Mel'nikov, V. K. (Institut Atomnoi Energii SSSR, Moscow). 1964. 11p. Dep. mn.

The perturbation of a helical magnetic field causes the escape of some part of the lines of force from the region bounded by the branches of the separatrix. Perceptible escape of the lines of force begins even at perturbations $h \cong H_0 \times 10^{-3}$ Oe. An idea for the compensation of the helical magnetic field perturbations was proposed previously. The conditions for compensation were confirmed experimentally, and it was shown that, in the case of the nonobservance of the conditions for compensation, the escape of lines of force becomes greater. (tr-auth)

41117 (LA-3306) STABILITY OF DETONATIONS FOR DISTURBANCES OF SMALL TRANSVERSE WAVELENGTH. Erpenbeck, Jerome J. (Los Alamos Scientific Lab., Univ. of California, N. Mex.). Mar. 1965. Contract W-7405-eng-36. 136p. Dep. mn; CFSTI $4.00 cy, $1.00.

The stability of one-dimensional, steady detonations to periodic disturbances transverse to the flow is examined in the limit of small wavelength, i.e., $2\pi/\epsilon \to 0$. It is found that any unstable disturbance grows in time. The asymptotic criterion for stability is found to depend largely upon the steady-state profile of $c_0^2 - u^2$ (where c_0 is the frozen sound speed and u is the mass velocity relative to the von Neumann shock) as a function of distance behind the shock. Detonations for which $c_0^2 - u^2$ decreases monotonically are found to be stable (in the $\epsilon \to \infty$ limit), but stability in cases in which this quantity increases either monotonically or up to a maximum (and decreases beyond) is determined through simple integral functions of the steady-flow variables. The asymptotic result can be readily applied to any detonation, irrespective of the number of chemical reactions which occur, provided knowledge of the equation of state and reaction kinetics is at hand. The criterion is applied to an idealized, one-reaction detonation. Unstable regimes are found only if the ratio of specific heats is less than 2, for which case all detonations are found to be unstable for sufficiently large values of the activation energy. For low heats of reaction, it is found that instability persists for all (positive) heats, unless the activation energy is also small. On the other hand, for more realistic heats of reaction, the criterion predicts stability for small activation energies. (auth)

41118 (LA-DC-6996) PHERMEX APPLICATIONS TO STUDIES OF DETONATION WAVES AND SHOCK WAVES. Venable, Douglas; Boyd, T. J. Jr. (Los Alamos Scientific Lab., Univ. of California, N. Mex.). [1965]. Contract W-7405-eng-36. 43p. (CONF-651003-1). Dep. mn; CFSTI, $2.00 cy, $0.50 mn.

For presentation at 4th Symposium on Detonation, Silver Spring, Md.

A 20-Mev, high intensity, high current, flash radiographic machine, PHERMEX, was built to complement other hydrodynamics facilities of the Los Alamos Scientific Laboratory. In many experimental situations, observations of hydrodynamic phenomena may be obtained by means of techniques unique to flash radiography. This device is used primarily to implement studies in areas related to detonation and shock waves, jet formation and the interaction of jets with matter, spalling and cratering. In certain simple geometries, shock wave and rarefaction wave velocities, particle velocities, and time variation of both edge positions and mass density distributions can be obtained. This facility and the choice of its design parameters are discussed. Radiographs illustrating typical experiments are included. Results of several experiments are presented; these include measurements of the Hugoniot pressure at zero particle velocity, and the particle velocity and sound speed behind a detonation wave in solid explosives. (auth)

41119 (MIT-36-P) APPROXIMATE SOLUTIONS FOR SKIN FRICTION AND HEAT TRANSFER IN MHD CHANNEL FLOWS. Project SQUID. Moffatt, W. Craig (Virginia Univ., Charlottesville. Dept. of Aerospace Engineering). June 1965. Contract Nonr 3623(00), NR-098-038. 36p. (CONF-650812-1).

From ASME-AIChE Heat Transfer Conference and Exhibit, Los Angeles.

Results are presented of a theoretical analysis of viscous and thermal boundary layer behavior on the electrically insulating wall of a rectangular MHD channel, using momentum and energy integral approximations. Steady, two-dimensional, constant-property, low magnetic Reynolds number flow is assumed with magnetic and electric fields imposed parallel to the short and long channel side-walls respectively. Analytical and numerical solutions are obtained for laminar skin friction and heat flux, and for turbulent skin friction, as a function of distance from the channel entrance. These results are compared with those for the case of no applied fields and possible reasons for the differences are set forth. (auth)

41120 (N64-30509) EXPERIMENTS WITH MAGNETOHYDRODYNAMICALLY SUPPORTED SHOCK LAYERS. Research Report No. 191. Locke, E.; Petschek, H. E.; Rose, P. H. (Avco-Everett Research Lab., Everett, Mass.). Aug. 1964. Contract NAS w-748. 42p. (NASA-CR-58823). CFSTI $2.00 cy, $0.50 mn.

Shock-tube experiments were performed to quantitatively determine the interaction of a hypersonic flow with the magnetic field of a straight current-carrying wire oriented perpendicular to the flow direction. Most of the experimental work was performed in a 50-50 mixture of argon and oxygen, at an initial pressure of 1-mm Hg, and in a range of shock velocities between 4.3 and 6 mm/μsec. Data were obtained by observing the flow luminosity, using an image converter and mirror camera looking both perpendicular to and along the wire. A circular shock front was observed to stand up to 5½ cm in front of a 1-cm-radius cylinder producing the magnetic field. The data on shock position vs current were in excellent agreement with theory. (auth)

41121 (N64-30658) IONIZATION OF CESIUM AND SODIUM CONTAMINATED AIR IN THE HYPERSONIC SLENDER BODY BOUNDARY LAYER. Lenard, M. (General Electric Co., Philadelphia, Pa. Missile and Space Div.). Aug. 1964. Contract AF04(694)-265. 30p. (R64SD22).

An approximate procedure is used to predict the effect on air ionization of small amounts of cesium and sodium in the ablating surface material of pointed cones. Ionization is assumed to occur due to finite rate gas phase chemical reactions in the laminar boundary layer. An 11-species (N_2, O_2, N, O, NO, Cs or Na, NO^+, Cs^+ or Na^+, O_2^-, O^-, e^-), 16-reaction chemical system is assumed. (auth)

41122 (N64-31207) THE ALGEBRAIC STRUCTURE OF THE N-BODY PROBLEM. Rauch, L. M. (Seton Hall Univ., South Orange, N. J.). Oct. 1964. 36p. (NASA-CR-111). CFSTI $1.00 cy, $0.50 mn.

It is found that the union of initially disparate subgroups leads to a group whose properties are the formal tools that formulate the explicit solutions of the n-body problem. A brief indication of the applications of this evolved algebra is given. (auth)

41123 (NASA-TR-R-225) ANALYSIS OF THE ERRORS ASSOCIATED WITH THE DETERMINATION OF PLANETARY ATMOSPHERE STRUCTURE FROM MEASURED ACCELERATIONS OF AN ENTRY VEHICLE. Peterson, Victor L. (National Aeronautics and Space Administration, Moffett Field, Calif. Ames Research Center). July 1965. 22p. CFSTI $1.00 cy, $0.50 mn.

An analytic method is developed for estimating the errors in the density and pressure structure of a planetary atmosphere constructed from measurements of accelerations experienced by an entry body. Among the sources of error considered both singly and collectively are the measuring accuracy of the accelerometers, the uncertainties in entry speed, entry angle, and aerodynamic coefficients, the frequency of data measurements, and the uncertainty of the attitude of entry bodies having nonzero lift-to-drag ratios. Results of sample calculations are presented to show the accuracy with which the extremes of a range of postulated model atmospheres for Mars can be defined from measurements of accelerations experienced by a spherically shaped entry body. It is found that if the accelerometer method were used only over that portion of the atmosphere traversed at speeds greater than sonic speed, then any of the atmospheres postulated for Mars can be defined reasonably well even when errors from all sources are combined in the most unfavorable manner. Some of the results obtained by the analytic method are compared with those from more precise numerical calculations and the agreement is found to be excellent. (auth)

41124 (NP-15108) RESEARCH IN PHYSICS OF ELECTRON EMISSION AND ELECTRON TUBE TECHNOLOGY. Interim Report No. 5, October 16, 1964-April 15, 1965. Anderson, D. E.; Laponsky, A. B.; Peria, W. T. (Minnesota Univ., Minneapolis. Physical Electronics Research Lab.). Contract AF33(657)-10475. 243p.

Several aspects of electron emission and electron tube technology were studied. The main topics under discussion are secondary emission, multilayer thin film tunnel devices, thermionic emitters, influence of adsorbed alkali on surface properties, surface cleaning, alkali antimonide, and the theory of low energy electron diffraction. Each of these topics is examined. (M.O.W.)

41125 (ORNL-TM-1185) A SOLUTION TO ELECTROMAGNETIC INDUCTION PROBLEMS. Dodd, Caius Vernon (Oak Ridge National Lab., Tenn.). Aug. 1965. Contract W-7405-eng-26. 31p. Dep. mn; CFSTI $2.00 cy, $0.50 mn.

Thesis submitted to Univ. of Tennessee, Knoxville.

A technique is described for solving electromagnetic induction problems. The differential equation for the vector potential is derived from Maxwell's equations. The various terms in the differential equation are approximated by finite difference equations, yielding an equation for the vector potential at a point in terms of the vector potential at surrounding points. By a relaxation technique, the vector potential for any axially symmetric induction problem can be calculated. Once this vector potential is known, any physically observable electromagnetic phenomenon, such as induced current, induction heating density, and coil impedance, can be calculated. These phenomena are calculated. Curves of calculated coil impedance agree with measured coil impedance. (auth)

41126 (SCL-DR-65-75) THEORY OF ONE-DIMENSIONAL SHOCK WAVE PROPAGATION. Taoka, G. T. (Sandia Corp., Livermore, Calif.). June 1965. Contract AT(29-1)-789. 49p. Dep. mn; CFSTI $2.00 cy, $0.50 mn.

The general theory of the one-dimensional propagation of shock waves in a continuous medium is presented. Initially, the theory is developed for the purely hydrodynamic case. Later, the effects of elastic-plastic flow are included. The finite difference form of the fundamental partial differential equations is also presented. (auth)

41127 (SUDAER-238) STATISTICAL THEORY OF HOMOGENEOUS HYDROMAGNETIC TURBULENCE. Hassan, Sayed D. (Stanford Univ., Calif. Dept. of Aeronautics and Astronautics). June 1965. 98p. (AROD-4284:4). CFSTI.

The existence of equilibrium ranges in homogeneous hydromagnetic turbulence is analyzed by using Fourier techniques. It is found that the reasons for believing in the existence of the equilibrium range in classical turbulence (non-conducting fluid) also hold for hydromagnetic turbulence. The asymptotic form of different correlation tensors at large separation distance in homogeneous hydromagnetic turbulence is considered. One assumes the convergence of velocity and magnetic field cumulants at an initial instant, then determines from the dynamical equations how they will evolve with time. The techniques used involve a great deal of tensor manipulation. A theory of weak turbulence where one can neglect the role of pressure forces in developing power laws, and thus have analytic spectrums is considered. The kinematics of the fluid motion then lead to certain asymptotic forms for different spectrums at small wave numbers, and the dynamics of the motion will lead to the permanence of large eddies and consequently to the invariance of Loitsainsky integrals in the case of isotropic turbulence. Lastly, the final period of decay was considered. The kinetic and magnetic energies are decaying at a rate proportional to $(t-t_0)^{-5/7}$ with time. The turbulence is approaching equipartition of energy at large times. A state of isotropy can be achieved in the final period of decay under certain circumstances, although the fluid was originally non-isotropic. (M.O.W.)

41128 (UCRL-12466) HIGH-PRESSURE SHOCK WAVE EXPERIMENTS IN ARGON AND XENON. Keeler, R. Norris; Alder, Berni J.; van Thiel, Mathias. Lawrence Radiation Lab., Univ. of California, Livermore). May 17, 1965. Contract W-7405-eng-48. 19p. (CONF-650435-1). Dep. mn; CFSTI, $1.00 cy, $0.50 mn.

From 5th Shock Tube Symposium, Silver Spring, Md.

The following were shown from work in expendable shock tubes: pairwise additivity for argon and xenon holds at close interatomic separations; the repulsive potential for argon and xenon is a universal function; an accurate intermolecular potential for argon and xenon was derived; deviations from classical behavior due to electronic effects are significant at the highest pressures for xenon; and the melting transition in argon was observed. (auth)

41129 HIGH-FREQUENCY SCATTERING BY AN IMPENETRABLE SPHERE. Nussenzveig, H. M. (New York Univ., New York). Ann. Phys. (N.Y.), 34: 23-95 (Aug. 1965).

The scattering of a scalar plane wave by a totally reflecting sphere (hardcore potential) at high frequencies is treated by a modified Watson transformation. The behavior of the solution both in the near and far regions of space is discussed, as well as the accuracy and domain of applicability of the WKB approximation and classical diffraction theory. It is shown that different transformations are required in the forward and backward half-spaces, and corresponding integral representations for the primary

wave are derived. The transformations are rigorously proved and the convergence of the residue series is discussed. In the shadow region, the physical interpretation of the complex angular momentum poles in terms of surface waves is in agreement with Keller's geometrical theory of diffraction. In the lit region, sufficiently far from the shadow boundary, the WKB expansion for the wave function is confirmed up to the second order. On the surface of the sphere, Kirchhoff's approximation is accurate, except in the penumbra region, where the behavior is described by Fock's function. The diffraction effects in the neighborhood of the shadow boundary are investigated and the corrections to classical diffraction theory are obtained. The shift of the shadow boundary is evaluated. The expression for the wave function in the Fresnel-Lommel region is derived and applied to the discussion of the Poisson spot and the behavior near the axis. The total scattering amplitude is evaluated for all angles, including the neighborhood of the forward and backward directions. The corrections to the forward diffraction peak and the transition to the region of geometrical reflection are discussed. The modified Watson transformation is also applied directly to the scattering amplitude. The connection between representations valid in different regions is established. (auth)

41130 CLASSICAL STATISTICAL MECHANICS OF THE PARTICLE MIXTURES WITH TYPE-DEPENDENT EXTENSIVE INTERMOLECULAR INTERACTIONS. Kelbg, G. (Universitaet, Rostock, Ger.). Ann. Physik (7), 14: 394-403(1964). (In German)

Formulas for the limit law and the radial distribution functions of a particle mixture with extensive general type-dependent intermolecular potential were derived. The method of auxiliary variables was used. Applications are given to the theory of strong electrolytes and quantum plasmas. (tr-auth)

41131 APPROXIMATE CALCULATION OF THE CLASSICAL TWO-PARTICLE COLLISION OPERATOR. Haubold, Karl. Bull. Classe Sci., Acad. Roy. Belg. (5), 50: 991-1008(1964). (In French).

A method is developed by which the eigenvalues of the classical two-body collision operator can be calculated to any order in the coupling constant. In particular, the dependence of these eigenvalues with respect to the eigenvalues $l(l+1)$ of the angular momentum operator in velocity space is shown. (D.C.W.)

41132 ON THE BOGOLUBOV ASYMPTOTIC CONDITION FOR NON-UNIFORM SYSTEMS. Nicolis, G. (Universite Libre, Brussels). Bull. Classe Sci., Acad. Roy. Belg. (5), 50: 1009-23(1964).

The Bogolubov boundary conditions for the weakening of initial-state correlations are used to write explicitly the equation in an inhomogeneous system and in the two-body collision approximation. The formalism employed is parallel to that developed by Prigogine, so that a comparison may be made with the equations derived by Prigogine and Severne. A complete identity of the results is established at least in the asymptotic limit ($t \to \infty$). Finally, a different form of the boundary condition is proposed which permits the direct establishment of the identity of the two theories in a much more general form; it is observed that, in addition, this boundary condition permits a treatment of Bogolubov's theory within the framework of the theory of Prigogine. (auth)

41133 LOW VOLTAGE DISCHARGE AT VERY HIGH INTENSITY INITIATED BY LASER PULSE. Chartier, Germain; Septier, Albert (Faculte des Sciences, Orsay, France). Compt. Rend., 260: 4685-8(May 3, 1965). (In French).

By focusing the luminous beam of a ruby laser on a titanium hydride target constituting one of the electrodes of a diode, current pulses with an intensity attaining several hundred amps for some microseconds were obtained. This procedure makes it possible to envisage the creation of very dense discharges or of high intensity ion sources. (tr-auth)

41134 PRODUCTION OF TROCHOIDAL ELECTRON BEAMS HAVING REDUCED ORBITAL MOTION. Prudkovskii, G. P. Elektron. Bol'shikh Moshchnostei, No. 3, 129-47(1964). (In Russian).

The production of electron beams using electron sources proposed by P. L. Kapitsa which make crossed-field oscillators more efficient is investigated. The electron-optical properties of emitters used in high-power c-w crossed-field oscillators—the planotron and nigotron—are discussed. The production and characteristics of trochoidal electron trajectories were investigated using an analog computer (a trajectograph) for the case in which a cylindrical electron emitter was placed inside a rectangular slot in the surface of a cathode. Such a system was found to be a focusing immersion-type lens. Its optical strength increased with the depth at which the emitter was located inside the slot. At a certain distance from the slot, the trajectories bunched together (like a focus), this bunching repeating itself with a period equal to the period of the cycloid. Conditions were also found under which the electron beam followed an equilibrium trajectory characterized by the absence of any orbital motion in mutually perpendicular electric and magnetic fields. (ATD)

41135 ON THE FLOW OF TWO CONDUCTING INCOMPRESSIBLE IMMISCIBLE FLUIDS BETWEEN TWO NON-CONDUCTING PLATES. Kapur, J. N.; Shukla, J. B. (Indian Inst. of Tech., Kanpur, India). Istanbul Univ., Fen Fak. Mecmuasi, Seri A, 27: 59-66(1962).

The steady flow of two conducting incompressible and immiscible fluids between two non-conducting parallel plates was considered in the presence of a transverse magnetic field. It was shown that as the Hartmann numbers for the two fluids increase, the flux, the interface velocity and the skin frictions at the two plates decrease. It was shown that unlike the case of non-conducting fluids where the velocity maximum occurs in the less viscous fluid, here the velocity-maximum can occur in the more viscous fluid also. (auth)

41136 INTERACTION OF ELECTROMAGNETIC SHOCK WAVES IN NONLINEAR TRANSMISSION LINES. Ostrovskii, L. A. (Gor'kii State Univ., USSR). Izv. Vysshikh Uchebn. Zavedenii, Radiofiz., 8: 285-91(1965). (In Russian).

The problem of shock-wave interaction in a line with an arbitrary, quasistatic, nonlinear characteristic is considered. The question of shock-wave propagation in a line with a step variation of parameters is also studied. (auth)

41137 TRANSIENT MAGNETOHYDRODYNAMIC FLOW IN AN ANNULAR CHANNEL. Narasimhan, M. N. L. (Mathematics Research Center, Madison, Wis.). J. Math. Mech., 14: 353-63(May 1965).

A transient solution is obtained for the problem of unsteady flow of a viscous incompressible electrically conducting fluid in an annular channel with an impressed radial transverse magnetic field. Expressions for the velocity distribution and the magnetic field components are obtained in terms of Bessel and Lommel functions and in the form of convolution integrals taking the longitudinal pressure as an arbitrary function of time. It is found that the response of the fluid in damped and the effect of the magnetic field is to shorten the flow development time further than in the nonmagnetic flow and also to flatten the velocity profile. (L.B.S.)

41138 REGISTRATION OF FISSION FRAGMENT TRACK ON SOLID SURFACE. Kikuchi, Takeo (Japan Atomic Energy Research Inst., Tokyo). Japan. J. Appl. Phys., 4: 386-7(May 1965).

Fission-fragment tracks were previously observed on a fractured surface of sintered UO_2 and on a surface of a LiF crystal. Relations between the two cases are considered. The relation between a dimension of a damaged region and a depth from which a track is registered on a surface is discussed. (D.C.W.)

41139 THE INFLUENCE OF MAGNETIC AND ELECTRIC FRINGING FIELDS ON THE TRAJECTORIES OF CHARGED PARTICLES. Wollnik, H.; Ewald, H. (Uni-

versitaet Giessen, Ger.). Nucl. Instr. Methods, 36: 93-104(Sept. 1965).

The effects of fringing fields of electric and magnetic sector fields on the trajectories of charged particles are determined in a second-order approximation. This means that all terms are included that are of the same magnitude as the second order aberrations of ideal fields. The effects are either equal for the whole beam of particle trajectories or they are almost independent of the special fringing field distribution. This result renders the possibility of calculating an apparatus corrected for image aberrations of second order without a very precise predetermination of the positions of the shielding diaphragms for the fringing fields. From the view of an experimentalist it is thus possible, to a certain amount, to adjust a sector field by changing the positions of the shielding diaphragms without disturbing the correction of the aberrations. (auth)

41140 THE EVALUATION OF TOTAL ABSORPTION CROSS-SECTION FOR PHOTONS IN HIGH DENSITY ELECTRON GAS. Thompson, C. (Marquardt Corp., Van Nuys, Calif.). Physik Kondensierten Materie, 3: 402-21(1965).

The total absorption cross section for a photon by an electron gas is calculated in the high density limit. The calculation uses the Green's function formulation applicable to many-body problems. Only the simplest final states leading to a non-vanishing cross section, consisting of an electron-hole pair and a plasmon are taken into consideration. The contributions arising due to this cross section have a threshold near the plasmon energy and are peaked because of the initial rapid rise of the available phase space, with a total cross section for real metals of 10^{-17}–10^{-19} cm^2 per electron. This compares favorably with other absorption mechanisms. (auth)

41141 TIME DEPENDENT BEHAVIOR OF SURFACE IONIZATION EFFICIENCIES OF Li AND LiF ON W. Andresen, S. G.; Shipley, C. A. (Univ. of Colorado, Boulder). Rev. Sci. Instr., 36: 858-9(June 1965).

The time dependence of the ionization efficiency of W filaments for Li and LiF beams is studied. The filament is flashed at 2000°C to remove surface deposits, and the ionization efficiency is then measured over a 2 hr period. The results are explainable in terms of the adsorption of residual O_2 and F_2 on the W filaments. (T.F.H.)

41142 SOME CONSIDERATIONS ON THE PHYSICS AND TECHNIQUES OF FREE ELECTRONS AND IONS. Bas, E. B. (Eidgenoeissisches Technische Hochschule, Zurich). Schweiz. Arch. Angew. Wiss. Tech., 31: 182-9 (June 1965). (In German).

Using a few simple but fundamental relations of the optics of corpuscles, some conclusions concerning the motion of charged particles in electromagnetic fields are formulated, from which the principles of some applications of charged-particle motion are derived. (auth)

41143 MOLECULAR BEAMS. Frisch, O. R. Sci. Am., 212: 58-72; 74(May 1965).

Studies involving coherent beams of atoms and molecules are reviewed, beginning with production of the first molecular beam by Dunoyer in 1911. The influence of these studies on the development of modern physics and applications of molecular-beam techniques in various branches of physics are pointed out. Modern results of these studies include masers, lasers, and atomic clocks. (A.G.W.)

41144 AERODYNAMIC CALCULATIONS OF A GAS FLAME IN MAGNETOHYDRODYNAMICS. Yarin, L. P. (Kazakh Scientific-Research Inst. of Power Engineering, USSR). Teplofiz. Vysokikh Temp., 3: 285-93(Mar.-Apr. 1965). (In Russian).

An analysis was made of diffusional combustion in the laminar boundary layer between two plane-parallel gas streams flowing concurrently at different velocities and in the presence of a transverse magnetic field. In such a combustion process, nonequilibrium plasma is produced which is of interest for use in MHD generators. To solve the system of magnetohydrodynamic and kinetic equations formulated for the flow of reacting and conducting gas, the assumption was made that the gas is conducting only in an effective, magnetohydrodynamic layer. Outside this narrow layer the conductivities of the fuel, oxidizer and combustion products are negligible. By introducing this effective layer the solution was reduced to the integration of equations for the boundary layer without a source, i.e., to the calculation of a nonisothermal jet at a given temperature and velocity at the boundary of the effective zone. Since the effective layer is a weak discontinuity, the transport equations were solved separately for the fuel and oxidizer regions. A system of equations was obtained for calculating the locations of the combustion zone and the temperatures and velocities in it. To evaluate the effect of the magnetic field on the flame structure, calculations were made for gases having an identical temperature (300°K), a heat release rate of 10^4 kcal/kg, and a velocity of 1 m/sec (given for one stream only). A plot of the ratios of the velocities in the combustion zone in the absence and in the presence of the magnetic field was obtained as a function of an interaction parameter in terms of magnetic induction, conductivity, and velocity. The calculations showed that even at low magnetic inductions (1 Weber/m^2) and at low electric conductivities, the magnetic field has considerable influence on the aerodynamics of the flame. Other calculations of diffusional combustion in crossed magnetic and electric fields showed that depending on the sign of the interaction parameter the gas in the combustion zone can be either accelerated or decelerated, which may result in elongation or shortening of the flame. The method can be also used for determining the effect of the magnetic field on the aerodynamic structure of a turbulent flame. (auth)

41145 DIFFERENCE EQUATIONS OF DYNAMICS IN HAMILTONIAN FORM. Savich, A. V. Vestn. Mosk. Univ., Ser. III: Fiz. Astron., No. 2, 81-91(Mar.-Apr. 1965). (In Russian).

Difference equations of dynamics of a system of material points in hamiltonian form are formulated using special operators of finite-difference relations, near in their properties to partial derivatives. These equations preserve the most important transformation properties of the corresponding differential equations and also give for the same conditions the laws of conservation of energy and momentum. The solution of these equations for small oscillations and for the motion of charged particles in a constant magnetic field is given. (tr-auth)

41146 DEVELOPMENT OF THE MAGNETOHYDRODYNAMIC BOUNDARY LAYER DUE TO THE SUDDEN INITIATION OF MOTION OR SUDDEN DECELERATION OF A SUPERSONIC FLOW ON THE SURFACE OF A HALF SPACE. Vatazhin, A. B. Zh. Prikl. Mekhan. i Tekhn. Fiz., No. 2, 3-14(Mar.-Apr. 1965). (In Russian).

The nonstationary flow of a viscous, compressible, conducting liquid over the surface of a half-space is studied. Starting from the standard boundary-layer equations, Maxwell's equations, and Ohm's law, the various terms are ordered in the limit of low viscosity. (D.C.W.)

41147 VISCOUS DRAG AND HEAT MOTION IN THE FLOW OF A PARTIALLY IONIZED MEDIUM ALONG A PLANE CHANNEL, ALLOWING FOR AN ANISOTROPIC TRANSPORT COEFFICIENT. Sakhovskii, E. G. (Physico-Technical Inst., USSR). Zh. Prikl. Mekhan. i Tekhn. Fiz., No. 2, 88-91(Mar.-Apr. 1965). (In Russian).

Previous results on wall skin friction and temperature gradients in a plane-channel MHD flow where the flow is assumed to be viscous, incompressible, of constant ionization, and under a strong magnetic field are reproduced. These results are calculated numerically and plotted as functions of the Hartman number M for a set of electron and ion Hall parameters. For $\omega_e\tau_\theta \ll 1$ increase in M^0 causes a decrease in the skin friction which has its maximum at M = 0. The joule heating, on the other hand, attains a maximum at M = 1.6. For $\omega_e\tau_\theta = 1$, $\omega_i\tau_i\theta \ll 1$, if one includes anisotropy effects of the electrical conductivity, only a slight change is noticed in the skin friction or heat flow as compared with the case of homogeneous electrical conductivity. Finally, electron and ion Larmor gyrations are shown to change the above curves considerably, especially as a function of the ionization level. (ATD)

41148 MODELING OF CURRENT DENSITY DISTRIBUTION IN A MAGNETOHYDRODYNAMIC CHANNEL, ACCOUNTING FOR ANISOTROPIC CONDUCTIVITY. Kovalev, A. I. Zh. Prikl. Mekhan. i Tekhn. Fiz., No. 2, 91-3(Mar.-Apr. 1965). (In Russian).

The effect of tensor conductivity on the current distribution in a rectangular channel MHD flow was investigated by using a special model. The model consisted of replacing the fluid by polycrystalline bismuth having the same general tensor conductivity characteristics as the fluid itself with a Hall parameter of 4000 $cm^2/v \cdot sec$ at room temperature. The applied magnetic field was 5000 gauss, and the electrodes were continuous and made of copper. Analytically, the generalized Ohm's law $j = \sigma(-\text{grad } V + v \times B)$ was reduced to the simple form $j = -\sigma \text{ grad } V$ by defining an irrotational electric field $E^* = -\text{grad } V + v \times B$. The current density was determined from the expression $j_* = [1/(1 + \mu^2B^2)] [(1/\mu B) (-\mu B/1)]\text{grad } V$, and the conversion to current densities with the moving fluid was accomplished by $j = j_* \sigma_0 W_0 / U_{OM} M$, where M is the ratio of apparatus dimensions to those of the model. The maximum scatter in equipotential lines did not exceed 3%. Comparing the potential distribution in the channel with exact numerical estimates showed a 10% scatter in the data. (ATD)

41149 ELECTROMAGNETIC PROCESSES IN ANISOTROPIC ELECTROCONDUCTING LIQUID IN ALTERNATING MAGNETIC FIELD. Kim, K. I. Zh. Prikl. Mekhan. i Tekhn. Fiz., No. 6, 93-6(Nov.-Dec. 1964). (In Russian).

The electromagnetic phenomena in a liquid passing through a channel of rectangular cross section are investigated in order to establish the basic facts associated with the anisotropy of conductance. In the case of anisotropic conductance, the normal character of the processes in the liquid is destroyed. In the relation for the determination of the magnetic field in the channel, the edge effects of the inductor are ignored. Given these and some other conditions, the induced field in the liquid is determined. The results of the computation of the truncated systems are given in tabular form. It is concluded that anisotropy of conductance results in: reduced fundamental-frequency currents; the generation of zero-frequency currents; and the generation of multiple-frequency currents, the most substantial of which are the double-frequency currents. The zero-frequency and double-frequency currents result in the formation of useless stresses and in increased joule losses. (ATD)

41150 TWO ELECTROSTATIC PROBLEMS FOR REGIONS BOUNDED BY CYLINDERS. Tsyrlin, L. E. Zh. Tekhn. Fiz., 35: 973-82(June 1965). (In Russian).

The solution of the Laplace equation is discussed for the electrostatic potential V under the following two different sets of boundary conditions (r, Θ, and z are cylindrical coordinates): 1) $V = 0$ on $r = b$, $V = U(z,\Theta)$ on $r = a$, $z > h$, and $V = \pm U(-z,\Theta)$ on $r = a$, $z < -h$; 2) $V = 0$ on $r = b$ and $V = U(z,\Theta)$ on $r = a$, $-h < z < h$. In both problems U is an arbitrary function of its arguments and $b > a$. The solution is sought by separation of variables. This leads to an expression for V as a Fourier series in Θ, each coefficient in which is an integral over a separation parameter of the product of an unknown function of the separation parameter, an exponential function of z, and an involved expression containing Bessel functions of r. Paired integral equations for the unknown functions are derived from the boundary conditions. The Wiener-Hopf method is not directly applicable to these paired integral equations, but an altered procedure is developed which leads ultimately to an expression for V as an infinite series. A feature of this solution is that the series converges the more rapidly the larger the gap 2h between the inner cylinders in problem 1 or the longer the inner cylinder in problem 2. The series break down in the limit $b \to \infty$, but a successive approximation method is applicable in this limit. (ATD)

41151 A CYLINDER IN THE FIELD OF CURRENT-CARRYING CONDUCTORS. Fomin, A. A. Zh. Tekhn. Fiz., 35: 983-9(June 1965). (In Russian).

The problem of a cylinder of magnetic material in the the field of a finite number of conductors parallel to its axis carrying alternating currents is treated. The problem has technical applications to the electrodynamic suspension of solid and liquid metals. The solution is obtained with the aid of a Green's function in a straightforward way, and in addition to the field the impedance of the conductors and the force on the cylinder are calculated. The conductors are assumed to be infinitely thin in the radial direction but to have finite extension in azimuth. The solutions are obtained in the form of finite sums over the conductors of infinite Fourier series. In case the conductors are infinitely thin also in azimuth, the infinite series can be summed and the results obtained in closed form. There is considerable discussion of the condition under which neglect of the finite azimuthal extent of the conductors is justified. (ATD)

41152 ROTATING MAGNETIC FIELD AND SURFACE CURRENTS IN A POLYPHASE SYSTEM WITH SKEW POLE PIECES. Kuznetskii, R. S. (Giprostal' Scientific Research and Design Inst., Khar'kov). Zh. Tekhn. Fiz., 35: 1154-5(June 1965). (In Russian).

The magnetic field within and the currents on the surface of a dielectric cylinder are calculated under the boundary conditions that on the surface of the cylinder the magnetic field is perpendicular to the axis, is proportional to $\cos(\omega t - k\varphi)$, and makes an arbitrary but constant angle with the radius vector. Here ω is a constant frequency, t is the time, k is an integer, and φ is the azimuth angle. The calculation is based on earlier calculation for a radial polyphase rotating magnetic field. (ATD)

41153 A COLLECTION OF PROBLEMS ON MATHEMATICAL PHYSICS. Budak, B. M.; Samarskii, A. A.; Tikhonov, A. N. A Pergamon Press Book. International Series of Monographs in Pure and Applied Mathematics. Volume 52. New York, The Macmillan Company, 1964. 780p. $11.50.

Translated by A. R. M. Robson from Sbornik Zadach po Matematicheskoi Fizike.

A collection of engineering and physical problems leading to partial differential equations is presented with detailed instructions and solutions. (D,C,W.)

41154 THE MOTION OF ELECTRICALLY CONDUCTING FLUID FOR GIVEN DISTRIBUTION CONDITIONS OF CONDUCTION AND EDDY CURRENT. Agostinelli, C. (Universita, Turin). p.281-97 of "High Temperatures in Aeronautics." New York, Pergamon Press and Milan, Tamburini Editore, 1964. (In Italian).

The determination of the velocity and the magnetic field in an incompressible conducting fluid moving in a fixed receptacle with conducting metallic walls was made when the conduction current and vortex are assigned at all points of the confined volume of the receptacle and at all times and when the normal component of the magnetic field at the surface is known. These conditions, together with that the velocity be tangent to the surface which limits the receptacle, assure the unity of the solution. It is shown how the question is reduced to the resolution of the Neumann problem for the harmonic functions and that the hydromagnetic problem can be reduced to the quadrature when the vortex and the conduction current verify two conditions which consist of two differential equations with partial derivatives of the first order; one of these is derived from the Maxwell field equations and the other from the Euler motion equation. The case in which the current line and the vortex line are both straight, but generally not parallel, and in which the conduction current and the vortex depend only on time and not on the point is considered, in particular. The results obtained are applied to the case in which the contained volume of the recipient is an ellipsoid with three axes. It is shown how in this case the problem is solved completely with quadrature. (tr-auth)

41155 SPECIAL PROBLEMS IN NON-EQUILIBRIUM STATISTICAL MECHANICS (thesis). Feiock, Frank Donald. Iowa City, Iowa, Univ. of Iowa, 1964. 134p.

An investigation was made on the conditions under which the Kubo method will be useful for calculational purposes in non-equilibrium statistical mechanics and to apply the method in some detail to two special cases. It is shown that the Kubo formulas entail solving the equations of mo-

tion of the unperturbed system. Hence the method will be useful if approximate or exact solutions of these equations can be obtained. As an example of an approximate solution a system of charged particles in a rapidly oscillating electric field is considered. The conductivity of the system is expanded in a power series of the inverse frequency of the field. The series diverges for the Coulomb potential, but is found to converge if the charges are not too dense and if they interact via a screened Coulomb potential. To fourth order in inverse frequency, the conductivity is diagonal and reduces to the zero-order inertial effect for particles with equal charge to mass ratios. The scalar field with fixed sources is considered as an example of a system which is exactly soluble. An external force field is applied, and the general question of surface effects is discussed. It was found that the surface terms vanish in the infinite volume limit if the potential is bounded by a polynomial or finite degree. Terms associated with the sources were also found to vanish in the infinite volume limit. The average current per unit volume was computed for a constant external field. (Dissertation Abstr.)

41156 SIMILARITY RULES IN MAGNETOHYDRODYNAMICS BASED ON MULTI-FLUID THEORY (thesis). Blech, Joab Jacob. East Lansing, Mich., Michigan State Univ., 1964. 115p.

Similarity rules were derived in magnetohydrodynamics, in the physical space, based on a multi-fluid theory. The basic hypothesis of the multi-fluid theory is that the fluid consists of a number of fluid components, each with its own intrinsic properties (such as molecular mass, charge, etc.). Each of the species is assumed to be inviscid and non-heat conducting. The postulated fundamental equations for each fluid component are: equation of state, first law of thermodynamics, conservation of mass, and conservation of momentum. In addition two Maxwell's vector equations, describing the electromagnetic field, were inserted into the system of equations. The flow is assumed to be multidiabatic, i.e., there is injection of momentum as well as energy (heat) by means of sources from outside into the various fluid components. A steady flow is assumed which depends only on two spatial coordinates; but in the present multi-fluid theory such a flow is not a two-dimensional flow in the usual sense. The velocity, the electric and the magnetic fields have three components. After a reduction of the number of fundamental equations is made, the system of equations is linearized, i.e., it is assumed that a first order small perturbation theory describes adequately the flow field. In the present case of MHD a mere linearization of the system of equations seems to be insufficient for obtaining similarity rules. An additional procedure, i.e., some sort of a smoothing process, is applied in which a criterion for neglecting very small terms is introduced, thus leading to a simplified system of equations which governs the flow. A correlation between this simplified system of equations of the compressible flow and corresponding systems of equations of the incompressible flow is established for the case of aligned fields, in which the velocity and the magnetic fields in the undisturbed stream are parallel, and for the case of crossed fields, where the velocity and the magnetic fields in the undisturbed stream are perpendicular. Pressure coefficients for the individual species and for the gross fluid are calculated and correlated. As a special numerical case, a fully ionized plasma is considered and the ion pressure coefficient is plotted vs. the ion free stream Mach number for various orientations of the magnetic field. (Dissertation Abstr.)

41157 THE PROPAGATION AND GROWTH OF DISCONTINUITIES IN MAGNETOGASDYNAMICS IN THE PRESENCE OF FINITE CONDUCTIVITY (thesis). Secrest, Bruce Gill. Ames, Iowa, Iowa State Univ., 1964. 69p.

Magnetogasdynamical problems were studied in the presence of finite conductivity for an inviscid, non heat-conducting fluid. It is first shown that, although conductivity is a dissipative parameter, its nature is distinct from that of other similar parameters such as viscosity. The distinctive feature of conductivity in magnetogasdynamics is that it allows the existence of certain singular surfaces. The singular surfaces defined are ones which admit of discontinuities in certain variables. The existence of a singular surface moving with the velocity of the gasdynamical speed of sound is proved, and it is shown that the discontinuities in density, velocity, and pressure are stronger than those for the magnetic field. Equations are obtained for the growth of the wave, and it is shown that the front may either terminate in a shock in a finite or infinite time, or may be damped out. The time for the formation of the shock is seen to depend on the direction of the normal to the wave-front. Next, the decay of a shock wave was studied. It is shown that an energy hypothesis is needed to determine the velocity of propagation of the shock wave. Such a hypothesis was made and a differential equation for the velocity of propagation was obtained. Since the resulting differential equation depends on the angle between the magnetic field and the normal to the surface, it is only integrated for the case of a cylindrical wave front with a perpendicular magnetic field. Finally, the compatibility conditions were again applied to the basic equations to obtain the jumps in the vorticity and the current across a shock wave. For completeness, the cases of both finite and infinite conductivity are given. It was observed that the jumps can be obtained in the finite conductivity case by use of only the equation of motion, whereas for the infinite conductivity case, the energy equation is also needed. Thus the finite conductivity result is purely kinematical in nature. (Dissertation Abstr.)

41158 POSITRON ANNIHILATION IN SODIUM TUNGSTEN BRONZE (thesis). Gustafson, Daniel Ray. Ames, Iowa, Iowa State Univ., 1964. 104p.

The angular correlations of positron annihilation radiation from positrons annihilating in sodium tungsten bronze (Na_xWO_3) were measured, for x = 0.75, for (1,0,0), (1,1,0), and (1,1,1) orientations of the samples. These angular correlations and the positron lifetimes in sodium tungsten bronze are interpreted in terms of a model for the electronic structure in which the conduction electrons are assumed to lie in states that are essentially tungsten 5d states. Both the angular correlations and the lifetimes are consistent with this model. (Dissertation Abstr.)

41159 MANY BODY THEORY OF THE POSITRON ANNIHILATION IN METALS (thesis). Yeh, William Wen. Iowa City, Iowa, Univ. of Iowa, 1964. 102p.

A general theory of positron annihilation in metal is proposed for the calculation of both the angular correlation and the mean lifetime. The general case of interaction of electrons in a periodic potential and Coulomb interaction between electrons, and electrons and positrons is considered. These terms cannot be neglected. A collective description of the motion was used to redescribe the motion of the electrons. Using a random phase approximation and a subsidiary condition, the system can be described in terms of a short range electron-positron interaction. The short range electron-positron interaction arises in a natural way. In this formulation both the angular correlation and lifetime can be calculated using the same matrix element of N electrons, M positrons to the N-1 electrons, M-1 positrons, and two photons states. Using the completeness relations, the total transition rate becomes a product of two-particle Green's function and another quantity which is the single electron-positron transition amplitude for Bloch states. Expanding the two particle Green's function results in an infinitive order of ladder diagrams. A technique is devised to sum up all these diagrams. As a zero approximation the experimentally incorrect free electron gas results are obtained. (Dissertation Abstr.)

41160 POSITRON ANNIHILATION RATE IN AN ELECTRON GAS (thesis). Bergersen, Birger. Waltham, Mass., Brandeis Univ., 1964. 137p.

A discussion is given of different computational methods for the evaluation of the positron annihilation rate in an electron gas, and a comparison is given with experimental data for positron annihilation in certain metals. Special emphasis is put on the consistency requirements

of the problem, these being the polarization cloud around the positron should have unit charge, the electron-positron and electron-electron pair correlation function be positive definite even if the positron charge is varied, and the Nozieres and Pines sum rule for the dielectric constant should be satisfied. A detailed discussion is given on how these requirements are taken into account in perturbation theory. Finally, a specific ansatz is made for the polarization cloud around the positron in terms of a bound-state wave function orthogonalized to a set of deformed plane waves. In the latter calculation, although quite close agreement is obtained with experimental annihilation rates, the results and the method should be considered tentative. Only the simpler case of a fixed heavy impurity is discussed in detail. (Dissertation Abstr.)

41161 ATOMIC THEORY OF GAS DYNAMICS. Bond, John W. Jr.; Watson, Kenneth M.; Welch, Jasper A. Jr. Addison-Wesley Series in Aerospace Science. Reading, Mass., Addison-Wesley, 1965. 527p. $16.75.

The text includes a large amount of material needed to develop the fundamentals of plasma physics; and it combines pertinent elements of kinetic theory of gases, statistical mechanics, theoretical physics, and atomic physics. The fundamental concepts of physics necessary for engineering applications are stressed, especially those pertaining to missile technology and high-altitude nuclear explosion phenomena. The development of transport processes in gases starts with the microscopic phenomena of atomic physics and presents the macroscopic phenomena of gas dynamics as particular limiting cases. Transport phenomena are discussed. (J.F.P.)

41162 PERFORMANCE OF DOUBLE-DRIVER SHOCK TUBE. Lemcke, Bo (Massachusetts Inst. of Tech., Cambridge). 30p. (CONF-650435-2). Gmelin, AED-CONF-65-097-1.

From 5th Shock Tube Symposium, Silver Spring, Md.

The double-driver shock tube was shown to be a useful experimental tool for producing a moving shock wave in a stationary flow field. The performance in terms of wave histories and shock strengths was found to agree reasonably well with theoretical predictions, at least under moderate operating conditions. The second shock wave was found to have the important feature of being almost plane across the tube through the wall boundary layer. This implies that a pressure peak should occur at the wall immediately behind the second shock. Such a peak was also noticed on pressure records as well as wall temperature records. A method based on the sudden rise of the stagnation pressure of a conventional hypersonic wind tunnel to produce a blast wave in the test section showed considerable promise for shock-on-shock studies. A double-driver shock tunnel would thus be a promising extension of both methods to make studies of blast effects at high Mach numbers as well as high enthalpy levels. (auth)

41163 A METHOD AND APPARATUS FOR PRODUCING X-RAYS OF PARTICULAR WAVE LENGTHS AND APPLICATIONS THEREFOR. Watt, John Stanley (to Australian Atomic Energy Commission). British Patent 997,338. July 7, 1965. Filed Oct. 30, 1963.

A method of producing x rays of a particular wavelength consists in causing a secondary material to emit its characteristic x-radiation by excitation with fairly low energy (less than 500 kev) gamma radiation from a gamma ray emitting radioisotope (primary source). The sources of primary and secondary radiation and a gamma ray shield are so arranged that the secondary radiation emerges fairly free of primary radiation. The radioisotope and the secondary material are so selected that the energy of at least some of the gamma rays is greater than that of the K (or L) absorption edge of the secondary material, and the secondary material is one such that the K (or L) x rays produced have the desired wavelengths. The radioisotope is selected from the group consisting of ^{153}Gd, ^{155}Eu, ^{145}Sm, ^{125}I, ^{170}Tm, or ^{241}Am. The gamma shield is placed in front of the isotope source; and the secondary emitting material is in the form of a hollow truncated cone, the narrow end of which is situated behind the isotope source and the inclined portions extend beyond the shield. The apparatus may be expanded to include the excitation of a tertiary material with the secondary radiation, in which case the secondary material itself may act as the gamma ray shield. Using the characteristic x rays from an apparatus of this type, measurement of the thickness of coatings or for the analysis of constituents of a material may be made by projecting the x-ray beam onto the coating or material and measuring the intensity of the emergent beam. (B.L.M.)

Accelerators

41164 (CEAL-1022) BEAM MONITOR—CALIBRATION MEASUREMENTS WITH THE 6-Gev EXTERNAL ELECTRON BEAM OF THE CAMBRIDGE ELECTRON ACCELERATOR. de Pagter, James; Fotino, Mircea (Cambridge Electron Accelerator, Mass. and Harvard Univ., Cambridge, Mass.). June 30, 1965. Contract AT(30-1)-2076. 29p. (CONF-650636-2). Dep. mn; CFSTI, $2.00 cy, $0.50 mn.

From International Symposium on Electron and Photon Interactions at High Energies, Hamburg.

Problems related to beam monitoring and calibrations pertinent to experiments performed with photon or electron beams in the multi-Bev range are discussed. The behavior of the Faraday cup and that of quantameters normally used for determining the total energy contained in a photon beam were studied in the electron beam with a secondary emission monitor as an intermediate standard. (M.O.W.)

41165 (LA-DC-7147) AN AUTOMATIC LIQUID NITROGEN DISTRIBUTION SYSTEM FOR TWENTY-FIVE COLD TRAPS. Fretwell, J. H.; Bartlit, J. R. (Los Alamos Scientific Lab., Univ. of California, N. Mex.). [1963]. Contract W-7405-eng-36. 12p. (CONF-650802-5). Dep. mn; CFSTI $1.00 cy, $0.50 mn.

From Cryogenic Engineering Conference, Houston, Tex.

Small amounts of liquid nitrogen were economically distributed by a 450 foot, foam-insulated pipeline to twenty five cold traps at an electrostatic accelerator building. The automatic filling system operates on two 40-minute cycles per day. An individual LN_2 level control and a gas/liquid phase separator were required at each cold trap location. Design and economic considerations are evaluated for economy of installation and operation. (auth)

41166 (ML-767) MEASUREMENT TECHNIQUES FOR PERIODIC STRUCTURES. Gallagher, W. J. (Microwave Lab., Stanford Univ., Calif.). Nov. 1960. Contract AT(04-3)-21. 61p. Dep. mn; CFSTI $3.00 cy, $0.75 mn.

A description is given of cavity-resonator test methods, matching of couplers, uniform structure measurements, and buncher measurements as applicable to particle accelerators using periodic accelerating structures. (T.F.H.)

41167 (NIRL/R/76) AUTOMATIC CONTROL OF THE ELECTROMAGNETIC FIELD IN LINAC RESONANT CAVITIES. Gallagher-Daggitt, G. E. (National Inst. for Research in Nuclear Science, Chilton (England)). Rutherford High Energy Lab.). Mar. 1, 1965. 42p. Dep. mn; BIS $1.40; HMSO 7s.

Results of experimental investigations of the beam dynamics in the 50 Mev Proton Linear Accelerator indicate the need for maintaining good amplitude control of the radio frequency accelerating field. The methods whereby such control is achieved are briefly described. Transfer functions of the elements which govern the dynamic behavior of the fast acting control system are given and plots in the frequency domain are used to determine system accuracy and stability on the basis of simple regeneration theory. (auth)

41168 (NP-15253) VLIYANIE MAGNITNYKH EKRANOV V PROMEZHTKAKH MEZHDU BLOKAMI NA RABOTY PROTONNOGO SINKHROTRONA ITEF. (The Effect of Magnetic Screens in the Spaces Between Blocks on the Operation of ITEF Proton Synchrotron). Report No. 270. Simonov, B. I.; Skachkov, S. V.; Shchegolev, V. A. (Gosudarstvennyi Komitet po Ispol'zovaniyu Atomnoi Energii

SSSR, Moscow. Inst. Teoreticheskoi i Eksperimental'noi Fiziki). 1964. 11p. Dep. mn.

The influence of beam screening from the stray magnetic field in the straight sections of ITEP proton synchrotron upon the acceleration process was investigated. It was shown, that the screening of two sections, which are 4 blocks apart one from another (i.e., approximately 0.5 wave length of 13th and 14th resonant harmonics), exerts no considerable influence upon the accelerator operation. (auth)

41169 (NYO-3364-7) INDUCED RADIOACTIVITY IN THE COLLIMATOR SYSTEM OF A 31 Mev BROWN BOVERI BETATRON. Stroemme, Aksel (Norsk Radiumhospital, Oslo). [nd]. Contract AT(30-1)-3364. 4p. Dep. mn; CFSTI, $1.00 cy, $0.50 mn.

The collimator system of the BBC 31-Mev betatron can be handled without noticeable radiation hazard if the field equalizer system is not touched directly with the hands, even after repeated irradiations. This can easily be obtained by means of a proper working technique or special handling tools. In more modern betatrons the collimator system and the different field equalizers are safely mounted inside the apparatus and remotely controlled. The radiation hazard problems due to collimator irradiation are therefore of no practical importance. (auth)

41170 (SLAC-42) TWO-MILE ACCELERATOR PROJECT. Quarterly Status Report, October 1-December 31, 1964. (Stanford Linear Accelerator Center, Stanford Univ., Calif.). Apr. 1965. Contracts AT(04-3)-400 and AT(04-3)-515. 116p. Dep. mn; CFSTI, $4.00 cy, $0.75 mn.

Development progress of the two-mile electron accelerator is presented. Information is given on plant engineering, systems engineering and installations, accelerator physics, instrumentation, heavy electronics, mechanical design and fabrication, klystron studies, beam switchyard, target area development, and pre-operations research and development. (M.O.W.)

41171 (N64-33402) DANGER CAUSED BY RADIATION IN THE BEAMS AND BEAM ZONES OF THE SYNCHROCYCLOTRON. Baarli, J. Translation of Dangers dus aux Radiations dans les Faisceaux et les Zones de Faisceaux au Synchrocyclotron, from a report of the MSC (Synchrocyclotron Machine) Meeting, June 21, 1963. 6p. (NASA-TT-F-9136). CFSTI, $1.00 fs, $0.50 mn.

The danger caused by synchrocyclotron radiations varies with the nature of the beams, their intensities, particle energies, and the extent of scattering. The biological effects and damage due to radiations are discussed, and dose limits are defined. The maximum permissible particle flux is given for various regions in the proton and neutron rooms for 600-Mev protons, 400-Mev neutrons, 50-Mev π^--mesons, and μ mesons. (CFSTI)

41172 THE RADIOFREQUENCY SYSTEM OF AN ISOCHRONOUS CYCLOTRON. Rosatelli, C. (Universita, Genoa). Alta Freq., 33: 337-45(June 1964). (In Italian).

The r-f system of the AVF cyclotron now under construction at the University of Milan is discussed. The accelerator is designed to accelerate protons up to 50 Mev. The resonator circuits and the r-f power supply are considered, together with measurements on a full-scale model of the resonator. (D.C.W.)

41173 AN EVALUATION OF THE ABERRATIONS OF FOCUSED BEAMS OF CHARGED PARTICLES CAUSED BY SPACE CHARGE. Kanaya, K.; Kawakatsu, H.; Yamazaki, H. (Electrotechnical Lab., Tokyo). Brit. J. Appl. Phys., 16: 991-1007(July 1965).

The aberrations caused by the space charge in both focused electron and ion beams, which prevent the attainment of highly resolved images in electron microscopy, and which set a limit to the maximum current density in electron or ion beam machines, are evaluated. The aberrations caused by space-charge defects, such as defocusing and change of magnification, as well as spherical aberration, coma, curvature of field, astigmatism, and distortion, are deduced by means of the eiconal method by use of the potential distribution of the space charge of the beam itself in the focusing lens. It is found that, although the defocusing effect due to space charge is a most important defect, the other aberrations caused by space charge are rarely as severe as the defocusing, because all aberrations owing to space charge act so as to reduce the normal Seidel aberrations. According to the numerical examples, even in electron microscopy and electron beam devices with a high current, the resolving power or the minimum spot size is not yet limited by the space-charge effect, but by the spherical aberration and astigmatism caused by manufacturing inaccuracy or inhomogeneity of the material. The caustic patterns of focused ion beams are, in general, much more affected by space charge than those of electron beams of the same incident energy, because of the large mass of the ion. It is experimentally ascertained that, even though the increase of focal length is certainly caused by the defocusing effect owing to space charge, a limit to the radius of least confusion of a focused ion beam with an accelerating potential of 30 kv and a beam current 500 μA is apparently not yet set by the space-charge effect, but by spherical aberration, because of the cancelling action of negative and positive aberrations. (auth)

41174 PRODUCTION OF INTENSE BEAMS OF NEUTRONS USING A CYCLOTRON WITH SEPARATED ORBITS. Bull. Inform. Sci. Tech. (Paris), No. 89, 53-8(Jan. 1965). (In French)

The design and principal parameters of a cyclotron with separated orbits are described. A critique of the project is given. The study of the production of intense neutron beams using such a cyclotron is summarized, with a consideration of possible improvements on the original design and its advantages and disadvantages. (J.S.R.)

41175 THE U. W. O. RACE-TRACK MICROTRON. Brannen, Eric; Froelich, H.; Sells, V. (Univ. of Western Ontario, London). Can. J. Phys., 43: 1555-7(Aug. 1965).

The use of a race-track design for the magnetic guide field of four sectors with uniform fields has advantages over a conventional microtron with a homogeneous field. The magnet gap between the sectors has a width of only 7.2 mm. The energy gain per orbit can be varied continuously, and synchronism can be obtained by adjusting the width of the central region between the sectors. A compact three-orbit machine (2.3 Mev 100ma) was designed and extension of the method indicates operation up to the 100 Mev region at least. (F.S.A.)

41176 PHYSICS WITH STORAGE RINGS. CERN Courier, 5: 103-6(July 1965).

Some indications are given of how the recent experiments on proton-proton scattering can be extended in scope by the construction of the proposed intersecting storage rings for the CERN proton synchrotron. The general characteristics of the rings are considered, and a diagram of the general layout of the ISR buildings is shown. (L.B.S.)

41177 RESULTS OBTAINED WITH A NEW TYPE OF SELF-FOCUSED LINEAR ACCELERATOR FOR HEAVY IONS. Boussard, Daniel (Faculte des Sciences, Orsay, France). Compt. Rend., 261: 345-8(July 12, 1965). (In French).

It was shown previously that it was possible to assure simultaneously the acceleration and focusing of particles in linear accelerators with slip tubes. A prototype accelerator with relatively low energy (200 kev) was constructed to determine the properties of this type of focusing. The characteristics of the prototype and preliminary results on the measurements of the current yield, beam acceleration, and phase acceptance are reported. (J.S.R.)

41178 IMPLANTATION OF THE 200-Gev SYNCHROTRON AT BERKELEY. Decae, Andre. Ind. At., 9: 51-65 (1965). (In French).

The study survey for the positioning of an accelerator of vast dimensions calls for studying the stability of the terrain on which it should be constructed and the development of suitable methods for the precise structural placement of the various elements of the machine. A first section reviews the diverse factors susceptible of affecting the stabil-

ity of the sub-soil for the foundations of the new Berkeley synchrotron with a radius of 704 meters (770 yards), and shows that the present site chosen seems capable of supporting a construction of this sort. A second section lists the metrological procedures developed for the positioning of the magnets. New metrological methods were developed and electronic measuring instruments capable of full automation were perfected to take care of the dimensions of the machine, and the need to perform these operations in the shortest possible time with a reduced staff, and above all the requirement of maintaining permanent control over the position of the elements during the operation of the accelerator. A final section lists the studies which must be worked out in Berkeley before the actual operations of construction can begin. (auth)

41179 SOME ASPECTS OF NUCLEAR PHYSICS AT 500 Mev. Lombard, Roland (C.N.R.S., Orsay, France). Ind. At., 9: 66-74(1965). (In French).

The study of nuclear structure with the aid of unstable elementary particles, such as the meson(π) or the meson (μ), will enable nuclear physics to take another great leap forward. Even a hasty survey of this field of investigation brings out the wealth of information contained in these new experiments. From the experimental point of view, all the tentatives made in this field run up against the problem of intensity: machines with a particle flux sufficiently great to enable exact measures to be made are still lacking. It is in this perspective that the project for a high intensity cyclotron at the Zurich Polytechnicum, which is the subject of this article, becomes most meaningful. (auth)

41180 RELATION BETWEEN DIOCHOTRON AND NEGATIVE MASS INSTABILITIES. Neil, V. Kelvin; Heckrotte, Warren (Univ. of California, Livermore). J. Appl. Phys., 36: 2761-6(Sept. 1965). (UCRL-12164).

A cylinder of electrons infinitely long and infinitesimally thin in the radial direction is used to show the equivalence of the diochotron and negative mass instabilities. The electrons have a unique relativistic velocity in the azimuthal direction. The external magnetic field has a radial gradient, and a criterion for stability is derived that places a lower limit on the field gradient. This criterion shows that the instability can occur at energies below the transition energy of the magnetic field. (auth)

41181 THE ELECTROSTATIC ION BEAM ACCELERATOR OF THE CENTRAL RESEARCH INSTITUTE FOR PHYSICS. Eroe, Janos; Klopfer, Ervin; Kostka, Pal; Kovacs, Istvan; Merey, Imre; Valyi, Laszlo; Varga, Laszlo. Magy. Tud. Akad. Kozp. Fiz. Kut. Int. Kozlemen., 13: 73-88(1965). (In Hungarian).

The Van de Graaff-type pressurized generator of the Central Research Institute for Physics is described. At present, the highest voltage of the generator is 3.3 Mv; up to now ions have been accelerated to energies of 2.1 Mev. Passing through 90° deflecting magnet, the ion beam can be focused onto any of the three target areas where the maximum intensity of the beam is found to be 4 to 5 μamp, the stability in energy being 1×10^{-3}. (auth)

41182 ON AN ACCELERATOR OF NEGATIVE IONS. Andrade E Silva, J.; Lochak, G. (University of Paris). Nucl. Instr. Methods, 36: 112-18(Sept. 1965). (In French).

The energy dispersion at different points of particle beams emanating from a negative ion accelerator is studied. Three simple methods permitting the reduction of this dispersion on a target located on either beam are suggested. (auth)

41183 A BEAM CURRENT INTEGRATOR FOR PULSED POSITIVE ION ACCELERATORS. Blignaut, E.; Kritzinger, J. J. (Southern Universities Nuclear Institute, Faure, Republic of South Africa). Nucl. Instr. Methods, 36: 176-8(Sept. 1965).

A current integrator capable of integrating and measuring positive currents in the range 100 μa to less than 1 na for direct and pulsed currents has been developed using the integrating capacitor principle. This has been made possible mainly by reducing the leakage current to less than 5×10^{-12} a by means of a simple electronic circuit. (auth)

41184 A HIGH-INTENSITY, PARTIALLY SEPARATED, BEAM OF ANTIPROTONS AND K-MESONS. Brautti, G. (Universita, Trieste, Italy and Istituto Nazionale di Fisica Nucleare, Trieste, Italy); Fidecaro, G.; Massam, T.; Morpurgo, M.; Muller, Th.; Petrucci, G.; Rocco, E.; Schiavon, P.; Schneegans, M.; Zichichi, A. Nuovo Cimento (10), 38: 1861-74(Aug. 16, 1965).

A beam of small production angle and large acceptance has been designed at the CERN Proton Synchrotron in order to yield partially separated, high-intensity beams of antiprotons and K-mesons. The features of the beam are discussed, together with the experimental results. (auth)

41185 IMPROVED SERIES OF ION GUN PARTS. Crawford, C. K. (Massachusetts Inst. of Tech., Cambridge). Rev. Sci. Instr., 36: 844(June 1965).

A set of standardized components and parts for ion sources is described. The components are particularly suited to large-diameter beams and right-angle intersections. The convenience, modular nature, ease of assembly, and other advantages of these components are outlined. (T.F.H.)

41186 SHUTTER FOR X-RAY OR ELECTRON BEAMS. Ritz, Victor H. (Naval Research Lab., Washington, D. C.). Rev. Sci. Instr., 36: 862-3(June 1965).

A mechanical shutter for x-ray or electron beams is described, whose purpose is to provide accurate control of exposure time of targets. The shutter inserts or removes a tungsten-alloy plug in the path of the beam by means of a solenoid-actuated drive. The exposure time using this system is found to be reproducible within 0.1%. (T.F.H.)

41187 STABILITY OF MOTION OF A CHARGED PARTICLE IN A MAGNETIC FIELD. Khapaev, M. M. (Moscow State Univ.). Soviet J. Nucl. Phys. (English Transl.), 1: 193-4(Aug. 1965).

Translated from Yadern. Fiz., 1: 274-6(Feb. 1965).

The motion of a charged particle in a straight helical magnetic field is studied by the methods of averaging. Adiabatic invariants are constructed and it is shown that the particle can be trapped in the vicinity of the axis of helical symmetry of the field. (auth)

41188 MEASUREMENTS OF BUNCH-INJECTOR OUTPUT PARAMETERS. Gross, V. F. Uskoriteli, No. 6, 51-5 (1964). (In Russian).

The output of a 2860 Mc magnetron generator is connected to a wave guide with a non-reflecting end. Power for the two resonating cavities of the injector-pulser and for the measuring resonator is tapped from the wave guide at appropriate intervals to maintain proper phase relationships. A hot tungsten needle serves as the electron source; the operating life of a needle is 10 hours. The maximum current per pulse is 80-110 ma; average current is 90-120 μa for 100-kev electrons. (TTT)

41189 MEASUREMENTS OF THE PHASE LENGTH OF AN ELECTRON PULSE PRODUCED BY AN INJECTOR-PULSER. Gross, V. F. Uskoriteli, No. 6, 56-61(1964). (In Russian).

With the proper electric field in an injector-pulser and proper phase shift, it is possible to obtain electron pulse lengths on the order of 2-3°. Two methods are described for measuring the pulse length by placing a toroidal measuring-resonator between the injector-pulser and a screen. In the first method the deflection and diameter of the electron beam is measured as a function of the distance L between the measuring-resonator and the screen. In the second case the measuring resonator is tilted by an angle α. Equations are presented for determining the phase shift $\Delta\phi$ in terms of L or α, and for determining the values of L or α for which $\Delta\phi$ is a minimum. (TTT).

41190 MEASUREMENT OF RESONATOR Q-VALUE CONSIDERING LOSSES IN THE COUPLING CIRCUIT. Shchedrin, I. S. Uskoriteli, No. 6, 62-4(1964). (In Russian).

The Q-value of a resonator is most easily measured by

measuring the quadrupole coupling between a driving circuit, the resonator circuit, and a detector circuit. If the reactive components of the coupling circuits are small, the measured Q-value will be accurate only if the driving and resonator circuits are closely matched; and such matching is difficult to obtain. Equations are presented for the Q-value in terms of the charge loads for two different degrees of coupling between the driving and resonator circuits. Using these equations the Q-value can be measured by arbitrary matching between the driving, resonator, and detector circuits. (TTT)

41191 INVESTIGATION OF MAGNETRON PERFORMANCE WITH A PAIRED RESONATOR SYSTEM. Milovanov, O. S.; Shchedrin, I. S. Uskoriteli, No. 6, 65-70 (1964). (In Russian).

The efficiency of an accelerating system can be improved by using the magnetron generator to drive more than one resonator. Equations are presented for matching the impedances when two resonators are driven by one generator. The results are extended to 2n generators. (TTT)

41192 APPARATUS FOR TESTING ION INJECTORS. Morozova, I. G. Uskoriteli, No. 6, 100-4(1964). (In Russian).

The apparatus consists of a vacuum system capable of maintaining pressures on the order of 10^{-6} mm Hg, a feed system for the operating gas, a 2000-volt power supply (maximum output current 150 ma), and a system to focus the beam. Ion injectors of various types can be mounted and tested with this system before they are mounted on the accelerator for which they are designed. Equipment is described for measuring various output parameters. (TTT)

41193 CYCLOTRON INJECTOR. Popov, B. M.; Vinogradova, L. I.; Kondrat'ev, A. S. Uskoriteli, No. 6, 112-15(1964). (In Russian).

Three types of ion injectors were studied to obtain high-intensity beams in a cyclotron: anode, extraction ring, dee; anode plus single lens; and anode, ring, grid, and dee. The first scheme is limited by discharges on the extraction ring, and requires extremely low residual gas pressures. In the second scheme the extraction ring is placed inside an insertion in the dee chamber, and the whole system acts as a single lens. With this scheme it is possible to increase the intensity of the ion beam by a factor of 1.2 to 1.5. In the third case the grid shields the extraction ring from the high-frequency field of the dee and reduces the chance of an induction discharge. Proper focusing with this scheme increased ion current by a factor of 20. With the third scheme it is possible to obtain shorter ion pulses of higher intensity than was previously possible with a cyclotron. Experiments were carried out with a deuteron beam. (TTT)

41194 SPECIFIC DISPERSION OF A MAGNETIC SECTOR FIELD WITH DOUBLE FOCUSING BEAM. Mizin, Yu. V. Uskoriteli, No. 6, 116-19(1964). (In Russian).

Equations and graphs are given for the specific dispersion $(E/\Delta E)$ as a function of the angle S between the axis of the beam outside the magnetic field and the boundaries of the magnetic field; the angular width of the magnet; and the ratio l/r, where l is the distance from the source to the magnet, and r is the radius of curvature of the beam inside the magnet. (TTT)

41195 MEASUREMENT AND ANALYSIS OF THE MAGNETIC CENTER PLANE IN A CYCLOTRON. Wang, Ta-chi; Wang, Chuan-ying. Yuan Tzu Neng, No. 1, 1-7 (1965).

The Hall effect method was used to measure the radial component of a magnetic field and the magnetic center plane. The magnetic center plane was found to coincide with the geometric center plane. (A.G.W.)

41196 CONCERNING THE INFLUENCE OF SPACE CHARGE ON BEAM FOCUSING AND ENERGY DISPERSION IN THE FIELD OF A PLANE CAPACITOR. Shapovalov, A. S. (Saratov State Univ., USSR). Zh. Tekhn. Fiz., 35: 1053-62(June 1965). (In Russian).

The influence of space charge on the motion of a plane charged-particle beam of finite angular divergence entering at 45° the uniform electric field of a plane capacitor is discussed. The calculations are nonrelativistic. With the aid of simplifying assumptions concerning the particle distribution in the beam cross section, nonlinear equations are derived for the motion of the limiting particles of the beam. These are solved by successive approximation to terms characterizing the space charge effects. The solutions are discussed, and the effects of space charge on the maximum displacement of the beam in the direction of the field and on the sharpness of focus are presented graphically for beams with angular divergences up to 20°. (ATD)

41197 CORRECTION OF THE ANGULAR ABERRATIONS OF A TWO-SECTOR ELECTROSTATIC ANALYZER. Zashkvara, V. V.; Korsunskii, M. I.; Kosmachev, O. S. Zh. Tekhn. Fiz., 35: 1063-7(June 1965). (In Russian).

A continuation of earlier work is presented. The aberrations of a 180° electrostatic analyzer due to angular divergences of the beam in the radial and axial directions were investigated experimentally with a 1 kev electron beam. The electrodes were laminated, and the potential on them varied linearly in the axial direction. The 180° sector was replaced by two identical 90° sectors of which the fields could be independently adjusted. The aberrations were minimized by separately adjusting the fields of the two sectors. It was found that the resolving power could be increased by a factor of 5 over that attainable with the one-sector instrument, and that the luminosity could be increased by an order of magnitude while decreasing the resolving power by a factor 1.7. It is concluded that other aberrations can also be corrected by employing more independently adjustable sectors. (ATD)

41198 SPHERICAL ABERRATION OF A COMBINED QUADRUPOLE LENS WITH A BELL-SHAPED FIELD DISTRIBUTION. Dymnikov, A. D.; Fishkova, T. Ya.; Yavor, S. Ya. (Inst. of Physics and Tech., Academy of Sciences, USSR). Zh. Tekhn. Fiz., 35: 1068-76(June 1965). (In Russian).

The spherical aberration of a combined electrostatic and magnetic quadrupole lens is calculated. Formulas for the spherical aberration are first derived for an arbitrary distribution of field strength on the axis and are then specialized to the case in which the electric and magnetic fields are both proportional to $1/(1 + (z/d)^2)^2$, where z is the axial coordinate and d is a constant. Curves are given showing the spherical aberration coefficients as functions of the total excitation and of the ratio of the electric to the magnetic field strength. The spherical aberration of a doublet consisting of two combined electrostatic and magnetic quadrupole lenses is discussed briefly, and it is shown that the spherical aberration can be compensated over the entire length of the linear image. (ATD)

41199 AUTOMATIC BETATRON GAMMA-RAY BEAM INTENSITY OPTIMIZATION. Balamatov, N. N.; Goryachev, B. I. Zh. Tekhn. Fiz., 35: 1091-7(June 1965). (In Russian).

An automatic control device for maintaining the gamma-ray beam from a betatron at peak intensity is described, its design is discussed, and its operation is explained in detail. Only the injection phase was controlled because the other relevant quantities, the injection energy and current, are relatively stable and do not require automatic regulation. The injection phase was moderated with a square wave of half the pulse repetition frequency, and the difference between the gamma-ray intensities for the even and odd pulses provided the error signal. The design was complicated by the presence of considerable random variations from pulse to pulse of the gamma-ray intensity, which made it necessary to employ a rather long time constant in the input circuit. This long time constant, on the other hand, made it possible to use a simple motor-driven potentiometer to control the injection phase. In the experiments with the MSU betatron it was found that the optimum values of the control system parameters (input time constant and modulation amplitude) were close to the calculated values, and it is concluded that the design equations presented are reliable. The efficiency of the control system can be further increased only by decreasing the rapid intensity

fluctuations, which present themselves to the control system as noise. (ATD)

41200 AN ELECTRODYNAMIC METHOD FOR DECELERATING MOLECULES. Kazachok, V. S. Zh. Tekhn. Fiz., 35: 1145-9(June 1965). (In Russian).

A method is proposed for decelerating a molecule having a large dipole moment by employing the force exerted on the molecule by a nonuniform electric field, in order to increase the efficiency of the molecular beam in a constant frequency oscillator. The electric field is obtained by applying potentials of opposite sign to the alternate elements of an array of equally spaced coaxial conducting rings. If the conductors near the center of the array are made larger in diameter than those near the ends the average force on the molecule is greater near the ends than near the center, and an axially moving molecule with insufficient energy to escape the array vibrates along the axis at a frequency calculated in terms of the geometry of the array, the applied potentials, and the mass and dipole moment of the molecule. Although the speed of a molecule traversing such an array is not reduced if the applied potentials are held constant, it is possible to effect a transfer of energy from the molecule to the field by introducing an appropriate time variation of the potentials. It is shown that it is possible in principle to reduce the velocity of the molecule to zero by causing the applied potentials to decrease exponentially with time. Specific numerical calculations are carried out for the deceleration of NH_3 molecules. (ATD)

41201 ULTRASONIC INSPECTION OF THE NIMROD POWER PLANT ALTERNATOR ROTORS. Brooks, H. C.; Brown, A. W.; Rankin, A. C. pp 196-202 of Non-Destructive Testing. London, Butterworths, 1964.

Ultrasonic inspection of the Nimrod proton synchrotron plant rotor forgings throughout the length of the forgings from the bores was attempted. The forgings have boreholes through the center. The probe units had to traverse 15 ft through the 2.75-in.-dia motor rotor bore, into the 25-ft 4.5-in.-dia alternator rotor bore, and on into the 25-ft 4.5-in.-dia flywheel half shaft bore. The equipment and methods are described. (M.C.G.)

41202 HIGH FIELD MEASUREMENTS AT 200 Mc/sec IN CONVENTIONAL PROTON LINEAR ACCELERATOR GEOMETRIES AT 5, 50, AND 125 Mev. Young, Donald E. 17p. (CONF-650410-13). Gmelin, AED-CONF-65-073-26.

From American Physical Society, Washington, D. C.

Measurements were made of axial accelerating fields E_0 in sparking and electron emission studies carried out in linear accelerator cavities of the Alvarez type, with 500 sec pulses and a 1% duty cycle. The experimental arrangement consists of a copper clad steel vacuum envelope pumped by a 400 l/s ion pump. A curve of the surface field on the drift tube in terms of E_0 is shown. Field emission and thermionic emission curves are shown. (L.B.S.)

Astrophysics and Cosmology

41203 (AD-600154) SEARCH FOR PLANETARY OPTICAL EMISSION, AND STUDY OF FLARE ACTIVITY OF NEARBY STARS. Final Report. Smith, Harlan J. (Yale Univ., New Haven, Conn.). May 20, 1964. 6p. (ONR-14-63). CFSTI $1.00 cy, $0.50 mn.

Accomplishments include: the construction of an effective 20-inch reflecting telescope at the Yale Observatory Bethany Station; the construction of a unique dual-channel pulse-counting photoelectric spectrophotometer, more sensitive than the best previously employed spectrophotometer by about three orders of magnitude, for variations lasting several seconds or longer (the new instrument is especially effective for a New England climate by being able to work without loss of accuracy through haze and thin clouds); testing of certain modern photomultipliers and the detection of hitherto unreported effects as to their behavior; the demonstration that Jovian H-alpha auroras are absent, to unexpectedly low levels, and that the search for Jovian auroras should now probably be carried out using other possible lines or bands; and preliminary indications that strong H-alpha flares are not of great frequency in late K dwarfs. (auth)

41204 (JINR-P-2174) PRETSESSIYA VOLCHKA V GRAVITATSIONNOM POLE. (The Precession of the Top in the Gravitational Field). Smorodinskii, Ya. A. (Joint Inst. for Nuclear Research, Dubna (USSR). Lab. of Theoretical Physics). 1965. 9p. Dep. mn.

The precession of the top in the gravitational field, the precession of the Mercury perihelion, and the motion of a planet in the field of the rotating sun are treated as different cases of the Thomas precession. This allows it to give an elementary derivation of the formulas for these effects. The top precession is also considered in a space with torsion (i.e. with $\Gamma^{\gamma}_{\alpha\beta}$ antisymmetrical in lower indexes) which can serve as a model of P- or T-parity nonconservation. (auth)

41205 (N64-31725) THE REDUCED THREE-BODY PROBLEM: A GENERALIZATION OF THE CLASSICAL RESTRICTED THREE-BODY PROBLEM. Herring, Gary P. (National Aeronautics and Space Administration, Huntsville, Ala. George C. Marshall Space Flight Center). July 16, 1964. 22p. (NASA-TM-X-53088). CFSTI $1.00 cy, $0.50 mn.

The restricted three-body problem is generalized to include the motion of the earth and moon on coplanar Keplerian ellipses of eccentricity ϵ, $(0 \leq \epsilon < 1)$. The equations of motion are written in a space fixed-coordinate system. After accomplishing a normalization of the equations in this system, the normalized equations are transformed to a rotating coordinate system. Transformations of the results to several other systems of interest are given. (auth)

41206 (N64-33291) GRAVITATIONAL RADIATION FROM BINARY SYSTEMS. Vishveshwara, C. V. (Maryland Univ., College Park. Dept. of Physics and Astronomy). [1964]. 14p. (NASA-CR-59249). CFSTI $1.00 cy, $0.50 mn.

The variation of the separation r and the angular velocity of rotation ω are investigated for two bodies of masses m_1 and m_2 moving in circular orbits about their common center of mass and acting as a source of gravitational waves that reduce the total energy of the system at a rate $(-de/dt)$. A formula for power loss to gravitational radiation is derived and applied to astronomical bodies. It is concluded that a binary system that has evolved out of the fission of a star can act as a powerful source of gravitational radiation, the rate of radiation increasing to values much higher than the initial luminosity within a short period of time. A comparison with radiation from spheroidal stars shows the importance of the effect of density on the emission rate of gravitational energy. (auth)

41207 (NEIC-RR-9) NUCLEAR ASTROPHYSICS. A BIBLIOGRAPHICAL SURVEY. PART II. Kuchowicz, B. (Nuclear Energy Information Center, Warsaw (Poland)). 1965. 190p. Dep.

A bibliography of papers on nuclear astrophysics which were published during and including the years 1335-1959 is presented. (M.O.W.)

41208 (ORNL-3827) ORBITS IN A MAGNETIC UNIVERSE. Melvin, M. A.; Wallingford, J. S. (Oak Ridge National Lab., Tenn.). July 1965. Contract W-7405-eng-26. 14p. Dep. mn; CFSTI $1.00 cy, $0.50 mn.

A cylindrically symmetric parallel bundle of magnetic lines of force, in equilibrium under their mutual gravitational attraction ("magnetic universe"), has recently received attention. While a Newtonian analysis suggests that the equilibrium is unstable, the complete general relativity analysis shows that the equilibrium is stable. This discrepancy may have to do with the unusually slow falloff of the gravitational field at large distances in this geometry. In order to understand the gravitational field of the static magnetic universe somewhat better, its time-like and lightlike geodesics (i.e., the orbits in it of electromagnetically neutral test particles with unit or zero rest mass)

are studied. Since the density of magnetic flux – and energy and stress and, therefore, "gravitating mass" – is approximately uniform in the vicinity of the axis, the motion of test particles there is like that in a Newtonian simple harmonic oscillator field. "Vicinity" here means within a small fraction ρ of the range radius $\bar{a} = (6.96/B_0) \times 10^{24}$ cm (B_0 is the magnetic field on the axis measured in gauss). As is to be expected from the universality of the angular frequency ω_0 in the harmonic oscillator field and the relation orbital velocity $\cong \omega_0\rho$, no motion can get too far from the axis. Otherwise the physical orbital velocity would exceed the speed of light. It is in this way that the strength of the attractive field, though it does not remain strictly of the harmonic oscillator type as one proceeds outward, implies that there is a critical straddling radius $\rho = 1/\sqrt{3}$. Circular or circular helical light tracks occur only at the critical radius, and with $B_0 = 10^5$ gauss, the time required for light to circumnavigate the critical circle is about 200 years. The cylinder marked out by this radius plays a unique limiting role: All particles, whether of zero or nonzero mass, and no matter what their initial positions and velocities (except in the one singular subcase of light tracks parallel to the cylindrical axis), must have their orbits lying wholly or partially within the cylindrical region $\rho < 1/\sqrt{3}$; hence the use of the adjective "straddling." Constants of motion which correspond closely to z-component linear momentum, angular momentum, and energy in Newtonian mechanics are defined. Bounds are placed on these dynamical constants and on the apsidal radii by the requirement that the range of motion be real. Finally, the magnetic universe is complete in the sense that "no news can enter or leave" – all orbits are of infinite duration. (auth)

41209 (N64-22932) RADIATION OF SOFT X-RAYS BY THE SOLAR CORONA. Fetisov, E. P. Translated from Kosmich. Issled., 1: 209-15(Sept.-Oct. 1963). 14p. (NASA-TT-F-8811). CFSTI, $1.00 fs, $0.50 mn.

The radiation flux of the solar corona in the spectral region shorter than 10 Å is studied. The concentrations of ions of the most prevalent elements are computed in the temperature interval of $1 \cdot 10^6$ to $4.5 \cdot 10^6$ °K. Radiation fluxes are obtained for free-free and free-bound transitions, as well as for radiations in the lines. In the temperature range of $1 \cdot 10^{6\circ}$ to $3 \cdot 10^{6\circ}$, the radiation is due primarily to the recombination of the ions of heavy elements. Calculations were carried out with the use of an electronic computer. (auth)

41210 (N64-25282) STELLAR EVOLUTION. I. A PROGRAM FOR THE SOLUTION OF THE TIME-DEPENDENT BASIC EQUATIONS. Hofmeister, E.; Kippenhahn, R.; Weigert, A. (Max-Planck-Institut fuer Physik und Astrophysik, Munich (West Germany)). Translated for National Aeronautics and Space Administration, Washington, D. C. from report MPI/PA/1/64. 41p. (NASA-TT-F-8740).

A program is described for stellar evolution computations, based on the Henyey method. The program shall be used for very different phases of stellar evolution. Therefore, the main program for the solution of the time dependent basic equations is kept as general as possible, while all assumptions about special physical conditions in the star occur only in subprograms. Hence the range of applicability of the program can easily be extended. The system of difference equations and details of the integration method used in the program are given. For a first test, the program was applied to the post main sequence evolution of a star of 7 M. Some technical details of these calculations are given and discussed. The program turned out to be applicable to calculations of the evolution near the main sequence, of phases of core contraction and of nuclear burning in shell sources. (auth)

41211 PLASMA FREQUENCY AND INTERNAL OPACITY OF STARS. Sofia, Sabatino (Observatorio Naval Juan Manuel Cagigal, Caracas). Acta Cient. Venezolana, 16: 34-5(1965). (In Spanish).

Several terms employed in the determination of χ the coefficient of absorption of a star, omit any dependence on the collective effects of the plasma; the infinite absorptivity for frequencies less than that of the plasma is ignored. It is necessary to calculate the limit below which such an effect might be important. The limit is chosen to be the point at which the maximum of the black-body radiation occurs at frequencies equal to or less than the frequency of the plasma. Equating the frequency from Wien's low and that for the frequency of the plasma, one obtains $\log T = \frac{1}{2} \log \rho + 5$. This result is not surprising; a similar expression could have been obtained by equating the interionic distance with the Debye length. The result is valid when energy transport is by radiation only, and not for degenerate plasmas. The region where the effect is important does not contain any of the stellar structures which have already been computed; this includes the non-degenerate atmosphere of the white dwarfs, in which the effect might be greater than in the sun and red giants. A figure illustrates the region of importance of the effect relative to computed structures. (BBB)

41212 ANTENNA IMPEDANCE IN A PLASMA: PROBLEMS RELEVANT TO RADIO ASTRONOMY MEASUREMENTS FROM SPACE VEHICLES. Walsh, D.; Haddock, F. T. (Univ. of Michigan, Ann Arbor). Ann. Astrophys., 28: 605-13(1965).

A critical review is given of the theory and experimental observations of antenna impedance behavior in a plasma as related to radio astronomy. The emphasis is on electrically small antennas. Three simplified cases of plasma are considered, namely, cold plasma without magnetic field, cold plasma with magnetic field, and warm plasma without magnetic field. Newly reduced experimental results are reported for the case of cold plasma without magnetic field, showing detailed agreement with theory in the neighborhood of a cutoff in the propagation of the extraordinary magnetoionic wave. (auth)

41213 ON X-RAY RADIATION OF THE QUIET SUN. Mandelshtam, S. L. (Lebedev Inst. of Physics, Moscow). Ann. Astrophys., 28: 614-22(1965).

The conditions of production of the solar x rays are briefly discussed. The comparison of the results of recent calculations and experimental measurements supports the assumption of a thermal origin of the x radiation. In the "tail" of the solar spectrum below 15 Å, the main contribution comes from the free-bound radiation of electrons and ions of carbon, nitrogen, oxygen and other elements. The solar radiation consist of a quasi-stable component, produced in undisturbed coronal regions and a slowly varying component generated in the active regions of the corona. (auth)

41214 FUNDAMENTAL PROPERTIES OF THE 11-YEAR CYCLE OF SOLAR ACTIVITY. Antalova, A.; Gnevyshev, M. N. Astron. Zh., 42: 253-8(1965).

Observations of solar corona outside eclipses made it possible to establish the rate of solar activity during a solar activity cycle. The usual concept of one maximum and one minimum is wrong. Careful investigations of the activity cycle from 1954 to 1963 proved the existence of two maxima from the intensity of the coronal line 5303 Å. The intensity of this line was measured from solar poles to the equator in both hemispheres. In the polar regions the line intensity showed one maximum; near the equator a second maximum appeared. The display of this phenomenon was symmetrical in both hemispheres. The existence of two maxima was proved by investigations of sunspot activity during eight solar cycles. The two maxima are correlated and determine the duration of the solar activity cycle. (ATD)

41215 MODEL OF CYCLIC SOLAR ACTIVITY. Gudzenko, L. I.; Chertoprud, V. E. Astron. Zh., 42: 267-75 (1965).

A model of sunspot formation was developed. The formation of sunspots depending upon the cycle of solar activity is considered to be a belt consisting of cells which are capable of separating under convective action. These separated cells emerge on the solar surface as a group or as individual spots. A mathematical theory is developed

for rectangular cells arranged in symmetric belts on both sides of the solar equator. The probability of separation of cells is expressed by a system of differential equations related to individual strips of the cell belt. By varying the equation system, one finds the moments of separation of cells. The ratio of cells departing from the belt in a given unit of time to the total number of cells in the belt is the measure of decomposition. The theory of decomposition agrees in some way with the spot formation during the solar activity cycle. The Coriolis force in the solar convection zone depends upon the heliographic latitude, which condition increases the magnetic field and the formation of cells. The cell belt is formed inside the convection zone, and cells emerge because of their magnetic state. The horizontal state of a separated cell is unstable and during the active cycle creates a magnetic field with a definite direction in spot groups. (ATD)

41216 QUASI-STATIONARY CORPUSCULAR STREAMS DURING THE DESCENDING PHASE OF THE 19TH CYCLE OF SOLAR ACTIVITY. Mustel', E. R. Astron. Zh., 42: 276-80(1965).

The fundamental source of solar corpuscular streams is the recurrent active M regions on the sun. A series of 14 passes of active solar regions through the central meridian are studied. These passes are compared with the state of the geomagnetic field. The stream emission from the sun is in a radial direction. The lag of geomagnetic disturbances behind the active region in the central meridian averages 5 days. The last phase of the observed active region is characterized by a local magnetic field and an absence of corpuscular emission. This state of the active region is termed the magnetic tail of the region. The minima and maxima of magnetic delay are represented graphically. The passes of active regions through the central meridian without geomagnetic disturbances are considered to be magnetic tails. The delay of magnetic disturbances after the passage of recurrent active regions through the central meridian corresponds to a corpuscular velocity of about 370 km/sec. The velocity of solar plasma measured by Mariner 2 reached 650 km/sec. The difference between the computed and the measured velocities is explained by a gradual increase in the velocity of the emitted stream. (ATD)

41217 ELEVEN-YEAR CYCLE OF SOLAR RADIO EMISSION. Gnevyshev, M. N. Astron. Zh., 42: 488-93 (1965).

The eleven-year activity cycle is characterized by two maxima. The first maximum of activity takes place at the 25° heliographic latitude in both hemispheres. Two or three years later a second maximum appears at the 10° latitude in both hemispheres. The maximum activity is observed in both the corona and the photosphere. During the IGY, IGC, and the IQSY, numerous data on solar radio emission are being collected on various frequencies. The rate of the solar radio emission during the activity cycle from 1953 to 1963 was determined and represented graphically. According to these curves, solar radio emission can be divided into three kinds or groups. The first group (wavelengths 3.2–30 cm) had one maximum in 1957 and 1958; the second group (wavelengths 150 and 370 cm) had two maxima, the second of which increases with the length of the wave; the third group with a wavelength of 450 cm contains only one maximum. The emission of the 30-cm wavelength is generated in the lower corona and the chromosphere. A table shows a comparison of the emission flux with the sunspot area on the disk for each station used. The maximum emission of the first group coincides with the maximum area of sunspots. The emission of the second and third groups is generated in the corona at a small solid angle. This condition makes it possible to distinguish between the maxima by the centers, which lie on different heliographic latitudes, so the emission does not represent an average of a large area. A comparison of the radio emission on the 150-cm wavelength with the intensity of the coronal 5303-Å line during the solar cycle shows good agreement. (ATD)

41218 ON SOME PROPERTIES OF SOLAR RADIO BURSTS OF SPECTRAL TYPE III. Elgaroy, Oystein; Rodberg, Harald. Astrophys. Norvegica, 8: 271-301 (Nov. 1963).

Solar type III bursts were observed with a swept frequency receiver in the 200 Mc/sec range. A mean frequency drift velocity of 60 Mc/sec^2 is found. The observed distribution of bursts of different drift velocities agrees with a calculated distribution curve based on other experimental data and simple assumptions. The time profile of the bursts is slightly asymmetrical, and it is possible to explain the profile from a simple model of the type III phenomenon. The analysis leads to a burst band-width of about 25 Mc/sec. If the band-width depends on the size of the exciting disturbance, the source size is about 0.05 $R_\odot$ at the 200 Mc/sec plasma level in the corona. Evidence of an increase in the source size on the way out through the corona is presented. The damping constant of the excited oscillations is larger than previously expected. If it is identified with the collision frequency between electrons and ions, a temperature of $2 \cdot 10^6$°K is found for the active region corona. (auth)

41219 RADIATIVE OSCILLATIONS IN STELLAR GASEOUS MASSES (RADIATIVE-ACOUSTIC WAVES). Ferrero, Giorgio M. Atti Accad. Sci. Torino: I. Classe Sci. Fis., Mat. Nat., 99: 709-22(1964-65). (In Italian).

When a perturbation determines small oscillations in a gaseous mass (as the Sun or certain Stars) with the respect to an initial state of equilibrium, a study is made upon the waves that so are formed under the action of the magnetic field, that there is present in the mass, with account of the heat for radiation and, besides the well known Alfvén's waves, radiative waves are observed. (auth)

41220 CONTOURS OF SPECTRAL LINES IN THE SOLAR CHROMOSPHERE. [PART] I. Krat, V. A. Izv. Gl. Astron. Observ. Pulkovo, 23: No. 5, 21-7(1964).

The study of the transfer of radiation in the chromosphere is based on the real distribution of the temperature, radiation density, electron concentration, and the gas density. Correct values of these parameters can be obtained by the diffusion of radiation in incoherent dispersion of light when the optical depth of the center of the line and the source function are taken into consideration. A differential equation of the radiation intensity is developed, the solution of which is obtained in the form of an integral equation. The equation can be transformed and solved by the method of Voltaire's equations. The analysis of the source function showed that it diminished rapidly at great optical depths on nearing the edge of the chromosphere. The lower layer of the chromosphere is called the inferior chromosphere; the radiation intensity found in it occurs under complicated conditions. The resonance lines of ionized calcium H and K have very great optical depth in the inner chromosphere. The flocculi of these lines are weak. Absorptions in them vary from place to place in the chromosphere revealing the high velocities of the gas masses which produce these lines. The weak radiation of lines is caused by a slowdown in the radiation diffusion. (ATD)

41221 MAGNETIC FIELDS AND MOTIONS IN AN UNDISTURBED PHOTOSPHERE. Vasil'eva, G. Ya. Izv. Gl. Astron. Observ. Pulkovo, 23: No. 5, 28-39(1964).

In the summers of 1960 and 1961 investigations of an undisturbed photosphere were carried out with the solar magnetograph at the Main Astronomical Observatory. The FeI line of 5250 Å was analyzed, and data obtained were processed by the correlation method. A structural function was used for eliminating errors in the correlation function. Six autocorrelation functions were composed for the fluctuations of the radial velocities and three functions for the fluctuations of the magnetic field. The Kolmogorov 2/3 exponential law for local turbulence was checked. An average structural function compiled from observation data showed a law of the first power instead of 2/3. A variable distribution of probabilities for the magnetic field was obtained. A compressed medium generates turbulence associated with energy emission in the form

of sound. The quantity of sonic energy and the energy dissipated in turbulence compose a part of the general flux of energy in photospheric motions. The sonic energy generated by the turbulence and the magnetic field and, because of viscosity, the dissipated energy in turbulent matter form a small part of the general energy that flows from the photosphere to the chromosphere. (auth)

41222 OBSERVATIONS OF RADIO ECLIPSE OF THE MOON AT MILLIMETER WAVES. Kamenskaya, S. A.; Kislyakov, A. G.; Krotikov, V. D. (and others) (Gor'kii State Univ., USSR). Izv. Vysshikh Uchebn. Zavedenii, Radiofiz., 8: 219-28(1965). (In Russian)

The effective temperature variation of the moon during the eclipses of July 7, 1963 and Dec. 30, 1963 was measured by observing lunar radio emission at millimeter wavelengths. The best agreement of the experimental results with theoretical prediction of the eclipse process for a uniform model of the moon was obtained when $\gamma/b = 6 \times 10^4(\gamma = (k\rho c)^{-0.5}$, k is the thermal conductivity, ρ is the density, c is the specific heat, and b is the specific angle of losses for lunar matter). The γ/b value obtained for the upper layer of lunar rock coincides, within the limits of experimental accuracy, with the value obtained previously from measurements of the phase dependence of lunar radio emission. (D.C.W.)

41223 THE USE OF THE PHASE TECHNICS FOR STUDYING POLARIZATION PHENOMENA OF RADIO-WAVES REFLECTION FROM THE METEOR TRAILS. Sidorov, V. V.; Pavlov, A. F.; Fakhrytdinov, P. Yu. (Kazan State Univ., USSR). Izv. Vysshikh Uchebn. Zavedenii, Radiofiz., 8: 234-43(1965). (In Russian)

The results are given of an investigation of polarization phenomena in radio-wave reflection from meteor trails by the direct-phase method. The observed magnification of resonance duration at the transition to denser trails provides evidence against the theory of "metallic" resonance. If the anisotropy in the trail giving the prolonged reflections is caused by the Earth's magnetic field, the structure of the trail must be looser than the structure in the case of purely ambipolar diffusion in the meteor trail. (D.C.W.)

41224 COMPARISONS OF POWER SPECTRUMS OF ARTIFICIAL TIME SERIES WITH SPECTRUM OF A SOLAR PLAGE INDEX. Shapiro, Ralph (Air Force Cambridge Research Labs., Bedford, Mass.). J. Geophys. Res., 70: 3581-6(Aug. 1, 1965).

A number of experiments are described whose purpose was to determine whether peaks in power spectrums of time series of solar indices reflect a tendency for equidistant separation in longitude of solar active regions or are produced by the analysis technique. From comparisons of power spectrums of artificial time series with the spectrum of a solar plage index it is clear that there is no appreciable tendency for equidistant spacing of active regions. (auth)

41225 COSMOGENIC AND RADIOGENIC HELIUM, NEON, AND ARGON IN AMPHOTERIC CHONDRITES. Heymann, Dieter. (Univ. of Chicago). J. Geophys. Res., 70: 3735-43(Aug. 1, 1965).

Cosmogenic and radiogenic rare gases were determined by mass spectrometry in 16 amphoterites. The radiation, U, Th-He, and K-Ar ages were calculated. Radiation ages of amphoterites vary from 0.9 to 58 m.y. They resemble the age distribution of the hypersthene chondrites in that few amphoterites have ages in the interval 2–6 m.y. The amphoterites Appley Bridge, Hamlet, and Soko-Banja have the same fall date, October 13, but very different radiation ages — 1, 31, and 58 m.y. — indicating that they did not belong to a periodic meteorite shower or stream. The same seems to be true also of Olivenza and Vavilovka, both of which fell on June 19. The ^{40}Ar contents of 4 amphoterites differ significantly from previous determinations by other authors, a finding that supports earlier conclusions that the K abundance in some amphoterites seems to be nonuniform. Although 2 of the amphoterites had U, Th-He ages as short as 1 b.y., most others are indeed quite old. Seventy-five per cent have ages greater than 3.0 b.y., whereas only 20% of the hypersthepe chondrites have ages above this limit. It is concluded that differences in chemistry and mineralogy cannot account for the systematic differences in gas-retention ages of bronzite, hypersthene, and amphoteric chondrites. Most, if not all, amphoterites seem to have escaped the reheating episode that hypersthene chondrites underwent late in their history. (auth)

41226 RADIO BRIGHTNESS CONTOURS OF 3C273. Hughes, M. P. (Harvard Radio Astronomy Sta., Ft. Davis, Tex.). Nature, 207: 178-9(July 10, 1965).

A contour map of the radio source 3C273, which consists of two components — a jet-like nebulosity and an object of stellar appearance — is presented, constructed from the analysis of five complete lunar occultations which occurred in 1963-4. The position angles of immersion and emersion for both source components and each occultation are given, and the method of reconstructing the radio brightness contours from the data of the ten scans across the source is described. (M.J.T.)

41227 CREATION RATE OF MATTER AND THE HEISENBERG UNCERTAINTY PRINCIPLE. Zupancic, A. O. (Univ. of Ljubljana, Yugoslavia). Nature, 207: 279 (July 17, 1965).

Equations are derived and numerical values found for the amount of matter created in the observable universe in the period of vibration corresponding to the largest possible wavelength and for the mean density of matter, assuming the steady-state theory of continuous creation of matter out of nothing and the hypothesis of a finite observable universe, and using Hubble's law and the Heisenberg uncertainty principle. (M.J.T.)

41228 PROPAGATION OF SOLAR PROTONS AND THE INTERPLANETARY MAGNETIC FIELD. Sakurai, Kunitomo (Kyoto Univ.). Planetary Space Sci., 13: 745-51 (Aug. 1965).

Solar proton events are classified into three types, F, F*, and S, based on the intensity time variation and related solar phenomena. The propagation mechanism for each is considered. The structure of the magnetic fields near the sun and in interplanetary space are deduced, and the structure of the flare nimbus is discussed. The influence of the interplanetary magnetic fields on the propagation of solar protons is examined in detail. (auth)

41229 RADIO EMISSION FROM SHOCK WAVES AND TYPE II SOLAR OUTBURSTS. Tidman, Derek A. (Goddard Space Flight Centre, Greenbelt, Md.). Planetary Space Sci., 13: 781-8(Aug. 1965).

A model for type II solar radio outbursts is discussed. The radiation is hypothesized to originate in the process of collective bremsstrahlung emitted by non-thermal electron and ion density fluctuations in a plasma containing a flux of energetic electrons. The source of radiation is assumed to be collisionless plasma-shock wave rising through the solar corona. It is also suggested that non-thermal electrons in the ionospheres of the earth and planets might be sources of the same type of radiation. (auth)

41230 SOLAR PROTON EVENT PRODUCTION BY HYDROMAGNETIC SHOCKS. Weddell, James B. (North American Aviation, Inc., Downey, Calif.). Planetary Space Sci., 13: 789-806(Aug. 1965).

The acceleration of solar wind protons by hydromagnetic shocks induced in the corona by heating due to flares is analyzed. Solution of the relativistic equations of motion of protons subject to the moving magnetic field accompanying a shock shows that the proton energies can reach several Mev to several hundred Mev. As the proton energies increase, their probability for scattering forward of the shock increases; this scattering is shown to be approximately random, so that the emergent protons are distributed isotropically. As the scattered protons remove energy from the shock, the shock weakens and vanishes. The times of flight of emergent protons through the interplanetary magnetic field were calculated as a function of heliocentric distance, flare position, emergent energy, and direction of emergence. These results were used to con-

struct the time-dependent angular distribution vs energy of protons reaching a point in the vicinity of the earth but outside the geomagnetic field. The calculations agree quantitatively in several respects with the observed characteristics of solar proton events. (auth)

41231 MEASUREMENTS OF SOLAR X-RAY FLUXES BY THE U. S. NAVAL RESEARCH LABORATORY SATELLITE 1964-01-D. Thomas, L.; Venables, F. H.; Williams, K. M. Planetary Space Sci., 13: 807-22(Aug. 1965).

Measurements of solar x rays were derived from telemetry received at Winkfield from satellite 1964-01-D during the period January to August 1964. The fluxes observed in the bands 0–8, 8–20, and 44–60 Å were about 0.3×10^{-3}, 2×10^{-3}, and 3×10^{-2} erg cm^{-2} sec^{-1} respectively. Observations beginning about 20 min after the visible termination of a flare of importance 1^{-} showed enhancements by factors of 2–3 in the fluxes for the 8–20 Å and 44–60 Å bands and these enhancements persisted for at least a further 20 min. Comparisons of fluxes in the 44–60 Å band and measurements of the E-layer critical frequency indicate that these x rays play little part in the production of the E layer during this period. Studies have been made of the atmospheric absorption of 44–60 Å x rays near sunrise and sunset. These studies have shown that atmospheric densities in the height range 120–200 km show large day-to-day changes. (auth)

41232 ON THE NUCLEAR ABUNDANCE AND RIGIDITY SPECTRA OF SOLAR COSMIC RAYS. Sakurai, Kunitomo (Kyoto Univ.). Planetary Space Sci., 13: 867-8(Aug. 1965).

An interpretation is given for the relation of the ratio of the relative abundance of solar protons to solar alpha particles. The time variation of this ratio may reflect upon the particle-acceleration mechanism in solar flares. The much greater power flux of μ-IV emission for both F and F* type events as compared with S type events suggests that the electron energy of the first two types is also greater. Thus the ratio p/α is greater than 1 when cosmic ray and solar-electron energies appear very high. This may indicate that during the initial phase of solar cosmic ray acceleration the acceleration rate of protons is much higher than that of the other heavier nuclei. The two facts that the proton to alpha ratio is much greater than 1 before onset of an SC magnetic storm and that the rigidity spectra of solar cosmic rays are exponential suggest that during the initial phase of solar cosmic ray acceleration, the Fermi mechanism is more effective than the betatron mechanism and that the acceleration originates from the plasma particles with thermal energy. (J.F.P.)

41233 AN EVOLUTIONAL TRACK OF GALAXIES IN L-(L/V) DIAGRAM. Aizu, Ko (Univ. of Rikkyo, Tokyo); Fujimoto, Yoichi; Hasegawa, Hiroichi; Taketani, Mituo. Progr. Theoret. Phys. (Kyoto), 33: 996-7(May 1965).

The shape of the evolutional track in the L-L/V diagram where L is radio luminosity and L/V is volume emissivity, is interpreted, assuming synchrotron emission of the radio waves and equipartition of energy among the three modes—cosmic rays, magnetic fields, and gas turbulent motion. The resulting relation between L and L/V is discussed for the cases of conservation of the total energy of magnetic fields and of adiabatic expansion. (M.J.T.)

41234 MEASUREMENTS OF ERUPTIVE PHENOMENA ON THE SOLAR LIMB. Chang, Ho-ch'i; Ts'ao, Tien-chun, Tien Wen Hsueh Pao, 12: 138-54(1964).

From a large number of H_α photographs of limb flares, fifteen were selected for reduction. The films were obtained with the standard Lyot-type Chromospheric patrol telescope at the Purple Mountain Observatory during the years 1959-1960. The following conclusions were made from the photometric and positional measurements of limb flares. There are violent radial ejections of matter during the flash-phase of the flare. Usually a part of the flare is ejected to distances ranging from 2×10^4 to 2.5×10^5 km above the base of the chromosphere. The main velocity of ejection is of the order of 30 km/sec to 400 km/sec. The maximum velocity appears in the initial stage of ejection and decreases later on. The acceleration of ejection is supergravitational. The ejective motions of flares are regular and apparently connected with the magnetic fields of the active regions. During the flash-phase of the flare the velocity of ejection varies directly with the rate of increase of brightness. It was also noted that the appearance of radio events is closely related to the ejection. (ATD)

41235 ORIGIN OF CHEMICAL ELEMENTS IN STARS: PART VI. Kuchowicz, Bronisław. Urania (Krakow), 36: 135-40(May 1965). (In Polish).

The process of element synthesis by neutron capture is examined. The neutron-capture nucleosynthesis process is studied from the point of view of rapid capture rate and slow capture rate. The relative abundance of the isotopes of Sm is treated as a case in point for determining the nature of nucleosynthesis for elements in the earth's crust. The evidence from the Sm isotope abundance and from the relative abundance of the transuranium elements points to a combination of slow and rapid neutron capture rate, or a synthesis that took place over a varied history of the parent star. The cosmological implications of this include a revision of the estimate of the age of the earth from 6.6×10^9 years to over 10^{10} years. (TTT)

41236 MAGNETIC MODEL OF THE UNIVERSE. Zel'dovich, Ya. B. Zh. Eksperim. i Teor. Fiz., 48: 986-8 (Mar. 1965). (In Russian).

Starting with the assumption that a primordial homogeneous magnetic field existed initially in the universe, various features of the corresponding cosmological solution are considered. It is assumed that the original field was uniform over the entire universe during that hypothetical stage of evolution when the distribution of matter was also uniform, and the features of the cosmological solution corresponding to the period when homogeneity was not yet destroyed are considered. The presence of a field destroys the symmetry (isotropy) of space, and a solution is considered in which the decrease in symmetry is minimal. The particular case of a flat world is considered, and it is shown that when the density of matter is both larger and smaller than the critical value (10^{-29} g/cm^3), the bending of the metric in a plane perpendicular to the field should lead to noticeable anisotropy distribution of far sources with a red shift close to unity. The hypothesis of a homogeneous magnetically anisotropic universe is thus compatible with observation only at critical density, which is much higher than the density of visible starts. The magnetic model is in full agreement with the presence of neutrinos in the early stage of evolution. (ATD)

41237 CENTRAL COOLING OF PARTIALLY DEGENERATE HELIUM CORES BY NEUTRINO LOSS (thesis). Mitalas, Romas. Ithaca, N. Y., Cornell Univ., 1964. 61p.

Temperature distributions in partially degenerate helium cores of population II red giants of approximately solar mass taking into account the plasmon neutrino energy loss mechanism of Adams et al. (1962) were approximately calculated. The outer layers were excluded from the calculation by assuming two core boundary conditions $V = 4$, $(n + 1) = 4$ at the outer edge of the helium-hydrogen discontinuity. Contribution of degenerate electrons to the opacity was considered. The plasmon neutrino energy loss dominates the gravitational energy release in the central portion of the core—the temperature gradient is positive there. The main result is that the ignition of helium takes place not centrally but at the position of maximum temperature in the core, where the neutrino and gravitational luminosities are equal. The degeneracy there is too low for the helium flash to start. But with increasing temperature of the hydrogen burning shell, the positive temperature gradient is wiped out, and helium flash will proceed along the usual lines. If larger neutrino energy loss mechanisms operating in this temperature-density regime were found, they would drastically reduce the intensity of the helium flash, or even prevent its occurrence. (Dissertation Abstr.)

41238 RECOMBINATION SPECTRA OF HYDROGEN AND HELIUM IN GASEOUS NEBULAE (thesis). Kaler,

James Bailey. Los Angeles, Univ. of California, 1964. 212p.

The validity of the theory of radiative recombination of an attenuated ionized gas (plasma) as applied to hydrogen and helium in gaseous nebulae is assessed. The emission line intensities for the Balmer and Paschen series of hydrogen, the Paschen, Pickering, and Pfund series of ionized helium, and the hydrogenic n^3D-2^3P and n^1D-2^1p series of neutral helium were considered. The observations were taken from three principal sources. The first and most important is a series of high dispersion spectrograms taken with the 100-inch and 120-inch telescopes for six planetary nebulae and the Orion Nebula. The second is a series of observations of lower dispersion of 10 planetary nebulae with the 120-inch telescope and the third source is a group of 17 planetaries. In addition, the works of others were used to obtain intensity data for lines which the new work did not cover. New values of the electron temperature and reddening constant for all the nebulae were obtained. After correction for interstellar reddening, the observations were compared with others. Several conclusions were made. The high Balmer lines, and the corresponding lines of other series can show marked deviation from theory. Roughly half the nebulae show deviations. Lines produced by transitions from the same upper level in hydrogen and ionized helium show the same percentage deviation. Lines produced by transitions from levels of hydrogen and neutral and ionized helium which have the same number of J-states show the same percentage deviation. Theoretical decrements appear to predict lower limits to the observed decrements. There appears to be no correlation between the degree of deviation and the physical parameters of the nebulae, except for the possibility of the presence of filamentary structure. (Dissertation Abstr.)

41239 GALAXY FORMATION IN A STEADY STATE UNIVERSE (thesis). Hunter, James Hardin Jr. Los Angeles, Univ. of California, 1964. 124p.

An investigation was made to determine what conditions of temperature and density must prevail in a steady-state universe in order to allow galaxies to form by the growth of small amplitude disturbances in the inverse Hubble constant time. The effects of self gravitation, radiation loss, and thermal conduction were included in the analysis. The effects of angular momentum and magnetic fields were ignored, because these phenomena will generally inhibit the development of a condensation. The universe is treated as a tenuous hydrogen plasma having constant density and temperature. Then, the equations of continuity, momentum transport, and conservation of thermal energy are derived by the moment method from a modified Boltzmann equation which contains a source term representing the continuous creation of matter. A modified Poisson equation with a nonzero cosmological constant is used to represent the body force per gram. The equations were linearized and solved to obtain stability conditions for the gas. In addition, approximate solutions were developed in order to follow the collapse of clouds that are linearly unstable into the nonlinear range. It was concluded that in order for large gas clouds to collapse gravitationally from the growth of small amplitude disturbances in a steady-state universe, the density of the intergalactic medium would have to be more than ten times greater than the density predicted by Hoyle. For certain ranges of temperature, thermal collapse can occur in a steady-state universe. However, in all cases studied, the end result of such a collapse is a partially ionized, thermally stable gas cloud. (Dissertation Abstr.)

41240 HeH^+ IN MODEL STELLAR ATMOSPHERES (thesis). Norton, Robert Henry. Pasadena, Calif., California Inst. of Tech., 1964. 176p.

Approximate quantum mechanical calculations for the two lowest $^1\Sigma^+$ states of the helium hydride molecule ion HeH^+ were made. The molecular potential energy curves resulting from these calculations were found to agree reasonably well with the results of others. Using classical statistics for the distribution of internuclear separations, approximate absorption coefficients for radiative transitions between these two states were obtained. A program to compute model stellar atmospheres in strict radiative equilibrium is described and was used to compute eight models with log g = 4.0 and effective temperatures between 9500 and 30,000°K. Total flux constant to within 1% was attained for these models excluding HeH^+ as a source of opacity. When the final models were re-computed including the opacity of HeH^+, radiative equilibrium was found to be destroyed by as much as 15%. Radiative equilibrium was re-established for the model with T_e = 16,000°K, and a comparison between this model with and without HeH^+ is given. It was found that HeH^+ introduces a striking discontinuity in the continuous spectrum of the model at 1130 A; the ratio of the emergent monochromatic flux on the red side of discontinuity to the flux on the violet side is 8.2 for the 16,000°K model. It was concluded that the wings of the Lyman lines, except L α, are probably weaker than previously supposed. In addition, numerical quadrature formulas of high accuracy and efficiency are given for integrals of the Schwarzschild-Milne type. (Dissertation Abstr.)

41241 ON THE GENERAL MAGNETIC FIELD OF THE SUN AND THE LIMIT OF CO-ROTATION OF THE CORONA (thesis). Tierney, Martin Stephen. Albuquerque, N. Mex., Univ. of New Mexico. 1964. 95p.

The question of the co-rotation of the corona was investigated within the framework of a model of the general magnetic field of the sun which could possibly enforce the co-rotation of the corona at great distances from the solar surface. The physical evidence for the existence of magnetic fields in the inner solar system is reviewed. From this evidence, a model of the sun's general magnetic field was constructed in which it is presumed that the field lines of a poloidal field emerge from one of the polar caps of the sun and return to the opposite polar cap after having looped over an extended, field-free region in the solar equatorial plane. It is furthermore assumed that the radial extent of the field-free region determines the radial distance from the sun to which the corona might be expected to participate in the solar rotation. Within 20 solar radii radial distance from the sun's surface, there is found to be a good agreement between the field and electron number density distribution resulting from the model and the field structure and electron density given by the observational evidence. However, under the assumptions made in the construction of the model of the general magnetic field of the sun, it was found that a magnetic field which is consistent with the currently available experimental data should be unable to enforce the rotation of the corona to distances much greater than 37 solar radii from the sun's surface. It was concluded that those modulation mechanisms proposed for the solar diurnal variation which require the rotation of the solar corona to great distances are invalid. Evidence for a diurnal cosmic-ray variation at primary particle energies in excess of 100 Bev is reviewed. It is shown that the most recently proposed modulation mechanism is unable to account for the experimentally observed amplitudes and phases of the variation. A way is suggested by which this mechanism could be modified to bring a closer agreement with the experimental evidence. Suggestions for further work on the problem are made. (Dissertation Abstr.)

41242 ON CERTAIN ASPECTS OF HYDROGEN AND HELIUM BURNING IN STARS (thesis). Caughlan, Georgeanne Robertson. Seattle, Univ. of Washington, 1964. 88p.

The fact that the ratio of the isotopic abundances of carbon, $^{13}C/^{12}C$, is observed to be from $\frac{1}{2}$ to $\frac{1}{4}$ in many carbon stars is an indication that hydrogen burning in the proton capture reactions defined as the CNO bi-cycle may have been active during the evolutions of these stars because the CNO equilibrium abundance ratio of $^{13}C/^{12}C$ is $\frac{1}{4}$. However, because of the long mean lifetime of ^{14}N for proton capture, the CNO bi-cycle processes CNO nuclei primarily into ^{14}N. There is no reason to believe that nitrogen is more abundant than carbon in carbon stars. In order to explain this probably lack of enhancement of

nitrogen in these stars, the reaction-rates differential equations of the CNO bi-cycle are solved and an analysis is made of the abundances of the carbon, nitrogen, and oxygen nuclei as functions of protons consumed per initial CNO nucleus in the approach to equilibrium of the CNO bi-cycle at temperatures of $10 \times 10^6 - 50 \times 10^6$°K. It is shown that if the CNO processes have been active for at least one half the mean lifetime of ^{12}C for proton capture, the $\frac{1}{3} - \frac{1}{5}$ ratio of $^{13}C/^{12}C$ can be explained, and if the bi-cycle has been active for no longer than one mean lifetime of ^{12}C for proton capture, nitrogen will be no more abundant than carbon. Three rules are established for low or intermediate mass stars ($M < 30M_\odot$) if abundances are to be attributed to hydrogen burning in the CNO bi-cycle. Because of the large amount of ^{16}O formed through helium burning in massive stars ($M > 30M_\odot$), the rules for explanation of CNO abundances on the basis of the CNO bi-cycle in massive stars require that although the $^{13}C/^{12}C$ ratio may be $\frac{1}{4}$, the N/C ratio must be greater than one and of the order 10–100 in the temperature range considered. Analysis is made of simple cases of carbon and nitrogen nuclei moving by convection through a star and of the effect this has on the CNO abundances. Summaries of the characteristics of carbon stars, of the mean lifetimes and equilibrium abundances of CNO nuclei, and of combined hydrogen and helium burning are presented to give a background for the study of the approach to equilibrium and for other reactions that may effect the abundances of the CNO nuclei in carbon stars. A table is given of the contributions to the ^{12}C, ^{13}C, and ^{14}N proton capture reactions of certain resonant levels in the respective compound nuclei ^{13}N, ^{14}N, and ^{15}O. These contributions become important when temperatures above 10×10^6°K are prevalent in the stars. (Dissertation Abstr.)

Atomic Physics

Refer also to abstracts 40552, 41967, and 41969.

41243 (FTD-TT-64–1368) CERTAIN PROBLEMS OF MASS SPECTROSCOPY AND THE SPECTROSCOPY OF ATOMIC NUCLEI. Zuk, W. Translated from Postepy Fiz., 14: 703-16(1963). 24p. CFSTI

A brief description of some of the applications of mass spectroscopy is given. The applications considered are: determination of the isotope composition of elements and of mass-spectrum peak ratios, investigation of phenomena of ionization in gases, separation of isotopes, and problems of measurement techniques and apparatus. (M.O.W.)

41244 COLLISIONAL EXCITATION OF AUTOIONIZING LEVELS. Goldberg, Leo (Harvard Coll. Observatory and Smithsonian Astrophysical Observatory, Cambridge, Mass.); Dupree, Andrea K.; Allen, John W. Ann. Astrophys., 28: 589-93(1965).

Collisional excitation of autoionizing levels is found to contribute significantly to the ionization rate for certain ions at temperatures characteristic of the solar corona. Preliminary calculations were carried out for O-IV, O-V, O-VI, Fe-XV and Fe-XVI. Autoionization may be of importance for O-IV and increases by approximately a factor of two the ionization rate of Fe-XV and -XVI. (auth)

41245 APPROXIMATION FORMULAS FOR THE FLUORESCENCE YIELDS OF THE L_2 AND L_3 SHELLS. Hohmuth, K. (Zentralinstitut fuer Kernforschung, Rossendorf, Ger.). Ann. Physik (7), 14: 129-36(1964). (In German)

By use of the known values for the total yield, the radiation width, and the fluorescence yield of the L_2 and L_3 levels, approximation formulas for the partial fluorescence yields ω_2 and ω_3 were derived. From both these relations, the fluorescence yield ω_{KL} was calculated and compared with the present experimental values. A satisfactory agreement was obtained between calculated and experimental values. (tr-auth)

41246 THE LUMINESCENCE OF THE RARE GAS MIXTURES Ar/Xe, Kr/Xe, Ar/Kr, AND THE MIXTURES Xe/N_2 AND Kr/N_2 IN EXCITATION WITH FAST ELECTRONS. Kugler, E. (Universitaet, Giessen, Ger.). Ann. Physik (7), 14: 137-46(1964). (In German).

The gas mixtures Ar/Xe, Kr/Xe, Ar/Kr, Xe/N_2, and Kr/N_2 were excited with 50-kev electrons, the emission was spectroscopically investigated, and the decay of narrow spectral ranges was measured by phase fluorimetry or oscillographically. In addition to arc and spark lines, bands of heteroatomic rare gas molecules were observed. The measured decay times permit conclusions on the mechanism of the molecule formation. (tr-auth)

41247 ABSORPTION AND SCATTERING OF QUANTUM MECHANICAL COHERENT BEAMS. I. INTERACTION WITH AN ATOM. Brunner, W.; Paul, H.; Richter, G. (Institut fuer Spezielle Probleme der Theoretischen Physik, Deutsche Akademie der Wissenschaften, Berlin). Ann. Physik (7), 14: 384-93(1964). (In German)

The alteration of the degree of coherence of a maximum coherent state, in the quantum electrodynamic sense, excited in a single self-oscillation, of the radiation field was investigated in absorption (by a single atom). The calculation was first carried out in perturbation theory approximation for short times and then for any times by omission of the matrix elements of the perturbation operators violating the energy law. For short times the coherence is maintained during absorption, for longer times a very slight coherence decrease occurs. For the case that a very great number of absorptions occur next to each other, no essential coherence deterioration is to be expected. For elastic scattering, it was shown in the perturbation theory approximation that the incident (quantum mechanical) coherent waves undergo no loss of coherence through scattering and that all scattering waves are also coherent. Also the calculation showed that the scattering beams arising from a (quantum mechanical) coherent primary radiation are independent of each other in the quantum mechanical sense. (tr-auth)

41248 ABSORPTION AND SCATTERING OF QUANTUM MECHANICALLY COHERENT BEAMS. II. INTERACTION WITH N ATOMS. Brunner, W.; Paul, H.; Richter, G. (Institut fur Spezielle Probleme der Theoretische Physik, Akademie der Wissenschaften, Berlin). Ann. Physik (7), 15: 17-29(1965). (In German).

Within the framework of the Gordon-Walker-Louisell model, the absorption and scattering of a light beam on idealized atoms were investigated with respect to whether in this process a change of the coherent properties of the radiation field occurs. In the case of scattering, it was assumed that the atoms which should represent in their totality a mirror surface are arranged randomly in a plane. The calculation shows that the "relative reduced scattering"—determining the coherent behavior—of the electrical field intensity of the radiation field remains practically unaltered in absorption and reflection; the classic electrodynamics with respect to coherent expressions is shown to be valid also in the microscopic range. (tr-auth)

41249 INVESTIGATION OF THE ISOTOPIC EFFECTS IN THE SECONDARY ELECTRON EMISSION ON METAL SURFACES BY POSITIVE IONS. Krebs, Karl Heinz (Humbolt-Universitat, Berlin). Ann. Physik (7), 15: 111-12(1965). (In German).

The secondary electron emission produced by Kr^+ and Xe^{2+} ions with energies between 12 and 25 kev at a pressure of 1×10^{-7} torr hitting a nickel target was determined. The results are plotted with respect to the isotopic mass in order to show the isotopic effect. The measurements satisfy neither the pure velocity dependence found by Ploch nor the correction factor proposed by Higatsberger et al. (J.S.R.)

41250 ON THE COLLISION MECHANISM OF BIMOLECULAR REACTIONS. PART I. THEORY AND EXPERIMENTAL METHOD FOR DETERMINATION OF THE VELOCITY SPECTRUM OF THE PRODUCTS FROM SIMPLE H-TRANSFER REACTIONS OF THE TYPE $X^+ + H_2 \rightarrow XH^+ + H$. Henglein, A.; Lacmann, K.; Jacobs, G. (Hahn-Meitner-Institut fuer Kernforschung, Berlin). Ber. Bunsenges. Physik. Chem., 69: 279-86(1965). (In German).

An apparatus is described with which the velocity spectra

of XH^+ or XD^+ ions, respectively, from ion-molecule reactions of the type $X^+ + H_2(D_2) \rightarrow XH^+ + H(XD^+ + D)$ can be measured. The secondary ions are not accelerated after their formation, and the incident X^+ ions have kinetic energies between 20 and 200 ev. Velocity spectra are calculated on the basis of two different collision models. (D.C.W.)

41251 ON THE COLLISION MECHANISM OF BIMOLECULAR REACTIONS. PART II. THE STRIPPING MECHANISM OF THE REACTION $Ar^+ + H_2(D_2) \rightarrow ArH^+ + H(ArD^+ + D)$ AT ENERGIES >20 ev. Lacmann, K.; Henglein, A. (Hahn-Meitner-Institut fuer Kernforschung, Berlin). Ber. Bunsenges. Physik. Chem., 69: 286-91(1965). (In German).

The bands of ArH^+ and ArD^+ ions were observed in the velocity spectra of the ions resulting from the interaction (chemical reaction and scattering) of Ar^+ ions with H_2 and D_2, respectively. The bands are practically located as expected from the stripping model. It is concluded that the Ar^+ ion does not collide with the whole hydrogen molecule in a completely inelastic manner as is the case at low kinetic energies, where the polarization theory of ion-molecule reactions is applicable. The Ar^+ ion interacts only with the captured hydrogen atom without transfer of momentum to the second atom. The cross section decreases with the relative kinetic energy of the collision partners rather than by the $1/\sqrt{E_s}$ law. The same function $\sigma(E_s)$ was obtained for the transfer of an H and of a D atom. The critical energies of the incident Ar^+ ions, above which the cross sections of the two reactions are zero, differ by a factor of about 2 and agree with the energies calculated from the stripping model. Some minor deviations from the stripping model are also mentioned. (auth)

41252 ON THE COLLISION MECHANISM OF BIMOLECULAR REACTIONS. PART III. INVESTIGATION OF THE REACTION $N_2^+ + H_2(D_2) \rightarrow N_2H^+ + H(N_2D^+ + D)$ AND $CO^+ + H_2(D_2) \rightarrow COH^+ + H(COD^+ + D)$. Lacmann, K.; Henglein, A. (Hahn-Meitner-Institut fuer Kernforschung, Berlin). Ber. Bunsenges. Physik. Chem., 69: 292-301(1965). (In German).

At moderate kinetic energies up to about 50 ev of the incident ion, the velocity spectra agree with the predictions of the stripping model. At higher energies, the bands of the product ions are shifted to somewhat higher velocities. This This indicates preferential forward scattering of the charged reaction product and less conversion of kinetic energy of the incident ion into internal energy of the products. As was expected, the cross sections for the transfer of an H and D atom are equal at the same relative kinetic energy. Over a wide range of energy, the cross section depends on the relative kinetic energy as $\sigma = k_1 \cdot e^{-k_2 E_s}$. Reactions could still be observed at relative kinetic energies which are larger than the dissociation energy of the product ion (up to 7 ev for N_2H^+ and N_2D^+ and up to 10 ev for COH^+ and COD^+). These details of the collision mechanism are tentatively explained by two hypotheses. (auth)

41253 RECENT PROGRESS IN THE STUDY OF ARC AND SPARK SPECTRA OF THULIUM. Blaise, Jean; Camus, Pierre (C.N.R.S., Bellevue, France). Compt. Rend., 260: 4693-6(May 3, 1965). (In French).

The measurement of Zeeman spectrograms at Argonne National Laboratory and a list of thulium wave lengths from 0.9 to 2.4 μ recently measured with a S.I.S.A.M. spectrometer have made it possible to calculate the J and the g values of almost all of the known levels and to find some new levels. These values are tabulated for both Tm I and Tm II. (J.S.R.)

41254 THE EXCITATION OF NEUTRAL ATOMS BY ELECTRON COLLISIONS. McCarroll, Ronald (Observatoire de Paris). Compt. Rend., 260: 6554-7(June 21, 1965). (In French).

A new method for the calculation of the collision cross sections for the excitation of neutral atoms by electrons, in which the interaction between the atomic electrons and the scattered electrons is considered, is described. The calculations made for the excitation of the 2s and 2p levels of hydrogen show a very good agreement with experiment. (tr-auth)

41255 FIELD DESORPTION OF THORIUM FROM A FIELD-EVAPORATED TUNGSTEN SURFACE. Young, Russell D. (National Bureau of Standards, Washington, D. C.). J. Appl. Phys., 36: 2656-7(Sept. 1965).

The field-desorption of thorium from a thermally smoothed tungsten substrate was previously investigated in the temperature range between 300° and 1090°K. The present work extends these measurements to 77°K and includes desorption from a field-evaporated surface as well as a thermally smoothed surface. For both types of surfaces at 77°K the desorption field strength was found to be 263×10^6 v/cm ± 10%. (auth)

41256 ELECTRON MICROSCOPE STUDY OF THE EFFECT OF OXYGEN ION IRRADIATION ON LITHIUM FLUORIDE. Carroll, Dennis B.; Birnbaum, H. K. (Univ. of Illinois, Urbana). J. Appl. Phys., 36: 2658-62(Sept. 1965). (COO-1198-227).

Large numbers of point defects were produced by the room-temperature bombardment of LiF by 100-kv oxygen ions. Clusters of these defects were studied in the electron microscope by means of their diffraction effects and their appearance in bright-field and dark-field images. Platelets of polycrystalline lithium were observed to form on $\{100\}_{LiF}$ planes. The mechanism of formation of these precipitates is discussed. (auth)

41257 SPUTTERING STUDIES OF INSULATORS BY MEANS OF LANGMUIR PROBES. Jorgenson, G. V.; Wehner, G. K. (Litton Systems, Inc., Minneapolis). J. Appl. Phys., 36: 2672-4(Sept. 1965).

The sputtering threshold energy and low-energy sputtering yields for films of sputtered quartz and Pyrex were measured with Langmuir probes. The probe characteristic is very sensitive to deposits of insulating material because even very thin insulating films cause radical changes in electron acceptance. A thin insulator film of known thickness is deposited on the probe by rf sputtering, and a known fraction of that film is removed by enforcing a dc bias voltage on the probe. Different bias voltages require different times to remove the same amount of material (as monitored in the probe characteristic), and one can use this as a very sensitive method for collecting sputtering yield data. Analysis of the deposit sputtered from a quartz target in a 10^{-2} Torr Ar discharge shows it to be $SiO_{1.8}$. The sputtering yield curve for this $SiO_{1.8}$ is presented and shows a yield of ~0.1 molecule/ion at 100 ev with a sputtering threshold of ~16 ev. (auth)

41258 STUDY OF ION-BOMBARDMENT DAMAGE ON A Ge(111) SURFACE BY LOW-ENERGY ELECTRON DIFFRACTION. Jacobson, R. L.; Wehner, G. K. (Litton Systems, Inc., Minneapolis). J. Appl. Phys., 36: 2674-81 (Sept 1965).

An atomically clean and highly ordered Ge(111) surface was bombarded with Ar^+ ions and the bombardment effects were studied by low-energy electron diffraction. Degradation characteristics of the (10) beam were most extensively investigated over an ion energy range from 10 ev to 1 kev with ion dosage ranging from 10^{12} to 10^{16} ions/cm^2. The degradation characteristics determine the mean area of damage per incident ion. This area is 7×10^{-14} cm^2 for a 1-kev Ar^+ ion and 1×10^{-15} cm^2 for a 40-ev ion. At low ion energies, some retention of (10) intensity is noted even for large dosages, indicating in this case that some short-range order is retained. The minimum ion energy for damage is ~20 ev. This value is close to the sputtering threshold energy and the reported displacement energy of Ge. A bombardment damage model is proposed to explain the low-energy ion-bombardment characteristics. Thermal recovery of the bombarded surface shows a dependence on ion energy and also on total bombardment dose. (auth)

41259 ANGULAR DISTRIBUTION OF SUBLIMED AND SPUTTERED PARTICLES FROM Ag SINGLE CRYSTALS. Cooper, C. Burleigh; Comas, James (Univ. of Delaware, Newark). J. Appl. Phys., 36: 2891-5(Sept. 1965).

When silver (100) and (110) single crystals were sputtered by 160 to 200-ev argon ions from an arc the well-known spot patterns appeared when the sputtered particles

were collected as a thin film on glass plates. To determine whether similar spot patterns would result from sublimation, the same crystals were sublimed at temperatures between 642° and 815°C under high-vacuum conditions. Optical transmission densitometer measurements on the resulting thin films indicated that during sublimation the emission was approximately cosine, and no evidence of preferential ejection of silver particles during sublimation was detected. It is estimated that if preferential ejection is taking place along the close-packed directions of the crystal during sublimation in this temperature range, this emission produced a thickness change of the collected silver films such that the transmitted light intensity varied from a cosinelike curve by less than 5% at those angles. (auth)

41260 EXCITATION OF THE H_β LINE OF HYDROGEN AND OF SOME MERCURY LINES BY COLLISION OF PROTONS AND H_2^+ IONS WITH MERCURY ATOMS. Bobashov, S. V.; Pop, S. S. Opt. Spectry. (USSR)(English Transl.), 18: 421-2(Apr. 1965).

Translated from Optika i Spektroskopiya, 18: 744-6 (Apr. 1965).

Measurements were made of the excitation cross section of the hydrogen H_β line for collisions of protons and H_2^+ ions (energies of 3–35 kev) with mercury atoms. The excitation cross section of the strongest mercury lines were also measured, and the dependence of the excitation cross section upon the energy of the ions H^+ and H_2^+ was obtained for energies ranging from 5 to 35 kev. The proton result confirmed the expectation that the excitation cross section of the H_β line increases with increasing atomic number of the atoms interacting with the protons; this increase, is, however, not very appreciable. In the case of single collisions of protons with mercury atoms, direct excitation ($H^+ + Hg \rightarrow H^+ + Hg$) is the only process that can lead to the emission of the Hg_I lines. The results are discussed. (P.C.H.)

41261 THE ENERGY SPECTRA OF ATOMS SLOWING DOWN IN STRUCTURELESS MEDIA. Robinson, Mark T. (Atomic Energy Research Establishment, Harwell, Berks.). Phil Mag. (8), 12: 145-56(July 1965). (AERE-R-4791).

Collision densities were computed for a uniform, isotropic source of mono-energetic atoms slowing down by elastic collisions with the atoms of an infinite, homogeneous, structureless medium. It is found that, because of the indistinguishability of the particles proceeding from a collision, the results are relatively insensitive to the shape of the differential elastic scattering cross section, whether this is described by a Legendre polynomial expansion, or by the interaction of the atoms through the Born-Mayer or the Thomas-Fermi potentials. For energies not too close to the source energy, the collision densities vary as $1/E^2$, in agreement with the result for hard-core scattering and with certain available experiments. (auth)

41262 SPIN-EXCHANGE LIGHT MODULATION BY ATOMIC HYDROGEN. Ruff, George A.; Carver, Thomas R. (Princeton Univ., N. J.). Phys. Rev. Letters, 15: 282-4(Aug. 16, 1965).

A transfer of coherence was observed from atomic hydrogen, which was driven in magnetic resonance, to optically pumped sodium vapor. The effect appears as a modulation of sodium monitoring light at a frequency corresponding to resonance in the hydrogen ground state. In the limit in which the exchange collision between hydrogen and sodium occurs in a time short compared to the Larmor period of either system, a simple theory of the exchange modulation and its line shape is given. The theory and experiment emphasize that the spin-exchange collision, though acting as a relaxation process for the driven system, is itself a driving interaction. (J.F.P.)

41263 INTERFERENCE OF FINE-STRUCTURE LEVELS IN HYDROGEN. Bashkin, S.; Bickel, W. S.; Fink, D.; Wangsness, R. K. (Univ. of Arizona, Tucson). Phys. Rev. Letters, 15: 284-5(Aug. 16, 1965).

Interference was observed between hydrogen fine-structure levels for n = 4, 5, 6, and 7. H_3^+ particles at 200 kev were sent through two successive foils; each foil was about 10 $\mu g/cm^2$ thick. Photographs were taken of the integrated light and of the individual Balmer lines, H_α through H_ϵ, which the foil-excited hydrogen atoms radiated. Then the spectrum from excited particles disturbed by electrostatic and magnetostatic fields was studied. Regularly-spaced bright spots were interpreted as arising from Stark-induced interference of hydrogen fine-structure levels. The results for Balmer lines and corresponding frequencies are tabulated. It appears that interference of closely spaced levels in hydrogen is identified. The electric field data also agree with the calculation. The helium lines showed no spots. (J.F.P.)

41264 INELASTIC SCATTERING OF ELECTRONS BY HELIUM. Chamberlain, G. E.; Heideman, H. G. M. (National Bureau of Standards, Washington, D. C.). Phys. Rev. Letters, 15: 337-8(Aug. 23, 1965).

The results are reported of extending the forward-scattering measurements to lower and higher energies than those previously reported. The extension to higher energies showed that the strongest resonances appear in pairs below each of the levels n = 3, 4, and 5. This clearly identified double series of resonances that previously appeared only dimly. The extension to lower energies permitted measurement of the energy dependence of the cross section in the neighborhood of threshold. It is believed that the cross section within a few electron volts of threshold is almost entirely due to resonance structures. These measurements are regarded not only as information on $e^- - He$ collisions but as a demonstration of new experimental capabilities. (J.F.P.)

41265 HIGHER ORDER CALCULATION OF THE LAMB SHIFT IN Li^{++}. Erickson, Glen W. (Univ. of California, Davis). Phys. Rev. Letters, 15: 338-41 (Aug. 23, 1965).

Calculations are given for the Lamb shift in $^6Li^{++}$, including higher order terms not considered previously as well as careful estimates of the limits of error in the calculation. These higher order terms are necessary for the comparison of theory with experiment because the largest ones are the most highly Z-dependent terms known and also because their magnitudes add up to more than the present difference between theory and experiment (although their algebraic sum is an order of magnitude smaller). The detailed error estimates are necessary in order to be able to say to what extent the various terms are actually tested. (J.F.P.)

41266 AN APPLICATION OF A VARIATIONAL PRINCIPLE TO THE CALCULATION OF FREE-FREE MATRIX ELEMENTS FOR H^-. Khare, S. P.; Rudge, M. R. H. (Queen's Univ., Belfast). Proc. Phys. Soc. (London), 86: 355-62(Aug. 1965).

A variational principle for the calculation of free–free matrix elements is described and applied to the case of an electron moving in the field of a hydrogen atom. It is shown that, even using very simple trial functions, the method gives good agreement with the results of more elaborate calculations. (auth)

41267 THE ELASTIC SCATTERING OF LOW ENERGY POSITRONS BY ATOMIC HYDROGEN. McEachran, R. P.; Fraser, P. A. (Univ. of Western Ontario). Proc. Phys. Soc. (London), 86: 369-73(Aug. 1965).

The elastic scattering of positrons by ground state hydrogen atoms, for positron energies below the threshold for positronium formation (6.8 ev), is investigated numerically, full allowance being made for the virtual excitation of all bound states of atomic hydrogen up to and including the 3d state. The phase shifts are obtained for the S, P, and D partial waves. The S-wave phases, when compared with those of Schwartz, point out the extremely slow convergence rate of the eigenfunction expansion approach to this problem. This slow rate of convergence also persists, especially at higher energies, for the P and D partial waves as well. (auth)

41268 STOPPING POWERS AND STRAGGLING IN NEON, ARGON AND KRYPTON. Bell, R. J. (National Physical Lab., Teddington, Middlesex, Eng.); Dalgarno, A. Proc. Phys. Soc. (London), 86: 375-7(Aug. 1965).

A semi-empirical procedure is used to calculate the mean excitation energies appropriate to stopping powers I and to straggling I_1 in neon, argon and krypton. The results are Ne: I = 150 ev; I_1 = 1200 ev; Ar: I = 220 ev, I_1 = 3200 ev; Kr: I = 360 ev, I_1 = 9600 ev. They are consistent with the experimental data. (auth)

41269 THE RANGES OF NITROGEN IONS IN NICKEL AND SILVER. Barker, P. H., Phillips, W. R. (The University, Manchester, Eng.). Proc. Phys. Soc. (London), 86: 379-85(Aug. 1965).

The ranges and range distributions of nitrogen ions in nickel and silver were determined for nitrogen ion energies of between 0.4 and 2.5 Mev. Values of the stopping cross sections for nickel and silver for these ions were determined from the (range, energy) curves and compared with present theories of the stopping processes. The range straggles provide information on atomic collision processes, and the observed straggles were compared with a simple model based on present approaches to stopping in the low velocity region. (auth)

41270 AUGER EJECTION OF ELECTRONS FROM SILVER. Morgan, C. G.; Jones, F. Llewellyn; Davies, D. Kenneth (University Coll. of Swansea, Wales). Proc. Phys. Soc. (London), 86: 403-7(Aug. 1965).

Values of the secondary ionization coefficient γ due to the Auger process of electron ejection caused by the incidence of atomic and molecular positive ions of helium on a silver cathode in low current discharges in the range $9 < E/p_0 < 41$ v cm^{-1} torr^{-1} of electric field E to gas pressure p_0 have been deduced from measurements of ionization growth times. For He^+ ions γ is found to be approximately 0.2 electrons per ion, but for He^+ ions the electron ejection efficiency is about 0.05 electrons per ion. The rate of conversion of atomic to molecular helium ions is deduced from the measurements to be approximately 160 p_0^3 sec^{-1}. Because of the p_0 and p_0^2 dependence of secondary processes at pressures in excess of about 20 torr the similarity principle for discharges is expected to fail in helium. (auth)

41271 DEPENDENCE OF SPUTTERING COEFFICIENT ON ION ENERGY. Martynenko, Yu. V. Soviet Phys.-Solid State (English Transl.), 6: 2827-30(June 1965).

Translated from Fiz. Tverd. Tela, 6: 3529-34(Dec. 1964).

A formula was obtained previously for the coefficient of sputtering of single crystals by ions having energies ranging from several kev to 10, 20, or more kev. At these energies, the interaction potential between the ions and the atoms is well approximated by the potential $\sim 1/r^2$. A generalization of this formula is obtained for large ion energies, where the interaction potential becomes coulombic. Further, by averaging the expression for the sputtering coefficient of the single crystals over all the structural parameters, a formula is found for the sputtering coefficient of polycrystalline materials, which, in spite of a number of simplifications, is in satisfactory agreement with the experimental data. (auth)

41272 AUGER EJECTION OF ELECTRONS FROM TUNGSTEN AND MOLYBDENUM BY MERCURY IONS. Dorozhkin, A. A.; Petrov, N. N. (Leningrad Polytechnical Inst.). Soviet Phys.-Solid State (English Transl.), 7: 88-91(July 1965).

Translated from Fiz. Tverd. Tela, 7: 118-22(Jan. 1965).

The method of ion-beam intensity modulation was used to study the ejection of electrons by mercury ions Hg^+ having energies from 500 to 2800 ev. It is shown that only the Auger ejection of electrons (which depended strongly on the target temperature) was observed for tungsten and molybdenum targets bombarded with these ions. It was established that both the kinetic and the Auger (potential) processes of electron ejection from tungsten by Ar^+ ions of 0.5–8 kev were independent of the metal's temperature over the whole range from 300 to 2100°K. A qualitative discussion of the data obtained is given. (auth)

41273 MULTIPLE SCATTERING OF 75- TO 200-Kev PROTONS ON SOLIDS. Bednyakov, A. A.; Svoretskii, V. N.; Savenko, I. A.; Tulinov, A. F. Vestn. Mosk. Univ., Ser. III: Fiz. Astron., No. 1, 55-63(Jan.-Feb. 1965). (In Russian).

The angular distributions of protons multiply scattered on thin films of Cu, Al, and polystyrene were measured. The data obtained are compared with the results of calculations made on the basis of the Moliere-Bethe theory. (tr-auth)

41274 MEASUREMENT OF FREE NEUTRON EXCITATION CROSS SECTIONS IN ALUMINUM AND BISMUTH. Triftshaeuser, Werner. Z. Physik, 186: 23-41(1965).

More accurate absolute determinations of the total neutron effective cross sections of Al and Bi were carried out (mean neutron wave length of 0.09 Å) using a special research installation at the FRM. From the measured values of 1.4207 ± 0.0010 and 9.2900 ± 0.0076 b for Al and Bi σ_{free} and the coherent scattering amplitudes of both elements were calculated as $3.4595 \pm 0.0017 \times 10^{-13}$ and $8.6253 \pm 0.0036 \times 10^{-13}$ cm with consideration for absorption, Doppler effect, crystal formation, and various other correction magnitudes. A comparison with the effective cross sections measured earlier shows a good agreement; however the accuracy obtained on the present study is better than the earlier measurements by a factor of 30 for Al and by a factor of 4 for Bi. The measurements are part of an experiment on the more accurate determination of the interaction of slow neutrons with electrons. (tr-auth)

41275 STUDY OF THE ENERGY EXCHANGE IN COLLISIONS OF MOLECULAR FLUX WITH A SURFACE. Leonas, V. B. Zh. Prikl. Mekhan. i Tekhn. Fiz., No. 2, 84-6(Mar.-Apr. 1965). (In Russian).

Apparatus is briefly described and some results are given for a study of the interaction of molecular beams with various metallic surfaces. Detailed descriptions of the experimental apparatus, the beam velocity selector, and the detector system are given in previous articles. The method of determining the molecular velocities by measuring the flight times for various known distances is discussed. The selected paths are such that the velocities of the incident and reflected molecules and the capture time of the molecules at the surface can be determined. Some results are given for molecular beams (Ar, CO_2) incident on metallic surfaces (Cu, Fe, Ta). It was found that for all combinations of molecular beams and surfaces, the velocity of the reflected beam corresponded to the mean velocity of the molecules at the temperature of the surface for all surface temperatures used in the range 300 to 1100°K. The capture times decreased with increasing surface temperature, depended on both the beam and the surface compositions, and were all in the range of 20 to 50 μsec. It was found, however, that the adsorption energy is practically independent of temperature and is about 1.8 ev. (ATD)

41276 MEASURING IONIZATION FUNCTION OF METAL ATOMS BY ELECTRON IMPACT. Beilina, G. M.; Pavlov, S. I.; Rakhovskii, V. I.; Sorokaletov, O. D. Zh. Prikl. Mekhan. i Tekhn. Fiz., No. 2, 94-6(Mar.-Apr. 1965). (In Russian).

A method is described for measuring the absolute ionization cross section of low-vapor-pressure metal atoms by electron impact. The apparatus used for this experiment involves a neutral atom source, an atomic beam chopper, an electron beam, a neutral atom collector, an ion collector, a thermopile, and a cooled collector for neutral atoms. The metal used was lead. An electrostatic selector was employed to make the electron beam monoenergetic. This was done successfully to within 0.35-ev electron energy. The ion current was measured by an electrometric amplifier U1-2 with an error of less than 8%. The ionization measurements were carried out from the threshold level up to 150 ev with a maximum ionization cross section of 8×10^{-16} cm^2 at 55 ev. The ionization cross section was determined from the expression Q = I₊ mtbv/I_M, where b is the atom beam width at the point of intersection with

the electron beam, t is the evaporation time and m is the atomic mass. A special effort was made to measure the neutral atom concentration accurately, condensing them on a collector cooled by liquid nitrogen. (ATD)

41277 INELASTIC ENERGY LOSS IN COLLISIONS OF NEON WITH ARGON, NEON WITH NEON, AND PROTONS WITH ARGON AT KILOVOLT ENERGIES (thesis). Flinchbaugh, David Edward. Storrs, Conn., Univ. of Connecticut, 1964. 93p.

The inelastic loss in kinetic energy for collisions of singly-ionized neon with argon atoms and with neon atoms, and protons with argon atoms, was measured as a function of the incident energy and scattering angle and energy. The Ne^+ on Ar collision processes were investigated at 3-, 6-, 12-, 25-, 50-, and 100 kev incident energies over an angular range of observation from 15 to 85° with respect to the incident beam. The other two ion-atom combinations were studied at 25 kev incident energy. Following a careful measurement of the single-collision parameters, the inelastic energy loss, or Q-value, for the reaction was computed for each defected charge state of both products of the collision utilizing the energy and momentum conservation equations. The energy loss was found, in most cases, to increase regularly with charge state, with incident particle energy, and with angle as the collision became more violent. The data for each incident energy are presented as plots of the mean energy loss Q_n for each charge state n versus the recoil angle ϕ for the target particle or versus the scattered incident particle angle θ. When the weighted mean inelastic energy loss $\overline{Q}'$ of all the data for each combination is plotted against the calculated distance of closest approach, r_θ, similar curves are obtained for each of the three cases. The best fit represents $\overline{Q}'$ as a function of r_θ to an inverse power, different for each case. The quantity $\overline{Q}'$ is also plotted against the average number of electrons lost, yielding a curve which rises above the boundary for net changes in total spectroscopic ionization energy. (Dissertation Abstr.)

41278 SPIN RELAXATION OF OPTICALLY PUMPED CESIUM (thesis). Franz, Frank Andrew. Urbana, Ill., Univ. of Illinois, 1964. 98p.

Spin relaxation of optically pumped cesium vapor was measured as a function of buffer gas pressure for various inert gases. Disorientation cross sections were found to be 5.3×10^{-24} cm² for neon, 8.0×10^{-23} cm² for argon, 2.1×10^{-21} cm² for krypton, and 4.6×10^{-20} cm² for xenon. The diffusion coefficients of cesium in neon and argon were found to be 0.40 and 0.23 cm²/sec, respectively. Disorientation cross sections and diffusion coefficients were also determined for molecular nitrogen. The results are $\sigma = 4.7 \times 10^{-23}$ cm², $D_0 = 0.22$ cm²/sec for $^{14}N_2$; $\sigma = 5.3 \times 10^{-23}$ cm², $D_0 = 0.20$ cm²/sec for $^{15}N_2$. The agreement of these values with existing theory is discussed. (Dissertation Abstr.)

41279 ROTATION AND VIBRATION IN N_2^+ FIRST NEGATIVE BANDS EXCITED BY ION IMPACT (thesis). Sheridan, John Roger. Seattle, Univ. of Washington, 1964. 101p.

Cross sections for excitation of the first negative bands of N_2^+ resulting from impact of H^+, D^+, He^+, Ne^+, and N^+ were measured in the energy range 10 to 65 kev, and at pressures such that radiation occurs much sooner than subsequent collisions of the excited molecule. Band ratios for the first negative system were measured directly and the rotational intensity distribution was determined in the 3914(0,0) and 4278(0,1) bands. Cross sections for excitation of Balmer radiation excited in charge exchange collisions of H^+ and D^+ with N_2 were measured in the same energy range. Supplementary measurements of total charge exchange cross sections and of relative band and rotational line intensities excited by e^- impact were also carried out. The measurements indicate a slight degree of enhancement of vibration for H^+, D^+, and e^- impact and a significant enhancement, varying with energy, for He^+, Ne^+, and N^+ impact. The rotational line intensities, however, show only a thermal distribution at room temperature. The measured cross sections are compared with theory and with experimental results of others where possible. Several models for describing production of vibration and rotation in ion impact collisions are discussed and related to the present experiment. (Dissertation Abstr.)

41280 ENERGY AND ANGULAR MEASUREMENTS OF RESONANT ELECTRON CAPTURE IN He^+ ON He COLLISIONS (thesis). Lockwood, Grant John. Storrs, Conn., Univ. of Connecticut, 1964. 68p.

Differential scattering of He^+ ions by He atoms in the energy range of 0.43 to 25.0 kev was studied as a function of scattering angle between 0.4 and 4.4°. The scattered ion was analyzed to determine if it had captured an electron after a single collision with a target atom. The limits in both energy and angle were chosen in order that a very wide variation in velocity and an impact parameter might be represented by the data. The high angular resolution needed in obtaining data at the small angles placed severe requirements on the beam-defining geometry and made precise determinations of the ion beam direction necessary. In addition, a spreading of the low energy ion beam, which would have prevented taking data at small angles, was observed. The use of a special high temperature collision chamber was necessary to prevent this spreading. Besides electron capture effects, electron stripping and electron double capture were also studied as represented by the He^{2+} and He^- components among the scattered particles. For this ion-atom combination, electron capture by the ion is a result of resonant charge transfer and the electron capture probability was observed to oscillate when plotted vs incident ion energy. However, the oscillation in electron capture probability which was found to be independent of scattering angle at the high ion energies, was observed to undergo a transition with the result that the electron capture probability oscillates rapidly with angle, independent of ion energy at low energies. From these data, relationships among electron capture probability, scattering angle, and ion energy are found and an empirical equation fitted to the data. These relationships are interpreted within the framework of the existing theory. (Dissertation Abstr.)

41281 THE ATOMIC SPECTRA OF ErI AND ErII (thesis). Marquet, Louis Carl. Berkeley, Calif., Univ. of California, 1964. 202p.

An intensive study of the optical spectrum of eribium was undertaken. Wavelengths of about 8000 lines were measured to an estimated accuracy of 0.015 cm^{-1}. Differentiation of the lines into first and second spectra is discussed. Self-reversal studies have identified over 350 lines in both spectra as transitions to low-lying levels. Analysis of these lines has led to the identification of the four lowest energy levels in ErI. These and the eight lowest levels of ErII reported by others have been well established by the Zeeman data of others and the high precision of the present wavenumber list. A total of 680 lines have been classified as transitions to one of these low levels, 172 in ErI and 508 in ErII. (Dissertation Abstr.)

41282 THE THEORY OF ELECTRON-ATOM COLLISIONS. Drukarev, G. F. New York, Academic Press, 1965. 169p. $6.50.

Translated from the Russian by S. Chomet.

The quantum theory of electron-atom collisions is expounded. Both the general theory and its application to specific problems are covered. (D.C.W.)

41283 ELASTIC DIFFERENTIAL SCATTERING OF He^+ IONS BY He IN THE 20-600 ev RANGE. Lorents, Donald C.; Aberth, William (Stanford Research Inst., Menlo Park, Calif.). 28p. (CONF-641210-21). Gmelin, AED-CONF-64-236-36.

From American Physical Society Meeting, Berkeley, Calif.

Absolute elastic differential scattering cross sections for He^+ on He were measured at relative energies of 20 to 600 ev over an angular range of 1–36°. The ions are extracted from an electron bombardment source, formed into a ribbon beam by a pair of slits, and scattered in a gas cell containing He. The scattered beam is energy-analyzed and

then detected by an electron multiplier. The relative data are normalized to absolute cross sections obtained at small angles using a Faraday cage in place of the multiplier. The effect of geometry, target particle motion, and inelastic scattering on the angular resolution of the elastic cross sections is discussed. Three distinct interference phenomena are observed: a series of smooth sinusoidal oscillations resulting from interference between the waves scattered from the gerade and ungerade potentials of the molecular ion, rainbow scattering, and secondary oscillations at large angles due to nuclear interchange. (auth)

41284 ELECTRON AND ION EMISSION FROM CESIATED AND VACUUM SURFACES. Wilson, R. G. 15p. (CONF-650410-17). Gmelin, AED-CONF-65-073-17.

From American Physical Society, Washington, D. C.

Vacuum thermionic emission, full temperature range cesiated electron emissive S curves, and cesium ion current densities were measured for various substrates which include refractory metals, nonrefractory metals, semiconductor refractory compounds, and one insulator. The influence of applied field, contamination, and temperature time, and field hystereses are studied. A brief description of the experimental techniques is given, and results for beryllium, copper, nickel, and 304 stainless steel are shown. (L.B.S.)

41285 POSITRON ANNIHILATION IN SOLID AND LIQUID METALS AND SEMI-CONDUCTORS. Kusmiss, J. H.; Stewart, A. T. (Univ. of North Carolina, Chapel Hill). 17p. (CONF-650410-19). Gmelin, AED-CONF-65-073-31.

From American Physical Society, Washington, D. C.

The angular correlation of the γ-ray pairs produced by the annihilation of positrons was studied in Bi, Ga, Hg, K, Sb, Sn, Te, Al, Cd, In, Pb, Zn, Na, Li, Se, and Tl. Results were obtained for each material at room temperature and at temperatures just above and below the melting point, in order to distinguish between effects due solely to the melting process and those due to increasing the temperature. (L.B.S.)

41286 POLARIZATION AND EXCHANGE EFFECTS IN SLOW ELECTRON SCATTERING FROM LITHIUM AND SODIUM. Garrett, W. R. (Univ. of Alabama, Huntsville). 24p. (CONF-758-47). Gmelin, AED-CONF-65-003-79.

From American Physical Society Meeting, New York, Jan. 1965.

Total elastic scattering cross sections were calculated for low energy electrons incident on lithium and sodium. The effects of target distortion by the electric field of the incident particle and electron exchange between incident and bound electrons were included through the adiabatic exchange approximation. In this method, the effect of the distortion induced in the target atom is computed through a polarization potential which is obtained by the method of polarized orbitals. The phase shifts and the total elastic scattering cross sections are obtained through the solution of a set of integrodifferential equations. The calculated polarization potential agrees asymptotically with experimental determinations of the dipole polarizability of Li and Na, and the total elastic scattering cross sections agree well with recent measurements over the entire experimental range. Results of both alkalis exhibit a small resonance at the experimental peak around 1 volt and a second peak at lower energies outside the present experimental range. (auth)

41287 SPECTROSCOPIC INVESTIGATIONS OF SOME HALIDE REACTIONS IN PLASMA-GENERATING DEVICES. Kana'an, Adli S.; Beguin, Claude P.; Margrave, John L. (Univ. of Wisconsin, Madison and Rice Univ., Houston, Tex.). 22p. (CONF-812-5). Gmelin, AED-CONF-64-207-7.

From Society for Applied Spectroscopy 3rd National Meeting, Cleveland, Sept.-Oct. 1964.

The behavior of some halides of carbon (CF_4, CCl_4, CF_3Cl, and Teflon), silicon (SiF_4 and $SiCl_4$), and boron (BF_3) in plasma jet reactors were investigated by emission spectroscopy. The emission spectra from these compounds were identified and arise from excited diatomic molecules SiF, SiO, BO, C_2, and CN and excited atoms of Si, B, and C. On the basis of the observed spectra and energetic and thermodynamic arguments it is concluded that dissociation, excitation and/or ionization processes requiring 25 to 30 ev are predominant in the plasma reactors under the experimental conditions of these studies. (auth)

Cosmic Radiation

See also Elementary Particles and Radiations. Nuclear Properties and Reactions.

Refer also to abstract 41571.

41288 (NASA-CR-58203) DATA REDUCTION AND ANALYSIS FOR HEAVY PRIMARY COSMIC RAY EXPERIMENT IN EXPLORER VII SATELLITE. Final Report, November 1, 1961–December 31, 1963. Pomerantz, M. A. (Bartol Research Foundation, Swarthmore, Pa.). June 24, 1964. Contract NASr-79. 75p. (N64-30518; N64-30519). CFSTI $3.00 cy, $0.75 mn.

Data taken from the heavy nucleus $Z \geq 6$ experiment aboard Explorer VII are examined. A comprehensive analysis of the data is presented after the completion of a rigorous data reduction process. Most of the results from the heavy nucleus experiment are presented. (M.O.W.)

41289 ON THE MECHANISM OF γ-RAY EMISSION IN SOLAR FLARES. Zheleznyakov, V. V. Astron. Zh., 42: 96-101(1964).

The solar flare of 20 March 1958 may be considered as an instance of joint emission of radio waves and gamma rays with energies of 0.2 to 0.5 Mev on one quantum. Its radio emission was probably based on magnetobremsstrahlung of relativistic electrons in local solar magnetic fields. There are other possibilities for generation of gamma-radiation, such as the annihilation of proton-electron pairs and the inverse Compton effect. The inverse Compton effect is meant to denote dispersion of energetic electrons on soft protons, transferring the energy of electrons to protons. The gamma-radiation becomes intense at the surface of the sun, where the energy of photons can increase to the level required for generation of gamma-radiation. The radio emission decreases with increased wavelength, as predicted from theoretical computations. A discrepancy was found between the theoretical and experimental data which is explained by strong gyroresonance absorption of waves in the corona. The great difference between the number of electrons necessary to generate gamma-radiation and that sufficient for radio emission verifies the impossibility of generating gamma-radiation by bremsstrahlung when the source is located in the corona. The third source of formation of gamma-quanta in the solar corona and chromosphere is the annihilation of electron-positron pairs. It can occur in the case of slow electrons and positrons when two gamma-quanta are created with energies of about 0.5 Mev in each event. This can occur when the energy of gamma-quanta is concentrated near the value of mc^2. X radiation by magnetobremsstrahlung seems to be only slightly probable, because a strong magnetic field and high-energy electrons cannot exist under solar conditions. (ATD)

41290 TREATMENT PROGRAM OF PENETRATING SHOWERS OF COSMIC RAYS WITH THE ENERGY OF 10^{10} TO 10^{12} ev. Gabunia, L. L., Mandrizkaya, K. W.; Razdolskaya, L. A.; Roinishvili, N. N.; Tatalashwili, N. N. Fiz. Chastits Vysokikh Energii, Akad. Nauk Gruz. SSR, Inst. Fiz., 1: 65-84(1965). (In Russian).

Several articles are presented concerning the problems of treatment of a single track and also geometric and kinematic analysis of penetrating showers in the whole. In the first paper a method is given for the exclusion of erroneous measurements at the treatment of data by the method of least squares, which appear with smoothing of measured trajectory traces. The second paper shows that errors in the coefficient of increase at the spatial reconstruction of single points of the trajectory has an essential influence on the measured momentum of the corresponding particles

and in the connection with this fact there is offered a method excluding errors of such a kind. The third paper describes the method of restoration of the place of a shower generation, exclusion of traces not taking part in the interaction, analysis of angular distributions and kinematics of a penetrating shower. (auth)

41291 THE ORIGIN OF HIGH-ENERGY PIONS, MUONS, AND PHOTONS. Grigorov, N. L.; Kotov, Yu. D.; Rozental, I. L. (Moscow State Univ. and Moscow Inst. of Engineering Physics). Izv. Akad. Nauk SSSR, Ser. Fiz., 28: 1815-20 (Nov. 1964). (In Russian).

Muon spectra may be derived from the pion spectra if it assumed that the pions are the basic source of muons and that the attenuation length and interaction range in air do not depend on energy and depth. The photon spectra are determined by the decay of the π^0 mesons, the number of which depends on the number of charged pions. This phenomenon was examined, using data on cosmic ray muons at sea level and stratospheric photons. The results showed that in the collision of nuclear-active particles with the nuclei of the atoms of air, a small number of pions take away about 1/5 of the energy of the elementary particles. In spite of their small number, the fast pions play a very important role in the formation of high-energy muons. In the pion–light nucleus interactions, in about 40% of the cases a negative pion is formed, carrying away 30 to 35% of the energy of the primary particle; a positive pion of the same energy is emitted in about 15% of the cases. The various theories developed in connection with the passage of cosmic ray components through the atmosphere, viz, the hyperon, isobaric, and pionization hypotheses and the Landau process are reviewed. (TTT)

41292 ENERGY SPECTRA OF COSMIC-RAY MUONS AT SEA LEVEL AND ENERGIES EXCEEDING 10^{11} ev. Krasil'nikov, D. D. (Inst. of Cosmic Studies and Aeronomics, Academy of Sciences, Siberian SSR). Izv. Akad. Nauk SSSR, Ser. Fiz., 28: 1854-6(Nov. 1964). (In Russian).

An analysis of large ionization bursts observed by means of shielded spherical cameras was extended to $n \cong 10^5$ cascade particles in Pb($E_0 \cong 10^{13}$ ev), proceeding from data obtained during the 8-year period of observing bursts at Yakutsk at a height of 100 m above the sea level. The muon-generated burst data were transformed into integral energy spectrum values of the total muon intensity at sea level, using an approximation method for integrating the equation of bursts formed by bremsstrahlung, knocking-out of electrons, pair formation, and nuclear interaction. The bremsstrahlung was found to be the most important process. The contribution of two opposite effects, viz, the fluctuation effect and the effect of the probable underestimation of the scattering of cascade particles, was neglected in the calculations. It is concluded that 10^{11} to 10^{12} muons are formed by means of π-μ decay; at higher energies other processes may be responsible. The total energy losses of muons in the ground as the result of pair formation, bremsstrahlung, and nuclear interaction amount to $>3 \times 10^{-6}$ E Mev g^{-1} cm^2. (TTT)

41293 ESSENTIAL MEASUREMENTS OF THE μ-MESON INTENSITY AT A GREAT DEPTH UNDER WATER. Vavilov, Yu. N. (Lebedev Inst. of Physics, Moscow). Izv. Akad. Nauk SSSR, Ser. Fiz., 28: 1857-60 (Nov. 1964). (In Russian).

Muon intensities, measured at underground depths corresponding to 6000m of water equivalent (mwe), were found to be dependent on their energy spectra at sea level at energies higher than 3×10^{12} ev. Knowledge of the muon energy losses and their absorption curve at various depths makes it possible to obtain the sea-level muon energy spectrum at energies $>10^{12}$ ev, thus helping to clarify the generation of muons possessing such energies. The energy losses were identified as electromagnetic and "nuclear" losses; they were different, depending on the medium (soil or water) in which the losses occurred. Even at 4000m in water, the muon intensity is found to be about 4 times higher than at the same depth in the soil. Cherenkov type or liquid scintillator counters are proposed for experimental work in this field. A model of a Cherenkov counter, with sea water as the emitter, has been constructed. Preliminary tests with this instrument at a depth of 17m during the trip of the research ship "Moskovskii Universitet" revealed that its efficiency for detecting muons exceeded 70%. (TTT)

41294 POLARIZATION OF COSMIC MUONS AT VARIOUS ENERGIES AND DETERMINATION OF THE RATIO $K^+/(K^+ + \pi^+)$. Asatiani, T. L.; Sharkhatunyan, R. O. (Inst. of Physics, State Committee on Utilization of Atomic Energy, USSR). Izv. Akad. Nauk SSSR, Ser. Fiz., 28: 1861-3(Nov. 1964). (In Russian).

The polarization of cosmic muons with a residual energy of E_μ of 140, 250, and 300 Mev, and 1.45 and 2 Bev was studied, the energy being determined from the thickness of the material above the apparatus. The measurements were carried out by rectangular and circular hodoscopes and a Wilson chamber. The polarization was calculated from the asymmetry in the angular distribution of the positrons formed by the decay of the muons at rest. About 90,000 and 20,750 decay events are observed with the rectangular and circular hodoscope respectively, and 1623 with the Wilson chamber. Data obtained at energies higher than 1 Bev indicated that the parent pions and kaons correspond to intervals from 4 to 7 and 4 to 87 Bev. Assuming that beyond 1 Bev the index of pion and kaon generation spectra $\gamma_\pi = \gamma_k = 2.65$, the following relation was obtained: $K^+/(K^+ + \pi^+) = 0.26 \pm 0.06$. (TTT)

41295 EMISSION OF ULTRA-HIGH ENERGY μ MESONS IN LAMINAR MEDIUM. Artyunyan, F. R.; Ispiryan, K. A.; Organesyan, O. G. (Inst. of Physics, State Committee on Utilization of Atomic Energy, USSR). Izv. Akad. Nauk SSSR, Ser. Fiz., 28: 1864-5(Nov. 1964). (In Russian).

The radiation generated by the passage of fast charged particles through a medium consisting of 300 paper layers is investigated. After passing through this medium, the μ mesons, which have an energy exceeding 10^{12} ev, are accompanied by 35 to 70 kev γ quanta. This radiation is allowed to pass through a Xe absorber kept at an overpressure of 5 cm of Hg in a Plexiglas container. After absorbing this radiation, the Xe emits its characteristic 35-kev γ quanta, which are recorded by 8 NaI scintillators in locations outside of the path of the μ mesons. The cosmic μ mesons are recorded by means of a GM-counter telescope. During a 2670-hour period, 47 events are recorded; only 3 events are found during a 1200-hour control test. The results seem to indicate that these events involve resonance emission of μ mesons with energies higher than 2×10^{12} ev in the laminar medium. (TTT)

41296 ON THE PRECISION OF CALCULATIONS OF FAST MUON ENERGY LOSSES. Kotov, Yu. D.; Rozental, I. L. (Moscow Inst. of Engineering Physics). Izv. Akad. Nauk SSSR, Ser. Fiz., 28: 1866-9(Nov. 1964). (In Russian).

The reliability of a previously developed method for computing the energy lost by fast muons is evaluated, taking into account inaccuracies in the perturbation theory calculations, the Born approximation, the photon formation in the atom electron field, screening, recoil effects, and radiation corrections. The calculated losses are tabulated. It is found that the effect of the medium becomes noticeable for muon energies $E_\mu \gg 10^{14}$ ev; the correction for pair formation is assumed to be of the same order of magnitude as the bremsstrahlung. The energy losses calculated on the basis of various form factors are found to be relatively small for shower formation; they are practically independent of the model used. The most probable value for losses in standard soil (Z = 10, A = 20) is 3.8×10^{-6} E g^{-1} cm^2; these values become 4.1 and 4.4×10^{-6} E g^{-1} cm^2 for soils with Z = 11, A = 22 and Z = 12, A = 24, respectively. (TTT)

41297 PROPERTIES OF A COMPONENT PENETRATING WIDE ATMOSPHERIC SHOWERS AT 200m DEPTH. Barnaveli, T. T.; Bibilashvili, M. F.; Grubelashvili, G. A.; Dzhavrishvili, A. K.; Kazarov, R. E.; Kuridze, R. V.; Khaldeeva, I. V. (Inst. of Physics, Academy of Sciences, Georgian SSR). Izv. Akad. Nauk SSSR, Ser. Fiz., 28: 1894-5(Nov. 1964). (In Russian).

A measuring system consisting of scintillation detectors

for determining the inclination of the axis of wide atmospheric showers, consisting of hodoscopes for measuring the coordinates of the axis with respect of the surface of the Earth and for establishing the total number of particles in the showers, and including 8 two-layer hodoscopic μ-meson detectors placed at an underground depth corresponding to 200m of water, was used for obtaining data on the irregularities in μ-meson fluxes. A law is found that is valid for the spatial distribution of the μ-meson flux. (TTT)

41298 FORMATION OF HIGH-ENERGY γ QUANTA IN WIDE 10^{15} ev ATMOSPHERIC SHOWERS IN THE UPPER ONE THIRD OF THE ATMOSPHERE. Antonov, R. A.; Smorodin, Yu. A.; Tulinova, Z. I. (Lebedev Inst. of Physics, Moscow and Moscow State Univ.). Izv. Akad. Nauk SSSR, Ser. Fiz., 28: 1896-8(Nov. 1964). (In Russian).

The formation of γ quanta in the upper layers of the atmosphere was studied for the purpose of obtaining data on the generation of pions in high-energy interactions. Ionization apparatus was used for recording the electron-photon showers formed by the γ quanta in the wide atmospheric showers above the recording devices. The 3.5-cm thick layer over the apparatus consisting of 15 cylindrical chambers with a total surface of 1.35m^2 ensured the recording of the particles in the 10^{11} to 10^{13} ev showers. It was found that an average of 1.3 showers reached the apparatus. Differences were found in the angular distribution of the showers which accompanied the recording of ionizing bursts ($\theta = 30 \pm 5°$) and atmospheric showers in general. If it is assumed that the showers are generated at the boundary of the atmosphere, it may be concluded from the calculations that the portion of scattered energy does not exceed one-third of the total energy. The gamma spectra generated by 10^{14} to 10^{15} ev particles exhibited a higher degree of energy dissipation during the pion formation in nuclear interactions than could have been expected from Landau's hydrodynamic theory. (TTT)

41299 X-RAY PHOTONS IN WIDE COSMIC SHOWERS IN THE STRATOSPHERE. Brazilevskaya, G. A.; Krasotkin, A. F.; Charakhch'yan, A. N. (Lebedev Inst. of Physics, Moscow). Izv. Akad. Nauk SSSR, Ser. Fiz., 28: 1899-1903 (Nov. 1964). (In Russian).

Comparison of the spectra of the low-energy (x-ray) photons formed in electron–photon cascade, calculated by the Klein-Nishina and Tamm formulas for the Compton scattering of photons, with the values derived from scintillation counter measurements in balloon probes, reveal that the actual intensity level of these photons in the stratosphere is much higher than the theoretical value, although there is an excellent agreement between experimental and calculated values for photons with energies in the Mev range. Recently, it has been suggested that these photons are generated by nuclear reactions. In order to resolve this question, the x-ray photons were investigated in wide atmospheric showers by means of 3 and 4-fold coincidences in scintillation and gas-discharge counters. The resolution of about 10^{-6} sec of the system made it possible to neglect random coincidences. The calculated values based on the equilibrium spectra of x-ray photons formed in electron–photon cascades agreed with the experimental data obtained in wide atmospheric showers. It is concluded that the intensity of the x-ray photons in the stratosphere should not be attributed exclusively to cascade processes. (TTT)

41300 CALCULATIONS OF WIDE ATMOSPHERIC SHOWER CURVES FOR NUCLEAR INTERACTIONS WITH VARIOUS MEAN FREE PATHS. Pomanskii, A. A.; Yudin, E. P. (Lebedev Inst. of Physics, Moscow). Izv. Akad. Nauk SSSR, Ser. Fiz., 28: 1904-6(Nov. 1964). (In Russian).

The interaction of nucleons with atoms of light materials indicates that λ, the mean free path of the interaction, may be 75 to 90 g cm^{-2}. Calculations are carried out to determine the effect of this numerical value on the fundamental characteristics of wide atmospheric showers, assuming that particles with energies of at least 3.7×10^9 ev are nuclear-active. The nucleons and $\pi^{\pm}$ lose their energy by forming π^0 mesons in nuclear interactions; the $\pi^{\pm}$ may decrease also by the $\pi^{\pm} \rightarrow \mu^{\pm}$ decay; no other processes are considered. The results supported a value of $\lambda = 90$ g cm^{-2}. Changing the contribution of baryons of all secondary particles generated in an elementary nuclear interaction act was found to affect strongly the number of nuclear-active particles in showers measured at sea level; the replacement of $\lambda = 75$ by $\lambda = 90$ g cm^{-2} did not affect this relationship or any of the other shower characteristics at sea level. (TTT)

41301 REDUCTION BY MEANS OF FINITE PASS BAND RADIOINTERFEROMETER. Balklav, A. (Astrophysical Lab., Academy of Sciences, Latvian SSR). Izv. Vysshikh Uchebn. Zavedenli, Radiofiz., 8: 244-50(1965). (In Russian)

The determination of the real distribution of radio brightness from a cosmic radiation source, taking into account the finite pass band of both the space and time interferometer frequencies, is studied. (D.C.W.)

41302 COSMIC RADIATION HELIUM SPECTRUM BELOW 90 Mev PER NUCLEON MEASURED ON IMP 1 SATELLITE. Fan, C. Y.; Gloeckler, George; Simpson, J. A. (Univ. of Chicago). J. Geophys. Res., 70: 3515-27(Aug. 1, 1965).

The differential spectrum of primary helium nuclei was measured over the energy range 30 to 90 Mev per nucleon in six energy intervals. The results are well-represented by the power spectrum $dJ/dE = 1.15 \times 10^{-5} E^{1.4 \pm 0.2}$ [m^2 sec ster Mev]$^{-1}$ where J is the integral flux of ^{3}He and ^{4}He, and E is the total kinetic energy. This is the time-averaged spectrum from November 27, 1963, to May 1, 1964, near the minimum of the solar activity cycle. There is evidence that this helium spectrum is the low-energy extension of the modulated, interstellar spectrum of cosmic helium: the the helium nuclei were continuously present over the 5-month period and not correlated with solar-flare phenomena; this helium spectrum extends smoothly into the higher-energy spectrum for cosmic-ray helium measured in balloons by others in 1963 and known to be of galactic origin; during this period the helium flux increased approximately 35% while the higher-energy cosmic radiation increased ~6%; this is the expected qualitative behavior for the solar modulation of an interstellar spectrum of helium during the decay phase of the interplanetary magnetic fields. Since the Imp 1 (Explorer 18) satellite had an apogee of 198,000 km, primary helium measurements were obtained over most of the orbital period. The experimental apparatus consisted of a solid-state, charged-particle telescope which measured the energy loss and total energy of protons, helium, and some components of higher charge. The novel use of semiconductor detectors, and their dynamic range, energy resolution, stability, and linearity as a function of particle charge, are discussed. (auth)

41303 NEAR-EARTH, POLAR-ORBITING SATELLITE MEASUREMENTS OF CHARGED PARTICLES. I. INSTRUMENTATION AND COSMIC RAYS. Seward, F. D.; Kornblum, H. N. Jr. (Univ. of California, Livermore). J. Geophys. Res., 70: 3557-70(Aug. 1, 1965).

A set of scintillation counters was carried on polar-orbiting Air Force satellites in the last half of 1961. Cosmic-ray effects were observed at high latitudes with good statistics. The L value of the "edge" of the cosmic-ray plateau was found to vary with longitude and to vary between L = 2.7 and L = 3.3. This corresponds to a "knee" at from L = 3.1 to L = 3.7. A "kneecap," consistently observed at the plateau edge, is interpreted as the appearance of reentrant albedo as the satellite moves to lower latitudes. The relative amount of this albedo was $8 \pm 2\%$ at an altitude of 300 km. A day-night effect in the observed high-latitude reentrant albedo cutoff is consistent with known day-night changes in the magnetosphere. The observed altitude dependence of flux at very high latitudes is used to derive an omnidirectional interplanetary flux of 2.6 ± 0.3 particles/cm^2 sec at this time. (auth)

41304 STUDY OF COSMIC-RAY INTENSITY MEASURED BY MARINER 2 AND BY GROUND NEUTRON

MONITORS DURING THE FORBUSH DECREASE OF SEPTEMBER 30, 1962. Rao, U. R. (Southwest Center for Advanced Studies, Dallas). J. Geophys. Res., 70: 3765-70(Aug. 1, 1965).

The study of cosmic-ray intensity measurements by Mariner 2 and by ground neutron monitors during the Forbush decrease yielded the following results. The neutron intensity at the ground recovers much faster than the ion chamber intensity, indicating that the intensity of low energy cosmic rays has not yet recovered to its pre-decrease value. Both the short-term variations, such as Forbush decreases and the long-term variations have similar spectrums of variation. The spectrum of variation during the Forbush decrease can be represented by $AE^{-0.45\pm0.04}$. The changes in cosmic-ray intensity are very well correlated with changes in solar wind velocity during the Forbush decrease. The experimental results are discussed. (J.F.P.)

41305 FINE STRUCTURE OF THE ENERGY SPECTRA OF FORBUSH DECREASES AND ITS DEPENDENCE ON SOLAR CYCLE. Kane, R. P. (Physical Research Lab., Ahmedabad, Israel). Nuovo Cimento (10), 38: 1457-66(Aug. 16, 1965).

The energy spectra of the Forbush decreases which occurred during May 1959 and September 1963 are studied. No significant difference in characteristics is observed, indicating no dependence on solar activity. Study of the fine structure indicates that for a spectrum of type $E^{-\nu}$, the ν values are ≥ 1.0 in the initial stages of the Forbush decrease, reduce to values 0.7 or less during the main phase and a part of the recovery, and increase to 1.0 or more during the later parts of recovery. Agreement with various theoretical models is discussed. (auth)

41306 EVIDENCE FOR HIGH-ENERGY COSMIC-RAY NEUTRINO INTERACTIONS. Reines, F. (Case Inst. of Tech., Cleveland); Crouch, M. F.; Jenkins, T. L.; Kropp, W. R.; Gurr, H. S.; Smith, G. R. Phys. Rev. Letters, 15: 429-33(Aug. 30, 1965).

Evidence is presented for the interactions of natural high-energy neutrinos obtained with a large area liquid scintillation detector (110 m^2) located at a depth of 3200 m (8800 mwe) in a South African gold mine. The essential idea of the experiment is to detect the energetic mesons (μ) produced in neutrino interactions in a mass of rock by means of a large area detector array embedded in it. It is concluded that if the seven events listed are all due to neutrinos, then either the neutrino flux is higher than anticipated or the interaction cross section rises more rapidly with energy above the region investigated by the accelerator groups. (J.F.P.)

41307 EFFECT OF MAGNETOSPHERIC TAIL ON COSMIC RAY CUT-OFFS. Michel, F. C. (Rice Univ., Houston, Tex.). Planetary Space Sci., 13: 753-60(Aug. 1965).

It is found that if the magnetospheric tail is longer than a characteristic length (estimated to be of the order of magnitude of one astronomical unit), then diffusion allows cosmic ray particles to enter the tail and appear essentially isotropically over the polar caps. The polar caps should then display no Stoermer-like latitude cut-offs whatsoever. For example, the recently observed fluxes of 3–12 Mev electrons should appear over the polar caps with the same intensity as in interplanetary space. Other available experimental data are compared with the theoretical prediction of zero cut-off energy for the polar caps. (auth)

41308 COHERENT RADIOEMISSION FROM COSMIC SHOWERS IN THE AIR AND DENSE MEDIA. Askar'yan, G. A. (Lebedev Inst. of Physics, Moscow). Zh. Eksperim. i Teor. Fiz., 48: 988-90(Mar. 1965). (In Russian).

Calculations based on the coherent radiation which results from the excess negative moving charge present in an electron-photon shower indicate the possibility of recording such showers by bursts of radiation. It is shown, in particular, that at small Cherenkov angles (shower in the atmosphere), the coherent radiation conditions are observed even for wavelengths much less than the dimensions of the shower particle clusters. The role of showers in the conduction of energy is noted in the registration of radiation in dense media. (CFSTI)

41309 THE NUCLEAR-ACTIVE COMPONENT OF EXTENSIVE AIR SHOWERS (thesis). Fletcher, Edward Royce. Albuquerque, N. Mex., Univ. of New Mexico, 1964. 102p.

The electron-photon and nuclear-active components of extensive air showers were studied at an intermediate altitude (1575 m.s.l.). A horizontal array of detectors was employed to measure the density of charged particles in the showers at several points so that the size, age, and the core location of the shower could be determined. Two large-area liquid scintillators were arranged to form a vertical telescope at the center of the array, in such a way that a variety of absorbing materials could be placed between them. When it was determined that the core of an extensive air shower had passed through this telescope, information about the nuclear-active component of the shower could be obtained by noting the number of particles in the lower scintillator which resulted from nuclear and subsequent electromagnetic interactions that took place in the composite filter between the two scintillators. Since the nuclear-active energy is confined to a region close to the core, a large portion of this energy can be expected to pass through a large-area detector when the core does. Thus, little information can be obtained about the number of nuclear-active particles with the present experimental arrangement. Approximately 2300 extensive air showers were recorded with each of four different arrangements of absorbers between the two liquid scintillators in the vertical telescope. When the distributions of observed multiplicities were studied, it was noted that the likelihood of multiplicities well above the average increases as the distance from the core decreases. This was particularly true in the arrangement where a low-Z material (water) was placed at an appropriate level in the composite filter to increase the number of particles produced in cascades initiated by nuclear-active particles. Those events where the observed multiplicity was greater than twice the predicted multiplicity were isolated as events containing possible nuclear interactions. The energy of the nuclear-active components passing through the vertical telescope was then computed from the number of particles in the lower scintillator in excess of that predicted by the electron-photon and nuclear-passive leakage through the composite filter. This nuclear-active energy as a function of shower size was shown to be in reasonable agreement with the results of others. (Dissertation Abstr.)

41310 SATELLITE OBSERVATIONS OF LOW ENERGY HEAVY COSMIC RAY NUCLEI. Fukui, Katsura; Lim, Yung K. 7p. (CONF-650410-18). Gmelin, AED-CONF-65-073-3.

From American Physical Society, Washington, D. C.

Stopping tracks of primary cosmic ray nuclei of charges equal and heavier than 6 were studied. The kinetic energy of each track was determined from range measurements, and the resulting spectra are shown for medium ($6 \leq Z \leq 9$), heavy ($10 \leq Z \leq 19$), and a very heavy ($20 \leq Z$) nuclei. The effect of solar modulation for medium and heavy nuclei was found to be similar to that of He nuclei. (L.B.S.)

41311 COSMIC RAY SEARCH FOR FRACTIONALLY CHARGED PARTICLES. DeLise, Donald A.; Bowen, Theodore (Univ. of Arizona, Tucson). 21p. (CONF-650410-9). Gmelin, AED-CONF-65-073-14.

From American Physical Society, Washington, D. C.

A mountain altitude search was made in the cosmic ray spectra for the hypothetical, fractionally charged particles known as quarks. These charge $\frac{1}{3}$ e and $\frac{2}{3}$ e particles have been theorized as the fundamental particles underlying one possible interpretation of the SU(3) classification schemes. A six element, liquid scintillator telescope, with the two central elements independent of the triggering requirements, was used in this search. The data were recorded in the form of differentially delayed pulses from the six photomultipliers. Using 90% confidence levels upper limits to the vertical intensities of $\frac{1}{3}$ e and $\frac{2}{3}$ e quarks at 760 gm/cm^2 atmospheric depth were found to be $I_O(\frac{1}{3}) \lesssim$

8.7×10^{-9} cm^{-2} sec^{-1} ster^{-1} and $I_Q(\frac{2}{3}) \lesssim 1.8 \times 10^{-8}$ cm^{-2} sec^{-1} ster^{-1}, respectively. The upper limits to the production cross sections were estimated as a function of the masses of these hypothetical particles and assumed values for attenuation mean free paths. If it is assumed that the quark production cross sections are of the order of 0.01 mb and that the quark removal cross sections are less than 15 mb/nucleon, then $M_Q(\frac{1}{3}) \lesssim 9$ Bev/c^2 and $M_Q(\frac{2}{3}) \lesssim 7$ Bev/c^2 are the lower limits. (auth)

41312 EFFECT OF A SOLAR FLARE ON THE OUTER RADIATION BELT. Paolini, F. R. (American Science and Engineering, Inc., Cambridge, Mass.); Theodoridis, G. C.; Katz, Ludwig. 13p. (CONF-758-30). Gmelin, AED-CONF-65-003-90.

From American Physical Society Meeting, New York, Jan. 1965.

The effect of the class 1^+ solar flare of 0734 UT 4 July 1963 on 0.7 to 4 Mev electrons and 1.5 to 4 Mev protons in the outer Van Allen belt was observed by the scintillation spectrometers flown on Hitch-hiker I. The outer belt was markedly depleted by this flare; at $(L, \lambda) \approx (5, 55°)$, electron intensities were reduced by more than an order of magnitude and proton intensities were reduced by about a factor of 3. Electron pitch angle distributions and electron and proton spectra observed following the flare and during the recovery period were similar in shape to those observed before. Electron intensities in this belt approached the pre-flare levels with a relaxation time of the order of 8 days. If a constant logarithmic loss mechanism and a constant source operative during the recovery period are assumed, a source strength of the order of 10^{13} erg/sec is implied for electrons of energy exceeding 1 Mev. The proton population of the outer belt recovered somewhat more slowly than the electron population. No perturbations in the inner belt, $L < 3$, were observed. (auth)

41313 ELECTROMAGNETIC INTERACTIONS OF 5-50 Gev/c COSMIC RAY MUONS WITH ELECTRONS. Kotzer, Peter. (Univ. of Washington, Seattle). 63p. (CONF-758-33). Gmelin, AED-CONF-65-003-57.

From American Physical Society Meeting, New York, Jan. 1965.

Quantum electrodynamic interactions between cosmic-ray muons and electrons are investigated in order to clarify previous results which showed that the data were not inconsistent with either a small admixture of spin $\frac{2}{3}$ muons or a possible refinement of the usual muon-electron scattering cross sections. Discussions are presented on theoretical muon-electron scattering cross section and two-body elastic-collision kinematic relations. Details are presented on the experimental arrangement, parameters, and data. The results are summarized and discussed along with previous results. (L.B.S.)

Direct Energy Conversion

Refer also to abstract 40566.

41314 (BNL-9329) STUDIES OF A REPETITIVE LIQUID METAL SLUG MHD GENERATOR. Powell, J. R.; Zucker, M. S.; Palmer, J. P.; Becker, W. W. (Brookhaven National Lab., Upton, N. Y.). June 1965. Contract AT-30-2-GEN-16. 42p. (CONF-650641-1). Dep. mn; CFSTI, $2.00 cy, $0.50 mn.

From American Society of Mechanical Engineers, International Conference on Energetics, Gatlinburg, Tenn.

Four major phases of a typical 5 Mwe MHD generator were investigated: (1) cycle thermodynamics, (2) electrical performance and efficiency, (3) slug injection, and (4) slug stability. (M.O.W.)

41315 MAGNETOPLASMADYNAMIC GENERATORS. Toschi, R. (EURATOM-CNEN, Rome). Alta Freq., 33: 125-43(Mar. 1964). (In Italian).

The conversion mechanism of the thermal energy of a plasma to electric energy via magnetoplasmadynamics is analyzed both from a simplified microscopic and macroscopic point of view. The electrical performances of different configurations of d-c and a-c MPD generators are derived and compared, and the state of art in this field is summarized. The fundamental equations of magnetoplasmadynamics are derived. (auth)

41316 A CONSIDERATION TO THE DESIGN OF MHD GENERATOR. Ito, Toshio; Morikawa, Tetsuya; Murai, Yutaka. Mitsubishi Denki Giho, 37: 1339-45(Nov. 1963). (In Japanese)

In an MHD generator duct, the temperature is extremely high, and the flow velocity is almost sonic. The thermal and frictional losses are very large. Taking these losses into account, theoretical considerations are given to the design of the MHD duct, and the effects on the efficiency of the MHD generator are considered. The results of calculations of the losses of open-cycle MHD generators with outputs of 200 kw to 400 mw are included. (D.C.W.)

41317 ON THE MOST EFFECTIVE REGIMES FOR THERMIONIC CONVERTORS. Dyuzhev, G. A.; Martsinovskii, A. M.; Pikus, G. E.; Yur'ev, V. G. Zh. Tekhn. Fiz., 35: 1160-2(June 1965). (In Russian).

The generally accepted view that, if only proper cathode materials could be produced, the direct-path plasma mode (vacuum with compensated space charge) would be the most effective method of thermionic energy conversion is thought to be questionable, and arguments are advanced to support the arc mode. The arc mode is considered to be superior in that it makes possible the use of low work-function emitters, whereas in the direct-path mode the space-charge neutralization is accomplished by ions generated in the volume. This advantage can become even more pronounced due to the presence of the anomalous Schottky effect. A comparison of published experimental data on the operation of the two modes demonstrates the superiority of the arc mode for the range of temperatures between 1400 and 2200°K. (ATD)

41318 THE TRANSIENT RESPONSE OF THE CESIUM DIODE TO POTENTIAL PULSES (thesis). Chung, Hui-Ying. Ames, Iowa, Iowa State Univ., 1964. 55p.

A theoretical analysis of the transport effects and the transient properties of the cesium plasma thermionic energy converters was made. The transport effects are due to the emitter sheath, the collector sheath, and the plasma resistance. The transient properties are related to the plasma resistance, inductance, and capacitance. These parameters are calculated for a simple model and checked against data reported elsewhere. The premise of these assumptions are to de-couple the related effects among these parameters and applying established theories to get a usable solution. The sheath thickness is in the order of Debye shielding distance, typically 10^{-4} cm for normal converter operation. The plasma resistance is mainly due to the electron scattering with the various particles in the plasma. For higher cesium pressure, the electron-neutral scattering was considered. The calculated resistivity for cesium plasma in the diode was less than one ohm-centimeter. The plasma reactance was calculated from reported current decay after a pulsed discharge. The origin of the plasma inductance is attributed to the electron-neutral scattering. When a high frequency emf was applied to the plasma diode, the latter reacted more like a perturbed resonant cavity. On the basis of oscillation modes an equation was derived for the plasma capacitor. The resulting capacitance varied with frequency and/or the sheath thickness. Plasma oscillations are interpreted in the discussion, and future possible research is mentioned. (Dissertation Abstr.)

41319 NEPOSRETSTVENNOE PREVRASCHCHENIE RAZLICHNYKH VIDOV ENERGII V ELECTRICHESKAYA I MEKHANICHESKUYU. (Direct Conversion of Various Types of Energy into Electrical and Mechanical Energy). Alekseev, T. N. Moscow-Leningrad, State Publishing House of Power Engineering, 1963. 334p.

General principles and theoretical premises of the direct conversion of chemical, nuclear, thermal, and solar energy into electrical and mechanical energy are presented. Various generators based on these principles are

described. Developments of designs for motors and electric generators are discussed. (M.J.T.)

41320 REVIEW OF MHD POWER GENERATION. Jackson, W. D. (Massachusetts Inst. of Tech., Cambridge). 9p. (CONF-414-8). Gmelin, AED-CONF-63-246-12.

From Conference on Direct Energy Conversion, Argonne, Ill., Nov. 1963.

A review is given of the development and characteristic features of MHD power generators. The economics of MHD central stations are compared with conventional power plants and non-MHD nuclear installations. Descriptions are given of a fossil fuel MHD system, gas-cooled reactor with combined MHD steam plant cycle, vapor MHD generator, single fluid with liquid metal MHD generator, two fluids with liquid metal generator, and linear and annular MHD induction generator. (L.B.S.)

Elementary Particles and Radiations

Refer also to abstracts 41306, 41666, and 41754.

41321 (AECD/TP/4) PHOTOPRODUCTION OF RHO- AND OMEGA-MESONS FROM NUCLEONS. Rashid, H. A. (Atomic Energy Centre, Dacca (Pakistan)). June 1965. 42p. Dep. mn.

Since the production of rho-and omega-mesons from nucleons by means of high energy photons are now experimentally possible, a detailed theoretical study of the photoproduction of these unstable vector particles will be very useful. The kinematics and the particular choice of the twelve invariant amplitudes of the process as well as the spin and helicity amplitudes of their inter-relations are described. The Mandelstam representation satisfied by the invariant amplitudes is obtained. Finally the one-particle intermediate state contributions to the various invariant amplitudes are obtained. For this purpose Feynman diagrams with nucleon exchange in s-channel, pseudo-scalar- and vector-meson exchange in the t-channel are considered. (auth)

41322 (BNL-9231) ON LINE DATA ANALYSIS OF HIGH ENERGY P-P SCATTERING EXPERIMENT. Fujii, T.; Anderson, E.; Bleser, E. (and others) (Brookhaven National Lab., Upton, N. Y.). May 11, 1965. Contract AT(30-2)-Gen-16. 15p. (CONF-650510-9). Dep. mn; CFSTI, $1.00 cy, $0.50 mn.

From Purdue Conference on Instrumentation for High Energy Physics, Lafayette, Ind.

In order to carry out a series of p-p inelastic scattering experiments at high energy, a system was developed which is capable of analyzing the data from 12 digitized spark planes on line to a PDP-6 computer. Some operational experiences obtained with this system are presented. (M.O.W.)

41323 (CALT-68-42) PHOTOPRODUCTION OF π^+ MESONS FROM HYDROGEN FROM 0.6 TO 1.2 Gev. Ecklund, S. D.; Walker, R. L. (California Inst. of Tech., Pasadena). [1960]. Contract AT(30-1)-844. 20p. (CONF-650636-1). Dep. mn; CFSTI, $1.00 cy, $0.50 mn.

From International Symposium on Electron and Photon Interactions at High Energies, Hamburg.

The reaction $\gamma p \rightarrow \pi^+ n$ was studied at the CIT Synchrotron with a magnetic spectrometer and counter system by identifying π^+ mesons of specific laboratory momentum and angle. Kinematics then determine the π^+ center of momentum angle θ and laboratory photon energy K. A sample of cross section data for 32 values of K between .578 and 1.248 Bev each with 14 to 20 values of θ is presented. (M.O.W.)

41324 (CERN-65-14) ETUDE EXPERIMENTALE DE LA PRODUCTION DE PARTICULES A PETIT ANGLE DANS LES COLLISIONS PROTON-PROTON ET PROTON-NOYAU A 20 Gev. (Experimental Study of the Production of Particles at Small Angles in Proton-Proton and Proton-Nucleus Collisions at 20 Gev). Jordan, B. (European Organization for Nuclear Research, Geneva (Switzerland)). Apr. 7, 1965. 116p. Dep.(mn).

An experimental study was made of the production of particles (π^+, π^-, K^+, K^-, antiprotons, and protons) in the collisions of protons at 20 Bev and with targets of liquid hydrogen, Be, and Pb. The experimental techniques used and the correction methods are described. The characteristic traits of the spectra obtained are emphasized and the spectra are compared with previous results. The information is coordinated to give angular distributions relative to the different particles. The basic hypotheses on nuclear models are reviewed and the results obtained from these models are discussed. The results obtained are compared with predictions of the various models and the disagreements and agreements are discussed in some detail. (J.S.R.)

41325 (CU-1932-245) ANNIHILATION OF ANTIPROTONS IN HYDROGEN AT REST. III. THE REACTIONS $\bar{p} + p \rightarrow \omega^0 + \pi^+ + \pi^-$ AND $\bar{p} + p \rightarrow \omega^0 + \rho^0$. Baltay, C.; Franzini, P.; Luetjens, G.; Severiens, J. C.; Steinberger, J.; Tycko, D.; Zanello, D. (Nevis Labs., Columbia Univ., Irvington-on-Hudson, N. Y.). July 1965. Contract AT(30-1)-1932. 15p. (NEVIS-139; R-511; CU-245). Dep. mn; CFSTI $1.00 cy, $0.50 mn.

The reactions (a) $\bar{p} + p \rightarrow \omega^0 + \pi^+ + \pi^-$ ($\pi^+\pi^-$ nonresonating), and (b) $\bar{p} + p \rightarrow \omega^0 + \rho^0$ were studied for antiprotons at rest. It is found that reaction (a) proceeds from the ^3S $\bar{p}p$ state whereas reaction (b) is allowed only for the ^1S state. Reaction (a) accounts for 0.039 ± 0.005 of all annihilations, and reaction (b) for 0.007 ± 0.003 of all annihilations. (auth)

41326 (HUX-2752-9) ON THE ELECTROMAGNETIC FORM FACTORS OF THE NEUTRON (thesis). Dunning, John Ray Jr. (Harvard Univ., Cambridge, Mass. Dept. of Physics). Nov. 1964. Contract AT(30-1)-2752. 140p. Dep. mn; CFSTI $4.00 cy, $1.00 mn.

The cross section for inelastic electron-deuteron scattering was measured in the four momentum transfer region corresponding to $q^2 = 0.389$ to 6.81 $(Bev/c)^2$ ($q^2 = 10$ to 175 f^{-2}). A liquid deuterium target was used in the internal beam of the Cambridge Electron Accelerator. The scattered electrons were detected with a spectrometer of 6.94% momentum acceptance centered on the quasi-elastic maximum. At $q^2 = 0.389$ to 1.17 $(Bev/c)^2$ and forward scattering angles the quasi-elastic recoil protons were also detected. An impulse approximation model for electron-deuteron scattering in the form given by Durand was used to interpret the deuterium cross sections as the sum of free proton and free neutron scattering cross sections. Using elastic electron-proton scattering cross sections obtained with a hydrogen target and the Rosenbluth equation, neutron form factors were obtained at $q^2 = 0.389$, 0.623, 0.857, 1.17 and 1.75 $(Bev/c)^2$. Upper limits on the form factors were extracted from the $q^2 = 2.92$, 3.89, and 6.81 $(Bev/c)^2$ data. (auth)

41327 (IC/65/63) GENERALIZED SPHERICAL FUNCTIONS FOR THE NON-COMPACT ROTATION GROUPS. Fischer, J.; Niederle, J.; Raczka, R. (International Centre for Theoretical Physics, Trieste (Italy)). June 1965. 20p. Dep. mn.

Special representations of arbitrary non-compact rotation groups labelled by one non-vanishing Casimir operator are considered. The explicit construction of the corresponding generalized spherical functions is given and the properties of these representations are discussed in detail. (auth)

41328 (IS-1187) STIMULATED COMPTON SCATTERING OF ELECTRONS BY LASER BEAM. Bartell, L. S.; Thompson, H. Bradford (Ames Lab., Iowa State Univ. of Science and Tech.). July 14, 1965. Contract W-7405-eng-42. 8p. (CONF-650638-1). Dep. mn; CFSTI, $1.00 cy, $0.50 mn.

From Physics of Quantum Electronics Conference, San Juan, Puerto Rico.

The scattering of a beam of electrons by intense standing waves of photons inside a laser cavity was recently observed. It is believed that this scattering corresponds to the stimulated Compton effect predicted by Kapitza and

Dirac many years ago. The analogy between this effect and its inverse, the scattering of photons by a periodic lattice of electrons, is discussed along with several experimental observations and possible applications. (auth)

41329 (JINR-P-2208) ELEKTROMAGNITNYE RASSHCHEPLENIYA MASS 70-PLETA V SKHEME SIMMETRII SU(6). (Electromagnetic Mass Splitting of 70-Plet in the Symmetry Scheme SU(6)). Dao Wong Duc; Cao Chi (Joint Inst. for Nuclear Research, Dubna (USSR). Lab. of Theoretical Physics). 1965. 6p. Dep. mn.

Relations were found for the electromagnetic mass splitting of the baryon resonances of the 70-plet in the SU(6) symmetry. (auth)

41330 (JINR-P-2213) KORRELYATSIONNYE FUNKTSII SLUCHAINYKH PROTSESSOV TIPA RAZMNOZHENIYA. (Correlation Functions for Processes of the Multiplication Type). Kozik, B. (Joint Inst. for Nuclear Research, Dubna (USSR). Lab. of Theoretical Physics). 1965. 5p. Dep. mn.

It is shown that the correlation functions, $K_{ik}(t',t)$ of Markov's multiplication processes involving r types of particles satisfy, for t (at $t > t'$), just the same system of equations as the average numbers $n_k(t)$ of the particles do. The Laplace transformation of these equations immediately determines the spectral power densities. (auth)

41331 (JINR-P-2219) BARIONNYE I MEZONNYE MUL'TIPLETY V GRUPPE SU(12), OB'EDINYAYUSHCHEI SIMPLEKTICHESKUYU I SPINOVUYU SIMMETRII. (Baryon and Meson Multiplets in the Group SU(12) Uniting Symplectic and Spin Symmetries). Fakirov, D. G. (Joint Inst. for Nuclear Research, Dubna (USSR). Lab. of Theoretical Physics). 1965. 30p. Dep. mn.

Quantum numbers of the baryon multiplet components are tabulated. These components comprise a 364-plet of the group SU(12) which was obtained as a unification of the symplectic group Sp(6) and the usual spin group. The components of the meson multiplet forming a 143-plet of the same SU(12) group are also listed. (auth)

41332 (JINR-P-2220) O RASSEYANII NAZAD CHASTITS VYSOKOI ENERGII. (On Backward Scattering of High Energy Particles). Blokhintsev, D. I. (Joint Inst. for Nuclear Research, Dubna (USSR). Lab. of Theoretical Physics). 1965. 5p. Dep. mn.

Using the optical model, under rather general assumptions it is shown that in the backward scattering there must occur a maximum of the width $\sim\lambda/R$ (R is the nucleon dimension). Unlike the forward scattering, the backward scattering cross section is constant or decreases with energy (depending upon a type of the optical model). (auth)

41333 (JINR-P-2227) DVOINOE N-N RASSEYANIE S POLYARIZOVANNYM PUCHKOM I POLYARIZOVANNOI MISHEN'YU. (Double N-N Scattering With a Polarized Beam and Polarized Target). Bilen'kii, S. M.; Lapidus, L. I.; Ryndin, R. M. (Joint Inst. for Nuclear Research, Dubna (USSR). Lab. of Nuclear Problems and Joint Inst. for Nuclear Research, Dubna (USSR). Lab. of Theoretical Physics). 1965. 20p. Dep. mn.

Experiments are discussed which concern measurements of nucleon polarization arising by scattering of a polarized beam by the polarized proton target. In these experiments it becomes possible for the first time to determine the components of the polarization tensor of the third rank M_{ikq}. The polarization correlation is treated in the case when one of the initial particles is polarized. The problem as to how to reconstruct the scattering matrix is being discussed. (auth)

41334 (JINR-P-2229) ELEKTRICHESKAYA I MAGITNAYA POLYARIZUEMOST CHASTITS VSLEDSTVIE NELINEINYKH EFFEKTOV ELEKTRODINAMIKI. (Electrical and Magnetic Polarizability of Particles Due to Nonlinear Effects of Electrodynamics). Gerasimov, S. B. (Joint Inst. for Nuclear Research, Dubna (USSR). Lab. of Theoretical Physics). 1965. 11p. Dep. mn.

Using dispersion relations for photon scattering and Lagrangian of nonlinear phenomenological electrodynamics, the coefficients of electric and magnetic polarizability of charged particles and particles with a magnetic moment due to nonlinear electrodynamic effects i.e., effects of vacuum polarization were calculated. The influence of the nonlinear electrodynamic effects in the processes of Coulomb neutron scattering and nuclei with large Z is discussed. Some qualitative features of the polarization of scalar and vector particles are indicated. (auth)

41335 (NP-15239) UNITARNAYA SIMMETRIYA I K_{e4} RASPAD. (Unitary Symmetry and K_{e4}-Decay). Report No. 320. Zakharov, V. I. (Gosudarstvennyi Komitet po Ispol'zovaniyu Atomnoi Energii SSSR, Moscow. Institut Teoreticheskoi i Eksperimental'noi Fiziki). 1965. 8p Dep. mn.

A relation between K_{e4} vector interaction coupling and $\eta \to \pi^+ + \pi^- \gamma$ coupling is derived in the limit of complete symmetry. Making use of this relation and experimental data available one can estimate the vector interaction contribution into observable effects in K_{e4} decay. The estimation leads to a considerable "right left" asymmetry. (auth)

41336 (NP-15335) PARTIAL WAVE DISPERSION RELATIONS FOR PIONIC DISINTEGRATION OF DEUTERON. Technical Report No. 436. Vasavada, Kashyap V. (Maryland Univ., College Park. Dept. of Physics and Astronomy). Feb. 1965. 88p.

A dispersion theoretic approach is made within the framework of partial wave dispersion relations to understand the pionic disintegration of the deuteron at low energies. The reaction amplitude is expressed in terms of six independent Lorentz invariant scalar functions which are free from kinematical singularities and the partial wave helicity amplitudes are obtained. Dispersion relations are written after removing kinematical singularities. After some approximations, the dispersion relations become soluble integral equations of the Omnes-Muskhelishvilli type. The contribution of the left hand single nucleon exchange cuts is evaluated exactly. The left hand anomalous contribution is evaluated approximately by replacing the cuts by poles in the appropriate channels. Analytic continuation in the deuteron mass gives the contribution of the right hand anomalous cut. Part of the right hand cut due to the two protons intermediate state is taken into account by using the experimental energy dependent phase shift parameters for proton proton scattering. The intermediate state containing two nucleons and one pion is effectively replaced by one particle and a resonance and model amplitudes are used to evaluate the contribution. The results of this calculation are numerically evaluated on IBM 7090 computer. For the angular distribution and the total cross section, a reasonable agreement is obtained with the results from low energy experiments. (auth)

41337 (NYO-2262-95) PROGRESS REPORT AND RENEWAL PROPOSAL FOR A RESEARCH PROGRAM IN EXPERIMENTAL AND THEORETICAL HIGH ENERGY PHYSICS. Feldman, David; Shapiro, Anatole M. (Brown Univ., Providence, R. I. Dept. of Physics). June 1, 1965. Contract AT(30-1)-2262. 40p. Dep. mn; CFSTI $2.00 cy, 1 mn.

Research in experimental and theoretical high-energy physics is discussed. A system for providing an electronic interface to the Brown University IBM 360/50 computer is described. (T.F.H.)

41338 (ORNL-TM-1149) A LOW PASS FILTER FOR COLD NEUTRONS TO BE USED IN A SEARCH FOR A NEUTRON ELECTRIC DIPOLE MOMENT. Miller, P. D. (Oak Ridge National Lab., Tenn.). June 1965. Contract W-7405-eng-26. 20p. Dep. mn; CFSTI, $1.00 cy, $0.50 mn.

An experiment to detect or set a new upper limit on the electric dipole moment of the neutron is being planned. Central to the apparatus is a bent neutron conducting tube to be installed at the HB-2 beam hole of the LITR. The dependence on various design parameters of the cold neutron spectrum from such a tube is investigated. (auth)

41339 (UCRL-11648) A FORTRAN PROGRAM FOR CALCULATING KINEMATICAL AND DYNAMICAL QUANTITIES OF PARTICLE INTERACTIONS AND DECAYS.

Trower, W. Peter (Lawrence Radiation Lab., Univ. of California, Berkeley). Sept. 3, 1964. Contract W-7405-eng-48. 3p. Dep. mn; CFSTI, $1.00 cy, $0.50 mn.

The application of special relativity to particle interactions is in general a straightforward but often tedious affair. A computer program is described that calculates relativistic kinematics and dynamics of particle interactions. (M.O.W.)

41340 (UR-875-53) TENSOR METHODS. II. MATRIX ELEMENTS OF THE DECUPLET OPERATOR OF SU_3. Pandit, L. K.; Mukunda, N. (Rochester Univ., N. Y. Dept. of Physics and Astronomy). Sept. 3, 1964. Contract AT(30-1)-875. 48p. Dep. mn; CFSTI, $2.00 cy, $0.50 mn.

In continuation of the work presented in an earlier paper on the tensor methods for SU_3, the nonvanishing matrix elements of the "decuplet operator" are derived. Simple derivations of some crossing and symmetry relations for the SU_3 Clebsch-Gordan-coefficients are given. It is further shown how the tensor methods lead to a simple understanding of the problem of reduction of direct products of arbitrary UIR's. (auth)

41341 ON THE ELECTROMAGNETIC CURRENT OPERATOR IN THE UNITARY SYMMETRY MODEL. Kapustsik, Edvard (JINR, Dubna, USSR). Acta Phys. Polon., 27: 633-6(1965). (In Russian).

The consequences of the assumption of scalarity of the photon relative to a subgroup of SU(3), the so-called U-spin group, are discussed. (tr-auth)

41342 A MODEL REQUIRING LIE GROUP SYMMETRIES. Polkinghorne, J. C. (Cambridge Univ., Eng.). Ann. Phys. (N. Y.), 34: 153-60(Aug. 1965).

Cutkosky's model of vector mesons in mutual interaction is rediscussed and extended by the introduction of further particles. The dynamical picture used is one based on the generation of Regge poles in scattering amplitudes in perturbation theory. It is found that particles of spin less than one must belong to representations of the Lie group of which the vector mesons form the adjoint representation. It is also found that the strength of the interaction of the lower spin particles is determined by the strength of the mutual interaction of the vector mesons, at least in the approximation discussed. (auth)

41343 A GENERALIZED ASYMPTOTIC CONDITION. I. Licht, A. L. (Naval Ordnance Lab., Silver Spring, Md. and Univ. of Maryland, College Park). Ann. Phys. (N.Y.), 34: 161-86(Aug. 1965).

The LSZ asymptotic condition is extended so as to apply to a class of fields that describe "particles" of indefinite mass. Sufficient conditions are given for the convergence of the asymptotic limits. These conditions are shown to be valid for several simple model field theories, including the generalized free field and the Zachariasen-Thirring model. (auth)

41344 PHOTOPRODUCTION OF π^+ AND π^- MESONS ON DEUTERIUM AT LOW ENERGY. Burq, Jean-Pierre (Faculte des Sciences, Orsay, France). Ann. Phys. (Paris), 10: 363-87(May-June 1965). (In French).

The differential cross sections for the photoproduction of π^+ and π^- mesons on deuterium was measured with great precision for photons with energy between 165 and 210 Mev and for pion emission angles of 155, 125, and 90°. The same ratio was measured for kinematic conditions so that the four-momentum transfer to the nucleon is constant and equal to the transfer at the reaction threshold. The particles emitted were analyzed with respect to charge and momentum. The rough results were corrected for the H contamination of the deuterium, the dead time of the coincident circuit and the gate circuit, the difference of nuclear absorption of π^+ and π^- mesons in matter, and of the contribution of electrons and positrons under the meson peak. The results are given and the implications are discussed. (J.S.R.)

41345 LOSS OF ENERGY BY ULTRA RELATIVISTIC MUONS. III. RANGE-ENERGY RELATION IN WATER AND ROCK. Castagnoli, Carlo; De Marco, Angelo; Scrimaglio, Renato. Atti Accad. Nazl. Lincei, Rend., Classe Sci. Fis., Mat. Nat. (8), 38: 201-6(Feb. 1965). (In Italian).

The range energy relation for ultra-relativistic muons in a condensed medium is calculated on the basis of an evaluation of the energy loss by pairs and nuclei and of the energy loss from collision. The two cases of water and rock are examined. (J.S.R.)

41346 ANALYTICAL EXPRESSIONS OF THE DEUTERON FORM FACTORS IN INDUCED DECAYS AS A FUNCTION OF THE DEUTERON PARAMETERS. Ballot, J.-Louis; Becker, Francois (Institut du Radium, Orsay, France). Compt. Rend., 260: 4714-16(May 3, 1965). (In French).

In a previous article (Compt. rend. 260: 4488(1965)), the deuteron form factors in induced decays were defined and their integral expressions were given as a function of the deuteron wave functions. In the present study these wave functions are defined and the method of integral calculation is presented. (tr-auth)

41347 ELASTIC n-p INTERACTION AT 3 TO 10 Bev. Besliu, Calin; Besliu, Tatiana; Constantinescu, Anisoara; (and others) (Universite, Bucharest). Compt. Rend., 260: 4495-8(May 10, 1965). (In French).

Elastic n-p reactions were studied using photographs of a propane chamber exposed to the neutron beam of the Dubna synchrophasotron. Eleven hundred events of the proton type associated with a star were selected. The elastic kinematics were varified using a χ^2 test. The dependence of using the elastic cross section of quadratransfer is graphed. The comparison of the values of the parameter b for proton-proton interaction with the present neutron-proton interactions indicates good agreement. This agreement proves the isotopic independence of these interactions. The elastic cross section is in agreement with the proton-proton elastic cross sections. (J.S.R.)

41348 NEUTRINOS AND SINGULAR ELECTROMAGNETIC FIELD. Moret-Bailly, Francoise (Faculte des Sciences, Dijon, France). Compt. Rend., 260: 6542-5 (June 21, 1965). (In French).

The fields of 1-spinors of the negative or positive type describing neutrinos have an isotropic associated current vector. Two of these spinor fields make it possible to construct a tensor field having the properties of the pure singular electromagnetic field. (tr-auth)

41349 WILLIAMS-WEIZSACKER COVARIANT METHODS FOR TWO VIRTUAL PHOTONS AND LIFETIME OF π_0. Le Guillou, Jean-Claude (Institut Henri-Poincare, Paris). Compt. Rend., 260: 326-9(July 12, 1965). (In French).

By using the results of a previous study, a covariant approximation method of the Williams-Weizsacker type for processes with two virtual photons was applied to the determination of the lifetime of π^0 as a function of the total production cross section of a π^0 in electron-electron collisions. (tr-auth)

41350 CHARGED SIGMA-HYPERONS GENERATED IN PHOTOEMULSION BY HIGH ENERGY PROTONS. Shakhulashvili, O. A. Fiz. Chastits Vysokikh Energii, Akad. Nauk Gruz. SSR, Inst. Fiz., 1: 1-27(1965). (In Russian).

Nuclear photoemulsion of the type BR—400 NIKFI irradiated by protons with the energy 9 Bev at the synchrocyclotron in Dubna was used to study generation and decay properties of $\Sigma^\pm$-hyperons. The energy distribution of charged Σ-hyperons below 350 Mev was obtained for $\Sigma^\pm$-hyperons generated both on heavy (72 $\Sigma^\pm$) and on light (25 $\Sigma^\pm$) nuclei of photoemulsion. There is a maximum in these spectra with rather a sharp slope towards high values of energy; it is situated in the energy range 100 to 200 Mev. The energy distribution of $\Sigma^\pm$-hyperons shows that, at least partially, the process of $\Sigma^\pm$-hyperon generation takes place at the peripheral collisions of nucleons. Using one dimensional approximation of secondary particle motion in the parent nucleus and the obtained data, the cross-section of $\Sigma^\pm$-hyperon generation in proton-nucleon interactions was found to be equal to 0.34 ± 0.08 mb. The

estimate showed that in the light nuclei of photoemulsion ≈35% of Σ^+-hyperons are generated by secondary π-mesons and in the heavy nuclei ≈50%. The study of angular distribution of π^+-mesons generated in decays of Σ^+-hyperons according to the scheme $\Sigma^+ \rightarrow n + \pi^+$ with respect to the normal to the plane of Σ^+-hyperon generation showed that in the system of hyperon generation this distribution is isotropic. The value 0.02 ± 0.02 of the coefficient of asymmetry was obtained. (auth)

41351 ANOMALOUS THRESHOLDS AND THE MASS SPECTRUM OF ELEMENTARY PARTICLES. Gedalin, E. V.; Kancheli, O. V.; Laperashvili, L. V.; Matinyan, S. G. Fiz. Chastits Vysokikh Energii, Akad. Nauk Gruz. SSR, Inst. Fiz., 1: 29-32(1965). (In Russian).

Attention is called to the fact that all stable particles, with respect to strong interactions, are characterized by an anomalous conditions on masses. In other words for any three different interconvertible particles of Gell-Mann—Nishijima scheme there are only vertices for which the following relations are valid: $M_0 < M_1 + M_2$, and $M_0^2 > M_1^2 + M_2^2$. An assumption is made that these relations regulate to a certain degree the spectrum, of masses of elementary particles and this principle, is used to obtain restriction for mass of particle predicted by Gell-Mann, but not yet discovered. (auth)

41352 REGGE POLES Y_1^* AND Y_0^* AND THE AMPLITUDE OF $\bar{K}N$-SCATTERING. Gedalin, E. V.; Laperashvili, L. V. Fiz. Chastits Vysokikh Energii, Akad. Nauk Gruz. SSR, Inst. Fiz., 1: 33-5(1965). (In Russian).

By means of a modified representation of Regge-Khuri total contributions of Regge poles Y_1^* (1385 Mev) and Y_0^* (1405 Mev) into the amplitudes of scattering of the two channel process $\pi Y \rightarrow \pi Y$, $\pi Y \rightarrow \bar{K}N$, $\bar{K}N \rightarrow \bar{K}N$ are found. The complex length of scattering of the process $\bar{K}N \rightarrow \bar{K}N$ is calculated in the state with isotopic spin T = 0 with the assumption that Y_0^* is a S-wave resonance. (auth)

41353 WEAK INTERACTION OF MESONS AND PERATIZATION. Kancheli, O. V.; Matinyan, S. G. Fiz. Chastits Vysokikh Energii, Akad. Nauk Gruz. SSR, Inst. Fiz., 1: 37-40(1965). (In Russian).

Weak scattering of mesons owing to W-meson exchange is considered in the ladder approximation. It is shown that all the contact terms disappear from the peratized allowed amplitude. (auth)

41354 ON THE SPECTRUM OF BURSTS GENERATED BY HIGH ENERGY μ-MESONS IN THICK ABSORBERS. Gedalin, E. V. Fiz. Chastits Vysokikh Energii, Akad. Nauk Gruz. SSR, Inst. Fiz., 1: 41-9(1965). (In Russian).

Large bursts caused by high energy muons are considered. The probability $P_\mu(n, E_\mu, E, t)$ was found of the fact that a shower generated by a muon of the energy E_μ, because of bremsstrahlung, will contain n charged particles with the energy larger than E at the depth t. It is shown that the spectrum of large bursts in thick absorbers practically coincides with the energy of incident muons. (auth)

41355 ON THE PROBLEM OF FLUCTUATIONS IN ELECTRON-PHOTON SHOWERS GENERATED BY HIGH-ENERGY μ-MESONS. Gedalin, E. V.; Mnatsakanova, M. N. Fiz. Chastits Vysokikh Energii, Akad. Nauk Gruz. SSR, Inst. Fiz., 1: 51-64(1965). (In Russian).

The third moment of distribution of the number of charged particles is calculated in showers generated by high energy μ-mesons. It is shown that the asymmetry of the function of probability distribution is great and it is not sufficient to know the first three moments for the reconstruction of the distribution function. The third moments of the numbers of particles are also calculated in electron-photon showers formed by electrons and photons. (auth)

41356 ON THE THEORY OF WEAK INTERACTIONS OF ELEMENTARY PARTICLES. Nagy, Karoly. Fiz. Szemle, 15: 100-7(Apr. 1965). (In Hungarian).

The development and status of the theory of weak interactions are briefly reviewed. (D.C.W.)

41357 AN ANALYSIS OF THE J-PHENOMENON IN SCATTERED X-RAYS. PART II. Pal, Hirendra Kumar (Univ. of Calcutta). Indian J. Phys., 39: 108-36(Mar. 1965).

Starting with Barkla's idea of radiation-atmosphere, where the different constituents of heterogeneous x-rays are considered as an integrated whole and taking into account the various effects due to (i) Compton scattering, (ii) interference of the scattered radiations (predominantly in the forward direction), (iii) absorption of the various constituents of the beam, (iv) narrowness of the primary beam in contrast with the width of the scattered beam, and (v) ionization produced by the radiations received in the ionization chambers, a theoretical analysis is given to explain, under suitable conditions, most of the experimental results of Barkla and Khastgir (1925-27), both qualitatively and quantitatively, on the comparative study of the primary and the scattered beams of heterogeneous x-rays, (i) when both the beams were filtered through the same increasing thickness of an absorbing material for a given average wavelength of the primary beam and (ii) when both the beams were unintercepted and intercepted by the same thickness of an absorbing material over a wide range of average wavelengths of the primary beam. The laws of the J-phenomenon formulated by Barkla are theoretically justified under certain conditions. Barkla's concept of discrete levels of x-ray activity associated with the J-phenomenon is not considered. (auth)

41358 INTERPRETATION OF EXPERIMENTAL DATA ON NUCLEON-NUCLEON INTERACTIONS AT ENERGY OF 300 Bev. Kuchin, I. A.; Usik, P. A. (Inst. of Nuclear Physics, Academy of Sciences, Kazakh SSR). Izv. Akad. Nauk SSSR, Ser. Fiz., 28: 1821-3(Nov. 1964). (In Russian).

The behavior of inelastic collision cross sections of nucleon–nucleon (NN) interactions follows the theoretical predictions, if the NN scattering with excitation of one of the nucleons resulting from the one-meson exchange is taken into account; at low energies this exchange possesses an isobaric character. At energies beyond 100 Bev, the $\pi\pi$ interaction plays an important role in the πN scattering. The strong anisotropy of the angular distribution of the secondary particles increases with increasing energy, so that the nucleons have a strong transverse pulse. On the basis of the agreement between theoretical and experimental results it is concluded that the behavior of high-energy NN collisions may be explained without assuming any contribution on the part of central NN and πN interactions. (TTT)

41359 APPLICATION OF THE METHOD OF MOMENTA FOR RESOLVING THE SOLID ANGLE PROBLEM IN ELECTROMAGNETIC CASCADE THEORY. Guzhavin, V. V.; Ivanenko, I. P. (Moscow State Univ.). Izv. Akad. Nauk SSSR, Ser. Fiz., 28: 1841-6(Nov. 1964). (In Russian).

Cosmic-ray experimentation requires the calculation of solid angle functions of the three-dimensional cascade theory. Data on wide atmospheric showers and those obtained by means of nuclear emulsions require the knowledge of the angular ($f(\theta)$) and spatial ($f(r)$) distributions of cascade particles, together with the complete $f(\theta,r)$ spatial-angular functions. The momentum method may be used to solve this problem by approximations. A more generally valid method is proposed for calculating the angular moments of solid angle functions, based on the distribution of the particles at short distances from the angle of the cascade shower in the A approximation of the cascade theory during various stages of the development of a cascade shower. It was found that the presence of cascade processes—radiative retardation of electrons and pair formation by protons—leads to slight qualitative changes in the dependence of the momenta while the absolute values are markedly changed. (TTT)

41360 INVESTIGATIONS ON NONRELATIVISTIC QUANTUM THEORY OF PARTICLE SCATTERING. Kamenetskii, V. D. (All-Union Correspondence Inst. of Textile and Light Industry, USSR). Izv. Vysshikh Uchebn. Zavedenii, Fiz., No. 3, 101-4(1965). (In Russian).

A previously proposed method for solving the radial equations for nonrelativistic quantum-mechanical problems on collisions is developed and studied. (tr-auth)

41361 ON THE DEGREE OF NONCONSERVATION OF PARITY IN Θ AND τ DECAYS. Tkachev, L. G. (Saratov State Univ., USSR). Izv. Vysshikh Uchebn. Zavedenii, Fiz., No. 3, 158-9(1965). (In Russian).

The final-state system for the radiative Θ and τ decays $K^+ \to \pi^+ + \pi^0 + \gamma$ and $K^+ \to 2\pi^+ + \pi^- + \gamma$ can be in either of two states, with opposite parity: positive parity for electric multipole radiation, and negative, for magnetic. The transition matrix element for the Θ decay, whose two terms correspond to electric and magnetic dipole radiation, is written in the dipole approximation, and the case for kaon at rest is considered. The Stokes parameters of the polarization matrix of the photon are calculated in terms of the form factors; it is found that circular polarization arises only if parity is not conserved, and that the degree of linear polarization depends on the degree of parity nonconservation and is 1 for the case of parity conservation. The transition matrix element for the τ decay has the same form as in the Θ decay, if it is considered that there are two identical Bose particles in the final state. (M.J.T.)

41362 SELECTION RULES AND MASS SPECTRUM OF PARTICLES. [PART] I. Nakamura, Seitaro (Tokyo Univ. and Nihon Univ., Tokyo). J. Phys. Soc. Japan, 20: 1101-3(July 1965).

In order to keep the independence of every quantum number describing the particles, three kinds of charge spins, U, τ, and ζ are introduced, and particles are considered to occupy the baryons and mesons with spin 0, eight kinds of fermions which we call superions and eight kinds of mesons with spin 0 should in our grouping be found in the future experiments. It is suggested that two kinds of the coupling types (derivative coupling and nonderivative coupling) are responsible for breaking the higher symmetry in the charge space. (auth)

41363 ON AN EXACT DISPERSION FORMULA. Dolinszky, Tamas. Magy. Tud. Akad. Kozp. Fiz. Kut. Int. Kozlemen., 13: 151-62(1965). (In Hungarian).

The elastic scattering is dealt with by the formal theory of scattering without recourse to Green operators. The dispersion structure is based on the eigenfunction expansion of the scattering state itself in terms of solutions to the force-free problem. By matching the homogeneous boundary conditions, both simplicity and uniform convergence are achieved. Particular features are the absence of non-resonant background and the one-term, many-pole correspondence. The poles are zeros of the resonance equations, formally identical with the boundary conditions. It is shown that theories working with unmatched boundary conditions necessarily fail in the exact evaluation of the singularities. (auth)

41364 CONVERGENCE PROPERTIES OF THE TIME-DEPENDENT PERTURBATION SERIES OF A N FERMION SYSTEM. Dahmen, H. D. (Technische Hochschule, Darmstadt, Ger.). Nucl. Phys., 72: 254-72(1965).

The convergence of the time-dependent perturbation series of a system of N fermions is shown under certain conditions of boundedness imposed on the potential representing the interaction. Furthermore, this proof gives the justification of the procedure of adiabatic switching. (auth)

41365 THE RANGE OF GAUGE FIELDS. Loos, Hendricus G. (Giannini Foundation, Indio, Calif.). Nucl. Phys., 72: 677-91(1965).

It is proved that all spherically symmetric gauge fields can by a gauge transformation be thrown in Coulomb form, for any gauge group. This generalizes Ikeda and Miyachi's result for O_3 and shows that the static condition may be left out. The investigation uses the interpretation of gauge fields as internal curvature and the group properties of curvature. It is shown that every spherically symmetric internal holonomy group with at least one source-free region is abelian. It is found that Ikeda and Miyachi's conditions for spherical symmetry of the gauge fields are sufficient but not necessary. There exists an overlooked family of spherically symmetric solutions which have a non-zero (θ,φ) component of internal curvature tensor operator. This component does not contribute to the field equation but it does appear in the rest energy of the field. The latter is calculated from a conjectured force law which is a generalization of the electro-magnetic force. Using a flat event space, the rest energy for a force-free spherically symmetric gauge field either diverges or vanishes; in the latter case the gauge group is non-compact. For two interacting particles, short-range effects show up in an example using as gauge group a subgroup of SU_3. At large distances the interaction is of Coulomb type. These findings give renewed hope that the gauge fields indeed have to do with strong interactions, notwithstanding the Coulomb like character of spherically symmetric solutions. (auth)

41366 UNITARY SYMMETRY BREAKING INTERACTIONS AND THE DECAYS OF VECTOR MESONS. Roy, B. Dutta; Mukherjee, C. S.; Roy, Salil (Saha Inst. of Nuclear Physics, Calcutta). Nucl. Phys., 72: 692-4(1965).

Several measurements were made of the partial decay widths of ρ, K* and φ corresponding to the decays $\rho \to \pi + \pi$, $K^* \to K + \pi$ and $\phi \to K + \bar{K}$. The experimental values seem to deviate much from the values predicted by SU_3. For example the theory predicts $\Gamma(K^* \to K\pi)/\Gamma(\varphi \to \pi\pi) = 0.29$, whereas experiments give $0.47 \pm 10\%$. This large deviation (about 62% from theoretical values) is explained by introducing symmetry breaking interactions. Comparison with experiment permits the determination of the strength of the symmetry breaking interactions. (auth)

41367 Λ^0-POLARIZATION FROM THE REACTION $\gamma + p = \Lambda^0 + K^+$ IN THE ENERGY RANGE (950/1050) Mev. Grilli, M. (Laboratori Nazionali, Frascati, Italy); Mezzetti, L.; Nigro, M.; Schiavuta, E. Nuovo Cimento (10), 38: 1467-88(Aug. 16, 1965).

Measurements of the Λ polarization in the reaction $\gamma + p = K^+ + \Lambda^0$ are reported, for $950 < E_\gamma < 1050$ Mev. The experimental apparatus and the detection techniques used are described. The results are compared with the theoretical predictions and other experimental values. (auth)

41368 SPIN AND PARITY OF THE 1320 Mev ρπ RESONANCE. Bettini, A.; Cresti, M.; Grigoletto, A.; Limentani, S.; Loria, A.; Peruzzo, L.; Santangelo, R. (Universita, Padua). Nuovo Cimento (10), 38: 1495-1504(Aug. 16, 1965).

The decay into $\rho^0\pi^\pm$ of the 1320 Mev resonance, the A_2, is analyzed, and it is shown that the spin of the resonance is 2 and its intrinsic parity is positive. (auth)

41369 ON THE DIFFERENCE IN THE RANGE-ENERGY RELATION FOR POSITIVE AND NEGATIVE PARTICLES. Cartacci, A. M. (Istituto Nazionale di Fisica Nucleare, Florence); Dagliana, M. G.; Corte, M. Della; Lamborizio, C.; Mora, S.; Ortalli, I. Nuovo Cimento (10), 38: 1515-18(Aug. 16, 1965).

Measurements were made on the final products of the reactions $K^- + p \to \Sigma^- + \pi^+$ and $K^- + p \to \Sigma^+ + \pi^-$, produced in nuclear emulsion by K^- mesons at rest. From measured pion momentum the expected energies for the hyperons were computed and the expected ranges for Σ^+ and Σ^- were obtained using existing range-energy relations. For Σ^+ the measured range was (822.0 ± 1.4) and the expected range (816 ± 11) μ; for Σ^- (709.2 ± 1) μ and (685 ± 6) μ respectively. For the Σ^- there is an evident disagreement between the two values. Such results confirm the hypothesis suggested by Barkas of a different behavior in the energy loss of negative and positive particles. (auth)

41370 THE SELF-CONSISTENT DETERMINATION OF THE ρ-MESON REGGE-POLE PARAMETERS. Anand, J. D.; Joshi, G. C. (Univ. of Delhi). Nuovo Cimento (10), 38: 1588-93(Aug. 16, 1965).

Within the framework of a method suggested by Bander and Shaw, the bootstrap calculations of a ρ-meson Regge pole in the π-π scattering are investigated, using a modified auxiliary partial-wave amplitude. A self-consistent value for the mass ($m_\rho^2 = 8m_\pi^2$) and the width ($\Gamma \approx 167$ Mev) of the ρ-meson Regge pole is obtained. (auth)

41371 CP VIOLATION AND SU_3 SYMMETRY. Morales, A.; Nunez-Lagos, R.; Soler, M. (CERN, Geneva). Nuovo Cimento (10), 38: 1607-15(Aug. 16, 1965).

A generalization of the Cabibbo rotation for the weak hadronic current is proposed with the SU_3 symmetry. The results of the Cabibbo theory are not modified. In leptonic processes CP violation appears only for $\Delta S = 1$. A parameter ω is defined through the difference of generalized rotations of the axial and vector parts, which measures the amount of CP violation. Leptonic and nonleptonic processes attain a maximum of CP violation for $\omega = \pi/2$, the violation being large for the former but only a few times per thousand for the latter as compared to CP-conserving processes. The decay of neutral K-mesons is studied and other experimental tests of the theory considered. (auth)

41372 ON A CLASSICAL THEORY OF CHARGED PARTICLES WITH SPIN AND THE CLASSICAL LIMIT OF THE DIRAC EQUATION. Dixon, W. G. (Cambridge Univ., Eng.). Nuovo Cimento (10), 38: 1616-43(Aug. 16, 1965).

Starting from the pole-dipole approximation to the equations of motion for an extended body in an electromagnetic field, a classical special-relativistic theory of a charged point particle with spin in an electromagnetic field is developed. This theory is seen to take an especially simple form for a gyromagnetic ratio $g = e/m$, and this case is treated in detail. The classical limit of the Dirac equation for an electron is studied in a new way, and for the Hamiltonian and equations of motion are found expressions which agree with the energy and equations of motion in the classical theory to first order in the charge. In the process, Poisson brackets between the dynamical variables are obtained that enable the equations of motion to be recovered from the classical expression for the energy, which may thus be regarded as the Hamiltonian in the classical theory. The assumptions of the classical theory are then discussed in detail. (auth)

41373 LIMITATIONS OF THE BOOTSTRAP METHOD FOR THE DETERMINATION OF VECTOR MESON PARAMETERS. Morel, A. (Centre d'Etudes Nucleaires de Saclay, Gif-sur-Yvette, France). Nuovo Cimento (10), 38: 1649-68(Aug. 16, 1965). (In French).

The conjecture that the observed P-wave resonances of two pseudoscalar mesons occur through the exchange of these resonant states is investigated in the framework of partial-wave dispersion relations. The idea is that the nearest singularities determine the major part of the behavior of amplitudes at low energy. In fact it is found that long-range forces corresponding to these singularities are not strong enough, and that the introduction of farther singularities, which are difficult to evaluate, is necessary to produce resonances. When such singularities are calculated by retaining only these forces which correspond to vector meson exchanges, the cross sections which are then obtained do not show the expected shape. A semi-quantitative agreement between the calculated and measured parameters of resonances must then be considered as fortuitous, and it is difficult to consider the vector mesons as solutions of a self-consistent bootstrap problem. (auth)

41374 RELATIVISTIC THEORY OF THE ELECTRODISINTEGRATION OF THE DEUTERON. II. NUMERICAL RESULTS AND NEUTRON FORM FACTORS DETERMINATION. Renard, F. M.; Tran Thanh Van, J.; Bellac, M. (Hautes Energies, Orsay). Nuovo Cimento (10), 38: 1688-1719(Aug. 16, 1965).

A covariant theory of the electrodisintegration of the deuteron has been constructed. Numerical results are given. The influence of various contributions often neglected in preceding calculations is discussed. The neutron form factors are determined by the quasi-elastic peak method to obtain: $F^N_{ch} \gtrsim 0$ and $F^N_{mag} \gtrsim F^P_{mag}$; these results are compared with those of coincidence experiments. It appears that the experimental status is not sufficient to give truly reliable values of the neutron form factors. In order to obtain further checks of the theory, new experiments are proposed, and compared with the present, and the results of the present theory. (auth)

41375 ON AN INCONSISTENCY IN TWO ONE-PARTICLE-EXCHANGE MODELS FOR π-N SCATTERING. Caprasse, H. (Institut de Physique Mathematique, Liege). Nuovo Cimento (10), 38: 1765-76(Aug. 16, 1965).

The consistency of the partial-wave amplitude dispersion relations in the one-nucleon and ρ exchange is examined. For both models, even if the correct threshold behavior is taken into account, it is found that an inconsistency arises whenever the forces are repulsive at high energy. For the ρ-exchange model, even if the force is attractive, there is also an inconsistency if the upper bound $g_{\rho\pi\pi}\, g_{\rho NN} \leq 4$ is violated. A plausible solution is presented to remedy the previous inconsistencies of the nucleon-exchange model. (auth)

41376 HIGH-ENERGY BEHAVIOR OF THE REAL PART OF THE SCATTERING AMPLITUDE. Igi, K. (Tokyo Univ. of Education). Nuovo Cimento (10), 38: 1815-23(Aug. 16, 1965).

The asymptotic behavior of the ratio (α) of the real part over the imaginary part of the forward scattering amplitude was investigated at high energies, by taking into account several high-ranking trajectories in the complex angular momentum plane (Pomeranchuk trajectory, cuts, and secondary poles). A simple relation is found between the real and imaginary part of the cut contribution, and use for discussing the behavior of α in pp, $p\bar{p}$, $\pi^{\pm}p$, and $K^{\pm}p$ scattering. Under general assumptions, it is found that $\alpha_{pp} < 0$, $\alpha_{\pi^+p} < 0$, and $|\alpha_{\pi^+p}| > |\alpha_{\pi^-p}|$, which is consistent with the experiment, and it is predicted that $|\alpha_{p\bar{p}}| < |\alpha_{pp}|$, $\alpha_{K^+p} < 0$, and $|\alpha_{K^-p}| < |\alpha_{K^+p}|$. In all the two-particle scatterings (A,B), it is found that the real part of the forward scattering amplitude approaches zero asymptotically from a negative value if $\sigma_{AB}(E) + \sigma_{A\bar{B}}(E) - 2\sigma_{AB}(\infty)$ is positive. (auth)

41377 ELECTROMAGNETIC MODELS OF ELEMENTARY PARTICLES. Smith, P. F. (Rutherford Lab., Chilton, Berks., Eng.). Nuovo Cimento (10), 38: 1824-34(Aug. 16, 1965).

The apparent numerical relationship between the elementary-particle mass spectrum and the electromagnetic coupling constant has led to proposals for models of the μ and π mesons consisting of relativistic systems of electrons and positrons, confined in localized quantum states by purely electromagnetic forces. These simple models do not appear to be in accordance with the known wave-mechanical behavior of electrons, and some possible ways of achieving closer compatibility are suggested. Preliminary calculations suggest that models based on a localized "plasma" of electron-positron pairs may offer a more satisfactory basis for a rigorous wave-mechanical investigation. Some difficulties associated with spin, strong interactions, and neutrinos are summarized. (auth)

41378 ON CP VIOLATION BY DERIVATIVE TERMS IN THE LEPTONIC CURRENT. Bergia, S.; Russo, G. (Universita, Modena, Italy). Nuovo Cimento (10), 38: 1849-53(Aug. 16, 1965).

CP-violating effects are introduced in the leptonic current by means of derivative couplings; in this model, a scalarlike and a tensorlike term arise. It is then shown that the $\pi \to (\mu + \nu)/(e + \nu)$ branching ratio and the muon decay rate impose upper bounds on such terms, if it is desired to preserve universality for the ordinary $\gamma_\alpha(1 + \gamma_5)$ coupling. A tensorlike CP-violating term could be present in muon decay and be revealed experimentally. (auth)

41379 π-α SCATTERING AND THE PIONIC FORM FACTOR. Sternheim, M. M. (Yale Univ., New Haven); Hofstadter, R. Nuovo Cimento (10), 38: 1854-60(Aug. 16, 1965).

Theoretical calculations are carried out on π^--α and π^+-α elastic scattering processes. Results are presented at a typical incident pion energy of 100 Mev. The results are sensitive to the pion's electromagnetic form factor since the form factor of the α-particle may be taken from electron scattering experiments. If the pion size is large the burden on the theoretical calculations is not great. However if the pion size is small the calculations must be refined. In any case the comparison of π^--α and π^+-α

scattering is worthwhile, and suggestions are made as to how to carry it out. (auth)

41380 A DYNAMICAL CALCULATION OF ρ^0-ω_8 TRANSITION MASS. Bose, Subir (Univ. of Allahabad, India). Nuovo Cimento (10), 38: 1881-2(Aug. 16, 1965).

A dynamical calculation of the ρ^0-ω_8 transition mass squared (m_T^2) yields $m_T^2(\rho^0-\omega_8) = 0.08\ m_\pi^2$. The calculation is based on a general method for calculating electromagnetic corrections to strong interactions. The electromagnetic interaction is parametrized by a phenomenological mixing, and the electromagnetic correction is sought in the pion-nucleon interaction. This correction gives a relation between the p-n mass difference and m_T^2, from which m_T^2 may be determined. (T.F.H.)

41381 A NOTE ON A CONJECTURE BY J. J. DE SWART. Babu, P. (Tata Inst. of Fundamental Research, Bombay and International Centre for Theoretical Physics, Trieste, Italy). Nuovo Cimento (10), 38: 1887-8(Aug. 16, 1965).

A relation, conjectured in order to simplify the evaluation of meson-meson and meson-baryon crossing matrices in various symmetry models, is proved. (T.F.H.)

41382 CAN THE COUPLING CONSTANT ASSUME ARBITRARY VALUE IN THE S-MATRIX THEORY? Sawada, T. (International Centre for Theoretical Physics, Trieste, Italy). Nuovo Cimento (10), 38: 1889-94(Aug. 16, 1965).

An explicit calculation is carried out of the restrictions imposed by maximal analyticity of the scattering amplitude upon the masses and coupling constants of elementary particles. The restrictions yield exact relations between masses and coupling constants. The starting point of the calculation is the assumptions that the scattering amplitude is unitary, and that it has the form of a spectral representation plus (possibly) subtraction terms. (T.F.H.)

41383 HIGH-ENERGY SCATTERING BY EXCHANGE OF MARKOV'S PARTICLE. Armoudian, G. A.; Ito, D.; Mori, K. (Louisiana State Univ., Baton Rouge). Nuovo Cimento (10), 38: 1895-8(Aug. 16, 1965).

The Markov field theory, in which the singularities of the propagation function are not on the light cone but on a hyperboloid, is used in an attempt to reproduce the distributions in large-angle p-p interactions. The results are compared with experimental data and distributions predicted by a Lorentz-contracted optical potential. (T.F.H.)

41384 RESONANT STATES Y*'S WITH M ≃ 1660 Mev. Minami, S. (Osaka City Univ.). Nuovo Cimento (10), 38: 1899-1992(Aug. 16, 1965).

A discussion is presented of an octet of resonant states having three elements ($Y_0^*(1662)$, $Y_1^*(1660)$, and $Y_0^*(1661)$) whose masses lie near 1660 Mev. Investigations are noted of several topics: the lack of evidence for the $Y_0^*(1661)$ in K^--p interactions at 1 to 2 Bev/c; means for verifying the existence of the two Y_0^* elements; forms for describing the two Y_0^* components; and explanation of the experimental results for the final $\Lambda\pi^+\pi^-$ configurations in $K^- + p \to \Lambda + \pi^+ + \pi^-$, taking contributions from the two Y_0^*'s into account. (T.F.H.)

41385 NUCLEON FORM FACTOR AND LARGE-ANGLE p-p SCATTERING. Armoudian, G. A.; Ito, D.; Mori, K. (Louisiana State Univ., Baton Rouge). Nuovo Cimento (10), 38: 1903-7(Aug. 16, 1965).

Starting from the nucleon form factors derived from pion-nucleon interactions, the second-order Born approximation of the T matrix for p-p scattering is written. The p-p angular distributions thus deduced are compared with experimental results and with results obtained using Markov theory with an exchange particle. (T.F.H.)

41386 RARE DECAY MODES OF THE ω-MESON. Greenberg, D. F. (Univ. of Chicago). Nuovo Cimento (10), 38: 1908-11(Aug. 16, 1965).

The feasibility of using colliding-electron and positron beams to verify the existence of a $\pi^+\pi^-$ decay mode for ω mesons is investigated, using a phenomenological Hamiltonian to account for $\omega\rho$ mixing effects. The use of this experiment to study $e^+ + e^- \to \pi^0 + \gamma$ is also discussed. (T.F.H.)

41387 NEUTRINO THEORY OF PHOTONS AND ITS IMPLICATION IN ELECTROMAGNETIC INTERACTION. Bandyopadhyay, P. (Indian Statistical Inst., Calcutta). Nuovo Cimento (10), 38: 1912-14(Aug. 16, 1965).

A Lagrangian is written for the absorption or emission of a photon, in the neutrino theory of photons. An identical mechanism is assumed for electromagnetic and weak interactions within the framework of this theory. The theory is shown to allow photons to undergo weak interactions. The Lagrangian for interactions between spinors and n photons is derived. It is shown that the spinor–n-photon interactions can be reduced to the proper electromagnetic interactions in limiting cases. (T.F.H.)

41388 ON THE NUMERICAL ANALYTIC CONTINUATION OF THE PROTON ELECTROMAGNETIC FORM FACTORS. Bertero, M.; Viano, G. A. (Universita, Genoa). Nuovo Cimento (10), 38: 1915-20(Aug. 16, 1965).

The conformal-mapping technique, as applied to the approximate numerical analytic continuation of the proton electromagnetic form factors, is shown to yield unstable solutions as the order of the approximating polynomial becomes unbounded. Upper-bound techniques are introduced for eliminating this instability. The proton form factors can be approximately analytically continued by this technique, under the assumptions only that they are bounded and analytic. (T.F.H.)

41389 THE WIGNER-INOENUE CONTRACTION AND POSSIBLE CONFORMAL INVARIANCE OF INTERNAL AND EXTERNAL MOTIONS OF ELEMENTARY PARTICLES. Prasad, R. (Institut Henri Poincare, Paris). Nuovo Cimento (10), 38: 1921-7(Aug. 16, 1965).

The conjecture is considered that for the elementary particles the real external group is not the universal covering of the usual Poincare group, but is rather the limit, in a certain sense, of the conformal group SO(4,1). This conjecture is investigated for the conformal group SO(4,2). It is shown that the conjecture is perfectly consistent from a mathematical and physical point of view. (T.F.H.)

41390 A REMARK TO A PAPER OF MOSES AND WANG. Raszillier, I. (Inst. of Physics of the Academy, Bucharest). Nuovo Cimento (10), 38: 1928-30(Aug. 16, 1965).

The kinematics of the angular momentum of a relativistic particle is considered, with particular reference to the effects of a particular class of transformations on a given state. An exact analytic solution is given for finding the probability distribution of the resulting final states. The method used is the same as that used to find the infinitesimal generators of the inhomogeneous Lorentz group. (T.F.H.)

41391 DIRAC MAGNETIC MONOPOLES AND SUPERCONDUCTIVITY. Tassie, L. J. (Indiana Univ., Bloomington). Nuovo Cimento (10), 38: 1935-7(Aug. 16, 1965).

The theoretical aspects and feasibility of using superconducting hollow cylinders for detecting Dirac magnetic monopoles are investigated. The magnetic field in such a cylinder is quantized in units of $\hbar c/2e$, which is exactly one-half the amount of flux carried by a Dirac monopole. Thus a monopole passing through the cylinder causes a quantum jump in the amount of trapped flux. (T.F.H.)

41392 CONFORMAL-GROUP SYMMETRY OF ELEMENTARY PARTICLES. Bohm, D. (Birkbeck Coll., London); Flato, M.; Sternheimer, D.; Vigier, J. P. Nuovo Cimento (10), 38: 1941-4(Aug. 16, 1965).

Several operations involving the conformal group are reviewed. The ability of this group to resolve problems in elementary particle theory is shown in several examples. Symmetries associated with this group are discussed. (T.F.H.)

41393 INDICATRIX OF THE RADIATION EMITTED BY A CHARGE IN AN EXTERNAL FIELD ACCORDING TO CLASSICAL THEORY. Bagrov, V. G. Opt. Spectry.

(USSR)(English Transl.), 18: 311-12(Apr. 1965).
Translated from Optika i Spektroskopiya, 18: 541-4 (Apr. 1965).

The instantaneous indicatrix (angular distribution) of the radiation emitted by an electron in an external field was investigated, taking account of polarization of the radiation. The investigation was carried out according to classical theory. (auth)

41394 APPROXIMATE SOLUTION OF PARTIAL-WAVE DISPERSION RELATIONS. Franklin, Jerrold (Univ. of California, Livermore). Phys. Rev., 139: B912-17(Aug. 23, 1965). (UCRL-12482-T).

An exact expression is derived for the solution of a partial-wave dispersion relation. This expression has the property that, when the zero-width-resonance approximation is made in all integrals where its use is valid, the solution of the dispersion relation is given by simple integrals and no further approximation is required. The result is shown to be independent of the subtraction point and symmetric when applied to a many-channel dispersion relation. Although it utilizes the inverse amplitude, the approximation can be used in some cases of zeros of the amplitude. As a sample calculation, the approximation is applied to the simple π-π-ρ bootstrap, and a self-consistent solution is obtained. (auth)

41395 BREAKDOWN OF UNITARY OCTET SYMMETRY IN A NONLINEAR SPINOR MODEL OF ELEMENTARY-PARTICLE THEORY. Byrne, N.; Iddings, C.; Shrauner, E. (Stanford Univ., Calif.). Phys. Rev., 139: B918-32(Aug. 23, 1965).

The spontaneous breakdown of unitary octet symmetry is considered in a nonlinear spinor model of elementary-particle theory. The model is an adaptation to unitary octet symmetry of a model originated by Nambu and Jona-Lasinio and contains $SU_3 \otimes SU_3$ symmetry in the same way that their model contained $SU_2 \otimes SU_2$ symmetry. An exact formula is derived for the physical baryon mass that reduces to the usual superconductor-type formula in the lowest order approximation. Nonperturbative solutions that leave the physical Λ and Σ masses degenerate are obtained. The presence in the nonperturbative solutions of massless pseudoscalar and scalar mesons transforming as components of F-type octets as predicted by the Goldstone theorem is confirmed. Massless pseudoscalar and scalar mesons that transform as components of unitary spin decimets are also found. It is explained that only the F octets are Goldstone mesons associated with the spontaneous breakdown of octet symmetry in the model, whereas the massless decimets are associated with the invariance of a restricted part of the lagrangian under a larger group and their masslessness is not a consequence of symmetry breakdown in the solutions. (auth)

41396 MESON STATES IN A NONLINEAR SPINOR MODEL OF ELEMENTARY-PARTICLE THEORY WITH SPONTANEOUS SYMMETRY BREAKDOWN. Byrne, N.; Iddings, C.; Shrauner, E. (Stanford Univ., Calif.). Phys. Rev., 139: B933-44(Aug. 23, 1965).

A self-coupled spinor model of elementary particles having $SU_2 \otimes SU_2$ symmetry is considered. It is demonstrated that for the case of complete spontaneous breakdown of the isospin symmetry the bubble approximation gives a method for treating the meson states that is compatible with symmetries of the model in that it gives the Goldstone bosons and Goldberger-Treiman relations exactly. It is shown that by a continuation in the parameter characterizing the isospin breakdown a transformation can be performed from a solution having isospin degeneracy to solutions in which the isospin, as well as the chiral symmetry, is spontaneously broken. Calculational techniques for the approximation are explicitly given. (auth)

41397 SOME SIMPLE CONSEQUENCES OF SU(4) SYMMETRY. Woo, Ching-hung; Dragt, Alex J. (Institute for Advanced Study, Princeton, N. J.). Phys. Rev., 139: B945-6(Aug. 23, 1965).

The electromagnetic properties of the nucleons and N*, as well as the meson-baryon coupling constants, are examined within the framework of an SU(4) symmetry combining spin and isospin. The motivation is to examine the consequences of such a symmetry at low energies without having to worry about the large mass differences within the SU(3) multiplets in the corresponding SU(6) theory. The coupling-constant ratios are in qualitative agreement with the experimental values. The arbitrariness in the proton-neutron magnetic-moment ratio is discussed. In the model where the electromagnetic interaction of the baryons is mediated by the vector mesons in the adjoint representation of SU(4), the magnetic-moment ratios agree with the SU(6) results. (auth)

41398 RELATIVISTIC MERGING OF SPIN AND ISOTOPIC SPIN. Barnes, K. J. (Cornell Univ., Ithaca, N. Y.). Phys. Rev., 139: B947-51(Aug. 23, 1965).

A calculation is presented in which spin and isotopic spin are combined within one larger symmetry. By treating the spin symmetry in a novel way the theory is made completely relativistic. Excellent agreement with experiment is achieved and, in particular, the experimentally well verified form equality between the electric and magnetic form factors of the proton emerges as a natural consequence of the theory. (auth)

41399 BROKEN SYMMETRIC COUPLINGS FOR DECUPLET DECAYS INTO BARYONS AND PSEUDOSCALARS. Johnson, Elizabeth (Imperial Coll. of Science and Tech., London and Battersea Coll. of Tech., London); McCliment, Edward R. Phys. Rev., 139: B951-5(Aug. 23, 1965).

In an approach to SU(3) symmetry breaking the point of view is adopted that perturbation theory may be used to calculate the corrections to the B*(10)BP coupling constants. The symmetry breaking is introduced via Gell-Mann-Okubo mass splittings of both the internal and external lines of the third-order vertex diagram. In this manner coupling constants which obey the sum rules of Gupta and Singh are obtained. This approach seems consistent with the notion that the Gell-Mann-Okubo formulas are themselves based on first-order symmetry breaking in the masses. The results are compared with those of other authors. (auth)

41400 ABSORPTIVE CORRECTIONS AND FORM FACTORS IN THE PERIPHERAL MODEL. Bander, Myron; Shaw, Gordon L. (Stanford Univ., Calif.). Phys. Rev., 139: B956-62(Aug. 23, 1965).

Absorptive corrections applied to the peripheral model provide a relatively successful interpretation of a variety of high-energy production processes. There exist, however, a number of difficulties associated with these calculations. The reaction $\pi N \to \rho N$, which is dominated by π exchange, is considered in order to study the following ambiguities: (i) the actual dependence of the absorptive corrections on the initial- and final-state elastic-scattering phase shifts, (ii) the role of a form factor, and (iii) the numerical values of the final-state elastic-scattering phase shifts. The comparison of the calculation with the experimental data, in particular the density matrix of the ρ, leads to the following results. The $j = 1/2$ partial waves must be totally suppressed by the absorptive corrections and the form factor must play a very minor role in order to fit the observed deviation of the ρ's density matrix from that predicted by the exchange of a π in the peripheral model. (A form factor cuts down the low partial waves in a manner which leaves the density matrix unmodified from the simple peripheral model and thus reduces the effect of absorption corrections on the density matrix.) Any form factor associated with π exchange is expected to have a weak t dependence, since there exists no resonance with the appropriate quantum numbers (to couple to the π) with energy $\lesssim 1.3$ Bev. It is plausible that form factors (in addition to the absorptive corrections), while unimportant for π exchange, may play a significant role in vector exchange (since there seems to be an abundance of high-spin resonances). (auth)

41401 NONLOCAL PROPERTIES OF STABLE PARTICLES. Fleming, Gordon N. (Univ. of Washington, Seattle). Phys. Rev., 139: B963-8(Aug. 23, 1965).

Some physical implications of the position operators

studied previously are presented. Lower limits on the dimensions, perpendicular to the momentum, of spinning particles are obtained, and the partial localization of massless particles by the center-of-mass operator is discussed. The lowest order correction to a local potential, from a potential which is spherically symmetric in terms of the nonlocal center of mass, is shown to be exactly the Thomas spin-orbit coupling interaction. (auth)

41402 BOOTSTRAP AND SU(3) ASSIGNMENT OF 2^+ MESONS. Hwa, Rudolph C.; Patil, Sharashchandra H. (Institute for Advanced Study, Princeton, N. J.). Phys. Rev., 139: B969-72(Aug. 23, 1965).

For meson-meson scattering, special properties of some submatrices of the total crossing matrix are derived. These properties are applied to the study of the bootstrap of 2^+ mesons in the scattering system of two pseudoscalar octets. It is found that self-consistency can be sustained by a 1^- octet, a 2^+ singlet, and a 2^+ octet. Assignments of $f^0(1250)$ to the 2^+ singlet and $A_2(1310)$ and $K^*(1415)$ to the 2^+ octet are made, leaving an $I = 0$, 2^+ particle yet to be found. Consequences of this assignment are discussed. (auth)

41403 MODEL FOR DYNAMICAL CALCULATION OF INELASTICITY. Islam, M. M.; Kang, Kyungsik (Brown Univ., Providence). Phys. Rev., 139: B973-81(Aug. 23, 1965). (NYO-2262-87).

A model is proposed in which inelasticity can be calculated dynamically. By this it is meant, given the left-hand cut contribution (or force), the model gives a prescription for calculating inelasticity $\eta_l (= e^{-2\delta_l^I}$ where δ_l^I is the imaginary part of the phase shift). The basic assumption of the model is that there is one inelastic v_1 above which a large number of reaction channels open, so that the partial-wave amplitude is essentially imaginary in the inelastic region. This amplitude satisfies elastic unitarity below the inelastic threshold and inelastic unitarity above it. The use of the model is illustrated by applying it to the π-π p-wave system, where the left-hand-cut contribution is approximated by one pole and by two poles. (auth)

41404 MEAN LIFETIME OF THE π^0 MESON. Evans, D. A. (Oxford Univ.). Phys. Rev., 139: B982-91(Aug. 23, 1965).

An experiment is described to measure the mean life of the π^0 meson using nuclear emulsions. The basic method was employed previously, viz., the determination of the flight distances of π^0 mesons produced at a unique velocity in the $K_{\tau 2}$ decay mode of the K^+ meson and decaying through the mode $\pi^0 \rightarrow \gamma e^+ e^-$. The coordinates of the grains composing the tracks in 67 such events were measured, and the flight distances of the π^0's determined by geometrical reconstruction of the events. It was considered that an accurate estimation of the various errors involved was essential to the correct computation of the lifetimes, and such estimations were attempted. The effect of the presence of a certain type of spurious event upon the final results is demonstrated. The value for the mean lifetime obtained is $\tau_\pi^0 = (1.6_{-0.5}{}^{/+0.6}) \times 10^{-16}$ sec. (auth)

41405 DIRECT AND Y_1^*-RESONANT PRODUCTION OF Λ^0 AND π^- AND Σ-Λ^0 CONVERSION FOLLOWING $\bar{K}$-MESON NUCLEAR ABSORPTION. FINAL-STATE INTERACTIONS IN THE $\bar{K} + {}^4He \rightarrow \pi^- + \Lambda^0 + {}^3He$ REACTION. Said, P.; Sawicki, J. (Universite de Paris, Orsay, France). Phys. Rev., 139: B991-1005(Aug. 23, 1965).

In the reaction of $\bar{K}$-meson nuclear absorption, three fundamental processes are considered: a direct (nonresonant) $\bar{K} + N \rightarrow \pi^- + \Lambda^0$ reaction, the same reaction with the Y_1^* resonance formation in the intermediate state, and the reaction with a Σ production in the first stage and its subsequent conversion into a Λ^0 in a successive collision with another nucleon. The zero-range impulse approximation is assumed. The initial $\bar{K}$ state is an nS or an mP Bohr mesoatomic orbit. Several forms of the Λ^0-nucleus final-state interaction are considered. For the case of the $K + {}^4He \rightarrow \pi^- + \Lambda^0 + {}^3He$ reaction the recoiling-^{3}He momentum distribution, the pion momentum distribution, and the $\pi^- + \Lambda^0$-^{3}He angular distribution are analyzed. It turns out that in order to explain the ^{3}He momentum distribution no elastic scattering distortion of the Λ^0-^{3}He wave is sufficient, and the Σ-Λ^0 conversion amplitude must be introduced, which is most important at high ^{3}He-momenta and which also improves pion momentum distribution. (auth)

41406 THREE-TRIPLET MODEL WITH DOUBLE SU(3) SYMMETRY. Han, M. Y. (Syracuse Univ., N. Y.); Nambu, Y. Phys. Rev., 139: B1006-10(Aug. 23, 1965). (NYO-3399-31).

With a view to avoiding some of the kinematical and dynamical difficulties involved in the single-triplet quark model, a model for the low-lying baryons and mesons based on three triplets with integral charges is proposed, somewhat similar to the two-triplet model introduced earlier by Nambu. It is shown that in a U(3) scheme of triplets with integral charges, one is naturally led to three triplets located symmetrically about the origin of I_3-Y diagram under the constraint that the Nishijima–Gell-Mann relation remains intact. A double SU(3) symmetry scheme is proposed in which the large mass splittings between different representations are ascribed to one of the SU(3), while the other SU(3) is the usual one for the mass splittings within a representation of the first SU(3). (auth)

41407 PADE APPROXIMANT IN POTENTIAL SCATTERING. Tani, S. (New York Univ., New York). Phys. Rev., 139: B1011-20(Aug. 23, 1965).

It is suggested that the Padé approximant be used as an approximation outside the radius of convergence of the Born series for scattering from a short-range potential free from a strong singularity. Following Weinberg's analysis of the Born series, the potential is approximated by a finite number of separable potentials in order to deal with a limited range of energy, and thus the associated K matrix can be evaluated without further approximation. When a number N of separable potentials are constructed by using the lowest 2N terms of the Born series, the result is identical to the (N,N) Padé approximant. If expanded formally into a power series in the potential strength, this approximation reproduces the original Born series exactly up to the 2Nth order; but without an expansion it takes a closed form for any finite potential strength, and therefore it is well defined outside the radius of convergence of the Born series. When the Weinberg eigenvalues and eigenfunctions on the energy shell are closely approximated with a suitably chosen N, the divergence difficulty of the conventional Born series can be overcome by the use of the Padé approximant, because the latter is correctly continued analytically outside the convergence radius of its Born series. (auth)

41408 STATISTICAL STUDY OF LINEAR MASS RELATIONS FOR ELEMENTARY PARTICLES. Fickinger, W. J.; Sternheimer, R. M. (Brookhaven National Lab., Upton, N. Y.). Phys. Rev., 139: B1021-2(Aug. 23, 1965). (BNL-9053).

In an empirical study of linear relations among the masses of the known elementary particles, the expression $m = pA + qB$, where p and q are integers, is compared, over a wide range of the constants A and B, with the set of the experimental mass values. (auth)

41409 SYSTEMATICS OF ANGULAR AND POLARIZATION DISTRIBUTIONS IN THREE-BODY DECAYS. Berman, S. M.; Jacob, M. (Stanford Univ., Calif.). Phys. Rev., 139: B1023-38(Aug. 23, 1965).

A general method is described for the measurement of the polarization and alignment of a particle of arbitrary spin from the analysis of its three-body decays. This method provides a procedure for the determination of spin and parity of the decaying system which is independent of the dynamics of the decay process. The procedure is closely related to the one currently used for two-body reactions except that the normal to the decay plane replaces the center-of-mass momentum as an analyzer. The general formalism is developed and illustrated by two examples: three-pion decays and baryon-two-pion decays. (auth)

41410 HYPERFINE STRUCTURE AND WEAK INTERACTIONS. Adams, J. Barclay (Stanford Univ., Calif.). Phys. Rev., 139: B1050-1(Aug. 23, 1965).

The contribution of possible four-fermion V–A weak interactions to the hyperfine splitting is considered for

the hydrogen-like bound systems (e^-,p^+), (μ^-,p^+), (e^-,μ^+), and (e^-,e^+). The effect might have experimental significance (19 parts per million) for the (μ^-,p^+) system. (auth)

41411 LORENTZ INVARIANCE AND INTERNAL SYMMETRY. O'Raifeartaigh, L. (Syracuse Univ., N. Y.). Phys. Rev., 139: B1052-62(Aug. 23, 1965). (NYO-3399-27).

One of the outstanding problems of elementary-particle physics is the problem of combining Lorentz invariance and internal symmetry in a nontrivial way. A general investigation of the possibilities of finding a Lie algebra of finite order E such that the Lie algebras of the Lorentz and internal symmetry groups appear in it as subalgebras is made, using some powerful standard results from the general theory of Lie algebras. The most relevant of these is Levi's result that any Lie algebra E is the semidirect product of a semisimple algebra G and an invariant solvable subalgebra S (called the radical). It is shown that if L, the algebra of the inhomogeneous Lorentz group, is a subalgebra of E, and M and P are the homogeneous and translation parts of L respectively, then either (a) M lies completely in G and P lies completely in S or (b) L has no intersection with S. Thus the ways in which L can be a subalgebra of E can be classified in a very simple way. The classification is carried out by subdividing case (a) into the three cases: (i) S = P, (ii) S Abelian but larger than, and containing P, and (iii) S solvable but not Abelian, and containing P; and by regarding case (b) as case (iv) $S \cap P = 0$. Each of these four cases is considered in detail. It turns out that case (i) is essentially a direct sum of L and a semisimple Lie algebra; case (ii) is possible, but has the disadvantage of introducing a translation group of more than four dimensions; and case (iii) seems to be rather unphysical. Case (iv) is possible but is equivalent to imbedding L in a simple Lie algebra. The over-all picture is that while there are a number of ways in which L can be imbedded in an E, none of these (except the direct sum) seems to be particularly attractive from the physical point of view. In particular, it seems that, while it may be possible to make SU(6) theory fully relativistic, it is probably not possible to do so within the context of a Lie algebra of finite order. (This does not contradict the $\tilde{U}(12)$ theory.) The question of explaining mass splitting within the context of a Lie algebra of finite order is considered, and it is shown that this can not be done. The various negative-type theorems obtained previously for special cases of E are rederived within the general framework, most of them from much weaker assumptions. (auth)

41412 π^+ DECAY OF $_{\Lambda}Li^7$. Bhowmik, B.; Chand, T.; Chopra, D. V.; Goyal, D. P. (Univ. of Delhi). Phys. Rev., 139: B1062-4(Aug. 23, 1965).

An event unambiguously identified as the π^+ decay of a ^{7}Li hyperfragment is reported. The event was observed in a stack of L_4 hypersensitized Ilford emulsions exposed to a 1.5-Bev/c K^- beam at CERN. The charge of the hyperfragment was uniquely determined as three, by comparing its measured mean track width with the curves (mean track width versus dip angle) established for Z = 1, 2, 3, 4, and 5 nuclides found in the same emulsions. The branching ratio R of the π^+/π^- decay modes for $_{\Lambda}Li^7$, on the basis of the present π^+ decay together with the available world data on π^- decays, is estimated as $R(_{\Lambda}Li^7) \sim 1\%$. (auth)

41413 SUGGESTED MEASUREMENTS OF NEUTRAL-KAON DECAY RATES. Kaplan, J. M. (Institut des Hautes Etudes Scientifiques, Bures-sur-Yvette, France). Phys. Rev., 139: B1065-7(Aug. 23, 1965).

A method which involves the use of K mesons produced in both the K^0 state and the $\bar{K}^0$ state is proposed to measure the decay rates of the short-lived and long-lived components of neutral kaons. A phenomenological analysis of these decay rates is carried out in the leptonic case, and a new test for CPT invariance is suggested. (auth)

41414 $K_{\mu 3}$ BRANCHING RATIO AND μ^+ ENERGY SPECTRUM. Bisi, V.; Borreani, G.; Marzari-Chiesa, A.; Rinaudo, G.; Vigone, M.; Werbrouck, A. E. (Universita, Turin and Istituto Nazionale di Fisica Nucleare, Turin). Phys. Rev., 139: B1068-72(Aug. 23, 1965).

The muon energy spectrum of $K_{\mu 3}$ decay was studied in heavy liquid and H_2 bubble chambers. The results favor vector coupling with a small negative value of the real part of the ratio ξ of the two vector form factors. The $K_{\mu 3}$ branching ratio obtained is $3.45 \pm 0.20\%$. (auth)

41415 QUARTET SCHEME AND WEAK INTERACTIONS. Lai, Chai S. (Univ. of Chicago). Phys. Rev., 139: B1072-8(Aug. 23, 1965).

A unified scheme of weak interactions is given within the framework of SU(4) by means of intermediate bosons. It is assumed that the fundamental entities—leptons, intermediate bosons, and quarks—are all quartets. The damping of the $|\Delta S| = 1$ transitions is introduced either through the breakdown of the strong-interaction symmetry or through a certain mixing of unphysical neutrinos. The theory possesses a complete symmetry between leptons and hadrons and accounts for the $|\Delta I| = \frac{1}{2}$ rule and the weak-interaction hamiltonian transforming like the sixth component of the unitary octet for the $|\Delta S| = 1$ part of the nonleptonic (noncharmed) decays. The problem of the absence of neutral lepton currents remains. (auth)

41416 NEW REDUCTION OF THE FADDEEV EQUATIONS AND ITS APPLICATION TO THE PION AS A THREE-PARTICLE BOUND STATE. Ahmadzadeh, A.; Tjon, J. A. (Univ. of California, San Diego, La Jolla). Phys. Rev., 139: B1085-92(Aug. 23, 1965).

A new separation of the angular momentum in the Faddeev equations is given. This separation makes use of two particles, which is combined with the angular momentum of the third particle in the over-all center-of-mass system. With the assumption that the two-body amplitudes factorize in the initial and final momenta, the Faddeev equations are reduced to a coupled set of integral equations in one variable. This set is furthermore simplified in the case of identical particles to only one integral equation. Thereby the statistics are correctly taken into account. The resulting equation is used to investigate possible bound states of three pions with total angular momentum zero, isospin one, and odd parity. The two-body amplitude which determines the kernel is approximated by the isospin-zero, s-wave effective-range formula of Chew and Mandelstam. Use is also made of relativistic kinematics. The pion is found as a bound state of three pions in this model. The outcome is, however, strongly dependent on a physical cutoff parameter in the two-body form factor. As a result a detailed investigation of the form factor is desirable. (auth)

41417 INTERPRETATION OF THE κ IN $K^+p \rightarrow K\pi\pi p$. Month, Melvin (Univ. of Illinois, Urbana). Phys. Rev., 139: B1093-7(Aug. 23, 1965).

The $K\pi$ mass distribution in the reaction $K^+p \rightarrow K\pi\pi p$ was computed using a triangle graph. A singularity of the triangle diagram is manifested as a peak in the mass spectrum at a $K\pi$ mass of slightly less than the $K^*\pi$ mass difference. A fit to the data at 3.0 Bev/c is obtained using a p-wave background constant interfering with the triangle amplitude. Some features which favor this description of the κ over a resonance explanation are (1) the absence of the κ bump in three- and four-body final states; (2) its isotropic production distribution; (3) the lack of $\kappa N^*\pi$ events; and (4) the decreasing magnitude of the peak with increasing incident energy. Two suggestions are made for further experimental analysis. Firstly, a study of the above reaction at energies lower than 3.0 Bev/c is predicted to show a similar κ enhancement (while at higher incident energies a diminution is anticipated). Secondly, the $K\pi\pi\pi$ mass distribution in the same five-body final state is predicted to show an enhancement at about 1080 Mev. (auth)

41418 STRANGE-PARTICLE PRODUCTION IN π^+-p COLLISIONS. Berley, David (Brookhaven National Lab., Upton, N. Y.); Gelfand, Norman. Phys. Rev., 139: B1097-1102(Aug. 23, 1965). (BNL-9050).

Strange particles produced in interactions of positive pions with protons were studied with the Brookhaven 20-in. bubble chamber, which was exposed to π^+ beams of 2.35, 2.62, and 2.90 Bev/c. Cross sections are presented, and the production of resonances is discussed. The outstanding feature of the multiparticle final states is that they are

dominated by K-π, K-$\overline{K}$, and Y-π resonances. The isotopic spin of the φ is confirmed to be zero, and no evidence is found for a φ decay into three pions. (auth)

41419 LOW-ENERGY Λ-d SCATTERING AND THE HYPERTRITON WITH SEPARABLE POTENTIALS. Hetherington, J. H.; Schick, L. H. (Univ. of Minnesota, Minneapolis). Phys. Rev., 139: B1164-9(Sept. 6, 1965).

The Λ-d scattering and ${}_{\Lambda}H^3$ binding-energy problems are solved exactly using nonlocal separable S-wave potentials and a multiple-scattering formalism of the Faddeev type. Λ-d scattering cross sections are presented for laboratory momenta in the range 100-250 Mev/c. No strong dependence of the Λ-d scattering cross sections upon the low-energy Λ-N scattering parameters is found. It is shown that the Λ-N scattering data and the ${}_{\Lambda}H^3$ binding energy can not both be adequately fitted with purely attractive two-body potentials of the form used. Results are presented which illustrate the energy dependence of the S matrix and the nonconvergence of the multiple-scattering series for the low-energy scattering amplitude when a three-body bound state is present. (auth)

41420 PROPERTIES OF WEAK AMPLITUDES IN BROKEN $\tilde{U}(12)$. Gatto, R. (Universita, Florence and Instituto Nazionale di Fisica Nucleare, Florence); Maiani, L.; Preparata, G. Phys. Rev., 139: B1294-6(Sept. 6, 1965).

Weak nonleptonic amplitudes are discussed in the $\tilde{U}(12)$ scheme on the assumption of octet dominance. The contributions to hyperon-decay S waves of spurions of representations higher than 143 of the current ⊗ current product are discussed in detail. In addition to Gell-Mann's relations for hyperon S waves, it is found that $\Sigma^+ \to n + \pi^+$ is forbidden in S waves apart from minor kinematical corrections. Possible modifications from a kinetic-energy spurion are also examined. Some remarks concerning consequences of CP invariance and concerning $K_{2\pi}$ decays are included. (auth)

41421 LONG-RANGE FORCES IN MESON-BARYON SYSTEMS. Golowich, E. (Cornell Univ., Ithaca, N. Y.). Phys. Rev., 139: B1297-1312(Sept. 6, 1965).

Single-particle-exchange forces were evaluated at low energies for all two-particle meson-baryon states with angular momentum from $S_{\frac{1}{2}}$ to $H_{\frac{11}{2}}$. Using real masses and SU(3) coupling constants normalized to experiment, the exchange of the following SU(3) multiplets was considered: baryon octet, $P_{\frac{1}{2}}$ decuplet, $Y_1^*(1520)$ singlet, vector-meson octet (vector and tensor coupling), and $D_{\frac{3}{2}}$ octet. The forces were classified in the direct channel according to SU(3) irreducible representations, an association which is inexact owing to mass splitting but which nevertheless allows us to relate resonant states thereby generated in various isospin and hypercharge channels. Strong attractive forces were found in the $P_{\frac{1}{2}}, F_{\frac{5}{2}}$ octet, $P_{\frac{3}{2}}, F_{\frac{7}{2}}$ decuplet, and $D_{\frac{3}{2}}$ singlet states. In particular, the exchange of vector mesons was observed to play a significant role in all these channels. The analysis suggests that the $D_{\frac{3}{2}}$ $Y_1^*(1765)$ be assigned to an octet, the other members of which are relatively inhibited by mass-splitting effects to the extent that they may not be observable experimentally as resonances. No forces likely to generate resonances in the multiplet 27 were found. (auth)

41422 RECIPROCAL BOOTSTRAP POSSIBILITIES FOR BARYONS. Balazs, L. A. P.; Singh, Virendra; Udgaonkar, B. M. (Tata Inst. of Fundamental Research, Bombay). Phys. Rev., 139: B1313-18(Sept. 6, 1965).

In πN scattering, using an N/D static model with linear approximation to the D function, the reciprocal bootstrap between the nucleon and the $(\frac{3}{2}, \frac{3}{2})$ resonance is shown to hold for any l, with an $I = \frac{1}{2}$, $j = l - \frac{1}{2}$ and an $I = \frac{3}{2}$, $j = l + \frac{1}{2}$ isobar supporting each other. It is also shown that this is in fact the only pair of multiplets capable of reciprocally bootstrapping. The following question is then raised: Given the existence of the pion, what is the simplest possible set of baryon multiplets which can support itself? It is found that the aforementioned pair is in fact the simplest set. All these results are then generalized to SU(3), where this pair becomes a $j = l - \frac{1}{2}$ octet and a $j = l + \frac{1}{2}$ decimet. (auth)

41423 PRECESSION OF RELATIVISTIC PARTICLES OF ARBITRARY SPIN IN A SLOWLY VARYING ELECTROMAGNETIC FIELD. Zwanziger, Daniel (Centre d'Etudes Nucleaires de Saclay, Gif-sur-Yvette, France). Phys. Rev., 139: B1318-22(Sept. 6, 1965).

It is shown that, under accelerator or bubble-chamber conditions, the passage of a particle of arbitrary spin through an electromagnetic field effects a Lorentz transformation on its momentum and polarization, and a linear differential equation determining this transformation is given. The decay-time dependence of the angular distribution that describes the decay of a particle moving in an electromagnetic field is also given explicitly; and a method, explained in detail, of measuring the magnetic moment of an unstable, higher spin particle like the Ω^- is obtained. It is noted that the gyromagnetic ratio $g = 2$ leads to particularly simple equations of motion for all spins, and not only for spin $\frac{1}{2}$. A novel covariant algebraic method is used to solve the equations of motion and obtain the finite Lorentz transformation in the case of a constant and homogeneous electromagnetic field. The method involves the introduction of an algebra of 4-by-4 matrices that plays the same role for 4-vectors as the Dirac algebra for 4-spinors. (auth)

41424 ELECTROMAGNETIC INTERACTIONS AND THE SUBGROUPS OF SU(6). Harari, H. (Soreq Nuclear Research Center, Yavne, Israel). Phys. Rev., 139: B1323-5 (Sept. 6, 1965). (IA-1023).

Various sets of relations concerning the electromagnetic properties of the constituents of the SU(6) supermultiplets were recently derived by various authors. A systematic study of these relations is presented here, using subgroups of SU(6) which are generalizations of the U-spin subgroup of SU(3). It is shown that two different assumptions on the transformation properties of the electromagnetic contributions to the particle masses are not in contradiction with the present data: invariance to all orders under $SU(2)_U \otimes SU(2)_R \otimes SU(2)_P$, where R and P are the total quark spins of the $Q = -\frac{1}{3}$ and $Q = \frac{2}{3}$ quarks, respectively; and second-order contributions from an $SU(2)_U$-invariant interaction which transforms like a 35. Moreover, the relation $p - n = N^{*+} - N^{*0}$ is obtained from all the various assumptions which are stronger than the usual U-spin invariance. This relation may serve as a criterion for the usefulness of any discussion of electromagnetic mass differences according to SU(6). (auth)

41425 COMPTON SCATTERING OF AN INTENSE PHOTON BEAM. Frantz, Lee M. (TRW Space Technology Labs., Redondo Beach, Calif.). Phys. Rev., 139: B1326-36(Sept. 6, 1965).

The fully quantum-mechanical description of the Compton scattering of a photon beam is shown to be equivalent under certain conditions to a semiclassical description, thereby confirming the prediction by Brown and Kibble and by Goldman of an intensity-dependent increment to the frequency shift. If the incident beam is in a coherent state, the equivalence is exact under all conditions. If it contains a definite number of photons, the equivalence is approximate, and requires many photons and convergence of the expansion in powers of the photon density. The demonstration is based upon the explicit use of wave packets to introduce the boundary conditions, and the equivalence is shown to hold in the sense that the transition probabilities, but not the transition amplitudes, are the same in the quantum and semiclassical treatments. The apparent failure of energy-momentum conservation implied by the incremental shift is seen to be accounted for by the energy-momentum uncertainty of the ensemble of localized wave packets even in the monochromatic limit. It is proved that the coherent states are the only kind for which the equivalence is exact. (auth)

41426 REGGE-POLE MODELS FOR HIGH-ENERGY πN, KN, AND $\overline{K}N$ SCATTERING. Phillips, Roger J. N. (Univ. of California, Berkeley); Rarita, William; Phys. Rev., 139: B1336-47(Sept. 6, 1965). (UCRL-16033).

It is shown that πN, KN, and $\overline{K}N$ elastic-scattering and

charge-exchange data at high energy and small momentum transfer can be well fitted by assuming that the amplitudes are dominated by a few Regge poles in the crossed channel. The constraints imposed by the factorization principle are included. Unitary symmetry (SU_3) is approximately satisfied. Sample predictions of πp polarization and $K^+ + n \rightarrow K^0 + p$ charge exchange are made. (auth)

41427 POLES AND RESONANCES IN THE PROCESS $\pi^+ + p \rightarrow \Sigma^+ + K^+$. Holladay, W. G. (Vanderbilt Univ., Nashville). Phys. Rev., 139: B1348-54(Sept. 6, 1965).

Several models considered in successively greater degrees of complexity are discussed for the $T = {}^3/_2$ process $\pi^+ + p \rightarrow \Sigma^+ + K^+$. The ingredients of the model are Λ and K^* poles, the $p_{3/2}$ 1238-Mev resonance, and an $f_{5/2}$ resonance at 1925 Mev. Although various combinations of these terms yield generally good results for the total and differential cross sections from threshold (beam momentum of 1021 Mev/c) to 1.76 Bev/c, calculated Σ^+ polarizations are too small. Much better agreement is found with the polarization if the pole terms are multiplied by $e^{i\delta}$ where δ is taken to be a constant of magnitude 40–50°. Such a term may arise from the presence of other open channels. The quantum numbers $f_{5/2}$ for the 1925-Mev resonance are consistent with the notion that this resonance is a Regge recurrence of the $p_{3/2}$, 1238-Mev state. (auth)

41428 RELATIVISTIC FORMULATION OF THE SU(6) SYMMETRY SCHEME. Sakita, Bunji; Wali, Kameshwar C. (Argonne National Lab., Ill.). Phys. Rev., 139: B1355-67 (Sept. 6, 1965).

A relativistic formulation of the SU(6) symmetry is presented, starting with the basic assumption that the fields corresponding to elementary particles are tensors of M(12) [or $\bar{U}(12)$ or $SU(12)'$]. In particular, a mixed second-rank tensor and a totally symmetric third-rank tensor are associated with the meson and baryon fields, respectively. It is shown that if these fields are required to satisfy prescribed free-field equations of motion, then one is led to a particle supermultiplet structure which corresponds to the 35⊕1 and 56-dimensional representations of SU(6) for the mesons and baryons. It is also shown that the spin-dependent and SU(3)-spin-dependent mass splittings can be included in the theory and that solutions in terms of physical particle fields can be obtained. Effective trilinear meson-meson and meson-baryon vertex functions, using these solutions and an interaction Lagrangian which is invariant under M(12), are calculated in the lowest order perturbation. The following results are noted: from the known pion-nucleon coupling constant, the width of the pion-nucleon (3,3) resonance is calculated to be 94 Mev; the ratio of the magnetic form factors for the neutron and proton is $-{}^2/_3$ for all momentum transfers and $\mu p = (1 + 2M_p/m_\rho)$ nuclear magnetons; and the charge form factor of the neutron is zero for all momentum transfers. (auth)

41429 SUMMING CERTAIN ϕ^4 GRAPHS USING INTEGRAL EQUATIONS. Nussinov, S. (Univ. of Washington, Seattle). Phys. Rev., 139: B1367-71(Sept. 6, 1965).

It is shown that the problem of summing certain graph chains occurring in ϕ^4 theory in which three (or four) particles are in the intermediate state is reducible to an integral equation. For forward scattering and zero-mass field, this equation can be solved exactly using a method for solving the Bethe-Salpeter equation which has been recently suggested. As an example, the case of the truss-bridge diagrams is worked out in detail. (auth)

41430 EFFECT OF MASS SPLITTINGS ON SYMMETRY RELATIONS BETWEEN SCATTERING AMPLITUDES. Everett, Allen E. (Tufts Univ., Medford, Mass.). Phys. Rev., 139: B1375-81(Sept. 6, 1965).

The question of the violation of relations predicted by SU(3) invariance between scattering amplitudes that is due to the kinematical effect of mass splittings alone, with no other symmetry breaking in the Hamiltonian, is considered. On the basis of qualitative considerations and a simple potential scattering model, it is argued that these effects can be very severe, and can produce order-of-magnitude disagreements with the theoretical predictions unless the total center-of-mass energy is large compared with the masses of the particles involved. It seems likely that all existing disagreements between SU(3) predictions and scattering experiments could be accounted for on the grounds of mass splittings alone. A study is also made of whether to compare cross sections at the same initial kinetic energies, or at the same Q values, as has been done heretofore. It appears that there is comparatively little to choose between the two methods, or between either of them and other procedures which might be used. If the result depends sensitively on the method adopted for comparing the cross sections, this in itself is an indication that the effects of mass splittings are so large that agreement with theory can not be expected. (auth)

41431 QUADRILOCAL MODEL OF BARYONS AND UNITARY SYMMETRY. Takabayasi, Takehiko (Nagoya Univ., Japan). Phys. Rev., 139: B1381-7(Sept. 6, 1965).

A unified theory of baryons is proposed based on a spinor wave equation that depends on four space-time points or equivalently on the center of mass and three relative-coordinate vectors. The associated subsidiary condition and the structure of the mass operator are such that the four-point association is maintained within a small region of Minkowski space-time with characteristic length and that the theory has U(9) symmetry in the full symmetry limit. By the couplings of internal motions, this symmetry is reduced to the direct product of the usual unitary-spin group U(3) and the other unitary group U(3)′ characteristic of spherical-oscillator-type motions, and then this latter is further reduced to simple rotational invariance. Baryonic states are assigned to the 165-dimensional irreducible representation (IR) of the U(9) corresponding to the first excited shell with respect to the oscillatory motions of relative coordinates. These states are subgrouped according to the IR of the usual SU(3) and to the eigenvalue of the relative angular momentum. Identifications with known levels are then made. The whole treatment is carried out covariantly, and minimum violation of causality is implied inside the particle. (auth)

41432 SELF-CONSISTENT PARTICLE SETS IN A BARYON BOOTSTRAP MODEL. Koerner, Juergen G.; Capps, Richard H. (Northwestern Univ., Evanston, Ill.). Phys. Rev., 139: B1388-93(Sept. 6, 1965).

An SU(n)-symmetric bootstrap model is considered in which the baryons are meson-baryon bound states. A postulate used previously in similar models of mesons is applied: that a solution to the dynamical equations should exist in which particles of the same type are degenerate. It is shown that this postulate is difficult to satisfy unless the baryons correspond to a single irreducible representation of the SU(n) group. The π-N-N* system is discussed in detail. The condition that the baryons correspond to a single irreducible representation does not favor a particular value of n for the underlying SU(n) symmetry, but does rule out the fundamental representation for the baryons and favors the group SU(mn) over SU(m)⊗SU(n). Several relations between SU(4) and SU(6) symmetry schemes are pointed out. (auth)

41433 DYNAMICAL BASIS FOR η-BARYON INTERACTIONS. Tuan, S. F. (Purdue Univ., Lafayette, Ind.). Phys. Rev., 139: B1393-1400(Sept. 6, 1965).

The recent experimental evidence for a rapid rise in η production near threshold in the reactions $\pi^- + p \rightarrow \eta^0 + n$ and $K^- + p \rightarrow \eta^0 + \Lambda$ is analyzed on the basis of a constant-K-matrix formalism. Representative scattering lengths for the η-baryon systems are introduced to illustrate pertinent features of the presently known experimental data. A dynamical basis for the physical situation is discussed in terms of possible new baryon states due to virtual or bound states of the η-baryon systems. Comparison of the results with expectations from a conjectured η octet of baryon ($^1/_2^-$) states for SU(3) symmetry is briefly referred to. (auth)

41434 NORMALIZATION CONDITION AND NORMAL AND ABNORMAL SOLUTIONS OF THE BETHE-SALPETER EQUATION. [PART] II. Nakanishi, Noboru (Brookhaven National Lab., Upton, N. Y.). Phys. Rev., 139: B1401-6(Sept. 6, 1965). (BNL–9079).

The normalization integrals of the Bethe-Salpeter am-

plitudes are calculated in the Wick-Cutkosky model in order to check the conjecture that the sign of the norm is $(-1)^\kappa$ for $0 < s < 4$. It is explicitly verified for the following solutions with $n = 1 + l$: (1) κ arbitrary, s infinitesimal; (2) $\kappa = 0$, $0 < s \leq 2$; (3) $\kappa = 1$, $0 < s \leq 2 + (n + 2)^{-1}$; (4) $\kappa = 0$, 4 − s infinitesimal. Here κ, n, l are the conventional quantum numbers and $s^{1/2}$ denotes the bound-state mass in units of the constituent-particle mass. Some speculations are presented concerning the existence of ghost states. (auth)

41435 SIMPLE ALTERNATIVES TO SU(6). Joseph, D. W. (Univ. of Nebraska, Lincoln). Phys. Rev., 139: B1406-10(Sept. 6, 1965).

A search is made for simple classical Lie groups which could serve as alternatives to SU(6). Among the groups with less than 140 generators, the most likely possibilities are found to be R(11), with 55 generators, and Sp(16), with 136 generators; but even these two have features which seem to discriminate against their use as particle symmetry groups. (auth)

41436 K^+p INTERACTIONS AT 2 Bev/c—ELASTIC SCATTERING AND TOTAL CROSS SECTIONS. Chinowsky, W.; Goldhaber, G.; Goldhaber, S.; O'Halloran, T.; Schwarzschild, B. (Univ. of California, Berkeley). Phys. Rev., 139: B1411-15(Sept. 6, 1965). (UCRL–11669).

A study of 1.96-Bev/c K^+p interactions in the Brookhaven 20-in. liquid-hydrogen bubble chamber yielded a measurement of the elastic-scattering cross section (7.5 ± 0.7 mb). A fit to the differential cross section versus momentum transfer of the form $\sigma_0 e^{-\alpha t}$ gives, for the interval $0.01 (\text{Bev/c})^2 < t < 0.60 (\text{Bev/c})^2$, $\alpha = 3.1 \pm 0.3 (\text{Bev/c})^{-2}$, and $\sigma_0 = 4.8 \pm 0.5$ mb/sr. The total cross section obtained is 19.4 ± 2.0 mb with single-pion production dominant. (auth)

41437 POSSIBLE C-NONINVARIANT EFFECTS IN THE 3π DECAY MODES OF η^0 AND ω^0. Lee, T. D. (Columbia Univ., New York). Phys. Rev., 139: B1415-20(Sept. 6, 1965). (TID–21821).

The observed CP noninvariance in $K_2^0 \rightarrow \pi^+ + \pi^-$ is assumed to be due to the existence of a new strangeness-conserving but C-noninvariant and T-noninvariant interaction called H_F, whose coupling constant F is $\sim 10^3 G$ where G is the Fermi coupling constant in the usual CP-invariant weak interaction. A phenomenological analysis of the possible forms of the energy asymmetry between π^+ and π^- in the 3π decay modes of η^0 and ω^0 is made. It is pointed out that a study of such an asymmetry can be used to test the possible existence of H_F as well as its isotopic-spin selection rules. (auth)

41438 ANTI-ISOBAR PRODUCTION IN $\bar{p}n$ INTERACTIONS. Bacon, T. C. (Brookhaven National Lab., Upton, N. Y.); Hopkins, H. W. K.; Robinson, D. K.; Salant, E. O.; Engler, A.; Fisk, H. E.; Meltzer, C. M.; Westgard, J. Phys. Rev., 139: B1420-7(Sept. 6, 1965). (BNL–9123).

Single-pion production in $\bar{p}n$ interactions was studied in the BNL 20-in. deuterium-filled bubble chamber at an incident $\bar{p}$ momentum of 1.96 Gev/c. Copious production of the $\frac{3}{2}$, $\frac{3}{2}$ anti-isobar was observed. The differential cross section of momentum transfer has a distribution consistent with that predicted by one-pion exchange (OPE). The experimental cross section of 5.1 ± 0.5 mb, however, is about half that predicted by the OPE model of Ferrari and Selleri. (auth)

41439 COUNTING THE BOUND STATES IN SHORT-RANGE CENTRAL POTENTIALS. Schey, Harry M.; Schwartz, Judah L. (Univ. of California, Livermore). Phys. Rev., 139: B1428-32(Sept. 6, 1965). (UCRL–14106).

For the case of a short-range central potential, the quantity α_l, defined as the zero-energy limit of $k^{2l+1}\cot\delta_l$, vanishes whenever the range and depth of the potential are such that there is a state of zero binding energy. By solving the zero-energy scattering problem, α_l is obtained as a function of range and depth, and the number of bound states supportable by a given central potential is determined as a function of the potential parameters without having to solve the associated and more difficult eigenvalue problem. The method is applied to the Debye-Huckel (Yukawa) and Woods-Saxon potentials. (auth)

41440 TRANSLATIONAL INERTIAL SPIN EFFECT WITH PHOTONS. de Beauregard, O. Costa (Institut Henri Poincare, Paris). Phys. Rev., 139: B1443-7(Sept. 6, 1965).

The Borgnis technique is used to solve the Maxwell equations under the following conditions: complex field strengths are used such that $H = \pm iE$, that is, circularly polarized waves of positive or negative helicity; there is only harmonic time dependence through a factor exp(iWt), that is, a pure energy state of the photons; there is no z dependence, that is, no k_z component of the photons' momentum; and there is no restriction on the x, y dependence of the solutions. It is then shown that the S_z component of the Poynting vector obeys the formula $\pm 2WS_z = \partial_x S_y = \partial_y S_x$ and is in general nonzero. This fact, together with the postulated nullity of k_z, is the expression of the translational inertial spin effect. An experiment using the limiting case of total reflection is proposed to test the effect. A discussion of gauge-dependent expressions of the effect, using potentials, is also given, in connection with de Broglie's formulas for the current-and spin-density 4-vectors of the photon waves. (auth)

41441 DIPION PRODUCTION AT LOW MOMENTUM TRANSFER IN π^--p COLLISIONS AT 1.5 Bev/c. Clark, A. R.; Christenson, J. H.; Cronin, J. W.; Turlay, R. (Princeton Univ., N. J.). Phys. Rev., 139: B1556-65 (Sept. 20, 1965).

Precision spark-chamber spectrometers were used to measure the dipion mass spectrum from the reaction $\pi^- + p \rightarrow \pi^- + \pi^+ + n$ at an incident momentum of 1.5 Bev/c. The spectrum was observed between 450 and 1000 Mev, with π-π scattering angles at 90 ± 30 deg, and with four-momentum transfer to the nucleon between the minimum Δ_{min} and $\Delta_{min} + 2\mu$. The mass resolution of the apparatus was ±4 Mev. With more than 6000 events a peak was observed in the π-π mass spectrum at ~750 Mev with a width $\Gamma \cong 130$ Mev. With these results an upper limit for the branching ratio $(\omega \rightarrow \pi^+\pi^-/\omega \rightarrow \pi^+\pi^-\pi^0)$ of ≤10%, was obtained, based on the assumption that there is no interference between the ρ and ω amplitudes. Interpreting the data with the one-pion exchange (OPE) model, the differential cross section $d\sigma_{\pi\pi}/d\cos\theta_{\pi\pi}$ at 90 deg was computed. This quantity shows a strong peak at the mass of the ρ^0 meson, but the peak is much larger than expected from a $J = 1$ π-π resonant state produced by OPE. Expressing the ρ decay intensity as $a + b\cos^2\theta_{\pi\pi}$, the data require $a/b \approx 0.06$, while the simple OPE model predicts $a/b = 0$. Other features of the data, the momentum-transfer distribution and the Treiman-Yang angular distribution, fit the OPE predictions fairly well. Some evidence that the effect of a 1.4-Bev, $T = \frac{1}{2}$ isobar can be seen in the data is discussed. (auth)

41442 PION-NUCLEON SCATTERING AMPLITUDES IN THE RANGE 300-700 Mev. Bransden, B. H. (Durham Univ., Eng.); O'Donnell, P. J.; Moorhouse, R. G. Phys. Rev., 139: B1566-84(Sept. 20, 1965). (NIRL-R-79).

The cross section for the scattering of π^+ and π^- by nucleons in the energy range 300 to 700 Mev was analyzed in terms of energy-independent parameters. The parameterization is based on a dispersion relation satisfied by the partial-wave amplitudes, by replacing the left cut by a superposition of poles and the inelasticity function $R_l = \sigma_l(\text{tot})/\sigma_l(\text{el})$ by a ratio of polynomials in the momentum. Detailed results are presented for the real and imaginary parts of the phase shifts with $l \leq 3$. The structure of the second resonance is more complicated than has heretofore been thought, p_{11}, s_{11}, and d_{13} waves all playing an important part. The width of the d_{13} resonance is found to be considerably smaller than previous values from total cross-section measurements. The role of the (possibly resonant) amplitudes p_{11} and s_{11} is discussed. (auth)

41443 BARYON BOOTSTRAP POSSIBILITIES IN SU(6). Singh, Virendra; Udgaonkar, Bhalchandra M. (Tata Inst. of Fundamental Research, Bombay). Phys. Rev., 139: B1585-7(Sept. 20, 1965).

The various bootstrap possibilities arising in meson-baryon scattering in SU(6) are discussed using the static model. The mesons are taken to belong to the 35-plet of

SU(6). It is shown that if the baryons are limited to the eightfold way-type representations, i.e., to the 20-plet, 56-plet, 70-plet, etc., then the simplest bootstrap possibility for baryons is the self-bootstrap of the 56-plet in the scattering of 56-plet baryons and mesons. No simpler possibility arises when the scattering of a lower dimensional 20-plet of baryons with mesons is considered. (auth)

41444 SECOND-ORDER PERTURBATION IN INTRINSICALLY BROKEN $\tilde{U}(12)$. River, R. J. (International Atomic Energy Agency, Trieste, Italy). Phys. Rev., 139: B1587-90(Sept. 20, 1965).

In second-order perturbation theory in intrinsically broken $\tilde{U}(12)$, it is found that in many cases the $\tilde{U}(12)$ symmetry is recovered in the forward direction. The consequences of this are discussed, as is the asymptotic behavior of amplitudes and differential cross sections for the case of octet-baryon-pseudoscalar-meson scattering. (auth)

41445 POSSIBLE EFFECTS OF CP VIOLATION IN $K^+ \to 3\pi$ DECAY. Ueda, Yoshiaki; Okubo, Susumu (Univ. of Rochester, N. Y.). Phys. Rev., 139: B1591-9(Sept. 20, 1965). (UR-875-82).

The effects of CP violation in $K \to 3\pi$ decay were investigated. In a linear energy approximation for the decay matrix elements, it is proved using the TCP theorem alone, that the partial decay rate of the τ (or τ') mode (and also θ modes) for the K^+ meson is nearly equal to that for the K^- meson, provided that contributions from the final I = 3 pion configuration are neglected. Also, effects of final pion-pion interactions were computed by extending the dispersion-theoretical treatment of Khuri and Treiman. (auth)

41446 EXPERIMENTAL STUDY OF $K^+_{\pi 4}$ DECAY. Birge, Robert W. (Univ. of California, Berkeley); Ely, Robert P. Jr.; Gidal, George (and others). Phys. Rev., 139: B1600-8(Sept. 20, 1965). (UCRL-16083).

A search was made for the rare $K^+_{\pi 4}$ decay modes $\pi^+\pi^-e^+\nu$, $\pi^+\pi^+e^-\bar{\nu}$, and $\pi^+\pi^+\mu^-\bar{\nu}$ in a sample of approximately 3×10^6 K^+ decays. A total of 69 events of the mode $\pi^+\pi^-e^+\nu$ were observed. The other two modes are forbidden by the $\Delta S = \Delta Q$ rule and no examples of them were found. The experiment gives an upper limit for the amplitude ratio $X = |[A(\Delta S = -\Delta Q)]/[A(\Delta S = \Delta Q)]|$, for the axial-vector current of 0.25, with the assumption of no final-state π-π interaction. The effects of final-state interactions in the π-π system modify the interpretation of this result and may be large. The rate for the $\pi^+\pi^-e^+\nu$ mode was determined to be $(2.9 \pm 0.6) \times 10^3$ sec^{-1}. The angular correlations between the planes formed by the lepton pair and the pion pair, and the angular distribution of π^+ with respect to the dipion line of flight in the dipion rest system for the 69 events, were studied. The dipion mass spectrum is presented for the 69 $\pi^+\pi^-e^+\nu$ events. The value of the ratio of the two form factors in $K_{\pi 4}$ decay (p wave to s wave) was found to be $\eta = 0.8 \pm 0.30$ from an analysis of these correlations. An estimate of the low-energy π-π phase shift was determined to be "$\delta_0 - \delta_1$" = 35° ± 30° from the angular correlations. The difference "$\delta_0 - \delta_1$" between the s-wave (δ_0) and p-wave (δ_1) phase shift is averaged over the π-π invariant mass spectrum. Since this spectrum is peaked at low-dipion invariant mass, the average pertains mainly to an invariant mass in the region of 179.2 to 350 Mev. The shape of the dipion invariant mass spectrum does not agree with the shape expected if a σ resonance exists and has a mass of approximately 400 Mev and a width of approximately 100 Mev. (auth)

41447 SPIN TESTS FOR BOSONS. Ademollo, M.; Gatto, R.; Preparata, G. (Universita, Florence; I.N.F.N., Florence). Phys. Rev., 139: B1608-18(Sept. 20, 1965).

Tests of spin for an unstable boson which decays into three spinless particles, or into a spin-1 and a spin-0 particle, or into two spin-½ particles, are presented. The proposed spin tests should be useful for the spin-parity determination of the new boson resonances. Spin tests linear in the experimental test functions are discussed in particular, in view of their general applicability independently of the production kinematics. Explicit expressions of the test functions are reported for the lower spin assignments. (auth)

41448 LONG-RANGE ELECTROMAGNETIC FORCES ON NEUTRAL PARTICLES. Feinberg, G. (Columbia Univ., New York); Sucher, J. Phys. Rev., 139: B1619-33 (Sept. 20, 1965). (TID-21813).

The long-range forces are considered, i.e., those falling off as a power of the distance, which may act between pairs of particles, one of which is neutral and spinless. It is shown that these forces may easily be calculated from the discontinuity function in the momentum transfer of the scattering amplitude for the two particles. In particular, the two-photon exchange force between two neutral, spinless systems, and the three-photon exchange force between a charged and a neutral, spinless system were investigated. In the former case, it is found that the potential behaves as r^{-7} for large r, in contradiction to the London expression for the Van der Waals force, and in agreement with the result of Casimir and Polder. For the latter case, the potential is odd under charge conjugation and hence can convert a K_2 meson to a K_1 meson. It is again found that the potential behaves as r^{-7}, and that such long-range electromagnetic interactions are presently unobservable in particle physics. (auth)

41449 LIE GROUPS, LIE ALGEBRAS, AND THE TROUBLES OF RELATIVISTIC SU(6). Lipkin, Harry J. (Weizmann Inst. of Science, Rehovoth, Israel). Phys. Rev., 139: B1633-7(Sept. 20, 1965).

Some of the difficulties of relativistic SU(6) are examined. Those arising from the use of continuous groups can be avoided by the use of algebras of finite sets of operators which are sufficient to give the desired properties of elementary particles. The nonconservation of probability associated with the relativistic separation of space and spin is pointed out. Quantum electrodynamics applied to atomic structure is shown to exhibit the type of peculiar symmetry which leaves the interaction invariant but is broken by free Dirac propagators. The implications of this analogy for SU(6) are discussed. The mixing of physical and nonphysical states (positive- and negative-energy quark states) leads to noninvariance of the vacuum under the symmetry group, and to a degenerate vacuum in the exact symmetry limit. The existence of open inelastic channels for low-mass boson production is relevant to unitarity calculations and is implied in all energy regions where the symmetry is not badly broken. (auth)

41450 CONSISTENCY CONDITIONS ON THE STRONG INTERACTIONS IMPLIED BY A PARTIALLY CONSERVED AXIAL-VECTOR CURRENT. II. Adler, Stephen L. (Harvard Univ., Cambridge, Mass.). Phys. Rev., 139: B1638-43(Sept. 20, 1965).

Consequences of the partially conserved axial-vector current (PCAC) hypothesis are explored. A set of simple rules is derived which relate the matrix element for any strong interaction process with the matrix element for the corresponding process in which an additional zero-mass, zero-energy pion is emitted or absorbed. A generalization to include lowest order electromagnetic processes is given. A theorem is stated and proved which shows how divergence equations of the form $\partial_\lambda J_\lambda = D$ are modified when a minimal electromagnetic interaction is switched on. (auth)

41451 LOW-ENERGY EQUIVALENT-POTENTIAL APPROACH FOR STRONG INTERACTIONS. II. Balazs, Louis A. P. (Tata Inst. of Fundamental Research, Bombay). Phys. Rev., 139: B1646-9(Sept. 20, 1965).

A method was previously presented for constructing the long-range part of an effective potential at any given energy. In certain problems, this potential is singular at small distances, requiring a cutoff or some other parameterization. The parameters thereby introduced can be determined by requiring that the amplitude at threshold be the same as that given by the Singh-Udgaonkar sum rule. (auth)

41452 POSSIBLE C,T NONINVARIANCE IN THE ELECTROMAGNETIC INTERACTION. Bernstein, J. (New York Univ., N. Y.); Feinberg, G.; Lee, T. D. Phys. Rev., 139: B1650-9(Sept. 20, 1965). (TID-21864).

The experimental foundation of the various discrete symmetry properties for the strong and the electromag-

netic interactions is reviewed. It is found that there is strong evidence that both interactions are invariant under P and CPT, and good evidence that the strong interaction is invariant under C and T. However, at present, there is a complete lack of evidence that the electromagnetic interaction of the strongly interacting particles is invariant under C and T. Possible experiments that can test such C, T invariance or noninvariance are discussed. It is pointed out that if the electromagnetic interaction of the strongly interacting particles has strong violations of C, T invariance, then, through second-order processes, C-violating and CP-violating effects can be observed in the usual strong and weak processes, respectively. In particular, the decay $K_2^0 \rightarrow \pi^+ + \pi^-$ may occur with an amplitude $\sim(\alpha/\pi)$ times that of $K_1^0 \rightarrow \pi^+ + \pi^-$. (auth)

41453 ELASTIC ELECTRON-DEUTERON SCATTERING AND POSSIBLE MESON-EXCHANGE EFFECTS. Buchanan, C. D.; Yearian, M. R. (Stanford Univ., Calif.). Phys. Rev. Letters, 15: 303-6(Aug. 16, 1965).

Data on elastic electron-deuteron scattering was obtained using a two-spectrometer coincidence-detection technique. Both electric and magnetic scattering were measured. A preliminary analysis of the data was compared with an impulse-approximation theory and permitted an investigation of possible meson exchange and/or relativistic effects. The conclusions are that simple impulse-approximation theory, without corrections, appears not to be adequate to explain the large observed magnetic scattering, electric scattering agrees with the uncorrected theory, the ρ-π-γ meson-exchange effect seems to be a good candidate for explaining the consistently large magnetic scattering observed. (J.F.P.)

41454 TEST FOR PARTICLE-MIXTURE THEORIES OF $K^0 \rightarrow 2\pi$ DECAY. Kabir, P. K. (Institut de Physique Nucleaire, Lyon); Lewis, R. R. Phys. Rev. Letters, 15: 306-8(Aug. 16, 1965).

In order to explain the long-lived $\pi^+\pi^-$ decays, which were previously confirmed, possible explanations of this effect are considered within the framework of CP invariance, since there is no clear indication of CP violation. A simple test is described for a class of such particle-mixture theories, which represent the only proposals advanced so far which maintain CP invariance without calling upon cosmological effects. It is believed that this experimental test proposed provides a more direct and clear-cut test of particle-mixture theories than other tests proposed. (J.F.P.)

41455 PION-PROTON ELASTIC SCATTERING AT HIGH MOMENTUM TRANSFERS. Orear, J. (Cornell Univ., Ithaca, N. Y.); Rubinstein, R.; Scarl, D. B.; White, D. H.; Krisch, A. D.; Frisken, W. R.; Read, A. L.; Ruderman, H. Phys. Rev. Letters, 15: 309-13(Aug. 16, 1965).

Measurements of 8 and 12 Bev/c π^+ and π^- elastic scattering on hydrogen which extend angular distributions well beyond the forward diffraction peak are reported. At an incident meson (π) momentum of 8 Bev/c the elastic differential cross sections were measured for values of the invariant four-momentum transfer squared, -t, from 1.2 to 6.0 Bev/c, corresponding to center-of-mass scattering angles from 33.8 to 81.2°. At 12-Bev/c incident meson (π) momentum the measurements covered a range of $-t$ from 1.2 to 3.5 Bev/c, corresponding to center-of-mass angles from 27.1 to 47.4°. For most of these momentum transfers, cross sections were measured for incident negative mesons (π), positive mesons (π), and protons. The shapes of the cross section curves for the scattered particles are discussed. (J.F.P.)

41456 BACKWARD ELASTIC SCATTERING OF HIGH-ENERGY PIONS BY PROTONS. Frisken, W. R. (Brookhaven National Lab., Upton, N. Y.); Read, A. L.; Ruderman, H.; Krisch, A. D.; Orear, J.; Rubinstein, R.; Scarl, D. B.; White, D. H. Phys. Rev. Letters, 15: 313-16(Aug. 16, 1965).

The backward elastic scattering of mesons (π) at 4 and 8 Bev/c was studied; and cross sections for positive and negative mesons (π) were measured at center-of-mass angles from 170 to 180° in the center of mass. A sharp peak was found in the backward direction for positive mesons (π) and a lower, flatter peak for negative mesons (π) at both 4 and 8 Bev/c. The measured values of the differential elastic cross section, versus the center-of-mass scattering angle are given and plotted. It is concluded that the backward peak in 8 Bev/c π^+-p scattering is narrower than the forward diffraction peak. The charge dependence of the backward peak seems to imply that the backward scattering may be due to a process more complicated than simple diffraction. (J.F.P.)

41457 RARE DECAY MODES OF THE η MESON AS A PROBE OF ELECTROMAGNETIC AND STRONG INTERACTIONS. Geffen, Donald A.; Young, Bing-lin (Univ. of Minnesota, Minneapolis). Phys. Rev. Letters, 15: 316-20 (Aug. 16, 1965). (COO-1371-15).

Since the rare decay modes of the meson (η) can provide a variety of valuable information about electromagnetic and strong interactions, the following phenomena are studied: A comparison is made of decay modes for the same values of the lepton-pair center-of-mass energy; tests are made for a difference between the meson (μ)-photon and electron-photon interaction for timelike virtual photon phenomena; the measurements of the distribution of events in the η decays as a function of lepton-pair center-of-mass energy, yields the electromagnetic form factor of the meson. The result can be compared with the predictions of SU(3). The branching ratio for one of the decay modes depends strongly upon the behavior of the $\eta \rightarrow 2\gamma$ vertex for large virtual photon momenta. (J.F.P.)

41458 B-MESON DECAY, ω-ϕ MIXING, AND SU(6). Capps, Richard H.; Koerner, Juergen G. (Northwestern Univ., Evanston, Ill.). Phys. Rev. Letters, 15: 320-1 (Aug. 16, 1965).

It is pointed out that if the preliminary experimental evidence that the spin-parity assignment of the 1215 Mev meson (B) is 1^+, is correct then the B may belong to an SU(6) multiplet. In this case the $\pi\phi/\pi\omega$ branching ratio of the B decay is a measure of the ω-ϕ mixing angle. It is assumed that the B is an axial-vector meson t at decays primarily into S-wave $\pi\omega$ and $\pi\phi$ states. It is also assumed that the relative coupling of the B to various $\mu\mu$ states (where μ denotes a member of the 35-fold multiplet of pseudoscalar and vector mesons) corresponds to Clebsch-Gordan coefficients of nonrelativistic SU(6).(J.F.P.)

41459 EXISTENCE AND PROPERTIES OF A NON-STRANGE MESON OF MASS 1500 Mev/c^2. Barnes, V. E. (Brookhaven National Lab., Upton, N. Y.); Culwick, B. B.; Guidoni, P. (and others). Phys. Rev. Letters, 15: 322-5 (Aug. 16, 1965).

Evidence is presented for the existence and properties of a nonstrange meson which is called f*. An enhancement is observed in the K_1K_1 system with mass $M \approx 1500$ Mev/c^2 and width $\Gamma \approx 85$ Mev/c^2. The existence of this decay mode requires that the f* be even under charge conjugation, C, or equivalently, that it have even spin and parity. The decay of the f* into KK*, which excludes a 0^+ spin-parity assignment, was also observed. K^-p interactions at 4.6 and 5.0 Bev/c incident K momentum were studied. The evidence for the existence of the f* meson comes from a study of the final states summarized. It is emphasized that the f* enhancement is due primarily to the shaded events, those with two visible K_1 decays. (J.F.P.)

41460 BRANCHING RATIOS FOR DECAYS OF THE f^0, A_2, AND K* (1400) MESONS. Chung, Suh Urk; Dahl, Orin I.; Hardy, Lyndon M.; Hess, Richard I.; Jacobs, Laurance D.; Kirz, Janos; Miller, Donald H. (Univ. of California, Berkeley). Phys. Rev. Letters, 15: 325-9(Aug. 16, 1965). (UCRL-16220).

Branching ratios for the f^0 and A_2 were estimated by using events produced in π^- + p interactions at 3.2 Bev/c. Since this momentum is near the threshold for Y + K* (1400), the branching ratios for K* (1400) were obtained using events produced at 3.9 and 4.2 Bev/c. Results on the branching fractions and cross sections are summarized. Since the f^0, A_2, and K*(1400) are all produced peripherally in π^- + p interactions, the low four-momentum transfer squared events were considered separately to reduce background. (J.F.P.)

41461 DECAY MODES OF SPIN-TWO MESONS. Glashow, Sheldon L.; Socolow, Robert H. (Univ. of California, Berkeley). Phys. Rev. Letters, 15: 329-33(Aug. 16, 1965).

The observed partial decay widths of the $J^P = 2^+$ mesons are compared with theoretical predictions based on SU(3). The results strongly support the assignment of these states to the reducible $1 \oplus 8$ representation of SU(3) with considerable f,f' mixing. Certain remarkable regularities characterize the nonets of $J^P = 1^-$ and $J^P = 2^+$ mesons, and a theoretical framework from which these regularities may be understood is represented. (J.F.P.)

41462 $SU(6)_W$ PHOTOPRODUCTION AND MESON-BARYON SCATTERING AMPLITUDES. Carter, J. C. (National Bureau of Standards, Washington, D. C.); Coyne, J. J.; Meshkov, S.; Horn, D.; Kugler, M.; Lipkin, H. J. Phys. Rev. Letters, 15: 373-7(Aug. 23, 1965).

W spin and $SU(6)_W$ are used to obtain many simple relations among photoproduction amplitudes and among scattering amplitudes which hold even when the particles involved are moving, as long as the motions are collinear. Amplitudes of the form ($\gamma\rho$/MB) and (MB/MB) are considered. The predictions obtained are relativistic but hold only in the forward or backward directions. (J.F.P.)

41463 $\tilde{U}(12)$ PREDICTIONS FOR $N\bar{N}$ ANNIHILATION AT REST INTO FOUR MESONS. Leung, Y. C.; Rashid, M. A. (International Atomic Energy Agency, Trieste, Italy). Phys. Rev. Letters, 15: 424-9(Aug. 30, 1965).

Predictions for annihilation modes are obtained where the final products consist entirely of pseudoscalar mesons, since experimental information on these is most easily accessible. Final products containing two K mesons are of special interest as these modes are forbidden in a previously considered case. Toward this aim conclusions are reached which are very specific. The annihilation amplitudes are considered to consist only of the regular couplings, which are $\tilde{U}(12)$-invariant quantities before an actual identification of the external lines with physical particles is made. The results are obtained that $N\bar{N}$ annihilation at rest into two mesons is forbidden and that the couplings for annihilations into three mesons is unique. However, since the $\tilde{U}(12)$ symmetry is intrinsically broken for a physical S-matrix element, there is no reason a priori to exclude couplings which contain symmetry-breaking kinetic-energy parts, referred to as irregular couplings. (J.F.P.)

41464 CHARGE CONJUGATION, DECAY OF VECTOR MESONS, AND SU(6) SYMMETRY. Konuma, Michiji (Scuola Normale Superiore, Pisa, Italy and Centro Ricerche Fisica e Matematica, Pisa, Italy); Remiddi, Ettore. Phys. Rev. Letters, 15: 433-6(Aug. 30, 1965).

A charge-conjugation operator in the SU(6) symmetry is introduced which reproduces the usual charge-conjugation properties of known elementary-particle states. Vector-meson decays into two mesons are treated with the requirement that this operator be conserved. Interesting predictions between decay amplitudes are obtained in good agreement with experimental data. (J.F.P.)

41465 PROTON COMPTON SCATTERING IN THE 2ND RESONANCE ENERGY REGION. Nagashima, Yorikiyo (Univ. of Tokyo). Progr. Theoret. Phys. (Kyoto), 33: 828-39(May 1965).

A phenomenological treatment based on the isobar model is applied to the elastic scattering of photons by protons around the second resonance energy region. The experimental evidence of the large cross section around 600 Mev and the relative shift of the 2nd resonance peak to lower energy side by 50 Mev is explained by the inclusion of $T = J = \frac{1}{2}$ resonance at 600 Mev. In contrast to the discussion based on the phase shift analysis of pion nucleon scattering, the analysis seems more favorable to the odd parity attached to that resonance. Effects of the scalar boson exchange term are discussed. (auth)

41466 SELECTION RULES IMPOSED BY THE SYMMETRICAL QUARK MODEL. Iso, Chikashi (Tokyo Inst. of Tech.). Progr. Theoret. Phys. (Kyoto), 33: 840-9 (May 1965).

Selection rules for strangeness-nonzero systems are discussed based on a symmetrical quark model, because of the conservation of $G_{ds}(G_{us})$ parity, where G_{ds} is defined by (exchange of d and s) × (charge conjugation) and G_{us} is defined by (exchange of u and s) × (charge conjugation). These selection rules are applied to the processes such as boson decays, $\Sigma^+ p$ annihilation, Ξp annihilation, $\Lambda' + \Lambda' \to K_1^0 + K_2^0$, etc. Some processes are useful for checking the symmetrical quark model (SU(3)). (auth)

41467 A RELATIVISTIC SU_6 SYMMETRY SCHEME. Suzuki, Mahiko (Univ. of Tokyo). Progr. Theoret. Phys. (Kyoto), 33: 850-3(May 1965).

A relativistically covariant assignment of particles in the SU_6 symmetry is proposed on the basis of the $U_6 \times U_6$ symmetry. Since, in contrast with the usual assignment, the present scheme contains the fourth components of spin-one and spin-$\frac{1}{2}$ particles, all matrix elements are SU_6-covariant as well as relativistically covariant. It is stressed that the Lorentz condition is not SU_6-invariant. (auth)

41468 MASS SPLITTING OF PSEUDOSCALAR OCTET CAUSED BY BARYON OCTET MASS DIFFERENCE. Kinoshita, Kisei (Univ. of Tokyo). Progr. Theoret. Phys. (Kyoto), 33: 854-63(May 1965).

The mass renormalization is expressed in terms of the proper vertex function under certain conditions on the propagator when $Z_3 \neq 0$. In the framework of the SU_3 symmetry, the effect of baryon mass difference on the mass splitting of the pseudoscalar octet is estimated with this formula, where the proper vertex function is calculated in the ω-, V_8-, P_8-exchange ladder approximation. With the maximum value of the meson-baryon coupling constant consistent with the condition $1 > Z_3 > 0$, experimental values are explained when F/D = 0.1. (auth)

41469 DOMINANCE THEOREM IN CROSSING MATRICES AND ITS PHYSICAL IMPLICATIONS IN HIGH ENERGY DIFFRACTION SCATTERING THEORY. Masuda, Naohiko (Nihon Univ., Tokyo). Progr. Theoret. Phys. (Kyoto), 33: 864-76(May 1965).

The following theorem is proved in SU(2) and SU(3) groups: the absolute magnitude of the nonzero crossing matrix element between s-channel amplitude in the singlet state and t- or u-channel amplitude in a given arbitrary multiplet state is never smaller than the absolute magnitude of the crossing matrix element between s-channel amplitude in an arbitrary multiplet state and t- or u-channel amplitude in a given arbitrary multiplet state. Possible implications of this theorem in high energy scattering are discussed. (auth)

41470 CP VIOLATION AND PT INVARIANCE. Hiida, Kichiro (Univ. of Tokyo). Progr. Theoret. Phys. (Kyoto), 33: 877-81(May 1965).

A theory of weak interactions is presented such that small CP violating weak interactions are invariant universally under PT, assuming the CPT theorem. The reason why PT invariance is assumed and results obtained from the theory are discussed. (auth)

41471 CP VIOLATION AND THE $|\Delta I| = \frac{1}{2}$ RULE. Yokoo, Yashimatsu (Osaka Univ.). Progr. Theoret. Phys. (Kyoto), 33: 882-8(May 1965).

The CP-violating processes and the decay modes violating the $|\Delta I| = \frac{1}{2}$ rule are investigated on the same footing by introducing a $|\Delta I| = \frac{3}{2}$ interaction which is assumed to violate maximally the CP invariance. It is shown that a new relation concerning a couple of branching ratios, $(K_2^0 \to \pi^+ + \pi^-)/(K_2^0 \to 2\pi) = (K_1^0 \to \pi^0 + \pi^0)/(K_1^0 \to 2\pi)$, should hold. Another interesting result is that the processes with $\Delta S/\Delta Q = -1$ such as $\Sigma^+ \to n + l^+ + \nu$ and $K^0 \to \pi^+ + l^- + \nu$, are suppressed by the factor 10^{-6} compared with ordinary ones ($\Delta S/\Delta Q = +1$). (auth)

41472 ON A CLASSICAL SPINNING PARTICLE MODEL OF DIRAC PARTICLE. Goto, Tetsuo (Univ. of Nihon, Tokyo). Progr. Theoret. Phys. (Kyoto), 33: 889-906(May 1965).

By using the momentum proper time, which coincides with the usual time in the momentum rest frame, the general lagrangian and hamiltonian formalism of classical relativistic spinning particles is developed. As an example of this

formalism, a classical model which directly corresponds to Dirac and Duffin-Kemmer particles is found. In connection with this example, differential operators are obtained which satisfy Bhabha's condition and, therefore, correspond to Dirac's γ-matrices if only the spin-$\frac{1}{2}$ states are considered. (auth)

41473 RIGID SPHERE MODEL OF ELEMENTARY PARTICLES AND THE ELECTROMAGNETIC FIELD. Hara, Osamu; Goto, Tetsuo (Univ. of Nihon, Tokyo). Progr. Theoret. Phys. (Kyoto), 33: 907-31(May 1965).

An attempt is made to derive the relation of the isospin with the electromagnetic field, based upon the rigid sphere model of elementary particles, starting from the five dimensional theory proposed by Kaluza and Klein. The field equation for the metric field is given uniquely by the requirement of general covariance. In the first approximation with respect to the square root of the gravitational constant, this equation reduces to Maxwell's equation with $Q = eI^3$, where Q is the electric charge and I^3 is the third component of the isospin given by Nakano, Takabayasi, and Vigier in their theories of the extended particle model of elementary particles. The fact that the electromagnetic field defines a special direction in the isospace follows very naturally from this field equation. Thus, all characteristic features of the electromagnetic field as well as the relation between the electromagnetic field and the isospin are derived as a necessary consequence of the theory, without any further specific assumptions. (auth)

41474 THEORY OF BOUND STATES. I. Kawaguchi, Masaaki (Univ. of Osaka; Australian National Univ., Canberra). Progr. Theoret. Phys. (Kyoto), 33: 932-45(May 1965).

Relativistic and nonrelativistic theories of bound states mediated by a finite mass meson are discussed. The Fredholm formula is applied to the Bethe-Salpeter equations. Difficulties concerned with divergent Fredholm traces are avoided by factorizing divergent terms which are independent of the eigenvalue problem. An eigenvalue of the coupling constant is found for a given binding energy of two scalar nucleons as well as spinor nucleons. In the nonrelativistic limit the same method is applied to the Schroedinger equation with the static Yukawa potential. The eigenvalue of the coupling constant is found for the real deuteron, and the eigenfunction turns out to be very similar to the Hulthén wave function. (auth)

41475 AN APPROACH IN THE CANONICAL FORMALISM OF QUANTUM FIELD THEORY. Watanabe, Ichie (Tokyo Medical and Dental Univ.). Progr. Theoret. Phys. (Kyoto), 33: 946-63(May 1965).

Vacuum and other states are studied by the canonical formalism of quantum field theory. At first the physical vacuum is defined by a free vacuum and creation operators of a Fock space, which is constructed from field variables at a fixed time. It is rewritten in such a way that a state obtained by applying an annihilation operator to the vacuum is equated with the state obtained by applying power series of creation operators to the vacuum. Parameters of this series (β parameters) characterize the vacuum and define new operators which annihilate the physical vacuum. If any state is considered to be represented by power series of adjoint of the new operators applied on the vacuum it can be proved that their coefficients (ρ parameters) are expectation values of field operators. β parameters are determined by the hamiltonian of the system. A method to obtain them from a given hamiltonian is shown by simple examples. Self-coupled neutral scalar fields are considered as an example. (auth)

41476 POSSIBLE CHOICE OF FUNDAMENTAL PARTICLE MODELS. Ishida, Shin (Univ. of Nihon, Tokyo). Progr. Theoret. Phys. (Kyoto), 33: 994-5(May 1965).

A possible criterion for the choice of an elementary-particle model using SU(3) symmetry is proposed. Mass splitting of multiplets is treated assuming that symmetry breakdown is due to small mass differences among the basic triplet. The quartet model—having four fundamental particles consisting of one triplet and one singlet—and the triplet model are used to estimate the mass splittings of the baryon octet, using the expectation values of the hamiltonian. Results from the triplet model are found to be very satisfactory. (M.J.T.)

41477 A NEW BARYON OCTET AND THE QUARK MODEL. Kunimasa, Tosaku (Univ. of Osaka). Progr. Theoret. Phys. (Kyoto), 33: 997-9(May 1965).

A modified quark model of baryons is proposed which gives a reasonable assignment of experimentally discovered particles to the unfamiliar octet and singlet states derived from the irreducible decomposition of the product states of three quarks. It is assumed that there exist three kinds of quarks bound by a strong force yielding S-state baryons. A sum rule for masses of the singlet, decuplet, and the two octets is obtained from an interaction hamiltonian representing the unitary-spin dependent force caused by the exchange of scalar-octet bosons between the two quarks. The baryons $N^*(1480)$, $Y_0^*(1660)$, $\Xi^*(1810)$, and the undiscovered $Y_0^*(1600)$ are assigned to the 8′ spin-$\frac{1}{2}$ octet, and the $Y_0^*(1405)$, to the singlet. (M.J.T.)

41478 ON THE INTERNAL STRUCTURE OF ELEMENTARY PARTICLES. Ono, Ken-Ichi (Tokyo Univ.). Sci. Papers Coll. Gen. Educ., Univ. Tokyo, 15: 35-42 (June 1965).

A discussion is given of properties of the structure of particles. This includes symmetry, antiparticles, transformation of field operators, chirality, strangeness, and helicity. A possible phenomenon is proposed concerning a transition between two levels of asymmetric vibration. A vibration of an electric charge along the spiral orbit raises an electric moment as well as a magnetic moment, and the two moments are in linear relation with a phase difference of $\pi/2$. This is considered the general feature of any asymmetric vibration. If such moments do arise, then the inevitable interaction is expressed by a hamiltonian. Experimentally, it is expected that the rotation of the polarization plane of the gamma ray when it passes through matter, and the change of the sense of rotation when the energy of the gamma ray passes over the value corresponding to the mass difference between the levels which have different strangeness will occur. If these phenomena exist, they are a powerful means of investigation. (J.F.P.)

41479 ANALYSIS OF PROTON-TRITIUM ELASTIC SCATTERING ABOVE THE $T(p,n)^3He$ THRESHOLD. Balashko, Yu. G.; Barit, I. Ya. (Lebedev Inst. of Physics, Moscow). Soviet J. Nucl. Phys. (English Transl.), 1: 153-4(Aug. 1965).

Translated from Yadern. Fiz., 1: 221-3(Feb. 1965).

A phase shift analysis is made of p-t elastic scattering at 1-3 Mev taking the reaction $T(p,n)^3He$ into account. The phase shift $^1\delta_0$ is extrapolated from the region below 1 Mev according to the single-level resonance formula. Appreciable contributions from spin-orbit splitting and d scattering are found. (auth)

41480 MICHEL PARAMETER IN $\mu^- - e^-$ DECAY. Pontecorvo, J. B.; Sulyaev, R. M. (Joint Inst. for Nuclear Research, Dubna, USSR). Soviet J. Nucl. Phys. (English Transl.), 1: 200-3(Aug. 1965).

Translated from Yadern. Fiz., 1: 283-7(Feb. 1965).

The energy spectrum of electrons formed in the decay of negative μ mesons from states of mesonic helium atoms was obtained. The momenta of 4090 electrons were measured. The experiment utilized a diffusion chamber placed in a stabilized magnetic field of 6100 Oe and filled with helium to a pressure of 20 atm. The Michel parameter calculated by the method of least squares turned out to be 0.867 ± 0.035. (auth)

41481 SCATTERING OF ANTINEUTRINOS BY ELECTRONS. Bogush, A. A.; Bolsun, A. I.; Satsunkevick, I. S. (Inst. of Physics, Academy of Sciences, Belorussian SSR). Soviet J. Nucl. Phys. (English Transl.), 1: 204-6(Aug. 1965).

Translated from Yadern. Fiz., 1: 288-90(Feb. 1965).

The differential and total cross sections for the process $\bar{\nu}_e + e \rightarrow e' + \bar{\nu}_e'$ are calculated assuming the existence of

intermediate vector mesons and taking account of a possible charge distribution of the antineutrino. Possible methods of determining the non-locality parameter due to the bosons and the Dirac charge form factor of the antineutrino are discussed. (auth)

41482 ON THE DECAY $\pi \rightarrow \mu + \nu + e^+ + e^-$. Pikin, S. A.; Kharkats, Yu. I. (Inst. of Engineering and Physics, Moscow). Soviet J. Nucl. Phys. (English Transl.), 1: 207-10(Aug. 1965).

Translated from Yadern. Fiz., 1: 291-5(Feb. 1965).

The decay $\pi \rightarrow \mu + \nu + e^+ + e^-$ is considered, where the e^+e^- pair is created by a virtual γ quantum from internal bremsstrahlung. The total decay probability, equal to 2.6×10^{-8} of the $\pi \rightarrow \mu + \nu$ probability, and the differential distribution with respect to energy and angle are obtained. The possibility of using this decay to determine the mass of the muonic neutrino is investigated. (auth)

41483 SUPERCHARGE AND SUPERCHARGED PARTICLES. Okun', L. B. (Inst. for Theoretical and Experimental Physics, State Commission for Atomic Energy, USSR). Soviet J. Nucl. Phys. (English Transl.), 1: 211-14 (Aug. 1965).

Translated from Yadern. Fiz., 1: 297-302(Feb. 1965).

Within the SU_3 symmetry scheme all hadrons can be characterized by their supercharge σ—an additive quantum number which is the same for all members of a supermultiplet. It is shown that for the supermultiplet $(p,q)Y^0$, with Y^0 the hypercharge of the isosinglet of the supermultiplet, the supercharge is $\sigma = p - q + \frac{3}{2} Y^0$. The known hadron octets and the decimet have $\sigma = 0$. Possible selection rules imposed by σ are discussed, as well as the possibility of manifestations of hadrons with $\sigma = 0$, in particular of unitary triplets, in neutrino experiments. A simple rule for the multiplication of supermultiplets is proposed. (auth)

41484 A POSSIBILITY FOR DETECTING THE INTERMEDIATE MESON WITH MASS LARGER THAN TWICE THE NUCLEON MASS. Zheleznykh, I. M.; Markov, M. A. (Lebedev Inst. of Physics, Moscow). Soviet J. Nucl. Phys. (English Transl.), 1: 215-18(Aug. 1965).

Translated from Yadern. Fiz., 1: 303-8(Feb. 1965).

Specific types of decay of an intermediate meson of large mass ($M_W > 2m_N$, where m_N is the mass of the nucleon) are considered. Possibilities for detecting the W meson in a resonance reaction of the type $\bar{p} + n \rightarrow W^- \rightarrow \mu^- + \bar{\nu}_\mu$ are discussed. (auth)

41485 THE ANGULAR CORRELATION BETWEEN π MESON AND LEPTONS AND THE DETERMINATION OF FORM-FACTORS IN $K_{\mu 3}$ DECAY. Tsukerman, I. S. Soviet J. Nucl. Phys. (English Transl.), 1: 221-2(Aug. 1965).

Translated from Yadern. Fiz., 1: 311-13(Feb. 1965).

It is shown that the shape of the angular correlation between the directions of emergence of the π meson and the leptons in $K_{\mu 3}$ decay is sensitive to the choice between two possible values of the ratio of the form-factors. (auth)

41486 THE PROCESS OF PAIR PRODUCTION BY FAST MUONS. Mikhailov, V. D. Soviet J. Nucl. Phys. (English Transl.), 1: 223-4(Aug. 1965).

Translated from Yadern. Fiz., 1: 314-16(Feb. 1965).

An estimate of the relativistic corrections to the process of production of electron-positron pairs by fast charged particles in an external field is made by means of the equivalent-photon method. The energy dependence of the corrections is examined for angles which are not too small. (auth)

41487 ELASTIC pp SCATTERING AT 1.45 Bev. Kruchinin, S. P.; Mukhin, K. N.; Romantseva, A. S.; Svetlolobov, I. A.; Sulkovskaya, M. M.; Chueva, S. A.; Shlyapnikov, R. S. Soviet J. Nucl. Phys. (English Transl.), 1: 225-9(Aug. 1965).

Translated from Yadern. Fiz., 1: 317-23(Feb. 1965).

Elastic pp scattering at 1.45 Bev was investigated with the help of a propane bubble chamber with a pulsed magnetic field. The differential cross section was obtained over the entire angular region 0–90° (c.m.s.). The results are compared with optical-model predictions and optimal values of the parameters are obtained. It is shown that the experimental dependence of $d\sigma/d\Omega$ on $p_\perp$ obtained for large $p_\perp$ is well approximated by the exponential dependence suggested by Orear: $d\sigma/d\Omega \sim \exp(-p_\perp/p_0)$. It is noted that the best agreement with the exponential approximation is obtained for c.m.s. scattering angles of $\chi = 90°$, when $p_\perp = p_{cms}$. In this case ($\chi = 90°$), $d\sigma/d\Omega = A \exp(-p_{cms}/p_0)$, A = 115 mb/sr, $p_0 = 143$ Mev/c, and the extrapolation is correct for all known data on elastic pp scattering in the energy region 0.38–30.9 Bev. (auth)

41488 BARYON RESONANCES IN π^-p INTERACTIONS AT 7.5 Bev WITH STRANGE-PARTICLE FORMATION. Belyakov, V. A.; Veksler, V. I.; Viryasov, N. M.; Kladnitskaya, E. N.; Kopylov, G. I.; Penev, V. N.; Solov'ev, M. I. (Joint Inst. for Nuclear Research, Dubna, USSR). Soviet J. Nucl. Phys. (English Transl.), 1: 240-8(Aug. 1965).

Translated from Yadern. Fiz., 1: 338-50(Feb. 1965).

The formation and properties of resonances decaying into Λ hyperons and π mesons were studied. Data are given on the cross sections for formation of $Y^+(1385)$ and $Y^+(1660)$ hyperons in π^-p interactions at 7.5 Bev/c. The properties and production characteristics of $Y^+(1385)$ hyperons and their decay products were also studied. The peak in the $M_{\Lambda\pi^+\pi^-}$ mass spectrum at ~1770 Mev is discussed. (auth)

41489 MESON RESONANCES IN π^-p INTERACTIONS AT 7.5 Bev WITH STRANGE PARTICLE PRODUCTION. Belyakov, V. A.; Veksler, V. I.; Viryasov, N. M.; Kladnitskaya, E. N.; Kopylov, G. I.; Penev, V. N.; Solov'ev, M. I. (Joint Inst. for Nuclear Research, Dubna, USSR). Soviet J. Nucl. Phys. (English Transl.), 1: 249-58(Aug. 1965).

Translated from Yadern. Fiz., 1: 351-65(Feb. 1965).

Resonances decaying into $K^0(\bar{K}^0,K^+)$ and π mesons were investigated. Cross sections are given for the production of K*(888) and k(730) mesons in π^-p interactions at 7.5 Bev/c in events with $\bar{K}K$ pairs, and the contribution (in %) of k^0 and K^{*0} mesons to events with ΛK^+ pairs is estimated. Properties and production characteristics of $K^{*\pm}$ mesons are described. Mass spectra of the $K2\pi$ and $K3\pi$ systems were investigated. The possibility of the production of a new resonance $U \rightarrow K^0 + \pi^+ + \pi^- + \pi^\pm$ with a mass of 1660 Mev is indicated. An attempt was made to determine its quantum numbers. Proofs are given of the production of a resonance with a mass of 1050 Mev, decaying into three π mesons ($\pi^\pm\pi^\pm\pi^\mp$), which can be identified as the A_1 meson. (auth)

41490 THE OKUBO MASS FORMULA IN HIGHER ORDERS. Rekalo, M. P. (Inst. of Physics and Tech., Academy of Sciences, Ukrainian SSR). Soviet J. Nucl. Phys. (English Transl.), 1: 259-60(Aug. 1965).

Translated from Yadern. Fiz., 1: 366-8(Feb. 1965).

Postulating a definite transformation character for the hamiltonian of the moderately strong interactions with respect to SU_3 transformations, and making use of the U-spin formalism, the Okubo mass formula is detained in higher orders of the moderately strong interaction and in arbitrarily high order with respect to the electromagnetic interaction. The total number of parameters in this formula, taking into account the moderately strong interaction to a sufficiently high order, coincides with the multiplicity of the U-multiplet. (auth)

41491 CONCERNING THE CALCULATION OF THE PARAMETERS OF SCATTERING BY A TENSOR POTENTIAL. Babikov, V. V. (Joint Inst. for Nuclear Research, Dubna, USSR). Soviet J. Nucl. Phys. (English Transl.), 1: 261-8(Aug. 1965).

Translated from Yadern. Fiz., 1: 369-79(Feb. 1965).

The method of phase functions is extended to include the case of non-central forces. Equations are obtained for the calculation of the phase shifts and the mixing parameters in different representations. The effective-radius theory is considered for scattering by a tensor potential, and equations are obtained which allow account of the effect of the tensor forces to be taken. (auth)

41492 POSSIBILITY OF THE EXISTENCE OF A BOSON 27-SUPERMULTIPLET 1^+. Vladimirskii, V. V. (Inst. of Theoretical and Experimental Physics, State Commision

for Atomic Energy, USSR). Soviet J. Nucl. Phys. (English Transl.), 1: 269-70(Aug. 1965).

Translated from Yadern. Fiz., 1: 380-2(Feb. 1965).

The existence of a 27-supermultiplet with spin and parity 1^+ or possibly 2^- is discussed. The main type of decay for such resonance states should be two-particle decay with $l = 0$ into particles with spin and parity 0^- and 1^-. The 27-supermultiplet consists of nine multiplets. For bosons the hypercharge is equal to the strangeness. Multiplets which differ in the sign of strangeness are charge conjugates, and have identical masses and types of decay. Owing to this there are only six essentially different types of particle. It is pointed out that the degree of assurance in the determination of the quantum numbers for the resonances in question, and serious doubts of the very existence of some of them, do not allow the proposed scheme to be regarded as anything more than a working hypothesis. (J.F.P.)

41493 THE CROSS SECTIONS FOR THE PROCESSES $e^+ + e^- \to e^+ + \mu^- + \nu_e + \bar{\nu}_\mu$. Badalyan, A. M. Soviet J. Nucl. Phys. (English Transl.), 1: 219-20(Aug. 1965).

Translated from Yadern. Fiz., 1: 309-10(Feb. 1965).

The cross sections for the processes $e^+ + e^- \to e^+ + \mu^- + \nu_e + \bar{\nu}_\mu$ are calculated. It is shown that these cross sections are proportional to $S \ln (S/2m^2)$ (S is the square of the total energy). (auth)

41494 ANGULAR CORRELATIONS BETWEEN FAST Σ HYPERONS AND FAST PROTONS EMITTED FROM INTERACTIONS OF K-MESONS AT REST IN NUCLEAR EMULSION. Burhop, E. H. S. • (London Univ.); Davis, D. H.; Jones, B. D.; Sacton, J.; Zakrzewski, J. Univ. Bruxelles, Inst. Phys., Bull., No. 17, 1-8(Sept. 1964).

The properties of interactions in which a fast charged hyperon (Σ) of energy greater than 50 Mev is emitted together with a fast proton of energy greater than 30 Mev are investigated. Such interactions can be attributed to the non-mesonic absorption of mesons (K^-) involving more than one nucleon. The appearance of both a fast hyperon (Σ) and a fast proton probably implies a primary meson (K^-) interaction with a neutron and a proton. From a sample of about 18,000 meson (K^-) capture stars, 89 containing a fast hyperon (Σ) and a fast proton were analyzed. The results indicate that the multi-nucleon absorption on a neutron-proton pair can occur in both the light and the heavy types of emulsion nuclei. (J.F.P.)

41495 DESCRIPTION OF STATIONARY STATES IN THE INTERACTION REPRESENTATION. Alekseev, V. V.; Grigorev, V. I. Vestn. Mosk. Univ., Ser. III: Fiz. Astron., No. 1, 42-6(Jan.-Feb. 1965). (In Russian).

The description in the interaction representation of those physical systems for which the method of adiabatic inclusion and interaction de-energizing does not appear satisfactory is examined. The equations for the S-matrix, whose eigenvalues determine energy, etc., are introduced. (tr-auth)

41496 BETA DECAY OF MOVING, LONGITUDINALLY POLARIZED NEUTRONS. Kerimov, B. K.; Alishev, S. A. Vestn. Mosk. Univ., Ser. III: Fiz. Astron., No. 1, 88-90 (Jan.-Feb. 1965). (In Russian).

The beta decay of moving, longitudinally polarized free neutrons and antineutrons is investigated according to the four-fermion V-A interaction scheme, taking into account the spin states of the product fermions. A closed formula describing the electron (positron) angular distribution from the decay in flight of a longitudinally polarized neutron (antineutron) is found as a result of integration of the differential decay probability over the solid angle of emission of the antineutrino (neutrino) and the energy of the emitted electron (positron). The calculated angular distributions of the longitudinally polarized electrons at various velocities of the left and right polarized decaying neutron are represented in the form of graphs. (M.J.T.)

41497 CLASSICAL SCALAR MESON FIELDS. Pytev, Yu. P. Vestn. Mosk. Univ., Ser. III: Fiz. Astron., No. 2, 53-8(Mar.-Apr. 1965). (In Russian).

The five-dimensional scalar field theory is examined. Corresponding classical particles are the singularities of the field. Dynamic variables of the particles are determined as dynamic variables of the singular part of the field; classical equations of motion are derived from the field equation. The spectral condition on the mass and the coupling of the five-dimensional field equations with the quantum mechanical equations are considered. (tr-auth)

41498 REGGE POLES AND $T = 3/2$, $J = 3/2$ π–N SCATTERING PHASE-SHIFT. Lo, Bae-ling; Lee, Hwa-chung. Wu Li Hsueh Pao, 21: 884-8(Apr. 1965). (In Chinese).

On the basis of the hypothesis that in the low-energy region between the threshold and the resonance, the main contribution of $T = 3/2$, $J = 3/2$ p-wave amplitude is from the Regge trajectory on which N^*_{33} lies, the Regge–Khuri representation is used to calculate the π–N scattering of δ_{33}. Because the approximations used in these calculations possess an accurate threshold behavior, the calculated values agree closely with the experimentally obtained data in the region between the threshold and 40 Mev; a reasonably good agreement was obtained in the region beyond 40 Mev. (TTT)

41499 QUANTUM THEORY OF CHERENKOV RADIATION IN ANISOTROPIC MEDIA. Lu, Chen-fa. (Nankai Univ., Tientsin, China). Wu Li Hsueh Pao, 21: 1049-60 (May 1965). (In Chinese).

Cherenkov radiation in anisotropic media is studied on the basis of quantization of the electromagnetic field. The intensities of radiation corresponding to the extraordinary wave as well as the ordinary wave are obtained. The effect of particle spin on the radiation intensity is explained. Quantum calculations differ from classical by taking particle spin into account. Radiation of both ordinary and extraordinary waves occurs in the case of movement along the optical axis. Results of the analysis are given for movement along the optical axis and in the direction perpendicular to the optical axis. (tr-auth)

41500 ON RADIATIVE CORRECTIONS IN PAIR PHOTOPRODUCTION. Fomin, P. I. (Inst. of Physics and Tech., Academy of Sciences, Ukrainian SSR). Zh. Eksperim. i Teor. Fiz., 48: 992-4(Mar. 1965). (In Russian).

It is shown that the deductions of Vekshteyn (ZhETF, 47: 678, (1964)) concerning an anomalously strong energy dependence of the relativistic radiative corrections to the cross section for pair photoproduction are in error. The source of the error lies in the fact that not all the diagrams describing the radiative corrections to the photoproduction were taken into account. (ATD)

41501 CLASSICAL APPROXIMATION FOR THE CHANGE OF POLARIZATION IN POTENTIAL SCATTERING (thesis). Lu, Pao. Ames, Iowa, Iowa State Univ., 1964. 70p.

The classical approximation for the cross section and change of polarization in potential scattering was obtained by solving the Thomas-Bargmann-Michel-Telegdi equation with fields $\vec{E} = -\vec{\nabla}\phi$ and $\vec{B} = 0$. It was found that the polarization vector precesses about the angular momentum, and the problem of finding the total precession angle is reduced to a quadrature. The criteria of validity of the approximation are discussed. Detailed results for the Coulomb potential were obtained. Both the cross section and the change of polarization in scattering agree with quantum mechanical results given by others in the appropriate limits. (Dissertation Abstr.)

41502 π^--p INTERACTIONS AT 2.0 Bev/c. Tuli, Shrawan Kumar. Tallahassee, Fla., Florida State Univ., 1964. 113p.

An experimental study of the interaction between negative pions and protons was made. A total of 3438 two-prong events obtained in an exposure of the 72 in. Berkeley liquid-hydrogen bubble-chamber to pions of momenta 1975 and 2035 Mev/c (±2%) were investigated. A sequence of spatial-reconstruction and kinematic fitting programs was used to classify the events into various hypotheses. An analysis of the processes involving elastic scattering and the inelastic processes which result in the production of a single pion was carried out in terms of phenomenological models. The values of the partial cross sections ob-

tained are: σ (elastic) = 6.95 ± 0.26, σ ($\pi^-p\pi^0$) = 3.40 ± 0.19, and σ ($\pi^-\pi^+n$) = 7.34 ± 0.27 mb. The elastic scattering differential cross section has a characteristic diffraction peak and involves partial waves at least up to l = 3. The inelastic processes are dominated by the formation of the di-pion system ρ (T = J = 1 at 757 Mev) and the pi-nucleon system $N^*_{3,3}$ (at 1238 Mev). The production mechanism for ρ is essentially peripheral. An application of the Trieman-Yang test, however, shows the inadequacy of a pure one-pion-exchange. The effects due to ω → 2π and the presence of kinematically overlapping $N^*_{3,3}$ are examined. There is evidence for a significant T = 0 s-wave π-π interaction. The production of the nucleon-isobar does not agree with a ρ-exchange mechanism. It was observed that the contributions from processes such as the transmission of two-pions (not necessarily in the resonant ρ state) and the formation of an intermediate state can not be ruled out. The data indicates a lack of any strong interference between the ρ resonance and the nucleon-isobar. (Dissertation Abstr.)

41503 PROTON-PROTON COLLISIONS AT 2.0 Bev (thesis). Ijaz, Mujaddid Ahmed. Athens, Ohio, Ohio Univ., 1964. 85p.

A 2.0 Bev proton beam from the Cosmotron was passed through the BNL 20 inches hydrogen bubble chamber. 57,000 pictures were recorded. A part of the film containing 20,000 pictures was scanned for two prong events and this yielded about 6000 events. These 6000 events were measured with the help of digitized projectors and their spatial reconstruction and kinematical analysis was achieved by the programs TRED and GUTS written for IBM-7094 computer. Events of the following type were selected for analysis: p + p → p + p; → p + n + π^+; and → p + p + π^0. The number of events included was elastic, 1894; pnπ^+, 2335; and ppπ^0, 603. The CMS momentum distributions of the pions and nucleons were plotted and compared with the isobar model. The momentum distributions agree very well in the neutron production events. The sharp peaks around 800 Mev/c in the neutron and proton spectrum is a consequence of the ($\frac{3}{2},\frac{3}{2}$) pion–proton resonance. The Q-value distribution for the pπ^+ system agrees with the isobar model. The CMS momentum distributions from pπ^0 isobar have low momentum, and this may be due to $N^*_{\frac{3}{2}}$ (1512 Mev) isobar, whose presence tends to increase the proportion of low momentum nucleons. The branching ratio σ(pnπ^+)/σ(ppπ^0) is equal to 4.077 ± 0.285, and this value indicates a small fraction of contribution from T = ½ state to the scattering process, in which T = ⅔ state is dominant. The partial cross sections are σe, 17.01 ± 0.96 mb; σpnπ^+, 16.18 ± 0.95 mb; and σppπ^0, 4.45 ± 0.42 mb. The absolute cross section for the neutrons as a function of the laboratory kinetic energy T is in close agreement with OPE model for $\Delta^2 \leq 0.1$ (Bev/c)^2, where $\Delta^2 = 2mT$, but the OPE theory predicts higher values of cross sections at high momentum transfer. Treiman-Yang test was applied to see the spin of the exchange particle. The events for low Δ^2 are approximately symmetric about 90°, which favors the spinless pion exchange hypothesis. The scattering of the virtual pion from the proton was treated as real pion–proton scattering. The events under the π^+-p resonant peak with 75 < Q < 225 Mev and $0 < \Delta^2 < 0.2$ (Bev/c)^2 follow nearly $1 + 1.75\cos^2\theta$ type distribution. For events with 475 < Q < 600 Mev and $0.2 < \Delta^2 < 0.8$ (Bev/c)^2 the angular distribution changes its character and corresponds to nearly $(1 - 0.6\cos^2\theta)$ distribution which is characteristic of the vector meson (ξ) exchange. (Dissertation Abstr.)

41504 NEUTRON-DEUTERON SCATTERING: SINGULARITIES OF THE PARTIAL WAVE AMPLITUDES (thesis). Morrison, James Leslie. Ithaca, N. Y., Cornell Univ., 1964. 81p.

Nonrelativistic and relativistic methods of locating singularities of scattering amplitudes are reviewed and applied to neutron-deuteron elastic scattering. The singularities of the partial wave amplitudes were found by projection. The proton-exchange pole in the amplitude was examined and from its partial wave projection the existence of the doublet S-wave scattering amplitude of a virtual bound state and a zero, which gives rise to a pole in k cot δ, were deduced. The effect of an excluded bound state in giving $\delta(0) - \delta(\infty) = \pi$ in the absence of a bound state was analyzed. A numerical solution of an integral equation for unitary N-D quartet S-wave scattering with inelastic effects neglected and singularities more distant than the proton-exchange cut approximated by a single pole was obtained. There are no free parameters and use of the previously determined proton-exchange discontinuity gave $a_Q = 6.31f$ and $r_Q = 1.8f$ in very good agreement with experiment. For this solution, the phase shift exhibited the excluded bound state behavior. The rate of change of an elastic S-wave phase shift at threshold with purely attractive forces is shown to obey $(d\delta_s/dk) \geq -(2/K_B)$. For doublet N-D scattering this inequality yields $a_D \leq 4.46f$ which suggests the correctness of one set of the experimentally possible N-D scattering lengths. (Dissertation Abstr.)

41505 PION-PION INTERACTION IN PAIR CREATION BY GAMMA-RAYS (thesis). Orenstein, Stephen. Waltham, Mass., Brandeis Univ., 1964. 111p.

The effects of pion-pion interaction on the purely electromagnetic pair creation process were studied. The method used to include such an effect is that given previously on the influence of final-state interaction on primary processes. It was assumed that the two pions will be produced in a T = J = 0 state, and near the threshold at the energy of the (ABC) particle. The applicability of the theorem to the particular set of conditions encountered in this problem is discussed in detail. The calculation of an integrated cross section for the creation of a pair of pi mesons on the basis of a kinematically allowed set of variables is included. Without final-state interactions, this cross section is $\sigma = 1.2 \times 10^{-34} Z^2 cm^2$. When the effect of final state interaction is included, $\sigma = 8.8 \times 10^{-34} Z^2 cm^2$, or an enhancement of about 6.5. Moreover, the effect of final-state interactions on the angular distribution was calculated. The angular distribution was found to be a sensitive test of the presence of final-state pion-pion interactions; that is there is a marked preference for the emission of the two-pions at small opening angles φ between the two pions when final-state interactions are included. The feasibility of an experiment which would exhibit the effect described above is also discussed. It was concluded that such an experiment would be difficult to perform due to the small cross sections involved and to the extraneous background of electron and muon pairs created along with the pions. (Dissertation Abstr.)

41506 K-MESON NUCLEON SCATTERING. Pande, Lalit Kumar. Waltham, Mass., Brandeis Univ., 1964. 146p.

A rather exhaustive covariant perturbation theoretical investigation was carried out for low energy meson(k)-nucleon scattering. Possible effects of π-π and κ-π resonances were considered. (Dissertation Abstr.)

41507 CHARGE EXCHANGE AND THE PRODUCTION OF π^0 AND η^0 MESONS IN π^--p COLLISIONS AT 1275 Mev/c (thesis). Crouch, Harry Randall Jr. (Providence, Brown Univ., 1964. 88p.

A heavy-liquid bubble chamber with an internal hydrogen target was used to study neutron meson production by π^--p collisions at a π^- momentum of 1275 Mev/c. The reactions considered are: $\pi^- + p \rightarrow \pi^0 + n$ (charge exchange); $\pi^- + p \rightarrow N\pi^0 + n$ (N = 2,3,4); and $\pi^- + p \rightarrow \eta^0 + n$, $\eta^0 \rightarrow \gamma + \gamma$. The neutral mesons were detected by observing the conversion of their decay gamma rays in the bubble chamber liquid. Cross sections obtained for the above reactions are tabulated. The angular distribution for the first reaction was found to contain terms of $\cos^6$ in the cm scattering angle. A pronounced forward peaking was evident in the η^0 angular distribution. By attributing the entire $3\pi^0$ cross section to η^0 decay by the $3\pi^0$ mode and taking account of a possible systematic error in $\sigma(\eta^0)$ due to background, a minimum value of (1.4 ± 1.1) was calculated for the η^0 decay branching ratio $[\Gamma(2\gamma)/\Gamma(3\pi^0)]$. (Dissertation Abstr.)

41508 A STUDY OF THE REACTION $\pi^- + P \rightarrow \pi^- + P + \pi^0$ AT 905 Mev (thesis). Massimo, Joseph Thomas. Providence, Brown Univ., 1964. 120p.

A study was made of the reaction $\pi^- + P \rightarrow \pi^- + P + \pi^0$ in a special bubble chamber containing an internal liquid hydrogen target. The laboratory kinetic energy of the incident pion was 905 Mev. A high-Z liquid mixture was used in the chamber to enhance the materilization of gamma rays from the decay of the π^0. Thus events are observed to which can be applied the constraints of hydrogen kinematics, and in which the gamma-ray directions are also measurable. Some of the advantages and disadvantages of this relatively new technique are discussed. The production of a neutral pion at 905 Mev was found to be in large part consistent with the description offered by the extended isobar model. This was particularly evident in the pion momentum distributions. However, the angular distribution of the proton strongly favored the backward direction of the center-of-mass system, suggesting that the interaction is essentially peripheral. Furthermore, the effective mass distribution of the two pions indicated that the influence of the ρ resonance, although strongly suppressed because of the available phase space, is probably not negligible. The statistics of the experiment did not permit a complete analysis of the relative influence of the different resonances, but it was concluded that in this energy region both the higher isobars and the ρ resonance compete with the 3-3 resonance in pion production. The total cross section for the above reaction was found to be 5.0 ± 0.7 mb. Rough estimates of other inelastic cross sections were made. (Dissertation Abstr.)

41509 A FINAL STATE INTERACTION MODEL IN THE REACTION $\pi + N \rightarrow \pi_1 + \pi_2 + N'$ BELOW 1 Bev (thesis). Olsson, Martin Godfrey. College Park, Univ. of Maryland, 1964. 159p.

A phenomenological model for the single pion production process in pion-nucleon reactions is presented. It is the purpose of this model to identify those aspects of the experimental data which are determined by the effects of known final-state interactions, and hence, to calculate some of the gross properties of the primary mechanism and its relation to the elastic pion-nucleon channel. In $T = \frac{1}{2}$ production reactions both $P_{\frac{1}{2}}^+$ and $D_{\frac{3}{2}}^-$ states are large and attractive below 700 Mev. The latter has a phase angle which is rapidly increasing, passing through 90° near 500 Mev. From the relation of this phase angle to the elastic scattering phase shift, a connection to the well-known 600-Mev resonance is established. Below 700 Mev the $T = \frac{3}{2}$ production occurs strongly through an attractive $D_{\frac{3}{2}}^-$ state and a repulsive $P_{\frac{3}{2}}^+$ state. Energy and angle distributions as well as the energy dependence of the cross sections are accounted for in the five experimentally known production reactions. The prominent exception to the preceding statement is the appearance of an anomaly in the pion-pion mass spectra in the two reactions in which the two pions might be in a $T = 0$ state. The model assumes that only those amplitudes are important in which there exists an attractive interaction between two of the three particles in the final state. Attempts were also made to construct a model which is close enough to reality to be able to fit the experimental data, but yet make a minimum of assumptions about the nature of underlying dynamics. (Dissertation Abstr.)

41510 A RELATIVISTIC HIGH ENERGY APPROXIMATION FOR ELASTIC SCATTERING OF DIRAC PARTICLES (thesis). Baker, Adolph. Waltham, Mass., Brandeis Univ., 1964. 52p.

A high-energy approximation is described for predicting the elastic scattering of Dirac particles from a scalar potential. The formal result was then applied to the specific problem of electron and positron scattering from nuclei. The predicted cross sections turned out to be in close agreement with those of partial-wave analysis, even at large scattering angles. (Dissertation Abstr.)

41511 S-MATRIX METHODS FOR ELECTROMAGNETIC CORRECTIONS TO STRONG INTERACTIONS WITH AN APPLICATION TO THE PROTON-NEUTRON MASS DIFFERENCE (thesis). Dashen, Roger Frederick. Pasadena, Calif., California Inst. of Tech., 1964. 49p.

An S-matrix method was developed for calculating the effect of small perturbations on a partial-wave amplitude, and, in particular, on the positions and residues of bound states. The method is applicable to both non-relativistic and relativistic problems. It has, as a particular virtue, rapid convergence of the dispersion integrals. Electromagnetic corrections to strong interactions will be an important application, and modifications useful for handling the infrared divergence that occurs in this case are described in detail. A detailed, quantitative application to the neutron-proton mass difference is also included. Neutrons and protons were treated as bound state poles in the π-N scattering amplitude, and the mass difference was obtained by finding the electromagnetic corrections to their binding energies. The results are in good agreement with experiment. No cutoffs or other purely theoretical parameters were involved. All the long-range corrections to the π-N interaction were investigated. Photon exchange turned out to be the most important. Form factors appear as short-range modifications of the photon exchange force. The results of the calculation are not sensitive to the detailed behavior of the form factors at large momentum transfer. (Dissertation Abstr.)

41512 ELEMENTARNYE CHASTITSY. (Elementary Particles. Second Expanded Edition). Novozhilov, Yu. V. Moscow-Leningrad, State Publishing House of Literature in Physics and Mathematics, 1963. 204p.

A popular presentation of basic ideas and achievements in the physics of elementary particles is given. Discoveries of the various particles and the various theories proposed to explain and classify them are discussed in their historical sequence. Discussions are given of conservation laws, quantum numbers, high-energy interactions, strange particles and antiparticles, parity nonconservation, and meson and baryon resonances and classifications. (M.J.T.)

41513 NUCLEAR INTERACTIONS OF THE HYPERONS. Dalitz, R. H. Tata Institute of Fundamental Research Studies in Physics. Oxford, Oxford University Press, 1965. 110p. $5.05.

The present evidence on the hyperon-nucleon interaction is discussed. Topics covered include a review of the data on Λ hypernuclei, the phenomenological analysis of binding energy data for hypernuclei, the spin-dependence of the Λ nucleon interaction, theoretical discussion of hyperon nucleon forces, hyperon-nucleon scattering and reaction processes, the decay modes of the light hypernuclei, and some problems for the future concerning hypernuclei. (J.F.P.)

41514 CORAL GABLES CONFERENCE ON SYMMETRY PRINCIPLES AT HIGH ENERGY. Second Conference, January 20-22, 1965, University of Miami. Kursunoglu, Behram; Perlmutter, Arnold; Sakmar, Ismail, eds. A Series of Books in Physics. San Francisco, W. H. Freeman and Co., 1965. 438p. $8.00. (CONF-650106)

Separate abstracts are prepared for 8 of the 19 papers presented. Abstracts of 11 papers previously appeared in NSA as 19: 4985, 20940, 21005, 23365, 25364, 27269, 29041, 29075, 30994, 30998, and 30999. (C.E.S.)

For abstracts of individual papers see: 41515–41522.

41515 REMARKS ON SYMMETRY PRINCIPLES. Oppenheimer, J. Robert (Inst. for Advanced Study, Princeton, N. J.). p.2-4 of Coral Gables Conference on Symmetry Principles at High Energy. San Francisco, W. H. Freeman and Co., 1965.

The application of SU(6) to the forward elastic scattering amplitudes and the connection of symmetries to bootstraps are discussed. (C.E.S.)

41516 SYMMETRY AND STRONG INTERACTION. Kursunoglu, Behram (Univ. of Miami, Coral Gables, Fla.). p.160-77 of Coral Gables Conference on Symmetry Principles at High Energy. San Francisco, W. H. Freeman and Co., 1965.

The possibility of some connection between internal and space-time symmetries is considered. The commuta-

tion relations of the group $L\tilde{U}(12)$ are obtained, and the results are valid for strongly interacting massive states. (C.E.S.)

41517 TESTS OF UNITARY SYMMETRY AND POSSIBLE HIGHER SYMMETRIES. Lipkin, Harry J. (Weizmann Inst. of Science, Rehovoth, Israel). p. 202-17 of Coral Gables Conference on Symmetry Principles at High Energy. San Francisco, W. H. Freeman and Co., 1965.

Tests of unitary and higher symetries are discussed as they relate to selection rules and quantum numbers of elementary particles. (J.F.P.)

41518 MESON DECAYS AND THE SIGMA HYPOTHESIS. Brown, Laurie M.; Faier, Harry (Northwestern Univ., Evanston, Ill.). p.219-48 of Coral Gables Conference on Symmetry Principles at High Energy. San Francisco, W. H. Freeman and Co., 1965.

A critical review is presented of the current evidence for the σ-hypothesis in meson decays, involving strong, weak, and electromagnetic types. It is seen that these various decays possess significant features in common, so that final state interaction is not unreasonable. The decay spectra and branching ratios of the meson decays $\eta \rightarrow 3\pi$, $K \rightarrow 3\pi$, $X^0(960) \rightarrow \eta 2\pi$ all appear to be consistent with the final state dominance of a scalar σ meson having I = 0, mass about 400 Mev and width about 100 Mev. (J.F.P.)

41519 DYNAMICAL SYMMETRIES AND FUNDAMENTAL FIELDS. Nambu, Y. (Univ. of Chicago). p.247-85 of Coral Gables Conference on Symmetry Principles at High Energy. San Francisco, W. H. Freeman and Co., 1965.

Fundamental fields and their associated particles are discussed together with the various related symmetries. The possibility of mesons and baryons being composite rather than simple systems is considered. (J.F.P.)

41520 THE PROBLEM OF GROUP EXTENSIONS OF THE POINCARE GROUP AND SU(6) SYMMETRY. Michel, Louis (Institut des Hautes Etudes Scientifiques, Bures-sur-Yvette, France). p.331-52 of Coral Gables Conference on Symmetry Principles at High Energy. San Francisco, W. H. Freeman and Co., 1965.

The problem of group extensions of the Poincare group is considered. Its applications to SU(6) symmetry is emphasized, and a possible group of invariance of a relativistic SU(6) theory is suggested. Also the group of invariance of Wigner's supermultiplet theory is discussed. (J.F.P.)

41521 PHENOMENOLOGICAL FIELD THEORY. Schwinger, Julian (Harvard Univ., Cambridge, Mass.). p.372-8 of Coral Gables Conference on Symmetry Principles at High Energy. San Francisco, W. H. Freemann and Co., 1965.

The problem of a field theory of matter making contact between the postulated attributes of fundamental field variables and the properties of the phenomenological fields that represent observed particles is investigated. While the problem defies direct dynamical attack, there is an indirect procedure for establishing a limited connection, through a technique of comparative kinematical transformation. Such a procedure is presented. (J.F.P.)

41522 A MODEL FOR PC VIOLATION IN THE FRAMEWORK OF UNITARY SYMMETRY. d'Espagnat, B.; Gaillard, M. K. (Laboratoire de Physique Theorique et Hautes Energies, Orsay, France). p.380-400 of Coral Gables Conference on Symmetry Principles at High Energy. San Francisco, W. H. Freeman and Co., 1965.

An elementary description of the construction of weak currents with an application to the leptonic decays of strange particles is dealt with and a comparison with the predictions of Cabbibo's version of a PC violation is made. A more formal approach which leads to a coherent description of both leptonic and non-leptonic interactions is also presented. (J.F.P.)

41523 DEUTERON PRODUCTION IN p-p COLLISIONS AT 1.55, 2.5, AND 2.9 Bev. Pellett, D. E. (Univ. of Michigan, Ann Arbor); Overseth, O. E.; Perl, M. L. 12p. (CONF-650410-22). Gmelin, AED-CONF-65-073-37.

From American Physical Society, Washington, D. C.

An experiment is described in which the deuteron production cross section was measured as a function of momentum at several fixed laboratory angles and for three energies of the incident proton. A peak corresponding to the rho meson was observed in plots of the cross section versus the invariant mass of the pion system. (L.B.S.)

41524 FURTHER EVIDENCE FOR A MOLECULAR STRUCTURE OF MESON AND BARYON RESONANCE STATES. Sternglass, E. J. (Westinghouse Electric Corp., Pittsburgh). 14p. (CONF-758-53). Gmelin, AED-CONF-65-003-72.

From American Physical Society Meeting, New York, Jan. 1965.

It was previously shown that the masses and spins of the heavy mesons and pion-resonances are well accounted for by quasi-molecular rotator models composed of pions with a single bond length and binding energy per bond. The extent to which these models have been further substantiated by the discovery of the predicted higher rotational levels is outlined, and it is shown that the same models account for the observed masses and angular momenta of the excited baryon states. (L.B.S.)

41525 THE COMPOSITE MODEL OF BOSONS. Levinger, J. S. (Rensselaer Polytechnic Inst., Troy, N. Y.). 9p. (CONF-758-42). Gmelin, AED-CONF-65-003-54.

From American Physical Society Meeting, New York, Jan. 1965.

The quantum numbers of bosons formed by bound states of the $N\bar{N}$, $N\bar{\Lambda}$, and $\Lambda\bar{\Lambda}$ systems are compared with a recent review of experimental boson properties by Rosenfeld et al. Many workers have noted agreement with experiment for the four S states of $N\bar{N}$, and the two S states of $N\bar{\Lambda}$. We identify four of the eight P states of $N\bar{N}$ as the B at 1215 Mev ($^1P_1$ isovector), the $K\bar{K}\pi$ at 1410 Mev ($^3P_1$ isoscalar), the f at 1253 Mev ($^3P_2$ isoscalar) and the A2 at 1310 Mev ($^3P_2$ isovector). We predict that the B and the $K\bar{K}\pi$ are each 1^{+-} (for J^{PC}). The other four P states are presumed to have very large decay widths into $\pi\pi$, $\pi\eta$, or $\pi\rho$ in S states. The two S states of $\Lambda\bar{\Lambda}$ are identified as the ϕ at 1019.5 Mev and the $\eta 2\pi$ at 960 Mev; this leads to a prediction that the $\eta 2\pi$ is 0^+. (auth)

41526 COVARIANT POLARIZATION THEORY OF SPIN ONE PARTICLES. Sankaranarayanan, A. (Ames Lab., Ames, Iowa). 26p. (CONF-758-38). Gmelin, AED-CONF-65-003-51.

From American Physical Society Meeting, New York, Jan. 1965.

A covariant theory of polarization effects in the scattering of spin one particles by spinless targets is developed. The most generally written covariant S matrix and density matrices $\rho(p)$ and $\rho'(p')$ before and after the scattering respectively are split into two parts so as not to mix up the energy states by using the hole-theory condition of STAPP. Finally by substituting thus obtained results in the scattering equation $\rho'(p') = S\,\rho(p)\,\bar{S}$ the polarization effects are studied and the corrections to the non-relativistic theory obtained. A brief discussion of some calculational aids for the spin one formalism is also included because of its pertinence to some nuclear reaction problems. (auth)

41527 PARTICLE IDENTIFICATION BY PULSE HEIGHT CORRELATION IN A RANGE TELESCOPE. Groom, D. E.; Marshall, J. H. 13p. (CONF-758-39). Gmelin, AED-CONF-65-003-50.

From American Physical Society Meeting, New York, Jan. 1965.

A method of identifying photoproduced K mesons is described, in which particles are stopped in plastic scintillators, and pulse height distributions were analyzed with a semi-on-line computer. An attempt was made to measure the polarization of the associated Λ particles, and to detect the decay proton. A schematic drawing is given of the counter array, along with a more detailed drawing on the range telescope. (L.B.S.)

41528 ρ AND ω PRODUCTION IN π^+d INTERACTIONS AT 1.7 Gev/c. Bacon, T. C.; Fickinger, W. J.; Hill, D. G.; Hopkins, H. W. K.; Robinson, D. K.; Salant, E. O. 11p. (CONF-758-52). Gmelin, AED-CONF-65-003-62.

From American Physical Society Meeting, New York, Jan. 1965.

The production of ρ and ω mesons were investigated in the $\pi^+ + n \rightarrow p + \pi^+ + \pi^-$ and $\pi^+ + n \rightarrow p + \pi^+ + \pi^- + \pi^0$ reactions, which were observed in a 20-inch bubble chamber filled with deuterium and exposed to 1.68 Bev/c pions. Cross sections and multi-pion effective mass distributions are shown. Decay angular distributions were measured in order to study the exchange mechanisms for the ρ and ω productions. The results are discussed. (L.B.S.)

Field Theory and Quantum Mechanics

41529 (N64-31206) THE THREE BODY PROBLEM. Lemaitre, C. G. (California Univ., Berkeley). Oct. 1964. 48p. (NASA-CR-110). CFSTI $1.25 cy, $0.50 mn.

Relative axes are introduced, which are the principal axes of inertia of the system of the three masses. They are related to a fixed axis by Euler's angles ϕ, Ψ, θ in the customary manner. The cartesian coordinates of the masses relative to the principal axes are defined by way of the three coordinates r, B, L, which are related in a simple way to the three distances r_1, r_2, r_3 of the masses. These formulas involve the three angles μ_1, μ_2, μ_3, depending on the masses. They are the angles of the triangle of the masses in the particular configuration for which the ellipse of inertia is a circle. The elimination of the nodes is made in the usual way by elimination of the Eulerian angle θ, and the hamiltonian is obtained. The relation of these coordinates with a variable introduced by Lagrange is shown, leading to simplification in the work of Lagrange. (auth)

41530 (N64-32432) THE REGULARIZED EXPLICIT SOLUTION OF THE ANALYTIC N-BODY PROBLEM. Rauch, L. M. (Seton Hall Univ., South Orange, N. J.). Oct. 1964. 29p. (NASA-CR-123). CFSTI $1.00 cy, $0.50 mn.

The regularized N-body problem is resolved in explicit form by the introduction of a pseudo-time parameter in the form of a Sundman and Levi-Civita transformation. The solution consists of two phases, namely, by the formal representation of the solution by a pseudo-time series and by the analytical justification of the process. A brief third part is added as a directive in the essential mode of numerization of the problem. (auth)

41531 (SLAC-PUB-44) ON THE PROBLEM OF HIDDEN VARIABLES IN QUANTUM MECHANICS. Bell, J. S. (Stanford Linear Accelerator Center, Stanford Univ., Calif.). Aug. 1964. Contract AT(04-3)-326. 22p. Dep. mn; CFSTI, $1.00 cy, $0.50 mn.

The demonstrations of von Neumann and others, that quantum mechanics does not permit a hidden variable interpretation, are reconsidered. It is shown that their essential axioms are unreasonable. It is urged that in further examination of this problem an interesting axiom would be that mutually distant systems are independent of one another. (auth)

41532 THE DETERMINATION OF THE ENERGY SPECTRUM FROM THE TIME BEHAVIOR OF THE DECAY OF A QUANTUM MECHANICAL SYSTEM. Gromes, D.; Petzold, J. (Universitaet, Marburg, Ger.). Ann. Physik (7), 14: 353-83(1964). (In German).

A study was made to determine which expressions of the energy spectrum of an unstable quantum-mechanical system could be obtained from its time behavior. (tr-auth)

41533 ON THE CALCULATION OF THE AVERAGE PERMEABILITY OF POTENTIAL WAVES. Christov, S. G. (Institut fur Physikalische Chemie, Bulgarische Akademie der Wissenschaften, Sofia). Ann. Physik (7), 15: 87-100(1965). (In German).

A method for the calculation of the average permeability of the potential waves in stable energy distribution of the incident particles is described. It is applicable under the following conditions: the wave can be approximated in the area of its maximum—over a given energy value E′—by a parabola; and for all particles with energy U larger than E′, a Boltzmann energy distribution is valid. It was shown that the magnitude E′ can be so determined that for larger energy values (U > E′) the parabolic approximation is valid, and for smaller energy (U > E′) the usual Wentzel-Brillouin-Kramers equation is valid. For the parabolic range (U > E′), formulas were given in quasi-classical approximation. The accuracy of the method was tested on the generalized Eckard wave which contains the pure parabolic wave as the limiting case. For the W-B-K range, (U > E′) the calculation was carried out under the assumption of a Boltzmann distribution with the help the saddle-point method. (tr-auth)

41534 GENERATOR KERNEL OF THE CREATION AND ANNIHILATION OPERATORS ON A STATIC SPACE-TIME. Combet, Edmond (Faculte des Sciences, Lille). Compt. Rend., 260: 6296-9(June 14, 1965). (In French).

The Schwartz theory of kernels is applied to the construction of creation and annihilation operators on a static space-time curve of $ds^2 = dt^2 - d\sigma_3^2$ metrics. The kernel G^1 obtained verifies the Lichnerowicz-Rideau conditions. (tr-auth)

41535 THE EXPERIMENTS OF MAGYAR AND MANDEL AND THE WAVE-CORPUSCLE DUALISM. Andrade e Silva, Joao (Institut Henri Poincare, Paris). Compt. Rend., 260: 6550-3(June 21, 1965). (In French).

From an analysis of the interference experiments of Magyar and Mandel, it is shown that, from the viewpoint of the Copenhagen School, the wave function should be regarded as a simple representation of our possible knowledge of the state of the system. This concept is used to interpret the Schroedinger "cat paradox" and the Renninger "negative result" experiment. (tr-auth)

41536 PROPAGATION OF WAVES IN A ONE-DIMENSIONAL RANDOM MEDIUM. Frisch, Uriel (Institut d'Astrophysique, Paris). Compt. Rend., 261: 55-7(July 5, 1965). (In French).

The stochastic equation governing the propagation of waves in a one-dimensional medium with Gaussian random function index of position was studied. It is shown that under certain conditions the index can be treated as a simple random variable. (tr-auth)

41537 THE EXTENSION OF THE NYQUIST THEOREM TO SYSTEMS WITH NEGATIVE TEMPERATURE. Convert, Guy (Laboratoire de la C. S. F., Orsay, France). Compt. Rend., 261: 58-61(July 5, 1965). (In French).

The fluctuations of a system with negative temperature are given by the Nyquist fluctuation-dissipation theorem. The power transmitted by these fluctuations to a cold dissipative medium mingles with the spontaneous emission or the acceleration radiation when the system consists of an assembly of quantum or classical oscillators. (tr-auth)

41538 ON THE MOTION OF PARTICLES IN SYMMETRICAL FIELDS. Klima, R. (Inst. for Plasma Physics, Prague). Czech. J. Phys., 15: 473-93(1965).

The hamiltonian of a charged particle in a general electromagnetic field transformed to time dependent curvilinear coordinates is discussed. From the assumption of the independence of the hamiltonian on one of the coordinates, the inequalities which the particle must satisfy in its motion are derived. The sets of points accessible to the given particle are thus determined in the space of the remaining two coordinates. The problem of the absolute maintenance of particles is paid special attention. The necessary and sufficient conditions fulfilled by a field intended for maintaining the particles are derived. (auth)

41539 ON THE DIFFRACTION OF THE FIELD OF AN ARBITRARILY MOVING PARTICLE IN A SEMIPLANE. Aivazyan, Yu. M. Dokl. Akad. Nauk Arm. SSR, 40: 155-8 (1965). (In Russian).

An exact solution is derived for the problem of the diffraction of the field of a charged particle, moving in space according to the law $\vec{r} = \vec{r}(t)$ in the cartesian system of coordinates (x, y, z) on an infinite conducting semiplane. (M.J.T.)

41540 THE USE OF DIRECT METHODS OF MATHEMATICAL PHYSICS IN THE THEORY OF QUANTUM TRANSITIONS. [PART] I. Kushnirenko, A. N. (Inst. of Problems of Metallography, Academy of Sciences, Ukrainian SSR). Izv. Vysshikh Uchebn. Zavedenii, Fiz., No. 3, 19-26(1965). (In Russian).

A previously developed method using mathematical physics to calculate the S-matrix in quantum field theory in the presence of strong or intermediate coupling between fields requires the solution of a system of integral equations for time-dependent functions. The method is modified to avoid the difficulties in solving a system of integral equations rather than a system of linear algebraic equations and the necessity of integrating to a variable upper limit. The moments method and the Bubnov-Galerkin method are used to obtain formulas of the usual perturbation theory in the weak coupling approximation. Algebraic equations giving the normalized wave vector and the unitary scattering matrix are developed by the Ritz and least-squares variational methods. (M.J.T.)

41541 UNIFIED DESCRIPTION OF INTERACTIONS. Sokolik, H. A.; Konopleva, N. P. (Research Inst. for Electrical Mechanics, Moscow). Nucl. Phys., 72: 667-76 (1965).

A generalization of gauge fields is found for the case of curved space. The results obtained permit the establishment of a connection between gravitation interaction and the fields induced by local gauge invariance. (auth)

41542 CONSERVATION LAWS OF THE GENERAL THEORY OF RELATIVITY. I. SPACE TIMES ADMITTING MOTIONS. Davis, W. R.; Moss, M. K. (North Carolina State Univ., Raleigh). Nuovo Cimento (10), 38: 57(Aug. 16, 1965).

A fundamental method of approach to the formulation of the conservation laws of the general theory of relativity is presented. This approach is based on the symmetry properties which are admitted by the specific physical space-times under consideration and which underlie the conservation laws in differential form that are shown to follow from a generally covariant generator. This method embraces procedures that permit the proper conservation laws of the field to be formulated in a consistent and well-defined manner. For example, if the total energy of a physical system characterized by a solution of Einstein's field equations is conserved, then this conserved quantity may be formulated in any other co-ordinate system or frame of reference related to the original co-ordinate representation by transformations of the general form $\bar{x}^i = x^i(x^1, x^2, x^3, x^4)$. Symmetry properties characterized by groups of motions (Killing vectors) of given space-times are considered in detail. The conservation laws of energy, linear momentum, and angular momentum of the theory of general relativity follow, if admitted, as an immediate consequence of these motions. (auth)

41543 CONSERVATION LAWS OF THE GENERAL THEORY OF RELATIVITY. II. SPACE-TIMES ADMITTING CERTAIN SYMMETRY PROPERTIES MORE GENERAL THAN MOTIONS. Davis, W. R.; Moss, M. K. (North Carolina State Univ., Raleigh). Nuovo Cimento (10), 38: 1558-69(Aug. 16, 1965).

Explicit formulations of field and particle conservation laws existing in consequence of the ability of the geometry of space-time to admit symmetry properties more general than motions are developed. In particular, space-times admitting affine and projective collineations and conform transformations are considered. Brief consideration is given to the application of some of these results to the Friedmann-Lemaître nonstatical cosmological space-time. (auth)

41544 THE GRAVITATION OF A CYLINDRICALLY SYMMETRIC MAGNETIC FIELD. Ghosh, R. (Barisha Vivekananda Coll., Calcutta); Sengupta, R. Nuovo Cimento (10), 38: 1579-87(Aug. 16, 1965).

The line element for a cylindrically symmetric magnetic field is obtained. The behaviors of light rays and test particles in this field are studied. (auth)

41545 INFRA-RED BEHAVIOUR OF THE WAVE FUNCTION RENORMALIZATION CONSTANT IN COVARIANT GAUGES. Perrin, R. (Massachusetts Inst. of Tech., Cambridge). Nuovo Cimento (10), 38: 1644-8(Aug. 16, 1965).

The techniques developed for treating soft photons in quantum electrodynamics, by coupling them to an equivalent classical current, are used to study the infrared behavior of Z_3. When the photon's Green's function is of the form $D_{\mu\nu}(k) = (g_{\mu\nu} - \lambda k_\mu k_\nu/k^2)\, d(k^2)$, it is found that the second-order infrared divergence of Z_2 exponentiates in such a way that, so far as infrared effects are concerned, Z_2 is zero for $\lambda < -2$, finite for $\lambda = -2$, and infinite for $\lambda > -2$. (auth)

41546 THE CONSTRUCTION OF A SEPARABLE HAMILTONIAN. Pearson, D. B. (Univ. of Hull, Eng.). Nuovo Cimento (10), 38: 1720-39(Aug. 16, 1965).

Assuming the scattering amplitude to have a particularly simple separable form, a method is given of constructing a Hamiltonian. Under quite general conditions, the Hamiltonian is shown to be hermitian, and to have simple analytic properties in the energy variable. (auth)

41547 SYMMETRY-BREAKING CORRECTIONS TO WEAK VECTOR CURRENTS. Furlan, G.; Lannoy, F. G.; Rossetti, C.; Segre, G. (CERN, Geneva). Nuovo Cimento (10), 38: 1747-54(Aug. 16, 1965).

A general method for calculating the renormalization of partially conserved vector currents due to symmetry breaking is discussed. As an application, the renormalization of the strangeness-changing weak vector current is calculated in the pole approximation and its effect on universality is discussed. (auth)

41548 FEYNMAN RULES AND FEYNMAN INTEGRALS FOR SYSTEM WITH HIGHER-SPIN FIELDS. Lam, C. S. (Univ. of Maryland, College Park). Nuovo Cimento (10), 38: 1755-64(Aug. 16, 1965).

It is known that Feynman rules for many systems may be expressed by replacing the interaction Hamiltonian in the Dyson formula by minus the interaction Lagrangian, provided suitable covariant changes of the time-ordered functions between some fields are made. The general conditions for which this is valid are investigated. In case this is not valid, a general, straightforward procedure for computing the extra vertices is given that is considerably simpler than the usual Dyson-Wick procedure. This procedure is illustrated by an explicit example dealing with charged vector electrodynamics. This example shows incidentally that an extra vertex persists even if an extra interaction is added. It follows from these investigations that the integrand for the Feynman path integral is not always simply the exponential of i times the action. This simple prescription fails whenever an extra vertex for the Feynman rule occurs, and the correct expressions in these cases are given. (auth)

41549 NONANALYTICAL PROPERTIES OF PROPAGATORS. The $g\varphi^4$ THEORY. Caianiello, E. R.; Campolattaro, A.; Marinaro, M. (Universita, Naples). Nuovo Cimento (10), 38: 1777-93(Aug. 16, 1965).

When perturbative expansions diverge the search for solutions of the equations for propagators is a problem in the real variable. It is shown, using the example of a neutral scalar field with $g\varphi^4$ self-coupling, that the coefficients of the divergent perturbative expansions can still be used in principle, heuristically, to obtain the wanted solutions. The proposed procedure, which is quite general, yields easily the known correct answer if applied to a solvable numerical model of this theory, giving solutions which are holomorphic in $1/\sqrt{g}$ and not uniquely determined by the knowledge of the perturbative coefficients. In the general case, the difference between any two such solutions would satisfy a bound state equation. A suitably regularized form of the

$g\varphi^4$ theory is studied in some detail; its solutions, if any exist, belong, like those of the model, to Hadamard's "class 2" of nonanalytical functions. (auth)

41550 THE SINGULARITIES OF THE SCATTERING AMPLITUDE IN POTENTIAL THEORY. Aks, S. O. (Univ. of Maryland, College Park), Nuovo Cimento (10), 38: 1794-1814(Aug. 16, 1965).

The analytic properties of the scattering amplitude are studied in potential theory. The connections between the singularities of the Born term are examined using the Lippman-Schwinger equation. The techniques can be applied to a wide class of potentials including square wells in combination with other potentials. It is not required that the potentials be superpositions of Yukawa wells. Expressions are given for all singularities in both the upper and lower half complex momentum planes. (auth)

41551 QUASI-BINOMIAL REPRESENTATION OF THE CLEBSCH-GORDAN COEFFICIENTS. Ansari, S. M. R. (Universitat, Tubingen, Ger.). Nuovo Cimento (10), 38: 1883-6(Aug. 16, 1965).

General expressions are derived for the Clebsch-Gordan coefficients for the case of angular momenta including spins. The representations of these coefficients can be deduced from a general expression by utilization of generalized factorials. The representations obtained allow extensions to be made in both the analytical and numerical tables of coefficients. The use of generalized factorials reduces the tabular space by a considerable amount. Tabulations are not included. (T.F.H.)

41552 INTRODUCTION TO THE N-QUANTUM APPROXIMATION IN QUANTUM FIELD THEORY. Greenberg, O. W. (Institute for Advanced Study, Princeton, N. J. and Univ. of Maryland, College Park). Phys. Rev., 139: B1038-49(Aug. 23, 1965).

The N-quantum approximation is designed to find approximate operator solutions of theories characterized by a specific hamiltonian. The Heisenberg field operators of the theory are approximated by finite-degree normal-ordered expansions in an irreducible set of in-fields. The c-number functions which are the coefficients of these expansions are the unknown quantities in the approximation. The approximation assumes that the dominant contributions to the vertex function, scattering function, and other low-order functions come from functions of similar low order. The c-number functions correspond to the connected graphs with a given number of external lines. Thus in graphical language the approximation assumes that the connected graphs with few external lines dominate. The N-quantum approximation is manifestly covariant, treats positive and negative frequencies in a symmetric way, allows a calculation of several different physical processes simultaneously, allows incorporation of bound states, and requires extrapolation off the mass shell in fewer variables than the usual Green's function approaches. After describing the N-quantum approximation, it is shown to be compatible with renormalization theory in first order of the approximation in the model with $\mathcal{H}_1 = gA^3$. It should be emphasized that all powers of the coupling constant occur in first order of the N-quantum approximation in this model. A quadratic integral equation is obtained for the vertex function, and it is shown that the vertex function satisfies the renormalization criteria that the particles in the theory have a given observed mass, and that the vertex function has a given coupling constant as the residue of a pole $(m^2 - k^2)^{-1}$ in the unphysical region. It is also shown that the power-series-expansion solution is finite term by term in all orders of the coupling contstant. (auth)

41553 QUANTUM EFFECTS ON THE ACCURACY OF MOMENTUM MEASUREMENTS. Woo, Ching-hung (Institute for Advanced Study, Princeton, N. J.). Phys. Rev., 139: B1103-6(Aug. 23, 1965).

It is shown in two examples that to measure the momentum of a particle with great accuracy, allowing for large uncertainties in the position, it is still necessary to consider additional quantum effects. For the case of measurements by electromagnetic means, the uncertainties in the measurability of field strengths and of charge-current densities should be considered. Within the framework of the Bohr-Rosenfeld analysis, uncertainties in the field measurements do not limit the accuracy of momentum measurements. What happens when the Bohr-Rosenfeld approximations are not made is an open question. (auth)

41554 DYNAMICS OF A BROKEN SU_N SYMMETRY FOR THE OSCILLATOR. Barut, A. O. (International Center for Theoretical Physics, Trieste). Phys. Rev., 139: B1433-6(Sept. 6, 1965). (IC/65/33)

All states of a one-dimensional harmonic oscillator are represented by a special unitary representation of the noncompact 2+1 Lorentz group. The direct product of N such representations leads to a degeneracy which is represented by the group SU_N, whereas all states of the N-dimensional oscillator are represented by the noncompact unitary group NU^N_{N+1} whose Casimir operator determines the energy spectrum. The anharmonic oscillator is represented by a broken symmetry, and mass-splitting formulas are obtained. It is shown how new quantum numbers arise from the direct products of basic dynamical groups, corresponding to composite structures. (auth)

41555 FUNCTION IN QUANTUM MECHANICS WHICH CORRESPONDS TO A GIVEN FUNCTION IN CLASSICAL MECHANICS. Daughaday, Hamilton (State Univ. of New York, Buffalo and Cornell Aeronautical Lab., Inc., Buffalo); Nigam, B. P. Phys. Rev., 139: B1436-42(Sept. 6, 1965).

A generalization of the procedures of Weyl and McCoy for making transition from a classical function to a quantum-mechanical operator function corresponding to it was carried out in order to include terms involving more than one pair of conjugate variables. An application of the method is made to the case of two spinless interacting charges—the Darwin interaction. This result is verified by solving directly for the quantum-mechanical Hamiltonian operator, starting from equations which were derived from the classical equations by replacing the classical Poisson brackets by commutators and by requiring the equality of the energy and the Hamiltonian operator. An alternative expression for a quantized Hamiltonian, reduces to the form given originally by Born and Jordon for a single set of conjugate variables. (auth)

41556 GAUGE-INVARIANT QUANTUM ELECTRODYNAMICS. II. Goldberg, I. (Clarkson Coll. of Tech., Potsdam, N. Y.). Phys. Rev., 139: B1665-?(Sept. 20, 1965).

A manifestly gauge-invariant formulation is introduced together with the procedure for quantizing the theory. This procedure is path-independent and leads to an electron operator which creates charged particles. The theory is nonlocal, but a procedure is introduced for determining the Hamiltonian of the theory. (auth)

41557 DERIVATION OF SUM RULES AND HYPERVIRIAL THEOREMS BY DIFFERENTIATION. Morgan, D. J.; Landsberg, P. T. (University Coll., Cardiff, Wales). Proc. Phys. Soc. (London), 86: 261-71(Aug. 1965).

Sum rules and hypervirial theorems are derived by using the simple technique of differentiating an eigenvalue equation with respect to parameters occurring in it. Various applications are discussed. (auth)

41558 ON THE POSSIBILITY OF THE CUT-PLANE ANALYTICITY OF THE MOMENTUM SPACE VERTEX FUNCTION. Minami, Masatsugu (Univ. of Kyoto). Progr. Theoret. Phys. (Kyoto), 33: 964-93(May 1965).

The analyticity property of the vertex function in momentum space, or, strictly, of the Fourier transform of the retarded function at three points, is considered. It is intended mainly to study the possibility that the entire plane of the third variable except a fixed portion of the real positive axis is in the holomorphic domain of the vertex function; this possibility corresponds to an extension of one result contained in the work of Kallen and Wightman. The problem is reduced to finding, first, the holomorphic domain of the absorptive part for the third variable fixed and real and, second, the intersection of all these domains when the variable varies from threshold to infinity. In the case where two threshold masses are equal, the boundary of the intersection is explicitly established, and it turns out that this

boundary is composed of a certain analytic hypersurface. On the contrary in the general case, it is seen that the boundary in question is pseudoconvex in the strict sense, i.e., the choice is not always limited by analytic hypersurfaces; however, the explicit formula remains unsolved. The new technique developed by mathematical physicists at Saclay, France, is used for the study of the holomorphic envelopment of the absorptive part. (tr-auth)

41559 PERTURBATION THEORY FOR SPIN SYSTEMS. **Giovannini, Bernard (Universite, Geneva). Sci. Papers Coll. Gen. Educ., Univ. Tokyo, 15: 49-62(June 1965).**

The modified Wick's theorem is proven, and corresponding diagrams are introduced. The technique is illustrated by a simple example. The generalized theorem for spin operators is discussed, and also the proof of the theorem for the simplest sets, the proof of the theorem for the general case, the diagram technique, and calculation rules. A simple application is given of the proof to the first order that this type of interaction gives neither shift nor broadening to the resonance line induced by a homogeneous alternating magnetic field perpendicular to the z axis. (J.F.P.)

41560 THE CONFLUENCE THEORY BASED ON HYPERCOMPLEX NUMBERS. Kurdgelaidze, D. F. Vestn. Mosk. Univ., Ser. III: Fiz. Astron., No. 1, 17-25 (Jan.-Feb. 1965). (In Russian).

The confluence theory of fields is developed on the basis of hypercomplex numbers. It is shown that the relativistic-invariant equation with $\Gamma_\mu = \gamma_\mu$, where $A(\gamma_\mu)$ is a Dirac algebra, can include the description of fields of spin s = 0, s = 1, and with $\Gamma_\mu = \beta_\mu$, where $A(\beta_\mu)$ is a Kemmer-Duffin algebra, the field of spin s = 2. In the latter case, the nonlinear generalization of the field equation is given, and it is shown that the structure of the field equation obtained by this means is very close to the structure of the Einstein equation for a free field. (tr-auth)

41561 A CANONICAL ANALYSIS OF GRAVITATIONAL RADIATION (thesis). Levin, Joel Melvin. Waltham, Mass., Brandeis Univ., 1964. 132p.

An investigation of gravitational radiation in terms of the full Einstein theory is presented with emphasis on radiation by axially symmetric systems. The general theory of relativity was examined in simpler cases (i.e., in spaces of fewer dimensions or greater symmetry), and it was found that these situations are too simple to admit gravitational radiation. It was found that in spaces of two or three dimensions there is no correspondence principle between general relativitiy and Newtonian gravitational theory, and that in three dimensions there are not even Coulomb forces in source-free regions. Thus gravitational radiation is seen to be inherently a four-dimensional phenomenon. The discussion of radiation from axially symmetric systems is introduced by a survey of previous studies of axially symmetric metrics in general relativity. Two of these (the time-symmetric metric of Brill and the radiating metric of Bondi) were analyzed in terms of the canonical formalism, thereby yielding some clarification of their physical interpretation. These calcuations were simplified by being carried out in terms of a redefinition of the orthogonal break-up of a symmetric three-tensor which was developed in the appendixes. The constraint equation was analyzed in the wave-zone for Brill's metric and yielded three interesting results. If $g_{ij} = \delta_{ij} + \ldots \theta(1/r)$ and if $g_{ij}^{TT} \sim$ wavy/r, the expansion of the metric in powers of $1/r$ can only be accomplished if the coefficients of $1/r^n$ are permitted to have polynomial behavior in r. This result imposes a limitation on the size of the wave-zone. Finally, this behavior implies that the strength of the radiation (i.e., the magnitude of the coefficient of $1/r$ in g_{ij}^{TT}) must be less than an explicit upperbound if the metric is to be real. These conclusions were generalized by investigating the constraint equations in terms of the canonical formalism. It is shown that if $g_{ij}^{TT} \sim$ wavy/r in the wave-zone for any radiating system, either the metric must contain logarithms or the coefficients of $1/r^n$ in the expansion of the metric in inverse powers of r must be polynomials in r. This conclusion is a direct consequence of the non-linearity of the theory. Applying this result to Bondi's radiating solution, it is shown that the absence of logarithms in his solution is achieved because of the presence of polynomials in r in the numerators of his expansion of the metric in powers of $1/r$. Bondi's conclusion that a radiating system is losing mass was verified by analyzing the Poynting vector of the canonical formalism. This result was generalized, and it is shown that for any outwardly radiating system, regardless of symmetry, there must be a negative-definite change of mass. The physical interpretation of Bondi's non-radiative, non-static solutions was clarified but not fully resolved. (Dissertation Abstr.)

41562 ON ALTERNATE COMMUTATION RELATIONS (thesis). Parks, William Frank. Iowa City, Iowa, Univ. of Iowa, 1964. 76p.

An alternate quantization procedure was investigated for scalar Bose fields. The basic commutation rules are $[a_i^\dagger, a_j] = 2/n_0\ \delta_{ij}\ \{N_i - n_0/2\}$, $[a_i, N_j] = \delta_{ij}\ a_i$, and $[a_i, a_j] = 0$ where i is a discrete variable labeling the single particle states. In the algebra defined by these rules N_i can be identified with the number operator for the state i; $a_i^\dagger$ and a_i, the creation and annihilation operators respectively in the i^{th} state. A theorem, corresponding to that proven for fermions, is proven demonstrating the existence of an infinite number of inequivalent irreducible representations of the algebra defined by the above relations. Furthermore, it is shown that, if one defines the space-time transformation and the particle-anti-particle conjugation properties in the usual, physically intuitive manner, the commutation rules are form invariant under these transformations. By investigation of a number of field theoretic models, it was found that the theories developed from the proposed commutation relations do not seem to lose any of the divergences intrinsic to the usual Bose quantization, even though the operators can be bounded. (Dissertation Abstr.)

41563 A VARIATIONAL PRINCIPLE IN GENERAL RELATIVITY AND THE STABILITY OF FLUID SPHERES (thesis). Cocke, William Johnston. Ithaca, N. Y., Cornell Univ., 1964. 64p.

The stability of gravitationally bound spheres of a perfect, relativistic fluid without heat flow was investigated via the following variational principle: Stable equilibrium requires that the total potential energy be a minimum relative to infinitesimal variations of the energy distribution which conserve total entropy. An expression for the proper entropy density of the perfect fluid is derived as an explicit function of the proper energy density, and it is shown that the vanishing of the covariant divergence of the energy-momentum tensor implies that this expression for the entropy density automatically satisfies the proper conservation (continuity) equation. This provides us with a non-trivial integral of the field equations for general, time-dependent fluid motions in space-time. It is shown that if a particle number density may be defined, then this number density is proportional to the derived entropy density. This interpretation provides an analogue to the Newtonian conservation of total mass. The above stability criterion is shown to yield the relativistic equation of hydrostatic equilibrium, and it is shown that the reciprocal variational principle (that the entropy be a maximum with respect to variations conserving potential energy) yields the same equilibrium equation. The expression for the second variation is much more manageable in the reciprocal problem, and it is shown that the requirement that the second variation of the entropy be negative for variations conserving energy gives a stability criterion which is equivalent to one derived from dynamical considerations. In an appendix it is proved that if the entropy is a maximum for variations conserving energy, then the energy cannot be a maximum for variations conserving entropy, and, contrariwise, if the energy is a maximum, then the entropy cannot also be a maximum. Applications to features of equilibrium models are considered. (Dissertation Abstr.)

41564 GRAVITATIONAL RADIATION AND THE MOTION OF TWO POINT MASSES (thesis). Peters, Philip Carl. Pasadena, Calif., California Inst. of Tech., 1964. 186p.

Expansion of the field equations of general relativity in powers of the gravitational coupling constant yield conservation laws of energy, momentum, and angular momentum. From these laws, the loss of energy, momentum, and angular momentum of a system due to the radiation of gravitational waves was found. Two techniques, radiation reaction and flux across a large sphere, were used in this calculation and are shown to be in agreement over a time average. The results were then applied to the system of two point masses moving in elliptical orbits around each other. The secular decays of the semi-major axis and eccentricity were found as functions of time and were integrated to specify the decay by gravitational radiation of such systems as functions of their initial conditions. For completeness, the secular change in the perihelion of the orbit for two arbitrary masses was found by a method which is in the spirit of the above calculations. The case of gravitational radiation when the bodies are relativistic was then considered, and an equation for the radiation similar to that of electromagnetic radiation was found. Also proof is given that, regardless of coordinate systems or conditions, the energy of a system must decrease as a result of the radiation of gravitational waves, providing the potentials are inversely proportional to the distance from the source for large distances. (Dissertation Abstr.)

41565 ASYMPTOTIC SOLUTION OF THE SCHROEDINGER EQUATION FOR THE THREE-BODY PROBLEM (thesis). Vezzetti, David Joseph. Hoboken, N. J., Stevens Inst. of Tech., 1964. 113p.

The WKB method was applied to determine the asymptotic expansion of the Schrödinger wave function for a system of three spinless particles which interact through central forces. By making a new assumption concerning the form of the WKB ansatz, a new set of equations for the asymptotic wave function was derived. These equations hold in a reduced, three-dimensional configuration space and are therefore, in some cases, easier to solve than the usual WKB equations which hold in a six-dimensional space. The phase, S, of the asymptotic wave function was found to satisfy a determinantal equation which is an analog of the Hamilton-Jacobi equation of classical mechanics. The amplitude of the asymptotic wave function may be expanded in a power series in h (Planck's constant divided by 2π) and the various terms in this expansion were found to satisfy a coupled set of linear partial differential equations. The general procedure for constructing the asymptotic wave function from the solutions of these equations is discussed in detail. The general method is specialized to the helium atom for S-states and P-states. In both cases, the equations in the three-dimensional configuration space may be solved by a perturbation procedure. To zero order in perturbation theory, the energy eigenvalues are just the energies of two independent electrons in the Coulomb field of the nucleus and are the same as those given by quantum mechanics. The asymptotic wave functions were also calculated to zero order in perturbation theory. These functions are an improvement over the usual wave functions of zero order perturbation theory in quantum mechanics in that they contain the proper angular symmetries for the angular momentum quantum state under consideration. Therefore, they are not simply the asymptotic expansions of the product of two hydrogenic Schrödinger wave functions. An examination of these functions shows that the two electrons are spacially correlated and therefore these solutions permit a semi-classical description of the various electronic motions in the helium atom. A perturbation procedure based on classical mechanics was carried out in order to obtain the first-order correction to the energy eigenvalues. It was found that the resulting correction is the asymptotic equivalent of the first order result of the usual Schrödinger perturbation theory of quantum mechanics. This result shows that the asymptotic method may be applied consistently to the helium atom and yields results which are in asymptotic agreement with those of quantum mechanics. The procedure for determining the first-order correction to the wave function was also developed. The method was applied to a system of three equally massive particles. The equilibrium energy and vibrational energy as well as the asymptotic wave functions were calculated to first order in perturbation theory. (Dissertation Abstr.)

41566 AN INTRODUCTION TO THE THEORY OF RELATIVITY. Rosser, W. G. V. Washington, D. C., Butterworths, 1964. 528p. $14.95.

A discussion is given of the theory of relativity. Topics include the history of Newtonian mechanics and ether, the Lorentz transformations, relativistic kinematics and mechanics, geometrical representations of the Lorentz transformation, electromagnetism as a second order effect, the relativistic transformation of Maxwell's equation and of the potentials. Also considered are development of the theory of electromagnetism, a critique of special relativity, and the theory of general relativity. (J.F.P.)

41567 LECTURES ON QUANTUM MECHANICS. Dirac, Paul A. M. Belfer Graduate School of Science Monographs Series Number Two. New York, Belfer Graduate School of Science, Yeshiva Univ., 1964. 90p.

Available in U. S. from Academic Press, New York, $3.50.

Four lectures are given in quantum mechanics. These are the Hamilton method, the problem of quantization, quantization on curved surfaces, and quantization on flat surfaces. (J.F.P.)

41568 MATRIX MECHANICS. Green, H. S. Groningen, Netherlands, P. Noordhoff Ltd., 1965. 125p. $5.50.

The mathematical and physical basis of quantum mechanics, the simple harmonic oscillator, angular momentum, and relativistic quantum mechanics are discussed. The physical foundations correspond roughly to Heisenberg's original ideas, and are later generalized to include Dirac's relativistic theory. Quantum-mechanical paradoxes are also treated. (J.F.P.)

Geophysics

Refer also to abstract 40433.

41569 (AD-426145) METHODS OF PROMOTING THE REMOVAL OF FREE ELECTRONS FROM AN IONIZED AND DISSOCIATED ATMOSPHERE. Final Report. NRA Report No. 113-400-4. Arthur, W.; Beiser, A. (NRA, Inc., Long Island City, N. Y.). June 1963. Contract AF19(628)-255. 20p. (AFCRL-63-380). CFSTI $2.60 cy.

A study of methods of promoting the removal of free electrons from an ionized and dissociated atmosphere is presented. This study included an analysis of the atomic and ionic processes relevant to the above (with special regard to the dependence of these processes upon electrical energy) and a quantitative assessment of the various possible means for removal of free electrons from such an atmosphere, including estimates of time scales, efficiencies, and power requirements. (auth)

41570 (CONF-765-11) SOME ASPECTS OF THE GENERAL CIRCULATION OF THE LOWER STRATOSPHERE. Newell, R. E.; Miller, A. J. (Massachusetts Inst. of Tech., Cambridge. Dept. of Meteorology). [1964]. Contract AT(30-1)-765. 18p. Dep. mn; CFSTI $1.00 cy, $0.50 mn.

From 2nd Conference on Radioactive Fallout from Nuclear Weapons Tests, Germantown, Md., Nov. 1964.

Climatological data make possible the construction of a broad general outline of the manner in which the lower stratosphere is driven from below. It would appear that the distribution of trace substances in the lower stratosphere is governed by the energy production and vertical flux of energy in the troposphere. We might therefore expect differences between hemispheres just as there are seasonal effects in each hemisphere. For example, if a good fraction of the driving energy is exported from the troposphere in the form of standing waves, we would expect smaller vertical fluxes in the southern hemisphere

where these waves are less important than in the northern hemisphere. Thus one might anticipate smaller amounts of total ozone in the southern hemisphere. As there is apparently not so much seasonal variation of the standing waves in the southern hemisphere one might also expect less marked spring maxima in ozone and also perhaps in fallout. (auth)

41571 (N64-29400) SEMIANNUAL REPORT ON NASA RESEARCH GRANT NSG 249-62, FOR THE PERIOD JANUARY 1, 1964–JUNE 30, 1964. Coleman, Paul J. Jr.; Farley, Thomas A. (California Univ., Los Angeles. Inst. of Geophysics and Planetary Physics). 17p. (NASA-CR-58669). CFSTI, $1.60 cy.

Work on space-instrument development has concentrated on charged-particles and magnetic-fields research. The charged-particle research program, which involves both trapped Van Allen radiation and interplanetary cosmic rays, includes these: (1) electron detectors for EGO-3; (2) an experiment to determine the isotopic abundance, flux, and energy spectra of the hydrogen and helium isotopes in solar and galactic cosmic rays; (3) a program to compute pitch-angle distribution from omnidirectional intensities; and (4) calibration of space-radiation monitoring instruments for the Department of Defense. The magnetic fields research program includes these: (1) reduction and analysis of data from the Mariner II magnetometer; (2) studies of related measurements; (3) preparations for Mariner-C magnetometer experiment; and (4) development of new instruments to study hydromagnetic disturbances and their effects on geomagnetically trapped particles. (auth)

41572 (NASA-CR-258) INVESTIGATION OF NONLINEAR INTERACTION PHENOMENA IN THE IONOSPHERE. Hsieh, H. C.; Lomax, R. J.; Rowe, J. E. (Michigan Univ., Ann Arbor). July 1965. 86p. CFSTI, $3.00 cy.

Three separate areas of investigation are presented: study of thermal radiation (noise) from the ionosphere, propagation of naturally occurring radio noise through the ionosphere, generation of VLF emissions in the exosphere by double-beam instability, and the generation of natural radio emission by plasma-oscillation. In addition, the Boltzmann equation and Lagrangian analysis methods are given. (M.O.W.)

41573 (RPU-S19) STATISTICAL CHARACTERISTICS OF SUDDEN IONOSPHERIC DISTURBANCES. Scientific Report No. 19. Mitra, A. P.; Subrahmanyam, C. V.; Karabin, Mirjana (Radio Propagation Unit, National Lab., New Delhi (India)). Feb. 15, 1965. 47p. Dep. mn.

The results of a detailed statistical examination made of the relation between optical observations of solar flares, solar radio noise bursts, magnetic crochets, and the various sudden ionospheric disturbances are described. The period covered is mostly that of the International Geophysical Year (July 1, 1957-December 31, 1958). The major conclusions are presented. (auth)

41574 (FTD-TT-65-101) DETERMINATION OF THE EFFECTIVE COLLISION FREQUENCY IN THE IONOSPHERE. Gusev, V. D. Translated from Vestn. Mosk. Univ., Ser. Mat., Mekhan, Astron., Fiz. i Khim., 14: No. 1, 105-8(1959). 6p. CFSTI.

A method is developed for determining the distribution of the collision frequency of electrons with neutral particles and ions in the ionosphere. This method considers the isotropic medium and the monotonic change of the ionosphere with altitude. (M.O.W.)

41575 (FTD-TT-65-112) CONNECTION OF BRIEF PERIODIC OSCILLATIONS (KPK) OF THE TERRESTRIAL ELECTROMAGNETIC FIELD WITH AURORA POLARIS ILLUMINATION INTENSITY VARIATIONS. Skrynnikov, R. G. Translation of p.29-38 from AN SSSR. Kol'skiy Filial. Polyarny Geofizicheskii Institut. Issledovanie Geofizicheskikh Yavleniy Elektromagnitnogo Kompleksa v Vysokikh Shirotakh, 1964. 16p. CFSTI.

Preliminary results of comparing the brief periodic oscillations of the terrestrial electromagnetic field with variations of aurora polaris glow intensities are presented. Observations were conducted in the winter season of 1961/1962. Conclusions from these observations are presented. (M.O.W.)

41576 (N64-21876) RESEARCH RESULTS OBTAINED DURING THE INTERNATIONAL GEOPHYSICAL YEAR. AURORAE AND AIRGLOW. ARTICLES, IV SECTION OF IGY PROGRAM NO. 9. Krasovskii, V. I. (ed.). Translation of Mezhduvedomstvennyi Geofizicheskii Komitet. IV Razdel Programmy MGG. Poliarnye Siyaniya i Svechenie Nochnogo Neba. Sbornik Statei, No. 9 (a publication of the Publishing House of the Academy of Sciences, Moscow, 1962). 91p. (NASA-TT-F-202). CFSTI, $2.25 cy.

The following topics are discussed: seasonal and annual variations in the intensity of the night airglow in Abastumani, variations in the populations of the vibrational levels of hydroxyl molecules, latitudinal and planetary variations of the hydroxyl emission, variations of the H_α profile, behavior of certain emissions in auroral rays, the emissions of molecular oxygen observed in Yakutsk, rotational temperature of OH bands, OH emission and the atmospheric band λ 8,645 Å of the O_2 molecule, the emission (NI) λ 5,200 Å based on observations made in Yakutsk, the twilight emission OI λ 8,446 Å, observation of a twilight burst of helium emission λ 10,830 Å with a Fabry-Perot standard, and certain features of the continuum in twilight. (M.O.W.)

41577 ON THE ORIGIN OF OUTER-BELT PROTONS. 1. Nakada, M. P.; Dungey, J. W.; Hess, W. N. (Goddard Space Flight Center, Greenbelt, Md.). J. Geophys. Res., 70: 3529-32(Aug. 1, 1965).

The variations in the energy spectrums with pitch angle and L of the relatively stable 0.1- to 5-Mev protons in the outer radiation belt have been found to be in good agreement with the results of a model that permits rapid motion of the protons in L space. In this model the third adiabatic invariant of the protons is violated, but not the first two adiabatic invariants. The variations in flux with L are found to indicate an external source and are discussed qualitatively. (auth)

41578 INWARD RADIAL DIFFUSION OF ELECTRONS OF GREATER THAN 1.6 MILLION ELECTRON VOLTS IN THE OUTER RADIATION ZONE. Frank, L. A. (Univ. of Iowa, Iowa City). J. Geophys. Res., 70: 3533-40 (Aug. 1, 1965).

Observations of the temporal variations of electron ($E > 1.6$ Mev) intensities near the geomagnetic equator in the outer radiation zone with Explorer 14 (October 2, 1962, to August 8, 1963) strongly suggest that replenishment of energetic electrons in the outer radiation zone during the several weeks following a period of geomagnetic activity proceeds by an inward radial motion of energetic electrons from $L > 5$. The apparent, inward radial velocity of the "wave" of electrons ($E > 1.6$ Mev) is ~0.4 earth radius $(\text{day})^{-1}$ at $L = 4.7$ and ~0.03 earth radius $(\text{day})^{-1}$ at $L = 3.4$, and varies as $\sim L^8$ between these L shells. These inward radial velocities for the several replenishment cycles of outer-zone electrons ($E > 1.6$ Mev) observed with Explorer 14 at a given L shell are equal to within experimental errors. These measurements provide evidence for a continually active mechanism for diffusing energetic electrons across L shells in the outer radiation zone. (auth)

41579 ANOMALOUS INCREASE IN THE NEUTRON FLUX AT AIRCRAFT ALTITUDES. Gauger, Joleroy (Boeing Scientific Research Labs., Seattle). J. Geophys. Res., 70: 3571-4(Aug. 1, 1965).

An anomalous increase in the flux of low-energy neutrons (0.02 ev to ~5 Mev) was detected at aircraft altitudes on January 21, 1964, between 0350 and 0400 UT. The aircraft (at an altitude of 39,000 feet and a geographic position between 38° and 35°S latitude in the region of the magnetic anomaly east of Buenos Aires) was instrumented with ionospheric sounding gear, three cosmic-ray neutron counters, and night airglow monitors. The increase in the neutron flux, which was detected by all three neutron counters, coincided with an increase in the intensity of the night airglow monitored in the same aircraft. (auth)

41580 EXPLORER 14 PLASMA PROBE OBSERVATIONS DURING THE OCTOBER 7, 1962, GEOMAGNETIC

DISTURBANCE. Wolfe, J. H.; Silva, R. W. (Ames Research Center, Moffett Field, Calif.). J. Geophys. Res., 70: 3575-9(Aug. 1, 1965).

The October 7, 1962, event, as seen by the plasma probe aboard Explorer 14, was characterized by the appearance of plasma approximately 2 minutes after the ground-level sudden impulse. The spacecraft at this time was outbound at 13.5 earth radii. Before this event no plasma was observed. The results presented are consistent with a compression of the magnetospheric boundary below the altitude of the spacecraft. Data are further presented to give evidence for momentary penetration by Explorer 14 of the postulated bow shock. Comparisions are made with Mariner 2 magnetometer and plasma probe data with consideration given to the time delay associated with the propagation of the disturbance from Mariner 2 to earth. (auth)

41581 EXCITATION OF EXTREMELY LOW FREQUENCY ELECTROMAGNETIC WAVES IN THE EARTH-IONOSPHERE CAVITY BY HIGH-ALTITUDE NUCLEAR DETONATIONS. Kahalas, Sheldon L. (Mt. Auburn Research Associates, Inc., Cambridge, Mass.). J. Geophys. Res., 70: 3587-94(Aug. 1, 1965).

The magnetic disturbances produced on a worldwide scale by high-altitude nuclear detonations are treated. The characteristics of the magnetic signals from Argus 3 and Starfish are briefly discussed. Particularly, the fast propagation time observed for the early part of the signal is explained by the magnetohydrodynamic-electromagnetic coupling mechanism. An idealized model is explored of excitation of extremely low frequency electromagnetic waves in a cylindrical vacuum cavity by magnetohydrodynamic waves incident from the surrounding plasma. It is found that there is a characteristic time needed for the cavity waves to respond to this external excitation: no matter how fast the excitation, the cavity wave amplitude changes in a time of the order of 2 seconds. (auth)

41582 DYNAMIC SPECTRAL CHARACTERISTICS OF MICROPULSATION PEARLS. Pope, Joseph H. (National Bureau of Standards, Boulder, Colo.). J. Geophys. Res., 70: 3595-3603(Aug. 1, 1965).

The dynamic spectrums of micropulsation pearls (type Pc 1) recorded at stations in various latitudes were studied to obtain the frequencies and the spacing times of the fine structure elements comprising pearl events. In confirmation of earlier results, the product of these two parameters is found to be nearly independent of latitude. However, the parameters are themselves functions of latitude, both the spacing time and the reciprocal of the frequency being almost proportional to the L value. These dependences are such as to account for the tendency of the frequency-spacing time product to be constant. An attempt to discriminate between Alfvén wave and particle bunch hypotheses for the generation of pearls was made by comparing the experimental results with computations of the travel time over the field line as a function of latitude. It appears that mirroring particle bunches with a velocity of about 1270 km/sec could account for the observed latitude effect. (auth)

41583 ADIABATIC MOTION OF AURORAL PARTICLES IN A MODEL OF THE ELECTRIC AND MAGNETIC FIELDS SURROUNDING THE EARTH. Taylor, Harold E.; Hones, Edward W. Jr. (Univ. of Iowa, Iowa City). J. Geophys. Res., 70: 3605-28(Aug. 1, 1965).

The motion of charged particles in the electric and magnetic fields constituting the earth's magnetosphere is calculated using the assumption that the first and second adiabatic invariants are conserved. The model of the magnetic field includes the effects of the solar wind pressure on the sunward side of the magnetosphere and of the newly discovered current sheet in the magnetospheric tail. The electric field is deduced in the ionosphere from the S_D current system which accompanies magnetic bays. The magnetic field lines are then assumed to be equipotentials, so that the electric field can be projected throughout the magnetosphere. The motion of low energy plasma is discussed qualitatively, and the motion of solar wind particles which become trapped on the surface of the magnetosphere is calculated in quantitative detail. It is found that solar wind electrons (kinetic energy at the magnetospheric surface <1 kev) will be accelerated to energies in the range of 1 to 40 kev and will be confined to a narrow latitudinal zone where extensive precipitation into the atmosphere will occur during local nighttime. Protons of similar energy will be confined to a region south of the electron region and will precipitate during local afternoon and evening. The conclusion is reached that auroral events are produced largely by electrostatic acceleration of solar wind particles and occur on lines of force which close in the tail of the magnetosphere within $50R_E$ of the earth. (auth)

41584 CLASSIFICATION OF MAGNETIC SHELLS. Stern, David (Goddard Space Flight Center, Greenbelt, Md.). J. Geophys. Res., 70: 3629-34(Aug. 1, 1965).

A new method of calculating the magnetic shell parameter L, based on Pennington's perturbation method for calculating the shape of magnetic shells, is presented. In this approach the shell passing a given point is characterized by two parameters, L and a function α_m of the local pitch angle. The dependence on θ_m is shown to be very weak, however, so that it may be neglected to a good approximation. Auxiliary functions necessary for this method are tabulated, including a 48-coefficient expansion of the geomagnetic potential in tilted-dipole coordinates, and the results are compared with those derived by McIlwain's method. The results are found to be, in general, within several per cent of those numerically integrated by McIlwain. (auth)

41585 AMBIPOLAR DIFFUSION IN THE GEOMAGNETIC FIELD. Holway, Lowell H. Jr. (Raytheon Research Div., Waltham, Mass.). J. Geophys. Res., 70: 3635-45(Aug. 1, 1965).

The effect of the earth's magnetic field on ambipolar diffusion at ionospheric heights is considered. It is shown that the geomagnetic field will increase the lifetime of an ionized cloud at 150-km altitude by more than an order of magnitude and that a spherically symmetrical cloud becomes markedly ellipsoidal in shape owing to the anisotropic diffusion. The electric and magnetic fields induced by the azimuthal current distribution are also discussed. (auth)

41586 AN EVALUATION OF THE MAIN GEOMAGNETIC FIELD, 1940-1962. Cain, Joseph C. (Goddard Space Flight Center, Greenbelt, Md.); Daniels, W. E.; Hendricks, Shirley J.; Jensen, Duane C. J. Geophys. Res., 70: 3647-74(Aug. 1, 1965).

A set of 21,695 selected survey and observatory annual mean data available for the interval 1940-1963 is used to make a new determination of the geomagnetic field and its secular change. The field is given by a series of 63 spherical harmonics (g_n^m and h_n^m to n = m = 7) and 35 time derivatives ($\dot{g}_n^m$ and $\dot{h}_n^m$ to n = m = 5). Although it is inferred from these results that a better fit could be made with existing data if more coefficients were used, the improvement is substantial enough for us to recommend that the coefficients be used as a replacement for previously derived coefficients to evaluate the field at the current epoch. One refinement in the present determination is the use of an oblate earth in place of the spherical approximation. It is illustrated that this modification is necessary to obtain meaningful extrapolations above the earth's surface. The standard errors and confidence levels are given for the coefficients to show that almost all are well determined. It is shown that, when the field components computed using this new series are compared with several weighted selections of survey data, the rms deviations average only 210 γ (1955-1963), a value smaller than that obtained by other spherical harmonic series known to us. (auth)

41587 STRUCTURE AND VARIATION OF THE TOPSIDE IONOSPHERE CLOSE TO THE FORT MONMOUTH LONGITUDE. Arendt, P. R.; Papayoanou, A. (U. S. Army Electronics Command, Fort Monmouth, N. J.). J. Geophys. Res., 70: 3675-85(Aug. 1, 1965).

Ionograms of the topside ionosphere obtained from the Alouette satellite during a period of more than a year

have been reduced to "real height" profiles. Data obtained between September 1963 and January 1964 have been studied in detail. The effective radio horizon of Fort Monmouth enables a study of the upper ionosphere between 15° and 65°N geographic latitude and 50° and 100°W longitude. Curves of plasma frequencies and of electron density at fixed altitudes have been prepared as a function of latitude, longitude, and time of day. Special attention has been given to the effects of magnetic disturbances as revealed on the contours. During the observed magnetic storms, the measured altitudes for specific plasma frequencies were decreased by more than 200 km. Another parameter, the integrated electron content in the topside ionosphere, has been compared with f_0F_2. The assistance of five bottomside sounding stations located within the radio horizon of Fort Monmouth and computer programs for reducing topside and bottomside ionograms to real height profiles made it possible to study the difficulties in matching topside and bottomside profiles. Many topside and bottomside profiles have been found to match closely when the observed f_0F_2 values of topside and bottomside ionograms differ by not more than 0.3 Mc/s. Matching was observed for differences of 1° to 2° of the geographic positions of the ground station and the subsatellite point. Discrepancies on topside and bottomside ionograms (different geographic locations, nonmatching f_0F_2) are exhibited. (auth)

41588 MASS SPECTROMETRIC MEASUREMENTS OF POSITIVE IONS AT ALTITUDES FROM 64 TO 112 KILOMETERS. Narcisi, R. S.; Bailey, A. D. (Air Force Cambridge Research Labs., Bedford, Mass.). J. Geophys. Res., 70: 3687-3700(Aug. 1, 1965).

A quadrupole mass spectrometer system employing a liquid nitrogen chilled zeolite pump was recently developed for sampling positive ions at altitudes above 50 km. This system was flown successfully on a Nike Cajun rocket on October 31, 1963, at local noon from Eglin Air Force Base, Florida, and has provided the first positive ion composition measurements in the D region. The predominant ions detected within the D region (64 to 82 km) were 19^+, 30^+, and $(37 \pm 1)^+$, with 32^+ rapidly rising above 75 km approaching the abundance of 30^+ at 83 km. At 82.5 km a sharp transition occurred in the spectrums, characterized by the rapid disappearance of 19^+ and 37^+ and instantaneous appearance of six new ion peaks. Five of these ion peaks are suggested to be the metallic ions of sodium (23^+), magnesium (24^+, 25^+, 26^+), and calcium (40^+). The metallic ions all exhibited an identical altitude profile: a 10-km-wide peak with a maximum at 95 km, a minimum at 105 km, and then a continuous increase until apogee at 112 km. Above 82 km the ions 30^+ and 32^+ appear to be the most predominant, although many other minor constituent ions are present. (auth)

41589 GEOMAGNETIC AND SOLAR DATA. Lincoln, J. Virginia (ed.) (National Bureau of Standards, Boulder, Colo.). J. Geophys. Res., 70: 3761-3(Aug. 1, 1965).

Data are presented for the principal geomagnetic storm sudden commencements for the period January to March 1965. Maximum activity and ranges of the storms are presented. Geomagnetic and solar range indices are given for March, 1965. (J.F.P.)

41590 ISOCONTOURS OF MAGNETIC SHELL PARAMETERS B AND L. Venkatesan, Bharathi. (Univ. of Iowa, Iowa City). J. Geophys. Res., 70: 3771-80 (Aug. 1, 1965).

A master grid of B-L values was prepared for the altitude range 0 to 2000 km, in steps of 100 km. The latitude belt covered the region 70°N to 70°S. Interpolations from the grid give the isocontours for selected values of L. These contours show where the lines of force corresponding to a particular magnetic shell meet the specified spherical surface. Graphs are also given for the study of the drift of trapped particles around the earth. The altitudes corresponding to selected pairs of values of B and L are shown as a function of longitude for both northern and southern hemispheres. (J.F.P.)

41591 ON THE DETERMINATION OF THE ELECTRON DENSITY WITHIN DISCRETE AURORAL FORMS IN THE E REGION. Hunsucker, Robert D. (National Bureau of Standards, Boulder, Colo.). J. Geophys. Res., 70: 3791-2(Aug. 1, 1965).

Values are given for the number of electrons/cm^3 from observations of sporadic-E ionization whose virtual height as a function of frequency is relatively constant at 110 km. (J.F.P.)

41592 INFRA-SONIC WAVES FROM AURORAE. Maeda, Kaichi (Goddard Space Flight Center, Greenbelt, Md.); Young, Jessie M. Nature, 207: 279-81(July 17, 1965).

The characteristics of auroral infrasonics, occurring during times of high geomagnetic activity, are pointed out, and an interpretation of the waveform and periodicity of these atmospheric travelling auroral pressure waves which are observed at the ground is given. The two types of atmospheric pressure waves—acoustic (sonic) and thermobaric (internal gravity) modes—are considered. (M.J.T.)

41593 DYNAMO ACTION IN THE IONOSPHERE AND MOTIONS OF THE MAGNETOSPHERIC PLASMA. II. DEFORMATION OF THE RADIATION BELTS DUE TO THE ELECTROSTATIC FIELD PRODUCED BY IONOSPHERIC WINDS. Dewitt, R. N.; Akasofu, S.-I. (Univ. of Alaska, College). Planetary Space Sci., 13: 729-36(Aug. 1965).

The distribution of the dynamo-induced electrostatic field obtained by Maeda and Kato is discussed in terms of ionospheric winds, and the motion of the magnetospheric plasma resulting from the field is further discussed. It is suggested that the ionospheric electrostatic field can affect the configuration of radiation belts and that a certain similarity exists between the flow patterns of the magnetospheric plasma and the observed day–night asymmetry of radiation belts. A possible significance of this regarding auroral phenomena is suggested. (auth)

41594 DYNAMO ACTION IN THE IONOSPHERE AND MOTIONS OF THE MAGNETOSPHERIC PLASMA. III. THE PEDERSEN CONDUCTIVITY, GENERALIZED TO TAKE ACCOUNT OF ACCELERATION OF THE NEUTRAL GAS. Akasofu, S.-I.; Dewitt, R. N. (Univ. of Alaska, College). Planetary Space Sci., 13: 737-44(Aug. 1965).

The generalized Pedersen conductivity is calculated by taking into account the mass motion of neutral particles in typical ionospheric conditions. It is shown that for electrostatic fields of periods more than 6 hr the generalized Pedersen conductivity is significantly less than the well-known Pedersen conductivity beyond 150 km in altitude. This suggests that the mass motion of neutral particles (namely a wind) is generated by the interaction between the charged particles and the neutral particles, resulting in dynamo action. The importance of this apparent reduction of the conductivity is discussed in the transmission of an electrostatic field from the magnetosphere (or from the dynamo effective region of the ionosphere) to the upper ionosphere. (auth)

41595 MICROPULSATION MODE PROPAGATION IN THE MAGNETOSPHERE. Dowden, R. L. (Univ. of Tasmania, Australia). Planetary Space Sci., 13: 761-72(Aug. 1965).

Propagation of extremely low-frequency (~1 c) waves along field lines in the magnetosphere in the "micropulsation mode" is considered. Expressions for phase and group refractive index for any wave-normal direction are derived. Although wave-normal angles are likely to be large, longitudinal expressions can be used with reasonable accuracy in calculating travel times and dispersion. The medium produces strong guiding without field-aligned columns. The maximum deviation of the ray path from a field line is shown to be small. (auth)

41596 THE USE OF MICROPULSATION WHISTLERS IN THE STUDY OF THE OUTER MAGNETOSPHERE. Dowden, R. L.; Emery, M. W. (Univ. of Tasmania, Australia). Planetary Space Sci., 13: 773-9(Aug. 1965).

Certain types of micropulsation dynamic spectra show

a series of rising tones thought to be caused by dispersion in the magnetosphere. Based on this idea and a previous analysis it is shown that these spectra can be used to evaluate the plasma density in the outer magnetosphere (five to eight earth radii) in a way analogous to that used for vlf whistlers. The method is applied to micropulsations observed at Hobart in April 1964. The results indicate a substantial decrease in plasma density beyond about five earth radii in broad agreement with previous vlf work. (auth)

41597 OBSERVATIONS OF IONOSPHERIC ELECTRON CONTENT USING A GEOSTATIONARY SATELLITE. Garriott, O. K. (Stanford Univ., Calif); Smith III, F. L.; Yuen, P. C. Planetary Space Sci., 13: 829-38(Aug. 1965).

Observations of the telemetry transmissions from Syncom III at the University of Hawaii and at Stanford University have permitted the diurnal variation of electron content to be calculated. Typical diurnal curves are shown for both stations and their characteristics are found to be markedly different. A diurnal range of at least 30:1 is found in Hawaii but only 10:1 at Stanford. Large day-to-day and even hour-to-hour variability is observed, especially in Hawaii. The nighttime levels at both stations are nearly constant and the sunrise increase is nearly identical every day. The diurnal variation of slab thickness is not properly understood. Several new studies are suggested, including the calculation of production rates, loss rates, and the correlation with airglow and other geophysical phenomena. (auth)

41598 THE RATE OF PRODUCTION OF ELECTRONS IN THE IONOSPHERE. Garriott, O. K.; Smith III, F. L. (Stanford Univ., Calif.). Planetary Space Sci., 13: 839-49(Aug. 1965).

Accurate measurements of the variation of electron content in the sunrise period have provided the means of calculating the integrated electron-production rate for an overhead sun. Based on Syncom III observations in Hawaii, the maximum integrated production rate Q_0 is about $1.4(\pm 0.3) \times 10^{14}$ electrons/m^2/sec, corresponding to a peak $q_0 \approx 1300 \times 10^6$ electrons/m^3/sec for a single constituent atmosphere. Observations from Stanford yield values about 25% higher, but there is less confidence in the results since the observations of Syncom III are made only 17° above the horizon. If rapid recombination of N_2^+ is assumed, the total production rate $Q_0(O^+ + N_2^+)$ at noon will be about 60% higher. These results are compared with some previous estimates of production rates and related photometer measurements above the production peak. (auth)

41599 BEHAVIOR OF SLOW ELECTRONS IN ATMOSPHERIC GASES. PART I. GENERAL CONSIDERATION OF ROTATIONAL EXCITATION AND APPLICATION TO THE OXYGEN MOLECULE. Takayanagi, Kazuo (Saitama Univ., Urawa, Japan and Tokyo Univ.). Rept. Ionosphere Space Res. Japan, 19: 1-15(1965).

Effective cross sections for the rotational transition of an oxygen molecule by slow electrons (<2 ev) are calculated by using the Born approximation. Validity of the approximation is discussed. The resulting cross sections are used to evaluate the stopping power of oxygen for slow electrons. (auth)

41600 BEHAVIOR OF SLOW ELECTRONS IN ATMOSPHERIC GASES. PART II. ROTATIONAL EXCITATION OF THE NITROGEN MOLECULE. Takayanagi, Kazuo (Saitama Univ., Urawa, Japan and Tokyo Univ.). Rept. Ionosphere Space Res. Japan, 19: 16-20(1965).

The specific stopping power of the nitrogen molecule for slow electrons due to rotational excitation is calculated. It is based on the cross section calculated by Takayanagi and Geltman using the distorted wave method. It is found that the stopping power of nitrogen is an order of magnitude larger than that of oxygen calculated previously. (auth)

41601 GEOMAGNETIC PULSATIONS AND THE EXOSPHERE. PART III. ION DENSITY DISTRIBUTION IN THE EXOSPHERE. Kitamura, Tai-ichi (Doshisha Univ., Kyoto). Rept. Ionosphere Space Res. Japan, 19: 21-9 (1965).

The ion density distribution in the exosphere, assuming the diffusive equilibrium type of distribution ($\rho = \rho_0 \exp\{mg_0/(kT \cdot R)\}$), is investigated, solving a spatial part of the fundamental equation of oscillation in the exosphere, with an assumption that geomagnetic pulsations in the polar regions (pc 5) are standing waves along the field lines of magnetic force. In the present, ρ_0 and T, cannot be determined independently, and they are related apparently by $\rho_0 = kT^\lambda$, where K and λ are constants. The relation between them depends on the oscillation modes along the lines of force. The estimated ion densities assuming a temperature of 1250°K in the exosphere are about 90-700 particles/cc at three earth radii, and 60-400 particles/cc at five earth radii, which are roughly consistent with values calculated from whistler observations. (auth)

41602 A NEW INDEX OF GEOMAGNETIC PULSATION AND ITS RELATION TO SOLAR M-REGION. PART III. ANNUAL VARIATION AND LATITUDINAL DEPENDENCE OF M-REGIONS. Saito, Takao (Tohoku Univ., Sendai). Rept. Ionosphere Space Res. Japan, 19: 30-46(1965).

Geomagnetic disturbances due to solar M regions often seem to show apparent annual variation; these are activated either near vernal or autumnal equinox. A geomagnetic pulsation index Kc3 from 1959 to 1964 and three-hour planetary index Kp from 1931 to 1934 are presented as examples of this variation, which is interpreted by the axial effect of the sun; in other words, an effect of the variation in the earth's heliographic latitude. In order to explain the reason why the clearest 27-day recurrence tendency of M disturbances appears only in the declining phase of the solar cycle, the following hypothesis is introduced. Although M regions are alive in all phases, they change their heliographic latitudes depending on the phase like other solar phenomena; M regions which appear in high latitudes in minimum phase shift their locations gradually to lower latitudes as the phase changes to inclining, maximum, declining, and again to minimum. By this hypothesis, the M-disturbances with the recurrence period of both fast and slow types which often appear in the minimum phase may easily be interpreted. Namely, if a solar wind ejected from a high latitudinal M region is deflected towards the earth, it will stir up the slow type of M-disturbances. This may also substantiate the deflection hypothesis previously proposed. The assumptions that both fast and slow types of M disturbances are simultaneously caused in minimum phase, that M regions are in high latitudes during the inclining phase, and that solar and interplanetary magnetic fields are disturbed in maximum phase, will deduce the clearest 27-day recurrence tendency only in a declining phase. (auth)

41603 CATALOGUE OF DISTURBANCES IN IONOSPHERE, GEOMAGNETIC FIELD, FIELD INTENSITY OF RADIO WAVE, COSMIC RAY, SOLAR PHENOMENA AND OTHER RELATED PHENOMENA. Rept. Ionosphere Space Res. Japan, 19: 61-119(1965).

The catalog of disturbances contains the observational data of remarkable disturbances during September, 1963. Data of the following elements are given: the ionosphere, the geomagnetic field, field intensity of radio waves, cosmic rays, solar phenomena and other related phenomena. Simultaneous observations of the remarkable disturbances during the 7 days from September 13 to 19, 1963, when a magnetic storm occurred are given. (J.F.P.)

41604 THERMAL ESCAPE OF NEUTRAL HYDROGEN AND ITS DISTRIBUTION IN THE EARTH'S THERMOSPHERE. Liwshitz, Mordehai (Goddard Space Flight Center, Greenbelt, Md.); Singer, S. F. 47p. (CONF-650410-14). Gmelin, AED-CONF-65-073-22.

From American Physical Society, Washington, D. C.

The effect of thermal escape on the distribution of neutral hydrogen in the upper thermosphere is investigated. A simplified model is proposed, which assumes an extended transition region between the collision dominated lower thermosphere, and the effectively collisionless exosphere. In this region collisions with the predominant constituent, oxygen, are still too frequent to be neglected, while the

effect of thermal escape is strong enough to impede the approach to local thermal equilibrium. The behavior of hydrogen in the transition region is investigated by means of the Monte Carlo method, for different oxygen temperatures. Results show that stationary conditions are attained in relatively short times varying from about one hour at 1500°K to about half an hour at 2500°K. The velocity distribution of hydrogen is seriously perturbed, and shows marked anisotropy as a result of escape. Consequently the loss rate of neutral hydrogen from the terrestrial atmosphere is reduced by a factor of three or more, in the range of temperatures considered. (auth)

41605 ADVANCES IN UPPER ATMOSPHERE RESEARCH. Papers Presented at the NATO Advanced Study Institute at Corfu, July 1960. Landmark, B. (Ed.). A Pergamon Press Book. New York, The Macmillan Company, 1963. 345p. $12.25. (CONF-600701).

Papers (20) are included on auroral phenomena, effects of high-altitude nuclear explosions, wave propagation in the ionosphere, and ionization in the ionosphere. (D.C.W.)

41606 NEUTRON ALBEDO MEASUREMENTS ON POLAR-ORBITING SATELLITES (thesis). Trainor, James Harold. Durham, N. H., Univ. of New Hampshire, 1964. 88p.

An experiment was designed to measure the neutron albedo flux and its spatial and time variations. The neutron detector was a $^{10}BF_3$ counter within a moderator and surrounded by a ring of charged-particle proportional counters to discriminate against possible neutrons produced in the detector assembly by the cosmic radiation. A transistorized electronics system amplified the counter pulses, provided the necessary logic functions, counted the output data, and fed this data to the satellite telemetry system. Three such payloads were flown on polar-orbiting Agena satellites in 1962. The results show an albedo flux of .085 ± .030 n/cm^2 sec at the equator at 300 km altitude. This is in agreement with rocket measurements and calculations of others. Applying a correction at middle latitudes the measured flux is in good agreement with the present measurements at middle latitudes also. An appendix outlines calculations that were carried out to estimate the neutron production in the detector assembly and on the Agena due to the primary cosmic radiation. These estimates compare well with the experimental measurements of production in the detector assembly. The third Agena was launched 12 days after the Starfish nuclear explosion and was in a unique position to monitor leakage of electrons and protons from the trapping regions. While the detector assembly was not designed for monitoring low-energy electrons and protons, significant results can be extracted in many instances. (Dissertation Abstr.)

Low Temperature Physics

Refer also to abstracts 40543, 40845, and 42004.

41607 (LA-3342) A REVIEW OF QUASIPARTICLE AND JOSEPHSON TUNNELING IN SUPERCONDUCTORS. Brout, Robert (Los Alamos Scientific Lab., Univ. of California, N. Mex.). Oct. 1964. Contract W-7405-eng-36. 56p. Dep. mn; CFSTI, $3.00 cy, $0.75 mn.

After a brief treatment of the general theory of quantum-mechanical tunneling, a review of electron tunneling which occurs across metal-insulator-metal junctions, with emphasis on the cases where one or both metals are superconductors is given. Quasiparticle tunneling is first described by means of a phenomenological approach resembling that used in the theory of electrons tunneling into semiconductors. Then the important features of quasiparticle tunneling are developed using a more refined, microscopic theory, and the predictions are compared with the results of published experimental work. Finally, the theory of Josephson tunneling is treated in detail, and the important effects — d.c. current, presence of external field, Josephson skin depth, a.c. potential effect — are discussed along with experiments. (auth)

41608 (MIT-QPR-57, pp 59-65) MAGNETIC IMPURITY EFFECT ON SUPERCONDUCTOR TRANSITION TEMPERATURE—EXTENSION OF NAKAOKA'S THEORY. Gunther, Leon (Massachusetts Inst. of Tech., Cambridge).

Nakaoka's theory is extended to the case of superconductors, thus calculating the effect on the superconducting transition temperature T_c at low temperature. Two unusual results are reported. First, a higher T_c than that previously reported for given impurity concentration. Secondly, it is found that there is no finite critical impurity concentration which brings T_c to zero. (M.O.W.)

41609 EXPERIMENTS WITH SUPERCONDUCTING NIOBIUM–TIN CYLINDERS. Smith, P. F.; Spurway, A. H.; Lewin, J. D. (Rutherford Lab., Chilton, Berks, Eng.). Brit. J. Appl. Phys., 16: 947-56(July 1965).

Measurements are described of flux jumping and current density in hollow superconducting cylinders of sintered niobium–tin alloy. The possibility of improving both strength and flux jumping behavior by impregnating the pores of the material with other metals has been investigated; the expected increase in strength was obtained, but in all cases flux jumping was more frequent. The current density was little affected by silver, indium, or lead, but was considerably reduced by copper or tin. The performance of both plain and impregnated cylinders was also measured in an environment of helium gas at 4.2°K, and compared with the results obtained with liquid helium for different rates of change of applied field. Flux jumping occurred more frequently in the poorer thermal environment, but was less affected by rate of change of field. The results support the suggestion that flux jumping is reduced by penetration of liquid helium into the porous material. Subsidiary measurements discussed include the observation of very rapid "transfer of current" between a pair of concentric cylinders. (auth)

41610 TEMPERATURE DEPENDENCE OF THE CRITICAL FIELDS OF A SUPERCONDUCTING Pb–Tl ALLOY. Sekula, S. T.; Kernohan, R. H. (Oak Ridge National Lab., Tenn.). J. Appl. Phys., 36: 2895-97(Sept. 1965). (ORNL-P-1184).

Using a conventional ballistic technique, magnetization curves of a superconducting Pb–27% Tl alloy were obtained from the transition temperature T_c = 6.43°K down to 1.70°K. The thermodynamic critical field curve indicates that this alloy is of the strong coupling type. The Ginzburg-Landau parameters deduced from several features of the magnetization curves are given and their temperature dependence is compared to theoretical models. (auth)

41611 NUCLEAR SPIN-LATTICE RELAXATION IN TYPE II SUPERCONDUCTORS. Asayama, Kunisuke (Osaka Univ.); Masuda, Yoshika. J. Phys. Soc. Japan, 20: 1290-1(July 1965).

The nuclear spin-lattice relaxation time of vanadium and of niobium in the hard superconductors V–Ti and Nb–Zr alloys was measured in the temperature range of 4.2 to 1.4°K respectively. This relaxation time provides information on the electronic structures near the Fermi surface, and it provides a test of any theory of superconductivity. It is expected that the penetration of flux in the intermediate magnetic field is via quantized vortices. The experimental results are shown. (J.F.P.)

41612 BEHAVIOUR OF TYPE-II SUPERCONDUCTING CYLINDERS OF SMALL RADIUS NEAR THE LOWER CRITICAL FIELD. Boebel, G. (Universita, Genoa). Nuovo Cimento (10), 38: 1740-6(Aug. 16, 1965).

By applying Abrikosov's theory to a type-II superconducting cylinder of small radius, the critical fields for the formation of the first four flux threads are calculated. When the radius is smaller than about ten times the penetration depth, each thread grows up singly at different values of the applied magnetic field. (auth)

41613 MAGNETIZATION OF SUPERCONDUCTORS OF THE SECOND KIND. Fournet, G. (L.C.I.E., Fontenay-aux-Roses, France). Phys. Letters, 17: 210-11(July 15, 1965). (In French)

Results obtained previously on the thermodynamics of superconductors are applied to a simple model. This model is defined by assuming that each vortex possesses a core in which the density of the superconductor electrons is strongly reduced. At the exterior of the core the Londen relation is applied, and it is assumed that only the density of superconductor determines the value. Each vortex occupies a circular cylinder whose base area is equal to the area of the right section attributed to each vortex. Using this hypothesis the distribution of the field at the interior of a vortex is determined. For a first approximation the case where $(1 - p)$ is 0 is considered, p designates the mean ratio of the superconductor electron density in the core to the constant density at the exterior. (J.S.R.)

41614 INVESTIGATION OF MICROWAVE RADIATION EMITTED BY JOSEPHSON JUNCTIONS. Langenberg, D. N.; Scalapino, D. J.; Taylor, B. N.; Eck, R. E. (Univ. of Pennsylvania, Philadelphia). Phys Rev. Letters, 15: 294-7(Aug. 16, 1965).

The results of an investigation of the microwave radiation from a Josephson junction is reported. This includes a discussion of the junction-waveguide-magnetic-field configuration and a theoretical estimate of the magnitude of the radiated power, experimental observation of 10^{-12} W of emitted radiation at 9.2 Bc with a spectral purity greater than 1 part in 10^4, and observation and explanation of harmonic and fractional subharmonic radiation. (J.F.P.)

41615 NONANALYTIC FORM OF THE COEXISTENCE CURVE OF HELIUM AT THE CRITICAL POINT. Edwards, M. H. (Stanford Univ., Calif.). Phys. Rev. Letters, 15: 348-51(Aug. 23, 1965).

The density of saturated helium-4 vapor was previously measured along the coexistence curve from 0.30 to 0.994 T_c by refractive index measurements. The data were analyzed on the coexistence curve between 0.98 and 0.994 T_c. If, as it is now believed, singularities occur at the critical point, the whole expansion procedure of analysis is questionable. A reanalysis of these same data is now presented. The result of this analysis confirms that the critical point is indeed a nonanalytic point. (J.F.P.)

41616 ASYMMETRY IN THE CRITICAL SURFACE CURRENT OF TYPE-2 SUPERCONDUCTORS. Park, J. G. (Imperial Coll., London). Phys. Rev. Letters, 15: 352-6(Aug. 23, 1965).

Recently Fink (Phys, Rev. Letters, 14: 309(1965)) described how the order parameter near the plane surface of a type II superconductor varies with position when a magnetic field is applied parallel to the surface. This calculation is extended in order to see in what way his surface solutions are altered by a current, and in particular to calculate the critical current and how it varies with magnetic field. Whatever the total current in the surface layer may be, there is a current at any point at some depth below the surface, which flows normal to the field. Only the situation is considered in which the total surface current is directed normal to the field. (J.F.P.)

41617 STANDING WAVES OF THIRD SOUND IN He II FILMS. Knudsen, W. C. (Lockheed Missiles and Space Co., Palo Alto, Calif.). Phys. Rev. Letters, 15: 379-81 (Aug. 30, 1965).

Corroborating evidence is reported for the existence of third sound, the He II film equivalent of a shallow-water wave. The evidence consists of an oscillatory phenomenon observed previously in experiments conducted to measure the thickness of the He II film at large heights above the reference bath. The phenomenon was correctly attributed to an oscillatory motion of the film, but the mechanics of the motion were incorrectly surmised. The evidence suggests that standing waves of third sound were observed at a frequency of approximately 0.2 cps. The oscillations were initiated by abruptly changing the equilibrium thickness of the film at the end of a quarter-wavelength resonator of 125 cm lengths. The oscillations were detected by observing the time required to re-establish the initial film conditions at various phases of the wave motion. (J.F.P.)

41618 AN INTERMEDIATE STATE BETWEEN He I AND He II. Revzen, Michael; Ron, Amiram; Rudnick, Isadore (Israel Inst. of Tech., Haifa). Phys. Rev. Letters, 15: 384-6(Aug. 30, 1965).

The consequences of the eventuality of a possible interpretation of the results of a recent experiment that there is a discontinuity in the magnitude of the velocity of sound at the λ transition of helium-4 at vapor pressure are considered. It is argued that this indicates the existence of an intermediate state between He I and He II at pressures higher than the vapor pressure. The proposed phase diagram is depicted. It is calculated that the slopes of the two λ lines differ by 1% at vapor pressure. For the analysis a general expression is obtained for the velocity of sound in a form which renders the reasoning simpler. From the experimentally known features of the λ transition at vapor pressure, the possibility of a second-order phase transition and its concomitant velocity-of-sound discontinuity is ruled out. Finally, the only other possibility that can give such a discontinuity is considered, namely the presence of an intermediate state between He I and He II. The width of this new phase is then calculated from the available data. The expected discontinuity of the specific heat at constant volume is also discussed. (J.F.P.)

41619 VELOCITY OF SOUND IN LIQUID HELIUM AT ITS LAMBDA POINT. Rudnick, Isadore; Shapiro, Kenneth A. (Univ. of California, Los Angeles). Phys. Rev. Letters, 15: 386-9(Aug. 30, 1965).

Sound velocity measurements near the λ point of liquid helium at 9.75 kc are reported. The experimental test is not affected by attenuation and dispersion at this frequency. The method consisted of the determination of a plane-wave-mode resonance of a cylindrical chamber using as exciting and sending transducers two exactly similar electrostatic units. The velocity of the first sound is plotted as a function of temperature through the λ point. The sound velocity is also plotted as a function of $1/C_p$. In helium-I the two quantities are linearly related fitting the given equation over a range of two decades in temperature. But in helium-II the temperature-dependence variation of the velocity does not fit the equation. The data are replotted according to an experimental equation which holds over three decades in temperature variation. These results raise a serious question about the nature of the phase change at elevated pressures. (J.F.P.)

41620 OBSERVATION OF STABLE SUPERFLUID CIRCULATION IN LIQUID-HELIUM II AT THE LEVEL OF ONE, TWO, AND THREE QUANTUM UNITS. Whitmore, S. C.; Zimmermann, W. Jr. (Univ. of Minnesota, Minneapolis). Phys. Rev. Letters, 15: 389-92(Aug. 30, 1965).

A repetition and extension of Vinen's experiment is reported in which the circulation around a fine wire immersed in superfluid helium was measured by means of the influence that the circulation exerts on the transverse vibrations of the wire. In the absence of circulation a cylindrically symmetric wire can be regarded as having as its lowest modes of transverse vibration two degenerate circularly polarized modes. With circulation around the wire the degeneracy of these modes is removed by the lift force resulting in a splitting between the angular frequencies of the two modes. If the two modes are excited simultaneously with equal amplitude, the result is vibration of the wire in a plane which precesses with angular frequency in the same sense as the fluid is circulating. The elements of the apparatus are immersed in a liquid helium bath; and the wire is a quartz fiber on which a conducting layer of gold was evaporated. The results show that the motion of the superfluid can persist for long periods of time with the assembly carrying the tube and wire stationary. Also the circulation around the wire tends to show markedly greater stability at the anticipated quantum levels than at other values. As the wire diameter increased the maximum value of stable circulation observed also increased. (J.F.P.)

41621 EXPERIMENTS ON THE CREATION OF CHARGED QUANTIZED VORTEX RINGS IN LIQUID HE-

LIUM AT 1 deg K. Careri, G.; Cunsolo, S.; Mazzoldi, P.; Santini, M. (Universita, Rome). Phys. Rev. Letters, 15: 392-6(Aug. 30, 1965).

The origin of charged vortex rings of one quantum of circulation are experimentally investigated at 1°K; and these processes are discussed in the frame of the theory of Huang and Olinto (Phys. Rev., 139: A1441(1965)) recently proposed. The experiment consists of the determination of the drift velocity of ions in liquid helium at different field strengths, the temperature and pressure being kept constant. In the range of the reduced electric field studied, two hydrodynamical regimes were observed and identified, at limiting low fields the motion of a bare ion in a rarefied roton gas, and at high fields the motion of a charged vortex ring in the same excitation gas. It is concluded that while the capture of the vortex ring by the ion to form the charged vortex ring is a process observed in the experiments reported and well described by the theory of Huang and Olinto, the origin of the quantized vortex rings is still a matter of speculation. (J.F.P.)

41622 RANGE OF PERTURBATION OF THE ORDER PARAMETER IN HOMOGENEOUS AND ZERO-FIELD SUPERCONDUCTORS. Caroli, C. (Universite de Paris). Physik Kondensierten Materie, 3: 345-8(1965). (In French).

The range of a small local deviation from the equilibrium value of the order parameter in a superconductor depends on the temperature and on the nature of the superconductor. This calculation, valid from absolute zero to T_c for pure metals and non-magnetic alloys shows that even at $T \approx 0$, this range is of the order of the coherence length ξ_0. (auth)

41623 ELECTRONIC EXCITATIONS IN SUPERCONDUCTORS FREE FROM A SECOND SPECIES. I. DENSITY OF STATES. Cyrot, M. (Universite de Paris). Physik Kondensierten Materie, 3: 374-9(1965). (In French).

In a pure superconductor of the second kind, with a $\kappa \gg 1$, one can consider the region far from vortex lines as a BCS superconductor with a local superfluid velocity. Calculations are made for local density of states due to the excitations in such a superconductor, then the density of states of the excitations for the whole superconductor, except for the core regions. This density of states remains finite even near the gap and takes a non-zero value below the gap. (auth)

41624 ELECTRONIC EXCITATIONS IN SUPERCONDUCTORS FREE FROM A SECOND SPECIES. II. EXCITATIONS OF LOW ENERGY. Caroli, C.; Matricon, J. (Universite de Paris). Physik Kondensierten Materie, 3: 380-401(1965). (In French).

The low energy spectrum of a type II superconductor are studied in the mixed state, with a low density of vortex lines ($H \ll H_{c2}$). The states which are localized in the core of a line cannot be described in the frame work of the local approximation. These states correspond precisely to the lowest part of the energy spectrum. The energy gap for these excitations of order $\Delta_\infty^2/2E_F$ (Δ_∞ is the gap in zero magnetic field, E_F the Fermi energy) is considerably smaller than the gap in zero field. The corresponding density of states is of order $N(0)B/H_{c2}$ (B being the macroscopic induction in the material). These states determine the low temperature ($T \ll T_c$) properties of the superconductor. In that range of temperature: the ultrasonic attenuation is anisotropic but extremely small; there are two regimes for the relaxation of nuclear spins, depending on whether the diffusion of the nuclear magnetization is slow or fast with respect to the direct relaxation. In both regimes the relaxation is much faster than in a superconductor in zero field. (auth)

41625 THE GINSBURG-LANDAU EQUATIONS FOR ANISOTROPIC ALLOYS. Tilley, D. R. (Mullard Research Labs., Redhill, Surrey, Eng.). Proc. Phys. Soc. (London), 86: 289-95(Aug. 1965).

The calculation of Gor'kov for isotropic alloys is extended to anisotropic superconductors. The results are equations of the form proposed by Ginzburg. The mass tensor is given by the same expression as that found for a pure anisotropic material by Gor'kov and Melik-Barkhudarov, except that the factor relating to anisotropy of the energy gap is absent. It is pointed out that the mass tensor is proportional to the normal-state conductivity tensor. In an anisotropic material the parameter κ depends on the direction of the magnetic field; however, it changes with impurity content in exactly the same way as does κ for an isotropic material. (auth)

41626 ECONOMICAL LIQUID HELIUM CRYOSTAT AND OTHER CRYOGENIC APPARATUS. Whitehouse, J. E.; Callcott, T. A.; Naber, J. A.; Raby, J. S. (Purdue Univ., Lafayette, Ind.). Rev. Sci. Instr. 36: 768-71(June 1965).

A liquid helium cryostat which is inexpensive and simple to build is described. Its main features originate from the use of spherical metal floats arranged concentrically to form the body of the vessel. The tailpiece used with the cryostat provides for liquid helium to circulate in the sample holder. A mechanical valve allows the flow of liquid to be interrupted so that temperatures above 4.2°K may be maintained. A typical combination of cryostat and tailpiece has a capacity of 2 liters of liquid helium and will store this charge for nearly 4 days. A liquid nitrogen vacuum system cold trap and a liquid helium transfer tube are also described. The former also features the use of metal floats in its construction. The transfer tube has a degree of flexibility and a very small outer diameter. (auth)

41627 ON THE ROLE OF THE COULOMBIC INTERACTIONS BETWEEN ELECTRONS IN A SUPERCONDUCTOR. Batyev, E. G. (Inst. of Radiophysics and Electronics, Academy of Sciences, Novosibirsk, USSR). Soviet Phys.-Solid State (English Transl.), 6: 2846-52(June 1965).

Translated from Fiz. Tverd. Tela, 6: 3554-62(Dec. 1964).

Calculation of the coulombic interactions of the electrons in a superconductor is carried out in the framework of the isotropic model. The interaction is not assumed to be weak. In contrast to the investigation of Bogolyubov, Tolmachev, and Shirkov, the change of the dispersion and the damping of electrons because of the interaction with phonons is taken into consideration. Under the assumption that the gap is small in comparison with the Debye frequency, one is able to explain the dependence of the gap on the quantities characterizing the interaction and on the ion mass. The expression for the gap agrees qualitatively with the result of Tolmachev. (auth)

41628 DENSITY OF A WEAK MIXTURE OF He^3-He^4. Ptukha, T. P. Ukr. Fiz. Zh., 10: 353(Jan. 1965). (In Ukrainian).

The density of a He isotope solution depends on its ^3He concentration, decreasing when the light isotope content is increased. All previous studies were carried out at relatively high ^3He concentrations, ranging from 10 to 100%. The scope of measurements was extended to ^3He concentrations down to 10^{-2}%, determining the density of the solution by a pycnometric method. The concentration, expressed as the molar fraction $\epsilon = {}^3He/({}^3He + {}^4He)$, was calculated with an error of 1%; the atomic weights of the isotopes were taken as $\mu_3 = 3.0170$ and $\mu_4 = 4.0039$. The results indicated that the density of the mixture containing 10^{-2}% of ^3He is almost identical with that of pure ^4He. At experimental temperatures ranging from 1.347 to 2.167°K, the density of the dilute solutions was found to be about 0.6% lower than that of pure ^4He; the temperature dependence of the density of these dilute solutions was also similar to that of ^4He. (TTT)

41629 A PROOF OF THE ASYMPTOTIC ACCURACY OF THE B. C. S. SUPERCONDUCTING GROUND STATE. Tour, Yung; Suen, Shin; Chow, Shih-hsun. Wu Li Hsueh Pao, 21: 880-3(Apr. 1965). (In Chinese).

It is shown that the Schrödinger perturbation theory series, perturbed by the interaction of residual terms of the hamiltonian treated by the uv linear transformation, is indeed convergent. On the basis, it is possible to prove the asymptotic accuracy of the superconducting ground state. The proof was carried out by using the convergence

conditions of Wigner's perturbation theory series and that of the ladder diagrams. (TTT)

41630 A NEW METHOD FOR MEASURING THE CRITICAL CHARACTERISTIC CURVES OF SUPERCONDUCTORS. Chen, Pu-fun; Cheng, Guo-kuang; Kuan, Wei-yen. Wu Li Hsueh Pao, 21: 879-96(May 1965). (In Chinese).

A persistent-current method for measuring critical characteristic curves of superconductors is described. In comparison with the usual four-probe method, this new method possesses the following advantages: The $I_c(H)$ curves thus determined have clear physical significance; the technical difficulty of introducing heavy current into the cryostat is avoided; there is no danger of burn-out of the specimen tested. The $I_c(H)$ curve of cold worked niobium wire has been determined with this method. The result confirms the existence of the peak in the $I_c(H)$ characteristic observed previously with the four-probe method. (auth)

41631 EXPERIMENTAL STUDIES OF THE TUNNEL EFFECT FOR PHOTON-EMITTING COOPER PAIRS. Yanson, I. K.; Svistunov, V. M.; Dmitrenko, I. M. (Inst. of Physics and Tech. of Low Temperatures, Academy of Sciences, Ukrainian SSR). Zh. Eksperim. i Teor. Fiz., 48: 976-9(Mar. 1965). (In Russian).

An experiment aimed at observing photon emission upon occurrence of alternating superconducting current in a structure of the type $Sn-SnO_2-Sn$ is described. Tin films of width 1.17 mm and thickness ~2000 Å were evaporated on a glass substrate at a right angle, and a thin oxide layer was formed between the films. The structure was placed in a rectangular waveguide parallel to its side wall, one of the films being parallel to the wave propagation vector in the guide. A small constant magnetic field was applied in the same direction. The entire system was placed in a liquid-helium cryostat, and the volt-ampere characteristic of the structure was plotted on an automatic potentiometer at 1.57°K for various values of the magnetic field. The step observed in the response of a tuned detector in a field of 1.5 gauss at a bias of 19.8 μv corresponding to a wavelength of the order of 3 cm, together with other steps observed at nearly the same voltage for various magnetic fields, is interpreted as direct experimental proof of the possibility of Cooper pairs tunneling between two superconductors with emission of photons. An inverse experiment in which the tunnel structure was irradiated by an external microwave generator was also performed and yielded similar evidence. (ATD)

41632 CALCULATION OF SUPERCONDUCTING SOLENOID CHARACTERISTICS. Manuilov, V. G. Zh. Tekhn. Fiz., 35: 1077-83(June 1965). (In Russian).

The stresses in a multilayer solenoid were calculated. The turns of the solenoid were treated as rings with rectangular cross sections and were assumed to be packed tightly. The field of each ring was calculated with a handbook formula and the field at any point was obtained by summing the contributions from all the turns. The sums were evaluated numerically with the aid of a computer; the field strength at the center of the solenoid, the maximum field strength on the inner surface, and the maximum radial stress in the solenoid are tabulated as functions of two shape parameters. The stresses were calculated under the assumption that the outer surface of the solenoid is constrained by a rigid force ring. The use of the tables for design calculations is illustrated by two numerical examples concerning superconducting solenoids. (ATD)

41633 MEGACYCLE FREQUENCY SECOND SOUND (thesis). Notarys, Harris Anthony. Pasadena, Calif., California Inst. of Tech., 1964. 39p.

Generation and detection of second sound were extended to 25 Mc/sec using a resonant cavity technique. Investigations show the attenuation coefficient of second sound is proportional to the square of the frequency up to 1.3 Mc/sec at 1.22°K, 4 Mc/sec at 1.47°K, and 10 Mc/sec at 1.9 to 2.1°K, in agreement with Khalatnikov's theoretical predictions and with previous low-frequency measurements. (Dissertation Abstr.)

41634 QUANTIZED VORTEX RINGS IN SUPERFLUID HELIUM (thesis). Rayfield, George William. Berkeley, Calif., Univ. of California, 1964. 90p.

Evidence is presented to show that charged particles in superfluid helium at low temperatures can be accelerated to create freely moving charge-carrying vortex rings in the liquid. The circulation of these vortex rings can be determined by measuring their energy and velocity; it was found to be equal to one quantum h/m, where h is Planck's constant and m is the mass of a helium atom. The core radius of the vortex is approximately 1Å. The dynamical properties of such a vortex ring moving under the influence of external forces can be described by a dispersion relation ($E \propto p^{\frac{1}{2}}$) connecting its energy E and momentum p; it can also be understood in detail in terms of the hydrodynamic Magnus force. Experiments are described which verify the essential validity of this dynamical analysis. Vortex rings can interact with various quasi-particles in the liquid, i.e., with rotons, phonons, and ^{3}He impurities. The scattering of these quasi-particles by vortex rings can be investigated by experiments designed to study the temperature dependence of the rate of energy loss of such rings moving through the liquid. In this way it is possible to measure the effective momentum-transfer cross sections for scattering of the various quasi-particles by vortex lines. The cross section thus deduced is 9.5 Å for scattering of rotons and 18.3Å for scattering of ^{3}He atoms. The experiments yield only scant information about scattering of phonons, but are not inconsistent with the magnitude of the phonon scattering cross section expected on theoretical grounds. (Dissertation Abstr.)

41635 AN ANALYTICAL INVESTIGATION OF FILM FREE CONVECTION HEAT TRANSFER TO LIQUID HELIUM II (thesis). Rivers III, William Jones. Lafayette, Ind., Purdue Univ., 1964. 200p.

Free convection heat transfer from a solid surface to liquid Helium II in the presence of a film of either liquid Helium I or helium gas was analyzed mathematically. The characteristics of this phenomenon were assumed to be the same in either case except for the film fluid properties and the involvement of latent heat at the film interface only when the film is helium gas. The analysis was restricted to only two heater shapes, a vertical flat plate and a horizontal circular cylinder, each with an isothermal surface; and the physical properties of the film fluid were assumed constant. The integral forms of the boundary layer equations were used to describe mathematically the convection process within the film. The velocity and temperature profiles in the film were approximated by fourth-degree polynomials whose coefficients were evaluated by applying a system of boundary conditions which were derived in the usual fashion but were based on assumed discontinuities in both the temperature and velocity profiles at the interface. The introduction of these profile expressions into the integral equations reduced them to a system of three first-order ordinary differential equations which were then integrated numerically on a digital computer using the Runge–Kutta integration technique. The results indicated that this phenomenon can occur in any one of three rather distinct modes depending upon the relative magnitudes of the temperature drop across the film and temperature drop across the interface. (Dissertation Abstr.)

41636 AN INTRODUCTION TO THE THEORY OF SUPERFLUIDITY. Khalatnikov, I. M. Frontiers in Physics. New York, W. A. Benjamin, Inc., 1965. 217p. $9.00.

Translated by Pierre C. Hohenberg.

A unified treatment of the theory of superfluidity is presented covering elementary excitations, hydrodynamics, kinetic phenomena, and impurities in helium II. (D.C.W.)

41637 DISTRIBUTION OF MAGNETIC FIELDS AND CURRENTS IN COLD-WORKED TYPE II SUPERCONDUCTORS. Coffey, Howard T. (Westinghouse Electric Corp., Pittsburgh). 16p. (CONF-758-45). Gmelin, AED-CONF-65-003-95.

From American Physical Society Meeting, New York, Jan. 1965.

The magnetic field was measured in the gap between two superconducting rods placed in a superconducting magnet. From these measurements the induced current density and the Lorentz force acting on the pinning centers is deduced. The phenomena of flux jumping and flux creeping are clearly illustrated. (auth)

41638 SUPERCONDUCTING MAGNET FOR VARIABLE BANDWIDTH TRAVELING WAVE MASERS. Troxel, L. M. (Bell Telephone Labs., Inc., Allentown, Penna.). 14p. (CONF-650403-5). Gmelin, AED-CONF-65-038-2.

From International Conference on Non-Linear Magnetics, Washington, D. D.

In order to amplify microwave signals with optimum gain, the ruby crystal of a 4 gc/s traveling wave maser requires a 3300 gauss magnetic field uniform to 0.1%. By properly varying the magnetic field along the length of the ruby crystal, the bandwidth of the maser amplifier can be increased at the expense of gain. A compact superconducting magnet is described which provides the required magnetic field. The field is obtained from a short solenoid, which is made to appear infinitely long through the use of a low reluctance enclosure. A portion of the resulting uniform field can be modified by a superconducting trimmer coil imbedded in the low reluctance enclosure. This coil produces an adjustable stepped magnetic field which allows for varying maser bandwidth. Alternatively, it can be used to operate two independent masers in a single magnetic structure. A high degree of reliability is attained. Problems of flux jumping have been avoided by a design in which the diamagnetic (magnetic insulating) properties of superconducting materials play a minor role. (auth)

41639 CRITICAL CURRENT DEGRADATION IN WIDE SAMPLES OF HIGH FIELD STRIP SUPERCONDUCTORS. Hoag, Ethan D. (Avco-Everett Research Lab., Everett, Mass.). 9p. (CONF-794-11). Gmelin, AEC-CONF-64-204-20.

From Magnetism Conference, Minneapolis, Nov. 1964.

Measurements of the magnetic anisotropy of critical current in samples wide enough for use in large magnets reveal a degradation effect in strip superconductors. The effect is manifested as a truncation or chopping off of the peaks of the anisotropy curves of these samples. With narrow samples the anisotropy curves (average critical current density plotted as a function of magnetic field direction) normally display a well defined peak centered about the direction parallel to the rolling plane of the strip. With wide samples, however, this peak appears progressively more truncated as the width is increased and the truncation level (i.e. maximum current density) is roughly inversely proportional to the width so that the total current tends to remain constant, independent of width. For Nb-25% Zr strip 0.051mm thick, this limiting current is approximately 150A at a field of 4 Wb/m^2 for widths between 1 and 10mm. 1.32mm wide samples display little or no truncation and have maximum current densities of 1.8×10^5 amp/cm^2 whereas 10mm wide samples show severe truncation and have maximum current densities of 1.5×10^4 amp/cm^2. (auth)

Neutron Physics

See also REACTOR TECHNOLOGY — Criticality Studies.

Refer also to abstract 41174.

41640 (GA-6323) INTEGRAL NEUTRON THERMALIZATION. Quarterly Progress Report for the Period Ending March 31, 1965. Beyster, J. R.; Huffman, D.; Koppel, J. U.; Naliboff, Y. D.; Neill, J. M.; Profio, A. E.; Russell, J. L. Jr.; Young, J. A.; Young, J. C. (General Atomic, San Diego, Calif. John Jay Hopkins Lab. for Pure and Applied Science). Apr. 22, 1965. Contract AT(04-3)-167. 44p. Dep. mn; CFSTI, $2.00 cy, $0.50 mn.

The results of the thermalization program are discussed. New differential scattering measurements for H_2O, D_2O, and $ZrH_{1.85}$ are compared with predictions based on the currently available molecular models used for these moderators. New experimental spectral measurements are reported as well as work in the compilation of the Neutron Spectrum Book. (M.O.W.)

41641 (MIT-2344-3, pp 137-54) OSCILLATING NEUTRON SOURCE EXPERIMENT. Sefchovich, E. (Massachusetts Inst. of Tech., Cambridge. Dept. of Nuclear Engineering).

The theoretical basis of the oscillating-neutron-source experiment is briefly reviewed and the results of the experimental work are presented. (M.O.W.)

41642 (NAA-SR-10853) ANALYSIS OF NEUTRON TRANSMISSION THROUGH SLABS OF LITHIUM HYDRIDE. Hubner, R. S. (Atomics International, Canoga Park, California). July 25, 1965. Contract AT-11-1-GEN-8. 80p. Dep. mn; CFSTI $1.00 cy, $0.50 mn.

The results of the analyses of the ORNL Tower Shielding experiments on fast neutron transmission through lithium hydride slabs are presented and compared to the experimental data. Satisfactory agreement in the scattered dose is noted in all cases with the maximum deviation at the 30-in. thickness being only 25%. The calculated transmitted spectra and n^{th} collision doses are presented. Modifications to the Monte Carlo techniques used in the analyses are presented in the Appendix. (auth)

41643 (ORNL-TM-1184) PROPAGATION OF NEUTRON WAVES THROUGH HETEROGENEOUS MULTIPLYING AND NONMULTIPLYING MEDIA. Cain, V. R. (Oak Ridge National Lab., Tenn.). Aug. 1965. Contract W-7405-eng-26. 110p. Dep. mn; CFSTI $4.00 cy, $0.75 mn.

Thesis submitted to Univ. of Florida, Gainesville.

Prediction of the behavior of neutron waves in heterogeneous media is performed using one-group diffusion theory and age-diffusion theory. The one-group theory is used in two different, finite geometries which allow reduction to a one-dimensional problem and to a two-dimensional problem. These cases result in diffusion kernels, or Green's functions, for the two finite configurations. The theory is then extended to include Fermi-age, or continuous slowing-down, theory for higher energy neutrons. The approach is similar to the Feinberg-Galanin heterogeneous reactor theory except that it is applied to a finite geometry and includes time dependence. A finite diffusion kernel is obtained which is similar to the results of the simpler calculations. In addition, a finite-medium, Fermi-age kernel results which describes the behavior of the slowing-down neutrons in the finite geometry. Both the one-group and the age-diffusion developments are used to calculate numerically sample configurations which are suitable for experimental verification. These include rectangular assemblies of graphite and heavy water which have poison or fuel rods inserted. In order to demonstrate better the improvements of this work over the Feinberg-Galanin theory, an extension to critical assemblies is made. This offers the possibility of doing criticality calculations for physically small assemblies which are not amenable to homogenization techniques. Using the age-diffusion theory results, it is also shown that data from neutron wave experiments may be processed in such a way as to give experimental measurements of both the diffusion and the slowing-down kernel. (auth)

41644 DERIVATION OF THE NORDHEIM EQUATION FROM THE DIFFUSION EQUATION. Oezemre, Ahmed Yuksel. Istanbul Univ., Fen Fak. Mecmuasi, Seri A, 27: 41-7(1962). (In French).

The Nordheim equation is derived, based uniquely on the diffusion equation of thermal neutrons by adding another term to account for the contribution of the delayed neutrons slowed by the other neutrons in the area. The consideration of a single differential equation for obtaining the Nordheim equation is an important simplification due to its agreement with the present method which uses the diffusion equation of thermal neutrons and the coupled equations giving the

densities of fission products which emit the delayed neutrons. (J.F.P.)

41645 SUGGESTION FOR THE DEMONSTRATION OF NEUTRON WAVE REFLECTION EFFECTS USING STATISTICAL CORRELATION TECHNIQUES IN ELLIPTIC SYSTEMS. Srinivasan, M. (Atomic Energy Establishment Trombay, India). J. Nucl. Sci. Technol. (Tokyo), 2: 272-3(July 1965).

Properties of an ellipse suggest that if a disturbance emanating from one of the foci gets reflected at the boundary, then all reflected waves would constructively interfere at the other focus. Construction of an experiment in which a pulse of neutrons is placed at one of the foci of a reflected elliptical medium and the reflected pulse is looked for at the other focus is discussed. (M.C.G.)

41646 NEUTRON-SPECTRUM MEASUREMENTS IN H_2O AND D_2O. Young, J. C.; Neill, J. M.; Houston, D. H.; Beyster, J. R. (General Atomic Div., General Dynamics Corp., San Diego, Calif.). Nucl. Sci. Eng., 23: 34-44 (Sept. 1965). (GA-6034).

Spatially dependent neutron-spectrum measurements were made in both light and heavy water, using the linear accelerator facility and standard time-of-flight techniques. The measurements were made with varying geometrical arrangements, and both 1/v and resonance absorbers were utilized to simulate reactor poisons. The measurements were compared to calculations performed with an S_N transport code utilizing the bound scattering models proposed for these moderators. The agreement between theory and experiment for the Nelkin model for H_2O and Honeck's extension of this model to D_2O is shown to be very satisfactory for the cases studied. (auth)

41647 PULSED-DECAY AND EXTRAPOLATION-LENGTH MEASUREMENTS IN GRAPHITE. Davis, S. K.; De Juren, J. A.; Reier, M. (Atomics International, Canoga Park, Calif.). Nucl. Sci. Eng., 23: 74-81(Sept. 1965).

Measurements of the shape of the fundamental mode of a thermalized neutron pulse in graphite for rectangular stacks has yielded a value of the extrapolation length, $d = 1.825 \pm 0.025$ cm. The pulsed-neutron decay constants in graphite were measured over a buckling range from 1.946×10^{-3} to 1.230×10^{-2} cm^{-2} and fitted to three- and four-term power series in the buckling. To fit points at bucklings greater than 6.0×10^{-3} cm^{-2}, a cubic fit is necessary. An iterative method of fitting the decay constants results in an extrapolation length of 1.78 ± 0.01 cm. The diffusion constant was $(2.0896 \pm 0.0093) \times 10^5$ cm^2/sec, and the diffusion cooling constant was $(3.77 \pm 0.35) \times 10^6$ cm^4/sec at a density of 1.689 g/cm^3. A technique of correcting the decay constants for the effect of spectral cooling was developed. The decay constants corrected to room temperature can be fitted as a linear function of the buckling. This method interates on the heat-transfer coefficient, γ, and gives a value of $\gamma = 1633 \pm 89$ sec^{-1} for graphite. The heat-transfer coefficient relates the rate of energy transfer from a moderator to a cooled-neutron spectrum. With this approach the entire buckling range can be fitted with three parameters. (auth)

41648 THERMOPYL, A PROGRAM FOR CALCULATING THE THERMAL NEUTRON ENERGY SPECTRUM IN HETEROGENEOUS LATTICE CELLS. Maerkl, H.; Raum, H. (Siemens-Schuckertwerke AG, Erlangen, Ger.). Nukleonik, 7: 247-57(May 1965).

A program for calculating the thermal neutron energy spectrum in heterogeneous lattice cells is described that is based on a collision probability theory. A simplified and yet sufficiently accurate method for computing the collision probabilities is derived. The program was extensively checked against activation experiments and calculation methods developed elsewhere. The THERMOPYL results are found to be in quite satisfactory agreement with the Chalk River measurements and in excellent agreement with the THERMOS and Monte Carlo results. (auth)

41649 PROGRAM SYSTEM FOR THE SOLUTION OF THE MULTI-GROUP NEUTRON DIFFUSION EQUATION. Warmbold, I.; Ehret, B.; Wolf, H.-P. (Siemens-Schuckertwerke AG, Erlangen, Ger.). Nukleonik, 7: 257-60(May 1965). (In German).

Programs for the numerical solution of the one- and two-dimensional diffusion equations are described, which were formulated with respect to multiple take-off and expansion possibilities. (tr-auth)

41650 MULTIPLE SCATTERING OF A NARROW BEAM OF FAST NEUTRONS. Budyanskii, G. M. (Moscow Engineering-Physics Inst.). Soviet J. Nucl. Phys. (English Transl.), 1: 155-8(Aug. 1965).

Translated from Yadern. Fiz., 1: 224-8(Feb. 1965).

The spatial and angular distributions are established for a narrow beam of fast neutrons passing through some layer of scattering matter. The inelastically scattered neutrons are regarded as being knocked out of the beam. A correlation exists between the angular and coordinate distributions. Starting from general distribution functions, formulas are derived for the distribution functions with respect to the plane and solid angles observed in the registration of neutrons with sufficiently long and short detectors, respectively. A spatial distribution function (independent of the deflection angles) is obtained for the beam. The distribution of the beam density with respect to the coordinate and to the radius is determined. Accurate to small terms of second order, the distribution functions are similar to a resonance curve and are not at all similar to the Gaussian distribution. (auth)

41651 APPROXIMATE SOLUTION FOR THE NONLINEAR TRANSPORT EQUATION. Moskalev, O. B. Zh. Vychislitel. Mat. i Mat. Fiz., 5: 561-5(May-June 1965). (In Russian)

The successive approximation method usually employed for solving the nonlinear stationary neutron transport equation necessitates lengthy calculations. In order to simplify the required computations, an approximation was developed, splitting the solution according to small parameters. The chief member of the operation is a constant, multiplied by the eigenfunction of the linear problem. The method was applied numerically in the case of a plane, one-dimensional reactor. The neutron distribution of the reactor was assumed to follow the one-group diffusion equation, with a coefficient dependent on the internal reactor temperature; the temperature distribution within the reactor was described by the heat transfer equation. The computed values were found to lie in the same order of magnitude as the actual physical data. By homogenizing the reactor temperature, a simple relation was derived between the Laplacian in the cold state and the Laplacian corresponding to operation at a given power level. (TTT)

41652 TEMPERATURE-DEPENDENT NEUTRON THERMALIZATION (thesis). Charyulu, Varada P. T. Ames, Iowa, Iowa State Univ., 1964. 76p.

A theoretical study was made of the effect of temperature on the spatial distribution of thermal neutron flux spectrum in a source-free absorbing medium. The medium consists of two dissimilar contiguous semi-infinite regions. A step-type temperature variation in the medium is considered with the discontinuity occurring at the interface of the two regions. The entire medium is treated as a heavy monoatomic gas whereby the scattering is taken to be isotropic in the laboratory system and the scattering cross section is assumed to be independent of energy. The absorption cross section is assumed to obey the 1/V law. Analytical solutions are presented for the second-order partial differential equation resulting from the stated assumptions. The boundary conditions imposed on the system are that the flux shall vanish at zero energy and have finite energy moments everywhere in the medium. Also, far from interface of the two temperature regions, the flux spectrum is assumed to be independent of position. Besides, at the temperature interface the flux together with its first derivative is assumed to be continuous. An analytical solution is developed by solving the equation separately in the two regions by the method of separation of variables and matching the solutions for each region as the interface

by the boundary conditions. The asymptotic behavior of the solution is investigated for large values of energy. The effect of the absorption parameter on the solutions for large order of eigenvalues was also investigated. Terms higher than second order in the absorption parameter were neglected. Approximate solutions were developed to the same problem as well as a similar problem in a non-absorbing medium. (Dissertation Abstr.)

41653 SOME THEOREMS ON NEUTRON FLUCTUATIONS AND FLUCTUATION SPECTRA. Osborn, R. K.; Akcasu, Z. (Univ. of Michigan, Ann Arbor). 23p. (CONF-650413-6). Gmelin, AED-CONF-65-042-12.

From Symposium on Neutron Dynamics and Control, Tucson, Ariz.

Three theorems based on the equations of neutron fluctuations are discussed. The first relates to the meaning of the notion of fluctuations in critical assemblies. It is shown that the implication of the point-reactor kinetic theory of fluctuations is not peculiar to point-reactor kinetics, but is equally inherent in phase-space kinetics. The second theorem establishes a connection between the singlet and doublet theories of fluctuations. It shows that an inhomogenous equation for the doublet density can be deduced from both theories. The third theorem establishes in general, though formal, terms the similarities and dissimilarities between the singlet and doublet interpretations of a fluctuation spectrum measurement. (L.B.S.)

41654 INVESTIGATION OF THE RISE PORTION OF PULSED NEUTRON CURVES. Leonard, B. E. (North Carolina State Univ., Raleigh). 27p. (CONF-650413-11). Gmelin, AED-CONF-65-042-6.

From Symposium on Neutron Dynamics and Control, Tucson, Ariz.

The possibility of the use of pulsed neutron curves to determine fast group and slowing-down constants is proposed. Two group and Fermi age theories are applied to study, in particular, the rise portion of pulse neutron curves. (L.B.S.)

Nuclear Properties and Reactions

Refer also to abstracts 40938, 41324, 41334, 41439, 41513, and 42154.

41655 (BNL-934) A STUDY OF GENERALIZED LEVEL DENSITY BY THE METHODS OF DIFFERENTIAL-RECURRENCE EQUATIONS. Kahn, Peter B.; Porter, Charles E. (Brookhaven National Lab., Upton, N. Y.). July 1965. Contract AT-30-2-GEN-16. 27p. Dep. mn; CFSTI, $2.00 cy, $0.50 mn.

Level density formulas are derived for certain unitary generalized ensembles. The results are in agreement with those derived by other methods of approximation. (auth)

41656 (BNL-9245) SEARCH FOR J-DEPENDENT NEUTRON STRENGTH FUNCTIONS IN THE RARE EARTH REGION. Chrien, R. E.; Mughabghab, S. F. (Brookhaven National Lab., Upton, N. Y.). May 1965. Contract AT-30-2-GEN-16. 7p. (CONF-650706-21). Dep. mn; CFSTI, $1.00 cy, $0.50 mn.

From International Conference on the Study of Nuclear Structure with Neutrons, Antwerp.

An investigation was carried out to detect a possible dependence of the strength function on target spin I in the rare earth region. Ten isotopes of gadolinium, dysprosium, and ytterbium ranging from A = 155 to A = 173, and from I = 0 to I = $\frac{5}{2}$, were investigated. The results are obtained from a measurement of the $E^{-\frac{1}{2}}$ energy dependence of the average cross section in the kev region, and from the parameters of resolved resonances in the ev region. (M.O.W.)

41657 (DP-986) RADIATION PROPERTIES OF CALIFORNIUM-252. Stoddard, Dean H. (Du Pont de Nemours (E. I.) and Co., Aiken, S. C. Savannah River Lab.). June 1965. Contract AT(07-2)-1. 12p. Dep. mn; CFSTI, $1.00 cy, $0.50 mn.

The radiation properties of californium (~72 wt % ^{252}Cf) produced by thermal neutron bombardment of transplutonium isotopes are presented. The gamma and neutron radiations associated with this material were converted to dose rate, for evaluation by isotope users. (auth)

41658 (IAE-655) REAKTSII $He^3(d,t)2p$ I $He^3(He^3,\alpha)2p$. (The Reactions $^3He(d,t)2p$ and $^3He(^3He,\alpha)2p$). Artemov, K. P.; Gol'dberg, V. Z.; Ogloblin, A. A.; Rudakov, V. P.; Serikov, I. N.; Chuev, V. I. (Institut Atomnoi Energii, Gosudarstvennyi Komitet po Ispol'zovaniyu Atomnoi Energii SSSR, Moscow). 1964. 9p. Dep. mn.

Energy spectra of tritons and alpha particles at small angles were obtained in the reactions $^3He(d,t)2p$ and $^3He(^3He,\alpha)2p$. Measurements were performed at deuteron energies of 20 to 25 Mev and ^3He ion energies of 16, 26, and 36 Mev. In their shape, the spectra are analogous to the spectrum of neutrons from the reaction D(p,n)2p. (tr-auth)

41659 (IAE-835) REAKTSIYA $He^4(He^3,n)Be^6$. (The Reaction $^4He(^3He,n)^6Be$). Gulyamov, M.; Rybakov, B. V.; Sidorov, V. A. (Institut Atomnoi Energii, Gosudarstevnnyi Komitet po Ispol'zovaniyu Atomnoi Energii SSSR, Moscow). 1965. 10p. Dep. mn.

The neutron spectrum from the reaction $^4He(^3He,n)^6Be$ at a ^3He-ion energy of 29.8 ± 0.3 Mev was investigated using a multichannel fast-neutron time-of-flight spectrometer. Neutron groups corresponding to the ground and first-excited states of the nucleus ^6Be were found. The energy of the ^6Be excited state ($E^* = 1.73 \pm 0.1$ Mev) and its width ($\Gamma = 1.7 \pm 0.3$ Mev) were determined. The differential cross sections for the production of both groups of neutrons were measured at angles of 0, 7.5, 15.0, 22.5, 30.0, and 45.0° to the incident beam. (tr-auth)

41660 (ISS-65/3) L'ESPERIENZA (e,e'p): RISULTATI OTTENUTI E SVILUPPI FUTURI. (The (e'e,p) Experiment: Results Obtained and Planned Proposals). Venuti, G. Campos; Salvadori, P. (Istituto Superiore di Sanita, Rome (Italy). Laboratori di Fisica). Jan. 22, 1965. 45p. Dep. mn.

After having briefly summarized the reasons for an (e'e,p) experiment, the apparatus which was used to study the binding energies of protons in 1s and 1p shells of ^{12}C, and in 1s, 1p and 2s 1d in ^{27}Al and ^{32}S, is extensively discussed. Experimental curves for these nuclei versus the energy of the incident electrons are then reported together with their graphical decompositions into components corresponding to the different levels. A new device to measure the binding energies and the angular distributions of the protons produced in the (e,e'p) reaction is shown. Finally, requests for the use of the synchrotron are presented in order to study a certain number of nuclei in a year's time. (auth)

41661 (JINR-P-2158) NEITRONNYE REZONANSY IZOTOPOV ITTERBIYA. (Neutron Resonances of Ytterbium Isotopes). Wang, Nai-yang; Karzhavina, E. N.; Popov, A. B.; Yazvitskii, Yu. S.; Chi-chuang, Yao (Joint Inst. for Nuclear Research, Dubna (USSR). Lab. of Neutron Physics). 1965. 12p. Dep. (mn).

A slow neutron spectrometer was used to make the transmission measurements of the natural mixture of ytterbium and the radiative capture of ^{171}Yb, ^{172}Yb, ^{173}Yb, ^{174}Yb, ^{176}Yb, isotopes in the energy range up to 150 ev. The resonances were indentified for the first time and their parameters were determined. The values of the strength function for ^{171}Yb and ^{173}Yb were obtained to be ($^{171}S_0 = (1.1 \pm 0.4) \cdot 10^{-4}$, $^{173}S_0 = (2.4 \pm 0.9) \cdot 10^{-4}$). The number of the observed levels in ^{171}Yb and ^{173}Yb allows the parameter σ in the Bethe formula, which shows a dependence of the level density on the excitation energy and on the compound nucleus spin (σ = 2.5), to be estimated. (auth)

41662 (JINR-P-2176) ENERGETICHESKAYA SHCHELY V YADERNOI MATERII DLYA POTENTSIALOV S MYAGKOI SERDTSEVINOI. (Energy Gap in Nuclear Matter in the Case of Soft Core Potentials). Boshan, P. (Joint Inst. for Nuclear Research, Dubna (USSR). Lab. of Theoretical Physics). 1965. 9p. Dep. mn.

An equation for the gap was solved in the case of soft

core potentials. For the potentials obtained from the scattering data the gap is absent. In the case of the effective potential the finite nuclei gap was obtained which coincides approximately with the experimental one. (auth)

41663 (JINR-P-2184) ISSLEDOVANIE YADERNYKH REAKTSII GELIYA-3 S UGLERODOM. (Investigation of Nuclear Reactions of Helium-3 With Carbon). Gromov, A. V.; Kashlik, K.; Kobzev, A. P.; Nedvedyuk, K.; Salatskii, V. I.; Sizov, I V. (Joint Inst. for Nuclear Research, Dubna (USSR). Lab. of Theoretical Physics). 1965. 24p. Dep. mn.

The differential cross sections and angular distributions of the following reaction channels: $^{12}C(^3He,\alpha_0)^{14}C$; $^{12}C(^3He,p_0)^{14}N$; $^{12}C(^3He,p_1)^{14*}N$; $^{12}C(^3He,p_2)^{14*}N$ were measured in the energy range of $^3He-1.0-1.8$ Mev. The excitation functions of all four channels show the resonance structure at $E_{^3He} = 1.3$ Mev which is assigned to the levels of the compound nucleus of ^{15}O. The angular distributions of the reaction products are asymmetrical with respect to 90° in the c.m.s. and have a complicated character. The total reaction cross sections were obtained. (auth)

41664 (JINR-P-2193) MEDLENNYE CHASTITSY ISPUSKAEMYE V REAKTSIYAKH RASSHCHEPLENIYA. (Slow Particles Emitted in Stripping Reactions). Mekhedov, V. N. (Joint Inst. for Nuclear Research, Dubna (USSR). Lab. of Nuclear Problems). 1965. 22p. Dep. mn.

Experimental data are considered on emission in stripping reactions of secondary slow particles (with energies below 20–30 Mev). The difference in the production of neutron-rich (^3H, ^6He) and neutron-deficient (^7Be, ^{11}C, ^{18}F etc) radioactive fragments can be qualitatively accounted for if one assumes that the surfaces of heavy nuclei are enriched in neutrons. (auth)

41665 (JINR-P-2209) OPREDELENIE SPINOV NEITRONNYKH REZONANSOV YADER Ho^{165} PO PROLUSKANIYU POLYARIZOVANNYKH NEITRONOV CHEREZ POLYARIZOVANNUYU MISHEN V OBLASTI ENERGII 0-55 ev. (Determination of Spins of Ho^{165} Neutron Resonances by Transmission of Polarized Neutrons Through a Polarized Target in the Energy Interval 0-55 ev). Alfimenkov, V. P.; Lushchikov, V. I.; Nikolenko, V. G.; Taran, Yu. V.; Shapiro, F. L. (Joint Inst. for Nuclear Research, Dubna (USSR). Lab. of Neutron Physics). 1965. 20p. Dep. mn.

Polarized neutron transmission measurements on a polarized target of polycrystalline metallic holmium were carried out. A polarized proton target of monocrystals of the double lanthanum magnesium nitrate with polarization of 44% was used for neutron polarization. The nuclear polarization of the sample was obtained by using the Rose-Gorter method at temperature of 0.35°K and magnetic field of 15 kOe. The spins of eleven excited states of compound nucleus ^{165}Ho corresponding to the neutron resonance at energies of 3.92; 8.1; 12.6; 18.1; 21.0; 35.3; 37.0; 39.4; 47.3; 51.24; 54 ev were found to be 4,3,4,3,4,3,3(4),4,3,3 and 3(4), respectively. (auth)

41666 (JINR-P-2233) DVOINOE pp-RASSEYANIE PRI 667 Mev. (Double pp-Scattering at 667 Mev). Azhgirei, L.; Kumekin, Yu.; Meshcheryakov, M.; Nurushev, S.; Solov'yanov, V.; Stoletov, G. (Joint Inst. for Nuclear Research, Dubna (USSR). Lab. of Nuclear Problems). 1965. 8p.

Experiments on double pp-scattering at 667 Mev are described. The data obtained are analyzed by expanding the product $\sigma(\theta) \cdot P(\theta)$ in Legendre polynomials. Together with other experimental data on pp-scattering they are used to make the phase shift analysis more accurate. (auth)

41667 (JINR-P-2239) O TREKHKVAZICHASTICHNOM SOSTOYANII V Er^{165}. (On Three-Quasiparticle State in ^{165}Er). Bonch-Osmolovskaya, N. A.; Wang, Chang-zhu; Gromov, K. Ya. (Joint Inst. for Nuclear Research, Dubna (USSR). Lab. of Nuclear Problems). 1965. 11p. Dep. mn.

An investigation of γ-rays emitted from the 1428 level in ^{165}Er is presented. The characteristics of the level are determined and the three-quasiparticle nature of the level predicted by V. G. Soloviev is confirmed by using the obtained data and those of Z. Preibisz et al. (auth)

41668 (KFK-306) REICHWEITEVERTEILUNG ISOBARER REIHEN UND REICHWEITE VON FRAGMENTEN BEI DER THERMISCHEN SPALTUNG VON Pu-239. (Isobaric Order of Particle Range and Range of Fragments from the Thermal Fission of Pu-239). Hollstein, Martin (Kernforschungszentrum, Karlsruhe (West Germany). Institut fur Radiochemie). Feb. 1965. 82p. Dep. (mn).

The range distributions of ^{140}Ba and ^{127}Sb in Al were investigated using the stripping method. The mean ranges were 2.95 ± 0.10 mg Al/cm² for ^{140}Ba and 3.6 ± 0.2 mg Al/cm² for ^{127}Sb. The relative dispersions of the range distributions were 20.3 ± 1.0% for ^{140}Ba and 23.1 ± 1.7% for ^{127}Sb. The width of the distributions is larger than the dispersion obtained with gaseous absorbers. A low energy background occurred in the differential range experiments in the experimental distributions. It was explained by scattering of the fission products on the collimator wall and in the material between target site and absorber. The contribution of both effects on the total distribution depends on the structure of the collimator. An investigation of the stripping method showed that electropositive elements are only partially dissolved by Al absorbers. Under the assumption of a constant delay the following delay factors k were determined; k = 0.80 ± 0.03 for Sb and k = 0.98 ± 0.01 for Ag. A critical comparison of the energy dispersion of primary fragments caused by the fission products gave a value of approximately 11%. In the calculation it was assumed that both the range and also the dispersion of all fragments of an isobaric series are equal. A new technique was developed that makes it possible with a thick target–thick absorber arrangement to detect ranges directly in Al. The target material consists of an alloy, for example ^{239}Pu (in Al). A newly developed separation method for ^{139}Ba and ^{139}Xe made it possible to separate these nuclides from the absorber and target foils in 30 or 20 seconds. Using these methods, the fragment ranges of ^{139}Ba and ^{139}Cs and the cumulative range of ^{139}Ba in Al was investigated. These ranges were (in mg Al/cm²): cumulative range for ^{139}Ba, 2.96 ± 0.03; fragment range for ^{139}Ba, 2.75 ± 0.06; and the fragment range for ^{139}Cs, 2.86 ± 0.20. The range of fragments within an isobaric series is not equal according to these experimental results. An evaluation showed that the relative range with respect to the isobaric series R_f/R_{is} of heavy fragments depends approximately linearly on the difference $Z - Z_p$; $R_f/R_{is} = 1.0 - 0.037\ (Z - Z_p)$. By consideration of this function and under the assumption the range dispersion for all terms for an isobaric series is constant, the dispersion of kinetic energy of primary fragments caused by the fission process was calculated from the results of others. The values determined earlier for this dispersion were too large by a factor of approximately 2. A testing of the results derived from this magnitude is therefore necessary. (tr-auth)

41669 (LA-DC-7096) HIGH RESOLUTION MEASUREMENTS OF GAMMA RAYS FROM NEUTRON INELASTIC SCATTERING. Day, Robert B.; Palms, John M. (Los Alamos Scientific Lab., Univ. of California, N. Mex.). [1964]. Contract W-7405-eng-36. 5p. (CONF-650706-20). Dep. mn; CFSTI, $1.00 cy, $0.50 mn.

From International Conference on the Study of Nuclear Structure with Neutrons, Antwerp.

A brief comparison of the new lithium-drifted germanium and the NaI neutron detector is presented. Gamma ray spectra from the neutron bombardment of gold-197, lead-206, and bismuth-209 at energies ranging from .4 to 4.1 Mev are included. (M.O.W.)

41670 (LA-DC-7097) HIGH ENERGY GAMMA-RAY SPECTRUM OF THERMAL NEUTRON CAPTURE IN HOLMIUM. Motz, H. T.; Jurney, E. T. (Los Alamos Scientific Lab., Univ. of California, N. Mex.). [1965]. Contract W-7405-eng-36. 6p. (CONF-650706-19). Dep. mn; CFSTI, $1.00 cy, $0.50 mn.

From International Conference on the Study of Nuclear Structure with Neutrons, Antwerp.

The experimental technique for obtaining high energy gamma ray spectra of thermal neutron capture in holmium is presented. A discussion of the data obtained is included. (M.O.W.)

41671 (LADC-6186) PIONS, MUONS AND NUCLEAR STRUCTURE. Critchfield, Charles L.; Heller, Leon; Lee, Clarence E.; Young, James E. (Los Alamos Scientific Lab., Univ. of California, N. Mex.). [1963]. Contract W-7405-eng-36. 30p. Dep. mn; CFSTI, $2.00 cy, $0.50 mn.

A summary of the papers presented at the pions, muons, and nuclear structure conference held at LASA in August 1963 is presented. The papers concern: muon interactions with nuclei, mesic x rays, pion-nucleon resonances effect on some simple nuclear reactions, pion optical potential, pion capture on complex nuclei, elementary particles and the boundary condition model, pion production facilities, and a discussion on neutrino experiments. (M.O.W.)

41672 (MIT-2344-3, pp 5-14) FAST FISSION MEASUREMENTS. Papay, L. T. (Massachusetts Inst. of Tech., Cambridge. Dept. of Nuclear Engineering).

Measurements of the ratio of the fission rate in ^{238}U to the fission rate in ^{235}U are discussed. Results are presented for lattices of .25 inch, 1.14% ^{235}U rods and for single rods in air. (M.O.W.)

41673 (NP-15251) SPEKTR ELEKTRONOV VNUTRENNEI KONVERSII SOPROVAKHDAYUSHCHIKH α-RASPAD Pu^{239} I SKHEMA UROVNEI U^{235}. (Spectrum of Internal Conversion Electrons in α-Decay of ^{239}Pu and Energy Levels of ^{235}U). Report No. 280. Tret'yakov, E. F.; Kondrat'ev, L. N. (Gosudarstvennyi Komitet po Ispol'zovaniyu Atomnoi Energii SSSR, Moscow. Institut Teoreticheskoi i Eksperimental'noi Fiziki). 1964. 20p. Dep. mn.

By means of a double ironless β-spectrometer with the toroidal field the spectrum of $\alpha - e_K$ coincidences of the ^{239}Pu sample in the region of electron energies 15-500 kev was investigated. The energies of the levels of the two known rotation bands ($K = 7/2^-$ and $K = 1/2^+$) were improved. A new rotation band appearing on the excited state of ^{235}U with the excitation energy 393.8 kev $K = 3/2^+$ was found. The scheme of excited levels of ^{235}U is discussed. (auth)

41674 (NYO-1930-44) ISOMERIC CROSS-SECTION RATIOS IN THE (p,pn) AND HEAVY-ION NEUTRON-TRANSFER REACTIONS (thesis). Gatrousis, Christopher (Clark Univ., Worcester, Mass. Dept. of Chemistry). [1964]. Contract AT(30-1)-1830. 137p. Dep.(mn); $4.00(cy), 3(mn) CFSTI.

The role of angular momentum in nuclear reactions was studied by measuring for the isomeric pairs ^{127m}Te and ^{127g}Te ($11/2^-$, $3/2^+$) and ^{129m}Te and ^{129g}Te ($11/2^-$, $3/2^+$) the cross-section ratios for their formation by the (p,pn) reaction in the energy range 40 to 150 Mev and by the heavy-ion neutron-transfer reactions of ^{128}Te induced by N-14 and C-12 ions having energies up to 10 Mev/nucleon. The isomeric cross-section ratio of ^{69m}Zn and ^{69g}Zn ($9/2^+$, $1/2^-$) was measured for the neutron-transfer reaction in ^{68}Zn induced by N-14 ions. Tellurium and zinc were separated from the irradiated targets by standard radiochemical methods and the activities of the isomeric pairs were resolved from the gross decay curves. The experimentally determined isomeric ratio, high-spin state to low-spin state, for the reaction $^{130}Te(p,pn)^{129m}Te$ and ^{129g}Te is about 0.65 and shows no variation with energy. The isomeric ratio for the $^{128}Te(p,pn)^{127m}Te$ and ^{127g}Te reaction is about 0.75 over the entire energy range studied. For the heavy-ion reactions, neutron transfers both to and from ^{128}Te were studied simultaneously. The isomeric ratios for the ^{128}Te(N-14, N-15) and the ^{128}Te(C-12, C-13) reactions are constant at about 0.4 from energies near the barrier up to 10 Mev/nucleon. The isomeric ratios for the ^{128}Te (N-14, N-13) and the ^{128}Te(C-12, C-11) reactions are constant at about 1.5 to 2. The isomeric ratio for the ^{68}Zn(N-14, N-13) reaction is about 2.2 between 80 and 140 Mev. The isomeric ratios in the (p,pn) reaction are believed to result from a direct interaction and they are analyzed in terms of a cascade-plus-evaporation process at the lower energies and a knock-on process at 150 Mev. For the cascade-plus-evaporation calculations the experimental values for the isomeric ratios were used to infer an initial angular-momentum distribution following a (P,P') cascade. A distribution characterized by a root-mean-square angular momentum of about $4\hbar$ is implied by the experimental ^{127m}Te and ^{127g}Te ratio. The distribution implied by the ^{129m}Te and ^{129g}Te ratio suggests a value lower perhaps by $1/2\hbar$. Calculations based on a knock-on mechanism were used to deduce the neutron levels in ^{128}Te and ^{130}Te. If the $1h_{11/2}$, $3s_{1/2}$, $1g_{7/2}$, and $2d_{3/2}$ neutron levels are occupied in ^{128}Te, the predicted ratios are consistent with the experimental data. The calculated values for ^{130}Te show agreement with the observed ratios only if the two additional neutrons occupy the $2d_{3/2}$ level. The heavy-ion neutron-transfer reactions were analyzed in terms of classical Rutherford scattering. The angular momenta thus calculated are in qualitative agreement with an observed decrease in total cross sections at lower bombarding energies. For the case in which a neutron is removed from the target nucleus, the calculations are also consistent with the observed isomeric ratios. To explain the ratios of isomers formed by neutron transfer to the target nucleus, the suggestion was made that the distance of closest approach is much smaller for excited-state transfers than for ground-state transfers. (auth)

41675 (ORNL-P-330) EXCITATION OF THE FIRST LEVEL OF ^{12}C BY 156 Mev PROTONS. Haybron, R. M. (Michigan State Univ., East Lansing and Oak Ridge National Lab., Tenn.); McManus, H. (Michigan State Univ., East Lansing). [1963]. Contract W-7405-eng-26. 14p. Dep. mn; CFSTI, $1.00 cy, $0.50 mn.

The inelastic cross section and polarization for the excitation of the 4.43 Mev of ^{12}C were calculated in the distorted wave impulse approximation using the Tamm-Dancoff and RPA wavefunctions of Gillet and also of Goswami and Pal. Comparison with experiment favors the RPA wavefunctions of Gillet. (auth)

41676 (ORNL-P-1468) $^{51}V(p,n)^{51}Cr$ CROSS SECTION FROM THRESHOLD TO 2.25 Mev. Gibbons, J. H.; Macklin, R. L. (Oak Ridge National Lab., Tenn.). [1965]. Contract W-7405-eng-26. 6p. (CONF-650635-1). Dep. mn; CFSTI, $1.00 cy, $0.50 mn.

From 2nd International Meeting on Accelerator Targets Designed for the Production of Neutrons, Grenoble, France.

The absolute (p,n) total cross section for $^{51}V(p,n)$ was measured from threshold to 2.25 Mev with an accuracy of 5%. The cross section measured with an ~15 kev thick target fluctuates appreciably despite the ~1 kev level spacing observed using a thin target. The small change of neutron energy with emission angle make this reaction a good 4π monoenergetic source. (auth)

41677 (ORNL-TM-1151) DWB DEUTERON STRIPPING PROGRAM. Smith, William R. (Oak Ridge National Lab., Tenn.). June 10, 1965. Contract W-7405-eng-26. 26p. Dep. mn; CFSTI, $2.00 cy, $0.50 mn.

A FORTRAN program is described which calculates (d,p) and (d,n) stripping angular cross sections with the inclusion of nuclear optical-model potentials and Coulomb interactions. The Q value is restricted to values greater than −2.226 Mev. Provision is also made for approximating the finite-range n-p interaction, the deuteron polarizability, and the nonlocality of the nuclear forces. The program is set up to run on a CDC-1604 computer but should be easily adaptable to other computers using FORTRAN. (auth)

41678 (PR-P-65) PHYSICS DIVISION. Progress Report January 1−March 31, 1965. Elliott, L. G. (Atomic Energy of Canada Ltd., Chalk River (Ontario)). 49p. (AECL-2256). Dep; $1.50 (AECL).

Work is reported on: nuclear physics research, solid state studies, developments in solid state radiation detectors, and developments in computation. (M.O.W.)

41679 (UCRL-11462(Rev.)) ANGULAR DISTRIBUTIONS OF CONVERSION ELECTRONS FROM ORIENTED Ce^{137m} NUCLEI. Stone, N. J.; Frankel, R. B.; Shirley, D. A. (Lawrence Radiation Lab., Univ. of California,

Berkeley). May 1965. Contract W-7405-eng-48. 6p. (CONF-650525-6). Dep. mn; CFSTI, $1.00 cy, $0.50 mn.

From International Conference on the Internal Conversion Process, Nashville, Tenn.

Experimental techniques are described which make possible the measurement of the energy dependence of charged-particle anisotropies from oriented nuclei. The application of these techniques to obtain the angular distribution of conversion electrons from oriented cerium-137m is discussed. (M.O.W.)

41680 (UCRL-16184) INTERNAL CONVERSION ELECTRONS FROM PRIMARY FISSION FRAGMENTS. Watson, R. L.; Bowman, H. R.; Thompson, S. G.; Rasmussen, J. O. (Lawrence Radiation Lab., Univ. of California, Berkeley). May 1965. Contract W-7405-eng-48. 15p. (CONF-650525-7). Dep. mn; CFSTI $1.00 cy, $0.50 mn.

From International Conference on the Internal Conversion Process, Nashville.

The experimental facilities and techniques for measuring the energies of conversion electrons from primary fission fragments are discussed. Some results are given for the mass intervals (103-105) and (143-145) in which the heavy fragment is in the region of barium. (M.O.W.)

41681 (ANL-Trans-205) NEUTRON EMISSION FROM U^{233}, U^{235} AND Pu^{239} FISSION FRAGMENTS. Apalin, V. F.; Gritsyuk, Yu. N.; Kutikov, I. E.; Lebedev, V. I.; Mikaelyan, L. A. (Institut Atomnoi Energii, Gosudarstvennyi Komitet po Ispol'zovaniyu Atomnoi Energii SSSR, Moscow). Translated by Elmar K. Wilip (Argonne National Lab., Ill.), from Preprint IAE-710. 1964. 13p. Dep. mn; CFSTI, $1.00 cy, $0.50 mn; JCL, $1.60 fs, $0.80 mf.

Quantitative data were obtained for the neutron emission in the symmetric fission region. The number of ghost events recorded in this region could be decreased to 15 + 20%. (auth)

41682 ELASTIC SCATTERING OF 10.5- AND 14.5-Mev POLARIZED PROTONS FROM NUCLEI AND THE OPTICAL MODEL POTENTIAL AT INTERMEDIATE ENERGIES. Rosen, Louis (Los Alamos Scientific Lab., N. Mex.); Beery, Jerome G.; Goldhaber, Alfred S.; Auerbach, Elliot H. Ann Phys. (N. Y.), 34: 96-152(Aug. 1965). (LA-DC-7063).

The results of extensive measurements of the angular distributions and azimuthal asymmetries for elastic scattering of 10.5 and 14.5 Mev polarized protons, from a wide range of nuclei, are presented. Attention is focused on the general features of these angular distributions and certain deviations from the general trends. The interpretations of both these aspects of the data are discussed. In addition, results are presented from an extensive search program designed to obtain fits to the data with a six-parameter local "optical" potential. From these individual fits to each nuclide have been obtained a set of average parameters at 10.5 Mev and another set at 14.5 Mev. The predictions of the optical model with the average parameters are compared not only to the polarization data but also to elastic differential cross sections and reaction cross sections for protons. With a modification of the magnitudes of the refractive and absorptive central potentials, as required to fit 14.5 Mev neutron elastic scattering cross sections, the potential has been used to predict differential elastic cross sections, reaction cross sections, total cross sections, and polarizations for neutrons, and the results compared with available experimental data. A study has been made of the dependence of the refractive central potential depth on proton energy and on the nuclear symmetry parameter, (N-Z)/A, obtaining reasonable agreement with the results of other workers. (auth)

41683 STUDY OF ^{9}Be BY ELECTRON SCATTERING. DISCRETE AND CONTINUUM STATES. Nguyen Ngoc, Hoan (Faculte des Sciences, Orsay, France). Ann. Phys. (Paris), 10: 315-61(May-June 1965). (In French).

The excited states (both the discrete states and the continuum states) of ^{9}Be were studied by inelastic scattering of electrons with energy from 70 to 250 Mev. The experimental technique and the principal theoretical formulas necessary for the analysis of the results are described. The technique for the analysis of the results is given with a detailed exposition of the formulas used. The experimental results are given and interpreted. Only three discrete levels at 1.6 ± 0.2, 2.47 ± 0.02, and 6.4 ± 0.1 Mev were observed. The calculations of the reduced probabilities of transition and the associated radiative lengths of transition showed the collective character of the 2.47 and 6.4 Mev levels. In order to verify the collective nature of these transitions the scattering cross section was calculated by using the shell model with intermediate coupling. The results are of an order 4 times weaker than the experimental cross section. By assuming the transitions are simply due to protons from the p shell, the cross sections were calculated phenomenologically by introducing the quadrupole moment as a parameter. Transitions were also studied within the framework of the α particle model. In the study of the continuum states the cross section for the Bremsstrahlung radiation was calculated in the first Born approximation and compared with the results of other workers. An approximation consisting of dividing the continuum into small bands of energy and considering them as discrete levels was used for the extraction of the nuclear cross sections. Two invariant functions of quadritransfer and of the energy of excitation were determined and adjusted to analytical form by analogy with the analysis of discrete excited states. Two tests were made to verify the coherence of the analytical technique. The Fermi gas model used for interpretation of the continuum spectrum was satisfactory for the spectra with large transfers. (J.S.R.)

41684 SOME (d,α) DIFFERENTIAL CROSS SECTIONS FOR Na^{23}, Al^{27}, AND P^{31} AT ABOUT 9.3 Mev. Cosper, S. W.; Lucas, B. T.; Johnson, O. E. (Purdue Univ., Lafayette, Ind.). Phys. Rev., 139: B763-9(Aug. 23, 1965). (COO-1420-115).

The differential cross sections for the (d,α) reactions which lead to various nuclear states in ^{21}Ne (ground, 1, and 2), ^{25}Mg (ground, 1, 2, 3, and 4), and ^{29}Si (ground, 1, 2, 3, 4, 5, and 6) were measured at nominal deuteron energies of 9.2, 9.2, and 9.5 Mev, respectively, using a silicon surface-barrier detector. Targets of various thicknesses ranging from 70 to 642 $\mu g/cm^2$ were used. In each case the differential cross section was determined at more than 34 angles from 10 to 172.5°. Although the shape of each angular distribution is different from any of the others in detail, all exhibit the following characteristics: pronounced forward and backward peaking; an over-all oscillatory structure; an asymmetry about 90°; and minima whose magnitudes differ significantly from zero. Comparisons are made with (d,α) results previously obtained by other investigators using deuteron energies in the 7-15-Mev range. No correlation could be established between any specific detail in shape or general feature of these angular distributions and any physical quantity associated with the nuclear states involved. Analyses of these differential cross sections are described using an expression consisting of the sum of an isotropic component and a plane-wave Born approximation component which arises from the coherent action of a two-nucleon pickup and a heavy-particle-stripping mechanism. (auth)

41685 SELF-CONSISTENT PERTURBATION OF HARTREE-FOCK-BOGOLIUBOV EQUATIONS AND NUCLEAR ROTATIONAL SPECTRA. [PART] I. Marshalek, Eugene R. (Brookhaven National Lab., Upton, N. Y.). Phys. Rev., 139: B770-89(Aug. 23, 1965).

The effect of a single-particle perturbation on the Hartree-Fock-Bogoliubov equations is considered. Corrections to the ground-state wave function, density matrix, and pairing tensor are obtained through third order, thus determining the energy through fourth order. The results are applied to rotational spectra of even-even atomic nuclei, in which the nucleons interact via pairing and quadrupole forces, and the single-particle perturbation is the Coriolis force in a rotating frame of reference. The energy levels of the ground-state band are obtained to order $I^2(I+1)^2$ in

the angular momentum. It is shown that the coefficient of the $I^2(I+1)^2$ term contains contributions arising from centrifugal stretching of the self-consistent quadrupole field and having the expected form of a rotation-vibration interaction. In addition, however, the coefficient contains terms arising from the Coriolis unpairing effect and also terms arising from the influence of the Coriolis force on independent quasiparticle motion. Approximate numerical estimates indicate that the contribution from the Coriolis unpairing is far greater than from the beta vibration-rotation interaction. (auth)

41686 NUCLEAR COUPLING SCHEMES WITH A SURFACE DELTA INTERACTION. Green, Ira M. (TRW Space Technology Labs., Redondo Beach, Calif.); Moszkowski, S. A. Phys. Rev., 139: B790-3(Aug. 23, 1965).

Recent work indicates that the major part of the residual interaction in nuclei, namely, both the quadrupole and pairing interactions, acts primarily when particles are near the nuclear surface. Since the one-particle radial wave functions at the surface are essentially state-independent, a surface interaction implies that all radial integrals are approximately the same. Thus for a surface delta function all radial integrals are assumed to be identical. For mixed two-particle configurations, e.g. $(s,d)^2$, the surface delta-function interaction gives a first excited 2+ state at a lower energy than a conventional delta function acting throughout the nuclear volume. For the $(s,d)^4T = 2$ configuration essentially a vibrational spectrum is obtained in both cases. However, for the $(s,d)^4T = 0$ configuration involving both neutrons and protons, the conventional delta function and surface delta function give quite different spectra. The former leads to a spectrum similar to the two-particle case, whereas for a surface delta-function interaction, the lowest states are 0+, 2+, and 4+ with a near-rotational spacing. It appears then that it is possible to obtain a rotational spectrum even with a short-range interaction, provided mixed configurations and both neutrons and protons are participating. (auth)

41687 FIVE-DIMENSIONAL QUASISPIN. EXACT SOLUTIONS OF A PAIRING HAMILTONIAN IN THE J-T SCHEME. Hecht, K. T. (Univ. of Michigan, Ann Arbor). Phys. Rev., 139: B794-817(Aug. 23, 1965).

The matrix elements of a charge-independent pairing hamiltonian spanning several single-particle states are expressed in terms of the matrix elements of the infinitesimal operators of R_5, the rotation group in a five-dimensional space. General algebraic expressions for these matrix elements are calculated for states with reduced isospin $t = 0, \frac{1}{2}$, and 1, in a scheme in which both nucleon number N and isospin T are good quantum numbers, making it possible to find exact solutions to the charge-independent pairing hamiltonian for states with individual level seniorities $v \leq 2$. Exact solutions are compared with perturbation-theory formulas for some simple models. The results indicate that perturbation theory may be used as a guide to an understanding of the charge-independent pairing interaction in its dependence on N and T. For relatively strong pairing and fixed T, the dependence on nucleon number N is similar to that for configurations of identical nucleons; while for fixed N, the T dependence is given mainly by a term of simple T(T + 1) form. (auth)

41688 STATES IN C^{12} BETWEEN 16.4 AND 19.6 Mev. Segel, R. E.; Hanna, S. S.; Allas, R. G. (Argonne National Lab., Ill.). Phys. Rev., 139: B818-30(Aug. 23, 1965).

The states of ^{12}C in the energy region 16.4 Mev $< E_x$ (C^{12*}) < 19.6 Mev were studied by bombarding ^{11}B with protons in the range 0.5 Mev $< E_p < 4.0$ Mev. Many angular distributions and yield curves were measured for the capture gamma rays forming the ground state and first excited state of ^{12}C and for the alpha-particle transitions to the ground state and first excited state of ^8Be. The total-neutron-yield curve was determined by measuring the yield of residual ^{11}C activity. The absolute inelastic proton-scattering cross section was also determined and used to normalize the relative-yield curve of other investigators. The elastic proton scattering was measured as a function of energy at several angles. Some γ-γ angular-correlation measurements were made at one resonance. In all, nine distinct resonances were studied and given spin, parity, and isospin assignments with varying degrees of completeness. In most cases in which earlier assignments existed, these assignments were confirmed. The observed levels are compared with those predicted by particle-hole calculations. It is concluded that the particle-hole model is consistent with most of the observed structure, and that all of the predicted levels in this region are at least tentatively identified. (auth)

41689 (p,t) GROUND-STATE L = 0 TRANSITIONS IN THE EVEN ISOTOPES OF Sn AND Cd AT 40 Mev, N = 62 TO 74. Bassani, G.; Hintz, Norton M.; Kavaloski, C. D.; Maxwell, J. R.; Reynolds, Glenn M. (Univ. of Minnesota, Minneapolis). Phys. Rev., 139: B830-?(Aug. 23, 1965).

The (p,t) reaction was used to investigate the ground-state L = 0 transitions in the seven even Sn isotopes and four even Cd isotopes with a 40-Mev proton beam. Angular distributions were taken in the range 7 to 25° in most cases, and the integrated cross sections used for comparison with the theory. The isotopes of Sn have a closed Z = 50 proton shell and should be rather well described in terms of the neutrons outside of the N = 50 shell. The detailed description of the neutron configurations is available from theoretical work and one-neutron transfer reactions. The agreement between pairing spectroscopic factors and the experimental cross sections is not good. It is clear that a distorted-wave Born-approximation analysis of the data is necessary, as well as, perhaps, a better understanding of the nuclear structure of the Sn isotopes. The Cd data show that an open proton shell decreases the number of J = 0 coupled neutron pairs in the ground state. (auth)

41690 (p,p'γ) ANGULAR CORRELATIONS IN Ti^{48}. Humes, Richard M.; Hausman, Hershel J. (Ohio State Univ., Columbus). Phys. Rev., 139: B846-51(Aug. 23, 1965).

The angular correlations between the protons inelastically scattered from the first excited state of ^{48}Ti and the associated de-excitation gamma rays were measured as absolute second differential cross sections at bombarding energies of 4.63 and 5.25 Mev. These measurements were made both in the scattering plane and at angles of 30, 45, 60, and 90° relative to the scattering plane. Special attention was directed to studies of the symmetry predictions of the compound nucleus and direct interaction processes, and comparison is made with the statistical-theory computations of Sheldon. For a given proton detector angle, the azimuthal symmetries agree in shape though not in magnitude with statistical-theory predictions. However, results for complementary proton-detector angles are incommensurate with the symmetries predicted by statistical theory. (auth)

41691 ABSOLUTE FISSION CROSS SECTION OF U^{235} FOR 2200-m/sec NEUTRONS. Maslin, E. E.; Moore, J. A.; Reichelt, J. M. A.; Crowden, J. B. (Atomic Weapons Research Establishment, Aldermaston, Berks, Eng.). Phys. Rev., 139: B852-63(Aug. 23, 1965).

A measurement of the fission cross section of ^{235}U is described. Neutrons of 2200-m/sec velocity were selected with a fast neutron chopper. Fission neutrons from a thick sample of ^{235}U were detected in capsules of liquid scintillator employing pulse-shape discrimination of fast neutrons from gamma rays. The neutron flux was measured by stopping the beam in a thick sample of ^{10}B and detecting the 478-kev gamma rays in a pair of sodium iodide crystals. The efficiency of the sodium iodide crystals for detecting gamma rays was established by observing coincidences between gamma-ray pulses from the detector and from disintegrations in a thin sample of ^{10}B contained within an ionization chamber. The efficiency of the liquid scintillators was determined in a similar manner using a thin foil of ^{235}U. A large correcting factor was discovered originating from the anisotropy introduced into the angular distribution of detected neutrons by the absorption of fission fragments in the ionization-chamber foil. The method yields an absolute value for the fission cross section, independent of any

reference cross sections. A value of $\sigma_F = 572 \pm 6$ b was obtained. (auth)

41692 CALCULATION OF INELASTIC ALPHA-PARTICLE SCATTERING BY Ni^{58}. Madsen, V. A. (Oregon State Univ., Corvallis); Tobocman, W. Phys. Rev., 139: B864-70(Aug. 23, 1965).

A distorted-wave calculation is presented for excitation of the 1.45 Mev 2^+ level of ^{58}Ni by inelastic scattering of 43-Mev alpha particles. The collective one-phonon state is taken to be an eigenfunction of the pairing plus $Q \cdot Q$ potential, and the finite-range alpha-nucleon interaction is taken from (p,α) elastic-scattering analysis. It is shown how the collective enhancement and the surface-peaked interaction form factor arise. Qualitative agreement with experimental differential cross sections and with the predictions of the vibrational nuclear model are obtained, but quantitative agreement for the angular distributions is lacking. The cause of the disagreement is discussed. The calculated absolute cross sections are in good agreement with experimental data. (auth)

41693 STUDY OF THE $Mg^{26}(p,p'\gamma)$ REACTION MECHANISM AT LOW ENERGIES. Hulubei, H.; Martalogu, N.; Ivascu, M.; Scintei, N.; Berinde, A.; Neamu, I.; Francz, J. (Institute for Atomic Physics, Bucharest). Phys. Rev., 139: B871-80(Aug. 23, 1965).

The angular distribution and p'-γ angular correlations of the protons inelastically scattered on the first two 2^+ excited states of ^{26}Mg were measured at several energies of the incident protons between 5.67 and 6.46 Mev. The angular correlation of the inelastically scattered protons on the ^{26}Mg second excited state is of the type $0^+ \rightarrow J^\pi \rightarrow 2^+ \rightarrow 2^+ \rightarrow 0^+$, where the heavy arrow indicates the unobserved cascade γ rays. The angular distributions and correlations corresponding to the second level of ^{26}Mg ($Q = -2.94$ Mev) are in good agreement with the predictions of the statistical model. In the case of the protons which populate the first level ($Q = -1.81$ Mev) the angular distribution varies strongly with the energy, indicating a violation of the hypotheses on which the statistical model are based. The angular correlations corresponding to the excitation of this level likewise agree only in some cases with the predictions of the statistical model. The difference in behavior of the angular distribution and angular correlations on the two levels is attributed to the differences in value of the transmission coefficients $T_l(E)$. Angular correlations for $^{26}Mg(p,p'\gamma)$, $Q = -1.81$ Mev at energies higher than 6 Mev also suggest some contribution of the direct-interaction mechanism. (auth)

41694 ELECTRON SCATTERING FROM NUCLEAR MAGNETIC MOMENTS. Griffy, T. A.; Yu, D. U. L. (Stanford Univ., Calif.). Phys. Rev., 139: B880-5(Aug. 23, 1965).

The elastic scattering of high-energy electrons from the magnetic dipole and magnetic octupole moments of light nuclei is calculated using shell-model wave functions. The results of the calculation are compared with recent experimental results for ^9Be and ^{11}B, and the possibility of obtaining a value for the magnetic octupole moment from an analysis of these experiments is discussed. (auth)

41695 CROSS-SECTION RATIOS OF ISOMERIC NUCLIDES PRODUCED IN MEDIUM-ENERGY (α,xn) REACTIONS. Matsuo, T.; Matuszek, J. M. Jr.; Dudey, N. D.; Sugihara, T. T. (Clark Univ., Worcester, Mass.). Phys. Rev., 139: B886-95(Aug. 23, 1965).

Cross-section ratios of isomeric nuclides produced in the reactions $^{41}K(\alpha,n)^{44}Sc$, $^{55}Mn(\alpha,n)^{58}Co$, $^{93}Nb(\alpha,n)^{96}Tc$, $^{93}Nb(\alpha,2n)^{95}Tc$, $^{93}Nb(\alpha,3n)^{94}Tc$, and $^{136}Ba(\alpha,3n)^{137}Ce$ are reported for the α-particle energy range from reaction threshold to 42 Mev. Recoil ranges of products were also determined. Range information was used to help establish the bombarding-energy region in which a particular reaction was likely to be compound-nuclear. The ratio of cross sections, high-spin product to low-spin product, was found to increase initially as the bombarding energy increased. In the three (α,n) reactions, the ratio goes through a maximum and decreases. The decreasing region is consistent with the onset of a process in which the product nucleus does not have all of the momentum of the incident α particle. In the $^{93}Nb(\alpha,2n)$ reaction the cross-section ratio also goes through a maximum, but the range measurements in this energy region suggest that in only a small fraction of events is the momentum transfer much less than complete. Both $(\alpha,3n)$ reactions show a monotonic increase in the cross-section ratio with increasing α-particle energy. Excitation functions of isomeric pairs indicate a shift to higher bombarding energy for the nuclide of higher spin. (auth)

41696 STATISTICAL-MODEL ANALYSIS OF ISOMERIC RATIOS IN (α,xn) COMPOUND NUCLEAR REACTIONS. Dudey, N. D. (Clark Univ., Worcester, Mass. and Columbia Univ., New York); Sugihara, T. T. Phys. Rev., 139: B896-904(Aug. 23, 1965). (NYO-1930-42).

Cross-section ratios of isomeric pairs produced in the compound nuclear reactions $^{41}K(\alpha,n)^{44}Sc$, $^{55}Mn(\alpha,n)^{58}Co$, $^{93}Nb(\alpha,n)^{96}Tc$, $^{93}Nb(\alpha,2n)^{95}Tc$, $^{93}Nb(\alpha,3n)^{94}Tc$, and $^{136}Ba(\alpha,3n)^{137}Ce$ are analyzed in terms of the statistical model. In this context Vandenbosch and Huizenga proposed a formalism for calculating isomer formation from compound nuclei of relatively low excitation energy and spin. It is assumed that the density of levels of spin J in residual nuclei is proportional to $(2J + 1)\exp[-J(J + 1)/2\sigma^2]$ and that in the case of a product formed by neutron evaporation the emission of charged particles is not of importance. Here σ is the spin cutoff parameter and is related to the effective moment of inertia j. The extension of such a model to compound nuclei of much higher excitation energy and spin is considered. Typically by this method the experimental isomeric ratios imply a value of j much smaller than that of a rigid sphere, j_R, even for nuclei excited to well above nucleon binding energies. The introduction of two additional factors in the formalism leads to more reasonable values of j/j_R. First, a principle of limiting spin is invoked. That is, the level density of a residual nucleus is not described by the expression above for all J; rather, above some critical J value, determined by a Fermi-gas model, the level density is taken to be zero. Secondly, we find charged-particle emission, particularly of α particles, to be of importance in many cases. With the inclusion of these factors experimental isomeric ratios are consistent with a j/j_R value of unity when the excitation energy E_f is greater than about 10 Mev. Below 10 Mev, j/j_R has essentially the same dependence on E_f for all of the reactions analyzed. (auth)

41697 INVESTIGATION OF THE $T = 3/2$ STATE AT 16.97 Mev IN Be^9. Imhof, W. L.; Chase, L. F. Jr.; Fossan, D. B. (Lockheed Missiles and Space Co., Palo Alto, Calif.). Phys. Rev., 139: B904-11(Aug. 23, 1965).

A resonance in the $^7Li + d$ reaction at a deuteron bombarding energy of 361 ± 2 kev, corresponding to a level in ^9Be at 16.97 Mev, was investigated. Total cross sections for $^7Li(d,p_0)^8Li$ were measured by detecting induced ^8Li activity for deuteron energies between 340 and 780 kev. In agreement with earlier work of Woods and Wilkinson, a resonance in this reaction was observed on a background rapidly decreasing with decreasing deuteron energy. This resonance and the surrounding region from 0.1 to 1.1 Mev were also studied with the $^7Li(d,\gamma)^9Be$ reaction by measuring the yield of the gamma-ray transitions to the lower states of ^9Be with a NaI crystal. The measured width of the level was less than 600 ev in the laboratory system. The angular distribution of the on-resonance gamma rays to the ground state was isotropic to within 7%. Branching ratios for the gamma rays to several states in ^9Be were measured with a NaI crystal, a scintillation pair spectrometer, and a NaI crystal surrounded by an anticoincidence shield. The relative intensities for the gamma-ray transitions to the ground state and to the states at 1.70, 2.43, 3.04, and 4.74 Mev were found to be 100, 8.5 ± 4.3, 10.6 ± 5.3, ≤ 4.5, and 9.6 ± 4.8, respectively. The 15.3-Mev gamma-ray transition indicates the existence of a level in the usual sense at 1.70 Mev in ^9Be. From the gamma-ray measurements below resonance at 300 kev an upper limit of 1.6×10^{-30} cm^2 was found for the direct (d,γ) cross section to low-energy states in ^9Be. For the $^7Li(d,n)$ reaction, the yield of neutrons with energies above 10 Mev showed a resonance at the same energy. From neutron time-of-flight measure-

ments relative to coincident gamma rays, neutron groups were seen corresponding to breakup of levels in ^{9}Be at 2.43 and 4.74 Mev. The ^{7}Li(d,d)^{7}Li and ^{7}Li(d,α)^{5}He reactions did not show observable resonance effects. From the above results, the reduced widths for neutron and alpha-particle emission are found to be considerably smaller than the corresponding width for protons, thus supporting the hypothesis that the state in ^{9}Be at 16.97 Mev has an isobaric spin of $3/2$. (auth)

41698 THE QUANTUM MECHANICAL FUNDAMENTALS OF THE THEORY OF γ-γ ANGULAR CORRELATIONS. Paul, Harry. Ann. Physik (7), 14: 166-75(1964). (In German).

In the theoretical treatment of γ-γ angular correlations, the problem occurs of describing quantum mechanically the state of a nucleus that immediately before had emitted a first γ quantum of given propagation direction n_1 and polarization p_1. For its solution the density matrix (to be expected easily from the Wigner-Weisskopf solution of the Schroedinger equation) for a nucleus was calculated. The nucleus after emission of a γ quantum (n_1p_1) occurring any time earlier is found in the intermediate state of the γ-γ cascade. The time alteration of this density matrix can be written as the sum of three terms, which refer to the three processes: (a) transition from the initial state of the cascade to the intermediate state after emission of a γ quantum (n_1p_1), (b) transition from the intermediate state into the final state after emission of a γ quantum of any direction polarization, and (c) unperturbed (with respect to the radiation interaction) time alteration of the density matrix. The term corresponding to (a) characterizes the state of a nucleus immediately after the irradiation of a γ quantum (n_1p_1). Therefore the initial condition for the Schroedinger equation is known, and this describes the second emission process. Its solution yields the known expression for the γ-γ correlation function in delayed coincidences. (tr-auth)

41699 THE DECAY OF CARBON-12 INTO THREE α PARTICLES IN THE NUCLEAR REACTION ^{11}B(p,α)2α. Dehnhard, D.; Kamke, D.; Kramer, P. (Universitaet, Marburg, Ger.). Ann. Physik, (7), 14: 201-20(1964). (In German).

Coincidence measurements on the reaction ^{11}B(p,α)2α for proton energies of 150 and 163 kev were reported. The measurements were made with two semiconductor detectors connected with a one-parameter, multichannel discriminator. The results were represented in Dalitz diagrams. Below the narrow resonance of the reaction at 163 kev ($\Gamma_{1\,ab}$ = 7 kev), the Dalitz diagram agrees with the expected distribution for a decay to ^{8}Be (ground state and first excited state at 2.9 Mev). Within the resonance the Dalitz diagram contains a high density in the center. This high density is incompatible with a cascade decay to ^{8}Be and can only be explained by a three-particle decay of ^{12}C into three α particles. (tr-auth)

41700 ON THE PROBABLE RADIOACTIVE DECAY OF ^{136}Ce. Hohmuth, Karl; Schintlmeister, Josef (Zentralinstitut fur Kernforschung, Rossendorf, Ger.). Ann. Physik (7), 15: 101-5(1965). (In German).

On the basis of the mass values for isobars with A = 136, it can be suspected that ^{136}Ce, which was assumed stable, is possibly unstable toward E capture. In order to test this supposition, 2 g of Ce_2O_3 were investigated in a proportional counter for the emission of the L x-ray line of ^{136}Ba. This line must be emitted on the basis of the decay of the daughter nucleus ^{136}La (9.25 min.) from the Ce preparation. The results of the study show no such line. Therefore, a lower limit for the half life of ^{136}Ce is 2.9×10^{11} yrs. (tr-auth)

41701 ELECTRIC OCTUPOLAR TRANSITION OF 71.2 kev IN THE DECAY OF HAFNIUM-171 INTO LUTETIUM-171. Barneoud, Daniel; Treherne, Jacqueline; Valentin, Jacques (Centre d'Etudes Nucleaires, Grenoble, France and Laboratoire Joliot-Curie, Orsay, France). Compt. Rend., 260: 4717-20(May 3, 1965). (In French).

An E_3 type 71.2-kev transition in the decay ^{171}Hf $\rightarrow$ ^{171}Lu was shown, and a theoretical interpretation of it was given. (tr-auth)

41702 VARIATIONAL CALCULATION OF THE COLLECTIVE STATES OF SPHERICAL NUCLEI. Touchard, Jean (Faculte des Sciences, Orsay, France). Compt. Rend., 260: 4937-9(May 10, 1965). (In French).

Variational calculation was made of the collective states of spherical nuclei. The study was limited to the case where all the eigenvalues of M are real, distinct, and not 0. Numerical results obtained using reference parameters for Sn isotopes are tabulated together with the exact solutions and the results of a perturbation calculation of the lowest order. The results show that the approximations are very close to the exact results. (J.S.R.)

41703 STUDY OF THE ANGULAR CORRELATION IN THE (p,pd) REACTION ON CARBON-12. Bachelier, Daniel; Bernas, Monique; Brissaud, Ivan; Detraz, Claude; Ganguly, Nripendra; Radvanyi, Pierre (Faculte des Sciences, Orsay, France). Compt. Rend., 260: 4987-90 (May 10, 1965). (In French).

The angular correlation between 155-Mev incident protons and emitted deuterons in the (p,pd) reaction on carbon was determined experimentally, with the purpose of separating the mechanisms of indirect pick-up and knock-out. The first results obtained for the angles of emission of deuterons at 28¼° and 38¼° and at relatively high deuteron energies show a maximum angular correlation near the angle of the free proton-deuteron scattering. (tr-auth)

41704 STUDY OF THE γ RADIATIONS OF ^{182}Ta USING GERMANIUM n-i-p. Henck, Roland; Stab, Lucien; Siffert, Paul; Coche, Andre (Centre de Recherches Nucleaires, Strasbourg). Compt. Rend., 260: 4991-4(May 10, 1965). (In French).

A lithium-compensated germanium diode was used to study the γ spectrum emitted during the decay ^{182}Ta $\rightarrow$ ^{182}W in the energy range from 850 to 1600 kev. (tr-auth)

41705 THE DECAY OF ^{169}Er. Duperrin, Jean-Claude; Gizon-Juillard, Andree (Faculte des Sciences, Grenoble, France; CEN, Grenoble, France). Compt. Rend., 261: 98-101(July 5, 1965). (In French).

The analysis of M conversion electrons from the 8.42-kev transition yields a mixing ratio E_2/M_1 of $1.4 \pm 0.3 \times 10^{-3}$. The branching ratio of the β spectrum at the 8.42-kev level is $(45 \pm 5)\%$. (tr-auth)

41706 STUDY OF THE EXCITATION CURVES OF THE REACTION ^{12}C(t,α_0)^{11}B. Seltz, Raymond; Gerardin, Claude; Wery, Michel; Magnac-Valette, Denise (CRN, Strasbourg). Compt. Rend., 261: 391-4(July 12, 1965). (In French).

The excitation curves of the reaction ^{12}C(t,α_0)^{11}B were determined at various angles with incident tritons with energy from 1.350 to 3.400 Mev. Eight of the excited levels of the compound nucleus ^{15}N found by other reactions are confirmed by the results obtained. (tr-auth)

41707 HIGH-ENERGY ELECTRON AND PHOTON PASSAGE THROUGH CONDENSED MEDIA. Pomanskii, A. A. (Lebedev Inst. of Physics, Moscow). Izv. Akad. Nauk SSSR, Ser. Fiz., 28: 1826-8(Nov. 1964). (In Russian).

Nuclear interactions of high-energy particles have been investigated using the photoemulsion method. The photons formed by the decay of π^0 mesons in these interactions were found to possess very high energies. Passage of such high-energy photons and electrons ($E > 10^{12}$ ev) through the photoemulsion cannot be described by the usual equations of the cascade theory, especially if it contains embedded heavy ions, such as W. The bremsstrahlung and pair formation theory does not apply to condensed media at high energies; polarization of the medium leads to the emission of a low-energy γ quantum. A. B. Migdal considered these effects from the view quantum theory viewpoint, taking into account the effect of multiple scattering and pair formation; he derived formulas for calculating the cross section for bremsstrahlung and pair formation which are valid at $E \gg mc^2$. Analytical expressions are given for the cross sections calculated on the basis of Migdal's formulas. The number of particles in a shower may be determined by a Monte-Carlo method, defining the behavior of a cascade shower at its first stage of development. (TTT)

41708 USE OF CONFORMING LOBACHEVSKII PLANE REFLECTION ON EUCLIDEAN BAND IN THE ANALYSIS OF MULTIPLE MESON PRODUCTION. Bubelev, E. G. (Joint Inst. for Nuclear Research, Dubna, USSR). Izv. Akad. Nauk SSSR, Ser. Fiz., 28: 1829-34(Nov. 1964). (In Russian).

The various types of interactions of relativistic particles may be determined not only by statistical methods but also by studying the interaction in individual cases. N. A. Chernikov developed the concept of the Lobachevskii velocity spaces which was used to evolve a method based on the reflection of a Lobachevskii plane on a Euclidean band. By means of a graphic method representing the velocities of pion showers formed by the collision of high-energy nucleons, the inelasticity coefficient of the target nucleon may be rapidly determined in the system at rest of the emitted nucleon. The interaction of high-energy nucleons in the fireballs or clusters formed by the annihilation of antinucleons is also examined. Lobachevskii velocity diagrams are shown for particle showers with energies of 0.1 to 1 Tev. (TTT)

41709 ANALYSIS OF HIGH-ENERGY PARTICLE FLUXES BY MEANS OF LOBACHEVSKII VELOCITY DIAGRAMS. Bubelev, E. G. (Joint Inst. for Nuclear Research, Dubna, USSR). Izv. Akad. Nauk SSSR, Ser. Fiz., 28: 1835-40(Nov. 1964). (In Russian).

The Lobachevskii velocity diagrams, applied to the analysis of meson production in the 10^{11} to 10^{12} ev range, was used to examine particle jets possessing energies of about $>10^{12}$ ev. In view of its invariance with respect to parallel transfers, this diagram is a convenient representation of the kinematics of a given particle jet, as it is unaffected by the choice of the counting system, once the direction of the axis of the jet has been established. Use of such diagrams for analysis facilitates the separation of the particles in the jet into genetically related groups, formed by pion fireballs and excited nucleons. The values obtained are more reliable than those obtained from log tgθ diagrams. As an example, the Lobachevskii diagrams of 5 jets with energies of $E_0 >$ 1 Tev, containing the most complete data on the angle of emission and pulses of the secondary particles, have been analyzed. Three cases involved neutral, ultrarelativistic pions, carrying 30 to 45% of the energy of the primary nucleon, which conserved only 20 to 40%. It was found that in these jets the ultrarelativistic pions represent the product of anisotropic decay of heavy mesons emitted by strongly excited nucleons with masses $M_i = 2$ to 3 Bev/c^2. Other vector mesons with a 2 or 3-particle decay scheme may participate in the transition of large portions of the energy of the primary nucleon to one neutral or charged pion. (TTT)

41710 INVERSE PROBLEM IN CASCADE THEORY. Astaf'ev, V. A.; Ivanenko, I. P. (Moscow State Univ.). Izv. Akad. Nauk SSSR, Ser. Fiz., 28: 1847-53(Nov. 1964). (In Russian).

Experimental data concerning high-energy showers, such as the number of particles of a given type, and their energy distribution at various depths in the atmosphere, are usually correlated with a specific nuclear interaction model. However, it is of interest to examine the elementary act of interaction without reference to any model. Within the framework of the cascade theory this can be achieved by solving the so-called inverse problem, expressing the energy spectra of the particles or differential interaction probabilities directly through the shower characteristics, which are assumed to be known from experimental studies. Several solutions are proposed for solving these problems, starting either from the cascade equations for the average differential spectra at various depths or from the first-collision equation. The cascade equations in their usual form are not suited for solving the inverse problem because some of the members of these equations are integrated according to the first, the others according to the second differential probability argument. Therefore, the first-collision equation seemed to offer a better approach for solving this problem. As an example, electron–photon showers generated by primary photons are considered. (TTT)

41711 FLUCTUATION OF PARTICLE NUMBER IN ELECTROMAGNETIC CASCADES AND ITS EFFECT ON THE SPECTRUM OF IONIZATION BURSTS INDUCED BY μ MESONS. Gerasimova, N. M. (Lebedev Inst. of Physics, Moscow). Izv. Akad. Nauk SSSR, Ser. Fiz., 28: 1870-2(Nov. 1964). (In Russian).

The strong fluctuations in the electron–photon showers as the result of interactions may exceed the average values of the showers; therefore, when analyzing experimental data on electromagnetic processes, the fluctuations must be calculated. Analytical formulas derived for the dispersion of the e-γ shower particles are illustrated for the case of showers formed by 1-Tev electrons and photons in Fe. Estimation of the fluctuations in the spectra of large bursts indicates that a corresponding attenuation coefficient must be introduced in the μ-meson spectrum. However, this factor is not sufficient to resolve the disagreement in the spectra derived from bursts and those based on spectroscopic measurements. (TTT)

41712 NUCLEAR PHOTOEFFECT IN THE LABORATORY. Kuz'menko, G. I. (Odessa Army Academy). Izv. Vysshikh Uchebn. Zavedenii, Fiz., No. 3, 145-6(1965). (In Russian)

A method for observing the nuclear photoeffect in the ordinary laboratory and in lecture demonstrations is described. The method enables the order of magnitude of the transverse cross section for the $D + \gamma \rightarrow H + n$ reaction to be obtained, using a ^{228}Th gamma source and a heavy water target. (M.J.T.)

41713 THE ENTROPY OF A NUCLEAR SPIN SYSTEM IN A MAGNETIC FIELD. AN APPLICATION OF STATISTICAL MECHANICS. Lee, J. (Univ. of Manchester, Eng.). J. Chem. Educ., 42: 340-1(June 1965).

An assembly of equivalent nuclei of spin $\frac{1}{2}$ is considered. An algebraic expression is obtained for the entropy as a function of magnetic field using two distinct approaches: firstly from the point of view of the number of a priori equally probable complexions; and secondly by use of the partition function concept. (L.B.S.)

41714 CROSS-SECTION RATIOS FOR THE ISOMERIC PAIR $^{44m/44}$Sc PRODUCED BY THE ^{45}Sc(d,t)^{44}Sc NUCLEAR REACTION. Mocoroa, A.; Vignau, H.; Caracoche, M. C.; Nassiff, S. J. (Comision Nacional de Energia Atomica, Buenos Aires; La Plata National Univ., Argentina). J. Inorg. Nucl. Chem., 27: 1719-22(Aug. 1965).

Yield ratios for the isomeric pair ^{44m}Sc and ^{44}Sc formed in the (d,t) reaction on ^{45}Sc were experimentally determined. By means of the stacked foils technique, deuterons energy was varied from the threshold for the studied reaction up to 28.6 Mev. (auth)

41715 CROSS-SECTION RATIOS FOR THE ISOMERIC PAIR ^{58m}Co, ^{58}Co PRODUCED BY THE (d,t) REACTION. Caracoche, M. C.; Mocoroa, A.; Nassiff, S. J.; Vignau, H. (Comision Nacional de Energia Atomica, Buenos Aires; La Plata National Univ., Argentina). J. Inorg. Nucl. Chem., 27: 1723-6(Aug. 1965).

The isomer yield ratios for the ^{58}Co isomers produced by (d,t) reactions were investigated from threshold to 26 Mev. Experimental results are briefly discussed. (auth)

41716 A SEARCH FOR 2.6-Hr ^{126m}I. Narang, V. P.; Sugihara, T. T. (Clark Univ., Worcester, Mass.). J. Inorg. Nucl. Chem., 27: 1727-8(Aug. 1965).

Attempts to produce 2.6-hr ^{126m}I in the reactions ^{127}I(p, pn), ^{127}I(n,2n), ^{123}Sb(α,n) were unsuccessful. The previous report of an iodine nuclide of 2.6-hr half life and mass 126 appeared to be in error. (auth)

41717 THE RADIOISOTOPES ^{117}I, ^{118}I, AND ^{119}I, AND ^{117}Te. Butement, F. D. S.; Qaim, S. M. (Univ. of Liverpool). J. Inorg. Nucl. Chem., 27: 1729-34(Aug. 1965).

The half lives of ^{117}I, ^{118}I, and ^{119}I were determined by milking the tellurium daughters, and were 14.5, 17.2, and 25.8 min respectively. ^{118}I emits 5.5-Mev positrons. ^{117}Te appears to have two isomers decaying independently, ^{117m}Te (1.9 hr) emitting 1.7-Mev positrons and ^{117}Te(1.1 hr) emitting gamma radiation of over 2 Mev but no positrons over 1 Mev. (auth)

41718 INELASTIC SCATTERING OF 14 Mev NEUTRONS TO LOW-LYING STATES OF Ta, W, Tl AND Pb. Pearlstein, S.; Winhold, E. J. (Rensselaer Polytechnic Inst., Troy, N. Y.). J. Nucl. Energy: Pts. A and B, 19: 497-500(July 1965). (BNL-8421).

Measurements of the scattered neutron energy spectra at 90° over the range 6 to 14 Mev for 14 Mev neutrons incident on Ta, W, Tl and Pb were made using a proton recoil neutron spectrometer. Integrated inelastic cross sections over this energy range vary from 11 ± 3 mb/sterad for W to 17 ± 3 for Pb. In all cases the spectra appear to go through a minimum in the vicinity of an excitation energy of 8 Mev before rising strongly toward the evaporation peak. (auth)

41719 HALF-LIFE MEASUREMENTS IN Rh^{101} AND Rh^{102m}. Hisatake, Kazuo; Matsuo, Shigeki; Kawakami, Hirokane (Tokyo Inst. of Tech.). J. Phys. Soc. Japan, 20: 1107-11(July 1965).

The half lives of ^{101}Rh and ^{102m}Rh were investigated by measuring the internal conversion electrons with a magnetic beta-ray spectrometer. The half life of ^{101}Rh and that of ^{102m}Rh are determined to be (3.0 ± 0.4)y and (2.1 ± 0.9)y, respectively. (auth)

41720 ALPHA PARTICLE GROUPS FROM THE DEUTERON BOMBARDMENT ON ^{16}O AND ^{40}Ca. Ishimatsu, Toshiyuki; Morita, Susumu; Tohei, Tsutomu; Kawai, Nawoyuki; Takano, Naoyuki; Kato, Norihisa; Yamanouchi, Yoshimaro (Tokyo Univ.). J. Phys. Soc. Japan, 20: 1112-20(July 1965).

Calcium oxide targets were bombarded with 15.14-Mev deuterons from a cyclotron. Alpha-particle spectra were obtained at angles of 45, 60, and 90° by means of a broad range magnetic spectrograph. In the 45 and 60° spectra none of the alpha-particle groups corresponding to T = 1 levels in ^{14}N up to an excitation of 10 Mev was observed with an appreciable intensity with the only exception of the alpha-particle group leading to the 9.17-Mev level. In the 90° spectrum, however, alpha-particle groups leading to some of the T = 1 levels in ^{14}N were observed evidently. Alpha-particle groups leading to somewhat doubtful levels in ^{14}N, i.e., 6.05-, 6.70-, 7.40-, and 7.60-Mev levels were not observed with appreciable intensities in all the spectra. Alpha-particle groups from the $^{40}Ca(d,\alpha)^{38}K$ reaction leading to several levels in ^{38}K below 4-Mev excitation and some ^{3}He groups from the $^{40}Ca(d,^{3}He)^{39}K$ reaction leading to the lowest levels in ^{38}K were observed. (auth)

41721 ENERGY DEPENDENCE OF THE ANGULAR DISTRIBUTION IN THE $^{12}C(d,p)^{13}C$ REACTION. Borbely, Imre; Dolinszky, Tamas; Eroe, Janos; Hrehuss, Gyula. Magy. Tud. Akad. Kozp. Fiz. Kut. Int. Kozlemen., 13: 89-98(1965). (In Hungarian).

Excitation functions at Θ/lab = 90° of the elastically scattered deuterons and of the p_0 and p_1 proton groups were measured at 10-kev steps in the range 900 to 2000 kev, and the absolute cross section was determined. Angular distributions of the ground-state protons were also taken at 34 different energies within the same energy range. No indication of any appreciable contribution from direct processes to the reaction pattern is observed. (auth)

41722 ANGULAR DISTRIBUTION OF GAMMA-RAYS FROM THE FISSION OF U-235. Graff, Gyoergy; Lajtai, Albert; Nagy, Laszlo. Magy. Tud. Akad. Kozp. Fiz. Kut. Int. Kozlemen., 13: 177-84(1965). (In Hungarian).

The angular distribution of gamma rays from thermal-neutron-induced fission was measured with respect to the axis of fission. The gamma intensities were found to be higher in the direction of fragment motion than in the direction normal to fragment motion. The anisotropy was found to be nearly identical for 120-kev and 600-kev threshold photon energies. (auth)

41723 METHOD FOR MEASURING TOTAL CROSS SECTIONS WITH NEUTRONS HAVING ENERGIES FROM 2.5 TO 15 Mev. Foster, D. G. Jr.; Glasgow, D. W. (General Electric Co., Richland, Wash.). Nucl. Instr. Methods, 36: 1-12(Sept. 1965). (BNWL-SA-92).

Pulsed-beam time-of-flight techniques, used in a transmission measurement with a continuous spectrum of neutron energies, permit moderate resolution (2.5 to 4.5 percent, without gaps) and moderate precision (1 to 3 percent) to be obtained in an investigation of neutron total cross sections between 2.5 and 15 Mev. Neutrons are produced by bombarding a thick lithium target with deuterons and are detected by a liquid scintillation counter. The use of small-diameter samples close to the source minimizes inscattering and permits the use of scarce samples. Calculations relative to the best position, diameter, and thickness for the samples are summarized. Sharp structure in the spectrum introduces some difficulties into the reduction of data and may cause systematic errors above 11 Mev. Tests for other systematic errors have shown them to be less than two percent. (auth)

41724 COMPUTATION OF MOESSBAUER SPECTRA. Gabriel, J. R.; Ruby, S. L. (Argonne National Lab., Ill.). Nucl. Instr. Methods, 36: 23-8(Sept. 1965).

Three new FORTRAN programs are described that can compute the spectrum to be expected in almost any Moessbauer experiment. Illustrations of its use are given, including results for the effect of an external magnetic field on a powdered sample with a crystalline electrostatic field. (auth)

41725 NEUTRON-CAPTURE GAMMA RAY STUDIES OF LOW-LYING ^{52}V LEVELS. White, D. H.; Saunders, B. G.; John, W.; Jewell, R. W. Jr. (Univ. of California, Livermore). Nucl. Phys., 72: 241-53(1965). (UCRL-12349).

Neutron-capture gamma rays from natural vanadium were studied by means of a bent crystal spectrometer and a NaI(Tl) coincidence spectrometer. Gammas attributed to ^{52}V were found at 124.454 ± 0.016, 125.083 ± 0.015, 147.841 ± 0.028, 294.97 ± 0.09, 419.54 ± 0.23, 436.49 ± 0.23, 645.70 ± 0.10, 794.2 ± 0.4, 824.4 ± 0.5, and 845.8 ± 1.5 kev, using the bent crystal spectrometer. Energies are calibrated from the 100.107 ± 0.001 kev ^{182}Ta gamma. An additional gamma was found at 17.0 ± 0.3 kev using a thin cleaved NaI(Tl) crystal with a thin window. An analysis was made based upon the energy differences, relative intensities, coincidence measurements, and published (d,p) results. A consistent level scheme is proposed with excited states at 17.0, 22.8, 141.5, 147.8, 436.5, 793.6, and 847.0 kev. Results are considered in terms of shell model predictions. (auth)

41726 THE LEVEL STRUCTURE OF ^{53}Cr AND ^{55}Cr. Bock, R.; Duhm, H. H.; Martin, S.; Ruedel, R.; Stock, R. (Max-Planck-Institut fuer Kernphysik, Heidelberg). Nucl. Phys., 72: 273-97(1965). (In German).

The reactions $^{52,54}Cr(d,p)^{53,55}Cr$ were studied with a magnetic spectrograph at E_d = 10 Mev. The Q values and absolute differential cross sections for many proton groups were measured. Angular momentum assignments and absolute spectroscopic factors for different levels given by means of the DWBA are compared with the results of calculations on the basis of the shell model and the unified model. The collective components in the wave functions of the unified model were observed in the reaction $^{53}Cr(p,p')$ at E_p = 11 Mev. A strong similarity between the low-lying states of ^{53}Cr and ^{63}Cu is found. (auth)

41727 Nb AND Rb NEUTRON RESONANCES AND RADIATION WIDTHS OF MEDIUM-MASS NUCLEI. Iliescu, N.; Kim, Hi San; Pikelner, L. B.; Sharapov, E. I.; Sirazhet, H. (Joint Inst. for Nuclear Research, Dubna, USSR). Nucl. Phys., 72: 298-304(1965).

The neutron resonance parameters for niobium and rubidium in the energy range up to 400 ev and 1300 ev, respectively, were determined by measuring the transmission, capture, scattering, and self-indication. The obtained values of the radiation widths for niobium s and p wave levels coincide within the measurement error. The radiation width for the magic nucleus of ^{87}Rb is less than that of the nonmagic ^{85}Rb. The experimental data on the radiation widths of medium nuclei show a minimum in the region of the closed shell with the number of neutrons equal to 50. (auth)

41728 OVERLAP INTEGRALS AND SINGLE-PARTICLE WAVE FUNCTIONS IN DIRECT INTERACTION THEORIES. **Berggren, Tore (Nordisk Institut for Teoretisk Atomfysik, Copenhagen). Nucl. Phys., 72: 337-51(1965).**

A formalism is given in which the overlap integrals between the eigenstates of an A particle system and those of an (A – 1) particle subsystem play the role of single-particle wave functions for the description of the system. These overlap integrals are the natural quantities to use in the treatment of processes in which one particle is added to or extracted from the system (capture and ionization processes). It is shown that they are also well suited for expressing matrix elements of any single-particle operator. Their transformation properties under space inversion and rotation are examined in detail. The relation between the overlap integrals and the shell model single-particle orbitals is discussed, and some possible generalizations are briefly described. (auth)

41729 STUDIES ON NUCLEAR STRUCTURE IN THE 2s-1d SHELL. I. METHODS OF GROUP THEORY AND A MODEL INTERACTION. **Flores, J.; Chacon, E.; Mello, P. A.; de Llano, M. (Universidad de Mexico, Mexico City). Nucl. Phys., 72: 352-78(1965).**

It is proposed to carry out systematic calculations in nuclear structure in the 2s – 1d shell, considering a model interaction which is a linear combination of a spin-orbit coupling ($W_{s.o.}$) plus a quadrupole-quadrupole (Q^2) and an orbital pairing (P) term, the last two terms taking into account, respectively, the long and short-range correlations of the residual central interaction. Methods of group theory are discussed that would allow the states to be classified in relation with a chain of subgroups in such a way that each of the interactions Q^2, P and $W_{s.o.}$ becomes diagonal. It is then considered how to obtain transformation brackets from states classified by one chain of subgroups to states classified by another, so that it is possible to obtain the matrix elements for the model interaction. (auth)

41730 STUDIES ON NUCLEAR STRUCTURE IN THE 2s-1d SHELL. II. APPLICATION TO NUCLEI WITH A = [18] AND A = 20. **de Llano, M.; Mello, P. A.; Chacon, E.; Flores, J. (Universidad de Mexico, Mexico City). Nucl. Phys., 72: 379-416(1965).**

A model interaction containing quadrupole-quadrupole, orbital pairing, and spin-orbit terms is used. The explicit matrices of the model interactions are obtained for systems of two and four particles in the 2s – 1d shell. The eigenvalues of these matrices are compared with the energy levels of ^{18}F, ^{18}O, ^{20}Ne, ^{20}O, and ^{20}F, obtaining the values of the parameters in the model interaction that give the best fit. Furthermore, the explicit expression of states of two and four particles in the 2s – 1d shell are given in the SU_3 classification, and the eigenstates of the model interaction are obtained in terms of these states. (auth)

41731 THE POLARIZATION OF PROTONS SCATTERED BY CARBON. **Moss, S. J.; Haeberli, W. (Univ. of Wisconsin, Madison). Nucl. Phys., 72: 417-35(1965). (COO-7-355).**

Angular distributions of polarization and cross section in p–^{12}C elastic scattering were measured in 10° intervals for laboratory scattering angles Ψ_1 = 20 to 140° at eight energies between 4.7 and 8.7 Mev. Polarizations and cross sections as a function of energy at Ψ_1 = 50° are also presented. At three angles of scattering (Ψ_1 = 50, 70, and 90°) the polarization measurements were extended to 11.3 Mev. A phase analysis of the data was carried out at the energies where angular distributions were measured. It is shown that the gross features of the energy dependence of the phase shifts agrees with the optical model. (auth)

41732 DIFFERENTIAL CROSS SECTIONS AT 0° AND ANGULAR DISTRIBUTIONS OF RESOLVED NEUTRONS FROM ^{11}B + d. **Almond, P. R.; Risser, J. R. (Rice Univ., Houston, Tex.). Nucl. Phys., 72: 436-48(1965). (TID-21763).**

Differential cross sections at 0° for the reactions $^{11}B(d,n_0)^{12}C$ and $^{11}B(d,n_1)^{12*}C$ (4.43 Mev state) were measured at deuteron bombarding energies from 1 to 11 Mev. Angular distributions were measured at 2.38, 3.58, 3.78, 4.23, 5.5, 7.0, 8.0, 8.8, 9.0, and 9.7 Mev. The 0° differential cross sections for the reaction $^{11}B(d,n_2)^{12*}C$ (7.66 Mev state) from 2 to 11 Mev and for the reaction $^{11}B(d,n_3)^{12*}C$ (9.64 Mev state) from 5.5 to 11 Mev were also measured. The data were taken by means of a neutron spectrometer consisting of a polyethylene radiator with gas proportional dE/dx and scintillation E counters operating in coincidence to detect recoil protons from the radiator. Above 6 Mev, the $^{11}B(d,n_0)^{12}C$ and $^{11}B(d,n_1)^{12*}C$ (4.43 Mev state) reactions appear to proceed mainly by deuteron stripping. Below about 6 Mev, some compound-nucleus formation may be indicated by the form of the angular distributions and by the broad resonance-like structure in the 0° excitation curves. Theoretical angular distributions were calculated in the distorted wave Born approximation for comparison with the experimental angular distributions. (auth)

41733 A STUDY OF THE (^3He,^7Be) REACTION IN ^{12}C. **England, J. B. A.; Reece, B. L. (Birmingham Univ., Eng.). Nucl. Phys., 72: 449-60(1965).**

Stacked-foil and catcher-foil techniques were used to determine the excitation function, angular distribution, and energy spectrum of ^7Be produced by ^3He bombardment of ^{12}C at a primary energy of 29.4 Mev. Carbon foils from 2 to 7 mg · cm^{-2} thick were used as targets, and the ^7Be was estimated by radioactive assay. A phenomenological analysis of the data, taking account of the absorption of the ^7Be fragments in the material of the target, suggests that the ^7Be is produced by a three-body process. (auth)

41734 EFFECT OF EXPERIMENTAL RESOLUTION ON THE MEASURED WIDTHS OF THE FLUCTUATION CORRELATION FUNCTION FOR NUCLEAR CROSS SECTIONS. **Lang, Donald W. (Bartol Research Foundation, Swarthmore, Penna.; Argonne National Lab., Ill.). Nucl. Phys., 72: 461-74(1965).**

The effect of experimental resolution on measurements involving fine structure in nuclear cross sections is considered. In energy regions where resonances overlap considerably, the average width of the fine-structure features is normally determined from a set of averages of products. The effect on the set, and hence on the resonance width, is investigated for several different forms of the resolution function. Both analysis and numerical results are presented. If the resolution function has a sufficiently narrow width and drops rapidly to zero away from the measured energy, then the average is unaffected. Curves are given to provide corrections in less optimal conditions. (auth)

41735 SHELL-MODEL CALCULATION FOR ^{212}Po. **Glendenning, Norman K.; Harada, Kichinosuke (Univ. of California, Berkeley). Nucl. Phys., 72: 481-508(1965). (UCRL-11945).**

A detailed shell-model calculation for the lower excited levels and high-spin, alpha-emitting isomer of ^{212}Po is reported. The result shows that the main configuration of the isomeric state of ^{212}Po is $[(h_{9/2})^2_9(g_{9/2}i_{11/2})_{10}]$ and has spin J = 18. The calculated spectrum also suggests the existence of a few low-lying levels which have not been observed experimentally, including a possible isomer with J = 10. Alpha reduced widths and electromagnetic transition probabilities were calculated and compared with those of the previous works, and with experiment. The results are generally satisfactory. The wave functions are strongly configuration admixed including non-negligible higher seniority components. (auth)

41736 OBSERVATION OF THE $[505]11/2^-$ NILSSON STATE AS AN ISOMER IN ^{159}Dy. **Borggreen, J.; Frahm, H. J.; Hansen, N. J. Sigurd; Bjoernholm, S. (Universitet, Copenhagen). Nucl. Phys., 72: 509-14(1965).**

The 115 ± 10 μsec isomer in ^{159}Dy was produced by bombardment of ^{159}Tb with pulsed beams of protons and deuterons. The delayed γ-rays were recorded with a NaI scintillation spectrometer and the delayed conversion lines with a magnetic spectrometer. The results are interpreted in terms of an isomeric level at 356 ± 3 kev with (K,I^π) equal to ($11/2, 11/2^-$), decaying by K-forbidden M1 and E2

transitions to the $^9/_2^-$ and $^7/_2^-$ members of the ground-state rotational band in ^{159}Dy. These properties serve to identify the isomeric level as the $[N,n_z,\Lambda]\Omega^\pi = [505]\ ^{11}/_2^-$ neutron state predicted by Nilsson. (auth)

41737 NEUTRON SCATTERING STUDIES OF ^{39}K. Towle, J. H.; Gilboy, W. B. (Atomic Weapons Research Establishment, Aldermaston, Berks, Eng.). Nucl. Phys., 72: 515-28(1965).

Differential scattering cross sections were measured at 1.49, 2.38, 3.00 and 3.76 Mev using a time-of-flight spectrometer. Fits were made to the differential elastic and total cross sections at each energy using a surface absorption optical model in which the real and imaginary well depths were allowed to vary, and good agreement was obtained at 3.00 and 3.76 Mev. Inelastic scattering was observed to the 2.53, 2.82 and 3.02 Mev levels of ^{39}K. Statistical model calculations were made at 3.76 taking into account the (n,n'), (n,p) and (n,α) reactions, and the results are compared with experiment. Transmission measurements of the total cross section were made between 2 and 3 Mev where there were no previous data. (auth)

41738 NEW BOUND LEVELS IN ^{43}Sc FROM RADIATIVE PROTON CAPTURE IN ^{42}Ca. Broman, L.; Dubois, J. (Chalmers Tekniska Hogskola, Goteborg). Nucl. Phys., 72: 529-36(1965).

The gamma radiation from the $^{42}Ca(p,\gamma)^{43}Sc$ reaction was studied at seven resonances with a lithium-drifted germanium solid state detector. The excellent resolving power and the good linearity of the detector made it possible to determine accurately the decay scheme of ^{43}Sc. The levels found at 150 ± 1, 472 ± 1, 844 ± 2, 877 ± 2, 1175 ± 4, 1649 ± 7 and 2089 ± 7 kev are in good agreement with earlier results obtained with NaI crystals. Additional new levels were found at 1959 ± 7, 2137 ± 7, 2200 ± 7, 2587 ± 10, 2676 ± 10, 2979 ± 10, 3297 ± 10 and 3809 ± 10 kev and new levels at 1150 ± 10 and 2382 ± 10 kev are suggested. The Q value of the reaction was determined to 4937 ± 5 kev. (auth)

41739 (d,p) AND (t,d) REACTIONS IN THE COULOMB FIELD. Goldfarb, L. J. B. (Univ. of Manchester, Eng.). Nucl. Phys., 72: 537-51(1965).

Arguments are put to show the unique role provided by measurements of differential cross sections below the Coulomb barrier for the determination of reduced widths or spectroscopic factors in stripping reactions. Corroboration is given by the results of DWBA calculations involving targets with Z = 20, 30, 40 and 50 where certain energies and angles are singled out as providing instances of high yields, (close to that expected above the Coulomb barrier in the forward hemisphere) and a fair degree of insensitivity to the effects of nuclear distortion and other uncertainties associated with the DWBA. This situation obtains for low Q values, and the relevance is then only to high states of excitation in a (d,p) transition. The (t, d) reaction, on the other hand, enables studies of transitions to the ground state and neighboring excited states. (auth)

41740 WEAKLY EXCITED RESONANCE LEVELS IN THE $^{13}C(p,\gamma)^{14}N$ REACTION. Detenbeck, R. W.; Armstrong, J. C.; Figuera, A. S.; Marion, J. B. (Univ. of Maryland, College Park). Nucl. Phys., 72: 552-76(1965).

Three midget resonances in the $^{13}C(p,\gamma)^{14}N$ reaction were observed at E_p = 1012 ± 2 kev, 1523 ± 2 kev and 1701 ± 1 kev corresponding to ^{14}N excitation energies of 8.489, 8.963 and 9.129 Mev, respectively. The 8.489 Mev state decays by γ-ray emission predominantly to the 5.10 Mev state with an angular distribution, $W(\theta) = 1 + (0.59 \pm 0.06)P_2(\cos\theta) - (0.46 \pm 0.10)P_4(\cos\theta)$. This angular distribution together with the observed γ-ray width ($\omega\Gamma_\gamma \cong 0.01$ ev) and branching ratios determine that $J^\pi = 4^-$, T = 0 for this level. The 8.963 Mev level decays by γ-ray emission at least two-thirds to the 6.44 Mev state. This fact and the small transition rate ($\omega\Gamma_\gamma \cong 0.003$ ev) identify the level as 5^+. The only observed transition (≥80%) from the 9.129 Mev level is to the ground state ($\omega\Gamma_\gamma \simeq 0.03$ ev) with an angular distribution, $W(\theta) = 1 + (0.22 \pm 0.09)P_2(\cos\theta)$. These data establish $J^\pi = 2^-$, T = 0 for this level. Arguments are given for shell model assignments to these levels. (auth)

41741 EVIDENCE FOR SHELL STRUCTURE AND ANGULAR MOMENTUM EFFECTS IN THE DECAY OF COMPOUND NUCLEI OF NICKEL. Ewart, Alan; Blann, Marshall (Univ. of Rochester, N. Y.). Nucl. Phys., 72: 577-92(1965).

Excitation functions resulting from the $^{56}Fe(\alpha,xnyp)$, $^{56}Fe(^3He,xnyp)$ and $^{54}Fe(\alpha,xnyp)$ reactions were compared with three sets of statistical theory calculations. The first set of calculations employed a level density expression of the form $\rho(E,J)\propto(2J+1)E^{-2}\exp 2\sqrt{aE}$, where the excitation energy was corrected for pairing effects. The excitation functions calculated with this level density expression grossly overestimate the yields of ^{56}Ni and ^{57}Ni, and all calculated excitation functions attain their maximum yields at lower energies than the corresponding experimental excitation functions. Results of a second set of calculations in which the shell effect suggested by Margenau is considered explicitly by using the level density model of Rosenzweig show that the discrepancies are quantitatively consistent with the expectations of a dependence of level densities on shell occupation. It is shown that the disagreement in energy at which calculated and experimental excitation functions attain their maximum yields shows a correlation with average angular momentum, but not with excitation energy or the number of particles emitted. A third set of calculations was performed with a level density of the form $\rho(E,J)\propto(2J+1)(E-E_{rot})^{-2}\exp 2\sqrt{a(E-E_{rot})}$ where for each value of J, $E_{rot} = J(J+1)\hbar^2/2\mathcal{I}_{rig}$ and where $\mathcal{I}_{rig}$ is the rigid body moment of inertia. Evaporation probabilities were summed for each impact parameter J, weighted as $(2J+1)T_J$ where T_J is the optical model transmission coefficient for formation of the compound nucleus. It was assumed that all rotational energy was dissipated by γ-ray de-excitation with no change in the spin distribution throughout the evaporation cascade. The results of the third set of calculations gave improved agreement with respect to energy dependence of excitation functions. In all three sets of calculations the pairing energy correction was taken from the masses of Everling et al., optical model nonelastic cross sections were used for inverse reaction cross sections, and the level spacing parameter was evaluated from the $^{59}Co(p,\alpha)$ spectral measurement of Sherr and Brady. (auth)

41742 REGIONS OF VALIDITY OF THE (d,p) COULOMB STRIPPING APPROXIMATION. Smith, William R. (Oak Ridge National Lab., Tenn.). Nucl. Phys., 72: 593-603(1965).

The validity of the Coulomb stripping approximation for (d, p) reactions was investigated numerically for six targets ranging from ^{16}O to ^{238}U. The investigation involved finding the region in (E_d, Q) space where DWBA calculations that include nuclear optical-model potentials yield agreement with calculations that include only the Coulomb potentials. For nuclei between ^{48}Ca and ^{238}U the boundary between valid and non-valid Coulomb stripping was found to have an E_d dependence proportional to Z and a Q dependence proportional to $Z/A^{\frac{1}{3}}$; and furthermore, this boundary can be approximated by a straight line which, for $^{90}Zr(d,p)^{91}Zr$, has the intercepts E_d = 4.2 Mev and Q = 5.2 Mev. (auth)

41743 LOW-ENERGY TRANSITIONS IN THE DECAY OF ^{132}I. Boyd, H. W.; Hamilton, J. H. (Vanderbilt Univ., Nashville). Nucl. Phys., 72: 604-16(1965).

The internal conversion electron spectrum of transitions below 1.4 Mev in the decay of ^{132}I was studied in an iron-free, -double-focussing spectrometer. Conversion electrons were observed for transitions of 147.2 ± 1.0, 262.8 ± 1.0, 504.0 ± 1.0, 507.6 ± 1.0, 523.0 ± 0.5, 630.7 ± 0.5, 651 (complex), 667.8 (complex, 727.3 ± 0.7, 729.2 ± 0.7, 772.9 ± 0.5, 995.0 ± 0.5, 1138.4 ± 1.0 and 1398.4 ± 1.0 kev. The relative intensities of the K conversion electrons were obtained for these transitions. The K conversion coefficient of the $2^+ \rightarrow 0^+$ 668 kev transition was measured by the internal-external conversion method to be 3.59 ±

0.30×10^{-3} which agrees with theory (3.65×10^{-3}). This conversion coefficient was used to normalize relative K electron and gamma-ray intensities to obtain conversion coefficients for the 727, 729, 773, 955 and 1398 kev transitions. All are M1 and/or E2. (auth)

41744 HIGH-ENERGY TRANSITIONS IN THE DECAY OF ^{132}I. Johnson, Noah R.; Wilsky, K.; Hansen, P. G.; Nielsen, H. L. (Atomenergikommissionen, Forsoegsinstitut, Risoe, Denmark). Nucl. Phys., 72: 617-24(1965).

A study of the high-energy gamma rays of ^{132}I with a three-crystal pair spectrometer disclosed the presence of several new transitions. In addition, it permitted more precise energy assignments for the previously observed gamma rays. Gamma rays having energies greater than the pair production threshold were found at 1.141 ± 0.009, 1.22 ± 0.02, 1.282 ± 0.008, 1.359 ± 0.012, 1.393 ± 0.008, 1.439 ± 0.014, 1.716 ± 0.017, 1.767 ± 0.012, 1.914 ± 0.009, 1.988 ± 0.009, 2.076 ± 0.016, 2.162 ± 0.016, 2.222 ± 0.016, 2.394 ± 0.012, 2.55 ± 0.04 and 2.68 ± 0.04 Mev. The electron spectrum was examined with a six-gap iron beta-ray spectrometer covering the energy range of 100 to 2200 kev. Electron lines were observed corresponding to transitions at 147.4 ± 0.9, 263.0 ± 0.9, 285.5 ± 1.1, 523.0 ± 1.2, 631.5 ± 1.4, 669.0 ± 1.2 (complex), 728.8 ± 1.7, 773.8 ± 1.6, 954.9 ± 1.9 and 1395 ± 8 kev. A careful study of the end-point region of the beta spectrum has shown that the maximum energy beta ray of ^{132}I is at 2118 ± 15 kev. (auth)

41745 ENERGY LEVELS IN ^{132}Xe. Hamilton, J. H. (Vanderbilt Univ., Nashville); Boyd, H. W.; Johnson, Noah R. Nucl. Phys., 72: 625-40(1965). (ORNL-P-1258).

The energy levels in ^{132}Xe populated by the decay of ^{132}I were analyzed in the light of recent internal conversion electron and three-crystal pair spectrometer studies. All previous information on the decay of ^{132}I as well as that on the decay of ^{132}Cs was considered. The energies in kev and the spins and parities of the following excited levels in ^{132}Xe are observed in the decay of ^{132}I: 667.8 ± 0.3,2^+; 1298.1 ± 0.4,2^+; 1440.7 ± 0.4,4^+; 1805.9 ± 0.7, $(2,3)^+$; 1963.7 ± 0.7 $(3,4)^+$; 2110.4 ± 0.5, $(2-5)^+$; 2112.2 ± 0.5 $(2-5)^+$; 2395.6 ± 0.5, $(3-5)^+$; 2584.3 ± 0.8, (3^-); 2658 ± 2, (2,3); 2762.4 ± 0.5, (3,4); and 2839.5 ± 0.5, $(3)^+$. Thirty-three transitions were assigned as depopulating these levels. The states at 667.8, 1298.1, 1440.7, and 1805.9 kev as well as one at 1987 ± 2.5 kev are observed in the decay of ^{132}Cs to ^{132}Xe. (auth)

41746 FORM FACTORS FOR NUCLEAR STRIPPING REACTIONS. Pinkston, W. T. (Bartol Research Foundation, Swarthmore, Penna.); Satchler, G. R. Nucl. Phys., 72: 641-56(1965). (ORNL-P-1087).

The wave function, or form factor, to be used for the captured particle in a stripping reaction is discussed. It is shown that the structure of the nucleus must be taken into account, and leads to a set of coupled equations for this form factor. Approximate solutions to these equations are studied, and their relations to various phenomenological prescriptions for the form factor are discussed. It is stressed that if an effective one-body potential well is used to generate the wave function, it is probably not sufficient merely to vary its depth, but changes in shape (particularly in radius) must be considered. The procedure of using an effective binding energy different from the separation energy is shown, in principle, to be wrong. (auth)

41747 0^+ STATES IN THE N = 82 NUCLEI. Christensen, Rex; Yang, Fu-Chia (Universitet, Copenhagen). Nucl. Phys., 72: 657-66(1965).

Targets of ^{140}Ce, ^{142}Nd and ^{144}Sm were bombarded with 12 Mev protons and deuterons. The spectra of high-energy conversion electrons were studied in a six-gap β-ray spectrometer, and the inelastically scattered particles from ^{142}Nd and ^{144}Sm were observed in a heavy-particle spectrograph. Four E0 transitions were observed, one in ^{140}Ce, one in ^{142}Nd and two in ^{144}Sm. These E0 transitions are interpreted as transitions from excited 0^+ states to the 0^+ ground state. The energies of the excited 0^+ states are ^{140}Ce 1.90 ± 0.02 Mev, ^{142}Nd 2.21 ± 0.02 Mev, ^{144}Sm 1.67 ± 0.02 Mev and 2.45 ± 0.02 Mev. The inelastic-particle spectra show five levels in ^{142}Nd below 2.8 Mev excitation energy and seven levels in ^{144}Sm below 2.8 Mev excitation energy. (auth)

41748 ENERGY DISTRIBUTIONS OF FISSION FRAGMENTS FROM URANIUM DIOXIDE FILMS. Kahn, Steve; Harman, Randall; Forgue, Vernon (Aerojet-General Nucleonics, San Ramon, Calif.). Nucl. Sci. Eng., 23: 8-20 (Sept. 1965).

Energy spectra were obtained experimentally for fission fragments escaping from backed films of enriched uranium dioxide that were less than 11 μm thick. The data were reduced to give values for the relative average escape energies (R), escape fractions (S) and energy deposition efficiencies (D). A mathematical model was developed to synthesize these results using a Monte-Carlo-type computer code. This code included the fission-fragment masses, yields, and initial energies, the experimental source-detector geometry, a range-energy relation, an energy-loss relation and a function for the pulse-height defect in surface-barrier detectors. Various functions for these last three parameters were used in combination to obtain results that duplicated the experimental spectra and R, S and D values. The agreement was obtained with range proportional to $(\text{energy})^{\frac{5}{3}}$, the square energy-loss function, and pulse-height defect = A (E) (M − B), where A and B are constants and E and M are energy and mass, respectively. The experimental detection functions were removed from the code, and the spectra and R, S and D values were calculated for a 2π geometry. These values agreed well with those calculated using weighted averages for range and initial energy. (auth)

41749 MEASUREMENT OF THE ^{235}U NEUTRON CAPTURE-TO-FISSION RATION, α, FOR INCIDENT NEUTRON ENERGIES FROM 3.25 ev TO 1.8 kev. deSaussure, G. (Oak Ridge National Lab., Tenn.); Weston, L. W.; Gwin, R.; Russell, J. E.; Hockenbury, R. W. Nucl. Sci. Eng., 23: 45-57(Sept. 1965). (ORNL-TM-1041).

The ratio of the neutron capture cross section to the fission cross section, α, for ^{235}U was measured for incident neutron energies from 3.25 ev to 1.8 kev. A pulsed and collimated neutron beam was passed through a ^{235}U fission chamber placed at the center of a large liquid scintillator, and both capture and fission events in the chamber were detected in the scintillator by means of their prompt gamma rays. A fission event was distinguished from a capture event by a coincidence of the scintillator signal with a signal with a signal from the fission chamber. The values of α obtained, after various efficiency and background corrections were applied, are in good agreement with data derived from other experiments. (auth)

41750 A SEARCH FOR A β-ACTIVE ^{5}H. Argan, P. E.; Meneghetti, L.; Vitale, S. (Universita, Naples). Nuovo Cimento (10), 38: 1489-94(Aug. 16, 1965).

A search is made for a β-active ^{5}H produced on a ^{7}Li target by the 1000-Mev bremsstrahlung beam of the Frascati synchrotron. A negative result is obtained, and an upper limit for the production cross section of $(1.3 \pm 0.4) \cdot 10^{-31}$ cm^2 is found. (auth)

41751 ON THE DESCRIPTION OF RELAXATION PROCESSES IN NUCLEAR MAGNETIC RESONANCE. Grunzweig-Genossar, J. (Israel Inst. of Tech., Haifa). Nuovo Cimento (10), 38: 1570-8(Aug. 16, 1965).

An attempt is made to discuss the general properties and structure of (linearized) equations describing the processes of relaxation in magnetic resonance experiments. A consistent interpretation is made using a geometrical model. (auth)

41752 RADIATIVE CORRECTIONS TO INELASTIC ELECTRON SCATTERING WITH DETECTION IN COINCIDENCE. de Calan, C.; Fuchs, G. (Centre de Physique Theorique de l'Ecole Polytechnique, Paris). Nuovo Cimento (10), 38: 1594-1606(Aug. 16, 1965).

Radiative corrections are calculated for reactions of the type e + A → e′ + B + C, where the outgoing electron e′ and

another particle are detected in coincidence. The result is expressed in the usual form of a fractional correction δ to the cross section of the basic process; δ is given as a function of the kinematics, of the energy width of the detection slit for e', and of the energy width of the observed spectrum of the other detected particle. Numerical values are specified for two experiments: electro-production of π mesons and electro-disintegration of deuterium. (auth)

41753 MUON CAPTURE BY THE VIRTUAL PIONS EXCHANGED BY PROTON PAIRS IN A NUCLEUS. Bertero, M.; Passatore, G.; Viano, G. A. (Universita, Genoa). Nuovo Cimento (10), 38: 1669-87(Aug. 16, 1965).

The rate for muon capture by pairs of protons in a nucleus is evaluated. The mechanism assumed for the process is the interaction (implied by the conserved vector current theory) between the muon and the virtual pions exchanged by the nucleons. Such a process can give protons outside the nucleus; the probability of proton emission is derived and the energy spectrum is also obtained. (auth)

41754 THE ENERGY DEPENDENCE OF INELASTIC NEUTRINO CROSS-SECTION IN RESONANCE MODEL. Kawakami, A.; Fukawa, M. (Tokyo Univ. of Education). Nuovo Cimento (10), 38: 1875-80(Aug. 16, 1965).

In neutrino reactions with intranuclear nucleons, it is observed that the π^+/π^0 production ratio is 1.9 ± 0.4, and that the cross section increases rapidly with neutrino energy. In a model in which baryon resonances having spins as high as $\frac{7}{2}$ are taken into account, the experimental observations are shown to be explicable. (T.F.H.)

41755 THE (n,d) REACTION ON ^{63}Cu AND ^{65}Cu ISOTOPES AT 14 Mev NEUTRON ENERGY. Fazio, M.; Iori, I.; Micheletti, S.; Molho, N.; Pignanelli, M. (Universita, Milan). Nuovo Cimento (10), 38: 1938-40(Aug. 16, 1965).

Angular distributions of deuterons to the ground and 2^+ first-excited states of ^{62}Ni from the ^{63}Cu(n,d)^{62}Ni reaction are measured at a neutron energy of 14 Mev. The results are compared with DWBA calculations using l = 1 (ground state) and a mixture of l = 1 and l = 3 (first-excited state). The shell-and optical-model parameters of ^{62}Ni are deduced. The results for ^{65}Cu(n,d)^{64}Ni are similar to those for ^{63}Cu(n,d). (T.F.H.)

41756 LEVEL SCHEME OF ^{69}Ga. Temperley, J. K.; McDaniels, D. K.; Wells, D. O. (Univ. of Oregon, Eugene). Phys. Rev., 139: B1125-34(Sept. 6, 1965).

The gamma spectrum from the decay of ^{69}Ga was studied with the aid of a lithium-drifted germanium detector. Gamma rays of 2023, 1922, 1893, 1576, 1525, 1349, 1335, 1206, 1107.2, 1052, 871.8, 788, 763, 587, 573.4, 553, 511, 320, and 237 kev were observed. A level scheme consistent with gamma-gamma coincidence measurements is presented for ^{69}Ga. The experimental results are compared with a calculation of the energy levels in ^{69}Ga based on the intermediate-coupling model. (auth)

41757 COLLECTIVE REPRESENTATION OF LOWER LYING STATES IN Ne^{21}, Na^{21}, AND Na^{23}. Howard, A. J.; Allen, J. P.; Bromley, D. A. (Yale Univ., New Haven). Phys. Rev., 139: B1135-48(Sept. 6, 1965).

Employing model parameters deduced from the observed static properties of the nuclear systems ^{21}Ne, ^{21}Na, and ^{23}Na, both total and partial gamma transition probabilities involving relevant states in the ground-state rotational bands are computed within the Nilsson strong-coupling collective-model framework and are compared with the respective observed values. Agreement within a factor of 2 is noted for all cases with the exception of the first-excited to ground-state ^{21}Ne transition. Similar comparisons of relative total gamma transition probabilities involving postulated $\frac{9}{2}^+$ members of these same rotational bands are also presented. The relative phases of coherently interfering magnetic-dipole and electric-quadrupole radiation amplitudes are predicted for the pertinent intraband transitions; agreement with the observed relative phases is found in three of the four cases available for unambiguous comparison. Model-predicted values for beta transition probabilities involving the ground states of these three nuclei are in good agreement with observations. These comparisons provide striking support for the model validity for the description of these nuclei; prolate deformations corresponding to $\eta \sim +4.0$ are indicated by these comparisons and in addition by examination of the total nuclear binding energy calculated as a function of deformation. (auth)

41758 MEAN LIVES OF THE 2.15- AND 1.74-Mev LEVELS IN ^{10}B. Lonergan, J. A.; Donahue, D. J. (Univ. of Arizona, Tucson). Phys. Rev., 139: B1149-52(Sept. 6, 1965).

The mean lives of the 2.15- and 1.74-Mev levels of ^{10}B were measured by the Doppler-shift attenuation method. The reaction ^{11}B(^{3}He, ^{4}He)^{10}B was used, and the direction of the recoiling ^{10}B nuclei was selected by a coincidence technique. The mean lives were found to be $1.41 \pm 0.17 \times 10^{-12}$ sec for the 2.15-Mev level and $1.52 \pm 0.24 \times 10^{-13}$ sec for the 1.74-Mev level. The results are compared with estimates based on the independent-particle model. The mean lives of allowed M1 transitions are found to agree with these estimates. Evidence was found for the inhibition of an M1 transition for which $\Delta T = 0$ in a self-conjugate nucleus, and for enhancement of an E2 transition. (auth)

41759 P- AND D-STATE CONTRIBUTIONS TO THE MAGNETIC MOMENT FORM FACTORS OF H^3 AND He^3. Gibson, B. F. (Stanford Univ., Calif.). Phys. Rev., 139: B1153-9(Sept. 6, 1965).

The effects of reasonable admixtures of P- and D-state ($J^P = \frac{1}{2}^+$, $T = \frac{1}{2}$) components to the ground-state wave function of ^{3}H and ^{3}He on their magnetic-moment form factors are calculated. It is found that these form factors can not be accounted for in this way. Inclusion of the S' state and a typical $T = \frac{3}{2}$ state still leaves the magnetic form factors unexplained, although such an admixture is shown to account for the difference between the observed charge form factors. The empirical isoscalar and isovector exchange magnetic-moment form factors that are needed to fit the experimental data are calculated. (auth)

41760 INELASTIC ALPHA-PARTICLE SCATTERING BY Mn^{55} AND Co^{59}. Broek, H. W. (Argonne National Lab., Ill.). Phys. Rev., 139: B1160-3(Sept. 6, 1965).

The angular distributions of 43-Mev alpha particles scattered by ^{55}Mn and ^{59}Co were measured. The angular distributions for reactions leading to the levels at 0.98 and 1.88 Mev in ^{55}Mn are out of phase with elastic scattering. The ^{55}Mn spectra lack the very strong collective quadrupole group. Eight peaks from ^{55}Mn and seven from ^{59}Co were resolved. The ^{59}Co spectra are similar to those from ^{60}Ni, except that the excitation energies are slightly smaller in ^{59}Co. The collective quadrupole group in ^{59}Co is at least 0.3 Mev wide. (auth)

41761 INVESTIGATION OF THE $Al^{27}(\alpha,p)$ REACTION BY CROSS-SECTION FLUCTUATION STUDIES. Dearnaley, G. (Atomic Energy Research Establishment, Harwell, Berks, Eng.); Gibbs, W. R.; Leachman, R. B.; Rogers, P. C. Phys. Rev., 139: B1170-84(Sept. 6, 1965). (LA-DC-6746).

Cross sections for the reaction ^{27}Al(α,p)^{30}Si were measured with energy resolutions which, in the incoming alpha-particle channel, are finer than the energy width of the overlapping levels of the compound system ^{31}P. Fluctuations in these cross sections were analyzed for the coherence widths of this compound nucleus and for details of the reaction mechanism, such as the behavior of reaction amplitudes as shown by the form of the frequency distribution of the cross section, the independence of the reactions leading to the different magnetic substates, and the amounts of compound-nucleus and direct-interaction processes. Cross sections were measured at 11 angles between 0 and 175° and at 5-kev energy steps for energies between 5.8 and 8.6 Mev. Lack of a cross correlation between the yields of protons to the ground (0^+) and first excited (2^+) states of ^{30}Si confirmed the expected overlapping of levels of the compound nucleus, which is a basic requirement of fluctuation analysis. The coherence width of the compound-nucleus ^{31}P was found to increase from 8 to 18 kev over the range of excitation energy 14.7 to 17.1

Mev. At the back angles of 175 and 170°, the frequency distributions of cross sections for protons to the ground state of ^{30}Si agree with x^2 distributions with only slightly more than two effective degrees of freedom. This number corresponds to the slightly more than one effective magnetic substate allowed by angular-momentum properties near 180°. This agreement substantiates cross-section fluctuation theory and indicates negligible direct interaction at these back angles. At 140 and 160°, direct interactions were assumed still to be negligible, and then from the frequency distributions of cross sections the number of independent magnetic quantum states at these angles was found to be less than expected from an analysis based on angular-momentum properties and a Hauser-Feshbach calculation. This difference is a consequence of the small orbital angular momenta involved in the (α,p) reaction at these energies. These effective numbers of magnetic substates were used at the corresponding forward angles to determine the amounts of compound-nucleus and direct-interaction processes from fluctuations in cross sections. At the lowest energies of incident alpha particles, the amount of direct interaction was too low to be determined with accuracy, but at the highest energies the maximum direct-interaction cross section was roughly equal to the compound-nucleus cross section. The direct-interaction cross section was found to vary with angle roughly as expected from distorted-wave Born-approximation calculations. (auth)

41762 FINITE-SAMPLE-SIZE EFFECTS IN NUCLEAR CROSS-SECTION FLUCTUATIONS. Gibbs, W. R. (Los Alamos Scientific Lab., N. Mex.). Phys. Rev., 139: B1185-6(Sept. 6, 1965). (LA-DC-7128).

The question of bias and error due to finite size is considered, and it is suggested that these effects may be computed by replacing the excitation function with a number of independent cross sections. It is argued that the effective number of independent cross sections is given by $n = (\Delta E/\pi\Gamma_\theta)+1$ as long as the energy range ΔE is not too great. The results of some Monte Carlo calculations are also given. (auth)

41763 REMARKS ON CHARGED-PARTICLE SCATTERING. Holdeman, J. T.; Thaler, R. M. (Case Inst. of Tech., Cleveland). Phys. Rev., 139: B1186-92(Sept. 6, 1965).

The scattering of charged particles from a shielded Coulomb potential is reviewed. The limit as the shielding radius becomes infinite is discussed. A method of determining reaction cross sections, recently introduced by the authors, is treated in detail and is applied to the scattering of protons from ^{4}He and ^{2}H at 40 Mev. (auth)

41764 CLUSTER TRANSFER REACTIONS BETWEEN COMPLEX NUCLEI. Dar, Arnon (Weizmann Inst. of Science, Rehovoth, Israel). Phys. Rev., 139: B1193-1206(Sept. 6, 1965).

Cluster transfer reactions between complex nuclei are discussed in a simple semiclassical approximation. For energies below the Coulomb barrier, nuclear distortions are neglected; and the results coincide with the tunneling-model predictions of Breit. For energies above the Coulomb barrier, distortions are taken into account by a finite-range diffraction model. Closed-form expressions are obtained for the angular distribution of the reaction products and for the transfer excitation function. Coulomb effects are shown to play a dominant role in determining the main features of the reaction. Good agreement with experimental data is obtained. (auth)

41765 PRODUCTION OF HEAVY NUCLEI IN THE PAR AND BARBEL DEVICES. Bell, George I. (Los Alamos Scientific Lab., N. Mex.). Phys. Rev., 139: B1207-16(Sept. 6, 1965). (LA-DC-7093).

In the Par and Barbel thermonuclear devices, heavy nuclei up to A = 257 were produced by the exposure of ^{238}U to intense neutron fluxes. If one tries to interpret the resulting abundance as a function of mass number by assuming that all higher nuclei resulted from multiple neutron capture in ^{238}U, there are difficulties in reconciling the high-A data with standard semiempirical mass formulas and neutron-capture cross-section theories. Neither the general trend of abundance as a function of A, nor the odd-even fluctuation (for A > 249) which is superimposed on this trend, is consistent with standard theory. The suggestion that the high-mass isotopes resulted from neutron capture in odd-Z nuclei (Pa and Np) is studied. A simplified model of the thermonuclear devices is adopted in which deuterium plus tritium burns to completion and resulting neutrons are captured by various heavy nuclei. The number of uranium nuclei which will be transformed to add Z by the reactions ^{238}U(n,p)^{238}Pa; ^{238}U(d,n)^{239}Np, and ^{238}U(d,2n)^{238}Np is estimated first. A production of about 10^{-3} Pa/U and $\leq 10^{-3}$ Np/U is found and it is estimated that roughly these ratios will be available as targets for multiple neutron capture. Statistical theory is used together with Seeger's semiempirical mass formula to calculate 20-kev neutron-capture cross sections for the nuclei $91 \leq Z \leq 93$, $238 \leq A \leq 257$. The average odd-Z cross sections are systematically larger than the even Z, and those of Np are larger than Pa. The mass-yield curve can then be calculated for various neutron-flux values, and the results are compared with experiment. For both Par and Barbel, good agreement with the experimental abundance data is found using a 20-kev exposure of 7×10^{24} neutrons/cm^2. For Par, a Np/U ratio of 10^{-3} is required, while for Barbel the corresponding ratio is about 5×10^{-4}. In both cases the light end of the mass curve (A < 248) is due to the uranium capture chain, while the heavy end (A ≥ 250) arises from capture by Np. A comparison is also made with less complete data from the Mike device, and it is found that for A ≥ 245 the data can be fit for $\varphi = 6 \times 10^{24}$ neutrons/cm^2 with Np/U ≃ 1.5×10^{-4}. It is concluded that the formation of odd-Z nuclei which undergo multiple neutron capture permits one to understand the mass-yield curves using standard semiempirical mass formulas and conventional capture-cross-section theory. (auth)

41766 MUON CAPTURE AND INELASTIC ELECTRON SCATTERING IN C^{12} AND O^{16}. deForest, Taber Jr. (Stanford Univ., Calif.). Phys. Rev., 139: B1217-26 (Sept. 6, 1965).

The dipole (first-forbidden) contribution to the muon-capture matrix elements, M_V, M_A, and M_P, is calculated using wave functions computed in the particle-hole theory. It is found that $(M_V{}^2)_D = (M_A{}^2)_D = (M_P{}^2)_D$ to within 13%. The assumption that the dipole part of the nuclear matrix element may be expressed as the unretarded dipole matrix element multiplied by the elastic form factor is found to hold to about 1%. Calculations of inelastic electron scattering from the 2^-, T = 1 states in these nuclei predict large cross sections for some of the states at about 100 Mev/c momentum transfer. These "giant-magnetic-quadrupole states" are identified with observed levels found in recent 180° electron-scattering experiments. (auth)

41767 STATIC FISSION-BARRIER CALCULATIONS OF A TWO-PARAMETER LIQUID DROP. Lawrence, James N. P. (Los Alamos Scientific Lab., N. Mex.). Phys. Rev., 139: B1227-31(Sept. 6, 1965). (LA-DC-7125).

Calculations based on a two-parameter description of a uniformly charged liquid drop are reported. Results include fission-barrier energy and other saddle-point properties. The electrostatic energy of the drop was computed by a novel and highly accurate method. The saddle-point properties and corresponding drop shapes are compared with calculations that use nine parameters. Agreement is best for fissionability parameters greater than 0.70, suggesting that these calculations may provide a few-parameter basis for dynamical calculations of adequate precision at the larger fissionability parameters. (auth)

41768 INELASTIC SCATTERING AND NEUTRON PICKUP FOR ^{12}C AND ^{16}O PROJECTILES ON ^{208}Pb. Wang, K. H.; McIntyre, J. A. (Yale Univ., New Haven). Phys. Rev., 139: B1231-8(Sept. 6, 1965). (TID-21524).

Some ^{208}Pb nuclei were bombarded with ^{12}C and ^{16}O projectiles under conditions in which a semiclassical

description of the process should be valid. In the bombardment of ^{208}Pb with 126.5-Mev ^{12}C ($\eta = ZZ'e^2/\hbar v = 24.5$), two inelastic-scattering peaks are observed corresponding to $Q = -2.7 \pm 0.3$ and -4.5 ± 0.3 Mev. The angular distributions of the inelastically scattered ^{12}C show a monotonic increase with decreasing angle until a maximum is reached at about $\theta_{c.m.} = 35°$. This angle corresponds to grazing collisions, assuming that particles follow Rutherford trajectories. The Q = −2.7-Mev peak is identified as the excitation of the 2.6-Mev state in ^{208}Pb. The Q = −4.5-Mev peak could be the excitation of the 4.4-Mev state in ^{12}C or the 4.3-Mev state in ^{208}Pb. The inelastic scattering cross section for the excitation of the 2.6-Mev ^{208}Pb state by ^{16}O projectiles having approximately the same velocity (166.4 Mev) is a factor of 2 smaller than when ^{12}C is used as a projectile; this result is somewhat surprising since the semiclassical conditions are similar and the elastic-scattering cross sections differ only by 20%. The cross section for the 4.5-Mev excitation is not observed and is smaller by more than a factor of 4. Therefore, in the ^{12}C + ^{208}Pb case, the major contribution to the 4.5-Mev excitation very likely originates from the excitation of the 4.4-Mev state in ^{12}C. The reactions ^{208}Pb(^{16}O, ^{17}O)^{207}Pb and ^{208}Pb(^{12}C, ^{13}C)^{207}Pb were also observed in these experiments. Both angular distributions have a maximum differential cross section of 100 mb/sr, which is considerably larger than those ordinarily observed in neutron-transfer reactions. The excitation energies are consistent in both reactions with neutrons being picked up by the projectiles into $d_{\frac{5}{2}}$ states. (auth)

41769 DECAY OF COLLECTIVE NUCLEAR STATES EXCITED IN MUON CAPTURE. Ueberall, H. (Catholic Univ. of America, Washington, D. C.). Phys. Rev., 139: B1239-45(Sept. 6, 1965).

Excitation of giant-dipole and related collective states has been found to give predominant contributions to muon capture. The present work obtains polarizations of the neutrons emitted in the subsequent decay of these states for capture in some 0^+ closed-shell nuclei (their angular distributions are shown to be isotropic). The polarization of the neutrons is due to the polarization of the captured muon and is obtained both according to type (longitudinal and transverse) and according to magnitude (it depends on the configuration mixing of the dipole states). The generalized Goldhaber-Teller model is used for the calculation of the excitation, and Boeker's form of the Wigner R-matrix theory for the decay, together with standard Racah methods. The longitudinal polarization of the directly emitted neutrons of highest energy following muon capture in nuclei, and its dependence on the weak coupling constants, are discussed briefly. (auth)

41770 RELATIVISTIC EFFECTS IN THE FORM FACTORS OF He^3 AND H^3. West, Geoffrey B. (Stanford Univ., Calif.). Phys. Rev., 139: B1246-52(Sept. 6, 1965).

Relativistic corrections to Schiff's nonrelativistic analysis of the three-body nuclei form factors are estimated. High-energy electron scattering from these nuclei is reexamined using an impulse approximation in which the intermediate nucleon states are taken to propagate and interact as free particles. It is concluded that the corrections to the form factors are small ($\lesssim 5\%$) for $-q^2 \lesssim 8F^{-2}$. However, it is shown that they assume great importance if the experiments are used to investigate the neutron charge form factor. Various effects arising from the use of the impulse approximation are discussed. These include considerations of current conservation, of the static limit ($q^2 \to 0$), and of the extraction of nuclear form factors from the impulse-approximation nuclear current. (auth)

41771 EXPERIMENTAL APPROACH TO THE NATURE AND CHARACTERISTICS OF PRIMARY FISSION FRAGMENTS. Stevenson, Peter C.; Hicks, Harry G. (Univ. of California, Livermore). Phys. Rev., 139: B1264-71(Sept. 6, 1965). (UCRL-6491(Rev. I)).

Positive ions of charges 1, 2, 3, and 4 were obtained for each of several masses in a beam of recoiling fission fragments from a thick ^{235}U target. The existence of such low-charged ions was demonstrated by resolving the beam after passing it through parallel electric and magnetic fields. The energies of these low-charged ions are approximately proportional to their charges. The abundances of the low-charged ions are of the order of 0.5% of the total number of emitted fission fragments. At higher charges, the charge on a fission fragment emitted from a thick source appears to be roughly proportional to its velocity. The abundances of low-charged ions appear to depend on their chemical properties. (auth)

41772 EXCITATION OF ISOBARIC ANALOG STATES IN MEDIUM-WEIGHT NUCLEI BY THE (d,p) REACTION AT 28 Mev. Sherr, R. (Princeton Univ., N. J.); Bayman, B. F.; Rost, E.; Rickey, M. E.; Hoot, C. G. Phys. Rev., 139: B1272-93(Sept. 6, 1965).

States of spin $\frac{7}{2}^-$ in ^{47}Ti, ^{49}Ti, ^{51}Cr, ^{53}Fe, ^{55}Fe, ^{57}Fe, ^{57}Ni, ^{59}Ni, and ^{61}Ni were observed by means of the (p,d) reaction with 28-Mev incident protons. In each case the highest $\frac{7}{2}^-$ state seen was found to be the isobaric analog of the the lowest $\frac{7}{2}^-$ state of the isobar with one more neutron. Coulomb displacement energies were obtained which are in excellent agreement with known values in this mass region. The lower $\frac{7}{2}^-$ states were interpreted as "configuration states," that is, states associated with the same configuration as the analog, but with isospin lower by unity. The angular distributions in all cases were in good agreement with distorted-wave calculations. Comparison of the spectroscopic factors for the analog and configuration states with the predictions of j-j-coupling sum rules revealed that the normal procedures used in distorted-wave calculations predict too large a Q dependence. However, by using radial wave functions for the picked-up neutron that are identical for all $1f_{\frac{7}{2}}$ states in a given nucleus, reasonable agreement with the sum rules was obtained. Reasonable agreement was also found with the strengths for various states computed from $1f_{\frac{7}{2}}$ shell-model calculations. The energy splitting between the analog state and the strength-weighted mean of the configuration states was also found to be in agreement with theoretical estimates. (auth)

41773 DOUBLE-CHARGE-EXCHANGE SCATTERING OF LOW-ENERGY PIONS BY NUCLEI. Koltun, D. S.; Reitan, A. (Univ. of Rochester, N. Y.). Phys. Rev., 139: B1372-4(Sept. 6, 1965). (UR-875-80).

The double-charge-exchange cross section for the scattering of low-energy pions by nuclei is calculated in second Born approximation, considering only s-wave scattering of the pions by individual nucleons. The differential cross section for pions of energy 20 to 40 Mev and a light target with two neutrons outside a closed shell is calculated to be ~ 7 μb/sr, with considerable enhancement for targets with larger neutron excess. The scattering to the isobaric analog of the target ground state is strongly favored. (auth)

41774 APPLICATION OF THE GOLDBERGER-TREIMAN RELATION TO THE BETA DECAY OF COMPLEX NUCLEI. Kim, C. W.; Primakoff, H. (Univ. of Pennsylvania, Philadelphia). Phys. Rev., 139: B1447-63(Sept. 20, 1965).

The theory of the beta decay of complex nuclei, $N_i \to N_f + e^- + \bar{\nu}_e$, is developed on the basis of a treatment which considers the nuclei involved (N_i and N_f) as "elementary" particles and applies the hypotheses of the conserved polar-vector hadron weak current (CVC) and the partially conserved axial-vector hadron weak current (PCAC) to determine the effective polar-vector and axial-vector weak coupling constants $G_V(N_i \to N_f)$ and $G_A(N_i \to N_f)$; the numerical values of $G_V(N_i \to N_f)$ and $G_A(N_i \to N_f)$ reflect in this treatment the complexity of internal nuclear structure. Using CVC, and supposing that $|N_i\rangle$ and $|N_f\rangle$ are sufficiently pure isospin eigenstates, $G_V(N_i \to N_f)$ can be calculated, while PCAC, together with a suitable pion-pole-dominance assumption, implies the Goldberger-Treiman (G-T) relation which expresses $G_A(N_i \to N_f)$ in terms of the pion–initial-nucleus–final-nucleus coupling constant $f_{\pi N_i N_f}$; this coupling constant can be found from a polological analysis of $n + N_f \to p + N_i$ nucleon charge-exchange scattering experiments. Since such experiments are not as yet available, the values of the $f_{\pi N_i N_f}$ are calculated in

terms of the known magnetic moments of N_i and N_f by means of a very crude theory, and are compared with the values of the $f_{zN_iN_f}$ calculated by means of the G-T relation from the $G_A(N_i \rightarrow N_f)$ deduced from observed beta-decay rates. The agreement is, in general, somewhat better than that found between calculated and observed rates in the customary impulse-approximation theory of beta decay. (auth)

41775 PROPERTIES OF THE 4.403-Mev EXCITED STATE OF ^{27}Al. Metzger, F. R. (Franklin Inst., Swarthmore, Penna.). Phys. Rev., 139: B1464-7(Sept. 20, 1965).

Using the Doppler-broadened 4.43-Mev gamma line from the reaction $^{15}N(p,\alpha)^{12*}C$, the 4.403-Mev level in ^{27}Al was excited by resonant absorption. The de-excitation of this level was found to lead to the 2.21-Mev (11%) and the 1.01-Mev (32%) excited states as well as directly to the ground state of ^{27}Al (57%). From a self-absorption study, a value $g\Gamma_0 = 0.24 \pm 0.03$ ev was obtained for the product of the statistical factor $g = (2J_{exc} + 1)/(2J_{gs} + 1)$ and the partial width Γ_0 of the ground-state transition. The angular distribution of the 4.403-Mev resonance radiation was observed to be $W(\theta) = 1 + (0.30 \pm 0.05) P_2(\cos\theta)$, and that of the 3.39-Mev radiation to the 1.01-Mev state $W(\theta) = 1 - (0.24 \pm 0.12) P_2(\cos\theta)$. Of the possible spin parity assignments, only $\frac{5}{2}^+$ and $\frac{7}{2}^+$ are compatible with the observed widths and the angular distributions, the most probable assignment being $\frac{5}{2}^+$, the least probable $\frac{7}{2}^+$. With a spin of $\frac{5}{2}$, the partial width for the 4.403-Mev ground-state transition becomes $\Gamma_0 = (0.24 \pm 0.03)$ ev, and the total width of the level $\Gamma = (0.42 \pm 0.06)$ ev. The fact that resonance scattering from the 4.504-Mev level was not observed points to a spin of either $\frac{1}{2}$ or $\geq \frac{9}{2}$ for that level. (auth)

41776 GAMMA-GAMMA DIRECTIONAL CORRELATION IN ^{143}Pr. Gopinathan, K. P. (Tata Inst. of Fundamental Research, Bombay). Phys. Rev., 139: B1467-71 (Sept. 20, 1965).

The directional correlations of four γ-γ cascades in ^{143}Pr fed from the decay of ^{143}Ce were studied. The correlation functions for the 293–57, 232–493, 591–293, and the 668–57-kev cascades are found to be: $W(\theta_{293-57}) = 1 + (0.112 \pm 0.009) P_2(\cos\theta) + (0.000 \pm 0.014) P_4(\cos\theta)$, $W(\theta_{232-493}) = 1 - (0.176 \pm 0.008) P_2(\cos\theta) - (0.001 \pm 0.012) P_4(\cos\theta)$, $W(\theta_{591-293}) = 1 + (0.146 \pm 0.015) P_2(\cos\theta) + (0.003 \pm 0.026) P_4(\cos\theta)$, and $W(\theta_{668-57}) = 1 + (0.063 \pm 0.018) P_2(\cos\theta)$, respectively. Knowing the spin of the ground state of ^{143}Pr as $\frac{7}{2}^+$ and the recently measured spin of the ground state of ^{143}Ce as $\frac{3}{2}^-$, and from the analysis of the angular-correlation results combined with the log ft values of β transitions from ^{143}Ce, the levels of ^{143}Pr were assigned spins and parities as follows: ground state, $\frac{7}{2}^+$; 57 kev, $\frac{5}{2}^+$; 351 kev, $\frac{3}{2}^+$; 493 kev, $\frac{7}{2}^+$; 725 kev, $\frac{5}{2}^+$; 942 kev, $\frac{3}{2}^+$ or $\frac{5}{2}^+$; 1160 kev, $\frac{1}{2}^+$, $\frac{3}{2}^+$, or $\frac{5}{2}^+$; and 1395 kev, $\frac{3}{2}^-$ or $\frac{5}{2}^-$. (auth)

41777 THREE-BODY MODEL FOR STRIPPING AND THE VALIDITY OF THE DISTORTED-WAVE BORN APPROXIMATION. Mitra, A. N. (Dehli Univ.). Phys. Rev., 139: B1472-8(Sept. 20, 1965).

A model is proposed, according to which a deuteron, consisting of two identical particles, interacts with a core nucleus, taken as an infinitely massive point particle which can form a bound state with either of the two particles. Assuming factorable interactions between the particles of all the three pairs, exact expressions for the scattering and stripping amplitudes are obtained. A comparison with the corresponding distorted-wave Born approximation (DWBA) amplitudes, which can also be obtained in the model, shows that DWBA is valid within the model. The model also predicts that the partial-wave scattering amplitudes a_l are small compared with the corresponding stripping amplitudes b_l. An (indirect) experimental test of this result is suggested on the basis of large angular momenta, which are needed to overcome the difficulties of finite nuclear size in actual situations. (auth)

41778 LEVEL STRUCTURE OF THE ODD-A ISOTOPES OF SAMARIUM. Kenefick, Robert A.; Sheline, Raymond K. (Florida State Univ., Tallahassee). Phys. Rev., 139: B1479-99(Sept. 20, 1965).

The levels of ^{145}Sm, ^{149}Sm, ^{151}Sm, ^{153}Sm, and ^{155}Sm were studied with 0.1% resolution by the (d,p) reaction at 12-Mev incident energy. Levels in ^{147}Sm were observed by (p,p′) reactions at 12 Mev. A large number of previously unknown levels were observed at excitation energies up to 4 Mev. Previously known levels from decay spectroscopy were, in general, verified. It is suggested that spherical and deformed nuclear shapes are in evidence close to the ground state in ^{151}Sm. This conclusion is based partly on these data, on the spectroscopic structure of the neighboring even-even nuclei ^{150}Sm and ^{152}Sm, and on the observed two-neutron separation energies (S_{2n}) of odd-A and even-A Sm isotopes in this transition region. A fragmentation of the (d,p) intensities among the increasing number of states is observed as one proceeds from ^{145}Sm (single closed shell plus one neutron) to ^{155}Sm (strongly deformed), as expected from the Nilsson model. Some of the levels below 2 Mev in ^{148}Sm are discussed in terms of shell-model configurations. Levels in ^{147}Sm are compared with the $(f_{\frac{5}{2}})^3$ coupling scheme and with the excited-core model. Using particularly the relative intensities of members of the rotational bands, which strongly characterize the assignments, but also the observed energies for the levels and systematics of other deformed odd-A nuclei, the following Nilsson orbitals and some of their associated rotational states were assigned in ^{153}Sm and ^{155}Sm: $\frac{3}{2}-(521)$, $\frac{5}{2}-(523)$, $\frac{1}{2}-(521)$, and $\frac{5}{2}+(642)$. The (d,p) spectra indicate that the ground state of ^{153}Sm is the $\frac{3}{2}+(651)$ configuration and not the $\frac{3}{2}-(521)$ as assumed previously. The ground state for ^{155}Sm is assigned as the $\frac{3}{2}-(521)$ orbital. The previously unobserved $(11/2)-(505)$ orbital, whose depopulation is hypothesized to cause the sudden onset of deformation at N = 90, has been tentatively assigned at 65 kev in ^{153}Sm. The ground-state Q values observed in the experiments are: $^{144}Sm(d,p)^{145}Sm$, Q = +4.533 ± 0.012 Mev; $^{148}Sm(d,p)^{149}Sm$, Q = +3.648 ± 0.012 Mev; $^{150}Sm(d,p)^{151}Sm$, Q = +3.369 ± 0.016 Mev; $^{152}Sm(d,p)^{153}Sm$, Q = +3.645 ± 0.012 Mev; $^{154}Sm(d,p)^{155}Sm$, Q = +3.584 ± 0.012 Mev. (auth)

41779 EFFECT OF INCREASING EXCITATION ENERGY ON NUCLEAR CHARGE DISTRIBUTION IN FISSION. Nethaway, D. R.; Levy, H. B. (Univ. of California, Livermore). Phys. Rev., 139: B1505-13(Sept. 20, 1965). (UCRL-12481).

The independent fractional chain yields of ^{90}Y, ^{96}Nb, and ^{140}La were measured from fission of ^{232}Th with alpha particles. The excitation energy was varied from about 20 to 40 Mev. Yields are also calculated for ^{136}Cs from data previously published. In addition, the independent fractional chain yields of ^{92}Y, ^{98}Nb, and ^{140}La were measured from fission of ^{235}U with 14.9-Mev neutrons. From these data, smoothly varying plots of independent yield versus excitation energy were constructed for ^{90}Y, ^{96}Nb, ^{136}Cs, and ^{140}La. The data from 14.9-Mev neutron fission of ^{235}U are in good agreement with those from alpha-particle fission of ^{232}Th at the same excitation energy. It is shown that, within the limits of certain assumptions regarding the charge dispersion curves, the shift in Z_p (the most probable charge for a given mass number) with increasing excitation energy varies among the nuclides studied. In particular, it appears that dZ_p/dE may be significantly greater for heavy fragments than for light fragments. The data for ^{90}Y, ^{96}Nb, and ^{140}La are consistent with linear plots of Z_p versus E^*, except that the value for ^{96}Nb for thermal-neutron fission of ^{235}U is off the curve by 0.1 charge unit. The value of dZ_p/dE for ^{136}Cs decreases with energy in this energy range, possibly because of shell effects at low excitation energies. (auth)

41780 CROSS SECTIONS FOR THE PRODUCTION OF ^{9}Li, ^{16}C, AND ^{17}N IN IRRADIATIONS WITH Gev-ENERGY PROTONS. Dostrovsky, I.; Davis, R. Jr.; Poskanzer, A. M.; Reeder, P. L. (Brookhaven National Lab., Upton, N. Y.). Phys. Rev., 139: B1513-24(Sept. 20, 1965). (BNL-9046).

Twenty-five targets ranging from boron to uranium were irradiated with 1.0- and 2.8-Bev-energy protons. Cross sections for the production of the nuclides ^{9}Li, ^{16}C, and ^{17}N were measured by counting the delayed neutrons which they emit. No longer lived delayed-neutron emitters were ob-

served except those produced as fission products from uranium. Cross sections for the latter are presented and interpreted in terms of low-deposition-energy processes. Cross sections for the nuclides ^{9}Li, ^{16}C, and ^{17}N from the lightest targets are interpreted as simple spallation products, mainly from (p,xp) reactions. Several pairs of targets with similar mass number and differing neutron-to-proton ratio were studied. A strong dependence of the cross sections on the neutron-to-proton ratio of the target was observed, especially for the lighter mass regions. Relative cross-section calculations were performed for the heavier targets assuming these and other light fragments were evaporated from excited knock-on cascade products. The effect of secondary evaporation from excited evaporated fragments was included. The experimental and calculated relative cross sections agree well with respect to their dependence on the mass number and neutron-to-proton ratios of the target. It is concluded that the mass-energy surface, which is included in the evaporation formalism, is important in determining the relative yields of light fragments. (auth)

41781 14-Mev-NEUTRON PRODUCTION OF ISOMERIC STATES FOR SEVERAL RARE-EARTH ELEMENTS. Broadhead, K. G.; Shanks, D. E.; Heady, H. H. (Department of the Interior, Reno, Nev.). Phys. Rev., 139: B1525-8(Sept. 20, 1965).

Fast-neutron cross sections were determined for the following reactions, using 14-Mev neutrons from the ^{3}H(d,n)^{4}He reaction: ^{89}Y(n,n'γ)^{89m}Y, 400 mb; ^{142}Nd(n,2n)^{141m}Nd, 545 mb; ^{144}Sm(n,2n)^{143m}Sm, 400 mb; ^{159}Tb(n,2n)^{158m}Tb, 160 mb; ^{168}Er(n,2n)^{167m}Er, 190 mb. Possible sources of error affecting the cross-section measurements are discussed and evaluated numerically. The overall accuracy was determined to be about ±12%. (auth)

41782 MUON CAPTURE BY DEUTERONS. Wang, I.-T. (Columbia Univ., New York). Phys. Rev., 139: B1539-44 (Sept. 20, 1965).

Rates of muon capture from the separate μd hyperfine states are computed. The dependence of the measurement of effective coupling constants on the neutron energy is explicitly demonstrated. The calculation of the neutron energy spectra includes mainly the following refinements: (1) use of two-nucleon wave functions with hard core, (2) corrections for the target-proton momentum, and (3) inclusion of certain induced pseudoscalar terms. The capture rates obtained are 334 and 15 sec^{-1} for the μd doublet and quartet states respectively. (auth)

41783 STUDY OF THE BREAKUP CHANNELS OF MUON CAPTURE BY ^{3}He. Wang, I.-T. (Columbia Univ., New York). Phys. Rev., 139: B1544-7(Sept. 20, 1965).

Neutron energy spectra are obtained for the processes of muon capture by ^{3}He into the "breakup" channels: $\mu + {}^{3}\text{He} \rightarrow \nu + n + d$ and $\mu + {}^{3}\text{He} \rightarrow \nu + 2n + p$. The chief approximations are the use of plane waves for the relative motions between the final nuclear particles and a Gaussian-type wave function for the ^{3}He nucleus. The rates obtained for the two breakup channels are, respectively, 988 and 272 sec^{-1}. (auth)

41784 POSSIBILITY OF OBSERVING A NONLINEAR ELECTROMAGNETIC EFFECT. Talman, James D. (Univ. of California, Davis; Univ. of Western Ontario, London). Phys. Rev., 139: B1644-5(Sept. 20, 1965).

A fourth-order electromagnetic effect which may be observable with present experimental techniques is discussed. The effect is the interaction of a photon with an electrostatic field to produce two photons. A low-energy approximation to the cross section is given and other coherent processes are discussed. (auth)

41785 SPONTANEOUS EMISSION OF ENERGETIC He^{6} PARTICLES FROM Cf^{252}. Whetstone, S. L. Jr.; Thomas, T. D. (Los Alamos Scientific Lab., N. Mex.). Phys. Rev. Letters, 15: 298-300(Aug. 16, 1965).

Helium-6 particles spontaneously emitted from a californium-252 source are observed. This is the first known observation of the spontaneous emission of particles (other than fission fragments) heavier than helium-4 from nuclei. The charged particles were detected in a $\Delta E - E$ counter telescope consisting of two silicon semiconductor detectors. The spectrum of helium-6 particles detected is shown. A relatively clean separation is observed between the helium-4 and helium-6 events. The absence of any events immediately above the helium-3 locus toward the helium-4 locus is further evidence that the helium-6 events observed are real. (J.F.P.)

41786 Li^{4} AND THE EXCITED LEVELS OF He^{4}. Cerny, Joseph; Detraz, Claude; Pehl, Richard H. (Univ. of California, Berkeley). Phys. Rev. Letters, 15: 300-3 (Aug. 16, 1965).

The technique of simultaneous observation of (p,t) and (p,^{3}He) transitions to analog final states is used to investigate the lithium-4 and helium-4 nuclei. This would aid in the location of the lowest T = 1 state of helium-4. For this investigation the reactions ^{6}Li(p,t)^{4}Li and ^{6}Li(p,^{3}He)^{4}He were used. The unbound ground state of lithium-4 was observed and the prediction is made that helium-4 must be unbound by 2 Mev. Angular distributions of the 20.1-Mev state of helium-4 which are consistent with its 0^{+} assignment are obtained and the lowest T = 1 state of helium-4 at an excitation of 22.5 ± 0.3 Mev was identified. (J.F.P.)

41787 CORRECTION TO THE (^{3}He,$2^{3}S_{1}$) TO (^{3}He^{3+}, $2^{3}S_{\frac{1}{2}}$) HYPERFINE-STRUCTURE RATIO. Sternheim, Morton M. (Yale Univ., New Haven). Phys. Rev. Letters, 15: 336-7(Aug. 23, 1965).

Since there was a discrepancy in the ratio of the $2^{3}S_{1}$ state hyperfine structure of the ^{3}He atom to the $2^{3}S_{\frac{1}{2}}$ state hyperfine structure of the ^{3}He^{+} ion, the calculated value being too large by 10 ppm. The omission of a correction of −4 ppm is pointed out in this theoretical ratio. The second-order radiative corrections to the hyperfine structure were calculated in powers of the Coulomb field. They give a correction to the hyperfine structure. (J.F.P.)

41788 DIRECTION AND ENERGY DISTRIBUTION OF CHARGED PARTICLES TRANSMITTED THROUGH SINGLE CRYSTALS. Gibson, W. M. (Bell Telephone Labs., Murray Hill, N. J. and Rutgers State Univ., New Brunswick, N. J.); Erginsoy, C.; Wegner, H. E.; Appleton, B. R. Phys. Rev. Letters, 15: 357-60(Aug. 23, 1965). (BNL-9311).

New observations are reported from a detailed study of the energy loss of 5-Mev protons incident on low-index planes in silicon crystals. The results show that transmitted particles with anomalously high energy loss have a strikingly different dependence on both the incidence and emergency angle than particles with anomalously low energy loss; that particles transmitted most nearly parallel to the planar direction exhibit a specific energy loss that depends on the characteristics on the plane; and that multiple Coulomb scattering plays an important role in the observed anisotropy. (J.F.P.)

41789 ANISOTROPIC EFFECTS IN INTERACTIONS OF ENERGETIC CHARGED PARTICLES IN A CRYSTAL LATTICE. Erginsoy, Cavid (Brookhaven National Lab., Upton, N. Y.). Phys. Rev. Letters, 15: 360-4(Aug. 23, 1965). (BNL-9317).

An outline is given of the theory of axial and planar channeling, including the effects of temperature. The motion of charged particles is treated classically since for the massive particles (proton, helium-3, and helium-4) with which most of the experiments were carried out, the wavelengths are of the order of 10^{-4} to 10^{-3} Å and a wave description of the observed transmission effects does not appear to be necessary at this stage. Next the observed angular widths connected with channeled particles are discussed. Finally, remarks are made on blocking effects which have to be distinguished from channeling. These effects provide a new source of anisotropy. (J.F.P.)

41790 TOTAL PHOTOPROTON CROSS SECTION AND BRANCHING RATIOS IN THE O^{16} GIANT RESONANCE. Morrison, R. C.; Stewart, J. R.; O'Connell, J. S. (Yale Univ., New Haven). Phys. Rev. Letters, 15: 367-8 (Aug. 23, 1965).

In order to measure the total photoproton cross section

and branching ratios in the ^{16}O giant resonance, a thin target of O_2 gas, with natural isotopic content was irradiated with bremsstrahlung produced by the electron linac, with end-point energies of 22 and 40 Mev. A proton spectrum was measured with 22-Mev bremsstrahling over the proton energy range of 5 to 10 Mev, yielding a true ground-state cross section from E_γ = 17 to 22 Mev. A supplementary run with 24-Mev bremsstrahlung extended the range to this measurement to 23 Mev. The entire measurement was then repeated under identical conditions with 40-Mev bremsstrahlung. The data analysis considered only transitions to 5.3 and 6.3 Mev. The results imply that there is no significant two-particle-two-hole contribution to the ^{16}O giant resonance. (J.F.P.)

41791 MÖSSBAUER SCATTERING: THE GYROMAGNETIC MOMENTS OF FIRST 2^+ STATES IN W^{182} AND W^{186} AND Os^{186} AND Os^{188}. Chow, Y. M.; Grodzins, L.; Barrett, P. H. (Massachusetts Inst. of Tech., Cambridge). Phys. Rev. Letters, 15: 369-73(Aug. 23, 1965).

The application of the technique for measuring the angular distribution of Mössbauer-scattered radiation to the measurement of the quadrupole interaction in osmium metal by the measurement of the attenuated angular correlation of the Mössbauer radiation scattered from the first 2^+ state of osmium-186, was previously described. The extension of that technique to the measurement of the magnetic moments of excited states by precessing the Mössbauer angular distribution with an external magnetic field is described. The method is applied to the first 2^+ states in the transition region from ^{182}W to ^{188}Os. The relevant experimental quantity is the gyromagnetic ratio, which is a measure of the magnetic properties of the rotation. The Mössbauer scattering aspects show a number of merits which can be exploited for the measurement of small perturbations. (J.F.P.)

41792 ACOUSTIC EXCITATION OF NUCLEAR SPIN RESONANCE IN SINGLE-CRYSTAL METALLIC TANTALUM. Gregory, E. H.; Boemmel, H. E. (Univ. of California, Los Angeles). Phys. Rev. Letters, 15: 404-6 (Aug. 30, 1965).

Both longitudinal and transverse waves were successfully employed to detect the nuclear spin resonance in tantalum. The samples were in the form of cylinders accurately oriented along the desired crystalline axis. Nuclear spin resonances were detected where the change in magnetic quantum number of the nucleus was 1 and 2. Two typical resonances are shown. A departure from the expected angular dependence was observed for both longitudinal and transverse waves which cannot be caused by an anisotropic line-shape factor. This is thought to be due to acoustic-mode conversion in the sample arising because of the relatively small ratio of sample diameter to sound-wave length. (J.F.P.)

41793 MOESSBAUER EFFECT RESULTING FROM THE REACTION $^{56}Fe(d,p)^{57}Fe$. Goldberg, D. A.; Keaton, P. W.; Lee, Y. K.; Madansky, L.; Walker, J. C. (Johns Hopkins Univ., Baltimore). Phys. Rev. Letters, 15: 418-19(Aug. 30, 1965).

A large Mössbauer effect in γ rays resulting from deuteron reactions (d,p) with iron-56 in a natural iron target. From the present result and from the previously reported Mössbauer effect from Coulomb-excited levels in iron-57, it is concluded that the conditions for recoilless emission are relatively insensitive to the reaction process leading to the excitation and to the amount of recoil momentum imparted to the nucleus during such reaction. Observation of a large effect with resolved hyperfine structure induced by (d,p) reactions is of particular interest in that the measurement of the hyperfine splitting in the target environment would shed additional insight into the still unknown process in which a recoiling nucleus with a large momentum is rapidly restored into a lattice before a recoilless γ emission occurs. The Mössbauer apparatus consisted of a loudspeaker driven by a parabolic wave form and a multichannel analyzer operated in a multiscaling mode. The study of the hyperfine structure by Mössbauer effect from the recoil nucleus will permit, under certain circumstances, the direct study of nuclear polarization following a nuclear reaction. (J.F.P.)

41794 ODD-PARITY ROTATIONAL BANDS IN ^{246}Cm. Stephens, F. S.; Asaro, Frank; Fried, Sherman; Perlman, I. (Univ. of California, Berkeley). Phys. Rev. Letters, 15: 420-4(Aug. 30, 1965).

An experimental study is reported of the sequence ^{246}Pu (β^-/11 day)^{246}Am(β^-/25 min)^{246}Cm. The interpretation of the levels observed is discussed. Although most levels agree well with the expectations of the existing theory, the $K = 2^-$ band observed in ^{246}Cm at 842 kev seems to be somewhat lower in energy and more collective in nature than was expected. The strongest evidence for the collective nature of the 2^- band in ^{246}Cm is the systematic occurrence of such levels at comparable energies in neighboring nuclei. These $K = 2^-$ bands presumably correspond to octupole vibrations similar to the well-known $K = 0^-$ bands in the Ra – Th – U region. (J.F.P.)

41795 NUCLEON-TRANSFER REACTIONS IN THE INTERACTION OF NUCLEI WITH HEAVY IONS. PART B. REACTIONS OF MANY-NUCLEON TRANSFER. Pomorski, Leon (Inst. of Nuclear Physics, Krakow). Postepy Fiz., 16: 69-83(1965). (In Polish)

The large negative Q-value that is characteristic of many-nucleon transfer reactions has restricted the scope of research in this area until recently, when modern heavy ion accelerators were built with ion excitation capabilities of the order of 10 Mev per nucleon. In many-nucleon transfer, the peripheral nucleons take part. Therefore, research in this area (especially with the transfer of protons, neutrons, and alphas) provides information relating to the spatial distribution of nucleons near the surface and to their energetic and spatial correlation. In part A of this series of articles, one-neutron transfer reactions were treated. This article treats many-nucleon transfer reactions. Excitation functions and angular distributions are reviewed for multi-nucleon transfer reactions. These include varying the target isotope for a given target element and studying the excitation function for a (+2n) transfer, varying the bombarding ion and target isotope but keeping fixed the product light-ion(^{17}N) for a (−3p2n) transfer, fixing both the bombarding ion and target nucleus, and obtaining the angular distribution for a variety of multi-nucleon transfers. Recent developments of one-nucleon transfer reactions are also reviewed. (TTT)

41796 COMMENT ON A PAPER BY M. K. F. WONG, ON THE MOESSBAUER EFFECT. Proc. Phys. Soc. (London), 86: 417-19(Aug. 1965).

The polarization factor for the interference between Rayleigh scattering and Mössbauer scattering from ^{57}Fe is shown to be cos θ for both an unsplit scatterer and a non-aligned split scatterer, a result which differs from that recently published by Wong. Polarization factors have no effect on the ratios of the absorption cross sections for the hyperfine components of a non-aligned split scatterer. (auth)

41797 THE 3.92 TO 1.98 Mev TRANSITION IN ^{18}O. Ellis, P. J. (Manchester Univ., Eng.); Wilmore, D. Proc. Phys. Soc. (London), 86: 422-3(Aug. 1965).

A correction is made to the theoretical M1 transition probability predicted by the shell model calculation of Flowers and Wilmore. Agreement with experiment is thereby improved. (auth)

41798 THE BRANCHING RATIO OF ^{212}Bi(ThC). Walker, J.; Salgir, T. (Univ. of Brimingham, Eng.). Proc. Phys. Soc. (London), 86: 423-5(Aug. 1965).

Surface barrier detectors were used to measure the branching ratio in ^{212}Bi(ThC); the average value obtained for the α branch is 36.00 ± 0.03%, which is higher than the latest counter measurements (35.81%) but in better agreement with the value from magnetic spectrometers (36.08%). Some information is given on the change in value which results from different methods of analysis. (auth)

41799 SEARCH FOR POSITRON EMITTERS AMONG THE PRODUCTS OF ^{235}U THERMAL NEUTRON FISSION.

Eismont, V. P.; Yurgenson, V. A. Soviet J. Nucl. Phys. (English Transl.), 1: 129-31(Aug. 1965).

Translated from Yadern. Fiz., 1: 185-8(Feb. 1965).

In order to provide direct experimental verification of the hypothesis of unequal charge distribution in ^{235}U thermal neutron fission symmetrical in mass distribution, a search was made for positron-active fission fragments. By observing $\gamma\gamma$ coincidences corresponding to annihilation radiation, it was established that the upper limit of the number of β^+ emitters is substantially less than the number expected on the basis of the above hypothesis. (auth)

41800 THE K-CAPTURE FRACTION OF ^{66}Ge, ^{69}Ge, AND ^{72}As. Zing, He-sung; Mal'tseva, N. S.; Mekhedov, V. N.; Rybakov, V. N. (Joint Inst. for Nuclear Research, Dubna, USSR). Soviet J. Nucl. Phys. (English Transl.), 1: 132(Aug. 1965).

Translated from Yadern. Fiz., 1: 189-90(Feb. 1965).

The probability ratios of K capture and β^+ decay were determined with the aid of a magnetic analyzer for several neutron-deficient isotopes of gallium, germanium, and arsenic by measuring the relative intensities and the decay curves of the corpuscular and x-radiation. The K-capture fraction of ^{66}Ge, ^{69}Ge, and ^{72}As was found to be 48 ± 20, 55 ± 10, and 20 ± 10 per cent, respectively. Control measurements of the K-capture fraction of ^{64}Cu, ^{66}Ga, ^{68}Ga, ^{71}As, and ^{72}As yielded values that agreed with the published data within the limits of experimental error. (auth)

41801 NEW DATA FOR THE ^{188}Re DECAY SCHEME. Vitman, V. D.; Voinova, N. A.; Dzhelepov, B. S. (Mendeleev All-Union Inst. of Metrology, USSR and Ioffe Inst. of Physics and Tech., Leningrad). Soviet J. Nucl. Phys. (English Transl.), 1: 133-7(Aug. 1965).

Translated from Yadern. Fiz., 1: 191-7(Feb. 1965).

The energies and relative intensities of ^{188}Re γ rays were determined using an electron magnetic γ spectrometer. The source was metallic rhenium activated by thermal neutrons. Of the 23 observed γ lines, those at 717, 1019, 1175, 1193, 1322, 1460, 1656, 1675, 1852, 1869, and 2026 kev were detected for the first time. The decay scheme of ^{188}Re is considered; three new levels, at 2026, 1828, and 1809 kev, are added to previously proposed schemes and their quantum characteristics are discussed. The intensities of γ transitions to ^{188}Os levels are determined from the balance of γ-transition intensities. (auth)

41802 NEW ISOMERS OF ^{43}Sc, ^{109}In, AND ^{125}Xe. Demin, A. G.; Kushakevich, Yu. P. Soviet J. Nucl. Phys. (English Transl.), 1: 138-9(Aug. 1965).

Translated from Yadern. Fiz., 1: 198-200(Feb. 1965).

New isomers of ^{43}Sc, ^{109}In, and ^{125}Xe were observed. The half lives, the energies, and the relative intensities of the gamma transitions were measured. The presence of a low-lying $3/2^+$ level in ^{43}Sc agrees with cluster-model deductions. The data obtained point to rather large spins and energies of the new isomer states of ^{109}In and ^{125}Xe. (auth)

41803 ON THE TWO-HOUR (7.7 ksec) ISOMER OF ^{168}Lu. Gromov, K. Ya.; Hnatowicz, V.; Danagulyan, A. S.; Strigachev, A. T.; Shpinel', V. S. (Joint Inst. for Nuclear Research, Dubna, USSR and Moscow State Univ.). Soviet J. Nucl. Phys. (English Transl.), 1: 140-2(Aug. 1965).

Translated from Yadern. Fiz., 1: 201-4(Feb. 1965).

The electron conversion lines previously ascribed to an 87.5-kev transition in the decay of a new ^{168}Lu isomer ($T_{1/2}$ = 2.15 hours = 7.7 ksec) were reinvestigated. It was determined from the energy differences of the K, L_2, L_3, M_2, M_3, and N lines that these lines are associated with an 88.3-kev transition in the Hf nucleus. Therefore the reasons for suggesting the existence of a two-hour ^{168}Lu isomer vanish. The 88.3-kev transition evidently results from the β^- decay of an isomeric ^{176}Lu state. (auth)

41804 CALCULATION OF MAGNETIC MOMENTS OF SPHERICAL NUCLEI. Troitskii, M. A.; Khodel', V. A. Soviet J. Nucl. Phys. (English Transl.), 1: 143-8(Aug. 1965).

Translated from Yadern. Fiz., 1: 205-14(Feb. 1965).

The magnetic moments of spherical nuclei are treated using the method of interacting quasiparticles. A solution is obtained of the equation for the effective magnetic field in the nucleus. The results are compared with experiment. The constant for the spin-spin interaction of quasiparticles is found from the experimental data. (auth)

41805 AN ANALYTICAL VERSION OF THE QUASI-CLASSICAL THEORY OF THE ANGULAR DISTRIBUTION OF THE PRODUCTS OF A ONE-NUCLEON TRANSFER REACTION. Grabowski, J.; Kalinkin, B. N. (Joint Inst. for Nuclear Research, Dubna, USSR). Soviet J. Nucl. Phys. (English Transl.), 1: 149-52(Aug. 1965).

Translated from Yadern. Fiz., 1: 215-20(Feb. 1965).

The angular distribution of the products of transfer reactions is investigated over the whole angular range by means of an analytical version of the quasiclassical theory. (auth)

41806 NEUTRON-CAPTURE CROSS SECTIONS IN SCANDIUM AND THE RADIATION WIDTHS OF THE ^{45}Sc AND ^{35}Cl RESONANCES. Romanov, S. A.; Shapiro, F. L. (Lebedev Inst. of Physics, Moscow). Soviet J. Nucl. Phys. (English Transl.), 1: 159-63(Aug. 1965).

Translated from Yadern. Fiz., 1: 229-34(Feb. 1965).

A plot is given of the cross section for radiative capture of neutrons by ^{45}Sc nuclei in the energy range 1 ev to 40 kev, obtained from measurements in a slowing-down-time spectrometer. Weak resonances are observed with energies of 450 ± 50 and 1000 ± 100 ev and neutron widths $2g\Gamma_n$ equal respectively to $(7.6 \pm 1.2) \times 10^{-3}$ and $(22 \pm 6) \times 10^{-3}$ ev, which apparently are p resonances. To determine the radiation widths of the resonances of ^{45}Sc and ^{35}Cl a new method involving the relation between the scattering amplitude, capture cross section, and radiation width, which follows from the multilevel Breit-Wigner formula, was used. The value $\Gamma_\gamma = 0.42 \pm 0.06$ ev is obtained for ^{45}Sc. The characteristics of the negative levels of ^{45}Sc and ^{35}Cl are discussed. (auth)

41807 GAMMA-RAY SPECTRA FROM THE (n,γ) REACTION IN ^{50}Cr, ^{52}Cr, AND ^{53}Cr. Rudak, E. A.; Firsov, E. I. (Inst. of Physics, Academy of Sciences, Belorussian SSR). Soviet J. Nucl. Phys. (English Transl.), 1: 164-74 (Aug. 1965).

Translated from Yadern. Fiz., 1: 235-49(Feb. 1965).

Spectra of γ rays accompanying the capture of thermal neutrons from the IRT reactor were investigated using a Compton magnetic γ spectrometer with 2% resolution and 0.3-Mev lower limit. The sample was placed in an extended tangential channel opposite the center of the reactor core. The thermal neutron flux at the sample was $\sim 10^{12}$ neutrons/cm^2-sec; the cadmium ratio was $R_{Cd} \approx 50$. The samples were separated Cr isotopes having $\sim$70 g-b for the product of the mass and (n,γ) cross section. Energies and intensities of observed γ rays from $^{51,53,54}Cr$ are given. Gamma-transition schemes from the capture states in $^{51,53,54}Cr$ are based on the data and their main features are discussed. (auth)

41808 SPECTRUM OF INTERNAL-CONVERSION ELECTRONS PRODUCED UPON CAPTURE OF THERMAL NEUTRONS BY INDIUM. Balodis, M. K.; Bondarenko, V. A.; Prokof'ev, P. T.; Simonova, L. I. (Inst. of Physics, Academy of Sciences, Latvian SSR). Soviet J. Nucl. Phys. (English Transl.), 1: 175-6(Aug. 1965).

Translated from Yadern. Fiz., 1: 250-1(Feb. 1965).

The spectrum of the internal-conversion electrons produced upon capture of thermal neutrons by indium was plotted with a β spectrograph of 0.4–0.5% resolution in the energy range 40–600 kev. Conversion lines were disclosed corresponding to γ transitions at 60.7, 85.5, 96.1, 115.0, 126.5, 141.2, 142.0, 155.6, 162.3, 171.0, 173.4, 186.2, 203.4, 234.8, 271.5, 284, 289, 335, and 384 kev. The internal-conversion coefficients were estimated for some of the transitions. The ratio of the cross section for isomer production was estimated from the intensity ratio of the 138.5 and 415 kev conversion lines ^{116}Sn and found to be σ(2 sec)/σ(54 min) = 0.8 ± 0.4. (auth)

41809 SEARCH FOR THE (n,α) REACTION IN HEAVY NUCLEI UNDER THE ACTION OF THERMAL NEUTRONS. Andreev, V. N.; Sirotkin, S. M. Soviet J. Nucl. Phys. (English Transl.), 1: 177-85(Aug. 1965).

Translated from Yadern. Fiz., 1: 252-63(Feb. 1965).

A number of nuclei in the rare-earth region, the isotopes of osmium and platinum, ^{210}Po, ^{235}U, and ^{239}Pu were investigated with the aim of detecting the (n,α) reaction induced by thermal neutrons. The existence of the (n,α) reaction in ^{143}Nd and ^{149}Sm was confirmed. The (n,α) reaction in ^{151}Eu and some α transitions in ^{143}Nd and ^{149}Sm were observed. In the remaining cases upper limits for the cross section were determined. The experimental results were compared with the single-particle and statistical theories of α decay. Satisfactory agreement with the statistical theory is found. (auth)

41810 NEUTRON SPECTRA IN INTERACTIONS OF HEAVY IONS WITH INTERMEDIATE NUCLEI. Kumpf, H.; Kumpf, L.; Shih, Shuang-hui (Joint Inst. for Nuclear Research, Dubna, USSR). Soviet J. Nucl. Phys. (English Transl.), 1: 186-90(Aug. 1965).

Translated from Yadern. Fiz., 1: 264-70(Feb. 1965).

The time-of-flight method was used to measure neutron spectra from Fe, Cu, Mo, Rh, and Sn targets irradiated with ^{40}Ar, ^{22}Ne, and ^{11}B ions, employing the natural modulation of the U-300 cyclotron beam. In the measurable energy range 5–12 Mev all the spectra have the form exp $(-E_{cm}/T)$, where the parameter T varies in the range 1.5–2.5 Mev. From this and earlier work it is concluded that about 40 Mev of the excitation energy of compound nuclei produced by ^{40}Ar irradiation is converted into γ radiation. (auth)

41811 CASCADE MECHANISM OF THE HIGH ENERGY NUCLEAR REACTIONS. I. TOTAL INELASTIC CROSS SECTIONS, ANGULAR AND ENERGY DISTRIBUTION OF THE FAST PARTICLES. Denisov, F. P.; Latipova, R. A.; Milovanov, V. P.; Cerenkov, P. A. (Lebedev Inst. of Physics, Moscow). Soviet J. Nucl. Phys. (English Transl.), 1: 234-9(Aug. 1965).

Translated from Yadern. Fiz., 1: 329-37(Feb. 1965).

The interactions of high energy protons with nuclei were calculated on the basis of the cascade theory of the nuclear reactions. The nuclear reactions induced by protons with energies 150, 340, and 660 Mev on ^{28}Si, (^{95}AgBr), and ^{197}Au were considered. The nuclear diffuse surface and the refraction and reflection of nucleons as they leave the nucleus were taken into account. The comparison results of the calculations with experiment allow the conclusion that principal initial suppositions of the cascade theory are valid. (auth)

41812 ELECTRIC MONOPOLE TRANSITIONS IN NONSPHERICAL ATOMIC NUCLEI. Davydov, A. A.; Rostovskii, V. S. Univ. of Moscow). Vestnk. Mosk. Univ., Ser. III, Fiz. Astron., No. 1, 64-77(1965).

Investigation was to calculate the energy levels, the wave functions, and the probabilities of E0 and E2 transitions, for nonspherical even-even atomic nuclei which have axial symmetry in the ground state, with full accounting for the interconnection between collective excitations of different types. It is shown that the wave functions and the relative energies of the excited states, when complete account is taken of the interaction between the rotation and the beta and gamma oscillations, can be expressed in terms of two parameters which characterize the amplitudes of the zero-point beta and gamma oscillations of the surface of the nucleus. The relative probabilities of the E0 and E2 transitions are calculated as functions of these parameters. The theoretical results are compared with experiment for a number of nuclei. (ATD)

41813 EXCITATION FUNCTIONS FOR (p,p′) ON ^{27}Al WITH EXCITATION OF LEVELS ABOVE 3.5 Mev. Vasilev, S. S.; Vorobev, Yu. A.; Mikhaleva, T. N.; Chuprunov, D. L. (Scientific-Research Inst. of Nuclear Physics, USSR). Vestn. Mosk. Univ., Ser. III: Fiz. Astron., No. 1, 87(Jan.-Feb. 1965). (In Russian).

Excitation curves for inelastic scattering of 6.15-to 6.7-Mev protons on ^{27}Al with excitation of levels at 3.74, 3.95, 4.05, 4.40, 4.80, and 5.15 Mev were measured at 90° in the laboratory system. The measured excitation functions are characterized by a strong fluctuation of the differential transverse cross section, indicating a compound-nucleus mechanism for this process. (M.J.T.)

41814 CORRELATION EFFECTS OF NUCLEAR REACTIONS AT GROUND STATE. Zhivopistsev, F. A.; Yudin, N. P. Vestn. Mosk. Univ., Ser. III: Fiz. Astron., No. 2, 30-4(Mar.-Apr. 1965). (In Russian).

The correlation effects in the ground state in nuclear reactions are investigated. It is shown that taking into account the backward Feynman diagrams can significantly reduce the width of the collective states. (tr-auth)

41815 SPALLATION OF HYPERFRAGMENTS IN A COULOMB FIELD. Vedrinskii, R. V.; Kolesnikov, N. N. Vestn. Mosk. Univ., Ser. III: Fiz. Astron., No. 2, 71-80 (Mar.-Apr. 1965).

It is shown that Coulomb disintegration can play an essential role in scattering of light hypernuclei on heavy nuclei. In the case of $^{3}H_{\Lambda}$, the cross section can reach tens of barns. The applicability of various approximations in the calculation of this process is discussed. (tr-auth)

41816 THE STRUCTURE OF THE EVEN PARITY STATES OF ^{16}O. [PART] I. Chang, Tsung-hua; Yu, Youwen; Tzu, Hsi-chuen. Wu Li Hsueh Pao, 21: 897-906(May 1965). (In Chinese).

The even parity states of ^{16}O are treated by taking into account the configuration of 2 ħω excitation in the L–S coupling scheme and using the δ-interaction of the Wigner type. An approximate method is suggested and the 0^+, 2^+, 4^+, states are solved. Rigorous solutions of the wave functions are obtained as well and compared with the approximate solutions. It is found that they are very close to each other. By using these approximate wave functions the monopole and E2 transition probabilities are calculated; and the results are in nice agreement with experiment, but do not show agreement for the energy level spacings. (auth)

41817 TWO-NUCLEON STRIPPING REACTIONS. Wang, Ju-lin; Chen, Sheng-chun. Wu Li Hsueh Pao, 21: 907-14(May 1965). (In Chinese).

The formulas for the differential cross sections of the (d,α) and (t,p) stripping reactions, derived assuming the plane-wave Born approximation and zero radius of action for nuclear forces, are considered following the development of Talmi. Comparison of results obtained using these formulas with calculations by a more exact approximation shows that, although the more exact approximation does not alter the shape of the differential cross sections, it strongly changes their absolute values. (tr-auth)

41818 VIBRATION-ROTATION INTERACTION OF EVEN-EVEN NUCLEI IN THE TRANSITION REGION. Liu, Tun-huan. Wu Li Hsueh Pao, 21: 952-60(May 1965). (In Chinese).

By using the Bohr-Mottelson model, and taking the vibration-rotation interaction into account more carefully, the energy spectra and the rates of electric quadrupole transitions of even-even nuclei in the transition region can be well explained. (auth)

41819 STUDIES OF STRUCTURAL FACTORS IN TWO-NUCLEON STRIPPING AND KNOCK-ON REACTIONS. Li, Yen-kuo; Chen, Sheng-chung. Wu Li Hsueh Pao, 21: 961-75(May 1965). (In Chinese).

Structure factors affecting the cross sections of stripping and knock-on reactions are investigated. The change of structure factors with changes in the number of nucleons outside of closed shells is considered, using collective-oscillation wave functions in a simple model and wave functions in the shell model. It is found that in the first case the variation of structure factors has an obvious regularity. (tr-auth)

41820 ISOMERIC CROSS-SECTION RATIOS FOR YTTRIUM-90 BY THE (a,n), (d,p) AND (^{3}He,p) REACTIONS, AND FOR SCANDIUM-44 BY THE (a,n) REACTION (thesis). Riley, Clyde. Tallahassee, Fla., Florida State Univ., 1964. 123p.

Absolute cross sections and isomer ratios were measured for the ^{87}Rb(a,n)^{90g,90m}Y, ^{89}Y(d,p)^{90g,90m}Y, ^{88}Sr(^{3}He,p)^{90g,90m}Y, and ^{41}K(a,n)^{44g,44m}Sc reactions. The irradiations were performed over various energy ranges at intervals of one Mev or less. The absolute cross sections were de-

termined by scintillation and beta counting. A sum peak determination was used to determine the excited state cross sections for the yttrium producing reactions. The isomer ratio functions for the three yttrium producing reactions were compared. Similarities and differences in the isomer ratio plots were seen to exist and are discussed in terms of the mechanisms for the nuclear reactions involved. Also, calculations of the Huizenga–Vandenbosch type were performed for the $^{87}Rb(a,n)^{90g,90m}Y$ and $^{41}K(a,n)^{44g,44m}Sc$ reactions. A value of 4–5 was obtained for σ, the spin cut off parameter, for ^{90}Y and a value of 1.7–1.8 was determined for ^{44}Sc. Difficulty was found to exist when applying the Huizenga–Vandenbosch formalism to the $^{87}Rb(a,n)$ reaction because of the effects of any possible direct interaction and competition from the ^{87}Rb (a,2n) reaction. The effects of these possibilities on the isomer ratios and spin cut off parameter for ^{90}Y are discussed. The effects of the (a,2n) reaction on the spin cut off parameter for the (a,n) reaction product were demonstrated by studying the $^{41}K(a,n)$ reaction below and above the $^{41}K(a,2n)$ threshold. It was concluded that care must be taken in applying the Huizenga–Vandenbosch formalism even to the simplest compound nucleus reaction such as an (a,n), because meaningless parameters will be obtained when a major competing reaction such as the (a,2n) is also taking place. (Dissertation Abstr.)

41821 THE EFFECT OF ANGULAR MOMENTUM ON ISOMERIC CROSS-SECTION RATIOS IN COMPOUND NUCLEAR REACTIONS (thesis). Dudey, Norman Dean. Worcester, Mass., Clark Univ., 1964. 197p.

The effects of angular momentum on compound nuclear reactions was investigated by measuring the formation cross section ratios of two isomeric pairs, ^{117}In and ^{137}Ce. The former was produced in the $^{115}In(\alpha,2p)$ reaction and the latter as the three-neutron evaporation product from the compound nucleus ^{140}Ce which was formed by the reactions $\alpha + {}^{136}Ba$, $p + {}^{139}La$, and $^{12}C + {}^{128}Te$. The experimentally determined isomeric ratio, high-spin state to low-spin state, for the reaction $^{115}In(\alpha,2p)^{117g,m}In$ is ~0.4 at 21 Mev, increases with energy to ~1.4 at 29 Mev, after which it is constant to 42 Mev. The excitation function for the $(\alpha,2p)$ reaction is constant at ~45 μb from 20 to 26 Mev; then it increases rapidly to ~800 μb at 42 Mev. The isomeric ratio for the $^{136}Ba(\alpha,3n)^{137g,m}Ce$ reaction is 3.5 at 29 Mev, increases slowly to 5.0 at 32 Mev, and then more rapidly to 11.3 at 40 Mev. The excitation function increases to a maximum value of 580 mb at 35 Mev and then decreases to ~240 mb at 40 Mev. Range measurements are also reported for this reaction; these support a compound nuclear mechanism. The isomeric ratio for the $^{139}La(p,3n)^{137g,m}Ce$ reaction is constant at ~1.9 from 25 to 35 Mev, increases slowly to a maximum of 3.6 at 55 Mev, and finally decreases to 3.0 at 70 Mev. The excitation function decreases rapidly with increasing proton energies up to about 50 Mev; above this energy it is constant at ~350 mb. The isomeric ratio for the (^{12}C, 3n) reaction increases very rapidly to a maximum of 12 at 46 Mev and then decreases with increasing energy to ~2 at 95 Mev. The increasing region is attributed to the increased angular momentum carried in by the ^{12}C ions with increasing energy. The isomeric ratios in the $(\alpha,2p)$, $(\alpha,3n)$, and several other alpha reactions were analyzed in terms of the formalism of Vandenbosch and Huizenga. This method was extended to include the effects of competing evaporation processes and the effects of γ emission competing against particle emission. The results were found to be consistent with the analysis of level counting and angular distribution experiments. However, average moments of inertia implied by the calculations were always less than that of a rigid sphere and sometimes much less. (Dissertation Abstr.)

41822 DIRECTIONAL CORRELATIONS OF THE GAMMA RAYS OF ^{140}La AND ^{140}Ce. Black, Walter Wayne. Bloomington, Ind., Indiana Univ., 1964. 120p.

The directional correlations of the gamma rays in ^{140}La and ^{140}Ce were measured. The apparatus used was a conventional fast-slow coincidence counting set in conjunction with a 200 channel analyzer. The resolving time of the apparatus is $2\tau = 20$ nanoseconds. NaI(Tl) crystals (cylinders, $1\frac{1}{2} \times 1\frac{1}{2}$ in.) were mounted on RCA 6810 A photomultiplier tubes. Ba-^{140}La equilibrium sources were used for the study of the gamma rays of ^{140}Ce, and ^{140}Ba sources for the study of the gamma rays of ^{140}La. The analysis of the complex gamma spectra involved was carried out with the help of an IBM-709 computer. The main objective of doing ^{140}La was to measure the correlations involving the 700–900 kev region of the spectrum. The energy of the gamma cascades (kev) and the values of A_2 and A_4 in that order follow: 487 – 1597, 0.097 ± 0.005, 0.016 ± 0.009; 923 – 1597, 0.24 ± 0.01, –0.005 ± 0.018; 815 – 1597, –0.099 ± 0.009, –0.008 ± 0.017; 329 – 1597, –0.104 ± 0.015, –0.005 ± 0.028; 329 – 487, –0.094 ± 0.014, –0.044 ± 0.007. The results for the 487 – 1597 kev correlation are in good agreement with theory which gives $A_2 = 0.102$ and $A_4 = 0.009$. The values of the correlation coefficients for the cascades including the 329- and 815-kev transitions indicate that these two transitions contain approximately 0.5% and 0.1% quadrupole content respectively. The correlation coefficients found for the 923–1597 kev correlation indicate a spin of 2 for the 2.52-Mev level. The experimental value places an upper limit of 0.1% of quadrupole content for the 923 kev transition. In the case of the ^{140}Ba decay, measurements of the 162–304 kev correlation were made. The experimental results gave $A_2 = 0.062 \pm 0.005$ and $A_4 = 0.015 \pm 0.008$. These results coupled with beta decay data indicate that the most probable spin sequence is $1^- \rightarrow 2^- \rightarrow 3^-$ in order of descending energy. (Dissertation Abstr.)

41823 TRANSITION PATHS OF μ^- MESONS CAPTURED IN SOLID LITHIUM (thesis). Johnson, Coates Richard. Berkeley, Calif., Univ. of California, 1963. 105p.

An investigation was made on the cascade down to the ground state of meson (μ^-) captured by an atom of solid lithium. The cascade takes place predominately through three processes. These are radiation transitions, Auger transitions involving the K-shell electrons of the mesonic atom, and Auger transitions involving the band electrons of the solid. It is assumed that the meson is captured in a state of high principal quantum number ($n \sim 15$). It is found, independent of the number of K-shell electrons remaining in the mesonic atom that the principal decay paths follow, at least approximately, and if the meson is captured in a high l state, the route $\Delta n = \Delta l = -1$. For mesons captured in low l states there is a tendency for the main paths to pass through states of higher l than that given by $\Delta n = -1$, $\Delta l = -1$. Because of the presence of Auger transitions where $\Delta n = -1$, $\Delta l = 0$ and where $\Delta n = 0$, $\Delta l = -1$, the cascades contain a rather large dispersion away from the main paths and towards both large and small l. Reasons are given for expecting the same qualitative description of mesonic cascades to hold also for mesons (π^-) captured in lithium, and for both mesons (μ^-) and (π^-) captured in other light solids ($Z < 6$). (Dissertation Abstr.)

41824 NUCLEAR El PHOTODISINTEGRATION IN THE 1s-SHELL (thesis). Davey, Paul Oliver. Lincoln, Neb., Univ. of Nebraska, 1964. 112p.

The integrated and bremsstrahlung-weighted El photoabsorption cross sections, σ_{int} and σ_b, were calculated for the lightest nuclei, ^2H, ^3H, and ^3He, within the framework of a second-order perturbation procedure. For the purpose of comparison, two gaussian nucleon-nucleon potentials were employed; one containing a repulsive core, central attractive, and tensor components, the other only central attractive and tensor terms. The results for σ_{int} indicate that while reasonable overall agreement with experiment may be achieved with either potential, the component contributions differ widely because of the admixture of the repulsive core. Furthermore, the results of σ_b for the deuteron seem to indicate a deficiency in the present choice of oscillator basis functions when applied to the loosely bound system. Considerable improvement for σ_b was noted for ^3H and ^3He where the nucleus is a more tightly bound and less extended structure. It was found

by analyzing exact and approximate third-order contributions to both the deuteron binding energy and integrated cross section that the use of a wave function containing parameters determined by minimization of the perturbation expansion through second order is probably not acceptable, at least for this nucleus. This was further substantiated by comparison with the binding energy results obtained from an exact numerical solution of the coupled S and D radial differential equations. In order to test the effects of a component of mixed spatial symmetry on σ_b for the three-body system, a calculation was carried out using the wave functions recently suggested by Schiff. The discrepancy between the result computed in this way and other theoretical and experimental values supports the need for a further study of this problem. (Dissertation Abstr.)

41825 K ELECTRON EJECTION ACCOMPANYING NUCLEAR K-CAPTURE (thesis). Intemann, Robert Louis. Hoboken, N. J., Stevens Inst. of Tech., 1964. 86p.

The momentum spectrum for the K electrons ejected during nuclear K-capture is calculated in the lowest order of perturbation theory using a nonrelativistic approximation for the electrons. A discussion of relativistic effects and effects due to atomic screening and nuclear recoil is given. The discrepancies existing between theories and experiments are also discussed. (Dissertation Abstr.)

41826 THE ENERGY GAP IN INTERACTING NUCLEON SYSTEMS (thesis). Kennedy, Roger Charles. Seattle, Univ. of Washington, 1964. 123p.

The BCS integral equation was applied to systems of interacting nucleons in an attempt to understand certain features of the spectra of finite nuclei. The approach here is to use a realistic nuclear interaction. This is in contrast to most of the previous work in which the interaction is represented by an empirically adjusted strength parameter. Of particular interest are the comparisons between the energy gap function for infinite nuclear systems and that for finite systems and the dependence of the gap function on the size of the finite systems. The kernel of the integral equation is the matrix element of the s-wave part of a phenomenological two-body potential acting between time-reversed states of the model in question. In all cases, this s-wave part of the potential consists of a separable or a sum of two separable terms fitted to the same three pieces of proton-proton scattering data: the scattering length, the effective range, and the singlet, s-wave phase shift at 310 Mev. Calculations were performed for three nuclear systems: infinite nuclear matter, and two nuclear slabs (which serve to introduce finiteness in one dimension). These slabs are defined by potential wells in one-dimension (the x-direction) and no restrictions in the other two. The specific wells considered are the infinite and finite symmetric square-wells. The infinite matter model is the only one in which calculations can be performed exactly. These exact solutions provide an important basis of comparison for the approximations which are used in the solutions of the remaining two models. In the limit that the extent of the finite systems becomes very large, the solutions should approach those of the infinite matter case. It is shown that this holds true for the infinite square-well but does not hold true for the finite well. This suggests that a reformulation of the basic theory is in order so that the proper limits obtain. Estimates of the actual energy gaps of finite nuclei can be made from comparisons of even-even nuclei and their odd-A neighbors. The importance of finite effects in determining the magnitude of the energy gap is emphasized. Finally, a short survey is given of appropriate numerical techniques. (Dissertation Abstr.)

41827 NEUTRON DIFFERENTIAL ELASTIC SCATTERING CROSS SECTIONS—ANGULAR DISTRIBUTIONS (thesis). Gerardo, Henry Alexander. Lafayette, Ind., Purdue Univ., 1964. 165p.

A nuclear optical model code incorporating spin-orbit coupling was used to theoretically calculate the differential elastic scattering cross section of a number of elements for incident neutron energies where no experimental measurements have been performed. Neutron angular distributions and tables of cumulative probability density distribution functions for Monte Carlo codes and specialized reactor-shield and nuclear probe programs have been generated for a twenty energy group structure (ranging from 0.13–20 Mev) for elements pertinent to mobile and aerospace applications. Curves and tables of the results are presented based on the parameters selected to best fit the experimental data available. (Dissertation Abstr.)

41828 MONOCHROMATOR STUDIES OF NUCLEAR RESONANCE FLUORESCENCE IN CARBON, SILICON, AND MAGNESIUM (thesis). Kuehne, Herbert Wayne. Urbana, Ill., Univ. of Illinois, 1964. 182p.

Experimental studies of isolated energy levels with the aid of the University of Illinois bremsstrahlung monochromator are described. The studies had as objectives both the development of techniques needed to make the monochromator a better tool for studying nuclear levels and the investigation of the properties of selected levels. There are three aspects of the monochromator performance that were improved or studied during the course of the experiment. The first consisted of the design of a very fast transistorized scalar to count random electron pulses coming at an average rate of about one per microsecond. The second monochromator improvement involved the energy stability and energy calibration. The third facet of the monochromator performance which was especially important was the energy resolution. The experimental results related to nuclear structure consisted of information about six different energy levels. The energies of five of these levels were determined precisely as 15.11 Mev in ^{12}C (standard), 11.40 ± 0.02 Mev in ^{28}Si, 12.31 ± 0.03 Mev in ^{28}Si, 10.64 ± 0.02 Mev in ^{24}Mg, and 9.90 ± 0.025 Mev in ^{24}Mg. The sixth level was found incidentally while studying the 9.90-Mev resonance. Its energy was estimated as 10.05 ± 0.05 Mev. The resonance is assumed to be due to ^{26}Mg. The level parameters for all resonances except the 12.31-Mev resonance were determined from measurements of the absolute scattering and the self absorption. The experiment did not clearly distinguish between elastic and inelastic scattering; however, the data for the 15.11- and 11.40-Mev resonances indicate little or no inelastic scattering. (Dissertation Abstr.)

41829 STRUCTURE OF MATTER. Finkelnburg, Wolfgang. New York, Academic Press, 1964. 520p. $14.50.

Translated from Einfuehrung in die Atomphysik.

The structure of matter is presented in a very broad sense. The structure of matter, its constituent elementary particles, their properties and reactions are considered. An attempt is made to explain the immense number of observed phenomena in a unified way, and this with as small a number as possible of elementary particles, of general basic laws, and of fundamental constants. Topics covered include atoms, ions, electrons, atomic nuclei, and photons, atomic spectra and structure, quantum mechanics, physics of atomic nuclei and elementary particles, molecular physics, and solid state from the atomistic point of view. (J.F.P.)

41830 NUCLIDES AND ISOTOPES. (INCLUDES REVISED "CHART OF THE NUCLIDES"). Eighth Edition. Goldman, David T. (Schenectady, N. Y., General Electric Co.). 1965. 8p.

An explanation of the eighth edition of the General Electric Chart of the Nuclides, which is based on data available up to March 15, 1965, is presented. (D.C.W.)

41831 EVIDENCE FOR NUCLEON CLUSTERING FROM HIGH-ENERGY REACTIONS. Lefort, M.; Cohen, J. P.; Dubost, H.; Tarrago, X. (Universite de Paris). 24p. (CONF-650401-7). Gmelin, AED-CONF-65-041-24.

From American Chemical Society, Detroit.

The telescope method was used with solid state detectors for measuring angular and energy distributions of complex particles emitted in nuclear reactions induced by 157-Mev protons on heavy nuclei (Ag, Au, Bi, Th). Both an isotropic and a forward-peaked emission were observed for ^4He, tritons and deuterons. Yields of ^3He were found to be very

low at the back-angles. The components of the above particle spectra emitted at forward angles are interpreted in terms of a direct interaction mechanism on α clusters in surface and a Monte Carlo calculation was performed to compute the yield of α clusters knocked out by prompt cascade nucleons. The tritons and ^{3}He particles might partly be ejected by a double pick-up process, partly by a stripping mechanism on alpha clusters. (auth)

41832 ANGULAR DISTRIBUTION OF THE D-D REACTION PRODUCTS. Beach, L. A.; Theus, R. B.; McGarry, W. I. (Naval Research Lab., Washington, D. C.). 11p. (CONF-758-43). Gmelin, AED-CONF-65-003-59.

From American Physical Society Meeting, New York, Jan. 1965.

Angular distributions of the reaction products of deuteron reactions with deuterium were measured at 20 to 300 kev. Branching ratios between the two reaction modes, D(d,n) ^{3}He and D(d,p)^{3}H, are determined within 1% and the asymmetry coefficients are determined within 5%. The angular distributions for the charged particles are shown for bombarding energies of 122.0 and 298.5 kev. An analysis of differences between the two reactions indicated an appreciable difference in the mass distributions of ^{3}H and ^{3}He. (L.B.S.)

41833 PHOTONEUTRONS FROM LEAD. Stubbins, Warren Fenton. 6p. (CONF-650410-6). Gmelin, AED-CONF-65-073-7.

From American Physical Society, Washington, D. C.

A fission counter using normal or depleted uranium is used as a threshold detector for studying photoneutron production from lead at 11.6 Mev. Two experimental arrangements are used, and preliminary results are given. Characteristics of the uranium fission counter are described. (L.B.S.)

41834 NEUTRON SPECTRA FROM BISMUTH PRODUCED BY MONOENERGETIC GAMMA-RAYS. Kuchnir, F. T.; Axel, P.; Criegge, L.; Drake, D. M.; Hanson, A. O.; Sutton, D. C. (Univ. of Illinois, Urbana). 10p. (CONF-650410-25). Gmelin, AED-CONF-65-073-42.

From American Physical Society, Washington, D. C.

A photon monochromator arrangement with a 25-Mev betatron was used to study the neutron spectra form the (γ,n) reaction in ^{209}Bi over the giant resonance region. Neutron time-of-flight spectra were measured at gamma energies of 12 to 16 Mev. A fast neutron group was observed with a width of approximately 1 Mev, which is consistent with transitions to levels from the ground state to about 1 Mev excitation in ^{208}Bi. Nuclear temperatures were determined from plots of $\ln(1/E_n dN/dE_n)$ versus the neutron energy for three γ-ray energies. Cross sections for neutrons with energy larger than 1 Mev and larger than 3 and 5 Mev are also plotted. It is concluded from the shape and thresholds of the three curves that the direct process is associated with the giant resonance. (L.B.S.)

41835 A STUDY OF THE EXCITED STATES OF ^{127}I POPULATED IN THE DECAY OF ^{127}Te AND ^{127m}Te. Auble, R. L.; Kelly, W. H. (Michigan State Univ., East Lansing). 20p. (CONF-650410-4). Gmelin, AED-CONF-65-073-2.

From American Physical Society, Washington, D. C.

Gamma ray singles, coincidence and angular correlation studies were performed to aid in determination of the spins of several excited states in ^{127}I and the multipolarities of the gamma ray transitions from these states. The results, when analyzed in conjunction with other recent findings, allow unique spin assignments of $5/2$, $7/2$, $3/2$ and $5/2$ to be made for the ground, 0.0576, 0.203 and 0.417 Mev states respectively. In addition, a state at 0.649 Mev was observed which had been unreported in previous studies. The close similarity between these states and those in ^{121}Sb is noted. (auth)

41836 GAMMA RATES AND INTENSITIES; l-FORBIDDEN M1 TRANSITIONS. Fossan, D. B.; Chase, L. F. Jr.; Coop, K. L. (Lockheed Missiles and Space Co., Palo Alto, Calif.). 35p. (CONF-641004-14). Gmelin, AED-CONF-64-220-42.

From American Physical Society, Chicago.

A search for l^1forbidden M1 transitions of the type ($1g_{9/2} \rightarrow 2d_{5/2}$) was made in Pm^{149}, Pm^{151}, and Sb^{125}. Lifetimes of the first excited states were obtained from beta-gamma and gamma-gamma time-delay distributions that were measured with a fast time-to-height converter. The measured half-life for the 114-kev level in Pm^{149} is (2.62 ± 0.10) nsec and that for the 326-kev level in Sb^{125} is ≤ 0.2 nsec; hinderance factors relative to Moszkowski limits for these transitions are 350 and ≤ 300, respectively. In the deformed nucleus Pm^{151}, the half-life of the 118-kev first excited state is ≤ 0.3 nsec and that of the 256-kev level was measured to be (0.91 ± 0.03) nsec. Lifetime limits for additional levels were obtained. Because of uncertainties in the level schemes of Pm^{149} and Pm^{151}, the gamma-ray intensities from the decay of Nd^{149} and Nd^{151} were measured with a Ge(Li) solid-state detector. From the 28h Pm^{151} daughter activity, a half-life of (0.48 ± 0.03) nsec was measured which is associated with the 105-kev level in Sm^{151} and an upper limit of ≤ 0.2 nsec was placed on the half-life of the 345-kev level. (auth)

41837 THE E_p = 1.278 Mev RESONANCE OF ^{22}Ne(p,γ)^{23}Na. Greene, M. Wayne. (Univ. of Iowa, Iowa City). 37p. (CONF-758-36). Gmelin, AED-CONF-65-003-60.

From American Physical Society Meeting, New York, Jan. 1965.

The subsequent gamma ray decay from the 10.013 Mev excited state of the compound nucleus ^{23*}Na formed by the resonant capture of 1.278 Mev protons by ^{22}Ne was investigated. The four principal modes of decay were: (1) to the first excited state E_γ = 9.58 Mev, (2) to the 2.98 Mev level E_γ = 7.03 Mev, (3) to the 3.85-3.92 Mev doublet E_γ = 6.04 Mev and E_γ = 6.16 Mev, and (4) to the 7.85 Mev level E_γ = 2.19 Mev. A direct transition to the ground state E_γ = 10.01 Mev was not observed. The absence of any energy dependent anomaly in the elastic scattering of protons observed at 90 degrees in the laboratory at the 1.278 Mev resonance indicates the angular momentum of the captured protons has the values l = 1, 3, 5 . . . and hence the resonance state has odd parity. (auth)

41838 AN INVESTIGATION OF GAMMA RAYS FROM THE REACTIONS ^{20}Ne(p,γ)^{21}Na, ^{21}Ne(p,p'γ)^{21}Ne, AND ^{22}Ne(p,γ)^{23}Na. Coop, Kenneth L. (Univ. of Iowa, Iowa City). 55p. (CONF-758-35). Gmelin, AED-CONF-65-003-61.

From American Physical Society Meeting, New York, Jan. 1965.

An investigation was made of gamma rays from reactions induced by proton bombardment of natural neon gas in the energy range E_p = 1.28 to 1.86 Mev. Gamma ray yield curves indicated seven new resonances in the ^{22}Ne(p,γ)^{23}Na reactions, and eight previously unreported resonances in ^{21}Ne(p,p'γ)^{21}Ne. No evidence was found from the ^{20}Ne(p,γ)^{21}Na yield curves for the existence of a previously reported 3.88 Mev level in ^{21}Na. Using single crystal, coincidence, and three crystal pair spectra, a study was made of the reaction ^{20}Ne(p,γ)^{21}Na at E_p = 1.17 Mev. The branching ratio and the gamma ray energies were determined for the decay of the 3.54 Mev level in ^{21}Na. The energies of the first and second excited states of ^{21}Na were determined to be 0.30 ± 0.01 Mev and 1.70 ± 0.03 Mev, respectively. (auth)

41839 THE GROUPS R(5) AND R(8) AND GENERALIZED QUASI-SPIN IN NUCLEAR STRUCTURE PROBLEMS. Hecht, K. T. 30p. (CONF-758-41). Gmelin, AED-CONF-65-003-55.

From American Physical Society Meeting, New York, Jan. 1965.

The quasi-spin formalism is briefly reviewed for fermions of one kind only, either neutrons or protons, in which case the quasi-spin group is the rotation group in three dimensions. Generalization is then made to proton-neutron configuration, in which the quasi-spin group is a rotation group in an abstract space of 5 dimensions in the case of j-j coupling, and in 8 dimensions in the case of L–S coupling. (L.B.S.)

41840 INTERMEDIATE STATE REORIENTATION IN THE NUCLEAR ALIGNMENT OF ^{139}Ce IN Ce–Mg NITRATE.

Sapp, R. C.; Carlson, E. R. (Univ. of Kansas, Manhattan). 10p. (CONF-650410-8). Gmelin, AED-CONF-65-073-15.

From American Physical Society, Washington, D. C.

A nuclear alignment experiment on ^{139}Ce in CeMg nitrate at the very low temperature attained by magnetic coiling is described. The possibility of an intermediate state reorientation effect similar to that found in angular correlation experiments is re-examined. The anisotropies were derived from the angular distributions obtained after demagnetizations from 24.5 and 7.2 kOe at 1.15°K. The hfs coupling, temperature scale, spin-spin interactions, and the degree of coherent mixing in the gamma transition were precisely determined in order to extract the attenuation coefficient. It is concluded that there is evidence for an enhancement of about 25%, in disagreement with an attenuation predicted on the basis of previous experiments. (D.B.S.)

41841 FAMILY OF VELOCITY-DEPENDENT NUCLEON-NUCLEON POTENTIALS FOR SINGLET-EVEN STATES. Pearson, J. M.; Trudeau, Fernand (Univ. of Montreal). 9p. (CONF-650410-11). Gmelin, AED-CONF-65-073-4.

From American Physical Society, Washington, D. C.

An expression is presented for the form of the singlet-even potential in which the first two terms represent the short-range phenomenological part of which the first is static and the second is momentum dependent. The variables in the expression are tabulated values of the peak-displacement parameter. Comparison is shown with experimental data. (L.B.S.)

41842 STUDY OF THE ^{6}Li(p,2p)^{5}He REACTION USING CLUSTER MODEL WAVEFUNCTIONS. Wittern, H. W.; Hansteen, J. M. (Florida State Univ., Tallahassee). 8p. (CONF-650410-5). Gmelin, AED-CONF-65-073-6.

From American Physical Society, Washington, D. C.

Calculations were made of the angular correlation distributions for s- and p-protons in ^{6}Li and are compared with experimental distributions from the ^{6}Li(p,2p) reaction. (L.B.S.)

41843 ON THE SUPERCONDUCTIVITY THEORY OF THE NUCLEAR PAIRING INTERACTION. Nogami, Yukihisa (McMaster Univ., Hamilton, Ont.). 9p. (CONF-650410-23). Gmelin, AED-CONF-65-073-38.

From American Physical Society, Washington, D. C.

A method is presented for which the superconductivity solution to the nuclear pairing interaction is found to exist for any interaction strength. In this method the gap parameter shows no sudden change as a function of the coupling constant G, and approaches zero smoothly as G tends to zero. A symmetric two-degenerate-level case is discussed as an illustration. (L.B.S.)

41844 DYNAMICAL CORRELATIONS AND THE NUCLEAR PHOTOEFFECT. Wang, Tso-Pin; Clark, John W. (Washington Univ., St. Louis). 82p. (CONF-758-34). Gmelin, AED-CONF-65-003-94.

From American Physical Society Meeting, New York, Jan, 1965.

The dipole sum rules of Levinger and Bethe are used to estimate the influence of strong dynamical correlations, generated by realistic 2-nucleon potentials, on the photoeffect in heavy nuclei. An asymptotic description of the nuclear ground state is given, based on a complete set of correlated functions $\{F\ \Phi_m\}$, where F is a product of 2-body correlation factors f appropriate to a system with strong short-range repulsions and $\{\Phi_m\}$ a complete set of Fermi-gas model functions satisfying periodic boundary conditions over a fundamental volume Ω identified with the (assumed large) nuclear volume. The integral of the photonuclear cross section over all photon energies, $\sigma_{int} = \int\sigma(w)dw$, is estimated in zeroth cluster order for Hamada-Johnston, Brueckner-Gammel-Thaler, Gammel-Christian-Thaler, and Ohmura-Morita-Yamada potentials, with a ground-state wave function constructed from the $F\Phi^m$ via a first-order perturbation theory. The bremsstrahlung-weighted cross section, $\sigma_{\perp} = \int\sigma(w)w^{-1}dw$, is calculated with the unperturbed wave function $F\Phi_0$, where Φ_0 is the wave function of the degenerate Fermi gas; here first-order cluster corrections are included. The first energy moment $\sigma_1 = \int\sigma(w)wdw$ of the cross section is also evaluated using $F\Phi_0$, but keeping only lowest cluster contributions. Variation of these three energy moments of $\sigma(w)$ with an inverse range parameter γ in f and with the nuclear radius parameter γ_0 is studied. It is found that σ_{int} and σ_1, which depend explicitly on the 2-nucleon potential and are sensitive to the short-range behavior of f, are substantially increased, and σ_b, which is sensitive to the long-range behavior of f, may be appreciably diminished, compared to their respective values for a Fermi-gas model and well-behaved central potentials fitting the low-energy scattering data. (In particular, for all potentials tested and for reasonable parameter choices, σ_{int} is enhanced by roughly a factor 2 over the TRK value). It is anticipated that, in the future, the Levinger-Bethe sum rules may emerge as important tools for probing the validity of favored models of the nuclear ground state and of the 2-nucleon potential. (auth)

41845 MEASUREMENTS BY SCATTERING TECHNIQUES. [PART] II. Debrunner, P. (Univ. of Illinois, Urbana). 15p. (CONF-650101-4). Gmelin, AED-CONF-65-006-2.

From Moessbauer Symposium, New York.

The application of a backscattering geometry for the measurement of Mössbauer transitions with very small recoilless fractions is discussed. A hypothetical experiment with no interfering background is considered in order to derive an upper limit for the signal to noise ratio for the geometries in a scattering and a transmission experiment. A detailed description is given of a backscattering system, and the features that are essential in the design are discussed. (L.B.S.)

41846 PARITY ASSIGNMENTS IN ^{200}Hg FROM LINEAR POLARIZATION CORRELATION OF THERMAL NEUTRON CAPTURE γ RAYS. Bartholomew, G. A.; Gunye, M. R.; Earle, E. D. 14p. (CONF-650410-7). Gmelin, AED-CONF-65-073-8.

From American Physical Society, Washington, D. C.

An experiment was performed on ^{199}Hg(n,γ)^{200}Hg in order to make independent determinations of the parities of the levels in ^{200}Hg which were assigned spin 1 from previous sum-coincidence and γ-γ correlation measurements, and to establish the multipolarities of the high energy primary γ-rays which make up the bulk of the anomalous part of the ^{199}Hg(n,γ)^{200}Hg high energy spectra. In particular, the hypothesis that the anomalously intense region above ~4 Mev in the spectra of nuclei of $180 < A < 200$ may contain a large contribution from an M1 giant resonance is tested. Linear polarization correlations of the secondary γ-rays were measured; the results are discussed. (L.B.S.)

41847 ENERGY LEVELS OF ^{158}Dy. Schroeer, D.; Jastram, P. S. (Ohio State Univ., Columbus). 10p. (CONF-650410-20). Gmelin, AED-CONF-65-073-33.

From American Physical Society, Washington, D. C.

The decay of ^{158}Tb to ^{158}Dy was studied using a separated ^{158}Tb source. With a plastic scintillator the β spectrum is found to have an energy endpoint of about 800 kev. These β particles are in coincidence with 100 and 220 kev γ-rays, which in turn are in coincidence with each other. The energy levels at 100 and 320 kev agree with those found via coulomb excitation of natural ^{158}Dy, and in the K-capture decay of ^{158}Ho to ^{158}Dy, and the energy ratio of 3.2 agrees well with the rotational model value of 3.33 if the 320 kev state has I = 4. The lifetime of the 100 kev level, found to be 1.84 ± 0.07 ns both by β-γ and γ-γ fast coincidence techniques, agrees with the value of 1.85 ns calculated from the B(E2) determined via coulomb excitation. Using a scintillation counter-proportional counter coincidence arrangement with a resolving time of 0.2 nsec, coincidences between the 100 kev γ-ray and a 725 γ-ray are found. This may be the first vibrational 2^+ level, corresponding 2^+ levels are found in neighboring even-even nuclei. (auth)

41848 MOESSBAUER TECHNIQUES USING HIGH FIELD WATER-COOLED SOLENOIDS. Blum, Norman A. (Massachusetts Inst. of Tech., Cambridge). 22p. (CONF-650101-2). Gmelin, AED-CONF-65-006-4.

From Moessbauer Symposium, New York.

Problems solved in the design and construction of a velocity spectrometer capable of performing with reasonably high resolution (0.1 mm/sec or better) at sample temperatures down to about 1°K using high-field solenoids with fields up to 150 kOe are discussed. A methane-xenon gas-filled proportional counter is used for detecting low-energy gamma rays. The velocity drive was designed to produce a continuously changing velocity, which varied linearly from zero to $V_{max\ 1}$ back through zero to $-V_{max\ 1}$ and then back to zero again. A technique was developed for overcoming the possibility of line broadening as a result of a change in the phase lag between the source motion and pickup signal with a change in acceleration. A multiscalar mode was used in operating the spectrometer. Methods were studied for reducing ambient noise and vibration levels. The sample was held inside a liquid-helium cryostat to provide a controlled-temperature environment from 1.1°K to room temperature. Modifications in the solenoid system improved the accuracy of magnetic field control to about ±0.5%. (M.C.G.)

Plasma Physics and Thermonuclear Processes

Refer also to abstract 41287.

41849 (AD-426079) CYCLOTRON-WAVE INSTABILITIES. Scientific Report No. 23. Maxum, B. J. (California Univ., Berkeley. Electronics Research Lab.). July 15, 1963. Contract AF19(628)-324. 169p. (AFCRL-63-550). CFSTI $13.00 cy, $1.00 mn.

Interactions of waves in electron streams or plasmas are studied for several geometric plasma configurations of finite cross section in a finite magnetic field. The plasma is assumed to be at zero temperature. Each of the constituents of the plasma is assumed to have a monoenergetic, nonrelativistic velocity parallel to the magnetic field. It is further assumed that either macroscopic neutrality exists or static space-charge forces are negligible. For the most part the quasi-static analysis is used. For the case of two drifting streams cyclotron waves act to give instabilities which are either convective (spatially growing) or nonconvective (time growing), depending upon whether the streams are drifting in the same or opposite directions. These instabilities, unlike the usual two-stream space-charge wave-interactions, exist for physically realizable un-neutralized electron streams without the requirement that the streams drift in the same direction with almost equal velocities. For oppositely directed streams with equal velocities, oscillations are predicted at approximately one-half the cyclotron frequency, and are observed at the output of the experimental tube in which two concentric coaxial electron streams were allowed to interact in an evacuated drift space. (auth)

41850 (AD-617386) STUDY OF COLLISION PROCESSES IN GASEOUS PLASMAS. Semi-Annual Technical Report No. 4. Oskam, H. J. (ed.) (Minnesota Univ., Minneapolis. Plasma Physics Lab.). July 1965. Contract Nonr 710(37). 9p.

Results are summarized with respect to ambipolar diffusion coefficient of He^+ and He_2^+ as obtained from mass spectrometer measurements. Modifications necessary in the SLEAMA II system in order to obtain a stronger ion signal are indicated. Recent results of mass spectrometric studies of diatomic molecular ions are summarized. (M.O.W.)

41851 (IAE-635) ISSLEDOVANIYA PLAZMY MALOI PLOTNOSTI, OBRAZUYUSHCHEISYA V OGRE PRI INZHEKTSII MOLEKULYARNYKH IONOV VODORODA. (Investigation of Low-Density Plasma Forming in Ogra During Injection of Molecular Hydrogen Ions (thesis)). Panov, D. A. (Institut Atomnoi Energii, Gosudarstvennyi Komitet po Ispol'zovaniyu Atomnoi Energii SSSR, Moscow). 1964. 127p. Dep. mn.

A study on low-density plasma such as produced in Ogra apparatus, with particular attention to the processes occurring during the initial stage of accumulation is presented. The topics dealt with are flute instability and its stabilization by an electrostatic method, the generation of high positive plasma potential, and anomalous electron losses. It is concluded that although the electron loss is the principle among the collective interactions occurring in the plasma, the charge resulting from the electron loss does not exert any direct influence on plasma containment in the trap. (auth)

41852 (IAE-676) O POLUCHENII GORYACHEI TERMOYADERNOI PLAZMY METODOM INZHEKTSII BYSTRYKH CHASTITS V MAGNITNUYU LOVUSHKU. (Obtaining a Hot Thermonuclear Plasma by Injection of Fast Particles into a Magnetic Trap). Artemenkov, L. I.; Bogdanov, G. F.; Golovin, I. N. (and others) (Institut Atomnoi Energii, Gosudarstvennyi Komitet po Ispol'zovaniyu Atomnoi Energii SSSR, Moscow). 1964. 116p. Dep. mn.

The possibility of accumulating dense hot plasma in a magnetic trap with mirrors upon injection of fast molecular ions and natural atoms is considered. Experiments carried out with the Ogra installation on the accumulation of plasma in the dissociation of molecular ions by residual gas and in a lithium arc are described. The experiments show that the radial electric field hinders greatly the development of flute instability, the suppression of which is the most important condition for the successful accumulation of plasma in magnetic traps. In the presence of a sufficiently strong radial field, produced by the space charge of the plasma, the time for all non-gas losses, due to all types of instability and to the non-adiabatic ion motion, exceeds 10 milliseconds. In dissociation by residual gas, a hot plasma with density 10^9 ion/cm^3 was obtained, and the only ion losses from the trap were due to charge exchange. It is pointed out that there are no principal physical obstacles to further increase in plasma density in all axially symmetrical magnetic traps such as Ogra. The major deduction drawn from the analysis of all the available data is that plasma stabilization can be effected using only the internal electric fields of the plasma. (auth)

41853 (LA-DC-6603) EFFECT OF INNER FIELD FLUCTUATIONS ON PLASMA IMPEDANCE. Theimer, O. (Los Alamos Scientific Lab., Univ. of California, N. Mex.). [1964]. Contract W-7405-eng-36. 25p. Dep. mn; CFSTI, $1.00 cy, $0.50 mn.

The effective field acting on the electrons in a plasma is studied by methods similar to those employed for analyzing the dielectric properties of neutral gases. The difference between incident and effective field is the polarization field which is associated with the displacement of ions relative to electrons. This latter field is found to be a sensitive function of the ion positions which fluctuates with the fluctuating ion density. The plasma impedance is averaged over these fluctuations and is shown to satisfy a formula of the form $Z = Z_1[1 + \Sigma_{\nu=1}^{\infty} C_\nu (n_0\alpha_0)^\nu]^{-1}$, where n_0 is the average electron density, $\alpha_0 = -\omega_p^2/4\pi\omega^2 n_0$ is the free electron polarizability, ω_p is the electron plasma frequency, and ω is the frequency of the driving field. The coefficients C_ν (which are zero if field fluctuations are neglected) have the magnitude $C_1 = 0$, $C_2 = 0.8[1 - 7.6(\omega/v_0 n_0^{1/3})^2 - i\ 11.2(\omega/v_0 n_0^{1/3})^3]$, where v_0 is the average thermal electron velocity. The frequency dependence of Z is quite different from that of the uncorrected impedance Z_1. (auth)

41854 (MATT-369) A MICROWAVE SYSTEM FOR LOW DENSITY MEASUREMENTS. Levine, A. M.; Kuckes, A. F.; Skislak, A. (Princeton Univ., N. J. Plasma Physics Lab.). July 1965. Contract AT(30-1)-1238. 9p. Dep. mn; CFSTI, $1.00 cy, $0.50 mn.

A simple microwave system for measuring very low densities is described. The noise level of the actual bridge was below .05° of phase shift. The technical details and theory of the bridge are presented. (M.O.W.)

41855 (NP-15142) ELECTROMAGNETIC STUDIES IN SHOCK PRODUCED PLASMAS. Technical Report No. 519. Final Report. Tomboulian, R. (General Applied

Science Labs., Inc., Westbury, N. Y.). Apr. 15, 1965. Contract Nonr-3475(00). 180p.

The important aspects of an analytical and experimental study concerned with non-uniform plasmas are considered. A detailed description of the experimental shock tube facility is presented. The development of a spatially resolving electron density microwave diagnostic technique is presented. This technique was used to measure electron density profiles behind normal air shocks in the range of Mach number 8.5-11 and initial pressure conditions of ~1 mm Hg. The microwave instrumentation for this technique is described. The analytical formulation correlating the measured properties to ascertain the electron density is given. A summary of the theoretical work conducted in conjunction with the experimental program is presented. A brief description of the generalized properties of non-uniform plasmas is given and referenced to the detailed formulations. (M.O.W.)

41856 (NP-15205) O DVIZHENII PLAZMENNYKH SGUSTKOV V SVOBODNOM OT POLEI PROSTRANSTVE. (Motion of Plasma Bunches in a Field-Free Space). Azovskii, Yu. S.; Guzhovskii, I. T.; Mazalov, Yu. P.; Pistryak, V. M. (Akademiya Nauk Ukrainskoi SSR, Kharkov. Fiziko-Tekhnicheskii Institut). 1964. 15p. Dep. mn.

The rate of mixing of layers of specified density in the leading part of a cluster during its motion in free space was determined. The mixing of layers was recorded using the Doppler effect during the reflection of microwave radiation from the moving cluster. The velocity of sound in the cluster, which characterizes its thermal expansion, was estimated from these measurements, using the analogy between the expansion of a gas cloud and a plasma cluster. (tr-auth)

41857 (NP-15206) MAGNITNYI MOMENT PLAZMENNOGO SGUSTKA, NALETAYUSHCHEGO NA ODNORODNOE PRODOL'NOE MAGNITNOE POLE. (The Magnetic Moment of a Plasma Bunch Impinging on a Homogeneous Longitudinal Magnetic Field). Khizhnyak, N. A. (Akademiya Nauk Ukrainskoi SSR, Kharkov. Fiziko-Tekhnicheskii Institut). 1964. 20p. Dep. mn.

The magnetic moment of a charged particle in the region of a homogeneous axially symmetric magnetic field is calculated as a function of the asymptotic behavior of the components of the field for $H \to 0$ and of the parameters of motion of the particle at infinity. The magnetic moment of a plasma cluster impinging on an axially symmetric magnetic field is investigated as a function of the particle density in the cluster. It is shown that for clusters of low density $n < 10^{12}/r^2$, where r is the radius of the cluster, there exists the conception of adiabaticity of motion, analogous to the conception of the adiabaticity of motion of the individual charged particle. For cluster densities $n > 10^{12}/r^2$, the character of motion is essentially different. The currents induced in the cluster distort the external magnetic field, moving the lines of force of the field apart, and the magnetic moment of the cluster is not conserved. (tr-auth)

41858 (NP-15217) LOVUSHKA S MAGNITNYMI PROBKAMI, RASSCHITANNAYA NA DLITEL'NOE YADERZHANIE ELEKTRONOV. (Trap With Magnetic Plugs Designed for Prolonged Holding of Electrons). Dubinina, A. I.; Trainin, L. Ya.; Chirikov, B. V. (Akademiya Nauk SSSR, Novosibirsk. Institut Yadernoi Fiziki). 1964. 10p. Dep. mn.

Design, arrangement and preliminary experiments with an electron mirror machine are described. A mean containment time up to 40 sec was observed for electron energy about 100 kev, magnetic induction in the mirror about 2.5 kG and mirror ratio 2.5. Dimensions of the cylindrical vacuum chamber are 1600 × 210 mm; the pressure was $\sim 8 \times 10^{-10}$ mm Hg. Under these conditions the number of electron oscillations between mirrors achieves 5×10^9 and the number of Larmor revolutions $\sim 10^{11}$. Significant decreasing of the containment time was observed for $\rho/R \gtrsim 0.1$ where ρ is electron orbit radius and R is magnetic line curvature radius. This result demonstrates a non-adiabaticity of electron motion in magnetic mirror geometry. A simple method of electron injection from outer electron gun is described. The capture is the result of fast switching of the special form electric field at the magnetic mirror. (auth)

41859 (NP-15218) ISSLEDOVANIE RASPREDELENIYA TOKA V KOAKSIAL'NOI PLAZMENNOI PUSHKE. (The Study of Current Distribution in a Coaxial Plasma Gun). Zolototrubov, I. M.; Kiselev, V. A.; Novikov, Yu. M. (Akademiya Nauk Ukrainskoi SSR, Kharkov. Fiziko-Tekhnicheskii Institut). 1964. 12p. Dep mn.

The current distribution in a coaxial plasma source was investigated using a differential magnetic probe. It was shown that in the initial stage the discharge in the gun is formed successively by several current layers. The discharge current of the capacitance battery flows through the last current layer, whose motion leads to the merging of the current layers and to the formation of a unique layer in the gun. Measurements of the velocity of the current layer within the gun and of the plasma clusters outside of it were performed. Comparison of these rates indicates that a fast plasma cluster does not owe its origin to electrodynamic acceleration of the current layer. It is assumed that a fast cluster is formed as a consequence of plasma drift in the crossed electric and magnetic fields behind the current layer. (tr-auth)

41860 (NP-15220) ISSLEDOVANIE PLAZMY Θ-PINCHA S AZIMUTAL'NYM MAGNITNYM POLEM. (Study of Plasma in Θ-Pinch With Azimuthal Magnetic Field). Volkov, Ya. F.; Dyatlov, V. G.; Mitina, N. I. (Akademiya Nauk Ukrainskoi SSR, Kharkov. Fiziko-Tekhnicheskii Institut). 1964. 11p. Dep. mn.

A theta-pinch plasma confined in an azimuthal magnetic field was studied to explore the possible existence of dense currents of accelerated electrons, transferring part of their energy to the plasma. The apparatus and measuring method are described. Measurements of the electron and ion temperatures were performed at He pressures in the discharge chamber of 1 to 2×10^{-3} mm Hg. Electron temperatures were found to reach values higher than 1 kev. Powerful radio noise was observed, indicating electron oscillations at frequencies on the order of the plasma frequency. The azimuthal field was found to stabilize the plasma and raise the ion temperature. Significant heating of the ions took place, caused by collisionless interaction between the plasma electrons and ions. (M.J.T.)

41861 (NP-15255) ISSLEDOVANIYA PO NAGREVU PLAZMY UDARNYMI VOLNAMI V LOVUSHKE S MAGNITNYMI PROBKAMI, PROVODIMYE V INSTITUTE YADERNOI FIZIKI SIBIRSKOGO OTDELENIYA AN SSSR. (Studies on Heating of Plasma by Shock Waves in a Trap With Magnetic Probes, Conducted at the Institute of Nuclear Physics, Siberian Department of the Academy of Sciences, USSR). Nesterikhin, Yu. E. (Akademiya Nauk SSSR, Novosibirsk. Institut Yadernoi Fiziki). 1964. 40p. Dep. mn.

Experiments aimed at heating a plasma by means of collisionless shock waves are described. The theory of the phenomenon is briefly outlined. The experiments were carried out on a plasma with ion density $\sim 10^{14}$ cm^{-3}, produced with the aid of a θ-pinch discharge by either internal or external injection in a pyrotron unit. The equipment, the injection methods, the behavior of the preliminary plasma prior to application of the shock waves, the shock-wave production, techniques used to determine the optical and magnetic characteristics of the shock-wave front, and the results of capturing and retaining the heated plasma in a magnetic-mirror trap are described. Among the illustrations are diagrams of the experimental equipment and oscillograms of the x-ray and neutron emission from the plasma. The publications where most of the tests results and equipment are described are cited in the references. It is deduced from the data that the experimenters succeeded in capturing hot plasma with ion energies 10–15 kev and of density $\sim 5 \times 10^{12}$ cm^{-3}. (auth)

41862 (NP-15256) VYSOKOCHASTOTNYI NAGREV PLAZMY. (High-Frequency Heating of Plasma). Tolok,

V. T. (Akademiya Nauk Ukrainskoi SSR, Kharkov. Fiziko-Tekhnicheskii Institut). 1964. 26p. Dep. mn.

The main results of high-frequency plasma heating, predominantly with the aid of ion cyclotron and fast magnetosonic waves, in bounded plasma of varying density and under different excitation conditions are reviewed. The theory of excitation and attenuation of natural plasma oscillations is briefly reviewed and the various experimental methods used are described, including the "Sneg," "Vikhr'," and "Grad" apparatus. The efficiency of the equipment and the behavior of the plasma heated by this equipment are analyzed in detail. Among the conclusions are: There is good agreement between theory and the experimental data on resonant excitation, propagation, and attenuation (collisional and collisionless) of waves in a dense plasma. Temperatures above 1 kev were attained at a plasma density 10^{13} cm^{-3}. Most experiments were concerned with fast heating of the plasma without proper attention to plasma confinement. Simultaneous use of both ion-cyclotron and fast magnetosonic waves is desirable for a more uniform heating of the ions and electrons in the plasma. Although many experimental facts can be interpreted with the aid of the theory as a result of "ionic two-stream" instability, it is felt that this conclusion needs further experimental clarification. (ATD)

41863 (NP-15302) THE ELECTRON PLASMA-EXPERIMENT THEORY AND APPLICATIONS. Levy, R. H.; Janes, G. S. (Avco-Everett Research Lab., Everett, Mass.). June 1965. Contract AF49(638)-659. 17p. (AMP-160).

The basic concepts involved in the production and control of pure electron and electron rich plasmas are reviewed, with particular reference to the different geometries in which equilibrium may be achieved. An inductive method of establishing arbitrary equilibrium profiles is described. Recent theoretical work on the stability of some particularly simple equilibria is then discussed. Instabilities considered are: 1) The so-called diocotron (or slipping stream) instability, this instability (whose importance in magnetron work is well understood) is related to the Kelvin-Helmholtz instability in fluid mechanics; 2) A new mode involving spontaneous coherent radiation into space as a result of bunching. This effect can be described as the "flexible antenna instability." Both these instabilities are considered for low density electron beams (that is, $\omega_p \ll \omega_c$). Two experiments are discussed. The object of the first is to produce a stable electron plasma in a simple geometry. The second is designed to test the practicability of the inductive charging scheme. A brief review of selected applications of the electron plasma is also given; these include space radiation shielding and certain high voltage laboratory devices. (auth)

41864 (ORNL-P-1244) ENGINEERING ASPECTS OF THE PRODUCTION OF EXCITED STATE H_2^+ FOR LORENTZ DISSOCIATION IN DCX-1. Edwards, R. S. (Oak Ridge National Lab., Tenn.). [1963]. Contract W-7405-eng-26. 10p. (CONF-650512-3). Dep. mn; CFSTI $1.00 cy, $0.50 mn.

From Symposium on Engineering Problems of Controlled Thermonuclear Research, Livermore, Calif.

DCX-1 is a steady state thermonuclear experiment. The experiment accumulates a plasma by means of high energy injection of diatomic ions into a magnetic mirror geometry. Some of the techniques and hardware used to produce this plasma, particularly those concerned with beam injection, are described. (M.O.W.)

41865 (TID-22050) NONLINEAR MODE INTERACTIONS IN UNIVERSAL PLASMA INSTABILITIES. Lashinsky, Herbert (Maryland Univ., College Park. Inst. for Fluid Dynamics and Applied Mathematics). May 1965. Contract AT(30-1)-2464. 10p. (BN-399). Dep. mn; CFSTI $1.00 cy, $0.50 mn.

The nonlinear mode interactions in a two mode system with incommensurate (i.e., not related by integer ratios) mode frequencies are investigated. (M.O.W.)

41866 (UCRL-12052) NOTE ON ELECTROSTATIC INSTABILITIES IN A PLASMA WITH ANISOTROPIC VELOCITY DISTRIBUTION. Shima, Yaakov; Hall, Laurence S. (Lawrence Radiation Lab., Univ. of California, Livermore). Aug. 4, 1964. Contract W-7405-eng-48. 7p. Dep. mn; CFSTI $1.00 cy, $0.50 mn.

An attempt is made to delimit as much as possible the location of possibly unstable roots to the dispersion equation for electrostatic waves in an infinite plasma situated in a constant magnetic field. (M.O.W.)

41867 (UCRL-12455-T) PLASMA CONFINEMENT PROPERTIES OF RELATIVISTIC ELECTRON COILS. Christofilos, N. (Lawrence Radiation Lab., Univ. of California, Livermore). July 6, 1965. Contract W-7405-eng-48. 11p. Dep. mn; CFSTI, $1.00 cy, $0.50 mn.

The most important property of the relativistic electron coil, which is known as the E-layer, created in the Astron, is the magnetic field configuration which is established by the combination of the external vacuum field and the self-field of the E-layer. The loading factor (ratio of the current/cm of the E-layer to the ampere turns/cm of the external field) of the E-layer required to provide plasma stability is examined. (M.O.W.)

41868 ON THE USE OF ELECTROSTATIC PROBES IN THE DIAGNOSTIC OF A PLASMA COLUMN. Marchesini, G. (Universita, Padua). Alta Freq., 33: 167-75 (Mar. 1964). (In Italian).

The main properties of the plasma column of a glow discharge and the principles of classical electrostatic probe theory are recalled to indicate the type of information available by this technique. The remarkable usefulness of electronic devices for fast recording of probe characteristics is outlined. The electronic circuits realized are described, and the results obtained are discussed and compared with those obtained analytically by the use of the classical Langmuir theory and the Schottky and modified Schottky theories. (auth)

41869 EFFECT OF TRANSPORT COEFFICIENTS ON THE DAMPING OF HYDROMAGNETIC WAVES. Malik, F. B.; Trehan, S. K. (Univ. of Delhi). Ann. Phys. (N.Y.), 34: 1-22(Aug. 1965).

The general theory of the propagation of hydromagnetic waves in a magnetized plasma is presented taking into account the finite ion-Larmor radius, the electrical and thermal conductivities, and the thermoelectric coefficients of the plasma. The dispersion relation is obtained as the exact solution of the linearized macroscopic moment equations of the Boltzmann equation derived by Marshall. The dispersion relation is solved in the special cases when the wave propagation is along the static magnetic field or transverse to it. The damping coefficient of the waves is given. It is found that in the case of propagation along the field lines, the damping of the acoustic mode is due to the electrical conductivity, the thermal conductivity and the thermoelectric coefficients while the damping of hydromagnetic mode is due to the electrical conductivity. In the case of propagation transverse to the field lines all the transport coefficients contribute to the damping of the hydromagnetic waves. (auth)

41870 KINETIC EQUATIONS AND MOMENTUM EQUATIONS FOR INHOMOGENEOUS PLASMAS. Ebeling, W. (Universitaet, Rostock, Ger.). Ann. Physik (7), 14: 404-6(1964). (In German)

By generalization of the results of an earlier work of Klimontowitsch and Ebeling (Wiss. Z. Univ. Rostock (Math.-Nat.), 11: 355(1962)) a general form of the kinetic equation for completely ionized slightly inhomogenous plasmas and a closed system of equations for moments of any order with respect to the Hermitic polynomial were derived. (tr-auth)

41871 DEVELOPMENT AND CONSTRUCTION OF ION SOURCES OF THE DUOPLASMATRON TYPE. Vincent, G.; Warnecke, R. J. Ann. Radioelec., 20: 101-14(Apr. 1965). (In French)

After a brief review of the operating principle of the duoplasmatron, two models of this type of ion source that are capable of producing in continuous or pulsed operation beams of high intensity (a few hundred milliamp) and of high energy (several tens of kev) are described.

Experimental results are given and are compared with results obtained elsewhere. (D.C.W.)

41872 THEORETICAL AND EXPERIMENTAL STUDY OF HOLLOW CESIUM PLASMA STRUCTURES, SOURCES OF IONS OR ELECTRONS. Le Bihan, R.; Maugis, D. Ann. Radioelec., 20: 126-58(Apr. 1965). (In French).

When a cesium vapor is introduced into a metal enclosure at a high temperature, the vapor is thermally ionized according to Saha's law, and a plasma is formed from which either electrons or ions can be extracted. Saha's law, which is demonstrated starting from electrochemical potentials, is considered, as well as the Saha-Langmuir law. The plasma and its connection to the metal by an ion or electron sheath are represented in a manner taken from the theory of semiconductors by identifying the electron electrochemical potential with the Fermi level. It is shown that the densities of the electron or ion current extracted depend on the relative dimensions of the sheaths and the enclosure orifice, this being confirmed by experiment and allowing conclusions to be drawn for ion or electron sources. The analogy with the case of hollow cathodes containing only electrons is demonstrated. (D.C.W.)

41873 SPECTRAL LINE INTENSITY DIFFERENCES BETWEEN ARC IN A TUBE AND A FREE-BURNING ARC. Vukanovic, M. V.; Georgijevic, M. V. Bull. Boris Kidrich Inst. Nucl. Sci., 16: 23-31(Jan. 1965).

An arc burning in a tube may give considerably lower line intensities than a free burning arc. This effect is greater the smaller the mass of the element and the higher the degree of ionization. (auth)

41874 THE OHM LAW FOR A PARTIALLY IONIZED PLASMA. Dolique, Jean-Michel (Faculte des Sciences Grenoble, France and E. I. E., Grenoble, France). Compt. Rend., 260: 3681-4(May 3, 1965). (In French).

Beginning with rigorous motion equations for partial fluids (electronic, ionic, and neutral) and for the total fluid, an expression for the Ohm law in partially ionized plasmas is established, which generalized the Cowling expression to the cases where: (a) the ionization is very strong; (b) the ions are multiply charged; (c) the mass of the ions differs significantly from that of the neutral particles (case of the ions coming from a "seed"); (d) the frequency of ion-neutral particle collision is not small owing to the frequency of electron-neutral particle collision (because of the Ramsauer effect for example); (e) the viscosity is not negligible; (f) the ion temperature is not small owing to the electron temperature; and (g) the propagation terms are not negligible. The range of validity of the Cowling formula is defined and also the significance of the collision frequencies that it contains: it is seen that it is a question of macroscopic frequencies. This point is important since the progress made in the measurement of the electric conductivity of gases has led some authors to go back from this conductivity to collision frequencies (and, from there, to cross sections), with the defining aid of the Cowling theoretical expression or equivalent expressions. (tr-auth)

41875 THE HIGH-FREQUENCY ARGON TORCH AT PRESSURES BELOW 1 ATM. Bohatiel, Teodor (Universite, Bucharest). Compt. Rend., 260: 4954-6(May 10, 1965). (In French).

The principal phenomena that maintain the high frequency discharge in an Ar torch are established. The experimental results are similar to those observed in air. As in air, the thermal excitation alone can not explain the great increase of the volume of the torch when the pressure of the Ar decreases. The principal phenomenon is electric excitation. At low pressures the mean free paths of the electrons and ions increase and so the absorbed energy of the electric field between two consecutive shocks increases. The appearance of brilliant plasmoids can be explained, not by thermal excitation, but by propagation phenomena in the ionized gases. (J.S.R.)

41876 DETECTION OF CENTIMETER WAVES IN A GAS DISCHARGE PLASMA. Sobol', G. A. Izv. Vysshikh Uchebn. Zavedenii, Radiofiz., 8: 420-2(1965).

The probe characteristic $I_p = f_1(V_p)$ and the detector characteristic $I_p = f_2(V_p)$ of a glow discharge in a plasma were measured simultaneously at 50, 10^9, and 10^{10} cps. The results are plotted. Comparison of the three detector characteristics under the same discharge conditions indicates that they are inherent in the plasma over a wide frequency range range. Thus a plasma detector of unlimited power can be constructed for frequencies ranging from 20 to 10^{10} cps. Tuning to the desired frequency can be accomplished by varying the probe voltage V_p of the appropriate anode. It is asserted that the detector effect is determined chiefly by processes occurring at the cathode when the latter is irradiated by a shf field. The following experimental facts serve to support this assertion. The detector effect is observed only when the cathode region of the discharge is irradiated by the shf field and is completely absent when other discharge regions are irradiated. The detector effect is not observed in air arc discharge. During irradiation of the cathode lead, I_d maximum is observed when antinode E~ of the shf field is present at the cathode. The size of the detector effect depends on both the cathode material and the type of gas in the discharge tube, but is independent of the anode and probe materials. (ATD)

41877 DISTRIBUTION FUNCTION OF THE ELECTRON VELOCITIES IN A CESIUM PLASMA IN OSCILLATION REGIME. Moreau, Jean-Baptiste. Compt. Rend., 260: 6314-17(June 14, 1965). (In French).

The distribution function of the electron velocities in a low pressure Cs plasma in the oscillation regime between 2.8 and 0 v was analyzed on the basis of the Medicus graphic method. The results show that the ionic oscillations observed are created by an interaction of the plasma with a beam of electrons accelerated by the sheath that borders the emitter. (J.S.R.)

41878 MEASUREMENTS OF THE CHARACTERISTICS OF A METALLIC PLASMA PULSE. Consoli, Terenzio; Gormezano, Claude; Slama, Lucien (CEN, Saclay). Compt. Rend., 261: 86-9(July 5, 1965). (In French).

The experimental determination of the density, temperature, and expansion speed of a plasma pulse produced in less than 10^{-7} sec very reproducibly by the collision of a ruby laser beam on an Al foil is described. (tr-auth)

41879 MIKHAILOVSKY'S FINITE LARMOR RADIUS EFFECTS AND GRAVITATIONAL INSTABILITY OF PLASMA, TREATED BY METHOD OF MOMENTS OF BOLTZMANN-VLASOV EQUATION. Sedlacek, Z. (Inst. of Plasma Physics, Prague). Czech. J. Phys., 15: 494-505(1965).

The effect of the stabilization of the gravitational instability of a hot rarefied plasma by the finite Larmor radius, established previously with the aid of the collisionless Boltzmann-Vlasov equation, was later derived from the magneto-hydrodynamic equations modified by terms describing the magnetic "viscosity" of the plasma. It is shown that even the effect of the disappearance of this stabilization at very low plasma density, as found by Mikhailovsky, may be derived from the two-fluid macroscopic equations (the method of moments of the Boltzmann-Vlasov equation) using a very simple iterative procedure in which directly figures the so-called "effective" electric field of perturbation employed for physical interpretation of the effects of the finite Larmor radius. (auth)

41880 CONTRIBUTION TO STUDY OF SPLITTING OF PLASMA SHOCK WAVES IN ACCELERATING TUBE. Sobra, K. (Inst. of Solid State Physics, Prague); Kalivoda, L'.; Hanitz, F. Czech. J. Phys., 15: 534-5(1965).

When the acceleration of plasmatic clusters in a Marshall jet was studied, it was found that two clusters leave its mouth with different velocities. A similar effect was observed in the study of the acceleration of a shock wave between straight conductors. A time-continuous recording of the motion of a shock wave of plasma is shown. In seeking common features between the Marshall jet and the tube with straight conductors, it was found that the magnetic field of each is nonuniform. It is this nonuniformity which is thought to have an analogous effect in both cases. (J.F.P.)

41881 PLASMA FUSION. Yoshimura, Hisamitsu; Saito, Masaji (Nippon Univ., Tokyo). Genshiryoku Kogyo, 11: No. 4, 56-60(Apr. 1965). (In Japanese)

Since the historic prediction of the potential use of plasma fusion made at the 1955 Geneva Conference, there has been great interest in this field of atomic research. The early history of effort in this field in Japan was limited to studying foreign work. In 1958 a society was formally organized which began publication of a monthly journal on "Plasma Fusion Research." A plasma laboratory was established at Nagoya in 1961 under Director Fushimi. Work along this line has been severely handicapped by the high cost of equipment, and the funds initially granted for this effort are expected to be completely spent by the end of this year. As a result, concrete results are rather scarce. Progress is reported on a sealed-in, high-temperature plasma generator. Plans for testing this plasma, following oscillation phenomena, studying plasma radiation, and diagnosing plasma are described. (TTT)

41882 EMISSION OF EXTRAORDINARY WAVE BY A CURRENT IN A LAYER OF MAGNETOACTIVE PLASMA. Samokhin, M. V. Izv. Vysshikh Uchebn. Zavedenii, Radiofiz., 8: 251-9(1965). (In Russian)

The problem is considered of the plane-layer radiation of a magnetoactive plasma with current. The magnetic field is assumed to be perpendicular to the layer boundaries, and the change of the magnetic field and plasma density is taken to be small. The refractive index for an extraordinary wave has the pole in the point where the radiation frequency coincides with the electron gyrofrequency so the wave equation reduces to the nonhomogeneous degenerated hypergeometric equation for which the solution and its asymptotic expansion have been found. A plot is given of the electric and magnetic field distribution in a layer. (auth)

41883 SPECTROSCOPIC TECHNIQUE FOR PROBING AN IONIZED GAS. Winocur, Joseph; Pyle, Robert V. (Univ. of California, Berkeley). J. Appl. Phys., 36: 2740-4(Sept. 1965). (UCRL-11532).

Ionized strontium is studied by the method of resonant absorption of optical radiation. Because of an accidental frequency overlap, normal rubidium can be used in a lamp as the source of resonant light. Spectral profiles of absorption were made with a scanning Fabry-Perot interferometer. The $5s_{\frac{1}{2}}-6p_{\frac{1}{2}}$ line of Rb and the $5s_{\frac{1}{2}}-5p_{\frac{1}{2}}$ line of Sr^+ are found to differ by 0.014 Å. Optical and Langmuir probe measurements of density compare favorably. Ion temperatures in a steady-state and a decaying plasma were determined from the Doppler width. Two different sources of ionized strontium plasma are described. Negative results were obtained in an attempt to optically pump strontium ions in a plasma. (auth)

41884 ABSOLUTE INSTABILITIES OF PERPENDICULARLY PROPAGATING CYCLOTRON HARMONIC PLASMA WAVES. Crawford, F. W.; Tataronis, J. A. (Stanford Univ., Calif.). J. Appl. Phys., 36: 2930-4(Sept. 1965).

Computed dispersion characteristics are presented for perpendicularly progagating electron cyclotron harmonic waves in an infinite plasma having a delta-function transverse electron velocity distribution and an arbitrary longitudinal velocity distribution. It is shown that in general the propagation occurs in passbands centered on the cyclotron harmonic frequencies and that a given mode can carry positive or negative r-f energy depending on the frequency and wavenumber. This suggests the possibility of growing waves in finite plasmas due to interaction with slow wave circuits. Even in an infinite plasma, as the ratio of plasma frequency to cyclotron frequency increases, modes in successive passbands couple to each other, leading to wave growth in time. This represents absolute instability of a type which may be closely related to effects observed in some thermonuclear fusion studies and other laboratory plasmas. There may also be important applications of these modes to the construction of practical microwave oscillators and amplifiers. (auth)

41885 PARTICLE ORBITS IN A HELIOTRON MAGNETIC FIELD. Amano, Tsuneo; Murakami, Masanori; Outi, Akizi (Kyoto Univ.). J. Phys. Soc. Japan, 20: 1239-50(July 1965).

The motion of individual charged particles in a Heliotron magnetic field, which is an axialsymmetrically corrugated field with zero-field points, is investigated. The effective potential is introduced to describe the motion in the (r,z) plane, and the conditions for the trapping of the particle inside the neutral line (the line of force passing through the zero-field points) are obtained in terms of the particle energy and canonical angular momentum. The particle orbits are calculated numerically on an electronic computer. The adiabaticity of the magnetic moment of the particle is examined from the calculations, and three classes of orbits: adiabatic, moderately adiabatic and non-adiabatic orbits are distinguished. The azimuthal drift and the longitudinal invariant of the particle are also examined. (auth)

41886 UNIFIED THEORY OF RELAXATIONS IN PLASMAS. V. FORMULATION FROM LIOUVILLE EQUATION. Aono, Osamu (Tokyo Univ.). J. Phys. Soc. Japan, 20: 1250-4(July 1965).

From the Liouville equation a kinetic equation is derived which is exact in the sense that exact numerical factors can be given in the arguments of the Coulomb logarithms. The kinetic equation is written in the form of the connection formula. The connection formula is generalized so as to make it possible to treat rapidly varying or inhomogeneous plasmas in external fields. (auth)

41887 THE INITIAL-PRESSURE DEPENDENCE OF THE INSTABILITIES IN A LOW B THETA PINCH PLASMA. Takeda, Yasumasa; Shiina, Shoichi (Nihon Univ., Tokyo). J. Phys. Soc. Japan, 20: 1275(July 1965).

The behavior of plasma was observed by high speed framing photographs taken from the axial direction. Helium gas was used in the pressure range of 25 to 100 mtorr. The maximum electron temperature in the earlier half cycles rose from 30 to 50 ev with lowering of the initial pressure from 100 to 25 mtorr. The corresponding electron density was expected to be of the order of 10^{15} to 10^{16}/cc. The Rayleigh-Taylor instability occurred in the radial oscillation state immediately after the maximum contraction. The instability was apparently weak at the lower initial pressure. At higher initial pressures the number of flutes was larger than 4 and then the plasma showed an irregular and complicated deformation and struck the wall. Noting that the plasma density may decrease and the ion temperature is expected to rise with lowering the initial pressure, it is concluded that the observed initial pressure dependence of the instability may be explained by viscous damping. (J.F.P.)

41888 MOVING STRIATION OF PLASMA IN A LONGITUDINAL MAGNETIC FIELD. Yatsui, Kiyoshi; Ohji, Takayoshi; Inuishi, Yoshio (Osaka Univ.). J. Phys. Soc. Japan, 20: 1281(July 1965).

Effects of longitudinal magnetic field on a moving striation were studied experimentally in the range of $0 \sim 2200$ gauss. The discharge was produced in a cylindrical tube with an inside diameter of 22mm and interelectrode distance of 270mm, filled with argon at 0.3 torr. A characteristic of moving striation is given as a function of applied longitudinal magnetic field, such as frequency measured by probes and phototransistor, wavelength by two axial phototransistors, and the resultant phase velocity calculated from the product of frequency and wavelength. It is concluded that generation of a moving striation is caused in the cathode part and that longitudinal magnetic field applied to the cathode end of the positive column is important for an analysis of this oscillation. (J.F.P.)

41889 THE GENERAL CONSERVATION LAWS IN A DILUTE PLASMA. Ong, R. S. B. (Univ. of Michigan, Ann Arbor). Nuovo Cimento (10), 38: 1835-48(Aug. 16, 1965).

The macroscopic conservation equations for a dilute, fully ionized plasma are derived directly from the B-B-G-K-Y hierarchy instead of from the kinetic equation involving only the single-particle distribution function. In this way it is possible to exhibit clearly the role which the two-par-

ticle correlation function plays in the various macroscopic quantities. (auth)

41890 SATURATION AND SHORT-TIME BEHAVIOUR OF UNSTABLE ION WAVES. Iannuzzi, M.; Righetti, G. B. (EURATOM-C.N.E.N., Frascati, Italy). Nuovo Cimento (10), 38: 1931-4(Aug. 16, 1965).

An axisymmetric cavity is used to study standing waves excited by collective effects in collisionless alkali plasma in thermal equilibrium at 2300°K. One electrode of the cavity is comprised by an axial wire, and the other is a cylindrical foil. The amplitudes of the current oscillations are studied as a function of interelectrode potential. The short-time behavior of these oscillations is also studied. (T.F.H.)

41891 EXPERIMENTAL DETERMINATION OF THE EFFECTIVE PROBABILITY OF PHOTON EMISSION BY PLASMA ATOMS. Uvarov, F. A.; Fabrikant, V. A. Opt. Spectry. (USSR)(English Transl.), 18: 323-7(Apr. 1965). Translated from Optika i Spektroskopiya, 18: 562-70 (Apr. 1965).

Rozhdestvenskii's hook method was used to measure the distribution of excited atoms over the cross section of a low-pressure discharge in mercury vapor and in a mercury vapor–argon mixture. The power of the 2537 Å resonance radiation was measured at the same time. The data thus obtained were used to determine A_{eff}, the effective probability of photon emission by plasma atoms. Addition of argon was found to increase A_{eff} by a factor of 1.5–2.5. This phenomenon may be explained by the broadening of the 2537 Å line due to collisions with argon atoms, as well as by redistribution of the radiating atoms over the cross section of the discharge. (auth)

41892 COLLISIONLESS ION-WAVE PROPAGATION AND THE DETERMINATION OF THE COMPRESSION COEFFICIENT OF PLASMA ELECTRONS. Alexeff, I.; Jones, W. D. (Oak Ridge National Lab., Tenn.). Phys. Rev. Letters, 15: 286-8(Aug. 16, 1965).

The adiabatic compression coefficient of the electron gas was investigated, since the subtleties of collisionless waves are such as to make such a study desirable. The plasma is formed under conditions such that it is collisionless, no external magnetic field is present, the effects of the walls are negligible, and there is negligible streaming of electrons relative to ions. The experimental results are listed and show that under the given conditions of operation, the value of the adiabatic compression coefficient best corresponds to 1. Thus the ion waves appear to propagate with collisionless, isothermal compression taking place in the electron gas. (J.F.P.)

41893 NEW INSTABILITIES DUE TO HALL EFFECT. Hosking, R. J. (The Univ. of Western Ontario, London). Phys. Rev. Letters, 15: 344-5(Aug. 23, 1965).

A simple situation is considered in which it appears that the Hall effect produces an aperiodic instability in a wave-number band which was previously stable. The situation chosen is similar to that where an infinitely conducting plasma occupies the half-space and is supported against gravity by magnetic pressure due to a jump in field strength at the plasma boundary. It is assumed that the plasma exhibits a significant Hall effect and that the seed field is uniform throughout all space. It is emphasized that resistive modes are precluded and that the viscosity-like finite gyroradius term in the equation of motion was neglected. (J.F.P.)

41894 HYPERSONIC BODY MOTION THROUGH RAREFIED PLASMA. Gurevich, A. V.; Pitayevsky, L. P. (Academy of Sciences, Moscow). Phys. Rev. Letters, 15: 346-8(Aug. 23, 1965).

The exact solution of the problem of rarefied flow near a body is considered in the case when the body size is much less than the electron mean free path, so the plasma can be considered collisionless. Moreover the flow velocity is supposed to be much greater than the ion thermal velocity, and the Debye radius much less than a typical body size. It is found that the agreement obtained exceeds the accuracy of both experiment and theory. (J.F.P.)

41895 SPECTRUM OF LOW-β PLASMA TURBULENCE. Chen, Francis F. (Princeton Univ., N. J.). Phys. Rev. Letters, 15: 381-3(Aug. 30, 1965).

Another experimental observation is reported on the theory of drift waves. This observation is the universality of the phenomenon in order to explain the shape of the frequency spectrum. In all cases observed anomalous transport was present. The universality of the spectrum under such diverse conditions suggests that the final turbulent state is independent of the excitation mechanism, provided that there is sufficient time for the instability involved to reach its limiting amplitude. It is believed that drift waves are the sole cause of anomalous transport in dense, low-β plasmas. This hypothesis is made along with the further one that the turbulent state is independent of the excitation mechanism. Thus to describe the turbulent state the universal instabilities may be eliminated and only gravitational ones considered. (J.F.P.)

41896 MOTION OF PLASMA AND LIFETIMES OF ENERGETIC IONS IN A TOROIDAL OCTUPOLE MAGNETIC FIELD. Kerst, D. W.; Dory, R. A.; Wilson, W. E.; Meade, D. M.; Erickson, C. W. (Univ. of Wisconsin, Madison). Phys. Rev. Letters, 15: 396-8(Aug. 30, 1965).

Simultaneous observations of the flow of plasma at numerous points in an octupole magnetic field revealed processes responsible for the injection and trapping of a collimated plasma stream in the system of closed magnetic field lines. Observations were made of the guiding of the plasma clouds around the toroid in both directions by the steering effect of the generated octupole electric field, and of phenomena occurring at the collision of the plasma clouds passing in opposite directions around the toroid, and the subsequent containment with no catastrophic depletion of electrons or ions to suggest instability of the plasma. These observations were made in plasmas of density $n = 10^{12}$/cc after the plasma had filled the remote parts of the confinement region. The electron temperature was 10 ev throughout the duration of the magnetic field, and the ion or proton-energy distribution extended from 50 to ~300 ev. (J.F.P.)

41897 GENERAL CRITERION FOR ELECTROSTATIC PLASMA INSTABILITIES WITH UNIFORM MAGNETIC FIELD. McCune, James E. (Massachusetts Inst. of Tech., Cambridge). Phys. Rev. Letters, 15: 398-401 (Aug. 30, 1965).

It is pointed out that the microscopic stability of a uniform plasma without magnetic field is completely determined by the properties of the projection of the distribution functions of the various species of the undisturbed plasma. This condition was previously derived in terms of a Nyquist-diagram technique in complex space. It is shown that a similar general criterion can be given for electrostatic (longitudinal) plasma oscillations in the presence of a uniform magnetic field. (J.F.P.)

41898 TECHNIQUE FOR MEASURING THE ABSORPTION COEFFICIENT OF A PLASMA. Braun, W. G. (Aerospace Research Labs., Wright-Patterson AFB, Ohio). Rev. Sci. Instr., 36: 802-5(June 1965).

Instrumentation for determining the absorption coefficient in a plasma in the optical wavelength region has been developed for the study of a hydrogen arc discharge. The arc column is scanned with a beam of its own radiation emitted from the central zone, which usually displays the highest brightness. The accuracy of the attenuation measurements near the edges of the plasma column is significantly increased over the accuracy obtainable with the double-path method. The described instrumentation produces a lateral scan of the plasma in digital form suitable for the computation of the spatial distribution of the absorption coefficient. (auth)

41899 PROTON BEAM TECHNIQUE FOR MEASURING THE ION DENSITY IN A PLASMA. Duclos, Donald P. (Electro-Optical Systems, Inc., Pasadena, Calif.). Rev. Sci. Instr., 36: 806-9(June 1965).

A technique is described for obtaining localized measurements of the ion density in a plasma that is not affected by the presence of a magnetic field or the absence of thermodynamic equilibrium. The technique consists basically of exciting the ions with a proton beam and relating the measured absolute intensity of certain spectral lines to the ion density. Three requirements are discussed which must be satisfied in order to apply the method to a particular gas. The technique appears to be well suited to measuring the density of helium ions. The possible sources of error are examined and, for helium plasmas, none of the errors are large provided that the gas pressure is less than 1 mm Hg and the temperature is over 10,000°K. A preliminary experiment is described. (auth)

41900 PLASMA. Seikel, George R. (Lewis Research Center, Cleveland). Space/Aeron., 43: No. 4, 40-5(Apr. 1965).

A general treatment is presented on the characteristics and technological applications of natural and man-made plasmas. A diagram for plasmas varying over a wide range of temperatures and pressures is presented, which shows the region in which gases of all elements change to plasma if their volume is large enough, the area of limits of physical containment of plasma, and the magnetic containment region. Plasma applications are tabulated along with the corresponding principle properties used, the mechanism or description, and the development status. (L.B.S.)

41901 ON THE DISPLACEMENT OF RESONANCE FREQUENCY OF THE INTERACTION OF A PLASMOID WITH A SPATIALLY MODULATED MAGNETIC FIELD. Marinin, V. G. Ukr. Fiz. Zh., 10: 343-6(Jan. 1965). (In Ukrainian).

It was noted earlier that when a low-density plasmoid is injected into a spatially modulated magnetic field, an energy redistribution occurs between the longitudinal and transverse directions, at a certain ratio between the velocity of the plasmoid and the ion cyclotron frequency. Further studies revealed that the value of the magnetic field at which the redistribution takes place is by 20 to 25% lower than the value of the magnetic field resonance calculated for a single particle. In order to resolve this discrepancy, the motion of the plasmoid in an axially symmetric field possessing specific field components was analyzed. The calculations indicated that the shift of the magnetic field at which the energy of the plasmoid was redistributed with respect of the magnetic field of the charged particles generated electric fields in a direction perpendicular to that of the magnetic field. Similar shifts of the electron resonance frequency as a function of the spatially modulated field in the presence of a perpendicular electromagnetic field have been observed previously. (TTT)

41902 ON THE EXCITATION OF WAVES IN AN ORGANIC PLASMA BY MODULATED CURRENT. Kondratenko, A. N. Ukr. Fiz. Zh., 10: 346-8(Jan. 1965). (In Ukrainian).

In previous studies on the excitation of waves by modulated currents, the plasma was assumed to be infinite, isothermic, and linear. It was deemed to be of interest to extend these studies by examining mathematically the excitation of waves in a confined, nonlinear plasma. The results indicated that for both low- and high-frequency oscillations, the amplitude of the field of the excited waves will be nonlinear. (TTT)

41903 INVESTIGATION OF THE H_{11} WAVE PASSAGE THROUGH BOUNDED PLASMA IN A CIRCULAR WAVEGUIDE. Gorokhov, Yu. V.; Modenov, V. P.; Prokofeva, S. V. Vestn. Mosk. Univ., Ser. III: Fiz. Astron., No. 1, 85-6(Jan.-Feb. 1965). (In Russian).

The dependence of the transmission coefficient T for a TE_{11} wave in a circular waveguide on the properties of gas-discharge plasma occupying a finite region of the waveguide length was investigated. The waveguide was of the conventional type; the plasma was homogeneous and took the form of a cylinder with a diameter close to that of the waveguide. The neon plasma was produced by uhf discharge of a pulse magnetron generator (50 kw). To keep plasma losses to a minimum, the measurements were carried out in a state of deionization; i.e., the temperature of the electrons was practically room temperature. Deionization time was 10^{-3} to 10^{-4} sec. The dependence of T^2 on electron concentration was observed at 9400 Mc. The resulting curves possessed maxima and minima whose positions were determined by the strength of the applied magnetic field and electron concentration in the plasma. The dependence of T^2 on the magnetic-field strength for various values of electron concentration is shown. (ATD)

41904 INVESTIGATIONS ON AN INVERSE PINCH. Groenig, H. (Technische Hochschule, Aachen). Z. Naturforsch., 20a: 606-10(Apr. 1965). (In German).

It was experimentally shown that the inverse pinch, because of its symmetrical properties, is very well suited for the production of cylindrical collision waves whose fronts are well defined and reproducible. A Kerr cell camera and a light conductor system was used for the measurement of the luminous front and a piezoelectric pressure probe was used for the study of the collision front. The results show that the luminous front and the collision waves agree and that propagation of the collision wave can be described well using a snow plow model. (tr-auth)

41905 STRUCTURE OF THE BOUNDARY LAYER BETWEEN RAREFIED PLASMA AND A MAGNETIC FIELD. Sigov, Yu. S. Zh. Prikl. Mekhan. i Tekhn. Fiz., No. 2, 15-22(Mar.-Apr. 1965). (In Russian).

The structure of a plane boundary layer between a magnetic field and a collisionless plasma is investigated under steady-state conditions. The problem is considered relativistically invariant with governing parameters $L = \sqrt{Rr}$ and the Debye radius (R,r correspond to the ion and electron Larmor radii). It is also assumed that upon reflection from a magnetic wall most of the kinetic energy is transmitted to the electrons. The plasma is assumed to be neutral with all physical magnitudes a function of the x-coordinate only. (ATD)

41906 ON PLASMA POLARIZATION IN AN ELECTRIC FIELD. Golovanivskii, K. S.; Pogosyan, V. A. Zh. Prikl. Mekhan. i Tekhn. Fiz., No. 2, 23-9(Mar.-Apr. 1965). (In Russian).

The electrostatic polarization of a plasma in an external electric field is investigated. A plane layer of homogeneous, two-component, partially ionized plasma of thickness d, bounded by impermeable dielectric walls at $x = o$ and $x = d$, is considered. The results show that the sudden application of an electric field to an otherwise quiescent plasma generates very complex motions between the ions and the electrons. It is also shown that the ratio n_p/n_e (density distributions of ions and electrons after application of the electric field) is of the order T_e/T_p for polarized plasma. (D.C.W.)

41907 ELECTRON OSCILLATIONS IN A PLASMA. Zaitsev, A. A.; Savchenko, I. A. Zh. Prikl. Mekhan. i Tekhn. Fiz., No. 2, 30-4(Mar.-Apr. 1965). (In Russian).

The conditions under which periodicity occurs in the spatial distribution of the intensity of plasma oscillations excited by an electron beam were studied experimentally. It was found that periodicity occurs in the presence of a boundary which reflects primary or emits secondary electrons to form a reflected wave. In the absence of such a boundary, the oscillations are amplified in accordance with the theory of convective plasma instability. The experiments were conducted with a plasma produced in several types of argon-filled discharge tubes. The role of the reflected wave in the formation of periodicity was considered first. The distribution of oscillation intensity along the discharge axis was determined for two different cases in which the reflector plane was perpendicular to the direction of the primary beam, the reflector formed an angle of 45° with the direction of the primary beam. In the first case, the intensity distribution had a distinct periodic structure, while there was none in the second. The distance from the cathode to the zone of maximum oscillation intensity, together with the growth factor, were next determined. Finally, the relation between the intensity of oscillations at a fixed frequency, based on data from elec-

tron concentration measurements with a Langmuir probe, showed that the maximum oscillation intensity is reached at a frequency approaching the frequency of the plasma electron oscillations. The typical spatial distribution of oscillation intensity is shown for a case in which the oscillations in the beam are caused by plasma-beam interactions. (ATD)

41908 ON PLASMOID STRUCTURE IN AN ELECTROMAGNETIC ACCELERATOR. Grigor'ev, V. N. Zh. Prikl. Mekhan. i Tekhn. Fiz., No. 2, 35-40(Mar.-Apr. 1965). (In Russian).

A detailed experimental study was made of the structure and acceleration of a high-density plasma cluster in an electromagnetic field. The apparatus consists of a pair of copper-plate electrodes 2 cm apart, connected to a 36-μf capacitor bank with a 4.5-kv discharge voltage. The tube pressure varied between 0.1 to 20 μ Hg. The discharge was measured by means of high-speed photorecording equipment. The records show that during the first half-period of current discharge the plasmoid consists of sharp layers moving at a speed of 6×10^6cm/sec. The speed and the diameter of the plasma clusters are found to be independent of the pressure and the type of gas used. The ion velocities were measured from Doppler shifts, using a spectrograph with 6-12 Å/mm dispersion in the interval 3900-4500 Å. The plasma temperature was measured from Si-ion line intensities and the known electron densities. Its value was $3.4 \times 10^{4\circ}$K. The plasma density was determined from Stark-broadening measurements, with a value of 2.5×10^{17} cm^{-3}. These results indicate that, upon acceleration, the plasma splits into layers and undergoes a pinch, as substantiated by the pinch parameter formula $N = (I^2/2c^2\pi r^2 kT) = 6.10^{17}$ cm^{-3}. From the expression for the plasma pinch radius $r_s = k(c^2/4\pi\sigma V)$, the value for r is calculated to be 8×10^{-2} cm. The pinch is shown to contain the materials from the glass wall (Si and O ions). (ATD)

41909 INVESTIGATION OF A LOW-TEMPERATURE PLASMA IN A LOW-VOLTAGE ARC. Lebedev, M. A. Zh. Prikl. Mekhan. i Tekhn. Fiz., No. 2, 41-6(Mar.-Apr. 1965). (In Russian).

An investigation was made of the electron temperature and distribution in a cesium plasma of a low-voltage arc discharge at pressures of 5×10^{-3} to 5×10^{-1} mm Hg and values of the discharge current of 1 to 3 amp. The double probe method was used for measurements at six points along the axis of the 9.8 mm interelectrode spacing. The temperature of the cathode and the anode was maintained at 700°C in all the experiments. At a discharge current value $I_d = 1.0$ amp, the electron temperature was found to be inversely proportional to pressure; it was highest at the cathode, then slowly decreased in the direction of the anode. A 25 to 30% energy loss within the gap was attributed to inelastic collisions with atoms and the braking effect of the electric field. The ignition potential necessary to sustain the discharge current at 1.0 amp decreased rapidly with increasing pressure, attained its minimum at p = 0.55 mm Hg, and then slowly increased. At low cesium pressures, an increase in the discharge current from 1.0 to 2.0 amp brought about an increase of T_e from 2400 to 3650°K at a distance of 0.7 mm from the cathode. If the pressure was increased along with the discharge current, the corresponding increase of T_e slowed down. The maximum dependence of the electron concentration on pressure in all experiments was at a distance of 2 mm from the cathode; pressure has virtually no effect on concentration in the interval from 4 to 9 mm. It is concluded that ions are formed in the interelectrode spacing by collisions of cesium atoms in excited states (that the mechanism of ion formation has a step-like character). (ATD)

41910 VISCOSITY OF PARTIALLY IONIZED TWO-TEMPERATURE PLASMA. Bisnovatyi-Kogan, G. S. Zh. Prikl. Mekhan. i Tekhn. Fiz., No. 2, 74-8(Mar.-Apr. 1965). (In Russian).

An expression is derived for the viscosity of a partially ionized, two-temperature plasma. (D.C.W.)

41911 EXCITATION OF STRONG COLLISIONLESS SHOCK WAVES IN PLASMA. Kurtmullaev, R. Kh.; Malinovskii, V. K.; Nesterikhin, Yu. Ye.; Ponomarenko, A. G. Zh. Prikl. Mekhan. i Tekhn. Fiz., No. 2, 79-83 (Mar.-Apr. 1965). (In Russian).

Experimental results were obtained on collisionless shock-wave excitation in a plasma. The plasma was created in a conical source by a pair of 17-μf, 10-kv capacitors. The discharge lasted 5 μsec at 350 kamps. The plasmoid was then accelerated through a 0–2 kgauss longitudinal magnetic field in a 5.2×200 cm glass tube. The shock-wave excitation was achieved by means of a copper coil supplied by a 0.6-μf, 50-kv capacitor bank. The discharge time was 10^{-6} μsec. The density of the plasmoid varied between 5×10^{14} to 5×10^{16} cm^{-3}. Spectrophotometric records indicated that after the excitation coil discharge, the plasma is set into periodic oscillations. X-ray measurements on the plasmoid showed a sharp drop in x-ray output as the electron density of the plasma increased from 10^{14} to 10^{16}. These x rays are shown to arise after the excitation of the plasma shock wave. Special collectors were used to measure the ion and electron currents, but it was not clear how the shock front was forming in the plasmoid. (ATD)

41912 ON MEASURING THE VELOCITY OF PLASMA JETS. Eremin, Yu. V.; Trokhan, A. M. Zh. Prikl. Mekhan. i Tekhn. Fiz., No. 2, 86-7(Mar.-Apr. 1965). (In Russian).

A photographic method was developed to measure the velocity of a luminous gas stream by using the time-shift in the plasma-jet brightness fluctuation. Near the flow are placed three prisms and a diaphragm with a slit opening. Light from two separate sections passes through the diaphragm and the objective and falls on the film placed on a rotating drum. The fluctuation change between the sections allows estimation of the stream velocity. This technique is adapted to an electrical signal system where the luminous pulse in the plasma jet is recorded at two positions by means of photomultipliers. The velocity measured in this manner is shown to be 10% higher than the values obtained by heat balance methods. (ATD)

41913 SOME CORRELATIONS IN THE INVESTIGATION OF ELECTRIC ARCS. Dautov, G. Yu.; Zhukov, M. F. Zh. Prikl. Mekhan. i Tekhn. Fiz., No. 2, 97-105 (Mar.-Apr. 1965). (In Russian).

A three-part report is presented on general analytical and experimental studies made of the electric arc in a plasmatron. The characteristics of a stabilized arc in a plasma arc chamber are discussed first. The mechanism of arc shunting is considered in some detail, with a sectioned cathode. Arc current traces recorded on two oscillograms indicate that the striking of a constant-current arc follows an unsteady process, and large-scale shunting techniques create changes in the arc length and generate large-scale current and voltage pulses. Current distributions along the length of the arc show that increasing the current strength causes a decrease in the maximum and the minimum arc length. A dimensional analysis is then made of the arc characteristics for the most general plasma-arc operation. This is subsequently simplified to a set of dimensionless combinations m_e/m_a, m_i/m_a, Q_{ae}/Q_a, Q_k/Q_a, U_j/U, $k/c_v m_a$. The analysis is further simplified by assuming a small magnetic Reynolds number, negligible kinetic energy relative to the arc thermal energy, ideal gas, and a zero magnetic field. This leads to the following volt-ampere characteristic $\lg(U_c d/I) = \alpha - \beta \lg (I^2/Gd)$. A final simplification is made in an argon plasma by neglecting the convective heat transfer rate compared to the conduction heat transfer rate. The motion of the arc is then considered in a transverse magnetic field. The following similarity conditions are obtained K = idem, (I/aH) = idem (vH^2/p) idem, (d/a) = idem. The nondimensional arc velocity is correlated with the criterion I/aH. Finally, similarity studies are made for a free atmospheric arc jet; the experimental data are correlated by the following current-voltage characteristic: $(I^2/a^{1.5})(U_c a^{0.5}/I) = (IU_c/a) = \text{idem}$. (ATD)

41914 APPLICATION OF THE THEORY OF THERMAL SIMILARITY TO THE STUDY OF AN ELECTRIC ARC. Krinberg, I. A. Zh. Prikl. Mekhan. i Tekhn. Fiz., No. 2, 105-10(Mar.-Apr. 1965). (In Russian).

The suitability of the theory of thermal similarity for studying electric arcs cooled by natural convection was analyzed. Previous investigations in this field gave inconclusive or negative results due to the nature of the assumptions taken. It is shown that, with a more exact approach, this method is valid. The arc is divided into an inner and outer zone separated by an isothermal surface of temperature T^*. There is no convective heat loss in the inner zone as the gas flows parallel to the arc axis, and the energy balance equation involves only the conduction and radiation losses and the energy of the electric field. In solving this equation, two boundary conditions are used: $dT/dr = 0$ at $r = 0$ (r is the distance from the arc axis), and $\chi\, dT/dr = -q$ at $T = T^*$, where χ is the thermal conductivity. Factor q involves the acceleration of gravity, the coefficient of volume expansion, the specific heat capacity at constant pressure, the density, the dynamic viscosity of the gas, and the heat transfer coefficient (α) found from the thermal similarity theory, between the Nusselt number, the Grashof number, and the Prandtl number. The previous assumption that $T^* = 3{,}000°K$ for various currents (I) results in constant values for χ, q, dT/dr, and IE/R (R is the radius of the isothermal surface), which was experimentally shown to be true only for a limited value of I. By studying data for carbon arcs in air with I of 10 amp and 200 amp, the general relation $T^* = \frac{1}{2}T_0$ (T_0 is the axis temperature) was indicated. This relation was verified for various conditions of the arc plasma by an indirect method (with the radiation losses considered negligible). While the principle of the thermal similarity theory can be adopted in full from the technique used in studying turbulent convection from a solid surface, the constants can not, but must be separately determined. Using information from other sources, the justification of this approach was confirmed. The relation of T_0 to I in various media was studied, and it was found that for argon, $T_0 = 8000 + 1800 \log I$ (T_0 in degrees K, I in amp). For nitrogen, the relation is more complex, with a sharp increase in the range from 10,000 to 11,000°K. It is concluded that the use of the thermal similarity theory in calculating the heat transfer from arcs with natural convection gives sufficiently accurate values for various arc plasma conditions and for currents of 1 to 300 amp. (ATD)

41915 STATIONARY NONLINEAR WAVE IN FINITE TEMPERATURE PLASMA. Zakharov, V. E. Zh. Prikl. Mekhan. i Tekhn. Fiz., No. 6, 96-8(Nov.-Dec. 1964). (In Russian).

Studies of stationary nonlinear waves propagating transverse to the magnetic field in a finite temperature plasma showed the presence of isolated rarefied waves with the characteristic length larger or of the order of the Larmor radius. The front of these waves has an oscillator-type structure expanding into the nonperturbed flow zone. Stationary nonlinear waves appeared in the media with competing dispersion processes and processes of nonlinear wave shape deformations. Magnetohydrodynamic equations were developed for these effects. (R.V.J.)

41916 ON THE INFLUENCE OF PLASMA RESONANCE ON THE PROPAGATION OF SURFACE WAVES IN A NON-UNIFORM PLASMA. Stepanov, K. N. Zh. Tekhn. Fiz., 35: 1002-14(June 1965). (In Russian).

The propagation of slow surface waves on the boundary between a plasma and the vacuum is discussed for the case in which the boundary is not sharp. The cases of a semi-infinite plasma, a thin plane plasma layer, and a plasma cylinder are treated separately. The plasma density is assumed to fall monotonically to zero in a surface layer that is thin compared with the wavelength, and the wave equation is solved by successive approximation in this region. The effect on the dispersion equation of first order terms in the ratio of the transition layer thickness to the wavelength is calculated. Only H waves (the magnetic field in the surface and normal to the propagation direction) are treated because the E-wave equation does not admit surface wave solutions in the case of a diffuse boundary. Resonance between the wave frequency and the Langmuir frequency within the transition layer strongly affects the propagation of the surface waves and can lead to large damping constants. By measuring the frequency dependence of the damping constant information concerning the density distribution within the transition layer can be derived. Spatial dispersion due to the thermal motions of the electrons can be derived. A criterion for the negligibility of spatial dispersion is derived, and the effects of spatial dispersion are calculated for the case when this criterion is not met. Spatial dispersion can contribute significantly to the damping when the electron collision frequency is low. (ATD)

41917 ON DAMPING OF WAVES PROPAGATING IN A BOUNDED PLASMA PERPENDICULAR TO A MAGNETIC FIELD. Kondratenko, A. N. (Inst. of Physics and Tech., Academy of Sciences, Ukrainian SSR). Zh. Tekhn. Fiz., 35: 1015-23(June 1965). (In Russian).

The propagation of electromagnetic waves in an infinite plasma layer of finite thickness located in an external magnetic field perpendicular to the layer is discussed. The calculations are based on the kinetic equations without the collision integrals. Specular reflection of the plasma particles is assumed at the boundaries of the plasma layer. The electron and ion distribution functions and the field strengths are expanded in Fourier series in the coordinate normal to the plasma layer, and the dielectric constants and dispersion equation are derived. Thermal velocities are neglected in certain stages of the derivation. The resulting dispersion equation can be factored in the following limiting cases: the external magnetic field is weak; the external magnetic field is strong; the phase velocity is small; the wave frequency is close to the electron or the ion Larmor frequency; or the wave frequency is low. Neglect of the thermal motions is not justified in the case of low wave frequency for weak external field. The limiting cases are discussed separately, and the damping constants are derived. (ATD)

41918 ON THE CYCLOTRON INSTABILITY OF A PLASMA WITH NONMONOTONIC ION DISTRIBUTION FUNCTION. Davydova, T. A. (Moscow State Univ.). Zh. Tekhn. Fiz., 35: 1024-31(June 1965). (In Russian).

The cyclotron instability of a magnetized plasma with an anisotropic ion velocity distribution function is discussed. The calculations are of interest in connection with plasmas in magnetic traps. The distribution function for the component of the ion velocity parallel to the magnetic field is assumed to be maxwellian and that for the transverse component v to be proportional to $\exp(-((v - w)/wL)^2)$, where w is a constant velocity and L is a dimensionless parameter. The distribution function for v reduces to a delta function in the limit $L = 0$. The dispersion equation is written in the form derived by Dnestrovskiy, and conditions for the stability of the plasma are derived from it. It is shown that as L increases, i.e., as the ion velocity distribution becomes less sharp, the critical velocity anisotropy for plasma instability increases. This effect of L on the critical anisotropy is greater for high electron temperatures than for low. If the plasma is finite in extent the instability for a fixed ion velocity anisotropy disappears when the plasma density exceeds a certain critical value, and this critical density increases with increasing size of the plasma. This effect of plasma size is absent in the case of a delta function transverse ion velocity distribution. (ATD)

41919 GRAVITY SEPARATION OF CHARGES IN PLASMA. Samokhin, M. V. Zh. Tekhn. Fiz., 35: 1032-4(June 1965). (In Russian).

A numerical solution is given for the problem of the separation of charges in a thermodynamic equilibrium plasma located in a constant field of gravity. The effect of the gravity field on the electrons is taken into account. Under the assumption that the gravity field is centrally symmetric, the electrostatic and gravitational potentials can remain finite in the whole space. Thus, with a suffi-

ciently high plasma temperature it is possible to linearize the barometric formula and to avoid laborious calculations. At a high plasma temperature and small Debye radius a thin layer of space charge forms close to the gravitational body. This charge decreases exponentially with the distance from the surface of the body. The electrostatic potential approaches a value $\frac{1}{2}\ \Phi_\infty$, where Φ_∞ is a dimensionless gravity potential at infinity. (ATD)

41920 ON THE INVESTIGATION OF PLASMA BY MEANS OF A RELATIVISTIC ELECTRON BEAM. Zhileiko, G. I.; Baskakov, S. I. Zh. Tekhn. Fiz., 35: 1035-8 (June 1965). (In Russian).

The use of a bunched beam of relativistic electrons for plasma diagnostics is discussed. The use of the electron beam depends on the radiation by the beam of high-frequency electromagnetic waves. The plasma is assumed to be in a uniform magnetic field and only magnetic bremsstrahlung at harmonics of the Larmor frequency is considered, although it is asserted that the results are fully applicable to the transition radiation due to plasma nonuniformities. Formulas are adduced from which the necessary characteristics of the beam can be calculated for given radiation requirements. It is assumed that the bunches are small enough to radiate coherently. The formulas are applied to a plasma with an electron density of 10^{16} cm^{-3} in a 10^4 Oe field. A radiation frequency of 10^{12} cps is required, and a detected power of 10^{-6} w is necessary to keep the signal above the noise. It is found that the optimum electron energy is 2.55 Mev, the energy dispersion must be kept down to 0.1%, and a beam current of 0.24 mamp is required. The size of the required bunches is such that the longitudinal debunching space charge field is 24.2 v/cm. To meet the energy dispersion requirement there must be a 51-gauss focusing field in the linear accelerator, and the accelerating field must exceed 1.54 kv/cm. (ATD)

41921 INVESTIGATION OF A THETA PINCH PLASMA IN AN AZIMUTHAL MAGNETIC FIELD. Volkov, Ya. F.; Dyatlov, V. G.; Mitina, N. I. Zh. Tekhn. Fiz., 35: 1039-43 (June 1965). (In Russian).

Ion and electron temperatures in a helium plasma in an external azimuthal magnetic field were measured. The plasmas were produced in a spherical glass vessel containing helium at approximately 10^{-3} mm Hg by 20-kv capacitor discharge. The period of the resulting magnetic field was 30 μsec and the amplitude reached 16 kOe. The azimuthal magnetic field was provided by a 3-kv capacitor discharge. The period of this system was 425 μsec and the current reached 100 kamp. The ion temperatures were determined from the Doppler broadening of several lines in the optical spectrum, and the electron temperatures were determined from the relative intensities of two or more lines. The time variation of the temperatures was followed by measuring at different phases of different discharges. The average ion temperatures were of the order of 40 to 60 ev. Electron temperatures exceeding 1 kev were observed. Soft x-ray absorption measurements indicated that electron temperatures greater than 4 kev did not occur. Radio noise of the order of 1 w was observed at 3 cm wavelength. The time dependence of the ion and electron temperatures was characterized by a rapid rise to a maximum within a few microseconds and a subsequent decrease. The electron temperature showed a small secondary maximum at about 6 μsec. The rapid rise of the ion temperature can not be accounted for by collisions with electrons; it is ascribed to plasma instability involving pulsations at approximately the Langmuir frequency. (ATD)

41922 MEASURING THE TEMPERATURE OF FREE ELECTRONS IN RAREFIED ACETYLENE-AIR FLAMES. Tverdokhlebov, V. I.; Tretenko, M. E. (Dnepropetrovsk Mining Inst., USSR). Zh. Tekhn. Fiz., 35: 1044-6(June 1965). (In Russian).

The temperature differences between electrons and gas molecules in rarefied acetylene-air flames measured by Soviet and non-Soviet authors are discussed. The curves of the dependence of the temperature of free electrons on the distance from the burner orifice at pressures from 20 to 40 mm Hg are given. Temperature measurements of free electrons by the two-probe method with allowance for relaxation phenomena indicate that this temperature inside the reaction zone is near the temperature of the gas molecules. (ATD)

41923 PRODUCTION OF AN INTENSE PULSED BEAM OF ACCELERATED TRITIUM ATOMS. Knyazyatov, A. S.; Mal'tsev, V. V. Zh. Tekhn. Fiz., 35: 1047-52(June 1965). (In Russian).

An apparatus is described with which 0.5- to 2-μsec pulses of 100-kev tritium atoms can be produced with an intensity equivalent to an ion current of 5 mamp at 1 m from the source. The apparatus was developed for plasma diagnostics (measurement of deuterium plasma densities by the neutron yield). The atom beam is produced from an ion beam by charge exchange on a gaseous target. A diagram of the apparatus is shown. The distinctive feature of the apparatus is the use of a pulsed gas jet charge exchange target; this considerably reduces the pumping requirements from those for the case of a continuous flow gas target. The apparatus is so constructed that the diffusion time from the target to the ion source exceeds the pulse duration; if the target gas pressure in the vicinity of the target rises to such a value as to result in electric breakdown, this occurs only after the pulse is over and does not interrupt operations. Hydrogen was employed as the target gas and an a-c charge exchange efficiency of 50% was achieved. The operation of the apparatus was investigated for different values of the parameters with deuterium as the target gas; this made it possible to follow the motions of the target gas by observing the neutron yield from the tritium ion beam. The beam intensity and profile were determined calorimetrically. The results are briefly discussed. (ATD)

41924 THE MEASURING OF ELECTRON CONCENTRATION IN A PLASMA BY MEANS OF INTERFEROMETER METHOD USING RUBY LASER. Mitsuk, V. E.; Savoskin, V. I.; Chernikov, V. A. Zh. Tekhn. Fiz., 35: 1156-8(June 1965). (In Russian).

A device for measuring the electron density of a plasma is described based on the use of a ruby laser with a Fabry-Perot etalon partially filled with plasma. A 12-cm-long ruby rod with a 10-mm diameter with dielectric coatings was utilized. A laser pulse 0.7 msec in duration was synchronous with a pulsed discharge from a LC circuit in a tube 1.3 cm in diameter filled with argon at a pressure of 10 mm Hg. The tube, located between the mirrors of the etalon, contained optical windows for passage of the probing laser beam perpendicular to the discharge axis. An interference filter was used to filter out plasma radiation. After its passage through the tube, the laser beam passed through a 3-mm diaphragm. The electron density was determined by comparing a sequence of interference patterns obtained prior to and after the discharge. It was established that variation of the refraction index due to variation of the gas density during discharge could be disregarded, that the plasma was optically thin to laser radiation, and that the effect of the laser beam on the plasma was negligible. (ATD)

41925 ON SUPERHEATING INSTABILITY OF A PLASMA. Sanochkin, Yu. V. Zh. Tekhn. Fiz., 35: 1163-4(June 1965). (In Russian).

The stability of a nonideal plasma with respect to the generation of acoustic waves is discussed. The linearized magnetohydrodynamic equations for the perturbations of a plasma in a magnetic field are written for the case that the transport coefficients depend only on the temperature, the magnetic viscosity is large compared with the heat conductivity, the mechanical viscosity is negligible, and the electron collision frequency is greater than the Larmor frequency. The dispersion equation is derived for the coupled diffuse and acoustic branches, and the stability conditions are obtained. An expression is given for the logarithmic increment of the waves, and their wavelength is estimated. If the electric conductivity of the plasma is independent of the temperature (or nearly so) and the power lost by radi-

ation increases with increasing temperature, the instability does not develop. Under anomalous radiation conditions, however, in which the radiated power decreases or the absorbed power increases with increasing temperature, the plasma can be unstable even if its conductivity vanishes. (ATD)

41926 EXPERIMENTAL OBSERVATIONS OF AN INTERACTION BETWEEN TWO COUNTERSTREAMING PLASMAS IN THE PRESENCE OF EXTERNAL MAGNETIC FIELDS (thesis). DiMarco, Joseph Nicola. Hoboken, N. J., Stevens Inst. of Tech., 1964. 102p.

Plasmas from pulsed conical copper guns are fired at each other in the presence of mirror- and cusp-geometry magnetic fields of up to 3000 gauss. The directed velocity of the plasma stream is approximately 3×10^6 cm/sec, and the electron temperature and density are of the order of 10 ev and 10^{14} particles/cc. The presence of an interaction between the two counter-streaming plasmas in a mirror-geometry magnetic field has been detected. The presence of an interaction between the two counter-streaming plasmas, does not improve the trapping and containment decay time of the plasma compared with a single gun firing, although the initial density in the former case is larger. The interaction is delayed approximately 20 μ sec. after the counter-streaming plasmas have initially interpenetrated one another, and measurements of the plasma density at the radial periphery of the system indicate the presence of large fluctuations in the plasma density which reach a maximum at approximately 100 μ sec. These fluctuations indicate that a portion of the plasma escapes radially across the magnetic field in the mirror-geometry configuration by some instability mechanism that is present when the two guns are fired at each other. The Kerr cell photographs of the interaction between the two counter-streaming plasmas in the mirror-geometry magnetic field indicate the presence of filamentary structures which are very likely due to velocity shear between interacting plasma streams. (Dissertation Abstr.)

41927 EXCITATION OF NONLINEAR CURRENTS AND GENERATION OF HARMONIC WAVES BY AN ELECTROMAGNETIC WAVE IN AN ISOTROPIC PLASMA (thesis). Tang, Ting-wei. Providence, Brown Univ., 1964. 96p.

The nonlinear polarization currents excited by a plane electromagnetic wave propagating in an isotropic, homogeneous, or inhomogeneous plasma medium is discussed. The nonlinear terms arise from Boltzmann's momentum transport equation, Maxwell's equations, and the continuity equation. Four different nonlinear effects, namely, the intrinsic electromagnetic interaction, temperature effects, space charge currents, and spatial dispersion are fully discussed and their importances in different situations are compared. An explicit expression of harmonic currents excited by the primary wave was obtained in each case by means of a perturbation method, with a proper perturbation parameter indicated. Radiation fields established by the harmonic currents generated inside the plasma were calculated. A model of an inhomogeneous plasma layer with a linearly increasing electron density is considered, both for normal and oblique incidence of a plane electromagnetic wave. The electron collision frequency is first neglected in the case of normal incidence, and it is shown in this case that the plasma excites a longitudinally oscillating second harmonic electric field without radiation into free space. The field intensity of the third harmonic wave radiated into the free space region is calculated for the extreme cases of a quasi-homogeneous plasma and a sharp plasma boundary. The result shows that the amplitude of the radiated field oscillates as a function of ω^3. In the case of oblique incidence of a plane wave, the collision frequency is taken into account. However, only the quasi-homogeneous plasma medium is considered, and the radiation intensity of the second harmonic wave is calculated. This time, the amplitude of the radiated field decreases according to $1/\omega^4$ as the frequency increases. Finally, the theory developed is applied to a model ionosphere. In the case of a strong field, the intensity of the second harmonic wave radiated into free space is found to be smaller than the primary wave by a factor 10^{-5}, if collisions are assumed to be infrequent, to 10^{-8} for larger collision frequencies. (Dissertation Abstr.)

41928 STRUCTURE OF A PLASMA SHOCK WAVE (thesis). Jaffrin, Michel Yves. Providence, Brown Univ., 1964. 70p.

The one-dimensional, steady state structure of a shock wave in a fully ionized plasma was investigated in the absence of external applied magnetic or electric fields. The structure was assumed to be described by the appropriate Navier-Stokes equations written for the electron and ion fluids, together with Poisson's equation for the self-induced electric field effects. The shock structure is shown to be described by a system of five coupled nonlinear ordinary differential equations of which three are of first order and two of second order. The collisional broadening mechanisms considered, along with their respective length scales, are: electron heat conduction and ion-electron energy and momentum transfer, $\epsilon^{-1}l_2$; ion heat conduction and viscosity, l_2; and electron viscosity, ϵl_2. The length l_2 is the ion-ion mean free path downstream of the shock and the small parameter ϵ is the square root of the ratio of the electron mass to ion mass. The other parameter which enters is the ratio l_2/λ_{D_2}, where λ_{D_2} is the Debye length downstream of the shock. It was found that when the free stream Mach number M_1 is less than 1.12, there is only one shock layer whose thickness is approximately $7l_2/\epsilon$. The plasma behaves like a single fluid. When $M_1 > 1.12$, an ion shock of approximate thickness $6l_2$ appears embedded in a wider thermal layer of thickness $2l_2/\epsilon$. In the thermal layer, the electrons are heated up first because of their higher thermal conductivity. Compression and heating of the ions take place in the ion shock while the electrons remain in local thermal equilibrium. The ion temperature overshoots its downstream value and the two temperatures equilibrate after the ion shock. Within the ion shock the electric field and charge separation each show a single damped oscillation with an amplitude proportional respectively to λ_{D_2}/l_2 and $(\lambda_{D_2}/l_2)^2$. Throughout the shock the electric potential increases continuously, though it rises more steeply within the ion shock. Numerical calculations are shown which illustrate these results. When the mean free path and the Debye length are of the same order of magnitude, the electrical effects are more important and interact directly with the flow in the two electric shock layers. (Dissertation Abstr.)

41929 IONIZATION PHENOMENA IN A GAS-PARTICLE PLASMA (thesis). Gibson, Edward George. Pasadena, Calif., California Inst. of Tech., 1964. 189p.

Several interesting and practically important types of ionization phenomena that occur in a plasma that is composed of thermionically emitting particles and an ionized gas, were investigated. There are many interactions that can take place between the particles and the gas which are able to alter the electron density of the plasma appreciably from what it would be in the absence of the particles. Several of these interactions were explored. Throughout all of the analysis, the emphasis was placed on gaining a physical understanding of the basic phenomena that are involved. In order to determine the nature of the potential and charge distributions that exist in a gas-particle plasma, the problem in which there is no gaseous ionization and equilibrium prevails was first thoroughly investigated. Using a family of numerical solutions to Poisson's equation, it was found that these distributions can be divided into two characteristic regimes and that a simple algebraic expression, which was derived, is a good approximation to the potential distribution in one of them. A readily applied method of calculation of the electron density in the plasma and a study of the dependence of this density on the initial parameters which enter the problem are presented. The relations that are required in order to analyze non-equilibrium ionization phenomena in a gas-particle plasma were formulated and then applied to various special cases. The case that has received the major emphasis is that in which the particles are hotter than the gas and an enhancement in the gaseous ionization results.

It is shown that this enhancement could be quite large. Electron absorption by the particles, particle quenching of the gaseous ionization, and the suppression of either particle or gas ionization, due to the presence of the other, were also investigated. (Dissertation Abstr.)

41930 A NEW SOLUTION OF THE KINETIC EQUATIONS FOR A PLASMA INCLUDING RADIATION. A CALCULATION OF THE SPECTRAL DENSITY OF RADIATION SCATTERED BY A NON-EQUILIBRIUM PLASMA WHICH IS VALID FOR ALL WAVENUMBERS. (VOLUMES 1 AND 2) (thesis). Fante, Ronald Louis. Princeton, N. J., Princeton Univ., 1964. 203p.

The Fokker-Planck equation and the rate of energy transfer from the particles to radiation field in an infinite, spatially homogeneous plasma, with and without an external magnetic field applied, were obtained. For a plasma with no external fields it was found that there is no transfer of energy from particles to the radiation field for time scales of order of the time between collisions. However, if an external magnetic field is applied it was found that there is a strong interchange of energy due to cyclotron and synchrotron effects. The emission and absorption coefficients for these processes were obtained. The behavior of the induction fields in the plasma were also examined and found that they approach their asymptotic values in times of order of a plasma oscillation (i.e. times of order $(\omega)^{-1}$, where ω is the electron plasma frequency). A formula for the spectral density $S(k,\omega)$ of radiation scattered by a non-equilibrium plasma which is valid for all wavenumbers k was also derived. It was found that the spectrum obtained is equal to the spectrum obtained by Rostoker and Rosenbluth (and Lamb) plus a correction term which is important for large k. (Dissertation Abstr.)

41931 TECHNIQUES FOR TREATING FULLY IONIZED TWO-PARTICLE PLASMA EQUATIONS (thesis). Hartle, Richard Eastham. University Park, Penna., Pennsylvania State Univ., 1964. 102p.

Analytical methods were developed for treating the Boltzmann-Maxwell or associated continuum equations for fully ionized two-particle plasma equations and to demonstrate their uses through specific examples. The descriptive equations are treated exactly; that is, the usual linearization approximation is not made. A time series expansion method along with the method of partial summation was applied to the cold plasma equations. More specifically, the dependent variables were expanded in time power series and the coefficients determined as functionals of the initial functions. Partial summation was applied to groups of terms in each expansion. The result is written in a convenient form comparable to that obtained by others and from which some plasma properties were obtained. Both the time series method and the method of characteristics were applied to the Boltzmann-Maxwell system. The general time series solution was demonstrated useful through application to a plasma in a uniform magnetic field. The method of characteristics is discussed in general and also applied to the problem of a plasma in a uniform magnetic field. The method of characteristics was applied to the Boltzmann equations for positive and negative ions to obtain general solutions for transverse electromagnetic waves. A general class of self-consistent solutions is defined when the above are coupled with the Maxwell equations. From this class two specific solutions and a result were obtained. (Dissertation Abstr.)

41932 EXPERIMENTAL STUDY OF PLASMA WAVE RESONANCES IN A HOT NONUNIFORM PLASMA COLUMN (thesis). Nickel, John Carl. Pasadena, Calif., California Inst. of Tech., 1964. 137p.

The relative frequency spectrum $\omega^2/\overline{\omega_p^2}$ of plasma wave resonances in the positive column of a low-pressure mercury discharge tube is shown to depend upon the parameter $r_w^2/\overline{\lambda_D^2}$ where r_w is the radius of the column, $\overline{\lambda_D^2}$ is the Debye length defined in terms of the average electron density, and $\overline{\omega_p^2}$ is the square of the average plasma frequency. Observations of both dipole and quadrupole resonance spectra made on several discharge tubes with r_w ranging from 0.30 to 0.87 cm are presented. For these measurements $r_w^2/\overline{\lambda_D^2}$ varies from about 10^2 to 10^5, and the best fit electron temperatures were found to be of the order of 3 ev. The average electron densities were directly measured using a cavity perturbation technique. The results of these observations were found to be in good agreement with the theory based upon the first two moments of the correlationless Boltzmann equation in conjunction with Parker's electron density profile for a low density positive column. The results of a preliminary investigation of the effects of an axial, static magnetic field on the dipole resonance spectrum are also presented. These results indicate that in the presence of an axial magnetic field not only does the lowest resonance (approximately predicted by the cold plasma theory) split, but the next higher order resonance also splits. For the lowest resonance, it was found that $\Delta\omega/\omega_g \approx .8 \pm .1$, while for the next higher order resonance $\Delta\omega/\omega_g \approx .5 \pm .2$, where ω_g is the cyclotron frequency. These preliminary results are in good accord with calculations made by others, again using the moment equation approach. (Dissertation Abstr.)

41933 INTERACTION OF FAST CHARGED PARTICLES WITH THE CORONAL PLASMA (thesis). Altschuler, Martin David. New Haven, Yale Univ., 1964. 260p.

Hydromagnetic equations were solved for the electrostatic field distribution of a charged test particle in a plasma. When electrons are accelerated by the electrostatic field of the test particle they emit electromagnetic radiation. The spectrum of this radiation was calculated. When the test particle moves slower than the thermal electron speed, the electrostatic field of the test particle is a shielded and distorted Coulomb potential (a distorted Debye potential). The resulting electromagnetic radiation has a spectrum that agrees in the low- and high-frequency limits with the results of others. When the test particle moves faster than the thermal electron speed, the plasma perturbations are contained within a Mach cone trailing the test particle. The resulting electromagnetic radiation has a resonance at $\omega_e[1 - V^2/u^2]^{-\frac{1}{2}} > \omega_e$ where ω_e is the plasma frequency and V and u are the thermal electron speed and test particle speed respectively. When two or more test particles move together supersonically through the plasma, even harmonics of the resonant frequency arise in a natural manner. Possible applications of this theory to non-thermal radio emission of solar bursts are pointed out. (Dissertation Abstr.)

41934 EXPERIMENTAL INVESTIGATIONS OF THE TEMPORALLY AND SPATIALLY RESOLVED ENERGY STATES OF A HIGH DENSITY GASEOUS PLASMA (thesis). Hirsch, Robert Louis. Urbana, Ill., Univ. of Illinois, 1964. 177p.

The energy states of a high-density gaseous plasma in low-pressure hydrogen were studied experimentally. The plasmas were produced by radial magnetic compression in a time varying longitudinal magnetic field. Particular attention was given to the highly reproducible compressed plasmas on the fourth, fifth, and sixth half cycles of the damped sinusoidal magnetic field (half period of 6.6 μ sec; fourth half cycle field peak of the order of 8 kilogauss). Electron density variations in space and time were determined using the Stark broadening of the H_β spectral line. Peak densities were found to be of the order of 10^{16} per cc for initial pressures of the order of 100 μ Hg. The spatial distributions of electron density were shown to agree well with a Bennett model for the theta pinch. Correlation of the results of magnetic probe, electric conductivity, spectral, and plasma expansion techniques yielded a detailed description of the compressed plasmas and showed the plasmas to be very nearly in a state of local thermodynamic equilibrium. Temperatures were found to be of the order of 50,000°K. A method for diagnostics in rapidly compressed plasmas was developed. It involved the study of a controlled plasma expansion and provided a measure of the energy of the compressed plasma. Two methods of analysis of the expansion were found to provide good correlation with the results of other techniques. The various diagnostic techniques were also

evaluated with regard to their flexibility and usefulness in high-density plasma studies. (Dissertation Abstr.)

41935 PHOTOIONIZATION UPSTREAM OF A STRONG SHOCK WAVE. Ferrari, C.; Clarke, J. H. (Brown Univ., Providence). p.239-61 of "High Temperatures in Aeronautics." New York, Pergamon Press and Milan, Tamburini Editore, 1964.

Explicit gasdynamic equations for unsteady, rectilinear motion are deduced for an ionizing and radiating gas, when both of these processes are out of equilibrium. An estimate is then given of the degree of ionization produced upstream of a strong normal shock wave by radiation from the hot nonequilibrium region downstream of the shock. (auth)

41936 STUDY OF SOME PLASMA JETS. Brun, E. A. (Faculte des Sciences, Paris). p.263-79 of "High Temperatures in Aeronautics." New York, Pergamon Press and Milan, Tamburini Editore, 1964. (In French).

The magnetically driven shock tube makes it possible to obtain velocities and temperatures higher than the classic diaphragm shock tube. It is, for example, possible to obtain with the magnetically driven tube, in the case of He, a velocity of 4×10^4 m/sec with a temperature of approximately 40,000°K. This temperature, obtained by a spectrometric measurement, is approximately double that given by the calculation based on the Rankine-Hugoniot equations. Experiments have made it possible to analyze phenomena appearing in a magnetically driven shock tube. These phenomena are notably different from those observed in the classical shock tube; some results are presented which support this point of view. A plasma flow in a pipe in the presence of an axial magnetic field was studied. The plasma generator is classical, but the presence of the magnetic field in the pipe makes possible a confinement of the jet which decreases the heat transmission of the plasma to the wall of the pipe. From this fact, as measurements of pressure along the tube show, the flow approaches adiabatic conditions. A simplification, therefore, occurs in the equations relative to this flow. From the practical point of view, the presence of the axial magnetic field stabilizes the functioning of the generator, reduces the wear of the pipe, and increases the energy yield. It is however necessary to take into consideration magnetohydrodynamic effects which cause the presence of the field. These effects modify the form of the lines of current of the plasma at the output of the pipe. Because of this curious cases of ablation have been obtained in the plasma jet leaving the pipe. (tr-auth)

41937 IONIZED GASES. SECOND EDITION. von Engel, A. Oxford, Oxford University Press, 1965. 334p. $8.80.

An introduction is given to the field of ionized gases with emphasis on the fundamental concepts and the limitations of the various treatments. The details of the theories, their applications to real discharges, and their more practical uses are less extensively dealt with. Included topics are conduction in feebly ionized gases, production of charged particles, mobility and charge transfer, diffusion and mutual repulsion, recombination, ionization and excitation in an electric field, glow discharge, and arc discharge. (J.F.P.)

41938 ELECTRON AVALANCHES AND BREAKDOWN IN GASES. Raether, H. Butterworths Advanced Physics Series. Monographs on Ionization and Electrical Discharges in Gases. Washington, D. C., Butterworths, 1964. 200p. $11.95.

A survey of the physics of the electron avalanche is presented, including an account of the results of experiments on series of avalanches together with a review of recent theoretical work. A review on the phenomena of breakdown is also included. (D.C.W.)

41939 WAVE PROPAGATION ALONG WARM PLASMA COLUMNS. Diament, Paul (Columbia Univ., New York); Granatstein, Victor L.; Schlesinger, S. Perry. 12p. (CONF-758-40). Gmelin, AED-CONF-65-003-56.

From American Physical Society Meeting, New York, Jan. 1965.

Dispersion curves for bound modes of propagation along warm plasma columns are presented, which show the effects of finite temperature on the surface wave of the cold case and also predict an infinite series of propagating modes corresponding to the Dattner scattering resonances. (L.B.S.)

41940 KINETIC EQUATIONS FOR SYSTEMS OF CHARGED PARTICLES AND PHOTONS. Chappell, Willard R. (Univ. of Colorado, Boulder). 246p. (CONF-758-50). Gmelin, AED-CONF-65-003-96.

From American Physical Society Meeting, New York, Jan. 1965.

Quantum kinetic equations are derived for systems of charged particles interacting with photons. In particular, two systems are considered: a homogeneous, multicomponent, fully ionized gas with no external fields present, and a homogeneous electron gas in the presence of a constant external magnetic field. (L.B.S.)

41941 STARK BROADENING OF IONIZED NITROGEN LINES IN A T-TUBE PLASMA. Day, R. A.; Griem, H. R. 9p. (CONF-758-51). Gmelin, AED-CONF-65-003-65.

From American Physical Society Meeting, New York, Jan. 1965.

The results of an experimental investigation of the Stark widths and shifts of lines emitted by nitrogen in an electromagnetic T-tube are reported. A comparison is made with predictions of the Stark broadening theory; agreement was found within 15% except for the intercombination line at 4553 Å. (L.B.S.)

41942 OBSERVATION OF NON-QUASISTATIC PLASMA SURFACE WAVES. Granatstein, V. L. (Bell Telephone Labs., Inc., Murray Hill, N. J.); Schlesinger, S. P. 15p. (CONF-641108-49). Gmelin, AED-CONF-64-196-71.

From American Physical Society, New York.

The propagation of surface waves along a dielectric plasma-filled tube imbedded in free space is considered. An experiment was performed in the afterglow of an argon positive plasma column, and an attempt was made to observe the non-quasistatic phenomenon of a forward dipole surface wave at values of phase velocity close to c. An open microwave cavity was used for detecting plasma surface wave resonances, and the behavior of the low-density and high-density peaks observed in oscilliscope displays of the probe signals vs. time are discussed. Comparison is made between the observed behavior of the resonance peaks and theoretical dispersion curves for surface waves. (L.B.S.)

41943 PLASMA GENERATION BY THE LASER ILLUMINATION OF A TUNGSTEN SURFACE. Gilmour, A. S. Jr.; Giori, F. A. (Cornell Aeronautical Lab., Inc., Buffalo). 13p. (CONF-641016-7). Gmelin, AED-CONF-64-223-15.

From 17th Annual Gaseous Electronics Conference, Atlantic City.

An experiment was performed to study ion generation by illumination of a tungsten surface with focused light from a pulsed ruby laser. The quantity and energy of emitted particles were measured over a wide range of conditions, and the electrical nature of the emission (charge to mass ratios and per cent ionization) was determined. It is concluded that the large electron and ion current densities obtained and which were controllable should make possible a large number of applications for this type of ionization process. (L.B.S.)

41944 MICROWAVE MEASUREMENT OF THE PROBABILITY OF COLLISION OF LOW ENERGY ELECTRONS IN NITROGEN. Noon, J. H.; Holt, E. H.; Quine, J. P. (Rensselaer Polytechnic Inst., Troy, N. Y.). 19p. (CONF-641016-6). Gmelin, AED-CONF-64-223-14.

From 17th Annual Gaseous Electronics Conference, Atlantic City.

The probability of collision for momentum transfer (P_c) of low energy electrons (< 1 ev) in nitrogen was experimentally determined using microwave transmission techniques. A bakeable cell constructed of X-band waveguide contained the plasma. A nitrogen discharge was produced by a pulsed d-c supply and the phase shift and attenuation of the microwave signal measured as a function of time in the afterglow

plasma. The change in electron temperature with time was monitored using a gated microwave radiometer. Assuming a Maxwellian velocity distribution for the electrons, P_c was calculated as a function of electron energy and values obtained agree with those of Phelps et. al but disagree with those of Anderson and Goldstein. However, the radiometer measurements indicate that the electron energy distribution is not Maxwellian in the early afterglow. This is important in explaining the disagreement between values of P_c calculated by earlier workers and in understanding the heating effect of nitrogen metastables in the afterglow. (auth)

41945 POSITRON ANNIHILATION AND ORTHOGONALIZED PLANE WAVES IN LITHIUM. Melngailis, J. (Carnegie Inst. of Tech., Pittsburgh). 32p. (CONF-758-46). Gmelin, AED-CONF-65-003-85.

From American Physical Society Meeting, New York, Jan. 1965.

Anisotropies in the momentum distribution of positron annihilation radiation have in the past been observed in several single crystal metals, most recently in Li. Interpretation of the results in terms of Fermi surface structure is complicated. The angular correlation pattern is affected not only by the Fermi surface shape but also by the necessary departure of the conduction electron wavefunction from a plane wave. The magnitude of these two effects is evaluated in Li. The OPW method with 19 waves is used to obtain the lowest band, $E(\underline{k})$, and the corresponding conduction electron wavefunctions. The numerically calculated angular correlation curves show anisotropies in agreement with the measured results if both the effect of the Fermi surface shape and the effect of the wavefunction are included. If the Fermi surface shape alone is considered, the observed anisotropies cannot be explained. Quantitative agreement with experiment can be obtained if, in addition to all other effects, the enhancement factor due to electron positron attraction calculated by Kahana is included. (auth)

41946 ELECTRON GUN FOR PLASMA-OSCILLATION STUDIES. Zieske, P. L.; Kofoid, M. J. 5p. (CONF-471-57). Gmelin, AED-CONF-63-268-67.

From American Physical Society 5th Annual Meeting, San Diego, Calif., Nov. 1963.

Recent improved experimental results, some conclusions, and summarizing comments are presented from the study of large-diameter low-voltage electron beams for use as an exciting stream in the production of longitudinal electron oscillations. (L.B.S.)

41947 OBSERVATION OF THE FARADAY EFFECT IN A THETA-PINCH PLASMA USING A He–Ne GAS LASER. Falconer, I. S.; Benesch, R.; Ramsden, S. A. (National Research Council, Ottawa). 7p. (CONF-641108-48). Gmelin, AED-CONF-64-196-74.

From American Physical Society, New York.

The observation of the Faraday effect rotation in a θ-pinch plasma, using the visible radiation 6328 Å from a He–Ne gas laser, is reported. A rotation of approximately five minutes of arc was observed. Evidence is presented to show that this is a true rotation of the plane of polarization of the laser beam. The order of magnitude of the rotation was found to be consistent with independent measurements of electron density and magnetic field along the path of the beam through the plasma. (L.B.S.)

41948 THEORY OF THE PLASMA WAVE PROBE. Fontheim, Ernest G. 21p. (CONF-650410-26). Gmelin AED-CONF-65-073-28.

From American Physical Society, Washington, D. C.

A general expression is derived for the a-c response of a probe to a plasma for the case of a low-frequency wave. Solutions are obtained for the accelerated and retarded a-c currents, both of which are proportional to $e^{-i\omega t}$. It is concluded that the current collected by the probe consists of the usual d-c component plus a superposed a-c component which oscillates with the frequency of the plasma wave. The derivation for the high-frequency case is planned. (L.B.S.)

41949 LOW-FREQUENCY IMPEDANCE CHARACTERISTICS OF A LANGMUIR PROBE IN A PLASMA. Crawford, F. W.; Grard, R. (Stanford Univ., Calif.). 30p. (CONF-641108-50). Gmelin, AED-CONF-64-196-69.

From American Physical Society, New York.

Measurement of the low-frequency impedance of a Langmuir probe in a plasma can give the local electron density and temperature. Such diagnostic methods have been employed in ionospheric probing, but the interpretation of the results based on simplified theory has not been entirely satisfactory. Laboratory plasma studies designed to investigate the validity of the simplified theory are described. Good agreement is obtained between results obtained by two different impedance techniques, and conventional Langmuir probe data reduction. It is concluded that the methods could provide additional methods of measurement in laboratory plasmas, with some inherent advantages, but that a more detailed theory and extensive experimental verification are required before they can be applied with confidence to more complicated conditions in the ionosphere. (auth)

41950 IMPROVEMENTS IN OR RELATING TO GAS PLASMA APPARATUS. (to Litton Industries Inc.). British Patent 997,960. July 14, 1965. Priority date Aug. 7, 1963, United States.

In a gas plasma apparatus means are provided for establishing a circularly polarized high frequency electromagnetic field adapted both to excite the plasma and to confine it in a potential well formed along the axis of the field rotation. The rotating electromagnetic field is established by at least two pairs of coaxial electrodes, each pair including a larger diameter and a smaller diameter coil in a common plane. The pairs of coils are mounted to lie in two parallel planes so that they define an annular space, and the coils of each pair are connected in series opposition and are energized in phase quadrature. The electromagnetic field has the shape of a toroid and rotates in radial planes through the axis of the toroid, and the frequency of the field is above the cyclotron resonance frequency of the plasma ions. (B.L.M.)

Shielding

Refer also to abstract 40834.

41951 (N64-30510) THE CALCULATION OF PROTON PENETRATION AND DOSE RATES. Burrell, Martin O. (National Aeronautics and Space Administration, Huntsville, Ala. George C. Marshall Space Flight Center). Aug. 17, 1964. 77p. (NASA-TM-X-53063). CFSTI $3.00 cy, $0.75 mn.

Computational methods are developed to determine the proton energy degradation and flux attenuation as a function of penetration depth in various materials. The primary purpose of this work is to estimate the energy deposition or tissue dose rate at a given depth or on the surface of a shielded object. Detailed analysis of the methods used and their accuracy are a prime part of this study. (auth)

41952 (N64-31552) ACTIVE SHIELDING CONCEPTS FOR THE IONIZING RADIATION IN SPACE. Final Report, September 1, 1962–August 31, 1963. Good, R. C.; Shen, S. P.; Dow, N. F. (General Electric Co., Philadelphia, Pa. Missile and Space Div.). Revised Jan. 31, 1964. Contract NASw-502. 94p. (NASA-CR-58950). CFSTI $3.00 cy, $0.50 mn.

An effort was made to find the optimum weight for a spacecraft active shield, using electromagnetic fields. Protons in the range of 100 to 1000 Mev were chosen as the most dangerous ionizing radiation in space that could be shielded. Particles in space are isotropic, and shielding must provide for this. Topics covered are these: (1) theoretical calculations of magnetic fields and their effects on the trajectory of incident particles; (2) determination of coil-design factors (size, position, material, and support) for various shapes of spacecraft; (3) calculations of the

weights for these configurations and selection of the optimum values considering the weight, supporting structure, and type of superconducting material; and (4) calculation of cascading effects of protons in iron, lucite, and chrondrites. An electromagnetic-field system, using a toroidal-shaped spacecraft with a confined magnetic field was shown to be the lightest among those considered. In general, the active shield weight was only 20% that of the passive shield for high-energy protons and for large spacecraft. The shield with a confined field weighed 30% of that for a shield using an unconfined field. If hatches were included, the use of spherical modules led to spacecraft lighter than spheres, cylinders, or tori. For spacecraft in the shape of a torus, a passively shielded hatch is not required because there are no junctions between oppositely directed magnetic fields. (auth)

41953 (NP-15131) UGLOVYE I ENERGETRICHESKIE RASPREDELENIIA γ-IZLUCHENIIA. (Angular and Energy Distribution of γ Emission Scattered in Water and Iron). Kazanskii, Yu. A. (Gosudarstvennyi Komitet po Ispol'zovaniyu Atomnoi Energii SSSR). 1960. 20p. Dep. mn.

A detailed study was made of multiple scattering of gamma rays and of their angular and energy distributions, allowing gamma attenuation to be calculated in complex geometrical conditions. Angular and energy distributions of ^{60}Co gamma rays were measured in water and iron in conditions of semi-infinite geometry, and it was determined that these distributions have a maximum near the energy corresponding to single scattering at minimum angle. It was shown that the intensity angular distributions bear an exponential character, the exponential coefficient depending linearly on the atomic number of the medium. The intensity energy distributions agree with previous calculations. (tr-auth)

41954 (NP-15338) COMPUTER PROGRAMS FOR SHIELDING PROBLEMS IN MANNED SPACE VEHICLES. Hill, C. W.; Douglass, C. C. Jr.; Ritchie, W. B.; Simpson, K. M. Jr. (Lockheed-Georgia Co., Marietta). Jan. 1964. Contract NAS 8-5180. 135p. (ER-6643).

The results of an effort to extend and refine certain space radiation shielding codes and detailed code descriptions and operating instructions are presented. In particular, the approximations in the proton penetration code were examined and improved where possible. Changes include a better attenuation kernel for evaporation neutrons, parabolic rather than linear interpolation in tables, arbitrary angle of incidence for monodirectional proton beams, removal of the assumption of constant cross section within a layer, and inclusion of a source term calculation for secondary gamma rays. Three new codes were written during the present effort. Program LIGHT computes gamma ray cascades from excited nuclei. Program MSGAM computes gamma ray dose due to the distributed sources developed in the proton penetration code. Program LRSPC computes improved proton range and stopping power data for use in the proton penetration code. The production of cascade gamma rays arising from inelastic nucleon collisions with shield nuclei was examined because of conflicting results of other investigators. (auth)

41955 (ORNL-TM-1121) THE NUCLEON-MESON CASCADE INITIATED BY 200-Gev PROTONS. Alsmiller, R. G. Jr.; Barish, J. (Oak Ridge National Lab., Tenn.). May 3, 1965. Contract W-7405-eng-26. 19p. Dep. mn; CFSTI, $1.00 cy, $0.50 mn.

One-dimensional nucleon-meson cascade calculations were carried out for the case of 200-Bev protons in iron. Since there is very little information concerning particle production at such high energies, two calculations using different assumptions about this production were performed. (auth)

41956 (SC-R-65-933) SOME ELECTROMAGNETIC EFFECTS OF HIGH DENSITY GAMMA FLUX INTERACTING WITH MATTER. Taylor, Clayborne Dudley (New Mexico State Univ., University Park). May 1965. Contract AT(29-1)-789. 71p. Dep. mn; CFSTI $3.00 cy, $0.75 mn.

Sandia Corp. Monograph.

A metal slab is considered to be bombarded normally by a flux of gamma rays. As a result of this bombardment electrons are scattered from the slab with a distribution of velocities. This distribution is determined by the energies of the incident gamma rays and the slab thickness. An approximation to the velocity distribution is obtained for the case of gamma rays with the energy of 1.02 Mev—corresponding to the average energy of the gamma rays emitted from a nuclear explosion. A nonlinear integral equation describing the motion of the electrons egressing from a slab is derived. It is found to depend on the flux density of electrons egressing from the slab, and the distribution of the forward components of the electrons' velocities upon egressing from the slab, i.e., the velocity components along the normal to the slab. It is proved that the nonlinear integral equation can be solved by a method of successive approximations. Two special cases are treated: the flux density of the egressing electrons is considered to be approximately the electron flux density that is scattered from the slab by the gamma flux from a nuclear explosion, and the electrons are considered to egress from the slab with the same velocity—the average velocity of the electrons scattered from the slab by the gamma flux from a nuclear explosion, and all the electrons are considered to egress from the slab at once with a distribution of forward components of the velocities which crudely approximates the distribution for electrons scattered from the slab by the gamma flux from a nuclear explosion. After obtaining these equations of motion, the resulting electric fields are then found. It is shown that the formulation for the treatment of a slab being bombarded by gamma rays can be applied in treating the r-f radiation from a high altitude nuclear explosion. The results of this treatment are compared with those of the theory by Karzas and Latter, and a discussion of factors determining the RF radiation is presented. A monopole antenna is considered to be bombarded by a flux of gamma rays propagating normally to the axis of the antenna. As a result of this bombardment, electrons are scattered from the antenna, thus charging the antenna positively. This induces a current in the load impedance of the antenna—appearing as if the antenna were receiving a transient r-f signal. An expression for the time dependent voltage across the load impedance of the antenna is obtained by assuming that every electron scattered from the antenna never returns and that the antenna capacitance is the d-c capacitance. (auth)

41957 (UCRL-14165) FOTRAC: A MONTE CARLO PHOTON TRACING COMPUTER PROGRAM. Davies, Nan; Terrall, John (Lawrence Radiation Lab., Univ. of California, Livermore). May 20, 1965. Contract W-7405-eng-48. 9p. Dep. mn; CFSTI $1.00 cy, $0.50 mn.

FOTRAC is a computer program for performing transport calculations on photons using the Monte Carlo method. It was originally conceived as part of a larger scheme in which neutrons, transporting themselves through a configuration of media, produced photons from nuclear reactions. As development proceeded it was decided that, in addition to this source of photons, it would be convenient to provide FOTRAC with its own source generator so that it could function independently as a complete program, as well as in association with the neutron transport calculation. Results from the photon calculation are produced in the form of tables and graphs, with the standard deviations included in both forms. The graphs show crosses which indicate energy spreads as well as the statistical deviations. (auth)

41958 INVESTIGATION OF γ-RADIATION PROPAGATION IN A SUBSTANCE BY THE SIMILARITY THEORY. Makhlis, F. A.; Breger, A. Kh. (Inst. of Resin Industry, Moscow). Inzh.-Fiz. Zh., Akad. Nauk Belorussk. SSR, 8: 516-22(Apr. 1965). (In Russian).

The main principles of the application of similarity theory to the investigation of problems of the passage of radiation through a substance are considered. Basic similarity numbers are obtained. It is shown that the similarity theory can serve as the basis for simulation of problems on the propagation of radiation in a substance. The possibility of taking into account the boundary condi-

tions and the extent of radiation sources is of particular interest. (D.C.W.)

41959 CALCULATION OF ABSORBED ENERGY OF γ RADIATION. Makhlis, F. A.; Sugak, L. A.; Galkina, N. N.; Rumyantsev, S. A. (Inst. of Resin Industry, Moscow). Inzh.-Fiz. Zh., Akad. Nauk Belorussk. SSR, 8: 675-9(May 1965). (In Russian).

The distribution of absorbed energy and gamma flux is considered for the case of an isotropic point source with an energy of 1.25 Mev placed in the center of both finite and infinite hemispheres of water. Results obtained by the Monte Carlo method and by numerical integration are compared. (D.C.W.)

41960 UNSCATTERED FLUX FROM SPHERICAL AND CYLINDRICAL SOURCES WITH SHELL-SHAPED SHIELDS. Tsuruo, Akira (Japan Atomic Energy Research Inst., Tokyo). J. Nucl. Sci. Technol. (Tokyo), 2: 261-9(July 1965).

The effect of a shell-shaped shield surrounding a spherical or cylindrical source is studied. The shapes of different shields with a common attenuation parameter μt were classified into six types according to the positions of the inner and outer surfaces with respect to the source and the detector. The exact equations and their approximate formulas for unscattered fluxes from sources with shell-shaped shields were derived. The difference between the results from the approximate and the exact calculations was less than ±2% for dense and/or large sources ($\mu_s R_0 \gtrsim 4$), and ±20% for small and/or thin sources ($\mu_s R_0 \approx 0.25$). Functions expressing the effect of shield shape were also derived. This effect was very large, and sometimes reached a factor of from 2 to 10. The results of calculation for spherical sources were compared with those by Ascoli, and it was found that his approximate method has a large error for large sources and/or dense shields ($\mu R_0 \gtrsim 4$). The results of calculation for cylindrical sources agreed well with those by Taylor and Obenshain, and also with Osanov's experiments. (auth)

41961 INELASTIC SCATTERING OF ELECTRONS IN THIN FILMS. Nakhodkin, N. G.; Ostroukhov, A. A.; Romanovskii, V. A. (Shevchenko State Univ., Kiev). Soviet Phys.-Solid State (English Transl.), 7: 161-5 (July 1965).

Translated from Fiz. Tverd. Tela, 7: 210-16(Jan. 1965).

The approximation of previous papers was used to solve the transport equation for normal and oblique beam incidence with accurate regard to the emission conditions. The dependence of the transmission coefficient on film thickness for normal-beam incidence was calculated. The relation between the total electron range and the extrapolated value was investigated and agreement was observed between the extrapolated range and the electron scattering length. The dependence of the coefficient of reflection on the atomic number of the target was calculated and agreement with experimental data for both small and large numbers was found. (auth)

Solid State Physics

See also CHEMISTRY — Inorganic and Physical Chemistry
METALS, CERAMICS, AND OTHER MATERIALS — Properties and Structure

Refer also to abstract 41678.

41962 (AERE-M-967) YORK 87—A 7090-FORTRAN PROGRAMME FOR ANALYSING PHONON DISPERSION CURVES. Low, G. G. E.; Taylor, D. W.; York, E. J. (Atomic Energy Research Establishment, Harwell (England)). Dec. 1961. 7p. Dep. mn.

A FORTRAN program is described for analyzing a set of phonon dispersion data all of which correspond to propagation along one particular direction of high symmetry in a crystal. (M.O.W.)

41963 (IS-1141) THE REDUCED CELL AND ITS CRYSTALLOGRAPHIC APPLICATIONS. Lawton, Stephen L.; Jacobson, Robert A. (Ames Lab., Iowa State Univ. of Science and Tech.). Apr. 1965. Contract W-7405-eng-82. 208p. Dep. mn; CFSTI $6.00 cy, $1.25 mn.

The reduced cell and its applications to structural crystallography are described. Typical applications are its use as the standard choice of the unit cell in a triclinic lattice and the use of its scalars in identifying the cell of highest symmetry in a lattice. Two FORTRAN computer programs, which may be used to locate the reduced cell in a lattice, to calculate its parameters, and to derive the matrix for the transformation of the original cell to the reduced cell, are described. (auth)

41964 (JINR-P-2201) EFFEKTIVNOE UREMYA ZHIZNI NOSITELEI TOKA V KREMNII, KOMPENSIROVANNOM LITIEM. (Effective Lifetime of Current Carriers in Lithium-Compensated Silicon). Vasilev, V. S. (Joint Inst. for Nuclear Research, Dubna (USSR). Lab. of Nuclear Problems). 1965. 21p. Dep. mn.

Using the photoelectric method the diffusion lengths of the photoinjected electrons and holes in the lithium-compensated p-silicon were determined. According to the data obtained with several samples, the experimental values of the effective lifetimes were found to be $\tau_{el} \approx 3$ to 4 ms for electrons and $\tau_h \approx 7$ to 8 ms for holes. (auth)

41965 (LA-3309) AN INTEGRATED SERIES OF CRYSTALLOGRAPHIC COMPUTER PROGRAMS. VII. INTERATOMIC DISTANCE AND ANGLE CALCULATIONS. Larson, A. C.; Roof, R. B. Jr.; Cromer, D. T. (Los Alamos Scientific Lab., Univ. of California, N. Mex.). Jan. 1965. Contract W-7405-eng-36. 41p. Dep. mn; CFSTI, $2.00 cy, $0.50 mn.

The procedures employed and the computer program used for determining the distances between atoms in a unit cell are described. Any three atoms may be characterized by two vectors, each with an end common to one of the three atoms. The program may also be used to determine the angle between these two vectors. (auth)

41966 (LA-3310) AN INTEGRATED SERIES OF CRYSTALLOGRAPHIC COMPUTER PROGRAMS. VIII. THERMAL ELLIPSOID ORIENTATION. Larson, Allen C.; Roof, R. B. Jr.; Cromer, Don T. (Los Alamos Scientific Lab., Univ. of California, N. Mex.). Nov. 1964. Contract W-7405-eng-36. 29p. Dep. mn; CFSTI $2.00 cy, $0.50 mn.

The procedures employed and the computer program used for determining the principal axes and the orientation of anisotropic thermal ellipsoids relative to crystallographic axes are described. This information is often useful in correlating the thermal vibrations of the atoms of a single crystal with its various other physical properties. (auth)

41967 (MIT-QPR-57) SOLID-STATE AND MOLECULAR THEORY GROUP QUARTERLY PROGRESS REPORT NO. 57. (Massachusetts Inst. of Tech., Cambridge). July 15, 1965. Contract Nonr-1841(34). 65p.

Individual abstracts were prepared for two of the papers included. Papers also are included on the cohesive structure of KCl and symmetry orbitals, closed shell interactions, and crystal field potential for some molecular clusters. (M.O.W.)

For abstracts of individual papers see: 41608 and 41968.

41968 (MIT-QPR-57, pp 22-42) THE BAND STRUCTURE OF BERYLLIUM. Terrell, J. H. (Massachusetts Inst. of Tech., Cambridge).

The results of an augmented plane wave (APW) calculation of the energy bands of hexagonal close packed beryllium are presented. The APW method of computation is briefly discussed. The potential is described and a discussion of the APW method from the viewpoint of scattering theory is presented. (M.O.W.)

41969 (ORNL-TM-1153) LOW ENERGY ELECTRON AND PROTON TRANSMISSION IN ALUMINUM AND SILVER. Garber, Floyd Wayne (Oak Ridge National Lab., Tenn.).

Aug. 1965. Contract W-7405-eng-26. 117p. Dep. mn; CFSTI, $4.00 cy, $0.75 mn.

Thesis submitted to Univ. of Tennessee, Knoxville.

A technique is presented for constructing a target system that can be used to study the energy losses of low energy electrons and protons. The target system consists of a thin (150-300 Å or greater) top foil of metal, vacuum evaporated onto a thick (>2000 Å) aluminum foil having a 75 Å Al_2O_3 insulating surface on it. The electrons or protons are normally incident on the top metallic foil. The currents collected in the top foil and the bottom foil give transmission of the top foil. Using this target system the transmission of aluminum was studied for both electrons and protons. Data are presented for the range of charge versus energy for 50% transmission of the proton beam. For electrons, data are presented for 150, 200, and 250 Å top foils. These data show absorption maxima that are attributed to surface plasma excitation, volume plasma and electron-electron excitation of the conduction electrons, and L shell ionization. The threshold energy for L shell ionization is estimated to be at 115 volts. A curve is presented showing the complete transmission length of the foil as a function of the primary beam energy. Finally these curves were analyzed to give values of the stopping power of aluminum for electrons in the kilovolt energy region. Data are given showing the absorption of electrons in silver foils. The absorption maxima are attributed to volume plasmon and electron-electron excitation and M and N shell excitation. (auth)

41970 (ORNL-TM-1224) MATHEMATICAL MODELS OF DIFFUSION IN GRAIN BOUNDARIES. Barrett, Lida K. (Oak Ridge National Lab., Tenn.). [1964]. Contract W-7405-eng-26. 11p. Dep. mn; CFSTI $1.00 cy, $0.50 mn.

The mathematical models by Fisher, Whipple, and Suzuoka for diffusion in grain boundaries are given in such a way that their derivations, physical assumptions, mathematical statements, and manners of solution can be readily compared. A summary is given of the results contained in various commentary and comparison papers, including a summary of the facts that can be of use in the interpretation of experimental results. (auth)

41971 (UCRL-7968-T) STIMULATED BRILLOUIN SCATTERING. Fleck, J. A. Jr. (Lawrence Radiation Lab., Univ. of California, Livermore). July 1964. Contract W-7405-eng-48. 24p. Dep. mn; CFSTI, $1.00 cy, $0.50 mn.

A quantum mechanical hamiltonian is derived to describe the interaction between a transverse electromagnetic field and the field of acoustic waves in an isotropic solid. The coupling mechanism between the two types of field is the dependence of the dielectric permitivity on density. First order perturbation theory based on this hamiltonian is used to derive Boltzmann or gain-loss equations for the scattered photon and phonon distribution functions. These equations enable a simple and straightforward derivation of the original cross-section formulas of Brillouin for the scattering of light by thermal acoustic waves as well as a determination of the rates of stimulated scattering of light and the associated production of phonons. Conditions, which depend on the power as well as the frequency and angular spread of the laser beam, are derived for the exponential buildup of the scattered beam and associated photon. (auth)

41972 VARIATION OF THE MAGNETIC SUSCEPTIBILITY OF IRON, GADOLINIUM, AND NICKEL NEAR THE CURIE POINT. Develey, Gerard (Institut Polytechnique, Grenoble, France). Compt. Rend., 260: 4951-3(May 10, 1965). (In French).

It was verified experimentally that near the Curie point (θ_f) the susceptibility (κ) of iron, gadolinium, and nickel obey the relation $(1/\kappa)^n = p(t - \theta_f)$, with $n = 3/4$ for iron and nickel and $6/7$ for gadolinium. (tr-auth)

41973 TRANSPORT PROPERTIES OF NEODYMIUM NITRIDE AT LOW TEMPERATURE. Veyssie, Jean-Jacques; Haen, Pierre; Chaussy, Jacques; Anselin, Francois (Centre de Recherches sur les Tres, Basses Temperatures, Grenoble, France and Centre d'Etudes Nucleaires, Fontenay-aux-Roses, France). Compt. Rend., 260: 4980-3(May 10, 1965).

The strong anomaly of resistivity observed in NdN (neodymium nitride) near the Curie point was interpreted by the hypothesis of critical electron diffusion. An approximate value of the number of free electrons, compatible with results from measurements of thermoelectric power, was deduced. (tr-auth)

41974 CHARGE STATE OF DEFECTS PRODUCED BY IRRADIATION WITH ^{60}Co γ RAYS IN THE CHARGE SPACE REGION OF A SILICON SEMICONDUCTOR JUNCTION. Messier, Jean (CEN, Saclay, France). Compt. Rend., 260: 6330-3(June 14, 1965). (In French).

The charge state of the defects produced by ^{60}Co γ rays in the charge-space zone of a NPP^+ silicon junction was studied. The formation of negatively charged defects was observed. These defects were the same as those responsible for the well-known energy level at 270 Mev above the valence band. The negative charge state is due to the presence of a supplementary electron on an energy level in the middle of the forbidden band. (tr-auth)

41975 RADIATION STABILITY OF ALKALI HALIDE CRYSTALS. Vorob'ev, A. A. (Tomsk Polytechnic Inst., USSR). Izv. Akad. Nauk SSSR, Ser. Fiz., 29: 361-5(Mar. 1965). (In Russian).

Properties of alkali halide crystals are discussed with some reference to their behavior under exposure to different types and amounts of radiation. Decrease of the binding energy and of the fraction of ionic bonding reduces the activation energy of thermal microdefects and the stability of the crystal against external influences. The processes in the crystal lattice involving displacement of particles and vacancies and the formation of various defects are uniquely determined by the lattice energy. Under comparable conditions the concentration of color centers is larger the greater the lattice energy. Crystals with large total atomic number of the constituents and low lattice energy absorb more radiation but store less energy than those with greater lattice energy. It is concluded that the regularities found for alkali halide crystals apply also to other ionic crystals with Coulomb binding and that properties of crystals measured at different temperatures and pressures can not be properly compared without employing the equations of state and reducing the data to some standard conditions. (ATD)

41976 RADIATION DAMAGE IN IONIC CRYSTALS. Andronikashvili, E. L.; Politov, N. G.; Getiya, M. Sh.; Vorozheikina, L. F. Izv. Akad. Nauk SSSR, Ser. Fiz., 29: 366-70(Mar. 1965). (In Russian).

The formation of dislocations and color centers in LiF and KCl crystals by thermal neutron irradiation was investigated. The specimens were irradiated in a reactor; they were subsequently etched and the dislocations were counted by microscopic examination. In each case two specimens were cut from the same crystal; one was irradiated, the other not. Both were then etched and examined. The relative color center concentrations were found by measuring the absorption coefficients at wavelengths near (but not at the centers of) the F and M bands for LiF and the F and U bands for KCl. Neither the dislocation nor color center concentrations increased monotonically with dose. The dislocation density curve for each substance had two maxima at approximately the same doses, namely, 0.4×10.16 nvt. In LiF the second maximum was the higher one; in KCl, the first. The absorption curves for LiF also had two maxima, one at the dose corresponding to the first maximum of the dislocation density curve, and one at the dose corresponding to the second minimum of this curve. The absorption curves for KCl showed only one maximum at 0.4×10^{16} nvt. The healing of the LiF dislocations by annealing was investigated. It was found that the dislocations corresponding to the first maximum were much more slowly healed by annealing than those formed by further irradiation. It was suggested that the dislocations responsible for the first maximum are due to interstitial atoms while those that are formed by further irradiation are due to vacancies. (ATD)

41977 INDUCED LUMINESCENCE OF SILVER-ACTIVATED ALKALI HALIDE PHOSPHORS. Parfianovich, I. A.; Penzina, E. E.; Penzin, Yu. G. (Irkutsk State

Univ., USSR). Izv. Akad. Nauk SSSR, Ser. Fiz., 29: 431-3 (Mar. 1965). (In Russian).

The luminescence of NaCl, KBr, and NaBr phosphors activated with 1 mole percent silver was investigated. These phosphors have two types of activator centers: type I, responsible for the short wavelength luminescence, and type II, responsible for a longer wavelength luminescence. The nature of the B and C centers is investigated. B centers were induced in KBr : Ag by x irradiation. The phosphorescence found previously for additive induced B centers was also found for x-ray induced B centers. The phosphorescence was excited both by B band radiation and by F band radiation, and the afterglow intensity was found to be strongly temperature dependent. The B centers were optically unstable. All these results are regarded as supporting the recombination mechanism for B center emission, proposed by Kats and Nikol'skiy. C centers were induced in NaCl : Ag phosphors by x-irradiation. The C center concentration was found to increase on heating or storage of x irradiated phosphors, from which it is concluded that ionic processes are involved. The C centers are thermally the most stable of all the induced color centers, and crystals were prepared containing practically no other induced centers. The behavior of these crystals confirmed the close relation between C centers and type II activator centers proposed by Gindina and Lushchik. X irradiation was found to reduce the luminescence from type II centers, while simultaneously increasing that from C centers, and destruction of C centers by heating was found to lead to a partial restoration of the type II center concentration. C center emission could be excited not only by C band radiation (310 mμ) but also by 245 mμ radiation, and the behavior of the emission band did not depend on how it was excited. This behavior is not understood; it is suggested that transfer of energy of the C centers is involved. A similar short wavelength band was observed in the C center excitation spectrum of NaBr : Ag phosphors. (ATD)

41978 TRAPPING CENTERS IN RARE EARTH-ACTIVATED CALCIUM, STRONTIUM, AND BARIUM FLUORIDE SINGLE CRYSTALS. Arkhangel'skaya, V. A. Izv. Akad. Nauk SSSR, Ser. Fiz., 29: 454-9(Mar. 1965). (In Russian).

Earlier experimental work on the thermoluminescence and thermal bleaching of Er^{3+}, Ho^{3+}, Dy^{3+}, Nd^{3+}, and Tm^{3+} activated CaF_2, SrF_2, and BaF_2 single crystals is reviewed. The possible nature of the luminescence centers and the mechanism of their activation are discussed. It is concluded that the trapping centers and emission centers are spatially separated, and the thermoluminescence is accordingly due to a recombination process; that direct recombination of a negative charge carrier with an activator ion is excluded, and the luminescence is accordingly a sensitized process; and that the kinetics of the luminescence are pseudomonomolecular in nature. (ATD)

41979 CONCERNING TWO MECHANISMS OF PHOTOSTIMULATED ELECTRON EMISSION FROM IONIC CRYSTALS. Belkind, A. I.; Kyaembre, Kh. F. (Inst. of Physics, and Astronomy, Academy of Sciences, Estonian SSR). Izv. Akad. Nauk SSSR, Ser. Fiz., 29: 466-8(Mar. 1965). (In Russian).

Earlier experimental work on photostimulated electron emission from colored alkali halide crystals is reviewed. Results are discussed in terms of the mechanisms of photoionization emission—an F center is directly ionized by the incident photon with the emission of an energetic electron—and photothermal emission—an F center is excited by the incident photon to the 2_p level, is subsequently thermally ionized, and the resulting electron is thermally ejected from the crystal. Which mechanism predominates in a given case depends on the diffusion length of a thermal electron, the distance an energetic electron can travel in the crystal before losing its energy, the thickness of the colored layer, and the electron affinity in the crystal. (ATD)

41980 EFFECT OF RADIATION ON PHOTOSTIMULATED EMISSION FROM ALKALI HALIDE CRYSTALS. Belkind, A. I. Izv. Akad. Nauk SSSR, Ser. Fiz., 29: 469-71(Mar. 1965). (In Russian).

The formation of F centers in NaCl by 70 kv x rays filtered through 1 mm of NaCl and the accompanying increase in the photostimulated emission were investigated in order to determine whether the latter effect can be employed to investigate the former. The curves of F center concentration and photostimulated emission current (stimulated by F band radiation) versus x-ray dose were found to be very similar in shape and to consist of a rapidly rising initial portion (ascribed to the formation of F centers from vacancies initially present in the crystal) followed by a less rapidly rising section. Analysis of the curves showed that proportionality was maintained between the F-center concentration and the photostimulated emission, and that no significant formation of anion vacancies occurred within a 10^4 Å thick surface layer. It is concluded that photostimulated emission can be used for study of color center formation processes. (ATD)

41981 ELECTROSTIMULATED LUMINESCENCE OF ACTIVATED ALKALI HALIDE COMPOUNDS. Denks, V. P. Izv. Akad. Nauk SSSR, Ser. Fiz., 29: 486-9(Mar. 1965). (In Russian).

The electroluminescence of alkali halide phosphors was studied; results are discussed for KBr : Tl. The crystal phosphors were activated by x-ray or ultraviolet irradiation and subsequently subjected to a slowly pulsed or low-frequency alternating electric field of 10^4 to 3×10^4 v/cm. During the prolonged phosphorescence following activation, application of a field caused an increase in the phosphorescence intensity. After decay of the phosphorescence, emission could be stimulated by illumination with F band radiation; during such stimulated emission, application of the electric field increased the intensity. The electric field also increased the intensity of subsequent thermostimulated emission. During the decay of the luminescence stimulated by F band radiation, the ratio of the luminescence intensity with the electric field to the intensity without the field was accurately constant; this ratio was a nonlinear function of the field strength and decreased with increasing concentration of color centers. These phenomena are interpreted on the basis of the hypothesis that a color center is ionized by collision with a free carrier accelerated to optical energies by the applied field. Evidence is presented that the electric field affects electron-hole processes but has little or no effect on excitons. (ATD)

41982 SPIN-LATTICE RELAXATION OF RARE EARTH IONS. Bogachev, G. A. (Lebedev Inst. of Physics, Moscow). Izv. Vysshikh Uchebn. Zavedenii, Fiz., No. 3, 95-100(1965). (In Russian).

Crystals in which the impurity ions are surrounded by a cube consisting of eight diamagnetic particles are considered. Spin-lattice relaxation of impurity rare-earth ions in these crystals, proceeding at the expense of single-phonon processes, is studied. The relaxation time of Yb^{3+} ions in a CaF_2 lattice is calculated. Some deviation between the theoretical calculations and the experimental data is discussed. (tr-auth)

41983 ENTROPY CONTRIBUTIONS TO THE RESTORING FORCE OF A DISLOCATION KINK CHAIN. Alefeld, Georg (General Atomic Div., General Dynamics Corp., San Diego, Calif.). J. Appl. Phys., 36: 2633-41(Sept. 1965).

The application of a shear stress to a dislocation segment causes not only energy changes of the dislocation but also entropy changes. For a dislocation kink chain, the entropy change leads to a significant increase in the restoring force for dislocations which have small angles against close-packed directions. For a dislocation string, the entropy contribution to the restoring force is negligible. (auth)

41984 VOLUME COMPRESSIBILITY OF BeO AND OTHER II–VI COMPOUNDS. Cline, Carl F.; Stephens, Douglas R. (Univ. of California, Livermore). J. Appl. Phys., 36: 2869-73(Sept. 1965). (UCRL-7706).

The volume compressibilities of BeO, ZnS, CdS, CdSe, and CdTe were measured to 45 kbar. Solid-solid transi-

tions were observed in CdS, CdSe, and CdTe at 17.5, 21.3, and 31.8 kbar, respectively, with corresponding volume changes of 16.0%, 16.4%, and 16.4%. (auth)

41985 THERMALLY STIMULATED CONDUCTIVITY OF NEUTRON-IRRADIATED SILICON. Wysocki, J. J. (RCA Labs., Princeton, N. J.). J. Appl. Phys., 36: 2968-9 (Sept. 1965).

An experiment was performed in which carriers are photo-excited into trapping levels in large bandgap semiconductors at low temperatures. Thermally stimulated conductivity (TSC) measurements were made on neutron irradiated p-type silicon in order to determine the location and number of trapping levels. TSC data, which were obtained for the temperature range 300 to 370°K, are shown for heating rates of 0.1 to 1°/sec, and an upper limit of 1.7×10^{18} trapping levels per cc was found. The energy level was determined by different methods and the results were found to be in acceptable agreement with one another. (L.B.S.)

41986 ELECTRON PARAMAGNETIC RESONANCE SPECTRUM OF Yb^{3+} IONS IN SYNTHETIC $PbMoO_4$ SINGLE CRYSTALS. Kurkin, I. N.; Shekun, L. Ya. Opt. Spectry. (USSR)(English Transl.), 18: 417-18(Apr. 1965).

Translated from Optika i Spektroskopiya, 18: 738-40 (Apr. 1965).

Studies were made on the EPR spectrum of Yb^{3+} ions in synthetic $PbMoO_4$. Investigation of the angular dependence showed that all of the Yb^{3+} ions are magnetically equivalent. In the orientation H⊥z the spectrum is completely symmetrical, the lines are narrow (~10 Oe) and easily identified. For H||z the spectrum is sharply asymmetrical, the lines are broad (~100 Oe) and frequently overlap. The Hamiltonian constants were estimated in order to identify the lines. (P.C.H.)

41987 INVESTIGATION OF THE MAGNON SPECTRUM WITH NEUTRONS. Wanic, Adam (Inst. of Nuclear Physics, Krakow). Postepy Fiz., 16: 86-104(1965). (In Polish).

Methods and results of observations of exciting singular groups of magnons or spin waves are discussed. The term magnon refers to the collective excitation of the spin lattice in magnetic materials near saturation. Magnons may be treated as pseudo-particles in many cases, somewhat like phonons, Bloch electrons, and polarons that are better known in solid-state physics. Although the magnetic properties at low temperatures are related to the magnon spectrum for a given structure, investigation of this region of crystal excitation was not feasible until slow-neutron inelastic scattering techniques were applied to this problem about a decade ago. This method of crystal-lattice excitation is covered, while the method of photoexcitation, which deals with a completely different part of the crystal-lattice excitation, will be treated in a separate article. The theoretical foundations for a description of the spin lattice in terms of spin-spin coupling and for a description of neutron scattering are reviewed. Following this, the techniques of research with slow neutrons are reviewed, and the results of published experimental results are presented and compared with theoretical predictions. (TTT)

41988 SPIN ECHOES IN SOLIDS. Butterworth, J. (Atomic Energy Research Establishment, Harwell, Berks., Eng.). Proc. Phys. Soc (London), 86: 297-304(Aug. 1965).

The formation of nuclear spin echoes in the presence of combined static or quasi-static magnetic and quadrupolar perturbations is analyzed. The perturbations are assumed small in comparison with the Zeeman splitting by the applied field, and nuclear dipolar coupling is neglected. Echoes are formed by two pulses of radio-frequency excitation separated by an interval τ. Echoes appear only at $t = 2\tau$. The quadrupolar echoes at $t \neq 2\tau$ discussed previously are suppressed by the magnetic inhomogeneity. The condition for their suppression is roughly $b\tau > 1$, where b is the magnetic inhomogeneity in nuclear frequency units. The dependence of the echo amplitude at $t = 2\tau$ on the nutation angle ϕ_2 induced by the second pulse was calculated for $I = 3/2$ and $5/2$, assuming an initial 90° pulse. The variation in amplitude with ϕ_2 of the echo from the combined perturbation is different from that of echoes arising out of either a purely magnetic or purely quadrupolar perturbation. The combined echo exhibits two main maxima as ϕ_2 increases from 0° to 180°. The echo shape at the first maximum is a hybrid of magnetic and quadrupolar parentage; the second at $\phi_2 = 180°$ is purely magnetic. The echo amplitude at the first maximum is substantially greater than that of the corresponding quadrupolar echo. Experimental confirmation of some of the analytical results has been obtained from observations of the ^{127}I signal from KI and the ^{63}Cu signal from Cu-4.4 at. % Zn and Cu-1 at. % Mn alloys. (auth)

41989 NUCLEAR MAGNETIC RELAXATION IN Nb–Mo ALLOYS. Noer, R. J. (Atomic Energy Research Establishment, Harwell, Berks., Eng.). Proc. Phys. Soc. (London), 86: 309-13(Aug. 1965).

The ^{93}Nb nuclear spin-lattice relaxation time T_1 was measured at 77°K in the body-centered cubic Nb–Mo alloy system from 0 to 60 at. % Mo. T_1T decreases from 0.32 sec deg K for 100% Nb to 0.31 at 5 at. % Mo, and then increases to about 1.13 at 60 at. % Mo. These results are compared with existing measurements of electronic specific heat in the Nb–Mo system, and it is found that both can be related by a rigid two-band model only if quantities other than the densities of states are allowed to vary with composition. (auth)

41990 INTERACTION OF CHARGED PARTICLES WITH A PIEZODIELECTRIC CRYSTAL. Bass, F. G.; Gredeskul, S. A.; Kaganov, M. I. (Khar'kov State Univ.). Soviet Phys.-Solid State (English Transl.), 6: 2863-8 (June 1965).

Translated from Fiz. Tverd. Tela, 6: 3577-84(Dec. 1964).

The Cherenkov radiation of sound waves of a charged particle is calculated for propagation along the axis of a piezodielectric crystal. The coherent interaction of a compensated beam of charged particles with a piezodielectric crystal is analyzed. (auth)

41991 RESONANT SCATTERING OF PHONONS BY IMPURITY ATOMS AND ONE-PHONON COHERENT SCATTERING OF SLOW NEUTRONS. Dzyub, I. P. (Inst. of Physics, Kiev). Soviet Phys.-Solid State (English Transl.), 6: 2955-61(June 1965).

Translated from Fiz. Tverd. Tela, 6: 3691-9(Dec. 1964).

A calculation is carried out of the broadening of the one-phonon peak in the spectrum of slow neutrons scattered coherently by disordered solid solutions. The calculation is made neglecting the difference between the coupling constants of an impurity atom and an atom of the crystal matrix. It is shown that the broadening of the one-phonon peak, associated with the scattering of phonons by impurity atoms, has a resonant character and may attain a value larger than the broadening due to anharmonicity. (auth)

41992 OBSERVATION OF ELECTRON-NUCLEAR DOUBLE RESONANCE OF F-CENTERS IN KCl. Ruban, M. A.; Deigen, M. F. (Inst. of Semiconductors, Kiev). Soviet Phys.-Solid State (English Transl.), 6: 2977-8(June 1965).

Translated from Fiz. Tverd. Tela, 6: 3715-17(Dec. 1964).

Electron-nuclear double resonance spectra for coordination spheres I and II of the F-centers in KCl are shown. Measurements were carried out at room temperature with an F-center concentration of 6×10^{17} cm^{-3}. (A.G.W.)

41993 THE EFFECT OF OXYGEN IMPURITY ON THE OPTICAL PROPERTIES OF CaF_2–Sm CRYSTALS. Krotova, L. V.; Osiko, V. V.; Udovenchik, V. T. (Lebedev Inst. of Physics, Moscow). Soviet Phys.-Solid State (English Transl.), 7: 181-5(July 1965).

Translated from Fiz. Tverd. Tela, 7: 238-43(Jan. 1965).

The existence of four types of CaF_2–Sm crystals containing oxygen as impurity is demonstrated, each type being characterized by a specific arrangement of point defects and optical centers in mutual equilibrium. The effects on the absorption spectra of reduction of the trivalent Sm in the crystals by additive coloring in Ca or Mg

vapors or by γ irradiation are shown. The mechanism of the reduction of the Sm and the role of oxygen in the process are discussed. (A.G.W.)

41994 ELECTRON PARAMAGNETIC RESONANCE OF Gd^{3+} IN SYNTHETIC $SrMoO_4$. Kurkin, I. N.; Stepanov, V. G. (Kazan State Univ., Tatar SSR). Soviet Phys.-Solid State (English Transl.), 7: 223(July 1965).

Translated from Fiz. Tverd. Tela, 7: 285-6(Jan. 1965).

Observations of the electron paramagnetic resonance (EPR) of the Gd^{3+} ion in the $SrMoO_4$ lattice led to the conclusion that all the Gd^{3+} ions were magnetically equivalent and the positions of the EPR lines of these ions were given by the usual spin hamiltonian of tetragonal symmetry with an effective spin $S = 1/2$. The spin-hamiltonian constants were determined; they are tabulated and compared with similar data for $PbMoO_4$. (A.G.W.)

41995 RELAXATION OF RARE-EARTH IONS. Bogachev, G. A. (Lebedev Inst. of Physics, Moscow). Soviet Phys.-Solid State (English Transl.), 7: 243-4(July 1965).

Translated from Fiz. Tverd. Tela, 7: 306-7(Jan. 1965).

A formula for the relaxation time of rare earth ions in the case of one-phonon processes is obtained by expanding the spin-phonon interaction hamiltonian in coordinates Q_0 of the normal vibration modes. The only parameter determined from experimental data is the effective charge of the diamagnetic ions of the surrounding medium. The formula is applied to Yb^{3+} in a fluorite lattice, and satisfactory agreement with experiment is obtained. (A.G.W.)

41996 INVESTIGATION OF THE THERMAL VIBRATIONS OF THE ATOMS IN COPPER BY NEUTRON SPECTROMETRY. Vintaikin, E. Z.; Gorbachev, V. V.; Gruzin, P. L. Soviet Phys.-Solid State (English Transl.), 7: 296-9(Aug. 1965).

Translated from Fiz. Tverd. Tela, 7: 367-71(Feb. 1965).

A description is given of the instrument used to determine the dispersion relations from inelastic neutron scattering. Results are given of a determination of the dispersion relations for the copper lattice in the [100], [110], and [111] directions. The results are compared with x-ray data. (auth)

41997 THEORY OF THE MOESSBAUER EFFECT IN NONIDEAL CRYSTALS. Dzyub, I. P. (Inst. of Physics, Kiev). Soviet Phys.-Solid State (English Transl.), 7: 300-4(Aug. 1965).

Translated from Fiz. Tverd. Tela, 7: 372-8(Feb. 1965).

The dependence of the Mössbauer line intensity and its temperature shift on the impurity atom concentration is investigated, considering only the difference between the masses of the impurity atom and of the atom of the crystal matrix. The theoretical results are compared with the existing experimental data. (auth)

41998 RADIATION DEFECTS IN VERY PURE SILICON CRYSTALS. Vavilov, V. S.; Vintovkin, S. I.; Lyutovich, A. S.; Plotnikov, A. F.; Sokolova, A. A. (Lebedev Inst. of Physics, Moscow). Soviet Phys.-Solid State (English Transl.), 7: 399-402(Aug. 1965).

Translated from Fiz. Tverd. Tela, 7: 502-5(Feb. 1965).

The photoconductivity spectra of very pure p-type Si single crystals both before and after irradiation by electrons with energy of about 1 Mev are described. It is shown that the purification process was very successful for all impurities except boron. Crystals grown by the floating zone method have oxygen concentrations of about 10^{16} atoms/cm^3. When such ultrapure crystals are irradiated by electrons at liquid-nitrogen temperature, a continuous distribution of allowed levels is introduced into the forbidden-energy gap; these levels are evidently associated with the point defects produced by irradiation. If a crystal with a low oxygen concentration is heated to room temperature, only one level, located at $E_v + 0.45$ ev, is detected. If the crystal has a considerable concentration of oxygen atoms, three levels, at $E_c - 0.16$, $E_v + 0.30$, and $E_v + 0.45$ ev, are observed in the crystal after heating. Special features of the effects on resistivity and minority-carrier lifetime of electron-irradiated ultrapure Si crystals are noted. (A.G.W.)

41999 ON THE NEW ELECTRON PARAMAGNETIC RESONANCE SPECTRUM OF NEODYMIUM IN CaF_2 SINGLE CRYSTALS. Kask, N. E.; Kornienko, L. S. (Moscow State Univ.). Soviet Phys.-Solid State (English Transl.), 7: 497-9 (Aug. 1965).

Translated from Fiz. Tverd. Tela, 7: 625-8(Feb. 1965).

A new electron paramagnetic resonance of Nd ions in CaF_2 was discovered. A resonance takes place between initially split levels. It is assumed that the spectrum pertains to a neodymium ion in the tetravalent state. Constants of the spin hamiltonian are measured, and the temperature dependence of the spin-lattice relaxation time is derived. (auth)

42000 RELAXATION PROCESSES IN PARAMAGNETIC RESONANCE OF U^{3+} AND Tb^{3+} IN CaF_2. Berulava, B. G.; Sanadze, T. I.; Khakhanashvili, O. G. (Tiflis State Univ., Georgian SSR). Soviet Phys.-Solid State (English Transl.), 7: 509-10(Aug. 1965).

Translated from Fiz. Tverd. Tela, 7: 640-2(Feb. 1965).

Spin-lattice relaxation processes were studied for U^{3+} and Tb^{3+} in CaF_2 crystals so selected that the added ions were located solely in a tetragonal environment. Concentrations of 0.02, 0.05, and 0.12% U^{3+} and 0.005 and 0.05% Tb^{3+} were used. Measurements of the relaxation times in the temperature range 1.5–4.2°K showed that for both ions the relaxation mechanism is due to direct one-phonon processes. In the temperature range 10–15°K the relaxation process goes through the upper excited level. (A.G.W.)

42001 SOME PROPERTIES OF DYNAMIC NUCLEAR ORIENTATION (thesis). Misra, Sushil Kumar. St. Louis, St. Louis Univ., 1964. 160p.

For the 28 cases of nuclear polarization investigated by Barker, calculations of the enhancement of the nuclear magnetic resonance and the steady-state entropy and heat capacity were carried out. These are valid for low temperatures where the linear approximation to the Boltzmann factor is not applicable. The results are consistent with the Gibbs relation and the third law of thermodynamics. The relative intensity ratio: $R(\nu) \equiv (I_\infty - I_t(\nu))/(I_\infty - I_t(-\nu))$ for a transmission-type Mössbauer spectrum was computed for the 14.4-kev gammas obtained in the decay of dynamically oriented ^{57}Co. The numerical results indicate that $R(\nu)$ is appreciably different for the oriented as compared to the unoriented case. The Mössbauer radiation host is assumed to supply unpaired electrons interacting with the ^{57}Co nuclei. A sufficiently strong magnetic field is assumed so that the Zeeman components of the Mössbauer radiation are well resolved. The hyperfine and quadrupole interaction admix the wave functions so that forbidden transitions may be induced in the ^{57}Co nuclear-electron spin coupled system by a pumping radiation field of frequency $\nu_e + 2\nu_n$. Theoretical expressions are obtained for a cold source and a warm absorber at arbitrary relative orientations of source and absorber quantization axes. Numerical results for a source temperature 1°K and a static field 100 kg indicate that the Mössbauer effect may be used to test the nature of the static and dynamic spin coupling of unstable nuclei in solids. (Dissertation Abstr.)

42002 DISLOCATION INTERSTITIAL INTERACTIONS IN SINGLE CRYSTAL TUNGSTEN AND TANTALUM (thesis). Carpenter, Steve Haycock. Salt Lake City, Univ. of Utah, 1964. 83p.

Dislocation-interstitial interactions were investigated in zone-melted single crystal tungsten and tantalum by means of internal friction measurements. A Marx piezoelectric composite oscillator resonating at 50 kc/sec was used to measure the log. decrement as a function of time, temperature, and strain amplitude. Measurements on slightly cold worked single crystal tungsten showed that at temperatures above 400°C the amplitude independent damping decreases with time and the strain amplitude necessary for breakaway increases. These effects are explained in terms of the diffusion of interstitial impurities, according to the $t^{\frac{1}{3}}$ law of Cottrell and Bilby, to the dislocation lines pinning them and rendering them immobile. An activation energy for the process was found to be 47,000 ± 5,000 cal/mole. The interstitial was not identified.

Damping measurements on single crystal tantalum indicate that two separate pinning processes occur in the 0 to 100°C temperature range. In the 0 to 25°C range, the amplitude independent damping measured immediately following deformation (~1%) was found to decrease with time. No change in the amplitude dependence was detected. This is called stage one pinning. The relaxation time for stage one pinning was found to be too short to allow for the long range diffusion of interstitials required for Cottrell type pinning. The activation energy for the stage one process was found to be 23,500 ± 3,000 cal/mole. A value consistent with the diffusional energy of oxygen in tantalum. Increasing the test temperature to the 75 to 100°C range was found to cause a further reduction of the amplitude independent damping with time. A decrease in the amplitude dependence was also observed. This is called stage two pinning. Stage two pinning was identified as the same type of pinning process as that observed in the tungsten. It is satisfactorily explained by the Cottrell type pinning of the dislocation lines by solute interstitial oxygen atoms. (Dissertation Abstr.)

42003 THE FERMI SURFACE OF TUNGSTEN AND MOLYBDENUM BY THE DE HAAS-VAN ALPHEN EFFECT (thesis). Sparlin, Don Merle. Evanston, Ill., Northwestern Univ., 1964. 139p.

Torsion measurements of the de Haas–van Alphen (dHvA) effect in single crystals of tungsten and molybdenum were made in fields to 34 kgauss. Manual methods of analysis are given for the complicated oscillatory curves obtained from these measurements; geometrical parameters of the Fermi surfaces were obtained as results. The Fermi surface parameters obtained from these measurements were compared with those obtained from measurements of the magnetoresistance, the magnetoacoustic attenuation, the anomalous skin effect, cyclotron resonance, the dHvA effect by pulsed fields, and other low-field torsion measurements of the dHvA effect. The Lomer topology for the Fermi surface of the group (VI) metals chromium, molybdenum, and tungsten was compared with the experimental results. The modifications to the Lomer model suggested by this comparison was found to be incorporated in a Fermi surface model obtained by a re-interpretation of the Lomer band diagrams. A semi-quantitative fit of this modified Fermi surface model was then made to the experimental results for tungsten and molybdenum. The resulting Fermi surface models for tungsten and molybdenum are shown to be in agreement with the number of carriers, connectivity of surfaces, total surface area, extremal dimensions, and cyclotron effective masses given as results by others. (Dissertation Abstr.)

42004 SOLID STATE AND LOW TEMPERATURE PHYSICS IN THE USSR. A Survey. Paris, Organisation for Economic Co-Operation and Development, 1964. 155p. $3.00; 17 s. 6d.; F 12; Sw fr. 12; DM 10.

A survey is given of work done in the USSR on several aspects of solid state and of low temperature physics. The discussion is more slanted toward theory than toward experiments. The topics discussed are liquid helium, superconductivity, magnetic resonance, Fermi surfaces, magnetism, semiconductors, and cryogenic techniques. Extensive lists of references are included. (J.F.P.)

42005 MAGNETIC BEHAVIOR OF RARE EARTH METALS AT HIGH PRESSURES. Robinson, Lawrence Baylor (Univ. of California, Los Angeles); Milstein, Frederick; Tan, Swie-In; Sterrett, K. F. 23p. (CONF-650423-3). Gmelin, AED-CONF-65-058-7.

From International Conference on Physics of Solids and High Pressures, Tucson, Ariz.

Experimental investigations were made of the effect of hydrostatic pressure on the magnetic transition temperatures of gadolinium, terbium, and dysprosium. Results are presented of the direct magnetic measurement of pressure effect on Néel temperature to 25 kilobars, measurement of magnetic transitions at 40°K and 25 kbar simultaneously, and observations of the disappearance of the Curie point on an element with increasing pressure. (L.B.S.)

REACTOR TECHNOLOGY

General

Refer also to abstract 40396.

42006 (IDO-10043(Vol. II) (Rev. 1)) ACCIDENT RECOVERY EQUIPMENT STUDY—AEC-DRD REACTORS. VOLUME II. (Babcock and Wilcox Co., Lynchburg, Va. Atomic Energy Div.). June 1965. Contract AT(10-1)-1202. 300p. Dep. mn; CFSTI $6.00 cy, 5 mn.

Past reactor accidents throughout the world are reviewed from the viewpoint of problems involved and equipment used in radioactivity recovery. Twenty-seven power, experimental and test, maritime and space propulsion, production, and power-prototype reactors are chosen for illustrative purposes, and for these reactors various information is surveyed, including: required recovery equipment; available recovery equipment; reactor parameters; problems associated with radioactivity recovery following accidents; and general safety aspects, as revealed by questionnaires. (T.F.H.)

42007 (MIT-2344-3) HEAVY WATER LATTICE PROJECT ANNUAL REPORT. Lanning, D. D.; Kaplan, I.; Clikeman, F. M. (eds.) (Massachusetts Inst. of Tech., Cambridge, Dept. of Nuclear Engineering). Sept. 30, 1964. Contract AT(30-1)-2344. 182p. (MITNE-60). Dep.(mn); $5.00(cy), 4(mn) CFSTI.

Separate abstracts were prepared for the nine sections of the report. (M.O.W.)

For abstracts of individual sections see: 41641, 41672, and 42043–42049.

42008 (ORNL-NSIC-5(Vol.I and II)) U. S. REACTOR CONTAINMENT TECHNOLOGY. A Compilation of Current Practice in Analysis, Design, Construction, Test, and Operation. Cottrell, William B.; Savolainen, A. W. (eds.) Oak Ridge National Lab., Tenn. and Bechtel Corp., San Francisco, Calif.). Aug. 1965. Contract W-7405-eng-26. 1447p. Dep. mn; CFSTI $14.00 cy, $5.75 mn.

A compilation of information on current practice in analysis, design, construction, test, and operation of reactors is presented. The included information attempts to describe the containment features of existing reactor installations, describe some of the calculational techniques that were employed to determine fluid dynamics and radiological loads on containment systems, present experimental data pertinent to items 1 and 2, describe pertinent details of the design, construction, and test of containment systems, present existing data on the cost of containment systems, and to review the current research and development pertinent to the above items. (M.O.W.)

42009 (WAPD-T-1811) HEAT TRANSFER ASPECTS OF THE LOSS OF COOLANT ACCIDENT. Margolis, S. G.; Redfield, J. A. (Bettis Atomic Power Lab., Pittsburgh, Pa.). Aug. 1965. Contract AT(11-1)-Gen-14. 7p. CONF-650920–1). Dep. mn; CFSTI, $1.00 cy, $0.50 mn.

From ASME–AIChE Heat Transfer Conference, Los Angeles.

A simple model for calculating what might occur during a loss of coolant accident is presented. An attempt was made to imbed explicit heat transfer calculations in an overall description of system behavior. (M.O.W.)

42010 A STUDY OF XENON POISONING IN A NUCLEAR REACTOR. Carlson, Alan (Electronic Associates, Inc.). Inst. Control Systems, 38: 165-7(May 1965).

Two nuclides of particular interest as reactor poisons because of their high cross sections are ^{135}Xe and ^{149}Sm. The xenon decay reaction involves over 5% of the direct fission products, as compared to ~1.5% in the case of samarium. For this reason, and the fact that the xenon cross section is ~100 times that of samarium, the effect of it alone is considered. When a reactor is started up and brought to a constant power level, the xenon concentration, initially zero, also rises to an equilibrium value. At this equilbrium concentration, the magnitude of which depends on the reactor flux (or power level), the rate of formation of ^{135}Xe from ^{135}I and direct fission products is counterbalanced by the rate of burnup (by capture of a neutron) to ^{136}Xe and decay to ^{135}Cs. Thus, the poison concentration will remain constant as long as the flux is constant. When the reactor is shut down, ^{135}Xe can no longer burnup to ^{136}Xe, and no more ^{135}I can be formed from the direct fission product, ^{135}Te. Since ^{135}I decays faster than ^{135}Xe, the ^{135}Xe concentration initially builds up, but eventually decreases. If reactor shutdown is for a short period of time (e.g., a few hours), it may not be possible to start the reactor again until the ^{135}Xe concentration is considerably reduced. This occurs when the built-in reactivity of the fuel is not sufficient to overcome the effect of the elevated xenon concentration. A mathematical model was developed and equations were derived to relate the following parameters to ^{135}Xe accumulation: the ratio of neutrons absorbed by poisons (or iodine) to neutrons absorbed by fuel (θ, or Γ), the decay constant of ^{135}Xe (or ^{135}I) (λ_1 or λ_2), the time scaling factor (β), and the thermal neutron flux (ϕ). These equations describe the formation of ^{135}I and ^{135}Xe for reactor startup and steady-state operation. Computer programming was used to investigate the system for fluxes of 2.5, 1.0, and 0.25×10^{14} neutrons/cm^2-sec, which are typical of modern reactors. The maximum value of θ occurs during the shutdown of the reactor when Γ is somewhere between its maximum and zero. Therefore, it was assumed that Γ was at one-half its maximum value. Equations were mechanized on a PACE TR-20 general-purpose analog computer; and results for 3 values of the neutron flux are shown. It is possible to ascertain from these results how long a reactor must be shut down due to the xenon buildup during this period. For example, if a reactor was designed so that its fuel produces a 10% excess of neutrons to compensate for reactor poisons, the maximum value of θ would be 0.10 when the reactor was critical. Thus, it would take shutdown periods of 36 and 50 hr for fluxes of 1.0 and 2.5×10^{15}, respectively, before startup could be effected. However, if the reactor was designed for a flux of 2.5×10^{13}, no waiting period would be necessary. This mechanization of the xenon-poisoning equations for the constant-flux case is applicable to more complex reactor simulations where the flux is a variable. (BBB)

42011 DETERMINATION OF A MIXING COEFFICIENT IN A FLUIDIZED-BED REACTOR. Burovoi, I. A.; Svetozarova, G. I. Inzh.-Fiz. Zh., Akad. Nauk Belorussk. SSR, 8: 627-31(May 1965). (In Russian).

The methods are described for determining the mixing coefficient in a fluidized-bed reactor by means of mathematical models. Using the mathematical model of the drying process of a granular material in a fluidized bed, mixing coefficients for three sizes of particles are determined by comparison of experimental curves of the moisture content distribution along the furnace length with predicted curves. (auth)

42012 ON ONE PROBLEM OF OPTIMIZATION OF A SYSTEM WITH DISTRIBUTED PARAMETERS. Volin, Yu. M.; Ostrovskii, G. M. Prikl. Mat. i Mekhan., 29: 593-8(1965).

The problem of optimizing a series of reactors is studied. Each reactor is described by a system of differential equations. The necessary optimal conditions are derived, and the application of an approximation method in finding optimal values of control variables is discussed. (L.B.S.)

42013 ON THE NUMERICAL SOLUTION OF ONE PROBLEM ON OPTIMUM NUCLEAR REACTOR CONTROL. Leonchuk, M. P.; Trofimov, A. S.; Kurbatov, I. M. Zh. Vychislitel. Mat. i Mat. Fiz., 5: 558-60(May-June 1965). (In Russian).

The optimization of a reactor described by a system of equations with partial derivatives is solved by means of direct and integral relations. The optimized transient operation of a reactor involves processes taking place for the shortest permissible time, during which the operating parameters are kept within preset limits. These limits may refer to critical phenomena in the reactor channels, maximum and minimum temperatures, and the load capacity of the plant and of the control system. Equations may be derived to protect the overall system against sudden heating of the coolant. A computer solution of an actual case is presented, assuming that the heat exchange process does not change. The derived curves indicated that the coolant temperature did not exceed the set limit at its exit from the reactor, as the parameters followed an asymptotic course. The method used may be of interest for determining the flow rate, thus optimizing the pumping conditions. (TTT)

42014 EXPERIMENTAL REACTOR ANALYSIS AND RADIATION MEASUREMENTS. Glower, Donald D. McGraw-Hill Series in Nuclear Engineering. New York, McGraw-Hill Book Co., 1965. 360p. $13.50.

An integrated experimental text for graduate level laboratory courses in nuclear science and engineering is presented. Basic quantum particle detection techniques are examined as pertinent to the particles found in a nuclear reactor. Different measuring techniques and basic concepts are illustrated. (J.F.P.)

42015 IMPROVEMENTS RELATING TO COOLANT FOR NUCLEAR REACTORS HAVING GRAPHITE MODERATORS. Tomlinson, Michael; Lind, Robert (to United Kingdom Atomic Energy Authority). British Patent 997,209. July 7, 1965. Filed Nov. 14, 1962.

In the operation of a graphite moderated reactor using CO_2 as a coolant contacting the graphite, a method is provided of inhibiting the reaction between the graphite moderator and the coolant. The addition of sulfur or iodine, preferably in the form of SO_2 or elemental iodine, in the range of up to 5 vol % and the addition of CO in the range of 0.5 to 10 vol % inhibits the reaction. (B.L.M.)

42016 LIQUID HOMOGENEOUS NUCLEAR REACTOR POWER LEVEL CONTROL. Kersten, Johannes A. H. (to Stichting Reactor Centrum). Canadian Patent 711,365. June 8, 1965. Priority date Dec. 30, 1960, Netherlands.

An apparatus is described for the fine control of the power level in a suspension nuclear reactor. When a change in the neutron flux occurs resulting from a power fluctuation, an electrolyte is added to the circulating suspension which affects H or D concentration. Small power fluctuations and the resulting undesirable temperature and pressure changes are eliminated. (F.S.A.)

Auxiliaries and Components

42017 (IS-1219) DESIGN CONSIDERATIONS FOR A SYSTEM TO INVESTIGATE SHORT-LIVED NUCLEI PRODUCED AT A REACTOR. Talbert, W. L. Jr.; Thomas, David (Ames Lab., Iowa State Univ. of Science and Tech.). [1964]. Contract W-7405-eng-42. 20p. (CONF-650627-2). Dep. mn; CFSTI, $1.00 cy, $0.50 mn.

From Conference on Electromagnetic Isotope Separators and Related Ion Accelerators, and Their Applications to Physics, Aarhus, Denmark.

A system for the precision study of the nuclear decays of short-lived nuclei produced by neutron irradiation is described. The system as envisioned will employ continuous introduction of irradiated material into the ion source of an electromagnetic isotope separator and subsequent "on-line" operation of the separator in connection with nuclear decay analysis apparatus. The results of an empirical study are presented regarding the characteristics of a vapor transport line used for the extraction of irradiated material from the vicinity of the reactor core and transport to the isotope separator ion source. Of particular interest in this study are the transit times achieved with the system and properties of the system associated with the presence of electrical discharge in the vapor transport line. Extensions of the results of this study to an actual system are discussed. (auth)

42018 (NAA-SR-10100) CONVENTIONAL BUILDINGS FOR REACTOR CONTAINMENT. (Atomics International, Canoga Park, Calif.). July 25, 1965. Contract AT-11-1-GEN-8. 453p. Dep. mn; CFSTI, $7.53 cy, $2.25 mn.

Measurements were made of the air-leakage rates through structural components of conventional metal-panel and concrete buildings which may serve as containment for nuclear reactors. The component measurements included structural penetrations such as doors and louvers as well as materials such as caulking compounds, gaskets, and paints. Specimens were sealed inside of test vessels. Pressure differentials were generated across the specimen with each component installed in the manner of typical construction techniques. From measurements of the pressure difference as a function of time, the volumetric leak rates were computed. After the major leak paths were determined, additional tests were made with improved methods of construction. A detailed description and the results of every completed test are presented. Leak-rate analytic expressions using the empirical constants resulting from these tests are presented; these predict the flow rates through building components as a function of size, method of construction, and pressure difference. The forms of the equations are such that the total leak rate of a building of any size can be computed for any excess pressure for which the component data are valid. Metal-panel and concrete models were constructed and tested; the results verified the calculations. Detailed design configurations are presented for applications of the tested specimens in constructing and/or estimating leakage of a real structure. Limitations in the applicability, design and construction of low-leakage conventional structures are delineated. Methods are described for estimating leak rates, locating leak paths, and measuring the leakage rate of completed structures. (auth)

42019 (ORNL-tr-669) PROCESS AND EQUIPMENT FOR THE CONTROL OF A NUCLEAR REACTOR. Clawley, William Edgar. Translated for Oak Ridge National Lab., Tenn. from French Patent No. 1,329,117. June 4, 1962. 9p. Dep. mn; JCL, $1.10 fs, $0.80 mf.

An invention is described for the process and equipment for the control of a nuclear reactor, and more particularly, a process permitting the control of a nuclear reactor during startup after a period of shutdown. The invention applies specifically to natural uranium, graphite-moderated and water-cooled nuclear reactors which contain more than the optimum quantity of moderator compared to the fuel. (M.O.W.)

42020 FOG COOLANT TECHNOLOGY AND ITS APPLICATION TO NUCLEAR REACTORS. Sofer, George A. (United Nuclear Corp., White Plains, N. Y.). Chem. Eng. Progr., 60: Symp. Ser., No. 51, 119-27(1964).

A comprehensive summary of fog coolant technology and potential applications to nuclear reactors is presented, incorporating burnout and hydrodynamic data. (auth)

42021 COMPUTER SIZES PARAMETERS OF A PNEUMATIC SCRAM SYSTEM. Larson, Ralph H. (Bendix Corp., Southfield, Mich.). Hydraulics Pneumatics, 17: No. 10, 94-101(Oct. 1964).

The parameters of a completely pneumatic scram system for use in an extreme environment (1200°F and 10^8 rads) were optimized by simulation on a digital computer. The system is described, and the mathematical model used in the simulation is summarized, together with the derivation of the equations. (D.C.W.)

42022 RELIABILITY CONSIDERATIONS FOR AUTOMATIC PROTECTIVE SYSTEMS. Green, A. E.; Bourne, A. J. Nucl. Eng., 10: 303-6(Aug. 1965).

Predictions of the reliability of automatic protective systems for reactors are dependent on mathematical techniques and probability distributions, which fit the observed facts. Safety assessments of the systems are based on performance such as response, accuracy, and efficacy. (F.J.H.)

42023 LONG-TIME OPERATIONAL BEHAVIOR OF A HIGH POWER PRESSURIZED WATER REACTOR WITH BORON TRIMMING (CHEMICAL SHIM). Frei, Gerhard; Orth, Karl-Heinz (Siemens-Schuckertwerke AG, Erlangen, Ger.). Nukleonik, 7: 231-6(May 1965). (In German).

Pressurized water reactors offer the possibility of equalizing high excess reactivities and slowly occurring reactivity changes by using an adjustable concentration of a neutron absorber dissolved in the coolant water. For various fuel loadings, the necessary concentration variations were introduced not by hand, but by a control system. The operational behavior of such a concentration control system was investigated. (tr-auth)

42024 DEVELOPMENT OF RADIOGRAPHIC AND ULTRASONIC METHODS OF INSPECTING NUCLEAR REACTOR PRESSURE VESSELS. Hanstock, R. F. pp 249-54 of Non-Destructive Testing. London, Butterworths, 1964.

The use of ^{60}Co sources and high-voltage x-ray generators for site radiography of welds in thick steel pressure vessels for nuclear reactors is discussed. The limitations of radiography for detection of cracks and the problems of shielding intense sources of gamma or x rays led to an examination and development of ultrasonic techniques for inspection of nozzle welds and butt welds in thick sections. The development of a four-probe system of inspecting butt welds by mechanical scanning is described. (auth)

42025 AUTOMATIC ULTRASONIC INSPECTION OF NOZZLE WELDS IN NUCLEAR REACTOR PRESSURE VESSELS. Hanstead, P. D.; McElwee, I. pp 255-60 of Non-Destructive Testing. London, Butterworths, 1964.

The steel pressure vessels of nuclear reactors used for power production have a number of nozzles welded into the top part of the vessel. A device is described, which permits the automatic inspection of these welds. An immersion technique is used and the information is recorded on film as a number of separate frames, each frame representing a pictorial cross section of the weld. The information recorded allows the magnitude of the echo from any defect to be determined as well as defining its position in three dimensions. (auth)

42026 PUMPS FOR NUCLEAR SERVICE. Bunke, A. L.; Ball, R. E. 15p. (CONF-650429-16). ORINS. From American Power Conference, Chicago.

Nuclear pumps for boiling water, pressurized water, sodium graphite, fast breeder, organic and gas-cooled graphite reactors are discussed. Basic design considerations and some manufacturing and testing procedures that insure reliability in severe operating conditions are presented. A brief description of the reactor system is given along with the corresponding pump requirements. Canned motor pumps, shaft-sealed pumps, mechanical face-type seals, breakdown throttle bushings, and breakdown throttle bushings with back-up mechanical face-type seals are discussed. (L.B.S.)

42027 IMPROVEMENTS IN OR RELATING TO GRABS. Bellinger, Ronald; Wills, Stanley Charles Frederick (to Strachan and Henshaw Ltd.). British Patent 997,413. July 7, 1965. Filed Jan. 27, 1961.

A mechanically operated grab having sequential movements gravitationally actuated includes a casing member carrying the nose of the grab. A movable jaw actuating member is mounted on the casing member for movement axially to the casing, and cam surfaces are provided on the actuating member. At least three jaws mounted in the casing member and operatively associated with the cam surfaces are provided for movement to and from the engaging and disengaging positions. A pawl is associated between the actuating member and the casing member to restrain movement of the casing member to the jaw engaging position. Pawl actuating means are provided in association with the actuating and casing members. Preferably, the pawl actuating means includes a resetting member mounted in and axially movable to the casing member and operated on disengagement from a load that has been disposed in the jaws. The pawl actuating means includes a two-arm lever pivoted coaxially with the pawl and a link pivoted at one end to one arm of the lever and pivotally and slidably mounted in the casing member to be moved into and out of contact relation of the actuating member. The other arm of the lever lies in the path of the resetting member. A cam-shaped surface and a second latch pivotally mounted in the casing member form the actuating member and serve to prevent the actuating member moving downwardly until the resetting member is lifted by engagement with a load disposed in the jaws. (B.L.M.)

42028 IMPROVEMENTS IN NUCLEAR REACTORS. (to Societe Anglo-Belge Vulcain S.A.). British Patent 998,540. July 14, 1965. Priority date May 24, 1961, Belgium.

The reactivity of a nuclear reactor is controlled by a liquid moderator and by movable elements adapted to penetrate into the core to a variable extent and having a moderating capacity different to that of the moderator inside which they are displaced. The movable elements may comprise solid masses of chambers containing a fluid moderator. The volume occupied by the movable elements, when being displaced, varies uniformly and similarly in cross sectional area along the direction of displacement of the elements. (B.L.M.)

42029 NUCLEAR REACTOR CONTROL SYSTEMS. Ashcroft, David John (to United Kingdom Atomic Energy Authority). British Patent 998,933. July 21, 1965. Filed Sept. 20, 1962.

A reactor control system consists of two control members containing neutron absorbing material and independent means for driving the members into and out from opposite ends of the reactor core through a channel. One member is a rigid rod, and the other is a flexible coherent train of bodies, preferably ball shaped, that enter the channel at the bottom end and may be driven through the channel by gas pressure. Associated with each train is an associated mechanism that serves as a combined locking means and a secondary drive means for the bodies. (B.L.M.)

42030 IMPROVEMENTS IN NUCLEAR REACTORS. (to Societe Anglo-Belge Vulcain S.A.). British Patent 999,005. July 21, 1965. Priority date Feb. 28, 1961, Belgium.

A method for controlling under normal operation the reactivity of a fluid moderated reactor consists of varying the temperature and composition of the moderator to retain the moderator temperature within a band defined by predetermined upper and lower temperature limits. With particular application to heavy water–light water reactors, the method eliminates the heavy water reconcentration plant on the reactor site or allows the substantial reduction in plant capacity. The moderator flows in a separate circuit by either natural or forced flow through the reactor. A heat exchanger is provided through which a fluid is passed to provide an exchange of heat between itself and the fluid moderator. A regulating circuit is provided in which flows either the moderator itself or a regulating fluid of an identical nature or of a different nature from that of the coolant and/or the moderator. At various stages of core burnup, the regulating circuit controls the reactivity by the variation of temperature so that the lower limit of temperature of at least a part of the moderator is chosen at a value still permitting a useful utilization of the heat absorbed by the moderator inside the core. The upper limit of temperature is equal to, or close to, the temperature of saturation of the moderator liquid under normal power operation. For a heavy water–light water reactor, as the core burnup proceeds from one stage to another, the concentration of light water is brought to a value at the commencement of each new stage that is higher than that existing during the previous stage. Shut-off rods are provided that may also be utilized as regulating rods. (B.L.M.)

42031 IMPROVEMENTS IN NUCLEAR REACTORS. (to Societe Anglo-Belge Vulcain, S.A.). British Patent 999,006. July 21, 1965. Priority date Feb. 28, 1961, Belgium.

In a method for operating a nuclear reactor with a fluid moderator the reactivity of the reactor is controlled by

deliberately varying the temperature of the moderator within a band defined between upper and lower temperature limits during normal operation. The coolant and moderator of the reactor must be seapaate and flow in separate circuits. (B.L.M.)

42032 METHOD OF AND DEVICE FOR OPERATING A LOADING MACHINE FOR ATOMIC REACTORS. Kumpt, Hermann; Weber, Robert; Ropers, Johann; Schubert, Franz (to Siemans-Schuckertwerke AG). Canadian Patent 703,560. Feb. 9, 1965. Priority date June 30, 1961, Germany.

A method is outlined for maintaining a flow of coolant gas or liquid in the loading device at approximately the same temperature as the reactor so that undesirable expansion or contraction will not occur at the locking-on faces. Means are provided for avoiding sudden pressure changes. Pressure can be maintained in the loading machine containing a fuel element while out of contact with the reactor face. Testing for leaks is carried out before the fuel change. (F.S.A.)

42033 NUCLEAR REACTOR CONTROL ROD OPERATING DEVICE. Filloleau, Etienne; Haffemayer, Marcel; Maulard, Jean (to Commissariat a l'Energie Atomique). Canadian Patent 712,250. June 22, 1965. Priority date June 27, 1961, France.

In a breeder reactor cooled by molten metal, each boron control rod is operated by a differential gear having an output element which produces the displacement of the rod. There is also a first input element adapted to be rotated in both directions and a second input element adapted for rotation in a direction that moves the control toward its safety position (downward) by a magnetic actuating mechanism. Silicones provide required lubrication. (F.S.A.)

Criticality Studies

See also PHYSICS — Criticality Studies.

Refer also to abstract 42077.

42034 (AAEC/E-134) A METHOD FOR CALCULATING THE REACTIVITY WORTH OF PARTIALLY INSERTED CONTROL RODS USING TWO-DIMENSIONAL GEOMETRY. Spinks, N. (Australian Atomic Energy Commission Research Establishment, Lucas Heights). Apr. 1965. 14p. Dep. mn.

The three-dimensional problem of a reactor with partially inserted control rods is reduced to a two-dimensional problem by a redistribution of control material within the reactor. The transformation is exact when the pitch circle radius of the rods and the depth of insertion of the rods into the reactor are large compared with the control rod pitch. The effect of variations in pitch on the accuracy of the transformation is investigated by calculation. (auth)

42035 (ANL-6590) SPECTRAL REPRESENTATION AND CRITICALITY PROBLEM OF A TWO-REGION CELL TRANSPORT OPERATOR. Pollack, Israel; Bareiss, Erwin (Argonne National Lab., Ill.). Mar. 1965. Contract W-31-109-eng-38. 41p. Dep. mn; CFSTI, $2.00 cy, $0.50 mn.

It is shown that the method introduced by K. M. Case (Ann. Phys., 9: 1 (1960)) can be used to determine the flux distribution and criticality condition for a two-region reactor cell with reflecting boundaries. An equation is derived that can be used to determine the accuracy of an approximate solution. A first-order approximation is shown to be equivalent to the P_1-approximation of the spherical harmonic method. (M.O.W.)

42036 (BNWL-95) PHYSICS RESEARCH QUARTERLY REPORT, JANUARY, FEBRUARY, MARCH, 1965. (Battelle-Northwest, Richland, Wash. Pacific Northwest Lab.). Contract AT(45-1)-1830. 55p. Dep. mn; CFSTI, $3.00 cy, $0.50 mn.

Individual abstracts were prepared for the five included papers on: comparison of measured and calculated spectra and average reaction rates, comparison of diffusion and transport calculations for NPR tube-in-tube fuel geometry, critical experiments with PuO_2-polystyrene compacts ^{240}Pu-8.0%, H/Pu = 15, prompt neutron decay using Monte Carlo methods of analysis, and interpretation of pulsed neutrons and reactor noise experiments in reflected reactors. (M.O.W.)

For abstracts of individual papers see: 42037—42040, and 42128.

42037 (BNWL-95, pp 4-17) REACTOR ANALYSIS. COMPARISON OF MEASURED AND CALCULATED SPECTRA AND AVERAGE REACTION RATES. Harris, R. A.; Reardon, W. A. (Battelle-Northwest, Richland, Wash. Pacific Northwest Lab.).

Measured thermal-neutron spectra for several homogeneous, light water and polyethylene moderated systems, were compared to spectra calculated by theoretical methods presently in use. Average thermal group cross sections (chosen as cross sections for neutrons between 0 and .683 ev) were obtained by integrating energy-dependent cross sections over the measured spectra. These were then compared with the corresponding parameters obtained using the theoretical spectra. (M.O.W.)

42038 (BNWL-95, pp 27-35) CRITICAL MASS PHYSICS. CRITICAL EXPERIMENTS WITH PuO_2-POLYSTYRENE COMPACTS ^{240}Pu = 8.0 PERCENT, H/Pu = 15. Richey, C. R.; White, J. D. (Battelle-Northwest, Richland, Wash. Pacific Northwest Lab.).

A series of critical experiments were completed with homogeneous PuO_2-polystyrene compacts (hydrogen-to-plutonium atomic ratio = 15) having 8.0% ^{240}Pu. These data are applicable to the intervening systems of wet powders, precipitates, slurries, polymers, and other highly concentrated plutonium mixtures encountered in chemical plants processing reactor fuels. (M.O.W.)

42039 (BNWL-95, pp 36-9) CRITICAL MASS PHYSICS. PROMPT NEUTRON DECAY USING MONTE CARLO METHODS OF ANALYSIS. Carter, L. L. (Battelle-Northwest, Richland, Wash. Pacific Northwest Lab.).

Equations were developed for determining the prompt neutron decay as a function of time and position from Monte Carlo techniques by analyzing one generation of neutrons. The assumption was made that the reactor geometry or fuel composition does not change with time. A simple calculation was successfully made to determine the integrated prompt neutron decay over the whole reactor using this method of analysis. (M.O.W.)

42040 (BNWL-95, pp 40-54) CRITICAL MASS PHYSICS. INTERPRETATION OF PULSED NEUTRON AND REACTOR NOISE EXPERIMENTS IN REFLECTED REACTORS. Albrecht, R. W. (Battelle-Northwest, Richland, Wash. Pacific Northwest Lab.).

A preliminary, theoretical investigation of reflected reactor kinetics is presented. The discussion concerns: two-node kinetics equations for reflected reactors, derivation of source transfer functions, decay constants for critical, two-region, reactor model, and computations of decay constants for critical, reflected, two-node reactor model. (M.O.W.)

42041 (GA-6286) EFFECTIVE THERMAL NEUTRON CROSS SECTIONS FOR MATERIALS WITH GRAIN STRUCTURE. Dyos, M. W.; Pomraning, G. C. (General Atomic, San Diego, Calif. John Jay Hopkins Lab. for Pure and Applied Science). May 27, 1965. Contract AT(04-3)-187. 25p. Dep. mn; CFSTI, $1.00 cy, $0.50 mn.

A method is given for the calculation of effective neutron cross sections for materials with grain structure. The method is particularly suited for the calculation of effective cross sections at thermal energies where the ratio of scattering to total cross section for absorbers is small. Application to a practical problem, the calculation of effective neutron cross sections and effective thermal neutron spectrum, was made. The problem in question is that of 200 micron diameter plutonium grains, containing 17% ^{240}Pu, homogeneously dispersed in BeO. It is shown that provided the centers of the grains are not less than 800

microns apart the method is applicable and gives excellent agreement with the results obtained from a P-1, S-8 neutron transport theory calculation. (auth)

42042 (JINR-P-2216) KORRELYATSIYA NEITRONOV V YADERNYKH REAKTORAKH S UCHETOM IKH PROSTRANSTVENNO-ENERGETICHESKOGO RASPREDELENIYA. (Neutron Correlation in Nuclear Reactors With Account of Their Space and Energy Distribution). Kozik, Ben'yamin (Joint Inst. for Nuclear Research, Dubna (USSR). Lab. of Neutron Physics). 1965. 10p. Dep. mn.

The basic theorem of the correlation theory of nuclear reactors is proved which states that the binary correlation density (correlation function) of neutrons in nuclear reactors satisfies the non-stationary homogeneous Boltzman equation. This equation together with the equations for the binary densities of the second order central moments allows to solve all the correlation problems of the statistical theory of reactors. More concrete results are given for diffusion approximation. (auth)

42043 (MIT-2344-3, pp 15-36) FAST NEUTRON DISTRIBUTIONS. Woodruff, G. (Massachusetts Inst. of Tech., Cambridge. Dept. of Nuclear Engineering).

Fast neutron distributions were studied by using threshold detector foils in five types of lattices: 1.25, 1.75, and 2.50 inch spacings of 1.03% ^{235}U, .25 inch diameter fuel rods, and 1.25 inch and 2.50 inch spacings of 1.14% ^{235}U, .25 inch diameter fuel rods. The reactions used include $^{64}Zn(n,p)^{64}Cu$, $^{58}Ni(n,p)^{58}Co$, $^{115}In(n,n')^{115m}In$, $^{238}U(n,f)$. (M.O.W.)

42044 (MIT-2344-3, pp 37-54) STUDIES OF EPITHERMAL NEUTRONS IN URANIUM, HEAVY WATER LATTICES. D'Ardenne, Walter H. (Massachusetts Inst. of Tech., Cambridge. Dept. of Nuclear Engineering).

Measurements related to reactor physics parameters were made in three heavy water lattices. The three lattices studied contained .25 inch diameter, 1.03% ^{235}U uranium metal rods in triangular arrays spaced at 1.25, 1.75, and 2.50 inches. The following four microscopic parameters were measured in each of the three lattices studied: (1) the ratio of the average epicadmium ^{238}U capture rate in the fuel rod to the average subcadmium ^{238}U capture rate in the fuel rod, (2) the ratio of the average epicadmium ^{235}U fission rate to the average subcadmium ^{235}U fission rate in the fuel rod, (3) the ratio of the average ^{238}U capture rate to the average ^{235}U fission rate in the fuel rod, and (4) the ratio of the average ^{238}U fission rate to the average ^{235}U fission rate in the fuel rod. (M.O.W.)

42045 (MIT-2344-3, pp 55-108) PULSED NEUTRON AND CONTROL ROD RESEARCH STUDIES OF REACTIVITY AND RELATED PARAMETERS. Malaviya, B. K. (Massachusetts Inst. of Tech., Cambridge. Dept. of Nuclear Engineering).

A pulsed neutron set-up was brought into operation for use in conjunction with heavy water lattice facilities. One phase of research, involving pulsed neutron experiments with multiplying and non-multiplying assemblies, was completed. Control rod studies by both pulsed neutron and steady-state methods were made. A new technique was developed for the study of lattice parameters by means of the pulsed neutron method. This technique makes possible the direct determination of such lattice parameters as k_∞ and L^2 in far subcritical lattices. The experimental set-up and the techniques are described and the results are presented. (M.O.W.)

42046 (MIT-2344-3, pp 109-14) MEASUREMENTS ON POISONED LATTICES. Harrington III, J. (Massachusetts Inst. of Tech., Cambridge. Dept. of Nuclear Engineering).

Exploration was started of a new technique for the experimental measurement, in a subcritical assembly, of the neutron multiplication factor for an infinite lattice (k_∞). An attempt to develop the technique and use it to obtain values of k_∞ for lattices of slightly enriched uranium in heavy water is made. The objectives of this work and the planning and preparation for the achievement of these objectives are presented. (M.O.W.)

42047 (MIT-2344-3, pp 115-24) SINGLE ROD MEASUREMENTS AND THEORY. Pilat, E. E. (Massachusetts Inst. of Tech., Cambridge. Dept. of Nuclear Engineering).

Radial and axial gold foil activations were measured around a single, 1 inch diameter, natural uranium rod placed at the center of a 3 foot diameter tank filled with heavy water. Axial foil activitions were made at three different radii: 10.8, 15.9, and 22.2 cm. The results of the innermost and outermost runs, plotted on arbitrary scales, are given. The theory dealing with neutron flux distributions around a single fuel rod immersed in moderator is discussed. (M.O.W.)

42048 (MIT-2344-3, pp 125-36) TWO-REGION LATTICES. Gosnell, J. (Massachusetts Inst. of Tech., Cambridge. Dept. of Nuclear Engineering).

Investigations of the validity of lattice parameter measurements in the center of two-region assemblies are being conducted by using the M. I. T. lattice facility. Determination of spectral changes across the two regions was the main object of the experiments. In addition, axial buckling measurements were made at various radial positions in the assemblies to ascertain whether or not the axial relaxation length is a function of radius. (M.O.W.)

42049 (MIT-2344-3, pp 155-64) MATERIAL BUCKLING AND INTRACELLULAR THERMAL NEUTRON DISTRIBUTIONS. Clikeman, F.; Barch, J.; Supple, A.; Berube, N.; Kelley, B. (Massachusetts Inst. of Tech., Cambridge, Dept. of Nuclear Engineering).

A standard system was developed previously for the measurement of the material buckling of lattices in the M. I. T. Lattice Facility. Results were obtained by using these techniques on new lattice arrangements. (M.O.W.)

42050 (NAA-SR-11368) REACTIVITY WORTHS OF SEVERAL FAST REACTOR CONTROL MATERIALS. Campbell, R. W.; Carpenter, S. G. (Atomics International, Canoga Park, Calif.). July 25, 1965. Contract AT(11-1)-Gen-8. 19p. Dep. mn; CFSTI, $1.00 cy, $0.50 mn.

A high sensitivity reactor oscillator was used to determine the reactivity worths of a series of control rod materials in a range of spectra having median fission energies from 8.5 ev to 422 kev. The control rod materials studied were natural B, ^{10}B, Eu_2O_3, Gd_2O_3, and Ta. Europium oxide was as good a poison as natural boron and better than Gd_2O_3 by a factor of 4 over the range studied. Tantalum showed good control capabilities at the higher energies and offers the advantage of a metallic form. (auth)

42051 (UCRL-12013) PULSED NEUTRON MEASUREMENTS ON SOLID-MODERATED, ENRICHED-URANIUM SUBCRITICAL ASSEMBLIES. Morton III, J. R.; Goldberg, E. (Lawrence Radiation Lab., Univ. of California, Livermore). July 1964. Contract W-7405-eng-48. 16p. Dep. mn; CFSTI, $1.00 cy, $0.50 mn.

Measurements were made of the prompt neutron decay constant, alpha, for several subcritical assemblies. These measurements included the determination of both the delayed critical alpha and the variation of alpha with buckling. These near-homogeneous assemblies were BeO- or graphite-moderated and were fueled with enriched uranium (93.2% ^{235}U). The following moderator-fuel molar ratios were studied: $BeO/^{235}U$ = 123, 247, 370, 493, 3830, and $C/^{235}U$ = 1145. A method is described by which the data can be used for a sensitive test of quality of the nuclear cross sections such as are found in multigroup diffusion calculations. (auth)

42052 THE CONTROL POISON AS AN EIGENVALUE OF THE DIFFUSION EQUATIONS. Buffoni, G.; Loizzo, P. (Centro di Studi Nucleari, Casaccia, Italy). Energia Nucl. (Milan), 12: 401-5(Aug. 1965).

The possibilities of solving the diffusion equations of a reactor directly for the quantities of poison that bring the reactor to criticality are discussed. The possiblity of formulating an eigenvalue problem in which the smallest eigenvalue is the one desirable is considered. This problem can always be solved when the reactor is subcritical. The

examples carried out by using a slightly modified version of the Equipoise-3 Code showed that there is always convergence of the iterative processes used when the reactor is subcritical. If the reactor is supercritical the processes may not converge. (auth)

42053 MEASUREMENT OF MIGRATION AREA AND MULTIPLICATION FACTOR OF UO_2–H_2O LATTICE. Kobayashi, Keisuke; Takeda, Seishi; Ukai, Seiji; Hoshino, Tsutomu; Matsuura, Shojiro (Kyoto Univ.). J. Nucl. Sci. Technol. (Tokyo), 2: 257-60(July 1965).

The migration area, multiplication factor, and axial as well as radial reflector savings of a light-water-moderated critical assembly fueled with UO_2 (enriched to 2.596 wt% in ^{235}U) were obtained through water height experiments applying the one group diffusion model. The water height was varied from 1.226 to 710 mm, while the core radius was changed from 183.3 to 196.8 mm in order to maintain criticality. The linear relation obtained between the water height h and $(\partial\rho/\partial h)^{-\frac{1}{2}}$ as well as between the radial buckling B_r^2 and the axial buckling B_z^2 indicated that the one group diffusion model is a good approximation for this core. (auth)

42054 CRITICALITY CALCULATIONS FOR UNIFORM WATER-MODERATED LATTICES. Strawbridge, L. E.; Barry, R. F. (Westinghouse Electric Corp., Pittsburgh). Nucl. Sci. Eng., 23: 58-73(Sept. 1965).

A procedure for calculating the neutron multiplication factor and few-group constants for water-moderated reactors was developed. The intent of this development was to produce a calculational procedure which could be used with confidence in the engineering design of water-moderated reactors. Analytic procedures that require large amounts of computer time were excluded from consideration. The proposed procedure includes a heterogeneous treatment of the fast-fission effect, resonance absorptions and the thermal utilization. The results of the procedure agree well with more rigorous calculations requiring orders of magnitude more computer time. The procedures were applied to 116 U-metal and UO_2 experimental lattices covering a wide range of parameters. The multiplication factor is calculated for all cases with a standard deviation about the mean of 0.86%. (auth)

42055 IMPROVEMENTS TO THE THEORY OF RESONANCE ESCAPE IN HETEROGENEOUS FUEL. II. THE DANCOFF FACTOR AND THE EQUIVALENCE THEOREM IN CLUSTER-TYPE FUEL. Leslie D. C. (Atomic Energy Establishment, Winfrith, Dorset, Eng.); Jonsson, A. Nucl. Sci. Eng., 23: 82-9(Sept. 1965).

A method for the rapid evaluation of the Dancoff factor in regular arrays of fuel rods was previously put forward. It was also shown how extended rational approximations to the fuel nonescape probability could be used to improve the form of the equivalence theorem based on Wigner's rational approximation. This form of equivalence asserts that the resonance integral is a function of the geometry through the excess potential scattering $1/N\bar{l}$ only, where N is the number density of the absorber and $\bar{l}$ is the mean chord. In the modification proposed, this function is generalized to $a/N\bar{l}$; the Bell factor a is found to vary with coolant density. By making use of an approximate analytic method for the calculation of collision probabilities in geometries more general than regular arrays, this work is extended to cluster-type fuel elements. The basic procedure is the same as in the work referred to above. An analytic expression for the fuel-to-fuel collision probability is derived using arguments about its behavior in the black and white limits (i.e. in the limits of high and low cross sections). The Dancoff factor is derived from the behavior in the black limit. It is shown, by comparison with exact calculations, that for two types of cluster geometry of current interest in fuel element design, the proposed Dancoff factor is in error by at most 2%. Improved equivalence relations for cluster geometry are also considered. It has been customary to assume that the cluster is equivalent to an isolated rod of diameter d_p/Γ, where d_p is the diameter of a single pin in the cluster and Γ is the Dancoff factor. Such a procedure implies that the Bell factor of the cluster is constant and equal to its value for an isolated rod. It is shown that the Bell factor is a function of coolant density and that, in a particular case, the cluster is almost equivalent to an isolated rod at low density. As the density increases, the Bell factor drops rapidly by 6% and then increases slowly. (auth)

42056 ON THE THEORY OF SPACE-DEPENDENT NEUTRON SPECTRA IN HETEROGENEOUS REACTORS. II. Kunze, Helmut (Institut fuer Struktur der Materie, Karlsruhe, Ger.). Nucl. Sci. Eng., 23: 90-7(Sept. 1965).

For the heavy-gas model, the stationary space-dependent neutron spectrum in one- and two-dimensional heterogeneous thermal reactors is determined in the diffusion approximation. The fuel elements, which are not necessarily identical, and absorbing slabs or rods are arranged arbitrarily. However, absorption in all of them is assumed to follow a 1/v law. The neutron flux is represented as a linear combination of the lowest eigenfunction of the Laplace operator for the geometry considered and a finite set of Green's functions for the stationary-wave equation for various, usually imaginary, wave numbers. The energy-dependent coefficients are determined by the method, developed earlier. The lowest eigenfunctions of the Laplace operator and Green's functions for the stationary-wave equation are given for some geometries of practical interest. Solutions found earlier for simple geometries may now be regarded as special representations of these Green's functions. But in these cases, too, other representations can be found which are to be preferred for numerical reasons. (auth)

42057 EFFECT OF RESONANCE CORRECTION TO GROUP FLUX IN FAST-REACTOR DOPPLER-EFFECT CALCULATION. Hummel, H. H.; Hwang, R. N. (Argonne National Lab., Ill.). Nucl. Sci. Eng., 23: 98-9 (Sept. 1965).

A clarification of the nature of the errors made when the effect on group fluxes of resonances in the total cross section is not allowed for in making fast-reactor Doppler-effect calculations is given. It is shown that in most cases of interest such errors will be small. The connection between this flux correction and the correction to be made to fission and capture cross sections because of overlap between resonances in fissile and fertile material is also discussed. (J.F.P.)

42058 COMMENT ON THE EFFECT OF RESONANCE CORRECTION TO GROUP FLUX IN FAST-REACTOR DOPPLER-EFFECT CALCULATION. Nicholson, R. B. (Univ. of California, Livermore). Nucl. Sci. Eng., 23: 103-4(Sept. 1965).

A disagreement is expressed with the point of view of Hummel and Hwang (Technical Note, Nucl. Sci. Eng., 23: 98-9(1965)) and (R. N. Hwang, Nucl. Sci. Eng., 21: 523 (1965)) regarding the importance of using flux correction factors and making resonance overlap corrections for the overlap between resonances in two different materials. It is stressed that the disagreement with Hwang's interpretation of overlap effects is only when the overlapping resonances are in two different materials or sequences. It is noted that he presents an original and apparently useful procedure for accounting for overlap among resonances within a given material. (J.F.P.)

42059 TRANSIENT REACTIVITY VARIATION OF A REACTOR CONTROLLED WITH THE TEMPERATURE OF THE MODERATOR. Palinski, Roman (EURATOM, Ispra, Italy). Nukleonik, 7: 241-7(May 1965). (In German).

In studies of reactor dynamics, the reactivity feedback due to a moderator temperature change with time was considered by using two terms. The first term was proportional to the variation of the mean temperature. The introduction of a second term, which considers moderator temperature variations in the core, is explained. It was found convenient to discuss "weight temperature coefficients" of the moderator. A system of ordinary differential equations was established for the properly defined temperature functions, describing the variation of the mean temperature, the outlet temperature, and the moderator temperature at the core center. For the inlet temperature of

a moderator at constant flow, every time function is admissible. In the core the moderator is heated by heat source with time-variable amplitude, that heats in accordance with a cosine distribution in the flow direction. (tr-auth)

42060 CALCULATION METHOD FOR HETEROGENEOUS REACTOR CELLS. Kuznetsov, E. S. Zh. Vychislitel. Mat. i Mat. Fiz., 5: 488-502(May-June 1965). (In Russian)

Most of the usual approximation methods for calculating heterogeneous reactor cells are based on the P-1 and P-2 approximations; however, it became obvious recently that more accurate solutions, derived from the kinetic equation, are desirable. The applicable methods include the S_N method of Carlson and the method developed by Vladimirov. For solving the problem by these methods, the cell is usually assumed to consist of an infinite cylinder, as stipulated by Wigner and Seitz, while the neutron scattering is considered to be isotropic, and the kinetic equation is solved by the one-group approximation. In addition, the neutron flux at the cell boundary is assumed to possess an isotropic angular distribution. Although in one-group calculations the neutron velocity is taken as the unity, in multigroup calculations the differences between the velocities of the groups can not be neglected. Special computer programs were developed for solving the problems, treating special cases taken from a paper by Amouyal (J. Nucl. Energy 6: 79-98(1957)); they involved 2-region cells consisting of an inner U block and an outer moderator region. In addition to the usual cell characteristics, the angular distribution of phase densities along the axis of the cylinder were also determined. The shape of the curves obtained reflected closely the properties of the cell, specifically the ratio of neutron densities in the directions parallel and perpendicular to the axis of the cylinder. (TTT)

42061 THE DYNAMIC REACTIVITY EFFECT—A FURTHER DEVELOPMENT. Campe, K. M.; Bailey, R. E. (Purdue Univ., Lafayette, Ind.). 40p. (CONF-650413-5). Gmelin, AED-CONF-65-042-13.

From Symposium on Neutron Dynamics and Control, Tucson, Ariz.

A prediction was previously made, based on some results obtained from simple diffusion theory, that there possibly may exist a dynamic reactivity effect in a compressible fissile medium whose geometric size is forced to change periodically. Within the assumptions inherent in the mathematical model representing the physical behavior of the system, it was found that, according to diffusion theory, if one is able to force the rate of change of the size of the system faster than the neutron population could adjust itself to the said change, a net reactivity gain could be obtained. Supporting studies have been made using the telegrapher's equation for the slab geometry and the diffusion equation for spherical and cylindrical geometries. The conditions for the dynamic reactivity effect (DRE) are presented for each geometry. Also some additional physical reasoning pertaining to the causes of the DRE is presented. (auth)

42062 INVESTIGATIONS ON NONLINEAR STABILITY OF COUPLED NUCLEAR SYSTEMS. Gage, Stephen J.; Adler, F. T.; Powers, P. N. (Purdue Univ., Lafayette, Ind.). 42p. (CONF-650413-9). Gmelin, AED-CONF-65-042-4.

From Symposium on Neutron Dynamics and Control, Tucson, Ariz.

An alternative model of the coupled-core reactor kinetics equations is derived from the fundamental transport equation. The applicability of this formulation to the analysis of nonlinear dynamic stability is discussed. An analysis of a two-core reactor in which the reactivity feedback mechanism is dependent on average core power is detailed. The behavior of the singular points for this simplified model is described for the cases when the delay times associated with coupling neutrons traveling from one core to another are neglected and when the time lags are approximately treated. Using the methods of Lur'e and Letov and of Aizerman, stability criteria are derived for the two-core reactor with nonlinear power-dependent feedback. The relative advantages of the two approaches are compared. (auth)

42063 A CALCULATION OF THE DISADVANTAGE FACTOR IN CYLINDRICAL GEOMETRY. Robinson, Alan H.; Ferziger, Joel H. (Stanford Univ., Calif.). 7p. (CONF-654-91). Gmelin, AED-CONF-64-219-109.

From American Nuclear Society Meeting, San Francisco, Nov.-Dec. 1964.

An attempt was made to extend calculations of disadvantage factors previously made for slab geometries to cylindrical geometries. Expressions for the neutron density in the inner and moderator regions are given, and an equation is obtained for the disadvantage factor which is the usual cylindrical geometry diffusion result with a correction factor from transport theory. Good agreement was found with results of other methods. (L.B.S.)

42064 DEVICE FOR DETERMINING THE RATE OF INCREASE OF THE NEUTRON FLUX IN A NUCLEAR REACTOR. Bolliet, Roger (to Commissariat a l 'Energie Atomique). British Patent 997,925. July 14, 1965. Priority date Nov. 7, 1962, France.

A device for determining the period, P, of a nuclear reactor and its doubling time, T, includes means for recording on an endless, flexible recording medium driven at a constant linear speed, V, around a closed path. Disposed around the path in the direction of medium movement are an eraser head, a recording head, and a first and second reading head. An electrical signal whose amplitude corresponds to the instantaneous amplitude of the neutron flux of the reactor is applied to the recording head. The first and second reading heads are separated by a distance, L, along the path corresponding to a movement in time of the medium equal to $4_2 - t_1 = \tau = L/V$. The levels corresponding to the neutron flux φ_1 and φ_2 at times t_1 and t_2 are passed after amplification to a calculating device for evaluating the period of the reactor according to the relation $P/\tau = 1/\log \varphi_2 - \log \varphi_1$. The calculating device includes two integrating and shaping channels producing at their outputs d-c signals whose amplitude is proportional to the number of pulses received. The calculating member mainly produces an a-c voltage whose amplitude is proportional to the difference between the d-c signals. Also included are amplifying stages and a two-phase motor operating the slider of a potentiometer receiving the d-c signal delivered by the first reading head, in order that the voltage applied to one part of the potentiometer bounded by the slider is equal to the voltage delivered by the first reading head. The two-phase motor is adapted to rotate a dial having a movable element, and the dial is graduated to give a direct reading of the doubling time or the reactor period for a given tape speed and for a given distance between the two reading heads. (B.L.M.)

Design and Feasibility

42065 A THERMAL NUCLEAR REACTOR. Mialki, Werner; Wille, Rudolf. British Patent 999,274. July 21, 1965. Priority date Nov. 2, 1961, Germany.

A thermal reactor for use in the temperature range of 1000 to 2000°C is described in which a diathermanous substance is used to radiate a substantial portion of the heat produced. Both the fissionable material and the moderator are contained in the diathermanous substance in one of the following manners: both dissolved in it; one or both held in suspension in it; the fissionable material in the shape of small particles surrounded by the envelope of moderator; or a graphite crucible forming the moderator and containing the fissionable material in the diathermanous material or fissionable material in the form of fuel rods immersed in the diathermanous substance. The diathermanous material may be a glass or a mixture of metallic oxides selected from the group consisting of MgO, BeO, Al_2O_3, CaO, and ZrO_2. Other preferred component materials are UO_2 fuel and BeO or graphite moderator. Means are provided for passing a gas flow through the diathermanous melt both to stir the melt and to absorb some of the heat. The gas stream is then passed through heat exchanger means. The mixture may be withdrawn from the crucible through a discharge aperture at the bottom or may be frozen by cooling prior to removal. The latter treat-

ment serves to trap some of the gaseous fission products. (B.L.M.)

42066 IMPROVEMENTS IN OR RELATING TO NUCLEAR REACTORS. Halliday, Dixon Brydsen (to United Kingdom Atomic Energy Authority). British Patent 999,699. July 28, 1965. Filed Nov. 20, 1962.

A nuclear reactor includes a pressure vessel, a plurality of elongate tubular fuel elements centrally located within the vessel to form the core, and means for passing heavy water into the vessel above the core to act as coolant, reflector, and moderator. The coolant is passed downwards between the core and the pressure vessel and upwards through the core to pressure vessel outlet means located above the core. The fuel elements are highly enriched U alloy fuel and are spaced so as to provide an undermoderated core. A fuel storage means comprising a rotatable magazine is located within the pressure vessel, and transfer means are provided for the fuel elements. A beam is radially mounted above the reactor, and a fuel element transfer flask is movable on the beam. Heat exchange means are associated with the flask so that a fuel element may be removed from the reactor into the flask while immersed in liquid coolant that is the same as the reactor coolant. Means for inserting and withdrawing a reactivity control element are provided. This type reactor is particularly useful as a neutron beam producing reactor with tubes for irradiation purposes being provided through the biological shield into the reactor or to allow the beam to pass to external experimental apparatus. (B.L.M.)

42067 LOW POWER NUCLEAR REACTORS. Biehl, Arthur T. (to Aerojet-General Nucleonics). Canadian Patent 698,037. Nov. 17, 1964.

These small reactors are designed to operate at a power of 1 kw or less and consist of a solid multiple-section core of fuel-impregnated resinous material, such as polyethylene, protected against melting caused by an excursion. This is accomplished by a device which allows the core sections to separate into less than critical masses if the temperature rises above a safe value. Such reactors adapted for use in education, research, medical diagnosis, and process control have a low cost compared with high-power reactors. The fuel is UO_2 enriched in ^{235}U with a graphite reflector. The critical mass is about 600 g ^{235}U. (F.S.A.)

42068 NUCLEAR REACTOR. Costes, Didier (to Commissariat a l'Energie Atomique). Canadian Patent 711,366. June 8, 1965. Priority date May 17, 1961, France.

A reactor is designed in which the reflector consists of a lining of canned and removable elements of solid moderator on the interior wall of the reactor tank. The release of Wigner energy from these elements is thus permitted. It is further claimed that a solid moderator is more economical than a liquid in the low flux regions. (F.S.A.)

42069 BOILING NEUTRONIC REACTOR SYSTEMS. Abbott, William E. (to Westinghouse Electric Corp.). Canadian Patent 712,678. June 29, 1965.

A reactor is described in which the fuel material is intimately mixed with the boiling coolant. The homogeneous or fluidized nuclear fuel is circulated as a slurry through the reactor vessel and through primary loops where the heat is extracted for steam generation. Temperature differential between the working fluid and the cooling fluid is eliminated. The coolant is a miscible mixture of higher and lower boiling hydrocarbons whereby a substantial portion of the lower boiling component is vaporized to provide a working fluid. An improved moderator system is also claimed. (F.S.A.)

Fuels

42070 THE INDUSTRIAL MANUFACTURE OF FUEL ELEMENTS IN FRANCE. Jeanpierre, G. Nucl. Eng., 10: S2-3(Aug. 1965).

Activities of the French nuclear fuel industry are discussed. The reactor systems served consist of gas-cooled graphite-moderated reactors and gas-cooled heavy-water-moderated reactors. Policies followed to meet the requirements of these reactors are discussed. (F.J.H.)

42071 MEASUREMENT AND APPLICATION OF X- AND GAMMA-RAY ATTENUATION TO REACTOR MATERIALS EVALUATION. Foster, B. E.; Snyder, S. D.; McClung, R. W. pp 339-42 of Non-Destructive Testing, London, Butterworths, 1964.

Non-destructive testing methods are used to evaluate reactor fuel homogeneity. Gamma or x-ray attenuation techniques were demonstrated to be feasible for this requirement. A constant-potential x-ray source was used. The detection equipment included a sodium iodide scintillator and photomultiplier tube. Scanning speeds were limited by the recorder-response time and the beam intensity that could be faithfully accepted by the detector. Applications to feed plates, fuel rods, and determination of mass attenuation coefficients are discussed. (M.C.G.)

42072 IMPROVEMENTS RELATING TO NUCLEAR REACTOR FUEL ELEMENT ASSEMBLIES. Williams, Ronald Peter; Ashcroft, David John (to United Kingdom Atomic Energy Authority). British Patent 998,624. July 14, 1965. Filed Sept. 5, 1962.

A nuclear fuel assembly for a reactor of the kind in which the fuel assembly is pervaded by a fluid moderator is made up of at least three rod-shaped fuel elements grouped around a rod without fuel but containing burnable poison. All the elements are arranged on parallel axes and with equal spacing from the burnable poison rod, and the elements and the poison rod are held together as a unitary structure. The poison concentration varies along the length of the burnable poison rod. A group of such assemblies together bound a vacancy in the reactor core for the introduction of a tubular neutron observer rod. The assemblies are arranged in parallel tubes in such a way that all fuel elements are equally spaced from a burnable poison rod. The fuel elements are composed of stacked pellets contained in a sheath, and at intervals along the length of the fuel elements there are spacer grids formed of metal strip such as a Zr alloy. The metal strip is bent transversely of its width to form a number of closed lobes that receive the fuel elements. (B.L.M.)

42073 HEATING ELEMENT SPACER GRIDS. Williams, Ronald Peter; Ashcroft, David John (to United Kingdom Atomic Energy Authority). British Patent 998,625. July 14, 1965. Filed Sept. 5, 1962.

A spacer element grid is provided to hold a number of heating elements on parallel axes equi-spaced around a circle. An endless length of metal strip arranged on edge in the direction of the elements is bent across its width to form portions extending substantially radially of the center of the circle. Between these portions, intermediate portions are in engagement alternately with the inner and outer members of closed shape so that with these members the strip defines cells into which to receive the heating elements. The grid construction may be employed with a number of concentric circles of elements so that the inner and outer members will lie between one circle and another. Instead of the spider arrangement, the metal strip may also be arranged to form straight portions extending substantially radially of the center of the circle. The portions between the straight portions are in engagement alternately with inner and outer members of closed shape, and the straight portions define wide angle sectors alternating with narrow angle sectors. The wide angle sectors are adapted to pinch elements received into them against the outer members. A stiffening means is provided in the narrow angle sectors to restrain bowing of the straight radial portions. (B.L.M.)

42074 A FUEL ELEMENT FOR A NUCLEAR REACTOR. Caillat, Roger; Elston, Jean (to Commissariat a l'Energie Atomique). British Patent 998,902. July 21, 1965. Priority date Apr. 26, 1962, France.

In a reactor fuel element made up of a slug of fertile material contained in a metal jacket closed at one end with a cap, the heat transfer from the fertile material to the cap is reduced while the heat transfer from the fertile material to the jacket is kept normal. A disc-shaped

spacer having a thermal conductivity axially of the slug lower than its thermal conductivity radially of the slug is disposed between the slug and the cap. The spacer is formed by coating the inside of the cap with a ceramic material, such as alumina or magnesia, sprayed against the cap by a plasma jet. Alternatively, the spacer may be formed by a sandwich of several layers of a metal of low neutron cross section, such as Mg, Al, or Mo, alternated with layers of an oxide of such a metal. The layers comprise an insulating and a conductive substance and may be deposited on the cap and be unitary with it or can be prepared separately and merely interposed. The layers of the sandwich are deposited in a conventional costing method, e.g. by torch spraying. The sandwich layer in contact with the slug is preferably formed by a refractory oxide and the one in contact with the cap may be either the refractory or the metal. (B.L.M.)

Power and Power-Breeder Reactors

42075 (ANL-6735) FUEL MANAGEMENT AND INVENTORY IN THE EBR-II FUEL CYCLE. Dillon, I. G.; Burris, L. Jr.; Levenson, M. (Argonne National Lab., Ill.). Mar. 1965. Contract W-31-109-eng-38. 19p. Dep. mn; CFSTI, $1.00 cy, $0.50 mn.

A fuel management study was made with the objective of minimizing fuel inventory by pinpointing factors that strongly affect fuel inventory. Included in the various fuel-cycle operating parameters that were investigated were cooling time of discharged fuel, time required for processing and fabrication of the fuel, time between reactor shutdowns for charging and discharging fuel, and reactor power level. A burnup of 2 at. % of the heavy elements in all fuel discharged from the reactor was assumed for all calculations, but the general effect of degree of fuel burnup on the fuel inventory was discussed qualitatively. (M.O.W.)

42076 (ANL-6751) NEUTRON-FLUX STUDIES IN THE EBWR DURING POWER OPERATION. Knapp, W. G. (Argonne National Lab., Ill.). Mar. 1965. Contract W-31-109-eng-38. 39p. Dep. mn; CFSTI $2.00 cy, $0.50 mn.

The neutron-flux distribution in the Experimental Boiling Water Reactor (EBWR) core during power operation was studied through the use of activation foil detectors. The method described was used for irradiation and analysis of the detectors. From data obtained with bare and cadmium-covered, cobalt-aluminum alloy foils, neutron-flux isogram plots were prepared. The effects of reactor power changes, soluble-poison concentration, and control rod positions on the thermal and resonance neutron-flux distribution are shown. (auth)

42077 (ANL-7014) AN ANALYSIS OF SIX AETR FAST CRITICAL EXPERIMENTS. Davey, William G. (Argonne National Lab., Idaho Falls, Idaho). Mar. 1965. Contract W-31-109-eng-38. 23p. Dep. mn; CFSTI, $1.00 cy, $0.50 mn.

Atomics International has constructed a series of multi-region fast-thermal critical assemblies as part of the Advanced Epithermal Thorium Reactor (AETR) program to obtain data on the physics of ^{233}U-Th-fueled reactors. In each case, the central test region was of a composition appropriate to a full-scale core. The physics data obtained in six cores, where the test regions simulated the cores of fairly large fast reactors, were analyzed using a cross-section set previously used in an analysis of ZPR-III fast critical assemblies. These data are central fission ratios, relative reactivities of certain materials, and the relative importance of neutron sources of different energies. Trends are identified in the differences between calculated and measured data, and these are compared with similar trends found in the ZPR-III assemblies. (auth)

42078 (ANL-7019) SOME PHYSICS ASPECTS OF THE PLUTONIUM EXPERIMENT IN EBWR. Toppel, B. J.; Avery, R. (Argonne National Lab., Ill.). Apr. 1965. Contract W-31-109-eng-38. 38p. Dep. mn; CFSTI, $2.00 cy, $0.50 mn.

Information concerning the plutonium experiment in EBWR is presented under several main headings: description of survey calculational methods, survey calculations, topics related to an improved calculational model, and arguments leading to the present configuration. (M.O.W.)

42079 (APDA-NTS-4) INVESTIGATION OF CORE REPRODUCIBILITY OF THE ENRICO FERMI REACTOR. Mueller, R. E.; Wilber, H. A. (Atomic Power Development Associates, Inc., Detroit, Mich.). Apr. 1965. 40p. Dep. mn; CFSTI $2.00 cy, $0.50 mn.

The reproducibility of the Enrico Fermi reactor core was studied. In the test, the fuel subassembly hold-down mechanism was raised, rotated, and returned to its original operating position a number of times. Critical rod and positive period reactivity measurements were made after each movement to determine whether any significant core perturbation resulted from operation of the hold-down mechanism. The primary purpose of the test was to determine whether an experimental error due to the movement of the hold-down mechanism will occur in those nuclear tests where fuel handling is required. The test results show that no significant change in the reactivity state of the reactor was caused by movement of the hold-down mechanism. The test, therefore, verified that the core configuration was highly reproducible, and that no error due to hold-down movement will occur in subsequent nuclear tests. (auth)

42080 (APDA-NTS-5) MEASUREMENT OF THE ISOTHERMAL TEMPERATURE COEFFICIENT OF REACTIVITY OF THE ENRICO FERMI REACTOR. Wilber, H. A.; Fischer, E. A.; Mueller, R. E. (Atomic Power Development Associates, Inc., Detroit, Mich.). June 1965. 54p. Dep. mn; CFSTI $3.00 cy, $0.50 mn.

The isothermal temperature coefficient of reactivity of the Enrico Fermi reactor was measured for various reasons on three different occasions during the reactor low-power nuclear test program. From the first measurements, an average isothermal temperature coefficient of −0.83 ih/F over the temperature range 400 to 520°F was obtained. The next measurements were made over the narrow temperature range 500 to 540°F and yielded a value of −0.84 ih/F. The third were detailed measurements made over the temperature range 400 to 600°F in 40°F increments. The magnitude of the temperature coefficient varied from −0.8436 ih/F at the average temperature of the lower temperature increment of the test (420°F) to −0.8665 ih/F at the average temperature of the upper temperature increment (580°F). During this portion of the test, it was also possible to measure, mechanically, the thermal expansion of the operating control rod drive extensions. The average expansion of the extensions was measured to be +0.0003 inch/F over the temperature range of 400°F to 600°F. The agreement between the measured and calculated values of the isothermal temperature coefficient of reactivity is considered satisfactory. The measured values are, on the average, about 7 per cent smaller than predicted. Because the calculations involved in the predictions are quite complex, a discrepancy larger than this would not have been unexpected. From the good agreement, it appears that the method used for calculating temperature-reactivity feedback effects in the reactor is probably accurate. This gives reason for optimism that the calculated power coefficients will also be sufficiently accurate. (auth)

42081 (CONF-193-11) BREEDING, SAFETY AND FUEL CYCLES. Okrent, David (Argonne National Lab., Ill.). 1963. Contract W-31-109-eng-38. 35p. Dep. mn; CFSTI $2.00 cy, $0.50 mn.

From 8th Nuclear Congress, Rome, June 1963.

The effects of fuel expansion, Doppler shifts, and sodium losses and expansion of the reactivity of heterogeneous, sodium-cooled, fast power breeder reactors are reviewed. The effects of these considerations on the design and per-

formance of U–Th and U–Pu power breeders are studied. (T.F.H.)

42082 (CONF-650633-1) DEVELOPMENT AND POTENTIALITIES OF THE HIGH TEMPERATURE PEBBLE BED REACTOR CONCEPT. Mueller, H.-W.; Lupberger, A. (Brown Boveri/Krupp Reaktorbau G.m.b.H., Duesseldorf (West Germany)). [1965]. 21p. Dep. mn.

From Forum Italiano Dell'Energia Nucleare, Rome.

A brief review of the AVR reactor design is given. The current status of the Thorium High Temperature Reactor THTR development is reported. Several aspects of the THTR are discussed. These include: fuel, graphite uses, purification of primary coolant, and some further design and development aspects. (M.O.W.)

42083 (COO-652-16) PIQUA NUCLEAR POWER FACILITY MONTHLY OPERATING REPORT NO. 26. (Piqua Nuclear Power Facility, Ohio). June 1965. Contract AT(11-1)-652. 23p. Dep. mn; CFSTI $1.00 cy, $0.50 mn.

Activities are summarized in sections on reactor operation, control and safety systems, and organic systems. (J.R.D.)

42084 (CVNA-239) MONTHLY OPERATNG REPORT, JUNE 1965. (Carolinas Virginia Nuclear Power Associates, Inc., Parr, S, C.). Contract AT(30-1)-2289. 36p. Dep. mn; CFSTI $2.00 cy, $0.50 mn.

Reactor operation continued during the first three weeks of the month at essentially the licensed power level of 44.3 Mw(t). On June 20, the power level was reduced and reactor was shutdown. The main reason for the shutdown was to remove Group VI control rods from the core since fuel burnup had reached the point that required their removal. Another reason was to complete and test changes made to improve the operation of the control rod drive system. A program of physics test work was also begun at this time. Down time was used to perform plant instrument, electrical, mechanical maintenance, and testing. Systems chemistry showed changes from the normal range due to shutdown conditions. The radiation exposure of plant personnel was maintained at a relatively low level and well within permissible limits. The shutdown was completed at the end of June. (auth)

42085 (EUR-2426.d) KERNKRAFTWERK GUNDREMMINGEN (KRB) JAHRESBERICHT 1964. (Gundremmingen (KRB) Nuclear Power Plant Annual Report, 1964). (Kernkraftwerk RWE-Bayerwerk G.m.b.H., Gundremmingen (West Germany)). May 1965. 59p. Dep.(mn).

The development, design, and construction work done at the Gundremmingen Nuclear Power Plant during 1964 is summarized. A time schedule for the completion of the work is included. The characteristics of the nuclear power plant installed are tabulated. (J.S.R.)

42086 (EUR-2427.i) CENTRALE ELETTRONUCLEARE DEL GARIGLIANO RELAZIONE ANNUALE 1964. (Garigliano Nuclear Power Plant Annual Report, 1964). (Ente Nazionale per l'Energia Elettrica, Rome (Italy)). May 1965. 133p. Dep.(mn).

The operation of the Garigliano Nuclear Power Plant during 1964 is reported. The startup program was completed. The data obtained on the operation of the power plant itself and the reactor in power production are summarized. The operation of the chemical plant, the processing of the water, and the monitoring of the installation by health physics are reported. The installation and programing of the computer for data processing are described. (J.S.R.)

42087 (EUR-2428.f) CENTRALE NUCLEAIRE DES ARDENNES. RAPPORT ANNUEL 1964. (Ardennes Nuclear Power Plant—Annual Report, 1964). (Societe d'Energie Nucleaire Franco-Belge des Ardennes, Chooz-Lez-Givet (France)). May 1965. 81p. Dep.(mn).

The design and construction work at the Ardennes Nuclear Power Station performed during 1964 is summarized. A time schedule for the completion of the work and the startup of the reactor is also included. A financial statement is presented for the nuclear power plant. (J.S.R.)

42088 (EUR-2430.n) KERNENERGIECENTRALE VAN 50 MWe TE DODEWAARD, JAARVERSLAG 1964. (50 MWe Dodewaard Nuclear Power Plant, Annual Report, 1964). (Samenwerkende Electriciteits-Productiebedrijven, N. V., Arnhem, Netherlands). 1965. 51p. Dep. mn.

The design, development, and construction of the Dodewaard Nuclear Power Plant performed during 1964 are summarized. The development of the nuclear steam supply system is described in some detail. The remainder of the installation is described in general. (J.S.R.)

42089 (GA-5938) DESIGN, CONSTRUCTION, AND INITIAL OPERATION OF GENERAL ATOMIC IN-PILE LOOP. Simon, R. H. (General Atomic, San Diego, Calif.). Feb. 16, 1965. Contract AT(04-3)-314. 150p. Dep. mn; CFSTI, $4.00 cy, $1.00 mn.

The test facility consists of a single full-diameter, quarter-length Peach Bottom fuel element, a closed-loop helium gas circulating system in which the heat generated is removed, a fission-product trapping system, provision for sampling both the main loop and the fission-product trapping system, and their required containment cubicles and shielding. The element was operated at a maximum measured fuel temperature of 2700°F. Some parts of the fuel reached calculated temperatures of 3000°F. (M.O.W.)

42090 (GA-6132) DEVELOPMENT OF THE GAS-COOLED FAST REACTOR CONCEPT. Fortescue, Peter; Shanstrom, R. T.; Fenech, Henri (General Atomic, San Diego, Calif. John Jay Hopkins Lab. for Pure and Applied Science). Feb. 12, 1965. Contract AT(04-3)-167. 11p. (CONF-650417-2) Dep.(mn); $1.00(cy), 1(mn) CFSTI

From American Nuclear Society, National Topical Meeting on Fast Reactor Technology, Detroit.

A description of the work carried out in several different areas is presented. These areas include: burnup studies leading to adoption of single batch fuel management as a practical and useful specification, water flooding studies, carbide fuel performance, more sophisticated fuel cycle cost analysis leading to core optimization, further thought on over-all plant proportions, and application extension including desalting. (M.O.W.)

42091 (GEAP-4852) CORE EVALUATION OF THE GARIGLIANO REACTOR. Macnabb, W. V. (General Electric Co., San Jose, Calif. Atomic Power Equipment Dept.). May 1, 1965. Contract AT(04-3)-189. 51p. (EURAEC-1444). Dep. mn; CFSTI $3.00 cy, $0.50 mn.

Work Performed Under United States–Euratom Joint Research and Development Program.

The Garigliano reactor is analyzed thermally, hydraulically, and mechanically in order to define improved modes of core operation. The results are presented as a set of parametric curves of MCHFR (minimum critical heat flux ratio) versus core power with the power distribution as a parameter. These calculations are intended primarily as a guide to uprating the core but also are used to evaluate alternatives for improving core performance. Two alternatives considered are (1) reducing core size and (2) changing fuel design. Conclusions are drawn which make recommendations and a suggested sequence of steps for action by SENN. (auth)

42092 (GEAP-4909) DEVELOPMENT PROGRAM ON THE GARIGLIANO NUCLEAR REACTOR. Quarterly Report No. 11. Howard, C. L. (General Electric Co., San Jose, Calif. Atomic Power Equipment Dept.). July 1, 1965. Contract AT(04-3)-189. 59p. (EURAEC-1436). Dep. mn; CFSTI, $3.00 cy, $0.75 mn.

Work Performed Under United States–Euratom Joint Research and Development Program.

All the individual program modules for the Garigliano on-line computer were satisfactorily tested at the site. The entire system is now being placed in on-line operation. The instrumented assembly and movable ion chamber designs were completed, and the fabrication of the first flowmeters was completed. The readout panel was fabricated. The plans were formulated for calibration of the completed instrumented assemblies in the heat transfer loop. The equipment for the fuel gamma scan using the $D_2O(\gamma,n)$ method was designed and ordered. Additional safeguards information was submitted as a topical report, "Final Safeguards Report, Garigliano Development Program,"

GEAP-4899. The rod oscillator drive mechanism was tested in San Jose and shipped to the reactor site. Preliminary calculations of control rod patterns during the reactor tests were completed. (auth)

42093 (GEAP-4912) PLUTONIUM SUBCRITICAL EXPERIMENT PROGRAM. Fourth Quarterly Report, April 1–June 30, 1965. Carver, J. G.; Robkin, M. A. (General Electric Co., San Jose, Calif. Vallecitos Atomic Lab.). July 1, 1965. Contract AT(04-3)-189. 22p. (EURAEC-1442). Dep. mn; CFSTI $1.00 cy, $0.50 mn.

Work Performed Under United States–Euratom Joint Research and Development Program.

Brief descriptions of work performed on the pressurized water system, fuel lattice, reaction rate measurements, theoretical studies, licensing, and schedules are given. A summary of progress to date and plans for future work are given. (M.O.W.)

42094 (NAA-SR-11314) 200-Mwe PROTOTYPE LARGE SGR—REACTOR STRUCTURE DESIGN AND EVALUATION. Anderson, D. R.; Foster, K. W. (eds.) (Atomics International, Canoga Park, Calif.). July 25, 1965. Contract AT(11-1)-Gen-8. 296p. Dep. mn; CFSTI, $6.00 cy, $1.50 mn.

The reactor structure design and evaluation for a 200-Mwe prototype large SGR is presented. The concept of the 1000-Mwe plant and its 200-Mwe prototype plant was completely described in December 1963. Additional analysis and studies completed since that time represent the thermo-mechanical design of the 200-Mwe prototype reactor structure. This document describes the expected operating environment for the 30-yr plant life, treats the steady-state and transient effects on the reactor structure, provides the basis for selection of materials, summarizes results of the mechanical-structural analysis, and describes calandria leak detection and remote maintenance techniques. The results of these studies indicate a highly reliable reactor, conservatively designed to fulfill operating requirements of the 200-Mwe SGR Prototype. (auth)

42095 (NAA-SR-11378(Vol.III)) FEASIBILITY STUDY OF A 1000-Mwe SODIUM-COOLED FAST REACTOR. VOLUME III. METHODS DEVELOPMENT. (Atomics International, Canoga Park, Calif.). July 25, 1965. Contract AT(11-1)-Gen-8. 184p. Dep. mn; CFSTI $5.00 cy, $1.00 mn.

The separate technical accomplishments in the area of methods development achieved during the modular flux-trap development are presented. Physics calculational techniques, hydrodynamic and thermodynamic calculational methods, kinetics calculation methods, and economics are discussed. In addition information is presented on sources of microscopic cross-section data, listing of 9W097 15-group cross-section library for use with CAESAR, listing of 9W088 15-group cross-section library for use with CAESAR, and preliminary 35-group ULCER library. (M.O.W.)

42096 (NAA-SR-11396) THE EFFECTS OF LONG-TERM OPERATION ON SRE Na SYSTEM COMPONENTS. Hansen, A. I. (Atomics International, Canoga Park, Calif.). Aug. 31, 1965. Contract AT(11-1)-Gen-8. 50p. Dep. mn; CFSTI $3.00 cy, $0.50 mn.

Major components from the main heat transfer system of the Sodium Reactor Experiment were subjected to a performance evaluation after seven years of in-system operation. Selected components were disassembled and/or sectioned for detailed examination and analysis. Retention of fission product in the cold trap and evidence of structural or mechanical weakness in mechanical components as a result of prolonged exposure to sodium were prime areas investigated. A partially saturated cold trap was found to contain fission products and a large number of other impurities in addition to oxides. The main intermediate heat exchanger showed no material defects or weaknesses. Although 24 out of the 316 tubes were found to be blocked by carbonaceous material, no thermal deficiency could be measured. A control rod was examined to determine the effect of prolonged exposure; the poison ring exposed to the highest integrated flux (3.3×10^{20} nvt) revealed a diameter growth of 0.56%. No major defects or weaknesses were discovered in any of the components examined. (auth)

42097 (ORNL-TM-1152) A PRELIMINARY INVESTIGATION OF LOW-TEMPERATURE, LIGHT WATER-COOLED AND MODERATED, SLIGHTLY-ENRICHED URANIUM METAL FUELED REACTORS FOR LARGE SINGLE-PURPOSE NUCLEAR DESALTING PLANTS. Chapman, R. H.; Gift, E. H. (Oak Ridge National Lab., Tenn.). Aug. 1965. Contract W-7405-eng-26. 42p. Dep. mn; CFSTI $2.00 cy, $0.50 mn.

Low-temperature, light water-cooled and moderated, slightly enriched uranium metal fueled reactors suggest significant savings in capital and fuel cycle costs in relatively large, single-purpose desalting plants. As this concept may be suitable for near-term application, a preliminary study was performed to determine current fuel limitations and approximate heat costs, based on a specified set of economic ground rules. Reactors of 1500 and 3500 Mwt (unit sizes) were selected for study. These reactor sizes are sufficient for producing 150 and 350 Mgd of fresh water, respectively, when coupled to water plants having performance ratios of about 10. (auth)

42098 (RT/PROT(65)24) SELEZIONE DEGLI OPERATORI DI CENTRALE ELETTRONUCLEARE. (Selection of Nuclear Power Station Operators). Giuliani, P.; Petrangeli, G. (Comitato Nazionale per l'Energia Nucleare, Rome (Italy)). June 1965. 38p. Dep. mn.

The problems connected with the selection of nuclear power station operators were examined in some detail. A discussion of the Italian situation as compared to that in other countries follows. A series of actual operator's examinations is included. (auth)

42099 (TID-22013) HALLAM NUCLEAR POWER FACILITY MONTHLY OPERATING REPORT NO. 33, APRIL 1965. (Consumers Public Power District, Hallam, Nebr.). Contract AT(11-1)-513. 54p. Dep. (mn); $3.00 (cy), $0.50 (mn) CFSTI.

Plant operation, testing, and performance during the month are summarized. Summaries are also included on plant maintenance, plant modifications, component transfers, moderator replacement, and radiation control. Procedure additions on moderator handling are included. (J.R.D.)

42100 (UNC-5092) SURVEY OF CURRENT METHODS FOR ANALYSIS OF FAST REACTOR TRANSIENTS INCLUDING MELTDOWN. Kazi, A. H.; Cherry, B. H. (United Nuclear Corp., White Plains, N. Y. Development Div.). Aug. 28, 1964. Contract AT(30-1)-2832. 120p. Dep. mn; CFSTI $4.00 cy, $0.75 mn.

A survey of current methods used in fast reactor transients and meltdown analyses is presented. The survey is not concerned with the calculation of reactivity coefficients such as Doppler, or in the problem of obtaining or calculating acceptable coolant void effects. Reactivity coefficients are assumed to be known in terms of various analytical formulations as given in the literature. The two principal and related areas studied are fast reactor transients and core meltdown. Also a discussion of specific fast reactor accidents is presented. (M.O.W.)

42101 (WAPD-PWR-1606(Add.2)) THE SHIPPINGPORT PRESSURIZED WATER REACTOR PROJECT CATALOG OF DOCUMENT ABSTRACTS. (Bettis Atomic Power Lab., Pittsburgh, Pa.). June 1965. Contract AT(11-1)-Gen-14. 58p. Dep. mn; CFSTI, $3.00 cy, $0.50 mn.

The abstracts included are contained in nine principal sections. The subjects are listed in chronological order. The pages are numbered consecutively in each of the nine sections: chemistry, core development, physics, reactor engineering, power plant, metallurgy, general, progress reports, and Duquesne light company test results. (auth)

42102 (WCAP-2385(Vol.I)) 1000 MWE CLOSED CYCLE WATER REACTOR STUDY. (Westinghouse Electric Corp., Pittsburgh, Pa. Atomic Power Div.). Mar. 1963. Contract AT(30-1)-3070. 322p. Dep. mn; CFSTI, $7.00 cy, $1.75 mn.

The feasibility study report of an all-nuclear 1000 Mwe

pressurized water reactor plant is presented. A report summary, conclusions, a detailed description of the reference plant design, consideration of two alternate core designs, and an analysis of the power generation costs are presented. (M.O.W.)

42103 (WCAP-2385(Vol.II)) 1000 MWE CLOSED CYCLE WATER REACTOR STUDY. VOLUME II. (Westinghouse Electric Corp., Pittsburgh, Pa. Atomic Power Div.). Mar. 1963. Contract AT(30-1)-3070. 181p. Dep. mn; CFSTI, $4.00 cy, $1.00 mn.

The feasibility study report of an all-nuclear 1000 Mwe pressurized water reactor plant is presented. A comprehensive nuclear evaluation of the reactor core, the feasibility report of the reactor vessel, minimum site requirements, a listing of recommended areas for continued study, and the proposed research and development program are included. (M.O.W.)

42104 (NP-tr-1234) DESCRIPTION OF THE FUEL ELEMENT FOR THE RAPSODIE REACTOR. Translated for Atomic Power Development Associates, Inc., Detroit, Mich., from the French. [nd]. 15p. Dep. mn; $1.60 fs, $0.80 mf, JCL.

A brief description of the fuel element for Rapsodie is presented. The core rod is obtained by placing mixed oxide pellets of UO_2 - PuO_2 containing 28 wt % PuO_2 in the interior of a can closed at its ends with helium-welded plugs. The cladding consists of steel of type AISI-316L. (M.O.W.)

42105 OBRIGHEIM NUCLEAR POWER PLANT—AS THE FUTURE OWNER CONCEIVED IT. Kallenbach, R. (Kernkraftwerk Obrigheim GmbH, Stuttgart). Atomwirtschaft, 10: 266-71(June 1965). (In German).

Partly because of experience gained from an earlier project, precise requirements were stipulated for the Obrigheim nuclear power station. The station was to be put up on a site at Obrigheim on the river Neckar. With base load operation and at maximum operational safety, the lowest possible cost per unit of power generated was to be achieved assuming conditions common to the German power utility industry (service life about 17 years; average plant factor 75%). The electrical output of the power plant was specified between 150 and 300 Mw. The plant, incorporating a pressurized-water reactor, is discussed. The conventional portion of the plant was designed for an output of 282.7 Mw. Gross output of the station will be 300 Mw. On the basis of a cost of DM 150,000 for each day of plant downtime it was determined to what extent it would be economically prudent, with a view to still higher plant availability, to duplicate plant components or to subdivide systems into several units with partial load assigned to each. A radiation level must be maintained permitting continued plant operation even in the event that one percent of the fuel elements become defective. (M.C.G.)

42106 PLANNING AND DESIGN OF THE 300 MW NUCLEAR POWER STATION AT OBRIGHEIM. Frewer, H.; Held, Chr.; Keller, W. (Siemens-Schuckertwerke AG, Erlangen, Ger.). Atomwirtschaft, 10: 272-82(June 1965). (In German).

In March 1965 a contract for construction at Obrigheim on the river Neckar of a nuclear power plant incorporating a pressurized-water reactor was awarded. On startup in 1968, with a gross electrical output of 300 Mw the plant will be the largest light-water cooled nuclear power station in Europe. The thermal output of the reactor will be 905 Mw. The fuel is UO_2 with an average enrichment of 3%, in Zircaloy cladding. The total weight of fuel inventory is 35 metric tons contained in 121 fuel elements holding 180 fuel rods each. Coolant outlet temperature is 310°C and pressure is 145 atm. Overall coolant flow rate is 22,000 metric tons/hr. The steam boiler produces saturated steam of 50 atm. abs. and 262.7°C. Improvements aim at an increased plant availability. Cost-saving design improvements were also included. The main coolant loop contains neither shut-off valves nor non-return flaps; pumps fitted with conventional motors are employed, and the size of the reactor pressure vessel was reduced by the use of novel control rod clusters. Another important objective is the achievement of a high mean fuel burnup. By means of fuel element reshuffling a flat distribution of the power density is to be maintained throughout the whole service life of the reactor plant. The achievement of high fuel burnup rates is facilitated through chemical shim control using boron. The reactor pressure vessel has an inside diameter of 3.27. The reactor building is designed as a containment and has a double safety shell: the inner one consists of a gas-tight steel sphere with a diameter of 44; the outer one is a reinforced concrete shell with a thickness of 0.80m at the bottom and 0.60m at the top, for screening off the environment in the event of a reactor incident. The steel containment is devised to withstand a pressure of 4.05 atm. abs. (auth)

42107 THE SUPERHEAT REACTOR AT GROSSWELZHEIM. Kornbichler, H. (Kernenergieanlagen, Frankfurt am Main). Atomwirtschaft, 10: 286-91 (June 1965). (In German).

Despite achievements by light-water reactors, the steam conditions obtained from these reactor types, wet steam of about 50 to 70 atm., are still unsatisfactory in terms of conventional power plant engineering. With the boiling-water reactor, nuclear superheating of the saturated steam generated can be achieved by passing it back in through the reactor core for absorption of additional thermal energy. The German medium-range program for the development of nuclear reactors incorporates an experimental plant with nuclear superheat. A contract was awarded to AEG for construction at Grosswelzheim of the superheat reactor (HDR), as developed and designed by AEG. This experimental reactor will have a thermal output of 100 Mw and reactor steam conditions of 500°C and 60 atm. It will operate on UO_2 fuel with 2.7% enrichment. The HDR was sited directly adjacent to the experimental nuclear power station at Kahl, and is scheduled to feed the steam produced into an existing 25 Mw(e) turbine generator of the Dettingen steam power plant, which is operated by RWE. As part of later extensions a separate superheat steam turbine set without intermediate steam converters is to be installed, whereby the electrical output of the plant will be raised to 35 Mw. Objective of building the HDR is to demonstrate that nuclear superheat can be adopted reliably for the production of electric power. Accordingly, the main purpose of the plant is to furnish operating experience, and in particular experience on fuel burnup, which represents a decisive basic criteron for an appraisal of the economics of nuclear reactor systems. This is why the initial core loading will comprise fuel elements of various designs and employ different canning materials. The startup of the HDR is planned for 1968. Construction was started recently. (auth)

42108 FUTURE DEVELOPMENT AND FUTURE OF THE D_2O PRESSURE BOILER REACTORS. Ziegler, A. (Siemens-Schuckertwerke AG, Erlangen, Ger.). Atomwirtschaft, 10: 390-2(July-Aug. 1965). (In German).

Heavy water reactors represent advanced types. They depend, however, essentially on already tested reactor technology. Especially the pressure boiler reactor has a future as a thermal breeder and for nuclear superheating. On economic grounds heavy water reactors can easily find a market as soon as they have reached the stage at which the individual power plants are competitive. (tr-auth)

42109 THE THORIUM FUEL CYCLE. Edlund, M. C. (Babcock and Wilcox Co., New York). Chem. Eng. Progr., 60: Symp. Ser., No. 51, 78-86(1964).

Fuel cycle costs for the thorium fuel cycle have been calculated for large, spectral-shift-control, pressurized-water reactors for 1968 and 1972. Recycle of the uranium-233 bred from thorium offers the potential of nuclear fuel cost as low as 1 mill/kwhr. (auth)

42110 HEAT TRANSFER IN ORGANIC-COOLED REACTORS. Shimazaki, T. T.; Huber, D. A.; Adler, K. L. (Atomics International, Canoga Park, Calif.). Chem. Eng. Progr., 60: Symp. Ser., No. 51, 128-36(1964).

The heat transfer aspects of organic-cooled nuclear power reactors are discussed. Data on convective heat transfer, boiling heat transfer, and critical heat flux are presented. Heat transfer limitations owing to pyrolytic

and radiolytic decomposition are discussed. Thermal and hydraulic data for a 300 Mw(e) organic-moderated and -cooled reactor are given. (auth)

42111 A VERSATILE STRATEGY OF THE NUCLEAR FUEL. Rollier, M. A. (Universita, Pavia, Italy). Chim. Ind. (Milan), 47: 291-302(Mar. 1965). (In Italian).

A versatile nuclear fuel strategy to be used in conventional reactors of today to produce in the Italian nuclear system an improvement in the conversion ratio bringing it to a near-breeding condition is discussed. It has an advantage from the standpoint of the balance of payments and with the possibility of reducing to a minimum the dependence on gaseous diffusion plants for fuel enrichment. The enriched fuel would be limited to the first fuel charge of the reactor. This nuclear fuel strategy requests a careful appraisal work on Th–^{233}U cycles, on thorium utilization systems in thermal converters, and on the feasibility of using new fuels made of a mixture of thorium and plutonium oxides. (auth)

42112 NIEDERAICHBACH NUCLEAR POWER STATION. EuroNuclear, 2: 281-3(June 1965).

The Niederaichbach power station is briefly described in which a gas-cooled, heavy-water-moderated, pressure-tube reactor will be used. The reactor, heating circuits, control system, reactor building, and equipment for fuel-element transport are covered. (D.C.W.)

42113 DEVELOPMENT OF THE DON PROJECT. EuroNuclear, 2: 283-4(June 1965).

The development and status of the organic-cooled heavy-water-moderated reactor are summarized covering measurements in an exponential assembly, fuel development, and research on SAP-stainless steel joints. (D.C.W.)

42114 A CALORIMETRIC DETERMINATION OF FISSION PRODUCT HEATING IN FAST REACTOR PLUTONIUM FUEL. Johnston, K. (Atomic Weapons Research Establishment, Aldermaston, Berks, Eng.). J. Nucl. Energy: Pts. A and B, 19: 527-39(July 1965).

Fission product heating in plutonium irradiated in the Dounreay Fast Reactor was measured using a Calvet microcalorimeter. By use of small, lightly canned samples and a γ-absorber, the β- and γ-power contributions were measured separately over a range of decay times between 40 and 150 days after shutdown. (auth)

42115 DESIGNED: THE PORTABLE POWER REACTOR. Luchter, Stephen (Aerojet-General Nucleonics, San Ramon, Calif.). Mech. Eng., 87: 32-5(June 1965).

The water-moderated multipurpose military portable power reactor is described including the buildings. The reactor assembly is packaged in an aluminum tank, which also serves as a support structure. Borated water is circulated within the annuli between the inner and outer lead shields and the interior of the tank. The control drive mechanisms are housed in cavities in the wall of the shield tank and operate the control blades by means of rotating shafts that extend into the core at right angles to the control blades. (D.C.W.)

42116 THE DOUNREAY FAST REACTOR. SUSTAINED FULL POWER OPERATION. PART II. Phillips, J. L. Nucl. Eng., 10: 291-3(Aug. 1965).

The operation efficiency and methods of feeding new elements and removal of irradiated elements were improved. The objectives were to make refueling time dependent solely on refueling machine operation, and to eliminate idle time of the machine. The refueling rate was increased from an uncertain fourteen per day to a firm twenty per day. The effects of oxide deposits on snout jaw operation of the charge machine were reduced by use of glove boxes. Over 2700 core and 600 breeder elements were recharged without any major difficulties or damage to any element. The control system, electro-magnetic pumps, control and safety circuits, normal operation, and use of vented fuel are discussed. (F.J.H.)

42117 MEASUREMENT OF GAMMA HEATING IN D.F.R. Dehn, R. (Dounreay Experimental Reactor Establishment, Caithness, Scotland). Nucl. Instr. Methods, 36: 141-52(Sept. 1965).

A series of experiments has been carried out in the Dounreay Fast Reactor at power levels from 1 to 60 Mw to measure the gamma heating (total energy deposition) in materials such as tungsten and stainless steel. Most of the measurements were made in the first row of the breeder, and in this position the mean value for the gamma heating in stainless steel was found to be 28 mw/g · Mw ± 15%. Several different calorimeter designs are discussed. The electrical calibration procedure is outlined. One standard type and the novel twin-bulb differential calorimeter are described in detail. (auth)

42118 THE HEAT-ENGINEERING DATA OF A PRESSURIZED WATER REACTOR WITH SPECIAL CONSIDERATION OF A POSSIBLE BREAKDOWN OF THE PRINCIPAL CIRCULATING PUMP. Kampfenkel, Ottomar; Ulrych, Gerhard (Siemens-Schuckertwerke AG, Erlangen, Ger.). Nukleonik, 7: 236-41(May 1965). (In German).

For the heat-engineering configuration of the core of a nuclear power plant, a series of conceivable operational perturbations and accidents are considered, in addition to the conditions of the plant in normal operation at stated outputs. After an introductory representation of the essential heat-engineering data for pressurized water reactors, the consequences of a possible breakdown of the principal circulating pump were considered. (tr-auth)

42119 THE SAINT-LAURENT-DES-EAUX NUCLEAR POWER STATION-SEALING BARRIERS AROUND THE FOUNDATION PITS. Maillard, R.; Couineau, P. Travaux, No. 355, 579-84(June 1964).

Construction at the Saint-Laurent-des-Eaux power station is described. The first unit of this station (EDF-4) will have an output of 500 Mwe. The pressure vessels, the subsoil characteristics, and the construction of the protecting barrier around the foundation pits are described in detail. (D.C.W.)

42120 LARGE NUCLEAR-POWERED SEA WATER REVERSE OSMOSIS PLANTS. Keilin, B.; Watson, E. R. 10p. (CONF-650401-8). Gmelin, AED-CONF-65-041-26.

From American Chemical Society, Detroit.

It is pointed out that reverse osmosis can be used in conjunction with a nuclear reactor to yield at least as much electrical power and, at the same time, produce a considerably greater quantity of water in a desalting plant than the distillation system under optimum conditions. (L.B.S.)

42121 NUCLEAR POWER AND SUPERCRITICAL STEAM CYCLES. MacMillan, John H. (Babcock and Wilcox Co., Lynchburg, Va.). 10p. (CONF-650429-12). ORINS.

From American Power Conference, Chicago.

The evolutionary steps in the technological progress of converting thermal energy to electricity in central power stations are reviewed. A summary is presented of steam cycle evolution, energy conversion precepts, reactor design evolution, steam cooled breeder reactors, and other major developments in reactor physics, fuel element materials, and components. (L.B.S.)

42122 NUCLEAR REACTOR VESSELS—1965 STATUS. Gaines, A. L. (Combustion Engineering, Inc., Chattanooga). 8p. (CONF-650429-13). ORINS.

From American Power Conference, Chicago.

The reactor vessel designers and fabricators have been shown capable of meeting the size requirements for single reactor stations having capacities up to 1,500,000 Kw(e). The next efforts of this industry will be directed toward producing vessels in the quantities required by the nuclear power plant market expansion and delivering them. The ability to furnish a vessel for a remote site remains to be demonstrated, but exists. The real news of the past decade is the increase in size of vessel the fabricators are capable of building— from a vessel size restricting power capacity to only 150,000 Kw(e) to a vessel size permitting 1,500,000-Kw(e) capacity in a single reactor. (auth)

42123 NUCLEAR STEAM GENERATORS. Davies, D. K. (Babcock and Wilcox Co., Barberton, Ohio). 25p. (CONF-650429-14). ORINS.

From American Power Conference, Chicago.

A review of the progress made in steam generator designs for central station plants in the past five years shows that much has been accomplished. New data have provided increased confidence in performance predictions and have, in some cases, permitted a significant reduction in capital costs or in station heat rate. A not insignificant factor in the progress which has been made has been the concurrent development of manufacturing skills and facilities. Many techniques necessary to the manufacture of nuclear steam generators are considered routine today whereas five years ago they were being used on an experimental or developmental basis. We are confident that the next five years will see comparable progress in manufacturing techniques as well as in design development. (auth)

42124 DUAL PURPOSE NUCLEAR PLANTS FOR WATER DESALINATION AND POWER. Lang, Peter M. (Allis-Chalmers Mfg. Co., Bethesda, Md.). 4p. (CONF-650429-11). ORINS.

From American Power Conference, Chicago.

With a nuclear dual purpose plant, operated at base load, the aim of obtaining desalted water from the ocean at costs within the 30-40¢/1000 gal. range while selling power at a normal price is attainable in the near future in those areas having large demands for both products. Converted water at this cost will replace few natural sources of water but will be acceptable for municipal and industrial uses where adequate natural sources do not exist. This cost of water is still too high for extensive agricultural use. The high present capital cost of water conversion plants is the main barrier to lowering the cost of desalted water. The aggressive development of water-conversion equipment now taking place should lead to future water costs significantly below those estimated here. (auth)

42125 IMPROVEMENTS IN NUCLEAR GENERATORS. (to Societe Rateau). British Patent 998,135. July 14, 1965. Priority date Feb. 3, 1961, France.

A nuclear power generator combines a direct cycle repressurizing of the operative fluid in the liquid phase with extraction of the heat in the gaseous phase. An operative fluid in the form of super-heated vapor is used for cooling the reactor and is divided, upon leaving the reactor, into two streams that flow through different circuits in the installation. In one circuit the fluid serves to generate power, and in the other it serves to cool the reactor. The power generation circuit includes a turbine with an associated condenser and a pump for recycling the condensed fluid in the liquid state. The other circuit includes a mixer and means for discharging the condensed liquid into the mixer to be vaporized before being returned to the reactor. A vessel is provided that is divided by a perforated partition into two chambers, one of which forms the mixer and the other that contains the reactor. A flow of vapor between the two chambers is possible through the perforated partition and through a conduit with a blower being provided for forcing movement through the conduit. Both the blower and the conduit may be disposed inside the vessel. Since the vapor in the different chambers of the vessel is at different temperatures, the partition is made of a material that is a poor conductor to act as a thermal screen between the chambers. (B.J.M.)

42126 NUCLEAR POWER PLANT. Kagi, Jakob (to Sulzer Freres). Canadian Patent 696,336. Oct. 20, 1964. Priority date Sept. 21, 1960, Switzerland.

The reactor core in this nuclear power plant is steam cooled. This steam coolant is divided into two streams; one does useful work in a turbine and is subsequently condensed, while the other stream is circulated by a blower and recooled by evaporating the condensate of the first stream. It is claimed that the power required for circulation of the coolant is considerably reduced by this arrangement. (F.S.A.)

Process Heat Reactors

42127 (TID-22009) HIGH-TEMPERATURE ENERGY SYSTEMS. Quarterly Progress Report, February 1-April 30, 1965. (Bureau of Mines, Morgantown, W. Va. Morgantown Coal Research Center). 43p. Dep. mn; CFSTI $2.00 cy, $0.50 mn.

The Atomic Energy Commission and the Bureau of Mines continued to cooperate in the development of closed-cycle (Brayton) gas turbine power systems. In the system under development, the turbine is to be driven by high-temperature inert gas that is heated by nuclear fuels or coal. Operation at high temperatures with radioactive materials or coal presents difficulties in construction materials, lubricants, and working fluid leakage. A possible solution to the difficulties lies in the use of turbomachinery with gas-lubricated bearings. During the year the Bureau contracted for the design and construction of a prototype closed-cycle gas turbine equipped with gas-lubricated bearings. After preliminary laboratory tests, the turbocompressor was installed in a test facility and was operated on a self-sustaining basis. Study was initiated on equipment items for a high-temperature closed-cycle gas turbine system fired by coal. Gas-solids suspensions appear promising as working fluids for various energy conversion systems, including the closed-cycle gas turbine. During the year it was found that addition of about 30% by weight of powdered stainless steel to graphite eliminated deposition on heat exchanger walls. Powdered metals were also circulated successfully. Powdered metals appear suitable for evaluating the heat-transfer capability of suspensions. A system was constructed for determining the energy required to circulate suspensions. Initial tests with this system indicate that the energy required is not proportional to total mass flow but is somewhat lower. Tests with a system for determining film coefficients of heat transfer for suspensions were initiated. Evaluation of suspensions was made more difficult by the absence of satisfactory flowmeters. A meter for measuring the flow of suspensions was developed. Work was continued on the gasification of bituminous coal using nuclear reactor heat. Emphasis was directed toward evaluation of fluidized-bed gasifiers heated by He, simulating nuclear systems. Alloys were tested to determine their suitability for use in externally heated, fluidized-bed coal gasifiers; only Hastelloy-X showed promise for use in this application. (J.R.D.)

Production Reactors

42128 (BNWL-95, pp 18-23) ENGINEERING PHYSICS. COMPARISON OF DIFFUSION AND TRANSPORT CALCULATIONS FOR NPR TUBE-IN-TUBE FUEL GEOMETRY. Bennett, C. L. (Battelle-Northwest, Richland, Wash. Pacific Northwest Lab.).

In fuel cycle calculations the use of diffusion theory coupled into an automatic burnup routine is found to be a great convenience. Diffusion theory is used in a study of a particular NPR fuel geometry and composition. The system studied is an NPR unit cell in cylindrical geometry with zirconium clad, uranium metal, tube-in-tube fuel. (M.O.W.)

42129 (DPSPU-65-30-27) SRP REACTOR ON-LINE COMPUTER—PROCESS. Field, F. R. Jr.; Butterworth, R. R.; Gimmy, K. L.; Hurley, T. J.; Hartshorn, W. R.; Ryder, F. D. (Du Pont de Nemours (E. I.) and Co., Aiken, S. C. Savannah River Plant). July 1965. Contract AT (07-2)-1. 6p. (CONF-650917-1). Dep. mn; CFSTI, $1.00 cy, $0.50 mn.

From International Conference on Industrial Electronics and Control Instrumentation, Philadelphia.

A GE 412 on-line computer has proved valuable in increasing safety and assisting operation of a large heavy-water-moderated nuclear reactor at the Savannah River Plant. Computed performance data close to operating control limits are displayed frequently for the reactor

operator; about 3250 sensor readings are made every 4½ minutes. Computer output (available >99% of the time) gives, with the existing system of comprehensive written procedures, improved reactor control. (auth)

42130 (HW-68387) REMOVAL OF RADIOISOTOPE PARENT MATERIAL BY PRODUCING HIGH PURITY PROCESS WATER. Perkins, R. W. (General Electric Co., Richland, Wash. Hanford Atomic Products Operation). Feb. 10, 1961. Contract AT(45-1)-1350. 5p. Dep. mn; CFSTI, $1.00 cy, $0.50 mn.

$Al(NO_3)_3 \cdot 9H_2O$ was used as flocculating agent in the treatment of water for one side of the H reactor, while $Al_2(SO_4)_3 \cdot 18H_2O$ was used for producing "normal" water for the other side of the reactor. The raw water and process water from both sides of the reactor were analyzed for 14 parent elements. Both treatments were found to increase the Na and Ga concentrations, but considerable reductions in the effluent radioisotopes were obtained with the $Al(NO_3)_3 \cdot 9H_2O$ treatment. (D.L.C.)

42131 (HW-77028) N-REACTOR, PRESSURIZER-HIGH PRESSURE INJECTION PUMP SIMULATION STUDY. PART II. SYSTEM RESPONSE TO SMALL DISTURBANCES. Robinson, R. K. (General Electric Co., Richland, Wash. Hanford Atomic Products Operation). June 25, 1963. Contract AT(45-1)-1350. 68p.

The results of an analog simulation study of the system response to the small disturbances of process tube diversion and return, reactor power level increase and decrease, and some instrumentation failures are presented. The data and conclusions derived from the simulation runs are presented. (M.O.W.)

Propulsion and Space

See also ENGINEERING — Space Propulsion.

Refer also to abstract 40703.

42132 (GE-TM-65-3-6) NUCLEAR DRY CARGO SHIPS VS. CONVENTIONAL. Blumberg, Ben Jr. (General Electric Co., Cincinnati, Ohio. Nuclear Materials and Propulsion Operation). Mar. 5, 1965. Contract AT(40-1)-2847. 20p. Dep. mn; CFSTI, $1.00 cy, $0.50 mn.

Conventional and nuclear power in a 13,000 DWT dry cargo vessel operating over a speed range from 18 to 28 knots are compared. Ship operating costs are shown for foreign flag (or U. S. subsidized) and United States flag ships operating without subsidy. The nuclear steam generator used is the 630A Mark V. A definite advantage for the nuclear ship vs. the conventional ship over a wide range of operating conditions is shown. This advantage reaches 28 percent on the operating cost of a ship per mile traveled. A potential reduction in the present U. S. subsidy of about 30 million dollars per year is shown to be possible assuming both the foreign flag and U. S. ship operators have optimum nuclear ships. (auth)

42133 (GEMP-340) 630A MARK III MARITIME NUCLEAR STEAM GENERATOR SUMMARY REPORT. (General Electric Co., Cincinnati, Ohio. Nuclear Materials and Propulsion Operation). Feb. 26, 1965. Contract AT (40-1)-2847. 11p. Dep.(mn), $1.00(cy), 1(mn) CFSTI.

The Mark III design concept of the 630A Maritime Nuclear Steam Generator is described. A bibliography of reports issued in connection with the design work is included. (J.R.D.)

42134 (IDO-17070) STEP PROJECT. Quarterly Technical Report, January–March 1964; April–June 1964. Dietz, K. A. (ed.) (Phillips Petroleum Co., Idaho Falls, Idaho. Atomic Energy Div.). June 1965. Contract AT(10-1)-205. 218p. Dep. mn; CFSTI $6.00 cy, $1.25 mn.

The Safety Test Engineering Program is concerned with the safety testing of the small aerospace SNAP 10A/2 reactors and with the loss-of-fluid testing of a typical pressurized water reactor. The Loss of Fluid Test Program (LOFT) will be performed on a 50 Mw(t) pressurized water reactor representative of commercial pressurized water reactor systems. Testing of the SNAPTRAN 2/10A-1 reactor was limited to a performance evaluation of the stepper and impulse drum drive-units and a critical loading of the reactor. Data acquisition systems were installed, evaluated, and calibrated for the SNAPTRAN 2/10A-3 destructive test which was performed. The test results are interpreted and presented. Technical progress in the Loss of Fluid Test Program included final selection of the test site and completion of the preliminary mechanical design of the reactor vessel and internals. Nuclear, heat-transfer, and hydraulic studies and a blowdown analysis were also completed. A preliminary investigation of the estimated contamination of the LOFT containment system and a radiological computer program (RSAC) for determining the inhalation doses were also completed. (auth)

42135 (LA-3304) INTEGRAL GAMMA AND NEUTRON MEASUREMENTS ON THE KIWI TNT. Lee, P. K.; Worman, F. C. V. (Los Alamos Scientific Lab., Univ. of California, N. Mex.). May 3, 1965. Contract W-7405-eng-36. 18p. Dep. mn; CFSTI, $1.00 cy, $0.50 mn.

Gamma and neutron doses and integral neutron fluxes produced by the Kiwi TNT nuclear destruct event were documented. Dosimetry stations were positioned close to the reactor for measurement of prompt and fission product radiation. In addition, gamma doses resulting from the effluent cloud were monitored at distances out to 50 miles downwind with dosimeter films. Total rad doses of gamma and neutron radiation were 1.91×10^4 rads 50 feet from the reactor and decreased to 46.9 rads at 1,000 feet. Fission product gamma activity was selectively dispersed by the winds and produced an anisotropic gamma dose distribution even as close as 100 feet from the reactor. Gamma doses downwind from the reactor were 250 mR at 8,000 feet, 330 mR at 16,000 ft, 150 mR at 6 miles, and 10 mR at 12 miles. (auth)

42136 (LA-DC-6941) HYDRAULIC CONTROL ROD ACTUATORS FOR THE KIWI-TNT NUCLEAR REACTOR. Frame, Roy A.; Milich, Charles P. (Los Alamos Scientific Lab., Univ. of California, N. Mex.). [June 1963]. Contract W-7405-eng-36. 12p. (CONF-651002-4). Dep. mn; CFSTI, $1.00 cy, $0.50 mn.

For Presentation at Instrument Society of America, 20th Annual Conference, Los Angeles.

A nuclear rocket reactor received severe structural damage during a planned experiment which consisted of withdrawing the control rods to the maximum reactivity position very rapidly. This experiment was aimed at providing insight into the mechanism whereby nuclear rocket reactor power excursions become self-limiting. Hydraulic actuators which rotated the control rods at a velocity of 4000°/sec are described along with experimental results for actuator velocity and torque. Delay circuits and simultaneity measurements for 12 control rods are also presented. (auth)

42137 (LA-DC-7313) THERMAL RADIATION FROM BURNING HYDROGEN PLUME. Martin, Paul E. (Los Alamos Scientific Lab., Univ. of California, N. Mex.). [nd]. Contract W-7405-eng-36. 5p. (CONF-651002-6). Dep. mn; CFSTI $1.00 cy, $0.50 mn.

From Instrument Society of America, 20th Annual Conference, Los Angeles.

Liquid hydrogen passes through a nuclear reactor, is ejected skyward, and ignited. Its thermal radiation pattern is to be studied so that expected heat radiations may be calculated for locations near the test pad. Several sensors — commercial and home made — are used to determine the thermal radiation received at discrete points. From measured radiation, range, assumed plume height, and sensor orientation and height, the average thermal emitting power per unit distance along the vertical plume is calculated. (auth)

42138 (N64-33780) INTRODUCTION TO NUCLEAR PROPULSION. Lecture 13 — Reactor Control. DeRosier, T. A. (General Electric Co., Cincinnati, Ohio Nuclear Materials and Propulsion Operation). Apr. 1963. Con-

tract NAS 8-5215. 53p. (NASA-CR-52943; GEMP-190h). $2.00(CFSTI).

Some of the peculiarities of reactor control are pointed out. Automatic and manual control along with safety requirements are discussed. Some reactor control characteristics such as reactivity coefficients are discussed. The reactor control process such as reactivity control, automatic flux control, automatic temperature control, startup control, and reactor safety are discussed. (M.O.W.)

42139 (N64-33784) INTRODUCTION TO NUCLEAR PROPULSION. LECTURE 21. NUCLEAR ROCKET SYSTEM. Motsinger, Russell E. (General Electric Co., Cincinnati, Ohio. Nuclear Materials and Propulsion Operation). 1963. Contract NAS 8-5215. 35p. (NASA-CR-52948; GEMP-190n(Pt.B)). CFSTI $3.00 cy, $0.50 mn.

Information is presented on reactor conditions in typical missions, reactor thermal design requirements, nuclear design requirements, and minimization of non-reactor engine components. Data and information are also included on thermodynamics of fuel elements, design and pressure loss relations for heat addition to H_2 in constant area ducts, and a method for converting nuclear information on critical mass for solid spherical geometries to cylindrical geometries with voids. (J.R.D.)

42140 (NAA-SR-11353) AEROSPACE SAFETY PROGRAM—SAFE DISPOSAL OF SNAP REACTORS. Determan, R. L.; Weitzberg, A.; Willis, C. A. (Atomics International, Canoga Park, Calif.). July 25, 1965. Contract AT-11-1-GEN-8. 41p. Dep. mn; CFSTI $2.00 cy, $0.50 mn.

Methods for safely disposing of SNAP reactors after space operation are evaluated. There are three principles which may be employed: decay, dilution, and recovery. Three basic methods have evolved for implementing the disposal principles; the basic methods are: (1) boost to a long-lived orbit, (2) destruct, and (3) controlled reentry. The value of each of the methods depends on the characteristics of the reactor. Combinations of these methods for the short orbit case are considered and several systems are found to be promising. For the long orbit case, it is found that a reliable end-of-life shutdown device coupled with intrinsic subcriticality effectively eliminates all safety problems for these missions. It is concluded that: (1) an effective destruct device should be developed, (2) practical aspects of boost and deboost systems should be investigated, (3) data should be obtained and used to provide a more realistic evaluation of fallout hazards, and (4) intact reentry systems appear undesirable. (auth)

42141 (NASA-CR-54422) DESIGN STUDY OF MODIFICATION OF M-1 LIQUID HYDROGEN TURBOPUMP FOR USE IN NUCLEAR REACTOR TEST FACILITY. Knuth, W. H.; Farquahr, J.; Lindley, B. (Aerojet-General Corp., Sacramento, Calif.). May 15, 1965. Contract NAS 3-2555. 123p. (AGC-8800-5).

A design study was conducted to determine the capability of adapting the M-1 fuel turbopump to satisfy the requirements of the PHOEBUS II Reactor Liquid Hydrogen Feed System. Appropriate design and performance analyses as well as mechanical design effort were performed to the extent needed to permit rapid transition into a development program. A 20% stall margin is predicted for the resulting pump hydraulic geometry at the nominal PHOEBUS operating point. A nominal speed of 11,500 rpm will be required to produce a 1400 psi pressure rise at a hydrogen weight flow of 350 lb/sec. The predicted nominal turbine weight flow is approximately 55-lb/sec. (auth)

42142 (R62FPD-252) 630A BLOWER FEASIBILITY STUDY. Gisslen, J. M. (General Electric Co., Cincinnati, Ohio. Large Jet Engine Dept.). June 26, 1962. Contract AT(40-1)-2847. 86p. Dep. mn; CFSTI $3.00 cy, $0.75 mn.

A feasibility study of a single stage axial blower for the 630A Nuclear Powered Steam Generator was carried out. The study results show a need for two different blowers, one for continuous duty and one for auxiliary duty, provided the requirements prescribed by NM & PO must be met. The study has confirmed the need for initiating a seal test program to develop the technology required to meet the tight seal requirements. It is suggested that the aerodynamics of the proposed blower be designed by aid of full scale testing, which also should include optimization of inlet, turns and exit. Bearings should be built and tested before the blower is put into service. Blade stress levels in the design are on the high side and the design should be adjusted to reduce these to values comparable with those of stationary gas and steam-powerplants. (auth)

42143 NUCLEAR PROPULSION IN MARITIME TRANSPORT: THE SHIP "SAVANNAH." Automazione Automatismi, 9: 27-40(Jan.-Feb. 1965). (In Italian).

The history of the development of the concept of nuclear propulsion for ships is traced from the first proposals by Fermi through the construction of the "Nautilus." The design and characteristics of the "Savannah" are then described. Proposals for the nuclear propulsion of ships are summarized. The problem of safety in nuclear ships and the preparation of nuclear fuels are indicated. (J.S.R.)

42144 TEST FACILITIES FOR NUCLEAR ROCKETS. Rose, B. F. Naval Engrs.' J., 77: 89-92(Feb. 1965).

The facilities of the first large-scale nuclear rocket engine test installation at the Nevada Test Site at Jackass Flats, Nevada, are described including the safety and shielding standards that were developed. The center will be used for ground testing of the hydrogen-fueled Nerva engines. (D.C.W.)

42145 THE NUCLEAR ROCKET. Space/Aeron., 43: No. 4, 32-9(Apr. 1965).

Developments in the Rover nuclear propulsion technology program are discussed. Nuclear rocket concepts are described according to core compositions, which include the dust bed and liquid core, gas core and solid core. Particular attention is given to developments for the solid-core Nerva engine. (L.B.S.)

42146 NON-DESTRUCTIVE INSPECTION OF FUEL ELEMENTS FOR NUCLEAR ROCKETS. Tenney, Gerold H. pp 43-7 of Non-Destructive Testing. London, Butterworths, 1964.

Some of the contributions made by non-destructive testing towards the development of the Kiwi-A fuel elements are described. Radiographic techniques developed for this purpose are outlined. By means of this inspection method, the uniformity of distribution of uranium in the graphite, inclusions, laminations, and other defects were studied. Radiation gages were used to obtain data on the density distribution. Special ultrasonic inspection techniques were developed for the detection of laminar cracks in fuel plates. Specifications were developed and established. The non-destructive inspection of tested, and thereby highly radioactive, fuel elements was carried out. The Rover program and selection of material are reviewed. (M.C.G.)

42147 FUNDAMENTALS OF NUCLEAR FLIGHT. Bussard, R. W.; DeLauer, R. D. New York, McGraw-Hill Book Co., 1965. 461p. $15.50.

A collection of applications of many various and different fields of engineering and physics are given in discussing the fundamentals of nuclear flight propulsion. The topics covered are nuclear flight propulsion, the principles of performance analysis, heat transfer and fluid flow, fission-reactor neutronics, nuclear radiations, radiation leakage, and shielding, materials, requirements, properties and problems, and reactor-design and engine-cycle considerations. (J.F.P.)

Research and Test Reactors

42148 (AECL-2216) THE NRU MONITOR COMPUTER AND SELF-POWERED NEUTRON FLUX DETECTORS. Morin, K. R. (Atomic Energy of Canada Ltd., Chalk River (Ontario)). May 1965. 45p. Dep.; AECL $4.50 cy.

The part played by the PDP-5 in the real-time dual computer system at the NRU reactor is described. The

PDP-5 basically digitizes signals from an analog multiplexer, checks the values against alarm levels, and then passes them on to the PDP-4, which uses them for display and control. Particular attention is paid to the computer usage of self-powered neutron flux detectors. The PDP-5 input-output equipment is described. The program organization is outlined, and the use of the program interrupt, establishment of priorities, and interlacing of printouts are discussed. The multiplexer programs are described in detail, including alarm printouts and the introduction of hysteresis into the digital alarm levels. The flux detector programs are described, including background corrections and the daily recalibration of the sensitivity factors. The detailed mathematics used with the rhodium detectors is given. Some alternatives to using a computer to follow detectors' decrease in sensitivity are outlined. Details of program sizes and execution times are given. (auth)

42149 (ANL-6961) EXPERIMENTS WITH CENTRAL SUPERHEATER CORE CSH-1, BORAX-V. (Argonne National Lab., Ill.). Jan. 1965. Contract W-31-109-eng-38. 151p. Dep. mn; CFSTI $5.00 cy, 3 mn.

The central-superheat core CSH-1 in Borax-V operated one week before a leak between superheated-steam and moderator-water systems forced its discontinuance. Several days of this operation included powers up to 10.2 Mwt. A review is given of reactivity measurements, neutron flux mapping, superheater-fuel experience, in-core instrumentation development and data, water chemistry measurements and catalytic recombination experiments, and overall plant performance. (T.F.H.)

42150 (ANL–7009) A FEASIBILITY STUDY OF THE APPLICATION OF A DIGITAL DATA ACQUISITION AND PROCESS CONTROL SYSTEM TO A RESEARCH REACTOR. Vellender, G. C. (Argonne National Lab., Ill.). Jan. 1965. Contract W-31-109-eng-38. 132p. Dep. mn; CFSTI, $4.00 cy, $1.00 mn.

The advantages of the digital data acquisition and control system are discussed. The digital data system characteristics and the techniques of application are considered in detail. Such topics as: accuracy, speed of data sampling, process-transducer characteristics, word length, equipment reliability, electrical noise susceptibility and emanation, input/output subsystems, programing, utility requirements, and service conditions are discussed. A test-evaluation installation is proposed. A complete system specification and cost estimate are also included. (auth)

42151 (CEA-R-2518(Vol. II)) RAPPORT DE SURETE DE REACTEUR PEGASE. TOME II. SURETE DES INSTALLATIONS. (Safety Report Concerning the Reactor PEGASE. Volume II. Safety of the Installations). Venezziano, Augusta (Societe d'Exploitation des Materiels Hispano-Suiza, Boid-Colombes (France)); Lacour, Jean (Commissariat a l'Energie Atomique, Saclay (France). Centre d'Etudes Nucleaires). Mar. 1965. 338p. Dep. mn.

Accidents are examined that could cause damage to the Pegase reactor installation. Among possible causes of accidents considered are the seismicity of the region, an excessive power excursion of the reactor, and a fracture in the sealing of an independent loop. Although all possible precautions have been taken to offset the effects of such accidents, their ultimate consequences are considered. The importance is stressed of the security action and regulations which, added to the precautions taken for the construction, assure the safety of the installations. (auth)

42152 (IDO–17088) REACTOR STABILITY TESTS IN THE SPERT IV FACILITY. Crocker, J. G.; Martinson, Z. R.; Potenza, R. M.; Stephan, L. A. (Phillips Petroleum Co. Idaho Falls, Idaho. Atomic Energy Div.). July 1965. Contract AT(10-1)-205. 70p. Dep. mn; CFSTI $3.00 cy, $0.75 mn.

A series of tests to investigate the stability characteristics of a highly enriched, water-moderated, plate-type core was performed in the Spert IV facility. Most of the tests were initiated at atmospheric pressure, ambient (≈20°C) bulk water temperature, and with only natural water circulation through the core. The results of these tests showed that, following rampwise reactivity insertions up to 5.0$ (the maximum used) at an average rate of about 0.15$/sec, the core under investigation would not become unstable as long as the inlet water temperature to the core remained near ambient. One test was performed in which the bulk water temperature of the system was increased by operation of the reactor at significant power levels with no heat removal equipment in operation. In this test, 4.0$ of reactivity was inserted in a ramp, and the reactor became unstable when the inlet water temperature reached approximately 70°C after about 12.5 minutes of reactor operation. Upon becoming unstable, the reactor power exhibited successive power oscillations with peaks of 7.5, 15, 25, and 50 Mw with a frequency of two cycles per second. A few tests were performed with 1.2 ft/sec forced coolant circulation through the core under ambient bulk water conditions. Under these conditions, the reactor was not made unstable because potential fuel plate burnout problems were encountered with reactivity insertions which were insufficient for obtaining divergent power oscillations. From the various tests which were performed, the rms value of the reactor power noise, special power densities, and spectral moment frequencies were determined in order to evaluate the usefulness of these quantities in determining reactor stability characteristics. The results showed that these quantities can be of value in predicting the onset of reactor instability. The experimental and analytical results obtained from the Spert IV stability tests are presented in this report. (auth)

42153 (JUL-235-RE) UBERPRUFUNG DER NOTKUHLANLAGE DES REAKTORS FRJ-2 (DIDO). (Testing of the Emergency Cooling System of the Reactor FRJ-2 (DIDO)). Paul, H.-G. (Kernforschungsanlage, Julich (West Germany)). June 1964. 18p. Dep.(mn).

Measurements made on a simulated tube break in the primary coolant circuit of the FRJ-2 reactor and the testing of the emergency coolant installation are reported. The velocity at which the heavy water leaves the reactor tank in the case of a break, the water mass necessary for the emergency coolant installation, the heavy water supply available for the emergency coolant, and the conditions for the startup of the emergency coolant installation were determined. (J.S.R.)

42154 (KFK–261) EINE METHODE ZUR UNTERSUCHUNG DER INELASTISCHEN STREUUNG LANGSAMER NEUTRONEN AN VIELTEILCHENSYSTEMEN. (A Method for Studying the Inelastic Scattering of Slow Neutrons in Many-Particle Systems). Glaeser, Wolfgang (Kernforschungszentrum, Karlsruhe (West Germany). Institut fuer Angewandte Kernphysik). Nov. 1964. 37p. Dep. mn.

For the production of pulsed monochromatic beams double choppers and rotary crystal spectrometers are used. These two types of monochromators are compared with respect to resolution and intensity. The background problem was discussed. The rotary crystal, time-of-flight spectrometric installation at the DIORIT reactor was described. Simple approximation formulas for primary and secondary energy resolution were derived. The Doppler effect was discussed, and a comparison with the measurement results was carried out. A simple measurement and evaluation method for the determination of two-fold differential scattering cross sections and for the determination of the scattering law was described. (J.S.R.)

42155 (NAA-SR-Memo-3196) PRE-CRITICAL ELECTRICAL AND MECHANICAL TESTING: THE CRITICAL ASSEMBLY, REACTOR PARAMETERS. Johnson, R. P. (Atomics International, Canoga Park, Calif.). Oct. 16, 1958. Contract AT(11-1)-Gen-8. 34p. Dep. mn; CFSTI, $2.00 cy, $0.50 mn.

All mechanical and electrical testing on the L-77 Vanowen reactor and console were completed by the Operations Unit and recommendations were made to the Manufacturing Department. Any rework that was incorporated on the L-77 Vanowen reactor was also incorporated on the assembly

line L-77 reactors by Manufacturing. The L-77 Vanowen reactor was loaded in two different cases with 90 and 20% enriched uranyl sulfate. Reactor parameters were studied with the varying core conditions. (auth)

42156 (UCRL-12476) MEASUREMENT OF THE LIVERMORE POOL-TYPE REACTOR (LPTR) TRANSFER FUNCTION USING REACTOR OSCILLATION TECHNIQUES. Cowan, Charles L. (Lawrence Radiation Lab., Univ. of California, Livermore). Mar. 30, 1965. Contract W-7405-eng-48. 26p. Dep. mn; CFSTI $2.00 cy, $0.50 mn.

The transfer function of the Livermore Pool Type Reactor was measured with the aid of a pile oscillator mechanism. A description of the oscillator construction is presented and the experimental transfer-function curves for phase lag and amplitude are indicated. The break frequency of the transfer function was determined from the measured curves and the ratio of the effective delayed neutron fraction to the effective neutron lifetime was found to be $\beta/l = 88 \pm 4\ sec^{-1}$. The transfer function was measured with both bare and cadmium-covered detectors. The frequency-response measurements were found to be identical for both detectors. (auth)

42157 GUARANTEES FOR MTR FUEL ELEMENTS. Eschnauer, H.; Warrikoff, A. (NUKEM, Wolfgang, Ger.). Atomwirtschaft, 10: 325-6(July-Aug. 1965). (In German).

A weighted guarantee formula for fuel elements of research reactors was worked out. The formula takes into consideration the possible sources of damage—errors in construction, in preparation, and in reactor operation. It also considers the actual and time limits of the guarantees in operation. (tr-auth)

42158 THE MZFR—A LANDMARK OF GERMAN REACTOR DEVELOPMENT. Finkelnburg, W. (Siemens-Schuckertwerke AG, Erlangen, Ger.). Atomwirtschaft, 10: 330-1(July-Aug. 1965). (In German).

The MZFR, constructed in only three and a half years, is a prototype heavy water pressure boiler reactor. With an output of 200 Mw(t) and 50 Mw(e) it is the largest heavy water power reactor in the world. Since a reactor of this size cannot produce current economically, the MZFR was also developed as a multipurpose reactor for fuel element and materials testing without the disadvantages arising through compromise. The factors that lead to the selection of a D_2O reactor and the individual characteristics of the MZFR are briefly indicated. (J.S.R.)

42159 MZFR—COST AND UTILIZATION. Brandl, J. (Gesellschaft fuer Kernforschung mbH/Geschaeftsfuehrung Versuchsanlagen, Karlsruhe, Ger.). Atomwirtschaft, 10: 331-2(July-Aug. 1965). (In German).

In the future operation of the MZFR a concrete cost analysis will be developed. Principally the scientific utilization of the special research devices of the reactor should contribute significantly to the cost reduction. The total cost, as calculated at the present, including fuel elements, D_2O, land, construction, and all secondary costs is 157,000,000 DM, that was contributed for the most part by the state. The electricity produced was connected with the public utility net. (tr-auth)

42160 MZFR—THE TOTAL INSTALLATION. Ruf, R. (Siemens-Schuckertwerke AG, Erlangen, Ger.). Atomwirtschaft, 10: 333-5(July-Aug. 1965). (In German).

A brief description of the MZFR prototype and reactor is presented. The reactor characteristics, coolant circuits, reactor vessel, and auxiliary circuits are briefly described. (J.S.R.)

42161 PHYSICAL DESIGN OF THE MZFR. Behrens, E.; Ritz, H.; Rupp, W. (Siemens-Schuckertwerke AG, Erlangen, Ger.). Atomwirtschaft, 10: 344-6(July-Aug. 1965). (In German).

The cell calculation program developed by Siemens in 1958 was the basis for the design calculations for the MZFR. It was supplemented by an experimental program including a zero power experiment. In addition to the design values for an economic optimum, the optimum loading arrangement for continuous loading of fuel elements during operation was determined. A final burnup of 5800 Mwd/t was obtained. (tr-auth)

42162 MZFR—CONSTRUCTION PRINCIPLES OF THE REACTOR. Kumpf, H. (Siemens-Schuckertwerke AG, Erlangen, Ger.). Atomwirtschaft, 10: 347-8(July-Aug. 1965). (In German).

The construction characteristics of the MZFR with respect to other pressure boiler reactors are described. These include a special moderator container with piled earth for the optimum distribution of the usable reactor volume, placement of each fuel element and control rod channel through suitable stages in the boiler cover, a pressure vessel cover forged from one stage that lets the plate for the loading machine be free over the reactor, and installations for the introduction of the research loops without extensive modification to the reactor. (tr-auth)

42163 MZFR—REACTOR PRESSURE VESSEL AND INSTALLED CONSTRUCTION. Dorner, H. (Siemens-Schuckertwerke AG, Erlangen, Ger.). Atomwirtschaft, 10: 348-51(July-Aug. 1965). (In German).

The MZFR vessel is probably the largest high pressure vessel prepared up to the present. It required therefore new methods of preparation, calculation, and construction. The 7.8-m high vessel with 4.1-m diameter was designed for 100 atm and 300°C. The cover is cast from a single piece. The installations consist essentially of moderator container, thermal shield, perpendicular coolant channels, and fillers. (tr-auth)

42164 MZFR—THE PRIMARY CIRCUIT AND ITS CONSTRUCTION. Rothe, R.; Sparhuber, R.; Winkler, F. (Siemens-Schuckertwerke AG, Erlangen, Ger.). Atomwirtschaft, 10: 351-5(July-Aug. 1965). (In German).

The construction of the primary circuit was significantly modified by the use of natural uranium as fuel element and D_2O as a coolant and by the separation of the fast-flowing coolant from the cold, slow-flowing moderator. The primary circuit consists of two principal coolant circuits and one moderator circuit, as well as a pressure vessel system. (tr-auth)

42165 MZFR FUEL ELEMENTS—DESIGN, CONSTRUCTION, AND RESEARCH. Holzer, R.; Morgenstern, F.; Stehle, H. (Siemens-Schuckertwerke AG, Erlangen, Ger.). Atomwirtschaft, 10: 355-7(July-Aug. 1965). (In German).

The fuel in each coolant channel is divided into two coupled fuel elements which consist of 37 rods. The rods contain uranium dioxide as sintered pellets. Design and construction were tested in numerous studies, including irradiation of a rod bundle in a pressurized water loop. (tr-auth)

42166 MZFR—DEVICES FOR FUEL ELEMENT EXCHANGE. Kumpf, H.; Weber, R. (Siemens-Schuckertwerke AG, Erlangen, Ger.). Atomwirtschaft, 10: 357-8 (July-Aug. 1965). (In German).

The system for loading and unloading fuel elements during operation was so constructed that as few as possible functional motions occur in the reactor region. Each fuel element column is transposed during its loading time only once. The essential devices for fuel element exchange are the loading machine with carrier, the unloading machine, the fuel element sluice, and the dismounting device in the basin. (tr-auth)

42167 MZFR SAFETY SHIELD WITH INSTALLATION FOR PRESSURE RELEASE. Aisch, D.; Petersen, G. (Siemens-Schuckertwerke AG, Erlangen, Ger.). Atomwirtschaft, 10: 359-60(July-Aug. 1965). (In German).

For the protection of the environment in a possible reactor incident, the MZFR has a gas-tight safety shield of steel. The cylinder is 27-m high and 24.4-m in diameter and is anchored in the concrete foundations of the reactor vessel. In addition there is an installation for the pressure release of the vessel that causes the immediate condensation of steam into the water container. (tr-auth)

42168 MZFR NUCLEAR TECHNICAL AUXILIARY INSTALLATIONS. Kausz, I. (Siemens-Schuckertwerke

AG, Erlangen, Ger.). Atomwirtschaft, 10: 360-2(July-Aug. 1965). (In German).

The nuclear technical auxiliary installations of the MZFR provide principally for cooling outside the power range, maintenance of the necessary chemical state of the coolant, the recovery of heavy water, and the prevention of radioactivity escape into the atmosphere. The design of installations for these purposes is described. (J.S.R.)

42169 MZFR—THE STEAM POWER INSTALLATION. Bald, A.; Schamburger, R. (Siemens-Schuckterwerke AG, Erlangen, Ger.). Atomwirtschaft, 10: 363-8(July-Aug. 1965). (In German).

The monel characteristic of the steam power installation is the careful separation of the steam and feed water circuits from the operational behavior of the reactor in order to obtain optimum efficiency. In both the steam generators and the moderator coolers, the heat of the primary circuit is transferred to the secondary circuit. The steam state before introduction to the turbines is 30.7 atm at 238°C. (tr-auth)

42170 MZFR ELECTROTECHNICAL INSTALLATIONS. v[on] Haebler, D.; Riemann, K.; Stein, H. (Siemens-Schuckertwerke AG, Erlangen, Ger.). Atomwirtschaft, 10: 369-73(July-Aug. 1965). (In German).

Included in the electrotechnical installations are instrumentation and control (with nuclear and conventional measurement channels, power control, and reactor protection), operation, interlocks and automatics, maintenance, high current installations, and the emergency power supply. Each of these is described briefly. (J.S.R.)

42171 MZFR STRUCTURAL INSTALLATIONS. Goepel, R.; Kuester, H.; Malinka, F. (Siemens-Schuckertwerke AG, Erlangen, Ger.). Atomwirtschaft, 10: 373-5(July-Aug. 1965). (In German).

The MZFR was constructed within the nuclear research center at Karlsruhe. The layout and construction of the reactor proper, the machine shops and auxiliary installations are briefly described. The basic concepts used in the design and establishment of the reactor complex are considered. (J.S.R.)

42172 MZFR—MANUFACTURE OF THE MOST ESSENTIAL PARTS OF THE PRIMARY INSTALLATION. Wawersik, H. (Kloeckner-Werke AG, Osnabrueck, [Ger]). Atomwirtschaft, 10: 376-9(July-Aug. 1965). (In German).

The cylinder and flange rings were manufactured as seamless forged rings for a pressure vessel of more than 2-m diameter for the first time in Germany. All surfaces coming in contact with D_2O had to be of refined steel or plated with it. (tr-auth)

42173 MZFR STEAM GENERATOR. Baberg, W. (Gutehoffnungshuette Sterkrade AG, Oberhausen-Sterkrade, Ger.); Mayer, H. Atomwirtschaft, 10: 379-81(July-Aug. 1965). (In German).

The peculiarities in the construction of the steam generator were the necessary thickness of the primary space, the coating of refined steel, and construction under conditions of nuclear purity. The drilling of thick pipe bottoms in connection with a new type of build-up welding presented the greatest difficulties. (tr-auth)

42174 MZFR PRINCIPAL COOLANT CIRCULATING PUMPS. Maiwald, H. (Klein Schanzlin and Becker AG, Frankenthal [Ger.]). Atomwirtschaft, 10: 381-2(July-Aug. 1965). (In German).

The primary coolant pumps of the MZFR are 4.5-m high pistonless pumps with a collimator motor in order to satisfy requirements of the greatest possible tightness and freedom from maintenance. The production problems occurred principally in the weldings. (tr-auth)

42175 MZFR FUEL ELEMENTS. Ploeger, F. (NUKEM, Wolfgang, Ger.); Schneider, G.; Zeller, W. Atomwirtschaft, 10: 382-4(July-Aug. 1965). (In German).

Whereas the assembly for all fuel elements for the MZFR took place in the Reactor Development Division of the Siemens-Schuckertwerke, the fuel rod preparation was divided between two other firms, which made possible a technical comparison. The treatment of the Zircaloy for the attainment of sufficient strength, the welding, and the preparation of black surfaces presented the most problems. (tr-auth)

42176 MZFR—COMPLETION OF THE CONSTRUCTION. Janovicz, W. (Siemens-Schuckertwerke AG, Erlangen, Ger.). Atomwirtschaft, 10: 385(July-Aug. 1965). (In German).

The MZFR was constructed in three years. In the first year the foundations and the crude buildings were erected; in the second year installations were begun. The reactor construction itself and the machine and electrical components were completed in the third year. (tr-auth)

42177 MZFR—CONSTRUCTION OF THE REACTOR BUILDING AND INSTALLATION OF THE PRESSURE VESSEL. Seyd, G. (Siemens-Schuckertwerke AG, Erlangen, Ger.). Atomwirtschaft, 10: 386-7(July-Aug. 1965). (In German).

At the end of 1962 the base plate of the reactor building was poured. In February 1964 a pressure test was made at 1.5 atm. With leak rate measurements on March 1, 1964, the construction was completed. The 105-ton reactor pressure vessel which offered special transportation problems, was installed at the end of 1964. (tr-auth)

42178 MZFR—THE ZERO POWER EXPERIMENT. Ritz, H. (Siemens-Schuckertwerke AG, Erlangen, Ger.). Atomwirtschaft, 10: 387-9(July-Aug. 1965). (In German).

The novelty of the MZFR reactor core made it necessary to support the theoretical calculations of the reactivity behavior with experimental measurements. Therefore an installation for a zero power experiment was constructed. It consisted of a reactor core of the same size and with the same installations. (tr-auth)

42179 RESEARCH INSTALLATIONS AT THE MZFR. Schabert, H.-P. (Siemens-Schuckertwerke AG, Erlangen, Ger.). Atomwirtschaft, 10: 389-90(July-Aug. 1965). (In German).

For carrying out irradiation research with the MZFR, 6 coolant channels distributed equally over the circumference of the reactor core were installed on the semi-core radius as special test positions. Construction provisions were made for the later installation of test loops. Three experimental areas are available. (tr-auth)

42180 THE LIQUID-HELIUM IRRADIATION FACILITY AT THE MUNICH RESEARCH REACTOR FRM. Meissner, H.; Schilling, W.; Wenzl, H. (Technische Hochschule, Munich). EuroNuclear, 2: 277-80(June 1965).

A low-temperature irradiation facility is described in which samples can be irradiated with neutrons at temperatures between 4.6 and 300°K in the core of the Munich Research Reactor. Safety considerations are summarized, together with experimental possibilities and operating experience. (D.C.W.)

42181 MEASUREMENT OF THE PLATE TEMPERATURE OF THE FUEL ELEMENTS OF THE BR-2 REACTOR. Delmas, R.; Denegre, G.; Mathieu, F.; Zelbstein, U. J. Nucl. Energy: Pts. A and B, 19: 501-13(July 1965). (In French).

The high flux material testing reactor BR-2 is situated at Mol in Belgium and is operated by Centre d'Etudes Nucléaires, Belgium, in association with Euratom. During the start-up period a certain number of methods for measuring the fuel-plate temperature were investigated. The reactor BR-2 has certain original nuclear and thermodynamic characteristics. The method of making the measurements, the results and useful conclusion are given. (auth)

42182 COUPLED REACTOR KINETICS. I. TRANSFER FUNCTION MEASUREMENT OF A COUPLED REACTOR. Kawai, Toshio (Hitachi Ltd., Ozenji, Kawasaki-shi, Kanagawa-ken, Japan). J. Nucl. Sci. Technol. (Tokyo), 2: 245-50(July 1965).

The transfer function of the two slab loading core of Argonaut was measured and analyzed by a coupling model. The measurement showed good agreement with predicted

behavior. The coupling constants and subcriticality of the component reactors were obtained and compared with the values obtained from independent statical measurements. (auth)

42183 NEUTRON FLUX MEASUREMENTS IN THE CORE OF THE VVR-S RESEARCH REACTOR. Frankl, Laszlo; Nemeth, Andras; Toth, Mihaly. Magy. Tud. Akad. Kozp. Fiz. Kut. Int. Kozlemen., 13: 109-26(1965). (In Hungarian).

The method for measuring both the conventional and the fast-neutron flux in the irradiating channels in the core of the VVR-S reactor is described. Results of the measurements are given. The investigations covered the absolute and relative distributions of the two kinds of flux, evaluating the results of measurements in terms of Westcott's formulation. Au foils as well as Cu and Dy wires in combination with a threshold detector were used in the experiments. (auth)

42184 AN ACCURATE DETERMINATION OF THE NEUTRON SPECTRUM IN THE THERMAL COLUMN OF THE TRIGA-REACTOR FIR:1. Palmgren, A. (Reactor Lab., Helsinki). Nucl. Instr. Methods, 36: 88-92(Sept. 1965).

An experimental determination of the neutron spectrum in the thermal column of the Triga Mark II reactor of the Institute of Technology is reported. Instrumental corrections are carefully determined for the time-of-flight spectrometer, and these are applied to the measured spectrum of the neutron beam from the thermal column. It is found that the spectrum can be accurately represented as a Maxwellian with the temperature of the graphite, when the effect of the flux gradient at the point of extraction is taken into account. (auth)

42185 IRRADIATION OF A MZFR TEST FUEL ELEMENT IN THE NRX REACTOR. Knaab, H.; Stehle, H. (Siemens-Schuckertwerke AG, Erlangen, Ger.). Nukleonik, 7: 209-17(May 1965). (In German).

In the X-5 loop of the NRX Reactor, Chalk River, Canada, a 7-rod test element with the construction characteristics of the MZFR fuel elements was irradiated for the duration of 2 reactor cycles. On the average, a burn-up of 1900 Mwd/t U at a maximum rod output of 405 w/cm was obtained. The research inset was provided with thermoelements and capillary wires for differential pressure measurements. The investigations after the irradiation include, in addition to visual appraisal, extensive dimension measurements and metallographic studies and hydrogen analyses. The study confirms the correctness of the MZFR fuel element construction and supported the initial data. (tr-auth)

42186 ZERO-ENERGY MEASUREMENTS ON THE CORE OF THE MULTI-PURPOSE RESEARCH REACTOR. Behrens, Ernst; Bronner, Gottfried; Dio, Wolf-Heiner; Gruen, Arnold E.; Ritz, Hilmar; Schlosser, Gerhard (Siemens-Schuckertwerke AG, Erlangen, Ger.). Nukleonik, 7: 221-31(May 1965). (In German).

Zero-energy measurements were made on the core of the multipurpose research reactor (MZFR) during construction. The core was introduced with the necessary instrumentation into a provisional structure. In the first phase of the measurement program, the charge of the core was increased by steps up to a complete charge; in the second phase the excess reactivity was analyzed by stepwise poisoning of the moderator with B. The measurement of the following magnitudes is described individually: excess reactivity, material buckling, temperature coefficient of reactivity, efficiency of the control rods individually and in groups, and coolant void coefficient. Emphasis was placed on a meticulous determination of excess reactivity. It is shown that these magnitudes can be very accurately determined by a stepwise homogeneous poisoning of the moderator with B. The most important results of the measurements and their theoretical interpretation and peculiarities of the measurement methods used were reported. (tr-auth)

42187 PROPERTIES OF THE ARGONAUT RING CORE WITH INCREASED H_2O:URANIUM RATIO. Stribel, Theodor (Siemens-Schuckertwerke AG, Erlangen, Ger.). Nukleonik, 7: 260-3(May 1965). (In German).

Research on the Siemens Argonaut Reactor has shown that with a ring core arrangement it is possible to increase the plate distance from 6.5 to 10 mm without increasing the critical mass in otherwise unaltered core construction. Measurements of critical magnitudes for safe operation temperature and void coefficients and reactivity values of control plates, gave rise to only small objections to operation with the charge modification. From the measured Cd ratio in the core, an approximately 33% higher ratio of thermal to epithermal flux was obtained than with 6.5-mm plate separation. The modified core construction is therefore of interest from a spectral standpoint. Further possibilities with respect to a 3-group spectrum are discussed. The prompt neutron lifetime, determined from Rossi α measurements, was about 7 to 8% smaller than the usual construction. (tr-auth)

42188 FEEDBACK EFFECTS DURING SHORT INTERVAL-SERIES PULSING. Miley, G. H.; Kurstedt, H. A.; Beck, G. P. (Univ. of Illinois, Urbana). 29p. (CONF-650413-7). Gmelin, AED-CONF-65-042-16.

From Symposium on Neutron Dynamics and Control, Tucson, Ariz.

Experimental results are reported for short interval-series pulsing with a TRIGA Mark II reactor using repetition rates from ½ to 3 pulses/minute. The influence of repetition rate, pulse rod drop time, and initial pulse reactivity on both the equilibrium pulse amplitude and the time to reach equilibrium is discussed. Results indicate that the reactivity coefficient associated with a water temperature increase has the opposite sign from the fuel coefficient. Some methods for optimization of series pulsing which do not involve major design modifications are noted. Also, a calculational model which is designed for rapid calculation of series pulsing is discussed. It utilizes an integral formulation to solve directly for the time dependent temperature. (auth)

42189 DEVICE FOR OPERATING A MOVABLE TROLLEY. Chabassier, Roger; Chaffiote, Pierre; Megret, Jean (to Commissariat a l'Energie Atomique). British Patent 997,387. July 7, 1965. Priority date Jan. 10, 1963, France.

A trolley that is movable on a stationary support is particularly applicable to use with swimming pool reactors for the purpose of displacing an irradiation loop relatively to the reactor core. The installation includes a main drive mechanism that serves to displace the trolley in two opposite directions. An auxiliary drive mechanism is synchronized under normal conditions with the main drive mechanism and serves to displace the trolley in at least one direction independently of the main drive. The trolley and the main drive are connected with a coupling and with a device that serves to release the coupling and set the auxiliary drive mechanism into operation alone. (B.L.M.)

42190 A MOVABLE PARTITION OR COFFERDAM. Saget, Pierre (to Commissariat a l'Energie Atomique). British Patent 998,944. July 21, 1965. Priority date Oct. 16, 1962, France.

A movable partition or cofferdam is provided for separating and mutually sealing-off two intercommunicating pools, such as the water-filled tank and the receiving pool for the fuel elements for a swimming pool reactor. The cofferdam comprises a metal apron with a peripheral reinforcement girder carrying a double annular piece of flexible material such that the material flattens and has a sealing action when pressure is applied to either side of the apron. Preferably, the apron is made up of a channeled plate made up of a series of channel irons assembled together side by side but sequentially in alternate directions so that the apron is made up of alternate concave and convex surfaces to achieve a satisfactory modulus of inertia. Abutments of elastic material are distributed over the height of the apron on either side of its surfaces so that when the pool is emptied, the apron may rest against the opposite edge of the recess in which the cofferdam is mounted. (B.L.M.)

WASTE DISPOSAL AND PROCESSING

See also BIOLOGY AND MEDICINE — Ecology.
CHEMISTRY — Radiochemistry.
CHEMISTRY — Separation Processes and Procedures.
HEALTH AND SAFETY.

Refer also to abstract 42140.

42191 (AEET/HP/TH-20) TEMPERATURE DISTRIBUTION IN RADIOACTIVE SOLIDS. PART II. GAMMA-ACTIVE SPHERES. Sundaram, V. K.; Gopinath, D. V.; Ganguly, A. K. (Atomic Energy Establishment, Trombay (India). Health Physics Div.). 1964. 22p. Dep. mn.

One of the ultimate methods proposed for high level radioactive waste disposal is to contain the activity in ceramic bodies and bury them underground or in deep sea. The limit of the activity that can be incorporated in such bodies is decided by the temperature rise in the body due to the absorption of nuclear radiation. The temperature distribution in a solid sphere containing long-lived gamma emitters and buried in a medium having the same thermal properties is discussed. Analytical expressions are given for heat source distribution and for calculations of temperature distribution in and out of a solid sphere containing gamma activity. Numerical values obtained with energies in the range of 0.5 to 3 Mev and in spheres of radii 10, 20, and 30 cm are presented. The results are compared with those of the beta case. (auth)

42192 (BNWL-80) SOLIDIFICATION OF HIGH LEVEL WASTES. PART IV. PHOSPHATE MELTS FOR FIXATION OF RADIOACTIVE RESIDUES FROM PUREX TYPE WASTES–THREE TO FIFTY PER CENT FISSION PRODUCT OXIDES. Barton, G. B. (Battelle-Northwest, Richland, Wash. Pacific Northwest Lab.). July 1965. Contract AT(45-1)-1830. 39p. Dep. mn; CFSTI, $2.00 cy, $0.50 mn.

The possible composition range for the high-level radioactive wastes generated from various power reactor fuels processed through a Purex-type process is very broad. A partial survey of this wide range was conducted in an effort to establish the composition limits that bound the operable range of the phosphate melt system. Two screening criteria were used: (a) drip temperature, an empirical measure of flow temperature at which a container could be filled, and (b) solubility. Measurements indicated the occurrence of two (or possibly more) optimum phosphate additions near M_2O/P_2O_5 ratios of 2.1 and 1.0. It was found that fission products equivalent to at least 50% of the weight of oxides in the plant waste can be successfully incorporated in a phosphate melt that can be transferred as a fluid into containers at less than 900°C. (auth)

42193 (BNWL-101) TESTING OF IMMERSION HEATERS FOR IN-TANK SOLIDIFICATION CIRCULATORS. Dunn, J. (Battelle-Northwest, Richland, Wash. Pacific Northwest Lab.). July 1965. Contract AT(45-1)-1830. 15p. Dep. mn; CFSTI $1.00 cy, $0.50 mn.

The use of direct immersion electric heaters is proposed for concentrating intermediate level wastes in underground tanks. A series of tests was completed to investigate the major technical concern with this concept (that of scale deposition on the heat transfer surfaces). Tests were performed with simulated coating wastes, concentrated up to four times the original volume, and containing either 0 or 1% added sodium sulfate or phosphate. Power density of the heaters ranged from 17 to 500 w/in.^{2}. No scale deposition on heated surfaces occurred in either bench- or pilot-scale tests during any of the tests; maximum test duration was approximately 2600 hr. Some solids buildup occurred on heater supports in the vapor space above the heaters during early stages of the test program. This problem was overcome by relocating the reflux return line to provide a washing action, and the deposit proved readily soluble in water. Periodic washes would be expected to minimize solids formation, which otherwise might occur with either the immersion heater or hot air system. Based on the heater performance and on the absence of scale on the heated surfaces, an electric heater prototype is recommended for testing under plant conditions. (auth)

42194 (NP-15267) WASTE MANAGEMENT RESEARCH ABSTRACTS NO. 1. (International Atomic Energy Agency, Vienna (Austria)). 1965. 75p. Dep. mn; IAEA Free.

Abstracts are presented on national waste management research projects which were completed in 1963–64 by Czechoslovakia, Germany, Italy, Japan, Sweden, United Kingdom, USA, and USSR. The abstracts are arranged into the following categories: gaseous waste treatment and disposal, liquid waste treatment, solid waste treatment, storage and discharge studies, and economic studies. (D.L.C.)

42195 (ORNL-P-1479) PROJECT SALT VAULT: RADIOACTIVE WASTE DISPOSAL IN A SALT MINE. Boegly, W. J. Jr.; Bradshaw, R. L.; Empson, F. M.; McClain, W. C.; Parker, F. L.; Schaffer, W. F. Jr. (Oak Ridge National Lab., Tenn.). [1964]. Contract W-7405-eng-26. 20p. (CONF-650539-1). Dep. mn; CFSTI $1.00 cy, $0.50 mn.

From 20th Annual Industrial Waste Conference, Lafayette, Ind.

The findings of studies on the disposal of high-level wastes in salt formations are summarized. Project Salt Vault is a field experiment for demonstrating the feasibility of storing solid wastes in a salt mine, and for determining any possible radiation effects or salt creep. The experiment will be carried out using irradiated ETR fuel assemblies to simulate solidified wastes. An engineering description of the experiment is given. (D.L.C.)

42196 THE HANFORD PROGRAM FOR MANAGEMENT OF HIGH-LEVEL WASTE. Tomlinson, Roy E. (General Electric Co., Richland, Wash.). Chem. Eng. Progr., 60: Symp. Ser. No. 53, 2-19(1964).

Process wastes containing fission products have been stored as alkaline slurries in underground tanks. A program is proposed to decrease the mobility of the stored materials. Wastes that self-heat significantly will be fractionized into long-lived heat emitters and residual salt waste. The cesium and strontium heat emitters will be stored separately in high-integrity containers, which can be made available for beneficial use on request; residual waste will be combined with other low-heating waste and evaporated to salt cakes in existing underground tanks. An obsolete canyon-type building will be reactivated and revised to conduct the chemical processing operations required. Solvent extraction will probably be used to isolate cesium, strontium, and cerium from acid waste and dissolved sludges. Cesium will be removed from the stored alkaline sludges supernatant solutions by adsorption on a zeolite. (auth)

42197 DEVELOPMENT OF RADIOACTIVE WASTE FRACTIONIZATION AND PACKAGING TECHNOLOGY. DeMier, Warren V.; Richardson, Gerald L.; Platt, Allison M.; Swift, Ward H. (General Electric Co., Richland, Wash.). Chem. Eng. Progr., 60: Symp. Ser. No. 53, 50-61(1964).

Solvent extraction, ion exchange, and precipitation processes are described for removing long-lived heat-generating fission products (strontium-90 and cesium-137) from high-level radioactive wastes. Packaging techniques for long-term storage of isolated strontium and cesium employ

ion exchange absorption on zeolites followed by thermal stabilization and encapsulation in small-volume, high-integrity containers. (auth)

42198 ACCELERATED DEFORMATION OF ROCK SALT AT ELEVATED TEMPERATURE. Lomenick, T. F.; Bradshaw, R. L. (Oak Ridge National Lab., Tenn.). Nature, 207: 158-9(July 10, 1965). (ORNL-P-1163).

Uniaxial tests of scale-model specimens of rock salt were performed to predict the effects on rock-salt mine stability of supporting-pillar stresses and elevated temperatures, in order to be able to design a radioactive waste disposal facility in a salt mine. Cylindrical specimens were tested for axial loads of 2000, 4000, 6000, 8000, and 10,000 lb/in^2 and at 22.5, 60, and 100°C, for a few hours to several thousand hours. It was found that pillar deformation increased markedly with increasing load, and creep rates of the salt were greatly accelerated at elevated temperatures. Sample data are presented. The results were fitted by empirical equations which predict strain rate and cumulative deformation. (M.J.T.)

GENERAL AND MISCELLANEOUS

42199 (BNL-8397) MEMBRANES, MATERIAL TRANSFER AND ENZYMES. Nims, Leslie F.; Butera, Regina; Schnappauf, Ursula (Brookhaven National Lab., Upton, N. Y.). [1963] Contract AT(30-2)-Gen-16. 14p. Dep. mn; CFSTI, $1.00 cy, $0.50 mn.

A material transfer system for membranes was constructed in which the energy required to maintain a nonequilibrium ionic distribution pattern was furnished by an enzyme catalyzed chemical reaction. The distribution was effected across a cellophane membrane by the urease catalyzed hydrolysis of urea. The system exhibited properties similar to those of living cells in that the individual ions to which the system can be considered closed occurred at different concentrations in the internal and external phases of the system when a stationary state was reached. Furthermore, in this system ions were accumulated against concentration gradients during the approach to the stationary state. (auth)

42200 (COO-1354-5) THE BEHAVIOR OF AQUEOUS SALTS IN CONTACT WITH OXIDE SURFACES. Maatman, Russell W. (Dordt Coll., Sioux Center, Iowa. Dept. of Chemistry). [1965]. Contract AT(11-1)-1354. 26p. (CONF-650902-5). Dep. mn; CFSTI, $2.00 cy, $0.50 mn.

From American Chemical Society, 150th National Meeting, Atlantic City.

A study was made of the nature of silica gel, alumina, and silica-alumina surfaces in the presence of aqueous electrolytes. General methods for treating surface-solution systems are discussed, and application is made to the above surfaces. The results for silica gel are interpreted in terms of ion exchange with surface hydrogen. The site densities are low for alumina and silica-alumina, and the reaction is cation exchange for surface aluminum. It is concluded that no physical adsorption occurs. (D.L.C.)

42201 (CU-2663-23) CIRCULATION NEAR THE SOUTHERN BERRY ISLANDS, BAHAMAS. Technical Report No. CU-23-65. Katz, Bernard (Columbia Univ., Palisades, N. Y. Lamont Geological Observatory). July 1965. Contract AT(30-1)-2663. 51p. Dep. mn; CFSTI $3.00 cy, $0.50 mn.

Dye tracers were used in the Bahamas to study circulation in the southern part of the Berry Island group and near New Providence Island. Current velocities were measured using aerial photographs of dye patches in time series to obtain net displacements as small as 0.1 nautical miles. The use of dye tracers also provided comparative estimates of mixing on the shelf and information on the exchange of water between the banks and the Tongue of the Ocean. (auth)

42202 (HW-64483) A CHEMICAL COMPOSITION AND PROCESS FOR REMOVING OXIDE AND SCALE FROM ALUMINUM METALS AND ALUMINUM ALLOYS. Richman, R. B.; Larrick, A. P. (General Electric Co., Richland, Wash. Hanford Atomic Products Operation). Mar. 28, 1960. Contract AT(45-1)-1350. 5p. Dep. mn; CFSTI $1.00 cy, $0.50 mn.

A method is given for removing oxide, film, and/or scale layers which were formed at high temperatures on Al and its alloys. The method comprises heating the metal to 300 to 500°C in air, quenching in air or water, and then immersing in a solution at 20 to 95°C until clean. The solution comprises 3 to 25% orthophosphoric acid, 0.5 to 30% sodium dichromate, 0.5 to 50% acetic acid, and balance water. The method does not remove any of the base metal or alter its structure. (D.L.C.)

42203 (LA-3297) A STUDY OF THE ONE-DIMENSIONAL, TIME-DEPENDENT REACTION ZONE OF NITROMETHANE AND LIQUID TNT. Mader, Charles L. (Los Alamos Scientific Lab., Univ. of California, N. Mex.). Apr. 6, 1965. Contract W-7405-eng-36. 51p. Dep. mn; CFSTI $3.00 cy, $0.50 mn.

The time-dependent reaction zones of nitromethane and liquid TNT were investigated using one-dimensional numerical hydrodynamics with Arrhenius chemical reaction and accurate equations of state. The formation of an overdriven stable detonation in nitromethane by various types of pistons was investigated. A piston whose velocity decreases abruptly to a lower value produces an initially short reaction zone which lengthens and decreases in pressure, when the second and lower velocity occurs, until the rate of release of chemical energy exceeds that necessary to sustain the wave. If the stepped-velocity piston has a sufficiently small lower step, failure of the detonation occurs in the time and space scale of interest. If the detonation is not sufficiently overdriven, the solution of the equations is nonsteady and periodic, oscillating about the steady-state (time-independent) solution. (auth)

42204 (LA-DC-6632) A UNIQUENESS THEOREM CONCERNING MOMENT DISTRIBUTIONS. Zeigler, R. K. (Los Alamos Scientific Lab., Univ. of California, N. Mex.). [1960]. Contract W-7405-eng-36. 5p. Dep. mn; CFSTI, $1.00 cy, $0.50 mn.

Let the random variable Y have the density function p(y). Let $f(x) = e^{tx}p(x)/E(e^{tx})$ where $E(e^{tx}) = \int_{-\infty}^{\infty} e^{tx}p(x)dx$, then f(x) is a density function. The random variables associated with these density functions have the same variances if and only if p(y) is a normal density function. (auth)

42205 (LA-DC-6990) INTERACTIONS OF DETONATION WAVES IN CONDENSED EXPLOSIVES. Gardner, S. D.; Wackerle, Jerry (Los Alamos Scientific Lab., Univ. of California, N. Mex.). [1965]. Contract W-7405-eng-36. 12p. (CONF-651003-6). Dep. mn; CFSTI $1.00 cy, $0.50 mn.

From 4th Symposium on Detonation, Silver Spring, Md.

Flow patterns similar to regular and Mach reflection resulting from the interaction of detonation waves in condensed explosives were observed with rotating mirror cameras and flash radiography. The principal emphasis of the study was with the oblique collision of plane detonation waves. In this configuration the assumptions of steady flow, infinitesimal reaction zone thicknesses, the Chapman-Jouguet hypothesis, and simple reaction-product equations of state permit an analytic solution for the detonation parameters for regular reflection and the computation of the critical angle for the onset of Mach reflection. These critical angles were measured for Composition B, 9404-03 PBX, Baratol, and nitromethane. Additional data obtained on Composition B include a measurement of Mach stem pressure and stem shape. In inhomogeneous explosives, Mach stems and reflected shocks displayed substantial curvatures, and flash x-ray studies revealed anomalous density regions in the symmetry planes in both regular and Mach reflection experiments. These observations, along with deviations in computed and measured critical angle values, have indicated a degree of failure of the simplified theory to provide an exact, detailed description of the interaction phenomena; this failure is currently believed to result primarily from the nonuniform structure of the detonation wave. (auth)

42206 (LA-DC-6992) ANALYSIS OF SHOCK WAVE AND INITIATION DATA FOR SOLID EXPLOSIVES. Ramsay, J. B.; Popolato, A. (Los Alamos Scientific Lab., Univ. of California, N. Mex.). [1965]. Contract W-7405-eng-36. 5p. (CONF-651003-3). Dep. mn; CFSTI, $1.00 cy, $0.50 mn.

From 4th Symposium on Detonation, Silver Spring, Md.

If the usual analysis of shock-wave data is made for polycrystalline plastic-bonded HMX and pressed TNT, the experimental data extrapolate to the detonation pressure point rather than to the peak spike pressure point. This is indicative of a reactive wave, which is to be expected. Limitations based on the assumptions and analysis are discussed to show that it is not possible to infer any infor-

mation about the shock properties of unreacted explosive from the available shock-wave data for solid explosives. Since no calculational model is available which will permit the computation of the details of initiation of solid explosives, empirical relationships are presented to summarize the data for engineering purposes. (auth)

42207 (LA-DC-6994) EXPERIMENTAL OBSERVATIONS OF INITIATION OF NITROMETHANE BY SHOCK INTERACTIONS AT DISCONTINUITIES. Travis, J. R. (Los Alamos Scientific Lab., Univ. of California, N. Mex.). [1965]. Contract W-7405-eng-36. 24p. (CONF-651003-5). Dep. mn; CFSTI $1.00 cy, $0.50 mn.

From 4th Symposium on Detonation, Silver Spring, Md.

Shock interactions at density discontinuities introduced into nitromethane compressed by a plane shock wave can reduce the induction time for initiation of detonation near the discontinuity. Experimental results are presented which illustrate this phenomenon and which corroborate the theoretical results presented by Mader in his paper in this symposium. The initiating efficacy of a discontinuity formed by a solid inclusion immersed in nitromethane is strongly dependent on the material used. It is also dependent on the dimensions of the object in the directions parallel and perpendicular to the front of the initiating shock when these dimensions are between a lower critical size and an upper effectively infinite size, and on the angle of incidence between the shock and the discontinuity. Data which relate the induction time to these parameters are presented. (auth)

42208 (NAA-SR-4527(Pt.2)) ANALYSIS OF STRESSES IN BELLOWS. PART II. MATHEMATICAL. Anderson, W. F. (Atomics International, Canoga Park, Calif.). May 27, 1965. Contract AT-11-1-GEN-8. 161p. Dep. mn; CFSTI, $5.00 cy, $0.75 mn.

A method of analysis for stresses in toroidal shells was developed which is applicable to a wide range in the geometrical parameters involved. Application of this method to the problem of analysis for stresses in bellows provided results consistent over a full range of the parameter μ with the results of other methods which are limited in application to the range of low or high values of μ. The method outlined can probably be applied with equal facility to other problems of toroidal shells. (auth)

42209 (NP-15356) 10 YEARS OF ATOMIC ENERGY IN INDIA, 1954-1964. (Department of Atomic Energy, Bombay (India)). 36p. Dep. mn.

An account is given of atomic energy activities in India prior to and after the establishment of a commission in 1948 and of a national program in 1954. The Apsara, CIR, and Zerlina reactors are described together with fuel production and reprocessing facilities. Radioisotopes, instrumentation, applications, health physics, and atomic power are also discussed. (D.L.C.)

42210 (NVO-98-8) INTERIM PROGRESS REPORT TASK IV LOCAL NEWPORT PIER TEST. Tucker, Charles T. (National Marine Consultants, Anaheim, Calif.). June 29, 1965. Contract AT(26-1)-98. 50p. Dep. mn; CFSTI $2.00 cy, $0.50 mn.

Results of tests on Type III shallow water system are reported. The tests were conducted to provide functional checks on the system including a data logging system, a data logging system test set, Amerograph cables, and differential pressure transducers. The ability of the system to detect Tsunami-like waves was evaluated. (J.R.D.)

42211 (NYO-1480-19) PATTERN RECOGNITION. Bianchini, R.; Shostak, M. (AEC Computing and Applied Mathematics Center, New York Univ., N. Y.). Dec. 15, 1964. Contract AT(30-1)-1480. 92p. Dep. mn; CFSTI $3.00 cy, $0.75 mn.

Report is made of a character recognition study and development of a digital computer input device for reading and translating handprinted FORTRAN programs. Based upon a 2000-specimen library, computer recognition programs were written to partition the 40 alphanumeric character classes used as input into a total of 20 classes with an accuracy of slightly over 90%. Further refinement of methods used in this study would probably lead to full 40-class partition, with an accuracy of about 90%. (auth)

42212 (NYO-3424-1) SEMINAR ON TOPICS IN BIOPHYSICS [HELD AT COLUMBIA UNIVERSITY], JUNE 29-JULY 17, 1964. Final Report. (Columbia Univ., New York). Contract AT(30-1)-3424. 37p. Dep. mn; CFSTI, $2.00 cy, $0.50 mn.

A program of informal lectures, discussions, and demonstrations was presented. Topics discussed included: the biochemical and physical aspects of photosynthesis; a conceptual system of molecular genetics with emphasis on the role of nucleic acids in the synthesis of enzymes from nucleic acids; the photochemistry and photobiology of nucleic acids in microorganisms; the properties, structure, and function of bacterial, plant, and animal viruses; the storage, replication, and transfer of genetic information in macromolecules with emphasis on the role of DNA and RNA in protein synthesis; physical mechanisms related to excitable cell membranes; physical aspects of biological movements, with emphasis on muscle physiology; physical studies of nucleic acids in solutions; nonchromosomal heredity, with emphasis on studies of the properties of nonchromosomal genes and mutations of a nonchromosomal genetic system in a single-celled algae, chlomydomonas; and the structures of nucleic acids, their physical properties, how the structures may be determined by physical methods, and the relation of physical properties to biological properties. (C.H.)

42213 (ORNL-TM-1164) OPTICAL PROPERTIES OF VACUUM EVAPORATED FILMS OF CADMIUM, THALLIUM, AND ZINC IN THE VACUUM ULTRAVIOLET. Jelinek, T. M.; Hamm, R. N.; Arakawa, E. T. (Oak Ridge National Lab., Tenn.). Aug. 1965. Contract W-7405-eng-26. 61p. Dep. mn; CFSTI $3.00 cy, $0.75 mn.

Thesis submitted by Thomas Milo Jelinek to Vanderbilt Univ., Nashville, Tenn.

The optical constants of vacuum evaporated films of Cd, Tl, and Zn were determined in the vacuum ultraviolet region from reflectance measurements made for monochromatic light incident at various angles of incidence. These optical constants, n and k, were then used to calculate values of the complex dielectric constant and the energy loss function, $\mathrm{Im}\frac{1}{\epsilon}$. The values of the energy loss functions were in good agreement with the characteristic electron energy losses. In addition, the optical constants were used in the transition radiation theory to calculate the optical emission spectra of electron bombarded metal films. The theoretical spectra agree well with those found experimentally. (auth)

42214 (RFP-397) A LABORATORY IGNITION SYSTEM. Thompson, M. A. (Rocky Flats Div., Dow Chemical Co., Golden, Colo.). June 8, 1964. Contract AT(29-1)-1106. 15p. Dep. mn; CFSTI $1.00 cy, 1 mn.

A simplified laboratory ignition system was built for measuring the ignition temperature of samples up to 1200°C in a controlled, static, or flowing atmosphere. The design of the ignition system and some of its applications are presented. (M.O.W.)

42215 (RFP-625) THE EFFECT OF TEMPERATURE ON RTV-20. Dietrich, D. E. (Rocky Flats Div., Dow Chemical Co., Golden, Colo.). Aug. 10, 1965. Contract AT(29-1)-1106. 11p. Dep. mn; CFSTI $1.00 cy, $0.50 mn.

The heat in the projector lamp beam of an optical comparator; the effect of this heat on RTV-20 and the reduction of these effects by use of an infrared filter are studied. (auth)

42216 (SC-DR-65-269) WEAR TESTING OF PLATED COATINGS. Jennings, C. W. (Sandia Corp., Albuquerque, N. Mex.). July 1965. Contract AT(29-1)-789. 32p. Dep. mn; CFSTI $2.00 cy, $0.50 mn.

An investigation was conducted to determine the wear characteristics of combinations of electroplated metals for use in rotary switches. From specimens electroplated under controlled conditions and tested for wear resistance with a wear tester which was similar in operation to a rotary switch, no apparent correlation was found between wear resistance and conditions of electroplating, other than

thickness of the deposits. A thin film of soft gold (approximately 30 millionths of an inch thick) electroplated on a hard substrate of rhodium or electroless nickel or bright nickel was found to provide better wear characteristics than a rhodium-on-nickel system. A few tests were also run on gold alloy boards and ion-plated gold on alumina substrates. The latter combination, which had excellent wear characteristics, shows considerable promise for high temperature or corrosive applications. (auth)

42217 (SC-RR-65-325) APPARATUS FOR THE MEASUREMENT OF THE HALL EFFECT IN METALS. Heckman, R. C. (Sandia Corp., Albuquerque, N. Mex.). Aug. 1965. Contract AT(29-1)-789. 17p. Dep. CFSTI $1.00 cy, $0.50 mn.

Apparatus for the measurement of the Hall effect in metals is described. The apparatus utilizes cross-modulation of the sample current and magnetic field. Comparison with other schemes of Hall effect measurement is presented. (auth)

42218 (SC-TM-64-509) BASIC UNCERTAINTIES IN ELECTRICAL MEASUREMENTS. McCallum, R. E. (Sandia Corp., Albuquerque, N. Mex.). Dec. 1964. Contract AT(29-1)-789. 28p. Dep. mn; CFSTI $2.00 cy, $0.50 mn.

Basic conceptions and definitions used by authorities in the fields of electrical measurements, metrology, and applied mathematics are presented. Their application to measurements of emf and resistance and reduction of errors in a laboratory concerned with high levels of accuracy is described. An attempt to minimize the number of concepts and the technical vocabulary employed was made. (auth)

42219 (TID-21177) SUBACUTE NECROTIZING ENCEPHALOMYELOPATHY. A CASE REPORT WITH SPECIAL EMPHASIS ON THE ASSOCIATED PATHOLOGY OF THE PERIPHERAL NERVOUS SYSTEM. Namiki, Hideo (Atomic Bomb Casualty Commission, Hiroshima (Japan)). [1960]. Contract AT(49-1)-Gen-72. 22p. Dep. mn; CFSTI, $1.00 cy, $0.50 mn.

A 15-year-old Japanese girl with a clinical history and postmortem findings of a subacute necrotizing encephalomyelopathy is reported. The patient's parents were consanguineous and a similar disease was also present in one sibling. This case and those available in the literature indicate that a severe peripheral neuropathy associated frequently with secondary degeneration of the dorsal white columns of the spinal cord constitutes an integral part of the disorder. The presence of peripheral neuropathy reminiscent of that due to deficiency of thiamine and pantothenic acid, frequent familial occurrence of the disorder, and consanguinity in some of the parents give support to the speculation of previous investigators that the disease may represent an inborn error of metabolism, especially of pyruvate metabolism. (auth)

42220 (TID-22023) SOME ASPECTS OF THE LIFE HISTORY OF THE BANDED SCULPIN, COTTUS CAROLINAE CAROLINAE, IN DOE RUN, MEADE COUNTY, KENTUCKY. [Final Report]. Craddock, James E. (Louisville Univ., Ky. Dept. of Biology). 1965. Contract AT(40-1)-2595. 193p. Dep. mn; CFSTI, $5.00 cy, $1.00 mn.

Results are reported from comparative biological studies of Cottus c. carolinae from four semi-isolated areas of Doe Run, Meade County, Kentucky, made from October 1959 through February 1964. Of the several aspects of life history and morphology of C. carolinae studied at Doe Run, there were many differences between "populations" at the four localities sampled, most especially with respect to growth, food habits, and meriatics. At which station of Doe Run the biological phenomena would best typify the species as a whole is unknown and, probably, irrelevant. Just as each stream is an "individual," the populations of fishes living in them, or in each part of them, are unique. (C.H.)

42221 (TIM-939) LAG—A LOAD AND GO ASSEMBLER WRITTEN FOR THE CDC-1604-B COMPUTER. Lawrence, R. (Pratt and Whitney Aircraft, Middletown, Conn. Connecticut Advanced Nuclear Engineering Lab.). July 22, 1965. Contract AT(30-1)-2789. 18p. Dep. mn; CFSTI, $1.00 cy, $0.50 mn.

LAG, a program written for the CDC-1604-B, is a one-pass load and go assembler which was designed to accept IBM-7090-FLOCO II instructions. LAG consists of a main program and 153 subroutines. Of the subroutines, 9 are written in CODAP-1 and are primitives used for address manipulation. Five of the programs were written in FORTRAN-63 and then assembled as CODAP-1 subroutines and altered so that variable length calling sequences could be used. An over-all description of the LAG code is presented. (M.O.W.)

42222 (TIM-940) CMPXMAT, A TRANSFER FUNCTION EVALUATION PROGRAM. Kvick, P. G. (Pratt and Whitney Aircraft, Middletown, Conn. Connecticut Advanced Nuclear Engineering Lab.). July 23, 1965. Contract AT(30-1)-2789. 12p. Dep. mn; CFSTI, $1.00 cy, $0.50 mn.

CMPXMAT written in FORTRAN-63 for the CDC-1604B Computer does a transfer function evaluation. A system of N linear equations derived from the Laplace transform of a set of linearized differential equations is solved for amplitude and phase angle as a function of frequency. For each frequency the coefficient matrix and its Crout reduction are used as constants for an iterative refinement of the solution vector. N must be less than or equal to 70. The program was checked out for N = 2, 3, 7, 44 and was used for production. It is run under the standard master control system with the FORTRAN-63 library and requires three tape units, the standard input, the standard output, and 32768 words of core storage. (auth)

42223 (UCRL-12006) RESCUE BASKET. Page, Roy (Lawrence Radiation Lab., Univ. of California, Livermore). Aug. 1964. Contract W-7405-eng-48. 7p. Dep. mn; CFSTI, $1.00 cy, $0.50 mn.

For the rescue of injured persons from inaccessible canyons, a basket and a simple procedure for its use were devised. The basket can also be used in excavations, mine and elevator shafts, etc. (D.L.C.)

42224 (UCRL-12041-T) ON NEW THEOREMS FOR ELEMENTARY NUMBER THEORY. Mullin, Albert A. (Lawrence Radiation Lab., Univ. of California, Livermore). [1963]. Contract W-7405-eng-48. 5p. Dep. mn; CFSTI, $1.00 cy, $0.50 mn.

The classical number-theoretic notions of multiplicative function and additive function are generalized. In addition to extending classes of functions it can be shown that certain specific functions such as Euler's quotient, Möbius' function, and Liouville's function have precise analogues within the theory. (auth)

42225 (UCRL-12050) DETERMINATION OF ERRORS IN A ONE-PARAMETER SYSTEM. Schroeder, R. (Lawrence Radiation Lab., Univ. of California, Livermore). Aug. 28, 1964. Contract W-7405-eng-48. 9p. Dep. mn; CFSTI, $1.00 cy, $0.50 mn.

A one-parameter system to define a smooth curve is assumed. From the errors which occur in the empirical determination of the locus of the curve, the errors in the system parameter and the functional representation are derived. The conditions for the independence of abscissa and ordinate errors are noted. (auth)

42226 (UCRL-12117-T) MODULAR, PLUG-IN CHASSIS SYSTEM PERMITS COMPATIBLE MOUNTING OF CONVENTIONAL CHASSIS, PRINTED CIRCUIT BOARDS, AND MICROMODULES. Pass, C. (Lawrence Radiation Lab., Univ. of California, Livermore). Aug. 17, 1964. Contract W-7405-eng-48. 19p. Dep. mn; CFSTI, $1.00 cy, $0.50 mn.

A plug-in chassis for standardization reasons, was developed which is compatible for use with the old, conventional chassis, the printed circuit board, and the micro-miniature module. The design and versatility of the system are discussed. (M.O.W.)

42227 RESEARCH CENTERS IN EUROPE. NO. 6. PETTEN. EuroNuclear, 2: 289-96(June 1965).

The activities, facilities, and organization of the two research centers at Petten are briefly described. The high-flux reactor and experiments thereon are considered, together with the low-flux reactor, the NERO marine

reactor project, and the laboratory for highly radioactive objects. (D.C.W.)

42228 RESEARCH CENTERS IN EUROPE. NO. 7. SIEMENS-SCHUCKERTWERKE. EuroNuclear, 2: 343-50 (July 1965).

The Siemens-Schuckertwerke Central Research and Development Laboratories at Erlangen are described. Research progress on reactor technology, fuel element development and assembly, zero energy experiments for the MZFR, radiation chemistry, radiochemistry neutron generators, plasma physics, superconductivity, and direct energy conversion is reported. (M.C.G.)

CORPORATE AUTHOR INDEX

This index contains entries for this period for all report literature and, in addition, for certain published literature items for which it is felt that a corporate approach is especially desirable, e.g., symposia, conference proceedings, and meetings.

Each entry under a corporate author is a shortened version of the title of the publication, followed by the *NSA* volume and abstract number. Report numbers are given in parentheses.

The phrase "Progress report" is abbreviated as "Prog. rpt.," permitting a more rapid and complete alphabetical arrangement of the titles without changing the location of the progress report titles in relation to the other titles.

A

ACF INDUSTRIES, INC., ALBUQUERQUE, N. MEX.
Filament-wound sphere with polar opening, 19: 40698 (ACF-9)
Physical property study of polystyrene foam (210-050), 19: 41000 (ACF-10)

AEC COMPUTING AND APPLIED MATHEMATICS CENTER, NEW YORK UNIV., N. Y.
Pattern recognition, 19: 42211 (NYO-1480-19)

AEROJET-GENERAL CORP., SACRAMENTO, CALIF.
Design study of modification of M-1 liquid H turbopump for use in reactor test facility, 19: 42141 (NASA-CR-54422)

AEROJET-GENERAL NUCLEONICS, SAN RAMON, CALIF.
Prog. rpt. on alkali metals evaluation program, 4–6/65, 19: 41001 (AGN-8154)

AEROPROJECTS, INC., WEST CHESTER, PA.
Prog. rpt. on ultrasonic instrumentation for nuclear applications, 6–7/65, 19: 40847 (NYO-2910-11)

AKADEMIYA NAUK SSSR, MOSCOW. RADIOTEKHNICHESKII INSTITUT.
Certain theoretical problems of wide-band oscillators, 19: 40846 (NP-15209)

AKADEMIYA NAUK SSSR, NOVOSIBIRSK. INSTITUT YADERNOI FIZIKI.
Heating of plasma by shock waves in a trap with magnetic probes, 19: 41861 (NP-15255)
Trap with magnetic plugs designed for prolonged holding of electrons, 19: 41858 (NP-15217)

AKADEMIYA NAUK UKRAINSKOI SSR, KHARKOV. FIZIKO-TEKHNICHESKII INSTITUT.
Current distribution in a coaxial plasma gun, 19: 41859 (NP-15218)
High-frequency heating of plasma, 19: 41862 (NP-15256)
Motion of plasma bunches in a field-free space, 19: 41856 (NP-15205)
Plasma in a θ-pinch with azimuthal magnetic, 19: 41860 (NP-15220)
The magnetic moment of a plasma bunch impinging on a homogeneous longitudinal magnetic field, 19: 41857 (NP-15206)

AMES LAB., IOWA STATE UNIV. OF SCIENCE AND TECH.
Application of metal coatings on uranium, 19: 40949 (ISC-640)
Application of vacuum metallurgy in the purification of rare-earth metals, 19: 40948 (IS-1195)
Deactivation of reaction complexes in the recoil chemistry of ^{11}C, 19: 40550 (IS-T-27)
Design considerations for a system to investigate short-lived nuclei produced at a reactor, 19: 42017 (IS-1219)
Heat contribution due to thermal excitation of 4F electrons of some di- and tri-valent lanthanide elements, 19: 40457 (IS-1156)
Single-crystal elastic constants of lead-thallium alloys, 19: 41012 (IS-T-16)
Solid solubility of magnesium in the close-packed modifications of some rare-earth metals, 19: 41011 (IS-T-15)
Stimulated Compton scattering of electrons by laser beam, 19: 41328 (IS-1187)
The reduced cell and its crystallographic applications, 19: 41963 (IS-1141)
Thermodynamic measurements on CsCl-type structures in rare earth-magnesium systems, 19: 41013 (IS-T-25)

ARGONNE NATIONAL LAB., IDAHO FALLS, IDAHO.
Analysis of six AETR fast critical experiments, 19: 42077 (ANL-7014)

ARGONNE NATIONAL LAB., ILL.
Application of digital data acquisition and process control system to research reactor, 19: 42150 (ANL-7009)
Breeding, safety and fuel cycles, 19: 42081 (CONF-193-11)
Convective MHD channel flow, 19: 41115 (ANL-6967)
Development of a process for manufacturing ZPR-III U–Pu–Mo test fuel elements, 19: 40978 (ANL-6955)
Experiments with central superheater core CSH-1, BORAX-V, 19: 42149 (ANL-6961)
Fuel management and inventory in the EBR-II fuel cycle, 19: 42075 (ANL-6735)
Innovations in bubble chamber devices, 19: 40869 (CONF-650510-14)
Neutron-flux studies in the EBWR during power operation, 19: 42076 (ANL-6751)
Physics aspects of the plutonium experiment in EBWR, 19: 42078 (ANL-7019)
Radiation safety technician training course. I., 19: 40801 (ANL-6991)
Spectral representation and criticality problem of a two-region cell transport operator, 19: 42035 (ANL-6590)

ARIZONA UNIV., TUCSON. GEOCHEMICAL SECTION.
Prog. rpt. on correlation and chronology of ore deposits, annual, 8/1/65, 19: 40778 (COO-689-50)

ARKANSAS UNIV., FAYETTEVILLE. DEPT. OF CHEMISTRY.
Fission products in the atmosphere and in rain, 19: 40785 (TID-21224)

ARMY ENGINEER NUCLEAR CRATERING GROUP, LIVERMORE, CALIF.
Crater measurements on Project Pre-Schooner, 19: 40707 (PNE-502F)

ARMY ENGINEER WATERWAYS EXPERIMENT STATION, VICKSBURG, MISS.
Investigation of manufacture of aggregate and riprap by nuclear means, 19: 40709 (PNE-5003)

ATLANTIC RESEARCH NUCLEAR CORP., ALEXANDRIA, VA.
Prog. rpt. on effects of electrical fields on boiling heat transfer, 5/26/64–9/30/64, 19: 40735 (NYO-2404-5)

ATOMENERGIKOMMISSIONEN, RISOE (DENMARK). FORSOEGSINSTITUT.
Facilities for mechanical testing of irradiated reactor materials at Risoe, 19: 40717 (RISO-98)
Thermoluminescence readout instrument for measurement of small doses, 19: 40877 (RISO-101)

ATOMIC BOMB CASUALTY COMMISSION, HIROSHIMA (JAPAN).
Subacute necrotizing encephalomyelopathy, 19: 42219 (TID-21177)

ATOMIC ENERGY CENTRE, DACCA (PAKISTAN).
Photoproduction of ρ and ω mesons from nucleons, 19: 41321 (AECD/TP/4)

ATOMIC ENERGY ESTABLISHMENT, TROMBAY (INDIA). HEALTH PHYSICS DIV.
Temperature distribution in radioactive solids. II., 19: 42191 (AEET/HP/TH-20)

ATOMIC ENERGY OF CANADA LTD., CHALK RIVER (ONTARIO).
NRU monitor computer and self-powered neutron flux detectors, 19: 42148 (AECL-2216)
Prog. rpt. on physics research, 1–3/65, 19: 41678 (PR-P-65)
Solid-state multiplexer for use with self-powered neutron flux detectors,

19: 40866 (AECL-2217)
ATOMIC ENERGY RESEARCH ESTABLISHMENT, HARWELL (ENGLAND).
Prog. rpt. on health physics, 1–12/64, 19: 40800 (AERE-PR/HPM-7)
The extraction of zinc by dithizone retained on cellulose acetate, 19: 40642 (AERE-R-4969)
YORK 87–A 7090-FORTRAN program for analyzing phonon dispersion curves, 19: 41962 (AERE-M-967)
ATOMIC INDUSTRIAL FORUM, INC., NEW YORK.
Investigation of core reproducibility of the Enrico Fermi reactor, 19: 42079 (APDA-NTS-4)
ATOMIC POWER DEVELOPMENT ASSOCIATES, INC., DETROIT, MICH.
Measurement of the isothermal temperature coefficient of reactivity of the Enrico Fermi reactor, 19: 42080 (APDA-NTS-5)
ATOMICS INTERNATIONAL, CANOGA PARK, CALIF.
Analysis of neutron transmission through slabs of LiH, 19: 41642 (NAA-SR-10853)
Analysis of stresses in bellows, 19: 42208 (NAA-SR-4527(Pt.II))
Conventional buildings for reactor containment, 19: 42018 (NAA-SR-10100)
Effects of long-term operation on SRE Na system components, 19: 42096 (NAA-SR-11396)
Equipment for fabrication and encapsulation of irradiated UO_2 pellets, 19: 40715 (NAA-SR-Memo-7438)
Feasibility study of 1000-Mwe sodium-cooled fast reactor, 19: 42095 (NAA-SR-11378(Vol.III))
Nonequilibrium uranium carbide phase relationships, 19: 41018 (NAA-SR-10768)
Pre-critical electrical and mechanical testing of reactor critical assembly, 19: 42155 (NAA-SR-Memo-3196)
Prog. rpt. on solubility studies in alkali metals, 1/3–4/3/65, 19: 40946 (AI-65-93)
Pyrochemical reprocessing of uranium carbide, 19: 40652 (NAA-SR-11340)
Pyrochemical reprocessing of UO_2 by airox, 19: 40653 (NAA-SR-11389)
Rapid pulse heating of modified zirconium-uranium hydrides to destruction, 19: 41017 (NAA-SR-10482)
Reactivity worths of several fast reactor control materials, 19: 42050 (NAA-SR-11366)
Safe disposal of SNAP reactors, 19: 42140 (NAA-SR-11353)
Sodium fires and release characteristics of particulates and fission products, 19: 40803 (NAA-SR-Memo-9719)
Study of instantaneous collapse and creep buckling characteristics of large SGR process tubes, 19: 41019 (NAA-SR-11323)
The thermal expansion of Al_2O_3, 19: 41020 (NAA-SR-Memo-2987)
Uranium–Mo fuel element irradiation in SRE, 19: 41090 (NAA-SR-11121)
200-Mwe prototype large SGR–reactor structure design and evaluation, 19: 42094 (NAA-SR-11314)
AUSTRALIAN ATOMIC ENERGY COMMISSION RESEARCH ESTABLISHMENT, LUCAS HEIGHTS.
Calculating reactivity worth of partially inserted control rods using two-dimensional geometry, 19: 42034 (AAEC/E-134)
Microhardness measurement of unirradiated and irradiated BeO, 19: 41087 (AAEC/E-135)
AVCO-EVERETT RESEARCH LAB., EVERETT, MASS.
Electron plasma-experiment theory and applications, 19: 41863 (NP-15302)
Experiments with magnetohydrodynamically supported shock layers, 19: 41120 (N64-30509)

B

BABCOCK AND WILCOX CO., LYNCHBURG, VA.
Prog. rpt. on irradiation performance of thoria–urania fuel materials, 1–3/65, 19: 41003 (BAW-6376-3)
BABCOCK AND WILCOX CO., LYNCHBURG, VA. ATOMIC ENERGY DIV.
Accident recovery equipment study reactors, 19: 42006 (IDO-10043(Vol. II) (Rev.1))
BARTOL RESEARCH FOUNDATION, SWARTHMORE, PA.
Prog. rpt. on cosmic ray experiment in Explorer VII, final, 11/61–12/63, 19: 41288 (NASA-CR-58203)
BATTELLE MEMORIAL INST., COLUMBUS, OHIO.
Characterization of pyrolytic-carbon fuel-particle coatings prepared with acetylene, 19: 41004 (BMI-1735)
Development of an improved method of sampling and analysis for atmospheric iodine, 19: 40402 (BMI-X-10137)
Reactor Materials, Vol. 8, No. 2, 19: 40957
BATTELLE-NORTHWEST, RICHLAND, WASH. PACIFIC NORTHWEST LAB.
Automated procedure for zirconium analysis in water, 19: 40403 (BNWL-SA-166)
Automated procedure for H_3BO_3 analysis in water, 19: 40404 (BNWL-SA-167)
Boron-11 neutron flux monitors–interim report, 19: 40867 (BNWL-64)
Corrosion in simulated PRTR fuel element surface crevices, 19: 40965 (BNWL-83)
Critical experiments with PuO_2–polystyrene compacts with ^{240}Pu = 8%, 19: 42038 (BNWL-95, pp 27-35)
Diffusion and transport calculations for NPR tube-in-tube fuel geometry, 19: 42128 (BNWL-95, pp 18-23)
Environmental tests of HTLTR materials, 19: 40966 (BNWL-92)
Fallout radionuclides in Alaskan food chains, 19: 40780 (BNWL-SA-242)
Formation of chemicals by reactor irradiation of oxygenated water and ammoniated water, 19: 40548 (BNWL-82)
Hot-cell studies on the separation of Pa-233 from irradiated thoria by coprecipitation with MnO, 19: 40644 (BNWL-78)
Interpretation of pulsed neutron and reactor noise experiments in reflected reactors, 19: 42040 (BNWL-95, pp 40-54)
MIDAS computation of waterdrop evaporation, 19: 41110 (BNWL-74)
Prog. rpt. on physics, 1–3/65, 19: 42036 (BNWL-95)
Prompt neutron decay using Monte Carlo methods of analysis, 19: 42039 (BNWL-95, pp 36-9)
Reactor analysis: measured and calculated spectra and average reaction rates, 19: 42037 (BNWL-95, pp 4-17)
Recovery of plutonium and uranium from reactor fuel metallurgical scrap, 19: 40643 (BNWL-57)
Solidification of high-level wastes. IV., 19: 42192 (BNWL-80)
Testing of immersion heaters for in-tank solidification circulators, 19: 42193 (BNWL-101)
Thermoluminescent dosimetry studies at Hanford, 19: 40868 (BNWL-SA-23)
BECHTEL CORP., SAN FRANCISCO, CALIF.
U. S. Reactor containment technology, 19: 42008 (ORNL-NSIC-5(Vol.I and II))
BELFER GRADUATE SCHOOL OF SCIENCE, YESHIVA UNIV., NEW YORK.
Prog. rpt. on stable isotope studies, annual, 9/15/64–7/15/65, 19: 40460 (NYO-3462-1)
BENDIX PRODUCTS AEROSPACE DIV., BENDIX CORP., SOUTH BEND, IND.
Prog. rpt. on improved strength and oxidation resistance of Cr composites, final, 3/64–3/65, 19: 41022 (NP-15292)
BETTIS ATOMIC POWER LAB., PITTSBURGH, PA.
Heat transfer aspects of the loss of coolant accident, 19: 42009 (WAPD-T-1811)
MO608–A FORTRAN program to evaluate radiochemical data, 19: 40636 (WAPD-TM-516)
Properties of a Hf control rod after exposure during three seed lives in PWR Core 1, 19: 41092 (WAPD-TM-457)
Shippingport PWR Project catalog of document abstracts, 19: 42101 (WAPD-PWR-1606(Add.2))
Ultrasonic testing characteristics of forged Inconel, 19: 41027 (WERL-0029-2)
BROOKHAVEN NATIONAL LAB., UPTON, N. Y.
Analysis of high energy p-p scattering experiment, 19: 41322 (BNL-9231)
Data processing method for a multidetector positron scanner, 19: 40390 (BNL-9384)
Ecological changes in insect community of a pitch pine-oak forest subjected to chronic γ irradiation, 19: 40307 (BNL-9253)
Membranes, material transfer and enzymes, 19: 42199 (BNL-8397)
Novel synthesis of carrier-free ^{106}Ru-labeled ruthenocene, 19: 40634 (BNL-8405)
Pathogenesis of radiolesions in the mature central nervous system, 19: 40349 (BNL-9345)
Search for J-dependent neutron strength functions in rare earth region, 19: 41656 (BNL-9245)
Slow neutron studies of molecular motions in condensed matter, 19: 40455 (BNL-9297)
Studies of a repetitive liquid metal slug MHD generator, 19: 41314 (BNL-9329)
Studies with DL-alanine-2-^{14}C of interaction of ethanol metabolism with pathways of hepatic gluconeogenesis in the rat, 19: 40308 (BNL-8379)
Study of generalized level density by the methods of differential-recurrence equations, 19: 41655 (BNL-934)
BROWN BOVERI/KRUPP REAKTORBAU G.M.B.H., DUESSELDORF (WEST GERMANY).
Development and potentialities of the high-temperature pebble-bed reactor concept, 19: 42082 (CONF-650633-1)
BROWN ENGINEERING CO., INC., HUNTSVILLE, ALA. RESEARCH LABS.
Analysis of radiators for space nuclear power systems, 19: 40731 (AD-609969)
BROWN UNIV., PROVIDENCE, R. I. DEPT. OF PHYSICS.

Prog. rpt. on experimental and theoretical high energy physics, 9/64–8/65, 19: 41337 (NYO-2262-95)
BROWN UNIV., PROVIDENCE, R. I. DIV. OF ENGINEERING.
Asymptotic theory of photoionization chamber. I., 19: 40552 (NP-15287)
BUNDESGESUNDHEITSAMT, BERLIN (WEST GERMANY). INSTITUT FUER WASSER-, BODEN- UND LUFTHYGIENE.
Alarm plan, 19: 40804 (NP-14925)
Application of radioactive luminous paints in navigational instruments of aircraft, 19: 40940 (NP-14924)
Treatment with Th-X, 19: 40391 (NP-14921)
BUREAU OF MINES, MORGANTOWN, W. VA. MORGANTOWN COAL RESEARCH CENTER.
Prog. rpt. on high-temperature energy systems, 2–4/65, 19: 42127 (TID-22009)

C

CALIFORNIA INST. OF TECH., PASADENA.
Photoproduction of π^+ mesons from hydrogen from 0.6 to 1.2 Bev, 19: 41323 (CALT-68-42)
CALIFORNIA INST. OF TECH., PASADENA. W. M. KECK LAB. OF ENGINEERING MATERIALS.
Study of CsCl type intermediate phases involving rare earth elements, 19: 41005 (CALT-221-11)
CALIFORNIA UNIV., BERKELEY.
The three body problem, 19: 41529 (N64-81206)
CALIFORNIA UNIV., BERKELEY. ELECTRONICS RESEARCH LAB.
Cyclotron-wave instabilities, 19: 41849 (AD-426079)
CALIFORNIA UNIV., LOS ANGELES. INST. OF GEOPHYSICS AND PLANETARY PHYSICS.
Prog. rpt. on geo- and planetary physics, 1–6/64, 19: 41571 (N64-29400)
CAMBRIDGE ELECTRON ACCELERATOR, MASS.
Accurate current integrator in the range of 10^{-5} to 10^{-9} amperes, 19: 40843 (CEAL-1021)
Calibration of beam monitor of Cambridge Electron Accelerator, 19: 41164 (CEAL-1022)
CARNEGIE INST. OF TECH., PITTSBURGH, PA.
Inovations in bubble chamber devices, 19: 40869 (CONF-650510-14)
CAROLINAS VIRGINIA NUCLEAR POWER ASSOCIATES, INC., PARR, S. C.
Prog. rpt. on CVTR operation, 6/65, 19: 42084 (CVNA-239)
CENTRE NATIONAL DE LA RECHERCHE SCIENTIFIQUE, PARIS (FRANCE).
Prog. rpt. on mechanical properties of steels, final, 1965, 19: 40947 (EURAEC-1403)
CHANTIERS DE L'ATLANTIQUE PENHOET-LOIRE, PARIS (FRANCE).
Prog. rpt. on vertical welding process under-electro-conducting on steel plates, 11/20/62, 19: 41007 (EURAEC-1400)
CLARK UNIV., WORCESTER, MASS. DEPT. OF CHEMISTRY.
Isomeric cross-section ratios in (p,pn) and heavy-ion neutron-transfer reactions, 19: 41674 (NYO-1930-44)
CLEARINGHOUSE FOR FEDERAL SCIENTIFIC AND TECHNICAL INFORMATION, SPRINGFIELD, VA.
Food preservation by irradiation, 19: 40941 (SB-403(Suppl.1)(Rev.))
COLORADO UNIV., BOULDER.
Separation of amines by ligand exchange. II., 19: 40647 (COO-499-1)
Separation of amines by ligand exchange. III., 19: 40648 (COO-499-2)
COLUMBIA UNIV., NEW YORK.
Seminar on biophysics, 6/29–7/17/64, 19: 42212 (NYO-3424-1)
COLUMBIA UNIV., PALISADES, N. Y. LAMONT GEOLOGICAL OBSERVATORY.
Circulation near the southern Berry Islands, Bahamas, 19: 42201 (CU-2663-23)
COMBUSTION ENGINEERING, INC., WINDSOR, CONN. NUCLEAR DIV.
Prog. rpt. on burnable poison additions to UO_2, 1–3/65, 19: 41006 (CEND-3107-238)
Prog. rpt. on in-pile thermal conductance testing, 1–3/65, 19: 40732 (CEND-3336-237)
COMITATO NAZIONALE PER L'ENERGIA NUCLEARE, ROME (ITALY).
Analog model for cylindrical nuclear fuel rods, 19: 40740 (RT/ING(64)16)
Bibliography on fouling research, 19: 40971 (RT/CHI(65)20)
Direct determination of some fission products in mixtures by γ spectrometry, 19: 40411 (RT/CHI(65)2)
Dissolution experiments of aluminum and SAP cladding material in a laboratory recirculation dissolver, 19: 40655 (RT/CHI(65)-1)
Selection of nuclear power station operators, 19: 42098 (RT/PROT(65)24)
Synthesis of some alkyl benzylamines of high molecular weight of the type $C_6H_5–CH_2–NH(R_1)(R_2)$, 19: 40540 (RT/CHI(64)16)
COMMISSARIAT A L'ENERGIE ATOMIQUE, GRENOBLE (FRANCE). CENTRE D'ETUDES NUCLEAIRES.
Irradiation of Cu–Co alloys, 19: 41095 (ORNL-tr-667)
COMMISSARIAT A L'ENERGIE ATOMIQUE, SACLAY (FRANCE). CENTRE D'ETUDES NUCLEAIRES.
Safety concerning reactor Pegase, 19: 42151 (CEA-R-2518(Vol.II))
Study of recombination processes for electron-hole pairs in germanium irradiated by γ rays from ^{60}Co using the photovoltaic effect in P-N junctions, 19: 40932 (CEA-R-2723)
CONSOLIDATION COAL CO., LIBRARY, PA. RESEARCH DIV.
Prog. rpt. on evaluation of β radiation as hydrogenation catalyst, 3/62–10/63, 19: 40553 (NYO-2978-34)
CONSUMERS PUBLIC POWER DISTRICT, HALLAM, NEBR.
Prog. rpt. on Hallam reactor operation, 4/65, 19: 42099 (TID-22013)

D

DEPARTMENT OF ATOMIC ENERGY, BOMBAY (INDIA).
Prog. rpt. on atomic energy, 1954–64, 19: 42209 (NP-15356)
DEUTSCHER WETTERDIENST, OFFENBACH AM MAIN (WEST GERMANY). ABT. KLIMA.
Annual precipitation and precipitation frequency for European community, 19: 41111 (EUR-2296.e)
DIVISION OF BIOLOGY AND MEDICINE (AEC), WASHINGTON, D. C.
Conference on late irradiation effects, USAEC, Washington, 12/63, 19: 40352 (WASH-1059)
DIVISION OF ISOTOPES DEVELOPMENT (AEC), WASHINGTON, D. C.
Development of safety performance criteria and tests standard for radioisotope sealed sources and devices, 19: 40802 (CONF-650616-5)
DIVISION OF RAW MATERIALS (AEC), WASHINGTON, D. C.
Reconnaissance for U in the Colimapu Formation of central Chile, 19: 40798 (RME-4571(Rev.))
DIVISION OF REACTOR DEVELOPMENT AND TECHNOLOGY (AEC), WASHINGTON, D. C.
Prog. rpt. on fissiochemical process development. I., 12/2/63–6/30/64, 19: 40547 (AGN-8137(Vol.I))
DORDT COLL., SIOUX CENTER, IOWA. DEPT. OF CHEMISTRY.
The behavior of aqueous salts in contact with oxide surfaces, 19: 42200 (COO-1354-5)
DU PONT DE NEMOURS (E. I.) & CO., AIKEN, S. C. SAVANNAH RIVER LAB.
Automated analyses for the characterization of heavy water moderator, 19: 40406 (CONF-650919-2)
Automated procedures for lithium, cobalt, and thorium and their applications in nuclear processes, 19: 40405 (CONF-650919-1)
Behavior of actinides and fission products in TBP and DABP, 19: 40645 (CONF-650918-1)
Radiation properties of californium-252, 19: 41657 (DP-986)
Selection, cost, and performance of n-paraffin diluents, 19: 40646 (CONF-650918-2)
Semiworks evaluation of manganese dioxide head-end step in the Thorex Process, 19: 40649 (DP-982)
DU PONT DE NEMOURS (E. I.) & CO., AIKEN, S. C. SAVANNAH RIVER PLANT.
SRP reactor on-line computer, 19: 42129 (DPSPU-65-30-27)

E

ENTE NAZIONALE PER L'ENERGIA ELETTRICA, ROME (ITALY).
Prog. rpt. on Garigliano nuclear power plant, annual, 1964, 19: 42086 (EUR-2427.i)
EUROPEAN ATOMIC ENERGY COMMUNITY.
Annual precipitation and precipitation frequency for European community, 19: 41111 (EUR-2296.e)
Prog. rpt. on Ardennes nuclear power plant, annual, 1964, 19: 42087 (EUR-2428.f)
Prog. rpt. on Garigliano nuclear power plant, annual, 1964, 19: 42086 (EUR-2427.i)
Prog. rpt. on Gundremminger nuclear power plant, annual, 1964, 19: 42085 (EUR-2426.d)
Set-up for registering data via a single cable utilizing passive components, 19: 40714 (EUR-2421.d)
EUROPEAN ATOMIC ENERGY COMMUNITY, ISPRA (ITALY). JOINT NUCLEAR RESEARCH CENTER.
Set-up for registering data via a single cable utilizing passive components, 19: 40714 (EUR-2421.d)
EUROPEAN ORGANIZATION FOR NUCLEAR RESEARCH, GENEVA (SWITZERLAND).
Production of particles at small angle in p-p and p-nucleus collisions at 20 Bev, 19: 41324 (CERN-65-14)

F

FLORIDA UNIV., GAINESVILLE.
Propagation of neutron waves through heterogeneous multiplying and nonmultiplying media, 19: 41643 (ORNL-TM-1184)
FORSVARETS FORSKNINGSANSTALT, STOCKHOLM (SWEDEN).
Observations on the particle properties of nuclear debris in the upper atmosphere, 19: 40783 (NP-15327)
Theoretical aspects on the formation of nuclear weapon debris, 19: 40782 (NP-15325)
FRANKLIN INST. RESEARCH LABS., PHILADELPHIA, PA.
Design guide for gas-lubricated tilting-pad journal and thrust bearings with special reference to high-speed rotors, 19: 40736 (NYO-2512-1)

G

GARRETT CORP., PHOENIX, ARIZ. AIRESEARCH MFG. DIV.
SNAP 50/SPUR program materials investigation—mechanical properties of TZM, 19: 41002 (APS-5157-R)
GCA TECHNOLOGY DIV., GCA CORP., BEDFORD, MASS.
Circulation processes and mixing mechanisms in upper atmosphere above 30 km, 19: 41112 (SC-DC-65-1312)
GENERAL APPLIED SCIENCE LABS., INC., WESTBURY, N. Y.
Electromagnetic studies in shock-produced plasmas, 19: 41855 (NP-15142)
GENERAL ATOMIC, SAN DIEGO, CALIF.
Design, construction, and operation of in-pile loop, 19: 42089 (GA-5938)
GENERAL ATOMIC, SAN DIEGO, CALIF. JOHN JAY HOPKINS LAB. FOR PURE AND APPLIED SCIENCE.
Development of the gas-cooled fast reactor concept, 19: 42090 (GA-6132)
Effective thermal neutron cross sections for materials with grain structure, 19: 42041 (GA-6286)
Prog. rpt. on integral neutron thermalization, 3/31/65, 19: 41640 (GA-6323)
GENERAL ELECTRIC CO., CINCINNATI, OHIO. LARGE JET ENGINE DEPT.
630A blower feasibility study, 19: 42142 (R62FPD-252)
GENERAL ELECTRIC CO., CINCINNATI, OHIO. NUCLEAR MATERIALS AND PROPULSION OPERATION.
Introduction to nuclear propulsion—reactor control, 19: 42138 (N64-33780)
Introduction to nuclear propulsion—nuclear rocket system, 19: 42139 (N64-33784)
NMPO blower shaft seal-test report, 19: 40701 (TID-22007)
Nuclear dry cargo ships vs. conventional, 19: 42132 (GE-TM-65-3-6)
Properties of some refractory metals, III., 19: 41009 (GEMP-375)
630A Mark III maritime nuclear steam generator summary report, 19: 42133 (GEMP-340)
GENERAL ELECTRIC CO., CINCINNATI, OHIO. SPACE POWER AND PROPULSION SECTION.
Prog. rpt. in alkali metal corrosion, 12/64–3/65, 19: 40970 (NASA-CR-54390)
GENERAL ELECTRIC CO., PHILADELPHIA, PA. MISSILE AND SPACE DIV.
Cyclotron resonance propulsion system, 19: 40764 (N65-27691)
Ionization of Cs and Na contaminated air in the hypersonic slender body boundary layer, 19: 41121 (N64-30658)
Performance study of a repetitively pulsed two-stage plasma propulsion engine, 19: 40763 (N64-31453)
Prog. rpt. on continuous-microwave magnetic accelerators 8/8/63–8/7/64, 19: 40761 (N64-30604)
Prog. rpt. on shielding for ionizing radiation space, final, 9/62–8/63, 19: 41952 (N64-81552)
GENERAL ELECTRIC CO., RICHLAND, WASH. HANFORD ATOMIC PRODUCTS OPERATION.
A chemical composition and process for removing oxide and scale from aluminum metals and aluminum alloys, 19: 42202 (HW-64483)
Correlation of rose bengal clearance and histopathological change of sheep livers damaged by Np-237, 19: 40350 (HW-SA-3723)
Criticality safety of fissile materials in the chemical processing department, 19: 40807 (RL-SEP-389(Rev.))
Development in continuous ion exchange contactors, 19: 40650 (HW-77805)
Industrial noise control is practical, 19: 40806 (RL-SA-37)
N-reactor, pressurizer-high pressure injection pump simulation study. II., 19: 42131 (HW-77028)
Removal of radioisotope parent material by producing high-purity process water, 19: 42130 (HW-68387)
Ultrasonic bond testing of irradiated fuel elements, 19: 41089 (HW-56028)
GENERAL ELECTRIC CO., SAN JOSE, CALIF. ATOMIC POWER EQUIPMENT DEPT.
Core evaluation of the Garigliano reactor, 19: 42091 (GEAP-4852)
Fission gas release from UO_2 fuel rods with gross central melting. I., 19: 41088 (GEAP-4572)
Prog. rpt. on Garigliano reactor, 7/65, 19: 42092 (GEAP-4909)
Prog. rpt. on two-phase flow and heat transfer, 1/26–4/25/65, 19: 40733 (GEAP-4863)
GENERAL ELECTRIC CO., SAN JOSE, CALIF. VALLECITOS ATOMIC LAB.
Prog. rpt. on Pu subcritical experiment, 4–6/65, 19: 42093 (GEAP-4912)
GENERAL TECHNOLOGY CORP., TORRANCE, CALIF.
Magnetic induction plasma engine, 19: 40762 (N64-31010)
GEOSCIENCE LTD., SOLANA BEACH, CALIF.
Prog. rpt. on heat transfer for space nuclear power, 12/64–2/65, 19: 40741 (SAN-409-23)
GOSUDARSTVENNYI KOMITET PO ISPOL'ZOVANIYU ATOMNOI ENERGII SSSR.
Angular and energy distribution of γ emission in H_2O and Fe, 19: 41953 (NP-15131)
Spectrometric characteristics of LSU-5k apparatus, 19: 40875 (NP-15254)
GOSUDARSTVENNYI KOMITET PO ISPOL'ZOVANIYU ATOMNOI ENERGII SSSR, MOSCOW. INSTITUT TEORETICHESKOI I EKSPERIMENTAL'NOI FIZIKI.
Spectrum of internal conversion electrons in α-decay of ^{239}Pu and energy levels of ^{235}U, 19: 41673 (NP-15251)
The effect of magnetic screens in the spaces between blocks on the operation of ITEF proton synchrotron, 19: 41168 (NP-15253)
Unitary symmetry and K_{e4}-decay, 19: 41335 (NP-15239)
GRAND JUNCTION OFFICE (AEC), COLO. PRODUCTION EVALUATION DIV.
Airborne radiometric surveying—office and field techniques, 19: 40784 (RME-129(Rev.))

H

HAHN-MEITNER-INSTITUT FUER KERNFORSCHUNG, BERLIN (WEST GERMANY).
Prog. rpt., annual, 1964, 19: 40396 (HMI-B-39)
HARVARD UNIV., CAMBRIDGE, MASS.
Accurate current integrator in the range of 10^{-5} to 10^{-9} amperes, 19: 40843 (CEAL-1021)
Calibration of beam monitor of Cambridge Electron Accelerator, 19: 41164 (CEAL-1022)
HARVARD UNIV., CAMBRIDGE, MASS. DEPT. OF PHYSICS.
Electromagnetic form factors of the neutron, 19: 41326 (HUX-2752-9)
HOLMES AND NARVER, INC., LOS ANGELES, CALIF.
Engineering and cost considerations for tunnel grid blast shelter concept, 19: 40759 (ORNL-TM-1183)
HUGHES RESEARCH LABS., MALIBU, CALIF.
Prog. rpt. on ion rocket engine development, 1–3/65, 19: 40765 (NP-15309)

I

IIT RESEARCH INST., CHICAGO, ILL.
Prog. rpt. on yield phenomena and fracture of hybrided Zr, 4–6/65, 19: 41010 (IITRI-578P27-10)
INSTITUT ATOMNOI ENERGII, GOSUDARSTVENNYI KOMITET PO ISPOL'ZOVANIYU ATOMNOI ENERGII SSSR, MOSCOW.
Compensation of helical magnetic field disturbances, 19: 41116 (IAE-668)
Investigation of low-density plasma forming in Ogra during injection of molecular hydrogen ions, 19: 41851 (IAE-635)
Neutron emission from ^{233}U, ^{235}U and ^{239}Pu fission fragments, 19: 41681 (ANL-Trans-205)
Obtaining a hot thermonuclear plasma by injection of fast particles into a magnetic trap, 19: 41852 (IAE-676)
Reaction ^{4}He(^{3}He,n)^{6}Be, 19: 41659 (IAE-835)
Stabilizing amplification channel of scintillation counter, 19: 40870 (IAE-695)
Technique of conversion of highly basic anion-exchange resins (type AV-17 and AM) from the chloride to the hydroxyl form by the method of two-stage regeneration, 19: 40456 (IAE-713)
The reactions ^{3}He(d,t)2p and ^{3}He(^{3}He,α)2p, 19: 41658 (IAE-655)
INSTITUT DE RECHERCHES DE LA SIDERURGIE, ST. GERMAINE-EN-LAYE (FRANCE).
Prog. rpt. on study of base metal for research on brittle fracture of large welded assemblies, annual, 5/64–5/65, 19: 41008 (EURAEC-1407)
INSTITUTE OF PUBLIC HEALTH, TOKYO (JAPAN). DEPT. OF RADIOLOGICAL HEALTH.
Prog. rpt. on common and radioactive Cs in nature and man, 4/62–3/65, 19: 40781 (NP-15179)

Prog. rpt. on distribution of common and radioactive Cs in nature and man, 9/64, 19: 40309 (NP-15180)

INSTITUTO DE INVESTIGACIONES GEOLOGICAS, SANTIAGO (CHILE).
Reconnaissance for U in the Colimapu Formation of central Chile, 19: 40798 (RME-4571(Rev.))

INTERNATIONAL ATOMIC ENERGY AGENCY, VIENNA (AUSTRIA).
Symposium on chemical effects of nuclear transformations, Vienna, 12/64. I., 19: 40614
Waste Management Research Abstracts, No. 1, 19: 42194 (NP-15267)

INTERNATIONAL CENTRE FOR THEORETICAL PHYSICS, TRIESTE (ITALY).
Generalized spherical functions for the non-compact rotation groups, 19: 41327 (IC/65/63)

ISTITUTO SUPERIORE DI SANITA', ROME (ITALY). LABORATORI DI FISICA.
The (e,e'p) experiment: results obtained and planned proposals, 19: 41660 (ISS-65/3)

J

JOINT INST. FOR NUCLEAR RESEARCH, DUBNA (USSR). LAB OF HIGH ENERGY.
Application of controlled photomultiplier as a separating element in the Nanosecond Coincidence Circuit, 19: 40872 (JINR-P-2203)
Optimal determination of the detecting efficiency (weight) of an event, 19: 40873 (JINR-P-2215)
Reconstruction of the spatial picture of an event in the bubble chamber, 19: 40871 (JINR-P-2179)

JOINT INST. FOR NUCLEAR RESEARCH, DUBNA (USSR). LAB. OF NEUTRON PHYSICS.
Determination of spins of ^{165}Ho neutron resonances by transmission of polarized neutrons through a polarized target in the energy interval 0–55 ev, 19: 41665 (JINR-P-2209)
Neutron correlation in nuclear reactors with account of their space and energy distribution, 19: 42042 (JINR-P-2216)
Neutron resonances of ytterbium isotopes, 19: 41661 (JINR-P-2158)

JOINT INST. FOR NUCLEAR RESEARCH, DUBNA (USSR). LAB OF NUCLEAR PROBLEMS.
Double n-a scattering with a polarized beam and polarized target, 19: 41333 (JINR-P-2227)
Double pp scattering at 667 Mev, 19: 41666 (JINR-P-2233)
Effective lifetime of current carriers in lithium-compensated silicon, 19: 41964 (JINR-P-2201)
Slow particles emitted in stripping reactions, 19: 41664 (JINR-P-2193)
Three-quasiparticle state in ^{165}Er, 19: 41667 (JINR-P-2239)

JOINT INST. FOR NUCLEAR RESEARCH, DUBNA (USSR). LAB OF NUCLEAR REACTIONS.
Investigation of complexes of Am, Cm, Cf, and Fm with lactic acid, 19: 40458 (JINR-P-2224)

JOINT INST. FOR NUCLEAR RESEARCH, DUBNA (USSR). LAB OF THEORETICAL PHYSICS.
Baryon and meson multiplets in the group SU(12) uniting symplectic and spin symmetries, 19: 41331 (JINR-P-2219)
Correlation functions for processes of the multiplication type, 19: 41330 (JINR-P-2213)
Double n-n scattering with a polarized beam and polarized target, 19: 41333 (JINR-P-2227)
Electrical and magnetic polarizability of particles due to nonlinear effects of electrodynamics, 19: 41334 (JINR-P-2229)
Electromagnetic mass splitting in symmetry scheme SU(6), 19: 41329 (JINR-P-2208)
Energy gap in nuclear matter in the case of soft-core potentials, 19: 41662 (JINR-P-2176)
Investigation of nuclear reactions of helium-3 with carbon, 19: 41663 (JINR-P-2184)
On backward scattering of high-energy particles, 19: 41332 (JINR-P-2220)
Precession of the top in the gravitational field, 19: 41204 (JINR-P-2174)

K

KERNFORSCHUNGSANLAGE, JUELICH (WEST GERMANY).
Geometry and statistical error in absolute counting with β-γ coincidence method, 19: 40874 (JUL-227-CA)
Testing emergency cooling system of reactor FRJ-2 (DIDO), 19: 42153 (JUL-235-RE)

KERNFORSCHUNGSZENTRUM, KARLSRUHE (WEST GERMANY). INSTITUT FUR ANGEWANDTE KERNPHYSIK.
Method for studying inelastic scattering of slow neutrons in many-particle systems, 19: 42154 (KFK-261)

KERNFORSCHUNGSZENTRUM, KARLSRUHE (WEST GERMANY). INSTITUT FUER RADIOCHEMIE.
Isobaric order of particle range and range of fragments from thermal fission of Pu-239, 19: 41668 (KFK-306)

KERNFORSCHUNGSZENTRUM, KARLSRUHE (WEST GERMANY). LABORATORIUM FUER STRAHLENCHEMIE.
Solvated electrons in γ-irradiated, frozen solutions, 19: 40551 (KFK-293)

KERNKRAFTWERK RWE-BAYERWERK G.M.B.H., GUNDREMMINGEN (WEST GERMANY).
Prog. rpt. on Gundremminger nuclear power plant, annual, 1964, 19: 42085 (EUR-2426.d)

L

LAWRENCE RADIATION LAB., UNIV. OF CALIFORNIA, BERKELEY.
A FORTRAN program for calculating kinematical and dynamical quantities of particle interactions and decays, 19: 41339 (UCRL-11648)
Alpha particle bombardment of Si and GaAs diodes; energy conversion and radiation damage, 19: 40937 (UCRL-11958)
Analysis of dislocation loops in quenched fcc metals, 19: 41026 (UCRL-16024)
Angular distributions of conversion electrons from oriented ^{137m}Ce nuclei, 19: 41679 (UCRL-11462(Rev.))
Concrete low-background counting enclosure, 19: 40721 (UCRL-11454)
Electron spin resonance studies of transition metal ion complexes, 19: 40465 (UCRL-16175)
Gas absorption by drops traveling on a vertical wire, 19: 40398 (UCRL-16047)
Internal conversion electrons from primary fission fragments, 19: 41680 (UCRL-16184)
Physical chemistry of glass-metal interfaces, 19: 40464 (UCRL-11816 (Rev.))
Sensitive differential pressure system for measuring depths of cryogenic liquids, 19: 40878 (UCRL-9672(Rev.))
Use of semiconductor detectors for internal-conversion coefficient measurements, 19: 40880 (UCRL-16035)

LAWRENCE RADIATION LAB., UNIV. OF CALIFORNIA, LIVERMORE.
Bibliography on thermal resistance of contacting surfaces, 19: 40744 (UCRL-14264)
Determination of errors in a one-parameter system, 19: 42225 (UCRL-12050)
FOTRAC: a Monte Carlo photon tracing computer program, 19: 41957 (UCRL-14165)
High-pressure shock wave experiments in argon and xenon, 19: 41128 (UCRL-12466)
Index to hazards control quarterly reports nos. 1 through 19, 19: 40833 (UCRL-14116)
Measurement of Livermore pool-type reactor (LPTR) transfer function using reactor oscillation techniques, 19: 42156 (UCRL-12476)
Modular, plug-in chassis system permits compatible mounting of conventional chassis, printed circuit boards, and micromodules, 19: 42226 (UCRL-12117-T)
New theorems for elementary number theory, 19: 42224 (UCRL-12041-T)
Note on electrostatic instabilities in a plasma with anisotropic velocity distribution, 19: 41866 (UCRL-12052)
Operating trans-curium element radiochemistry facility, 19: 40719 (UCRL-7844-T)
Plasma confinement properties of relativistic electron coils, 19: 41867 (UCRL-12455-T)
Pre-Schooner base surge and cloud formation, 19: 40708 (PNE-503F)
Prog. rpt. on hazards control, 1–3/65, 19: 40834 (UCRL-14151)
Pulsed neutron measurements on solid-moderated, enriched-uranium subcritical assemblies, 19: 42051 (UCRL-12013)
Remotely-operated trans-plutonium chemical process cells, 19: 40720 (UCRL-7845-T)
Rescue basket, 19: 42223 (UCRL-12006)
Spectrophotometric determination of trace amounts of Ta, 19: 40414 (UCRL-7967)
Stimulated Brillouin scattering, 19: 41971 (UCRL-7968-T)
The sulfides of Sr, Ca, and Mg in infrared stimulated luminescence dosimetry, 19: 40879 (UCRL-12371)

LOCKHEED–GEORGIA CO., MARIETTA.
Computer programs for shielding problems in manned space vehicles, 19: 41954 (NP-15338)

LOS ALAMOS SCIENTIFIC LAB., UNIV. OF CALIFORNIA, N. MEX.
A uniqueness theorem concerning moment distributions, 19: 42204 (LA-DC-6632)
Analysis of shock wave and initiation data for solid explosives, 19: 42206 (LA-DC-6992)
Automatic liquid nitrogen distribution system for twenty-five cold traps, 19: 41165 (LA-DC-7147)
Effect of inner field fluctuations on plasma impedance, 19: 41853 (LA-

DC-6603)
Experimental observations of initiation of nitromethane by shock interactions at discontinuities, 19: 42207 (LA-DC-6994)
Feasibility of brazed joints between Nb-1 Zr alloy and alumina ceramics, 19: 40980 (LA-3302)
High-energy γ spectrum of thermal neutron capture in holmium, 19: 41670 (LA-DC-7097)
High resolution measurements of γ rays from neutron inelastic scattering, 19: 41669 (LA-DC-7096)
Hydraulic control rod actuators for Kiwi-TNT reactor, 19: 42136 (LA-DC-6941)
Integral gamma and neutron measurements on Kiwi-TNT, 19: 42135 (LA-3304)
Integrated series of crystallographic computer programs. VII., 19: 41965 (LA-3309)
Integrated series of crystallographic computer programs. VIII., 19: 41966 (LA-3310)
Interactions of detonation waves in condensed explosives, 19: 42205 (LA-DC-6990)
Phase relationships of the high carbon portion of the lanthanide dicarbides, 19: 41014 (LA-DC-6819)
Phermex applications to studies of detonation waves and shock waves, 19: 41118 (LA-DC-6996)
Pions, muons and nuclear structure, 19: 41671 (LADC-6186)
Review of quasiparticle and Josephson tunneling in superconductors, 19: 41607 (LA-3342)
Solubility of selected elements in liquid plutonium. V., 19: 40950 (LA-3338)
Stability of detonations for disturbances of small transverse wavelength, 19: 41117 (LA-3306)
Study of one-dimensional, time-dependent reaction zone of nitro methane and liquid TNT, 19: 42203 (LA-3297)
Thermal radiation from burning hydrogen plume, 19: 42137 (LA-DC-7313)
X-ray fluorescence spectrometric determination of plutonium in uranium–plutonium–manganese alloys, 19: 40408 (LA-3333)

LOUISVILLE UNIV., KY. DEPT. OF BIOLOGY.
Life history of banded sculpin, Meade Co., Kentucky, 19: 42220 (TID-22023)

M

MARYLAND UNIV., COLLEGE PARK. DEPT. OF PHYSICS AND ASTRONOMY.
Gravitational radiation from binary systems, 19: 41206 (N64-33291)
Partial-wave dispersion relations for pionic disintegration of deuterons, 19: 41336 (NP-15335)

MARYLAND UNIV., COLLEGE PARK. INST. FOR FLUID DYNAMICS AND APPLIED MATHEMATICS.
Nonlinear mode interactions in universal plasma instabilities, 19: 41865 (TID-22050)

MASSACHUSETTS INST. OF TECH., CAMBRIDGE.
Magnetic impurity effect on superconductor transition temperature–extension of Nakaoka's theory, 19: 41608 (MIT-QPR-57, pp 59-65)
Prog. rpt. on solid-state and molecular theory, 4–6/65, 19: 41967 (MIT-QPR-57)
The band structure of beryllium, 19: 41968 (MIT-QPR-57, pp 22-42)

MASSACHUSETTS INST. OF TECH., CAMBRIDGE. DEPT. OF METEOROLOGY.
Some aspects of general circulation of the lower stratosphere, 19: 41570 (CONF-765-11)

MASSACHUSETTS INST. OF TECH., CAMBRIDGE. DEPT. OF NUCLEAR ENGINEERING.
Epithermal neutrons in U–D_2O lattices, 19: 42044 (MIT-2344-3, pp 37-54)
Fast fission measurements, 19: 41672 (MIT-2344-3, pp 5-14)
Fast neutron distributions, 19: 42043 (MIT-2344-3, pp 15-36)
Material buckling and intracellular thermal neutron distributions, 19: 42049 (MIT-2344-3, pp 155-64)
Measurements on poisoned lattices, 19: 42046 (MIT-2344-3, pp 109-14)
Oscillating neutron source experiment, 19: 41641 (MIT-2344-3, pp 137-54)
Prog. rpt. on Heavy Water Project, annual, 9/30/64, 19: 42007 (MIT-2344-3)
Pulsed neutron and control rod research studies of reactivity and related parameters, 19: 42045 (MIT-2344-3, pp 55-108)
Single-rod measurements and theory, 19: 42047 (MIT-2344-3, pp 115-24)
Two-region lattices, 19: 42048 (MIT-2344-3, pp 125-36)

MASSACHUSETTS INST. OF TECH., CAMBRIDGE, MASS. INSTRUMENTATION LAB.
Improvement of U–Mo alloys for gyroscope wheel rims, 19: 41023 (NP-15334)

MASSACHUSETTS UNIV., AMHERST.
Ecological changes in insect community of a pitch pine-oak forest subjected to chronic γ irradiation, 19: 40307 (BNL-9253)

MAX-PLANCK-INSTITUT FUR PHYSIK UND ASTROPHYSIK, MUNICH (WEST GERMANY).
Stellar evolution. I., 19: 41210 (N64-25282)

MICHIGAN STATE UNIV., EAST LANSING.
Excitation of first level of ^{12}C by 156-Mev protons, 19: 41675 (ORNL-P-330)

MICHIGAN UNIV., ANN ARBOR.
Investigation of nonlinear interaction phenomena in the ionosphere, 19: 41572 (NASA-CR-258)

MINNESOTA UNIV., MINNEAPOLIS. DEPT. OF CHEMICAL ENGINEERING.
Recombination of hydrogen and oxygen in the presence of water vapor under the influence of radiation, 19: 40549 (COO-1032-1)

MINNESOTA UNIV., MINNEAPOLIS. PHYSICAL ELECTRONICS RESEARCH LAB.
Prog. rpt. on physics of electron emission and electron tube technology, 10/16/64–4/15/65, 19: 41124 (NP-15108)

MINNESOTA UNIV., MINNEAPOLIS. PLASMA PHYSICS LAB.
Prog. rpt. on collision processes in gaseous plasmas, 1–6/65, 19: 41850 (AD-617386)

MSA RESEARCH CORP., CALLERY, PA.
Prog. rpt. on effect of high-temperature Na on steels, 4–6/65, 19: 40969 (MSAR-65-96)
Prog. rpt. on measurement of impurities in Na, 4–5/65, 19: 40409 (MSAR-65-95)

N

NATIONAL AERONAUTICS AND SPACE ADMINISTRATION, CLEVELAND, OHIO. LEWIS RESEARCH CENTER.
Bend transition temperature of arc-cast molybdenum and molybdenum-0.5-percent-titanium sheet in worked, recrystallized, and welded conditions, 19: 41016 (N64-80997)

NATIONAL AERONAUTICS AND SPACE ADMINISTRATION, HUNTSVILLE, ALA. GEORGE C. MARSHALL SPACE FLIGHT CENTER.
Calculation of proton penetration and dose rates, 19: 41951 (N64-30510)
Reduced three-body problem: a generalization of the classical restricted three-body problem, 19: 41205 (N64-31725)

NATIONAL AERONAUTICS AND SPACE ADMINISTRATION, MOFFETT FIELD, CALIF. AMES RESEARCH CENTER.
Analysis of errors associated with the determination of planetary atmosphere structure from measured accelerations of an entry vehicle, 19: 41123 (NASA-TR-R-225)

NATIONAL BUREAU OF STANDARDS, WASHINGTON, D. C.
Fluid amplification, 19: 40739 (OTR-112)

NATIONAL INST. FOR RESEARCH IN NUCLEAR SCIENCE, CHILTON (ENGLAND). RUTHERFORD HIGH ENERGY LAB.
Automatic control of electromagnetic field in linac resonant cavities, 19: 41167 (NIRL/R/76)

NATIONAL MARINE CONSULTANTS, ANAHEIM, CALIF.
Prog. rpt. on Task IV local Newport pier test, 6/29/65, 19: 42210 (NVO-98-8)

NAVAL CIVIL ENGINEERING LAB., PORT HUENEME, CALIF.
Ground-motion effects on the contents of buried structures, 19: 40758 (AD-426249)

NAVAL RADIOLOGICAL DEFENSE LAB., SAN FRANCISCO, CALIF.
Calorimeters and radiometers for measurement of large thermal irradiances, 19: 40882 (USNRDL-TR-839)

NAVAL RESEARCH LAB., WASHINGTON, D. C.
Optical techniques for electron probe analysis, 19: 40951 (NRL-6290)

NEVIS LABS., COLUMBIA UNIV., IRVINGTON-ON-HUDSON, N. Y.
Annihilation of anti-protons in hydrogen at rest. III., 19: 41325 (CU-1932-245)

NEW MEXICO STATE UNIV., UNIVERSITY PARK.
Electromagnetic effects of high-density γ flux interacting with matter, 19: 41956 (SC-R-65-933)

NEW MEXICO UNIV., ALBUQUERQUE. ENGINEERING EXPERIMENT STATION.
Prog. rpt. on inverter applications, 6/63–5/64, 19: 40845 (N64-33676)

NEW SOUTH WALES UNIV., KENSINGTON (AUSTRALIA). DEPT. OF NUCLEAR AND RADIATION CHEMISTRY.
Environmental radioactivity in New South Wales, 19: 40805 (NRS-30)

NORSK RADIUMHOSPITAL, OSLO.
Induced radioactivity in the collimator system of a 31-Mev Brown Boveri betatron, 19: 41169 (NYO-3364-7)
Induced radioactivity caused by therapeutic use of high-energy radiation, 19: 40392 (NYO-8364-6)

NRA, INC., LONG ISLAND CITY, N. Y.
Methods of promoting the removal of free electrons from an ionized and

dissociated atmosphere, 19: 41569 (AD-426145)
NUCLEAR ENERGY INFORMATION CENTER, WARSAW (POLAND).
Bibliography on nuclear astrophysics. II., 19: 41207 (NEIC-RR-9)
NUCLEAR MATERIALS AND EQUIPMENT CORP., APOLLO, PA.
Morphological characteristics of coprecipitated $(U,Pu)O_2$ powders by electron microscopy, 19: 41024 (NUMEC-2389-5)
Sintering behavior of PuO_2, 19: 40981 (NUMEC-2389-6)
NUCLEAR METALS, WEST CONCORD, MASS.
Prog. rpt. on dispersion-strengthened alloys, 4–6/65, 19: 41021 (NMI-8002.1)
NUCLEAR UTILITY SERVICES, INC., WASHINGTON, D. C.
Calculational models for beta dose from spherical particles, 19: 40635 (NUS-217)

O

OAK RIDGE NATIONAL LAB., TENN.
A comparison of multistage flash and long-tube vertical multiple-effect evaporators under identical conditions, 19: 40699 (ORNL-TM-826)
An unconventional ultra-high vacuum facility, 19: 40772 (ORNL-P-1465)
Chemical applications of nuclear explosions (CANE), 19: 40706 (ORNL-TM-1191)
Development of pulse-heating calorimetric technique for measuring the specific heat of electrical conductors and its application to pure iron from 100 to 1400°C, 19: 40700 (ORNL-TM-1187)
DWB deuteron stripping program, 19: 41677 (ORNL-TM-1151)
Engineering and cost considerations for tunnel grid blast shelter concept, 19: 40759 (ORNL-TM-1183)
Excitation of first level of ^{12}C by 156-Mev protons, 19: 41675 (ORNL-P-330)
Iodine transport and deposition in a high-temperature, helium loop first test series, 19: 40397 (ORNL-TM-1134)
Joint National Institutes of Health-Atomic Energy Commission zonal centrifugation on project. I., 19: 40654 (ORNL-3613)
Low-energy electron and proton transmission in Al and Ag, 19: 41969 (ORNL-TM-1153)
Low pass filter for cold neutrons to be used in a search for a neutron electric dipole moment, 19: 41338 (ORNL-TM-1149)
Low-temperature H_2O-cooled and -moderated reactors for desalting, 19: 42097 (ORNL-TM-1152)
Mathematical models of diffusion in grain boundaries, 19: 41970 (ORNL-TM-1224)
Motion of spheres in smooth rotating drums and applications to the coating of nuclear fuel particles, 19: 40982 (ORNL-3819)
Nucleon-meson cascade initiated by 200-Bev protons, 19: 41955 (ORNL-TM-1121)
Optical properties of vacuum-evaporated films of Cd, Tl, and Zn, 19: 42213 (ORNL-TM-1164)
Orbits in a magnetic universe, 19: 41208 (ORNL-3827)
Procurement and quality evaluation of Nb-1 percent Zr stock for boiling alkali metal corrosion studies, 19: 40952 (ORNL-TM-1179)
Production of excited state H_2 for Lorentz dissociation in DCX-1, 19: 41864 (ORNL-P-1244)
Project Salt Vault, 19: 42195 (ORNL-P-1479)
Propagation of neutron waves through heterogeneous multiplying and nonmultiplying media, 19: 41643 (ORNL-TM-1184)
Properties of thorium, its alloys, and its compounds, 19: 41025 (ORNL-TM-1144)
Radio-release methods for the evaluation of atmospheric pollution. Sulfur dioxide, 19: 40410 (ORNL-P-494)
Solution to electromagnetic induction problems, 19: 41125 (ORNL-TM-1185)
Some fluorine compounds of Re and Tc, 19: 40461 (ORNL-P-491)
U. S. reactor containment technology, 19: 42008 (ORNL-NSIC-5(Vol.I and II))
$^{51}V(p,n)^{51}Cr$ cross section from threshold to 2.25 Mev, 19: 41676 (ORNL-P-1468)
OHIO STATE UNIV. RESEARCH FOUNDATION, COLUMBUS.
Prog. rpt. on stress-corrosion cracking in Fe–Ni–Cr system, 3/17–6/16/65, 19: 40967 (COO-1319-27)

P

PADUCAH GASEOUS DIFFUSION PLANT, KY.
Chromatograph for analysis of highly reactive and corrosive compounds, 19: 40407 (KY-485)
PARIS UNIV. (FRANCE).
Study of recombination processes for electron-hole pairs in germanium irradiated by γ rays from ^{60}Co using the photovoltaic effect in P-N junctions, 19: 40932 (CEA-R-2723)
PHILLIPS PETROLEUM CO. IDAHO FALLS, IDAHO., ATOMIC ENERGY DIV.
Decontamination of radioactive effluent with clinoptilolite, 19: 40651 (IDO-14657)
Prog. rpt. on STEP Project, 1–6/64, 19: 42134 (IDO-17070)
Reactor stability tests in Spert IV facility, 19: 42152 (IDO-17088)
PIQUA NUCLEAR POWER FACILITY, OHIO.
Prog. rpt. on Piqua reactor operation, 6/65, 19: 42083 (COO-652-16)
PRATT AND WHITNEY AIRCRAFT, MIDDLETOWN, CONN. CONNECTICUT ADVANCED NUCLEAR ENGINEERING LAB.
CMPXMAT, a transfer function evaluation program, 19: 42222 (TIM-940)
Compact 1900°F resistance-wound combustion furnace for remote operation, 19: 40413 (TIM-948)
Direct current electromagnetic pump analysis, 19: 40743 (TIM-929)
LAG–a load and go assembler written for the CDC-1604-B computer, 19: 42221 (TIM-939)
Single-film journal bearing tests in water, 19: 40703 (TIM-916)
Summary of shaft face seal development program, 19: 40718 (TIM-909)
The electron microprobe and light element analysis, 19: 40412 (TIM-924)
Utilization of yttrium in gettering oxygen and nitrogen in Nb-base materials, 19: 40953 (PWAC-441)
Water tests of high-speed centrifugal dynamic shaft seals, 19: 40702 (TIM-914)
PRINCETON UNIV., N. J. PLASMA PHYSICS LAB.
A microwave system for low-density measurements, 19: 41854 (MATT-369)
High-voltage radio frequency variable capacitor using a liquid di-electric, 19: 40844 (MATT-341)

R

RADIO PROPAGATION UNIT, NATIONAL PHYSICAL LAB., NEW DELHI (INDIA).
Statistical characteristics of sudden ionospheric disturbances, 19: 41573 (RPU-S19)
RENSSELAER POLYTECHNIC INST., TROY, N. Y.
Investigation of transient radiation damage in semiconductor materials, 19: 40933 (NP-15300)
Investigation of transient radiation damage in semiconductor materials, 19: 40934 (NP-15301)
REYNOLDS ELECTRICAL AND ENGINEERING CO., INC., MERCURY, NEV. RADIOLOGICAL SCIENCES DEPT.
Remote radiation monitoring at the Nevada Test Site, 19: 40876 (NVO-162-5(Rev.))
ROCHESTER UNIV., N. Y. ATOMIC ENERGY PROJECT.
Effect of wide x-ray beam and finite phantom thickness on 1000-kvp x-ray depth dose, 19: 40881 (UR-667)
ROCHESTER UNIV., N. Y. DEPT. OF PHYSICS AND ASTRONOMY.
Tensor methods. II., 19: 41340 (UR-875-53)
ROCKETDYNE, CANOGA PARK, CALIF.
Application of thin-film electron microscopy to refractory metal processing, 19: 41015 (MIL-TDR-64-282)
Hydrogen heat transfer data compilation, 19: 40734 (NP-15331)
Prog. rpt. on liquid-metal-lubricated bearings, 3/15–6/15/65, 19: 40716 (NP-15280)
ROCKY FLATS DIV., DOW CHEMICAL CO., GOLDEN, COLO.
Laboratory ignition system, 19: 42214 (RFP-397)
The effect of temperature on RTV-20, 19: 42215 (RFP-625)
ROENTGEN TECHNISCHE DIENST N. V., ROTTERDAM (NETHERLANDS).
Prog. rpt. on nondestructive welding tests, 10–12/64, 19: 40753 (EURAEC-1378)
RUTGERS–THE STATE UNIV. OF NEW JERSEY, NEW BRUNSWICK. BUREAU OF ENGINEERING RESEARCH.
Prog. rpt. on gas-solid suspensions, 3–5/65, 19: 40742 (TID-22002)

S

SAMENWERKENDE ELECTRICITEITS-PRODUCTIEBEDRIJVEN, N. V., ARNHEM (NETHERLANDS).
Prog. rpt. on Dodewaard power plant, annual, 1964, 19: 42088 (EUR-2430.n)
SANDIA CORP., ALBUQUERQUE, N. MEX.
A study of the neutron-induced base current component in silicon transistors, 19: 40936 (SC-R-65-912)
Analytical approach to study vehicle collisions, 19: 40817 (SC-RR-65-98, pp 243-60)
Apparatus for measurement of the Hall effect in metals, 19: 42217 (SC-RR-65-325)
Approximate calculative assessment made relating to wall temperatures and behavior of cask in fire tests, 19: 40832 (SC-RR-65-98, pp 732-5)
Aspects of transportation of radioactive materials, 19: 40812 (SC-RR-65-

98, pp 74-8)
Basic uncertainties in electrical measurements, 19: 42218 (SC-TM-64-509)
Can we model a fire test, 19: 40815 (SC-RR-65-98, pp 133-40)
Circulation processes and mixing mechanisms in upper atmosphere above 30 km, 19: 41112 (SC-DC-65-1312)
Compilation of crater data, 19: 40711 (SC-RR-65-220)
Computer aided circuit reliability analysis, 19: 40848 (SC-R-65-935)
Conductivity induced in polystyrene by pulsed γ rays, 19: 41091 (SC-R-65-943)
Criticality safety evaluation of packages for the transport of fissile material, 19: 40828 (SC-RR-65-98, pp 679-90)
Description and evaluation of four $Pu(NO_3)_4$ shipping containers, 19: 40821 (SC-RR-65-98, pp 423-41)
Design of containers for shipment of radioactive materials, 19: 40823 (SC-RR-65-98, pp 450-72)
Design of plutonium oxide and plutonium nitrate shipping containers, 19: 40825 (SC-RR-65-98, pp 609-19)
Dimensions of a crater from a 500-ton TNT hemisphere detonated on rock, 19: 40712 (SC-RR-65-277)
Dispersion of radioisotopes caused by transport fires, 19: 40830 (SC-RR-65-98, pp 719-22)
Experimental studies of cask impact resistance, 19: 40818 (SC-RR-65-98, pp 261-82)
Fire test of 15-ton shipping container, 19: 40827 (SC-RR-65-98, pp 631-50)
Fire tests of packagings for radioactive materials, 19: 40814 (SC-RR-65-98, pp 114-18)
Introduction rate of electrically active defects in n-type silicon by nuclear radiation, 19: 40935 (SC-DC-65-1247)
New developments in accident-resistant shipping containers for radioactive materials, 19: 40816 (SC-RR-65-98, pp 141-86)
Nuclear explosives--tool for engineer, 19: 40710 (SC-DC-65-1485)
Packaging standards, 19: 40810 (SC-RR-65-98, pp 32-44)
Progress report on a class-II container for low-assay uranium compounds, 19: 40819 (SC-RR-65-98, pp 330-56)
Regulatory packaging standards, 19: 40811 (SC-RR-65-98, pp 45-54)
Resistance to fire of lead-lined casks, 19: 40813 (SC-RR-65-98, pp 107-13)
Special problems in packaging and transportation of radioactive materials, 19: 40826 (SC-RR-65-98, pp 625-9)
Studies on fire resistivities of radioisotope containers, 19: 40831 (SC-RR-65-98, pp 723-31)
Survey of research in the transportation of radioactive materials, 19: 40809 (SC-RR-65-98, pp 17-31)
Symposium on packaging and transporting radioactive materials, Albuquerque, 1/65, 19: 40808 (SC-RR-65-98)
Testing of 10-ton capacity UF_6 shipping containers, 19: 40824 (SC-RR-65-98, pp 580-608)
Testing shipping containers for slightly enriched uranium billets, ingots, and fuel cores, 19: 40820 (SC-RR-65-98, pp 357-76)
The kinetics of the reactions of KO_2 and KOH with water, 19: 40462 (SC-TM-65-183)
The problem of container interchangeability, 19: 40822 (SC-RR-65-98, pp 442-9)
The transport container for irradiated fuel from civil power stations in the UK, 19: 40829 (SC-RR-65-98, pp 711-18)
Wear testing of plated coatings, 19: 42216 (SC-DR-65-269)

SANDIA CORP., LIVERMORE, CALIF.
Theory of one-dimensional shock wave propagation, 19: 41126 (SCL-DR-65-75)

SETON HALL UNIV., SOUTH ORANGE, N. J.
Algebraic structure of the n-body problem, 19: 41122 (N64-31207)
Regularized explicit solution of the analytic n-body problem, 19: 41530 (N64-82432)

SOCIETE D'ENERGIE NUCLEAIRE FRANCO-BELGE DES ARDENNES, CHOOZ-LEZ-GIVET (FRANCE).
Prog. rpt. on Ardennes nuclear power plant, annual, 1964, 19: 42087 (EUR-2428.f)

SOCIETE D'EXPLOITATION DES MATERIELS HISPANO-SUIZA, BOIS-COLOMBES (FRANCE).
Safety concerning reactor Pegase, 19: 42151 (CEA-R-2518(Vol.II))

SOUDOMETAL, S. A., BRUSSELS (BELGIUM).
Prog. rpt. on stainless steel cladding of very thick steels, 1–3/65, 19: 40979 (EURAEC-1351)

SPACE TECHNOLOGY LABS., INC., LOS ANGELES, CALIF.
Electron bombardment of silicon solar cells, 19: 40931 (AD-609424)

STANFORD LINEAR ACCELERATOR CENTER, STANFORD UNIV., CALIF.
On the problem of hidden variables in quantum mechanics, 19: 41531 (SLAC-PUB-44)

Prog. rpt. on two-mile accelerator project, 10–12/64, 19: 41170 (SLAC-42)

STANFORD RESEARCH INST., MENLO PARK, CALIF.
Prog. rpt. on sorption of gases on metal surfaces, 2/15–5/15/65, 19: 40463 (SRIA-425-5)
Summary of the Soviet papers on the high pressure equation of state of metals, 19: 40459 (NP-15324)

STANFORD UNIV., CALIF. DEPT. OF AERONAUTICS AND ASTRONAUTICS.
Singular-perturbation methods applied to magneto-gasdynamics and plasma problems, 19: 41114 (AD-617258)
Statistical theory of homogeneous hydromagnetic turbulence, 19: 41127 (SUDAER-238)

STANFORD UNIV., CALIF. MICROWAVE LAB.
Measurement techniques for periodic structures, 19: 41166 (ML-767)

STATE UNIV. OF NEW YORK, BROOKLYN. DOWNSTATE MEDICAL CENTER.
Prog. rpt. on radiation effects on calcifying mechanism of epiphyseal cartilage, final, 2/62, 19: 40351 (NYO-1913-1)

STEIN SEAL CO., PHILADELPHIA, PA.
NMPO blower shaft seal-test report, 19: 40701 (TID-22007)

T

TENNESSEE UNIV., KNOXVILLE.
Development of pulse-heating calorimetric technique for measuring the specific heat of electrical conductors and its application to pure iron from 100 to 1400°C, 19: 40700 (ORNL-TM-1187)
Low-energy electron and proton transmission in Al and Ag, 19: 41969 (ORNL-TM-1153)
Solution to electromagnetic induction problems, 19: 41125 (ORNL-TM-1185)

TENNESSEE UNIV., KNOXVILLE. DEPT. OF CHEMISTRY.
Some fluorine compounds of Re and Tc, 19: 40461 (ORNL-P-491)

THAYER SCHOOL OF ENGINEERING, DARTMOUTH COLL., HANOVER, N. H.
Prog. rpt. on two-phase flow and boiling heat transfer, 1–3/65, 19: 40738 (NYO-3114-7)
Two-phase flow and boiling heat transfer. The separate-cylinders model of two-phase flow, 19: 40737 (NYO-3114-6)

TRW ELECTROMECHANICAL DIV., THOMPSON RAMO WOOLDRIDGE INC., CLEVELAND, OHIO.
Summary report on electron bombardment ion engine development, 19: 40760 (N64-25008)

TRW SPACE TECHNOLOGY LABS., THOMPSON RAMO WOOLDRIDGE INC., REDONDO BEACH, CALIF.
Shock spectrum measurements, Project Gnome, 19: 40713 (VUF-2401)

U

UNION CARBIDE CORP., OAK RIDGE, TENN. Y-12 PLANT.
Providing real-time information on production schedules and costs, 19: 40704 (Y-KA-9)

UNITED NUCLEAR CORP., WHITE PLAINS, N. Y. DEVELOPMENT DIV.
Analysis of fast reactor transients including meltdown, 19: 42100 (UNC-5092)

UNITED STATES--EURATOM JOINT RESEARCH AND DEVELOPMENT PROGRAM.
Core evaluation of the Garigliano reactor, 19: 42091 (GEAP-4852)
Fission gas release from UO_2 fuel rods with gross central melting. I., 19: 41088 (GEAP-4572)
Prog. rpt. on burnable poison additions to UO_2, 1–3/65, 19: 41006 (CEND-3107-238)
Prog. rpt. on Garigliano reactor, 7/65, 19: 42092 (GEAP-4909)
Prog. rpt. on in-pile thermal conductance testing, 1–3/65, 19: 40732 (CEND-3336-237)
Prog. rpt. on mechanical properties of steels, final, 1965, 19: 40947 (EURAEC-1403)
Prog. rpt. on nondestructive welding tests, 10–12/64, 19: 40753 (EURAEC-1378)
Prog. rpt. on Pu subcritical experiment, 4–6/65, 19: 42093 (GEAP-4912)
Prog. rpt. on stainless steel cladding of very thick steels, 1–3/65, 19: 40979 (EURAEC-1351)
Prog. rpt. on stress corrosion of austenitic stainless steels, 6/65, 19: 40968 (EURAEC-1424)
Prog. rpt. on study of base metal for research on brittle fracture of large welded assemblies, annual, 5/64–5/65, 19: 41008 (EURAEC-1407)
Prog. rpt. on vertical welding process under-electro-conducting on steel plates, 11/20/62, 19: 41007 (EURAEC-1400)
Prog. rpt. on yield phenomena and fracture of hydrided Zr, 4–6/65,

19: 41010 (IITRI-578P27-10)
Two-phase flow and boiling heat transfer. The separate-cylinders model of two-phase flow, 19: 40737 (NYO-3114-6)
USTAV JADERNEHO VYZKUMU, CESKOSLOVENSKA AKADEMIE VED, REZ.
General acidobasicity. III. Explanation of the author's conception, 19: 40466 (UJV-1209/65)

V

VANDERBILT UNIV., NASHVILLE, TENN.
Efficiency of high pressure electric shock tubes, 19: 40849 (TID-22061)
Optical properties of vacuum-evaporated films of Cd, Tl, and Zn, 19: 42213 (ORNL-TM-1164)
VIRGINIA POLYTECHNIC INST., BLACKSBURG. DEPT. OF METALS AND CERAMIC ENGINEERING.
Prog. rpt. on stress corrosion of austenitic stainless steels, 6/65, 19: 40968 (EURAEC-1424)
VIRGINIA UNIV., CHARLOTTESVILLE. DEPT. OF AEROSPACE ENGINEERING.
Skin friction and heat transfer in MHD channel flows, 19: 41119 (MIT-36-P)

W

WESTINGHOUSE ELECTRIC CORP., PITTSBURGH, PA. ATOMIC POWER DIV.
1000-Mwe closed-cycle water reactor study, 19: 42102 (WCAP-2385 (Vol.I))
1000-Mwe closed-cycle water reactor study, 19: 42103 (WCAP-2385 (Vol.II))
WESTINGHOUSE RESEARCH LABS., PITTSBURGH, PA.
Ultrasonic testing characteristics of forged Inconel, 19: 41027 (WERL-0029-2)

Y

YALE UNIV., NEW HAVEN, CONN.
Planetary optical emission and flare activity of nearby stars, 19: 41203 (AD-600154)

PERSONAL AUTHOR INDEX

Each entry after an author's name is a shortened version of the title of the report or article, followed by the *NSA* volume and abstract number. Report numbers are given in parentheses.

The phrase "Progress report" is abbreviated as "Prog. rpt.," permitting a more rapid and complete alphabetical arrangement of the titles without changing the location of the progress report titles in relation to the other titles.

Because of problems involving the mechanical preparation of this index, all accent marks are omitted. The following changes in spelling have been introduced to reduce some of the confusion which might result from omitting the accents:

ä	becomes	ae
ö		oe
ø		oe
ü		ue (except in transliterated Chinese names)

A

ABBOTT, William E., Boiling neutronic reactor systems, 19: 42069

ABERTH, William, Elastic differential scattering of He^+ ions by He in the 20–600 ev range, 19: 41283

ACETO, Henry Jr., Therapeutic possibilities of π^- mesons, 19: 40395

ACHENER, P. Y., Prog. rpt. on alkali metals evaluation program, 4–6/65, 19: 41001 (AGN-8154)

ADAM, Andres, On angular correlation measurements between fast neutrons, 19: 40894

ADAMS, J. Barclay, Hyperfine structure and weak interactions, 19: 41410

ADAMS, R. E., Properties of thorium, its alloys, and its compounds, 19: 41025 (ORNL-TM-1144)

ADAMYAN, V. E., Magnetic susceptibility of SmS, 19: 41060

ADCOCK, F. E., Design of plutonium oxide and plutonium nitrate shipping containers, 19: 40825 (SC-RR-65-98, pp 609–19)

ADEMOLLO, M., Spin tests for bosons, 19: 41447

ADLER, F. T., Investigations on nonlinear stability of coupled nuclear systems, 19: 42062

ADLER, K. L., Heat transfer in organic-cooled reactors, 19: 42110

ADLER, Stephen L., Consistency conditions on strong interactions. II., 19: 41450

AFANAS'EV, A. M., X-ray studies of polyamide films cast from irradiated solutions, 19: 40595

AFANAS'EV, Yu. A., Enthalpy variations during extraction according to standard enthalpy of formation, 19: 40669

AGOSTINELLI, C., Motion of electrically conducting fluid for given distribution conditions of conduction and eddy current, 19: 41154

AGULLO-LOPEZ, F., Plastic flow induced by partial x irradiation of NaCl, 19: 40594

AHMADZADEH, A., New reduction of the Faddeev equations and its application to the pion as a three-particle bound state, 19: 41416

AHRENS, L. H., Geochemistry of rare earths, 19: 40793

AISCH, D., MZFR safety shield with installation for pressure release, 19: 42167

AISMILLER, R. G. Jr., Nucleon–meson cascade initiated by 200-Bev protons, 19: 41955 (ORNL-TM-1121)

AIVAZYAN, Yu. M., Diffraction of field of an arbitrarily moving particle in semiplane, 19: 41539

AIZU, Ko, An evolutional track of galaxies in L-(L/V) diagram, 19: 41233

AKASOFU, S.-I., Dynamo action in ionosphere and motions of magnetospheric plasma. II., 19: 41593

AKASOFU, S.-I., Dynamo action in ionosphere and motions of magnetospheric plasma. III., 19: 41594

AKCASU, Z., Some theorems on neutron fluctuations and fluctuation spectra, 19: 41653

AKOPOVA, A. B., Effects of corrective substances on the treatment of nuclear emulsions with ultrasonic oscillations, 19: 40884

AKS, S. O., Singularities of scattering amplitude in potential theory, 19: 41550

ALBESCU, Ileana, Refractometric study of formation of complex Pr halides in aqueous solution, 19: 40469

ALBRECHT, R. W., Interpretation of pulsed neutron and reactor noise experiments in reflected reactors, 19: 42040 (BNWL-95, pp 40-54)

ALDER, Berni J., High-pressure shock wave experiments in argon and xenon, 19: 41128 (UCRL-12466)

ALEFELD, Georg, Entropy contributions to restoring force of dislocation Kink chain, 19: 41983

ALEKSEEV, T. N., Direct conversion of various types of energy into electrical and mechanical energy, 19: 41319

ALEKSEEV, V. V., Description of stationary state interactions, 19: 41495

ALEKSSENKO, L. A., Rare earth perchlorates, 19: 40509

ALEXA, J., Ion exchange chromatography of rare earths in aqueous organic media. I., 19: 40663

ALEXA, J., Ion exchange chromatography of rare earths in aqueous organic media. II., 19: 40664

ALEXA, J., Ion exchange chromatography of rare earths in aqueous organic media. III., 19: 40665

ALEXA, J., Ion exchange chromatography of rare earths in aqueous organic media. IV., 19: 40666

ALEXEFF, I., Collisionless ion-wave propagation and the determination of the compression coefficient of plasma electrons, 19: 41892

ALFIMENKOV, V. P., Determination of spins of Ho-165 neutron resonances by transmission of polarized neutrons through a polarized target in the energy interval 0–55 ev, 19: 41665 (JINR-P-2209)

ALISHEV, S. A., Beta decay of moving longitudinally polarized neutrons, 19: 41496

ALLAS, R. G., States in ^{12}C between 16.4 and 19.6 Mev, 19: 41688

ALLEN, B. O., Computer aided circuit reliability analysis, 19: 40848 (SC-R-65-935)

ALLEN, J. P., Collective representation of lower lying states in ^{21}Ne, ^{21}Na, and ^{23}Na, 19: 41757

ALLEN, John W., Collisional excitation of autoionizing levels, 19: 41244

ALLENDEN, Dennis, Improvements relating to measuring apparatus, 19: 40454

ALLISY, Andre, The utilization of a magnetic induction field in the exposure measurements of x and γ rays, 19: 40838

ALLKOFER, O. C., The behavior of spark discharge chambers by triggering by the primary ionization and the avalanche, 19: 40898

ALMOND, P. R., Cross sections at 0° and angular distributions of resolved neutrons from $^{11}B + d$, 19: 41732

ALONSO-LOPEZ, J., Electrochemical behavior of Cd in the H_2O–D_2O system. I., 19: 40427

ALTSCHULER, Martin David, Interaction of fast charged particles with the coronal plasma, 19: 41933

ALVAREZ RIVAS, J. L., Plastic flow induced by partial x irradiation of NaCl, 19: 40594

AMANO, Tsuneo, Particle orbits in a heliotron magnetic field, 19: 41885

ANAND, J. D., Self-consistent determination of the ρ-meson Regge-pole parameters, 19: 41370

ANDERSON, D. E., Prog. rpt. on physics of electron emission and electron tube technology, 10/16/64–4/15/65, 19: 41124 (NP-15108)

ANDERSON, D. R., 200-Mwe prototype large SGR—reactor structure design and evaluation, 19: 42094 (NAA-SR-11314)
ANDERSON, E., Analysis of high energy p-p scattering experiment, 19: 41322 (BNL-9231)
ANDERSON, Gordon D., Summary of the Soviet papers on the high pressure equation of state of metals, 19: 40459 (NP-15324)
ANDERSON, H. G., Joint National Institutes of Health-Atomic Energy Commission zonal centrifugal project. I., 19: 40654 (ORNL-3613)
ANDERSON, W. F., Analysis of stresses in bellows, 19: 42208 (NAA-SR-4527(Pt.II))
ANDRADE E SILVA, J., Accelerator of negative ions, 19: 41182
ANDRADE E SILVA, Jose, Experiments of Magyar and Mandel and the wave-corpuscle dualism, 19: 41535
ANDREEV, V. N., Search for the (n,α) reaction in heavy nuclei under the action of thermal neutrons, 19: 41809
ANDRESEN, S. G., Time-dependent behavior of surface ionization efficiencies of Li and LiF on W, 19: 41141
ANDRIANOV, A. S., Influence of an electric field on luminescence of alkali halide compounds, 19: 40572
ANDRONIKASHVILI, E. L., Radiation damage in ionic crystals, 19: 41976
ANIKIN, V. S., Determination of the number of fissions in natural uranium mixture irradiated by neutrons, 19: 40640
ANNENKOV, B. N., Accumulation and distribution of Sr-90 in swine after prolonged administration of radiostrontium, 19: 40328
ANNENKOV, B. N., Accumulation of Sr-90 in cattle during the embryonal and postembryonal periods of development, 19: 40330
ANNENKOV, B. N., Effect of some constituents of food products (Ca, Mg, protein, fat) on accumulation of Sr-90 in animals, 19: 40342
ANNENKOV, B. N., Migration of radioactive Sr through the fodder-cow-milk chain, 19: 40332
ANNO, George H., Calculational models for beta dose from spherical particles, 19: 40635 (NUS-217)
ANSARI, S. M. R., Quasi-binomial representation of the Clebsch-Gordan coefficients, 19: 41551
ANSELIN, Francois, Transport properties of Nd nitride at low temperature, 19: 41973
ANTALOVA, A., Fundamental properties of the 11-year cycle of solar activity, 19: 41214
ANTONIJEVIC, V. G., Extraction of copper and uranium with 2-methyl-heptane-4,6-dione and hexane-2,4-dione, 19: 40423
ANTONOV, R. A., Formation of high-energy γ quanta, 19: 41298
ANTONOVA, L. I., Roentgenographic studies of lanthanum tellurides La_3Te_y, 19: 41070
AOKI, Rei, Prompt cascade gamma peak efficiencies of well-type NAI for fission products, 19: 40891
AOKI, Ryozo, Neutron energy spectrometers, 19: 40928
AOKI, Ryozo, Prompt cascade gamma peak efficiencies of well-type NAI for fission products, 19: 40891
AONO, Osamu, Unified theory of relaxations in plasmas. V., 19: 41886
APALIN, V. F., Neutron emission from ^{233}U, ^{235}U, and ^{239}Pu fission fragments, 19: 41681 (ANL-Trans-205)
APANASENKO, Z. I., Combined action of whole-body vibration and ionizing radiations on central nervous system, 19: 40354 (FTD-TT-65-48 pp 38-9)
APELGOT, Sonia, Self-decomposition and radiolysis, at low temperature, of tritiated thymidine in aqueous solution, 19: 40583
APPLEBY, E. R., Effect of thermal cycling on α-β transformation temperature of Pu, 19: 41028 (BNWL-tr-4)
APPLETON, B. R., Direction and energy distribution of charged particles transmitted through single crystals, 19: 41788
APPLETON, G. J., Packaging standards, 19: 40810 (SC-RR-65-98, pp 32–44)
ARAKAWA, E. T., Optical properties of vacuum-evaporated films of Cd, Tl, and Zn, 19: 42213 (ORNL-TM-1164)
ARENDT, P. R., Structure and variation of the topside ionosphere close to the Fort Monmouth longitude, 19: 41587
ARGAN, P. E., Search for a β-active ^5H, 19: 41750
ARKHANGEL'SKAYA, V. A., Trapping centers in rare earth-activated Ca, Sr, and Ba fluoride single crystals, 19: 41978
ARMOUDIAN, G. A., High-energy scattering by exchange of Markov's particle, 19: 41383
ARMOUDIAN, G. A., Nucleon form factor and large-angle p-p scattering, 19: 41385
ARMSTRONG, J. C., Weakly excited resonance levels in reaction $^{13}C(p,\gamma)^{14}N$, 19: 41740
ARNOLD, J. L., Uranium–Mo fuel element irradiation in SRE, 19: 41090 (NAA-SR-11121)
ARONSON, S., Thermodynamic properties of nonstoichiometric ThC, 19: 40485
ARTEMENKOV, L. I., Obtaining a hot thermonuclear plasma by injection of fast particles into a magnetic trap, 19: 41852 (IAE-676)
ARTEMOV, K. P., The reactions $^3He(d,t)2p$ and $^3He(^3He,\alpha)2p$, 19: 41658 (IAE-655)
ARTHUR, W., Methods of promoting the removal of free electrons from an ionized and dissociated atmosphere, 19: 41569 (AD-426145)
ARTYUNYAN, F. R., Emission of ultra-high energy μ mesons, 19: 41295
ASARO, Frank, Odd-parity rotational bands in ^{246}Cm, 19: 41794
ASATIANI, T. L., Polarization of cosmic muons at various energies, 19: 41294
ASAYAMA, Kunisuke, Nuclear spin-lattice relaxation in type II superconductors, 19: 41611
ASHCROFT, David John, Heating element spacer grids, 19: 42073
ASHCROFT, David John, Improvements relating to nuclear reactor fuel element assemblies, 19: 42072
ASHCROFT, David John, Nuclear reactor control systems, 19: 42029
ASKAR'YAN, G. A., Coherent radioemission from cosmic showers, 19: 41308
ASTAF'EV, V. A., Inverse problem in cascade theory, 19: 41710
AUBLE, R. L., Excited states of ^{127}I populated in decay of ^{127}Te and ^{127m}Te, 19: 41835
AUERBACH, Elliot H., Elastic scattering of 10.5- and 14.5-Mev polarized protons and optical model potential, 19: 41682
AUPETIT, A., Resistance to fire of lead-lined casks, 19: 40813 (SC-RR-65-98, pp 107-13)
AVERY, R., Physics aspects of the plutonium experiment in EBWR, 19: 42078 (ANL-7019)
AVVAKUMOV, E. G., Separation coefficients for radioactive fission elements in the directional process of sodium nitrate crystallization, 19: 40683
AWWAL, M. A., Extraction of uranyl salts by TTA in CCl_4, 19: 40682
AXEL, P., Neutron spectra from Bi produced by monoenergetic γ rays, 19: 41834
AZHGIREI, L., Double pp scattering at 667 Mev, 19: 41666 (JINR-P-2233)
AZOVSKII, Yu. S., Motion of plasma bunches in a field-free space, 19: 41856 (NP-15205)

B

BAARLI, J., Danger caused by radiation in the beams and beam zones of the synchrocyclotron, 19: 41171 (N64-33402)
BABAEVA, E. P., Systems of fluorides of sodium, potassium, and scandium, 19: 40512
BABELAY, E. F., Joint National Institutes of Health-Atomic Energy Commission zonal centrifugation project. I., 19: 40654 (ORNL-3613)
BABERG, W., MZFR steam generator, 19: 42173
BABICHENKO, S. I., Spectrometric characteristics of LSU-5k apparatus, 19: 40875 (NP-15254)
BABIKOV, V. V., Concerning the calculation of the parameters of scattering by a tensor potential, 19: 41491
BABU, P., Note on a conjecture by J. J. De Swart, 19: 41381
BACCAREDDA, M., Structural modifications in irradiated 1,4 trans-polybutadiene, 19: 40561
BACHELIER, Daniel, Angular correlation in (p,pd) reaction on C-12, 19: 41703
BACON, T. C., Anti-isobar production in $\bar{p}n$ interactions, 19: 41438
BACON, T. C., ρ and ω production in π^+d interactions at 1.7 Bev/c, 19: 41528
BADALYAN, A. M., The cross sections for the processes $e^\pm + e^- \rightarrow e^\pm + \mu^- + \nu_e + \nu_\mu$, 19: 41493
BAGROV, V. G., Indicatrix of the radiation emitted by a charge in an external field according to classical theory, 19: 41393
BAHADORI, Mohdi Nejed, Laminar duct flow of a partially ionized gas, 19: 40749
BAILEY, A. D., Mass spectrometric measurements of positive ions at altitudes from 64 to 112 kilometers, 19: 41588
BAILEY, R. E., Dynamic reactivity effect—a further development, 19: 42061
BAISOGOLOV, G. D., Hematopoiesis in dogs during subacute intoxication induced by Pu-239, 19: 40379
BAKER, Adolph, Relativistic high-energy approximation for elastic scattering of Dirac particles, 19: 41510
BAKHAREVA, Z. A., Accumulation and distribution of Sr-90 in swine after prolonged administration of radiostrontium, 19: 40328
BAKHAREVA, Z. A., Accumulation of Sr-90 in cattle during the embryonal and postembryonal periods of development, 19: 40330
BALAMATOV, N. N., Automatic betatron γ beam intensity optimization, 19: 41199
BALARIN, M., Radiation saturation and defect structure in solids, 19: 41102
BALASHKO, Yu. G., Analysis of proton-tritium elastic scattering above the $T(p,n)^3He$ threshold, 19: 41479
BALAZS, L. A. P., Reciprocal bootstrap possibilities for baryons, 19: 41422

BALAZS, Louis A. P., Low-energy equivalent-potential approach for strong interactions. II., 19: 41451
BALD, A., MZFR—the steam power installation, 19: 42169
BALKLAV, A., Reduction by means of finite pass band radiointerferometer, 19: 41301
BALL, R. E., Pumps for nuclear service, 19: 42026
BALLARD, R. E., Transfer of triplet state energy from acetophenone to rare earth ions, 19: 40504
BALLOT, J.-Louis, Analytical expressions of deuteron form factors in induced decays, 19: 41346
BALODIS, M. K., Spectrum of internal-conversion electrons produced upon capture of thermal neutrons by indium, 19: 41808
BALTAY, C., Annihilation of antiprotons in hydrogen at rest. III., 19: 41325 (CU-1932-245)
BANDAMALIEVA, E., Recombination processes in CdS during excitations by α particles, 19: 40565
BANDER, Myron, Absorptive corrections and form factors in the peripheral model, 19: 41400
BANDYOPADHYAY, P., Neutrino theory of photons and its implication in electromagnetic interaction, 19: 41387
BANKS, D. C., Investigation of manufacture of aggregate and riprap by nuclear means, 19: 40709 (PNE-5003)
BANTYSH, A. N., Certain regularities in isotopic exchange equilibrium, 19: 40505
BARAKAT, M. F., The interaction of ^{14}C recoil atoms in binary mixtures, 19: 40627
BARAN, V., General acidobasicity. III. Explanation of the author's conception, 19: 40466 (UJV-1209/65)
BARCELO, Jose R., Isotopic effect on the infrared spectrum and molecular structure of trimethyl borate ester, 19: 40470
BARCH, J., Material buckling and intracellular thermal neutron distributions, 19: 42049 (MIT-2344-3, pp 155-64)
BAREISS, Erwin, Spectral representation and criticality problem of a two-region cell transport operator, 19: 42035 (ANL-6590)
BARISH, J., Nucleon–meson cascade initiated by 200-Bev protons, 19: 41955 (ORNL-TM-1121)
BARIT, I. Ya., Analysis of proton-tritium elastic scattering above the $T(p,n)^3He$ threshold, 19: 41479
BARKER, P. H., The ranges of nitrogen ions in nickel and silver, 19: 41269
BARKER, Robert F., Regulatory packaging standards, 19: 40811 (SC-RR-65-98, pp 45–54)
BARLOW, Anthony, Determination of vinyl acetate in ethylene vinyl acetate copolymers, 19: 40556
BARNAVELI, T. T., Properties of component penetrating atmospheric showers, 19: 41297
BARNEOUD, Daniel, Electric octupolar transition of 71.2-kev in decay of Hf-171, 19: 41701
BARNES, K. J., Relativistic merging of spin and isotopic spin, 19: 41398
BARNES, V. E., Existence and properties of a non-strange meson of mass 1500 Mev/c^2, 19: 41459
BARNETT, C. F., An unconventional ultra-high vacuum facility, 19: 40772 (ORNL-P-1465)
BARRETT, Lida K., Mathematical models of diffusion in grain boundaries, 19: 41970 (ORNL-TM-1224)
BARRETT, P. H., Moessbauer scattering: The gyromagnetic moments of first 2^+ states in ^{182}W and ^{186}W and ^{186}Os and ^{188}Os, 19: 41791
BARRINGER, H. P., Joint National Institutes of Health-Atomic Energy Commission zonal centrifugation project. I., 19: 40654 (ORNL-3613)
BARRY, R. F., Criticality calculations for uniform water-moderated lattices, 19: 42054
BARTELL, L. S., Stimulated Compton scattering of electrons by laser beam, 19: 41328 (IS-1187)
BARTHOLOMEW, G. A., Parity assignments in ^{200}Hg from linear polarization correlation of thermal neutron capture γ rays, 19: 41846
BARTLETT, A. A., A new double focusing beta spectrometer. II., 19: 40904
BARTLIT, J. R., Automatic liquid nitrogen distribution system for twenty-five cold traps, 19: 41165 (LA-DC-7147)
BARTON, G. B., Solidification of high-level wastes. IV., 19: 42192 (BNWL-80)
BARTON, J. P., Radiographic examination using cold neutrons, 19: 40722
BARTON, M. V., Shock spectrum measurements, Project Gnome, 19: 40713 (VUF-2401)
BARUT, A. O., Dynamics of broken SU symmetry for the oscillator, 19: 41554
BAS, E. B., Some considerations on the physics and techniques of free electrons and ions, 19: 41142
BASHKIN, S., Interference of fine-structure levels in hydrogen, 19: 41263
BASIN, Ya. N., Modernization of radioactivity logging apparatus, 19: 40794 (AEC-tr-6577)

BASKAKOV, S. I., Investigation of plasma by means of relativistic electron beam, 19: 41920
BASS, F. G., Interaction of charged particles with a piezodielectric crystal, 19: 41990
BASSANI, G., (p,t) Ground-state L = 0 transitions in the even isotopes of Sn and Cd at 40 Mev, N = 62 to 74, 19: 41689
BASSI, A., Structure and recrystallization of cold-rolled and annealed Zircaloy-2, 19: 41034
BASU, D. K., Sulfur-35: its radiochemical estimation in sea water, 19: 40431
BATE, L. C., Separation of traces of metals from uranium by chromatography on cellulose column, 19: 40687
BATSANOVA, L. R., Solubility of LaF_3 in $Be(NO_3)_2$ solutions, 19: 40870
BATYEV, E. G., Role of the Coulombic interactions between electrons in a superconductor, 19: 41627
BAUSCHMANN, Walter, Method of manufacture of UO_2 having a high density, 19: 40996
BAYBARZ, R. D., Dissociation constants of transplutonium element chelates, 19: 40676
BAYMAN, B. F., Excitation of isobaric analog states in medium-weight nuclei by (d,p) reaction at 28 Mev, 19: 41772
BEACH, L. A., Angular distribution of the d-d reaction products, 19: 41832
BEARD, E. L., The sulfides of Sr, Ca, and Mg in infrared stimulated luminescence dosimetry, 19: 40879 (UCRL-12371)
BEARDMORE, P., Deformation and fracture of tungsten single crystals, 19: 41046
BEARDSLEY, D. A., Substoichiometric determination of traces of gold by neutron-activation analysis, 19: 40437
BECHTEL, Richard, Prog. rpt. on inverter applications, 6/63–5/64, 19: 40845 (N64-33676)
BECIRSPAHIC, S., Heat transfer of reactor fuel element model with polyzonal-spiral finning, 19: 40748
BECK, E. J., Ground-motion effects on the contents of buried structures, 19: 40758 (AD-426249)
BECK, F. H., Prog. rpt. on stress-corrosion cracking in Fe–Ni–Cr system, 3/17–6/16/65, 19: 40967 (COO-1319-27)
BECK, G. P., Feedback effects during short interval-series pulsing, 19: 42188
BECKER, Francois, Analytical expressions of deuteron form factors in induced decays, 19: 41346
BECKER, W., Set-up for registering data via a single cable utilizing passive components, 19: 40714 (EUR-2421.d)
BECKER, W. W., Studies of a repetitive liquid metal slug MHD generator, 19: 41314 (BNL-9329)
BECKER, Warren E., Isotopic exchange reactions of difluoramine with deuterium oxide and trifluoroacetic acid, 19: 40537
BEDNYAKOV, A. A., Multiple scattering of 75- to 200-kev protons on solids, 19: 41273
BEERY, Jerome G., Elastic scattering of 10.5- and 14.5-Mev polarized protons and optical model potential, 19: 41682
BEGUIN, Claude P., Spectroscopic investigations of some halide reactions in plasma-generating devices, 19: 41287
BEHRENS, E., Physical design of the MZFR, 19: 42161
BEHRENS, Ernst, Zero-energy measurements on core of the multi-purpose research reactor, 19: 42186
BEILINA, G. M., Measuring ionization function of metal atoms by electron impact, 19: 41276
BEISER, A., Methods of promoting the removal of free electrons from an ionized and dissociated atmosphere, 19: 41569 (AD-426145)
BELKIND, A. I., Concerning two mechanisms of photostimulated electron emission from ionic crystals, 19: 41979
BELKIND, A. I., Effect of radiation on photostimulated emission from alkali halide crystals, 19: 41980
BEL'KOVA, M. M., Rare earth perchlorates, 19: 40509
BELL, George I., Production of heavy nuclei in Par and Barbel devices, 19: 41765
BELL, J. S., On the problem of hidden variables in quantum mechanics, 19: 41531 (SLAC-PUB-44)
BELL, R. J., Stopping powers and straggling in neon, argon, and krypton, 19: 41268
BELL, Robert, Improvements in or relating to concrete pressure vessels, 19: 40728
BELL, Walter Lee, Analysis of dislocation loops in quenched FCC metals, 19: 41026 (UCRL-16024)
BELLINGER, Ronald, Improvements in or relating to grabs, 19: 42027
BELOV, S. V., Determination of the number of fissions in natural uranium mixture irradiated by neutrons, 19: 40640
BELYAEV, Yu. A., Effectiveness of DTPA after intratracheal administration of Pu to rats, 19: 40346
BELYAEV, Yu. A., Oral administration of some complexing agents to remove

Pu from rats, 19: 40345
BELYAKOV, V. A., Baryon resonances in π-p interactions at 7.5 Bev with strange-particle formation, 19: 41488
BELYAKOV, V. A., Meson resonances in π-p interactions at 7.5 Bev with strange-particle production, 19: 41489
BENESCH, R., Observation of the Faraday effect in a θ-pinch plasma using He–Ne gas laser, 19: 41947
BENFORADO, Joseph M., Response to norepinephrine of isolated rat myocardium following ^{131}I-induced hypothyroidism, 19: 40368
BENJAMIN, B. M., Recombination of hydrogen and oxygen in the presence of water vapor under the influence of radiation, 19: 40549 (COO-1032-1)
BENNETT, C. L., Diffusion and transport calculations for NPR tube-in-tube fuel geometry, 19: 42128 (BNWL-95, pp 18-23)
BEONE, G., Dissolution experiments of aluminum and SAP cladding material in a laboratory recirculation dissolver, 19: 40655 (RT/CHI(65)-1)
BERANOVA, H., Studies on the effect of some polyhydric alcohols on ion-exchange and separation of rare earths with the aid of α-hydroxyisobutyric acid, 19: 40662
BERDONOSOV, S. S., Bromination of microquantities of Pa-233 in carriers, 19: 40501
BERGER, A. R., Multichannel system for analysis of pulses from ionization calorimeters, 19: 40854
BERGERSEN, Birger, Positron annihilation rate in an electron gas, 19: 41160
BERGGREN, Tore, Overlap integrals and single-particle wave functions in direct interaction theories, 19: 41728
BERGIA, S., CP violation by derivative terms in the leptonic current, 19: 41378
BERGSNOV-HANSEN, B., Prog. rpt. on sorption of gases on metal surfaces, 2/15–5/15/65, 19: 40463 (SRIA-425-5)
BERINDE, A., Reaction ^{26}Mg(p,p'γ) mechanism at low energies, 19: 41693
BERLEY, David, Strange-particle production in π^+-p collisions, 19: 41418
BERLIN, I. K., Production and application of niobium carbide parts, 19: 40988
BERMAN, S. M., Systematics of angular and polarization distributions in three-body decays, 19: 41409
BERNAS, Monique, Angular correlation in (p,pd) reaction on C-12, 19: 41703
BERNSTEIN, J., Possible C,T noninvariance in the electromagnetic interaction, 19: 41452
BERNSTEIN, S., Testing of 10-ton capacity UF_6 shipping containers, 19: 40824 (SC-RR-65-98, pp 580–608)
BERSIN, Richard L., Radiometric sensing of atomic hydrogen in trace quantities, 19: 40433
BERTERO, M., Muon capture by the virtual pion exchanged by proton pairs in a nucleus, 19: 41753
BERTERO, M., Numerical analytic continuation of proton electromagnetic form factors, 19: 41388
BERUBE, N., Material buckling and intracellular thermal neutron distributions, 19: 42049 (MIT-2344-3, pp 155-64)
BERULAVA, B. G., Relaxation processes in paramagnetic resonance of U^{3+} and Tb^{3+} in CaF_2, 19: 42000
BESLIU, Calin, Elastic n-p interaction at 3 to 10 Bev, 19: 41347
BESLIU, Tatiana, Elastic n-p interaction at 3 to 10 Bev, 19: 41347
BESSONOV, A. I., Unit for gas-phase radiation-induced graft polymerization, 19: 40596
BETHKE, George W., Cyclotron resonance propulsion system, 19: 40764 (N65-27691)
BETTENHAEUSER, K., A new nuclear-medical multi-channel measuring device used for the diagnosis of one-sided deficiency of renal function in the isotope nephrogram, 19: 40913
BETTERIDGE, Walter, Process for making workable ruthenium and product thereof, 19: 40999
BETTINI, A., Spin and parity of 1320 Mev $\rho\pi$ resonance, 19: 41368
BEYSTER, J. R., Neutron-spectrum measurements in H_2O and D_2O, 19: 41646
BEYSTER, J. R., Prog. rpt. on integral neutron thermalization, 3/31/65, 19: 41640 (GA-6323)
BHARATHI, Venkatesan, Isocontours of magnetic shell parameters B and L, 19: 41590
BHOWMIK, B., π^+ Decay of lambda Li-7, 19: 41412
BIANCHINI, R., Pattern recognition, 19: 42211 (NYO-1480-19)
BIANCIFIORI, M. A., Bibliography on fouling research, 19: 40971 (RT/CHI(65)20)
BIBILASHVILI, M. F., Properties of component penetrating atmospheric showers, 19: 41297
BICKEL, W. S., Interference of fine-structure levels in hydrogen, 19: 41263
BIEHL, Arthur T., Low power nuclear reactors, 19: 42067
BILEN'KII, S. M., Double N-N scattering with a polarized beam and polarized target, 19: 41333 (JINR-P-2227)
BIRGE, Robert W., Experimental study of $K^+_{\mu 4}$ decay, 19: 41446
BIRNBAUM, H. K., Electron microscope study of the effect of oxygen ion irradiation on LiF, 19: 41256
BISI, V., $K_{\mu 3}$ branching ratio and μ^+ energy spectrum, 19: 41414
BISNOVATYI-KOGAN, G. S., Viscosity of partially ionized two-temperature plasma, 19: 41910
BJOERNHOLM, S., Observation of $[505]\frac{11}{2}^-$ Nilsson state as isomer in Dy-159, 19: 41736
BLACK, Walter Wayne, Directional correlations of γ rays of ^{140}La and ^{140}Ce, 19: 41822
BLACK, Wayne Edward, Biosynthesis of radioactive ubiquinone-50, 19: 40641
BLAISE, Alain, Irradiation of Cu–Co alloys, 19: 41095 (ORNL-tr-667)
BLAISE, Jean, Recent progress in arc and Spark spectra of Tm, 19: 41253
BLAKE, C. A. Jr., Chemical applications of nuclear explosions (CANE), 19: 40706 (ORNL-TM-1191)
BLAKE, K. R., The measurement of surface contamination of high-purity beryllium samples, 19: 40453
BLANN, Marshall, Shell structure and angular momentum effects in decay of compound nuclei of nickel, 19: 41741
BLANTON, Roy W. Jr., Analysis of radiators for space nuclear power systems, 19: 40731 (AD-609969)
BLASIUS, E., Chelating resins. VI., 19: 40674
BLAZEK, D. R., Computer aided circuit reliability analysis, 19: 40848 (SC-R-935)
BLECH, Joab Jacob, Similarity rules in magnetohydrodynamics based on multi-fluid theory, 19: 41156
BLESER, E., Analysis of high energy p-p scattering experiment, 19: 41322 (BNL-9231)
BLIGNAUT, E., Beam current integrator for pulsed positive ion accelerators, 19: 41183
BLOCHER, John M. Jr., Characterization of pyrolytic-carbon fuel-particle coatings prepared with acetylene, 19: 41004 (BMI-1735)
BLOCK, F. E., Tungsten- and molybdenum-coated nonmetallic powder, 19: 40986
BLOCK, Seymour, Index to hazards control quarterly reports nos. 1 through 19, 19: 40833 (UCRL-14116)
BLOKHINTSEV, D. I., On backward scattering of high-energy particles, 19: 41332 (JINR-P-2220)
BLUM, Norman A., Moessbauer techniques using high field water-cooled solenoids, 19: 41818
BLUMBERG, Ben Jr., Nuclear dry cargo ships vs. conventional, 19: 42132 (GE-TM-65-3-6)
BOBASHOV, S. V., Excitation of the H_β line of hydrogen and of some mercury lines by collision of protons and H_2^+ ions with mercury atoms, 19: 41260
BOCK, R., Level structure of ^{53}Cr and ^{55}Cr, 19: 41726
BODDY, Keith, Improvements relating to measuring apparatus, 19: 40454
BODINE, J. E., Equipment for fabrication and encapsulation of irradiated UO_2 pellets, 19: 40715 (NAA-SR-Memo-7438)
BOEBEL, G., Behavior of type-II superconducting cylinders of small radius near the lower critical field, 19: 41612
BOEGLY, W. J. Jr., Project Salt Vault, 19: 42195 (ORNL-P-1479)
BOEMMEL, H. E., Acoustic excitation of nuclear spin resonance in single-crystal Ta, 19: 41792
BOGACHEV, G. A., Relaxation of rare-earth ions, 19: 41995
BOGACHEV, G. A., Spin-lattice relaxation of rare earth ions, 19: 41982
BOGDANOV, G. F., Obtaining a hot thermonuclear plasma by injection of fast particles into a magnetic trap, 19: 41852 (IAE-676)
BOGDANOV, R. V., Separation of radiophosphine from mixed KCl–$CaCl_2$ crystals irradiated with high-energy protons, 19: 40606
BOGDANOVSKAYA, R. L., Solubility in $Ce(NO_3)_3$–$LiNO_3$–H_2O, 19: 40519
BOGUSH, A. A., Scattering of antineutrinos by electrons, 19: 41481
BOHATIEL, Teodor, High-frequency Ar torch at pressures below 1 atm, 19: 41875
BOHM, D., Conformal-group symmetry of elementary particles, 19: 41392
BOISVERT, Gregory L., Irradiation of Cu–Co alloys, 19: 41095 (ORNL-tr-667)
BOKISH, K. P., Ultrasonic bond testing of irradiated fuel elements, 19: 41089 (HW-56028)
BOLLIET, Roger, Device for determining rate of increase of neutron flux in a reactor, 19: 42064
BOLSUN, A. I., Scattering of antineutrinos by electrons, 19: 41481
BONCH-OSMOLOVSKAYA, N. A., Three-quasiparticle state in ^{165}Er, 19: 41667 (JINR-P-2239)
BOND, A. F., Summary report on electron bombardment ion engine development, 19: 40760 (N64-25008)
BOND, John W. Jr., Atomic theory of gas dynamics, 19: 41161
BONDARENKO, V. A., Spectrum of internal-conversion electrons produced

upon capture of thermal neutrons by indium, 19: 41808
BOON, G., Precision (0.1°C) vacuum cryostat and furnace for Moessbauer experiments, 19: 40858
BORBELY, Imre, Angular distribution in $^{12}C(d,p)^{13}C$ reaction, 19: 41721
BORDONALI, C., Bibliography on fouling research, 19: 40971 (RT/CHI(65)20)
BORGGREEN, J., Observation of $[505]\frac{11}{2}^{-}$ Nilsson state as isomer in Dy-159, 19: 41736
BORISOV, V. P., Change of isotopic ratio in a mixture of U fission products after absorption from the intestinal tract, 19: 40322
BORISOV, V. P., Comparison of the distribution of Mo-99 and P-32 in animals, 19: 40319
BORISOV, V. P., Evaluation of some drugs for emergency use in case of injury by radioactive substances, 19: 40339
BOROM, Marcus P., Physical chemistry of glass-metal interfaces, 19: 40464 (UCRL-11816(Rev.))
BORREANI, G., $K_{\mu 3}$ branching ratio and μ^+ energy spectrum, 19: 41414
BOSE, Subir, Dynamical calculation of ρ^0-ω transition mass, 19: 41380
BOSHAN, P., Energy gap in nuclear matter in the case of soft-core potentials, 19: 41662 (JINR-P-2176)
BOUCHER, R. J., Transient radiation environment of nuclear weapon detonations, 19: 40938
BOURNE, A. J., Reliability considerations for automatic protective systems, 19: 42022
BOURRASSE, André, Improvements in or relating to metal oxide powder sintering, 19: 40995
BOUSSARD, Daniel, Results obtained with a new type of self-focused linear accelerator for heavy ions, 19: 41177
BOUTILLON, Mireille, The utilization of a magnetic induction field in the exposure measurements of x and γ rays, 19: 40838
BOWEN, Theodore, Cosmic-ray search for fractionally charged particles, 19: 41311
BOWERSOX, D. F., Solubility of selected elements in liquid plutonium. V., 19: 40950 (LA-3338)
BOWES, William A., Reconnaissance for U in the Colimapu Formation of central Chile, 19: 40798 (RME-4571(Rev.))
BOWMAN, H. R., Internal conversion electrons from primary fission fragments, 19: 41680 (UCRL-16184)
BOWMAN, M. G., Phase relationships of the high carbon portion of the lanthanide dicarbides, 19: 41014 (LA-DC-6819)
BOYD, H. W., Energy levels in Xe-132, 19: 41745
BOYD, H. W., Low-energy transitions in I-132 decay, 19: 47143
BOYD, T. J. Jr., Phermex applications to studies of detonation waves and shock waves, 19: 41118 (LA-DC-6996)
BOYLE, Thomas L., Airborne radiometric surveying—office and field techniques, 19: 40784 (RME-129(Rev.))
BOZZO, S. R., Data processing method for a multidetector positron scanner, 19: 40390 (BNL-9384)
BRADSHAW, A. L., Calorimetric measurement of absorbed dose with 15 Mev electrons, 19: 40910
BRADSHAW, R. L., Accelerated deformation of rock salt at elevated temperature, 19: 42198
BRADSHAW, R. L., Project Salt Vault, 19: 42195 (ORNL-P-1479)
BRAND, G. E., Pyrochemical reprocessing of uranium carbide, 19: 40652 (NAA-SR-11340)
BRAND, G. E., Pyrochemical reprocessing of UO_2 by Airox, 19: 40653 (NAA-SR-11389)
BRANDL, J., MZFR—cost and utilization, 19: 42159
BRANDT, A. A., Investigation of plasma frequency multiplier, 19: 40860
BRANDT, H. L., Development in continuous ion exchange contactors, 19: 40650 (HW-77805)
BRANNEN, Eric, University of Western Ontario race-track microtron, 19: 41175
BRANSDEN, B. H., Pion-nucleon scattering amplitudes in the range 300 to 700 Mev, 19: 41442
BRAUER, G., Crystal chemistry of rare earth oxides, 19: 40533
BRAUER, G., Synthesis and properties of red Ta_3N_5, 19: 40472
BRAUN, W. G., Technique for measuring the absorption coefficient of a plasma, 19: 41898
BRAUTTI, G., High-intensity, partially separated, beam of antiprotons and K mesons, 19: 41184
BRAYER, R. C., Prog. rpt. on burnable poison additions to UO_2, 1–3/65, 19: 41006 (CEND-3107-238)
BRAZILEVSKAYA, G. A., X-ray photons in cosmic showers in stratosphere, 19: 41299
BREGER, A. Kh., Investigation of γ propagation in substances by similarity theory, 19: 41958
BRETSCHER, Egon, Temperature dependence of dielectric polarization in some benzene derivatives, 19: 40468 (SC-T-65-721)
BREWER, George R., Physical electronic phenomena in ion propulsion engines, 19: 40766

BREY, Wallace S. Jr., Physical methods for determining molecular geometry, 19: 40530
BREZINA, František, Chemistry of the rare earth metals. VIII., 19: 40491
BRICARD, Jean, Mobility spectrum of small radioactive ions of the air, 19: 40787
BRIGGS, G. R., 5-Mc magnetic tunnel-semiconductor logic for nuclear radiation environments, 19: 40939
BRIL, K. J., Mass extraction and separation, 19: 40690
BRISCOE, G. B., Substoichiometric determination of traces of gold by neutron-activation analysis, 19: 40437
BRISSAUD, Ivan, Angular correlation in (p,pd) reaction on C-12, 19: 41703
BROADHEAD, K. G., 14-Mev-neutron production of isomeric states for several rare-earth elements, 19: 41781
BROCKLEHURST, James Ernest, Method of testing graphite, 19: 41109
BROEK, H. W., Inelastic α-particle scattering by Mn-55 and Co-59, 19: 41760
BROMAN, L., New bound levels in Sc-43 from radiative proton capture in Ca-42, 19: 41738
BROMIDGE, Noel Arthur Clifford, Joints between tubular members, 19: 40705
BROMLEY, D. A., Collective representation of lower lying states in ^{21}Ne, ^{21}Na, and ^{23}Na, 19: 41757
BRONNER, Gottfried, Zero-energy measurements on core of the multi-purpose research reactor, 19: 42186
BROOK, A. J., Approximate calculative assessment made relating to wall temperatures and behaviour of cask in fire tests, 19: 40832 (SC-RR-65-98, pp 732–5)
BROOKS, H. C., Ultrasonic inspection of Nimrod power plant alternator rotors, 19: 41201
BROUT, Robert, Review of quasiparticle and Josephson tunneling in superconductors, 19: 41607 (LA-3342)
BROWER, John H., Ecological changes in insect community of a pitch pine-oak forest subjected to chronic γ irradiation, 19: 40307 (BNL-9253)
BROWN, A. W., Ultrasonic inspection of Nimrod power plant alternator rotors, 19: 41201
BROWN, B. L., Remote radiation monitoring at the Nevada Test Site, 19: 40876 (NVO-162-5(Rev.))
BROWN, K. B., Chemical applications of nuclear explosions (CANE), 19: 40706 (ORNL-TM-1191)
BROWN, Laurie M., Meson decays and the sigma hypothesis, 19: 41518
BROWNING, Melvin F., Characterization of pyrolytic-carbon fuel-particle coatings prepared with acetylene, 19: 41004 (BMI-1735)
BROZIO, B., Chelating resins. VI., 19: 40674
BRUN, E. A., Study of plasma jets, 19: 41936
BRUNER, F., Gas chromatographic separation of deuterated methanes, 19: 40672
BRUNNER, W., Absorption and scattering of quantum mechanical coherent beams. I., 19: 41247
BRUNNER, W., Absorption and scattering of quantum beams. II., 19: 41248
BUBELEV, E. G., Analysis of multiple meson production, 19: 41708
BUBELEV, E. G., Analysis of high-energy particle fluxes by Lobachevskii velocity diagrams, 19: 41709
BUBEN, N. Ya., Radicals formed in radiolysis of certain benzene derivatives, 19: 40607
BUCHANAN, C. D., Elastic electron-deuteron scattering and possible meson-exchange effects, 19: 41453
BUDAK, B. M., A collection of problems on mathematical physics, 19: 41153
BUDESINSKY, B., Certain new Asenazo III analogs and their analytical properties, 19: 40426
BUDYANSKII, G. M., Multiple scattering of a narrow beam of fast neutrons, 19: 41650
BUELTEMANN, H.-J., High-temperature high-vacuum valves with gold-wire sealing, 19: 40775
BUFFONI, G., Control poison as an eigenvalue of the diffusion equations, 19: 42052
BUKHALOVA, G. A., Systems of fluorides of sodium, potassium, and scandium, 19: 40512
BUKHTYAROV, V. V., System $SmCl_3$–NaCl–KCl, 19: 40517
BULDAKOV, L. A., Accumulation of Sr in the skeleton of calves, 19: 40329
BULDAKOV, L. A., Biological effects of Sr-90, Co-137, and Pm-147 after chronic oral administration of low doses, 19: 40335
BULDAKOV, L. A., Distribution of Y-91, Zr-95, and Nb-95 in rats after inhalation, 19: 40314
BULDAKOV, L. A., Effect of food Ca on metabolism of Sr-90 in fodder-milk link in cows, 19: 40341
BULDAKOV, L. A., Metabolism and biological effects of Cs-137 in sheep, 19: 40334
BULDAKOV, L. A., Penetration of Sr-90 through the placental barrier of

sheep, 19: 40331
BULDAKOV, L. A., Strontium-90 content in rats after chronic oral administration, 19: 40323
BULLOT, Jacques, Thermoluminescence of molecular solids irradiated by γ rays at 77°K. Evidence of T → S and S → S emissions, 19: 40563
BULLOUGH, R., Formation of interstitial loops in bcc metals, 19: 41056
BUNCH, W. L., Boron-11 neutron flux monitors—interim report, 19: 40867 (BNWL-64)
BUNKE, A. L., Pumps for nuclear service, 19: 42026
BURDG, C. E., Prog. rpt. on in-pile thermal conductance testing, 1–3/65, 19: 40732 (CEND-3336-237)
BURGER, C. L., Joint National Institutes of Health-Atomic Energy Commission zonal centrifugation project. I., 19: 40654 (ORNL-3613)
BURHOP, E. H. S., Angular correlations between fast Σ hyperons and fast protons, 19: 41494
BUROV, N. I., Accumulation of Sr in the skeleton of calves, 19: 40329
BUROV, N. I., Effect of food Ca on metabolism of Sr-90 in fodder-milk link in cows, 19: 40341
BUROV, N. I., Penetration of Sr-90 through the placental barrier of sheep, 19: 40331
BUROVOI, I. A., Determination of mixing coefficient in a fluidized-bed reactor, 19: 42011
BURQ, Jean-Pierre, Photoproduction of π^+ and π^- mesons on deuterium at low energy, 19: 41344
BURRELL, Martin O., Calculation of proton penetration and dose rates, 19: 41951 (N64-30510)
BURRIS, L. Jr., Fuel management and inventory in the EBR-II fuel cycle, 19: 42075 (ANL-6735)
BURTON, G. Jr., Development of a process for manufacturing ZPR-III U–Pu–Mo test fuel elements, 19: 40978 (ANL-6955)
BURYKINA, L. N., Distribution of Sr-90 in the skeleton of dogs after chronic exposure, 19: 40324
BURYKINA, L. N., Passage of Sr-90 from mother to offspring in dogs under conditions of chronic uptake, 19: 40327
BUSH, Spencer H., Irradiation effects in cladding and structural materials, 19: 41107
BUSSARD, R. W., Fundamentals of nuclear flight, 19: 42147
BUTEMENT, F. D. S., Radioisotopes I-117, -118, and -119, and Te-117, 19: 41717
BUTERA, Regina, Membranes, material transfer and enzymes, 19: 42199 (BNL-8397)
BUTTA, E., Structural modifications in irradiated 1,4 trans-polybutadiene, 19: 40561
BUTTERWORTH, J., Spin echoes in solids, 19: 41988
BUTTERWORTH, R. R., SRP reactor on-line computer, 19: 42129 (DPSPU-65-30-27)
BUTZOW, James J., Interactions of metal ions with polynucleotides and related compounds. III., 19: 40474
BYAKHOVA, N. I., Enthalpy of the γ-UO_3 reaction with HF and enthalpy of formation of γ-UO_3, 19: 40521
BYK, D. S., Crystalline structure of certain ternary compounds in Nb–Co–Si system, 19: 41069
BYRNE, N., Breakdown of unitary octet symmetry in a nonlinear spinor model of elementary-particle theory, 19: 41395
BYRNE, N., Meson states in a nonlinear spinor model of elementary-particle theory with spontaneous symmetry breakdown, 19: 41396

C

CAIANIELLO, E. R., Nonanalytical properties of propagators. The $g\phi^4$ theory, 19: 41549
CAILLAT, Roger, Fuel element for a nuclear reactor, 19: 42074
CAILLAT, Roger, Improvements in or relating to metal oxide powder sintering, 19: 40995
CAIN, Joseph C., An evaluation of the main geomagnetic field, 1940–1962, 19: 41586
CAIN, V. R., Propagation of neutron waves through heterogeneous multiplying and nonmultiplying media, 19: 41643 (ORNL-TM-1184)
CALLCOTT, T. A., Economical liquid He cryostat and other cryogenic apparatus, 19: 41626
CALLIHAN, Dixon, Safety in handling fissionable materials, 19: 40840
CAMIN, L., Determination of iodides in the preparations of ^{131}I-Rose Bengal ^{131}I-Triolein, ^{131}I-Globulin, and ^{131}I-Iodoalbumin and preliminary separation by thin-layer chromatography, 19: 40656 (CEA-tr-X-609)
CAMONA, G., Structure and recrystallization of cold-rolled and annealed Zircaloy-2, 19: 41034
CAMPBELL, Darrell A., Tissue tolerance and systemic toxicity of 5-fluorouracil, external radiation, and drug-radiation combination in rabbits, 19: 40394
CAMPBELL, R. W., Reactivity worths of several fast reactor control materials, 19: 42050 (NAA-SR-11368)
CAMPBELL, T. T., Freeze-dry technique for making ultra-fine metal powder, 19: 40987
CAMPBELL, T. T., Tungsten- and molybdenum-coated nonmetallic powder, 19: 40986
CAMPE, K. M., Dynamic reactivity effect—a further development, 19: 42061
CAMPOLATTARO, A., Nonanalytical properties of propagators. The $g\phi^4$ theory, 19: 41549
CAMUS, Pierre, Recent progress in arc and Spark spectra of Tm, 19: 41253
CANNING, R. E., Joint National Institutes of Health-Atomic Energy Commission zonal centrifugation project. I., 19: 40654 (ORNL-3613)
CAO CHI, Electromagnetic mass splitting in symmetry scheme SU(6), 19: 41329 (JINR-P-2208)
CAPPS, Richard H., B-meson decay, ω-φ mixing, and SU(6), 19: 41458
CAPPS, Richard H., Self-consistent particle sets in a baryon bootstrap model, 19: 41432
CAPRASSE, H., Inconsistency in two one-particle-exchange models for π-N scattering, 19: 41375
CARACOCHE, M. C., Cross-section ratios for isomeric pair $^{44m/44}$Sc produced by ^{45}Sc(d,t)^{44}Sc reaction, 19: 41714
CARACOCHE, M. C., Cross-section ratios for isomeric pair $^{58m/58}$Co produced by ^{59}Co(d,t) reaction, 19: 41715
CARDER, Dean S., Travel times from central Pacific nuclear explosions and inferred mantle structure, 19: 40779
CARERI, G., Experiments on the creation of charged quantized vortex rings in liquid helium at 1°K, 19: 41621
CARLSON, Alan, Study of Xe poisoning in a nuclear reactor, 19: 42010
CARLSON, C. E., Utilization of yttrium in gettering oxygen and nitrogen in Nb-base materials, 19: 40953 (PWAC-441)
CARLSON, E. R., Intermediate state reorientation in nuclear alignment of ^{139}Ce in Ce–Mg nitrate, 19: 41840
CARLSON, Walter Berndt, Improvements in or relating to nuclear reactors, 19: 40993
CARO, Paul, Displacement of halogens from rare earths and Y by means of Mg, 19: 40955
CAROLI, C., Electronic excitations in superconductors free from second species. II., 19: 41624
CAROLI, C., Range of perturbation of the order parameter in homogeneous and zero-field superconductors, 19: 41622
CARPENTER, S. G., Reactivity worths of several fast reactor control materials, 19: 42050 (NAA-SR-11368)
CARPENTER, Steve Haycock, Dislocation interstitial interactions in single-crystal W and Ta, 19: 42002
CARRIERE, M., Optimum processing of spectrometric information by numerical adapted filters, 19: 40906
CARRINGTON, A., Isotope effects in electron spin resonance: the negative ion of cyclo-octatetraene-1-d, 19: 40541
CARROLL, Dennis B., Electron microscope study of the effect of oxygen ion irradiation on LiF, 19: 41256
CARTACCI, A. M., Difference in range-energy relation for positive and negative particles, 19: 41369
CARTER, J. C., $SU(6)_W$ photoproduction and meson-baryon scattering amplitudes, 19: 41462
CARTER, L. L., Prompt neutron decay using Monte Carlo methods of analysis, 19: 42039 (BNWL-95, pp 36–9)
CARTONI, G. P., Gas chromatographic separation of deuterated methanes, 19: 40672
CARVER, J. G., Prog. rpt. on Pu subcritical experiment, 4–6/65, 19: 42093 (GEAP-4912)
CARVER, Thomas R., Spin-exchange light modulation by atomic hydrogen, 19: 41262
CASTAGNOLI, Carlo, Loss of energy by ultra-relativistic muons. III., 19: 41345
CAUGHLAN, Georgeanne Robertson, Hydrogen and helium burning in stars, 19: 41242
CERENKOV, P. A., Cascade mechanism of the high-energy nuclear reactions. I., 19: 41811
CERNY, Joseph, Lithium-4 and the excited levels of He-4, 19: 41786
CERRE, P., Intervention-decontamination building, Centre d'Etudes Nucleaires de Fontenay-aux-Roses, 19: 40836
CERVASEK, Jiri, Effect of neutron radiation on certain mechanical and structural properties of austenitic chrome nickel steel, 19: 41093 (FTD-TT-65-125)
CHABASSIER, Roger, Device for operating a movable trolley, 19: 42189
CHACHATY, Claude, EPR study of PMR of free radicals in γ irradiation of nitromethane, 19: 40579
CHACON, E., Nuclear structure in the 2s-1d shell. I., 19: 41729
CHACON, E., Nuclear structure in the 2s-1d shell. II., 19: 41730
CHAFFIOTE, Pierre, Device for operating a movable trolley, 19: 42189
CHAMBERLAIN, G. E., Inelastic scattering of electrons by helium, 19: 41264

CHAND, T., π^+ Decay of lambda Li-7, 19: 41412
CHANDEBOIS, Rosine, Variations of the regenerating capacity of irradiated planaria (dugesia subtentaculata) as a function of the x-ray dose, 19: 40366
CHANDRA, P., Sensitivity of pyrimidines and purines towards neutron irradiation, 19: 40557
CHANG, Ho-ch'i, Measurements of eruptive phenomena on the solar limb, 19: 41234
CHANG, I-Dee, Singular-perturbation methods applied to magneto-gasdynamics and plasma problems, 19: 41114 (AD-617258)
CHANG, Tsung-hua, Structure of even parity states of ^{16}O. [Part] I., 19: 41816
CHAO, C. C., Study of CaCl type intermediate phases involving rare earth elements, 19: 41005 (CALT-221-11)
CHAPIRO, Adolphe, Rectification of apparent effect of an electric field on radiochemical polymerization of solid acrylonitrile, 19: 40582
CHAPMAN, R. H., Low-temperature H_2O-cooled and -moderated reactors for desalting, 19: 42097 (ORNL-TM-1152)
CHAPPELL, Willard R., Kinetic equations for systems of charged particles and photons, 19: 41940
CHARAKHCH'YAN, A. N., X-ray photons in cosmic showers in stratosphere, 19: 41299
CHARTIER, Germain, Low-voltage discharge at very high intensity initiated by laser pulse, 19: 41133
CHARYULU, Vorada P. T., Temperature-dependent neutron thermalization, 19: 41652
CHASE, L. F. Jr., Gamma rates and intensities; l-forbidden M1 transitions, 19: 41836
CHASE, L. F. Jr., Investigation of the T = ⅔ state at 16.97 Mev in ^9Be, 19: 41697
CHAUDRON, G., Prog. rpt. on mechanical properties of steels, final, 1965, 19: 40947 (EURAEC-1403)
CHAUSSY, Jacques, Transport properties of Nd nitride at low temperature, 19: 41973
CHEBOTARYOV, E. E., Combined treatment of acute radiation sickness (BK-8, vitamin B_{12}, butylic alcohol, bicillin-3), 19: 40387
CHEN, Francis F., Spectrum of low-β plasma turbulence, 19: 41895
CHEN, Ko-yun, Use of I-131 peanut oil in assessing lipid metabolism in coronary atherosclerosis, 19: 40393
CHEN, Pu-lun, Measuring critical characteristic curves of superconductors, 19: 41630
CHEN, Sheng-chun, Two-nucleon stripping reactions, 19: 41817
CHEN, Sheng-chung, Studies of structural factors in two-nucleon stripping and knock-on reactions, 19: 41819
CHENG, Goo-kuang, Measuring critical characteristic curves of superconductors, 19: 41630
CHERKESOV, A. I., New reagents for zirconium, 19: 40441
CHERNIKOV, V. A., Measuring of electron concentration in plasma, 19: 41924
CHERNOCK, W. P., Prog. rpt. on burnable poison additions to UO_2, 1–3/65, 19: 41006 (CEND-3107-238)
CHERNOROTOV, E. S., Technique of conversion of highly-basic anion-exchange resins (type AV-17 and AM) from the chloride to the hydroxyl form by the method of two-stage regeneration, 19: 40456 (IAE-713)
CHERRY, B. H., Analysis of fast reactor transients including meltdown, 19: 42100 (UNC-5092)
CHERSTVENKOVA, E. P., Thermal properties of binary sodium sulfates of certain cerium sub-group rare earths, 19: 40511
CHERTOPRUD, V. E., Model of cyclic solar activity, 19: 41215
CHERVINSKAYA, A. F., Effect of P-32 on higher nervous activity of dogs, 19: 40356 (FTD-TT-65-48, pp 469.70)
CHERY, R., Optimum processing of spectrometric information by numerical adapted filters, 19: 40906
CHIANG, Tai-wang, Reactions of hot tritium atoms with alcohols and with some of their binary hydrocarbon mixtures, 19: 40622
CHI-CHUANG, Yuo, Neutron resonances of ytterbium isotopes, 19: 41661 (JINR-P-2158)
CHIEN, Chien-hua, Use of I-131 peanut oil in assessing lipid metabolism in coronary atherosclerosis, 19: 40393
CHIKASHI, Iso, Selection rules imposed by the symmetrical quark model, 19: 41466
CHIKOVANI, G. E., A spark chamber with a big discharge gap, 19: 40886
CHIKOVANI, G. E., Multichannel analyzer of pulses for ionization calorimeter at capacity memory cells and the system of information output, 19: 40853
CHIKOVANI, G. E., Multichannel system for analysis of pulses from ionization calorimeters, 19: 40854
CHIKOVANI, G. E., Semi-automatic device for treatment of track photos in a cloud chamber, 19: 40888
CHIN, S. H., IBM 1620 reconstruction of bubble chamber interactions, 19: 40915

CHINOWSKY, W., K+p interactions at 2 Bev/c—elastic scattering and total cross sections, 19: 41436
CHIOTTI, P., Application of metal coatings on uranium, 19: 40949 (ISC-640)
CHIRIKOV, B. V., Trap with magnetic plugs for holding electrons, 19: 41858 (NP-15217)
CHKHEIDZE, I. I., Radicals formed in radiolysis of certain benzene derivatives, 19: 40607
CHLENOV, M. A., Radiochemistry of carbons. III. Effects of y radiation on the aqueous solutions of α-methyl-D-glucoside, 19: 40605
CHOPRA, D. V., π^+ Decay of lambda Li-7, 19: 41412
CHORNII, Z. P., Roentgenoluminescence and thermoluminescence of Tl-activated NaI crystal phosphors, 19: 40568
CHOW, Shih-hsun, B.C.S. superconducting ground state, 19: 41629
CHOW, Y. M., Moessbauer scattering: The gyromagnetic moments of first 2^+ states in ^{182}W and ^{186}W and ^{188}Os and ^{188}Os, 19: 41791
CHRIEN, R. E., Search for J-dependent neutron strength functions in rare earth region, 19: 41656 (BNL-9245)
CHRISTENSEN, Per Rox, 0^+ states in N = 82 nuclei, 19: 41747
CHRISTENSON, J. H., Dipion production at low momentum transfer in π^--p collisions at 1.5 Bev/c, 19: 41441
CHRISTMAN, A. M., Providing real-time information on production schedules and costs, 19: 40704 (Y-KA-9)
CHRISTOFILOS, N., Plasma confinement properties of relativistic electron coils, 19: 41867 (UCRL-12455-T)
CHRISTOV, S. G., Calculation of average permeability of potential waves, 19: 41533
CHUEV, V. I., The reactions $^3He(d,t)2p$ and $^3He(^3He,\alpha)2p$, 19: 41658 (IAE-655)
CHUEVA, S. A., Elastic pp scattering at 1.45 Bev, 19: 41487
CHUKHIN, S. G., Accumulation and distribution of Sr-90 in swine after prolonged administration of radiostrontium, 19: 40328
CHUKHLANTSEV, V. G., Subsolidus structure of Li_2O–ZrO_2–SiO_2 and its properties, 19: 41038
CHUNG, Hui-Ying, Transient response of the Cs diode to potential pulses, 19: 41318
CHUNG, Suh Urk, Branching ratios for decays of the f^0, A_2, and K*(1400) mesons, 19: 41460
CHUPRUNOV, D. L., Excitation functions for (p,p') on Al-27, 19: 41813
CLARK, A. R., Dipion production at low momentum transfer in π^--p collisions at 1.5 Bev/c, 19: 41441
CLARK, Anne Vincent, Thermal relaxation in oxygen with H_2O, HDO, and D_2O vapors as impurities, 19: 40483
CLARK, John W., Dynamical correlations and the nuclear photoeffect, 19: 41844
CLARK, W. G. Jr., Ultrasonic testing characteristics of forged Inconel, 19: 41027 (WERL-0029-2)
CLARKE, H. G. Jr., Experimental studies of cask impact resistance, 19: 40818 (SC-RR-65-98, pp 261–82)
CLARKE, J. H., Photoionization upstream of strong shock wave, 19: 41915
CLARKE, Joan R., McKelveyite, a new hydrous U carbonate mineral, 19: 40799
CLAWLEY, William Edgar, Process and equipment for control of reactor, 19: 42019 (ORNL-tr-669)
CLIKEMAN, F., Material buckling and intracellular thermal neutron distributions, 19: 42049 (MIT-2344-3, pp 155-64)
CLIKEMAN, F. M., Proj. rpt. on Heavy Water Project, annual, 9/30/64, 19: 42007 (MIT-2344-3)
CLINE, Carl F., Volume compressibility of BeO and other II–VI compounds, 19: 41984
COCHE, André, Study of y radiations of Ta-182, 19: 41704
COCKE, William Johnston, Variational principle in general relativity, 19: 41563
COERDT, R. J., Summary report on electron bombardment ion engine development, 19: 40760 (N64-25008)
COFFEY, Howard T., Distribution of magnetic fields and currents in cold-worked type II superconductors, 19: 41637
COFFMAN, Robert E., Thermoluminescent formation of Cr^{2+} in magnesium oxide, 19: 40631
COHEN, Ira M., Asymptotic theory of photoionization chamber. I., 19: 40552 (NP-15287)
COHEN, J. P., Evidence for nucleon clustering from high-energy reactions, 19: 41831
COLE, A. J., Effects of temperature and pressure on hot-atom reactions in bromoethane, 19: 40626
COLEMAN, Paul J. Jr., Prog. rpt. on geo- and planetary physics, 1–6/64, 19: 41571 (N64-29400)
COLLINS, Gaston, The oxysulfides and sesquisulfides of terbium, holmium, thulium, and lutetium, 19: 40475
COLVEN, T. J., Economics of fuel processing, 19: 40661
COMAS, James, Angular distribution of sublimed and sputtered particles

from Ag single crystals, 19: 41259
COMBET, Edmond, Generator kernel of creation and annihilation operators on a static space-time, 19: 41534
COMPSTON, W., Strontium isotope composition and K–Rb ratios in some rocks from Reunion and Rodriguez, Indian Ocean, 19: 40791
CONNELLY, D. J., Prog. rpt. on heat transfer for space nuclear power, 12/64–2/65, 19: 40741 (SAN-409-23)
CONSOLI, Terenzio, Measurements of the characteristics of metallic plasma pulse, 19: 41878
CONSTANTINESCU, Anisoara, Elastic n-p interaction at 3 to 10 Bev, 19: 41347
CONVERT, Guy, Extension of Nyquist theorem to systems with negative temperature, 19: 41537
CONWAY, J. B., Properties of some refractory metals. III., 19: 41009 (GEMP-375)
COOK, K. V., Ultrasonic detection of non-bond in clad structures, 19: 40756
COOP, K. L., Gamma rates and intensities; l-forbidden M1 transitions, 19: 41836
COOP, Kenneth L., Investigation of γ rays from reactions $^{20}Ne(p,\gamma)^{21}Na$, $^{21}Ne(p,p'\gamma)^{21}Ne$, and $^{22}Ne(p,\gamma)^{23}Na$, 19: 41838
COOPER, C. Burleigh, Angular distribution of sublimed and sputtered particles from Ag single crystals, 19: 41259
COOPS, M. S., Operating trans-curium element radiochemistry facility, 19: 40719 (UCRL-7844-T)
COOPS, M. S., Remotely-operated trans-plutonium chemical process cells, 19: 40720 (UCRL-7845-T)
COPLIN, D. H., Fission gas release from UO_2 fuel rods with gross central melting. I., 19: 41088 (GEAP-4572)
COPPAGE, F. N., Conductivity induced in polystyrene by pulsed γ rays, 19: 41091 (SC-R-65-943)
CORELLI, John C., Investigation of transient radiation damage in semiconductor materials. Quarterly progress report 11/1/64–1/31/65, 19: 40934 (NP-15301)
CORTE, M. Dalla, Difference in range-energy relation for positive and negative particles, 19: 41369
COSPER, S. W., Some (d,α) differential cross sections for ^{23}Na, ^{27}Al, and ^{31}P at about 9.3 Mev, 19: 41684
COSTES, Didier, Nuclear reactor, 19: 42068
COTE, Owen, Circulation processes and mixing mechanisms in upper atmosphere above 30 km, 19: 41112 (SC-DC-65-1312)
COTTRELL, William B., U. S. reactor containment technology, 19: 42008 (ORNL-NSIC-5(Vol.I and II))
COUINEAU, P., Saint-Laurent-des-Eaux nuclear power station sealing barriers around foundation pits, 19: 42119
COULTER, C. Alton, Fine structure of optical absorption bands in neutron-irradiated MgO, 19: 40632
COUVILLION, J., Prog. rpt. on ion rocket engine development, 1–3/65, 19: 40765 (NP-15309)
COWAN, Charles L., Measurement of Livermore pool-type reactor (LPTR) transfer function using reactor oscillation techniques, 19: 42156 (UCRL-12476)
COWLEY, R. A., The crystal dynamics of uranium dioxide, 19: 41032
COYNE, J. J., $SU(6)_W$ photoproduction and meson-baryon scattering amplitudes, 19: 41462
CRADDOCK, James E., Life history of banded sculpin, Meade Co., Kentucky, 19: 42220 (TID-22023)
CRAWFORD, C. K., Improved series of ion gun parts, 19: 41185
CRAWFORD, F. W., Absolute instabilities of perpendicularly propagating cyclotron harmonic plasma waves, 19: 41884
CRAWFORD, F. W., Low-frequency impedance characteristics of Langmuir probe in plasma, 19: 41949
CRAWFORD, R. L., Stable linear pulse-summing circuit, 19: 40726
CRAWFORD, Richard Lyle, The design criteria of a phoswich transducer 19: 40921
CREER, K. M., Radiometric age of the Serra Geral Formation, 19: 40796
CRESTI, M., Spin and parity of 1320 Mev $p\pi$ resonance, 19: 41368
CRIEGGE, L., Neutron spectra from Bi produced by monoenergetic γ rays, 19: 41834
CRITCHFIELD, Charles L., Pions, muons, and nuclear structure, 19: 41671 (LADC-6186)
CROCKER, J. G., Reactor stability tests in Spert IV facility, 19: 42152 (IDO-17088)
CROMER, D. T., Integrated series of crystallographic computer programs. VII., 19: 41965 (LA-3309)
CROMER, Don T., Integrated series of crystallographic computer programs. VIII., 19: 41966 (LA-3310)
CRONIN, J. W., Dipion production at low momentum transfer in π^--p collisions at 1.5 Bev/c, 19: 41441
CROUCH, E. A. C., Separation of fission product and actinide elements from fuels, 19: 40675
CROUCH, Harry Randall Jr., Production of π^0 and η^0 mesons in π^--p collisions, 19: 41507
CROUCH, M. F., Evidence for high-energy cosmic-ray neutrino interactions, 19: 41306
CROWDEN, J. B., Absolute fission cross section of ^{235}U for 2200-m/sec neutrons, 19: 41691
CULWICK, B. B., Existence and properties of a non-strange meson of mass 1500 Mev/c^2, 19: 41459
CUNSOLO, S., Experiments on the creation of charged quantized vortex rings in liquid helium at 1°K, 19: 41621
CUTHRELL, R. E., The kinetics of the reactions of KO_2 and KOH with water, 19: 40462 (SC-TM-65-183)
CUTRELL, R. E., Application of metal coatings on uranium, 19: 40949 (ISC-640)
CUYPERS, Marc, Systematic analysis of copper of very high purity after irradiation by thermal neutrons, 19: 40422
CYROT, M., Electronic excitations in superconductors free from second species. I., 19: 41623

D

DAGLIANA, M. G., Difference in range-energy relation for positive and negative particles, 19: 41369
DAHL, Orin I., Branching ratios for decays of the f°, A_2, and K*(1400) mesons, 19: 41460
DAHMEN, H. D., Convergence properties of the time-dependent perturbation series of a N fermion system, 19: 41364
DAHMER, Lionel H., Cation exchange separation of Mo, W, Nb, and Ta from other metal ions, 19: 40658
DALGARNO, A., Stopping powers and straggling in neon, argon, and krypton, 19: 41268
DALITZ, R. H., Nuclear interactions of the hyperons, 19: 51413
DAMON, Paul E., Prog. rpt. on correlation and chronology of ore deposits, annual, 8/1/65, 19: 40778 (COO-689-50)
DANAGULYAN, A. S., Two-hour (7.7 ksec) isomer of ^{168}Lu, 19: 41803
DANIELS, W. E., An evaluation of the main geomagnetic field, 1940–1962, 19: 41586
DAO WONG DUC, Electromagnetic mass splitting in symmetry scheme SU(6), 19: 41329 (JINR-P-2208)
DAR, Arnon, Cluster transfer reactions between complex nuclei, 19: 41764
D'ARDENNE, Walter H., Epithermal neutrons in U–D_2O lattices, 19: 42044 (MIT-2344-3, pp 37-54)
DAS, P. K., Hydrogen adsorption on zirconium borate and dioxide, 19: 40484
DASHEN, Roger Frederick, Electromagnetic corrections to strong interactions, 19: 41511
DAUGHADAY, Hamilton, Function in quantum mechanics which corresponds to a given function in classical mechanics, 19: 41555
DAUTOV, G. Yu., Some correlations in investigation of electric arcs, 19: 41913
DAVEY, Paul Oliver, Nuclear E1 photodisintegration in the 1s-shell, 19: 41824
DAVEY, William G., Analysis of six AETR fast critical experiments, 19: 42077 (ANL-7014)
DAVIES, Bea, Refractories and methods of manufacture therefor, 19: 40997
DAVIES, D. K., Nuclear steam generators, 19: 42123
DAVIES, D. Kenneth, Auger ejection of electrons from silver, 19: 41270
DAVIES, Nan, FOTRAC: a Monte Carlo photon tracing computer program, 19: 41957 (UCRL-14165)
DAVIES, Robert, Symposium on cavitation in real liquids, Warren, Mich., 1962, 19: 40751
DAVIES, W., Determination of nitrogen in uranium–plutonium dioxides, 19: 40438
DAVIS, D. H., Angular correlations between fast Σ hyperons and fast protons, 19: 41494
DAVIS, P. J., Microhardness measurement of unirradiated and irradiated BeO, 19: 41087 (AAEC/E-135)
DAVIS, R. Jr., Cross sections for the production of ^9Li, ^{16}C, and ^{17}N in irradiations with Bev-energy protons, 19: 41780
DAVIS, S. S., Pulsed-decay and extrapolation-length measurements in graphite, 19: 41647
DAVIS, W. R., Conservation laws of general theory of relativity. I., 19: 41542
DAVIS, W. R., Conservation laws of general theory of relativity. II., 19: 41543
DAVTYAN, I. A., Studies of Nd_2O_3–ZrO_2. Investigations of regions rich with ZrO_2, 19: 41037
DAVYDOV, A. A., Electric monopole transitions in nonspherical atomic nuclei, 19: 41812
DAVYDOVA, T. A., On the cyclotron instability of a plasma with non-monotonic distribution function, 19: 41918
DAY, R. A., Stark broadening of ionized nitrogen lines in a T-tube plasma, 19: 41941

DAY, Ralph K., Thermal conductivity of high conductivity materials. I., 19: 41029
DAY, Robert B., High resolution measurements of γ rays from neutron inelastic scattering, 19: 41669 (LA-DC-7096)
DAYTON, R. W., Reactor materials, Vol. 8, No. 2, 19: 40957
DEARNALEY, G., Investigation of $^{27}Al(\alpha,p)$ reaction by cross-section fluctuation studies, 19: 41761
DE BARROS, S., Treatment of capture gamma ray spectra obtained with the aid of a central crystal in association with an annular crystal, 19: 40896
DE BEAUREGARD, O. Costa, Translational inertial spin effect with photons, 19: 41440
DEBEAUVAIS, Monique, Determination of thresholds of sensitivity for recording of different ionizing particles in solid-state polymers, 19: 40564
DEBRUNNER, P., Measurements by scattering techniques. II., 19: 41845
DECAE, Andre, Implantation of 200-Bev synchrotron at Berkeley, 19: 41178
DE CALAN, C., Radiative corrections to inelastic electron scattering with detection in coincidence, 19: 41752
DECEV, G., Comparative studies of radioactively labeled precursors in the RNA of x-irradiated non-diploid yeast, 19: 40367
DEEM, H. W., Thermal radiative properties, 19: 41074
DE FOREST, Taber Jr., Muon capture and inelastic electron scattering in C-12 and O-16, 19: 41766
DEHN, R., Measurement of DFR γ heating, 19: 42117
DEHNHARD, D., Decay of C-12 into three α particles in reaction $^{11}B(p,\alpha)2\alpha$, 19: 41699
DEIGEN, M. F., Observation of electron-nuclear double resonance of F centers in KCl, 19: 41992
DEITZ, Allen, High-voltage radio frequency variable capacitor using a liquid dielectric, 19: 40844 (MATT-341)
DE JUREN, J. A., Pulsed-decay and extrapolation-length measurements in graphite, 19: 41647
DEL ARENAL, R., Geochemistry and radioactivity of waters in Lourdes, San Luis Potosi, Mexico, 19: 40835
DE LAUER, R. D., Fundamentals of nuclear flight, 19: 42147
DELGROSSO, E. J., Utilization of yttrium in gettering oxygen and nitrogen in Nb-base materials, 19: 40953 (PWAC-441)
DELIBRIAS, G., Age measurements using the C-14 method, 19: 40795
DE LISE, Donald A., Cosmic-ray search for fractionally charged particles, 19: 41311
DE LLANO, M., Nuclear structure in the 2s-1d shell. I., 19: 41729
DE LLANO, M., Nuclear structure in the 2s-1d shell. II., 19: 41730
DELMAS, R., Measurement of the plate temperature of fuel elements of BR-2, 19: 42181
DELMAS, Roger, Improvements in or relating to metal oxide powder sintering, 19: 40995
DELNAY, R. L., Description and evaluation of four $Pu(NO_3)_4$ shipping containers, 19: 40821 (SC-RR-65-98, pp 423–41)
DE LOTTO, I., Counting of events from pulsed sources, 19: 40885
DE MARCO, Angelo, Loss of energy by ultra-relativistic muons. III., 19: 41345
DE MARTINI, F., Sensitivity and admissible field inhomogeneity of a nuclear magnetometer, 19: 40851
DE MIER, Warren V., Development of radioactive waste fractionization and packaging technology, 19: 42197
DEMIN, A. G., New isomers of ^{43}Sc, ^{109}In, and ^{128}Xe, 19: 41802
DEMMITT, T. F., Automated procedure for zirconium analysis in water, 19: 40403 (BNWL-SA-166)
DEMMITT, T. F., Automated procedure for H_3BO_3 analysis in water, 19: 40404 (BNWL-SA-167)
DENEGRE, G., Measurement of the plate temperature of fuel elements of BR-2, 19: 42181
DENISOV, E. P., Cascade mechanism of the high-energy nuclear reactions. I., 19: 41811
DENKS, V. P., Electrostimulated luminescence of activated alkali halide compounds, 19: 41981
DENNIS, Wolcott, Krypton–xenon separation from a gas mixture, 19: 40695
DENNISON, David H., Heat contribution due to thermal excitation of 4F electrons of some di- and tri-valent lanthanide elements, 19: 40457 (IS-1156)
DE PAGTER, James, Calibration of beam monitor of Cambridge Electron Accelerator, 19: 41164 (CEAL-1022)
DE ROSIER, T. A., Introduction to nuclear propulsion—reactor control, 19: 42138 (N64-33780)
DERRY, L. W., Activation sintering of tungsten, 19: 40985
DE SAUSSURE, G., Measurement of the U-235 neutron capture-to-fission ratio from 3.25 ev to 1.8 kev, 19: 41749
DE S. BARROS, F., Moessbauer studies of inequivalent ferrous ion sites in ferrous formate, 19: 40542
D'ESPAGNAT, B., Model for PC violation in framework of unitary symmetry, 19: 41522
DETENBECK, R. W., Weakly excited resonance levels in reaction $^{13}C(p,\gamma)^{14}N$, 19: 41740
DETRAZ, Claude, Angular correlation in (p,pd) reaction on C-12, 19: 41703
DETRAZ, Claude, Lithium-4 and the excited levels of He-4, 19: 41786
DE TREZVINSKY, B., Determination of permanent gases by gaseous chromatography, 19: 40415 (CEA-tr-R-1839)
DETTERMAN, R. L., Safe disposal of SNAP reactors, 19: 42140 (NAA-SR-11353)
DETTORE, Joseph F., Characterization of pyrolytic-carbon fuel-particle coatings prepared with acetylene, 19: 41004 (BMI-1735)
DEUTSCH, F., Linear electromagnetic brake, 19: 40724
DEVELEY, Gerard, Variation of magnetic susceptibility of Fe, Gd, and Ni near the Curie point, 19: 41972
DE VOE, James R., Activation analysis program and facilities at the National Bureau of Standards, 19: 40450
DE VOE, James R., Simultaneous determination of copper and zinc in human lung tissue by neutron activation analysis, 19: 40452
DE WET, W. J., Separation of fission product and actinide elements from fuels, 19: 40675
DEWITT, R. N., Dynamo action in ionosphere and motions of magnetospheric plasma. II., 19: 41593
DEWITT, R. N., Dynamo action in ionosphere and motions of magnetospheric plasma. III., 19: 41594
DIAMENT, Paul, Wave propagation along warm plasma columns, 19: 41939
DIETHRICH, Edward B., Tissue tolerance and systematic toxicity of 5-fluorouracil, external radiation, and drug-radiation combination in rabbits, 19: 40394
DIETRICH, D. E., The effect of temperature on RTV-20, 19: 42215 (RFP-625)
DIETZ, John P., Compilation of crater data, 19: 40711 (SC-DC-65-220)
DIETZ, K. A., Prog. rpt. on STEP Project, 1–6/64, 19: 42134 (IDO-17070)
DILLON, I. G., Fuel management and inventory in the EBR-II fuel cycle, 19: 42075 (ANL-6735)
DI MARCO, Joseph Nicola, Experimental observations of an interaction between two counterstreaming plasmas in presence of external magnetic fields, 19: 41926
DI MARTINI, Raymond G., Gamma-radiation-induced decomposition of alkali nitrate crystals (thesis), 19: 40609
DIO, Wolf-Heiner, Zero-energy measurements on core of the multi-purpose research reactor, 19: 42186
DIRAC, Paul A. M., Lectures on quantum mechanics, 19: 41567
DIXON, W. G., Classical theory of charged particles with spin and classical limit of the Dirac equation, 19: 41372
DMITRENKO, I. M., Tunnel effect for photon-emitting Cooper pairs, 19: 41631
DMITRIEV, M. T., On the problem of utilization of heavy nuclei fission energy for ionizing the air, 19: 40604
DOBRZHANSKII, G. F., Some data on the luminescent properties of Eu-activated NaCl and KCl phosphors, 19: 40567
DODD, C. V., Recent eddy-current development at ORNL, 19: 40757
DODD, Caius Vernon, Solution to electromagnetic induction problems, 19: 41125 (ORNL-TM-1185)
DOLINSZKY, Tamas, Angular distribution in $^{12}C(d,p)^{13}C$ reaction, 19: 41721
DOLINSZKY, Tamas, Exact dispersion formula, 19: 41363
DOLIQUE, Jean-Michel, The ohm law for a partially ionized plasma, 19: 41874
DOLLING, G., The crystal dynamics of uranium dioxide, 19: 41032
DONAHUE, D. J., Mean lives of 2.15- and 1.74-Mev levels in ^{10}B, 19: 41758
DONDES, S., Promotion of chemical processes with reactor radiation, 19: 40559
DORNER, H., MZFR—reactor pressure vessel and installed construction, 19: 42163
DORONINA, V. P., Solubility of LaF_3 in $Be(NO_3)_2$ solutions, 19: 40670
DOROZHKIN, A. A., Auger ejection of electrons from tungsten and molybdenum by mercury ions, 19: 41272
DORY, R. A., Motion of plasma and lifetimes of energetic ions in a toroidal octupole magnetic field, 19: 41896
DOSHI, K. D., Analytical approach to study vehicle collisions, 19: 40817 (SC-RR-65-98, pp 243–60)
DOSTROVSKY, I., Cross sections for the production of ^{9}Li, ^{16}C, and ^{17}N in irradiations with Bev-energy protons, 19: 41780
DOUGLAS, D. A. Jr., Properties of thorium, its alloys, and its compounds, 19: 41025 (ORNL-TM-1144)
DOUGLASS, C. C. Jr., Computer programs for shielding problems in manned

space vehicles, 19: 41954 (NP-15338)
DOW, N. F., Prog. rpt. on shielding for ionizing radiation space, final, 9/62–8/63, 19: 41952 (N64-31552)
DOWDEN, R. L., Micropulsation mode propagation in the magnetosphere, 19: 41595
DOWDEN, R. L., Micropulsation whistlers in study of outer magnetosphere, 19: 41596
DOWNING, R. G., Electron bombardment of silicon solar cells, 19: 40931 (AD-609424)
DOYLE, N. J., Constitution diagram of tungsten–molybdenum–osmium system, 19: 41048
DOYLE, N. J., Solid solubility limits of Y and Sc in the elements W, Ta, Mo, Nb, and Cr, 19: 41050
DRAGOMIR, Eugenia, Refractometric study of formation of complex Pr halides in aqueous solution, 19: 40469
DRAGT, Alex J., Some simple consequences of SU(4) symmetry, 19: 41397
DRAKE, D. M., Neutron spectra from Bi produced by monoenergetic γ rays, 19: 41834
DRAN, Jean-Claude, Adsorption of CO and O_2 on ZnO and NiO, 19: 40578
DRAN, Jean-Claude, Oxidation of CO on NiO and ZnO, 19: 40577
DRANOVA, Zh. I., Reestablishment of contacts between fragments of a tungsten microcrystal, 19: 41061
DRIGO, L., Performance and properties of a proton polarimeter, 19: 40905
DROBOT, D. V., System $SmCl_3$–NaCl–KCl, 19: 40517
DRUKAREV, G. F., Theory of electron-atom collisions, 19: 41282
DRUSKINA, L. S., Radiophotoluminescence of polycrystalline pellets of Ag-activated NaCl, 19: 40569
DUBININA, A. I., Trap with magnetic plugs for holding electrons, 19: 41858 (NP-15217)
DUBOIS, J., New bound levels in Sc-43 from radiative proton capture in Ca-42, 19: 41738
DUBOST, H., Evidence for nucleon clustering from high-energy reactions, 19: 41831
DUBRIN, J., Reactions of nucleogenic C atoms with hydrocarbons, 19: 40617
DUCLOS, Donald P., Proton beam technique for measuring the ion density in a plasma, 19: 41899
DUDEY, N. D., Cross-section ratios of isomeric nuclides produced in medium-energy (α,xn) reactions, 19: 41695
DUDEY, N. D., Statistical-model analysis of isomeric ratios in (α,xn) compound nuclear reactions, 19: 41696
DUDEY, Norman Dean, Effect of angular momentum on isomeric cross-section ratios in compound nuclear reactions, 19: 41821
DUHM, H. H., Level structure of ^{53}Cr and ^{55}Cr, 19: 41726
DUNAWAY, D. L., Testing shipping containers for slightly enriched uranium billets, ingots, and fuel cores, 19: 40820 (SC-RR-65-98, pp 357–76)
DUNGEY, J. W., Origin of outer-belt protons. I., 19: 41577
DUNINA, A. A., X-ray luminescence of the NaI(Tl) phosphor, 19: 40908
DUNN, J., Testing of immersion heaters for in-tank solidification circulators, 19: 42193 (BNWL-101)
DUNNING, John Ray Jr., Electromagnetic form factors of the neutron, 19: 41326 (HUX-2752-9)
DUPERRIN, Jean-Claude, Decay of Er-169, 19: 41705
DUPREE, Andrea K., Collisional excitation of autoionizing levels, 19: 41244
DVORINA, L. A., Scandium monsilicide and its crystal structure, 19: 40479
DWORNIK, Edward J., McKelveyite, a new hydrous U carbonate mineral, 19: 40799
DYATKINA, M. E., Theoretical investigation of stereochemistry of complex compounds with f-electrons. II., 19: 40522
DYATLOV, V. G., Investigation of a θ pinch plasma in an azimuthal magnetic field, 19: 41921
DYATLOV, V. G., Plasma in a θ-pinch with azimuthal magnetic field, 19: 41860 (NP-15220)
DYMNIKOV, A. D., Spherical aberration of combined quadrupole lens with bell-shaped field distribution, 19: 41198
DYOS, M. W., Effective thermal neutron cross sections for materials with grain structure, 19: 42041 (GA-6286)
DYUZHEV, G. A., Most effective regimes for thermionic convertors, 19: 41317
DZANTIEV, B. G., Development of methods for hot synthesis of ^{35}S-labeled biologically active substances, 19: 40619
DZANTIEV, B. G., The formation of polymeric products in reactions of polyvalent recoil atoms, 19: 40628
DZHAVRISHVILI, A. K., Properties of component penetrating atmospheric showers, 19: 41297
DZHELEPOV, B. S., New data for ^{188}Re decay scheme, 19: 41801
DZYUB, I. P., Resonant scattering of phonons by impurity atoms and one-phonon coherent scattering of slow neutrons, 19: 41991
DZYUB, I. P., Theory of Moessbauer effect in nonideal crystals, 19: 41997

E

EARLE, E. D., Parity assignments in ^{200}Hg from linear polarization correlation of thermal neutron capture γ rays, 19: 41846
EBELING, W., Kinetic equations and momentum equations for inhomogeneous plasmas, 19: 41870
ECK, R. E., Investigation of microwave radiation emitted by Josephson junctions, 19: 41614
ECKERT, A. C., Summary report on electron bombardment ion engine development, 19: 40760 (N64-25008)
ECKLUND, S. D., Photoproduction of π^+ mesons from hydrogen from 0.6 to 1.2 Bev, 19: 41323 (CALT-68-42)
EDLOW, Samuel, Special problems in packaging and transportation of radioactive materials, 19: 40826 (SC-RR-65-98, pp 625–9)
EDLUND, M. C., The thorium fuel cycle, 19: 42109
EDVARSON, K., Observations on the particle properties of nuclear debris in the upper atmosphere, 19: 40783 (NP-15327)
EDVARSON, K., Theoretical aspects on the formation of nuclear weapon debris, 19: 40782 (NP-15325)
EDWARDS, J. W., Transfer of triplet state energy from acetophenone to rare earth ions, 19: 40504
EDWARDS, M. H., Nonanalytic form of coexistence curve of He at critical point, 19: 41615
EDWARDS, R. S., Production of excited state H_1^+ for Lorentz dissociation in DCX-1, 19: 41864 (ORNL-P-1244)
EFIMOV, B. V., Stabilizing amplification channel of scintillation counter, 19: 40870 (IAE-695)
EGUCHI, Tamotsu, The effects of preirradiation on the activities of solid acidic catalysts, 19: 41099
EHRET, B., Program system for solution of the multigroup neutron diffusion equation, 19: 41649
EIBEN, Klaus, Solvated electrons in γ-irradiated, frozen solutions, 19: 40551 (KFK-293)
EICHELBERGER, R. L., Prog. rpt. on solubility studies in alkali metals, 1/3–4/3/65, 19: 40946 (AI-65-93)
EICHHORN, Gunther L., Interactions of metal ions with polynucleotides and related compounds. III., 19: 40474
EISMONT, V. P., Search for positron emitters among the products of ^{235}U thermal neutron fission, 19: 41799
EISSENBERG, D. M., Iodine transport and deposition in a high-temperature, helium loop first test series, 19: 40397 (ORNL-TM-1134)
EKERT, Bernard, Self-decomposition and radiolysis, at low temperature, of tritiated thymidine in aqueous solution, 19: 40583
ELEKES, Istvan, Aseptic production of sterile pyrogen-free human albumin, labeled with ^{131}I, 19: 40639
ELGAROY, Oystein, Some properties of solar radio bursts of spectral type III, 19: 41218
ELINSON, S. V., New photometric methods for determining Nb and Ta in metals and alloys. IV., 19: 40442
ELISEEV, A. A., Crystal structure of $LaTe_2$, 19: 40476
ELISEEV, A. A., Roentgenographic studies of lanthanum tellurides La_4Te_7, 19: 41070
ELISEEV, A. A., Roentgenographic studies of lanthanum ditelluride, 19: 41071
ELLIOTT, L. G., Prog. rpt. on physical research, 1–3/65, 19: 41678 (PR-P-65)
ELLIS, P. J., Transition in O-18 (3.92 to 1.98 Mev), 19: 41797
ELSTON, Jean, Fuel element for a nuclear reactor, 19: 42074
ELSTON, Jean, Improvements in or relating to metal oxide powder sintering, 19: 40995
ELY, Robert P. Jr., Experimental study of $K_{\mu 4}^+$ decay, 19: 41446
EMERY, M. W., Micropulsation whistlers in study of outer magnetosphere, 19: 41596
EMPSON, F. M., Project Salt Vault, 19: 42195 (ORNL-P-1479)
ENDOW, N., Prog. rpt. on sorption of gases on metal surfaces, 2/15–5/15/65, 19: 40463 (SRIA-425-5)
ENDRES, G. W. R., Thermoluminescent dosimetry studies at Hanford, 19: 40868 (BNWL-SA-23)
ENGEL, J. David, Liquid scintillation counting of C-14 in aqueous digests of whole tissues, 19: 40418
ENGELMANN, R. J., MIDAS computation of waterdrop evaporation, 19: 41110 (BNWL-74)
ENGLAND, J. B. A., Study of $(^3He,^7Be)$ reaction in ^{12}C, 19: 41733
ENGLER, A., Anti-isobar production in $\bar{p}n$ interactions, 19: 41438
ERDTMANN, Gerhard, Geometry and statistical error in absolute counting with β-γ coincidence method, 19: 40874 (JUL-227-CA)
EREMIN, Yu. V., Measuring the velocity of plasma jets, 19: 41912
ERGINSOY, C., Direction and energy distribution of charged particles transmitted through single crystals, 19: 41788
ERGINSOY, Cavid, Anisotropic effects in interactions of energetic charged particles in crystal lattice, 19: 41789

ERICKSON, C. W., Motion of plasma and lifetimes of energetic ions in a toroidal octupole magnetic field, 19: 41896
ERICKSON, Glen W., Higher order calculation of Lamb shift in Li^{++}, 19: 41265
ERMAKOV, V. A., Investigation of complexes of Am, Cm, Cf, and Fm with lactic acid, 19: 40458 (JINR-P-2224)
ERNSTENE, M. P., Surface ionization engine development, 19: 40769
EROE, Jones, Angular distribution in $^{12}C(d,p)^{13}C$ reaction, 19: 41721
EROE, Jones, Electrostatic ion beam accelerator, 19: 41181
EROKHIN, R. A., Plutonium-239 in rat lung and liver and morphological changes after intratracheal administration, 19: 40317
EROKHIN, R. A., Strontium-90 content in rats after chronic oral administration, 19: 40323
ERPENBECK, Jerome J., Stability of detonations for disturbances of small transverse wavelength, 19: 41117 (LA-3306)
ESCHNAUER, H., Guarantees for MTR fuel elements, 19: 42157
ESCUDIE, B., Optimum processing of spectrometric information by numerical adapted filters, 19: 40906
ESTRADA, J., Determination of mass transfer coefficients for the liquid film in the system UO_2SO_4–anion exchange resins, 19: 40660
ETTER, D. E., Phase equilibria in plutonium–cerium–copper system, 19: 41054
EVANS, A. G., Role of grain boundaries in plastic deformation of CaF_2, 19: 40536
EVANS, C. A. Jr., Computer programs to optimize times of irradiation and decay in multielement activation analysis, 19: 40451
EVANS, D. A., Mean lifetime of the π^0 meson, 19: 41404
EVANS, Donald B., Equilibria of nitrogen with the refractory metals titanium, zirconium, columbium, vanadium, and tantalum in liquid iron, 19: 41065
EVERED, S., Hydrolysis of neutron-irradiated U and U–Pu monocarbides, 19: 40586
EVERETT, Allen E., Effect of mass splittings on symmetry relations between scattering amplitudes, 19: 41430
EWALD, H., Influence of magnetic and electric fringing fields on the trajectories of charged particles, 19: 41139
EWART, Alan, Shell structure and angular momentum effects in decay of compound nuclei of nickel, 19: 41741
EWERS, J., High-temperature high-vacuum valves with gold-wire sealing, 19: 40775
EWING, C. T., Instability of refractory metal thermocouples, 19: 40859
EYRE, B. L., Formation of interstitial loops in bcc metals, 19: 41056
EYRING, LeRoy, Science and technology of the rare earths. I., 19: 40399

F

FABRIKANT, V. A., Experimental determination of effective probability of photon emission by plasma atoms, 19: 41891
FAENHRICH, J., Influence of uv radiation on thermionic converters, 19: 40566
FAIER, Horry, Meson decays and the sigma hypothesis, 19: 41518
FAKHRYTDINOV, P. Yu., Use of phase technics for studying polarization phenomena of radiowave reflection from meteor trails, 19: 41223
FAKIROV, D. G., Baryon and meson multiplets in the group SU(12) uniting symplectic and spin symmetries, 19: 41331 (JINR-P-2219)
FALCONER, I. S., Observation of the Faraday effect in a θ-pinch plasma using He–Ne laser, 19: 41947
FAN, C. Y., Cosmic radiation helium spectrum below 90 Mev per nucleon measured on Imp 1 satellite, 19: 41302
FANTE, Ronald Leon, New solution of kinetic equations for a plasma, 19: 41930
FARLEY, Thomas A., Prog. rpt. on geo- and planetary physics, 1–6/64, 19: 41571 (N64-29400)
FARMELO, D. R., Compact 1900°F resistance-wound combustion furnace for remote operation, 19: 40413 (TIM-948)
FARQUAHR, J., Design study of modification of M-1 liquid H turbopump for use in reactor test facility, 19: 42141 (NASA-CR-54422)
FARRINGTON, Wayne A., Prog. rpt. on improved strength and oxidation resistance of Cr composites, final, 3/64–3/65, 19: 41022 (NP-15292)
FAUGERAS, P., Chemical treatment of irradiated nuclear fuels, 19: 40667
FAVREAU, Louis J., Cataphoretic coating La boride on Re filaments, 19: 40725
FAZIO, M., Reaction (n,d) on ^{63}Cu and ^{65}Cu isotopes at 14 Mev, 19: 41755
FEDOROV, A. A., Determination of Sm, Gd, Dy, Er, and Sc (0.01–0.6 percent) in steels and alloys by a chemicospectrographic method, 19: 40445
FEIGENBUTZ, L. V., Prog. rpt. on heat transfer for space nuclear power, 12/64–2/65, 19: 40741 (SAN-409-23)
FEINBERG, G., Long-range electromagnetic forces on neutral particles, 19: 41448
FEINBERG, G., Possible C,T noninvariance in the electromagnetic interaction, 19: 41452
FEIOCK, Frank Dongld, Special problems in non-equilibrium statistical mechanics, 19: 41155
FELDMAN, David, Prog. rpt. on experimental and theoretical high energy physics, 9/64–8/65, 19: 41337 (NYO-2262-95)
FELTEN, Edward J., Binary oxide systems of niobium pentoxide with oxides of common niobium alloying elements, 19: 41049
FENECH, Henri, Development of the gas-cooled fast reactor concept, 19: 42090 (GA-6132)
FERRARI, C., Photoionization upstream of strong shock wave, 19: 41935
FERRARI, Carlo, Symposium on high temperatures in aeronautics, Turin, 9/62, 19: 40767
FERRERO, Giorgio M., Radiative oscillations in stellar gaseous masses (radiative-acoustic waves), 19: 41219
FERRY, B. N., Prog. rpt. on stress corrosion of austenitic stainless steels, 6/65, 19: 40968 (EURAEC-1424)
FERZIGER, Joel H., Calculation of disadvantage factor in cylindrical geometry, 19: 42063
FETISOV, E. P., Radiation of soft x rays by the solar corona, 19: 41209 (N64-22932)
FICKINGER, W. J., ρ and ω production in π^+d interactions at 1.7 Bev/c, 19: 41528
FICKINGER, W. J., Statistical study of linear mass relations for elementary particles, 19: 41408
FIDECARO, G., High-intensity, partially separated, beam of antiprotons and K mesons, 19: 41184
FIELD, F. R., Jr., SRP reactor on-line computer, 19: 42129 (DPSPU-65-30-27)
FIGUERA, A. S., Weakly excited resonance levels in reaction $^{13}C(p,\gamma)^{14}N$, 19: 41740
FILATOV, E. S., Reactions of hot tritium atoms with alcohols and with some of their binary hydrocarbon mixtures, 19: 40622
FILATOV, Z. S., Chemical effects of nuclear transformations and energy transfer processes, 19: 40620
FILLOLEAU, Etienne, Nuclear reactor control rod operating device, 19: 42033
FINCH, R. A., Rapid pulse heating of modified zirconium-uranium hydrides to destruction, 19: 41017 (NAA-SR-10482)
FINIKOV, V. G., Isotopic exchange of oxygen in gas-melt systems at 700 to 955°C, 19: 40506
FINK, D., Interference of fine-structure levels in hydrogen, 19: 41263
FINKELNBURG, W., MZFR—a landmark of German reactor development, 19: 42158
FINKELNBURG, Wolfgang, Structure of matter, 19: 41829
FIQUET-FAYARD, Florence, Isotopic effects in dissociation of triatomic molecules by electron collision. III., 19: 40581
FIRSOV, E. I., Gamma spectra from the (n,γ) reaction in ^{50}Cr, ^{52}Cr, and ^{58}Cr, 19: 41807
FIRSOVA, L. P., The interaction of ^{14}C recoil atoms in binary mixtures, 19: 40627
FISCHER, E. A., Measurement of the isothermal temperature coefficient of reactivity of the Enrico Fermi reactor, 19: 42080 (APDA-NTS-5)
FISCHER, J., Generalized spherical functions for the non-compact rotation groups, 19: 41327 (IC-65/63)
FISHER, C. R., Prog. rpt. on alkali metals evaluation program, 4–6/65, 19: 41001 (AGN-8154)
FISHKOVA, T. Ya., Spherical aberration of combined quadrupole lens with bell-shaped field distribution, 19: 41198
FISK, H. E., Anti-isobar production in $\bar{p}n$ interactions, 19: 41438
FLAMM, H. J., Motion of spheres in smooth rotating drums and applications to the coating of nuclear fuel particles, 19: 40982 (ORNL-3819)
FLATO, M., Conformal-group symmetry of elementary particles, 19: 41392
FLECK, J. A. Jr., Stimulated Brillouin scattering, 19: 41971 (UCRL-7968-T)
FLEMING, Gordon N., Nonlocal properties of stable particles, 19: 41401
FLETCHER, Edward Royce, Nuclear-active component of extensive air showers, 19: 41309
FLETCHER, J. M., Partition coefficients of nitratonitrosylruthenium complexes between nitric acid and TBP phases, 19: 40677
FLINCHBAUGH, David Edward, Inelastic energy loss in collisions, 19: 41277
FLORES, J., Nuclear structure in the 2s-1d shell. I., 19: 41729
FLORES, J., Nuclear structure in the 2s-1d shell. II., 19: 41730
FOELSCHE, Trutz, Ionizing radiations in supersonic transport flights, 19: 40842
FOMICHENKI, K. V., Cardiac metabolism in radiation injuries, 19: 40357 (FTD-TT-65-48, pp 552-3)
FOMICHEV, V. V., Influence of an electric field on luminescence of alkali halide compounds, 19: 40572
FOMIN, A. A., A cylinder in the field of current-carrying conductors,

19: 41151
FOMIN, P. I., Radiative corrections in pair photoproduction, 19: 41500
FONTANA, M. G., Prog. rpt. on stress-corrosion cracking in Fe–Ni–Cr system, 3/17–6/16/65, 19: 40967 (COO-1319-27)
FONTHEIM, Ernest G., Theory of the plasma wave probe, 19: 41948
FOOKES, R. A., Airborne observations of natural radioactivity in the atmosphere, 19: 40790
FORGUE, Vernon, Energy distributions of fission fragments from UO_2 films, 19: 41748
FORMBY, C. L., The strain-ageing and quench-ageing of tantalum, 19: 41042
FORNWALT, D. E., The electron microprobe and light element analysis, 19: 40412 (TID-924)
FORRESTER, A. T., Surface ionization engine development, 19: 40769
FORTESCUE, Peter, Development of the gas-cooled fast reactor concept, 19: 42090 (GA-6132)
FORYS, M., The interaction of ^{14}C recoil atoms in binary mixtures, 19: 40627
FOSSAN, D. B., Gamma rates and intensities; l-forbidden M1 transitions, 19: 41836
FOSSAN, D. B., Investigation of the T = ½ state at 16.97 Mev in ^{9}Be, 19: 41697
FOSTER, B. E., Measurement and application of x- and gamma-ray attenuation to reactor materials evaluation, 19: 42071
FOSTER, D. G. Jr., Method for measuring total cross sections with neutrons having energies from 2.5 to 15 Mev, 19: 41723
FOSTER, K. W., 200-Mwe prototype large SGR—reactor structure design and evaluation, 19: 42094 (NAA-SR-11314)
FOTINO, Mircea, Calibration of beam monitor of Cambridge Electron Accelerator, 19: 41164 (CEAL-1022)
FOURNET, G., Magnetization of type II superconductors, 19: 41613
FRAGA, H., Determination of iodides in the preparations of ^{131}I-Rose Bengal, ^{131}I-Triolein, ^{131}I-Globulin, and ^{131}I-Iodoalbumin and preliminary separation by thin-layer chromatography, 19: 40656 (CEA-tr-X-609)
FRAHM, H. J., Observation of $[505]\frac{11}{2}^-$ Nilsson state as isomer in Dy-159, 19: 41736
FRAME, Roy A., Hydraulic control rod actuators for Kiwi-TNT reactor, 19: 42136 (LA-DC-6941)
FRANC, Z., Preparation of samples of biological material for liquid scintillation measurement of low-energy β-emitters, 19: 40425
FRANCOIS, Bernard, Improvements in or relating to metal oxide powder sintering, 19: 40995
FRANCOVA, V., Preparation of samples of biological material for liquid scintillation measurement of low-energy β-emitters, 19: 40425
FRANCZ, J., Reaction $^{26}Mg(p,p'\gamma)$ mechanism at low energies, 19: 41693
FRANK, L. A., Inward radial diffusion of electrons of greater than 1.6 Mev in the outer radiation zone, 19: 41578
FRANKEL, R. B., Angular distributions of conversion electrons from oriented ^{137m}Ce nuclei, 19: 41679 (UCRL-11462(Rev.))
FRANKL, Laszlo, Neutron flux measurements in core of the VVR-S research reactor, 19: 42183
FRANKLIN, Jerrold, Approximate solution of partial-wave dispersion relations, 19: 41394
FRANTZ, Lee M., Compton scattering of an intense photon beam, 19: 41425
FRANZ, Frank Andrew, Spin relaxation of optically pumped cesium, 19: 41278
FRANZINI, P., Annihilation of antiprotons in hydrogen at rest. III., 19: 41325 (CU-1932-245)
FRASER, P. A., Elastic scattering of low-energy positrons by atomic hydrogen, 19: 41267
FRECK, David Vernon, Improvements relating to measuring apparatus, 19: 40454
FREI, Gerhard, Long-time operational behavior of a high power pressurized water reactor with boron trimming (chemical shim), 19: 42023
FREIDMAN, G. I., On influence of fine splitting of lower level Cr^{+3} in a ruby upon some characteristics of coherent radiation, 19: 40574
FREISE, E. J., Slip systems in single crystals of WC, 19: 41055
FRETWELL, J. H., Automatic liquid nitrogen distribution system for twenty-five cold traps, 19: 41165 (LA-DC-7147)
FREWER, H., Planning and design of the 300-Mw nuclear power station at Obrigheim, 19: 42106
FRIED, Sherman, Odd-parity rotational bands in ^{246}Cm, 19: 41794
FRISCH, O. R., Molecular beams, 19: 41143
FRISCH, Uriel, Propagation of waves in one-dimensional random medium, 19: 41536
FRISKEN, W. R., Backward elastic scattering of high-energy pions by protons, 19: 41456
FRISKEN, W. R., Pion-proton elastic scattering at high momentum transfers, 19: 41455
FRITZ, James S., Cation exchange separation of Mo, W, Nb, and Ta from other metal ions, 19: 40658
FROELICH, H., University of Western Ontario race-track microtron, 19: 41175
FROMM, E., Gas-metal reactions during annealing and melting of niobium and tantalum, 19: 40490
FROSINI, V., Structural modifications in irradiated 1,4 trans-polybutadiene, 19: 40561
FRY, L. M., Fission products in the atmosphere and in rain, 19: 40785 (TID-21224)
FU, Chi-hsi, Ionization characteristics of an electromagnetic ion source, 19: 40861
FUCHS, G., Radiative corrections to inelastic electron scattering with detection in coincidence, 19: 41752
FUJII, T., Analysis of high energy p-p scattering experiment, 19: 41322 (BNL-9231)
FUJIMOTO, Yoichi, An evolutional track of galaxies in L-(L/V) diagram, 19: 41233
FUKAWA, M., Energy dependence of inelastic neutrino cross section in resonance model, 19: 41754
FUKUI, Katsuro, Satellite observations of low-energy heavy cosmic ray nuclei, 19: 41310
FULLER, Dudley D., Design guide for gas-lubricated tilting-pad journal and thrust bearings with special reference to high-speed rotors, 19: 40736 (NYO-2512-1)
FURLAN, G., Symmetry-breaking corrections to weak vector currents, 19: 41547
FURSIKOV, M. M., Optical properties of CaF_2–Dy^{3+}, 19: 40600

G

GABRIEL, J. R., Computation of Moessbauer spectra, 19: 41724
GABUNIA, L. L., Treatment program of penetrating showers of cosmic rays with the energy of 10^{10} to 10^{12} ev, 19: 41290
GADDY, R. H., Automated procedures for lithium, cobalt, and thorium and their applications in nuclear processes, 19: 40405 (CONF-650919-1)
GADDY, R. H., Automated analyses for the characterization of heavy water moderator, 19: 40406 (CONF-650919-2)
GAGARINSKII, Yu. V., Phase transitions of UF_4 and UCl_4, 19: 40481
GAGE, Stephen J., Investigations on nonlinear stability of coupled nuclear systems, 19: 42062
GAILLARD, M. K., Model for PC violation in framework of unitary symmetry, 19: 41522
GAINES, A. L., Nuclear reactor vessels—1965 status, 19: 42122
GALBRAITH, Frank W., Shock spectrum measurements, Project Gnome, 19: 40713 (VUF-2401)
GALKINA, N. N., Calculation of absorbed energy of γ radiation, 19: 41959
GALLAGHER, W. J., Measurement techniques for periodic structures, 19: 41166 (ML-767)
GALLAGHER-DAGGITT, G. E., Automatic control of electromagnetic field in linac resonant cavities, 19: 41167 (NIRL/R/76)
GAMBLE, F. R., Chemical enhancement of superconductivity, 19: 40543
GANDOLFO, F. W., Equipment for fabrication and encapsulation of irradiated UO_2 pellets, 19: 40715 (NAA-SR-Memo-7438)
GANGULY, A. K., Temperature distribution in radioactive solids. II., 19: 42191 (AEET/HP/TH-20)
GANGULY, Nripendra, Angular correlation in (p,pd) reaction on C-12, 19: 41703
GARBER, Floyd Wayne, Low-energy electron and proton transmission in Al and Ag, 19: 41969 (ORNL-TM-1153)
GARBER, R. I., Reestablishment of contacts between fragments of a tungsten microcrystal, 19: 41061
GARDNER, S. D., Interactions of detonation waves in condensed explosives, 19: 42205 (LA-DC-6990)
GARIBASHVILI, D. I., Multichannel analyzer of pulses for ionization calorimeter at capacity memory cells and the system of information output, 19: 40853
GARIBASHVILI, D. I., Multichannel system for analysis of pulses from ionization calorimeters, 19: 40854
GARRETT, W. R., Polarization and exchange effects in slow electron scattering from Li and Na, 19: 41286
GARRIOTT, O. K., Observations of ionospheric electron content using geostationary satellite, 19: 41597
GARRIOTT, O. K., The rate of production of electrons in the ionosphere, 19: 41598
GARVIN, H. L., Prog. rpt. on ion rocket engine development, 1–3/65, 19: 40765 (NP-15309)
GARWIN, R. L., Proton magnetometer and stable oscillator for remote measurement of strong magnetic fields, 19: 40857
GATROUSIS, Christopher, Isomeric cross-section ratios in (p,pn) and heavy-ion neutron-transfer reactions, 19: 41674 (NYO-1930-44)
GATTO, R., Properties of weak amplitudes in broken U(12), 19: 41420
GATTO, R., Spin tests for bosons, 19: 41447

GAUGER, Jeleroy, Anomalous increase in the neutron flux at aircraft altitudes, 19: 41579
GAUME-MAHN, F., Inorganic and organic compounds, 19: 40400
GAVRYUCHENKOV, F. G., Vapor phase complexing of $ErCl_3$–KCl, 19: 40516
GEDALIN, E. V., Anomalous thresholds and mass spectrum of elementary particles, 19: 41351
GEDALIN, E. V., Fluctuations in electron-photon showers generated by high-energy μ mesons, 19: 41355
GEDALIN, E. V., Regge poles Y_1^+ and Y_0^+ and amplitude of KN scattering, 19: 41352
GEDALIN, E. V., Spectrum of bursts generated by high-energy μ mesons in thick absorbers, 19: 41354
GEFFEN, Donald A., Rare decay modes of the η meson as a probe of electromagnetic and strong interactions, 19: 41457
GELFAND, Norman, Strange-particle production in π^+-p collisions, 19: 41418
GEORGE, T. C., Aspects of transportation of radioactive materials, 19: 40812 (SC-RR-65-98, pp 74–8)
GEORGIJEVIC, M. V., Spectral line intensity differences between arc in a tube and a free-burning arc, 19: 41873
GERARDIN, Claude, Study of excitation curves of reaction $^{12}C(t,\alpha_0)^{11}B$, 19: 41706
GERARDO, Henry Alexander, Neutron differential elastic scattering cross sections—angular distributions, 19: 41827
GERASIMOV, A. B., Current oscillations in Ge containing radiation defects, 19: 41105
GERASIMOV, S. B., Electrical and magnetic polarizability of particles due to nonlinear effects of electrodynamics, 19: 41334 (JINR-P-2229)
GERASIMOVA, N. M., Fluctuation of particle number in electromagnetic cascades, 19: 41711
GERRARD, Martha, Equilibrium between cerium and its di- and trivalent ions in a molten eutectic mixture of lithium and potassium chlorides, 19: 40467 (ORNL-tr-578)
GETIYA, M. Sh., Radiation damage in ionic crystals, 19: 41976
GHIRARDI, A., Counting of events from pulsed sources, 19: 40885
GHOSH, R., Gravitation of cylindrically symmetric magnetic field, 19: 41544
GIBBONS, J. H., $^{51}V(p,n)^{51}Cr$ cross section from threshold to 2.25 Mev, 19: 41676 (ORNL-P-1468)
GIBBS, W. R., Finite-sample-size effects in nuclear cross-section fluctuations, 19: 41762
GIBBS, W. R., Investigation of $^{27}Al(\alpha,p)$ reaction by cross-section fluctuation studies, 19: 41761
GIBSON, B. F., P- and d-state contributions to magnetic moment form factors of ^3H and ^3He, 19: 41759
GIBSON, Edward George, Ionization phenomena in gas-particle plasma, 19: 41929
GIBSON, W. M., Direction and energy distribution of charged particles transmitted through single crystals, 19: 41788
GIDAL, George, Experimental study of $K^0_{2\pi}$ decay, 19: 41446
GIFT, E. H., Low-temperature H_2O-cooled and -moderated reactors for desalting, 19: 42097 (ORNL-TM-1152)
GILBERT, A., Deformation and fracture of thoria, 19: 41058
GILBOY, W. B., Neutron scattering studies of K-39, 19: 41737
GILDSETH, Wayne Merlyn, Volume-temperature relationships of some rare-earth chloride solutions, 19: 40523
GILL, K. J., Application of metal coatings on uranium, 19: 40949 (ISC-640)
GILLET, C., Early induction by x rays of discoloration of foliar spots in Maranta Leuconeura, 19: 40362
GILMOUR, A. S. Jr., Plasma generation by the laser illumination of a tungsten surface, 19: 41943
GIMMY, K. L., SRP reactor on-line computer, 19: 42129 (DPSPU-65-30-27)
GIORDANO, P., Analog model for cylindrical nuclear fuel rods, 19: 40740 (RT/ING(64)16)
GIORI, F. A., Plasma generation by the laser illumination of a tungsten surface, 19: 41943
GIOVANNINI, Bernard, Perturbation theory for spin systems, 19: 41559
GIROD, Paul, Mobility spectrum of small radioactive ions of the air, 19: 40787
GISSLEN, J. M., 630A blower feasibility study, 19: 42142 (R62FPD-252)
GITTUS, John Henry, Improvements in or relating to nuclear reactor fuel elements, 19: 40994
GIULIANI, P., Selection of nuclear power station operators, 19: 42098 (RT/PROT(65)24)
GIZON-JUILLARD, Andree, Decay of Er-169, 19: 41705
GLADYSHEVSKII, E. I., Crystalline structure of La_3Si_3, Ce_3Si_3, Pr_3Si_3, Nd_3Si_3, Sm_3Si_3, 19: 40477
GLADYSHEVSKII, E. I., Crystalline structure of La_3Si_2, Ce_3Si_2, and Pr_3Si_2 compounds, 19: 40478
GLADYSHEVSKII, E. I., Crystalline structure of certain ternary compounds in Nb–Co–Si system, 19: 41069
GLADYSHEVSKII, E. N., Scandium monsilicide and its crystal structure, 19: 40479
GLAESER, Wolfgang, Method for studying inelastic scattering of slow neutrons in many-particle systems, 19: 42154 (KFK-261)
GLASGOW, D. W., Method for measuring total cross sections with neutrons having energies from 2.5 to 15 Mev, 19: 41723
GLASHOW, Sheldon L., Decay modes of spin-two mesons, 19: 41461
GLAZUNOV, P. Ya., Unit for gas-phase radiation-induced graft polymerization, 19: 40596
GLENDENNING, Norman K., Shell-model calculation for Po-212, 19: 41735
GLOECKLER, George, Cosmic radiation helium spectrum below 90 Mev per nucleon measured on Imp 1 satellite, 19: 41302
GLOERSEN, P., Performance study of a repetitively pulsed two-stage plasma propulsion engine, 19: 40763 (N64-31453)
GLOWER, Donald D., Experimental reactor analysis and radiation measurements, 19: 42014
GLUSHKOVA, V. B., Studies of Nd_2O_3–ZrO_2. Investigations of regions rich with ZrO_2, 19: 41037
GNAUCK, G., Determination of permanent gases by gaseous chromatography, 19: 40415 (CEA-tr-R-1839)
GNEVYSHEV, M. N., Eleven-year cycle of solar radio emission, 19: 41217
GNEVYSHEV, M. N., Fundamental properties of the 11-year cycle of solar activity, 19: 41214
GOBEN, C. A., A study of the neutron-induced base current component in silicon transistors, 19: 40936 (SC-R-65-912)
GOEFEL, R., MZFR structural installations, 19: 42171
GOGITIDZE, O. A., 340-Liters expansion-condensing chambers used to study nuclear interactions of high energy particles, 19: 40887
GOLD, L., Chemical potentials by direct summation of Fermi-Dirac functions, 19: 40493
GOLD, Raymond, Calculation of spectral distortion due to pile-up effect, 19: 40914
GOLDBERG, D. A., Mössbauer effect resulting from the reaction $^{56}Fe(d,p)^{57}Fe$, 19: 41793
GOLDBERG, E., Pulsed neutron measurements on solid-moderated, enriched-uranium subcritical assemblies, 19: 42051 (UCRL-12013)
GOLDBERG, I., Gauge-invariant quantum electrodynamics. II., 19: 41556
GOLDBERG, Leo, Collisional excitation of autoionizing levels, 19: 41244
GOL'DBERG, V. Z., The reactions $^3He(d,t)2p$ and $^3He(^3He,\alpha)2p$, 19: 41658 (IAE-655)
GOLDFARB, L. J. B., Reactions (d,p) and (t,d) in the Coulomb field, 19: 41739
GOLDHABER, Alfred S., Elastic scattering of 10.5- and 14.5-Mev polarized protons and optical model potential, 19: 41682
GOLDHABER, G., K+p interactions at 2 Bev/c—elastic scattering and total cross sections, 19: 41436
GOLDHABER, S., K+p interactions at 2 Bev/c—elastic scattering and total cross sections, 19: 41436
GOLDMAN, David T., Nuclides and Isotopes, 8th Ed., 19: 41830
GOLLING, E., Spectral analytical trace determination in UO_2 nuclear fuel elements using radiochemical controlled standard probes, 19: 40434
GOLOVANIVSKII, K., Plasma polarization in an electric field, 19: 41906
GOLOVIN, I. N., Obtaining a hot thermonuclear plasma by injection of fast particles into a magnetic trap, 19: 41852 (IAE-676)
GOLOWICH, E., Long-range forces in meson-baryon systems, 19: 41421
GOLUBKOV, A. V., Magnetic susceptibility of SmS, 19: 41060
GOMBOS, Peter, Investigation of an r-f ion source, 19: 40855
GOMOYUNOVA, M. V., Inelastic scattering of electrons by alkali-halide compounds, 19: 40502
GOMOYUNOVA, M. V., Secondary electron emission of alkali-halide compounds, 19: 40503
GONSER, U., Application of Moessbauer effect to biological systems, 19: 40306
GONSER, U., Moessbauer effect in hemoglobin and iron-containing biological compounds, 19: 40305
GOOD, R. C., Prog. rpt. on shielding for ionizing radiation space, final, 9/62–8/63, 19: 41952 (N64-31552)
GOPINATH, D. V., Temperature distribution in radioactive solids. II., 19: 42191 (AEET/HP/TH-20)
GOPINATHAN, K. P., Gamma-gamma directional correlation in ^{143}Pr, 19: 41776
GORBACHEV, V. V., Investigation of thermal vibrations of atoms in Cu by neutron spectrometry, 19: 41996
GORBAN', A. N., Some questions concerning radical-luminescence of crystals, 19: 40480
GORDUS, A. A., Gas-phase reactions of (n,γ) and isomeric transition-activated ^{80}Br with alkanes and haloalkanes, 19: 40618
GORIN, E., Prog. rpt. on evaluation of β radiation as hydrogenation catalyst, 3/62–10/63, 19: 40553 (NYO-2978-34)

CORNEZANO, Claude, Measurements of the characteristics of metallic plasma pulse, 19: 41878
COROKHOV, Yu. V., H_{11} wave penetration through plasma in circular waveguide, 19: 41903
COROWITZ, B., Performance study of a repetitively pulsed two-stage plasma propulsion engine, 19: 40763 (N64-31453)
CORYACHEV, B. I., Automatic betatron γ beam intensity optimization, 19: 41199
COSHELL, J., Two-region lattices, 19: 42048 (MIT-2344-3, pp 125-36)
COTO, Tetsuo, Classical spinning particle model of Dirac particle, 19: 41472
COTO, Tetsuo, Rigid sphere model of elementary particles and the electromagnetic field, 19: 41473
COWEN, Maynard Jr., Device for the measurement of liberated energy in explosion, 19: 40850 (ORNL-tr-588)
COYAL, D. P., π^+ Decay of lambda Li-7, 19: 41412
CRABOWSKI, J., Analytical version of quasiclassical theory of angular distribution of products of one-nucleon transfer reaction, 19: 41805
CRAFF, Gyoergy, Angular distribution of γ rays from fission of U-235, 19: 41722
CRANATSTEIN, V. L., Observation of non-quasistatic plasma surface waves, 19: 41942
CRANATSTEIN, Victor L., Wave propagation along warm plasma columns, 19: 41939
CRANNEMANN, W. W., Prog. rpt. on inverter applications 6/63–5/64, 19: 40845 (N64-33676)
CRANT, R. W., Application of Moessbauer effect to biological systems, 19: 40306
CRANT, R. W., Moessbauer effect in hemoglobin and iron-containing biological compounds, 19: 40305
CRARD, R., Low-frequency impedance characteristics of Langmuir probe in plasma, 19: 41949
CRAY, D. L., Iodine transport and deposition in a high-temperature, helium loop first test series, 19: 40397 (ORNL-TM-1134)
CREDESKUL, S. A., Interaction of charged particles with a piezodielectric crystal, 19: 41990
CREEN, A. E., Reliability considerations for automatic protective systems, 19: 42022
CREEN, H. S., Matrix mechanics, 19: 41568
CREEN, Ira M., Nuclear coupling schemes with a surface delta interaction, 19: 41686
CREEN, J. H., Environmental radioactivity in New South Wales, 19: 40805 (NRS-30)
CREENBERG, D. F., Rare decay modes of the ω-meson, 19: 41386
CREENBERG, O. W., Introduction to N-quantum approximation in quantum field theory, 19: 41552
CREENE, M. Wayne, $E_p = 1.278$ Mev resonance of $^{22}Ne(p,\gamma)^{23}Na$, 19: 41837
CREENE, N. D., Prog. rpt. on heat transfer for space nuclear power, 12/64–2/65, 19: 40741 (SAN-409-23)
CREENWOOD, G. W., Mechanism of cavitation in Mg during creep, 19: 41057
CREGORY, E. H., Acoustic excitation of nuclear spin resonance in single-crystal Ta, 19: 41792
CRIBANOVA, I. N., Phospho-organic complexing resins, 19: 40668
CRIEM, H. R., Start broadening of ionized nitrogen lines in a T-tube plasma, 19: 41941
CRIFFY, T. A., Electron scattering from nuclear magnetic moments, 19: 41694
CRIGOLASHVILI, T. S., Multichannel analyzer of pulses for ionization calorimeter at capacity memory cells and the system of information output, 19: 40853
CRIGOLETTO, A., Spin and parity of 1320 Mev $p\pi$ resonance, 19: 41368
CRIGOR'EV, A. I., Ammoniated Be, Mg, Ca, Al, Sc, and Y acetates, 19: 40507
CRIGOR'EV, A. T., Constitution diagrams of systems V–Ta–Nb and V–Ta–Mo, 19: 41036
CRIGOREV, V. I., Description of stationary state interactions, 19: 41495
CRIGOR'EV, V. N., Plasmoid structure in an em accelerator, 19: 41908
CRIGOROV, N. L., Origin of high-energy pions, muons, and photons, 19: 41291
CRILLI, M., Lambda^0 polarization from $\gamma + p \rightarrow \Lambda^0 + K^+$ at 950 to 1050 Mev, 19: 41367
CRITSYUK, Yu. N., Neutron emission from ^{233}U, ^{235}U, and ^{239}Pu fission fragments, 19: 41681 (ANL-Trans-205)
CRITZNER, G., Polarographic behavior of lanthanoids in dimethylsulfoxide and dimethylformamide, 19: 40681
CRJEBINE, T., Cosmic dusts. Recent C.E.A. studies, 19: 41113
CRODZINS, L., Moessbauer scattering: The gyromagnetic moments of first 2^+ states in ^{182}W and ^{186}W and ^{186}Os and ^{188}Os, 19: 41791
CROENIG, H., Investigations on an inverse pinch, 19: 41904
CROMES, D., Determination of energy spectrum from time behavior of decay of quantum mechanical system, 19: 41532
CROMOV, A. V., Investigation of nuclear reactions of helium-3 with carbon, 19: 41663 (JINR-P-2184)
CROMOV, B. V., Reaction of $U(SO_4)_2 \cdot 4H_2O$ with tri-n-octylamine sulfates and bisulfates, 19: 40688
CROMOV, K. Ye., Three-quasiparticle state in ^{165}Er, 19: 41667 (JINR-P-2239)
CROMOV, K. Ye., Two-hour (7.7 ksec) isomer of ^{169}Lu, 19: 41803
CROOM, D. E., Particle identification by pulse height correlation in a range telescope, 19: 41527
CROSS, V. F., Measurements of bunch-injector output parameters, 19: 41188
CROSS, V. F., Measurements of extension of electron bunch, 19: 41189
CROSSI, G., Synthesis of some alkyl benzylamines of high molecular weight of the type $C_6H_5–CH_2–NH(R_1)(R_2)$, 19: 40540 (RT/CHI(64)16)
CROSSO, J., Optical techniques for electron probe analysis, 19: 40951 (NRL-6290)
CROTHE, Karl Heinz, X-ray fluorescence spectral analysis in micro amounts. II., 19: 40440
CRUBELASHVILI, G. A., Properties of component penetrating atmospheric showers, 19: 41297
CRUEN, Arnold E., Zero-energy measurements on core of the multi-purpose research reactor, 19: 42186
CRUNZWEIG-GENOSSAR, J., Description of relaxation processes in nuclear magnetic resonance, 19: 41751
CRUSHIN, V. F., Effect of design parameters on the characteristics of Cerenkov's shower gamma-spectrometers, 19: 40897
CRUZIN, P. L., Investigation of thermal vibrations of atoms in Cu by neutron spectrometry, 19: 41996
GSCHNEIDNER, K. A. Jr., Gold-rich rare-earth-gold solid solutions, 19: 41062
GSCHNEIDNER, Karl A. Jr., Application of vacuum metallurgy in the purification of rare-earth metals, 19: 40948 (IS-1195)
GSCHNEIDNER, Karl A. Jr., Heat contribution due to thermal excitation of 4F electrons of some di- and tri-valent lanthanide elements, 19: 40457 (IS-1156)
GUDZENKO, L. I., Model of cyclic solar activity, 19: 41215
GUEDES DE CARVALHO, R. A., Electrophoresis of lanthanides, Sc, Th, U and Zr in glycolic acid, 19: 40671
GUIDONI, P., Existence and properties of a non-strange meson of mass 1500 Mev/c^2, 19: 41459
GUILLIER, M.-T., Age measurements using the C-14 method, 19: 40795
GULYAMOV, M., Reaction $^4He(^3He,n)^6Be$, 19: 41659 (IAE-836)
GUNTER, Edgar J. Jr., Design guide for gas-lubricated tilting-pad journal and thrust bearings with special reference to high-speed rotors, 19: 40736 (NYO-2512-1)
GUNTHER, Leon, Magnetic impurity effect on superconductor transition temperature—extension of Nakaoka's theory, 19: 41608 (MIT-QPR-57, pp 59-65))
GUNYE, M. R., Parity assignments in ^{200}Hg from linear polarization correlation of thermal neutron capture γ rays, 19: 41846
GUON, J., Equipment for fabrication and encapsulation of irradiated UO_2 pellets, 19: 40715 (NAA-SR-Memo-7438)
GUREVICH, A. V., Hypersonic body motion through rarefied plasma, 19: 41894
GURR, H. S., Evidence for high-energy cosmic-ray neutrino interactions, 19: 41306
GUSEV, V. D., Determination of effective collision frequency in the ionosphere, 19: 41574 (FTD-TT-65-101)
GUSEVA, N. K., Roentgenoluminescence and thermoluminescence of Tl-activated NaI crystal phosphors, 19: 40568
GUSTAFSON, Daniel Ray, Positron annihilation in sodium tungsten bronze, 19: 41158
GUTMAN, Thomas, Progress report on a class-II container for low-assay uranium compounds, 19: 40819 (SC-RR-65-98, pp 330–56)
GUTMANN, V., Polarographic behavior of lanthanoids in dimethylsulfoxide and dimethylformamide, 19: 40681
GUYON, Paul-Marie, Isotopic effects in dissociation of triatomic molecules by electron collision. III., 19: 40581
GUZHAVIN, V. V., Resolving solid-angle problem in electromagnetic cascade theory, 19: 41359
GUZHOVSKII, I. T., Motion of plasma bunches in a field-free space, 19: 41856 (NP-15205)
GWIN, R., Measurement of the U-235 neutron capture-to-fission ratio from 3.25 ev to 1.8 kev, 19: 41749

H

HAAS, K., Certain new Asenazo III analogs and their analytical properties, 19: 40426

HADDOCK, F. T., Antenna impedance in a plasma: problems relevant to radioastronomy measurements from space vehicles, 19: 41212
HAEBERLI, W., Polarization of protons scattered by carbon, 19: 41731
HAEN, Pierre, Transport properties of Nd nitride at low temperature, 19: 41973
HAESELER, Guenther, Thermal decomposition of the chlorohydrates of the rare earth elements, 19: 40489
HAFFEMAYER, Marcel, Nuclear reactor control rod operating device, 19: 42033
HAI, F., Frequency modulation of large cavities, 19: 40723
HAJDUKOVIC, S., Changes in the growth of progeny of male rats exposed to low x-ray doses in the infantile period, 19: 40365
HAKKILA, E. A., X-ray fluorescence spectrometric determination of plutonium in uranium–plutonium–manganese alloys, 19: 40408 (LA-3333)
HALL, Lourence S., Note on electrostatic instabilities in a plasma with anisotropic velocity distribution, 19: 41866 (UCRL-12052)
HALLIDAY, Dixon Brydsen, Improvements in or relating to nuclear reactors, 19: 42066
HALTEMAN, E. K., Morphological characteristics of coprecipitated $(U,Pu)O_2$ powders by electron microscopy, 19: 41024 (NUMEC-2389-5)
HAMADA, Tetsuji, Study on radiocarbon dating. I., 19: 40920
HAMAGUCHI, Hiroshi, Rare earth separation by anion exchange chromatography in salt solution, 19: 40659
HAMAMOTO, Yoshito, The effects of preirradiation on the activities of solid acidic catalysts, 19: 41099
HAMER, W. J., Testing of 10-ton capacity UF_6 shipping containers, 19: 40824 (SC-RR-65-98, pp 580–608)
HAMILTON, J. H., Energy levels in Xe-132, 19: 41745
HAMILTON, J. H., Low-energy transitions in I-132 decay, 19: 41743
HAMM, R. N., Optical properties of vacuum-evaporated films of Cd, Tl, and Zn, 19: 42213 (ORNL-TM-1164)
HAMMOND, J. M., Prog. rpt. on ion rocket engine development, 1–3/65, 19: 40765 (NP-15309)
HAN, M. Y., Three-triplet model with double SU(3) symmetry, 19: 41406
HANITZ, F., Splitting of plasma shock waves in accelerating tube, 19: 41880
HANNA, S. S., States in ^{12}C between 16.4 and 19.6 Mev, 19: 41688
HANSEN, A. I., Effects of long-term operation on SRE Na system components, 19: 42096 (NAA-SR-11396)
HANSEN, N. J. Sigurd, Observation of $[505]\frac{11}{2}^-$ Nilsson state as isomer in Dy-159, 19: 47136
HANSEN, P. G., High-energy transitions in I-132 decay, 19: 41744
HANSON, A. O., Neutron spectra from Bi produced by monoenergetic γ rays, 19: 41834
HANSON, C. L., Operating trans-curium element radiochemistry facility, 19: 40719 (UCRL-7844-T)
HANSON, C. L., Remotely-operated trans-plutonium chemical process cells, 19: 40720 (UCRL-7845-T)
HANSON, W. C., Fallout radionuclides in Alaskan food chains, 19: 40780 (BNWL-SA-242)
HANSTEAD, P. D., Automatic ultrasonic inspection of nozzle welds in nuclear reactor pressure vessels, 19: 42025
HANSTEEN, J. M., Study of the $^6Li(p,2p)^6He$ reaction using cluster model wavefunctions, 19: 41842
HANSTOCK, R. F., Development of radiographic and ultrasonic methods of inspecting nuclear reactor pressure vessels, 19: 42024
HARA, Osamu, Rigid sphere model of elementary particles and the electromagnetic field, 19: 41473
HARADA, Kichinosuke, Shell-model calculation for Po-212, 19: 41735
HARARI, H., Electromagnetic interactions and the subgroups of SU(6), 19: 41424
HARBOTTLE, Garman, Novel synthesis of carrier-free ^{106}Ru-labeled ruthenocene, 19: 40634 (BNL-8405)
HARDY, Lyndon M., Branching ratios for decays of the f^0, A_2, and K*(1400) mesons, 19: 41460
HARMAN, Randall, Energy distributions of fission fragments from UO_2 films, 19: 41748
HARRINGTON III, J., Measurements of poisoned lattices, 19: 42046 (MIT-2344-3, pp 109-14)
HARRIS, I. R., Rare earth intermediate phases. I., 19: 41041
HARRIS, J. E., Nucleation of creep cavities in magnesium, 19: 41063
HARRIS, R. A., Reactor analysis: measured and calculated spectra and average reaction rates, 19: 42037 (BNWL-95, pp 4–17)
HARRISON, R. W., Prog. rpt. in alkali metal corrosion, 12/64–3/65, 19: 40970 (NASA-CR-54390)
HART, F. A., Lanthanide complexes. III., 19: 40487
HARTECK, P., Promotion of chemical processes with reactor radiation, 19: 40559
HARTLE, Richard Eastham, Techniques for treating fully ionized two-particle plasma equations, 19: 41931
HARTSHORN, W. R., SRP reactor on-line computer, 19: 42129 (DPSPU-65-30-27)
HASEGAWA, Hiroichi, An evolutional track of galaxies in L-(L/V) diagram, 19: 41233
HASSAN, Sayed D., Statistical theory of homogeneous hydromagnetic turbulence, 19: 41127 (SUDAER-238)
HATUDA, Zin'itiro, Trial method of determining uranium and thorium content in rocks, 19: 40432
HAUBOLD, Karl, Approximate calculation of the classical two-particle collision operator, 19: 41131
HAUFF, A., Design and function of hydraulically actuated ultra vacuum through-way valve, 19: 40776
HAUSER, O., Radiation saturation and defect structure in solids, 19: 41102
HAUSMAN, Harshel J., $(p,p'\gamma)$ Angular correlations in ^{48}Ti, 19: 41690
HAWK, R. W., Remotely-operated trans-plutonium chemical process cells, 19: 40720 (UCRL-7845-T)
HAWKE, J. G., ESR spectra of γ-irradiated polycrystalline glycolic acid, 19: 40592
HAYBRON, R. M., Excitation of first level of ^{12}C by 156-Mev protons, 19: 41675 (ORNL-P-330)
HAYES, Dennis B., Compilation of crater data, 19: 40711 (SC-DC-65-220)
HAYMANN, P., Oxidation of iron surfaces under ion bombardment, 19: 40973
HEADY, H. H., 14-Mev-neutron production of isomeric states for several rare-earth elements, 19: 41781
HECHT, K. T., Five-dimensional quasispin, 19: 41687
HECHT, K. T., Groups R(5) and R(8) and generalized quasi-spin in nuclear structure problems, 19: 41839
HECKMAN, R. C., Apparatus for measurement of the Hall effect in metals, 19: 42217 (SC-RR-65-325)
HECKROTTE, Warren, Relation between dichotron and negative mass instabilities, 19: 41180
HEFLINGER, Lee, Magnetic induction plasma engine, 19: 40762
HEIDEMAN, H. G. M., Inelastic scattering of electrons by helium, 19: 41264
HELD, Chr., Planning and design of the 300-Mw nuclear power station at Obrigheim, 19: 42106
HELLER, Leon, Pions, muons, and nuclear structure, 19: 41671 (LADC-6186)
HENCK, Roland, Study of γ radiations of Ta-182, 19: 41704
HENDERSON, Malcolm C., Thermal relaxation in oxygen with H_2O, HDO, and D_2O vapors as impurities, 19: 40483
HENDRICKS, Shirley J., An evaluation of the main geomagnetic field 1940–1962, 19: 41586
HENGLEIN, A., Collision mechanism of bimolecular reactions. I., 19: 41250
HENGLEIN, A., Collision mechanism of bimolecular reaction. II., 19: 41251
HENGLEIN, A., Collision mechanism of bimolecular reactions. III., 19: 41252
HENNEL, Jacek W., Nuclear magnetic relaxation, 19: 40499
HENNINGS, K. E., New single-walled high-vacuum evaporator with very low cycling times, 19: 40774
HENSHAW, Paul S., Conference on late irradiation effects, USAEC, Washington, 12/63, 19: 40352
HERMAN, Jan A., Polymerization by x rays of mixtures of vinyl chloride and noble gases, 19: 40584
HERRING, Gary P., Reduced three-body problem: a generalization of the classical restricted three-body problem, 19: 41205 (N64-31725)
HESS, Richard I., Branching ratios for decays of the f^0, A_2, and K*(1400) mesons, 19: 41460
HESS, W. N., Origin of outer-belt protons. I., 19: 41577
HETHERINGTON, J. H., Low-energy Λ-d scattering and the hypertriton with separable potentials, 19: 41419
HETWER, K., Response of semiconductor surface barrier detectors to fission fragments, 19: 40901
HEYMANN, Dieter, Cosmogenic and radiogenic He, Ne, and Ar in amphoteric chondrites, 19: 41225
HICKAM, W. M., Solid solubility limits of Y and Sc in the elements W, Ta, Mo, Nb, and Cr, 19: 41050
HICKS, Harry G., Experimental approach to nature and characteristics of primary fission fragments, 19: 41771
HIGGINS, Irwin R., Radioactive decontamination of milk, 19: 40697
HIIDA, Kichiro, Cp violation and Pt invariance, 19: 41470
HIKAWA, Ikuko, Rare earth separation by anion exchange chromatography in salt solution, 19: 40659
HILL, Ann Gertrude, Separation of amines by ligand exchange. III., 19: 40648 (COO-499-2)
HILL, C. W., Computer programs for shielding problems in manned space vehicles, 19: 41954 (NP-15338)
HILL, D. G., ρ and ω production in π^+d interactions at 1.7 Bev/c,

19: 41528
HILL, John H., Spectrophotometric determination of trace amounts of Ta, 19: 40414 (UCRL-7967)
HILL, R. W., Remote radiation monitoring at the Nevada Test Site, 19: 40876 (NVO-162-5(Rev.))
HILLEMANN, Howard H., Light-tight, dust-free drying box for autoradiography, 19: 40304
HINKLE, James G., Design guide for gas-lubricated tilting-pad journal and thrust bearings with special reference to high-speed rotors, 19: 40736 (NYO-2512-1)
HNS, A. G., Development of a process for manufacturing ZPR-III U–Pu–Mo test fuel elements, 19: 40978 (ANL-6955)
HINTZ, Norton M., (p,t) Ground-state L = 0 transitions in the even isotopes of Sn and Cd at 40 Mev, N = 62 to 74, 19: 41689
HIRSCH, Robert Louis, Spatially resolved energy states of a high density gaseous plasma, 19: 41934
HIRSCHMAN, Albert, Prog. rpt. on radiation effects on calcifying mechanism of epiphyseal cartilage, final, 6/65–2/62, 19: 40351 (NYO-1913-1)
HIRTH, J. P., Conference on deformation twinning, Gainesville, 3/63, 19: 41076
HIRTH, J. P., Prog. rpt. on stress-corrosion cracking in Fe–Ni–Cr system, 3/17–6/16/65, 19: 40967 (COO-1319-27)
HISATAKE, Kozuo, Half-life measurements in ^{101}Rh and ^{102m}Rh, 19: 41719
HITCH, James W., Development of safety performance criteria and tests standard for radioisotope sealed sources and devices, 19: 40802 (CONF-650616-5)
HNATOWICZ, V., Two-hour (7.7 ksec) isomer of ^{168}Lu, 19: 41803
HOAG, Ethan D., Critical current degradation in wide samples of high field strip superconductors, 19: 41639
HOCKENBURY, R. W., Measurement of the U-235 neutron capture-to-fission ratio from 3.25 ev to 1.8 kev, 19: 41749
HOFFMAN, B. M., Chemical enhancement of superconductivity, 19: 40543
HOFMEISTER, E., Stellar evolution. I., 19: 41210 (N64-25282)
HOFSTADTER, R., π-α scattering and the pionic form factor, 19: 41379
HOHMUTH, K., Approximation formulas for fluorescence yields of the L_2 and L_3 shells, 19: 41245
HOHMUTH, Karl, Decay of Ce-136, 19: 41700
HOLDEMAN, J. T., Remarks on charged-particle scattering, 19: 41763
HOLLADAY, W. G., Poles and resonances in the process $\pi^+ + p \to \Sigma^+ + K^+$, 19: 41427
HOLLANDER, J. M., Use of semiconductor detectors for internal-conversion coefficient measurements, 19: 40880 (UCRL-16035)
HOLLSTEIN, Martin, Isobaric order of particle range and range of fragments from thermal fission of Pu-239, 19: 41668 (KFK-306)
HOLT, E. H., Microwave measurement of the probability of collision of low energy electrons in nitrogen, 19: 41944
HOLT, P. D., The response of photographic film dosemeters to high energy gamma radiation, 19: 40909
HOLWAY, Lowell H. Jr., Ambipolar diffusion in the geomagnetic field, 19: 41585
HOLZER, R., MZFR fuel elements—design, construction, and research, 19: 42165
HONDLIK, J., Preparation of samples of biological material for liquid scintillation measurement of low-energy β-emitters, 19: 40425
HONES, Edward W. Jr., Adiabatic motion of auroral particles in model of electric and magnetic fields surrounding the earth, 19: 41583
HOOT, C. G., Excitation of isobaric analog states in medium-weight nuclei by (d,p) reaction at 28 Mev, 19: 41772
HOPKINS, Donald R., Regulatory packaging standards, 19: 40811 (SC-RR-65-98, pp 45–54)
HOPKINS, H. W. K., Anti-isobar production in $\bar{p}n$ interactions, 19: 41438
HOPKINS, H. W. K., ρ and ω production in π^+d interactions at 1.7 Bev/c, 19: 41528
HORN, D., $SU(6)_w$ photoproduction and meson-baryon scattering amplitudes, 19: 41462
HOSAKA, Yoshimbo, Reaction of ethylene with phosgene induced by γ radiation, 19: 40589
HOSHINO, Tsutomu, Measurement of migration area and multiplication factor of UO_2–H_2O lattice, 19: 42053
HOSKING, R. J., New instabilities due to Hall effect, 19: 41893
HOUSTON, B. J., Investigation of manufacture of aggregate and riprap by nuclear means, 19: 40709 (PNE-5003)
HOUSTON, C. R., The measurement of surface contamination of high-purity beryllium samples, 19: 40453
HOUSTON, D. H., Neutron-spectrum measurements in H_2O and D_2O, 19: 41646
HOUSTON, M. D., Sintering behavior of PuO_2, 19: 40981 (NUMEC-2389-6)
HOWARD, A. J., Collective representation of lower lying states in ^{21}Ne, ^{21}Na, and ^{23}Na, 19: 41757
HOWARD, C. L., Prog. rpt. on Garigliano reactor, 7/65, 19: 42092 (GEAP-4909)
HOWES, J. E., Development of an improved method of sampling and analysis for atmospheric iodine, 19: 40402 (BMI-X-10137)
HOY, Gilbert R., Moessbauer studies of inequivalent ferrous ion sites in ferrous formate, 19: 40542
HREHUSS, Gyula, Angular distribution in ^{12}C(d,p)^{13}C reaction, 19: 41721
HSIEH, H. C., Investigation of nonlinear interaction phenomena in the ionosphere, 19: 41572 (NASA-CR-258)
HUANG, Sueі-rong, Radiolysis of alkali metal sulfates, 19: 40610
HUBER, D. A., Heat transfer in organic-cooled reactors, 19: 42110
HUBNER, R. S., Analysis of neutron transmission through slabs of LiH, 19: 41642 (NAA-SR-10853)
HUFFMAN, D., Prog. rpt. on integral neutron thermalization, 3/31/65, 19: 41640 (GA-6323)
HUGHEL, Thomas J., Symposium on liquids, Warren, Mich., 9/63, 19: 40538
HUGHES, M. P., Radio brightness contours of 3C273, 19: 41226
HUGHES, T., Prog. rpt. on stable isotope studies, annual, 9/15/64–7/15/65, 19: 40460 (NYO-3462-1)
HULL, D., Deformation and fracture of tungsten single crystals, 19: 41046
HULLIGER, F., $EuGd_2S_4$, a new ferromagnetic semiconductor, 19: 40496
HULUBEI, H., Reaction ^{26}Mg(p,p'γ) mechanism at low energies, 19: 41693
HUMES, Richard M., (p,p'γ) Angular correlations in ^{48}Ti, 19: 41690
HUMMEL, H. H., Effect of resonance correction to group flux in fast-reactor Doppler-effect calculation, 19: 42057
HUMPHREYS, L. L., Hot-cell studies on the separation of Pa-233 from irradiated thoria by coprecipitation with MnO, 19: 40644 (BNWL-78)
HUNSUCKER, Robert D., Determination of the electron density within discrete auroral forms in the E region, 19: 41591
HUNT, Larry H., Activation analysis for ^{18}O isotope abundance utilizing recoil protons, 19: 40419
HUNT, Stanley Ernest, Improvements relating to measuring apparatus, 19: 40454
HUNTER, James Hardin Jr., Galaxy formation in steady-state universe, 19: 41239
HUPIN, Pierre M., Polymerization by x rays of mixtures of vinyl chloride and noble gases, 19: 40584
HURLEY, R. G., X-ray fluorescence spectrometric determination of plutonium in uranium–plutonium–manganese alloys, 19: 40408 (LA-3333)
HURLEY, T. J., SRP reactor on-line computer, 19: 42129 (DPSPU-65-30-27)
HUTTON, P. H., Industrial noise control is practical, 19: 40806 (RL-SA-37)
HUYNH, V. C., Treatment of capture gamma ray spectra obtained with the aid of a central crystal in association with an annular crystal, 19: 40896
HUZIMURA, Ryoitiro, Radiation quenching of radio- and radiothermoluminescence of ZnS phosphors. I., 19: 40587
HWA, Rudolph C., Bootstrap and SU(3) assignment of 2$^+$ mesons, 19: 41402
HWANG, R. N., Effect of resonance correction to group flux in fast-reactor Doppler-effect calculation, 19: 42057
HYMOWITZ, Theodore, Studies on guar-cyamopsis tetragonoloba (L.) taub, 19: 40376

I

IANDELLI, A., Atomic size of rare earths in intermetallic compounds, 19: 41040
IANNUZZI, M., Saturation and short-time behavior of unstable ion waves, 19: 41890
IDDINGS, C., Breakdown of unitary octet symmetry in a nonlinear spinor model of elementary-particle theory, 19: 41395
IDDINGS, C., Meson states in a nonlinear spinor model of elementary-particle theory with spontaneous symmetry breakdown, 19: 41396
IGI, K., High-energy behavior of the real part of the scattering amplitude, 19: 41376
IJAZ, Mujaddid Ahmed, Proton-proton collisions at 2.0 Bev, 19: 41503
ILIESCU, N., Niobium and Rb neutron resonances and radiation widths of medium-mass nuclei, 19: 41727
ILMAS, E. R., Photon multiplication in crystals. II., 19: 40495
IMHOF, W. L., Investigation of the T = ½ state at 16.97 Mev in ^{9}Be, 19: 41697
IMPASTATO, Fred J., Isotopic exchange reactions of difluoramine with deuterium oxide and trifluoroacetic acid, 19: 40537
INGRAM, Blanche, McKelveyite, a new hydrous U carbonate mineral, 19: 40799
INOUE, Miyoko, Rectification of apparent effect of an electric field on radiochemical polymerization of solid acryloaitrile, 19: 40582
INTEMANN, Robert Louis, K electron ejection accompanying nuclear K-capture, 19: 41825
INUISHI, Yoshio, Moving striation of plasma in a longitudinal magnetic field, 19: 41888
IORI, I., Reaction (n,d) on ^{63}Cu and ^{65}Cu isotopes at 14 Mev, 19: 41755

IPPOLITOVA, E. A., Enthalpy of the γ-UO_3 reaction with HF and enthalpy of formation of γ-UO_3, 19: 40521
ISBIN, H. S., Recombination of hydrogen and oxygen in the presence of water vapor under the influence of radiation, 19: 40549 (COO-1032-1)
ISENHOUR, T. L., Computer programs to optimize times of irradiation and decay in multielement activation analysis, 19: 40451
ISHCHUK, V. A., Investigation of interaction of oxygen with tungsten by electron-stimulated desorption, 19: 41103
ISHIDA, Koji, Cation-exchange separation of Pa-233 from irradiated Th, 19: 40673
ISHIDA, Koji, Rare earth separation by anion exchange chromatography in salt solution, 19: 40659
ISHIDA, Shin, Possible choice of fundamental particle models, 19: 41476
ISHIKAWA, Sumio, Chemical reaction by ionizing radiation. III., 19: 40599
ISHIMATSU, Toshiyuki, Alpha particle groups from deuteron bombardment of ^{16}O and ^{40}Ca, 19: 41720
ISLAM, M. M., Model for dynamical calculation of inelasticity, 19: 41403
ISMAILZADE, I. G., Determination of Curie point of ferroelectrics $YMnO_3$ and $YbMnO_3$, 19: 41059
ISPIRYAN, K. A., Emission of ultra-high energy μ mesons, 19: 41295
ITO, D., High-energy scattering by exchange of Markov's particle, 19: 41383
ITO, D., Nucleon form factor and large-angle p-p scattering, 19: 41385
ITO, Toshio, A consideration to the design of MHD generator, 19: 41316
IVANENKO, I. P., Inverse problem in cascade theory, 19: 41710
IVANENKO, I. P., Resolving solid-angle problem in electromagnetic cascade theory, 19: 41359
IVANNIKOV, A. T., Effect of N,N,N',N'-tetra-acetic acid 2,2'-diamino-diethylsulfide (DDSTA) on the excretion of uranyl nitrate and course of uranium poisoning in rats, 19: 40348
IVASCU, M., Reaction $^{26}Mg(p,p'\gamma)$ mechanism at low energies, 19: 41693
IZRAEL', Yu. A., Determination of the fractioning coefficients and the biological availability of the products of nuclear explosions in radioactive fallouts, 19: 40786 (JPRS-30500)

J

JACKSON, Ross Jones, Structures and transformation kinetics of phases in U–Re alloy, 19: 41079
JACKSON, W. D., Review of MHD power generation, 19: 41320
JACOB, M., Systematics of angular and polarization distributions in three-body decays, 19: 41409
JACOBS, G., Collision mechanism of bimolecular reactions. I., 19: 41250
JACOBS, Lawrence D., Branching ratios for decays of the f^0, A_2, and K*(1400) mesons, 19: 41460
JACOBSON, R. L., Study of ion-bombardment damage on a Ge(111) surface by low-energy electron diffraction, 19: 41258
JACOBSON, Robert A., The reduced cell and its crystallographic applications, 19: 41963 (IS-1141)
JAFFRIN, Michel Yves, Structure of a plasma shock wave, 19: 41928
JAGODIV, V., Synthesis of some alkyl benzylamines of high molecular weight of the type $C_6H_5-CH_2-NH(R_1)(R_2)$, 19: 40540 (RT/CHI(64)16)
JAMES, E. L., Surface ionization engine development, 19: 40769
JANES, G. S., Electron plasma-experiment theory and applications, 19: 41863 (NP-15302)
JANOVICZ, W., MZFR—completion of the construction, 19: 42176
JARRETT, A. A., Sodium fires and release characteristics of particulates and fission products, 19: 40803 (NAA-SR-Memo-9719)
JASTRAM, P. S., Energy levels of ^{155}Dy, 19: 41847
JEANPIERRE, G., Industrial manufacture of fuel elements in France, 19: 42070
JEHN, H., Gas-metal reactions during annealing and melting of niobium and tantalum, 19: 40490
JELINEK, T. M., Optical properties of vacuum-evaporated films of Cd, Tl, and Zn, 19: 42213 (ORNL-TM-1164)
JENKINS, R. J., Calorimeters and radiometers for measurement of large thermal irradiances, 19: 40882 (USNRDL-TR-839)
JENKINS, R. O., Conductivity induced by electron bombardment, 19: 41097
JENKINS, T. L., Evidence for high-energy cosmic-ray neutrino interactions, 19: 41306
JENNINGS, A. S., Behavior of actinides and fission products in TBP and DABP, 19: 40645 (CONF-650918-1)
JENNINGS, C. W., Wear testing of plated coatings, 19: 42216 (SC-DR-65-269)
JENSEN, Duane C., An evaluation of the main geomagnetic field, 1940–1962, 19: 41586
JEWELL, R. W. Jr., Neutron-capture γ-ray studies of low-lying ^{52}V levels, 19: 41725
JEWETT, R. P., Application of thin-film electron microscopy to refractory metal processing. Final report, 19: 41015 (MIL-TDR-64-282)
JIH, T., Dispersion of radioisotopes caused by transport fires, 19: 40830 (SC-RR-65-98, pp 719–22)
JIN, T., Studies on fire resistivities of radioisotope containers, 19: 40831 (SC-RR-65-98, pp 723–31)
JODRA, L. G., Determination of mass transfer coefficients for the liquid film in the system UO_2SO_4–anion exchange resins, 19: 40660
JOHN, W., Neutron-capture γ-ray studies of low-lying ^{52}V levels, 19: 41725
JOHNSON, C. M., Chromatograph for analysis of highly reactive and corrosive compounds, 19: 40407 (KY-485)
JOHNSON, Coates Richard, Transition paths of μ^- mesons captured in solid Li, 19: 41823
JOHNSON, E. B., Safety in handling fissionable materials, 19: 40840
JOHNSON, Elizabeth, Broken symmetric couplings for decuplet decays into baryons and pseudoscalars, 19: 41399
JOHNSON, Noah R., Energy levels in Xe-132, 19: 41745
JOHNSON, Noah R., High-energy transitions in I-132 decay, 19: 41744
JOHNSON, O. E., Some (d,α) differential cross sections for ^{23}Na, ^{27}Al, and ^{31}P at about 9.3 Mev, 19: 41684
JOHNSON, R. P., Pre-critical electrical and mechanical testing of reactor critical assembly, 19: 42155 (NAA-SR-Memo-3196)
JOHNSTON, K., Calorimetric determination of fission product heating in fast reactor Pu fuel, 19: 42114
JOHNSTON, K. W. H., The transport container for irradiated fuel from civil power stations in the UK, 19: 40829 (SC-RR-65-98, pp 711–18)
JONES, B. D., Angular correlations between fast Σ hyperons and fast protons, 19: 41494
JONES, F. Llewellyn, Auger ejection of electrons from silver, 19: 41270
JONES, W. D., Collisionless ion-wave propagation and the determination of the compression coefficient of plasma electrons, 19: 41892
JONSSON, A., Improvements to theory of resonance escape in heterogeneous fuel. II., 19: 42055
JORDAN, B., Production of particles at small angle in p-p and p-nucleus collisions at 20 Bev, 19: 41324 (CERN-65-14)
JORDAN, E. C., Electromagnetic theory and antennas, 19: 40862
JORGENSON, G. V., Sputtering studies of insulators by means of Langmuir probes, 19: 41257
JOSEPH, D. W., Simple alternatives to SU(6), 19: 41435
JOSEPH, Robert Roderick, Solid solubility of magnesium in the close-packed modifications of some rare-earth metals, 19: 41011 (IS-T-15)
JOSHI, G. C., Self-consistent determination of the ρ-meson Regge-pole parameters, 19: 41370
JOUBERT, S. M., Studies with DL-alanine-2-^{14}C of interaction of ethanol metabolism with pathways of hepatic gluconeogenesis in the rat, 19: 40308 (BNL-8379)
JOVANOVIC, M. M., Influence of repeated ^{60}Co γ irradiation on urinary excretion of taurine in rats, 19: 40364
JOVIC, V., Heat transfer through vertical annular gas layer, 19: 40747
JULIEN, J., Treatment of capture gamma ray spectra obtained with the aid of a central crystal in association with an annular crystal, 19: 40896
JURNEY, E. T., High-energy γ spectrum of thermal neutron capture in holmium, 19: 41670 (LA-DC-7097)

K

KABIR, P. K., Test for particle-mixture theories of $K^0 \to 2\pi$ decay, 19: 41454
KAGANOV, M. I., Interaction of charged particles with a piezodielectric crystal, 19: 41990
KAGI, Jakob, Nuclear power plant, 19: 42126
KAHALAS, Sheldon L., Excitation of low-frequency EM waves in earth-ionosphere cavity by high-altitude nuclear detonations, 19: 41581
KAHN, Peter B., Study of generalized level density by the methods of differential-recurrence equations, 19: 41655 (BNL-934)
KAHN, S., Prog. rpt. on fissiochemical process development. I., 12/2/63–6/30/64, 19: 40547 (AGN-8137(Vol.I))
KAHN, Steve, Energy distributions of fission fragments from UO_2 films, 19: 41748
KAKAURIDZE, D. B., Multichannel system for analysis of pulses from ionization calorimeters, 19: 40854
KAKHIDZE, G. M., Multichannel system for analysis of pulses from ionization calorimeters, 19: 40854
KAKHIDZE, G. P., Multichannel analyzer of pulses for ionization calorimeter at capacity memory cells and the system of information output, 19: 40853
KAKUK, Janos, Investigation of an r-f ion source, 19: 40855
KALER, James Bailey, Recombination spectra of hydrogen and helium in gaseous nebulae, 19: 41238
KALINA, V. K., Change of thyroid gland activity after whole-body x irradiation, 19: 40374
KALINKIN, B. N., Analytical version of quasiclassical theory of angular distribution of products of one-nucleon transfer reaction, 19: 41805

KALIVODA, L'., Splitting of plasma shock waves in accelerating tube, 19: 41880
KALLENBACH, R., Obrigheim nuclear power plant—as the future owner conceived it, 19: 42105
KALMYKOVA, Z. I., Oxygen saturation of blood of rats after inhalation of Pu-239, 19: 40380
KAMATH, P. M., Determination of vinyl acetate in ethylene vinyl acetate copolymers, 19: 40556
KAMENETSKII, V. D., Investigations on nonrelativistic quantum theory of particle scattering, 19: 41360
KAMENSKAYA, S. A., Observations of radio eclipse of the moon at millimeter waves, 19: 41222
KAMI, S., Prog. rpt. on ion rocket engine development, 1–3/65, 19: 40765 (NP-15309)
KAMINSKII, V. N., Investigation of plasma frequency multiplier, 19: 40860
KAMKE, D., Decay of C-12 into three α particles in reaction $^{11}B(p,\alpha)2\alpha$, 19: 41699
KAMPFENKEL, Ottomar, Heat-engineering data of PWR with special consideration of possible breakdown of principal circulating pump, 19: 42118
KANA'AN, Adli S., Spectroscopic investigations of some halide reactions in plasma-generating devices, 19: 41287
KANAREK, T., Reconstruction of the spatial picture of an event in the bubble chamber, 19: 40871 (JINR-P-2179)
KANAYA, K., Evaluation of aberrations of focused beams of charged particles caused by space charge, 19: 41173
KANCHELI, O. V., Anomalous thresholds and mass spectrum of elementary particles, 19: 41351
KANCHELI, O. V., Weak interaction of mesons and peratization, 19: 41353
KANDER, Lois Nash, Prog. rpt. on stable isotope studies, annual, 9/15/64–7/15/65, 19: 40460 (NYO-3452-1)
KANE, R. P., Fine structure of the energy spectra of Forbush decreases and its dependence on solar cycle, 19: 41305
KANG, Kyungsik, Model for dynamical calculation of inelasticity, 19: 41403
KAPLAN, I., Prog. rpt. on Heavy Water Project, annual, 9/30/64, 19: 42007 (MIT-2344-3)
KAPLAN, J. M., Suggested measurements of neutral-kaon decay rates, 19: 41413
KAPUR, J. N., On the flow of two conducting incompressible immiscible fluids between two nonconducting plates, 19: 41135
KAPUSTSIK, Edvard, Electromagnetic current operator in the unitary symmetry model, 19: 41341
KARABIN, Mirjana, Statistical characteristics of sudden ionospheric disturbances, 19: 41573 (RPU-S19)
KARAGEORGE, G. K., Investigation of "scotchlite" as a reflective surface in a liquid hydrogen bubble chamber, 19: 40917
KARAPETYAN, Sh. A., Unit for gas-phase radiation-induced graft polymerization, 19: 40596
KARMANOV, F. V., Compensation of helical magnetic field disturbances, 19: 41116 (IAE-663)
KARPOV, V. L., X-ray studies of polyamide films cast from irradiated solutions, 19: 40595
KARZHAVINA, E. N., Neutron resonances of ytterbium isotopes, 19: 41661 (JINR-P-2156)
KASHLIK, K., Investigation of nuclear reactions of helium-3 with carbon, 19: 41663 (JINR-P-2184)
KASK, N. E., Electron paramagnetic resonance of irradiated single crystals of fluorite containing Nd addition, 19: 40602
KASK, N. E., New EPR spectrum of Nd in CaF_2 single crystals, 19: 41999
KASS, S., Properties of a Hf-control rod after exposure during three seed lives in PWR Core 1, 19: 41092 (WAPD-TM-457)
KATHREN, Ronald, Index to hazards control quarterly reports nos. 1 through 19, 19: 40833 (UCRL-14116)
KATO, Norihisa, Alpha particle groups from deuteron bombardment of ^{16}O and ^{40}Ca, 19: 41720
KATOH, Kazuki, Energy response of BF_3 counter using paraffin moderators, 19: 40890
KATS, M. L., Influence of an electric field on luminescence of alkali halide compounds, 19: 40572
KATSANOS, N. A., Thermal annealing phenomena in neutron-irradiated liquid organic bromides, 19: 40576
KATZ, Bernard, Circulation near the southern Berry Islands, Bahamas, 19: 42201 (CU-2663-23)
KATZ, Ludwig, Effect of solar flare on outer radiation belt, 19: 41312
KAURANEN, Pentti, Fission products in the atmosphere and in rain, 19: 40785 (TID-21224)
KAUSZ, I., MZFR nuclear technical auxiliary installations, 19: 42168
KAVALOSKI, C. D., (p,t) Ground-state L = 0 transitions in the even isotopes of Sn and Cd at 40 Mev, N = 62 to 74, 19: 41689
KAWAGUCHI, Masaaki, Theory of bound states. I., 19: 41474
KAWAI, Naoyuki, Alpha particle groups from deuteron bombardment of ^{16}O and ^{40}Ca, 19: 41720
KAWAI, Toshio, Coupled reactor kinetics. I., 19: 42182
KAWAKAMI, A., Energy dependence of inelastic neutrino cross section in resonance model, 19: 41754
KAWAKAMI, Hirokane, Half-life measurements in ^{101}Rh and ^{102m}Rh, 19: 41719
KAWAKATSU, H., Evaluation of aberrations of focused beams of charged particles caused by space charge, 19: 41173
KAZACHOK, V. S., Electrodynamic method for decelerating molecules, 19: 41200
KAZANSKII, Yu. A., Angular and energy distribution of γ emission in H_2O and Fe, 19: 41953 (NP-15131)
KAZAROV, R. E., Properties of component penetrating atmospheric showers, 19: 41297
KAZI, A. H., Analysis of fast reactor transients including meltdown, 19: 42100 (UNC-5092)
KAZINTSEVA, M. D., Some data on the luminescent properties of Eu-activated NaCl and KCl phosphors, 19: 40567
KEATON, P. W., Mössbauer effect resulting from the reaction $^{56}Fe(d,p)^{57}Fe$, 19: 41793
KEELER, R. Norris, High-pressure shock wave experiments in argon and xenon, 19: 41128 (UCRL-12466)
KEENAN, Robert G., Simultaneous determination of copper and zinc in human lung tissue by neutron activation analysis, 19: 40452
KEILIN, B., Large nuclear-powered sea water reverse osmosis plants, 19: 42120
KEITH, J., A new double focusing beta spectrometer. II., 19: 40904
KELBG, G., Classical statistical mechanics of the particle mixtures with type-dependent extensive intermolecular interactions, 19: 41130
KELLER, Roy A., The in situ identification of phosphate species in multispot chromatograms by neutron activation analysis, 19: 40429
KELLER, W., Planning and design of the 300-Mw nuclear power station at Obrigheim, 19: 42106
KELLEY, B., Material buckling and intracellular thermal neutron distributions, 19: 42049 (MIT-2344-3, pp 155-64)
KELLY, B. T., Basal plane contraction in graphite due to mono-vacancies, 19: 41100
KELLY, W. H., Excited states of ^{127}I populated in decay of ^{127}Te and ^{127m}Te, 19: 41835
KENEFICK, Robert A., Level structure of the odd-A isotopes of Sm, 19: 41778
KENNEDY, Roger Charles, Energy gap in interacting nucleon systems, 19: 41826
KENNEY, J., Performance study of a repetitively pulsed two-stage plasma propulsion engine, 19: 40763 (N64-31453)
KERIMOV, B. K., Beta decay of moving longitudinally polarized neutrons, 19: 41496
KERNOHAN, R. H., Temperature dependence of critical fields of superconducting Pb–Tl, 19: 41610
KERST, D. W., Motion of plasma and lifetimes of energetic ions in a toroidal octupole magnetic field, 19: 41896
KERSTEN, Johannes A. H., Liquid homogeneous nuclear reactor power level control, 19: 42016
KESSEL, F., Treatment with Th–X, 19: 40391 (NP-14921)
KHAKHANASHVILI, O. G., Relaxation processes in paramagnetic resonance of U^{3+} and Tb^{3+} in CaF_2, 19: 42000
KHALATNIKOV, I. M., Introduction to theory of superfluidity, 19: 41636
KHALDEEVA, I. V., Properties of component penetrating atmospheric showers, 19: 41297
KHALKIN, V. A., Microchromatographic column with remote control, 19: 40685
KHAN, A. S., Hydrogen adsorption on zirconium borate and dioxide, 19: 40484
KHANSEVAROV, R. Yu., Energy spectrum of defects appearing in indium antimonide at low-temperature γ-irradiation, 19: 41096
KHAPAEV, M. M., Stability of motion of a charged particle in a magnetic field, 19: 41187
KHARE, S. P., Application of a variational principle to the calculation of free-free matrix elements for H^-, 19: 41266
KHARKATS, Yu. I., Decay $\pi \to \mu + \mu + e^+ + e^-$, 19: 41482
KHIZHNYAK, N. A., The magnetic moment of a plasma bunch impinging on a homogeneous longitudinal magnetic field, 19: 41857 (NP-15206)
KHODEL', V. A., Calculation of magnetic moments of spherical nuclei, 19: 41804
KHOMUTOVSKII, O. A., Changes in pancreas after administration of radioactive Sr, 19: 40358 (FTD-TT-65-48, pp 577-8)
KHRIPIN, L. A., Phase transitions of UF_4 and UCl_4, 19: 40481
KHUNDKAR, M. H., Hydrogen adsorption on zirconium borate and dioxide, 19: 40484
KIEFFER, Fernand, Thermoluminescence of molecular solids irradiated by

γ rays at 77°K. Evidence of T → S and S → S emissions, 19: 40563

KIENEL, G., Design and function of hydraulically actuated ultra vacuum through-way valve, 19: 40776

KIIMA, R., Motion of particles in symmetrical fields, 19: 41538

KIKUCHI, Takeo, Registration of fission fragment track on solid surface, 19: 41138

KILER, E. K., Studies of Nd_2O_3–ZrO_2. Investigations of regions rich with ZrO_2, 19: 41037

KILLGROVE, T., Prog. rpt. on ion rocket engine development, 1–3/65, 19: 40765 (NP-15309)

KIM, C. W., Application of Goldberger-Treiman relation to β decay of complex nuclei, 19: 41774

KIM, Hi Sen, Niobium and Rb neutron resonances and radiation widths of medium-mass nuclei, 19: 41727

KIM, K. I., Electromagnetic processes in anisotropic electroconducting liquid, 19: 41149

KINNEY, W. E., Calculated tissue current-to-dose conversion factors for nucleons below 400 Mev, 19: 40372

KINOSHITA, Kisei, Mass splitting of pseudoscalar octet caused by baryon octet mass difference, 19: 41468

KIPPENHAHN, R., Stellar evolution. 1., 19: 41210 (N64-25282)

KIRBY, R. S., Feasibility of brazed joints between Cb-1 Zr alloy and alumina ceramics, 19: 40980 (LA-3302)

KIRGINTSEV, A. N., Separation coefficients for radioactive fission elements in the directional process of sodium nitrate crystallization, 19: 40683

KIRILLOV, L. A., Influence of an electric field on luminescence of alkali halide compounds, 19: 40572

KIROV, K., Recombination processes in CdS during excitations by α particles, 19: 40565

KIRZ, James, Branching ratios for decays of the f0, A_2, and K*(1400) mesons, 19: 41460

KISELEV, V. A., Current distribution in a coaxial plasma gun, 19: 41859 (NP-15218)

KISER, Donald Lee, Ion exchange separations in ammonium thiocyanate–organic solvent–water systems (thesis), 19: 40447

KISHBAUGH, Albert A., Semiworks evaluation of manganese dioxide head-end step in the Thorex Process, 19: 40649 (DP-982)

KISHII, Toru, Polarization of radio-photoluminescence of fluoro-dosimeter glass, 19: 40588

KISLYAKOV, A. G., Observations of radio eclipse of the moon at millimeter waves, 19: 41222

KITAMURA, Toi-ichi, Geomagnetic pulsations and the exosphere. III., 19: 41601

KIZHAEV, S. A., Determination of Curie point of ferroelectrics $YMnO_3$ and $YbMnO_3$, 19: 41059

KLADNITSKAYA, E. N., Baryon resonances in π⁻p interactions at 7.5 Bev with strange-particle formation, 19: 41488

KLADNITSKAYA, E. N., Meson resonances in π⁻p interactions at 7.5 Bev with strange particle production, 19: 41489

KLEINSTUECK, K., Low-temperature chamber for neutron-diffraction studies, 19: 40852

KLEMENC-SEBEK, S., Plasma pepsinogen after whole-body irradiation of rat, 19: 40363

KLEPFER, H. H., Application of metal coatings on uranium, 19: 40949 (ISC-640)

KLINE, D. E., Effect of nuclear radiation on the thermal conductivity of polyethylene, 19: 40603

KLOHN H., Erik, Reconnaissance for U in the Colimapu Formation of central Chile, 19: 40798 (RME-4571(Rev.))

KLOPFER, Ervin, Electrostatic ion beam accelerator, 19: 41181

KNAAB, H., Irradiation of a MZFR test fuel element in the NRX, 19: 42185

KNAPP, W. G., Neutron-flux studies in the EBWR during power operation, 19: 42076 (ANL-6751)

KNOWLES, Paul H., Reconnaissance for U in the Colimapu Formation of central Chile, 19: 40798 (RME-4571(Rev.))

KNUDSEN, W. C., Standing waves of third sound in He II films, 19: 41617

KNUTH, W. H., Design study of modification of M-1 liquid H turbopump for use in reactor test facility, 19: 42141 (NASA-CR-54422)

KNYAZEV, D. A., Certain regularities in isotopic exchange equilibrium, 19: 40505

KNYAZYATOV, A. S., Production of intense pulsed beam of accelerated tritium atoms, 19: 41923

KOBAYASHI, Keisuke, Measurement of migration area and multiplication factor of UO_2–H_2O lattice, 19: 42053

KOBZEV, A. P., Investigation of nuclear reactions of helium-3 with carbon, 19: 41663 (JINR-P-2184)

KOCHETOV, N. K., Radiochemistry of carbons. III. Effects of γ radiation on the aqueous solutions of α-methyl-D-glucoside, 19: 40605

KOEHLER, G., Nitryl nitrato complexes of indium and thorium, 19: 40471

KOERNER, Juergen G., B-meson decay, ω-φ mixing, and SU(6), 19: 41458

KOERNER, Juergen G., Self-consistent particle sets in a baryon bootstrap model, 19: 41432

KOFOID, M. J., Electron gun for plasma-oscillation studies, 19: 41946

KOFSTAD, P., High temperature metallographic microscope studies of initial oxidation of tantalum, 19: 40972

KOLCHIN, O. P., Production and application of niobium carbide parts, 19: 40988

KOLESNIKOV, N. N., Spallation of hyperfragments in Coulomb field, 19: 41815

KOLLIE, Thomas Gilmon, Development of pulse-heating calorimetric technique for measuring the specific heat of electrical conductors and its application to pure iron from 100 to 1400°C, 19: 40700 (ORNL-TM-1187)

KOLTUN, D. S., Double-charge-exchange scattering of low-energy pions by nuclei, 19: 41773

KONAREV, N. I., Thermal properties of binary sodium sulfates of certain sub-group rare earths, 19: 40511

KONDRATENKO, A. N., Damping of waves propagating in a bounded plasma perpendicular to a magnetic field, 19: 41917

KONDRATENKO, A. N., Excitation of waves in an organic plasma, 19: 41902

KONDRAT'EV, A. S., Cyclotron injector, 19: 41193

KONDRAT'EV, L. N., Spectrum of internal conversion electrons in α-decay of ^{239}Pu and energy levels of ^{235}U, 19: 41673 (NP-15251)

KONECNY, E., Response of semiconductor surface barrier detectors to fission fragments, 19: 40901

KONOPLEVA, N. P., Unified description of interactions, 19: 41541

KONSTANTINOV, V. A., Thermal treatment of Ti–Al–Mo–Zr–Sn alloys, 19: 41052

KONSTANTINOVA, M. S., Reaction of the endocrine organs to fractional irradiation with small doses of x rays, 19: 40360 (FTD-TT-65-48, pp 666)

KONTIS, S. S., Chemical effects of nuclear recoil in organic halide systems, 19: 40624

KONUMA, Michiji, Charged conjugation, decay of vector mesons, and SU(6) symmetry, 19: 41464

KOONTZ, R. L., Sodium fires and release characteristics of particulates and fission products, 19: 40803 (NAA-SR-Memo-9719)

KOPPEL, J. U., Prog. rpt. on integral neutron thermalization, 3/31/65, 19: 41640 (GA-6323)

KOPYLOV, G. I., Baryon resonances in π⁻p interactions at 7.5 Bev with strange-particle formation, 19: 41488

KOPYLOV, G. I., Meson resonances in π⁻p interactions at 7.5 Bev with strange-particle production, 19: 41489

KORITSANSZKY, Denes, Aseptic production of sterile pyrogen-free human albumin, labeled with ^{131}I, 19: 40639

KORNBICHLER, H., Superheat reactor at Grosswelzheim, 19: 42107

KORNBLUM, H. N. Jr., Near-earth, polar-orbiting satellite measurements of charged particles. I., 19: 41303

KORNIENKO, L. S., Electron parametric resonance of irradiated single crystals of fluorite containing Nd addition, 19: 40602

KORNIENKO, L. S., New EPR spectrum of Nd in CaF_2 single crystals, 19: 41999

KOROBKOV, V. I., Influence of length of α-particle track in nuclear photoemulsion in relation to pH of impregnating solution, 19: 40597

KOROLEV, G. K., Distribution of Sr-90 in rats after intratracheal administration, 19: 40312

KOROLEV, G. K., Distribution of Ce-144 in rats after intratracheal administration, 19: 40313

KORSHUNOV, B. G., System $SnCl_2$–NaCl–KCl, 19: 40517

KORST, Donald R., Tissue tolerance and systemic toxicity of 5-fluorouracil, external radiation, and drug-radiation combination in rabbits, 19: 40394

KORSUNSKII, M. I., Correction of angular aberrations of two-sector electrostatic analyzer, 19: 41197

KOSA, Somogyi Istvan, The effect of the type of radiation on the radiolysis of diphenyl–methane, 19: 40591

KOSA SOMOGYI, Istvan, Investigation of radiation chemical processes with cryoscopic method, 19: 40370

KOSHURNIKOVA, N. A., Effect of additional pathological agents on peripheral blood of rats exposed to Pu-239, 19: 40338

KOSHURNIKOVA, N. A., Long-term effects of aseptic inflammation in rats exposed to Pu-239, 19: 40381

KOSHURNIKOVA, N. A., Plutonium-239 in rat lung and liver and morphological changes after intratracheal administration, 19: 40317

KOSIKHIN, V. F., Aftereffects of F band illumination of x-ray-irradiated alkali halide phosphors, 19: 40570

KOSMACHEV, O. S., Correction of angular aberrations of two-sector electrostatic analyzer, 19: 41197

KOSTKA, Pal, Electrostatic ion beam accelerator, 19: 41181

KOSTROMINA, N. A., Acid dissociation constants of rare earth gluconates, 19: 40508

KOTOV, Yu. D., Origin of high-energy pions, muons, and photons, 19: 41291

KOTOV, Yu. D., Precision of calculations of fast muon energy losses, 19: 41296
KOTZER, Peter, Electromagnetic interactions of 5- to 50-Bev/c cosmic ray muons with electrons, 19: 41313
KOVACEVICH, E. A., SNAP 50/SPUR program materials investigation—mechanical properties of TZM, 19: 41002 (APS-5157-R)
KOVACS, Istvan, Electrostatic ion beam accelerator, 19: 41181
KOVALENKO, V. Ya., Medical defense against nuclear weapons, 19: 40361 (ORNL-tr-437)
KOVALEV, A. I., Modeling of current density distribution in a MHD channel, accounting for anisotropic conductivity, 19: 41148
KOVAL'SKAYA, M. P., Uranium extraction from Hf–HNO_3 by ternary amines in benzene, 19: 40684
KOYNER, D. S., Experimental liquid-metal gallium loop for MHD investigations, 19: 40727
KOZIK, B., Correlation functions for processes of the multiplication type, 19: 41330 (JINR-P-2213)
KOZIK, Ben'yamin, Neutron correlation in nuclear reactors with account of their space and energy distribution, 19: 42042 (JINR-P-2216)
KOZMA, Gyula, On angular correlation measurements between fast neutrons, 19: 40894
KRAFT, E., The behavior of spark discharge chambers by triggering by the primary ionization and the avalanche, 19: 40898
KRAMER, P., Decay of C-12 into three α particles in reaction $^{11}B(p,\alpha)2\alpha$, 19: 41699
KRASIL'NIKOV, D. D., Energy spectra of cosmic-ray muons at sea levels, 19: 41292
KRASIL'NIKOV, E. Yu., Experimental liquid-metal gallium loop for MHD investigations, 19: 40727
KRASNOV, Yu. N., Equilibrium between cerium and its di- and trivalent ions in a molten eutectic mixture of lithium and potassium chlorides, 19: 40467 (ORNL-tr-578)
KRASOTKIN, A. F., X-ray photons in cosmic showers in stratosphere, 19: 41299
KRASOVSKII, V. I., Research on aurorae and airglow, 19: 41576 (N64-21876)
KRAT, V. A., Contours of spectral lines in the solar chromosphere. I., 19: 41220
KREBS, Karl Heinz, Isotopic effects in secondary electron emission, 19: 41249
KRESTOV, G. A., Thermodynamic characteristics of electrode processes with participating rare earth and actinide elements, 19: 40500
KRIKORIAN, N. H., Phase relationships of the high carbon portion of the lanthanide dicarbides, 19: 41014 (LA-DC-6819)
KRINBERG, I. A., Application of the theory of thermal similarity to the study of an electric arc, 19: 41914
KRIPYAKEVICH, P. I., Crystalline structure of La_5Si_3, Ce_5Si_3, Pr_5Si_3, Nd_5Si_3, Sm_5Si_3, 19: 40477
KRISCH, A. D., Backward elastic scattering of high-energy pions by protons, 19: 41456
KRISCH, A. D., Pion-proton elastic scattering at high momentum transfers, 19: 41455
KRISTIANSON, Bryant Neil, Computed effect of neutron irradiation on the concentration of interstitials and vacancies in Nb, 19: 41106
KRISTOFF, J., Thermal-vacuum behavior of lithium-drifted silicon detectors, 19: 40902
KRITZINGER, J. J., Beam current integrator for pulsed positive ion accelerators, 19: 41183
KRIVCHENKOVA, R. S., Evaluation of some drugs for emergency use in case of injury by radioactive substances, 19: 40339
KROPP, W. R., Evidence for high-energy cosmic-ray neutrino interactions, 19: 41306
KROTIKOV, V. D., Observations of radio eclipse of the moon at millimeter waves, 19: 41222
KROTOVA, L. V., The effect of oxygen impurity on the optical properties of CaF_2–Sm crystals, 19: 41993
KRTIL, J., Sorption of Sr, Ce, Ru and Zr on tungsten ferrocyanide, 19: 40679
KRUCHININ, S. P., Elastic pp scattering at 1.45 Bev, 19: 41487
KRUDTAA, O. J., High temperature metallographic microscope studies of initial oxidation of tantalum, 19: 40972
KRUGLOV, A. A., Thermal properties of binary sodium sulfates of certain cerium sub-group rare earths, 19: 40511
KRUMHOLZ, P., Solution chemistry [of rare earths], 19: 40531
KRYLOVA, L. F., Phospho-organic complexing resins, 19: 40668
KRYNOV, L. N., Spectrometric characteristics of LSU-5k apparatus, 19: 40875 (NP-15254)
KUAN, Wei-yen, Measuring critical characteristic curves of superconductors, 19: 41630
KUCHIN, I. A., Experimental data on N-N interactions at 300 Bev, 19: 41358
KUCHNIR, F. T., Neutron spectra from Bi produced by monoenergetic γ rays, 19: 41834
KUCHOWICZ, B., Bibliography on nuclear astrophysics. II., 19: 41207 (NEIC-RR-9)
KUCHOWICZ, Bronislaw, Origin of chemical elements in stars. VI., 19: 41235
KUCKES, A. F., A microwave system for low-density measurements, 19: 41854 (MATT-369)
KUDASHEVA, N. P., Effect of additional pathological agents on peripheral blood of rats exposed to Pu-239, 19: 40338
KUDRYASHOV, L. I., Radiochemistry of carbons. III. Effects of γ radiation on the aqueous solutions of α-methyl-D-glucoside, 19: 40605
KUEHNE, Herbert Wayne, Nuclear resonance fluorescence in C, Si, and Mg, 19: 41828
KUESTER, H., MZFR structural installations, 19: 42171
KUGLER, E., Luminescence of rare gas mixtures in excitation with fast electrons, 19: 41246
KUGLER, M., $SU(6)_W$ photoproduction and meson-baryon scattering amplitudes, 19: 41462
KUKHARENKO, N. K., Modernization of radioactivity logging apparatus, 19: 40794 (AEC-tr-6577)
KULES, Ivan, The effect of the type of radiation on the radiolysis of diphenyl–methane, 19: 40591
KULESHOV, I. M., Separation coefficients for radioactive fission elements in the directional process of sodium nitrate crystallization, 19: 40683
KULINSKII, V. I., Catecholamine content in macacus tissues immediately after whole-body γ irradiation, 19: 40373
KULUNDZIC, P., Heat transfer of reactor fuel element model with polyzonal-spiral finning, 19: 40748
KUMEKIN, Yu., Double pp scattering at 667 Mev, 19: 41666 (JINR-P-2233)
KUMPF, H., MZFR—construction principles of the reactor, 19: 42162
KUMPF, H., MZFR—devices for fuel element exchange, 19: 42166
KUMPF, H., Neutron spectra in interactions of heavy ions with intermediate nuclei, 19: 41810
KUMPF, L., Neutron spectra in interactions of heavy ions with intermediate nuclei, 19: 41810
KUMPT, Hermann, Device for operating a loading machine for reactors, 19: 42032
KUNIMASA, Tosaku, New baryon octet and the quark model, 19: 41477
KUNZE, Helmut, Theory of space-dependent neutron spectra in heterogeneous reactors, 19: 42056
KURBATOV, I. M., Numerical solution of one problem on optimum nuclear reactor control, 19: 42013
KURDGELAIDZE, D. F., Confluence theory based on hypercomplex numbers, 19: 41560
KURIDZE, R. V., Properties of component penetrating atmospheric showers, 19: 41297
KURKIN, I. N., Electron paramagnetic resonance of Gd^{3+} in synthetic $SrMoO_4$, 19: 41994
KURKIN, I. N., EPR spectrum of Yb^{3+} ions in synthetic $PbMoO_4$ single crystals, 19: 41986
KURODA, P. K., Fission products in the atmosphere and in rain, 19: 40785 (TID-21224)
KURODA, Rokuro, Cation-exchange separation of Pa-233 from irradiated Th, 19: 40673
KURODA, Rokuro, Rare earth separation by anion exchange chromatography in salt solution, 19: 40659
KURSTEDT, H. A., Feedback effects during short interval-series pulsing, 19: 42188
KURSUNOGLU, Behram, Conferences on symmetry principles at high energy, Coral Gables, 1/65., II., 19: 41514
KURSUNOGLU, Behram, Symmetry and strong interaction, 19: 41516
KURTMULLAEV, R. Kh., Excitation of strong collisionless shock waves in plasma, 19: 41911
KUSHAKEVICH, Yu. P., New isomers of ^{43}Sc, ^{109}In, and ^{125}Xe, 19: 41802
KUSHNEVA, V. S., Accumulation of Sr-90 in the skeleton of dogs after chronic administration, 19: 40325
KUSHNIRENKO, A. N., Use of direct methods of mathematical physics in theory of quantum transitions. I., 19: 41540
KUSIAN, Ross, Index to hazards control quarterly reports Nos. 1 through 19, 19: 40833 (UCRL-14116)
KUSMISS, J. H., Positron annihilation in solid and liquid metals and semiconductors, 19: 41285
KUTIKOV, I. E., Neutron emission from ^{233}U, ^{235}U, and ^{239}Pu fission fragments, 19: 41681 (ANL-Trans-205)
KUTKA, Jan, Effect of neutron radiation on certain mechanical and structural properties of austenitic chrome nickel steel, 19: 41093 (FTD-TT-65-125)
KUZ'MA, Yu. B., Crystalline structure of certain ternary compounds in Nb–Co–Si system, 19: 41069

KUZ'MENKO, G. I., Nuclear photoeffect in the laboratory, 19: 41712
KUZNETSKII, R. S., Rotating magnetic field and surface currents in a polyphase system with skew pole pieces, 19: 41152
KUZNETSOV, E. S., Calculation method for heterogeneous reactor cells, 19: 42060
KUZNETSOV, F. A., Enthalpy variations during extraction according to standard enthalpy of formation, 19: 40669
KUZNETSOV, V. G., Crystal structure of $LaTe_2$, 19: 40476
KUZNETSOV, V. G., Roentgenographic studies of lanthanum tellurides La_4Te_7, 19: 41070
KUZNETSOV, V. G., Roentgenographic studies of lanthanum ditelluride, 19: 41071
KUZNETSOVA, M. A., Combined action of whole-body vibration and ionizing radiations on central nervous system, 19: 40354 (FTD-TT-65-48, pp 38-9)
KUZNETSOVA, Z. M., Photocolorimetric determination of uranium(VI) with Arsenazo III in presence of fluoride, 19: 40428
KVICK, P. G., CMPXMAT, a transfer function evaluation program, 19: 42222 (TIM-940)
KYAEMBRE, Kh. F., Concerning two mechanisms of photostimulated electron emission from ionic crystals, 19: 41979

L

LABEYRIE, J., Age measurements using the C-14 method, 19: 40795
LACMANN, K., Collision mechanism of bimolecular reactions. I., 19: 41250
LACMANN, K., Collision mechanism of bimolecular reaction. II., 19: 41251
LACMANN, K., Collision mechanism of bimolecular reactions. III., 19: 41252
LACOUR, Jean, Safety concerning reactor Pegase, 19: 42151 (CEA-R-2518(Vol.II))
LADNER, H.-A., Prophylactic effect of histamine in whole-body irradiated rats, 19: 40389
LADNER, H.-A., Radioprotection effectiveness of serotonin in rats, 19: 40388
LAI, Chai S., Quartet scheme and weak interactions, 19: 41415
LAJTAI, Albert, Angular distribution of γ rays from fission of U-235, 19: 41722
LAL, D., A versatile two-element low-background flow-type beta-counter, 19: 40903
LA LIBERTE, Bernard R., Process for preparing radiation-stabilized polyethylene and food package utilizing same, 19: 40633
LAM, C. S., Feynman rules and Feynman integrals for system with higher-spin fields, 19: 41548
LAMBORIZIO, C., Difference in range-energy relation for positive and negative particles, 19: 41369
LAMING, F. P., Lanthanide complexes. III., 19: 40487
LA MOTTE, J. D., Feasibility of brazed joints between Cb-1 Zr alloy and alumina ceramics, 19: 40980 (LA-3302)
LANDMARK, B., Conference on upper atmosphere research, Corfu, 7/60, 19: 41605
LANDSBERG, A., Freeze-dry technique for making ultra-fine metal powder, 19: 40987
LANDSBERG, A., Tungsten- and molybdenum-coated nonmetallic powder, 19: 40986
LANDSBERG, P. T., Derivation of sum rules and hypervirial theorems by differentiation, 19: 41557
LANG, Donald W., Effect of experimental resolution on measured widths of fluctuation correlation function for nuclear cross sections, 19: 41734
LANG, Peter M., Dual-purpose nuclear plants for water desalination and power, 19: 42124
LANGENBERG, D. N., Investigation of microwave radiation emitted by Josephson junctions, 19: 41614
LANGERON, Jean-Paul, Application of zone fusion method to purification of Zr, 19: 41030
LANGHAAR, J. W., Shipping and storing power fuels prior to reprocessing, 19: 40837
LANGRIDGE, Eric Graham, Improvements in or relating to conveyor systems, 19: 40729
LANNING, D. D., Prog. rpt. on Heavy Water Project, annual, 9/30/64, 19: 42007 (MIT-2344-3)
LANNOY, F. G., Symmetry-breaking corrections to weak vector currents, 19: 41547
LAPERASHVILI, L. V., Anomalous thresholds and mass spectrum of elementary particles, 19: 41351
LAPERASHVILI, L. V., Regge poles Y_1^+ and Y_1^- and amplitude of KN scattering, 19: 41352
LAPIDUS, L. I., Double N-N scattering with a polarized beam and polarized target, 19: 41333 (JINR-P-2227)
LAPITSKII, A. V., Bromination of microquantities of Pa-233 in carriers, 19: 40501
LAPONSKY, A. B., Prog. rpt. on physics of electron emission and electron tube technology, 10/16/64–4/15/65, 19: 41124 (NP-15108)
LARRICK, A. P., A chemical composition and process for removing oxide and scale from aluminum metals and aluminum alloys, 19: 42202 (HW-64483)
LARSON, A. C., Integrated series of crystallographic computer programs. VII., 19: 41965 (LA-3309)
LARSON, Allen C., Integrated series of crystallographic computer programs. VIII., 19: 41966 (LA-3310)
LARSON, Ralph H., Computer sizes parameters of a pneumatic scram system, 19: 42021
LASHINSKY, Herbert, Nonlinear mode interactions in universal plasma instabilities, 19: 41865 (TID-22050)
LASUK, S. R., Radiation safety technician training course. I., 19: 40801 (ANL-6991)
LATIPOVA, R. A., Cascade mechanism of the high energy nuclear reactions. I., 19: 41811
LATTERELL, J. J., Separation of amines by ligand exchange. II., 19: 40647 (COO-499-1)
LATYPOVA, R. A., Effect of design parameters on the characteristics of Cerenkov's shower gamma-spectrometers, 19: 40897
LAUBEN, G. N., Sodium fires and release characteristics of particulates and fission products, 19: 40803 (NAA-SR-Memo-9719)
LA VALLE, D. E., Some fluorine compounds of Re and Tc, 19: 40461 (ORNL-P-491)
LAW, Lewis Arthur, Accurate current integrator in the range of 10^{-5} to 10^{-9} amperes, 19: 40843 (CEAL-1021)
LAWRENCE, James N. P., Static fission-barrier calculations of two-parameter liquid drop, 19: 41767
LAWRENCE, R., LAG—a load and go assembler written for the CDC-1604-B computer, 19: 42221 (TIM-939)
LAWTON, Stephen L., The reduced cell and its crystallographic application, 19: 41963 (IS-1141)
LEACHMAN, R. B., Investigation of $^{27}Al(\alpha,p)$ reaction by cross-section fluctuation studies, 19: 41761
LEARY, J. A., Solubility of selected elements in liquid plutonium. V., 19: 40950 (LA-3338)
LEBEDEV, M. A., Investigation of a low-temperature plasma in a low-voltage arc, 19: 41909
LEBEDEV, N. A., Microchromatographic column with remote control, 19: 40685
LEBEDEV, V. L., Neutron emission from ^{233}U, ^{235}U, and ^{239}Pu fission fragments, 19: 41681 (ANL-Trans-205)
LEBEDEVA, K. A., Changes in mammary-gland activity after irradiation, 19: 40353 (FTD-TT-65-48, pp 16-17)
LE BELLAC, M., Relativistic theory of electrodisintegration of the deuteron. II., 19: 41374
LE BIHAN, R., Theoretical and experimental study of hollow Cs plasma structures, sources of ions, or electrons, 19: 41872
LEE, Clarence E., Pions, muons, and nuclear structure, 19: 41671 (LADC-6186)
LEE, E. K. C., Kinetic isotope effects in recoil tritium reactions, 19: 40615
LEE, Hwa-chung, Regge poles and T = 3/2, J = 3/2 π-N scattering phase shift, 19: 41498
LEE, J., Entropy of nuclear spin system in magnetic field, 19: 41713
LEE, P. K., Integral gamma and neutron measurements on Kiwi-TNT, 19: 42135 (LA-3304)
LEE, T. D., Possible C-noninvariant effects in the 3π decay modes of η^0 and ω^0, 19: 41437
LEE, T. D., Possible C,T noninvariance in the electromagnetic interaction, 19: 41452
LEE, Y. K., Mössbauer effect resulting from the reaction $^{56}Fe(d,p)^{57}Fe$, 19: 41793
LEFORT, M., Evidence for nucleon clustering from high-energy reactions, 19: 41831
LE GUENEC, Rose, Mechanical manipulators, 19: 40730
LE GUILLOU, Jean-Claude, Williams-Weizsacker covariant methods for two virtual photons and lifetime of π^0, 19: 41349
LEIKIN, E. M., Effect of design parameters on the characteristics of Cerenkov's shower gamma-spectrometers, 19: 40897
LEINHARDT, T. E., Crystal structure and resistivity of Ce as determined by temperature, 19: 41083
LEINHARDT, T. E., Temperature dependence of optical reflectivity of Ce metal, 19: 41082
LEITSINA, V. G., Reactions of lanthanum and yttrium oxides with ferric oxide, 19: 40515
LEMAITRE, C. G., The three body problem, 19: 41529 (N64-81206)
LEMBERG, V. K., Bone tumors in dogs exposed to Pu-239, 19: 40382
LEMBERG, V. K., Effectiveness of DTPA after intratracheal administration

of Pu to rats, 19: 40346
LEMBERG, V. K., Long-term effects of aseptic inflammation in rats exposed to Pu-239, 19: 40381
LEMCKE, Bo, Performance of double-driver shock tube, 19: 41162
LEMCOE, M., Study of instantaneous collapse and creep buckling characteristics of large SGR process tubes, 19: 41019 (NAA-SR-11323)
LENARD, M., Ionization of Cs and Na contaminated air in the hypersonic slender body boundary layer, 19: 41121 (N64-30658)
LENNOX, C. G., Solid-state multiplexer for use with self-power neutron flux detectors, 19: 40866 (AECL-2217)
LEONARD, B. E., Investigation of rise portion of pulsed neutron curves, 19: 41654
LEONAS, V. B., Energy exchange in collisions of molecular flux with a surface, 19: 41275
LEONCHUK, M. P., Numerical solution of one problem on optimum nuclear reactor control, 19: 42013
LE POITTEVIN, G., Treatment of capture gamma ray spectra obtained with the aid of a central crystal in association with an annular crystal, 19: 40896
LESLIE, D. C., Improvements to theory of resonance escape in heterogeneous fuel. II., 19: 42055
LETUNOV, N. A., Inelastic scattering of electrons by alkali-halide compounds, 19: 40502
LETUNOV, N. A., Secondary electron emission of alkali-halide compounds, 19: 40503
LEUNG, Y. C., Ū(12) predictions for $N\bar{N}$ annihilation at rest into four mesons, 19: 41463
LEVENSON, M., Fuel management and inventory in the EBR-II fuel cycle, 19: 42075 (ANL-6735)
LEVIN, Iddo, Electrolytic dissolution of U fuel elements, 19: 41086
LEVIN, Joel Melvin, Canonical analysis of gravitational radiation, 19: 41561
LEVINE, A. M., A microwave system for low-density measurements, 19: 41854 (MATT-369)
LEVINGER, J. S., Composite model of bosons, 19: 41525
LEVY, H. B., Effect of increasing excitation energy on nuclear charge distribution in fission, 19: 41779
LEVY, R. H., Electron plasma-experiment theory and applications, 19: 41863 (NP-15302)
LEWIN, J. C., Experiments with superconducting niobium–tin cylinders, 19: 41609
LEWIS, R. R., Test for particle-mixture theories of $K^0 \to 2\pi$ decay, 19: 41454
LI, Yen-kuo, Studies of structural factors in two-nucleon stripping and knock-on reactions, 19: 41819
LICHT, A. L., Generalized asymptotic condition. I., 19: 41343
LICHTENSTEIN, Roland M., Investigation of transient radiation damage in semiconductor materials, 19: 40933 (NP-15300)
LICHTENSTEIN, Roland M., Investigation of transient radiation damage in semiconductor materials. Quarterly progress report 11/1/64–1/31/65, 19: 40934 (NP-15301)
LIDIYA, G. G., Photon multiplication in crystals. II., 19: 40495
LILEEV, I. S., Synthesis of La silicates from aqueous solutions, 19: 40518
LIH, Yung K., Satellite observations of low-energy heavy cosmic ray nuclei, 19: 41310
LIMENTANI, S., Spin and parity of 1320 Mev $\rho\pi$ resonance, 19: 41368
LINCOLN, J. Virginia, Geomagnetic and solar data, 19: 41589
LIND, Robert, Improvements relating to coolant for nuclear reactors having graphite moderators, 19: 42015
LINDEKEN, Carl, Index to hazards control quarterly reports Nos. 1 through 19, 19: 40833 (UCRL-14116)
LINDLEY, B., Design study of modification of M-1 liquid H turbopump for use in reactor test facility, 19: 42141 (NASA-CR-54422)
LINDLEY, Bryon Charles, Improvements in and relating to tubular heat exchangers, 19: 40752
LINTZ, Paul R., Thermal relaxation in oxygen with H_2O, HDO, and D_2O vapors as impurities, 19: 40483
LIPKIN, H. J., SU(6)$_W$ photoproduction and meson-baryon scattering amplitudes, 19: 41462
LIPKIN, Harry J., Lie groups, Lie algebras, and the troubles of relativistic SU(6), 19: 41449
LIPKIN, Harry J., Tests of unitary symmetry, 19: 41517
LIPOVSKA, M., Preparation of samples of biological material for liquid scintillation measurement of low-energy β-emitters, 19: 40425
LIPPERT, J., Thermoluminescence readout instrument for measurement of small doses, 19: 40877 (RISO-101)
LIU, Tsu-huan, Vibration-rotation interaction of even-even nuclei in transition region, 19: 41818
LIVETT, R. K., Prog. rpt. on heat transfer for space nuclear power, 12/64–2/65, 19: 40741 (SAN-409-23)
LIVINGSTON, H. D., Estimation of vanadium in biological material by neutron activation analysis, 19: 40421
LIVSHITS, N. N., Combined action of whole-body vibration and ionizing radiations on central nervous system, 19: 40354 (FTD-TT-65-48, pp 38-9)
LIWSHITZ, Mordehai, Thermal escape of neutral hydrogen and its distribution in earth's thermosphere, 19: 41604
LO, Bae-ling, Regge poles and T = 3/2, J = 3/2 π-N scattering phase shift, 19: 41498
LOBANOV, N. I., Complex compounds of rare earths with 1,10-phenanthroline, 19: 40514
LOCHAK, G., Accelerator of negative ions, 19: 41182
LOCKE, E., Experiments with magnetohydrodynamically supported shock layers, 19: 41120 (N64-30509)
LOCKINGTON, N. A., Activation sintering of tungsten, 19: 40985
LOCKWOOD, Grant John, Energy and angular measurements of resonant electron capture in He^+ on He collisions, 19: 41280
LOGINOV, G. M., Magnetic susceptibility of SmS, 19: 41060
LOIZZO, P., Control poison as an eigenvalue of the diffusion equations, 19: 42052
LOMAX, R. J., Investigation of nonlinear interaction phenomena in the ionosphere, 19: 41572 (NASA-CR-258)
LOMBARD, Roland, Aspects of nuclear physics at 500 Mev, 19: 41179
LOMENICK, T. F., Accelerated deformation of rock salt at elevated temperature, 19: 42198
LONERGAN, J. A., Mean lives of 2.15- and 1.74-Mev levels in ^{10}B, 19: 41758
LONGO, John M., Some new ternary oxides of Re (thesis), 19: 40525
LONGUA, K. J., Properties of a Hf-control rod after exposure during three seed lives in PWR Core 1, 19: 41092 (WAPD-TM-457)
LONGUET-HIGGINS, H. C., Isotope effects in electron spin resonance: the negative ion of cyclo-octatetraene-1-d, 19: 40541
LOOS, Hendricus G., Range of gauge fields, 19: 41365
LORENTS, Donald C., Elastic differential scattering of He^+ ions by He in the 20–600 ev range, 19: 41283
LORIA, A., Spin and parity of 1320 Mev $\rho\pi$ resonance, 19: 41368
LORIERS, Jean, Analytical chemistry of rare earths, 19: 40448
LORIERS, Jean, The oxysulfides and sesquisulfides of terbium holmium, thulium, and lutetium, 19: 40475
LOU, Fu-ching, Use of I-131 peanut oil in assessing lipid metabolism in coronary atherosclerosis, 19: 40393
LOW, G. G. E., YORK 87—a 7090-FORTRAN program for analyzing phonon dispersion curves, 19: 41962 (AERE-M-967)
LU, Chen-fo, Quantum theory of Cherenkov radiation in anisotropic media, 19: 41499
LU, Pao, Change of polarization in potential scattering, 19: 41501
LUCAS, B. T., Some (d,α) differential cross sections for ^{23}Na, ^{27}Al, and ^{31}P at about 9.3 Mev, 19: 41684
LUCHTER, Stephen, Portable power reactor, 19: 42115
LUCKS, C. F., Thermal radiative properties, 19: 41074
LUETJENS, G., Annihilation of antiprotons in hydrogen at rest. III., 19: 41325 (CU-1932-245)
LUK'YANOVA, L. A., Phase transitions of UF_4 and UCl_4, 19: 40481
LUK'YANOVA, L. D., Combined action of whole-body vibration and ionizing radiations on central nervous system, 19: 40354 (FTD-TT-65-48, pp 38-9)
LUNDBERG, Max, Analysis of the concentrations of Cr, Ag, Fe, Co, Pt, and Rb in normal human dentine, 19: 40435
LUNDIN, C. E., Heats of mixing in Pr–Nd solid solutions, 19: 41044
LUNDY, T. S., Diffusion of Nb-95 and Ta-182 in niobium (columbium), 19: 41064
LUPBERGER, A., Development and potentialities of the high-temperature pebble-bed reactor concept, 19: 42082 (CONF-650633-1)
LUSHCHIK, Ch. B., Photon multiplication in crystals. II., 19: 40495
LUSHCHIKOV, V. I., Determination of spins of Ho-165 neutron resonances by transmission of polarized neutrons through a polarized target in the energy interval 0–55 ev, 19: 41665 (JINR-P-2209)
LYON, C. E., Partition coefficients of nitratonitrosylruthenium complexes between nitric acid and TBP phases, 19: 40677
LYON, W. S., Radio-release methods for the evaluation of atmospheric pollution. Sulfur dioxide, 19: 40410 (ORNL-P-494)
LYONS, M. F., Fission gas release from UO_2 fuel rods with gross central melting. I., 19: 41088 (GEAP-4572)
LYSKOVICH, A. B., Roentgenoluminescence and thermoluminescence of Tl-activated NaI crystal phosphors, 19: 40568
LYUBCHANSKII, E. R., Behavior of citrate complex of Pu-239 in rats after inhalation, 19: 40316
LYUBCHANSKII, E. R., Behavior of Pu-239 citrate in rats after single and repeated intraperitoneal injection, 19: 40326
LYUBCHANSKII, E. R., Plutonium-239 in rat lung and liver and morphological changes after intratracheal administration, 19: 40317
LYUTOVICH, A. S., Radiation defects in very pure silicon crystals, 19: 41998

M

MAA, Jer Ru, Fission-fragment-induced oxidation of light hydrocarbons (thesis), 19: 40611

MAATMAN, Russell W., The behavior of aqueous salts in contact with oxide surfaces, 19: 4200 (COO-1354-5)

MAC KAY, C., Reactions of nucleogenic C atoms with hydrocarbons, 19: 40617

MAC KENZIE, K. R., Frequency modulation of large cavities, 19: 40723

MACKLIN, R. L., $^{51}V(p,n)^{51}Cr$ cross section from the threshold to 2.25 Mev, 19: 41676 (ORNL-P-1468)

MAC MILLAN, John H., Nuclear power and supercritical steam cycles, 19: 42121

MACNABB, W. V., Core evaluation of the Garigliano reactor, 19: 42091 (GEAP-4852)

MADANSKY, L., Mössbauer effect resulting from the reaction $^{56}Fe(d,p)^{57}Fe$, 19: 41793

MADER, Charles L., Study of one-dimensional, time-dependent reaction zone of nitromethane and liquid TNT, 19: 42203 (LA-3297)

MADSEN, V. A., Calculation of inelastic α-particle scattering by Ni-58, 19: 41692

MAEDA, Koichi, Infrasonic waves from aurorae, 19: 41592

MAERKL, H., THERMOPYL—program for calculating the thermal neutron energy spectrum in heterogeneous lattice cells, 19: 41648

MAGAGNINI, P. L., Structural modifications in irradiated 1,4 trans-polybutadiene, 19: 40561

MAGARIL, I. G., Some data on the luminescent properties of Eu-activated NaCl and KCl phosphors, 19: 40567

MAGNAC-VALETTE, Denise, Study of excitation curves of reaction $^{12}C(t,\alpha_0)^{11}B$, 19: 41706

MAHER, R., Shipping and storing power fuels prior to reprocessing, 19: 40837

MAIANI, L., Properties of weak amplitudes in broken U(12), 19: 41420

MAILLARD, R., Saint-Laurent-des-Eaux nuclear power station sealing barriers around foundation pits, 19: 42119

MAILLIE, H. D., Effect of wide x-ray beam and finite phantom thickness on 1000-kvp x-ray depth dose, 19: 40881 (UR-667)

MAIWALD, H., MZFR principal coolant circulating pumps, 19: 42174

MAJOR, J. K., Measurements by scattering techniques. [Part] I., 19: 40922

MAJOR, R. W., Crystal structure and resistivity of Ce as determined by temperature, 19: 41083

MAKHLIS, F. A., Calculation of absorbed energy of γ radiation, 19: 41959

MAKHLIS, F. A., Investigation of γ propagation in substances by similarity theory, 19: 41958

MAKSIMOVA, N. D., Aftereffects of F band illumination of x-ray-irradiated alkali halide phosphors, 19: 40570

MAKSIMOVA, N. D., Investigation of thermal de-excitation processes in x-rayed alkali-halide phosphors, 19: 41101

MALAVIYA, B. K., Pulsed neutron and control rod research studies of reactivity and related parameters, 19: 42045 (MIT-2344-3, pp 55-108)

MALIK, F. B., Effect of transport coefficients on damping of hydromagnetic waves, 19: 41869

MALINKA, F., MZFR structural installations, 19: 42171

MALINOVSKII, V. K., Excitation of strong collisionless shock waves in plasma, 19: 41911

MAL'TSEV, V. V., Production of intense pulsed beam of accelerated tritium atoms, 19: 41923

MAL'TSEVA, N. S., K-capture fraction of ^{66}Ge, ^{69}Ge, and ^{72}As, 19: 41800

MANDELSHTAM, S. L., X radiation of the quiet sun, 19: 41213

MANDLE, H. H., Uses and applications of rare earths, 19: 40401

MANDLE, Richard M., Uses and applications of rare earths, 19: 40401

MANDRIZKAYA, K. W., Treatment program of penetrating showers of cosmic rays with the energy of 10^{10} to 10^{12} ev, 19: 41290

MANDUCHI, C., Performance and properties of a proton polarimeter, 19: 40905

MANFREDI, D. V., Summary of shaft face seal development program, 19: ~0718 (TIM-909).

MANFREDI, P. F., Counting of events from pulsed sources, 19: 40885

MANIG, M., Annual precipitation and precipitation frequency for European community, United Kingdom, Denmark, and Alps 1921-1950, 19: 41111 (EUR-2296.e)

MANUILOV, V. G., Calculation of superconducting solenoid characteristics, 19: 41632

MANZHAVIDZE, Z. Sh., 340-Liters expansion-condensing chambers used to study nuclear interactions of high energy particles, 19: 40887

MANZIONE, A. V., The electron microprobe and light element analysis, 19: 40412 (TIM-924)

MARCHESINI, G., Use of electrostatic probes in diagnostics of a plasma column, 19: 41868

MARCUS, Judith H., Simultaneous determination of copper and zinc in human lung tissue by neutron activation analysis, 19: 40452

MARGOLIS, S. G., Heat-transfer aspects of the loss-of-coolant accident, 19: 42009 (WAPD-T-1811)

MARGRAVE, John L., Spectroscopic investigations of some halide reactions in plasma-generating devices, 19: 41287

MARINARO, M., Nonanalytical properties of propagators. The g ^{4} theory, 19: 41549

MARININ, V. G., Displacement of resonance frequency of interaction of a plasmoid with spatially modulated magnetic field, 19: 41901

MARINOVA, Ts., Comparative studies of radioactively labeled precursors in the RNA of x-irradiated non-diploid yeast, 19: 40367

MARION, J. B., Weakly excited resonance levels in reaction $^{13}C(p,\gamma)^{14}N$, 19: 41740

MARKELS, Michael Jr., Prog. rpt. on effects of electrical fields on boiling heat transfer, 5/26/64–9/30/64, 19: 40735 (NYO-2404-5)

MARKOV, M. A., Possibility for detecting the intermediate meson with mass larger than twice the nucleon mass, 19: 41484

MARQUET, Louis Carl, Atomic spectra of Er I and Er II (thesis), 19: 41281

MARSH, William Robert, Improvements in or relating to the purification of gaseous helium, 19: 40539

MARSHALEK, Eugene R., Self-consistent perturbation of Hartree-Fock-Bogoliubov equations and nuclear rotational spectra, 19: 41685

MARSHALL, J. H., Particle identification by pulse height correlation in a range telescope, 19: 41527

MARSTON, A. L., Selection, cost, and performance of n-paraffin diluents, 19: 40646 (CONF-650918-2)

MARTALOGU, N., Reaction $^{26}Mg(p,p'\gamma)$ mechanism at low energies, 19: 41693

MARTIN, J. P., Improvement of resolution in large area photomultipliers, 19: 40895

MARTIN, Paul E., Thermal radiation from burning hydrogen plume, 19: 42137 (LA-DC-7313)

MARTIN, S., Level structure of ^{53}Cr and ^{55}Cr, 19: 41726

MARTIN, T. C., The measurement of surface contamination of high-purity beryllium samples, 19: 40453

MARTINSON, Z. R., Reactor stability tests in Spert IV facility, 19: 42152 (IDO-17088)

MARTSINOVSKII, A. M., Most effective regimes for thermionic convertors, 19: 41317

MARTYNENKO, Yu. V., Dependence of sputtering coefficient on ion energy, 19: 41271

MARX, Rose, Reactions of radicals formed by γ irradiation of solid mixtures of methyl methacrylate with paraffin oil, 19: 40580

MARZARI-CHIESA, A., $K_{\mu 3}$ branching ratio and μ^+ energy spectrum, 19: 41414

MASHOVETS, T. V., Energy spectrum of defects appearing in indium antimonide at low-temperature γ-irradiation, 19: 41096

MASLIN, E. E., Absolute fission cross section of ^{235}U for 2200-m/sec neutrons, 19: 41691

MASON, Edward A., Relative roles of pyrolysis and radiolysis in degradation of terphenyls, 19: 40630

MASSAM, T., High-intensity, partially separated, beam of antiprotons and K mesons, 19: 41184

MASSIMO, Joseph Thomas, Reaction $\pi^- + p \rightarrow \pi^- + p + \pi^0$, 19: 41508

MASUDA, Naohiko, Dominance theorem in crossing matrices, 19: 41469

MASUDA, Yoshiko, Nuclear spin-lattice relaxation in type II superconductors, 19: 41611

MATHIEU, F., Measurement of the plate temperature of fuel elements of BR-2, 19: 42181

MATHIS, A., Analog model for cylindrical nuclear fuel rods, 19: 40740 (RT/ING(64)16)

MATINYAN, S. G., Anomalous thresholds and mass spectrum of elementary particles, 19: 41351

MATINYAN, S. G., Weak interaction of mesons and peratization, 19: 41353

MATRICON, J., Electronic excitations in superconductors free from second species. II., 19: 41624

MATSUO, Shigeki, Half-life measurements in ^{101}Rh and ^{102m}Rh, 19: 41719

MATSUO, T., Cross-section ratios of isomeric nuclides produced in medium-energy (α,xn) reactions, 19: 41695

MATSUURA, Shojiro, Measurement of migration area and multiplication factor of UO_2–H_2O lattice, 19: 42053

MATTHES, Franz, Thermal decomposition of the chlorohydrates of the rare earth elements, 19: 40489

MATUSZEK, J. M. Jr., Cross-section ratios of isomeric nuclides produced in medium-energy (α,xn) reactions, 19: 41695

MAUGIS, D., Theoretical and experimental study of hollow Cs plasma structures, sources of ions, or electrons, 19: 41872

MAULARD, Jean, Nuclear reactor control rod operating device, 19: 42033

MAXUM, B. J., Cyclotron-wave instabilities, 19: 41849 (AD-426079)

MAXWELL, J. R., (p,t) Ground-state L = 0 transitions in the even isotopes of Sn and Cd at 40 Mev, N = 62 to 74, 19: 41689

MAYER, H., MZFR steam generator, 19: 42173

MAYES, Terrill Wayne, Efficiency of high pressure electric shock tubes, 19: 40849 (TID-22061)

MAYO, T. J., Chromatograph for analysis of highly reactive and corrosive compounds, 19: 40407 (KY-485)

MAZALOV, Yu. P., Motion of plasma bunches in a field-free space, 19: 41856 (NP-15205)

MAZZOLDI, P., Experiments on the creation of charged quantized vortex rings in liquid helium at 1°K, 19: 41621

MC CALLUM, R. E., Basic uncertainties in electrical measurements, 19: 42218 (SC-TM-64-509)

MC CANDLESS, T. D., Physical property study of polystyrene foam (210-050), 19: 41000 (ACF-10)

MC CARROLL, Ronald, The excitation of neutral atoms by electron collisions, 19: 41254

MC CARTHY, J. R., Hydrogen heat transfer data compilation, 19: 40734 (NP-15331)

MC CLAIN, W. C., Project Salt Vault, 19: 42195 (ORNL-P-1479)

MC CLIMENT, Edward R., Broken symmetric couplings for decuplet decays into baryons and pseudoscalars, 19: 41399

MC CLUNG, R. W., Measurement and application of x- and gamma-ray attenuation to reactor materials evaluation, 19: 42071

MC CLUNG, R. W., Ultrasonic detection of non-bond in clad structures, 19: 40756

MC CONNELL, H. M., Chemical enhancement of superconductivity, 19: 40543

MC CONVILLE, J. H., Direct current electromagnetic pump analysis, 19: 40743 (TIM-929)

MC CUNE, James E., General criterion for electrostatic plasma instabilities with uniform magnetic field, 19: 41897

MC DANIELS, D. K., Level scheme of Ga-69, 19: 41756

MC DOUGALL, Ian, Strontium isotope composition and K–Rb ratios in some rocks from Reunion and Rodriguez, Indian Ocean, 19: 40791

MC EACHRAN, R. P., Elastic scattering of low-energy positrons by atomic hydrogen, 19: 41267

MC ELWEE, I., Automatic ultrasonic inspection of nozzle welds in nuclear reactor pressure vessels, 19: 42025

MC GARRY, W. I., Angular distribution of the d-d reaction products, 19: 41832

MC HARGUE, C. J., Diffusion of Nb-95 and Ta-182 in niobium (columbium), 19: 41064

MC INTYRE, J. A., Inelastic scattering and neutron pickup for ^{12}C and ^{16}O projectiles on ^{208}Pb, 19: 41768

MC KEE, W., Prog. rpt. on ion rocket engine development, 1–3/65, 19: 40765 (NP-15309)

MC KISSON, R. L., Prog. rpt. on solubility studies in alkali metals, 1/3–4/3/65, 19: 40946 (AI-65-93)

MC LAUGHLIN, Edwin F., Sensitive differential pressure system for measuring depths of cryogenic liquids, 19: 40878 (UCRL-9672(Rev.))

MC MANUS, H., Excitation of first levels of ^{12}C by 156-Mev protons, 19: 41675 (ORNL-P-330)

MC MASTERS, O. D., Gold-rich rare-earth-gold solid solutions, 19: 41062

MC MULLEN, A. G., Transformation in zirconium–niobium alloys, 19: 41033

MC MULLEN, William Dale, Evaporation behavior of zirconium beryllides, 19: 41078

MC MURTRY, Carl H., Preparation of UC on pilot-plant scale, 19: 40954

MEAD, J. B., Improvement of resolution in large area photomultipliers, 19: 40895

MEADE, D. M., Motion of plasma and lifetimes of energetic ions in a toroidal octupole magnetic field, 19: 41896

MEDVEDEV, S. S., Transformations in EPR spectra of irradiated polyisobutylene, 19: 40608

MEGRET, Jean, Device for operating a movable trolley, 19: 42189

MEINADIER, J. P., Treatment of capture gamma ray spectra obtained with the aid of a central crystal in association with an annular crystal, 19: 40896

MEISSNER, H., Liquid-He irradiation facility at the Munich research reactor FRM, 19: 42180

MEJDAHL, V., Thermoluminescence readout instrument for measurement of small doses, 19: 40877 (RISO-101)

MEKHEDOV, V. N., K-capture fraction of ^{66}Ge, ^{69}Ge, and ^{72}As, 19: 41800

MEKHEDOV, V. N., Slow particles emitted in stripping reactions, 19: 41664 (JINR-P-2193)

MELEKHOVA, A. M., Influence of radiation on individual neurons of cortex, 19: 40355 (FTD-TT-65-48, pp 111-12)

MELHUISH, K. R., Determination of nitrogen in uranium–plutonium dioxides, 19: 40438

MELLO, P. A., Nuclear structure in the 2s-1d shell. I., 19: 41729

MELLO, P. A., Nuclear structure in the 2s-1d shell. II., 19: 41730

MELNGAILIS, J., Position annihilation and orthogonalized plane waves in lithium, 19: 41945

MEL'NIKOV, V. K., Compensation of helical magnetic field disturbances, 19: 41116 (IAE-663)

MELTZER, C. M., Anti-isobar production in $\bar{p}n$ interactions, 19: 41438

MELVIN, M. A., Orbits in a magnetic universe, 19: 41208 (ORNL-3827)

MENEGHETTI, L., Search for a β-active ^{5}H, 19: 41750

MENON, K. K., Fission products in the atmosphere and in rain, 19: 40785 (TID-21224)

MENSE, E. U., Prog. rpt. on stable isotope studies, annual, 9/15/64–7/15/65, 19: 40460 (NYO-3462-1)

MEREY, Imre, Electrostatic ion beam accelerator, 19: 41181

MERMAGEN, H., Effect of wide x-ray beam and finite phantom thickness on 1000-kvp x-ray depth dose, 19: 40881 (UR-667)

MESHCHERYAKOV, M., Double pp scattering at 667 Mev, 19: 41666 (JINR-P-2233)

MESHKOV, S., $SU(6)_w$ photoproduction and meson-baryon scattering amplitudes, 19: 41462

MESHKOVA, S. B., Rare earth complexes with sulfosalicylic acid in aqueous solutions, 19: 40513

MESICH, Frank Gerald, Deactivation of reaction complexes in the recoil chemistry of ^{11}C, 19: 40550 (IS-T-27)

MESSIER, Jean, Charge state of defects produced by irradiation in silicon semiconductor junction, 19: 41974

MESTRE, E., Intervention-decontamination building, Centre d'Etudes Nucleaires de Fontenay-aux-roses, 19: 40836

METHERELL, A. J. F., The characteristics of the moellenstedt velocity analyser, 19: 40883

METZGER, F. R., Properties of 4.403-Mev excited state of ^{27}Al, 19: 41775

MEYER, P., Prog. rpt. on two-phase flow and boiling heat transfer, 1–3/65, 19: 40738 (NYO-3114-7)

MEYER, W., High-temperature high-vacuum valves with gold-wire sealing, 19: 40775

MEYZEROV, E. S., Combined action of whole-body vibration and ionizing radiations on central nervous system, 19: 40354 (FTD-TT-65-48, pp 38-9)

MEZZETTI, L., Lambda^0 polarization from $\gamma + p \rightarrow \Lambda^0 + K^+$ at 950 to 1050 Mev, 19: 41367

MIA, M. D., Effects of temperature and pressure on hot-atom reactions in bromoethane, 19: 40626

MIALKI, Werner, Thermal nuclear reactor, 19: 42065

MICHEL, F. C., Effect of magnetospheric tail on cosmic ray cut-offs, 19: 41307

MICHEL, Louis, Problem of group extensions of Poincare group and SU(6) symmetry, 19: 41520

MICHELETTI, S., Reaction (n,d) on ^{63}Cu and ^{65}Cu isotopes at 14 Mev, 19: 41755

MIKAELYAN, L. A., Neutron emission from ^{233}U, ^{235}U, and ^{239}Pu fission fragments, 19: 41681 (ANL-Trans-205)

MIKHAILOV, V. A., A spark chamber with a big discharge gap, 19: 40886

MIKHAILOV, V. D., The process of pair production by fast muons, 19: 41486

MIKHAILOVSKII, I. M., Reestablishment of contacts between fragments of a tungsten microcrystal, 19: 41061

MIKHALEVA, T. N., Excitation functions for (p,p′) on Al-27, 19: 41813

MIKLER, J., Ion exchange separation of rare earth metals. III., 19: 40680

MILEY, G. H., Feedback effects during short interval-series pulsing, 19: 42188

MILICH, Charles P., Hydraulic control rod actuators for Kiwi-TNT reactor, 19: 42136 (LA-DC-6941)

MILLER, A. J., Some aspects of general circulation of the lower stratosphere, 19: 41570 (CONF-765-11)

MILLER, David B., Cyclotron resonance propulsion system, 19: 40764 (N65-27691)

MILLER, David B., Prog. rpt. on continuous-microwave magnetic accelerators, 8/8/63–8/7/64, 19: 40761 (N64-30604)

MILLER, Donald H., Branching ratios for decays of the f^0, A_2, and K*(1400) mesons, 19: 41460

MILLER, G., The stereochemistry of the reactions of (n,γ) halogen atoms with alkyl halides in the liquid phase, 19: 40625

MILLER, G. E., Effects of temperature and pressure on hot-atom reactions in bromoethane, 19: 40626

MILLER, J. A., Radiometric age of the Serra Geral Formation, 19: 40796

MILLER, K. J., Uranium–Mo fuel element irradiation in SRE, 19: 41090 (NAA-SR-11121)

MILLER, P. D., Low pass filter for cold neutrons to be used in a search for a neutron electric dipole moment, 19: 41338 (ORNL-TM-1149)

MILLER, R. R., Instability of refractory metal thermocouples, 19: 40859

MILLER, T. G., Determination of P/β ratio for plastic scintillator,

19: 40916
MILLER, W. S., Hydrogen heat transfer data compilation, 19: 40734 (NP-15331)
MILLER, Warren W., Activation analysis for ^{18}O isotope abundance utilizing recoil protons, 19: 40419
MILLHOUSE, A. H., Temperature dependence of optical reflectivity of Ce metal, 19: 41082
MILLICHAMP, James W., Characterization of the voltage fluctuation in the direct current arc for spectrochemical analysis, 19: 40416
MILLIGAN, V. M., Remote radiation monitoring at the Nevada Test Site, 19: 40876 (NVO-162-5(Rev.))
MILOVANOV, O. S., Magnetron performance with a paired-resonator system, 19: 41191
MILOVANOV, V. P., Cascade mechanism of the high-energy nuclear reactions. I., 19: 41811
MILSTEIN, Frederick, Magnetic behavior of rare earth metals at high pressures, 19: 42005
MILTON, Charles, McKelveyite, a new hydrous U carbonate mineral, 19: 40799
MINAMI, Masatsugu, Possibility of cut-plane analyticity of momentum space vertex function, 19: 41558
MINAMI, S., Resonant state Y^{*0}'s with M ≈ 1660 Mev, 19: 41384
MINASYAN, S. M., Serum protein fractions of blood of irradiated animals, 19: 40385 (FTD-TT-65-48, pp 134-5)
MIRONOV, O. M., Experimental liquid-metal gallium loop for MHD investigations, 19: 40727
MISRA, Sushil Kumar, Some properties of dynamic nuclear orientation, 19: 42001
MITALAS, Roman, Central cooling of partially degenerate He cores by neutrino loss, 19: 41237
MITINA, N. I., Investigation of a θ pinch plasma in an azimuthal magnetic field, 19: 41921
MITINA, N. I., Plasma in a θ-pinch with azimuthal magnetic field, 19: 41860 (NP-15220)
MITRA, A. N., Three-body model for stripping and the validity of the distorted-wave born approximation, 19: 41777
MITRA, A. P., Statistical characteristics of sudden ionospheric disturbances, 19: 41573 (RPU-S19)
MITSUK, V. E., Measuring of electron concentration in plasma, 19: 41924
MITSUTANI, Akio, The effects of preirradiation on the activities of solid acidic catalysts, 19: 41099
MITTA, E. A., Determination of iodides in the preparations of ^{131}I-Rose Bengal, ^{131}I-Triolein, ^{131}I-Globulin, and ^{131}I-Iodoalbumin and preliminary separation by thin-layer chromatography, 19: 40656 (CEA-tr-X-609)
MIZIN, Yu. V., Dispersion of magnetic sector field with double focusing beam, 19: 41194
MLADENOV, I., Recombination processes in CdS during excitations by α particles, 19: 40565
MNATSAKANOVA, M. N., Fluctuations in electron-photon showers generated by high-energy μ mesons, 19: 41355
MOCOROA, A., Cross-section ratios for isomeric pair $^{44m}/^{44}Sc$ produced by $^{45}Sc(d,t)^{44}Sc$ reaction, 19: 41714
MOCOROA, A., Cross-section ratios for isomeric pair $^{58m}/^{58}Co$ produced by $^{59}Co(d,t)$ reaction, 19: 41715
MODENOV, V. P., H_{11} wave penetration through plasma in circular waveguide, 19: 41903
MOE, H. J., Radiation safety technician training course. I., 19: 40801 (ANL-6991)
MOELLER, Roger D., Method of forming molybdenum silicide coating on molybdenum, 19: 40998
MOFFATT, W. Craig, Skin friction and heat transfer in MHD channel flows, 19: 41119 (MIT-36-P)
MOKHIR, Yu. M., Influence of unitol on biochemical indices of tissue after x irradiation, 19: 40386 (FTD-TT-65-48, pp 661-2)
MOLCHANOVA, E. K., Thermal treatment of Ti–Al–Mo–Zr–Sn alloys, 19: 41052
MOLHO, N., Reaction (n,d) on ^{63}Cu and ^{65}Cu isotopes at 14 Mev, 19: 41755
MONNIN, Michel, Determination of thresholds of sensitivity for recording of different ionizing particles in solid-state polymers, 19: 40564
MONTH, Melvin, Interpretation of the κ in $K^+p \to Kmmp$, 19: 41417
MOORE, Fletcher L., Liquid-liquid extraction of metal ions from aqueous solutions of organic acids, 19: 40657
MOORE, J. A., Absolute fission cross section of ^{235}U for 2200-m/sec neutrons, 19: 41691
MOORE, Robert A., Electric propulsion ground testing, 19: 40771
MOORHOUSE, R. G., Pion-nucleon scattering amplitudes in the range 300 to 700 Mev, 19: 41442
MORA, S., Difference in range-energy relation for positive and negative particles, 19: 41369
MORAGA B., Aldo, Reconnaissance for U in the Colinapu Formation of central Chile, 19: 40798 (RME-4571(Rev.))
MORALES, A., CP violation and SU_3 symmetry, 19: 41371
MOREAU, Jean-Baptiste, Distribution function of electron velocities in Cs plasma in oscillation regime, 19: 41877
MOREL, A., Limitations of the bootstrap method for the determination of vector meson parameters, 19: 41373
MORET-BAILLY, Francoise, Neutrinos and singular electromagnetic field, 19: 41348
MORETON-SMITH, M. J., Hydrolysis of neutron-irradiated U and U–Pu monocarbides, 19:40586
MORGAN, C. G., Auger ejection of electrons from silver, 19: 41270
MORGAN, D. J., Derivation of sum rules and hyperviral theorems by differentiation, 19: 41557
MORGAN, I. L., The measurement of surface contamination of high-purity beryllium samples, 19: 40453
MORGAN, James M. Jr., Survey of research in the transportation of radioactive materials, 19: 40809 (SC-RR-65-98, pp 17–31)
MORGENSTERN, F., MZFR fuel elements—design, construction, and research, 19: 42165
MORGENSTERN, J., Treatment of capture gamma ray spectra obtained with the aid of a central crystal in association with an annular crystal, 19: 40896
MORI, K., High-energy scattering by exchange of Markov's particle, 19: 41383
MORI, K., Nucleon form factor and large-angle p-p scattering, 19: 41385
MORIKAWA, Tetsuya, A consideration to the design of MHD generator, 19: 41316
MORIN, K. R., NRU monitor computer and self-powered neutron flux detectors, 19: 42148 (AECL-2216)
MORIN, K. R., Solid-state multiplexer for use with self-powered neutron flux detectors, 19: 40866 (AECL-2217)
MORITA, Susumu, Alpha particle groups from deuteron bombardment of ^{16}O and ^{40}Ca, 19: 41720
MORIYA, T., Dispersion of radioisotopes caused by transport fires, 19: 40830 (SC-RR-65-98, pp 719–22)
MORIYA, T., Studies on fire resistivities of radioisotope containers, 19: 40831 (SC-RR-65-98, pp 723–31)
MORIZE, Pierre, Improvements in or relating to metal oxide powder sintering, 19: 40995
MOROZ, V. I., Optimal determination of the detecting efficiency (weight) of an event, 19: 40873 (JINR-P-2215)
MOROZOVA, I. G., Bench for testing ion injectors, 19: 41192
MORPURGO, M., High-intensity, partially separated, beam of antiprotons and K mesons, 19: 41184
MORRISON, G. H., Computer programs to optimize times of irradiation and decay in multielement activation analysis, 19: 40451
MORRISON, James Leslie, Neutron-deuteron scattering, 19: 41504
MORRISON, R. C., Total photoproton cross section and branching ratios in the O-16 giant resonance, 19: 41790
MORTON III, J. R., Pulsed neutron measurements on solid-moderated, enriched-uranium subcritical assemblies, 19: 42051 (UCRL-12013)
MOSCICKI, Wladzimierz, Utilization of radiocarbon ^{14}C in the investigation of atmospheric movements, 19: 40797
MOSKALEV, O. B., Approximate solution for the nonlinear transport equation, 19: 41651
MOSKALEV, Yu. I., Biological effects of Sr-90 in relation to the duration and frequency of uptake, 19: 40336
MOSKALEV, Yu. I., Distribution, biological effects, and rapid excretion of radioactive isotopes, 19: 40311
MOSKALEV, Yu. I., Distribution of Y-91, Zr-95, and Nb-95 in rats after inhalation, 19: 40314
MOSKALEV, Yu. I., Distribution of radium isotope thorium-x, 19: 40315
MOSKALEV, Yu. I., Distribution of Sb-124 and Te-127, 19: 40318
MOSKALEV, Yu. I., Distribution of tin-113, 19: 40320
MOSKALEV, Yu. I., Distribution of a mixture of Ce-144 and Sr-89, -90, 19: 40321
MOSKALEV, Yu. I., Distribution of lead (thorium B) after intra-arterial and intravenous injection, 19: 40333
MOSS, A., Isotope effects in electron spin resonance: the negative ion of cyclo-octatetraene-1-d, 19: 40541
MOSS, M. K., Conservation laws of general theory of relativity. I., 19: 41542
MOSS, M. K., Conservation laws of general theory of relativity. II., 19: 41543
MOSS, S. J., Polarization of protons scattered by carbon, 19: 41731
MOSSOTTI, Victor Giovani, Atomic absorption spectra of lanthanide elements (thesis), 19: 40526
MOSZKOWSKI, S. A., Nuclear coupling schemes with a surface delta interaction, 19: 41686
MOTSINGER, Russell E., Introduction to nuclear propulsion—nuclear rocket system, 19: 42139 (N64-33784)

MOTZ, H. T., High-energy γ spectrum of thermal neutron capture in holmium, 19: 41670 (LA-DC-7097)
MUELLER, H.-W., Development and potentialities of the high-temperature pebble-bed reactor concept, 19: 42082 (CONF-650633-1)
MUELLER, Horst, Chemical results of nuclear processes in mixed crystals. I., 19: 40585
MUELLER, M. W., Summary report on electron bombardment ion engine development, 19: 40760 (N64-25008)
MUELLER, R. E., Investigation of core reproducibility of the Enrico Fermi reactor, 19: 42079 (APDA-NTS-4)
MUELLER, R. E., Measurement of the isothermal temperature coefficient of reactivity of the Enrico Fermi reactor, 19: 42080 (APDA-NTS-5)
MUELLER, William M., Seminar on energetics in metallurgical phenomena, Denver, 1962. I., 19: 41075
MUELLER-BUSHBAUM, G., Fluorescence of rare earths. II., 19: 40494
MUGHABGHAB, S. F., Search for J-dependent neutron strength functions in rare earth region, 19: 41656 (BNL-9245)
MUKHERJEE, C. S., Unitary symmetry breaking interactions and decays of vector mesons, 19: 41366
MUKHIN, K. N., Elastic pp scattering at 1.45 Bev, 19: 41487
MUKUNDA, N., Tensor methods. II., 19: 41340 (UR-875-53)
MULLER, Th., High-intensity, partially separated, beam of antiprotons and K mesons, 19: 41184
MULLER, W. C., Prog. rpt. on dispersion-strengthened alloys, 4–6/65, 19: 41021 (NMI-8002.1)
MULLIN, Albert A., New theorems for elementary number theory, 19: 42224 (UCRL-12041-T)
MUNIR, B. A., IBM 1620 reconstruction of bubble chamber interactions, 19: 40915
MURAI, Yutaka, A consideration to the design of MHD generator, 19: 41316
MURAKAMI, Masanori, Particle orbits in a heliotron magnetic field, 19: 41885
MURBACH, E. W., Pyrochemical reprocessing of uranium carbide, 19: 40652 (NAA-SR-11340)
MURBACH, E. W., Pyrochemical reprocessing of UO_2 by Airox, 19: 40653 (NAA-SR-11389)
MURIN, A. N., Separation of radiophosphine from mixed KCl–$CaCl_2$ crystals irradiated with high-energy protons, 19: 40606
MURRAY, B. W., Instrumentation for Moessbauer-effect experiments at low temperatures, 19: 40863
MURRAY, J. L., Correlation of rose bengal clearance and histopathological change of sheep livers damaged by Np-237, 19: 40350 (HW-SA-3723)
MUSTEL', E. R., Quasi-stationary corpuscular streams during the descending phase of the 19th cycle of solar activity, 19: 41216
MUZZARELLI, R. A. A., Separation of traces of metals from uranium by chromatography on cellulose, 19: 40687
MYERS, J. L., Testing of 10-ton capacity UF_6 shipping containers, 19: 40824 (SC-RR-65-98, pp 580–608)
MYERS, J. R., Influence of zirconium additions on epsilon phase of titanium–aluminum system, 19: 41053

N

NABER, J. A., Economical liquid He cryostat and other cryogenic apparatus, 19: 41626
NAD, L., Application of controlled photomultiplier as a separating element in the nanosecond coincidence circuit, 19: 40872 (JINR-P-2203)
NAEUMANN, R., Separation of iodine anions by glass fibre paper chromatography, 19: 40430
NAGASHIMA, Yorikiyo, Proton compton scattering in 2nd resonance energy region, 19: 41465
NAGY, Karoly, Theory of weak interactions of elementary particles, 19: 41356
NAGY, Laszlo, Angular distribution of γ rays from fission of U-235, 19: 41722
NAKADA, M. P., Origin of outer-belt protons. I., 19: 41577
NAKAMURA, Seitaro, Selection rules and mass spectrum of particles. I., 19: 41362
NAKANISHI, Nobuo, Normalization condition and normal and abnormal solutions of the Bethe-Salpeter equation. II., 19: 41434
NAKHODKIN, N. G., Inelastic scattering of electrons in thin films, 19: 41961
NALIBOFF, Y. D., Prog. rpt. on integral neutron thermalization, 3/31/65, 19: 41640 (GA-6323)
NAMBU, Y., Dynamical symmetries and fundamental fields, 19: 41519
NAMBU, Y., Three-triplet model with double SU(3) symmetry, 19: 41406
NAMIKI, Hideo, Subacute necrotizing encephalomyelopathy, 19: 42219 (TID-21177)
NARANG, V. P., Search for 2.6-hr iodine-126m, 19: 41716
NARASIMHAM, M. N. L., Transient MHD flow in an annular channel, 19: 41137
NARCISI, R. S., Mass spectrometric measurements of positive ions at altitudes from 64 to 112 kilometers, 19: 41588
NARDELLI, G. C., Performance and properties of a proton polarimeter, 19: 40905
NARVER, David L. Jr., Engineering and cost considerations for tunnel grid blast shelter concept, 19: 40759 (ORNL-TM-1183)
NASSIFF, S. J., Cross-section ratios for isomeric pair $^{44m/44}$Sc produced by ^{45}Sc(d,t)^{44}Sc reaction, 19: 41714
NASSIFF, S. J., Cross-section ratios for isomeric pair $^{58m/58}$Co produced by ^{59}Co(d,t) reaction, 19: 41715
NAZAROV, A. S., Reaction of $U(SO_4)_2 \cdot 4H_2O$ with tri-n-octylamine sulfates and bisulfates, 19: 40688
NEAMU, I., Reaction ^{26}Mg(p,p′γ) mechanism at low energies, 19: 41693
NEDVEDYUK, K., Investigation of nuclear reactions of helium-3 with carbon, 19: 41663 (JINR-P-2184)
NEEB, K. H., Spectral analytical trace determination in UO_2 nuclear fuel elements using radiochemical controlled standard probes, 19: 40434
NEFEDOV, A. P., Constitution diagrams of systems V–Ta–Nb and V–Ta–Mo, 19: 41036
NEIL, D. E., Promotion of chemical processes with reactor radiation, 19: 40559
NEIL, V. Kelvin, Relation between diochotron and negative mass instabilities, 19: 41180
NEILL, F. H., Iodine transport and deposition in a high-temperature, helium loop first test series, 19: 40397 (ORNL-TM-1134)
NEILL, J. M., Neutron-spectrum measurements in H_2O and D_2O, 19: 41646
NEILL, J. M., Prog. rpt. on integral neutron thermalization, 3/31/65, 19: 41640 (GA-6323)
NELSON, R. C., Fission gas release from UO_2 fuel rods with gross central melting. I., 19: 41088 (GEAP-4572)
NEMETH, Andras, Neutron flux measurements in core of the VVR-S research reactor, 19: 42183
NEMETH, Geza, Chebyshev expansion of integral sine and integral cosine functions, 19: 40944
NEMETH, Geza, Polynomial approximation to the function PSI(A, C, X), 19: 40943
NESMEYANOV, An. N., Chemical effects of nuclear transformations and energy transfer processes, 19: 40620
NESMEYANOV, An. N., Reactions of hot tritium atoms with alcohols and with some of their binary hydrocarbon mixtures, 19: 40622
NESMEYANOV, An. N., Reactions of hot tritium atoms with amino acids, 19: 40629
NESMEYANOV, An. N., The interaction of ^{14}C recoil atoms in binary mixtures, 19: 40627
NESTERIKHIN, Yu. E., Excitation of strong collisionless shock waves in plasma, 19: 41911
NESTERIKHIN, Yu. E., Heating of plasma by shock waves, 19: 41861 (NP-15255)
NESTEROV, V. E., Monitoring of cosmic radiation during flight of Vostok satellites, 19: 40841
NETHAWAY, D. R., Effect of increasing excitation energy on nuclear charge distribution in fission, 19: 41779
NETTER, F., Treatment of capture gamma ray spectra obtained with the aid of a central crystal in association with an annular crystal, 19: 40896
NEUMANN, J. P., On the deformation of tungsten single crystals by rolling, 19: 41066
NEWELL, R. E., Some aspects of general circulation of the lower stratosphere, 19: 41570 (CONF-765-11)
NEWMAN, K., Measurement of density of concrete and soils with γ radiation, 19: 40755
NEY, L. A., Filament-wound sphere with polar opening, 19: 40698 (ACF-9)
NGUYEN NGOC, Hoan, Beryllium-9 study by electron scattering, 19: 41683
NICHOLAS, John F., Atlas of models of crystal surfaces, 19: 41072
NICHOLLS, Jack, Variable guard, 19: 40930
NICHOLS, Charles R., Prog. rpt. on effects of electrical fields on boiling heat transfer, 5/26/64–9/30/64, 19: 40735 (NYO-2404-5)
NICHOLSON, R. B., Comment on the effect of resonance correction to group flux in fast-reactor Doppler-effect calculation, 19: 42058
NICKEL, John Carl, Study of plasma wave resonances, 19: 41932
NICOLIS, G., Bogolubov asymptotic condition for non-uniform systems, 19: 41132
NIEDERLE, J., Generalized spherical functions for the non-compact rotation groups, 19: 41327 (IC/65/63)
NIELSEN, H. L., High-energy transitions in I-132 decay, 19: 41744
NIFATOV, A. P., Biological effects of Sr-90, Co-137, and Pm-147 after chronic oral administration of low doses, 19: 40335
NIFATOV, A. P., Plutonium-239 in rat lung and liver and morphological changes after intratracheal administration, 19: 40317
NIGAM, B. P., Function in quantum mechanics which corresponds to a given function in classical mechanics, 19: 41555

NIGRO, M., Lambda° polarization from $\gamma + p \rightarrow \Lambda^0 + K^+$ at 950 to 1050 Mev, 19: 41367
NIKOLAEV, A. V., Enthalpy variations during extraction according to standard enthalpy of formation, 19: 40669
NIKOLAEV, A. V., Phospho-organic complexing resins, 19: 40668
NIKOLAEVA, N. M., Reactions of uranyl nitrate solution with sodium malonate solution, 19: 40482
NIKOLENKO, V. G., Determination of spins of Ho-165 neutron resonances by transmission of polarized neutrons through a polarized target in the energy interval 0–55 ev, 19: 41665 (JINR-P-2209)
NIMS, Leslie F., Membranes, material transfer and enzymes, 19: 42199 (BNL-8397)
NISHIMURA, Susumu, Trial method of determining uranium and thorium content in rocks, 19: 40432
NOELL, G. L., Water tests of high-speed centrifugal dynamic shaft seals, 19: 40702 (TIM-914)
NOER, R. J., Nuclear magnetic relaxation in Nb–Mo alloys, 19: 41989
NOGAMI, Yukihisa, Superconductivity theory of the nuclear pairing interaction, 19: 41843
NOON, J. H., Microwave measurement of the probability of collision of low energy electrons in nitrogen, 19: 41944
NORDEMANN, Daniel, Radioactivity of the Granes meteorite measured by γ spectrometry, 19: 40788
NORTON, Robert Henry, HeII+ in model stellar atmospheres, 19: 41240
NOTARYS, Harris Anthony, Megacycle-frequency second sound, 19: 41633
NOVAKOVIC, M., Heat transfer through vertical annular gas layer, 19: 40747
NOVIKOV, G. I., Vapor phase complexing of $ErCl_3$–KCl, 19: 40516
NOVIKOV, Yu. M., Current distribution in a coaxial plasma gun, 19: 41859 (NP-15218)
NOVOSILOVA, A. V., Ammoniated Be, Mg, Ca, Al, Sc, and Y acetates, 19: 40507
NOVOZHILOV, Yu. V., Elementary particles, 19: 41512
NUNEZ-LAGOS, R., CP violation and SU_3 symmetry, 19: 41371
NUNLEY, C. E., Joint National Institutes of Health-Atomic Energy Commission zonal centrifugation project. I., 19: 40654 (ORNL-3613)
NURUSHEV, S., Double pp scattering at 667 Mev, 19: 41666 (JINR-P-2233)
NUSSENZVEIG, H. M., High-frequency scattering by an impenetrable sphere, 19: 41129
NUSSINOV, S., Summing certain ϕ^4 graphs using integral equations, 19: 41429

O

O'CONNELL, J. S., Total photoproton cross section and branching ratios in the O-16 giant resonance, 19: 41790
O'DONNELL, P. J., Pion-nucleon scattering amplitudes in the range 300 to 700 Mev, 19: 41442
OEZEMRE, Ahmed Yuksel, Derivation of the Nordheim equation from the diffusion equation, 19: 41644
OGGERO, M., Electric propulsion by thermoelectric motors, 19: 40768
OGLOBLIN, A. A., The reactions $^3He(d,t)2p$ and $^3He(^3He,\alpha)2p$, 19: 41658 (IAE-655)
OGREN, John Roger, Thermodynamic measurements on CaCl-type structures in rare earth-magnesium systems, 19: 41013 (IS-T-25)
O'HALLORAN, T., K+p interactions at 2 Bev/c—elastic scattering and total cross sections, 19: 41436
OHJI, Takuyoshi, Moving striation of plasma in a longitudinal magnetic field, 19: 41888
OHNO, Shinichi, Oxidation of CO on NiO and ZnO, 19: 40577
O'KEEFE, D. P., Environmental tests of HTLTR materials, 19: 40966 (BNWL-92)
OKHRIMENKO, L., Reconstruction of the spatial picture of an event in the bubble chamber, 19: 40871 (JINR-P-2179)
OKRENT, David, Breeding, safety and fuel cycles, 19: 42081 (CONF-193-11)
OKUBO, Susumu, Possible effects of CP violation in $K^\pm \rightarrow 3\pi$ decay, 19: 41445
OKUDA, A. S., Hydrogen heat transfer data compilation, 19: 40734 (NP-15331)
OKUN', L. B., Supercharge and supercharged particles, 19: 41483
OLIVER, D. A., Silicon nitride: review of properties for use at elevated temperatures, 19: 41081
OLSON, P. W., Hollow metal single crystal for NMR experiments, 19: 40990
OLSSON, Martin Godfrey, Final-state interaction model in the reaction $\pi + N \rightarrow \pi_1 + \pi_2 + N$ below 1 Bev, 19: 41509
ONDRISH, L., Application of controlled photomultiplier as a separating element in the nanosecond coincidence circuit, 19: 40872 (JINR-P-2203)
ONG, R. S. B., General conservation laws in a dilute plasma, 19: 41889
ONO, Ken-ichi, Internal structure of elementary particles, 19: 41478
OPALOVSKII, A. A., Photocolorimetric determination of uranium(VI) with Arsenazo III in presence of fluoride, 19: 40428

OPAUSZKY, Istvan, The effect of the type of radiation on the radiolysis of diphenyl–methane, 19: 40591
OPPENHEIMER, J. Robert, Remarks on symmetry principles, 19: 41515
O'RAIFEARTAIGH, L., Lorentz invariance and internal symmetry, 19: 41411
OREAR, J., Backward elastic scattering of high-energy pions by protons, 19: 41456
OREAR, J., Pion-proton elastic scattering at high momentum transfers, 19: 41455
ORENSTEIN, Stephen, Pion-pion interaction in pair creation by gamma-rays, 19: 41505
ORGANESYAN, O. G., Emission of ultra-high energy μ mesons, 19: 41295
ORLOVA, K. B., Determination of nitrogen in metals by an isotope-dilution method, 19: 40444
ORTALLI, I., Difference in range-energy relation for positive and negative particles, 19: 41369
ORTH, Karl-Heinz, Long-time operational behavior of a high power pressurized water reactor with boron trimming (chemical shim), 19: 42023
OSBORN, R. K., Some theorems on neutron fluctuations and fluctuation spectra, 19: 41653
OSIKO, V. V., Optical properties of CaF_2–Dy^{3+}, 19: 40600
OSIKO, V. V., The effect of oxygen impurity on the optical properties of CaF_2–Sm crystals, 19: 41993
OSKAM, H. J., Prog. rpt. on collision processes in gaseous plasmas, 1–6/65, 19: 41850 (AD-617366)
OSTROUKHOV, A. A., Inelastic scattering of electrons in thin films, 19: 41961
OSTROVSKII, G. M., Problem of optimization of system with distributed parameters, 19: 42012
OSTROVSKII, L. A., Interaction of electromagnetic shock waves in nonlinear transmission lines, 19: 41136
OUTI, Akizi, Particle orbits in a heliotron magnetic field, 19: 41885
OVERSETH, O. E., Deuteron production in p-p collisions at 1.55, 2.5, and 2.9 Bev, 19: 41523
OWEN, W. S., The strain-ageing and quench-ageing of tantalum, 19: 41042

P

PAGANINI, L., Structure and recrystallization of cold-rolled and annealed Zircaloy-2, 19: 41034
PAGE, John P., Method of forming molybdenum silicide coating on molybdenum, 19: 40998
PAGE, Roy, Rescue basket, 19: 42223 (UCRL-12006)
PAK, Sang So, Prog. rpt. on inverter applications, 6/63–5/64, 19: 40845 (N64-33676)
PAL, Hiroadra Kumar, Analysis of J phenomenon in scattered x-rays. II., 19: 41357
PALENZONA, A., Atomic size of rare earths in intermetallic compounds, 19: 41040
PALEVSKY, Harry, Slow neutron studies of molecular motions in condensed matter, 19: 40455 (BNL-9297)
PALINSKI, Roman, Transient reactivity variation of reactor controlled with temperature of the moderator, 19: 42059
PALLISTER, E. T., Environmental radioactivity in New South Wales, 19: 40805 (NRS-30)
PALMER, B. D., Fission products in the atmosphere and in rain, 19: 40785 (TID-21224)
PALMER, J. P., Studies of a repetitive liquid metal slug MHD generator, 19: 41314 (BNL-9329)
PALMGREN, A., An accurate determination of neutron spectrum in thermal column of Triga reactor, 19: 42184
PALMS, John M., High resolution measurements of γ rays from neutron inelastic scattering, 19: 41669 (LA-DC-7096)
PALOTAY, J. L., Correlation of rose bengal clearance and histopathological change of sheep livers damaged by Np-237, 19: 40350 (HW-SA-3723)
PANDE, Lalit Kumar, K-meson nucleon scattering, 19: 41506
PANDIT, L. K., Tensor methods. II., 19: 41340 (UR-875-53)
PANOV, D. A., Low-density plasma forming in Ogra during injection of molecular hydrogen ions, 19: 41851 (IAE-635)
PAO, Chin-liang, Use of I-131 peanut oil in assessing lipid metabolism in coronary atherosclerosis, 19: 40393
PAOLINI, F. R., Effect of solar flare on outer radiation belt, 19: 41312
PAPADOPOULOS, L., Operation of a transistor in saturation state and a linear gate, 19: 40856
PAPAY, L. T., Fast fission measurements, 19: 41672 (MIT-2344-3, pp 5-14)
PAPAYOANOU, A., Structure and variation of the topside ionosphere close to the Fort Monmouth longitude, 19: 41587
PAPPAS, W. S., Constriction response analyzer and its application to continuous UF_6 determination, 19: 40417
PARFANOVICH, B. N., Unit for gas-phase radiation-induced graft polymer-

zation, 19: 40596
PARFENOV, Yu. D., Passage of Sr-90 from mother to offspring in dogs under conditions of chronic uptake, 19: 40327
PARFIANOVICH, I. A., Induced luminescence of Ag-activated alkali halide phosphors, 19: 41977
PARFIANOVICH, I. A., On the memory effect in the action of an electric field on the luminescence of alkali halide phosphors, 19: 40571
PARFIANOVICH, I. A., Some data on the luminescent properties of Eu-activated NaCl and KCl phosphors, 19: 40567
PARK, J. G., Asymmetry in the critical surface current of type-II superconductors, 19: 41616
PARKER, F. L., Project Salt Vault, 19: 42195 (ORNL-P-1479)
PARKS, William Frank, Alternate commutation relations, 19: 41562
PARR, E. D., Prog. rpt. on alkali metals evaluation program, 4–6/65, 19: 41001 (AGN-8154)
PARR, J. Gordon, Transformation in zirconium–niobium alloys, 19: 41033
PASCARD, Roger, Method of manufacture of UO_2 having a high density, 19: 40996
PASK, Joseph A., Physical chemistry of glass-metal interfaces, 19: 40464 (UCRL-11816(Rev.))
PASS, C., Modular, plug-in chassis system permits compatible mounting of conventional chassis, printed circuit boards, and micromodules, 19: 42226 (UCRL-12117-T)
PASSATORE, G., Muon capture by the virtual pions exchanged by proton pairs in a nucleus, 19: 41753
PASTERNAK, R. A., Prog. rpt. on sorption of gases on metal surfaces, 2/15–5/15/65, 19: 40463 (SRIA-425-5)
PATCH, R. W., Radiative transfer studies and opacity calculations for heated gases, 19: 40750
PATEL, K. C., Ascorbic acid and ascorbic acid oxidase of γ-irradiated Momordica charantia, 19: 40371
PATEL, R. D., Ascorbic acid and ascorbic acid oxidase of γ-irradiated Momordica charantia, 19: 40371
PATIL, Shareshchandra H., Bootstrap and SU(3) assignment of 2^+ mesons, 19: 41402
PATLACH, A. M., Proton magnetometer and stable oscillator for remote measurement of strong magnetic fields, 19: 40857
PATTERSON, D. E., The problem of container interchangeability, 19: 40822 (SC-RR-65-98, pp 442–9)
PAUL, H., Absorption and scattering of quantum mechanical coherent beams. I., 19: 41247
PAUL, H., Absorption and scattering of quantum beams. II., 19: 41248
PAUL, H.-G., Testing emergency cooling system of reactor FRJ-2 (DIDO), 19: 42153 (JUL-235-RE)
PAUL, Harry, Quantum mechanical fundamentals of theory of γ-γ angular correlations, 19: 41698
PAUL, Roger A., Crater measurements on Project Pre-Schooner, 19: 40707 (PNE-502F)
PAVLOV, A. F., Use of phase technics for studying polarization phenomena of radiowave reflection from meteor trails, 19: 41223
PAVLOV, S. A., X-ray studies of polyamide films cast from irradiated solutions, 19: 40595
PAVLOV, S. I., Measuring ionization function of metal atoms by electron impact, 19: 41276
PAVLYUCHENKO, M. M., Reactions of lanthanum and yttrium oxides with ferric oxide, 19: 40515
PAWEL, R. E., Diffusion of Nb-95 and Ta-182 in niobium (columbium), 19: 41064
PEARLSTEIN, S., Inelastic scattering of 14-Mev neutrons to low-lying states of Ta, W, Tl, and Pb, 19: 41718
PEARSON, D. B., Construction of a separable Hamiltonian, 19: 41546
PEARSON, J. B., Transient radiation environment of nuclear weapon detonations, 19: 40938
PEARSON, J. M., Family of velocity-dependent nucleon-nucleon potentials for singlet-even states, 19: 41841
PECK, P. F., The extraction of zinc by dithizone retained on cellulose acetate, 19: 40642 (AERE-R-4969)
PEDIGO, W. R., Testing of 10-ton capacity UF_6 shipping containers, 19: 40824 (SC-RR-65-98, pp 580–608)
PEERS, Arthur M., Adsorption of CO and O_2 on ZnO and NiO, 19: 40578
PEERS, Arthur Mackenzie, Oxidation of CO on NiO and ZnO, 19: 40577
PEHL, Richard H., Lithium-4 and the excited levels of He-4, 19: 41786
PEHLKE, Robert D., Equilibria of nitrogen with the refractory metals titanium, zirconium, columbium, vanadium, and tantalum in liquid iron, 19: 41065
PEISACH, Max, Use of semi-conductor detectors for surface analysis by elastic scattering of accelerated charged particles, 19: 40962
PELLETT, D. E., Deuteron production in p-p collisions at 1.55, 2.5, and 2.9 Bev, 19: 41523
PENEV, V. N., Baryon resonances in π-p interactions at 7.5 Bev with strange-particle formation, 19: 41488
PENEV, V. N., Meson resonances in π-p interactions at 7.5 Bev with strange-particle production, 19: 41489
PENNER, S. S., Radiation transfer studies and opacity calculations for heated gases, 19: 40750
PENZIN, Yu. G., Induced luminescence of Ag-activated alkali halide phosphors, 19: 41977
PENZINA, E. E., Induced luminescence of Ag-activated alkali halide phosphors, 19: 41977
PENZINA, E. E., Investigation of the processes occurring in excited Tl-activated KI phosphors upon application of an electric field, 19: 40573
PEPPARD, D. F., Fractionation of rare earths, 19: 40693
PERIA, W. T., Prog. rpt. on physics of electron emission and electron tube technology, 10/16/64–4/15/65, 19: 41124 (NP-15108)
PERKINS, M. A., Thermal-vacuum behavior of lithium-drifted silicon detectors, 19: 40902
PERKINS, R. W., Removal of radioisotope parent material by producing high-purity process water, 19: 42130 (HW-68387)
PERL, M. L., Deuteron production in p-p collisions at 1.55, 2.5, and 2.9 Bev, 19: 41523
PERLMAN, I., Odd-parity rotational bands in ^{246}Cm, 19: 41794
PERLMUTTER, Arnold, Conferences on symmetry principles at high energy, Coral Gables, 1/65., II., 19: 41514
PERMYAKOVA, T. V., Synthesis of La silicates from aqueous solutions, 19: 40518
PERRIN, R., Infrared behavior of the wave function renormalization constant in covariant gauges, 19: 41545
PERTSEV, A. N., Measurement of absolute yield of alkali-halide crystals in case of γ luminescence, 19: 40593
PERUZZO, L., Spin and parity of 1320 Mev $p\pi$ resonance, 19: 41368
PETERS, Philip Carl, Gravitational radiation and the motion of two point masses, 19: 41564
PETERSEN, G., MZFR safety shield with installation for pressure release, 19: 42167
PETERSON, F. C., Conductivity induced in polystyrene by pulsed γ rays, 19: 41091 (SC-R-65-943)
PETERSON, R. M., Uranium–Mo fuel element irradiation in SRE, 19: 41090 (NAA-SR-11121)
PETERSON, Reuben W., Design of containers for shipment of radioactive materials, 19: 40823 (SC-RR-65-98, pp 450–72)
PETERSON, Sigfred, Properties of thorium, its alloys, and its compounds, 19: 41025 (ORNL-TM-1144)
PETERSON, Victor L., Analysis of errors associated with the determination of planetary atmosphere structure from measured accelerations of an entry vehicle, 19: 41123 (NASA-TR-R-225)
PETRANGELI, G., Selection of nuclear power station operators, 19: 42098 (RT/PROT(65)24)
PETRANYI, Gyozoo, The importance of the quantitative alterations of the extracellular space in the water-embalances of the experimental intestinal x-ray death, 19: 40369
PETRARCA, S., Analog model for cylindrical nuclear fuel rods, 19: 40740 (RT/ING(64)16)
PETROV, K. I., System $SmCl_3$–NaCl–KCl, 19: 40517
PETROV, N. N., Auger ejection of electrons from tungsten and molybdenum by mercury ions, 19: 41272
PETROVICH, I. K., Changes in blood system of dogs intravenously injected with Y-91, 19: 40377
PETROVICH, I. K., Changes in blood content of pregnant animals after administration of Sr-90, 19: 40378
PETRUCCI, G., High-intensity, partially separated, beam of antiprotons and K mesons, 19: 41184
PETSCHEK, H. E., Experiments with magnetohydrodynamically supported shock layers, 19: 41120 (N64-30509)
PETZOLD, J., Determination of energy spectrum from time behavior of decay of quantum mechanical system, 19: 41532
PEWITT, E. G., Innovations in bubble chamber devices, 19: 40869 (CONF-650510-14)
PHILLIPS, J. L., Dounreay fast reactor. Sustained full power operation. II., 19: 42116
PHILLIPS, Roger J. N., Regge-pole models for high-energy πN, KN, and $\bar{K}$N scattering, 19: 41426
PHILLIPS, W. R., The ranges of nitrogen ions in nickel and silver, 19: 41269
PIAZZI, Marcello, Thermal decomposition of explosives exposed to γ rays, 19: 40562
PIERCE, T. B., The extraction of zinc by dithizone retained on cellulose acetate, 19: 40642 (AERE-R-4969)
PIERONI, J. J., Electron spin resonance determination of the radiolytic yields of trapped electrons and other species in an organic glass, 19: 40558
PIETRA, Francesco, Kinetic deuterium isotope effect in the reaction of 2,4-dinitrophenyl phenyl ether with piperidine in benzene, 19: 40544

PIGNANELLI, M., Reaction (n,d) on ^{63}Cu and ^{65}Cu isotopes at 14 Mev, 19: 41755
PIKE, R. W., Measurement of void fraction in two-phase flow by x-ray attenuation, 19: 40745
PIKELNER, L. B., Niobium and Rb neutron resonances and radiation widths of medium-mass nuclei, 19: 41727
PIKIN, S. A., Decay $\pi \to \mu + \mu + e^+ + e^-$, 19: 41482
PIKUS, G. E., Most effective regimes for thermionic convertors, 19: 41317
PILARSKI, E. M., Development of a process for manufacturing ZPR-III U–Pu–Mo test fuel elements, 19: 40978 (ANL-6955)
PILAT, E. E., Single-rod measurements and theory, 19: 42047 (MIT-2344-3, pp 115-24)
PILLOTON, R. L., Motion of spheres in smooth rotating drums and applications to the coating of nuclear fuel particles, 19: 40982 (ORNL-3819)
PINAJIAN, J. J., Use of ethanol in isolating ^{22}Na from cyclotron targets, 19: 40637 (ORNL-tr-625)
PINKAU, Klaus, Errors in electromagnetic cascade measurements due to the transition effect, 19: 40912
PINKSTON, W. T., Form factors for nuclear stripping reactions, 19: 41746
PIROGOVA, G. N., Effects of radiation on Yakutian diamonds, 19: 41098
PISARENKO, N. F., Monitoring of cosmic radiation during flight of Vostok satellites, 19: 40841
PISAREVSKII, A. N., Measurement of absolute yield of alkali-halide crystals in case of γ luminescence, 19: 40593
PISLAR, V., Heat transfer through vertical annular gas layer, 19: 40747
PISTRYAK, V. M., Motion of plasma bunches in a field-free space, 19: 41856 (NP-15205)
PITAYEVSKY, L. P., Hypersonic body motion through rarefied plasma, 19: 41894
PLATT, Allison M., Development of radioactive waste fractionization and packaging technology, 19: 42197
PLOEGER, F., MZFR fuel elements, 19: 42175
PLOTNIKOV, A. F., Radiation defects in very pure silicon crystals, 19: 41998
POBEDINA, L. I., New photometric methods for determining Nb and Ta in metals and alloys. IV., 19: 40442
POCTA, Bohumil, Change in the wall thickness of tubes during drawing, 19: 40983 (ANL-Trans-189)
PODGORODETSKAYA, V. N., Hematopoiesis in dogs during subacute intoxication induced by Pu-239, 19: 40379
POENARU, D. N., Analysis of some circuits used in amplifiers for semiconductor nuclear particle detectors, 19: 40899
POGODILOVA, E. G., Ammoniated Be, Mg, Ca, Al, Sc, and Y acetates, 19: 40507
POGOSYAN, V. A., Plasma polarization in an electric field, 19: 41906
POINDEXTER, Edward, Differential dynamic polarization of fluorine and hydrogen nuclei, 19: 40497
POINDEXTER, John Marion, Electronic shielding by closed shells in thulium compounds, 19: 40528
POLATTY, J. M., Investigation of manufacture of aggregate and riprap by nuclear means, 19: 40709 (PNE-5003)
POLEZHAEV, Yu. M., Subsolidus structure of $Li_2O–ZrO_2–SiO_2$ and its properties, 19: 41038
POLITOV, N. G., Radiation damage in ionic crystals, 19: 41976
POLKINGHORNE, J. C., Model requiring Lie group symmetries, 19: 41342
POLLACK, Israel, Spectral representation and criticality problem of a two-region cell transport operator, 19: 42035 (ANL-6590)
POLOGRUDOV, V. V., Investigation of the processes occurring in excited Tl-activated KI phosphors upon application of an electric field, 19: 40573
POLOGRUDOV, V. V., On the memory effect in the action of an electric field on the luminescence of alkali halide phosphors, 19: 40571
POLUEKTOV, N. S., Rare earth complexes with sulfosalicylic acid in aqueous solutions, 19: 40513
POMANSKII, A. A., Calculations of atmospheric shower curves, 19: 41300
POMANSKII, A. A., High-energy electron and photon passage through condensed media, 19: 41707
POMERANTZ, M. A., Prog. rpt. on cosmic ray experiment in Explorer VII, final, 11/61–12/63, 19: 41283 (NASA-CR-58203)
POMORSKI, Leon, Nucleon-transfer reactions in interaction of nuclei with heavy ions. B., 19: 41795
POMPEI, V., Direct determination of some fission products in mixtures by γ spectrometry, 19: 40411 (RT/CHI(65)2)
POMRANING, G. C., Effective thermal neutron cross sections for materials with grain structure, 19: 42041 (GA-6286)
PONOMARENKO, A. G., Excitation of strong collisionless shock waves in plasma, 19: 41911
PONTECORVO, J. B., Michel parameter in $\mu^- \to e^-$ decay, 19: 41480
POOL, M. J., Heats of mixing in Pr–Nd solid solutions, 19: 41044
POOLE, Durrell O., Use of semi-conductor detectors for surface analysis by elastic scattering of accelerated charged particles, 19: 40962

POP, S. S., Excitation of the H_β line of hydrogen and of some mercury lines by collision of protons and H_2^+ ions with mercury atoms, 19: 41260
POPE, Joseph H., Dyhamic spectral characteristics of micropulsation pearls, 19: 41582
POPE, William L., Sensitive differential pressure system for measuring depths of cryogenic liquids, 19: 40878 (UCRL-9672(Rev.))
POPEA, Florica, Separation of thorium from uranium, 19: 40439
POPOLATO, A., Analysis of shock wave and initiation data for solid explosives, 19: 42206 (LA-DC-6992)
POPOV, A. B., Neutron resonances of ytterbium isotopes, 19: 41661 (JINR-P-2158)
POPOV, B. M., Cyclotron injector, 19: 41193
POPOVICI, M., Choice of collimators for neutron powder diffractometry, 19: 40492
POPPENDIEK, H. F., Prog. rpt. on heat transfer for space nuclear power, 12/64–2/65, 19: 40741 (SAN-409-23)
PORETSKII, L. B., Irradiation of n-type Ge with fast neutrons, 19: 41104
PORTER, Charles E., Study of generalized level density by the methods of differential-recurrence equations, 19: 41655 (BNL-934)
POSEY, Lawrence D., Alpha particle bombardment of Si and GaAs diodes; energy conversion and radiation damage (thesis), 19: 40937 (UCRL-11958)
POSKANZER, A. M., Cross sections for the production of ^9Li, ^{16}C, and ^{17}N in irradiations with Bev-energy protons, 19: 41780
POTENZA, R. M., Reactor stability tests in Spert IV facility, 19: 42152 (IDO-17088)
POWELL, J. R., Studies of a repetitive liquid metal slug MHD generator, 19: 41314 (BNL-9329)
POWELL, Jack E., Separation of rare earths by ion exchange, 19: 40691
POWERS, P. N., Investigations on nonlinear stability of coupled nuclear systems, 19: 42062
PRADEL, Jacques, Mobility spectrum of small radioactive ions of the air, 19: 40787
PRASAD, R., Wigner-Inoenue contraction and possible conformal invariance of internal and external motions of elementary particles, 19: 41389
PRATT, P. L., Role of grain boundaries in plastic deformation of CaF_2, 19: 40536
PRAVEDNIKOV, A. N., Transformations in EPR spectra of irradiated polyisobutylene, 19: 40608
PREISS, K., Measurement of density of concrete and soils with γ radiation, 19: 40755
PREPARATA, G., Properties of weak amplitudes in broken U(12), 19: 41420
PREPARATA, G., Spin tests for bosons, 19: 41447
PRESENTI, Pierre, Mechanical manipulators, 19: 40730
PRIMAKOFF, H., Application of Goldberger-Treiman relation to β decay of complex nuclei, 19: 41774
PROFIO, A. E., Prog. rpt. on integral neutron thermalization, 3/31/65, 19: 41640 (GA-6323)
PROKOF'EV, P. T., Spectrum of internal-conversion electrons produced upon capture of thermal neutrons by indium, 19: 41808
PROKOFEVA, S. V., H_{11} wave penetration through plasma in circular waveguide, 19: 41903
PROTASOV, V. S., Scandium monosilicide and its crystal structure, 19: 40479
PRUDKOVSKII, G. P., Production of trochoidal electron beams having reduced orbital motion, 19: 41134
PTUKHA, T. P., Density of weak mixture of $^3He–^4He$, 19: 41628
PURDUE, C. H., Computer aided circuit reliability analysis, 19: 40848 (SC-R-65-935)
PURMAL, G. W., Surface ionization engine development, 19: 40769
PUSHINOV, Yu. V., New reagents for zirconium, 19: 40441
PYLE, Robert V., Spectroscopic technique for probing an ionized gas, 19: 41883
PYTEV, Yu. P., Classical scalar meson fields, 19: 41497

Q

QAIM, S. M., Radioisotopes I-117, -118, and -119, and Te-117, 19: 41717
QUINE, J. P., Microwave measurement of the probability of collision of low energy electrons in nitrogen, 19: 41944
QUITTNER, Pal, On angular correlation measurements between fast neutrons, 19: 40894

R

RABY, J. S., Economical liquid He cryostat and other cryogenic apparatus, 19: 41626
RACHAL, Lawrence H., The thermal expansion of Al_2O_3, 19: 41020 (NAA-SR-Memo-2987)

RACZKA, R., Generalized spherical functions for the non-compact rotation groups, 19: 41327 (IC/65/63)
RADVANYI, Pierre, Angular correlation in (p,pd) reaction on C-12, 19: 41703
RAETHER, H., Electron avalanches and breakdown in gases, 19: 41938
RAIKOV, V. S., Spectrometric characteristics of LSU-5k apparatus, 19: 40875 (NP-15254)
RAJAGOPALAN, G., A versatile two-element low-background flow-type beta-counter, 19: 40903
RAJAN, S. M., Gas absorption by drops travelling on a vertical wire, 19: 40398 (UCRL-16047)
RAJANGAM, K. B., Frequency modulation of large cavities, 19: 40723
RAKHOVSKII, V. I., Measuring ionization function of metal atoms by electron impact, 19: 41276
RALPH, John Charles, Improvements in or relating to conveyor systems, 19: 40729
RAMAUT, J., Early induction by x rays of discoloration of foliar spots in Nicotiana leuconeura, 19: 40362
RAMSAY, J. B., Analysis of shock wave and initiation data for solid explosives, 19: 42206 (LA-DC-6992)
RAMSDEN, S. A., Observation of the Faraday effect in a θ-pinch plasma using He–Ne laser, 19: 41947
RANKIN, A. C., Ultrasonic inspection of Nimrod power plant alternator rotors, 19: 41201
RANKIN, C. T., Joint National Institutes of Health-Atomic Energy Commission zonal centrifugation project. I., 19: 40654 (ORNL-3613)
RAO, B. N. Subba, Finite solid angle attenuation factors in angular correlation functions, 19: 40900
RAO, Modicherla Jagannadha, Electron spin resonance in irradiated hydroxylated organic compounds, 19: 40613
RAO, U. R., Cosmic-ray intensity measured by Mariner 2 and by ground neutron monitors during Forbush decrease of September 30, 1962, 19: 41304
RARITA, William, Regge-pole models for high-energy πN, KN, and $\bar{K}$N scattering, 19: 41426
RASHID, H. A., Photoproduction of ρ- and ω-mesons from nucleons, 19: 41321 (AECD/TP/4)
RASHID, M. A., $\bar{U}(12)$ predictions for $N\bar{N}$ annihilation at rest into four mesons, 19: 41463
RASMUSSEN, J. O., Internal conversion electrons from primary fission fragments, 19: 41680 (UCRL-16184)
RASZILLIER, I., Remark to a paper of Moses and Wang, 19: 41390
RATCLIFFE, R. T., Mechanism of cavitation in Mg during creep, 19: 41057
RAUB, Ernst, The influence of additions on the properties of tantalum, 19: 41067
RAUCH, L. M., Algebraic structure of the n-body problem, 19: 41122 (N64-31207)
RAUCH, L. M., Regularized explicit solution of the analytic N-body problem, 19: 41530 (N64-82432)
RAUM, H., THERMOPYL—program for calculating the thermal neutron energy spectrum in heterogeneous lattice cells, 19: 41648
RAVIV, Samuel, Electrolytic dissolution of U fuel elements, 19: 41086
RAWSON, B. J., ESR spectra of γ-irradiated polycrystalline glycolic acid, 19: 40592
RAY, J. A., An unconventional ultra-high vacuum facility, 19: 40772 (ORNL-P-1465)
RAYFIELD, George William, Quantized vortex rings in superfluid helium, 19: 41634
RAYMOND, L., On the deformation of tungsten single crystals by rolling, 19: 41066
RAYNOR, G. V., Rare earth intermediate phases. I., 19: 41041
RAZBITNAYA, L. M., Effect of N,N,N',N'-tetra-acetic acid 2,2'-diamino-diethylsulfide (DDSTA) on the excretion of uranyl nitrate and course of uranium poisoning in rats, 19: 40348
RAZDOLSKAYA, L. A., Treatment program of penetrating showers of cosmic rays with the energy of 10^{10} to 10^{12} ev, 19: 41290
RAZUMOVSKII, N. O., Effect of hypocalcemia and subcutaneous inflammatory foci on the level of radioactive Sr in the skeleton, 19: 40343
RAZUMOVSKII, N. O., Effect of complexing agents on the amount of radioactive Sr deposited in bones, 19: 40344
RAZUMOVSKII, N. O., Oral administration of complexing agents to remove rare-earth elements (Ce-144) from rats, 19: 40347
READ, A. L., Backward elastic scattering of high-energy pions by protons, 19: 41456
READ, A. L., Pion-proton elastic scattering at high momentum transfers, 19: 41455
REARDON, W. A., Reactor analysis: measured and calculated spectra and average reaction rates, 19: 42037 (BNWL-95, pp 4–17)
REBEV, S., Comparative studies of radioactively labeled precursors in the RNA of x-irradiated non-diploid yeast, 19: 40367
REDFIELD, J. A., Heat transfer aspects of the loss-of-coolant accident, 19: 42009 (WAPD-T-1811)
REECE, B. L., Study of (^{3}He,^{7}Be) reaction in ^{12}C, 19: 41733
REEDER, P. L., Cross sections for the production of ^{9}Li, ^{16}C, and ^{17}N in irradiations with Bev-energy protons, 19: 41780
REED-HILL, R. E., Conference on deformation twinning, Gainesville, 3/63, 19: 41076
REICHELT, J. M. A., Absolute fission cross section of ^{235}U for 2200-m/sec neutrons, 19: 41691
REID, G., Cesium electron bombardment ion engines, 19: 40770
REIER, M., Pulsed-decay and extrapolation-length measurements in graphite, 19: 41647
REILLEY, Charles N., Advances in analytical chemistry and instrumentation, 19: 40446
REINES, F., Evidence for high-energy cosmic-ray neutrino interactions, 19: 41306
REITAN, A., Double-charge-exchange scattering of low-energy pions by nuclei, 19: 41773
REKALO, M. P., Okubo mass formula in higher orders, 19: 41490
REMIDDI, Ettore, Charged conjugation, decay of vector mesons, and SU(6) symmetry, 19: 41464
RENNER, J., Determination of the structure of tantalum suboxides TaO_2(Ta_2O_5) with electron diffraction, 19: 41047
RESHETOV, G. N., Plutonium-239 in rat lung and liver and morphological changes after intratracheal administration, 19: 40317
REVZEN, Michael, Intermediate state between He I and He II, 19: 41618
REYNOLDS, Glenn M., (p,t) Ground-state L = 0 transitions in the even isotopes of Sn and Cd at 40 Mev, N = 62 to 74, 19: 41689
REZOVA, A. T., New photometric methods for determining Nb and Ta in metals and alloys. IV., 19: 40442
RHODES, D. W., Decontamination of radioactive effluent with clinoptilolite, 19: 40651 (IDO-14657)
RICCI, R. C., 5-Mc magnetic tunnel-semiconductor logic for nuclear radiation environments, 19: 40939
RICE, Andrew C., Process for separating rare earth elements by means of solvent extraction, 19: 40696
RICHARDSON, Gerald L., Development of radioactive waste fractionization and packaging technology, 19: 42197
RICHEY, C. R., Critical experiments with PuO_2–polystyrene compacts with ^{240}Pu = 8%, 19: 42038 (BNWL-95, pp 27–35)
RICHMAN, R. B., A chemical composition and process for removing oxide and scale from aluminum metals and aluminum alloys, 19: 42202 (HW-64483)
RICHTER, G., Absorption and scattering of quantum mechanical coherent beams. I., 19: 41247
RICHTER, G., Absorption and scattering of quantum beams. II., 19: 41248
RICKEY, M. E., Excitation of isobaric analog states in medium-weight nuclei by (d,p) reaction at 28 Mev, 19: 41772
RIDER, J. L., MO608—A FORTRAN program to evaluate radiochemical data, 19: 40636 (WAPD-TM-516)
RIDER, P. E., Gold-rich rare-earth-gold solid solutions, 19: 41062
RIEMANN, K., MZFR electrotechnical installations, 19: 42170
RIGHETTI, G. B., Saturation and short-time behavior of unstable ion waves, 19: 41890
RILEY, Clyde, Isomeric cross-section ratios for Y-90 by (a,n), (d,p), and (^{3}He,p) reactions, and for Sc-44 by (a,n) reaction, 19: 41820
RIMSHAW, S. J., Use of ethanol in isolating ^{22}Na from cyclotron targets, 19: 40637 (ORNL-tr-625)
RINAUDO, G., $K_{\mu 3}$ branching ratio and μ^+ energy spectrum, 19: 41414
RISSER, J. R., Cross sections at 0° and angular distributions of resolved neutrons from ^{11}B + d, 19: 41732
RITCHIE, E. E., Nonequilibrium uranium carbide phase relationships, 19: 41018 (NAA-SR-10768)
RITCHIE, W. B., Computer programs for shielding problems in manned space vehicles, 19: 41954 (NP-15338)
RITSCHARD, Ronald L., Light-tight, dust-free drying box for autoradiography, 19: 40304
RITZ, H., MZFR—the zero power experiment, 19: 42178
RITZ, H., Physical design of the MZFR, 19: 42161
RITZ, Hilmar, Zero-energy measurements on core of the multi-purpose research reactor, 19: 42186
RITZ, Victor H., Shutter for x-ray or electron beams, 19: 41186
RIVERS, R. J., Second-order perturbation in intrinsically broken U(12), 19: 41444
RIVERS III, William Jones, Analytical investigation of film free convection heat transfer to liquid helium II, 19: 41635
RJENARD, F. M., Relativistic theory of electrodisintegration of the deuteron. II., 19: 41374
ROBBINS, Donald T., Engineering and cost considerations for tunnel grid blast shelter concept, 19: 40759 (ORNL-TM-1183)
ROBERTSON, J. S., Data processing method for a multidetector positron

scanner, 19: 40390 (BNL-9384)
ROBINSON, Alan H., Calculation of disadvantage factor in cylindrical geometry, 19: 42063
ROBINSON, D. K., Anti-isobar production in $\bar{p}n$ interactions, 19: 41438
ROBINSON, D. K., ρ and ω production in $\pi^+ d$ interactions at 1.7 Bev/c, 19: 41528
ROBINSON, Lawrence Boyler, Magnetic behavior of rare earth metals at high pressures, 19: 42005
ROBINSON, Mark T., The energy spectra of atoms slowing down in structureless media, 19: 41261
ROBINSON, N. W., Use of mass spectrometer during output measurements of sputtering pumps, 19: 40777
ROBINSON, R. K., N-reactor, preasurizer-high pressure injection pump simulation study. II., 19: 42131 (HW-77028)
ROBKIN, M. A., Prog. rpt. on Pu subcritical experiment, 4–6/65, 19: 42093 (GEAP-4912)
ROBOTTI, A. C., Electric propulsion by thermoelectric motors, 19: 40768
ROBSON, A. R. M., A collection of problems on mathematical physics, 19: 41153
ROCCO, E., High-intensity, partially separated, beam of antiprotons and K mesons, 19: 41184
ROCHE, T. K., Procurement and quality evaluation of Nb-1 percent Zr stock for boiling alkali metal corrosion studies, 19: 40952 (ORNL-TM-1179)
RODBERG, Harold, Some properties of solar radio bursts of spectral type III, 19: 41218
ROESCHEL, Erich, The influence of additions on the properties of tantalum, 19: 41067
ROGERS, H. C., Conference on deformation twinning, Gainesville, 3/63, 19: 41076
ROGERS, P. C., Investigation of $^{27}Al(\alpha,p)$ reaction by cross-section fluctuation studies, 19: 41761
ROGERS, P. C., Stable linear pulse-summing circuit, 19: 40726
ROHRER, Robert, Pre-Schooner base surge and cloud formation, 19: 40708 (PNE-503F)
ROINISHVILI, N. N., Treatment program of penetrating showers of cosmic rays with the energy of 10^{10} to 10^{12} ev, 19: 41290
ROINISHVILI, V. N., A spark chamber with a big discharge gap, 19: 40886
ROLLIER, M. A., Versatile strategy of the nuclear fuel, 19: 42111
ROMANOV, S. A., Neutron-capture cross sections in Sc and radiation widths of the ^{45}Sc and ^{35}Cl resonances, 19: 41806
ROMANOVSKII, V. A., Inelastic scattering of electrons in thin films, 19: 41961
ROMANTSEVA, A. S., Elastic pp scattering at 1.45 Bev, 19: 41487
ROMMEL, Marjorie A., The in situ identification of phosphate in multispot chromatograms by neutron activation analysis, 19: 40429
RON, Amiram, Intermediate state between He I and He II, 19: 41618
ROOF, R. B. Jr., Integrated series of crystallographic computer programs. VII., 19: 41965 (LA-3309)
ROOF, R. B. Jr., Integrated series of crystallographic computer programs. VIII., 19: 41966 (LA-3310)
ROOSZ, Jozsef, Investigation of an r-f ion source, 19: 40855
ROOT, J. W., Kinetic isotope effects in recoil tritium reactions, 19: 40615
ROPERS, Johann, Device for operating a loading machine for reactors, 19: 42032
ROSATELLI, C., Radiofrequency system of an isochronous cyclotron, 19: 41172
ROSE, B. F., Test facilities for nuclear rockets, 19: 42144
ROSE, P. H., Experiments with magnetohydrodynamically supported shock layers, 19: 41120 (N64-30509)
ROSEN, Louis, Elastic scattering of 10.5- and 14.5-Mev polarized protons and optical model potential, 19: 41682
ROSENBERG, H., Reactions of nucleogenic C atoms with hydrocarbons, 19: 40617
ROSENBERG, H. S., Development of an improved method of sampling and analysis for atmospheric iodine, 19: 40402 (BMI-X-10137)
ROSENBERG, Henry Ernest, Szilard-Chalmers (n,γ) recoil reactor ions in metalloporphines, 19: 40612
ROSICKY, Jaroslav, Chemistry of the rare earth metals. VIII., 19: 40491
ROSS, H. H., Radio-release methods for the evaluation of atmospheric pollution. Sulfur dioxide, 19: 40410 (ORNL-P-494)
ROSSER, W. G. V., Introduction to the theory of relativity, 19: 41566
ROSSETTI, C., Symmetry-breaking corrections to weak vector currents, 19: 41547
ROSSMASSLER, W. R., Chromatograph for analysis of highly reactive and corrosive compounds, 19: 40407 (KY-485)
ROST, E., Excitation of isobaric analog states in medium-weight nuclei by (d,p) reaction at 28 Mev, 19: 41772
ROSTOVSKII, V. S., Electric monopole transitions in nonspherical atomic nuclei, 19: 41812
ROTH, J., Morphological characteristics of coprecipitated $(U,Pu)O_2$ powders by electron microscopy, 19: 41024 (NUMEC-2389-5)
ROTH, R. S., Phase equilibria studies in rare earth and other oxides, 19: 40534
ROTHE, R., MZFR—the primary circuit and its construction, 19: 42164
ROWE, J. E., Investigation of nonlinear interaction phenomena in the ionosphere, 19: 41572 (NASA-CR-258)
ROWLAND, F. S., Kinetic isotope effects in recoil tritium reactions, 19: 40615
ROWLAND, F. S., The stereochemistry of the reactions of (n,γ) halogen atoms with alkyl halides in the liquid phase, 19: 40625
ROY, B. Dutta, Unitary symmetry breaking interactions and decays of vector mesons, 19: 41366
ROY, C., Role of grain boundaries in plastic deformation of CaF_2, 19: 40536
ROY, Rustum, Crystal chemistry of rare earth sesquioxides, aluminates, and silicates, 19: 40535
ROY, Salil, Unitary symmetry breaking interactions and decays of vector vector mesons, 19: 41366
ROZENTAL, I. L., Origin of high-energy pions, muons, and photons, 19: 41291
ROZENTAL, I. L., Precision of calculations of fast muon energy losses, 19: 41296
ROZHNOV, A. P., Complex compounds of cerium(III) and europium(III) with tartaric acid, 19: 40510
RUBAN, M. A., Observation of electron-nuclear double resonance of F centers in KCl, 19: 41992
RUBINCHIK, Ya. S., Reactions of lanthanum and yttrium oxides with ferric oxide, 19: 40515
RUBINSTEIN, R., Backward elastic scattering of high-energy pions by protons, 19: 41456
RUBINSTEIN, R., Pion-proton elastic scattering at high momentum transfers, 19: 41455
RUBTSOV, M. V., System $SmCl_3$–NaCl–KCl, 19: 40517
RUBY, S. L., Computation of Moessbauer spectra, 19: 41724
RUDAK, E. A., Gamma spectra from the (n,γ) reaction in ^{50}Cr, ^{52}Cr, and ^{53}Cr, 19: 41807
RUDAKOV, V. P., The reactions $^3He(d,t)2p$ and $^3He(^3He,\alpha)2p$, 19: 41658 (IAE-655)
RUDERMAN, H., Backward elastic scattering of high-energy pions by protons, 19: 41456
RUDERMAN, H., Pion-proton elastic scattering at high momentum transfers, 19: 41455
RUDGE, M. R. H., Application of a variational principle to the calculation of free-free matrix elements for H^-, 19: 41266
RUDMAN, P. S., Lattice parameters of tantalum–osmium alloys, 19: 41046
RUDNICK, Isadore, Intermediate state between He I and He II, 19: 41618
RUDNICK, Isadore, Velocity of sound in liquid He at its λ point, 19: 41619
RUEDEL, R., Level strucutre of ^{53}Cr and ^{55}Cr, 19: 41726
RUESS, A., Performance study of a repetitively pulsed two-stage plasma propulsion engine, 19: 40763 (N64-31453)
RUF, R., MZFR—the total installation, 19: 42160
RUFF, George A., Spin-exchange light modulation by atomic hydrogen, 19: 41262
RUMYANTSEV, S. A., Calculation of absorbed energy of γ radiation, 19: 41959
RUNGE, D., Prog. rpt. on two-phase flow and boiling heat transfer, 1–3/65, 19: 40738 (NYO-3114-7)
RUPP, W., Physical design of the MZFR, 19: 42161
RUSISHVILI, N. S., 340-Liters expansion-condensing chambers used to study nuclear interactions of high energy particles, 19: 40887
RUSSELL, J. E., Measurement of the U-235 neutron capture-to-fission ratio from 3.25 ev to 1.8 kev, 19: 41749
RUSSELL, J. L. Jr., Prog. rpt. on integral neutron thermalization, 3/31/65, 19: 41640 (GA-6323)
RUSSELL, R. B., Prog. rpt. on dispersion-strengthened alloys, 4–6/65, 19: 41021 (NMI-8002.1)
RUSSO, G., CP violation by derivative terms in the leptonic current, 19: 41378
RUSSO-MANDUCHI, M. T., Performance and properties of a proton polarimeter, 19: 40905
RUZICKA, J., Substoichiometric determination of non-isotopic radioactive admixtures and the content of isotopic carrier in radioactive preparations, 19: 40424
RUZICKA, J., Substoichiometric determination of traces of gold by neutron-activation analysis, 19: 40437
RYABCHIKOV, D. I., Analytical chemistry of rare earths, 19: 40449
RYABCHIKOV, D. I., Chemistry of rare earth complexes, 19: 40532
RYABCHIKOVA, G. G., Unit for gas-phase radiation-induced graft polymerization, 19: 40596
RYABUKHIN, V. A., Analytical chemistry of rare earths, 19: 40449

RYBAKOV, B. V., Reaction $^{4}He(^{3}He,n)^{6}Be$, 19: 41659 (IAE-836)
RYBAKOV, V. N., K-capture fraction of ^{66}Ge, ^{69}Ge, and ^{72}As, 19: 41800
RYBALTOVSKII, A. O., Electron paramagnetic resonance of irradiated single crystals of fluorite containing Nd addition, 19: 40602
RYBASOV, V. A., Medical defense against nuclear weapons, 19: 40361 (ORNL-tr-437)
RYDER, F. D., SRP reactor on-line computer, 19: 42129 (DPSPU-65-30-27)
RYNDIN, R. M., Double N-N scattering with a polarized beam and polarized target, 19: 41333 (JINR-P-2227)
RYVKIN, S. M., Current oscillations in Ge containing radiation defects, 19: 41105

S

SABIN, C. M., Prog. rpt. on heat transfer for space nuclear power, 12/64–2/65, 19: 40741 (SAN-409-23)
SACH, Roger Stuart, Improvements in or relating to the purification of gaseous helium, 19: 40539
SACTON, J., Angular correlations between fast Σ hyperons and fast protons, 19: 41494
SADOFSKY, J., Thermodynamic properties of nonstoichiometric ThC, 19: 40485
SAGET, Pierre, A movable partition or cofferdam, 19: 42190
SAID, P., Direct and Y_1^*-resonant production of Λ^o and π^- and Σ-Λ^o conversion following K-meson nuclear absorption, 19: 41405
SAITO, Masuji, Plasma fusion, 19: 41881
SAITO, Takeo, New index of geomagnetic pulsation and its relation to solar M-region. III., 19: 41602
SAKHOVSKII, E. G., Viscous drag and heat motion in the flow of a partially ionized medium along a plane channel, allowing for an anisotropic transport coefficient, 19: 41147
SAKITA, Bunji, Relativistic formulation of the SU(6) symmetry scheme, 19: 41428
SAKMAR, Ismail, Conferences on symmetry principles at high energy, Coral Gables, 1/65., II., 19: 41514
SAKURADA, Ichiro, Osaka Lab. research, 19: 40555 (AEC-tr-6565, pp.1-7)
SAKURAI, Juuji, Polarization of radio-photoluminescence of fluorodosimeter glass, 19: 40588
SAKURAI, Kunitomo, Nuclear abundance and rigidity spectra of solar cosmic rays, 19: 41232
SAKURAI, Kunitomo, Propagation of solar protons and the interplanetary magnetic field, 19: 41228
SALANT, E. O., Anti-isobar production in $\bar{p}n$ interactions, 19: 41438
SALANT, E. O., ρ and ω production in π^+d interactions at 1.5 Bev/c, 19: 41528
SALATSKII, V. I., Investigation of nuclear reactions of helium-3 with carbon, 19: 41663 (JINR-P-2184)
SALGIR, T., Branching ratio of ^{212}Bi(ThC), 19: 41798
SALLEY, R. L., SNAP 50/SPUR program materials investigation—mechanical properties of TZM, 19: 41002 (APS-5157-R)
SALVADORI, P., The (e,e'p) experiment: results obtained and planned proposals, 19: 41660 (ISS-65/3)
SALVAGGIO, G. J., Properties of a Hf-control rod after exposure during three seed lives in PWR Core 1, 19: 41092 (WAPD-TM-457)
SAMARSKII, A. A., A collection of problems on mathematical physics, 19: 41153
SAMODELOV, A. P., Solubility of Sc chloride in HCl at 25°C, 19: 40520
SAMODELOV, A. P., Sorption and extraction of scandium by phosphoorganic compounds, 19: 40689
SAMOKHIN, M. V., Emission of extraordinary wave by a current in layer of magnetoactive plasma, 19: 41882
SAMOKHIN, M. V., Gravity separation of charges in, 19: 41919
SAMOUR, C., Treatment of capture gamma ray spectra obtained with the aid of a central crystal in association with an annular crystal, 19: 40896
SAMS, John R., Two-dimensional second virial coefficients of Kr on graphic carbon, 19: 40956
SAMSONOV, Grigorii Valentinovich, High-temperature compounds of rare earth metals with nonmetals, 19: 41073
SAMADZE, T. I., Relaxation processes in paramagnetic resonance of U^{3+} and Tb^{3+} in CaF_2, 19: 42000
SANBORN, E. N., The sulfides of Sr, Ca, and Mg in infrared stimulated luminescence dosimetry, 19: 40879 (UCRL-12371)
SANDER, Howard H., Device for the measurement of liberated energy in explosion, 19: 40850 (ORNL-tr-588)
SANITWONGS, P., Chemical effects of nuclear recoil in organic halide systems, 19: 40624
SANKARANARAYANAN, A., Covariant polarization theory of spin-one particles, 19: 41526
SANOCHKIN, Yu. V., Superheating instability of a plasma, 19: 41925
SANTANGELO, R., Spin and parity of 1320 Mev $\rho\pi$ resonance, 19: 41368
SANTINI, M., Experiments on the creation of charged quantized vortex rings in liquid helium at 1°K, 19: 41621
SAPP, R. C., Intermediate state reorientation in nuclear alignment of ^{139}Ce in Ce–Mg nitrate, 19: 41840
SATCHLER, G. R., Form factors for nuclear stripping reactions, 19: 41746
SATO, Toichi, Extraction of U(VI) from hydrochloric acid solutions by di-(2-ethylhexyl)-phosphoric acid, 19: 40678
SATSUNKEVICK, I. S., Scattering of antineutrinos by electrons, 19: 41481
SAUER, J. A., Effect of nuclear radiation on the thermal conductivity of polyethylene, 19: 40603
SAUNDERS, B. G., Neutron-capture γ-ray studies of low-lying ^{52}V levels, 19: 41725
SAVCHENKO, I. A., Electron oscillations in a plasma, 19: 41907
SAVENKO, I. A., Monitoring of cosmic radiation during flight of Vostok satellites, 19: 40841
SAVENKO, I. A., Multiple scattering of 75- to 200-kev protons on solids, 19: 41273
SAVICH, A. V., Difference equations of dynamics in Hamiltonian form, 19: 41145
SAVITSKII, E. M., Investigation of ternary W–Mo–Zr phase diagram, 19: 41035
SAVKOVIC, N., Changes in the growth of progeny of male rats exposed to low x-ray doses in the infantile period, 19: 40365
SAVOLAINEN, A. W., U. S. reactor containment technology, 19: 42008 (ORNL-NSIC-5(Vol.I and II))
SAVOSKIN, V. I., Measuring of electron concentration in plasma, 19: 41924
SAWADA, T., Can the coupling constant assume arbitrary value in the S-matrix theory?, 19: 41382
SAWICKI, J., Direct and Y_1^*-resonant production of Λ^o and π^- and Σ-Λ^o conversion following K-meson nuclear absorption, 19: 41405
SAXER, R. K., Influence of zirconium additions on epsilon phase of titanium–aluminum system, 19: 41053
SCARL, D. B., Backward elastic scattering of high-energy pions by protons, 19: 41456
SCARL, D. B., Pion-proton elastic scattering at high momentum transfers, 19: 41455
SCHABERT, H.-P, Research installations at the MZFR, 19: 42179
SCHAFFER, Allan, Magnetic induction plasma engine, 19: 40762
SCHAFFER, W. F. Jr., Project Salt Vault, 19: 42195 (ORNL-P-1479)
SCHAMBURGER, R., MZFR—the steam power installation, 19: 42169
SCHELL, Robert Aloysius, Studies of photoeffects occurring with anodized niobium electrodes, 19: 41080
SCHEY, Harry M., Counting the bound states in short-range central potentials, 19: 41439
SCHIAVON, P., High-intensity, partially separated, beam of antiprotons and K mesons, 19: 41184
SCHIAVUTA, E., Lambda^o polarization from $\gamma + p \rightarrow \Lambda^o + K^+$ at 950 to 1050 Mev, 19: 41367
SCHICK, L. H., Low-energy Λ-d scattering and the hypertriton with separable potentials, 19: 41419
SCHIESSER, Robert J., Improvement of U–Mo alloys for gyroscope wheel rims, 19: 41023 (NP-15334)
SCHILLER, Robert, The effect of the type of radiation on the radiolysis of diphenyl–methane, 19: 40591
SCHILLING, W., Liquid-He irradiation facility at the Munich research reactor FRM, 19: 42180
SCHIMMELFENNIG, Victor, Index to hazards control quarterly reports nos. 1 through 19, 19: 40833 (UCRL-14116)
SCHINEIZER, Michele, Radioactivity of the Granes meteorite measured by γ spectrometry, 19: 40788
SCHINTLMEISTER, Josef, Probable radioactive decay of Ce-136, 19: 41700
SCHIRMER, H., Annual precipitation and precipitation frequency for European community, United Kingdom, Denmark, and Alps 1921-1950, 19: 41111 (EUR-2296.e)
SCHLEA, C. S., Behavior of actinides and fission products in TBP and DABP, 19: 40645 (CONF-650918-1)
SCHLEIN, Herbert N., Process for preparing radiation-stabilized polyethylene and food package utilizing same, 19: 40633
SCHLESINGER, S. P., Observation of non-quasistatic plasma surface waves, 19: 41942
SCHLESINGER, S. Perry, Wave propagation along warm plasma columns, 19: 41939
SCHLOSSER, Gerhard, Zero-energy measurements on core of the multipurpose research reactor, 19: 42186
SCHMEISSER, M., Nitryl nitrato complexes of indium and thorium, 19: 40471
SCHMIER, H., Treatment with Th–X, 19: 40391 (NP-14921)
SCHMIER, Herbert, Alarm plan, 19: 40804 (NP-14925)
SCHNAPPAUF, Ursula, Membranes, material transfer and enzymes, 19: 42199 (BNL-8397)
SCHNEEGANS, M., High-intensity, partially separated beam of antiprotons and K mesons, 19: 41184

SCHNEIDER, G., MZFR fuel elements, 19: 42175
SCHNEIDER, J., Radioprotection effectiveness of serotonin in rats, 19: 40388
SCHOEBER, G., Polarographic behavior of lanthanoids in dimethylsulfoxide and dimethylformamide, 19: 40681
SCHONE, H. E., Hollow metal single crystal for NMR experiments, 19: 40990
SCHORNICK, James Leslie, The synthesis and evaluation of some 2-arylidenes and 2-aryl-3H-benz(e)indenes as liquid scintillation solutes 19: 40546
SCHRIEMPF, J. T., Electron beam zone refining of ruthenium, 19: 40984
SCHROEDER, R., Determination of errors in a one-parameter system, 19: 42225 (UCRL-12050)
SCHROEER, D., Energy levels of ^{158}Dy, 19: 41847
SCHUBERT, Franz, Device for operating a loading machine for reactors, 19: 42032
SCHUETZE, H. J., New single-walled high-vacuum evaporator with very low cycling times, 19: 40774
SCHULZ, W. W., Recovery of plutonium and uranium from reactor fuel metallurgical scrap, 19: 40643 (BNWL-57)
SCHWARTZ, Judah L., Counting the bound states in short-range central potentials, 19: 41439
SCHWARTZ, P. E., Prog. rpt. on heat transfer for space nuclear power, 12/64–2/65, 19: 40741 (SAN-409-23)
SCHWARZCHILD, B., K$^+$p interactions at 2 Bev/c—elastic scattering and total cross sections, 19: 41436
SCHWINGER, Julian, Phenomenological field theory, 19: 41521
SCINTEI, N., Reaction ^{26}Mg(p,p′γ) mechanism at low energies, 19: 41693
SCRIBNER, V. E., Operating trans-curium element radiochemistry facility, 19: 40719 (UCRL-7844-T)
SCRIBNER, V. E., Remotely-operated trans-plutonium chemical process cells, 19: 40720 (UCRL-7845-T)
SCRIMAGLIO, Renato, Loss of energy by ultra relativistic muons. III., 19: 41345
SEADER, J. D., Hydrogen heat transfer data compilation, 19: 40734 (NP-15331)
SECREST, Bruce Gill, Discontinuities in magnetogasdynamics in the presence of finite conductivity, 19: 41157
SEDGLEY, Robert, Separation of amines by ligand exchange. III., 19: 40648 (COO-499-2)
SEDLACEK, Z., Mikhailovsky's finite Larmor radius effects and gravitational instability of plasma, treated by method of moments of Boltzmann-Vlasov equation, 19: 41879
SEELENTAG, Application of radioactive luminous paints in navigational instruments of aircraft cockpit, 19: 40940 (NP-14924)
SEELENTAG, W., Treatment with Th–X, 19: 40391 (NP-14921)
SEELENTAG, Walter, Alarm plan, 19: 40804 (NP-14925)
SEFCHOVICH, E., Oscillating neutron source experiment, 19: 41641 (MIT-2344-3, pp 137-54)
SEGEL, R. E., States in ^{12}C between 16.4 and 19.6 Mev, 19: 41688
SEIKEL, George R., Plasma, 19: 41900
SEKULA, S. T., Temperature dependence of critical fields of superconducting Pb–Tl, 19: 41610
SELLA, C., Reactions of gases with graphite, 19: 40975
SELLE, J. E., Phase equilibria in plutonium–cerium–copper system, 19: 41054
SELLS, V., University of Western Ontario race-track microtron, 19: 41175
SELTZ, Raymond, Study of excitation curves of reaction ^{12}C(t,α_0)^{11}B, 19: 41706
SEMENOV, D. I., Distribution of Y-91, Zr-95, and Nb-95 in rats after inhalation, 19: 40314
SEMENOV, L. F., Catecholamine content in macacus tissues immediately after whole-body γ irradiation, 19: 40373
SENGUPTA, R., Gravitation of cylindrically symmetric magnetic field, 19: 41544
SEPTIER, Albert, Low-voltage discharge at very high intensity initiated by laser pulse, 19: 41133
SERGE, G., Symmetry-breaking corrections to weak vector currents, 19: 41547
SERGIEVSKII, V. V., Reaction of $U(SO_4)_2 \cdot 4H_2O$ with tri-n-octylamine sulfates and bisulfates, 19: 40688
SERIKOV, I. N., The reactions ^{3}He(d,t)2p and ^{3}He(^{3}He,α)2p, 19: 41658 (IAE-655)
SERRANO C., Mario, Reconnaissance for U in the Colimapu Formation of central Chile, 19: 40798 (RME-4571(Rev.))
SERVANT, J. Y., Packaging standards, 19: 40810 (SC-RR-65-98, pp 32–44)
SEVERIENS, J. C., Annihilation of antiprotons in hydrogen at rest. III., 19: 41325 (CU-1932-245)
SEWARD, F. D., Near-earth, polar-orbiting satellite measurements of charged particles. I., 19: 41303
SEYD, G., MZFR—construction of the reactor building and installation of the pressure vessel, 19: 42177
SHAKHBAZYAN, B. A., Optimal determination of the detecting efficiency (weight) of an event, 19: 40873 (JINR-P-2215)
SHAKHULASHVILI, O. A., Charged Σ-hyperons generated in photoemulsion by high-energy protons, 19: 41350
SHAMOVSKII, L. M., Investigation of thermal de-excitation processes in x-rayed alkali-halide phosphors, 19: 41101
SHAMOVSKII, L. M., X-ray luminescence of the NaI(Tl) phosphor, 19: 40908
SHANKS, D. E., 14-Mev-neutron production of isomeric states for several rare-earth elements, 19: 41781
SHANSTROM, R. T., Development of the gas-cooled fast reactor concept, 19: 42090 (GA-6132)
SHAPIRO, Anatole M., Prog. rpt. on experimental and theoretical high energy physics, 9/64–8/65, 19: 41337 (NYO-2262-95)
SHAPIRO, F. L., Determination of spins of Ho-165 neutron resonances by transmission of polarized neutrons through a polarized target in the energy interval 0–55 ev, 19: 41665 (JINR-P-2209)
SHAPIRO, F. L., Neutron-capture cross sections in Sc and radiation widths of the ^{45}Sc and ^{35}Cl resonances, 19: 41806
SHAPIRO, Kenneth A., Velocity of sound in liquid He at its λ point, 19: 41619
SHAPIRO, Ralph, Comparisons of power spectrums of artificial time series with spectrum of a solar plage index, 19: 41224
SHAPOVALOV, A. S., Influence of space charge on beam focusing and energy dispersion in field of plane capacitor, 19: 41196
SHARAPOV, E. I., Niobium and Rb neutron resonances and radiation widths of medium-mass nuclei, 19: 41727
SHARIPOV, R. K., Catalytic waves of reduction of a peroxide niobium complex in sulphuric acid, 19: 40443
SHARKHATUNYAN, R. O., Polarization of cosmic muons at various energies, 19: 41294
SHARPATYI, V. A., Transformations in EPR spectra of irradiated polyisobutylene, 19: 40608
SHARVIN, Yu. V., Possible method for studying Fermi surfaces, 19: 41068
SHATAS, Romas A., Fine structure of optical absorption bands in neutron-irradiated MgO, 19: 40632
SHATAS, Romas A., Phonon-induced infrared absorption spectrum in irradiated MgO, 19: 41108
SHAUER, P., Plasma pepsinogen after whole-body irradiation of rat, 19: 40363
SHAVRIN, P. I., Monitoring of cosmic radiation during flight of Vostok satellites, 19: 40841
SHAW, Gordon L., Absorptive corrections and form factors in the peripheral model, 19: 41400
SHAW, P. F. D., Effects of temperature and pressure on hot-atom reactions in bromoethane, 19: 40626
SHCHEDRIN, I. S., Magnetron performance with a paired-resonator system, 19: 41191
SHCHEDRIN, I. S., Measurements of resonator quality, 19: 41190
SHCHEGOLEV, V. A., The effect of magnetic screens in the spaces between blocks on the operation of proton synchrotron, 19: 41168 (NP-15253)
SHCHELKONOGOVA, M. I., Changes in blood system of dogs intravenously injected with Y-91, 19: 40377
SHEKUN, L. Ya., EPR spectrum of Yb^{3+} ions in synthetic $PbMoO_4$ single crystals, 19: 41986
SHELINE, Raymond K., Level structure of the odd-A isotopes of Sm, 19: 41778
SHEN, S. P., Prog. rpt. on shielding for ionizing radiation space, final, 9/62–8/63, 19: 41952 (N62-31552)
SHEPARD, Marion LaVerne, Single-crystal elastic constants of lead-thallium alloys, 19: 41012 (IS-T-16)
SHERIDAN, John Roger, Rotation and vibration in N_2^+ first negative bands excited by ion impact, 19: 41279
SHERR, R., Excitation of isobaric analog states in medium-weight nuclei by (d,p) reaction at 28 Mev, 19: 41772
SHEVELEVA, A. D., Solubility in $Ce(NO_3)_3$–$LiNO_3$–H_2O, 19: 40519
SHIH, Shuang-hui, Neutron spectra in interactions of heavy ions with intermediate nuclei, 19: 41810
SHIINA, Shoichi, Initial-pressure dependence of instabilities in a low B theta pinch plasma, 19: 41887
SHIMA, Yaskov, Note on electrostatic instabilities in a plasma with anisotropic velocity distribution, 19: 41866 (UCRL-12052)
SHIMAZAKI, T. T., Heat transfer in organic-cooled reactors, 19: 42110
SHIPLEY, C. A., Time-dependent behavior of surface ionization efficiencies of Li and LiF on W, 19: 41141
SHIRATO, Shoji, On the pulse-height defects in semiconductor detectors for fission fragments, 19: 40892
SHIRLEY, D. A., Angular distributions of conversion electrons from oriented ^{137m}Ce nuclei, 19: 41679 (UCRL-11462(Rev.))

SHISHKOV, A. V., Development of methods for hot synthesis of ^{35}S-labeled biologically active substances, 19: 40619
SHISHKOV, A. V., The formation of polymeric products in reactions of polyvalent recoil atoms, 19: 40628
SHLYAPNIKOV, R. S., Elastic pp scattering at 1.45 Bev, 19: 41487
SHOSTAK, M., Pattern recognition, 19: 42211 (NYO-1480-19)
SHPINEL', V. S., Two-hour (7.7 ksec) isomer of ^{168}Lu, 19: 41803
SHRABSHTEIN, S. A., Multichannel analyzer of pulses for ionization calorimeter at capacity memory cells and the system of information output, 19: 40853
SHRABSHTEIN, S. A., Semi-automatic device for treatment of track photos in a cloud chamber, 19: 40888
SHRAUNER, E., Breakdown of unitary octet symmetry in a nonlinear spinor model of elementary-particle theory, 19: 41395
SHRAUNER, E., Meson states in a nonlinear spinor model of elementary-particle theory with spontaneous symmetry breakdown, 19: 41396
SHREEVE, W. W., Studies with DL-alanine-2-^{14}C of interaction of ethanol metabolism with pathways of hepatic gluconeogenesis in the rat, 19: 40308 (BNL-8379)
SHTAERMAN, A. Yu., 340-Liters expansion-condensing chambers used to study nuclear interactions of high energy particles, 19: 40887
SHUCK, A. B., Development of a process for manufacturing ZPR-III U–Pu–Mo test fuel elements, 19: 40978 (ANL-6955)
SHUKLA, J. B., On the flow of two conducting incompressible immiscible fluids between two nonconducting plates, 19: 41135
SHURALEVA, E. I., Some data on the luminescent properties of Eu-activated NaCl and KCl phosphors, 19: 40567
SHVEDCHIKOV, A. P., The formation of polymeric products in reactions of polyvalent recoil atoms, 19: 40628
SHVEDOV, V. P., Complex compounds of cerium(III) and europium(III) with tartaric acid, 19: 40510
SIDOROV, V. A., Reaction $^4He(^3He,n)^6Be$, 19: 41659 (IAE-836)
SIDOROV, V. V., Use of phase technics for studying polarization phenomena of radiowave reflection from meteor trails, 19: 41223
SIFFERT, Paul, Study of γ radiations of Ta-182, 19: 41704
SIGOV, Yu. S., Structure of the boundary layer between rarefied plasma and a magnetic field, 19: 41905
SILVA, R. W., Explorer 14 plasma probe observations, 19: 41580
SIMON, R. H., Design, construction, and operation of in-pile loop, 19: 42089 (GA-5938)
SIMONOV, B. I., The effect of magnetic screens in the spaces between blocks on the operation of proton synchrotron, 19: 41168 (NP-15253)
SIMONOV, E. F., Reactions of hot tritium atoms with amino acids, 19: 40629
SIMONOVA, L. I., Spectrum of internal-conversion electrons produced upon capture of thermal neutrons by indium, 19: 41808
SIMONS, E. M., Reactor materials, Vol. 8, No. 2, 19: 40957
SIMPSON, J. A., Cosmic radiation helium spectrum below 90 Mev per nucleon measured on Imp 1 satellite, 19: 41302
SIMPSON, K. M. Jr., Computer programs for shielding problems in manned space vehicles, 19: 41954 (NP-15338)
SINCLAIR, John H., Bend transition temperature of arc-cast molybdenum and molybdenum-0.5-percent-titanium sheet in worked, recrystallized, and welded conditions, 19: 41016 (N64-30997)
SINCLAIR, V. M., Determination of nitrogen in uranium–plutonium dioxides, 19: 40438
SINGER, Ralph M., Convective MHD channel flow, 19: 41115 (ANL-6967)
SINGER, S. F., Thermal escape of neutral hydrogen and its distribution in earth's thermosphere, 19: 41604
SINGH, Virendra, Baryon bootstrap possibilities in SU(6), 19: 41443
SINGH, Virendra, Reciprocal bootstrap possibilities for baryons, 19: 41422
SIRAZHET, H., Niobium and Rb neutron resonances and radiation widths of medium-mass nuclei, 19: 41727
SIROTKIN, S. M., Search for the (n,α) reaction in heavy nuclei under the action of thermal neutrons, 19: 41809
SISEFSKY, J., Observations on the particle properties of nuclear debris in the upper atmosphere, 19: 40783 (NP-15327)
SISLER, J. A., New developments in accident-resistant shipping containers for radioactive materials, 19: 40816 (SC-RR-65-98, pp 141-86)
SIZOV, I. V., Investigation of nuclear reactions of helium-3 with carbon, 19: 41663 (JINR-P-2184)
SKACHKOV, S. V., The effect of magnetic screens in the spaces between blocks on the operation of proton synchrotron, 19: 41168 (NP-15253)
SKADCHENKO, N. M., Effect of K_3PO_4 and $Ca(OH)_2$ on accumulation of Sr-90 in plants, 19: 40310
SKISLAK, A., A microwave system for low-density measurements, 19: 41854 (MATT-369)
SKRYNNIKOV, R. G., Connection of brief periodic oscillations of terrestrial EM, 19: 41575 (FTD-TT-65-112)
SLAMA, Lucien, Measurements of the characteristics of metallic plasma pulse, 19: 41878
SLOT, C., Liquid scintillation counting of non-volatile water-soluble compounds, 19: 40436
SLOTNICK, Herbert, Kinetics of hydrofluorination of zirconium oxide in a fluidized bed, 19: 40529
SMILEY, S. D., Shipping and storing power fuels prior to reprocessing, 19: 40837
SMIRNOV, M. V., Equilibrium between cerium and its di- and trivalent ions in a molten eutectic mixture of lithium and potassium chlorides, 19: 40467 (ORNL-tr-578)
SMIRNOVA, E. A., Uranium extraction from Hf–HNO_3 by ternary amines in benzene, 19: 40684
SMIRNOVA, V. A., Complex compounds of rare earths with 1,10-phenanthroline, 19: 40514
SMITH, A. Gilbert, Radiometric age of the Serra Geral Formation, 19: 40796
SMITH, Alan R., Concrete low-background counting enclosure, 19: 40721 (UCRL-11454)
SMITH, D. R., Electron spin resonance determination of the radiolytic yields of trapped electrons and other species in an organic glass, 19: 40558
SMITH, David R., Criticality safety evaluation of packages for the transport of fissile material, 19: 40828 (SC-RR-65-98, pp 679–90)
SMITH III, F. L., Observations of ionospheric electron content using geostationary satellite, 19: 41597
SMITH III, F. L., The rate of production of electrons in the ionosphere, 19: 41598
SMITH, G. R., Evidence for high-energy cosmic-ray neutrino interactions, 19: 41306
SMITH, Gilbert W., Activation analysis program and facilities at the National Bureau of Standards, 19: 40450
SMITH, Hamilton, Estimation of vanadium in biological material by neutron activation analysis, 19: 40421
SMITH, Harlan J., Planetary optical emission and flare activity of nearby stars, 19: 41203
SMITH, J., Prog. rpt. on ion rocket engine development, 1–3/65, 19: 40765 (NP-15309)
SMITH, P. F., Electromagnetic models of elementary particles, 19: 41377
SMITH, P. F., Experiments with superconducting niobium–tin cylinders, 19: 41609
SMITH, V. A., Testing of 10-ton capacity UF_6 shipping containers, 19: 40824 (SC-RR-65-98, pp 580–608)
SMITH, William R., DWB deuteron stripping program, 19: 41677 (ORNL-TM-1151)
SMITH, William R., Regions of validity of (d,p) Coulomb stripping approximation, 19: 41742
SMITH, Wm. T. Jr., Some fluorine compounds of Re and Tc, 19: 40461 (ORNL-P-491)
SMOLIN, D. D., Effect of N,N,N',N'-tetra-acetic acid 2,2'-diaminodiethylsulfide (DDSTA) on the excretion of uranyl nitrate and course of uranium poisoning in rats, 19: 40348
SMOOT, Thomas W., Refractories and methods of manufacture therefor, 19: 40997
SMORODIN, Yu. A., Formation of high-energy γ quanta, 19: 41298
SMORODINSKII, Yu. A., Precession of the top in the gravitational field, 19: 41204 (JINR-P-2174)
SNEESBY, George V., Method of forming molybdenum silicide coating on molybdenum, 19: 40998
SNYDER, S. D., Measurement and application of x- and gamma-ray attenuation to reactor materials evaluation, 19: 42071
SNYTSYN, V. I., Effects of radiation on Yakutian diamonds, 19: 41098
SOBOL', G. A., Detection of centimeter waves in a gas discharge plasma, 19: 41876
SOBRA, K., Splitting of plasma shock waves in accelerating tube, 19: 41880
SOCOLOW, Robert H., Decay modes of spin-two mesons, 19: 41461
SOEREMARK, Rune, Analysis of the concentrations of Cr, Ag, Fe, Co, Pt, and Rb in normal human dentine, 19: 40435
SOFER, George A., Fog coolant technology and its application to nuclear reactors, 19: 42020
SOFIA, Sabatino, Plasma frequency and internal opacity of stars, 19: 41211
SOHL, G., Cesium electron bombardment ion engines, 19: 40770
SOKOLIK, H. A., Unified description of interactions, 19: 41541
SOKOLOVA, A. A., Radiation defects in very pure silicon crystals, 19: 41998
SOKOLOVA, I. G., Constitution diagrams of systems V–Ta–Nb and V–Ta–Mo, 19: 41036
SOKOLOVSKAYA, E. M., Constitution diagrams of systems V–Ta–Nb and V–Ta–Mo, 19: 41036
SOKOLOVSKII, Yu. S., Equilibrium between cerium and its di- and trivalent ions in a molten eutectic mixture of lithium and potassium chlorides, 19: 40467 (ORNL-tr-578)
SOKOLOWSKA, A., Reactions of tritium recoil atoms in liquid organic mixtures, 19: 40621

SOLER, M., CP violation and SU_3 symmetry, 19: 41371
SOLOV'EV, M. I., Baryon resonances in π-p interactions at 7.5 Bev with strange-particle formation, 19: 41488
SOLOV'EV, M. I., Meson resonances in π-p interactions at 7.5 Bev with strange-particle production, 19: 41489
SOLOV'YANOV, V., Double pp scattering at 667 Mev, 19: 41666 (JINR-P-2233)
SONGINA, O. A., Catalytic waves of reduction of a peroxide niobium complex in sulphuric acid, 19: 40443
SOROKALETOV, O. D., Measuring ionization function of metal atoms by electron impact, 19: 41276
SOROKINA, N. N., Determination of Sm, Gd, Dy, Er, and Sc (0.01–0.6 percent) in steels and alloys by a chemicospectrographic method, 19: 40445
SOSHIN, L. D., Measurement of absolute yield of alkali-halide crystals in case of γ luminescence, 19: 40593
SOTNIKOV, S. K., Stabilizing amplification channel of scintillation counter, 19: 40870 (IAE-695)
SOUCEK, Branko, Stored program computer as an associative radiation analyzer, 19: 40918
SOUDAIN, Georges, Theoretical and technical aspects of photographic dosimetry, 19: 40889
SOUSSELIER, Yves, Fire tests of packagings for radioactive materials, 19: 40814 (SC-RR-65-98, pp 114–18)
SOWDEN, R. G., Hydrolysis of neutron-irradiated U and U–Pu monocarbides, 19: 40586
SPACU, P., Refractometric study of formation of complex Pr halides in aqueous solution, 19: 40469
SPACU, Petru, Separation of thorium from uranium, 19: 40439
SPARHUBER, R., MZFR—the primary circuit and its construction, 19: 42164
SPARLIN, Don Merle, Fermi surface of W and Mo, 19: 42003
SPEISER, R. C., Cesium electron bombardment ion engines, 19: 40770
SPENCER, John Brocket, Electron spin resonance studies of transition metal ion complexes, 19: 40465 (UCRL-16175)
SPICER, L. D., Gas-phase reactions of (n,γ) and isomeric transition-activated ^{80}Br with alkanes and haloalkanes, 19: 40618
SPINDEL, W., Prog. rpt. on stable isotope studies, annual, 9/15/64–7/15/65, 19: 40460 (NYO-3462-1)
SPINKS, N., Calculating reactivity worth of partially inserted control rods using two-dimensional geometry, 19: 42034 (AAEC/E-134)
SPRAGINS, S. V., Influence of zirconium additions on epsilon phase of titanium–aluminum system, 19: 41053
SPRIET, B., Effect of thermal cycling on α-β transformation temperature of Pu, 19: 41028 (BNWL-tr-4)
SPRUILL, Joseph L., Crater measurements on Project Pre-Schooner, 19: 40707 (PNE-502F)
SPURLOCK, Jack M., Prog. rpt. on effects of electrical fields on boiling heat transfer, 5/26/64–9/30/64, 19: 40735 (NYO-2404-5)
SPURWAY, A. H., Experiments with superconducting niobium–tin cylinders, 19: 41609
SRINIVASAN, M., Demonstration of neutron wave reflection effects using statistical correlation techniques in elliptic systems, 19: 41645
STAB, Lucien, Study of γ radiations of Ta-182, 19: 41704
STAEHLE, R. W., Prog. rpt. on stress-corrosion cracking in Fe–Ni–Cr system, 3/17–6/16/65, 19: 40967 (COO-1319-27)
STANDERFER, F. R., Prog. rpt. on fissiochemical process development. I., 12/2/63–6/30/64, 19: 40547 (AGN-8137(Vol.I))
STANWOOD, D. E., Equipment for fabrication and encapsulation of irradiated UO_2 pellets, 19: 40715 (NAA-SR-Memo-7438)
STAROSTIN, K. L., Irradiation of n-type Ge with fast neutrons, 19: 41104
STARY, I., Investigation of complexes of Am, Cm, Cf, and Fm with lactic acid, 19: 40458 (JINR-P-2224)
STEEB, S., Determination of the structure of tantalum suboxides TaO_2(TaO_2) with electron diffraction, 19: 41047
STEELE, R. M., Some fluorine compounds of Re and Tc, 19: 40461 (ORNL-P-491)
STEHLE, H., Irradiation of a MZFR test fuel element in the NRX, 19: 42185
STEHLE, H., MZFR fuel elements—design, construction, and research, 19: 42165
STEIN, H., MZFR electrotechnical installations, 19: 42170
STEIN, H. J., Introduction rate of electrically active defects in n-type silicon by nuclear radiation, 19: 40935 (SC-DC-65-1247)
STEINBERGER, J., Annihilation of antiprotons in hydrogen at rest. III., 19: 41325 (CU-1932-245)
STEINHOUSER, H., Promotion of chemical processes with reactor radiation, 19: 40559
STEPANOV, A. V., Complex compounds of cerium(III) and europium(III) with tartaric acid, 19: 40510
STEPANOV, K. N., The influence of plasma resonance on the propagation of surface waves in a non-uniform plasma, 19: 41916
STEPANOV, V. G., Electron paramagnetic resonance of Gd^{3+} in synthetic $SrMoO_4$, 19: 41994
STEPHAN, L. A., Reactor stability tests in Spert IV facility, 19: 42152 (IDO-17088)
STEPHENS, Douglas R., Volume compressibility of BeO and other II–VI compounds, 19: 41984
STEPHENS, F. S., Odd-parity rotational bands in ^{246}Cm, 19: 41794
STERN, David, Classification of magnetic shells, 19: 41584
STERNGLASS, E. J., Further evidence for a molecular structure of meson and baryon resonance states, 19: 41524
STERNHEIM, M. M., π-α scattering and the pionic form factor, 19: 41379
STERNHEIM, Morton M., Correction to the (^{3}He,^{2}^{3}S$_1$) to (He^{3+},^{2}^{2}S$_{1/2}$) hyperfine-structure ratio, 19: 41787
STERNHEIMER, D., Conformal-group symmetry of elementary particles, 19: 41392
STERNHEIMER, R. M., Statistical study of linear mass relations for elementary particles, 19: 41408
STERRETT, K. F., Magnetic behavior of rare earth metals at high pressures, 19: 42005
STETTLER, John D., Phonon-induced infrared absorption spectrum in irradiated MgO, 19: 41108
STEVANCEVIC, D. B., Extraction of copper and uranium with 2-methyl-heptane-4,6-dione and hexane-2,4-dione, 19: 40423
STEVENS, R. E., Preparation and properties of $Cs_3Pu_3Cl_9 \cdot 2H_2O$, 19: 40488
STEVENSON, Peter C., Experimental approach to nature and characteristics of primary fission fragments, 19: 41771
STEWART, A. T., Positron annihilation in solid and liquid metals and semiconductors, 19: 41285
STEWART, J. R., Total photoproton cross section and branching ratios in the O-16 giant resonance, 19: 41790
STOCK, R., Level structure of ^{53}Cr and ^{55}Cr, 19: 41726
STODDARD, Dean H., Radiation properties of californium-252, 19: 41657 (DP-986)
STOFFEL, A. M., Magneto-optic measurements on magnetic rare earth–cobalt alloy films, 19: 41084
STOLETOV, G., Double pp scattering at 667 Mev, 19: 41666 (JINR-P-2233)
STONE, N. J., Angular distributions of conversion electrons from oriented ^{137m}Ce nuclei, 19: 41679 (UCRL-11462(Rev.))
STONE, R. L., Investigation of manufacture of aggregate and riprap by nuclear means, 19: 40709 (PNE-5003)
STOUT, C. D., Medical defense against nuclear weapons, 19: 40361 (ORNL-tr-437)
STRAMBI, E., Control of U in urine for the prevention of professional intoxication: a statistic contribution, 19: 40839
STRAWBRIDGE, L. E., Criticality calculations for uniform water-moderated lattices, 19: 42054
STREL'TSOVA, V. N., Biological effects of Sr-90 in relation to the duration and frequency of uptake, 19: 40336
STREL'TSOVA, V. N., Pathological anatomy of radiation injury induced by Pm-147, 19: 40383
STREL'TSOVA, V. N., Pathological anatomy of radiation injury induced by Nb-95, 19: 40384
STRETTA, E. J. P., Geochemistry and radioactivity of waters in Lourdes, San Luis Potosi, Mexico, 19: 40835
STRIBEL, Theodor, Properties of Argonaut ring core in the increase of the H_2O : uranium ratio, 19: 42187
STRIGACHEV, A. T., Two-hour (7.7 ksec) isomer of ^{168}Lu, 19: 41803
STRNAT, K., Magneto-optic measurements on magnetic rare earth–cobalt alloy films, 19: 41084
STROEMME, Aksel, Induced radioactivity in the collimator system of a 31-Mev Brown Boveri betatron, 19: 41169 (NYO-3364-7)
STROEMME, Aksel, Induced radioactivity caused by therapeutic use of high-energy radiation, 19: 40392 (NYO-3364-6)
STUBBINS, Warren Fenton, Photoneutrons from lead, 19: 41833
STUKAN, B. G., The formation of polymeric products in reactions of polyvalent recoil atoms, 19: 40628
STURGEON, George Dennis, Rare earth borides: samarium–boron system, 19: 40524
SU, Shih-chun, Ionization characteristics of an electromagnetic ion source, 19: 40861
SUBRAHMANYAM, C. V., Statistical characteristics of sudden ionospheric disturbances, 19: 41573 (RPU-S19)
SUCHER, J., Long-range electromagnetic forces on neutral particles, 19: 41448
SUEN, Shin, B.C.S. superconducting ground state, 19: 41629
SUGAK, L. A., Calculation of absorbed energy of γ radiation, 19: 41959
SUGIHARA, T. T., Cross-section ratios of isomeric nuclides produced in medium-energy (α,xn) reactions, 19: 41695

SUGIHARA, T. T., Search for 2.6-hr iodine-126m, 19: 41716
SUGIHARA, T. T., Statistical-model analysis of isomeric ratios in (α,xn) compound nuclear reactions, 19: 41696
SULKOVSKAYA, M. M., Elastic pp scattering at 1.45 Bev, 19: 41487
SULLIVAN, R. J., Equipment for fabrication and encapsulation of irradiated UO_2 pellets, 19: 40715 (NAA-SR-Memo-7438)
SULYAEV, R. M., Michel parameter in $\mu^- \rightarrow e^-$ decay, 19: 41480
SUNDARAM, V. K., Temperature distribution in radioactive solids. II., 19: 42191 (AEET/HP/TH-20)
SUNDERMAN, D. N., Development of an improved method of sampling and analysis for atmospheric iodine, 19: 40402 (BMI-X-10137)
SUPPLE, A., Material buckling and intracellular thermal neutron distributions, 19: 42049 (MIT-2344-3, pp 155-64)
SUTTON, D. C., Neutron spectra from Bi produced by monoenergetic γ rays, 19: 41834
SUZUKI, Mahiko, Relativistic SU_6 symmetry scheme, 19: 41467
SVETLOLOBOV, I. A., Elastic pp scattering at 1.45 Bev, 19: 41487
SVETOZAROVA, G. I., Determination of mixing coefficient in a fluidized-bed reactor, 19: 42011
SVISTUNOV, V. M., Tunnel effect for photon-emitting Cooper pairs, 19: 41631
SVOBODOVA, J., Preparation of samples of biological material for liquid scintillation measurement of low-energy β-emitters, 19: 40425
SVORETSKII, V. N., Multiple scattering of 75- to 200-kev protons on solids, 19: 41273
SWIFT, Ward H., Development of radioactive waste fractionization and packaging technology, 19: 42197
SYNDER, Donald D., Pairs of CdS crystals with matched photoresponses, 19: 40598
SZEBOEK, Zoltan, The importance of the quantitative alterations of the extracellular space in the water-embalances of the experimental intestinal x-ray death, 19: 40369

T

TAKABAYASI, Takehiko, Quadrilocal model of baryons and unitary symmetry, 19: 41431
TAKAHASHI, T., Slip systems in single crystals of WC, 19: 41055
TAKANO, Naoyuki, Alpha particle groups from deuteron bombardment of ^{16}O and ^{40}Ca, 19: 41720
TAKAYANAGI, Kazuo, Behavior of slow electrons in atmospheric gases. I., 19: 41599
TAKAYANAGI, Kazuo, Behavior of slow electrons in atmospheric gases. II., 19: 41600
TAKEDA, Soishi, Measurement of migration area and multiplication factor of UO_2–H_2O lattice, 19: 42053
TAKEDA, Yasumasa, Initial-pressure dependence of instabilities in a low B theta pinch plasma, 19: 41887
TAKEHISA, Masaaki, Reaction of ethylene with phosgene induced by γ radiation, 19: 40589
TAKEHISA, Masaaki, Reaction of ethylene with 1,2-dichloroethane induced by γ radiation, 19: 40590
TAKETANI, Mituo, An evolutional track of galaxies in L-(L/V) diagram, 19: 41233
TALBERT, W. L. Jr., Design considerations for a system to investigate short-lived nuclei produced at a reactor, 19: 42017 (IS-1219)
TALMAN, James D., Possibility of observing a nonlinear electromagnetic effect, 19: 41784
TAN, Swie-In, Influence of hydrostatic pressure on the magnetic transitions in Tb and Dy, 19: 41077
TAN, Swie-In, Magnetic behavior of rare earth metals at high pressures, 19: 42005
TANG, Ting-wei, Generation of harmonic waves by EM wave in an isotropic plasma, 19: 41927
TANI, S., Pade approximant in potential scattering, 19: 41407
TANTON, George A., Fine structure of optical absorption bands in neutron-irradiated MgO, 19: 40632
TANTON, George A., Phonon-induced infrared absorption spectrum in irradiated MgO, 19: 41108
TAOKA, G. T., Theory of one-dimensional shock wave propagation, 19: 41126 (SCL-DR-65-75)
TARAN, Yu. V., Determination of spins of Ho-165 neutron resonances by transmission of polarized neutrons through a polarized target in the energy interval 0–55 ev, 19: 41665 (JINR-P-2209)
TARRAGO, X., Evidence for nucleon clustering from high-energy reactions, 19: 41831
TASSIE, L. J., Dirac magnetic monopoles and superconductivity, 19: 41391
TATALASHWILI, N. N., Treatment program of penetrating showers of cosmic rays with the energy of 10^{10} to 10^{12} ev, 19: 41290
TATARONIS, J. A., Absolute instabilities of perpendicularly propagating cyclotron harmonic plasma waves, 19: 41884
TATSUTA, Hatsumi, Energy response of BF_3 counter using paraffin moderators, 19: 40890
TAVENDALE, A. J., Reduction of carrier trapping in germanium lithium-drift γ ray spectrometers, 19: 40919
TAYLOR, A., Constitution diagram of tungsten–molybdenum–osmium system, 19: 41048
TAYLOR, A., Solid solubility limits of Y and Sc in the elements W, Ta, Mo, Nb, and Cr, 19: 41050
TAYLOR, B. N., Investigation of microwave radiation emitted by Josephson junctions, 19: 41614
TAYLOR, Brian, Process for making workable ruthenium and product thereof, 19: 40999
TAYLOR, Clayborne Dudley, Electromagnetic effects of high-density γ flux interacting with matter, 19: 41956 (SC-R-65-933)
TAYLOR, D. W., YORK 87—a 7090-FORTRAN program for analyzing phonon dispersion curves, 19: 41962 (AERE-M-967)
TAYLOR, Harold E., Adiabatic motion of auroral particles in model of electric and magnetic fields surrounding the earth, 19: 41583
TEAGUE, H. J., Approximate calculative assessment made relating to wall temperatures and behaviour of cask in fire tests, 19: 40832 (SC-RR-65-98, pp 732–5)
TEKUTOV, P. F., Effect of P-32 on higher nervous activity of dogs, 19: 40356 (FTD-TT-65-48, pp 469-70)
TELESHOV, E. N., Transformations in EPR spectra of irradiated polyisobutylene, 19: 40608
TEMPERLEY, J. K., Level scheme of Ga-69, 19: 41756
TENNEY, Gerold H., Non-destructive inspection of fuel elements for nuclear rockets, 19: 42146
TEPLINSKAYA, G. N., Biological effects of Sr-90 in relation to the duration and frequency of uptake, 19: 40336
TERAO, Nobuzo, Structure of niobium nitrides, 19: 41051
TERENTYEVA, E. A., Chemistry of rare earth complexes, 19: 40532
TERRALL, John, FOTRAC: a Monte Carlo photon tracing computer program, 19: 41957 (UCRL-14165)
TERRELL, J. H., The band structure of beryllium, 19: 41968 (MIT-QPR-57, pp 22–42)
TERRIEN, Jean-Francois, Relative roles of pyrolysis and radiolysis in degradation of terphenyls, 19: 40630
TESTA, C., Control of U in urine for the prevention of professional intoxication: a statistic contribution, 19: 40839
THALER, R. M., Remarks on charged-particle scattering, 19: 41763
THANKI, R. J., Ascorbic acid and ascorbic acid oxidase of γ-irradiated momordica charantia, 19: 40371
THAYER, V. R., Economics of fuel processing, 19: 40661
THEIMER, O., Effect of inner field fluctuations on plasma impedance, 19: 41853 (LA-DC-6603)
THEODORIDIS, G. C., Effect of solar flare on outer radiation belt, 19: 41312
THEUS, R. B., Angular distribution of the d-d reaction products, 19: 41832
THOMAS, D. D., Chemical enhancement of superconductivity, 19: 40543
THOMAS, David, Design considerations for a system to investigate short-lived nuclei produced at a reactor, 19: 42017 (IS-1219)
THOMAS, David G., Forced convection mass transfer. II., 19: 40746
THOMAS, G., Preparation of single crystal spheres of refractory metals and alloys, 19: 40991
THOMAS, L., Measurements of solar x-ray fluxes by the U. S. Naval Research Lab. satellite 1964-01-D, 19: 41231
THOMAS, T. D., Spontaneous emission of energetic He-6 particles from Cf-252, 19: 41785
THOMPSON, C., Evaluation of total absorption cross-section for photons in high-density electron gas, 19: 41140
THOMPSON, Don D., Differential dynamic polarization of fluorine and hydrogen nuclei, 19: 40497
THOMPSON, H. Bradford, Stimulated Compton scattering of electrons by laser beam, 19: 41328 (IS-1187)
THOMPSON, J. Truman, Survey of research in the transportation of radioactive materials, 19: 40809 (SC-RR-65-98, pp 17–31)
THOMPSON, M. A., Laboratory ignition system, 19: 42214 (RFP-397)
THOMPSON, S. A., Prog. rpt. on ion rocket engine development, 1–3/65, 19: 40765 (NP-15309)
THOMPSON, S. G., Internal conversion electrons from primary fission fragments, 19: 41680 (UCRL-16194)
THUN, H., Stability of some lanthanide complexes, 19: 40486
TIDMAN, Derek A., Radio emission from shock waves and type II solar outbursts, 19: 41229
TIERNEY, Martin Stephen, General magnetic field of the sun and the limit of co-rotation of the corona, 19: 41241
TIKHONOV, A. N., A collection of problems on mathematical physics, 19: 41153
TILLEY, D. R., Ginsburg-Landau equations for anisotropic alloys,

19: 41625
TIMMINS, Tom H., Relative roles of pyrolysis and radiolysis in degradation of terphenyls, 19: 40630
TING, C. T., The stereochemistry of the reactions of (n,γ) halogen atoms with alkyl halides in the liquid phase, 19: 40625
TJON, J. A., New reduction of the Faddeev equations and its application to the pion as a three-particle bound state, 19: 41416
TKACHEV, L. G., Degree of nonconservation of parity in θ and τ decays, 19: 41361
TOBAILEM, Jacques, Radioactivity of the Granes meteorite measured by γ spectrometry, 19: 40788
TOBOCMAN, W., Calculation of inelastic α-particle scattering by Ni-58, 19: 41692
TOCHIN, V. A., Photoconductivity in irradiated aromatic compounds, 19: 40601
TODD, P. F., Isotope effects in electron spin resonance: the negative ion of cyclo-octatetraene-1-d, 19: 40541
TOEVS, J. W., Stable linear pulse summing circuit, 19: 40726
TOHEI, Tsutomu, Alpha particle groups from deuteron bombardment of ^{16}O and ^{40}Ca, 19: 41720
TOLMIE, Ronald W., Radioisotope identifier, 19: 40929
TOLOK, V. T., High-frequency heating of plasma, 19: 41862 (NP-15256)
TOLSTOI, N. S., Microchromatographic column with remote control, 19: 40685
TOMBOULIAN, R., Electromagnetic studies in shock-produced plasmas, 19: 41855 (NP-15142)
TOMKOVA, E., Influence of uv radiation on thermionic converters, 19: 40566
TOMLINSON, J. N., Effect of nuclear radiation on the thermal conductivity of polyethylene, 19: 40603
TOMLINSON, Michael, Improvements relating to coolant for nuclear reactors having graphite moderators, 19: 42015
TOMLINSON, Roy E., Hanford program for management of high-level waste, 19: 42196
TOPPEL, B. J., Physics aspects of the plutonium experiment in EBWR, 19: 42078 (ANL-7019)
TORCHINSKAYA, O. L., Effect of hypocalcemia and subcutaneous inflammatory foci on the level of radioactive Sr in the skeleton, 19: 40343
TORCHINSKAYA, O. L., Effect of complexing agents on the amount of radioactive Sr deposited in bones, 19: 40344
TORCHINSKAYA, O. L., Oral administration of complexing agents to remove rare-earth elements (Ce-144) from rats, 19: 40347
TORNIELLI, G., Performance and properties of a proton polarimeter, 19: 40905
TOSCHI, R., Magnetoplasmadynamic generators, 19: 41315
TOTH, I. J., Activation sintering of tungsten, 19: 40985
TOTH, Mihaly, Neutron flux measurements in core of the VVR-S research reactor, 19: 42183
TOUCHARD, Jean, Variational calculation of collective states of spherical nuclei, 19: 41702
TOUR, Yung, B.C.S. superconducting ground state, 19: 41629
TOURNOUX, Michel, Systems tin(IV)-oxygen-potassium and zirconium-oxygen-potassium, 19: 41031
TOWLE, J. H., Neutron scattering studies of K-39, 19: 41737
TRAININ, L. Ya., Trap with magnetic plugs for holding electrons, 19: 41858 (NP-15217)
TRAINOR, James Harold, Neutron albedo measurements on polar-orbiting satellites, 19: 41606
TRAN THANH VAN, J., Relativistic theory of electrodisintegration of the deuteron. II., 19: 41374
TRAVIS, J. R., Experimental observations of initiation of nitromethane by shock interactions at discontinuities, 19: 42207 (LA-DC-6994)
TREHAN, S. K., Effect of transport coefficients on damping of hydromagnetic waves, 19: 41869
TREHERNE, Jacqueline, Electric octupolar transition of 71.2-kev in decay of Hf-171, 19: 41701
TRETENKO, M. E., Measuring the temperature of free electrons in rarefied acetylene–air flames, 19: 41922
TRET'YAKOV, E. F., Spectrum of internal conversion electrons in α-decay of ^{239}Pu and energy levels of ^{235}U, 19: 41673 (NP-15251)
TRIFTSHAEUSER, Werner, Measurement of free neutron excitation cross sections in Al and Bi, 19: 41274
TRILLAT, J. J., Oxidation of iron surfaces under ion bombardment, 19: 40973
TRILLAT, J. J., Reactions of gases with graphite, 19: 40975
TRODDEN, W. G., Conductivity induced by electron bombardment, 19: 41097
TROFIMOV, A. S., Numerical solution of one problem on optimum nuclear reactor control, 19: 42013
TROFIMOV, V. I., Radicals formed in radiolysis of certain benzene derivatives, 19: 40607

TROITSKII, M. A., Calculation of magnetic moments of spherical nuclei, 19: 41804
TROKHAN, A. M., Measuring the velocity of plasma jets, 19: 41912
TROWER, W. Peter, A FORTRAN program for calculating kinematical and dynamical quantities of particle interactions and decays, 19: 41339 (UCRL-11648)
TROXEL, L. M., Superconducting magnet for variable bandwidth traveling wave masers, 19: 41638
TRUDEAU, Fernand, Family of velocity-dependent nucleon-nucleon potentials for singlet-even states, 19: 41841
TRUNOVA, N. M., Reactions of the retina to ionizing radiation, 19: 40359 (FTD-TT-65-48, pp 590-1)
TS'AO, T'sien-chun, Measurements of eruptive phenomena on the solar limb, 19: 41234
TSERELOV, A. A., 340-Liters expansion-condensing chambers used to study nuclear interactions of high energy particles, 19: 40887
TSITOVICH, A. P., Stabilizing amplification channel of scintillation counter, 19: 40870 (IAE-695)
TSUKERMAN, I. S., Angular correlation between the π meson and leptons and the determination of form-factors in $K_{\mu 3}$ decay, 19: 41485
TSURUO, Akira, Unscattered flux from spherical and cylindrical sources with shell-shaped shields, 19: 41960
TSYBUL'KO, I. A., Reactions of lanthanum and yttrium oxides with ferric oxide, 19: 40515
TSYPIN, A. B., Reactions of the retina to ionizing radiation, 19: 40359 (FTD-TT-65-48, pp 590-1)
TSYRLIN, L. E., Two electrostatic problems for regions bounded by cylinders, 19: 41150
TUAN, S. F., Dynamical basis for η-baryon interactions, 19: 41433
TUCKER, Charles T., Prog. rpt. on Task IV local Newport pier test, 6/29/65, 19: 42210 (NVO-98-8)
TUCKER, P. A., Phase equilibria in plutonium–cerium–copper system, 19: 41054
TULI, Shrawan Kumar, π⁻p interactions at 2.0 Bev/c, 19: 41502
TULINOV, A. F., Multiple scattering of 75- to 200-kev protons on solids, 19: 41273
TULINOVA, Z. I., Formation of high-energy γ quanta, 19: 41298
TUREK, S., Preparation of samples of biological material for liquid scintillation measurement of low-energy β-emitters, 19: 40425
TURLAY, R., Dipion production at low momentum transfer in π⁻-p collisions 1.5 Bev/c, 19: 41441
TURNER, J. M., Prog. rpt. on two-phase flow and boiling heat transfer, 1–3/65, 19: 40738 (NYO-3114-7)
TURNER, J. M., Two-phase flow and boiling heat transfer. The separate-cylinders model of two-phase flow, 19: 40737 (NYO-3114-6)
TURNER, W. Richard, The polarography and analytical applications of 8-substituted quinaldines and quinaldinic acids (thesis), 19: 40545
TUTUROV, Yu. F., Irradiation of n-type Ge with fast neutrons, 19: 41104
TUZZOLINO, A. J., Thermal-vacuum behavior of lithium-drifted silicon detectors, 19: 40902
TVERDOKHLEBOV, V. I., Measuring the temperature of free electrons in rarefied acetylene–air flames, 19: 41922
TYAGUNOV, A. V., Investigation of plasma frequency multiplier, 19: 40860
TYCKO, D., Annihilation of antiprotons in hydrogen at rest. III., 19: 41325 (CU-1932-245)
TYE, Russell, Liquid scintillation counting of C-14 in aqueous digests of whole tissues, 19: 40418
TZU, Hsi-chuen, Structure of even parity states of ^{16}O. [Part] I., 19: 41816

U

UDGAONKAR, B. M., Reciprocal bootstrap possibilities for baryons, 19: 41422
UDGAONKAR, Bhalchandra M., Baryon bootstrap possibilities in SU(6), 19: 41443
UDOVENCHIK, V. T., Optical properties of CaF_2–Dy^{3+}, 19: 40600
UDOVENCHIK, V. T., The effect of oxygen impurity on the optical properties of CaF_2–Sm crystals, 19: 41993
UEBERALL, H., Decay of collective nuclear states excited in muon capture, 19: 41769
UEDA, Yoshiaki, Possible effects of CP violation in $K^+ \to 3\pi$ decay, 19: 41445
UKAI, Seiji, Measurement of migration area and multiplication factor of UO_2–H_2O lattice, 19: 42053
UKHANOVA, V. A., Effect of food Ca on metabolism of Sr-90 in fodder-milk link in cows, 19: 40341
ULRYCH, Gerhard, Heat-engineering data of PWR with special consideration of possible breakdown of principal circulating pump, 19: 42118
URANO, Yukichi, Reaction of ethylene with 1,2-dichloroethane induced by γ radiation, 19: 40590

URCH, D. S., Reactions of hot tritium atoms with hydrocarbons, 19: 40616
USIK, P. A., Experimental data on N-N interactions at 300 Bev, 19: 41358
UTEKHIN, A. P., Spectrometric characteristics of LSU-5k apparatus, 19: 40875 (NP-15254)
UVAROV, F. A., Experimental determination of effective probability of photon emission by plasma atoms, 19: 41891

V

VALENTIN, Jacques, Electric octupolar transition of 71.2-kev in decay of Hf-171, 19: 41701
VALYI, Laszlo, Electrostatic ion beam accelerator, 19: 41181
VALYI, Laszlo, Investigation of an r-f ion source, 19: 40855
VANDERLEEN, W., Stability of some lanthanide complexes, 19: 40486
VAN DER WOUDE, F., Precision (0.1°C) vacuum cryostat and furnace for Moessbauer experiments, 19: 40858
VAN LANDUYT, J., Aspects of initial stage of oxidation of niobium, 19: 40974
VAN THIEL, Mathias, High-pressure shock wave experiments in argon and xenon, 19: 41128 (UCRL-12466)
VAN TORNE, L. I., Preparation of single crystal spheres of refractory metals and alloys, 19: 40991
VAN WINKLE, R., A comparison of multistage flash and long-tube vertical multiple-effect evaporators under identical conditions, 19: 40699 (ORNL-TM-826)
VARGA, Laszlo, Electrostatic ion beam accelerator, 19: 41181
VARUKHA, E. A., Effect of P-32 on higher nervous activity of dogs, 19: 40356 (FTD-TT-65-48, pp 469-70)
VARVOGLIS, A. G., Thermal annealing phenomena in neutron-irradiated liquid organic bromides, 19: 40576
VASAROS, L., Reactions of hot ^{38}Cl atoms in mixtures of CCl_4 with aliphatic alcohols, 19: 40623
VASAVADA, Keshyap V., Partial-wave dispersion relations for pionic disintegration of deuterons. Technical Report No. 436, 19: 41336 (NP-15335)
VASILEV, S. S., Excitation functions for (p,p′) on Al-27, 19: 41813
VASILEV, V. S., Effective lifetime of current carriers in lithium-compensated silicon, 19: 41964 (JINR-P-2201)
VASIL'EVA, G. Ya., Magnetic fields and motions in an undisturbed photosphere, 19: 41221
VATAZHIN, A. B., Development of MHD boundary layer due to sudden initiation of motion or sudden deceleration of supersonic flow, 19: 41146
VAUGHAN, Dale A., Characterization of pyrolytic-carbon fuel-particle coatings prepared with acetylene, 19: 41004 (BMI-1735)
VAVILOV, V. S., Radiation defects in very pure silicon crystals, 19: 41998
VAVILOV, Yu. N., Measurements of μ-meson intensity at great depth under water, 19: 41293
VAVREJN, B., Preparation of samples of biological material for liquid scintillation measurement of low-energy β-emitters, 19: 40425
VDOVENKO, V. M., Uranium extraction from Hf–HNO_3 by ternary amines in benzene, 19: 40684
VEDRINSKII, R. V., Spallation of hyperfragments in Coulomb field, 19: 41815
VEHAUC, A., Heat transfer of reactor fuel element model with polyzonal-spiral finning, 19: 40748
VEKSLER, V. I., Baryon resonances in π-p interactions at 7.5 Bev with strange-particle formation, 19: 41488
VEKSLER, V. I., Meson resonances in π-p interactions at 7.5 Bev with strange-particle production, 19: 41489
VELLENDER, G. C., Application of digital data acquisition and process control system to a research reactor, 19: 42150 (ANL-7009)
VENABLE, Douglas, Phermex applications to studies of detonation waves and shock waves, 19: 41118 (LA-DC-6996)
VENABLES, F. H., Measurements of solar x-ray fluxes by the U. S. Naval Research Lab. satellite 1964-01-D, 19: 41231
VENEZZIANO, Augusto, Safety concerning reactor Pegase, 19: 42151 (CEA-R-2518(Vol.II))
VENUTI, G. Campos, The (e,e′p) experiment: results obtained and planned proposals, 19: 41660 (ISS-65/3)
VERBEEK, F., Stability of some lanthanide complexes, 19: 40486
VERMEULEN, L. W., Recovery of Th from U process solutions, 19: 40694
VEYSSIE, Jean-Jacques, Transport properties of Nd nitride at low temperature, 19: 41973
VEZZETTI, David Joseph, Asymptotic solution of the Schroedinger equation for the three-body problem, 19: 41565
VIANO, G. A., Muon capture by the virtual pions exchanged by proton pairs in a nucleus, 19: 41753
VIANO, G. A., Numerical analytic continuation of proton electromagnetic form factors, 19: 41388
VIDAVSKII, L. M., Enthalpy of the γ-UO_3 reaction with HF and enthalpy of formation of γ-UO_3, 19: 40521
VIDONI, Carlotta M., Bibliography on thermal resistance of contacting surfaces, 19: 40744 (UCRL-14264)
VIDULICH, George Anthony, Absolute dielectric constants of H_2O and D_2O and transference numbers of LiCl and $CdCl_2$, 19: 40527
VIGIER, J. P., Conformal-group symmetry of elementary particles, 19: 41392
VIGNAU, H., Cross-section ratios for isomeric pair $^{44m}/^{44}Sc$ produced by $^{45}Sc(d,t)^{44}Sc$ reaction, 19: 41714
VIGNAU, H., Cross-section ratios for isomeric pair $^{58m}/^{58}Co$ produced by the $^{59}Co(d,t)$ reaction, 19: 41715
VIGONE, M., $K_{\mu 3}$ branching ratio and μ^+ energy spectrum, 19: 41414
VILCOV, N., Analysis of some circuits used in amplifiers for semiconductor nuclear particle detectors, 19: 40899
VINCENT, G., Development and construction of ion sources of duoplasmatron type, 19: 41871
VINOGRADOVA, L. I., Cyclotron injector, 19: 41193
VINTAIKIN, E. Z., Investigation of thermal vibrations of atoms in Cu by neutron spectrometry, 19: 41996
VINTOVKIN, S. I., Radiation defects in very pure silicon crystals, 19: 41998
VIRYASOV, N. M., Baryon resonances in π-p interactions at 7.5 Bev with strange-particle formation, 19: 41488
VIRYASOV, N. M., Meson resonances in π-p interactions at 7.5 Bev with strange-particle production, 19: 41489
VISHNEVSKII, V. F., Optimal determination of the detecting efficiency (weight) of an event, 19: 40873 (JINR-P-2215)
VISHVESHWARA, C. V., Gravitational radiation from binary systems, 19: 41206 (N64-33291)
VITALE, S., Search for a β-active ^5H, 19: 41750
VITMAN, V. D., New data for ^{188}Re decay scheme, 19: 41801
VITOL, E. N., Determination of nitrogen in metals by an isotope-dilution method, 19: 40444
VITSMAN, G., Fluorescence of rare earths. II., 19: 40494
VITTITOE, C. N., IBM 1620 reconstruction of bubble chamber interactions, 19: 40915
VITUSHKIN, N. I., Unit for gas-phase radiation-induced graft polymerization, 19: 40596
VLADIMIRSKII, V. V., Possibility of the existence of a boson 27–supermultiplet 1^+, 19: 41492
VODOP'YANOV, F. A., Certain theoretical problems of wide-band oscillators, 19: 40846 (NP-15209)
VOEDROES, Daniel, Activity measurement on the basis of the gamma spectrum, 19: 40893
VOGT, O., $EuGd_2S_4$, a new ferromagnetic semiconductor, 19: 40496
VOINOVA, N. A., New data for ^{188}Re decay scheme, 19: 41801
VOITOVICH, R. F., Oxidation of Nb–Cu and Zr–Cu alloys, 19: 40976
VOJTECH, O., Studies on the effects of some polyhydric alcohols on ion-exchange and separation of rare earths with the aid of α-hydroxyisobutyric acid, 19: 40662
VOLGER, J., Paramagnetic resonance of Eu(II) in Pb chloride, 19: 40498
VOLIN, Yu. M., Problem of optimization of system with distributed parameters, 19: 42012
VOLKOV, V. M., Theoretical investigation of stereochemistry of complex compounds with f-electrons. II., 19: 40522
VOLKOV, Yu. F., Investigation of a θ pinch plasma in an azimuthal magnetic field, 19: 41921
VOLKOV, Yu. F., Plasma in a θ-pinch with azimuthal magnetic field, 19: 41860 (NP-15220)
VOLOVIK, M. P., X-radiation-induced cytochemical changes in rabbits, 19: 40375
VON DUESTERLHO, R., Prophylactic effect of histamine in whole-body irradiated rats, 19: 40389
VON ENGEL, A., Ionized Gases, 2nd Ed., 19: 41937
V[ON] HAEBLER, D., MZFR electrotechnical installations, 19: 42170
VOROB'EV, A. A., Radiation stability of alkali halide crystals, 19: 41975
VOROBEV, Yu. A., Excitation functions for (p,p′) on Al-27, 19: 41813
VORON'KO, Yu. K., Optical properties of CaF_2–Dy^{3+}, 19: 40600
VOROZHEIKINA, L. F., Radiation damage in ionic crystals, 19: 41976
VORTMAN, L. J., Dimensions of a crater from a 500-ton TNT hemisphere detonated on rock, 19: 40712 (SC-RR-65-277)
VORTMAN, L. J., Nuclear explosives—tool for engineer, 19: 40710 (SC-DC-65-1485)
VREHEN, Q. H. F., Paramagnetic resonance of Eu(II) in Pb chloride, 19: 40498
VRZALOVA, D., Certain new Asenazo III analogs and their analytical properties, 19: 40426
VUKANOVIC, M. V., Spectral line intensity differences between arc in a tube and a free-burning arc, 19: 41873
VYAS, D. N., Ascorbic acid and ascorbic acid oxidase of γ-irradiated momordica charantia, 19: 40371
VYSOCHANSKII, M., Application of controlled photomultiplier as a

separating element in the nanosecond coincidence circuit, 19: 40872 (JINR-P-2203)

W

WACHTELL, George Peter, Can we model a fire test, 19: 40815 (SC-RR-65-98, pp 133–40)
WACHTELL, George Peter, Fire test of 15-ton shipping container, 19: 40827 (SC-RR-65-98, pp 631–50)
WACKER, A., Sensitivity of pyrimidines and purines towards neutron irradiation, 19: 40557
WACKERLE, Jerry, Interactions of detonation waves in condensed explosives, 19: 42205 (LA-DC-6990)
WADE, Marvon A., Microdetermination of fluoride using an improved distillation procedure, 19: 40420
WAGNER, Paul, Loss of UO_2 from Mo–UO_2 cermets by high-temperature diffusion, 19: 41043
WAI, C. M., The stereochemistry of the reactions of (n,γ) halogen atoms with alkyl halides in the liquid phase, 19: 40625
WAIN, A. G., Partition coefficients of nitratonitrosylruthenium complexes between nitric acid and TBP phases, 19: 40677
WALDBURGER, C., Oxidation of iron surfaces under ion bombardment, 19: 40973
WALI, Kameshwar C., Relativistic formulation of the SU(6) symmetry scheme, 19: 41428
WALKER, B. E. Jr., Instability of refractory metal thermocouples, 19: 40859
WALKER, J., Branching ratio of ^{212}Bi(ThC), 19: 41798
WALKER, J. C., Mössbauer effect resulting from the reaction $^{56}Fe(d,p)^{57}Fe$, 19: 41793
WALKER, R. L., Photoproduction of π^+ mesons from hydrogen from 0.6 to 1.2 Bev, 19: 41323 (CALT-68-42)
WALLACE, T. C., Phase relationships of the high carbon portion of the lanthanide dicarbides, 19: 41014 (LA-DC-6819)
WALLINGFORD, J. S., Orbits in a magnetic universe, 19: 41208 (ORNL-3827)
WALLIS, G. B., Prog. rpt. on two-phase flow and boiling heat transfer, 1–3/65, 19: 40738 (NYO-3114-7)
WALLIS, G. B., Two-phase flow and boiling heat transfer. The separate-cylinders model of two-phase flow, 19: 40737 (NYO-3114-6)
WALSH, D., Antenna impedance in a plasma: problems relevant to radio-astronomy measurements from space vehicles, 19: 41212
WALTON, H. F., Separation of amines by ligand exchange. II., 19: 40647 (COO-499-1)
WALTON, Herold F., Separation of amines by ligand exchange. III., 19: 40648 (COO-499-2)
WAMSER, A., Design and function of hydraulically actuated ultra vacuum through-way valve, 19: 40776
WANG, Chang-zhu, Three-quasiparticle state in ^{165}Er, 19: 41667 (JINR-P-2239)
WANG, Chuan-ying, Measurement and analysis of the magnetic center plane in a cyclotron, 19: 41195
WANG, I. T., Muon capture by deuterons, 19: 41782
WANG, I. T., Study of breakup channels of muon capture by ^3He, 19: 41783
WANG, Ju-lin, Two-nucleon stripping reactions, 19: 41817
WANG, K. H., Inelastic scattering and neutron pickup for ^{12}C and ^{16}O projectiles on ^{208}Pb, 19: 47168
WANG, Nai-yang, Neutron resonances of ytterbium isotopes, 19: 41661 (JINR-P-2158)
WANG, Te-chi, Measurement and analysis of the magnetic center plane in a cyclotron, 19: 41195
WANG, Tse-Pin, Dynamical correlations and the nuclear photoeffect, 19: 41844
WANGSNESS, R. K., Interference of fine-structure levels in hydrogen, 19: 41263
WANIC, Adam, Investigation of the magnon spectrum with neutrons, 19: 41987
WARBURTON, J. A., Airborne observations of natural radioactivity in the atmosphere, 19: 40790
WARD, H. C., Measurement of void fraction in two-phase flow by x-ray attenuation, 19: 40745
WARMBOLD, I., Program system for solution of the multigroup neutron diffusion equation, 19: 41649
WARNECKE, R. J., Development and construction of ion sources of duo-plasmatron type, 19: 41871
WARREN, J. H., Criticality safety of fissile materials in the chemical processing department, 19: 40807 (RL-SEP-389(Rev.))
WARRIKOFF, A., Guarantees for MTR fuel elements, 19: 42157
WARSHAW, Israel, Crystal chemistry of rare earth sesquioxides, aluminates, and silicates, 19: 40535
WATANABE, Ichie, Approach in canonical formalism of quantum field theory, 19: 41475
WATERBURY, G. R., X-ray fluorescence spectrometric determination of plutonium in uranium–plutonium–manganese alloys, 19: 40408 (LA-3333)
WATKINS, Robert V., Prog. rpt. on improved strength and oxidation resistance of Cr composites, final, 3/64–3/65, 19: 41022 (NP-15292)
WATKINS, Robert V., Prog. rpt. on improved strength and oxidation resistance of Cr composites, final, 3/64–3/65, 19: 41022 (NP-15292)
WATSON, E. R., Large nuclear-powered sea water reverse osmosis plants, 19: 42120
WATSON, Kenneth M., Atomic theory of gas dynamics, 19: 41161
WATSON, R. L., Internal conversion electrons from primary fission fragments, 19: 41680 (UCRL-16184)
WATT, J. S., Airborne observations of natural radioactivity in the atmosphere, 19: 40790
WATT, John Stanley, A method and apparatus for producing x rays of particular wave lengths and applications therefor, 19: 41163
WAWERSIK, H., MZFR—manufacture of the most essential parts of the primary installation, 19: 42172
WEAVER, Boyd, Liquid-liquid extraction of rare earths, 19: 40692
WEBER, C. W., Constriction response analyzer and its application to continuous UF_6 determination, 19: 40417
WEBER, R., MZFR—devices for fuel element exchange, 19: 42166
WEBER, Robert, Device for operating a loading machine for reactors, 19: 42032
WEDDELL, James B., Solar proton event production by hydromagnetic shocks, 19: 41230
WEGNER, H. E., Direction and energy distribution of charged particles transmitted through single crystals, 19: 41788
WEHNER, G. K., Sputtering studies of insulators by means of Langmuir probes, 19: 41257
WEHNER, G. K., Study of ion-bombardment damage on a Ge(111) surface by low-energy electron diffraction, 19: 41258
WEIDENBAUM, B., Fission gas release from UO_2 fuel rods with gross central melting. I., 19: 41088 (GEAP-4572)
WEIDLEIN, J. R., Synthesis and properties of red Ta_3N_5, 19: 40472
WEIGERT, A., Stellar evolution. I., 19: 41210 (N64-25282)
WEINBERG, B., Single-film journal bearing tests in water, 19: 40703 (TIM-916)
WEINBERG, J. G., Properties of a Hf-control rod after exposure during three seed lives in PWR Core 1, 19: 41092 (WAPD-TM-457)
WEINREICH, Marcel I., Temperature dependence of dielectric polarization in some benzene derivatives, 19: 40468 (SC-T-65-721)
WEINSTEIN, Joel, Accurate current integrator in the range of 10^{-5} to 10^{-9} amperes, 19: 40843 (CEAL-1021)
WEINSTOCK, Jacques J., Fabrication and utilization of large β sources, 19: 40560
WEISS, L., Low-temperature chamber for neutron-diffraction studies, 19: 40852
WEITZBERG, A., Safe disposal of SNAP reactors, 19: 42140 (NAA-SR-11353)
WELBER, Benjamin, Direct charge transfer by x irradiation in CaF_2:Eu, Tm, 19: 40575
WELCH, Jasper A. Jr., Atomic theory of gas dynamics, 19: 41161
WELCH, M. J., Reactions of hot tritium atoms with hydrocarbons, 19: 40616
WELLS, D. O., Level scheme of Ga-69, 19: 41756
WENZL, H., Liquid-He irradiation facility at the Munich research reactor FRM, 19: 42180
WERBROUCK, A. E., $K_{\alpha 3}$ branching ratio and μ^+ energy spectrum, 19: 41414
WERNER, K., A pulse method for investigation of time behavior of dynamic proton polarization, 19: 40473
WERTZ, John E., Thermoluminescent formations of Cr^{2+} in magnesium oxide, 19: 40631
WERY, Michel, Study of excitation curves of reaction $^{12}C(t,\alpha_0)^{11}B$, 19: 41706
WEST, D. L., Selection, cost, and performance of n-paraffin diluents, 19: 40646 (CONF-650918-2)
WEST, Geoffrey B., Relativistic effects in form factors of ^3He and ^3H, 19: 41770
WESTGARD, J., Anti-isobar production in $\bar{p}n$ interactions, 19: 41438
WESTON, L. W., Measurement of the U-235 neutron capture-to-fission ratio from 3.25 ev to 1.8 kev, 19: 41749
WESTON, M., Chemical effects of nuclear recoil in organic halide systems, 19: 40624
WHEATLEY, B. M., Dose equivalent estimation in health physics instrumentation, 19: 40911
WHELAN, M. J., The characteristics of the moellenstedt velocity analyser, 19: 40883
WHETSTONE, S. L. Jr., Spontaneous emission of energetic He-6 particles from Cf-252, 19: 41785
WHITE, D. H., Backward elastic scattering of high-energy pions by protons, 19: 41456

WHITE, D. H., Neutron-capture γ-ray studies of low-lying ^{52}V levels, 19: 41725
WHITE, D. H., Pion-proton elastic scattering at high momentum transfers, 19: 41455
WHITE, G. R., Radioactive hydrogen, 19: 40638
WHITE, J. D., Critical experiments with PuO_2–polystyrene compacts with ^{240}Pu = 8%, 19: 42038 (BNWL-95, pp 27–35)
WHITE, Stuart C., Device for the measurement of liberated energy in explosion, 19: 40850 (ORNL-tr-588)
WHITE, William Paul, Joints between tubular members, 19: 40705
WHITEHOUSE, J. E., Economical liquid He cryostat and other cryogenic apparatus, 19: 41626
WHITMORE, S. C., Observation of stable superfluid circulation in liquid He II at level of 1, 2, and 3 quantum units, 19: 41620
WIGGINS, L. L., Response to norepinephrine of isolated rat myocardium following ^{131}I-induced hypothyroidism, 19: 40368
WILBER, H. A., Investigation of core reproducibility of the Enrico Fermi 19: 42079 (APDA-NTS-4)
WILBER, H. A., Measurement of the isothermal temperature coefficient of reactivity of the Enrico Fermi reactor, 19: 42080 (APDA-NTS-5)
WILDING, M. W., Decontamination of radioactive effluent with clinoptilolite, 19: 40651 (IDO-14657)
WILHITE, R. N., Selection, cost, and performance of n-paraffin diluents, 19: 40646 (CONF-650918-2)
WILIP, Elmar K., Neutron emission from ^{233}U, ^{235}U, and ^{239}Pu fission fragments, 19: 41681 (ANL-Trans-205)
WILKINS, Bert Jr., Measurement of void fraction in two-phase flow by x-ray attenuation, 19: 40745
WILLARD, H. James Jr., Investigation of transient radiation damage in semiconductor materials. Quarterly progress report 11/1/64–1/31/65, 19: 40934 (NP-15301)
WILLE, Rudolf, Thermal nuclear reactor, 19: 42065
WILLIAMS, K. M., Measurements of solar x-ray fluxes by the U. S. Naval Research Lab. satellite 1964-01-D, 19: 41231
WILLIAMS, Kenneth John, Improvements in or relating to conveyor systems, 19: 40729
WILLIAMS, M., Substoichiometric determination of traces of gold by neutron-activation analysis, 19: 40437
WILLIAMS, Ronald Peter, Heating element spacer grids, 19: 42073
WILLIAMS, Ronald Peter, Improvements relating to nuclear reactor fuel element assemblies, 19: 42072
WILLIAMSON, E. L., Chromatograph for analysis of highly reactive and corrosive compounds, 19: 40407 (KY-485)
WILLIS, C. A., Safe disposal of SNAP reactors, 19: 42140 (NAA-SR-11353)
WILLS, Stanley Charles Frederick, Improvements in or relating to grabs, 19: 42027
WILMORE, D., Transition in O-18 (3.92 to 1.98 Mev), 19: 41797
WILSKY, K., High-energy transitions in I-132 decay, 19: 41744
WILSON, R. G., Electron and ion emission from cesiated and vacuum surfaces, 19: 41284
WILSON, W. E., Motion of plasma and lifetimes of energetic ions in a toroidal octupole magnetic field, 19: 41896
WINEGARDNER, W. K., Corrosion in simulated PRTR fuel element surface crevices, 19: 40965 (BNWL-83)
WINEGARDNER, W. K., Formation of chemicals by reactor irradiation of oxygenated water and ammoniated water, 19: 40548 (BNWL-82)
WINHOLD, E. J., Inelastic scattering of 14-Mev neutrons to low-lying states of Ta, W, Tl, and Pb, 19: 41718
WINKLER, F., MZFR—the primary circuit and its construction, 19: 42164
WINOCUR, Joseph, Spectroscopic technique for probing an ionized gas, 19: 41883
WINSLOW, F. R., Diffusion of Nb-95 and Ta-182 in niobium (columbium), 19: 41064
WINTER, J., Intervention-decontamination building, Centre d'Etudes Nucleaires de Fontenay-aux-Roses, 19: 40836
WINTHER, A. C., Facilities for mechanical testing of irradiated reactor materials at Risoe, 19: 40717 (RISO-98)
WITTENBERG, L. J., Phase equilibria in plutonium–cerium–copper system, 19: 41054
WITTERN, H. W., Study of the $^6Li(p,2p)^5He$ reaction using cluster model wavefunctions, 19: 41842
WOERNER, P. F., Application of metal coatings on uranium, 19: 40949 (ISC-640)
WOLF, H.-P., Program system for solution of the multigroup neutron diffusion equation, 19: 41649
WOLFE, J. H., Explorer 14 plasma probe observations, 19: 41580
WOLFGANG, R., Reactions of nucleogenic C atoms with hydrocarbons, 19: 40617
WOLLENBERG, Harold A., Concrete low-background counting enclosure, 19: 40721 (UCRL-11454)
WOLLNIK, H., Influence of magnetic and electric fringing fields on the trajectories of charged particles, 19: 41139
WOLLSCHLAEGER, G., Radioprotection effectiveness of serotonin in rats, 19: 40388
WOO, Ching-hung, Quantum effects on accuracy of momentum measurements, 19: 41553
WOO, Ching-hung, Some simple consequences of SU(4) symmetry, 19: 41397
WOOD, D. H., Correlation of rose bengal clearance and histopathological change of sheep livers damaged by Np-237, 19: 40350 (HW-SA-3723)
WOOD, M. R., Boron-11 neutron flux monitors—interim report, 19: 40867 (BNWL-64)
WOOD, W. D., Thermal radiative properties, 19: 41074
WOODRUFF, G., Fast neutron distributions, 19: 42043 (MIT-2344-3, pp 15-36)
WOODS, A. D. B., The crystal dynamics of uranium dioxide, 19: 41032
WORLOCK, R. M., Surface ionization engine development, 19: 40769
WORLOCK, Robert, Electric propulsion ground testing, 19: 40771
WORMAN, F. C. V., Integral gamma and neutron measurements on Kiwi-TNT, 19: 42135 (LA-3304)
WYSOCKI, J. J., Thermally stimulated conductivity of neutron-irradiated Si, 19: 41985

Y

YAKOVLEVA, N. I., Phospho-organic complexing resins, 19: 40668
YAKUBOVICH, A. A., Unit for gas-phase radiation-induced graft polymerization, 19: 40596
YAKUBOVSKAYA, V. I., Influence of unitol on biochemical indices of tissue after x irradiation, 19: 40386 (FTD-TT-65-48, pp 661-2)
YAMAGATA, Noboru, Prog. rpt. on common and radioactive Cs in nature and man, 4/62–3/65, 19: 40781 (NP-15179)
YAMAGATA, Noboru, Prog. rpt. on distribution of common and radioactive Cs in nature and man, 9/64, 19: 40309 (NP-15180)
YAMAMURA, Stanley S., Microdetermination of fluoride using an improved distillation procedure, 19: 40420
YAMANOUCHI, Yoshimaro, Alpha particle groups from deuteron bombardment of ^{16}O and ^{40}Ca, 19: 41720
YAMAZAKI, H., Evaluation of aberrations of focused beams of charged particles caused by space charge, 19: 41173
YANG, Fu-Chia, 0^+ states in N = 82 nuclei, 19: 41747
YANKOVSKAYA, Ts. L., Reaction of the endocrine organs to fractional irradiation with small doses of x rays, 19: 40360 (FTD-TT-65-48, pp 666)
YANSON, I. K., Tunnel effect for photon-emitting Cooper pairs, 19: 41631
YAREMBASH, E. I., Roentgenographic studies of lanthanum tellurides La_4Te_7, 19: 41070
YAREMBASH, E. I., Roentgenographic studies of lanthanum ditelluride, 19: 41071
YARIN, L. P., Gas flame in magnetohydrodynamics, 19: 41144
YAROSHINSKII, V. I., Thermal properties of binary sodium sulfates of certain cerium sub-group rare earths, 19: 40511
YARTSEV, E. I., Distribution of Sr-90 in the skeleton of dogs after chronic exposure, 19: 40321
YASUMOTO, Masahiko, Reaction of ethylene with phosgene induced by γ radiation, 19: 40589
YASUMOTO, Masahiko, Reaction of ethylene with 1,2-dichloroethane induced by γ radiation, 19: 40590
YATSUI, Kiyoshi, Moving striation of plasma in a longitudinal magnetic field, 19: 41888
YAVOR, S. Yu., Spherical aberration of combined quadrupole lens with bell-shaped field distribution, 19: 41198
YAVORSKY, P. M., Prog. rpt. on evaluation of β radiation as hydrogenation catalyst, 3/62–10/63, 19: 40553 (NYO-2978-34)
YAZVITSKII, Yu. S., Neutron resonances of ytterbium isotopes, 19: 41661 (JINR-P-2158)
YEARIAN, M. R., Elastic electron-deuteron scattering and possible meson-exchange effects, 19: 41453
YEH, William Wen, Many-body theory of positron annihilation in metals, 19: 41159
YEN, Wu-kuang, Optimal determination of the detecting efficiency (weight) of an event, 19: 40873 (JINR-P-2215)
YOKOO, Yoshimatsu, Cp violation and the $|\Delta| = \frac{1}{2}$ rule, 19: 41471
YORK, E. J., YORK 87—a 7090-FORTRAN program for analyzing phonon dispersion curves, 19: 41962 (AERE-M-967)
YOSHIDA, Yoshikazu, Energy response of BF_3 counter using paraffin moderators, 19: 40890
YOSHIMURA, Hisamitsu, Plasma fusion, 19: 41881
YOUNG, Bing-lin, Rare decay modes of the η meson as a probe of electromagnetic and strong interactions, 19: 41457
YOUNG, Donald E., High field measurements at 200 Mc/sec in conventional proton linear accelerator geometries at 5, 50, and 125 Mev, 19: 41202
YOUNG, J. A., Prog. rpt. on integral neutron thermalization, 3/31/65, 19: 41640 (GA-6323)

YOUNG, J. C., Neutron-spectrum measurements in H_2O and D_2O, 19: 41646
YOUNG, J. C., Prog. rpt. on integral neutron thermalization, 3/31/65, 19: 41640 (GA-6323)
YOUNG, James E., Pions, muons, and nuclear structure, 19: 41671 (LADC-6186)
YOUNG, Jessie M., Infrasonic waves from aurorae, 19: 41592
YOUNG, Russell D., Field desorption of Th from a field-evaporated W surface, 19: 41255
YU, D. U. L., Electron scattering from nuclear magnetic moments, 19: 41694
YU, You-wen, Structure of even parity states of ^{16}O. [Part] I., 19: 41816
YUDIN, E. P., Calculations of atmospheric shower curves, 19: 41300
YUDIN, N. P., Correlation effects of nuclear reactions at ground state, 19: 41814
YUEN, P. C., Observations of ionospheric electron content using geostationary satellite, 19: 41597
YUR'EV, V. G., Most effective regimes for thermionic convertors, 19: 41317
YURGENSON, V. A., Search for positron emitters among the products of ^{235}U thermal neutron fission, 19: 41799

Z

ZABORENKO, K. B., Influence of length of α-particle track in nuclear photoemulsion in relation to pH of impregnating solution, 19: 40597
ZAHEDI-MOGHADAM, Ali-Asghar, Study of recombination processes for electron-hole pairs in germanium irradiated by γ rays from ^{60}Co using the photovoltaic effect in p-n junctions, 19: 40932 (CEA-R-2723)
ZAHN, Ursel, Novel synthesis of carrier-free ^{106}Ru-labeled ruthenocene, 19: 40634 (BNL-8405)
ZAITSEV, A. A., Electron oscillations in a plasma, 19: 41907
ZAITSEVA, L. L., Thermal properties of binary sodium sulfates of certain cerium sub-group rare earths, 19: 40511
ZAKHAROV, A. M., Investigation of ternary W–Mo–Zr phase diagram, 19: 41035
ZAKHAROV, V. E., Stationary nonlinear wave in plasma, 19: 41915
ZAKHAROV, V. I., Unitary symmetry and K_{e4}-decay. Report No. 320, 19: 41335 (NP-15239)
ZAKRZEWSKI, J., Angular correlations between fast Σ hyperons and fast protons, 19: 41494
ZANELLO, D., Annihilation of antiprotons in hydrogen at rest. III., 19: 41325 (CU-1932-245)
ZANNONI, G., Performance and properties of a proton polarimeter, 19: 40905
ZASHKVARA, V. V., Correction of angular aberrations of two-sector electrostatic analyzer, 19: 41197
ZEIGLER, R. K., A uniqueness theorem concerning moment distributions, 19: 42204 (LA-DC-6632)
ZELBSTEIN, U., Measurement of the plate temperature of fuel elements of BR-2, 19: 42181
ZEL'DOVICH, Ya. B., Magnetic model of the universe, 19: 41236
ZELLER, W., MZFR fuel elements, 19: 42175
ZEMAN, Wolfgang, Pathogenesis of radiolesions in the mature central nervous system, 19: 40349 (BNL-9345)
ZERBY, C. D., Calculated tissue current-to-dose conversion factors for nucleons below 400 Mev, 19: 40372
ZHELEZNYAKOV, V. V., Mechanism of γ emission in solar flares, 19: 41289
ZHELEZNYKH, I. M., Possibility for detecting the intermediate meson with mass larger than twice the nucleon mass, 19: 41484
ZHILEIKO, G. I., Investigation of plasma by means of relativistic electron beam, 19: 41920
ZHIVOPISTSEV, F. A., Correlation effects of nuclear reactions at ground state, 19: 41814
ZHUKOV, M. F., Some correlations in investigation of electric arcs, 19: 41913
ZHUKOVSKAYA, A. S., Use of ethanol in isolating ^{22}Na from cyclotron targets, 19: 40637 (ORNL-tr-625)
ZHUKOVSKAYA, A. S., Use of ethanol in separation of sodium-22 from cyclotron target, 19: 40686
ZHURAVLEV, E. F., Solubility in $Ce(NO_3)_3$–$LiNO_3$–H_2O, 19: 40519
ZHURAVLEV, V. F., Experimental therapy of rabbits poisoned by tritium oxide, 19: 40340
ZHURAVLEV, V. F., Toxicity of tritium under experimental conditions, 19: 40337
ZICHICHI, A., High-intensity, partially separated, beam of antiprotons and K mesons, 19: 41184
ZIEGLER, A., Future development and future of D_2O pressure boiler reactors, 19: 42108
ZIESKE, P. L., Electron gun for plasma-oscillation studies, 19: 41946
ZIMMERMAN, R. L., Prog. rpt. on ion rocket engine development, 1–3/65, 19: 40765 (NP-15309)
ZIMMERMANN, W. Jr., Observation of stable superfluid circulation in liquid He II at level of 1, 2, and 3 quantum units, 19: 41620
ZING, He-sung, K-capture fraction of ^{66}Ge, ^{69}Ge, and ^{72}As, 19: 41800
ZINGERMAN, Ya. P., Investigation of interaction of oxygen with tungsten by electron-stimulated desorption, 19: 41103
ZOLOTOTRUBOV, I. M., Current distribution in a coaxial plasma gun, 19: 41859 (NP-15218)
ZUCKER, M. S., Studies of a repetitive liquid metal slug MHD generator, 19: 41314 (BNL-9329)
ZUK, W., Certain problems of mass spectroscopy and the spectroscopy of atomic nuclei, 19: 41243 (FTD-TT-64-1368)
ZUPANCIC, A. O., Creation rate of matter and the Heisenberg uncertainty principle, 19: 41227
ZURMUEHLE, R. W., A scattering chamber for charged particle work, 19: 40907
ZVEREV, B. L., X-ray studies of polyamide films cast from irradiated solutions, 19: 40595
ZWANZIGER, Daniel, Precession of relativistic particles of arbitrary spin in a slowly varying electromagnetic field, 19: 41423

SUBJECT INDEX

Main entries in this index are generally specific materials, things, and processes. These are followed by modifiers that describe the properties of, and processes applied to, the main entries.

The number preceding the colon is the *NSA* volume number, and the number following is the abstract number. The designation (R) following the abstract number indicates that the abstract is of a progress report; (P) indicates a patent; and (T) indicates a translation. Abstracts for reports other than progress reports carry no letter designation. References to report numbers, where appropriate, are included after the abstract number of the citation. Published literature (journal article or book) is identifiable by the absence of a report number.

The user should bear in mind that the ideas presented in the original literature, rather than key words, have been indexed. The indexers have tried to select what seemed the most probable and logical place to look for typical information. Since it is not possible to anticipate where a user would look for information, numerous cross references are included to assist him in his search.

Experience in using an index of this type will be the best guide in obtaining the desired information, and a consideration of synonymous or closely related terms will prove valuable.

Information must be so indexed as to be of the greatest use to the greatest number of users. This requires that a topic be indexed to headings that most specifically describe it and not ordinarily to the headings that describe its ultimate use, nor to the general class headings that include the specific headings. For example, information on the treatment of thyroid disease with I-131 would be indexed under Thyroid Diseases and under Iodine Isotopes I-131, but not necessarily under Radiotherapy. A study of the effects of x radiation on hair would be indexed under both X Radiation and Hair.

The broad, general class headings are used only for general information or for comprehensive reports or articles.

Subject Heading Styles

Generally, the direct form of subject entry is used rather than inverted headings or, in some cases, subheadings; e.g., Amino Acids rather than Acids, amino; Helium Isotopes He-4 rather than Helium — isotopes He-4 or Helium — He-4 isotopes. Note, however, that in some cases modifying terms are used parenthetically in preference to a more direct type of entry which would result in the scattering of information. Organic compounds, however, are usually entered in the index in the inverted form so that substituted compounds can be listed near the parent compound; e.g., Benzene, Bromo- rather than Bromobenzene. In general, the style of nomenclature used is that of *Chemical Abstracts*, except that some items listed in that publication as subheadings are elevated to form part of the main heading; e.g., Butyric Acid, Methyl Ester rather than Butyric Acid — methyl ester.

Alphabetization

Main headings are arranged according to the widely accepted word-by-word alphabetic system. A parenthetic qualifier following a main heading is disregarded in alphabetizing unless there are two or more headings identical except for the parenthetic qualifier, in which case the qualifier determines the order. Headings involving Greek letters are arranged as if the names of the letters were spelled out, e.g., Mesons (π), Mesons (ζ).

Nomenclature of Inorganic Compounds

Inorganic compounds are indexed in the direct form, listing cations in the order of increasing valence in the case of polycationic salts of varying valence and in alphabetic order for polycationic salts in which all cations have the same valence; e.g., Sodium Aluminum Silicates and Potassium Sodium Sulfates.

Multicomponent Systems

Multicomponent alloys, except well-known trade names, are indexed under each element in the alloy.

Example: Aluminum–Chromium Alloys are indexed

ALUMINUM ALLOYS
Al–Cr ...
CHROMIUM ALLOYS
Al–Cr ...

Well-known alloys such as Hastelloy are indexed directly. Cross references appear in the index cumulations. Multicomponent systems of elements are indexed similarly.

Example: Silicon–Tungsten Systems are indexed

SILICON SYSTEMS
Si–W ...
TUNGSTEN SYSTEMS
Si–W ...

Multicomponent systems of compounds are similarly indexed under the compound.

Physical States of Materials

Specification of the physical state of the material, if other than normal, is included in the modifying phrase.

Modifying Phrases (Subheadings)

Whenever it appears that such information would be useful, descriptive phrases (modifiers), rather than ordinary subheadings, are used under the main headings to give a better indication of the material covered in an abstract. Such phrases are written so that the idea considered most important is presented first. However, when using this index, the reader is advised to scan all modifiers under a main heading to determine whether any abstracts in addition to the most obvious should be consulted for the desired information. Many of the modifiers are designed to be read in inverted order or to be read with the main heading inserted at the position of the comma in order to obtain a meaningful phrase; e.g., Uranium–allotropic transformation temperatures of, effect of cooling rate on is read "effect of cooling rate on allotropic transformation temperatures of uranium." In many cases, the prepositions have been

omitted from such phrases provided no ambiguity results from the omission.

For entries concerned with physics, if the modifier does not indicate whether the reference is experimental or theoretical, a symbol E or T or E/T is given.

Conferences

Proceedings of conferences and conference papers are included in the Report Number Index.

A

ABSTRACTS
on fluid amplification, 19: 40739 (OTR-112)
on Shippingport Pressurized Water Reactor Project, 19: 42101 (WAPD-PWR-1606(Add.2))
on waste management research, 19: 42194 (NP-15267)
ACCELERATORS
beam bunch injector for, electron pulse length from, (T), 19: 41189
beam current integrators for positive-ion, (E), 19: 41183
beam motion in cyclic, stability of, (T), 19: 41187(T)
beam-injector pulser for, output parameters of, (E), 19: 41188
beams from, statistical problems of particle detection in, 19: 40885
cavity resonators for, magnetron performance for, 19: 41191
design and performance of negative-ion, (E), 19: 41182
diagnostic methods for periodic buncher, cavity, and coupler systems in, (E), 19: 41166 (ML-767)
ion injectors for, testing apparatus for, 19: 41192
magnetic field dispersion with double focusing beam in, sector, (T), 19: 41194
radiation monitoring system for, 19: 40924
ACCIDENTS
dosimetry of criticality, 19: 40800(R) (AERE-PR/HPM-7)
radioactivity recovery following reactor, (E), 19: 42006 (IDO-10043 (Vol.II)(Rev.1))
rescue basket for injured persons in canyons, 19: 42223 (UCRL-12006)
vehicle collisions, analysis of shipping container response to, 19: 40817 (SC-RR-65-98, pp 243-60)
ACETIC ACID
preparation of actinides and lanthanides from, by solvent extraction using amines, 19: 40657
ACETIC ACID, [(CARBOXYMETHYLIMINO)BIS(ETHYLENENITRILO)] TETRA-
effects on excretion of cerium-144 in rats, 19: 40347
effects on plutonium excretion in rats, 19: 40345
effects on plutonium excretion in rats, 19: 40346
solvent properties for rare earths, 19: 40696(P)
solvent properties for rare earths and transplutonium elements, 19: 40676
ACETIC ACID, (1,2-CYCLOHEXYLENEDINITRILO) TETRA-
solvent properties for rare earths, 19: 40696(P)
ACETIC ACID, (ETHYLENEDIAMINE) TETRA-
effects on excretion of cerium-144 in rats, 19: 40347
preparation of actinides and lanthanides from, by solvent extraction using amines, 19: 40657
solvent properties for rare earths, 19: 40696(P)
ACETIC ACID, (*N*-HYDROXYETHYLETHYLENEDIAMINE) TRI-
solvent properties for rare earths, 19: 40696(P)
ACETIC ACID, NITRILOTRI-
solvent properties for rare earths, 19: 40696(P)
ACETIC ACID, THIOBIS(ETHYLENENITRILO)TETRA-
effects on uranyl excretion and uranium poisoning in rats, 19: 40348
ACETIC ACID, TRIFLUORO-
isotopic exchange of deuterated with fluorimide, 19: 40537
ACETIC ACID, VINYL ESTER
determination in ethylene vinyl acetate copolymers by radiolysis and carbon monoxide yield, 19: 40556
ACETIC ACID, VINYL ESTER POLYMERS
with ethylene, radiolysis of, determination of vinyl acetate content by, 19: 40556
ACETONE
effects on ion exchange separation of rare earths using α-hydroxyisobutyric acid, 19: 40663
ACETONE, THENOYLTRIFLUORO-
benzene–thenoyltrifluoroacetone, solvent properties for transplutonic elements, 19: 40458 (JINR-P-2224)
carbon tetrachloride–thenoyltrifluoroacetone, solvent properties for uranyl salts, 19: 40682
ACETOPHENONE
energy transfer from triplet state of, to rare earth ions, 19: 40504
ACETYLENE
acetylene–air, electron and molecule temperatures in flames of, (E), 19: 41922
ACOUSTIC WAVES
emission in charged-particle interactions with piezodielectric crystals, (T), 19: 41990(T)
production in nonideal plasma, superheating instability from, (T), 19: 41925
propagation of infrasonic auroral, in atmosphere, 19: 41592
scattering by an impenetrable sphere, h-f, (T), 19: 41129
ACRYLONITRILES
radioinduced polymerization of, effect of electric field on, 19: 40582
ACTINIDES
reactions of, thermodynamics of electrode, 19: 40500
separation from irradiated fuel elements, 19: 40675
separation of transcurium elements, radiochemistry facility for, 19: 40719 (UCRL-7844-T)
ACTIVATION ANALYSIS
developments and standards in, techniques and facilities at National Bureau of Standards for, 19: 40450
methods for teeth, 19: 40435
sensitivity of, computer programs to optimize irradiation and decay times for, 19: 40451
substoichiometric separation procedures in, 19: 40424
ACTIVATION DETECTORS
analysis of aluminum–cobalt neutron flux monitor wires for cobalt, automated, 19: 40405 (CONF-650919-1)
design and performance of boron-11, for neutrons, (E), 19: 40867 (BNWL-64)
use for neutron flux measurements, design of multiplexer system for, 19: 40866 (AECL-2217)
use for neutron flux measurements, 19: 42148 (AECL-2216)
ADENINE
radiation effects on incorporation of carbon-14-labeled, in RNA in diploid yeast, 19: 40367
ADENOSINEPHOSPHORIC ACIDS
reactions of polyribonucleotides of, with cerium, lanthanum, and lutetium, 19: 40474
ADRENALINE
effects on blood pressure in rats, 19: 40360(T) (FTD-TT-65-48, pp 666)
ADVANCED EPITHERMAL THORIUM REACTOR
criticality studies, 19: 42077 (ANL-7014)
AERIAL SURVEYING
for radioactivity in western U. S., AEC techniques and results, 19: 40784 (RME-129(Rev.))
AEROSOLS
inhalation of radioactive, hazards of, 19: 40805 (NRS-30)
preparation and particle size of chromium-51-polystyrene, 19: 40800(R) (AERE-PR/HPM-7)
properties of radioactive, 19: 40800(R) (AERE-PR/HPM-7)
AGE ESTIMATION
ore deposit and volcanic rock, research program on, 19: 40778(R) (COO-689-50)
AIR
corrosive effects on chromium–magnesia composites, 19: 41022(R) (NP-15292)
cosmic-ray spectra in, analysis of high-energy, (E/T), 19: 41291
ionization in space vehicle hypersonic re-entry flight, effects of cesium and sodium contaminated cone materials on, 19: 41121 (N64-30658)
radioactive ions in, mobility spectra of small, 19: 40787
separation of krypton and xenon from, 19: 40695(P)
acetylene–air, electron and molecule temperatures in flames of, (E), 19: 41922
air–water, two-phase flow pressure drops in annular test section, 19: 40733(R) (GEAP-4863)
AIRCRAFT
instruments in, use of radioactive luminous paints in, 19: 40940 (NP-14924)
radiation hazards to passengers and crew of supersonic, galactic and solar cosmic, 19: 40842
ALANINE
metabolism in rat liver, tracer study, 19: 40308 (BNL-8379)
ALARM SYSTEMS
design of radiation, factors in, 19: 40804 (NP-14925)
ALASKA
fallout monitoring, 1959 to 1965, 19: 40780 (BNWL-SA-242)
ALBUMINS
preparation of iodine-131-labeled sterile pyrogene-free human serum, 19: 40639
separation of iodide from iodine-131-labeled, chromatographic, 19: 40656(T)
ALCOHOLS
reactions with recoil tritium atoms with and without benzene and cyclohexane, energy transfer in, 19: 40622
alcohol–cyclohexane, energy transfer processes in reactions with tritium recoil atoms, 19: 40622
alcohol–benzene, energy transfer processes in reactions with tritium recoil atoms, 19: 40622
ALGAE
genetic system for mutations of Chlamydomonas, nonchromosomal, 19: 42212 (NYO-3424-1)
ALKALI METAL HALIDES
electron inelastic scattering at 0.2 to 4 kev, (E/T), 19: 40502(T)

electron reactions with, secondary electron emission coefficients in, 19: 40503(T)
photoelectron emission from colored, mechanisms for, 19: 41979
radiation effects on electroluminescence of activated, uv and x, 19: 41981
radiation stability of crystals of, 19: 41975

ALKALI METAL HYDROXIDES
radiolysis of frozen solutions of, formation of solvated electrons in gamma, 19: 40551 (KFK-293)

ALKALI METAL NITRATES
radiolysis of, electron trapping in, 19: 40609

ALKALI METALS
solvent properties of pure, for pure transition metals, research program on, 19: 40946(R) (AI-65-93)
thermophysical properties of, research program on, 19: 41001(R) (AGN-8154)

ALKANES
alkane–TBP, performance as solvent in Purex Process, 19: 40646 (CONF-650918-2)

ALLOYS
book: *Thermal Radiative Properties*, 19: 41074
deformation twinning in, conference on, 19: 41076

ALLYL PHOSPHATES
sorptive properties of polymers of, for iron chlorides and lanthanum, neodymium, and uranyl nitrates, 19: 40668

ALPHA PARTICLES
angular distributions from aluminum-27, phosphorus-31, and sodium-23 (d,α) reactions at 9.3 Mev, (E), 19: 41684
detection and measurement of, design of proportional detector for, 19: 40834(R) (UCRL-14151)
effects on cadmium sulfide crystals, electron recombination processes in, 19: 40565
effects on gallium arsenide and silicon diodes, 19: 40937 (UCRL-11958)
emission from proton reactions with heavy nuclei at 157 Mev, (E), 19: 41831
emission in deuteron reactions (d,α) with calcium-40 and oxygen-16 at 15.14 Mev, selection rules from, (E), 19: 41720
energy spectra from helium-3 (He-3,α) reactions at 16 to 36 Mev, (E), 19: 41658 (IAE-655)
flux and rigidity spectra of solar, (T), 19: 41232
interactions with mesons (π), meson (π) form factors from, (T), 19: 41379
pathological effects on respiration in rats of, from inhaled plutonium-239 deposited in lungs, 19: 40380
pathological effects of, from injected plutonium-239 in dog bones, 19: 40382
reactions (α,n) with antimony-123, search for 2.6-hr iodine-126m in, 19: 41716
reactions (α,n) with potassium-41 and rubidium-87, isomeric cross section ratios for, (E), 19: 41820
reactions (α,p) with aluminum-27 at 5.8 to 8.6 Mev, cross-section fluctuations in, (E/T), 19: 41761
reactions (α,xn) with nuclei at threshold to 42 Mev, isomeric cross-section ratios from, (E), 19: 41695
reactions (α,xn) with nuclei, statistical model for isomeric ratios in, 19: 41696
reactions (α,xnyp) with iron-54 and -56, shell structure effects in nickel compound nuclei decay in, (T), 19: 41741
reactions (α,2p) with indium-115, angular momentum effects on isomeric cross section ratios in, (E), 19: 41821
reactions (α,3n) with barium-136 angular momentum effects on isomeric cross section ratios in, (E), 19: 41821
reactions with calcium, silver, and tellurium at 22 Mev, isomers from, (E), 19: 41802(T)
reactions with nuclear emulsions, effects of pH of impregnating solution on track length in, 19: 40597
reactions with thorium-232 at 20 to 40 Mev, yttrium-90, niobium-96, and lanthanum-140 yields from fission, (E), 19: 41779
scattering by cobalt-59 and manganese-55 at 43 Mev, inelastic, (E), 19: 41760
scattering by nickel-58 at 43 Mev, distorted-wave calculation of inelastic, 19: 41692

ALPHA SPECTROMETERS
design for determination of airborne radon-thoron daughters, 19: 40834(R) (UCRL-14151)

ALUMINUM
bonding to magnesium, zinc, and copper–magnesium alloy, hot-press, 19: 40949 (ISC-640)
cleaning of surfaces of, method for, 19: 42202 (HW-64483)
corrosive effects on tantalum at 800 to 1100°C, 19: 40961
corrosive effects on Inconel, niobium, and yttrium at 800 to 1100°C, 19: 40961
determination by spectrochemical methods, voltage-fluctuations patterns in, 19: 40416
dissolution in potassium or sodium hydroxide solutions, electrolytic, 19: 41086(P)
dissolution of tubes of, by mercuric sulfate–sulfuric acid in recirculation dissolver, 19: 40655 (RT/CHI(65)-1)
effects on manganese–molybdenum steel, 19: 41085(P)
electron transmission in foils of, low-energy, (E), 19: 41969 (ORNL-TM-1153)
fission fragment range distributions in, (E), 19: 41668 (KFK-306)
neutron reactions (n,γ) at 0.025 ev, spectra from, 19: 40896
neutron scattering in, excitation cross sections for, (E), 19: 41274
plasma pulse in, density, expansion velocity, and temperature of, (E), 19: 41878
positron annihilation in, angular correlations from, (E), 19: 41285
proton multiple scattering by thin films of, at 75 to 200 kev, (E/T), 19: 41273
proton spectra in, near surfaces, (T), 19: 41951 (N64-30510)
proton transmission in foils of, low-energy, (E), 19: 41969 (ORNL-TM-1153)
radiation damage rate in, effects of crystal defects and impurities on, 19: 40961
reactor criticality effects per atom, (E), 19: 42077 (ANL-7014)
thermodynamic properties at high pressures and temperatures, 19: 40459 (NP-15324)

ALUMINUM ACETATES
preparation and crystal structure of ammoniated, 19: 40507

ALUMINUM ALLOYS
analysis for niobium and tantalum, photometric method for, 19: 40442
cleaning of surfaces of, method for, 19: 42202 (HW-64483)
properties of weldments of cast-to-wrought, 19: 40989
welding of, 19: 40989
Al–Co, analysis of neutron flux monitor wires for cobalt, automated, 19: 40405 (CONF-650919-1)
Al–Cr–Fe–Y, corrosion by steam at 500 to 1300°C, 19: 40961
Al–Cr–Fe–Y, impact properties of, 19: 40961
Al–Mg, creep cavities in, nucleation of, 19: 41063
Al–Mo–Ti–Sn–Zr, mechanical properties of, effects of heat treatments on, 19: 41052
Al–Pu, criticality studies, 19: 42093 (GEAP-4912)
Al–Ti–Zr, effect of zirconium on lattice parameters of epsilon phase of, 19: 41053
Al–U, corrosive effects on tantalum at 800 to 1100°C, 19: 40961
Al–Zn, corrosion by aluminum–silicon and water of coatings of, on uranium, 19: 40949 (ISC-640)
Al–Zn, deposition on uranium, hot dip, 19: 40949 (ISC-640)

ALUMINUM ISOTOPES Al-27
alpha reactions (α,p) at 5.8 to 8.6 Mev, cross-section fluctuations in, (E/T), 19: 41761
deuteron reactions (d,α) at 9.3 Mev, differential cross sections for, (E), 19: 41684
energy levels of, properties of 4.403 Mev excited, (E), 19: 41775
proton binding energy in, measurement of, 19: 41660 (ISS-65/3)
proton inelastic scattering at 6.15 to 6.7 Mev, excitation functions for, (E), 19: 41813

ALUMINUM NITRATES
use in water purification, 19: 42130 (HW-68387)

ALUMINUM NITRIDES
compatibility with graphite–nitrogen environment at 1000 and 1200°C, 19: 40966 (BNWL-92)
effects on manganese–molybdenum steel, 19: 41085(P)

ALUMINUM OXIDES
bonding to niobium–1 zirconium of metallized, brazing alloy for, 19: 40980 (LA-3302)
coating with molybdenum or tungsten by chloride and oxide processes, evaluation of, 19: 40986
effects on oxidation resistance and strength of chromium–magnesia composites, 19: 41022(R) (NP-15292)
radiation effects on activities of activated solid, in acid catalyzed reactions, 19: 41099
sintering powders of, 19: 40995(P)
sorptive properties of surfaces of, for ions from aqueous solutions, 19: 42200 (COO-1354-5)
thermal conductivity of, evaluation of cut bar method for measuring, 19: 41029
thermal expansion coefficients parallel and normal to c axis, at 24 to 1100°C, 19: 41020 (NAA-SR-Memo-2987)
use as a diathermanous substance in thermal reactors, 19: 42065(P)
Al–Al_2O_3, photoelectric effect in tunnel junctions of, 19: 41124(R) (NP-15108)
Al–Al_2O_3–Sb, photoelectric effect in tunnel junctions of, 19: 41124(R)

(NP-15108)
Al_2O_3–Cr_2O_3, formation of refractories of, 19: 40997(P)
Al_2O_3–Nb_2O_5, phase studies, 19: 41049
Al_2O_3–PuO_2, phase studies, 19: 40958
Al_2O_3–SiO_2, radiation effects on activities in acid-catalyzed reactions, 19: 41099
Al_2O_3–SiO_2, sorptive properties of surfaces of, for ions from aqueous solutions, 19: 42200 (COO-1354-5)
Al_2O_3–Y_2O_3, bonding to niobium–1 zirconium, brazing alloy for, 19: 40980 (LA-3302)
ALUMINUM PHOSPHATES
$Al(PO_3)_3$–$LiPO_3$–$AgPO_3$, radio-photoluminescence polarization of glasses of, 19: 40588
ALUMINUM SYSTEMS
Al–Al_2O_3, photoelectric effect in tunnel junctions of, 19: 41124(R) (NP-15108)
Al–Al_2O_3–Sb, photoelectric effect in tunnel junctions of, 19: 41124(R) (NP-15108)
Al–Fe–Si–U, hot hardness and microstructure of, effects of heat treatments on, 19: 40958
Al–Fe–Si–U, properties of, effects of chromium and molybdenum on high-temperature, 19: 40958
Al–graphite, heat transfer from colloidal gas suspensions of, 19: 42127(R) (TID-22009)
Al–Si, corrosion by aluminum–silicon and water of coatings of, on uranium, 19: 40949 (ISC-640)
Al–Si–U, hot hardness and microstructure of, effects of heat treatments on, 19: 40958
ALUMS
effects of aluminum–potassium, on distortion in development of nuclear emulsions, 19: 40884
AMERICIUM
separation from aqueous solutions of organic acids by solvent extraction using high-molecular-weight amines, 19: 40657
separation from rare earths by solvent extraction using DTPA, 19: 40676
solvent extraction by thenoyltrifluoroacetone in benzene, 19: 40458 (JINR-P-2224)
AMERICIUM COMPLEXES
with lactic acid, stability constants, 19: 40458 (JINR-P-2224)
AMERICIUM ISOTOPES Am-246
gamma spectra of, (E), 19: 41794
AMIDE POLYMERS
radiation effects on, gamma, 19: 40595
AMINES
separation by ligand exchange on cation exchangers, 19: 40647 (COO-499-1)
solvent properties for rare earths in sulfate solutions, 19: 40696(P)
solvent properties of high-molecular-weight, for actinides and lanthanides, 19: 40657
solvent properties for uranium in hydrofluoric acid-nitric acid solutions, 19: 40684
AMINO ACIDS
reactions with tritium recoil atoms, yields in, 19: 40629
AMMINES
complexes with copper, electron spin resonance spectra, 19: 40465 (UCRL-16175)
AMMONIA
determination in heavy water moderator, automated, 19: 40406 (CONF-650919-2)
deuterium exchange with hydrogen, heavy water production by, 19: 40942(P)
radiolysis of, effects of physical variables on yields from, 19: 40547(R) (AGN-8137(Vol. I))
reactions with tantalum pentoxide to prepare red tantalum nitride, 19: 40472
NH_3–H_2, effects of ratio of, on nitrogen solubility in stainless steel, 19: 40968(R) (EURAEC-1424)
AMMONIUM ACETATES
solvent properties for europium and yttrium, 19: 40680
AMMONIUM THIOCYANATES
NH_4SCN–methanol–H_2O, distribution coefficients of metals in, 19: 40447
AMPLIFIERS
circuitry design for, for use in semiconductor detectors, (E), 19: 40899
efficiency of plasma microwave frequency, (E), 19: 40860
review of fluid, 19: 40739 (ORT-112)
stabilization of scintillation-detector, reference light pulse for, 19: 40870 (IAE-695)
AMYL ALCOHOL
reactions with tritium recoil atoms, with and without benzene and cyclohexane, energy transfer in, 19: 40622
ANALYSIS
equipment for relative abundance, of mixtures, 19: 40454(P)
ANILINE
radiolysis of, ESR of radicals in, 19: 40607
trimethyl-, radiolysis of, ESR of radicals in, 19: 40607
aniline-indole, labeled yields in reactions with carbon-14 recoil atoms, 19: 40627
aniline–picoline, labeled yields in reactions with carbon-14 recoil atoms, 19: 40627
ANIMAL CELLS
excitation of membranes of, physical mechanisms for, 19: 42212 (NYO-3424-1)
material transfer across membranes of, biological model of, 19: 42199 (BNL-8397)
radiation effects on rabbit, biochemical, 19: 40375
ANIMAL RESPIRATION
effects of inhaled plutonium-239 on, in rats, 19: 40380
radiation effects on, synergistic effects of stress induced by vibration, 19: 40354(T) (FTD-TT-65-48, pp 38–9)
ANIMALS
radiation effects on physiology of thyroid gland in, tracer study, 19: 40374
ANION EXCHANGE MATERIALS
conversion of highly basic AV-17 and AM from chloride to hydroxyl form, 19: 40456 (IAE-713)
ANISOLE
radiolysis of, ESR of radicals in, 19: 40607
ANTENNAS
conference, 19: 40862
impedance behavior in plasma, 19: 41212
ANTIMONY
determination in copper by activation, 19: 40422
positron annihilation in, angular correlations from, (E), 19: 41285
separation from uranium by chromatography on cellulose columns, tracer studies, 19: 40687
ANTIMONY ALLOYS
Sb–In, radiation effects on, gamma, 19: 41096
Sb–Na, electric conductivity of Na_3Sb, temperature dependence of, 19: 41124(R) (NP-15108)
ANTIMONY ISOTOPES Sb-123
alpha reactions (α,n) with, search for 2.6-hr iodine-126m in, 19: 41716
ANTIMONY ISOTOPES Sb-124
content in northern stratosphere, 1962-63, 19: 40785 (TID-21224)
metabolism in rats of, after intravenous or oral administration, 19: 40318
ANTIMONY ISOTOPES Sb-125
content in northern stratosphere, 1962-63, 19: 40785 (TID-21224)
gamma transitions in, lifetime and intensities of I-forbidden M1, (E), 19: 41836
ANTIMONY ISOTOPES Sb-127
range distributions of fission fragments of, in aluminum, (E), 19: 41668 (KFK-306)
ANTIMONY SYSTEMS
Al–Al_2O_3–Sb, photoelectric effect in tunnel junctions of, 19: 41124(R) (NP-15108)
ANTINEUTRINOS
interactions with electrons, differential and total cross sections for, (T), 19: 41481(T)
ANTINEUTRONS
beta decay of moving longitudinally polarized free, angular distributions from, (T), 19: 41496
ANTINUCLEONS
interactions with nucleons at rest, U(12) predictions for four-meson production in annihilation, (T), 19: 41463
ANTIPROTON BEAMS
production of high-intensity, using CERN PS, 19: 41184
ANTIPROTONS
interactions with protons, annihilation at rest, (E), 19: 41325 (CU-1932-245)
interactions with neutrons at 1.96 Bev/c, $\bar{N}^*$ production in, (E), 19: 41438
interactions with neutrons, intermediate vector boson production in, (T), 19: 41484(T)
interactions with protons at high energies, forward amplitudes for, (T), 19: 41376
ARCHAEOLOGICAL SPECIMENS
age estimation using carbon-14, 19: 40795
ARGON
charged-particle stopping power and straggling in, excitation energy for, (T), 19: 41268
content in amphoteric meteorites, (E), 19: 41225
electric discharges in torch of, effect of pressure on high-frequency, (E), 19: 41875
flow of partially ionized, laminar, (T), 19: 40749

neon ion collisions with atoms of, inelastic energy loss in, (E), 19: 41277
plasma surface waves in, non-quasistatic, (E), 19: 41942
proton collisions with atoms of, inelastic energy loss in, (E), 19: 41277
radioinduced polymerization of, with vinyl chloride and, 19: 40584
shock propagation in, properties of, 19: 41128 (UCRL-12466)

ARGON IONS
reactions with deuterium and hydrogen molecules, spectra of ArD^+ and ArH^+ in, (E), 19: 41251
reactions with germanium at 10 ev to 1 kev, electron diffraction studies of, 19: 41258
reactions with iron, oxidation mechanisms following, 19: 40973
reactions with molybdenum and tungsten surfaces, electron injection in, (E), 19: 41272(T)
sputtering on quartz and pyrex, silicon oxide yield from, (E), 19: 41257
sputtering on silver at 160 to 200 ev, angular distributions from, 19: 41259

ARGON ISOTOPES Ar-40
reactions with nuclei at 5 to 12 Mev, neutron spectra from, (E), 19: 41810(T)

ARGON SYSTEMS
Ar–Hg, photon emission by atoms in plasma of, (E), 19: 41891(T)
Ar–Kr, electron reactions at 50 kev, luminescence from, (E), 19: 41246
Ar–Xe, electron reactions at 50 kev, luminescence from, (E), 19: 41246

ARGONAUT REACTOR
core configuration for, properties of ring, 19: 42187
neutron flux distribution and transfer function of, with two-slab-loading, 19: 42182

ARIZONA
ore deposits and volcanic rocks of, geological studies of, 19: 40778(R) (COO-689-50)

ARKANSAS
fallout content of rain at Fayetteville, 19: 40785 (TID-21224)

ARMY REACTORS
design of multipurpose portable, 19: 42115

ARSENAZO III
analytical uses of derivatives of, 19: 40426

ARSENIC
determination in copper by activation, 19: 40422

ARSENIC ISOTOPES As-71
decay of, probability ratio of electron-capture, 19: 41800(T)

ARSENIC ISOTOPES As-72
decay of, probability ratio of electron-capture, 19: 41800(T)

ARSENIC ISOTOPES As-74
use for determining hydrogen atoms in upper atmosphere, 19: 40433

ASCORBIC ACID
radiation effects on content in *Momordica charantia* seeds, 19: 40371

ASPHALT
asphaltine–benzene–hexafluorobenzene–carbon disulfide, differential dynamic polarization of fluorine and hydrogen nuclei in, (E), 19: 40497
asphaltine–benzene-d_6–hexafluorobenzene–carbon disulfide, differential dynamic polarization of fluorine and hydrogen nuclei in, (E), 19: 40497
asphaltine–α,α,α–trifluorotoluene–carbon disulfide, differential dynamic polarization of fluorine and hydrogen nuclei in, (E), 19: 40497

ASTROPHYSICS
bibliography on nuclear, 19: 41207 (NEIC-RR-9)
element formation mechanisms in stars, (T), 19: 41235
flare activity of nearby stars, (E), 19: 41203 (AD-600154)
temperature distributions in partially degenerate helium cores in stars, neutrino loss effects on, (T), 19: 41237

ATHEROSCLEROSIS
coronary, tracer study of lipid metabolism using iodine-131-peanut oil, 19: 40393

ATMOSPHERE
airglow in, research on, 19: 41576(T) (N64-21876)
analysis for iodine, development of sampling method for, 19: 40402 (BMI-X-10137)
analysis for sulfur dioxide, 19: 40410 (ORNL-P-494)
carbon-14 content and diffusion in, 19: 40797
conference on upper, 19: 41605
cosmic-nucleon nuclear reactions in, showers from, (T), 19: 41300
electron removal from, methods for, (T), 19: 41569 (AD-426145)
electron stopping by oxygen in, due to rotational excitation, (T), 19: 41599
electron stopping by nitrogen in, due to rotational excitation, (T), 19: 41600
fallout particles in upper, 19: 40783 (NP-15327)
hydrogen content in upper, radiometric method for determining, 19: 40433
hydrogen distribution in, effect of thermal escape on, (T), 19: 41604
infrasonic-wave propagation in, from aurorae, 19: 41592
neutron albedo flux from, (E), 19: 41606
neutron flux at aircraft altitudes in, anomalous increases in, (E), 19: 41579
particle dispersion and sedimentation in upper, 19: 41112 (SC-DC-65-1312)
radioactivity in, over Japan, 19: 40792
radioactivity to 3.6 km, natural, 19: 40790
structure of planetary, errors in space vehicle acceleration measurements of, (T), 19: 41123 (NASA-TR-R-225)

ATOMIC BEAMS
review of studies involving, 19: 41143

ATOMIC ENERGY
activities in India, 19: 42209(R) (NP-15356)

ATOMIC ENERGY COMMISSION
airborne radiometric surveying in western U. S., techniques and results, 19: 40784 (RME-129(Rev.))

ATOMIC EXPLOSIONS
biological effects on populations of Hiroshima and Nagasaki, 19: 40361(T) (ORNL-tr-437)
chemical applications of underground, research program on, 19: 40706 (ORNL-TM-1191)
craters produced by, data compilation on dimensions of, 19: 40711 (SC-RR-65-220)
energy liberation of, device for measuring, 19: 40850(T) (ORNL-tr-588)
fallout from in-air, theory, 19: 40782 (NP-15325)
gamma emission in, electromagnetic effects in metal slabs, 19: 41956 (SC-R-65-933)
ground shock spectra from Gnome event, 19: 40713 (VUF-2401)
radiation doses from, gamma and neutron, (T), 19: 40938
radiation monitoring of, equipment for remote, 19: 40876 (NVO-162-5 (Rev.))
rock crushing by, for manufacture of aggregate and riprap, 19: 40709 (PNE-5003)
seismic wave travel times from central Pacific, 19: 40779
thermal radiation from, detectors for, (E), 19: 40882 (USNRDL-TR-839)
uses of, engineering, 19: 40710 (SC-DC-65-1485)

ATOMIC STRUCTURE
molecular-beam uses in study of, 19: 41143

ATOMS
book: *Atomic Theory of Gas Dynamics*, 19: 41161
book: *The Theory of Electron-Atom Collisions*, 19: 41282(T)
electron excitation of neutral, cross sections for, (T), 19: 41254
interactions with light beams, (T), 19: 41248
ionization cross sections of metallic, measurement by electron impact, (E), 19: 41276
motion and position in crystals, 19: 41966 (LA-3310)
radiation absorption and scattering by, coherent, (T), 19: 41247
reactions with atoms in structureless media, slowing-down spectra of, (T), 19: 41261
x-ray yields from L_2 and L_3 shells of, approximation formulas for, (T), 19: 41245

AUGER ELECTRONS
ejection from silver during helium ion scattering, (T), 19: 41270

AURORAL STORMS
infrasonic waves from, periodicity and waveform of, 19: 41592
intensity variations of, correlation with terrestrial electromagnetic field oscillations, 19: 41575(T) (FTD-TT-65-112)
properties of, research on, 19: 41576(T) (N64-21876)

AUTORADIOGRAPHY
design of drying box for, 19: 40304

AVR REACTOR
design of, review of pebble bed concept for, 19: 42082 (CONF-650633-1)

AZOBENZENE
radiolysis of, ESR of radicals in, 19: 40607

B

BARIUM
separation from uranium by chromatography on cellulose columns, tracer studies of, 19: 40687

BARIUM ALLOYS
Ba–Ru, process for improving workability of, 19: 40999(P)

BARIUM FLUORIDES
luminescence centers in rare-earth activated, 19: 41978

BARIUM ISOTOPES Ba-136
alpha reactions (α,3n) to 42 Mev, isomeric ratios from, (E), 19: 41695
alpha reactions (α,3n), statistical model for isomeric ratios in, 19: 41696
alpha reactions (α,3n), angular momentum effects on isomeric cross section ratios in, (E), 19: 41821

BARIUM ISOTOPES Ba-139
range distributions of fission fragments of, in aluminum, (E), 19: 41668

(KFK-306)
BARIUM ISOTOPES Ba-140
content in rain at Fayetteville, Arkansas, 19: 40785 (TID-21224)
determination in uranium fission products, 19: 40640
range distributions of fission fragments of, in aluminum, (E), 19: 41668 (KFK-306)
BARIUM OXIDES
content in McKelveyite uranium mineral, 19: 40799
thermionic emission, 19: 41124(R) (NP-15108)
$BaO-B_2O_3$, emission spectra of cerium- and samarium-activated phosphors of, 19: 40494(T)
BARYONS
bootstrap model for, reciprocal, (T), 19: 41422
bootstrap model of, self-consistent particle sets in, (T), 19: 41432
interactions with mesons, long-range forces in, (T), 19: 41421
interactions with mesons, bootstrap model in SU(6) for, 19: 41443
interactions with pseudoscalar mesons, second-order perturbation in U(12) for, (T), 19: 41444
interactions with mesons, $SU(6)_w$ for amplitudes of, (T), 19: 41462
interactions with mesons, evaluation of crossing matrices for, (T), 19: 41381
interactions with mesons, SU(4) symmetry for coupling constants in, 19: 41397
interactions with mesons (η), (T), 19: 41433
mass differences of octet, effects on pseudoscalar-meson octet mass splitting, 19: 41468
mass formula for, (T), 19: 41424
mass splittings of octet, quartet and triplet SU(3) models for, 19: 41476
model for low-lying, double SU(3) symmetry in three-triplet quark, 19: 41406
properties of, composite, (T), 19: 41519
quantum numbers for multiplet components of, 19: 41331 (JINR-P-2219)
structure of, internal, 19: 41478
symmetries of, electromagnetic mass splitting in SU(6), 19: 41329 (JINR-P-2208)
symmetry group for, mass spectra and selection rules in, (T), 19: 41362
theory of, unified, 19: 41431
BARYONS, RESONANCE
decay of N* and Y*, SU(6) symmetry for partial width of, (T), 19: 41515
decay of SU(3) decuplet, broken symmetric couplings in baryon-pseudoscalar, 19: 41399
electromagnetic properties of N*, SU(4) symmetry for, 19: 41397
model for N* (1480), Y_8^* (1405), Y_8^* (1600), Y_8^* (1660), and Ξ^* (1810), SU(3) quark, (T), 19: 41477
models for, quasi-molecular rotator, 19: 41524
production in neutrino-nucleon interactions, (T), 19: 41754
production of N*, in antiproton-neutron interactions at 1.96 Bev/c, (E), 19: 41438
production of (Y_1^*), in meson (K⁻)-neutron interactions, (T), 19: 41405
production of $Y\pi$, in meson (π^+)-proton interactions at 2.35 to 2.90 Bev/c, (E), 19: 41418
production of Y^* (1385) and Y^* (1660) in π^-p interactions at 7.5 Bev/c, (T), 19: 41488(T)
properties of $Y_0^*(1661)$, $Y_0^*(1662)$, and $Y_1^*(1660)$, (T), 19: 41384
quark model for SU(3) second-octet and singlet, 19: 41477
Regge pole contributions of Y_1^* and Y_0^* to meson (K)–nucleon scattering amplitude, (T), 19: 41352
BEARINGS
design and testing of potassium-lubricated journal and thrust, 19: 40716(R) (NP-15280)
design of gas-lubricated thrust, for high-speed rotors, 19: 40736 (NYO-2512-1)
testing liquid-metal-lubricated, equipment design for, 19: 40716(R) (NP-15280)
BELGIAN REACTOR-2
fuel plate temperature measurement in, 19: 42181
BELLOWS
stress analysis, 19: 42208 (NAA-SR-4527(Pt.II))
BENTONITES
effects on fast neutron radioinduced swelling in beryllia, 19: 40959
BENZALDEHYDE
radiolysis of, ESR of radicals in, 19: 40607
BENZENE
radiation effects on photoconductivity of, electron, 19: 40601(T)
radiolysis of, ESR of radicals in, 19: 40607
radiolysis of, G-values of products in, (E), 19: 40370
reactions with recoil carbon-11, 19: 40550 (IS-T-27)
reactions with tritium recoil atoms, abstraction and substitution in, 19: 40621
alcohol–benzene, energy transfer processes in reactions with tritium recoil atoms, 19: 40622
asphaltine–benzene–hexafluorobenzene–carbon disulfide, differential dynamic polarization of fluorine and hydrogen nuclei in, (E), 19: 40497
asphaltine–benzene-d_6–hexafluorobenzene–carbon disulfide, differential dynamic polarization of fluorine and hydrogen nuclei in, (E), 19: 40497
benzene–CCl_4, formation of polymeric yields in reactions with carbon-14 and sulfur-35 recoil atoms, 19: 40628
benzene–diphenylpicrylhydrazyl–hexafluorobenzene, differential dynamic polarization of fluorine and hydrogen nuclei in, (E), 19: 40497
benzene-d_6–hexafluorobenzene–diphenylpicrylhydrazyl, differential dynamic polarization of fluorine and hydrogen nuclei in, (E), 19: 40497
benzene–thenoyltrifluoroacetone, solvent properties for transplutonic elements, 19: 40458 (JINR-P-2224)
BENZENE, BROMO-
radiation effects on, thermal annealing of neutron, 19: 40576
Br–bromobenzene–bromoethane, neutron radiation effects on labeled organic retentions in, 19: 40624
BENZENE, BUTYL-
radiolysis of, ESR of radicals in, 19: 40607
BENZENE, CHLORO-
radiolysis of, ESR of radicals in, 19: 40607
BENZENE, *o*-DIETHOXY-
dielectric polarization in decalin, temperature dependence, 19: 40468(T) (SC-T-65-721)
BENZENE, DIFLUORO-
difluorobenzene–diphenylpicrylhydrazyl, differential dynamic polarization of fluorine and hydrogen nuclei in, (E), 19: 40497
BENZENE, HEXAFLUORO-
asphaltine–benzene-d_6–hexafluorobenzene–carbon disulfide, differential dynamic polarization of fluorine and hydrogen nuclei in, (E), 19: 40497
asphaltine–benzene–hexafluorobenzene–carbon disulfide, differential dynamic polarization of fluorine and hydrogen nuclei in, (E), 19: 40497
benzene–diphenylpicrylhydrazyl–hexafluorobenzene, differential dynamic polarization of fluorine and hydrogen nuclei in, (E), 19: 40497
benzene-d_6–hexafluorobenzene–diphenylpicrylhydrazyl, differential dynamic polarization of fluorine and hydrogen nuclei in, (E), 19: 40497
BENZENE, NITRO-
radiolysis of, ESR of radicals in, 19: 40607
BENZOIC ACID
radiolysis of, ESR of radicals in, 19: 40607
BENZOIC ACID, BENZYL ESTER
dielectric polarization in decalin, temperature dependence, 19: 40468(T) (SC-T-65-721)
BENZYL ALCOHOL
radiolysis of, ESR of radicals in, 19: 40607
BENZYLAMINE
synthesis of alkylated secondary, 19: 40540 (RT/CHI(64)16)
BERKELIUM
separation from rare earths by solvent extraction using DTPA, 19: 40676
BERYLLIUM
analysis for carbon, nitrogen, and oxygen surface contamination, by activation methods, 19: 40453
effects on properties of tantalum, 19: 41067
electron and ion emission from cesiated and vacuum surfaces of, (E), 19: 41284
electron band structure of, augmented plane wave calculations for, 19: 41968(R) (MIT-QPR-57, pp 22-42)
fabrication, 19: 40959
powder metallurgy, 19: 40959
proton reactions at 20 Bev, production of antiprotons, mesons, and protons in, 19: 41324 (CERN-65-14)
purification, 19: 40959
thermal conductivity of, evaluation of cut bar method for measuring, 19: 41029
BERYLLIUM ACETATES
preparation and crystal structure of ammoniated, 19: 40507
BERYLLIUM ALLOYS
Be–Cu, surface cleaning of, procedure for, 19: 40989
Be–La, vaporization of $LaBe_{13}$, 19: 40959
Be–Ti–Zr, brazing alloy for alumina-to-niobium alloy seals, 19: 40980 (LA-3302)
Be–Y, vaporization of YBe_{13}, 19: 40959
Be–Zr, phase studies and thermodynamics of intermetallic compounds in, 19: 41078
BERYLLIUM ISOTOPES Be-6
energy levels from helium-4 (He-3,n) reactions, first-excited, (E), 19: 41659 (IAE-835)
BERYLLIUM ISOTOPES Be-7
angular distributions and energy spectra from carbon-12 (He-3,Be-7) reactions at 29.4 Mev, (E), 19: 41733
BERYLLIUM ISOTOPES Be-9
electron elastic scattering by magnetic moments of, shell model for high-

energy, 19: 41694
electron scattering at 70 to 250 Mev, discrete and continuum states from, (E/T), 19: 41683
energy levels from lithium-7 (d,γ) reactions at 340 to 780 kev, (E), 19: 41697
BERYLLIUM NITRATES
solvent properties of solutions of, for lanthanum fluorides, 19: 40670
BERYLLIUM OXIDES
compressibility of, volume, (E), 19: 41984
hardness of, effects of crystal orientation on, 19: 41087 (AAEC/E-135)
radiation effects on modulus-of-rupture of, fast neutron, 19: 40959
radiation effects on hardness of, neutron, 19: 41087 (AAEC/E-135)
radioinduced swelling in, fast neutron, 19: 40959
radioinduced swelling in, effects of bentonite additives on fast neutron, 19: 40959
sintering powders of, 19: 40995(P)
thermal conductivity of, evaluation of cut bar method for measuring, 19: 41029
use as a diathermanous substance in thermal reactors, 19: 42065(P)
$BeO-B_2O_3$, emission spectra of cerium- and samarium-activated phosphors of, 19: 40494(T)
BeO–Pu, neutron cross sections for dispersions of, effects of grain structure on, (T), 19: 42041 (GA-6286)
$BeO-PuO_2$, phase studies, 19: 40958
$BeO-ThO_2$, phase studies, 19: 40958
BERYLLIUM SYSTEMS
Be–C–U, phase studies, 19: 40958
BETA DECAY
theory of Goldberger-Treiman relations in, 19: 41774
BETA PARTICLES
detection and measurement of, design of proportional detector for, 19: 40834(R) (UCRL-14151)
detection and measurement using Geiger counters, (E), 19: 40903
detection and measurement using Pilot B plastic scintillation counters, (E), 19: 40916
detection and measurement of low-energy, using liquid scintillation counters, 19: 40425
detection and measurement in biological materials, liquid scintillation, 19: 40436
detection and measurement of, from tritium decay, 19: 40638
dose from spherical radionuclide particles, calculational models for, 19: 40635 (NUS-217)
effects of activities of solid acidic catalysts, 19: 41099
effects on heating in fast reactor plutonium fuel, (E), 19: 42114
effects on hydrogenation of coal extract and aromatic compounds, catalytic, 19: 40553(R) (NYO-2978-34)
effects on pancreatic function and structure, 19: 40358(T) (FTD-TT-65-48, pp 577–8)
effects on tritiated thymidine in aqueous solutions at 0 to –75°C, 19: 40583
neurological effects of small doses of, in dogs, 19: 40356(T) (FTD-TT-65-48, pp 469–70)
spectra in decay of iodine-132, 19: 41744
BETA SOURCES
design as hydrogenation catalyst at high pressures and temperatures, 19: 40553(R) (NYO-2978-34)
fabrication and uses of planar isotopic, (E), 19: 40560
radioactivity of, carbon dioxide-filled proportional detector for measuring, 19: 40920
BETA SPECTROMETERS
characteristics of Moellenstedt velocity analyzer, (E), 19: 40883
performance of double-focusing magnetic, (E), 19: 40904
BETATRONS
bremsstrahlung-beam intensity optimization in, automatic device for, (E/T), 19: 41199
radioactivity induced in collimator of 31-Mev, 19: 41169 (NYO-3364-7)
therapeutic use of, radioactivity induced in patients during, 19: 40392 (NYO-3364-6)
BEVERAGES
strontium-90 content in Australian tea, 19: 40805 (NRS-30)
BIBLIOGRAPHIES
on analytical chemistry of rare earths, (E), 19: 40448
on analytical chemistry of rare earths, 19: 40449
on crystal chemistry of rare earth oxides, 19: 40533
on crystal chemistry of rare earth aluminates, sesquioxides, and silicates, 19: 40535
on fissiochemical processes, 19: 40547(R) (AGN-8137(Vol.I))
on fluid amplification, 19: 40739 (OTR-112)
on fouling research, 19: 40971 (RT/CHI(65)20)
on geochemistry of rare earths, 19: 40793
on Mk III maritime nuclear steam generator, 19: 42133 (GEMP-340)
on Mössbauer effect in biological materials, 19: 40306
on nuclear astrophysics, 19: 41207 (NEIC-RR-9)
on phase equilibria in rare earth oxide–oxide mixtures, 19: 40534
on properties of inorganic and organic rare-earth compounds, (E), 19: 40400
on properties of thorium and its alloys and compounds, 19: 41025 (ORNL-TM-1144)
on radiation processing of food, 19: 40941 (SB-403(Suppl.1)(Rev.))
on radiation protection, 19: 40801 (ANL-6991)
on rare earth separation from raw materials, 19: 40690
on rare earth separation by ion exchange, 19: 40691
on rare earth separation by organophosphorus extractants, 19: 40693
on solution chemistry of rare earths, 19: 40531
on Soviet studies of rare earth complexes, 19: 40532
on thermal resistance of contacting surfaces, 19: 40744 (UCRL-14264)
on uses of rare earths, 19: 40401
on waste management research, 19: 42194 (NP-15267)
BIOLOGICAL MATERIALS
analysis for carbon-14, iodine-131, phosphorus-32, sulfur-35, and tritium by beta counting, 19: 40425
analysis for carbon-14, 19: 40436
analysis for strontium, spectrographic, 19: 40309(R) (NP-15180)
analysis for vanadium by neutron activation methods, 19: 40421
Mössbauer effect in, uses of, 19: 40306
BIOLOGICAL MODELS
of material transfer across cell membranes, 19: 42199 (BNL-8397)
BIOLOGICAL STRESS
effects of, due to pain stimulation, on blood pressure in rats, 19: 40360(T) (FTD-TT-65-48, pp 666)
effects on response of rats to low doses of plutonium-239, 19: 40338
induced by vibration, effects on radiosensitivity of rats and guinea pigs, 19: 40354(T) (FTD-TT-65-48, pp 38–9)
BIOLOGICAL SYSTEMS
radiation effects in, delayed, 19: 40352 (WASH-1059)
BIOMETRY
tissue current-to-dose conversion factors for depth-dose measurements of nucleons below 400 Mev, 19: 40372
BIOPHYSICS
lectures on, 19: 42212 (NYO-3424-1)
BIPHENYL
radiation effects on photoconductivity of, electron, 19: 40601(T)
radioinduced hydrogenation of, beta, 19: 40553(R) (NYO-2978-34)
radioinduced thermoluminescence of, gamma, 19: 40563
BIPYRIDINES
complexes with rare earth acetates, chlorides, nitrides, and thiocyanates, preparation and properties, 19: 40487
BISMUTH
determination in copper by activation, 19: 40422
neutron scattering in, excitation cross sections for, (E), 19: 41274
positron annihilation in, angular correlations from, (E), 19: 41285
proton reactions at 157 Mev, nucleon clustering from, (E), 19: 41831
thermodynamic properties at high pressures and temperatures, 19: 40459 (NP-15324)
BISMUTH ALLOYS
Bi–Ru, process for improving workability of, 19: 40999(P)
BISMUTH ISOTOPES Bi-209
gamma reactions (γ,n) at 12 to 16 Mev, spectra from, (E), 19: 41834
neutron reactions (n,n'γ) at 2.5 to 4.1 Mev, gamma spectra from, (E), 19: 41669 (LA-DC-7096)
BISMUTH ISOTOPES Bi-212
decay of, branching ratio of alpha and beta, (E), 19: 41798
BLAST EFFECTS
on contents of buried shelters, 19: 40758 (AD-426249)
BLOOD
cesium content in human, 19: 40781(R) (NP-15179)
cesium-137 content in human, relation to body content, 19: 40781(R) (NP-15179)
plutonium-239 effects on oxygen content of, in rats, 19: 40380
radiation effects on lipid content in rat, effects of unitol on, 19: 40386(T) (FTD-TT-65-48, pp 661–2)
radiation effects on cholesterol content in rat, effects of unitol on, 19: 40386(T) (FTD-TT-65-48, pp 661–2)
strontium-90 content in rat, after intratracheal administration, 19: 40312
BLOOD PICTURE
effects of low doses of plutonium-239 in, effects of additional biological stresses on, 19: 40338
BLOOD PLASMA
radiation effects on pepsinogen content of, in rats, 19: 40363
BLOOD PLASMA SUBSTITUTES
therapeutic effects for radiation sickness in dogs, synergistic effects of butyl alcohol, vitamin B_{12}, and antibiotic therapy in dogs,

19: 40387
BLOOD PRESSURE
radiation effects on, in rats, 19: 40360(T) (FTD-TT-65-48, pp 666)
BLOOD SERUM
radiation effects on protein metabolism in, effects of bone marrow injections, 19: 40385(T) (FTD-TT-65-48, pp 134–5)
BLOWERS
seal test for NMPO shaft, 19: 40701 (TID-22007)
BODY WATER
radiation effects on, in rats, 19: 40369
BOILERS
design of Mk III maritime nuclear, 19: 42133 (GEMP-340)
developments in nuclear, 19: 42123
fabrication for MZFR, 19: 42173
BOILING
detection in metals and salts by ultrasonics, 19: 40847(R) (NYO-2910-11)
heat transfer at 300 psi, effects of electric fields on, 19: 40736(R) (NYO-2404-5)
heat transfer in liquid metals, research program on high-acceleration-field, 19: 40741(R) (SAN-409-23)
BOILING REACTOR EXPERIMENTS
operating experience with central-superheat core CSH-1 in Borax-V, (E), 19: 42149 (ANL-6961)
BOILING REACTORS
design using boiling coolant and fuel, 19: 42069(P)
BONE MARROW
protective effects against radiation injuries in dogs of injections of, 19: 40385(T) (FTD-TT-65-48, pp 134–5)
BONE TUMORS
radioinduced by injected plutonium-239, in dogs, 19: 40382
BONES
calcium content of human, 19: 40781(R) (NP-15179)
radium-224 content in rat, after intravenous injection, 19: 40315
strontium content of human, 19: 40781(R) (NP-15179)
strontium content in human rib, spectrographic method for determining, 19: 40309(R) (NP-15180)
strontium-89 metabolism in rat, effects of complexing agents on, 19: 40344
strontium-90 content in rat, after intratracheal administration, 19: 40312
BORATES
spectra of cerium- and samarium-activated, emission, 19: 40494(T)
BORIC ACID
determination in water, automated colorimetric, 19: 40404 (BNWL-SA-167)
BORON
reactivity worths of, reactor oscillator for measurement of, 19: 42050 (NAA-SR-11368)
reactor control using, chemical shim, 19: 42023
spectra of atomic, in plasma jets, (E), 19: 41287
BORON CARBIDES
compatibility with nickel at 1200°C, 19: 40966 (BNWL-92)
B_4C–UO_2, thermal testing for use as fuel, 19: 41006(R) (CEND-3107-238)
BORON ISOTOPES B-10
effects on infrared spectrum and molecular structure of trimethyl borate, 19: 40470
energy levels of, lifetimes of, (E), 19: 41758
exchange equilibrium with boron-11, 19: 40505
reactivity worths of, reactor oscillator for measurement of, 19: 42050 (NAA-SR-11368)
reactor criticality effects per atom, (E), 19: 42077 (ANL-7014)
BORON ISOTOPES B-11
deuteron reactions (d,n) at 1 to 11 Mev, angular distributions from, (E/T), 19: 41732
effects on infrared spectrum and molecular structure of trimethyl borate, 19: 40470
electron elastic scattering by magnetic moments of, shell model for high-energy, 19: 41694
exchange equilibrium with boron-10, 19: 40505
performance in neutron activation detectors, (E), 19: 40867 (BNWL-64)
proton reactions (p,γ) and (p,p) at 0.5 to 4.0 Mev, carbon-12 energy levels from, (E), 19: 41688
proton reactions (p,α) at 150 and 163 kev, coincidence measurements for, (E), 19: 41699
reactions with nuclei at 5 to 12 Mev, neutron spectra from, (E), 19: 41810(T)
BORON NITRIDES
compatibility with graphite–nitrogen environment at 1000 and 1200°C, 19: 40966 (BNWL-92)
BORON OXIDES
spectra of diatomic, in plasma jets, (E), 19: 41287
B_2O_3–CaO, emission spectra of cerium- and samarium-activated phosphors of, 19: 40494(T)
B_2O_3–MgO, emission spectra of cerium- and samarium-activated phosphors of, 19: 40494(T)
B_2O_3–SrO, emission spectra of cerium- and samarium-activated phosphors of, 19: 40494(T)
B_2O_3–ZrO_2, preparation and sorptive properties for hydrogen, 19: 40484
BaO–B_2O_3, emission spectra of cerium- and samarium-activated phosphors of, 19: 40494(T)
BeO–B_2O_3, emission spectra of cerium- and samarium-activated phosphors of, 19: 40494(T)
BORON SYSTEMS
B–H_2O, neutron spectra in, thermal, 19: 42037(R) (BNWL-95, pp 4-17)
B–polyethylene neutron spectra in, thermal, 19: 42037(R) (BNWL-95, pp 4-17)
BOROSILICATE GLASS
sputtering in argon discharge, threshold energy and yields for, (E), 19: 41257
BOSONS
decay of intermediate vector, (T), 19: 41484(T)
decay of, spin-parity tests for, (T), 19: 41447
model for, composite, 19: 41525
production of intermediate vector, in antiproton-neutron interactions, (T), 19: 41484(T)
production of, SU(6) symmetry for, 19: 41449
quantization of scalar Bose fields, (T), 19: 41562
spin tests for, (T), 19: 41447
symmetry for, 27-supermultiplet in, (T), 19: 41492(T)
use of intermediate vector, in SU(4) quartet scheme of weak interactions, 19: 41415
BRAIN
radiosensitivity of neurons in rabbit cortex, 19: 40355(T) (FTD-TT-65-48, pp 111–12)
BRAIN TUMORS
radiodiagnosis by positron scanning technique, 19: 40390 (BNL-9384)
BRAKES
design of linear electromagnetic, for halting metallic tubes, (E), 19: 40724
BRAZING ALLOYS
development for bonding alumina to niobium alloys, 19: 40980 (LA-3302)
properties of, for René 62 nickel alloy, 19: 40989
BREEDER REACTORS
control rod drive mechanism for, 19: 42033(P)
BREMSSTRAHLUNG
exposure dose measurements in air, magnetic induction field for, 19: 40838
intensity optimization of betatron beam of, automatic device for, (E/T), 19: 41199
interactions of internal, in meson (π) decay, (T), 19: 41482(T)
reactions (γ,n) with bismuth-209 at 12 to 16 Mev, spectra from, (E), 19: 41834
reactions (γ,p) with oxygen-16 at 22 to 40 Mev, branching ratios and cross sections for, (E), 19: 41790
reactions with lithium-7, beta-active hydrogen-5 from, (E), 19: 41750
BROMINE
effects on sintering of tungsten, 19: 40985
reactions with protactinium on hafnium oxide and tantalum oxide carriers, 19: 40501
sorption on polycrystalline graphite, determination of radiation effects by, 19: 41109(P)
BROMINE ISOTOPES Br-79
exchange equilibrium with bromine-80, 19: 40505
BROMINE ISOTOPES Br-80
exchange equilibrium with bromine-79, 19: 40505
recoil reactions with alkanes and haloalkanes, radioactivity in organic yields in, 19: 40618
recoil reactions with bromoethane, pressure and temperature effects on, 19: 40626
BROMINE ISOTOPES Br-82
diffusion and retention in thermal annealing of irradiated n-propylbromide, bromobenzene, 4-bromo-o-xylene, and benzylbromide, 19: 40576
dispersion of, caused by fire, 19: 40830 (SC-RR-65-98, pp 719-22)
leakage from radioisotope packages after fire tests, 19: 40831 (SC-RR-65-98, pp 723-31)
BROMINE SYSTEMS
Br–bromobenzene–bromethane, neutron radiation effects on labeled organic retentions in, 19: 40624
Br–bromoethane–CCl_4, neutron radiation effects on labeled organic retentions in, 19: 40624
BUBBLE CHAMBERS
design and performance of, 19: 40869 (CONF-650510-14)
elementary particle interactions in, detection efficiency for, 19: 40873

(JINR-P-2215)
illumination of liquid-hydrogen, testing Scotchlite reflective material for, (E), 19: 40917
particle track analysis in, using desk computer, (E), 19: 40915
particle tracks in xenon, reconstruction of spatial picture of, 19: 40871 (JINR-P-2179)
BUBBLES
rise velocity in inclined tubes, 19: 40738(R) (NYO-3114-7)
BUILDING MATERIALS
leak analysis for reactor containment, 19: 42018 (NAA-SR-10100)
BUTADIENE POLYMERS
radiation effects on structure of, neutron, 19: 40561
BUTANE
reactions with recoil tritium, kinetic isotope effects in, 19: 40615
reactions with recoil tritium in presence of helium, energy loss and reactivity values of, 19: 40616
butane–ethane, energy loss and reactivity in reactions with recoil tritium in presence of helium, 19: 40616
BUTANE, 1-CHLORO-
reactions with chlorine-38 recoil atoms, stereochemistry in, 19: 40625
BUTANE, 2-CHLORO-
reactions with chlorine-38 recoil atoms, stereochemistry in, 19: 40625
BUTANE, 2,3-DICHLORO-
reactions with chlorine-38 recoil atoms, stereochemistry in, 19: 40625
BUTANE, 2-METHYL-
reactions with recoil carbon-11, 19: 40550 (IS-T-27)
1-BUTANOL
reactions with tritium recoil atoms, with and without benzene and cyclohexane, energy transfer in, 19: 40622
butanol–ethanol, coagulation of thorium hydroxide particle in, 19: 40963(P)
2-BUTANOL
reactions with tritium recoil atoms, with and without benzene and cyclohexane, energy transfer in, 19: 40622
BUTYL PHOSPHATES
effects on solvent properties of DEHAP for uranium, 19: 40678
solvent properties for actinides and fission products in short-residence contactors, 19: 40645 (CONF-650918-1)
solvent properties for ruthenium nitrosyl nitrates, 19: 40677
alkane–TBP, performance as solvent in Purex Process, 19: 40646 (CONF-650918-2)
CCl_4–TBP, solvent properties for plutonium, thorium, and uranium from fuel scrap feed, 19: 40643 (BNWL-57)
dibutyl butylphosphonate–TBP, solvent properties for thorium and uranium, 19: 40643 (BNWL-57)
BUTYLAMINE
separation from other amines by ligand exchange on cation exchanger, 19: 40648 (COO-499-2)

C

CABLES
design for remote measurements in radiation environment, (E), 19: 40714 (EUR-2421.d)
testing of oceanographic, in shallow water, 19: 42210(R) (NVO-98-8)
CADARACHE REACTORS
safety hazards and precautions at Pegase installation, 19: 42151 (CEA-R-2518(Vol.II))
CADARACHE REACTORS (RAPSODIE)
fuel element for, description of, 19: 42104(T) (NP-tr-1234)
fuel rod testing for, 19: 41094(T) (NP-tr-1235)
CADMIUM
determination in copper by activation, 19: 40422
electrochemical behavior of, in water–water-d_2 system, 19: 40427
optical properties of films of, in vacuum ultraviolet region, 19: 42213 (ORNL-TM-1164)
positron annihilation in, angular correlations from, (E), 19: 41285
reactor criticality effects of rods of, in heavy water lattices, (E), 19: 42045(R) (MIT-2344-3, pp 55-108)
separation from uranium by chromatography on cellulose columns, tracer studies of, 19: 40687
solvent distribution in ammonium thiocyanate–methanol–water systems, distribution coefficients for, 19: 40447
thermodynamic properties at high pressures and temperatures, 19: 40459 (NP-15324)
CADMIUM ALLOYS
Cd–Gd, phase studies, 19: 40960
Cd–Pu, phase studies, 19: 40958
Cd–rare earths, crystal structure of intermetallic compounds in, 19: 41040
Cd–Ru, process for improving workability of, 19: 40999(P)
CADMIUM CHLORIDES
electric conductivity in methanol, transference numbers for, 19: 40527
CADMIUM FLUORIDES
electric properties of single crystals of, 19: 41124(R) (NP-15108)
CADMIUM ISOTOPES Cd-110
reactions (p,t) at 40 Mev, ground-state L = 0 transitions in, (E), 19: 41689
CADMIUM ISOTOPES Cd-112
reactions (p,t) at 40 Mev, ground-state L = 0 transitions in, (E), 19: 41689
CADMIUM ISOTOPES Cd-114
reactions (p,t) at 40 Mev, ground-state L = 0 transitions in, (E), 19: 41689
CADMIUM ISOTOPES Cd-116
reactions (p,t) at 40 Mev, ground-state L = 0 transitions in, (E), 19: 41689
CADMIUM SELENIDES
compressibility of, volume, (E), 19: 41984
CADMIUM SULFIDES
compressibility of, volume, (E), 19: 41984
effects of electron bombardment on electric conductivity of, 19: 41097
photoluminescence of, feasibility of obtaining pairs with matched response, (E), 19: 40598
radiation effects on, electron recombination processes in alpha, 19: 40565
CADMIUM TELLURIDES
compressibility of, volume, (E), 19: 41984
CALCIUM
content in diet of cattle, effects on strontium-90 transfer to milk, 19: 40341
content in man, blood analysis method for determining, 19: 40309(R) (NP-15180)
dietary content of, effects on strontium-90 absorption by cattle, 19: 40332
effects of dietary, on strontium-90 metabolism in animals, 19: 40342
effects of dietary, on strontium-90 metabolism, 19: 40343
metabolism by swine, effects on strontium-90 absorption, 19: 40328
metabolism in cattle, effects on strontium-90 absorption, 19: 40330
separation from rare earth metals, techniques for, 19: 40948 (IS-1195)
separation from strontium using pyridine-2,6-dicarboxylic acid resins, chromatographic, 19: 40674
CALCIUM ACETATES
preparation and crystal structure of ammoniated, 19: 40507
CALCIUM ALLOYS
Ca–Nb–Zr, corrosion by superheated steam, 19: 40977(P)
CALCIUM CHLORIDES
$CaCl_2$–KCl, radioinduced formation of phosphorus-32-labeled phosphine in, 19: 40606
CALCIUM FLUORIDES
electron paramagnetic resonance of neodymium ions in, (E), 19: 41999(T)
electron paramagnetic resonance of terbium and uranium in, relaxation in, (E), 19: 42000(T)
luminescence centers in rare-earth activated, 19: 41978
optical properties of samarium-containing, effects of samarium valence on, 19: 41993(T)
plastic deformation of, effects of grain boundaries in, 19: 40536
radiation effects on absorption spectra of samarium-containing, gamma and uv, (E), 19: 41993(T)
radiation effects on optical properties of dysprosium-containing crystals of, gamma, 19: 40600(T)
radiation effects on EPR in neodymium-containing crystals of, gamma, 19: 40602(T)
radioinduced charge transfer between europium and thulium ions in, x-, 19: 40575
samarium valency in, effects of oxygen on, 19: 41993(T)
ytterbium-ion spin-lattice relaxation time in, (T), 19: 41982
ytterbium-ion spin-lattice relaxation time in, (T), 19: 41995(T)
CALCIUM ISOTOPES Ca-40
alpha reactions (α,p) at 22 Mev, isomer production in, (E), 19: 41802(T)
deuteron reactions (d,α) and (d,He-3) at 15.14 Mev, isobaric spin selection rules from, (E), 19: 41720
deuteron reactions (d,p) with, DWBA and Coulomb stripping approximations for, (E), 19: 41742
meson (μ^-) capture by proton pairs in, (E/T), 19: 41753
CALCIUM ISOTOPES Ca-42
proton reactions (p,γ) with, scandium-43 energy levels from, (E), 19: 41738
CALCIUM OXIDES
content in McKelveyite uranium mineral, 19: 40799
effects on oxidation resistance and strength of chromium–magnesia composites, 19: 41022(R) (NP-15292)

use as a diathermanous substance in thermal reactors, 19: 42065(P)
B_2O_3–CaO, emission spectra of cerium- and samarium-activated phosphors of, 19: 40494(T)
CALCIUM SULFATES
performance of manganese activated, for gamma dosimetry, 19: 40877 (RISO-101)
CALCIUM SULFIDES
luminescence properties for gamma dosimetry, infrared-stimulated, 19: 40879 (UCRL-12371)
CALIFORNIUM
separation from aqueous solutions of organic acids by solvent extraction using high-molecular-weight amines, 19: 40657
separation from rare earths by solvent extraction using DTPA, 19: 40676
solvent extraction by thenoyltrifluoroacetone in benzene, 19: 40458 (JINR-P-2224)
CALIFORNIUM COMPLEXES
with lactic acid, stability constants, 19: 40458 (JINR-P-2224)
CALIFORNIUM ISOTOPES Cf-252
fission fragments of, conversion electron spectra from, 19: 41680 (UCRL-16184)
helium-6 spontaneous emission from, (E), 19: 41785
radioactivity of, dose rate and energy spectra of alpha, gamma, and neutron, 19: 41657 (DP-986)
CALORIMETERS
description of, for thermodynamic measurements on liquid metals, 19: 41001(R) (AGN-8154)
design for measuring thermal radiation from nuclear explosions, (E), 19: 40882 (USNRDL-TR-839)
pulse analyzers for ionization, multichannel, 19: 40853
pulse analyzers for ionization, design of multichannel, 19: 40854
use in electron dosimetry at 15 Mev, 19: 40910
CALORIMETRY
method of pulse heating, for specific heat measurements in electrical conductors, 19: 40700 (ORNL-TM-1187)
CAMBRIDGE SYNCHROTRON
beam monitoring and calibration in, equipment for, 19: 41164 (CEAL-1022)
CANDU REACTOR
coolants for, evaluation of performance of fog as, (E), 19: 42020
CARBIDES
analysis for carbon, electron microprobe, 19: 40412 (TIM-924)
CARBOHYDRATES
metabolism in rat liver, tracer study, 19: 40308 (BNL-8379)
CARBON
addition to alkali metal bath for coating of molybdenum with silicides, 19: 40998(P)
deposition of pyrolytic, on particulate reactor fuels and poisons, 19: 40992(P)
determination in liquid sodium, methods for, 19: 40409(R) (MSAR-65-95)
determination in refractory metals, combustion furnace for, 19: 40413 (TIM-948)
determination on beryllium surface by deuteron activation methods, 19: 40453
determination, electron microprobe, 19: 40412 (TIM-924)
diffusion into uranium nitride, 19: 40412 (TIM-924)
effects on corrosion of type 316 stainless steel by sodium, 19: 40969(R) (MSAR-65-96)
effects on mechanical properties of TZM molybdenum alloy, 19: 41002 (APS-5157-R)
electron absorption in ionization chamber, calorimetric measurement of, 19: 40910
nuclear resonance fluorescence in, (E), 19: 41828
oxidation properties of vitreous, 19: 40959
properties of coatings of pyrolytic, effects of preparation conditions on, 19: 41004 (BMI-1735)
proton spectra in, near surfaces, (T), 19: 41951 (N64-30510)
radiation effects on coatings of pyrolytic, on fuel particles, 19: 40958
reactor criticality effects per atom, (E), 19: 42077 (ANL-7014)
sorptive properties for krypton, two-dimensional second virial coefficients for, 19: 40956
spectra of atomic and molecular, in plasma jets, (E), 19: 41287
CARBON DIOXIDES
absorption by oil drops traveling on vertical wire, mass transfer, 19: 40398 (UCRL-16047)
content in McKelveyite uranium mineral, 19: 40799
reactions with graphite moderators, inhibition of, 19: 42015(P)
reactions with hydrogen, kinetics of, 19: 40959
reactions with potassium superoxide, kinetics, 19: 40462 (SC-TM-65-183)
yields from radiolysis of ethylene vinyl acetate copolymers, 19: 40556
CARBON ISOTOPES
radioactivity of, carbon dioxide-filled proportional detector for measuring, 19: 40920
CARBON ISOTOPES C-11
production in man during high-energy radiotherapy, 19: 40392 (NYO-3364-6)
reactions with ethane–neon and ethylene neon systems, kinetic energy effects on, 19: 40617
recoil reactions of, in liquid hydrocarbons, 19: 40550 (IS-T-27)
CARBON ISOTOPES C-12
abundance in massive stars, effects of helium and hydrogen burning on, (T), 19: 41242
decay of, three-alpha, (E), 19: 41699
deuteron reactions (d,p) at 0.9 to 2.0 Mev, angular distribution for, (E), 19: 41721
electron inelastic scattering by, (T), 19: 41766
energy levels, (E), 19: 41828
energy levels from 16 to 20 Mev, from boron-11 (p,γ) reactions, (E), 19: 41688
gamma reactions (γ,n) in liquid hydrocarbons, recoil reactions of carbon-11 produced in, 19: 40550 (IS-T-27)
helium-3 reactions (He-3,α) and (He-3,p) at 1.0 to 1.8 Mev, total cross sections for, (E), 19: 41663 (JINR-P-2184)
helium-3 reactions (He-3,Be-7) at 29.4 Mev, angular distributions and energy spectra from, (E), 19: 41733
meson (μ) capture by, (T), 19: 41766
proton binding energy in, measurement of, 19: 41660 (ISS-65/3)
proton elastic scattering at 4.7 to 11.3 Mev, angular distributions and polarization in, (E), 19: 41731
proton scattering at 156 Mev, 4.43-Mev level excitation in, (T), 19: 41675 (ORNL-P-330)
reactions (C-12, C-13) with tellurium-128 at 40 to 150 Mev, isomeric pair production ratios in, 19: 41674 (NYO-1930-44)
reactions (C-12,C-13) with lead-208, (E), 19: 41768
reactions (C-12,3n) with tellurium-128, angular momentum effects on isomeric cross section ratios in, 19: 41821
reactions (p,pd) at 155 Mev, angular correlations in, (E), 19: 41703
scattering by lead-208, inelastic, (E), 19: 41768
triton reactions (t,α) at 1.35 to 3.4 Mev, excitation curves for, (E), 19: 41706
CARBON ISOTOPES C-13
abundance in massive stars, effects of helium and hydrogen burning on, (T), 19: 41242
exchange equilibrium with carbon-14, 19: 40505
proton reactions (p,γ) at 0.60 to 1.8 Mev, nitrogen-14 energy levels from, (E), 19: 41740
CARBON ISOTOPES C-14
content and diffusion in atmosphere, 19: 40797
determination in animal tissues and excreta by liquid scintillation counting, 19: 40418
determination in biological material by scintillation counting of beta decay, 19: 40426
determination in biological materials, 19: 40436
exchange equilibrium with carbon-13, 19: 40505
incorporation in glutamic acid in rat liver, 19: 40308 (BNL-8379)
incorporation in ubiquinone-50, method for, 19: 40641
recoil reactions with liquid mixtures of heterocyclic compounds, labeled yields in, 19: 40627
recoil reactions with organic compounds, formation of polymeric products in, 19: 40628
use in age estimation in archeology and geology, 19: 40795
CARBON ISOTOPES C-16
production in proton reactions at 1.0 and 2.8 Bev, cross sections for, (E), 19: 41780
CARBON MONOXIDES
addition to carbon dioxide cooling streams to inhibit reaction with graphite moderators, 19: 42015(P)
determination in products from radiolysis of ethylene vinyl acetate copolymers by gas chromatography, 19: 40556
radiation effects on catalytic oxidation of, on nickel oxide at 25°C and zinc oxide at 270°C, 19: 40577
radiation effects on sorption of, on zinc oxide and nickel oxide, 19: 40578
reactions with deuterium and hydrogen molecules, spectra of COD^+ and COH^+ in, (E), 19: 41252
CARBON STEEL
sorptive properties of surfaces of, for iodine in high-temperature helium loop, 19: 40397 (ORNL-TM-1134)
CARBON SULFIDES
asphaltine–α,α,α–trifluorotoluene–carbon disulfide, differential dynamic polarization of fluorine and hydrogen nuclei in, (E), 19: 40497
asphaltine–benzene–hexafluorobenzene–carbon disulfide, differential

dynamic polarization of fluorine and hydrogen nuclei in, (E), 19: 40497
asphaltine–benzene-d_6–hexafluorobenzene–carbon disulfide, differential dynamic polarization of fluorine and hydrogen nuclei in, (E), 19: 40497

CARBON SYSTEMS
Be–C–U, phase studies, 19: 40958
C–N, spectra of diatomic, in plasma jets, (E), 19: 41287
C–Nb–Ti, analysis for carbon, electron microprobe, 19: 40412 (TIM-924)
C–Nb–W–Zr, properties of welds in D-43, 19: 40989
C–Nb–W–Zr, stress corrosion of D-43 by boiling potassium, research program on, 19: 40970(R) (NASA-CR-54390)
C–Nb–W–Zr, stress-rupture properties of D-43, 19: 40961
C–U, analysis for carbon, electron microprobe, 19: 40412 (TIM-924)

CARBON TETRACHLORIDE
carbon tetrachloride–thenoyltrifluoroacetone, solvent properties for uranyl salts, 19: 40682
reactions with bromine-80 recoil atoms, radioactivity in organic yields in, 19: 40618
benzene–CCl_4, formation of polymeric yields in reactions with carbon-14 and sulfur-35 recoil atoms, 19: 40628
Br–bromoethane–CCl_4, neutron radiation effects on labeled organic retentions in, 19: 40624
CCl_4–cyclohexane, formation of polymeric yields in reactions with carbon-14 and sulfur-35 recoil atoms, 19: 40628
CCl_4–cyclohexene, formation of polymeric yields in reactions with carbon-14 and sulfur-35 recoil atoms, 19: 40628
CCl_4–dibutyl butylphosphonate, solvent properties for plutonium and thorium from fuel scrap feed, 19: 40643 (BNWL-57)
CCl_4–ethanol, mechanism of chemical processes in reactions with chlorine-38 recoil atoms, 19: 40623
CCl_4–methanol, mechanism of chemical processes in reactions with chlorine-38 recoil atoms, 19: 40623
CCl_4–TBP, solvent properties for plutonium, thorium, and uranium from fuel scrap feed, 19: 40643 (BNWL-57)
CCl_4–1–propanol, mechanism of chemical processes in reactions with chlorine-38 recoil atoms, 19: 40623
CCl_4–2–propanol, mechanism of chemical processes in reactions with chlorine-38 recoil atoms, 19: 40623

CARBON TETRAFLUORIDE
reactions with bromine-80 recoil atoms, radioactivity of organic yields in, 19: 40618

CARBOX PROCESS
evaluation for reprocessing of uranium carbide fuel, 19: 40652 (NAA-SR-11340)

CARCINOMAS
radiotherapy of, effects of 5-fluorouracil in breast, 19: 40394

CAROLINAS-VIRGINIA TUBE REACTOR
operation, June 1965, 19: 42084(R) (CVNA-239)

CARTILAGE
radiation effects on calcification of, in rats, 19: 40351(R) (NYO-1913-1)

CASCADE SHOWERS
analysis of, by solving inverse problem, (T), 19: 41710
distributions in electron-photon, in condensed media, (T), 19: 41707
distributions in electromagnetic, for primary energies around 1 Tev, (T), 19: 41711
electromagnetic cascade theory, angular distribution functions in, (T), 19: 41359
gamma spectra in 1000-Tev extensive air showers, (T), 19: 41298
measurement of electromagnetic, transition effect on, 19: 40912
production of extensive air, by primary nucleons, (T), 19: 41300
x-ray spectra in cosmic electromagnetic, at high altitudes, (E/T), 19: 41299

CAST IRON
radiation effects on graphitization of white, gamma, 19: 40961

CATHODES
electron yields from nickelate, 19: 41124(R) (NP-15108)
fabrication of lanthanum-hexaboride-coated rhenium, (E), 19: 40725

CATION EXCHANGE MATERIALS
use for separation of amines by ligand exchange, 19: 40647 (COO-499-1)
use of nickel-loaded, for separation of amines by ligand exchange, 19: 40648 (COO-499-2)

CATIONS
diet, effects of calcium content on strontium-90 transfer to milk, 19: 40341

CATTLE
strontium-90 metabolism in calf skeleton, after ingestion by mother or self, effects of age, 19: 40329
strontium-90 metabolism in fetus of, after ingestion by the mother, 19: 40330
strontium-90 metabolism in milk cows, after chronic ingestion, 19: 40332

CAVES
description of beta-gamma, for mechanical testing of irradiated reactor materials, 19: 40717 (RISO-98)
description of transcurium element radiochemistry facility, 19: 40719 (UCRL-7844-T)
description of transplutonium chemical process cells, 19: 40720 (UCRL-7845-T)
development of concrete low-background, 19: 40721 (UCRL-11454)
equipment for, remote-control, 19: 40730(P)

CAVITATION
book: *Cavitation in Real Liquids*, 19: 40751

CAVITY RESONATORS
characteristics of, measurement in accelerators, (E), 19: 41166 (ML-767)
design for isochronous cyclotron, 19: 41172
electromagnetic field control in proton linac, 19: 41167 (NIRL/R/76)
field emission at 200 Mc/sec in linear accelerator, (E), 19: 41202
frequency modulation of large, (E), 19: 40723
Q-value of, measurement of, (T), 19: 41190

CELLOPHANE
ion transfer across membrane of, analysis by enzyme catalyzed chemical reaction, 19: 42199 (BNL-8397)

CELLULOSE PHOSPHATES
sorptive properties for scandium, 19: 40689

CENTRIFUGAL PUMPS
design for PHOEBUS reactor, 19: 42141 (NASA-CR-54422)

CENTRIFUGES
rotor development for zonal, low-speed, 19: 40654 (ORNL-3613)

CERAMIC BODIES
effects of high rates of heat transfer on, 19: 40961

CERAMIC COATINGS
deposition on aggregated reactor fuel particles, 19: 40994(P)

CERAMIC MATERIALS
book: *Thermal Radiative Properties*, 19: 41074

CERIUM
analysis for nitrogen, isotope-dilution method for, 19: 40444
determination by spectrochemical methods, voltage-fluctuation patterns in, 19: 40416
effects as coactivator with samarium on emission spectra of borate phosphors, 19: 40494(T)
electric conductivity of, at 20 to 300°K, effects of crystal structure on, 19: 41083
equilibrium between di- and trivalent cerium ions and, in molten salt, 19: 40467(T) (ORNL-tr-578)
optical reflectivity of annealed, at 80 and 300°K, 19: 41082
physical and thermodynamic properties, 19: 40948 (IS-1195)
polarographic behavior in dimethylformamide and dimethylsulfoxide, 19: 40681
preparation and purification, 19: 40948 (IS-1195)
reactions with polyribonucleotides of adenylic, cytidylic, and uridylic acids, mechanism of degradation in, 19: 40474
separation from aqueous solutions of organic acids by solvent extraction using high-molecular-weight amines, 19: 40657
sorption on tungsten ferrocyanide, tracer studies of, 19: 40679
viscosity of liquid, 19: 40958

CERIUM ALLOYS
Ce–Au, phase studies of solid solutions in, 19: 41062
Ce–Cu–Pu, phase studies, 19: 41054
Ce–Mg, phase studies, 19: 41011 (IS-T-15)
Ce–Ni, phase studies, 19: 40961
Ce–Pu, viscosity of liquid, 19: 40958
Ce–Ru, process for improving workability of, 19: 40999(P)

CERIUM CARBIDES
eutectic temperature between carbon and dicarbide, 19: 41014 (LA-DC-6819)
lattice parameters and phase transformation temperatures in, 19: 41014 (LA-DC-6819)
microhardness, 19: 41014 (LA-DC-6819)

CERIUM CHLORIDES
complexes with phenanthroline, preparation and properties, 19: 40514
formation of di-, 19: 40467(T) (ORNL-tr-578)

CERIUM COMPLEXES
with tartaric acids, composition and stability, 19: 40510

CERIUM IONS
equilibrium between cerium and di- and trivalent, in molten salt, 19: 40467(T) (ORNL-tr-578)

CERIUM ISOTOPES Ce-136
decay, (E), 19: 41700

CERIUM ISOTOPES Ce-137
cross section ratios from barium-136 (α,3n) reactions to 42 Mev, isomeric, (E), 19: 41695
cross-section ratios from barium-136 (α,3n) reactions, statistical model

for isomeric, 19: 41696
decay of oriented metastable, conversion electron distributions from, (E), 19: 41679 (UCRL-11462(Rev.))
production in barium-136(α,3n) reactions, angular momentum effects on isomeric cross section ratios in, (E), 19: 41821
production in lanthanum-139(p,3n) reactions, angular momentum effects on isomeric cross section ratios in, (E), 19: 41821
production in tellurium-128(C-12,3n) reactions, angular momentum effects on isomeric cross section ratios in, (E), 19: 41821
CERIUM ISOTOPES Ce-139
nuclear alignment in magnesium cerium nitrate, intermediate state reorientation in, 19: 41840
CERIUM ISOTOPES Ce-140
deuteron reactions (d,p) with, DWBA and Coulomb stripping approximations for, (E), 19: 41742
deuteron reactions (d,d'γ) at 12 Mev, 0+ states from, 19: 41747
energy levels from (p,p'γ) and (d,d'γ) reactions at 12 Mev, 0+, (E), 19: 41747
gamma directional correlations in, (E), 19: 41822
proton reactions (p,p'γ) at 12 Mev, 0+ states from, (E), 19: 41747
CERIUM ISOTOPES Ce-141
content in rain at Fayetteville, Arkansas, 19: 40785 (TID-21224)
CERIUM ISOTOPES Ce-143
decay of, promethium-143 energy levels from gamma-gamma directional correlations in, (E), 19: 41776
CERIUM ISOTOPES Ce-144
content in rain at Fayetteville, Arkansas, 19: 40785 (TID-21224)
excretion in rats, effects of complexing agents on, 19: 40347
metabolism in rats of, after intratracheal administration, 19: 40313
metabolism in rats of, after oral or intravenous administration, 19: 40321
metabolism in rats of, after oral administration of mixed uranium fission products, 19: 40322
poisoning by, drug evaluation for emergency treatment, 19: 40339
processing into planar beta sources, (E), 19: 40560
CERIUM NITRATES
$Ce(NO_3)_3$–$LiNO_3$–H_2O, solubility ratios in, at 10, 20, and 30°C, 19: 40519
CERIUM OXIDES
content in McKelveyite uranium mineral, 19: 40799
CERIUM PERCHLORATES
stability constants of, thermal, 19: 40509
CERIUM SILICIDES
crystal structure, 19: 40477
crystal structure, 19: 40478
CERIUM SULFATES
$Ce_2(SO_4)_3$–Na_2SO_4, thermal stability, 19: 40511
CERMETS
development and testing for liquid-metal pump seals, 19: 40718 (TIM-909)
CESIUM
content in blood and body of man, 19: 40781(R) (NP-15179)
determination by spectrochemical methods, voltage-fluctuations patterns in, 19: 40416
determination in copper by activation, 19: 40422
diffusion in inert gases, (E), 19: 41278
effects of sorbed, on germanium work function, 19: 41124(R) (NP-15108)
effects on air ionization in space vehicle hypersonic re-entry flights, 19: 41121 (N64-30658)
electron-velocity distribution function in low-pressure plasma of, in oscillation regime, (E), 19: 41877
performance in electron bombardment ion engines, 19: 40770
plasma of, electron distribution and temperature in low-voltage arc, (E), 19: 41909
radioinduced ionization in thermionic converters uv, (E), 19: 40566
reactions with boride and carbide coatings at 500°C, 19: 40765(R) (NP-15309)
separation from uranium by chromatography on cellulose columns, tracer studies of, 19: 40687
spin relaxation of optically pumped, in inert gases, (E), 19: 41278
CESIUM BROMIDES
radiation effects on electroluminescence of, x, 19: 40572
CESIUM CHLORIDES
complexes with praseodymium, properties of, 19: 40469
radiation effects on electroluminescence of, x, 19: 40572
CESIUM IODIDES
luminescence yields of, absolute gamma, 19: 40593(T)
radiation effects on electroluminescence of, x, 19: 40572
CESIUM IONS
emission from cesiated beryllium, copper, nickel, and 304 stainless steel surfaces, (E), 19: 41284
extraction from hollow cathode containing plasma, (E/T), 19: 41872
production by contact ionization on porous tungsten, 19: 40765(R) (NP-15309)
CESIUM ISOTOPES Cs-132
decay of, xenon-132 energy levels from, (E), 19: 41745
radiation hazards of inhalation and ingestion by man of, 19: 40805 (NRS-30)
CESIUM ISOTOPES Cs-137
biological effects in rats, after chronic low-dose oral administration, 19: 40335
content in Alaskan Arctic biota, 1959 to 1965, 19: 40780 (BNWL-SA-242)
content in blood and body of man, 19: 40781(R) (NP-15179)
content in food chains in Alaska, 1959 to 1965, 19: 40780 (BNWL-SA-242)
content in man, blood analysis method for determining, 19: 40309(R) (NP-15180)
metabolism in sheep of, after oral administration, 19: 40334
pathological effects of, in sheep, 19: 40334
separation from fuel storage basin effluent by ion exchange, 19: 40651 (IDO-14657)
CESIUM ISOTOPES Cs-139
range distributions of fission fragments of, in aluminum, (E), 19: 41668 (KFK-306)
CESIUM PLUTONIUM CHLORIDES
preparation and properties of dihydrate, 19: 40488
CHARGED PARTICLE BEAMS
aberrations of, evaluation of space-charge-produced, (T), 19: 41173
current integrators for positive, design of accurate, (E), 19: 41183
energy dispersion and focusing in plane-capacitor field, space-charge effects on, (T), 19: 41196
focusing by electromagnetic fields, (T), 19: 41142
interactions with piezodielectric crystals, equations for, 19: 41990(T)
motion in electric and magnetic fringing fields, (T), 19: 41139
spectroscopy in two-sector electrostatic analyzer, angular aberrations in, (E), 19: 41197
CHARGED PARTICLES
acceleration in superfluid helium at low temperatures, vortex ring production by, (E), 19: 41634
conservation equations for, in dilute plasma, (T), 19: 41889
density and energy in cosmic showers, (E), 19: 41309
diffusion in geomagnetic fields, ambipolar, (T), 19: 41585
interactions of spinless, (T), 19: 41555
interactions with coronal plasma, (T), 19: 41933
interactions with photons, kinetic equations for, 19: 41940
motion in conducting semiplane, diffraction of electromagnetic field during, 19: 41539
motion in constant magnetic field, difference equations for, 19: 41145
motion in electric and magnetic fringing fields, (T), 19: 41139
motion in electromagnetic fields, (T), 19: 41142
motion in geomagnetic fields, magnetic shell classification by, (T), 19: 41584
motion in Heliotron magnetic field, orbital, (T), 19: 41885
motion in oscillating electric fields, (T), 19: 41155
motion in symmetrical fields, hamiltonian for, (T), 19: 41538
motion of auroral, in magnetosphere, (T), 19: 41583
motion stability in magnetic field, (T), 19: 41187(T)
polarization of, electrodynamic effects on, (T), 19: 41334 (JINR-P-2229)
production of showers of, from high-energy mesons in thick absorbers, (T), 19: 41354
reactions in crystal lattices, anisotropic effects in, (T), 19: 41789
reactions in exosphere, v-l-f emissions from, 19: 41572 (NASA-CR-258)
reactions with nuclei, slow particle emission in stripping, (T), 19: 41664 (JINR-P-2193)
scattering by shielded Coulomb potential, (T), 19: 41763
scattering of Dirac particles by scalar potential, elastic, (T), 19: 41510
scattering of, design of chambers for, (E), 19: 40907
stopping and straggling in rare gases, excitation energy for, (T), 19: 41268
stopping in matter, computer program for calculation of, 19: 41954 (NP-15338)
theory for elementary, derivation of classical relativistic, 19: 41372
CHELATES
effects of complexing agents on deposition of strontium-89 in bones of rats, 19: 40344
CHEMICAL ANALYSIS
book: *Advances in Analytical Chemistry and Instrumentation*, Vol. 4, 19: 40446
equipment for, using constriction response, 19: 40417
of rare earths, review, (E), 19: 40448
of rare earths, review of Soviet studies on, 19: 40449
CHEMICALS AND REAGENTS

production by reactor irradiation of aqueous solutions, 19: 40548 (BNWL-82)
CHEMISTRY
chemical potentials in, calculation by summation of Fermi-Dirac functions, (T), 19: 40493
CHERENKOV DETECTORS
design for cosmic meson (μ) detection as deep as 6000 Mwe, (E), 19: 41293
response to 50- to 1000-Mev photons, (E), 19: 40897
CHERENKOV RADIATION
emission in anisotropic media, quantum theory of intensity of, 19: 41499
CHICKENS
strontium-90 metabolism in, effects of dietary constituents on, 19: 40342
CHILE
uranium reconnaissance of Colimapu formation in central, 19: 40798 (RME-4571(Rev.))
CHLORIDE COMPLEXES
with chromium, electron spin resonance spectra, 19: 40465 (UCRL-16175)
CHLORIDES
determination in heavy water moderator, automated, 19: 40406 (CONF-650919-2)
CHLORINE ISOTOPES Cl-34
production in man during high-energy radiotherapy, 19: 40392 (NYO-3364-6)
CHLORINE ISOTOPES Cl-35
exchange equilibrium with chlorine-36, 19: 40505
neutron capture cross sections and radiation widths, (E), 19: 41806(T)
CHLORINE ISOTOPES Cl-36
exchange equilibrium with chlorine-35, 19: 40505
CHLORINE ISOTOPES Cl-38
recoil reactions with alcohol–carbon tetrachloride mixtures, mechanisms of chemical processes in, 19: 40623
recoil reactions with chloroalkanes, stereochemistry in, 19: 40625
CHLOROFORM
reactions with bromine-80 recoil atoms, radioactivity in organic yields in, 19: 40618
$CHCl_3$–H_2O, dissociation of 2,4-hexanedione and 6-methyl-2,4-heptanedione in, 19: 40423
CHOLESTEROL
radiation effects on content in blood and liver of rats, 19: 40386(T) (FTD-TT-65-48, pp 661–2)
CHROMATOGRAPHIC SEPARATIONS
resin preparation for use in, 19: 40674
CHROMATOGRAPHY
equipment for analysis of corrosive gases, 19: 40407 (KY-485)
equipment for radioisotopic separation by remotely controlled, 19: 40685
gas, purification of helium for, 19: 40539(P)
use of beta ionization detector for analysis of permanent gases, 19: 40415(T) (CEA-tr-R-1839)
CHROMIUM
analysis for nitrogen, isotope-dilution method for, 19: 40444
corrosion by aluminum–silicon and water of coatings of, on uranium, 19: 40949 (ISC-640)
deposition on zinc-coated uranium, electrolytic, 19: 40949 (ISC-640)
determination by spectrochemical methods, voltage-fluctuation patterns in, 19: 40416
determination in copper by activation, 19: 40422
determination in heavy water moderator, automated, 19: 40406 (CONF-650919-2)
effects on high-temperature properties of aluminum–iron–silicon–uranium systems, 19: 40958
separation from uranium by chromatography on cellulose columns, tracer studies of, 19: 40687
CHROMIUM ALLOYS
Al–Cr–Fe–Y, corrosion by steam at 500 to 1300°C, 19: 40961
Al–Cr–Fe–Y, impact properties of, 19: 40961
Cr–Co–Fe–Mn–Mo–Ni–W, corrosion of Raonel, by coal gasification products at high temperatures, 19: 42127(R) (TID-22009)
Cr–Fe–Ni, corrosion films on, structure of oxide, 19: 40967(R) (COO-1319-27)
Cr–Fe–Ni, stress-corrosion cracking in, effects of fourth-component additions on, 19: 40967(R) (COO-1319-27)
Cr–Fe–Ni, stress-corrosion by chlorides, oxygen, and water, 19: 40967(R) (COO-1319-27)
Cr–Fe–Ni, tensile properties to 1200°F, effects of composition on, 19: 40967(R) (COO-1319-27)
Cr–Ni, diffusion in, activation energy and frequency factor for self-, 19: 40961
Cr–Sc, phase studies of solid solution formation in, 19: 41050
Cr–Ti, brazing alloy for niobium-based alloys, 19: 40989
Cr–Y, phase studies of solid solution formation in, 19: 41050
CHROMIUM COMPLEXES
chloroaquo-, electron spin resonance spectra, 19: 40465 (UCRL-16175)
pentacyanonitrosyl-, electron spin resonance spectra, 19: 40465 (UCRL-16175)
CHROMIUM IONS
radiation emission in ruby, level splitting effects on, (T), 19: 40574
radioinduced thermoluminescent reduction of, in magnesium oxide crystals, 19: 40631
CHROMIUM ISOTOPES Cr-50
neutron reactions (n,γ) with, gamma spectra from thermal, (E), 19: 41807(T)
CHROMIUM ISOTOPES Cr-51
deposition, computer program for evaluating radiochemical data on, 19: 40636 (WAPD-TM-516)
energy levels of, angular momentum, parity, and spin of, (E), 19: 41807(T)
CHROMIUM ISOTOPES Cr-52
deuteron reactions (d,p) at 10 Mev, energy levels from, (E), 19: 41726
neutron reactions (n,γ) with, gamma spectra from thermal, (E), 19: 41807(T)
CHROMIUM ISOTOPES Cr-53
energy levels from chromium-52 (d,p) reactions at 10 Mev, (E), 19: 41726
energy levels of, angular momentum, parity, and spin of, (E), 19: 41807(T)
neutron reactions (n,γ) with, gamma spectra from thermal, (E), 19: 41807(T)
proton inelastic scattering at 11 Mev, cross sections from, (E), 19: 41726
CHROMIUM ISOTOPES Cr-54
deuteron reactions (d,p) at 10 Mev, energy levels from, (E), 19: 41726
energy levels of, angular momentum, parity, and spin of, (E), 19: 41807(T)
CHROMIUM ISOTOPES Cr-55
energy levels from chromium-54 (d,p) reactions at 10 Mev, (E), 19: 41726
CHROMIUM OXIDES
Al_2O_3–Cr_2O_3, formation of refractories of, 19: 40997(P)
Cr_2O_3–MgO, formation of refractories of, 19: 40997(P)
Cr_2O_3–Nb_2O_5, phase studies, 19: 41049
Cr_2O_3–ZrO_2, formation of refractories of, 19: 40997(P)
CHROMIUM STEEL
analysis for samarium, 19: 40445
electric conductivity of, effects of carbon on, 19: 40409(R) (MSAR-65-95)
magnetic properties of, effects of carbon on, 19: 40409(R) (MSAR-65-95)
performance in measuring carbon in sodium, 19: 40409(R) (MSAR-65-95)
Cr–Mo–Ni, properties of Super-Elso, 19: 41008 (EURAEC-1407)
CHROMIUM SULFATES
radiolysis of hydrated, yields in, 19: 40610
CHROMIUM SYSTEMS
Cr–MgO_2, development of ductile composites of, with improved strength and oxidation resistance, 19: 41022(R) (NP-15292)
CIRCUITS
design for amplifiers in semiconductor detectors, (E), 19: 40899
design of chassis mounting standardization system for, 19: 42226 (UCRL-12117-T)
design of numerical adapted filters for analyzing spectrometer data, (E), 19: 40906
design of stable linear pulse-adding, (E), 19: 40726
measurements in, uncertainties of, 19: 42218 (SC-TM-64-509)
operations of transistorized, in saturation state, (E), 19: 40856
performance reliability of, computer program for analysis of, 19: 40848 (SC-R-65-935)
CITRIC ACID
preparation of actinides and lanthanides from, by solvent extraction using amines, 19: 40657
CLEANING SOLUTIONS
for removing oxide and scale from aluminum and its alloys, 19: 42202 (HW-64483)
CLOUD CHAMBERS
design of 340-liter expansion-condensing, 19: 40887
particle track photographs from, semiautomatic device for measurement of, 19: 40888
CLOUDS
dispersion and sedimentation of particulate, in upper atmosphere, 19: 41112 (SC-DC-65-1312)
COAL
gasification of, development of reactor-powered system for, 19: 42127(R) (TID-22009)
radioinduced hydrogenation, hydrocracking, and hydrofining of extract of, beta, 19: 40553(R) (NYO-2978-34)
COATINGS
bonding to substrate, ultrasonic methods of inspecting, 19: 40756

book: *Irradiation Effects in Cladding and Structural Materials*, 19: 41107
compatibility with graphite–nitrogen environment at 1000 and 1200°C, 19: 40966 (BNWL-92)
deposition of shock absorbing, on reactor fuel material or poisons, 19: 40992(P)
deposition on nuclear fuel particles, rotating-drum method for, 19: 40982 (ORNL-3819)
thickness measurements on, method for production of x rays of particular wavelengths for, 19: 41163(P)
wear characteristics of plated, for use in rotary switches, 19: 42216 (SC-DR-65-269)

COBALT
determination in copper by activation, 19: 40422
determination in neutron flux monitor wires, automated, 19: 40405 (CONF-650919-1)
effects on phase transformation in plutonium, 19: 40958
effects on phase transformations in delta-stabilized gallium–plutonium alloys, 19: 40958
magneto-optic properties, 19: 41084
separation from uranium by chromatography on cellulose columns, tracer studies of, 19: 40687
solvent distribution in ammonium thiocyanate–methanol–water systems, distribution coefficients for, 19: 40447

COBALT ALLOYS
analysis for niobium and tantalum, photometric method for, 19: 40442
Al–Co, analysis of neutron flux monitor wires for cobalt, automated, 19: 40405 (CONF-650919-1)
Co–Cu, radiation effects on properties of, fast neutron, 19: 41095(T) (ORNL-tr-667)
Co–Gd, magneto-optic properties of intermetallic compound $GdCo_5$ in, 19: 41084
Co–Nd, magneto-optic properties of intermetallic compound $NdCo_5$ in, 19: 41084
Co–Sm, magneto-optic properties of intermetallic compound $SmCo_5$ in, 19: 41084
Co–W, temper hardening properties, 19: 40961
Co–Y, magneto-optic properties of intermetallic compound YCo_5 in, 19: 41084
Cr–Co–Fe–Mn–Mo–Ni–W, corrosion of Ruonel, by coal gasification products at high temperatures, 19: 42127(R) (TID-22009)

COBALT COMPLEXES
with α, β, γ, δ-tetraphenylporphines, retentions in Szilard-Chalmers (n,γ) recoil reactions in, 19: 40612

COBALT ISOTOPES Co-57
Mössbauer spectra for 14.4-kev gamma rays from, nuclear polarization effect on, (T), 19: 42001

COBALT ISOTOPES Co-58
cross section ratios from manganese-55 (α,n) reactions to 42 Mev, isomeric, (E), 19: 41695
cross-section ratios from manganese-55 (α,n) reactions, statistical model for isomeric, 19: 41696
yields of isomer pairs of, from deuteron reactions with cobalt-59, 19: 41715

COBALT ISOTOPES Co-59
alpha inelastic scattering at 43 Mev, (E), 19: 41760
deuteron reactions (d,t) at 18.1 to 26 Mev, yields of cobalt-58 isomer pairs in, 19: 41715

COBALT ISOTOPES Co-60
deposition, computer program for evaluating radiochemical data on, 19: 40636 (WAPD-TM-516)

COBALT ISOTOPES Co-64
decay of, probability ratio of electron-capture, 19: 41800(T)

COBALT SULFATES
radiolysis of hydrated, yields in, 19: 40610

COBALT SYSTEMS
Co–Nb–Si, crystal structure of compounds in, 19: 41069
Co–TaC–TiC–WC, properties for liquid-metal pump seals, 19: 40718 (TIM-909)
Co–WC, properties for liquid-metal pump seals, 19: 40718 (TIM-909)

COINCIDENCE CIRCUITS
design for measurement of fast-neutron correlations, 19: 40894
separation element for nanosecond, photomultipliers for, 19: 40872 (JINR-P-2203)

COINCIDENCE COUNTERS
performance of β-γ, geometrical and statistical errors in, 19: 40874 (JUL-227-CA)
performance, for detection of gamma radiation produced by positron annihilation reaction, 19: 40390 (BNL-9384)

COINCIDENCE MEASUREMENTS
equipment design for, 19: 40927(P)

COLLIMATORS
radioactivity induced in 31-Mev Brown Boveri Betatron, 19: 41169 (NYO-3364-7)

COMPRESSORS
development of turbo-, with gas lubricated bearings, 19: 42127(R) (TID-22009)

COMPUTER PROGRAMS
AARDVARK, for optimization of irradiation and decay times in multi-element activation analysis, 19: 40451
BIJ, for determining position and thermal motion of atoms in crystals, FORTRAN II, 19: 41966 (LA-3310)
CMPXMAT, for transfer function evaluation, in FORTRAN-63 for CDC-1604-B, 19: 42222 (TIM-940)
DISAGL, for crystallographic interatomic distance and angle calculations, FORTRAN II and FAP, 19: 41965 (LA-3309)
FIEND, for fission energy deposition, 19: 40547(R) (AGN-8137(Vol.I))
for depth dose calculations for neutrons and protons, 19: 40372
for design analysis of direct-current electromagnetic pumps, FORTRAN 63 for CDC 1604, 19: 40743 (TIM-929)
for deuteron stripping angular cross section calculations, in FORTRAN for CDC-1604, 19: 41677 (ORNL-TM-1151)
for Moessbauer-spectrum analysis and calculation, (T), 19: 41724
for multigroup neutron diffusion equation, 19: 41649
for stellar evolution time-dependent calculations, 19: 41210(T) (N64-25282)
FOTRAC, for photon transport calculations, 19: 41957 (UCRL-14165)
input device for reading and translating handprinted FORTRAN, 19: 42211 (NYO-1480-19)
KINE, for particle interactions and decay analysis, in FORTRAN, 19: 41339 (UCRL-11648)
LAG, load and go assembler for accepting IBM-7090-FLOCO II instructions, in FORTRAN-63 for CDC-1604-B, 19: 42221 (TIM-939)
LEBC, for photon dosage calculations behind electron shields, for IBM 7090, 19: 41954 (NP-15338)
LIGHT, for gamma spectra from inelastic nucleon-nucleus collisions, for IBM 7090, 19: 41954 (NP-15338)
LMFC, for electron flux densities in Van Allen region, for IBM 7090, 19: 41954 (NP-15338)
LMFC, for proton flux densities in Van Allen region, for IBM 7090, 19: 41954 (NP-15338)
LPPC, for radiation dosage calculations behind proton shields, for IBM 7090, 19: 41954 (NP-15338)
LRSPC, for charged particle energy losses in matter, for IBM 7090, 19: 41954 (NP-15338)
LSSC, for proton spectral data conversion to differential number flux versus energy, for IBM 7090, 19: 41954 (NP-15338)
MIDAS, for waterdrop evaporation calculations, IBM 7090, 19: 41110 (BNWL-74)
MO608, for evaluating radiochemical data, FORTRAN, 19: 40636 (WAPD-TM-516)
MSGAM, for gamma dosage at exit face of proton shields, for IBM 7090, 19: 41954 (NP-15338)
MULTIOPT, for optimization of activation, 19: 40451
NET-1, for circuit reliability analysis, 19: 40848 (SC-R-65-935)
OPTIMIZE, for optimization of activation analysis, 19: 40451
OPTIPLOT, for optimization of activation analysis, 19: 40451
PARIS, analysis of bubble-chamber tracks, FORTRAN II for IBM 1620, (E), 19: 40915
RCELL, for crystal lattice transformation and cell reduction, FORTRAN for IBM 7074, 19: 41963 (IS-1141)
THERMOPYL, for calculating thermal neutron energy spectra in heterogeneous lattice cells, 19: 41648
TRACER, for crystal lattice transformation and cell reduction, FORTRAN for IBM 7074, 19: 41963 (IS-1141)
use in design of pneumatic scram system for reactors, 19: 42021
YORK-87, for phonon dispersion analyzing, in FORTRAN for IBM 7090, 19: 41962 (AERE-M-967)

COMPUTERS
feasibility of digital, for reactor control and data acquisition, 19: 42150 (ANL-7009)
input device for pattern recognition for handprinted FORTRAN programs, 19: 42211 (NYO-1480-19)
interface design for IBM 360/50, (E), 19: 41337 (NYO-2262-95)
programming for Garigliano Power Reactor data, 19: 42086(R) (EUR-2427.i)
teletype control from CDC-6600, engineering drawings of equipment for, 19: 40864
use for stress analysis in bellows, 19: 42208 (NAA-SR-4527(Pt.II))
use in NRU reactor control, 19: 42148 (AECL-2216)
use on-line for proton-proton scattering experiment analysis, 19: 41322 (BNL-9231)
use on-line with Savannah River Production reactors, 19: 42129

(DPSPU-65-30-27)
uses for on-line associative radiation analysis, (E), 19: 40918
CONCRETES
density measurements by gamma scattering, 19: 40755
leak analysis for reactor containment, 19: 42018 (NAA-SR-10100)
radioactivity of, development of low gamma background, 19: 40721 (UCRL-11454)
use of prestressed, in pressure vessels, 19: 40728(P)
CONFERENCES
see also introduction to Report Number Index
Advances in Upper Atmosphere Research, Corfu, July 1960, 19: 41605
Chemical Effects of Nuclear Transformations, Vienna, Dec. 7-11, 1964, Vol. 1., 19: 40614 (STI/PUB/91(Vol.I))
Deformation Twinning, Gainesville, Florida, March 21–22, 1963, 19: 41076
Electromagnetic Theory and Antennas, Symposium on, Copenhagen, June 25–30, 1962, Pt. 1, 19: 40862
Late Irradiation Effects Conference, Inventory of Capability, Germantown, 1963, 19: 40352 (WASH-1059)
Liquids, Structure, Properties, Solid Interactions, Warren, Mich. Sept. 1963, 19: 40538
Physics of Thin Ferromagnetic Films, Second All-Union Symposium on, Irkutsk, July 10–15, 1964, 19: 41039
Tenth Congress of the All-Union Pavlov Physiological Society, Erevan, 1964, 19: 40403(T) (FTD-TT-65-48)
topics in Biophysics, Columbia Univ., New York, 1964, 19: 42212 (NYO-3424-1)
CONSTANTS AND CONVERSION FACTORS
tissue current to dose, for nucleons below 400 Mev, 19: 40372
CONVECTION (FORCED)
through laminar boundary layers on flat plate, effects of wires near outer edge on, 19: 40746
CONVERSION ELECTRONS
angular distributions from oriented metastable cerium-137, 19: 41679 (UCRL-11462(Rev.))
spectra of iodine-132, (E), 19: 41743
spectra of, from fission fragments, 19: 41680 (UCRL-16184)
CONVEYERS
design of pneumatic, 19: 40729(P)
COPPER
analysis of, by activation, 19: 40422
corrosion by aluminum–silicon and water of coatings of, on uranium, 19: 40949 (ISC-640)
deposition on zinc-coated uranium, electrolytic, 19: 40949 (ISC-640)
deposition on Zircaloy-2, method of, 19: 40989
determination by spectrochemical methods, voltage-fluctuation patterns in, 19: 40416
determination in human lung tissue by neutron activation methods, 19: 40452
dislocation loops in quenched, 19: 41026 (UCRL-16024)
effects on superconductivity of niobium–tin alloys, (E), 19: 41609
electron and ion emission from cesiated and vacuum surfaces of, (E), 19: 41284
ion reactions at 5 to 12 Mev, neutron spectra from, (E), 19: 41810(T)
neutron reactions (n,γ) at 0.025 ev, spectra from, 19: 40896
neutron scattering by, dispersion relations for lattice vibrations from, (E), 19: 41996(T)
proton multiple scattering by thin films of, at 75 to 200 kev, (E/T), 19: 41273
separation by solvent extraction using 2A-hexanedione and 2-methylheptane-4,6-dione, 19: 40423
separation from uranium by chromatography on cellulose columns, tracer studies of, 19: 40687
sorptive properties of surfaces of, for iodine in high-temperature helium loop, 19: 40397 (ORNL-TM-1134)
thermal conductivity of, evaluation of cut bar method for measuring, 19: 41029
thermodynamic properties at high pressures and temperatures, 19: 40459 (NP-15324)
COPPER ALLOYS
Be–Cu, surface cleaning of, procedure for, 19: 40989
Ce–Cu–Pu, phase studies, 19: 41054
Co–Cu, radiation effects on properties of, fast neutron, 19: 41095(T) (ORNL-tr-667)
Cr–Ni, diffusion in, activation energy and frequency factor for self-, 19: 40961
Cu–Mg, bonding to aluminum, hot-press, 19: 40949 (ISC-640)
Cu–Mg, corrosion by aluminum–silicon and water of coatings of, on uranium, 19: 40949 (ISC-640)
Cu–Mg, deposition on uranium, hot dip, 19: 40949 (ISC-640)
Cu–Mn, copper-63 nuclear spin echoes in, (E/T), 19: 41988
Cu–Ni, brazing alloy for metallized alumina-to-niobium alloy seals, 19: 40980 (LA-3302)
Cu–rare earths, crystal structure of intermetallic compounds in, 19: 41040
Cu–rare earth, electric conductivity of CsCl-type phases in, 19: 41005 (CALT-221-11)
Cu–Zr, copper-63 nuclear spin echoes in, r-f excitation of, (E/T), 19: 41988
COPPER COMPLEXES
with α, β, γ, δ-tetraphenylporphines, retentions in Szilard-Chalmers (n,γ) recoil reactions in, 19: 40612
with ammonia, electron spin resonance spectra, 19: 40465 (UCRL-16175)
COPPER IONS
spectra in ammonia and water, electron spin resonance, 19: 40465 (UCRL-16175)
COPPER ISOTOPES
Cu–Nb, oxidation at 500 to 900°C, 19: 40976
Cu–Zr, oxidation at 500 to 900°C, 19: 40976
COPPER ISOTOPES Cu-63
neutron reactions (n,d) with, angular distributions from, (E/T), 19: 41755
nuclear spin echoes in copper–manganese and copper–zinc alloys, (E/T), 19: 41988
COPPER ISOTOPES Cu-65
neutron reactions (n,d) with, angular distributions from, (E/T), 19: 41755
COPPER SULFATES
radiolysis of hydrated, yields in, 19: 40610
CORROSION FILMS
structure of, on chromium–iron–nickel alloys, 19: 40967(R) (COO-1319-27)
COSMIC MESONS
intensities of K^+ and π^+, above 4 Bev, (E), 19: 41294
COSMIC MESONS (μ)
detection and measurement to 6000 mwe, (E), 19: 41293
detection at 200 mwe, from extensive air showers, (E), 19: 41297
energy loss calculations for, below 100 Tev, (T), 19: 41296
interactions in laminar media, gamma photons from, (E), 19: 41295
interactions with electrons at 5 to 50 Bev/c, (E/T), 19: 41313
polarization of, energy dependence of, (E), 19: 41294
production of high-energy, in air, (E/T), 19: 41291
reactions with nuclei around 1 Tev, particle distributions from, (T), 19: 41711
spectra above 100 Bev, during ionization bursts, (E), 19: 41292
COSMIC MESONS (π)
production in extensive air showers, by primary nucleons, (T), 19: 41300
production of high-energy, in air, (E/T), 19: 41291
COSMIC NEUTRINOS
flux of primary, (E), 19: 41306
interactions with nucleons, meson (μ) production in, (E), 19: 41306
COSMIC NEUTRONS
intensity variations during Forbush decrease, (E), 19: 41304
COSMIC NUCLEONS
interactions with atmospheric nuclei, showers from, (T), 19: 41300
COSMIC PARTICLES
energy spectra of primary helium, at 30 to 90 Mev/nucleon, (E), 19: 41302
intensity variations of nuclei $Z \geq 6$, 19: 41288(R) (NASA-CR-58203)
spectra of $(6 \leq Z \leq 20)$, satellite observations of, (E), 19: 41310
COSMIC PHOTONS
production in 1000-Tev extensive air showers, (T), 19: 41298
production of high-energy, in air, (E/T), 19: 41291
COSMIC RADIATION
cutoff of, magnetospheric tail effects on, (T), 19: 41307
detection of penetrating component of extensive air showers, at 200 Mwe, (E), 19: 41297
gamma spectra in 1000-Tev extensive air showers, (T), 19: 41298
hazards to passengers and crew of, in supersonic transport flight, 19: 40842
intensity distribution of r-f, determination using finite-pass-band spectrometer, (T), 19: 41301
intensity variations of, data for Sept. 1963, 19: 41603
intensity variations during Forbush decrease, (E), 19: 41304
intensity variations at high latitudes, (E), 19: 41303
monitoring on Kosmos and Vostok satellites, 19: 40841
properties of, research on, 19: 41571(R) (N64-29400)
quark production in, cross sections and intensities for, (E), 19: 41311
spectra in Forbush decreases, solar-cycle effects on, (E), 19: 41305
variations in, solar diurnal, (T), 19: 41241
COSMIC SHOWERS
analyses of, methods for geometric and kinematic, 19: 41290
detection of penetrating component of extensive air, at 200 Mwe, (E), 19: 41297

detection using coherent radiation from, (T), 19: 41308
distributions in electromagnetic, for primary energies around 1 Tev, (T), 19: 41711
gamma spectra in 1000-Tev extensive air, (T), 19: 41298
meson (μ) spectra above 100 Bev during ionization bursts, (E), 19: 41292
particle density and energy in extensive, (E), 19: 41309
production of extensive air, by primary nucleons, (T), 19: 41300
x-ray spectra in electromagnetic, at high altitudes, (E/T), 19: 41299
COSMOLOGY
matter in universe, Heisenberg uncertainty principle for creation rate of, 19: 41227
model of universe, (T), 19: 41236
COUNTING DEVICES
design and operation of automatic, for filter paper, 19: 40834(R) (UCRL-14151)
CRATER MISSILES
from Pre-Schooner detonations, 19: 40707 (PNE-502F)
CRATERS
dimensions of explosion-produced, compilation of data on, 19: 40711 (SC-RR-65-220)
dimensions of, from Pre-Schooner detonations, 19: 40707 (PNE-502F)
dimensions of, from 500-ton explosion on rock, 19: 40712 (SC-RR-65-277)
ejecta from Danny Boy, aggregate characteristics of, 19: 40709 (PNE-5003)
o-CRESOL
effects on use of chromogenic polymer for gamma dosimetry, 19: 40599
p-CRESOL
effects on use of chromogenic polymer for gamma dosimetry, 19: 40599
CRITICAL ASSEMBLIES
criticality studies in AETR, 19: 42077 (ANL-7014)
fuel element design and fabrication for ZPR-III, 19: 40978 (ANL-6955)
neutron decay constants in enriched-uranium, heavy water, pulsed, (E), 19: 42045(R) (MIT-2344-3, pp 55-108)
neutron kinetics in reflected, decay constants for, 19: 42040(R) (BNWL-95, pp 40-54)
neutron lattice parameters of two-region, enriched-uranium heavy water, 19: 42048 (MIT-2344-3, pp 125-36)
neutron migration area, multiplication factor, and reflector savings in TCA, 19: 42053
research programs on, at Siemens-Schuckertwerke laboratories, Erlangen, Germany, 19: 42228
CRITICALITY STUDIES
method for safety evaluation of packages for transport of fissile materials, 19: 40828 (SC-RR-65-98, pp 679-90)
neutron diffusion equation for, use of poison in direct solution of, 19: 42052
of low-assay uranium compounds in array of containers, 19: 40819 (SC-RR-65-98, pp 330-56)
CROSS SECTIONS
fluctuations of nuclear, finite-sample-size effects in, (T), 19: 41762
CRYOGENICS
book: *Solid State and Low Temperature Physics in the USSR*, 19: 42004
liquid depth measurement system for, 19: 40878 (UCRL-9672(Rev.))
CRYOSTATS
design for Mössbauer experiments at low temperatures, 19: 40863
design for neutron-diffraction studies, 19: 40852
design of liquid-helium, (E), 19: 41626
design of precision vacuum, for Moessbauer measurements, (E), 19: 40858
CRYSTAL STRUCTURE
book: *An Atlas of Models of Crystal Surfaces*, 19: 41072
dislocation kink chain in, entropy contributions to restoring force of, 19: 41983
CRYSTALLOGRAPHY
computer program for, 19: 41966 (LA-3310)
crystal lattice transformations, computer programs for, 19: 41963 (IS-1141)
interatomic distance and angle calculations, computer program for, 19: 41965 (LA-3309)
reduced cells in structural, 19: 41963 (IS-1141)
CRYSTALS
atom position and thermal motion in, 19: 41966 (LA-3310)
book: *An Atlas of Models of Crystal Surfaces*, 19: 41072
charged-particle reactions in lattices of, anisotropic effects in, (T), 19: 41789
Mössbauer effect in nonideal, theory of, 19: 41997(T)
phonon dispersion in, computer program for analyzing, 19: 41962 (AERE-M-967)
preparation of hollow cylindrical single, of tin, (E), 19: 40990
radiation stability of, with Coulomb binding, 19: 41975
radical luminescence of phosphor, electron-hole mechanism for, 19: 40480
rare-earth-ion spin-lattice relaxation time in, (T), 19: 41982
x-ray diffraction patterns of, engineering drawings of equipment for obtaining, 19: 40865
CURIUM
separation from aqueous solutions of organic acids by solvent extraction using high-molecular-weight amines, 19: 40657
separation from rare earths by solvent extraction using DTPA, 19: 40676
solvent extraction by thenoyltrifluoroacetone in benzene, 19: 40458 (JINR-P-2224)
CURIUM COMPLEXES
with lactic acid, stability constants, 19: 40458 (JINR-P-2224)
CURIUM ISOTOPES Cm-246
energy levels of, odd-parity rotational, (E), 19: 41794
CURRENT INTEGRATORS
design for use in pulsed-positive-ion accelerators, 19: 41183
design of nano-to-milliamp, (E), 19: 40843 (CEAL-1021)
CYANIDE COMPLEXES
spectra of pentacyanonitrosylchromium(II) ion, electron spin resonance, 19: 40465 (UCRL-16175)
CYANIDE IONS
exchange with pentacyanonitrosylchromium(II) ion, 19: 40465 (UCRL-16175)
CYCLOHEXANE
reactions with tritium recoil atoms, abstraction and substitution in, 19: 40621
alcohol–cyclohexane, energy transfer processes in reactions with tritium recoil atoms, 19: 40622
CCl_4–cyclohexane, formation of polymeric yields in reactions with carbon-14 and sulfur-35 recoil atoms, 19: 40628
CYCLOHEXENE
CCl_4–cyclohexene, formation of polymeric yields in reactions with carbon-14 and sulfur-35 recoil atoms, 19: 40628
CYCLOOCTATETRAENE
electron spin resonance of anionic, isotope effects in, 19: 40541
CYCLOPENTADIENE
reactions with ruthenium-106 trichloride, 19: 40634 (BNL-8405)
CYCLOPENTANE
reactions with recoil carbon-11, 19: 40550 (IS-T-27)
CYCLOPENTENE
reactions with recoil carbon-11, 19: 40550 (IS-T-27)
CYCLOTRON RADIATION
emission by electrons in homogeneous magnetic fields, (T), 19: 41393(T)
CYCLOTRONS
circuit design for isochronous, r-f, 19: 41172
development of 500-Mev, 19: 41179
ion injectors for, performance of, (E), 19: 41193
magnet design for Western Ontario microtron, 19: 41175
magnetic center plane in, Hall-effect measurement of, 19: 41195
use of separated-orbit, in production of high-intensity neutron beams, 19: 41174
CYLINDERS
electric surface currents and rotating magnetic field in polyphase dielectric, with skew pole pieces, (T), 19: 41152
magnetic field of, in field of current-carrying conductors, (T), 19: 41151
magnetic flux penetration into type-II superconducting, (E/T), 19: 41612
CYMENE
dielectric polarization of, temperature dependence, 19: 40468(T) (SC-T-65-721)
CYTIDYLIC ACIDS
reactions of polyribonucleotides of, with cerium, lanthanum, and lutetium, 19: 40474
CYTOPLASM
radiation effects on rabbit, biochemical, 19: 40375

D

DATA RECORDING SYSTEMS
development for use with 32-position positron scanner, 19: 40390 (BNL-9384)
performance of oceanographic, in shallow-water tests, 19: 42210(R) (NVO-98-8)
DATA TABULATIONS
book: *Thermal Radiative Properties*, 19: 41074
cosmic, geophysical, and solar data for Sept. 1963, 19: 41603
craters produced by explosions, dimensions of, 19: 40711 (SC-RR-65-220)
on radioactivity of atmosphere and sea water, 19: 40792
thermal capacity of rare earths, 4f electronic contributions to, 19: 40457 (IS-1156)
thermodynamic properties of metals at high pressures and temperatures, 19: 30359 (NP-15324)
DECONTAMINATION

methods for fissiochemical products, 19: 40547(R) (AGN-8137(Vol.I))
of light equipment, facility for, 19: 40836
of storage basin water from cesium-137 and strontium-90, 19: 40651 (IDO-14657)
procedures for, following reactor accidents, 19: 42006 (IDO-10043(Vol.II) (Rev.1))
DECONTAMINATION OF EQUIPMENT
facility for, design of, 19: 40836
procedures for, following reactor accidents, 19: 42006 (IDO-10043(Vol.II) (Rev.1))
DECONTAMINATION OF PERSONNEL
procedures for, following reactor accidents, 19: 42006 (IDO-10043(Vol.II) (Rev.1))
DENSITOMETERS
design and calibration of gamma radiometric, 19: 40755
DETONATION WAVES
hydrodynamic properties of, technique for observing, 19: 41118 (LA-DC-6996)
interactions in condensed explosives, 19: 42205 (LA-DC-6990)
stability of, analysis of asymptotic, (T), 19: 41117 (LA-3306)
DEUTERIUM
argon ion reactions with molecular, spectra of ArD^+ in, (E), 19: 41251
carbon monoxide ion reactions with molecular, spectra of COD^+ in, (E), 19: 41252
deuteron reactions (d,n) and (d,p) at 20 to 300 kev, angular distribution from, (E), 19: 41832
diagnostics of plasma of, using tritium pulsed atomic beam, (E), 19: 41923
effects in reaction of 2,4-dinitrophenyl phenyl ether with piperidine in benzene, kinetics of, 19: 40544
effects in recoil tritium reactions, molecule yield measurements of kinetic, 19: 40615
effects on chromatographic behavior of methane, 19: 40672
effects on ESR in cyclooctatetraene anions, 19: 40541
electron reactions with, relativistic theory for fission, 19: 41374
electron reactions with, radiative corrections to fission, (T), 19: 41752
exchange between fluorimide and heavy water or deuterated trifluoroacetic acid, 19: 40537
exchange between liquid ammonia and hydrogen for production of heavy water, 19: 40942(P)
gamma reactions (γ,n), laboratory observation of, 19: 41712
gamma reactions at 165 to 210 Mev, meson (π) production in, (E), 19: 41344
ion reactions with molecular, spectra of XD^+ in, (T), 19: 41250
nitrogen ion reactions with molecular, spectra of N_2D^+ in, (E), 19: 41252
proton scattering by, (T), 19: 41763
sorption by molybdenum at room temperature, 19: 40463(R) (SRIA-425-S)
DEUTERIUM IONS
reactions with molecular nitrogen ions at 10 to 65 kev, rotational and vibrational excitation in, (E), 19: 41279
DEUTERIUM SYSTEMS
D–H, sorption by molybdenum at room temperature, 19: 40463(R) (SRIA-425-S)
DEUTERONS
angular correlations in carbon-12 (p,pd) reactions at 155 Mev, (E), 19: 41703
binding energy of, nonrelativistic and relativistic theories for, 19: 41474
emission from proton relations with heavy nuclei at 157 Mev, (E), 19: 41831
form factors in induced decays, wave functions for, (T), 19: 41[illegible]
interactions with electrons, neutron electromagnetic form factors from, (E), 19: 41326 (HUX-2752-9)
interactions with hyperons (Λ) at low energies, (T), 19: 414[illegible]
interactions with electrons, meson-exchange effects in, (E), 19: 41453
interactions with neutrons, singularities of amplitudes for elastic, (T), 19: 41504
interactions with mesons (π^+), partial wave dispersion relations for disintegration in, 19: 41336 (NP-15335)
interactions with electrons, relativistic theory for fission, 19: 41374
meson (μ) capture by, neutron spectra from, (T), 19: 41782
photodisintegration cross sections for, (T), 19: 41824
production in proton-proton interactions at 1.5, 2.5, and 2.9 Bev, cross sections for, (E), 19: 41523
reactions (d,α) and (d,He-3) with calcium-40 at 15.14 Mev, isobaric spin selection rules from, (E), 19: 41720
reactions (d,α) with aluminum-27, phosphorus-31, and sodium-23 at 9.3 Mev, (E), 19: 41684
reactions (d,α) with oxygen-16 at 15.14 Mev, isobaric spin selection rules from, (E), 19: 41720
reactions (d,α) with nuclei, differential cross sections for, (T), 19: 41817
reactions (d,d'γ) with cerium-140, neodymium-142, and samarium-144, 0+ states from, (E), 19: 41747
reactions (d,n) and ^{3}(d,p) with nuclei, computer program for stripping angular cross section in, 19: 41677 (ORNL-TM-1151)
reactions (d,n) and (d,p) with deuterium at 20 to 300 kev, angular distribution from, (E), 19: 41832
reactions (d,n) with boron-11 at 1 to 11 Mev, angular distributions from, (E/T), 19: 41732
reactions (d,p) in nuclear Coulomb field, spectroscopic factors for, (T), 19: 41739
reactions (d,p) with carbon-12 at 0.9 to 2.0 Mev, angular distribution for, 19: 41721
reactions (d,p) with chromium-52 and -54 at 10 Mev, energy levels from, (E), 19: 41726
reactions (d,p) with nuclei, DWBA and Coulomb stripping approximations for, (E), 19: 41742
reactions (d,p) with medium-weight nuclei at 28 Mev, isobaric analog states from, (E/T), 19: 41772
reactions (d,p) with even-A samarium isotopes at 12 Mev, energy level structure of odd-A isotopes from, (E), 19: 41778
reactions (d,p) with yttrium-89, isomeric cross section ratios for, (E), 19: 41820
reactions (d,p) with iron-56, at 2.8 Mev, Mössbauer effect from, (E), 19: 41793
reactions (d,t) with helium-3 at 20 and 25 Mev, energy spectra from, (E), 19: 41658 (IAE-655)
reactions (d,t) with scandium-45 at 19 to 28.6 Mev, yields of scandium-44 isomer pairs in, 19: 41714
reactions (d,t) with cobalt-59 at 18.1 to 26 Mev, yields of cobalt isomer pairs in, 19: 41715
reactions with lithium-7 at 340 to 780 kev, resonances in, (E), 19: 41697
DIAMONDS
radiation effects on absorption spectra in infrared, ultraviolet, and visible regions, 19: 41098
DIDO REACTORS
cooling system testing for FRJ-2, secondary, 19: 42153 (JUL-235-RE)
DIET
calcium content of cattle, effects on strontium-90 transfer to milk, 19: 40341
effects of constituents in, on strontium-90 metabolism in animals, 19: 40342
effects on strontium-90 absorption by milk cows, 19: 40332
mineral content of Japanese and U. S., cesium, iron, and manganese, 19: 40781(R) (NP-15179)
radioactivity of Alaskan, fallout, 19: 40780 (BNWL-SA-242)
strontium content in seafood, population contamination by, 19: 40309(R) (NP-15180)
DIFFERENTIAL EQUATIONS
book: *A Collection of Problems on Mathematical Physics*, 19: 41153(T)
book: *Differential Equations and Their Applications*, 19: 40945
difference equations of dynamics in hamiltonian form, 19: 41145
DIFFUSION
book: *Energetics in Metallurgical Phenomena*. Vol. I, 19: 41075
DILATOMETERS
construction of, for density change measurements in liquids or solutions, 19: 40523
DILATOMETRY
method for refractory metals at high temperatures, optical, 19: 41009 (GEMP-375)
DIMETHYLAMINE
separation from other amines by ligand exchange on cation exchanger, 19: 40648 (COO-499-2)
DIODES
charge carrier trapping in lithium-drifted germanium, in gamma detection, (E), 19: 40919
radiation effects on gallium arsenide and silicon, alpha, 19: 40937 (UCRL-11958)
radiation effects on 5-Mc magnetic germanium tunnel, neutron, 19: 40939
response of cesium to potential pulses, (T), 19: 41318
DIRECT ENERGY CONVERSION DEVICES
review, 19: 41319
DISEASES
case history of encephalomyelopathy, 19: 42219 (TID-21177)
DITHIZONE
use in cellulose acetate column to extract zinc from aqueous solution, 19: 40642 (AERE-R-4969)
DODECANE
reactions with iodine compounds, 19: 40402 (BMI-X-10137)
DODECANE, 1-CYCLOHEXYL-1-PHENYL–

radiolysis of, ESR of radicals in, 19: 40607
DOGS
pathological effects of injected yttrium-91 in, 19: 40377
pathological effects of injected strontium-90 in, 19: 40378
pathological effects of injected plutonium-239 on hematopoietic system of, 19: 40379
pathological effects of injected plutonium-239 in, 19: 40382
radiation effects on nervous system activity in, chronic, 19: 40356(T) (FTD-TT-65-48, pp 469–70)
radiation injuries, protective effects of bone marrow injections, 19: 40385(T) (FTD-TT-65-48, pp 134–5)
radiation sickness in, treatment of, 19: 40387
strontium-90 metabolism in, after chronic ingestion, 19: 40324
strontium-90 metabolism in, after chronic ingestion, 19: 40325
strontium-90 metabolism in, after chronic ingestion, 19: 40327
strontium-90 transfer by milk and placenta of female, to offspring, 19: 40327
DOSIMETERS
calibration of film, for high energy gamma radiation, 19: 40909
design for building monitoring for gamma radiation, engineering drawings of, 19: 40926
development of infrared-stimulated luminescent, 19: 40879 (UCRL-12371)
health physics, dose equivalent estimation in, 19: 40911
performance and properties of emulsion, 19: 40889
performance of gamma and neutron, 19: 40868 (BNWL-SA-23)
performance of lithium fluoride gamma, in high neutron fluxes, 19: 40834(R) (UCRL-14151)
radiation effects on fluoro-, 19: 40588
readout instrument for lithium fluoride and manganese-activated calcium sulfate thermoluminescent, 19: 40877 (RISO-101)
DOUNREAY FAST REACTOR
fuel of, fission product heating of plutonium, (E), 19: 42114
gamma heating of materials in, (E), 19: 42117
operation efficiency, 19: 42116
DRAWING
wall thickness changes during sink, factors influencing, 19: 40983(T) (ANL-Trans-189)
DRESDEN POWER REACTOR
coolants for, evaluation of performance of fog as, (E), 19: 42020
DROPS
evaporation of water, computer program for, 19: 41110 (BNWL-74)
gas absorption by traveling, on vertical wire, 19: 40398 (UCRL-16047)
DRUGS
evaluation of effectiveness of several, for treatment of poisoning by radioactive metals, 19: 40339
DRY BOXES
design for fabrication and encapsulation of irradiated urania pellets, 19: 40715 (NAA-SR-Memo-7438)
DUSTS
composition, distribution, and origin of cosmic, 19: 41113
DYSPROSIUM
determination by spectrochemical methods, voltage-fluctuation patterns in, 19: 40416
determination in iron–rare earth alloys and medium alloyed steels, 19: 40445
effects on properties of tantalum, 19: 41067
magnetic properties at high pressures, (E), 19: 42005
magnetic transitions in, effects of hydrostatic pressure on, 19: 41077
neutron reactions (n,α) with, cross sections for thermal, (E), 19: 41809(T)
physical and thermodynamic properties, 19: 40948 (IS-1195)
polarographic behavior in dimethylformamide and dimethylsulfoxide, 19: 40681
preparation and purification, 19: 40948 (IS-1195)
radiation effects on optical properties of calcium fluoride crystals containing, gamma, 19: 40600(T)
DYSPROSIUM ALLOYS
Dy–Au, phase studies of solid solutions in, 19: 41062
Dy–Mg, phase studies, 19: 41011 (IS-T-15)
Dy–Mg, thermodynamic properties, 19: 41013 (IS-T-25)
DYSPROSIUM CARBIDES
eutectic temperature between carbon and dicarbide, 19: 41014 (LA-DC-6819)
lattice parameters and phase transformation temperatures in, 19: 41014 (LA-DC-6819)
microhardness, 19: 41014 (LA-DC-6819)
DYSPROSIUM CHLORIDES
complexes with phenanthroline, preparation and properties, 19: 40514
DYSPROSIUM COMPLEXES
with gluconic acids, stability constants, 19: 40508
DYSPROSIUM IONS
spectra in acetophenone, energy transfer in, 19: 40504
DYSPROSIUM ISOTOPES Dy-158
energy levels from beta decay of terbium-158, (E), 19: 41847
DYSPROSIUM ISOTOPES Dy-159
energy levels from gamma and conversion spectra of, isomeric, (E), 19: 41736
DYSPROSIUM ISOTOPES Dy-160
energy levels of, vibration-rotation interactions in, (T), 19: 41818
DYSPROSIUM ISOTOPES Dy-161
neutron strength functions for, target spin dependence of, 19: 41656 (BNL-9245)
DYSPROSIUM ISOTOPES Dy-162
neutron strength functions for, target spin dependence of, 19: 41656 (BNL-9245)
DYSPROSIUM ISOTOPES Dy-163
neutron strength functions for, target spin dependence of, 19: 41656 (BNL-9245)
DYSPROSIUM OXIDES
content in McKelveyite uranium mineral, 19: 40799
DYSPROSIUM PERCHLORATES
stability constants of, thermal, 19: 40509

E

EARTH
space vehicle motion under influence of moon and, (T), 19: 41205 (N64-31725)
ECOLOGY
of fish in Kentucky stream, 19: 42220 (TID-22023)
of insect populations in irradiated forest, 19: 40307 (BNL-9253)
of northern Alaska, 19: 40780 (BNWL-SA-242)
EINSTEINIUM
separation from rare earths by solvent extraction using DTPA, 19: 40676
ELECTRIC ARCS
heat transfer from, by natural convection, (T), 19: 41914
light absorption coefficient of, measurement of, (E), 19: 41898
properties in plasmatron, (E/T), 19: 41913
voltage fluctuations in d-c, in spectrochemical analysis, 19: 40416
ELECTRIC CHARGES
distribution in gas-particle plasma, (T), 19: 41929
separation in thermodynamic-equilibrium plasma in constant gravity field, (T), 19: 41919
ELECTRIC CONDENSERS
charged-particle beam in field of, space-charge effects on energy dispersion and focusing of, (T), 19: 41196
design of high-voltage high-current r-f, with Q above 2000, (E), 19: 40844 (MATT-341)
ELECTRIC CONDUCTORS
magnetic field of current-carrying, induced in cylinder, (T), 19: 41151
thermal capacity measurement in, pulse heating calorimetric method for, 19: 40700 (ORNL-TM-1187)
ELECTRIC CURRENTS
configuration of surface, in polyphase system with skew pole pieces, (T), 19: 41152
distribution in coaxial plasma gun, (E), 19: 41859 (NP-15218)
ELECTRIC DISCHARGE
book: *Electron Avalanches and Breakdown in Gases*, 19: 41938
ELECTRIC FIELDS
charged particle motion in, effects of fringing fields on, (T), 19: 41139
charged-particle motion in, (T), 19: 41142
charged-particle motion in oscillating, (T), 19: 41155
distribution in current-carrying layer of magnetoactive plasma, (T), 19: 41882
effects on boiling heat transfer at 300 psi, 19: 40735(R) (NYO-2404-5)
effects on radioinduced polymerization of solid acrylonitrile, 19: 40582
plasma polarization in, (T), 19: 41906
ELECTRIC INSULATORS
effects of electron bombardment on electric conductivity of, 19: 41097
ELECTRIC POTENTIAL
distribution in gas-particle plasma, (T), 19: 41929
ELECTRIC PROBES
impedance of Langmuir, in plasma, (E/T), 19: 41949
plasma flow around, hypersonic rarefied, (T), 19: 41894
response to plasma, equations for low-frequency, 19: 41948
use in diagnostics of plasma column, (E/T), 19: 41868
ELECTROCHEMISTRY
thermodynamics of electrode processes, 19: 40500
ELECTRODES
design and testing for ion rocket engines, 19: 40765(R) (NP-15309)
ELECTROLYTES
statistical mechanics of, with type-dependent intermolecular potentials,

(T), 19: 41130
ELECTROMAGNETIC FIELDS
charged-particle motion in symmetrical, hamiltonian for, (T), 19: 41538
charged-particle motion in, (T), 19: 41142
control of, in proton linac resonant cavities, 19: 41167 (NIRL/R/76)
diffraction of, from charged particle moving in conducting semiplane, 19: 41539
elementary-particle motion in slowly varying, relativistic, (T), 19: 41423
equations for isospin and, in rigid-sphere model of elementary particles, 19: 41473
induction problems in, solutions for i-f, (T), 19: 41125 (ORNL-TM-1185)
oscillations of terrestrial, connection with aurora polaris intensity variations, 19: 41575(T) (FTD-TT-65-112)
plasma acceleration in, plasmoid structure in, (E), 19: 41908
tensor field for, from neutrino 1-spinor fields, (T), 19: 41348
ELECTROMAGNETIC LENSES
spherical aberration of combined quadrupole electrostatic and, with bell-shaped field distribution, (T), 19: 41198
ELECTROMAGNETIC PUMPS
analysis of direct-current, 19: 40743 (TIM-929)
testing of, gallium loop for, 19: 40727
ELECTROMAGNETIC SEPARATION PLANT (Y-12)
control of production schedules and costs at, real-time information system for, 19: 40702 (Y-KA-9)
ELECTROMAGNETIC SHIELDING
development for space vehicles, 19: 41952(R) (N64-31552)
ELECTROMAGNETIC WAVES
conference, 19: 40862
emission by electrons in plasma, (T), 19: 41933
excitation in earth-ionosphere cavity by high altitude nuclear explosions, (T), 19: 41581
interactions in nonlinear transmission lines, (T), 19: 41136
interactions with electron beams and plasma, effects on stability, (T), 19: 41849 (AD-426079)
interactions with isotropic plasma, harmonic current and wave excitation in, (T), 19: 41927
propagation in bounded plasma perpendicular to magnetic field, damping in, (T), 19: 41917
propagation of surface, in nonuniform plasma, resonance effects in, (T), 19: 41916
propagation of TE_{11}, through plasma in circular waveguide, (E), 19: 41903
ELECTROMAGNETISM
elementary particle models in, (T), 19: 41377
induction problems in, solutions for i-f, (T), 19: 41125 (ORNL-TM-1185)
ELECTRON BEAMS
aberrations of, evaluation of space-charge-produced, (T), 19: 41173
effects of 500-kev, on efficiency of silicon solar cells, 19: 40931 (AD-609424)
effects on conductivity of n-type silicon, 19: 40935 (SC-DC-65-1247)
effects on graft-polymerization, 19: 40596
effects on photoconductivity of silicon semiconductors, 19: 40933(R) (NP-15300)
effects on photoconductivity of silicon semiconductors, 19: 40934(R) (NP-15301)
effects on photoconductivity of aromatic compounds, 19: 40601(T)
effects on ultrapure silicon crystals, 19: 41998(T)
electromagnetic waves in, effects on stability, (T), 19: 41849 (AD-426079)
interactions with laser beams, Compton scattering in, (E), 19: 41328 (IS-1187)
monitoring and calibration of, CEA, equipment for, 19: 41164 (CEAL-1022)
performance of pulsed relativistic, for plasma diagnostics, (T), 19: 41920
phase length measurement in pulsed, (T), 19: 41189
production of trochoidal, with reduced orbital motion, (T), 19: 41134
shutter design for accurate exposure timing of, (E), 19: 41186
spectroscopy in two-sector electrostatic analyzer, angular aberrations in, (E), 19: 41197
velocity measurement instruments for, characteristics of Moellenstedt, (E), 19: 40883
ELECTRON MICROSCOPY
analysis of dislocation loops in quenched fcc metals, 19: 41026 (UCRL-16024)
use in morphological study of coprecipitated plutonium dioxide–uranium dioxide powders, 19: 41024 (NUMEC-2389-5)
ELECTRON PAIRS
photoproduction of, radiative corrections to cross section for, (T), 19: 41500
production by fast mesons (μ), relativistic corrections for, (T), 19: 41486(T)
production by internal bremsstrahlung in meson (π) decay, (T), 19: 41482(T)
ELECTRON SHOWERS
analysis of cascade showers by solving inverse problem, (T), 19: 41710
distributions in electron-photon, in condensed media, (T), 19: 41707
distributions in, for primary energies around 1 Tev, (T), 19: 41711
electromagnetic cascade theory, angular distribution functions in, (T), 19: 41359
spectra in extensive a showers from 1000-Tev primaries, 19: 41298
x-ray spectra in, in cosmic showers at high altitudes, (E/T), 19: 41299
ELECTRON SOURCES
design for secondary emission studies, 19: 41124(R) (NP-15108)
performance of hollow-cathode, (E/T), 19: 41872
performance of large-diameter low-voltage, in plasma oscillation studies, (E), 19: 41946
ELECTRON TUBES
development, 19: 41124(R) (NP-15108)
performance of klystron, for Stanford electron accelerator, 19: 41170 (SLAC-42)
performance of magnetron with paired resonator system, 19: 41191
performance of 2860 Mc magnetron in bunch injector, (E), 19: 41188
ELECTRONIC EQUIPMENT
design for remote measurements in radiation environment, (E), 19: 40714 (EUR-2421.d)
design for use in proton-resonance measurements, (E), 19: 40857
design of chassis mounting standardization system for, 19: 42226 (UCRL-12117-T)
design of linear gate using transistors operating in saturation state, (E), 19: 40856
design of multiplexers, for use with self-powered neutron flux detectors, 19: 40866 (AECL-2217)
design of numerical adapted filters for analyzing spectrometer data, (E), 19: 40906
design of stable linear pulse-adding circuits, (E), 19: 40726
design of standardized modular, for ion sources, (E), 19: 41185
electromagnetic wave interactions in nonlinear transmission lines, (T), 19: 41136
radiation effects on, nuclear explosion, (T), 19: 40938
ELECTRONICS
measurements in, uncertainties of, 19: 42218 (SC-TM-64-509)
research programs on, 19: 40396(R) (HMI-B-39)
ELECTRONS
acceleration and precipitation of solar wind, in magnetosphere, (T), 19: 41583
Auger emission from molybdenum and tungsten surfaces by argon and mercury ions, (E), 19: 41272(T)
book: *Electron Avalanches and Breakdown in Gases*, 19: 41938
book: *The Theory of Electron-Atom Collisions*, 19: 41282(T)
capture by helium ions in scattering by helium atoms, resonant, (E), 19: 41280
compression coefficient in collisionless plasma, (E), 19: 41892
containment in magnetic mirror machines, 19: 41858 (NP-15217)
content in ionosphere, diurnal variations of, (E), 19: 41597
content in topside ionosphere, (E/T), 19: 41587
cyclotron radiation in homogeneous magnetic fields, (T), 19: 41393(T)
density and energy in cosmic showers, (E), 19: 41309
density in plasma, microwave system for measurement of, 19: 41854 (MATT-369)
density in sporadic-E region, (E), 19: 41591
diffusion in outer radiation zone, inward radial, (E), 19: 41578
distribution and temperature in cesium plasma, in low-voltage arc, (E), 19: 41909
distribution in high-energy meson (μ) showers, 19: 41355
distributions in outer radiation belts, effect of solar flare on, (E), 19: 41312
dosimetry of 15-Mev, calorimetric measurement of, 19: 40910
effect on pyrolysis of terphenyls, 19: 40630
effects on absorption spectra of Yakutian diamonds, 19: 41098
effects on electric conductivity of cadmium sulfide, 19: 41097
effects on oxygen desorption from tungsten, 19: 41103(T)
effects on positive oxygen ion production in light and heavy water, 19: 40581
effects on zinc sulfide luminescence, (E), 19: 40587
electromagnetic radiation from, in plasma, (T), 19: 41933
emission by gamma-irradiated metal slabs at 1.02 Mev, 19: 41956 (SC-R-65-933)
emission by nuclei, angular correlation measurements in, (T), 19: 40900
emission during K-electron capture, (T), 19: 41825
emission from cesiated beryllium, copper, nickel, and 304 stainless steel

surfaces, (E), 19: 41284
emission in mesons (μ^-) decay from mesonic helium atoms, Michel parameter for, (E), 19: 41480(T)
emission in reactions of positive ions with nickel surfaces, isotopic effects in, (E), 19: 41249
flux densities in Van Allen region, computer program for mapping, 19: 41954 (NP-15338)
gases of, kinetic equations for photon interactions in, 19: 41940
interactions in nitrogen afterglow plasma, probability of momentum-transfer in, (E/T), 19: 41944
interactions in superconductors, isotropic model for coulombic, 19: 41627(T)
interactions of bound, with neutrons, (E), 19: 41274
interactions with deuterons, neutron electromagnetic form factors from, (E), 19: 41326 (HUX-2752-9)
interactions with deuterons, meson-exchange effects in, (E), 19: 41453
interactions with photons in meson (η) decay, (T), 19: 41457
interactions with antineutrinos, differential and total cross sections for, (T), 19: 41481(T)
interactions with electrons and positrons in crossed beams at 1 to 250 Bev, cross sections for, (T), 19: 41493(T)
interactions with cosmic mesons (μ) at 5 to 50 Bev/c, (E/T), 19: 41313
interactions with electrons, Williams-Weizsacker covariant method for virtual-photon and meson (π^0) production in, (T), 19: 41349
interactions with deuterons, relativistic theory for fission, 19: 41374
interactions with positrons, meson (π) resonance effects in, (T), 19: 41386
motion in field of hydrogen atom, free-free matrix elements for, (T), 19: 41266
motion in helium atom, asymptotic solution of Schroedinger equation for, (T), 19: 41565
motion in magnetic fields, diochotron and negative mass instabilities in, 19: 41180
motion in plasma, inner field fluctuation effects on impedance of, (T), 19: 41853 (LA-DC-6603)
oscillations in plasma, (E), 19: 41907
photoemission from colored alkali halide crystals, mechanisms for, 19: 41979
photon absorption in high-density gases of, total cross section for, (T), 19: 41140
production and stability of plasma of, 19: 41863 (NP-15302)
production rate in ionosphere from overhead sun, (E/T), 19: 41598
radio emission by nonthermal, in ionosphere, (T), 19: 41229
radioinduced formation of solvated, in ice and frozen solutions, 19: 40551
reactions (e,e′p) with aluminum-27, carbon-12, and sulfur-32, proton binding energy from, 19: 41660 (ISS-65/3)
reactions in condensed matter at high energies, (T), 19: 41707
reactions with alkali metal halides at 0.2 to 4 kev, secondary emission in, 19: 40503(T)
reactions with atmospheric atoms and ions, removal, (T), 19: 41569 (AD-426145)
reactions with deuterium, relativistic theory for fission, 19: 41374
reactions with deuterium, radiative corrections to fission, (T), 19: 41752
reactions with ions and neutral particles in ionosphere, method for determination of frequency of, (T), 19: 41574(T) (FTD-TT-65-101)
reactions with molecular nitrogen ions, rotational and vibrational excitation in, (E), 19: 41279
reactions with neutral atoms, cross sections for excitation, (T), 19: 41254
reactions with rare gas mixtures at 50 kev, luminescence from, (E), 19: 41246
recombination and relaxation in partially ionized argon in laminar duct flow, (T), 19: 40749
scattering by alkali metal halides at 0.2 to 4 kev, inelastic, (E/T), 19: 40502(T)
scattering by beryllium-9, at 70 to 250 Mev, discrete and continuum states from, (E/T), 19: 41683
scattering by carbon-12 and oxygen-16, (T), 19: 41766
scattering by helium at 19.3 to 24.5 ev, resonances in inelastic, (E), 19: 41264
scattering by lithium and sodium at 0.003 to 25.0 ev, exchange effects and polarization in, (T), 19: 41286
scattering by magnetic moments of light nuclei at high energies, shell model for elastic, 19: 41694
scattering by nuclei, cross sections for, (T), 19: 41510
scattering by particles, radiative corrections to inelastic, (T), 19: 41752
scattering from germanium crystals, effects of sorbed sodium on, 19: 41124(R) (NP-15108)
scattering in thin films, calculation of inelastic, 19: 41961(T)
stopping by atmospheric oxygen due to rotational excitation, (T), 19: 41599
stopping by atmospheric nitrogen due to rotational excitation, (T), 19: 41600
temperature in acetylene–air flames, (E), 19: 41922
temperatures in helium theta-pinch plasma in azimuthal magnetic field, (E), 19: 41921
temperatures in theta-pinch plasma, (E), 19: 41860 (NP-15220)
transmission and reflection in thin films, measurement apparatus for, 19: 41124(R) (NP-15108)
transmission in aluminum- and silver foils at low energies, (E), 19: 41969 (ORNL-TM-1153)
tunneling in superconductors, theoretical review for Josephson, 19: 41607 (LA-3342)
tunneling in superconductors with photon emission, Cooper-pair, (E), 19: 41631
velocity distribution function in low-pressure cesium plasma in oscillation regime, (E), 19: 41877
velocity measurement instruments for, characteristics of Moellenstedt, (E), 19: 40883
yields from nickelate cathodes, 19: 41124(R) (NP-15108)

ELECTROSTATIC ANALYZERS
angular aberrations of two-sector, 19: 41197

ELECTROSTATIC FIELDS
charged-particle motion in, (T), 19: 41142
distribution from charged particle in plasma, (T), 19: 41933
Laplace equation for regions bounded by cylinders, solutions of, 19: 41150
production in ionosphere due to wind dynamo action, (T), 19: 41593

ELECTROSTATIC GENERATORS
cold traps for, liquid nitrogen distribution system for, 19: 41165 (LA-DC-7147)

ELECTROSTATIC LENSES
spherical aberration of combined quadrupole magnetic and, with bell-shaped field distribution, (T), 19: 41198

ELEMENTARY PARTICLES
bound states in short-range central potentials, (T), 19: 41439
bound states of, Faddeev-equation reduction for three-particle, 19: 41416
correlation functions for multiplication processes of, 19: 41330 (JINR-P-2213)
coupling constant relations for, in S-matrix theory, 19: 41382
decay amplitudes in U(12) symmetry, nonleptonic, (T), 19: 41420
decay of, computer program for analysis of, 19: 41339 (UCRL-11648)
decay of, systematics of angular and polarization distributions in three-body, 19: 41409
detection and measurement of Dirac magnetic monopoles, (E), 19: 41391
discoveries and theories in field of, review of, 19: 41512
electromagnetic properties in SU(6) symmetry, (T), 19: 41424
field theory for indefinite mass, generalized asymptotic condition in, (T), 19: 41343
field theory for, phenomenological, (T), 19: 41521
field-theory canonical formalism for vacuum and nonvacuum states, quantum, 19: 41475
interaction amplitudes for, normalization integrals of Bethe-Salpeter, (T), 19: 41434
interaction representation for stationary states of, 19: 41495
interactions of relativistic, multiple meson production in, (T), 19: 41708
interactions of spin-½, phase functions for noncentral, (T), 19: 41491(T)
interactions of spin-1, covariant polarization theory for, 19: 41526
interactions of strongly interacting, CT invariance in electromagnetic, 19: 41452
interactions of, absorptive corrections and form factors in peripheral model for high-energy, 19: 41400
interactions of, computer program for analysis of, 19: 41339 (UCRL-11648)
interactions of, CP violation and PT invariance in weak, 19: 41470
interactions of, cut-plane analyticity of momentum-space vertex function in, 19: 41558
interactions of, CP violations in SU(3) field theory for, (T), 19: 41371
interactions of, CP and $|\Delta I| = \frac{1}{2}$ violations in, 19: 41471
interactions of, detecting efficiency for, 19: 40873 (JINR-P-2215)
interactions of, dominance theorem in SU(2) and SU(3) groups for crossing matrices in, 19: 41469
interactions of, dynamical calculations of inelasticity in, 19: 41403
interactions of, effective potential for strong, (T), 19: 41451
interactions of, gauge groups for, (T), 19: 41365
interactions of, internal and space-time symmetries for strong, 19: 41516
interactions of, nonrelativistic and relativistic theories of bound states in, 19: 41474
interactions of, neutrino theory for electromagnetic and weak, (T), 19: 41387
interactions of, partially conserved axial-vector current for strong, (T),

19: 41450
interactions of, research on, (E/T), 19: 41337 (NYO-2262-95)
interactions of, review on theory of weak, 19: 41356
interactions of, radial equations for nonrelativistic quantum theory of, 19: 41360
interactions of, symmetrical quark model for selection rules in, 19: 41466
interactions of, S-matrix method for electromagnetic corrections to strong, (T), 19: 41511
interactions of, solution of partial-wave dispersion relations for, 19: 41394
interactions of, SU(4) symmetry for quartet scheme of weak, 19: 41415
interactions on neutral, long-range electromagnetic, (T), 19: 41448
interactions with electrons, radiative corrections to inelastic, (T), 19: 41752
mass formula in higher orders for, Okubo, (T), 19: 41490(T)
mass relations for, statistical study of linear, 19: 41408
mass spectrum of, anomalous thresholds and, (T), 19: 41351
model for, broken symmetry in oscillator, (T), 19: 41554
model for, electromagnetic-current operator in U-spin subgroup of SU(3), 19: 41341
model for, relativistic symmetry with isospin and spin in, 19: 41398
model for, SU(4) symmetry with isospin and spin in, 19: 41397
model of classical relativistic spinning, hamiltonian and lagrangian formalism for, 19: 41472
model of, electromagnetic field and isospin in rigid-sphere, 19: 41473
models for, description of electromagnetic, (T), 19: 41377
models of, Lie algebras for Lorentz invariance and internal symmetry in, 19: 41411
models of, mass splittings from quartet and triplet SU(3), 19: 41476
momentum measurements of, quantum effects on accuracy of, (T), 19: 41553
motion of relativistic, in slowly varying electromagnetic fields, (T), 19: 41423
polarization of scalar and vector, electrodynamic effects on, (T), 19: 41334 (JINR-P-2229)
position operators of nonlocal spinning stable, (T), 19: 41401
production of quarks in cosmic radiation, cross sections and intensities for, (E), 19: 41311
scattering amplitudes for, mass-splitting effects on symmetry relations between, (T), 19: 41430
scattering by soft core potential, energy gap equation for, 19: 41662 (JINR-P-2176)
scattering of, cross section and polarization change in potential, (T), 19: 41501
scattering of, dispersion relation for elastic, (T), 19: 41363
spinor model for, unitary-octet-symmetry breakdown in nonlinear, 19: 41395
spinor model of, meson states in symmetry-breaking SU(2) nonlinear, 19: 41396
structure of, internal, 19: 41478
symmetries for, dynamic, (T), 19: 41519
symmetries for, test of, (T), 19: 41517
symmetries of, matrix elements of the decuplet operator of SU_3, 19: 41340 (UR-875-53)
symmetry for, charge-conjugation operator in SU(6), (T), 19: 41464
symmetry for, supercharge in SU_3, (T), 19: 41483(T)
symmetry for, 27-supermultiplet in, (T), 19: 41492(T)
symmetry group for, spherical functions of non-compact rotational, 19: 41327 (IC/65/63)
symmetry group for, mass spectra and selection rules in, (T), 19: 41362
symmetry groups for, (T), 19: 41435
symmetry groups for, extensions of Poincare and SU(6), (T), 19: 41520
symmetry principles at high energy, conference on, 19: 41514
symmetry scheme for, relativistically covariant SU(6), 19: 41467
symmetry SU(6) for, Lie groups, Lie algebras and, 19: 41449
symmetry theory SU(6) for, relativistic formulation of, 19: 41428
theory for charged, derivation of classical relativistic, 19: 41372
theory for, symmetries in conformal-group, 19: 41392
theory for, using Poincare group and SO(4,2), 19: 41389
transitions of relativistic, distributions from, (T), 19: 41390

ELEMENTS
burning temperature measurements, ignition system for, 19: 42214 (RFP-397)
isotopic content of, mass spectroscopy techniques for determining, 19: 41243(T) (FTD-TT-64-1368)
neutron elastic scattering by, optical model calculations for, (T), 19: 41827
synthesis in stars, mechanisms for, (T), 19: 41235

ENDOCRINE GLANDS
radiation effects on function of, in rats, 19: 40360(T) (FTD-TT-65-48, pp 666)

EQUIPMENT AND PROCEDURES
rescue basket for injured persons in canyons, 19: 42223 (UCRL-12006)

ERBIUM
determination in iron–rare earth alloys and medium alloyed steels, 19: 40445
neutron reactions (n,α) with, cross sections for thermal, (E), 19: 41809(T)
physical and thermodynamic properties, 19: 40948 (IS-1195)
polarographic behavior in dimethylformamide and dimethylsulfoxide, 19: 40681
preparation and purification, 19: 40948 (IS-1195)
spectra of, atomic, (E), 19: 41281

ERBIUM ALLOYS
Er–Au, phase studies of solid solutions in, 19: 41062
Er–Mg, thermodynamic properties, 19: 41013 (IS-T-25)
Er–Ni, preparation for solid solubility studies, 19: 41021(R) (NMI-8002.1)
Er–Ru, process for improving workability of, 19: 40999(P)

ERBIUM CARBIDES
eutectic temperature between carbon and dicarbide, 19: 41014 (LA-DC-6819)
lattice parameters and phase transformation temperatures in, 19: 41014 (LA-DC-6819)
microhardness, 19: 41014 (LA-DC-6819)

ERBIUM CHLORIDES
complexes with phenanthroline, preparation and properties, 19: 40514

ERBIUM COMPLEXES
with gluconic acids, stability constants, 19: 40508

ERBIUM ISOTOPES Er-165
energy levels of, three-quasiparticle, (E), 19: 41667 (JINR-P-2239)

ERBIUM ISOTOPES Er-166
energy levels of, vibration-rotation interactions in, (T), 19: 41818

ERBIUM ISOTOPES Er-167
production of isomeric states in yttrium-89 (n,n'γ) reactions at 14 Mev, cross sections for, (E), 19: 41781

ERBIUM ISOTOPES Er-168
energy levels of, vibration-rotation interactions in, (T), 19: 41818
neutron reactions (n,2n) at 14 Mev, cross sections for erbium-167 isomeric states from, (E), 19: 41781

ERBIUM ISOTOPES Er-169
beta decay of, branching ratio for, (E), 19: 41705

ERBIUM OXIDES
content in McKelveyite uranium mineral, 19: 40799

ERBIUM PERCHLORATES
stability constants of, thermal, 19: 40509

ETHANE
ethane-O, oxidation induced by fission fragments in, 19: 40611
reactions with bromine-80 recoil atoms, radioactivity in organic yields in deuterated and normal, 19: 40618
reactions with recoil tritium in presence of helium, energy loss and reactivity values of, 19: 40616
butane–ethane, energy loss and reactivity in reactions with recoil tritium in presence of helium, 19: 40616
ethane–HCl, formation of polymeric yields in reactions with carbon-14 and sulfur-35 recoil atoms, 19: 40628
ethane–Ne, kinetic energy effects on carbon-11 reactions with, 19: 40617
2,2-dimethylpentane–ethane, energy loss and reactivity in reactions with recoil tritium in presence of helium, 19: 40616

ETHANE, BROMO-
reactions with bromine-80 recoil atoms, pressure and temperature effects on, 19: 40626
Br–bromoethane–CCl_4, neutron radiation effects on labeled organic retentions in, 19: 40624
Br–bromobenzene–bromoethane, neutron radiation effects on labeled organic retentions in, 19: 40624

ETHANE, 1,2-DICHLORO-
radioinduced reactions with ethylene, yields in, 19: 40590

ETHANE, HEXAFLUORO-
reactions with bromine-80 recoil atoms, radioactivity of organic yields in, 19: 40618

ETHANOL
effects of aqueous solutions of, on sorption of europium and yttrium by cation exchanger, 19: 40664
effects on ion exchange separation of rare earths using α-hydroxyisobutyric acid, 19: 40663
effects on ion exchange separation of europium and yttrium, 19: 40666
effects on sorption of europium and yttrium on ion exchangers, tracer studies of, 19: 40665
reactions with tritium recoil atoms, with and without benzene and cyclohexane, energy transfer in, 19: 40622

solvent properties for sodium-22 in cyclotron targets, 19: 40637(T) (ORNL-tr-625)
solvent properties for sodium, 19: 40686
butanol–ethanol, coagulation of thorium hydroxide particle in, 19: 40963(P)
CCl_4–ethanol, mechanism of chemical processes in reactions with chlorine-38 recoil atoms, 19: 40623
ETHANOL, 2-AMINO-
separation from other amines by ligand exchange on cation exchanger, 19: 40648 (COO-499-2)
ETHANOL, 2-ETHOXY-
dimethyl–effects on ion exchange separation of rare earths using α-hydroxyisobutyric acid, 19: 40663
ETHANOL, 2,2-IMINODI-
separation from other amines by ligand exchange on cation exchanger, 19: 40648 (COO-499-2)
ETHYLENE
ethylene-O, oxidation induced by fission fragments in, 19: 40611
radioinduced reactions with phosgene, yields in, 19: 40589
radioinduced reactions with 1,2-dichloroethane, yields in, 19: 40590
reactions with recoil tritium, kinetic isotope effects in, 19: 40615
ethylene–Ne, kinetic energy effects on carbon-11 reactions with, 19: 40617
ETHYLENE, CHLORO-
radioinduced polymerization of with argon, krypton, or xenon, 19: 40584
ETHYLENE, DICHLORO-
reactions with chlorine-38 recoil atoms, sterochemistry in, 19: 40625
ETHYLENE GLYCOL
effects on ion exchange separation of rare earths using α-hydroxyisobutyric acid, 19: 40663
ETHYLENE POLYMERS
radiation effects on thermal conductivity of, at 0 to 170°C, 19: 40603
radioinduced odor of, addition of 2,2′-methylene-bis-(4-methyl-6-*t*-butylphenol) to prevent, 19: 40633(P)
with vinyl acetate, radiolysis of, determination of vinyl acetate content by, 19: 40556
B–polyethylene, neutron spectra in, thermal, 19: 42037(R) (BNWL-95, pp 4-17)
ETHYLENE, TETRACHLORO-
dielectric polarization of, temperature dependence, 19: 40468(T) (SC-T-65-721)
ETHYLENIMINE POLYMERS
use in preparation of chromatographic resins, 19: 40674
EUROPE
precipitation amount and frequency, 1921 to 1950, 19: 41111 (EUR-2296.e)
EUROPIUM
physical and thermodynamic properties, 19: 40948 (IS-1195)
polarographic behavior in dimethylformamide and dimethylsulfoxide, 19: 40681
preparation and purification, 19: 40948 (IS-1195)
separation from aqueous solutions of organic acids by solvent extraction using high-molecular-weight amines, 19: 40657
separation from promethium and yttrium by ion exchange, effects of media on, 19: 40663
separation from yttrium by ion exchange, effects of alcohols on, 19: 40666
separation from yttrium by ion exchange using ammonium acetate eluant, 19: 40680
sorption by strongly acidic cation exchanger, effects of aqueous solutions of alcohols on, 19: 40664
sorption on ion exchanger, effects of glycols on, 19: 40662
sorption on ion exchanger, tracer studies of effects of alcohol solutions on, 19: 40665
EUROPIUM CHLORIDES
complexes with phenanthroline, preparation and properties, 19: 40514
EUROPIUM COMPLEXES
with gluconic acids, stability constants, 19: 40508
with tartaric acids, composition and stability, 19: 40510
EUROPIUM IONS
paramagnetic resonance of divalent, in lead chloride, 19: 40498
radioinduced charge transfer to thulium ions in calcium fluoride crystals, x, (E), 19: 40575
spectra in acetophenone, energy transfer in, 19: 40504
EUROPIUM ISOTOPES Eu-151
neutron reactions (n,α) with, cross sections for thermal, (E), 19: 41809(T)
EUROPIUM OXIDES
content in McKelveyite uranium mineral, 19: 40799
reactivity worths of, reactor oscillator for measurement of, 19: 42050 (NAA-SR-11368)
EUROPIUM SULFIDES
EuS–Gd_2S_3, magnetic properties of $EuGd_2S_4$, (E), 19: 40496
EVAPORATORS
economic comparison of multi-stage flash and long-tube vertical multiple-effect, for water desalination, 19: 40699 (ORNL-TM-826)
EXOSPHERE
charged-particle reactions in, v-l-f emissions from, 19: 41572 (NASA-CR-258)
ion density distribution in, (T), 19: 41601
EXPERIMENTAL BOILING WATER REACTOR
criticality studies, 19: 42093 (GEAP-4912)
fuel element testing for, physics aspects of plutonium recycle, 19: 42078 (ANL-7019)
neutron flux distributions during power operation, (E), 19: 42076 (ANL-6751)
EXPERIMENTAL BREEDER REACTOR-II
fuel management and inventory, 19: 42075 (ANL-6735)
reactivity transients including meltdown, methods for analysis of, 19: 42100 (UNC-5092)
EXPERIMENTAL GAS COOLED REACTOR
coolants for, evaluation of performance of fog as, (E), 19: 42020
EXPLOSION CLOUDS
formation of base surge, by Pre-Schooner detonations in basalt, 19: 40708 (PNE-503F)
EXPLOSIONS
crater dimensions from 500-ton, on rock, 19: 40712 (SC-RR-65-277)
energy liberation of, device for measuring, 19: 40850(T) (ORNL-tr-588)
stability of, analysis of asymptotic, (T), 19: 41117 (LA-3306)
EXPLOSIVES
detonation wave interactions in condensed, 19: 42205 (LA-DC-6990)
radiation effects on thermal decomposition of, gamma, 19: 40562
shock initiation of plastic-bonded HMX, 19: 42206 (LA-DC-6992)
EXPONENTIAL PILES
neutron decay constants for solid-moderated enriched uranium, 19: 42051 (UCRL-12013)
neutron multiplication factor in poisoned lattices of enriched uranium and heavy water, 19: 42046(R) (MIT-2344-3, pp 109-14)
EYES
radiation effects on electrical reactions of retina, in frogs and rabbits, 19: 40359(T) (FTD-TT-65-48, pp 590–1)

F

FALLOUT
analysis, 1963 to 1965, 19: 40789
biological accessibility and fractionation coefficients of, 19: 40786(T) (JPRS-30500)
content in stratosphere and in rain at Fayetteville, Arkansas, 19: 40785 (TID-21224)
from nuclear explosions in air, theory, 19: 40782 (NP-15325)
monitoring in Alaska, 1959 to 1965, 19: 40780 (BNWL-SA-242)
particles in upper atmosphere, 19: 40783 (NP-15327)
production in ground-level nuclear explosions, 19: 40786(T) (JPRS-30500)
FAST CERAMIC REACTOR
reactivity transients including meltdown, methods for analysis of, 19: 42100 (UNC-5092)
FAST REACTORS
development of gas cooled, economics of, 19: 42090 (GA-6132)
feasibility of sodium-cooled 1000 Mw(e), calculational methods development for, 19: 42095 (NAA-SR-11378(Vol.III))
neutron Doppler-effect calculations for, resonance corrections to, (T), 19: 42057
neutron Doppler-effect calculations for, resonance corrections to, (T), 19: 42058
reactivity and safety of sodium-cooled power breeders, (E), 19: 42081 (CONF-193-11)
reactivity transients including meltdown, methods for analysis of, 19: 42100 (UNC-5092)
FATTY ACIDS
effects of dietary, on strontium-90 metabolism in animals, 19: 40342
FECES
analysis for carbon-14 by liquid scintillation counting, 19: 40418
FERMI FAST BREEDER REACTOR
reactivity measurements in, core reproducibility study of, 19: 42079 (APDA-NTS-4)
reactivity of, measurement of isothermal temperature coefficient for, 19: 42080 (APDA-NTS-5)
FERMIONS
perturbation series of system of N, convergence properties of time-dependent, 19: 41364

symmetry group for, mass spectra and selection rules in, (T), 19: 41362
FERMIUM
separation from rare earths by solvent extraction using DTPA, 19: 40676
solvent extraction by thenoyltrifluoroacetone in benzene, 19: 40458 (JINR-P-2224)
FERMIUM COMPLEXES
with lactic acid, stability constants, 19: 40458 (JINR-P-2224)
FERROMAGNETIC MATERIALS
physics of thin films of, conference on, 19: 41039
FERTILIZERS
effects on strontium-90 uptake by plants from soils, 19: 40310
FETUSES
strontium-90 content of dog, after chronic ingestion by mother, 19: 40327
strontium-90 content of cattle, after ingestion by mother, effects of age, 19: 40329
strontium-90 content of cattle, after ingestion by mother, 19: 40330
strontium-90 metabolism in sheep, after intravenous or oral administration to mother, effects of age, 19: 40332
FIELD THEORY
bootstrap analysis of vector mesons in, limitations of, 19: 41373
canonical formalism of quantum, vacuum and particle states in, 19: 41475
conservation laws in relativistic, in space-times admitting motion, (T), 19: 41542
conservation laws in relativistic, in space-times admitting general transformations, 19: 41543
coupling constant relations in S-matrix, 19: 41382
diagrams containing multi-particle intermediate states, method for summing, 19: 41429
electromagnetic theory for elementary particles in, (T), 19: 41377
elementary particle interactions in SU(3), CP violations in, (T), 19: 41371
elementary particle interactions in, evaluation of crossing matrices for, 19: 41381
elementary particle interactions in, neutrino theory for electromagnetic and weak, (T), 19: 41387
elementary particle theory in, using Poincare group and SO(4,2), 19: 41389
elementary particle properties in conformal-group, 19: 41392
equations of five-dimensional classical scalar meson, 19: 41497
Feynman integrals and Feynman rules for high-spin fields, 19: 41548
gauge fields in, Coulomb form for, (T), 19: 41365
gravitation interactions in, gauge invariance for, 19: 41541
hamiltonians in, construction of separable, 19: 41546
lepton currents in, CP-violating terms in, (T), 19: 41378
operator solutions of quantum, N-quantum approximation for, 19: 41552
particles of indefinite mass in, generalized asymptotic condition for, (T), 19: 41343
propagators in $g\phi^4$, nonanalytic properties of, (T), 19: 41549
quantization of scalar Bose fields, (T), 19: 41562
relativistic-invariant equations for confluence, using hypercomplex numbers, 19: 41560
renormalization of partially conserved vector currents in, 19: 41547
scattering amplitude singularities in potential theory, (T), 19: 41550
scattering matrix in quantum, mathematical-physics methods for, 19: 41540
symmetry group for oscillator, (T), 19: 41554
transitions of relativistic particles, distributions from, (T), 19: 41390
vertex function in quantum, cut-plane analyticity of momentum-space, 19: 41558
FILMS
deposition of thin, design of ultrahigh vacuum evaporator for, 19: 40774
detection on metallic surfaces by charged particle elastic scattering, 19: 40962
electron scattering in thin, calculation of inelastic, 19: 41961(T)
physics of thin ferromagnetic, conference on, 19: 41039
radiation effects on polyamide, gamma, 19: 40595
FILTER PAPERS
analysis of air-monitor, automatic counting system for, 19: 40834(R) (UCRL-14151)
FINNED TUBES
machining from cylindrical cans, 19: 40993(P)
FIRES
effects on lead cask, calculations, 19: 40832 (SC-RR-65-98, pp 732-5)
effects on lead-lined casks, analysis, 19: 40813 (SC-RR-65-98, pp 107-13)
effects on lead-shielded containers and radioisotope packages, 19: 40831 (SC-RR-65-98, pp 723-31)
effects on shielded packagings for radioactive materials, tests of, 19: 40814 (SC-RR-65-98, pp 114-18)
effects on shipping containers, modeling of tests of, 19: 40815 (SC-RR-65-98, pp 133-40)
effects on shipping containers for slightly enriched uranium fuel cores, 19: 40820 (SC-RR-65-98, pp 357-76)
effects on 15-ton shipping container and finned box, 19: 40827 (SC-RR-65-98, pp 631-50)
radioisotope dispersion caused by, 19: 40830 (SC-RR-65-98, pp 719-22)
sodium, particle and iodine release from, 19: 40803 (NAA-SR-Memo-9719)
thermal radiation from plume of hydrogen, 19: 42137 (LA-DC-7313)
FISH
life history of the banded sculpin in Kentucky, 19: 42220 (TID-22023)
FISSION
energy and shape calculations in liquid-drop model, (T), 19: 41767
FISSION FRAGMENTS
charge distribution of uranium-238, (E), 19: 41771
conversion electrons from, measurement technique for spectra of, 19: 41680 (UCRL-16184)
detection and measurement by semiconductor surface-barrier detectors, (E), 19: 40901
detection using semiconductor detectors, pulse-height defects in, 19: 40892
energy distributions from uranium dioxide, (E), 19: 41748
neutron emission from, (E/T), 19: 41681(T) (ANL-Trans-205)
production of positron-active, from uranium-235 thermal fission, (E), 19: 41799(T)
reactions with ammonia, effects of physical variables on, 19: 40547(R) (AGN-8137(Vol. I))
sources of, performance and preparation of uranium oxide, 19: 40547(R) (AGN-8137(Vol.I))
track registration on surfaces of solids, (E/T), 19: 41138
use in oxidation of atmospheric nitrogen for nitric acid production, (E), 19: 40604
FISSION PRODUCTS
determination in irradiated fuels, gamma spectrometric, 19: 40411 (RT/CHI(65)2)
diffusion from urania at 1650 to 2800°C, 19: 41088 (GEAP-4572)
disposal and processing methods for, at Hanford plant, (E), 19: 42196
effect on heating in fast reactor plutonium fuel, (E), 19: 42114
effects on oxidation of light alkanes, dose rate and free radical diffusion effects on, 19: 40611
effects on radioinduced swelling in uranium, 19: 40958
gamma radiation from uranium-235, detection using thallium-activated sodium iodide crystals, (E/T), 19: 40891
metabolism of mixed uranium, after oral administration to rats, 19: 40322
production in nuclear explosion in rock, 19: 40706 (ORNL-TM-1191)
release from uranium-235, inventory of, 19: 42008 (ORNL-NSIC-5(Vol.I and II))
release from uranium-dioxide, analysis of, 19: 42008 (ORNL-NSIC-5 (Vol.I and II))
separation from spent fuel elements, scheme for, 19: 40675
separation in directional crystallization of sodium nitrate from melts, 19: 40683
separation of long- and short-lived, in high-level waste, (E), 19: 42197
separation of, scheme for sequential, 19: 40675
transport behavior in containment buildings, 19: 42008 (ORNL-NSIC-5 (Vol. I and II))
FISSIONABLE MATERIAL
handling standards for, 19: 40840
shipping of, criticality safety procedures for, 19: 40807 (RL-SEP-389 (Rev.))
transportation of, criticality evaluation of packages for, 19: 40828 (SC-RR-65-98, pp 679-90)
FISSIUM
fissium–Pu–U, creep at 650, 750, and 850°C, compressive, 19: 40958
fissium–Pu–U, phase transformations in, 19: 40958
fissium–Pu–U, reactions with titanium–vanadium at 600 to 750°C, 19: 40958
FLAMES
aerodynamics of gas, in MHD cells, (T), 19: 41144
FLOWMETERS
development for gas-solid suspensions, 19: 42127(R) (TID-22009)
development of isokinetic probes, 19: 40733(R) (GEAP-4863)
FLUID FLOW
amplification of, review, 19: 40739 (OTR-112)
in rectangular MHD channel, current distribution in, (T), 19: 41148
magnetohydrodynamic, convective channel, (T), 19: 41115 (ANL-6967)
magnetohydrodynamic, boundary layer separation in, (T), 19: 41114 (AD-617258)
magnetohydrodynamic, in annular channel with radial magnetic field, (T), 19: 41137
of conducting fluid in receptacle with conducting walls, (T), 19: 41154
two-phase, equations for pipe, 19: 40737 (NYO-3114-6)

two-phase, in multirod geometries, research program on, 19: 40733(R) (GEAP-4863)
two-phase, studies, 19: 40738(R) (NYO-3114-7)
void fraction measurement in two-phase, by x-ray attenuation, 19: 40745
FLUID FLOW (TURBULENT)
heat transfer in hydrogen in heated tubes, data compilation, 19: 40734 (NP-15331)
in gas–solid suspensions, research program on, 19: 40742(R) (TID-22002)
magnetohydrodynamic, statistical theory for homogeneous, 19: 41127 (SUDAER-233)
FLUID FUEL REACTORS
design of boiling, 19: 42069(P)
development of Dodewaard 50 Mw(e), 19: 42088(R) (EUR-2430.n)
mixing coefficients in fluidized-bed, (T), 19: 42011
FLUIDIZATION
mixing coefficients in fluidized-bed reactors, (T), 19: 42011
FLUIDS
stability of gravitationally bound spheres of perfect, (T), 19: 41563
FLUORIDES
determination in heavy water moderator, automated, 19: 40406 (CONF-650919-2)
determination of trace amounts of, distillation procedure for removing impurities in colorimetric, 19: 40420
effects on photocolorimetric determination of uranium, 19: 40428
FLUORINE
determination in gases, chromatographic, 19: 40407 (KY-485)
determination, electron microprobe, 19: 40412 (TIM-924)
polarization of nuclei of, differential dynamic, (E), 19: 40497
production by fissiochemical processes, design of loop for, 19: 40547(R) (AGN-8137(Vol. I))
separation from rare earth metals, techniques for, 19: 40948 (IS-1195)
FLUORINE ISOTOPES F-18
matrices for 2s-1d shell of, model-interaction, 19: 41730
FLUORINE ISOTOPES F-19
proton reactions (p,$\alpha\gamma$) at 1.4 Mev, gamma spectra from, (E), 19: 40896
FLUORINE ISOTOPES F-20
matrices for 2s-1d shell of, model-interaction, 19: 41730
FLUOROFORM
reactions with bromine-80 recoil atoms, radioactivity of organic yields in, 19: 40618
FOOD
packaging of, modification of irradiated polyethylene films for, 19: 40633(P)
radiation processing of, bibliography on, 19: 40941 (SB-403(Suppl.1) (Rev.))
FORESTS
radiation effects on ecology of insect populations in, chronic gamma exposure, 19: 40307 (BNL-9253)
FORMALDEHYDE
use in preparation of chromatographic resins, 19: 40674
FRANCE
nuclear fuel industry development in, 19: 42070
FREE RADICALS
radioinduced formation of solvated electrons in ice and frozen solutions, gamma, 19: 40551 (KFK-293)
radioinduced in single crystals of hydroxylated organic compounds, ESR spectra of, 19: 40613
radioinduced in 2-methyltetrahydrofuran, ESR spectra of, 19: 40558
yields from gamma radiolysis of solid mixtures of methyl methacrylate and paraffin oil, 19: 40580
FREQUENCY MODULATION
design of system for modulating large resonant cavities, (E), 19: 40723
FROGS
radiation effects on electrical reactions of retina, 19: 40359(T) (FTD-TT-65-48, pp 590–1)
FUEL CELLS
energy conversion in, review, 19: 41319
research programs on, at Siemens-Schuckertwerke laboratories, Erlangen, Germany, 19: 42228
FURAN
2-methyltetrahydro-, ESR spectra of radiolytic yields of trapped electrons and radicals in, 19: 40558
FURAN, TETRAHYDRO-
naphthalene–tetrahydrofuran, solvent properties for alkali metals, 19: 40409(R) (MSAR-65-95)

G

GADOLINIUM
determination in iron–rare earth alloys and medium alloyed steels, 19: 40445
magnetic properties at high pressures, (E), 19: 42005
magnetic properties near Curie point, (E), 19: 41972
neutron reactions (n,α) with, cross sections for thermal, (E), 19: 41809(T)
physical and thermodynamic properties, 19: 40948 (IS-1195)
physical and thermodynamic properties, 19: 40948 (IS-1195)
polarographic behavior in dimethylformamide and dimethylsulfoxide, 19: 40681
preparation and purification, 19: 40948 (IS-1195)
GADOLINIUM ALLOYS
Cd–Gd, phase studies, 19: 40960
Co–Gd, magneto-optic properties of intermetallic compound $GdCo_5$ in, 19: 41084
Gd–Au, phase studies of solid solutions in, 19: 41062
Gd–Mg, phase studies, 19: 41011 (IS-T-15)
Gd–Mg, thermodynamic properties, 19: 41013 (IS-T-25)
Gd–Ni, preparation for solid solubility studies, 19: 41021(R) (NMI-8002.1)
Gd–Ru, process for improving workability of, 19: 40999(P)
GADOLINIUM CARBIDES
eutectic temperature between carbon and dicarbide, 19: 41014 (LA-DC-6819)
lattice parameters and phase transformation temperatures in, 19: 41014 (LA-DC-6819)
microhardness, 19: 41014 (LA-DC-6819)
GADOLINIUM CHLORIDES
complexes with phenanthroline, preparation and properties, 19: 40514
GADOLINIUM COMPLEXES
with gluconic acids, stability constants, 19: 40508
GADOLINIUM IONS
electron paramagnetic resonance of, in strontium molybdates, 19: 41994(T)
GADOLINIUM ISOTOPES Gd-154
energy levels of, vibration-rotation interactions in, (T), 19: 41818
GADOLINIUM ISOTOPES Gd-155
neutron strength functions for, target spin dependence of, 19: 41656 (BNL-9245)
GADOLINIUM ISOTOPES Gd-156
energy levels of, vibration-rotation interactions in, (T), 19: 41818
neutron strength functions for, target spin dependence of, 19: 41656 (BNL-9245)
GADOLINIUM ISOTOPES Gd-157
neutron strength functions for, target spin dependence of, 19: 41656 (BNL-9245)
GADOLINIUM ISOTOPES Gd-158
energy levels of, vibration-rotation interactions in, (T), 19: 41818
GADOLINIUM OXIDES
content in McKelveyite uranium mineral, 19: 40799
reactivity worths of, reactor oscillator for measurement of, 19: 42050 (NAA-SR-11368)
GADOLINIUM PERCHLORATES
stability constants of, thermal, 19: 40509
GADOLINIUM SULFATES
$Gd_2(SO_4)_3$–Na_2SO_4, thermal stability, 19: 40511
GADOLINIUM SULFIDES
EuS–Gd_2S_3, magnetic properties of $EuGd_2S_4$, (E), 19: 40496
GADOLINIUM SYSTEMS
Gd–H_2O, neutron spectra in, thermal, 19: 42037 (BNWL-95, pp 4-17)
GAGES
design for remote measurements in radiation environment, (E), 19: 40714 (EUR-2421.d)
GALAXIES
evolutional track of, in L–L/V diagram, (T), 19: 41233
formation in steady-state universe, density and temperature conditions for, (T), 19: 41239
GALLIUM
determination by spectrochemical methods, voltage-fluctuation patterns in, 19: 40416
determination in copper by activation, 19: 40422
flow in test loops, magnetohydrodynamic, 19: 40727
positron annihilation in, angular correlations from, (E), 19: 41285
GALLIUM ALLOYS
Ga–Pu, density of liquid, at 682 to 847°C, 19: 40958
Ga–Pu, phase transformations in delta-stabilized, effects of cobalt or iron on, 19: 40958
GALLIUM ARSENIDES
radiation effects on diodes of, alpha, 19: 40937 (UCRL-11958)
GALLIUM ISOTOPES Ga-66
decay of, probability ratio of electron-capture, 19: 41800(T)

GALLIUM ISOTOPES Ga-68
decay of, probability ratio of electron-capture, 19: 41800(T)
GALLIUM ISOTOPES Ga-69
energy levels, (E), 19: 41756
GAMMA RADIATION
absorption in water hemispheres, from central point source, (T), 19: 41959
angular correlations from positron annihilation in liquid and solid metals and semiconductors, (E), 19: 41285
angular correlations in decay of cerium-143, promethium-143 energy levels from, (E), 19: 41776
angular distribution from thermal-neutron fission of uranium-235, (E), 19: 41722
detection and measurement of, produced by positron annihilation reaction, 19: 40390 (BNL-9384)
detection and measurement in high neutron fluxes, design of dosimeter for, 19: 40834(R) (UCRL-14151)
detection and measurement of, engineering drawings of ionization chamber for, 19: 40923
dosage calculations behind proton shields, computer programs for, 19: 41954 (NP-15338)
dosimetry of high energy, calibration of photographic film for, 19: 40909
dosimetry of nuclear explosion, (T), 19: 40938
dosimetry of, thermoluminescence readout instrument for, 19: 40877 (RISO-101)
dosimetry using chromogenic polymer after-effect, effects of phenol compounds on, 19: 40599
dosimetry using infrared-stimulated luminescence, 19: 40879 (UCRL-12371)
dosimetry using thermoluminescent phosphors, 19: 40868 (BNWL-SA-23)
ecological effects on insect populations in forest exposed to chronic irradiation, 19: 40307 (BNL-9253)
effect on pyrolysis of terphenyls, 19: 40630
effects of activities of solid acidic catalysts, 19: 41099
effects of pulsed, on photoconductivity in polystyrene, 19: 41091 (SC-R-65-943)
effects on absorption spectra of Yakutian diamonds, 19: 41098
effects on absorption spectra of samarium-containing calcium fluoride crystals, (E), 19: 41993(T)
effects on aqueous solutions in reactors, production of chemicals by, 19: 40548 (BNWL-82)
effects on aqueous solutions of α-methyl-D-glucoside, 19: 40605
effects on catalytic oxidation of carbon monoxide on nickel oxide at 25°C and zinc oxide at 270°C, 19: 40577
effects on decomposition of alkali nitrate crystals, electron trapping in, 19: 40609
effects on defect charge state of silicon semiconductor junction, 19: 41974
effects on electron-hole recombination in germanium, 19: 40932 (CEA-R-2723)
effects on EPR of neodymium-containing calcium fluoride crystals, 19: 40602(T)
effects on ESR spectra of polycrystalline glycolic acid, 19: 40592
effects on ethylene vinyl acetate copolymers, vinyl acetate content determination from, 19: 40556
effects on fluoro-dosimeter glass, 19: 40588
effects on graphitization of white cast iron, 19: 40961
effects on heating in fast reactor plutonium fuel, (E), 19: 42114
effects on hydrated alkali metal and alkaline earth sulfates, yields in, 19: 40610
effects on ice and frozen solutions, 19: 40551 (KFK-293)
effects on indium antimonide, 19: 41096
effects on induction of ethylene reactions with phosgene, yields in, 19: 40589
effects on mixtures of methyl methacrylate and paraffin oil, reaction of free radicals formed in, 19: 40580
effects on nitromethane at 77°K, EPR study of free radicals formed in, 19: 40579
effects on optical properties of dysprosium-containing calcium fluorides, 19: 40600(T)
effects on polyamide films, 19: 40595
effects on reactions of ethylene with 1,2-dichloroethane, yields in, 19: 40590
effects on recombination of hydrogen with oxygen, 19: 40549 (COO-1032-1)
effects on single crystals of hydroxylated organic compounds, ESR spectra of, 19: 40613
effects on sorption of carbon monoxide on zinc oxide and carbon monoxide and oxygen on nickel oxide, 19: 40578
effects on synthesis of ruthenium-106-labeled ruthenocene, 19: 40634 (BNL-8405)
effects on temperatures of materials in DFR, (E), 19: 42117
effects on thermal decomposition of explosives and propellants, 19: 40562
effects on thermoluminescence of crystalline biphenyl containing naphthalene, 19: 40563
effects on urinary excretion of taurine in rats, 19: 40364
emission by cosmic meson (μ) reactions in paper, (E), 19: 41295
emission by nuclei, angular correlation measurements in, (T), 19: 40900
emission by nuclei, angular correlations in, (T), 19: 41698
emission from KIWI-TNT destruct, dose measurements of, 19: 42135 (LA-3304)
emission from neodymium-149 and -151, half life and intensity of, (E), 19: 41836
emission in proton reactions (p,p′γ) with neon-21 at 1.28 to 1.86 Mev, (E), 19: 41838
emission in proton reactions (p,γ) with neon-20 and -22, at 1.28 to 1.86 Mev, 19: 41838
emission in solar flares, mechanism of, 19: 41289
energy transfer to radiation field in spatially homogeneous, (T), 19: 41930
exposure dose measurements in air, magnetic induction field for, 19: 40838
heating effects on gamma-active spheres, (T), 19: 42191 (AEET/HP/TH-20)
interactions with protons at 950 to 1050 Mev, hyperon (Λ^0) polarization from, (E), 19: 41367
monitor for, engineering drawings of, 19: 40926
pathological effects in nervous system of man, 19: 40349 (BNL-9345)
physiological effects on mammary gland activity, 19: 40353(T) (FTD-TT-65-48, pp 16–17)
physiological effects in guinea pigs and rats, effects of stress induced by vibration, 19: 40354(T) (FTD-TT-65-48, pp 38–9)
physiological effects on retina in eyes of frogs and rabbits, 19: 43059(T) (FTD-TT-65-48, pp 590–1)
physiological effects on pepsinogen content in rat plasma, 19: 40363
physiological effects on content of ascorbic acid and ascorbic acid oxidase in seeds, 19: 40371
physiological effects on pyrocatechol metabolism in Macacus monkeys, 19: 40373
polarization correlations from mercury-199 (n,γ) reactions, mercury-200 parity assignments from, 19: 41846
production in proton shields, computer programs for calculation of, 19: 41954 (NP-15338)
propagation in matter, investigation using similarity theory, 19: 41958
reactions (γ,n) with deuterium, laboratory observation of, 19: 41712
reactions with deuterium at 165 to 210 Mev, meson (π) production in, (E), 19: 41344
reactions with metal slabs at 1.02 Mev, electromagnetic effects, 19: 41956 (SC-R-65-933)
resonant absorption by 4.403 Mev level of aluminum-27, (E), 19: 41775
scattering by concretes and soils, density measurements by, 19: 40755
scattering by iron-57, interference between Mössbauer and Rayleigh, (T), 19: 41796
scattering by iron and water, angular and energy distributions in, (E), 19: 41953 (NP-15131)
scattering of, measurement techniques for resonant and nonresonant, (E), 19: 40922
spectra from beta decay of tantalum-182, (E), 19: 41704
spectra from proton reactions (p,γ) with calcium-42, scandium-43 energy levels from, (E), 19: 41738
spectra in decay of iodine-132, 19: 41744
spectra of dysprosium-159, isomeric levels from, (E), 19: 41736
uses of reactor, for commercial radiation chemistry, (E/T), 19: 40559
GAMMA SOURCES
activity of, use of spectrum characteristics in determination of, 19: 40893
use in production of selected wavelength x rays, 19: 41163(P)
GAMMA SPECTRA
analysis and calculation of Moessbauer, computer programs for, (T), 19: 41724
measurement in inelastic nucleon-nucleus collisions, computer program for, 19: 41954 (NP-15338)
GAMMA SPECTROMETERS
charge carrier trapping in lithium-drifted germanium, (E), 19: 40919
design of annular-crystal scintillation, for neutron-capture analysis, (E), 19: 40896
design using phoswich transducer, 19: 40921
design using water-cooled solenoids, for Mössbauer experiments, 19: 41848
response of Cherenkov-shower, at 50 to 1000 Mev, (E), 19: 40897

stability of LSU-5k, (E/T), 19: 40875 (NP-15254)
vacuum systems for Moessbauer, design of, (E), 19: 40858
GAMMA SPECTROSCOPY
techniques for neutron-capture, using scintillation detectors, (E), 19: 40896
use in direct determination of fission products, 19: 40411 (RT/CHI(65)2)
GARIGLIANO POWER REACTOR
core performance of, evaluation of hydraulic, mechanical, and thermal, 19: 42091 (GEAP-4852)
development, 19: 42092(R) (GEAP-4909)
operation of, 1964 summary on, 19: 42086(R) (EUR-2427.i)
GAS COOLED REACTORS
coolant-moderator reactions in, inhibition of, 19: 42015(P)
development of fast, economics of, 19: 42090 (GA-6132)
fuel manufacture for, in France, 19: 42070
iodine isotope release to atmosphere by, 19: 40800(R) (AERE-PR/HPM-7)
GAS FLOW (LAMINAR)
of partially ionized argon in duct, (T), 19: 40749
GASES
analysis of corrosive, chromatograph for, 19: 40407 (KY-485)
book: *Atomic Theory of Gas Dynamics*, 19: 41161
book: *Electron Avalanches and Breakdown in Gases*, 19: 41938
book: *Ionized Gases*, 19: 41937
combustion in MHD cells, aerodynamics of, (T), 19: 41144
corrosive effects of coal, on refractory alloys at high temperatures, 19: 42127(R) (TID-22009)
heat transfer in heated, radiative, 19: 40750
heat transfer through vertical annular layer of, (E), 19: 40747
ionization of, mass spectroscopy techniques for studying, 19: 41243(T) (FTD-TT-64-1368)
kinetic theory of, 19: 41132
magnetic field effects on ionized, hydrodynamic turbulence in, (T), 19: 41114 (AD-617258)
motion of ionized, around spheres, (T), 19: 41114 (AD-617258)
Ohm law for partially ionized, 19: 41874
photoionization of, upstream of shock waves, 19: 41935
photoionization of, asymptotic theory for, 19: 40552 (NP-15287)
photon interactions in electron and fully ionized, kinetic equations for, 19: 41940
positron annihilation rate in electron, (T), 19: 41160
stability in galactic evolution, (T), 19: 41239
gas–solid, fluid mechanics and heat transfer in turbulent suspensions of, research program on, 19: 40742(R) (TID-22002)
GASTROINTESTINAL TRACT
radiosensitivity of, in rats, 19: 40369
GATING SYSTEMS
design of linear gate using transistors operating in saturation state, (E), 19: 40856
GEIGER-MUELLER TUBES
performance in two-element low-noise flow-type beta detector, (E), 19: 40903
GENERATORS
energy conversion in, review, 19: 41319
GENES
nonchromosomal, properties of, 19: 42212 (NYO-3424-1)
GENETICS
information transfer systems for, 19: 42212 (NYO-3424-1)
role in encephalomyelopathy, in man, 19: 42219 (TID-21177)
GEOCHEMISTRY
of curative waters in Lourdes Spa, San Luis Potosi, Mexico, 19: 40835
GEOLOGY
age estimation using carbon-14, 19: 40795
GEOMAGNETIC FIELDS
charged-particle ambipolar diffusion in, (T), 19: 41585
cosmic radiation spectra in Forbush decreases, solar-cycle effects on, (E), 19: 41305
disturbances during magnetic storm, data for Sept. 1963, 19: 41603
intensity secular variations of, oblate earth model for, 19: 41586
properties of, research on, 19: 41571(R) (N64-29400)
pulsation pearls in, dynamic spectral characteristics of micro-, 19: 41582
structure of, isocontours of shell parameters B and L for, 19: 41590
structure of, shell classification for, (T), 19: 41584
GEOMAGNETIC STORMS
data from Jan. to March 1965, 19: 41589
solar plasma flux correlations with, (E), 19: 41580
solar radiation effects on latitudinal dependence and annual variation of M-region, (E), 19: 41602
GEOPHYSICS
stratospheric properties in, (T), 19: 41570 (CONF-765-11)
GERMAN REACTORS
auxiliary installations for MZFR, design of, 19: 42168
building construction and pressure vessel installation for MZFR, 19: 42177
construction of MZFR, 19: 42176
containment of MZFR, 19: 42167
coolant and moderator circuits of MZFK, construction of, 19: 42164
coolant pumps for MZFR, 19: 42174
description of MZFR, 19: 42160
design and fabrication principles for MZFR, 19: 42162
design, of MZFR, for economic optimum, 19: 42161
development of MZFR, 19: 42158
economics and utilization of MZFR, 19: 42159
experimental facilities of MZFR, 19: 42179
fuel elements for MZFR, design, construction, and testing of, 19: 42165
fuel rod fabrication for MZFR, 19: 42175
instrumentation and controls for MZFR, 19: 42170
loading equipment for MZFR, 19: 42166
MZFR structural design of, 19: 42171
pressure vessel for MZFR, design, construction, and installation of, 19: 42163
pressure vessel for MZFR, fabrication of, 19: 42172
reactivity measurements in MZFR, zero-energy, 19: 42186
reactivity of MZFR, zero-power experiment for, 19: 42178
steam generator for MZFR, construction of, 19: 42173
steam power installation for MZFR, 19: 42169
GERMANIUM
argon-ion reactions at 10 ev to 1 kev with, electron diffraction studies of, 19: 41258
Auger electron ejection from, 19: 41124(R) (NP-15108)
determination by spectrochemical methods, voltage-fluctuation patterns in, 19: 40416
electron scattering from crystals of, effects of sorbed sodium on, 19: 41124(R) (NP-15108)
radiation effects on electric conductivity and Hall coefficients of n-type, neutron, 19: 41104(T)
radiation effects on current oscillations in, 19: 41105(T)
radiation effects on electron-hole recombination in, gamma, 19: 40932 (CEA-R-2723)
radiation effects on tunnel diodes of, neutron, 19: 40939
thermionic work function of, effects of sorbed sodium on, 19: 41124(R) (NP-15108)
thermionic work function of, effects of sorbed alkali metals on, 19: 41124(R) (NP-15108)
GERMANIUM ALLOYS
Ge–Ru, process for improving workability of, 19: 40999(P)
GERMANIUM ISOTOPES Ge-66
decay of, probability ratio of electron-capture, 19: 41800(T)
GERMANIUM ISOTOPES Ge-69
decay of, probability ratio of electron-capture, 19: 41800(T)
GLASS
shielding properties in solar cells, 19: 40931 (AD-609424)
thermodynamics of interfaces with metals, 19: 40464 (UCRL-11816(Rev.))
use as a diathermanous substance in thermal reactors, 19: 42065(P)
GLASS TEXTILES
fiberglass coating of wood ladders using, inspection of, 19: 40834(R) (UCRL-14151)
GLOBULIN
separation of iodide from iodine-131-labeled, chromatographic, 19: 40656(T)
GLOW DISCHARGES
oscillations in cathode region of plasma, detection of centimeter, 19: 41876
plasma column in, diagnostics using electric probes, (E/T), 19: 41868
GLUCONIC ACIDS
complexes with rare earths, stability constants, 19: 40508
GLUCOSIDE, α-METHYL-
determination using paper chromatography, 19: 40605
radiation effects on aqueous solutions of, gamma, 19: 40605
GLUTAMIC ACID
metabolism in rat liver, tracer study, 19: 40308 (BNL-8379)
GLYCEROL
effects on ion exchange separation of rare earths using α-hydroxyisobutyric acid, 19: 40663
GLYCOLIC ACID
properties for use in electrophoresis of lanthanides, scandium, thorium, uranium, and zirconium, 19: 40671
radiation effects on ESR spectra of polycrystalline, gamma, 19: 40592
GLYCOLIC ACID COMPLEXES
with rare earths, stability and composition, 19: 40486
GLYCOLS
effects on separation of rare earths, by ion exchange, tracer studies of,

19: 40662
GOATS
radiation effects on mammary gland activity in, 19: 40353(T) (FTD-TT-65-48, pp 16–17)
GOLD
determination by spectrochemical methods, voltage-fluctuation patterns in, 19: 40416
determination in copper by activation, 19: 40422
determination in lead, rocks, silicon, and kale by neutron activation analysis, 19: 40437
proton reactions at 157 Mev, nucleon clustering from, (E), 19: 41831
radiation damage rate in, effects of crystal defects and impurities on, 19: 40961
thermodynamic properties at high pressures and temperatures, 19: 40459 (NP-15324)
wear characteristics of plated coatings of, for use in rotary switches, 19: 42216 (SC-DR-65-269)
GOLD ALLOYS
Au–La, phase studies of solid solutions in, 19: 41062
Au–Lu, phase studies of solid solutions in, 19: 41062
Au–Nd, phase studies of solid solutions in, 19: 41062
Au–rare earth, electric conductivity of CsCl–type phases in, 19: 41005 (CALT-221-11)
Au–Sc, phase studies of solid solutions in, 19: 41062
Au–Sm, phase studies of solid solutions in, 19: 41062
Au–Tb, phase studies of solid solutions in, 19: 41062
Au–Tm, phase studies of solid solutions in, 19: 41062
Au–Y, phase studies of solid solutions in, 19: 41062
Au–Yb, phase studies of solid solutions in, 19: 41062
Ce–Au, phase studies of solid solutions in, 19: 41062
Dy–Au, phase studies of solid solutions in, 19: 41062
Er–Au, phase studies of solid solutions in, 19: 41062
Gd–Au, phase studies of solid solutions in, 19: 41062
GOLD ISOTOPES Au-197
neon-20 reactions at 127 Mev, angular distributions from one-nucleon transfer, (T), 19: 41805(T)
neutron reactions (n,n'γ) at .4 to 1.2 Mev, gamma spectra from, (E), 19: 41669 (LA-DC-7096)
proton reactions at 150, 340, and 660 Mev, cascade theory for, (T), 19: 41811(T)
GONADS
radiation effects on rabbit, biochemical, 19: 40375
GRAIN-BOUNDARY DIFFUSION
mathematical models for, 19: 41970 (ORNL-TM-1224)
GRAPHITE
molds of, preparation of, 19: 40989
neutron decay and extrapolation length in, pulsed, (E), 19: 41647
oxidation of, mechanism of formation of corrosion patterns in, 19: 40975
radiation effects on properties of reactor-grade, neutron, 19: 40959
radiation effects on dimensions of polycrystalline, method of testing for, 19: 41109(P)
radioinduced basal plane contraction in, fast-neutron, (T), 19: 41100
reactions with carbon dioxide, inhibition of, 19: 42015(P)
sorptive properties for krypton, two-dimensional second virial coefficients for, 19: 40956
GRAPHITE MODERATED REACTORS
control equipment for, 19: 42019(T) (ORNL-tr-669)
coolant-moderator reactions in, inhibition of, 19: 42015(P)
fuel manufacture for, in France, 19: 42070
GRAPHITE SYSTEMS
Al–graphite, heat transfer from colloidal gas suspensions of, 19: 42127(R) (TID-22009)
graphite–N, effects on candidate HTLTR materials at 1000 and 1200°C, 19: 40966 (BNWL-92)
graphite–stainless steel, heat transfer from colloidal gas suspensions of, 19: 42127(R) (TID-22009)
GRAVITATION
generation by axisymmetric magnetic fields, 19: 41544
gravitational radiation in, canonical analysis of, (T), 19: 41561
gravitational radiation in system of two point masses, (T), 19: 41564
precession in fields of, (T), 19: 41204 (JINR-P-2174)
radiation from binary stellar systems, (T), 19: 41206 (N64-33291)
stability of gravitationally bound spheres of perfect fluid, (T), 19: 41563
GREEN RIVER FORMATION (WYO.)
uranium occurrence in McKelveyite in, 19: 40799
GROSSWELZHEIM SUPERHEAT REACTOR
design, 19: 42107
GROUND
cosmic meson (μ) spectra at great depths in, (E), 19: 41293
cosmic meson (μ) energy losses in, below 100 Tev, (T), 19: 41296
motion effects on contents of buried shelters, 19: 40758 (AD-426249)
shock spectra from Gnome explosion, 19: 40713 (VUF-2401)
GUINEA PIGS
radiation effects from injected strontium-89 and strontium-90 on pancreas of, 19: 40358(T) (FTD-TT-65-48, pp 577–8)
GUNDREMMINGEN POWER REACTOR
design and development of, 1964, 19: 42085(R) (EUR-2426.d)

H

HAFNIUM
determination in copper by activation, 19: 40422
diffusion coefficient for nitrogen and oxygen in, 19: 40960
radiation effects on mechanical properties of, fast neutron, 19: 41092 (WAPD-TM-457)
radiation effects on corrosion and tensile properties of welded joints of Zircaloy-2-to-, fast neutron, 19: 41092 (WAPD-TM-457)
HAFNIUM ALLOYS
Hf–Ir, phase studies, 19: 40960
Hf–Nb, phase studies, 19: 40960
Hf–Nb–W–Y, properties of welds in C-129Y, 19: 40989
Hf–Ru, process for improving workability of, 19: 40999(P)
Hf–Ta, phase studies, 19: 40960
Hf–Ta–W, properties of welds in T-111, 19: 40989
Hf–Ta–W, stress-rupture properties of T-111, 19: 40961
HAFNIUM CARBIDES
heats of formation, 19: 40961
HfC–HfH, properties, 19: 40959
HAFNIUM HYDRIDES
HfC–HfH, properties, 19: 40959
HAFNIUM IONS
reactions with derivatives of Arsenazo III, spectrophotometric studies of, 19: 40426
HAFNIUM ISOTOPES Hf-171
decay of, electric octupolar transition of 71.2 kev in, 19: 41701
HAFNIUM ISOTOPES Hf-178
energy levels of, vibration-rotation interactions in, (T), 19: 41818
HALL EFFECT
efficiency of multiterminal generator, for inverter applications, 19: 40845(R) (N64-33676)
measurement in metals, equipment for, 19: 42217 (SC-RR-65-325)
use in cyclotron magnetic-field measurements, 19: 41195
HALLAM POWER REACTOR
fuel for core I of, irradiation tests of molybdenum–uranium alloy, 19: 41090 (NAA-SR-11131)
maintenance, operation, and testing, April 1965, 19: 42099(R) (TID-22013)
HANDBOOKS AND MANUALS
for radiation safety technician training course, 19: 40801 (ANL-6991)
for use of nuclide chart, 19: 41830
HANDLING AND STORAGE
regulations for, for spent reactor fuels, (E), 19: 40837
safety criteria for, of sealed radioisotope sources, 19: 40802 (CONF-650616-5)
safety standards for, of fissionable materials, 19: 40840
HANFORD PRODUCTION REACTORS (H)
coolant purification for, reduction of radioisotopes in effluent by, 19: 42130 (HW-68387)
HANFORD PRODUCTION REACTORS (N)
coolant high pressure injection pump simulation study, system response to small disturbances in, 19: 42131 (HW-77028)
neutron diffusion and transport in tube-in-tube fuel geometry in, (T), 19: 42128(R) (BNWL-95, pp 18-23)
HANFORD WORKS, RICHLAND, WASH.
criticality safety in Chemical Processing Department, 19: 40807 (RL-SEP-389(Rev.))
waste disposal and processing methods used at, (E), 19: 42196
HARWELL SYNCHROTRON
power plant alternator for, ultrasonic inspection of, 19: 41201
HASTELLOY B
compatibility with graphite–nitrogen environment at 1000 and 1200°C, 19: 40966 (BNWL-92)
HASTELLOY X
carburization by methane at 1120°C, 19: 40961
compatibility with graphite–nitrogen environment at 1000 and 1200°C, 19: 40966 (BNWL-92)
corrosion by coal gasification products at high temperatures, 19: 42127(R) (TID-22009)
HAYNES 25 ALLOY
carburization by methane at 1120°C, 19: 40961
HEALTH PHYSICS

activities at CVTR, June 1965, 19: 42084(R) (CVNA-239)
dosimetry in, dose equivalent estimation in instruments for, 19: 40911
radiation hazards of synchrocyclotrons, 19: 41171(T) (N64-33402)
radiation hazards from luminous paints used in aircraft instruments, 19: 40940 (NP-14924)
technician training for, manual for, 19: 40801 (ANL-6991)
HEART
function, effects of iodine-131-induced hypothyroidism in isolated rat, 19: 40368
radiation effects on metabolism in, 19: 40357(T) (FTD-TT-65-48, pp 552–3)
HEART DISEASES
lipid metabolism in atherosclerosis, tracer study using iodine-131-peanut oil, 19: 40393
HEAT EXCHANGERS
design for cooling gas containing metal vapors, 19: 40752(P)
performance of liquid sodium, 19: 42096 (NAA-SR-11396)
spacer grid for multitube, 19: 42073(P)
HEAT-RESISTING ALLOYS
performance as thermocouples at 1000 to 2000°C, (E), 19: 40859
preparation of monocrystalline spheres of, (E), 19: 40991
HEAT TRANSFER
analysis in organic-cooled and -moderated power reactors, (E), 19: 42110
between contacting surfaces, bibliography on, 19: 40744 (UCRL-14264)
from electric arcs by natural convection, (T), 19: 41914
from reactor cylindrical fuel rods, analog models for, 19: 40740 (RT/ING(64)16)
from reactor fuel element with polyzonal-spiral finning, at low gas flow rates, (E), 19: 40748
from solid surface to helium II, film-free convective, (T), 19: 41635
in gas–solid suspensions, research program on, 19: 40742(R) (TID-22002)
in heated gases, radiative, 19: 40750
in laminar duct flow of partially ionized argon, (T), 19: 40749
in magnetohydrodynamic channel flows, (T), 19: 41119 (MIT-36-P)
in MHD flow of partially ionized medium along plane channel, (T), 19: 41147
in reactor coolant loss accidents, model for calculation of, 19: 42009 (WAPD-T-1811)
in turbulent flow of hydrogen through heated tubes, data compilation, 19: 40734 (NP-15331)
through vertical annular gas layer, (E), 19: 40747
HEATERS
tests of immersion, for in-tank solidification of wastes, 19: 42193 (BNWL-101)
HEAVY WATER REACTORS
design with undermoderated core, for neutron beam production, 19: 42066(P)
development, 19: 42007 (MIT-2344-3)
development of pressure boiler, 19: 42108
economics of spectral-shift pressurized-water thorium power breeders, (E), 19: 42109
fuel manufacture for, in France, 19: 42070
neutron parameters in lattices of, epithermal, 19: 42044(R) (MIT-2344-3, pp 37-54)
HELIUM
burning in stars, effects on carbon, nitrogen, and oxygen isotopic abundances, (T), 19: 41242
content in amphoteric meteorites, (E), 19: 41225
electron and ion temperatures in theta-pinch plasma of, in azimuthal magnetic field, (E), 19: 41860 (NP-15220)
electron and ion temperatures in theta-pinch plasma of, in azimuthal magnetic field, (E), 19: 41921
electron inelastic scattering at 19.3 to 24.5 ev, resonances in, (E), 19: 41264
electron motion in, asymptotic solution of Schroedinger equation for, (T), 19: 41565
heat transfer from solid surface to liquid II, film-free convective, (T), 19: 41635
helium ion scattering by atoms of, resonant electron capture in, (E), 19: 41280
helium-ion elastic differential scattering at 20 to 600 ev, cross sections for, (E), 19: 41283
performance as propellant in plasma engines, 19: 40762 (N64-31010)
phase state between liquid I and II, intermediate, (T), 19: 41618
purification of, method and equipment for, 19: 40539(P)
sound standing waves in films of liquid II, third, (E), 19: 41617
sound velocity at lambda point in liquid, (E), 19: 41619
spectra in gaseous nebulae, recombination, (T), 19: 41238
stability of low B theta pinch plasma of, pressure dependence of, (E), 19: 41887
superfluid circulation at quantum level units in, (E), 19: 41620
vortex rings in liquid, origin of charged quantized, (E/T), 19: 41621
vortex rings in superfluid, interactions with quasiparticles, (E), 19: 41634
vortex rings in superfluid, production by charged particle acceleration, (E), 19: 41634
HELIUM HYDRIDES
effects of ionic, in model stellar atmospheres, (T), 19: 41240
energy levels of ionic, (T), 19: 41240
HELIUM IONS
diffusion of diatomic molecular, in plasma, 19: 41850(R) (AD-617386)
reactions with molecular nitrogen ions at 10 to 65 kev, rotational and vibrational excitation in, (E), 19: 41279
scattering by helium atoms, resonant electron capture in, (E), 19: 41280
scattering by helium at 20 to 600 ev, cross sections for elastic differential, (E), 19: 41283
scattering by silver, Auger electron emission from, (T), 19: 41270
HELIUM ISOTOPES He-3
deuteron reactions (d,t) at 20 and 25 Mev, energy spectra from, (E), 19: 41658 (IAE-655)
differential energy spectra of primary cosmic, at 30 to 90 Mev per nucleon, (E), 19: 41302
form factors of, d- and p-state contributions to magnetic-moment, (T), 19: 41759
form factors of, relativistic effects in, (T), 19: 41770
He-3–He-4, density at low temperatures, (E), 19: 41628
hyperfine structure of atomic and ionic, correction to ratio of, (T), 19: 41787
meson (μ) capture by, neutron spectra from, (T), 19: 41783
photodisintegration cross sections for, (T), 19: 41824
reactions (He-3,α) with helium-3 at 16 to 36 Mev, energy spectra from, (E), 19: 41658 (IAE-655)
reactions (He-3,α) and (He-3,p) with carbon-12 at 1.0 to 1.8 Mev, total cross sections for, (E), 19: 41663 (JINR-P-2184)
reactions (He-3,Be-7) with carbon-12 at 29.4 Mev, angular distributions and energy spectra from, (E), 19: 41733
reactions (He-3,n) with helium-4 at 29.8 Mev, neutron spectra from, (E), 19: 41659 (IAE-835)
reactions (He-3,p) with strontium-88, isomeric cross section ratios for, (E), 19: 41820
reactions (He-3,xnyp) with iron-56, shell structure effects in nickel-59 decay in, (T), 19: 41741
use of liquid, as scintillator in neutron spectrometers, 19: 40928(P)
HELIUM ISOTOPES He-4
density at critical point of, (T), 19: 41615
differential energy spectra of primary cosmic, at 30 to 90 Mev per nucleon, (E), 19: 41302
energy levels of, excited, (E), 19: 41786
He-3–He-4, density at low temperatures, (E), 19: 41628
helium-3 reactions (He-3,n) at 29.8 Mev, neutron spectra from, (E), 19: 41659 (IAE-835)
meson (K^-) reactions (K^-,$\Lambda\pi^-$), final-state interactions in, (T), 19: 41405
proton elastic scattering by, polarization from, (E), 19: 40905
proton scattering by, (T), 19: 41763
HELIUM ISOTOPES He-6
emission from californium-252, spontaneous, (E), 19: 41785
HEMATINS
Mössbauer effect in, studies on, 19: 40305
Mössbauer effect in, studies on, 19: 40306
HEMATOPOIETIC SYSTEM
pathological effects of injected yttrium-91 in, of dogs, 19: 40377
pathological effects of injected strontium-90 in, of dogs, 19: 40378
pathological effects of injected plutonium-239 in dogs, 19: 40379
radiation injuries, effects of bone marrow transfusions in dogs, 19: 40385(T) (FTD-TT-65-48, pp 134-5)
HEMINS
Mössbauer effect in, studies on, 19: 40305
Mössbauer effect in, studies on, 19: 40306
HEMOGLOBIN
Mössbauer effect in, studies on, 19: 40305
Mössbauer effect in, studies on, 19: 40306
2,4-HEPTANEDIONE, 6-METHYL-
dissociation in chloroform–water system, constants for, 19: 40423
solvent properties for copper and uranium, 19: 40423
HETEROGENEOUS REACTORS
neutron distributions in, method for calculating, 19: 42060
neutron space-dependent spectra in thermal, diffusion approximation for, (T), 19: 42056
reactivity and safety of sodium-cooled fast power breeders, (E), 19: 42081 (CONF-193-11)

2,4-HEXANEDIONE
dissociation in chloroform–water system, constants for, 19: 40423
solvent properties for copper and uranium, 19: 40423
HIGH-ALTITUDE EXPLOSIONS
electromagnetic wave excitation in earth-ionosphere cavity by, (T), 19: 41581
HIGH ENERGY INJECTION DEVICES
ion Lorentz dissociation in DCX-1, excited-state diatomic hydrogen, 19: 41864 (ORNL-P-1244)
HIGH TEMPERATURE LATTICE TEST REACTOR
materials for, environmental tests of candidate, 19: 40966 (BNWL-92)
HIGH-TEMPERATURE OXIDATION
ignition system for studies of, 19: 42214 (RFP-397)
HIGH TEMPERATURE SEPARATION PROCESSES
development of AIROX, for reprocessing irradiated uranium dioxide fuel, 19: 40653 (NAA-SR-11389)
evaluation of pyrochemical, for reprocessing irradiated uranium carbide fuel, 19: 40652 (NAA-SR-11340)
HIROSHIMA
effects of atomic explosion on population of, 19: 40361(T) (ORNL-tr-437)
HISTAMINE
protective effects of injected, against radiation injuries in rats, 19: 40389
HOLMIUM
determination by spectrochemical methods, voltage-fluctuation patterns in, 19: 40416
neutron reactions (n,γ), gamma spectra from thermal, 19: 41670 (LA-DC-7097)
neutron reactions (n,α) with, cross sections for thermal, (E), 19: 41809(T)
physical and thermodynamic properties, 19: 40948 (IS-1195)
polarographic behavior in dimethylformamide and dimethylsulfoxide, 19: 40681
preparation and purification, 19: 40948 (IS-1195)
HOLMIUM ALLOYS
Ho–Mg, thermodynamic properties, 19: 41013 (IS-T-25)
Ho–Ru, process for improving workability of, 19: 40999(P)
HOLMIUM CARBIDES
eutectic temperature between carbon and dicarbide, 19: 41014 (LA-DC-6819)
lattice parameters and phase transformation temperatures in, 19: 41014 (LA-DC-6819)
microhardness, 19: 41014 (LA-DC-6819)
HOLMIUM CHLORIDES
complexes with phenanthroline, preparation and properties, 19: 40514
HOLMIUM COMPLEXES
with gluconic acids, stability constants, 19: 40508
HOLMIUM ISOTOPES Ho-165
neutron reactions with polarized at 0 to 55 ev, resonance spins from, (E), 19: 41665 (JINR-P-2209)
HOLMIUM ISOTOPES Ho-166
energy levels of, parity and spin of, 19: 41670 (LA-DC-7097)
energy levels of, spins of, (E), 19: 41665 (JINR-P-2209)
HOLMIUM OXIDES
content in McKelveyite uranium mineral, 19: 40799
HOLMIUM OXYSULFIDES
preparation and crystal structure, 19: 40475
HOLMIUM PERCHLORATES
stability constants of, thermal, 19: 40509
HOLMIUM SULFIDES
preparation and crystal structure, 19: 40475
HOMOGENEOUS REACTORS
design of boiling, 19: 42069(P)
power level control in, 19: 42016(P)
HYDRAZINE
production by fissiochemical processes, design of loop for, 19: 40547(R) (AGN-8137(Vol.I))
production by irradiation of ammoniated water, 19: 40548 (BNWL-82)
radioinduced production from ammonia using fission fragments, G values for, 19: 40547(R) (AGN-8137(Vol.I))
HYDRAZYL, DIPHENYLPICRYL-
benzene-d_6–hexafluorobenzene–diphenylpicrylhydrazyl, differential dynamic polarization of fluorine and hydrogen nuclei in, (E), 19: 40497
benzene–diphenylpicrylhydrazyl–hexafluorobenzene, differential dynamic polarization of fluorine and hydrogen nuclei in, (E), 19: 40497
difluorobenzene–diphenylpicrylhydrazyl, differential dynamic polarization of fluorine and hydrogen nuclei in, (E), 19: 40497
diphenylpicrylhydrazyl–α,α,α–trifluorotoluene, differential dynamic polarization of fluorine and hydrogen nuclei in, (E), 19: 49497
HYDRIODIC ACID
reactions with dodecane and sodium bisulfite, 19: 40402 (BMI-X-10137)
HYDROCARBONS
yields from radiolysis of ethylene vinyl acetate copolymers, 19: 40556
HYDROCHLORIC ACID
separation of scandium from, by solvent extraction using alkyl phosphates, 19: 40689
solubility of scandium chloride in, at 25°C, 19: 40520
ethane–HCl, formation of polymeric yields in reactions with carbon-14 and sulfur-35 recoil atoms, 19: 40628
HCl–methane, formation of polymeric yields in reactions with carbon-14 and sulfur-35 recoil atoms, 19: 40628
HYDRODYNAMICS
shock propagation in, one-dimensional, (T), 19: 41126 (SCL-DR-65-75)
use for analysis of asymptotic stability of detonations, (T), 19: 41117 (LA-3306)
HYDROFLUORIC ACID
determination in gases, chromatographic, 19: 40407 (KY-485)
reactions with gamma-uranium(VI) oxide, enthalpy of, 19: 40521
reactions with zirconium oxide in fluidized bed, kinetics of, 19: 40529
HYDROGEN
argon ion reactions with molecular, spectra of ArH^+ in, (E), 19: 41251
burning in stars, effects on carbon, nitrogen, and oxygen isotopic abundances, (T), 19: 41242
carbon monoxide ion reactions with molecular, spectra of COH^+ in, (E), 19: 41252
determination in cover gases for liquid metals, methods for, 19: 40409(R) (MSAR-65-95)
determination in upper atmosphere, radiometric method for, 19: 40433
determination, use of beta ionization detector in chromatographic, 19: 40415(T) (CEA-tr-R-1839)
deuterium exchange with ammonia, heavy water production by, 19: 40942(P)
distribution in atmosphere, effect of thermal escape on, (T), 19: 41604
effects of hydridation on properties of niobium–zirconium alloy, 19: 40959
effects on sintering of tungsten, 19: 40985
effects on yield point of zirconium, 19: 41010(R) (IITRI-578P27-10)
electron excitation of 2s and 2p levels of atomic, cross sections for, (T), 19: 41254
electron motion in field of atomic, free-free matrix elements for, (T), 19: 41266
energy levels of, interference of fine-structure, (E), 19: 41263
heat transfer in turbulent flow through heated tubes, data compilation, 19: 40734 (NP-15331)
hyperfine splitting of, four-fermion V-A weak interactions in, (T), 19: 41410
ion reactions with molecular, spectra of XH^+ in, (T), 19: 41250
light absorption by electric arcs in, measurement of, (E), 19: 41898
motion of plasma of, in toroidal octupole fields, (E), 19: 41896
nitrogen ion reactions with molecular, spectra of N_2H^+ in, (E), 19: 41252
polarization of nuclei of, differential dynamic, (E), 19: 40497
positron elastic scattering at low energies, phase shifts for, (T), 19: 41267
production of plasma of, in Ogra, 19: 41851 (IAE-635)
radioinduced recombination with oxygen in presence of water vapor, gamma, 19: 40549 (COO-1032-1)
reactions with carbon dioxide, kinetics of, 19: 40959
reactions with optically pumped sodium, light modulation in spin-exchange, (E), 19: 41262
sorption by molybdenum at room temperature, 19: 40463(R) (SRIA-425-5)
sorption on zirconium borate or dioxide, 19: 40484
spectra in gaseous nebulae, recombination, (T), 19: 41238
spectral lines excitation in collisions of hydrogen ions and protons with mercury atoms, (E), 19: 41260
thermal radiation from burning plume of, in Kiwi reactor run, 19: 42137 (LA-DC-7313)
yields from radiolysis of ethylene vinyl acetate copolymers, 19: 40556
HYDROGEN IONS
diffusion of diatomic molecular, in plasma, 19: 41850(R) (AD-617386)
injection in Ogra, properties of plasma production from, 19: 41851 (IAE-635)
production of excited diatomic, for Lorentz dissociation in DCX-1, 19: 41864 (ORNL-P-1244)
reactions with mercury atoms, hydrogen and mercury spectral line excitation in, (E), 19: 41260
reactions with molecular nitrogen ions at 10 to 65 kev, rotational and vibrational excitation in, (E), 19: 41279
spectral lines in solar chromosphere, (T), 19: 41220
HYDROGEN ISOTOPES H-5
detection of beta-active, from bremsstrahlung reactions with lithium-7, (E), 19: 41750
HYDROGEN PEROXIDES
production by fissiochemical processes, design of loop for, 19: 40547(R)

(AGN-8137(Vol.I))
production by irradiation of oxygenated water, 19: 40548 (BNWL-82)
HYDROGEN SYSTEMS
D–H, sorption by molybdenum at room temperature, 19: 40463(R) (SRIA-425-5)
H–Ne, performance in bubble chambers, 19: 40869 (CONF-650510-14)
H–Pt–PuO_2, reactions at 1050°C, 19: 40958
H–Pu, neutron spectra in, thermal, 19: 42037 (BNWL-95, pp 4-17)
NH_3–H_2, effects of ratio of, on nitrogen solubility in stainless steel, 19: 40968(R) (EURAEC-1424)
HYDROGENATION
radioinduced in coal extract and aromatic compounds, beta, 19: 40553(R) (NYO-2978-34)
HYDROMAGNETIC WAVES
damping in magnetized plasma, effect of transport coefficients on, (T), 19: 41869
propagation along warm plasma columns, (T), 19: 41939
propagation of low frequency micropulsation, in magnetosphere, (T), 19: 41595
propagation of non-quasistatic surface, in argon plasma, 19: 41942
HYDROQUINONE
effects on use of chromogenic polymer for gamma dosimetry, 19: 40599
HYPERFRAGMENTS
binding energy of $_{\Lambda}H^{3}$, (T), 19: 41419
decay of lambda-lithium-7, meson (π^{+}), (E), 19: 41512
properties of, book on, 19: 41513
scattering of $^{3}H_{\Lambda}$, on heavy nuclei, Coulomb spallation in, (T), 19: 41815
scattering on heavy nuclei, Coulomb spallation in, (T), 19: 41815
HYPERONS
book: *Nuclear Interactions of the Hyperons*, 19: 41513
decay amplitudes in U(12) symmetry, nonleptonic, (T), 19: 41420
decays of, PC violation in unitary symmetry for leptonic, (T), 19: 41522
properties of resonant states of, (T), 19: 41384
HYPERONS (Λ)
interactions with deuterons at low energies, (T), 19: 41419
HYPERONS (Λ^{0})
decay of lithium-7 hyperfragment with, meson (π^{+}), (E), 19: 41412
production in meson (K⁻)-neutron interactions, (T), 19: 41405
production of polarized, in photon–proton interactions at 950 to 1050 Mev, (E), 19: 41367
HYPERONS (Σ)
production in meson (K⁻)-neutron interactions, (T), 19: 41405
HYPERONS (Σ^{-})
production and decay in proton interactions with emulsion nuclei at 9 Mev, (E), 19: 41350
production in meson (K⁻) interactions with neutrons and protons at rest, (E), 19: 41494
range-energy relation for, difference from hyperons (Σ^{+}), (E), 19: 41369
HYPERONS (Σ^{+})
production and decay in proton interactions with emulsion nuclei at 9 Mev, (E), 19: 41350
production in meson (π^{+})-proton interactions, (T), 19: 41427
range-energy relation for, difference from hyperons (Σ^{-}), (E), 19: 41369

I

ICE
radiolysis of, formation of solvated electrons in gamma, 19: 40551 (KFK-293)
IMIDES
fluor-, isotopic exchange with heavy water and deuterated trifluoroacetic acid, 19: 40537
IMPACT SHOCK
effects on casks for irradiated fuel, 19: 40818 (SC-RR-65-98, pp 261-82)
effects on shipping containers for slightly enriched uranium fuel cores, 19: 40820 (SC-RR-65-98, pp 357-76)
effects on 10-ton capacity uranium hexafluoride shipping containers, 19: 40824 (SC-RR-65-98, pp 580-608)
IN-PILE LOOPS
displacement of, design of device for operating trolley for, 19: 42189(P)
INCOLOY
corrosion of 804, by coal gasification products at high temperatures, 19: 42127(R) (TID-22009)
INCONEL
compatibility of 600 and 625, with graphite–nitrogen environment at 1000 and 1200°C, 19: 40966 (BNWL-92)
corrosion by aluminum, lead, tin, and zinc at 800 to 1100°C, 19: 40961
corrosion of 702, by coal gasification products at high temperatures, 19: 42127(R) (TID-22009)
properties of forged, ultrasonic testing, 19: 41027 (WERL-0029-2)
welding to Zircaloy-2 of type 600, joint design for explosive, 19: 40989
INDENE
2-aryl- and 2-aryl-3H-benz(e)-, preparation and properties as scintillation phosphors and solutes, 19: 40546
INDEXES
of UCRL hazards control quarterly reports, 19: 40833 (UCRL-14116)
on Shippingport Pressurized Water Reactor Project, 19: 42101 (WAPD-PWR-1606(Add.2))
INDIA
atomic energy activities in, 19: 42209(R) (NP-15356)
INDIUM
determination in copper by activation, 19: 40422
effects on superconductivity of niobium–tin alloys, (E), 19: 41609
positron annihilation in, angular correlations from, (E), 19: 41285
separation from uranium by chromatography on cellulose columns, tracer studies of, 19: 40687
INDIUM ALLOYS
In–rare earths, crystal structure and thermal expansion of intermetallic compounds in, 19: 41041
In–Th, hardness at 30 to 800°C, effects of indium on, 19: 40958
In–Th, tensile properties at 800°C, 19: 40958
Sb–In, radiation effects on, gamma, 19: 41096
INDIUM COMPLEXES
nitryl nitrate, preparation and infrared spectra, 19: 40471
INDIUM ISOTOPES In-109
gamma spectra and half life of isomeric, (E), 19: 41802(T)
production of isomeric, (E), 19: 41802(T)
INDIUM ISOTOPES In-115
alpha reactions (α,2p) with, angular momentum effects on isomeric cross section ratios in, 19: 41821
neutron capture by conversion-electron spectra from thermal, (E), 19: 41808(T)
INDIUM ISOTOPES In-116
beta decay of, conversion electron spectra from, (E), 19: 41808(T)
INDIUM ISOTOPES In-117
production in indium-115(α,2p) reactions, angular momentum effects on isomeric cross section ratios in, (E), 19: 41821
INDOLE
aniline–indole, labeled yields in reactions with carbon-14 recoil atoms, 19: 40627
indole–pyridine, labeled yields in reactions with carbon-14 recoil atoms, 19: 40627
5-INDOLOL, 3-(2-AMINOETHYL)-
protective effects of injected, against radiation injuries in rats, synergistic effects of tryptophan, 19: 40388
INDUSTRIAL HYGIENE
noise control methods, 19: 40806 (RL-SA-37)
INDUSTRIAL MANAGEMENT
control of production schedules and costs at Y-12, real-time information system for, 19: 40704 (Y-KA-9)
INFLAMMATION
aseptic, effects on incidence of tumors induced by plutonium-239 in rats, 19: 40381
effects on strontium-90 metabolism in skeleton, 19: 40343
INFRARED RADIATION
quantum electrodynamics of, 19: 41545
INSECTS
ecology of, in irradiated forest, 19: 40307 (BNL-9253)
INSPECTION
of wood-core fiberglass, ladders, methods for, 19: 40834(R) (UCRL-14151)
INSTRUMENTATION
book: *Advances in Analytical Chemistry and Instrumentation*. Vol. 4, 19: 40446
design for Mössbauer experiments at low temperatures, 19: 40863
design of 6600-Octopus interface control for computer teletype control and remotely driving plotters, engineering drawings of, 19: 40864
development for ion engine control console, 19: 40765(R) (NP-15309)
development for Stanford electron accelerator, 19: 41170 (SLAC-42)
INSTRUMENTS
design for remote measurements in radiation environment, (E), 19: 40714 (EUR-2421.d)
design of standardized modular, for ion sources, (E), 19: 41185
design of ultrasonic, for liquid metal and liquid salt level measurements, 19: 40847(R) (NYO-2910-11)
luminous dials for, radiation hazards of radioactive, 19: 40940 (NP-14924)
INTERFEROMETERS
performance of ruby laser with, for plasma electron-density measurements, 19: 41924
INTERNAL CONVERSION

coefficients measurements for, performance of semiconductor detectors for, 19: 40880 (UCRL-16035)
INULIN SPACE
radiation effects on, in rats, 19: 40369
IODATES
separation from iodides and periodates by paper chromatography, tracer studies of, 19: 40430
IODIDES
separation from iodates and periodates by paper chromatography, tracer studies of, 19: 40430
separation from iodine-131-labeled organic compounds, chromatographic, 19: 40656(T) (CEA-tr-X-609)
IODINE
deposition on surfaces at 300 to 600°F in helium loop, 19: 40397 (ORNL-TM-1134)
determination in atmosphere, development of sampling method for, 19: 40402 (BMI-X-10137)
reactions with dodecane and sodium bisulfite, 19: 40402 (BMI-X-10137)
release in sodium fires, 19: 40803 (NAA-SR-Memo-9719)
use in carbon dioxide reactor cooling streams to inhibit reaction with graphite moderator, 19: 42015(P)
IODINE COMPOUNDS
chemical properties, 19: 40800(R) (AERE-PR/HPM-7)
IODINE ISOTOPES
production in man during high-energy radiotherapy, 19: 40392 (NYO-3364-6)
release to atmosphere by gas-cooled reactor accident, 19: 40800(R) (AERE-PR/HPM-7)
IODINE ISOTOPES I-117
half life, 19: 41717
IODINE ISOTOPES I-118
decay scheme, 19: 41717
half life, 19: 41717
IODINE ISOTOPES I-119
half life, 19: 41717
IODINE ISOTOPES I-126
production of 2.6-hr isomer of, attempts at, 19: 41716
IODINE ISOTOPES I-127
energy levels from tellurium-127 decay, (E), 19: 41835
exchange equilibrium with iodine-128, 19: 40505
neutron reactions (n,2n) with, search for 2.6-hr iodine-126m in, 19: 41716
nuclear spin echoes in potassium iodide crystals, (E/T), 19: 41988
proton reactions (p,pn) with, search for 2.6-hr iodine-126m in, 19: 41716
IODINE ISOTOPES I-128
exchange equilibrium with iodine-127, 19: 40505
IODINE ISOTOPES I-131
analytical use in detection of sulfur dioxide in atmosphere, 19: 40410 (ORNL-P-494)
content in food chains in Alaska, 1959 to 1965, 19: 40780 (BNWL-SA-242)
determination in biological material by scintillation counting of beta decay, 19: 40425
diagnostic use of, in irradiated patients, 19: 40374
effects on response to norepinephrine of rats, 19: 40368
effects on thyroid function in rats, 19: 40368
incorporation in sterile pyrogene-free human serum albumin, 19: 40639
separation from milk by moving bed ion exchange columns, 19: 40697(P)
IODINE ISOTOPES I-132
decay of, conversion electron spectra in, (E), 19: 41743
decay of, high-energy gamma transitions in, 19: 41744
decay of, xenon-132 energy levels from, (E), 19: 41745
thyroid activity of, from inhalation of labeled methyl iodide, 19: 40800(R) (AERE-PR/HPM-7)
ION BEAMS
aberrations of, evaluation of space-charge-produced, (T), 19: 41173
acceleration and focusing of heavy, in linear accelerator with slip tubes, (E), 19: 41177
accelerator design for negative, (E), 19: 41182
collector system testing for ion rockets, 19: 40765(R) (NP-15309)
ionization of lithium and lithium-fluoride, on tungsten electrodes, (E), 19: 41141
ION EXCHANGE MATERIALS
use of clinoptilolite in decontamination of storage basin water, 19: 40651 (IDO-14657)
ION EXCHANGE PROCESSES
for rare earth separation, review, 19: 40691
uses for separating long- and short-lived radioisotopes in wastes, (E) 19: 42197
ION EXCHANGERS
resin pump development for continuous contactors, 19: 40650(R) (HW-77805)
use of moving bed, in milk decontamination, 19: 40697(P)
ION PUMPS
performance of sputter, use of mass spectrometer in measuring, 19: 40777
ION SOURCES
components for, design of standardized modular, (E), 19: 41185
design and performance of negative-ion accelerators, (E), 19: 41182
design and performance of duoplasmatron, 19: 41871
development for space propulsion, 19: 40771
development of surface ionization, 19: 40769
ionization characteristics of electromagnetic, 19: 40861
performance of cesium electron-bombardment, for ion engines, 19: 40770
performance of hollow-cathode, (E/T), 19: 41872
performance of pulsed r-f, 19: 40855
performance of three anode, for cyclotrons, (E), 19: 41193
testing apparatus for, 19: 41192
IONIZATION
efficiency of, for lithium and lithium-fluoride ion beams on tungsten electrodes, (E), 19: 41141
of gas-particle plasma, (T), 19: 41929
of solvents, acido-basic reactions in, 19: 40466 (UJV-1209/65)
IONIZATION CHAMBERS
design for gamma and neutron monitoring, engineering drawings of, 19: 40923
design for monitoring radioisotopes packaged for shipment, engineering drawings of, 19: 40925
electromagnetic cascades in, transition effect on measurement of, 19: 40912
ionization in, in electric and magnetic fields, 19: 40861
performance in depth dose measurements on wide x-ray beam in finite phantom thickness, 19: 40881 (UR-667)
use in remote radiation monitoring at Nevada Test Site, 19: 40878 (NVO-162-5(Rev.))
IONOSPHERE
charged particle ambipolar diffusion in geomagnetic fields in, (T), 19: 41585
conference, 19: 41605
disturbances during magnetic storm, data for Sept. 1963, 19: 41603
disturbances in, statistical characteristics of sudden, 19: 41573 (RPU-S19)
electron collision frequency in, method for determination of, (T), 19: 41574(T) (FTD-TT-65-101)
electron content in, diurnal variations of, (E), 19: 41597
electron density in sporadic-E region of, (E), 19: 41591
electron production rate in, from overhead-sun, (E/T), 19: 41598
electrostatic field production by wind dynamo action in, (T), 19: 41593
gas motion in, Pedersen conductivity for neutral, (T), 19: 41594
ion density in D region of, positive, (E), 19: 41588
plasma oscillations in, r-f emission from, 19: 41572 (NASA-CR-258)
radio wave propagation in, analysis of, 19: 41572 (NASA-CR-258)
structure of topside, ionogram data for, (E/T), 19: 41587
IONS
density distribution in exosphere, (T), 19: 41601
density of positive, in ionospheric D region, (E), 19: 41588
distributions in plasma, measurement using proton scattering, (E), 19: 41899
mobility spectra of small radioactive, in air, 19: 40787
model transport by biological membranes, 19: 42199 (BNL-8397)
oscillations in alkali-metal plasma in thermal equilibrium, (E), 19: 41890
reactions with deuterium and hydrogen molecules, spectra of XD^+ and XH^+ in, (T), 19: 41250
reactions with nuclei, many-nucleon transfer in, 19: 41795
sorption from aqueous solutions by alumina, alumina–silica, and silica gel surfaces, 19: 42200 (COO-1354-5)
sputtering reactions with crystals, energy dependence of, (T), 19: 41271(T)
temperatures in helium theta-pinch plasma in azimuthal magnetic field, (E), 19: 41921
temperatures in theta-pinch plasma, (E), 19: 41860 (NP-15220)
IRIDIUM ALLOYS
Hf–Ir, phase studies, 19: 40960
IRON
analysis for nitrogen, isotope-dilution method for, 19: 40444
determination in copper by activation, 19: 40422
determination in heavy water moderator, automated, 19: 40406 (CONF-650919-2)
effects on phase transformation in plutonium, 19: 40958
effects on phase transformations in delta-stabilized gallium–plutonium alloys, 19: 40958

gamma angular and energy distributions in, cobalt-60, (E), 19: 41953 (NP-15131)
ion reactions at 5 to 12 Mev, neutron spectra from, (E), 19: 41810(T)
ionization of, collisional excitation in auto-, (T), 19: 41244
magnetic properties near Curie point, (E), 19: 41972
neutron reactions (n,γ) at 0.025 ev, spectra from, 19: 40896
oxidation of, effects of ion bombardment on, 19: 40973
proton reactions at 200 Bev, nucleon–meson cascade production in, (T), 19: 41955 (ORNL-TM-1121)
proton spectra in, near surfaces, (T), 19: 41951 (N64-30510)
reactions of boride and carbide coated, with cesium at 500°C, 19: 40765(R) (NP-15309)
separation from uranium by chromatography on cellulose columns, tracer studies of, 19: 40687
solubility in pure potassium at 1000°C, 19: 40946(R) (AI-65-93)
solvent distribution in ammonium thiocyanate–methanol–water systems, distribution coefficients for, 19: 40447
thermal capacity of pure, at 100 to 1400°C, 19: 40700 (ORNL-TM-1187)
thermodynamic properties at high pressures and temperatures, 19: 40459 (NP-15324)

IRON ALLOYS
analysis for niobium and tantalum, photometric method for, 19: 40442
Al–Cr–Fe–Y, corrosion by steam at 500 to 1300°C, 19: 40961
Al–Cr–Fe–Y, impact properties of, 19: 40961
Cr–Co–Fe–Mn–Mo–Ni–W, corrosion of Rasonel, by coal gasification products at high temperatures, 19: 42127(R) (TID-22009)
Cr–Fe–Ni, corrosion films on, structure of oxide, 19: 40967(R) (COO-1319-27)
Cr–Fe–Ni, stress-corrosion cracking in, effects of fourth-component additions on, 19: 40967(R) (COO-1319-27)
Cr–Fe–Ni, stress-corrosion by chlorides, oxygen, and water, 19: 40967(R) (COO-1319-27)
Cr–Fe–Ni, tensile properties to 1200°F, effects of composition on, 19: 40967(R) (COO-1319-27)
Fe–Nb, solubility of nitrogen in, 19: 41065
Fe–Pu, eutectic temperature of, effects of nickel on, 19: 40958
Fe–Pu–U, oxidation and ignition behavior of, 19: 40958
Fe–rare earths, analysis for erbium, dysprosium, gadolinium, and scandium, 19: 40445
Fe–Ta, solubility of nitrogen in, 19: 41065
Fe–Ti, solubility of nitrogen in, 19: 41065
Fe–U, phase studies, 19: 40958
Fe–V, solubility of nitrogen in, 19: 41065
Fe–Zr, solubility of nitrogen in, 19: 41065

IRON CHLORIDE COMPLEXES
spectra, electron spin resonance spectra, 19: 40465 (UCRL-16175)

IRON(III) CHLORIDES
sorption by phospho-organic resins, 19: 40668

IRON FORMATES
ion sites in, Mössbauer studies of inequivalent iron, (E/T), 19: 40542

IRON IONS
coupling at inequivalent sites in iron(II) formates, quadrupole, (E/T), 19: 40542

IRON ISOTOPES Fe-54
alpha reactions (α,xnyp) with, shell structure effects in nickel-58 decay in, (T), 19: 41741

IRON ISOTOPES Fe-55
deposition, computer program for evaluating radiochemical data on, 19: 40636 (WAPD-TM-516)

IRON ISOTOPES Fe-56
alpha reactions (α,xnyp) with, shell structure effects in nickel-60 decay in, (T), 19: 41741
deuteron reactions (d,p) at 2.8 Mev, Mössbauer effect from, (E), 19: 41793
helium-3 reactions (He-3,xnyp) with, shell structure effects in nickel-59 decay in, (T), 19: 41741

IRON ISOTOPES Fe-57
gamma scattering by, interference between Mössbauer and Rayleigh, (T), 19: 41796
Mössbauer effect in, from iron-56 (d,p) reactions at 2.8 Mev, (E), 19: 41793

IRON ISOTOPES Fe-59
deposition, computer program for evaluating radiochemical data on, 19: 40636 (WAPD-TM-516)

IRON OXIDES
effects on oxidation resistance and strength of chromium–magnesia composites, 19: 41022(R) (NP-15292)

IRON(III) OXIDES
properties of electron multiplier resistance-strip of, 19: 41124(R) (NP-15108)
reactions with lanthanum and yttrium oxides at 700 to 1400°C, 19: 40515

IRON SYSTEMS
Al–Fe–Si–U, hot hardness and microstructure of, effects of heat treatments on, 19: 40958
Al–Fe–Si–U, properties of, effects of chromium and molybdenum on high-temperature, 19: 40958

IRRADIATION FACILITIES
conveyor system for, pneumatic, 19: 40729(P)
design of low-temperature neutron, 19: 42180
design of strontium-90-, for hydrogenation of coal extract, 19: 40553(R) (NYO-2978-34)

ISOTOPE EFFECTS
in recoil tritium reactions through measurement of isotopic molecule yields, kinetic, 19: 40615
of deuterium on chromatographic behavior of methane, 19: 40672
on yields of positive oxygen ions from electron bombardment of light and heavy water, 19: 40581

ISOTOPES
separation of, mass spectroscopy techniques for, 19: 41243(T) (FTD-TT-64-1368)

ISOTOPIC EQUILIBRATION
of uranium fission products in rats, after oral administration of mixture, 19: 40322
substoichiometric separation procedures in, 19: 40424

ISOTOPIC EXCHANGE
mechanism and rates of, in molecules, 19: 40505
of deuterium between fluorimide and heavy water or deuterated trifluoroacetic acid, 19: 40537
of oxygen in gas-melt systems at 700 to 900°C, 19: 40506

J

JAPAN
radioisotopes in sea water in, dietary contamination by, 19: 40309(R) (NP-15180)

JOURNAL BEARINGS
design of gas-lubricated tilting-pad, for high-speed rotors, 19: 40736 (NYO-2512-1)
testing of fluid-film, for SNAP-50/SPURE liquid metal pumps, 19: 40703 (TIM-916)

K

KENTUCKY
life history of banded sculpin in stream in, 19: 42220 (TID-32023)

KIDNEYS
radiodiagnosis of one-sided deficiency in isotope nephrogram of, design of multichannel detector for, 19: 40913
radium-224 content in rat, after intravenous injection, 19: 40315

KRYPTON
cesium spin relaxation in, (E), 19: 41278
charged-particle stopping power and straggling in, excitation energy for, (T), 19: 41268
radioinduced polymerization of, with vinyl chloride and, 19: 40584
separation from gas mixtures, 19: 40695(P)
sorption on graphitic carbon, two-dimensional second virial coefficients for, 19: 40956

KRYPTON IONS
reactions with nickel surfaces, isotopic effect in secondary electron emission in, (E), 19: 41249

KRYPTON SYSTEMS
Ar–Kr, electron reactions at 50 kev, luminescence from, (E), 19: 41246
Kr–N, electron reactions at 50 kev, luminescence from, (E), 19: 41246
Kr–Xe, electron reactions at 50 kev, luminescence from, (E), 19: 41246

L

LABORATORIES
radiation monitoring in high-voltage, engineering drawings of equipment for, 19: 40924
research programs at Siemens-Schuckertwerke, Erlangen, Germany, 19: 42228

LABORATORY EQUIPMENT
design for handling irradiated materials, 19: 40715 (NAA-SR-Memo-7438)
design for radiation-chemistry studies, 19: 40370

LACTIC ACID COMPLEXES
with transplutonic elements, stability constants, 19: 40458 (JINR-P-2224)

LACTIC ACID, 2-METHYL-
preparation of actinides and lanthanides from, by solvent extraction using amines, 19: 40657
use in chromatographic separation of europium-152, 154 and yttrium-90, 19: 40662

use in ion exchange separation of rare earths, 19: 40665
use in ion exchange separation of rare earths, 19: 40666
uses in ion exchange separation of rare earths, 19: 40663
LANTHANUM
analysis for nitrogen, isotope-dilution method for, 19: 40444
determination by spectrochemical methods, voltage-fluctuations patterns in, 19: 40416
physical and thermodynamic properties, 19: 40948 (IS-1195)
polarographic behavior in dimethylformamide and dimethylsulfoxide, 19: 40681
preparation and purification, 19: 40948 (IS-1195)
reactions with polyribonucleotides of adenylic, cytidylic, and uridylic acids, mechanism of degradation in, 19: 40474
LANTHANUM ALLOYS
Au–La, phase studies of solid solutions in, 19: 41062
Be–La, vaporization of $LaBe_{13}$, 19: 40959
La–Mg, phase studies, 19: 41011 (IS-T-15)
La–Ni, preparation for solid solubility studies, 19: 41021(R) (NMI-8002.1)
La–Ru, process for improving workability of, 19: 40999(P)
LANTHANUM BORIDES
deposition of coatings of, on rhenium filaments, (E), 19: 40725
LANTHANUM CARBIDES
eutectic temperature between carbon and dicarbide, 19: 41014 (LA-DC-6819)
lattice parameters and phase transformation temperatures in, 19: 41014 (LA-DC-6819)
microhardness, 19: 41014 (LA-DC-6819)
LANTHANUM CHLORIDES
complexes with phenanthroline, preparation and properties, 19: 40514
temperature-volume relations in aqueous solutions of, 19: 40523
LANTHANUM COMPLEXES
tartrate, composition and stability, 19: 40491
with gluconic acids, stability constants, 19: 40508
LANTHANUM FLUORIDES
solubility in beryllium nitrate solutions, 19: 40670
LANTHANUM IONS
reactions with derivatives of Arsenazo III, spectrophotometric studies of, 19: 40426
LANTHANUM ISOTOPES La-139
proton reactions (p,3n), angular momentum effects on isomeric cross section ratios in, (E), 19: 41821
LANTHANUM ISOTOPES La-140
determination in uranium fission products, 19: 40640
gamma directional correlations in, (E), 19: 41822
yield in alpha fission of thorium-232 at 20 to 40 Mev, (E), 19: 41779
yield in neutron fission of uranium-235 at 14.9 Mev, (E), 19: 41779
LANTHANUM NITRATES
sorption by phospho-organic resins, 19: 40668
LANTHANUM OXIDES
content in McKelveyite uranium mineral, 19: 40799
reactions with ferric oxide at 700 to 1400°C, 19: 40515
LANTHANUM PERCHLORATES
stability constants of, thermal, 19: 40509
LANTHANUM SILICATES
preparation of, by reaction of lanthanum sulfate with sodium silicates, 19: 40518
LANTHANUM SILICIDES
crystal structure, 19: 40477
crystal structure, 19: 40478
LANTHANUM SULFATES
reactions with sodium silicates, preparation of lanthanum silicates by, 19: 40518
$La_2(SO_4)_3$–Na_2SO_4, thermal stability, 19: 40511
LANTHANUM TELLURIDES
crystal structure, 19: 40476
crystal structure of, x-ray studies of, 19: 41070
crystal structure of $LaTe_2$, 19: 41071
LAVA
age of Serra-Geral, potassium–argon estimation of, 19: 40796
LEAD
analysis for traces of gold by neutron activation methods, 19: 40437
bremsstrahlung reactions in, neutron production from, (E), 19: 41833
corrosive effects on Inconel and yttrium at 800 to 1100°C, 19: 40961
determination by spectrochemical methods, voltage-fluctuation patterns in, 19: 40416
effects on superconductivity of niobium–tin alloys, (E), 19: 41609
ionization cross sections of atoms of, measurement by electron impact, 19: 41276
melting in exposure of lead-lined casks to fire, 19: 40813 (SC-RR-65-98, pp 107-13)
melting in fire test of cask, calculations, 19: 40832 (SC-RR-65-98, pp 732-5)
neutron inelastic scattering at 14 Mev, cross sections for, (E), 19: 41718
neutron total cross sections of, (E), 19: 41723
performance of screens of, for radiography of steel welds, 19: 40753(R) (EURAEC-1378)
positron annihilation in, angular correlations from, (E), 19: 41285
proton reactions at 20 Bev, production of antiprotons, mesons, and protons in, 19: 41324 (CERN-65-14)
thermodynamic properties at high pressures and temperatures, 19: 40459 (NP-15324)
LEAD ALLOYS
Pb–Tl, critical fields of superconducting, temperature dependence of, (E), 19: 41610
Pb–Tl, Debye temperature and entropy of formation of, 19: 41012 (IS-T-16)
Pb–Tl, elastic constants of single-crystal, 19: 41012 (IS-T-16)
LEAD CHLORIDES
europium ion paramagnetic resonance in, divalent, (E/T), 19: 40498
LEAD ISOTOPES Pb-206
deuteron reactions (d,p) with, DWBA and Coulomb stripping approximations for, (E), 19: 41742
neutron reactions (n,n'γ) at 1.5 to 3.5 Mev, gamma spectra from, (E), 19: 41669 (LA-DC-7096)
LEAD ISOTOPES Pb-208
carbon-12 inelastic scattering by, (E), 19: 41768
carbon-12 reactions (C-12,C-13) with, (E), 19: 41768
meson (μ^-) capture by proton pairs in, (E/T), 19: 41753
oxygen-16 inelastic scattering by, (E), 19: 41768
oxygen-16 reactions (O-16,O-17) with, (E), 19: 41768
LEAD ISOTOPES Pb-212
metabolism in rabbits of, after intra-arterial, intravenous, or subcutaneous injection, 19: 40333
metabolism in rats of, after intra-arterial or intravenous injection, 19: 40333
LEAD MOLYBDATES
ytterbium ion EPR spectra in single crystals of, (E), 19: 41986(T)
LEAK DETECTORS
performance of vacuum system, 19: 40773
LEAKS
analysis of, in reactor containment buildings, 19: 42018 (NAA-SR-10100)
LECTURES
book: *Lectures on Quantum Mechanics*, 19: 41567
on nuclear rocket systems, 19: 42139 (N64-33784)
on reactor control, 19: 42138 (N64-33780)
LEPTONS
emission in meson ($K_{\mu 3}$) decay, angular correlation in, (T), 19: 41485(T)
theory for, CP-violating terms in field-theoretical lepton currents, (T), 19: 41378
LEVEL INDICATORS
description of differential-pressure, for cryogenic liquids, 19: 40878 (UCRL-9672(Rev.))
development of ultrasonic, for boiling metals and salts, 19: 40847(R) (NYO-2910-11)
LIFE SPANS
radiation effects on dog, effects of bone marrow transfusions, 19: 40385(T) (FTD-TT-65-48, pp 134–5)
LIGHT
absorption of rubidium, by ionized strontium, (E), 19: 41883
effects on synthesis of ruthenium-106-labeled ruthenocene, 19: 40634 (BNL-8405)
interactions with atoms, (T), 19: 41248
physiological effects on retina in eyes of frogs and rabbits, 19: 40359(T) (FTD-TT-65-48, pp 590–1)
scattering by density of fluctuations in matter, (T), 19: 41971 (UCRL-7968-T)
testing Scotchlite reflective material for illuminating bubble chambers, 19: 40917
LIGHT SOURCES
design of stroboscopic, for photoconductivity measurements, 19: 40933(R) (NP-15300)
LINEAR ACCELERATORS
accelerating fields at 200 Mc/sec in, (E), 19: 41202
beam acceleration and self-focusing in heavy-ion, with slip tubes, (E), 19: 41177
electromagnetic field control for resonant cavities of proton, 19: 41167 (NIRL/R/76)
performance of PHERMEX, for detonation and shock wave studies, 19: 41118 (LA-DC-6996)
LIPIDS
metabolism in coronary atherosclerosis, tracer study using iodine-131-

peanut oil, 19: 40393
radiation effects on content in blood and liver of rats, 19: 40386(T) (FTD-TT-65-48, pp 661–2)
LIQUID FLOW
magnetohydrodynamic, between nonconducting plates, (T), 19: 41135
LIQUID METAL COOLED REACTORS
feasibility of 1000 Mw(e) sodium, calculational methods development for, 19: 42095 (NAA-SR-11378(Vol.III))
reactivity and safety of sodium-cooled fast power breeders, (E), 19: 42081 (CONF-193-11)
LIQUIDS
book: *Cavitation in Real Liquids*, 19: 40751
book: *Liquids: Structure, Properties, Solid Interactions*, 19: 40538
electromagnetic processes in anisotropically conducting, in alternating magnetic fields, (T), 19: 41149
nuclear magnetic relaxation in, (T), 19: 40499
LITHIUM
corrosive effects on niobium and tantalum, 19: 40961
determination by spectrochemical methods, voltage-fluctuation patterns in, 19: 40416
determination in Tramex process samples, automated, 19: 40405 (CONF-650919-1)
electron scattering at 0.003 to 25.0 ev, exchange effects and polarization in, (T), 19: 41286
ionization of beams of, on tungsten electrodes, (E), 19: 41141
meson (μ^-) capture in solid, transition paths in, (T), 19: 41823
performance of lithium-drifted silicon radiation detectors in thermal-vacuum environment, (E), 19: 40902
positron annihilation in, angular correlations from, (E), 19: 41285
positron annihilation in, orthogonal plane waves in, (T), 19: 41945
use of vaporous, as getter in helium purification, 19: 40539(P)
LITHIUM CHLORIDES
electric conductivity in methanol, transference numbers for, 19: 40527
LiCl–KCl, equilibrium between cerium and its ions in molten eutectic, 19: 40467(T) (ORNL-tr-578)
LITHIUM FLUORIDES
ionization of beams of, on tungsten electrodes, (E), 19: 41141
performance as gamma and neutron dosimeters, 19: 40868 (BNWL-SA-23)
performance for gamma dosimetry, 19: 40877 (RISO-101)
radioinduced color centers and dislocations in, thermal-neutron, (E), 19: 41976
reactions with oxygen ions at 100 kv, effects of, (E), 19: 41256
LITHIUM HYDRIDES
neutron transmission through slabs of, Monte Carlo analysis of, 19: 41642 (NAA-SR-10853)
LITHIUM ISOTOPES Li-4
energy levels of, unbound, (E), 19: 41786
LITHIUM ISOTOPES Li-6
electron energy levels of, Lamb shift in, (T), 19: 41265
proton reactions (p,t) at 43.7 Mev, angular distributions from, (E), 19: 41786
proton reactions (p,He-3) at 43.7 Mev, angular distributions from, (E), 19: 41786
proton reactions (p,2p) with, angular correlations from, (T), 19: 41842
LITHIUM ISOTOPES Li-7
bremsstrahlung reactions with, beta-active hydrogen-5 from, (E), 19: 41750
decay of lambda hyperfragment, meson (π^+), (E), 19: 41412
deuteron reactions at 340 to 780 kev, resonances in, (E), 19: 41697
LITHIUM ISOTOPES Li-9
production in proton reactions at 1.0 and 2.8 Bev, cross sections for, (E), 19: 41780
LITHIUM NITRATES
$Ce(NO_3)_3$–$LiNO_3$–H_2O, solubility ratios in, at 10, 20, and 30°C, 19: 40519
LITHIUM OXIDES
Li_2O–SiO_2–ZrO_2, phase studies, 19: 41038
LITHIUM PHOSPHATES
$Al(PO_3)_3$–$LiPO_3$–$AgPO_3$, radio-photoluminescence polarization of glasses of, 19: 40588
LIVER
cerium-144 content in rat, after intratracheal administration, 19: 40313
function tests of, using iodine-131-rose bengal, 19: 40350 (HW-SA-3723)
metabolism of carbohydrates in rat, tracer study, 19: 40308 (BNL-8379)
radiation effects on rabbit, biochemical, 19: 40375
radiation effects on lipid content in rat, effects of unitol on, 19: 40386(T) (FTD-TT-65-48, pp 661–2)
radiation effects on cholesterol metabolism in rat, effects of unitol on, 19: 40386(T) (FTD-TT-65-48, pp 661–2)
radiation injuries of, induced by injected neptunium-237 in sheep, 19: 40350 (HW-SA-3723)
LIVERMORE POOL TYPE REACTOR
radiation from, measurement of gamma, 19: 40834(R) (UCRL-14151)
reactivity transfer function measurement in reactor oscillator technique for, 19: 42156 (UCRL-12476)
LOOPS
design for fissiochemical processing, 19: 40547(R) (AGN-8137(Vol.I))
design of high-pressure water, for testing liquid-metal lubricated bearings, 19: 40716(R) (NP-15280)
design of liquid-gallium, 19: 40727
LUMINESCENT DETECTORS
development of infrared-stimulated, using calcium, magnesium, and strontium sulfides, 19: 40879 (UCRL-12371)
LUMINESCENT MATERIALS
use of radioactive, in aircraft instruments, 19: 40940 (NP-14924)
LUNG INJURIES
pathology of, induced by deposited cerium-144 in rats, 19: 40313
LUNGS
analysis of tissue of, for copper and zinc, by neutron activation methods, 19: 40452
pathological effects of deposited plutonium-239 in rat, 19: 40380
radiation dose to, from polonium-210 in tobacco smoke, 19: 40805 (NRS-30)
strontium-90 content in rat, after intratracheal administration, 19: 40312
LUTETIUM
neutron reactions (n,α) with, cross sections for thermal, (E), 19: 41809(T)
physical and thermodynamic properties, 19: 40948 (IS-1195)
preparation and purification, 19: 40948 (IS-1195)
reactions with polyribonucleotides of adenylic, cytidylic, and uridylic acids, mechanism of degradation in, 19: 40474
LUTETIUM ALLOYS
Au–Lu, phase studies of solid solutions in, 19: 41062
Lu–Mg, phase studies, 19: 41011 (IS-T-15)
Lu–Mg, thermodynamic properties, 19: 41013 (IS-T-25)
LUTETIUM CARBIDES
eutectic temperature between carbon and dicarbide, 19: 41014 (LA-DC-6819)
lattice parameters and phase transformation temperatures in, 19: 41014 (LA-DC-6819)
microhardness, 19: 41014 (LA-DC-6819)
LUTETIUM CHLORIDES
complexes with phenanthroline, preparation and properties, 19: 40514
LUTETIUM COMPLEXES
with gluconic acids, stability constants, 19: 40508
LUTETIUM IONS
reactions with derivatives of Arsenazo III, spectrophotometric studies of, 19: 40426
LUTETIUM ISOTOPES Lu-168
energy levels of, nonexistence of isomeric, (E), 19: 41803(T)
LUTETIUM OXIDES
content in McKelveyite uranium mineral, 19: 40799
LUTETIUM OXYSULFIDES
preparation and crystal structure, 19: 40475
LUTETIUM PERCHLORATES
stability constants of, thermal, 19: 40509
LUTETIUM SULFIDES
preparation and crystal structure, 19: 40475

M

MAGNESIUM
bonding to aluminum, hot-press, 19: 40949 (ISC-640)
corrosion by aluminum–silicon and water of coatings of, on uranium, 19: 40949 (ISC-640)
creep cavities in, nucleation of, 19: 41063
creep of, cavitation along grain boundaries during, 19: 41057
deposition on uranium, hot dip, 19: 40949 (ISC-640)
diffusion of plutonium in, coefficients for, 19: 40961
neutron total cross sections of, (E), 19: 41723
nuclear resonance fluorescence in, (E), 19: 41828
processing deuteron-irradiated, for separation of sodium-22, 19: 40637(T) (ORNL-tr-625)
separation from sodium by solvent extraction using ethanol, 19: 40686
MAGNESIUM ACETATES
preparation and crystal structure of ammoniated, 19: 40507
MAGNESIUM ALLOYS
Al–Mg, creep cavities in, nucleation of, 19: 41063
Ce–Mg, phase studies, 19: 41011 (IS-T-15)
Cu–Mg, bonding to aluminum, hot-press, 19: 40949 (ISC-640)
Cu–Mg, corrosion by aluminum–silicon and water of coatings of, on uranium, 19: 40949 (ISC-640)

Cu–Mn, deposition on uranium, hot dip, 19: 40949 (ISC-640)
Dy–Mg, phase studies, 19: 41011 (IS-T-15)
Dy–Mg, thermodynamic properties, 19: 41013 (IS-T-25)
Er–Mg, thermodynamic properties, 19: 41013 (IS-T-25)
Gd–Mg, phase studies, 19: 41011 (IS-T-15)
Gd–Mg, thermodynamic properties, 19: 41013 (IS-T-25)
Ho–Mg, thermodynamic properties, 19: 41013 (IS-T-25)
La–Mg, phase studies, 19: 41011 (IS-T-15)
Lu–Mg, phase studies, 19: 41011 (IS-T-15)
Lu–Mg, thermodynamic properties, 19: 41013 (IS-T-25)
Mg–Nd, phase studies, 19: 41011 (IS-T-15)
Mg–Ni, production of splatcooled, 19: 41021(R) (NMI-8002.1)
Mg–Pr, phase studies, 19: 41011 (IS-T-15)
Mg–rare earths, crystal structure of intermetallic compounds in, 19: 41040
Mg–rare earth, phase studies, 19: 41011 (IS-T-15)
Mg–rare earth, preparation by magnesium salt reduction of halides, 19: 40955
Mg–Sm, thermodynamic properties, 19: 41013 (IS-T-25)
Mg–Tb, thermodynamic properties, 19: 41013 (IS-T-25)
Mg–Th, thermodynamic properties, 19: 41013 (IS-T-25)
Mg–Y, preparation by magnesium salt reduction of halides, 19: 40955

MAGNESIUM ALUMINATES
effects on oxidation resistance and strength of chromium–magnesia composites, 19: 41022(R) (NP-15292)

MAGNESIUM CERIUM NITRATES
cerium-139 nuclear alignment in, intermediate state reorientation in, 19: 41840

MAGNESIUM CHLORIDES
corrosive effects on high purity stainless steel, 19: 40947(R) (EURAEC-1403)

MAGNESIUM COMPOUNDS
effects of dietary, on strontium-90 metabolism in animals, 19: 40342
reactions of molten, with rare earth halides, 19: 40955

MAGNESIUM ISOTOPES Mg-24
energy levels, (E), 19: 41828

MAGNESIUM ISOTOPES Mg-26
energy levels, (E), 19: 41828
proton inelastic scattering at 5.67 to 6.46 Mev, angular correlations and distribution in, (E/T), 19: 41693

MAGNESIUM NITRATES
separation of rare earths from solutions of, by anion exchange chromatography, 19: 40659

MAGNESIUM OXIDES
coating with molybdenum or tungsten by chloride and oxide processes, evaluation of, 19: 40986
effects on electron emission ratio enhancement from iron oxides, 19: 41124(R) (NP-15108)
radiation effects on fine structure of optical absorption bands in, neutron, 19: 40632
radioinduced phonon infrared absorption spectrum in, neutron, 19: 41108
radioinduced thermoluminescent reduction of chromium ions in, 19: 40631
use as a diathermanous substance in thermal reactors, 19: 42065(P)
B_2O_3–MgO, emission spectra of cerium- and samarium-activated phosphors of, 19: 40494(T)
Cr–MgO_2, development of ductile composites of, with improved strength and oxidation resistance, 19: 41022(R) (NP-15292)
Cr_2O_3–MgO, formation of refractories of, 19: 40997(P)
MgO–PuO_2, phase studies, 19: 40958

MAGNESIUM SULFATES
radiolysis of hydrated, yields in, 19: 40610

MAGNESIUM SULFIDES
luminescence properties for gamma dosimetry, infrared-stimulated, 19: 40879 (UCRL-12371)

MAGNET COILS
design and performance for plasma engines, 19: 40762 (N64-31010)

MAGNETIC FIELDS
boundary layer between rarefied plasma and, structure of, (T), 19: 41905
charged particle motion in, effects of fringing fields on, (T), 19: 41139
charged particle orbits in Heliotron, (T), 19: 41885
charged-particle motion in, (T), 19: 41142
charged-particle motion in constant, difference equations for, 19: 41145
charged-particle motion in helical, (T), 19: 41187(T)
configuration of rotating, in polyphase system with skew pole pieces, (T), 19: 41152
cyclotron radiation from electrons in homogeneous, (T), 19: 41393(T)
design of linear electromagnetic brake, (E), 19: 40724
dispersion of sector, with double-focusing beam, (T), 19: 41194
distribution in current-carrying layer of magnetoactive plasma, (T), 19: 41882
effects in fluid flow boundary layer separation, (T), 19: 41114 (AD-617258)
effects of interplanetary, on solar proton propagation, (T), 19: 41228
effects on dipole resonance spectrum of plasma waves in hot nonuniform column, (E), 19: 41932
effects on impure sodium, 19: 40409(R) (MSAR-65-95)
effects on ionized gases, hydrodynamic turbulence in, (T), 19: 41114 (AD-617258)
effects on plasma flow, (E), 19: 41936
effects on resistors, for inverter applications, 19: 40845(R) (N64-33676)
effects on solar corona, (T), 19: 41241
electron motion in, diochotron and negative mass instabilities in, 19: 41180
equilibrium of parallel lines of, particle orbits in, 19: 41208 (ORNL-3827)
fluctuations in undisturbed photosphere, 19: 41221
gravitation properties of axisymmetric, 19: 41544
interactions of spatially modulated, with plasmoids, (T), 19: 41901
introduction into type-II superconducting cylinders, (E/T), 19: 41612
measurement of center plane and radial components of, in cyclotron, 19: 41195
measurement of inhomogeneous, using nuclear resonance, (E/T), 19: 40851
perturbation of helical, compensation of, (E), 19: 41116 (IAE-668)
plasma containment in, electrostatic instabilities in, (T), 19: 41866 (UCRL-12052)
plasma containment by toroidal rotating, 19: 41950(P)
plasma interactions in, counterstreaming, (E), 19: 41926
plasma motion in toroidal octupole, (E), 19: 41896
plasma moving striation in longitudinal, (E), 19: 41888
shock wave interactions with, MHD supported, 19: 41120 (N64-30509)

MAGNETIC MATERIALS
spin-wave excitation in, by neutron inelastic scattering, 19: 41987

MAGNETIC MIRROR MACHINES
design and performance for electron containment, 19: 41858 (NP-15217)

MAGNETIC MIRRORS
plasma production in, hot thermonuclear, 19: 41852 (IAE-676)

MAGNETIC MOMENTS
molecular-beam uses in study of, 19: 41143

MAGNETIC MONOPOLES
detection and measurement of Dirac, using superconducting cylinders, (E), 19: 41391

MAGNETIC RESONANCE
electron spin spectra of transition metal ion complexes, 19: 40465 (UCRL-16175)
magnetometer design for measurement of proton, (E), 19: 40857
molecular-beam uses in study of, 19: 41143

MAGNETOHYDRODYNAMIC CELLS
development for power generation, review on, 19: 41320
duct design for, (T), 19: 41316
efficiency, (T), 19: 41316
gas flames in, aerodynamics of, (T), 19: 41144
heat exchanger for, design of, 19: 40752(P)
performance, (E/T), 19: 41315
performance of liquid metal slug, 19: 41314 (BNL-9329)
research programs on, at Siemens-Schuckertwerke laboratories, Erlangen, Germany, 19: 42228

MAGNETOHYDRODYNAMICS
discontinuities in conducting inviscid fluid, (T), 19: 41157
flow in channels, skin friction and heat transfer in, (T), 19: 41119 (MIT-36-P)
flow of anisotropically conducting liquid in alternating magnetic field, (T), 19: 41149
flow of conducting fluid in receptacle with conducting walls, (T), 19: 41154
flow of liquid gallium in test loops, 19: 40727
flow of partially ionized medium along plane channel, viscous drag and heat transfer in, (T), 19: 41147
flow of viscous conducting liquid over surface of half-space, boundary layer in, (T), 19: 41146
fluid flow between nonconducting plates in, incompressible, (T), 19: 41135
fluid flow in annular channel with radial magnetic field, transient, (T), 19: 41137
fluid flow in convective channel, (T), 19: 41115 (ANL-6967)
fluid flow in rectangular channel, current distribution in, (T), 19: 41148
fluid flow in, statistical theory for homogeneous turbulence in, 19: 41127 (SUDAER-233)
fluid flow-magnetic field interactions in, hypersonic, 19: 41120 (N64-30509)

similarity rules in, based on multi-fluid theory, (T), 19: 41156
MAGNETOMETERS
design for inhomogeneous fields, 19: 40851
design for use in proton-resonance measurements, (E), 19: 40857
MAGNETOSPHERE
boundary compression, of solar plasma flux correlation with, 19: 41580
charged particle motion in, model for auroral, (T), 19: 41583
effects of tail of, on cosmic-ray cutoffs, (T), 19: 41307
plasma density in, micropulsation whistlers for diagnostics of, (T), 19: 41596
plasma motion in, effects of ionospheric electrostatic fields on, (T), 19: 41593
wave propagation in, low-frequency micropulsation, (T), 19: 41595
MAGNETS
design of linear electromagnetic brake, (E), 19: 40724
design of superconducting, for variable bandwidth traveling wave masers, 19: 41638
field dispersion of sector, with double-focusing beam, (T), 19: 41194
performance of superconducting, for bubble chambers, 19: 40869 (CONF-650510-14)
MALATES
radiation effects on single crystals of ammonium, ESR spectra of, 19: 40613
MALONIC ACID, DERIVATIVES
uranyl, stability and composition, 19: 40482
MAMMALS
radiation effects on cardiac metabolism, 19: 40357(T) (FTD-TT-65-48, pp 552–3)
MAMMARY GLAND
radiation effects on activity of, 19: 40353(T) (FTD-TT-65-48, pp 16–17)
radiotherapy of carcinomas of, effects of 5-fluorouracil on, 19: 40394
strontium-90 excretion by, after chronic ingestion by milk cows, 19: 40332
MAN
analysis after neutron activation, radiometric, 19: 40800(R) (AERE-PR/HPM-7)
analysis for copper and zinc in lung tissue of, by neutron activation methods, 19: 40452
calcium content of bone of, 19: 40781(R) (NP-15179)
cesium content in, 19: 40781(R) (NP-15179)
cesium-137 content of Alaskan, whole-body, 19: 40780 (BNWL-SA-242)
cesium-137 content of, relation to blood content, 19: 40781(R) (NP-15179)
cesium-137 content in, blood analysis determination of, 19: 40309(R) (NP-15180)
radiation effects on nervous system of, 19: 40349 (BNL-9345)
radioactivity induced in, during high-energy radiotherapy, 19: 40392 (NYO-3364-6)
radioactivity induced in, by exposure to high-energy betatron beams, 19: 40392 (NYO-3364-6)
radioactivity of Alaskan, effects of diet on, 19: 40780 (BNWL-SA-242)
strontium content of bone of, 19: 40781(R) (NP-15179)
strontium content in ribs of, spectrographic method for determining, 19: 40309(R) (NP-15180)
MAN (STANDARD)
blood content and weight of Japanese, 19: 40781(R) (NP-15179)
MANGANESE
determination by spectrochemical methods, voltage-fluctuation patterns in, 19: 40416
determination in copper by activation, 19: 40422
effects on oxidation resistance and strength of chromium–magnesia composites, 19: 41022(R) (NP-15292)
separation from uranium by chromatography on cellulose columns, tracer studies of, 19: 40687
MANGANESE ALLOYS
Cr–Co–Fe–Mn–Mo–Ni–W, corrosion of Rhonel, by coal gasification products at high temperatures, 19: 42127(R) (TID-22009)
Cu–Mn, copper-63 nuclear spin echoes in, (E/T), 19: 41988
Mn–Pu–U, analysis for plutonium, x-ray fluorescence spectrometric, 19: 40408 (LA-3333)
MANGANESE ISOTOPES Mn-54
content in northern stratosphere, 1962-63, 19: 40785 (TID-21224)
deposition, computer program for evaluating radiochemical data on, 19: 40636 (WAPD-TM-516)
MANGANESE ISOTOPES Mn-55
alpha inelastic scattering at 43 Mev, (E), 19: 41760
alpha reactions (α,n) to 42 Mev, isomeric ratios from, (E), 19: 41695
alpha reactions (α,n), statistical model for isomeric ratios in, 19: 41696
MANGANESE OXIDES
use in head-end step in Thorex Process, 19: 40649 (DP-982)
use in separation of protactinium-233 from irradiated thoria, 19: 40644 (BNWL-78)
MANGANESE STEEL
Mn–Mo, addition of metallic aluminum and aluminum nitride to, for improved mechanical properties, 19: 41085(P)
MANGANESE SULFATES
radiolysis of hydrated, yields in, 19: 40610
MARITIME NUCLEAR STEAM GENERATOR
blower design feasibility study for 630 A, 19: 42142 (R62FPD-252)
boiler design for Mark III, 19: 42133 (GEMP-340)
performance of 630A Mark V, 19: 42132 (GE-TM-65-3-6)
MARITIME PRESSURIZED WATER REACTOR
design, 19: 42143
MARITIME REACTORS
development at Petten research centers, Netherlands, 19: 42227
MARTENSITES
determination in stainless steel, method for, 19: 40947(R) (EURAEC-1403)
MASERS
development and uses, review of, 19: 41143
magnet design for variable bandwidth traveling wave, superconducting, 19: 41638
MASERS (OPTICAL)
beam interactions with electron beams, Compton scattering in, (E), 19: 41328 (IS-1187)
beam interactions with θ-pinch plasma, Faraday effect in He–Ne, 19: 41947
beam reactions on tungsten surface, ion generation by, (E), 19: 41943
beam reactions with titanium hydrides, low-voltage discharges from, (E), 19: 41133
performance in interferometric measurements of plasma electron density, 19: 41924
MASS SPECTROGRAPHY
uses, 19: 41243(T) (FTD-TT-64-1368)
MASS SPECTROMETERS
use for speed measurements on sputter ion pumps, 19: 40777
MASS TRANSFER
of forced convection through laminar boundary layers on flat plate, effects of wires near outer edge on, 19: 40746
MATERIALS TESTING
conference on nondestructive, London, Sept. 9 to 13, 1963, 19: 40754
methods of eddy-current, development and uses of, 19: 40757
methods of nondestructive, gamma and x-ray attenuation, 19: 42071
nondestructive methods of, for Kiwi reactor fuel elements, 19: 42146
nondestructive methods, summary of new developments in, 19: 40989
steel welds, evaluation of variables of radiographic, 19: 40753(R) (EURAEC-1378)
ultrasonic inspection, properties of, 19: 40989
ultrasonic testing properties of forged Inconel, 19: 41027 (WERL-0029-2)
MATHEMATICS
algebraic structure of n-body problem, (T), 19: 41122 (N64-31207)
book: *Matrix Mechanics*, 19: 41568
equations for fully ionized two-particle, methods for treating Boltzmann-Maxwell, (T), 19: 41931
error determination in one-parameter systems, 19: 42225 (UCRL-12050)
expansion of integral sine and integral cosine functions, 19: 40944
number theory, theorems for elementary, 19: 42224 (UCRL-12041-T)
polynomial approximation to confluent hypergeometric function, 19: 40943
research programs on, 19: 40396(R) (HMI-B-39)
MATTER
book: *Structure of Matter*, 19: 41829(T)
charged-particle stopping by, computer program for calculations of, 19: 41954 (NP-15338)
creation rate in universe, Heisenberg uncertainty principle for, 19: 41227
electron and photon reactions in, at high energies, (T), 19: 41707
gamma propagation in, investigation using similarity theory, 19: 41958
MCKELVEYITE
composition and occurrence in Green River Formation, Wyoming, 19: 40799
MEATS
cesium-137 content in caribou, moose, and reindeer, consumed by Alaskan natives, 1962 to 1965, 19: 40780 (BNWL-SA-242)
MECHANICS
algebraic structure of n-body problem, (T), 19: 41122 (N64-31207)
book: *Matrix Mechanics*, 19: 41568
difference equations of dynamics in hamiltonian form, 19: 41145
fluctuations of system of anharmonic charged oscillators at negative temperature, Nyquist theorem for, 19: 41537
perturbation method for treating ensemble averages in nonequilibrium statistical, 19: 41155

wave scattering by totally reflecting spheres, scalar plane, (T), 19: 41129
MEMBRANES
excitation of cell, physical mechanisms for, 19: 42212 (NYO-3424-1)
material transfer across cell, biological model of, 19: 42199 (BNL-8397)
MERCHANT VESSELS
nuclear propulsion of, development of, 19: 42143
nuclear-powered, economic comparisons with conventional ships, 19: 42132 (GE-TM-65-3-6)
MERCURY
determination in copper by activation, 19: 40422
plasma of, photon emission by atoms of, (E), 19: 41891(T)
positron annihilation in, angular correlations from, (E), 19: 41285
spectral line excitation by collisions with hydrogen ions and protons, (E), 19: 41260(T)
MERCURY ALLOYS
Hg–rare earths, crystal structure of intermetallic compounds in, 19: 41040
MERCURY IONS
reactions with molybdenum and tungsten surfaces, electron injection in, (E), 19: 41272(T)
MERCURY ISOTOPES
$HgSO_4$–H_2SO_4, solvent properties for aluminum tubes, 19: 40655 (RT/(CHI(65)-1)
MERCURY ISOTOPES Hg-198
energy levels of, vibration-rotation interactions in, (T), 19: 41818
neutron reactions (n,γ) at resonance energies, spectra from, (E), 19: 40896
MERCURY ISOTOPES Hg-199
neutron reactions (n,γ) at resonance energies, spectra from, (E), 19: 40896
neutron reactions (n,γ), mercury-200 parity assignments from, 19: 41846
MERCURY ISOTOPES Hg-200
energy levels from mercury-199 (n,γ) reactions, parities of, 19: 41846
MERCURY ISOTOPES Hg-201
neutron reactions (n,γ) at resonance energies, spectra from, (E), 19: 40896
MERCURY SYSTEMS
Ar–Hg, photon emission by atoms in plasma of, (E), 19: 41891(T)
MESIC ATOMS
hyperfine splitting of (μ–ρ), four-fermion V-A weak interactions in, (T), 19: 41410
meson (μ^-) capture by proton pairs in, (E/T), 19: 41753
meson (μ) capture by deuterons, neutron spectra from, (T), 19: 41782
meson (μ) capture by helium-3, neutron spectra from, (T), 19: 41783
MESON BEAMS
production of high-intensity meson (K^-), using CERN PS, 19: 41184
radiation hazards of synchrocyclotron, 19: 41171(T) (N64-33402)
use in radiotherapy of tumors, 19: 40395
MESON SHOWERS
production and properties of high-energy, (T), 19: 41709
production of nucleon–meson cascade by 200-Bev proton reactions with iron, (T), 19: 41955 (ORNL-TM-1121)
MESONS
decay of vector, conservation of charge-conjugation operator in SU(6) for, (T), 19: 41464
energy levels in symmetry-breaking SU(2) nonlinear spinor model, 19: 41396
field theory of scalar, five-dimensional classical, 19: 41497
interactions of two pseudoscalar-octet, bootstrap and SU(3) assignment of 2^+ mesons from, (T), 19: 41402
interactions of, peratization in weak, 19: 41353
interactions with baryons, long-range forces in, (T), 19: 41421
interactions with baryons, bootstrap model in SU(6) for, 19: 41443
interactions with baryons, second-order perturbation in U(12) for, (T), 19: 41444
interactions with baryons, $SU(6)_w$ for amplitudes of, (T), 19: 41462
interactions with baryons, SU(4) symmetry for coupling constants in, 19: 41397
interactions with baryons and mesons, evaluation of crossing matrices for, (T), 19: 41381
mass splitting of pseudoscalar-octet, baryon mass-difference effect on, 19: 41468
model for low-lying, double SU(3) symmetry in three-triplet quark, 19: 41406
photoproduction on protons, $SU(6)_w$ for amplitudes of, (T), 19: 41462
production of many, in relativistic elementary-particle interactions, (T), 19: 41708
properties of vector, limitations in bootstrap analysis of, (T), 19: 41373
properties of, composite, (T), 19: 41519
quantum numbers for multiplet components of, 19: 41331 (JINR-P-2219)
symmetries for vector, Lie group, (T), 19: 41342
symmetry group for, mass spectra and selection rules in, (T), 19: 41362
MESONS, RESONANCE
bootstrap and SU(3) assignment of 2^+, from scattering of two pseudoscalar octets, (T), 19: 14402
bootstrap and SU(3) assignment of A_2(1310), f°(1250), and K*(1415) to 2^+ multiplets, 19: 41402
decay modes of spin-two, partial widths in SU(3) for, (T), 19: 41461
decay of A_2, branching ratios for, (E), 19: 41460
decay of f*, KK* and K_1K_1, (E), 19: 41459
decay of K*, branching ratios for, (E), 19: 41460
decay of K*, unitary symmetry breaking in, (E/T), 19: 41366
energy levels in symmetry-breaking SU(2) nonlinear spinor model, 19: 41396
mass difference ρ^0–ω_0, from meson (π)–nucleon interactions, (T), 19: 41380
model for, composite, 19: 41525
models for, quasi-molecular rotator, 19: 41524
parity and spin determinations for, (T), 19: 41447
production in meson (π^-)-proton interactions at 7.5 Bev/c, cross sections for, (E), 19: 41489(T)
production of KK̄ and Kπ, in meson (π^+)-proton interactions at 2.35 to 2.90 Bev/c, (E), 19: 41418
properties of nonstrange meson (f*(1500), (E), 19: 41459
spin and parity of 1320-Mev A_2 π-ρ, (E/T), 19: 41368
symmetry for, 27-supermultiplet in, (T), 19: 41492(T)
MESONS (B)
decay of, ω–ϕ mixing angle from, (T), 19: 41458
model for, composite, 19: 41525
MESONS (η)
decay of electromagnetic and strong interactions in rare modes of, (T), 19: 41457
decay of, coupling effects in unitary symmetry, 19: 41335 (NP-15239)
decay of, meson (σ) hypothesis for, (T), 19: 41518
interactions with baryons, (T), 19: 41433
MESONS (η^0)
decay of, C-noninvariant effects in 3π, (T), 19: 41437
production in meson (K^-)-proton and meson (π^-)-proton interactions, (T), 19: 41433
production in meson (π^-)-proton interactions at 1275 Mev/c, (E), 19: 41507
MESONS (f)
decay modes of, partial widths in SU(3) for, (T), 19: 41461
model for, composite, 19: 41525
MESONS (f°)
decay of, branching ratios for, (E), 19: 41460
MESONS (K)
decay of K*, unitary symmetry breaking in, (E/T), 19: 41366
decay of, meson (σ) hypothesis for, (T), 19: 41518
interactions with mesons (K) and (π), resonance production in, (E), 19: 41418
interactions with nucleons at high energies, Regge-pole model for, (T), 19: 41426
interactions with nucleons, resonance effects in, (T), 19: 41506
interactions with nucleons, Regge poles Y_1^* and Y_0^* in scattering amplitude for, (T), 19: 41352
photoproduction of, method of identification of, 19: 41527
MESONS (K^-)
decay of, effects of CP violation in 3π, (T), 19: 41445
interactions of, SU(6) symmetry for forward amplitudes in, (T), 19: 41515
interactions with protons, meson (η^0) production in, (T), 19: 41433
interactions with protons at 4.6 and 5.0 Bev/c, f* (1500) production in, (E), 19: 41459
interactions with neutrons and protons at rest, hyperon (Σ^-) production in, (E), 19: 41494
interactions with protons at high energies, forward amplitudes for, (T), 19: 41376
interactions with protons, baryon resonances from, (T), 19: 41384
interactions with neutrons, final-state interactions in ($\Lambda\pi^-$), (T), 19: 41405
interactions with protons, range-energy relations for hyperons (Σ^-) and (Σ^+) from (E), 19: 41369
production in proton reactions with nuclei at 20 Bev, 19: 41324 (CERN-65-14)
production of high-intensity beams of, using CERN PS, 19: 41184
MESONS (K^0)
decay of K_1^0 and K_2^0, CT invariance in, 19: 41452
decay of K_2^0, CP violation in 2π, (T), 19: 41437
decay of, CP and $|\Delta I| = \frac{1}{2}$ violations in, (T), 19: 41471
decay of, SU(3) model for CP-violating, (T), 19: 41371
decay of, test for particle-mixture theories in 2π, (T), 19: 41454

decay rate of, CPT-invariance test and measurement method for, 19: 41413
interactions of, SU(6) symmetry for forward amplitudes in, (T), 19: 41515
MESONS (K^0)
decay rate of, CPT-invariance test and measurement method for, 19: 41413
interactions of, SU(6) symmetry for forward amplitudes in, (T), 19: 41515
interactions with nucleons at high energies, Regge-pole model for, (T), 19: 41426
MESONS (K^+)
decay of, branching ratio and meson (μ^+) energy spectrum in, (E), 19: 41414
decay of, effects of CP violation in 3π, (T), 19: 41445
decays of, parity nonconservation in ($2\pi\gamma$) and ($3\pi\gamma$), (T), 19: 41361
intensity of cosmic, above 4 Bev, (E), 19: 41294
interactions of, SU(6) symmetry for forward amplitudes in, (T), 19: 41515
interactions with protons, mass-spectrum κ singularity in ($Kmmp$), (T), 19: 41417
interactions with protons at 2 Bev/c, (E), 19: 41436
interactions with protons at high energies, forward amplitudes for, (T), 19: 41376
production in proton reactions with nuclei at 20 Bev, 19: 41324 (CERN-65-14)
MESONS (K_{e4})
decay modes of, analyses of rare, (E), 19: 41446
decay of, vector interaction effects in unitary symmetry, 19: 41335 (NP-15239)
MESONS ($K_{\mu 3}$)
branching ratio and meson (μ^+) energy spectrum, (E), 19: 41414
decay of, meson (π)-lepton angular correlation in, (T), 19: 41485(T)
MESONS ($K_{\pi\mu}$)
decay, (T), 19: 41420
MESONS (μ)
capture by carbon-12 and oxygen-16, (T), 19: 41766
capture by deuterons, neutron spectra from, (T), 19: 41782
capture by helium-3, neutron spectra from, (T), 19: 41783
capture by nuclei, decay of collective states excited in, (T), 19: 41769
decay of, CP violation in, (T), 19: 41378
energy loss of ultra-relativistic, in rock and water, (E/T), 19: 41345
interactions in thick absorbers at high energy, charged-particle showers from, (T), 19: 41354
interactions of high-energy, electron-photon showers from, 19: 41355
interactions with photons in meson (η) decay, (T), 19: 41457
models for, description of electromagnetic, (T), 19: 41377
reactions with nuclei as probe of nuclear structure, conference on, 19: 41671 (LADC-6186)
reactions with nuclear Coulomb field, electron pair production in, (T), 19: 41486(T)
reactions with nuclei around 1 Tev, particle distributions from, (T), 19: 41711
MESONS (μ^-)
capture by proton pairs in nuclei, (E/T), 19: 41753
capture in solid lithium, transition paths in, (T), 19: 41823
decay from mesonic helium atoms, Michel parameter for, (E), 19: 41480(T)
MESONS (μ^+)
energy spectra from meson ($K_{\mu 3}$) decay, (E), 19: 41414
production in proton-proton interactions at 2.0 Bev, (E/T), 19: 41503
MESONS (ω)
decay into two charged mesons (π), methods for detecting, (T), 19: 41386
emission in meson (β) decay, ω–ϕ mixing angle from, (T), 19: 41458
mass difference ρ^0–ω_8, from meson (π)–nucleon interactions, (T), 19: 41380
photoproduction on nucleons, (T), 19: 41321 (AECD/TP/4)
production in meson (π^+) interactions with neutrons at 1.7 Bev/c, (E), 19: 41528
MESONS (ω^8)
decay of, C-noninvariant effects in 3π, (T), 19: 41437
MESONS (ϕ)
decay of, unitary symmetry breaking in, (E/T), 19: 41366
emission in meson (β) decay, ω–ϕ mixing angle from, (T), 19: 41458
model for, composite, 19: 41525
production in meson (π^+)-proton interactions at 2.35 to 2.90 Bev/c, isospin from, (E), 19: 41418
MESONS (π)
bound states of, Faddeev-equation reduction for three-particle, 19: 41416
decay of, CP violation in leptonic, (T), 19: 41378
decay of, total probability for electron pair production in, (T), 19: 41482(T)
electromagnetic structure of charged, analysis using α–π interactions, (T), 19: 41379
emission in meson ($K_{\mu 3}$) decay, angular correlation in, (T), 19: 41485(T)
interactions of, meson (ρ) Regge pole effects on, (T), 19: 41370
interactions with nucleons, reciprocal bootstrap in, (T), 19: 41422
interactions with nucleons at high energies, Regge-pole model for, (T), 19: 41426
interactions with nucleons at low energies, (T), 19: 41498
interactions with mesons (π) in electromagnetic pair production, (T), 19: 41505
interactions with nucleons below 1 Bev, single meson (π) production in, (T), 19: 41509
interactions with nucleons at high energies, optical model for backward, (T), 19: 41332 (JINR-P-2220)
interactions with deuterons, partial wave dispersion relations for disintegration in, 19: 41336 (NP-15335)
interactions with nucleons, effects on nucleon–nucleon interactions at 300 Bev, (T), 19: 41358
interactions with mesons (ρ), spin-parity of 1320-Mev A_2 resonance in, (E/T), 19: 41368
interactions with nucleons, one-particle-exchange models for, (T), 19: 41375
interactions with nucleons, meson (ρ^0) and meson (ω_8) effects in, (T), 19: 41380
interactions with nucleons, form factors from, (T), 19: 41385
interactions with mesons (π), partial-wave dispersion relations for mesons (ρ) bootstrap in, 19: 41394
interactions with nucleons, absorptive corrections and form factors in peripheral model for ($N\rho$), 19: 41400
interactions with mesons (π), dynamical calculation of inelasticity in, 19: 41403
models for, description of electromagnetic, (T), 19: 41377
production by electrons on nuclei, radiative corrections to, (T), 19: 41752
production in mesons (π)-nucleon interactions below 1 Bev, model for single, (T), 19: 41509
production in neutrino-nucleon interactions, (T), 19: 41754
production of pairs of charged, in meson (ω) decay, (T), 19: 41386
reactions with nuclei as probe of nuclear structure, conference on, 19: 41671 (LADC-6186)
MESONS (π^-)
interactions of, SU(6) symmetry for forward amplitudes in, (T), 19: 41515
interactions with protons, meson (η^0) production in, (T), 19: 41433
interactions with protons at 1.5 Bev/c, dipion production in, (E), 19: 41441
interactions with nucleons at 300 to 700 Mev, amplitudes for, (E), 19: 41442
interactions with protons at 8 and 12 Bev/c, differential cross sections for elastic, (E), 19: 41455
interactions with protons hydrogen at 4 and 8 Bev/c, backward elastic, (E), 19: 41456
interactions with protons at 7.5 Bev, baryon resonances and strange particle production in, (T), 19: 41488(T)
interactions with protons at 2.0 Bev/c, (E), 19: 41502
interactions with protons at 1275 Mev/c, charge exchange in, (E), 19: 41507
interactions with protons at 905 Mev, mesons (π^-) and (π^0) production in, (E), 19: 41508
interactions with protons at high energies, forward amplitudes for, (T), 19: 41376
interactions with alpha particles, meson (π) form factors from, (T), 19: 41379
interactions with protons at 7.5 Bev/c, meson resonances and strange particle production in, (E), 19: 41489(T)
interactions with protons at 1275 Mev/c, meson (η^0) and meson (π^0) production in, (E), 19: 41507
photoproduction on deuterium at 165 to 210 Mev, angular distributions and cross sections for, (E), 19: 41344
production in meson (K^-)-neutron interactions, (T), 19: 41405
production in meson (π^-)-proton interactions at 905 Mev, (E), 19: 41508
production in proton reactions with nuclei at 20 Bev, 19: 41324 (CERN-65-14)
scattering by nuclei at low energies, double-charge-exchange, (T), 19: 41773
use in radiotherapy of tumors, 19: 40395
MESONS (π^0)
lifetime of, mean, (E), 19: 41404
lifetime of, Williams-Weizsacker covariant method for, (T), 19: 41349
production in meson (π^-)-proton interactions at 1275 Mev/c, (E), 19: 41507
production in meson (π^-)-proton interactions at 905 Mev, (E), 19: 41508
production in proton-proton interactions at 2.0 Bev, (E/T), 19: 41503
MESONS (π^+)

intensity of cosmic, above 4 Bev, (E), 19: 41294
interactions of, SU(6) symmetry for forward amplitudes in, (T), 19: 41515
interactions with protons at 2.35 to 2.90 Bev/c, resonance production in, (E), 19: 41418
interactions with protons, poles and resonances in, (T), 19: 41427
interactions with nucleons at 300 to 700 Mev, amplitudes for, (E), 19: 41442
interactions with protons at 8 and 12 Bev/c, differential cross sections for elastic, (E), 19: 41455
interactions with protons hydrogen at 4 and 8 Bev/c, backward elastic, (E), 19: 41456
interactions with neutrons at 1.7 Bev/c, meson (ρ) and (ω) production in, (E), 19: 41528
interactions with deuterons, partial wave dispersion relations for disintegration in, 19: 41336 (NP-15335)
interactions with protons at high energies, forward amplitudes for, (T), 19: 41376
interactions with alpha particles, meson (π) form factors from, (T), 19: 41379
photoproduction on protons at .6 to 1.2 Bev, angular distributions of, 19: 41323 (CALT-68-42)
photoproduction on deuterium at 165 to 210 Mev, angular distributions and cross sections for, (E), 19: 41344
production in proton reactions with nuclei at 20 Bev, 19: 41324 (CERN-65-14)
scattering by nuclei at low energies, double-charge-exchange, (T), 19: 41773

MESONS (ρ)
decay of, unitary symmetry breaking in, (E/T), 19: 41366
exchange in deuteron-electron interactions, (E), 19: 41453
interactions of, effects on meson (π)–nucleon interactions, (T), 19: 41375
interactions of, Regge-pole parameters for, (T), 19: 41370
interactions with mesons (π), spin-parity of 1320-Mev A_2 resonance in, (E/T), 19: 41368
photoproduction on nucleons, (T), 19: 41321 (AECD/TP/4)
production in meson (π^-) interactions with protons at 1.5 Bev/c, (E), 19: 41441
production in meson (π^+) interactions with neutrons at 1.7 Bev/c, (E), 19: 41528
production in meson (π)–nucleon interactions, absorptive corrections and form factors in peripheral model for, 19: 41400
production in meson (π)–meson (π) interactions, partial-wave dispersion relations for bootstrap, 19: 41394
production in proton-proton interactions at 1.5, 2.5, and 2.9 Bev, (E), 19: 41523

MESONS (ρ^0)
mass difference with resonance meson (ω_0), in meson (π)–nucleon interactions, (T), 19: 41380

MESONS (σ)
production in meson decays, (T), 19: 41518

MESONS (X^0)
decay of, meson (σ) hypothesis for, (T), 19: 41518

METABOLIC DISEASES
pathology of necrotizing encephalomyelopathy, familial occurrence of, 19: 42219 (TID-21177)

METABOLISM
radiation effects on pyrocatechal, in macacus monkeys, 19: 40373

METAL COATINGS
deposition on aggregated reactor fuel particles, 19: 40994(P)

METALLOGRAPHY
optical microscopic techniques for electron probe analysis, 19: 40951 (NBL-6290)
sample preparation in, 19: 40964(P)

METALLURGY
book: *Energetics in Metallurgical Phenomena*, Vol. I, 19: 41075

METALS
boiling heat transfer in high-acceleration fields, research program on, 19: 40741(R) (SAN-409-23)
book: *An Atlas of Models of Crystal Surfaces*, 19: 41072
book: *Energetics in Metallurgical Phenomena*, Vol. I, 19: 41075
book: *Irradiation Effects in Cladding and Structural Materials*, 19: 41107
book: *Thermal Radiative Properties*, 19: 41074
deformation twinning in, conference on, 19: 41076
dislocation loops in quenched fcc, electron microscopic analysis, 19: 41026 (UCRL-16024)
electron structure of, method for studying, 19: 41068
gamma reactions at 1.02 Mev, electromagnetic effects from, 19: 41956 (SC-R-65-933)
Hall effect in, apparatus for measurement of, 19: 42217 (SC-RR-65-325)
ionization cross sections of atoms of, measurement by electron impact, (E), 19: 41276
loop formation in bcc, interstitial, (T), 19: 41056
molecular beam interactions with surfaces of, energy exchange in, (E), 19: 41275
positron annihilation in, many-body theory of, 19: 41159
pumps for liquid, development and testing seals for, 19: 40718 (TIM-909)
radiation effects on, defect structure and saturation from, 19: 41102
solvent distribution in ammonium thiocyanate–methanol–water systems, distribution coefficients for, 19: 40447
surface analysis for films by proton elastic scattering, (E), 19: 40962
thermodynamic properties at high pressures and temperatures, 19: 40459 (NP-15324)
thermodynamics of interfaces with glass, 19: 40464 (UCRL-11816(Rev.))

METEORITES
age determination of amphoteric, 19: 41225
gamma activity in Granes stone, 19: 40788
rare gas content in amphoteric, (E), 19: 41225

METEOROLOGY
waterdrop evaporation, computer program for, 19: 41110 (BNWL-74)

METEORS
radio-wave reflection from trails of, polarization phenomena in, (E), 19: 41223

METERS
design for accurate timing of electron and x-ray exposures, (E), 19: 41186
design for remote measurements in radiation environment, (E), 19: 40714 (EUR-2421.d)

METHACRYLIC ACID, METHYL ESTER
radiolysis of mixtures of, with paraffin oil, reactions of free radicals formed in, 19: 40580

METHANE
chromatographic behavior of, effects of deuterium on, 19: 40672
corrosive effects on Hastelloy X and Haynes 25 alloy, 19: 40961
determination, use of beta ionization detector in chromatographic, 19: 40415(T) (CEA-tr-R-1839)
methane-O, oxidation induced by fission fragments in, 19: 40611
reactions with bromine-80 recoil atoms, radioactivity in organic yields in deuterated and normal, 19: 40618
reactions with recoil tritium, kinetic isotope effects in, 19: 40615
separation of deuterated, by gas chromatography, 19: 40672
HCl–methane, formation of polymeric yields in reactions with carbon-14 and sulfur-35 recoil atoms, 19: 40628

METHANE, BROMO-
reactions with bromine-80 recoil atoms, radioactivity of organic yields in, 19: 40618

METHANE, BROMOTRIFLUORO-
reactions with bromine-80 recoil atoms, radioactivity of organic yields in, 19: 40618

METHANE, CHLORO-
reactions with bromine-80 recoil atoms, radioactivity in organic yields in, 19: 40618
reactions with chlorine-38 recoil atoms, stereochemistry in, 19: 40625

METHANE, DICHLORO-
reactions with bromine-80 recoil atoms, radioactivity in organic yields in, 19: 40618

METHANE, DIFLUORO-
reactions with bromine-80 recoil atoms, radioactivity of organic yields in, 19: 40618

METHANE, DIPHENYL-
radiolysis of, effects of type of radiation on, (E), 19: 40591
radiolysis of, G-values of products in, (E), 19: 40370

METHANE, IODO-
metabolism of inhaled, 19: 40800(R) (AERE-PR/HPM-7)
reactions with dodecane and sodium bisulfite, 19: 40402 (BMI-X-10137)

METHANE, NITRO-
detonation initiation of, by shock interactions at discontinuities, 19: 42207 (LA-DC-6994)
detonation of, one-dimensional time-dependent reaction zone in, (T), 19: 42203 (LA-3297)
detonation wave interactions in condensed, 19: 42205 (LA-DC-6990)
radioinduced free radical formation in, electron paramagnetic resonance study of, 19: 40579

METHANOL
effects of aqueous solutions of, on sorption europium and yttrium by cation exchanger, 19: 40664
effects on ion exchange separation of rare earths using α-hydroxyisobutyric acid, 19: 40663
effects on ion exchange separation of europium and yttrium, 19: 40666
effects on sorption of europium and yttrium on ion exchangers, tracer studies of, 19: 40665
reactions with tritium recoil atoms with and without benzene and cyclohexane, energy transfer in, 19: 40622

CCl_4–methanol, mechanism of chemical processes in reactions with chlorine-38 recoil atoms, 19: 40623
NH_4SCN–methanol–H_2O, distribution coefficients of metals in, 19: 40447
METHIONINE
preparation of sulfur-35-labeled, by reactions with sulfur-35 recoil atoms, 40619
METHYL BORATES
molecular structure and infrared spectra of, isotope effects on, 19: 40470
METHYL RADICALS *(Free Radicals)*
yields from gamma radiolysis of nitromethane at 77°K, EPR studies of, 19: 40579
MEXICO
geochemistry and radioactivity of curative waters in Lourdes Spa, San Luis Potosi, Mexico, 19: 40835
MICE
radiation effects on mammary gland activity in, 19: 40353(T) (FTD-TT-65-48, pp 16–17)
MICROANALYSIS
optical microscopic techniques for electron-probe, 19: 40951 (NBL-6290)
use of electron-probe, to determine light elements in alloys, diffusion couples, and carbides, 19: 40412 (TIM-924)
MICROORGANISMS
photochemical reactions of nucleic acids in, 19: 42212 (NYO-3424-1)
MICROSCOPES
use for cloud chamber track photographs, semiautomatic device for, 19: 40888
MICROSCOPY
optical techniques for electron-probe analysis, 19: 40951 (NBL-6290)
MICROWAVE EQUIPMENT
design for plasma electron density measurements, 19: 41854 (MATT-369)
design for plasma diagnostics, nonuniform, 19: 41855 (NP-15142)
MICROWAVES
detection of centimeter, in gas discharge plasma, 19: 41876
emission from Josephson junctions, (E/T), 19: 41614
MILK
iodine-131 removal from, by moving bed ion exchange columns, 19: 40697(P)
strontium-90 content of, after chronic ingestion by milk cows, 19: 40332
strontium-90 content in, effects of dietary calcium consumed by cows, 19: 40341
strontium-90 removal from, by moving bed ion exchange columns, 19: 40697(P)
strontium-90 transfer by, after chronic ingestion by female dogs, 19: 40327
strontium-90 transfer in, to nursing calves, 19: 40329
strontium-90 transfer in, to nursing calves, 19: 40330
MINING
use of nuclear explosives to break copper ore deposits, 19: 40706 (ORNL-TM-1191)
MIT RESEARCH REACTOR
development, 19: 42007 (MIT-2344-3)
MITOSIS
radiation effects on Planaria, dose effects on regenerating capacity in, 19: 40366
MOLDING MATERIALS
temperature effects on RTV-20, 19: 42215 (RFP-625)
MOLECULAR BEAMS
deceleration of large-dipole-moment, electrodynamic method of, (T), 19: 41200
interactions with metallic surfaces, energy exchange in, (E), 19: 41275
review of studies involving, 19: 41143
MOLECULAR STRUCTURE
book: *Physical Methods for Determining Molecular Geometry*, 19: 40530
MOLECULES
motions in condensed matter, slow neutron studies of, 19: 40455 (BNL-9297)
properties of, research on, 19: 41967(R) (MIT-QPR-57)
reactions in mixtures of, statistical mechanics of, 19: 41130
temperature in acetylene–air flames, (E), 19: 41922
MOLYBDENUM
analysis for nitrogen, isotope-dilution method for, 19: 40444
argon-ion reactions with, Auger-electron emission in, (E), 19: 41272(T)
coating with silicides, 19: 40998(P)
compatibility with graphite–nitrogen environment at 1000 and 1200°C, 19: 40966 (BNWL-92)
deposition on ceramic powders by chloride and oxide processes, evaluation of, 19: 40986
determination in copper by activation, 19: 40422
dislocation structure in, effects of cold working on, 19: 41015 (MIL-TDR-64-282)
ductile-to-brittle transition temperature of sheet of, effects of recrystallization and welding on, 19: 41016 (N64-30997)
effects on high-temperature properties of aluminum–iron–silicon–uranium systems, 19: 40958
effects on oxidation resistance and strength of chromium–magnesia composites, 19: 41022(R) (NP-15292)
effects on properties of tantalum, 19: 41067
Fermi surface of single crystals of, (E/T), 19: 42003
ion reactions at 5 to 12 Mev, neutron spectra from, (E), 19: 41810(T)
mercury-ion reactions with, Auger-electron injection in, (E), 19: 41272(T)
microstructure of evaporated films of, 19: 40463(R) (SRIA-425-5)
oxidation kinetics at 1300 to 2400°C, 19: 40961
plastic deformation of, mechanisms of, 19: 40961
properties of electron multiplier resistance-strip of, 19: 41124(R) (NP-15108)
radiation effects on stored energy release in, fast neutron, 19: 40961
reactor criticality effects per atom, (E), 19: 42077 (ANL-7014)
separation from other metal ions by ion exchange, 19: 40658
solubility in pure potassium at 1000°C, 19: 40946(R) (AI-65-93)
sorptive properties of evaporated films of, for nitrogen and xenon, 19: 40463(R) (SRIA-425-5)
sorptive properties for deuterium, hydrogen, and deuterium–hydrogen mixtures at room temperature, 19: 40463(R) (SRIA-425-5)
stress-rupture properties, 19: 40961
tensile-ductility transition in, mechanism of, 19: 40961
thermal expansion to 2500°C, 19: 41009 (GEMP-375)
thermoelectric properties at 1000 to 2000°C, (E), 19: 40859
Mo–Ti–Zr, mechanical properties of TZM, effects of carbon content on, 19: 41002 (APS-5157-R)
Mo–Ti–Zr, mechanical properties of TZM, effects of forging schedule and ingot processing on, 19: 41002 (APS-5157-R)
MOLYBDENUM ALLOY COUPLES
Mo–Re/Re, stability of thermocouples of, (E), 19: 40859
Mo–Re/Re–W, stability of thermocouples of, (E), 19: 40859
MOLYBDENUM ALLOYS
analysis for niobium and tantalum, photometric method for, 19: 40442
Al–Mo–Ti–Sn–Zr, mechanical properties of, effects of heat treatments on, 19: 41052
Cr–Co–Fe–Mn–Mo–Ni–W, corrosion of Raonel, by coal gasification products at high temperature e 19: 42127(R) (TID-22009)
Mo–Nb, niobium-93 nuclear magnetic relaxation in, (E), 19: 41989
Mo–Nb–U, isothermal transformations of gamma-phase, 19: 40958
Mo–Nb–V–Zr, properties of welds in B-66, 19: 40989
Mo–Nb–V–Zr, stress-rupture properties of B-66, 19: 40961
Mo–Os–W, phase diagrams at 1600, 2000, and 2375°C, 19: 41048
Mo–Pu–U, casting procedures for, 19: 40978 (ANL-6955)
Mo–Re, creep and stress-rupture properties at 1600°C, 19: 40961
Mo–Re, thermal expansion to 2500°C, 19: 41009 (GEMP-375)
Mo–Re, thermoelectric properties at 1000 to 2000°C, (E), 19: 40859
Mo–Re–W, properties, 19: 40961
Mo–Re–W, stress-rupture properties, 19: 40961
Mo–Sc, phase studies of solid solution formation in, 19: 41050
Mo–Ta–V, phase diagram, 19: 41036
Mo–Ti, coating with silicides, 19: 40998(P)
Mo–Ti, ductile-to-brittle transition temperature of sheet of, effects of recrystallization and welding on, 19: 41016 (N64-30997)
Mo–Ti–Zr, coating with silicides, 19: 40998(P)
Mo–Ti–Zr, dislocation structure in, effects of cold working on, 19: 41015 (MIL-TDR-64-282)
Mo–U, elastic modulus of, effects of heat treatments on, 19: 41023 (NP-15334)
Mo–U, isothermal transformations of gamma-phase, 19: 40958
Mo–U, properties, 19: 41023 (NP-15334)
Mo–U, radiation effects on fuel elements of, 19: 41090 (NAA-SR-11121)
Mo–U–Zr, isothermal transformations of gamma-phase, effects of zirconium on, 19: 40958
Mo–W, phase studies, 19: 41035
Mo–W–Zr, phase studies, 19: 41035
Mo–Y, phase studies of solid solution formation in, 19: 41050
Mo–Zr, phase studies, 19: 41035
MOLYBDENUM COUPLES
Mo/Re–W, stability of thermocouples of, (E), 19: 40859
Mo/W, stability of thermocouples of, (E), 19: 40859
MOLYBDENUM ISOTOPES Mo-99
metabolism in rats of, 19: 40319
MOLYBDENUM OXIDES
MoO_3–Nb_2O_5, phase studies, 19: 41049
MOLYBDENUM SILICIDES
oxidation protection properties of, 19: 40961

MOLYBDENUM STEEL
Cr–Mo–Ni, properties of Super-Elso, 19: 41008 (EURAEC-1407)
Mn–Mo, addition of metallic aluminum and aluminum nitride to, for improved mechanical properties, 19: 41085(P)
MOLYBDENUM SYSTEMS
Mo–UO_2, diffusion of uranium dioxide from, at 1700 to 2500°C, 19: 41043
MONKEYS
radiation effects on pyrocatechol content in tissues of Macacus, 19: 40373
MONOCHROMATORS
use for energy level measurements, 19: 41828
MONTE CARLO METHOD
use for photon transport calculations, 19: 41957 (UCRL-14165)
use for prompt neutron decay analysis, 19: 42039(R) (BNWL-95, pp 36-9)
MOON
space vehicle motion under influence of earth and, (T), 19: 41205 (N64-31725)
temperature variations during eclipses, measurement using lunar radio emission, (E), 19: 41222
MORTARS
age estimation using carbon-14, 19: 40795
MOSSBAUER EFFECT
in biological materials, 19: 40306
in iron-57, from iron-56 (d,p) reactions at 1.8 Mev, (E), 19: 41793
instrumentation for, at low temperatures, 19: 40863
intensity and temperature shift in nonideal crystals, (T), 19: 41997(T)
measurement of, backscattering technique for, (T), 19: 41845
measurement of, design of vacuum cryostat and furnace for, (E), 19: 40858
measurement of, scattering techniques for, (E), 19: 40922
measurements of, use of water-cooled solenoids in spectrometer for, 19: 41848
spectra from, computer analysis and calculation of, (T), 19: 41724
spectra of, effects of nuclear polarization on, (T), 19: 42001
use for determining gyromagnetic ratio of nuclear excited states, (E), 19: 41791
use for studying hemoglobin and iron-containing biological compounds, 19: 40305
use in determining electronic shielding by closed shells in thulium compounds, 19: 40528
MUCOSA
radium-224 content in rat, after intravenous injection, 19: 40315
MULTIPLICATION FACTOR
calculation for uniform water-moderated lattices, 19: 42054
measurement for poisoned infinite lattices of enriched uranium and heavy water, 19: 42046(R) (MIT-2344-3, pp 109-14)
MUONIUM
hyperfine splitting of, four-fermion V-A weak interactions in, (T), 19: 41410
MUSCLES
physiology of movement of, 19: 42212 (NYO-3424-1)
MUTATIONS
nonchromosomal genetic system for, in algae, 19: 42212 (NYO-3424-1)
radioinduced in Tradescantia by neutrons, 19: 40800(R) (AERE-PR/HPM-7)

N

NAGASAKI
effects of atomic explosion on population of, 19: 40361(T) (ORNL-tr-437)
NAPHTHALENE
methyl-, radioinduced hydrogenation of, beta, 19: 40553(R) (NYO-2978-34)
radioinduced thermoluminescence of, in crystalline biphenyl, 19: 40563
naphthalene–tetrahydrofuran, solvent properties for alkali metals, 19: 40409(R) (MSAR-65-95)
NAPHTHALENE, DECAHYDRO-
dielectric polarization of, temperature dependence, 19: 40468(T) (SC-T-65-721)
NAPHTHALENE, 1,2,3,4-TETRAHYDRO-
radioinduced hydrogenation of, beta, 19: 40553(R) (NYO-2978-34)
2,7-NAPHTHALENEDISULFONIC ACID, 4,5-DIHYDROXY-
analytical uses of derivatives of, 19: 40426
NATURAL WATERS
geochemistry and radioactivity of Lourdes Spa, San Luis Potosi, Mexico, 19: 40835
NEBULAE
spectra of helium and hydrogen in gaseous, recombination, (T), 19: 41238
NEODYMIUM
determination by spectrochemical methods, voltage-fluctuation patterns in, 19: 40416
determination of micro amounts of, in rare earth oxides by x-ray fluorescence, 19: 40440
heat of solution in liquid tin, 19: 41044
neutron total cross sections of, (E), 19: 41723
physical and thermodynamic properties, 19: 40948 (IS-1195)
polarographic behavior in dimethylformamide and dimethylsulfoxide, 19: 40681
preparation and purification, 19: 40948 (IS-1195)
radiation effects on EPR of calcium fluoride crystals containing, 19: 40602(T)
NEODYMIUM ALLOYS
Au–Nd, phase studies of solid solutions in, 19: 41062
Co–Nd, magneto-optic properties of intermetallic compound $NdCo_5$ in, 19: 41084
Mg–Nd, phase studies, 19: 41011 (IS-T-15)
Nd–Pr, heat of solution in liquid tin, 19: 41044
NEODYMIUM CARBIDES
eutectic temperature between carbon and dicarbide, 19: 41014 (LA-DC-6819)
lattice parameters and phase transformation temperatures in, 19: 41014 (LA-DC-6819)
microhardness, 19: 41014 (LA-DC-6819)
NEODYMIUM CHLORIDES
complexes with phenanthroline, preparation and properties, 19: 40514
temperature-volume relations in aqueous solutions of, 19: 40523
NEODYMIUM COMPLEXES
with gluconic acids, stability constants, 19: 40508
NEODYMIUM FLUORIDES
solubility in beryllium nitrate solutions, 19: 40670
NEODYMIUM IONS
electron paramagnetic resonance of tetravalent, in calcium fluorides, (E), 19: 41999(T)
NEODYMIUM ISOTOPES Nd-141
production of isomeric states in yttrium-89 (n,n′γ) reactions at 14 Mev, cross sections for, (E), 19: 41781
NEODYMIUM ISOTOPES Nd-142
deuteron reactions (d,d′γ) at 12 Mev, 0+ states from, 19: 41747
energy levels from (p,p′γ) and (d,d′γ) reactions at 12 Mev, 0+, (E), 19: 41747
neutron reactions (n,2n) at 14 Mev, cross sections for neodymium-141 isomeric states from, (E), 19: 41781
proton reactions (p,p′γ) at 12 Mev, 0+ states from, (E), 19: 41747
NEODYMIUM ISOTOPES Nd-143
neutron reactions (n,α) with, cross sections for thermal, (E), 19: 41809(T)
NEODYMIUM ISOTOPES Nd-149
decay of, gamma intensities and half life from, (E), 19: 41836
NEODYMIUM ISOTOPES Nd-151
decay of, gamma intensities and half life from, (E), 19: 41836
NEODYMIUM NITRATES
sorption by phospho-organic resins, 19: 40668
NEODYMIUM NITRIDES
electric conductivity near Curie point, electron critical diffusion theory of, 19: 41973
NEODYMIUM OXIDES
content in McKelveyite uranium mineral, 19: 40799
Nd_2O_3–ZrO_2, phase studies, 19: 41037
NEODYMIUM PERCHLORATES
stability constants of, thermal, 19: 40509
NEODYMIUM SILICIDES
crystal structure, 19: 40477
NEODYMIUM SULFATES
$Nd_2(SO_4)_3$–Na_2SO_4, thermal stability, 19: 40511
NEON
charged-particle stopping power and straggling in, excitation energy for, (T), 19: 41268
content in amphoteric meteorites, (E), 19: 41225
diffusion and spin relaxation of cesium in, (E), 19: 41278
neon ion collisions with atoms of, inelastic energy loss in, (E), 19: 41277
ethylene–Ne, kinetic energy effects on carbon-11 reactions with, 19: 40617
NEON IONS
collisions with argon and neon atoms, inelastic energy loss in, (E), 19: 41277
reactions with molecular nitrogen ions at 10 to 65 kev, rotational and vibrational excitation in, (E), 19: 41279
NEON ISOTOPES Ne-20
matrices for 2s-1d shell of, model-interaction, 19: 41730
proton reactions (p,γ) at 1.28 to 1.86 Mev, gamma energies and yield, (E), 19: 41838

proton reactions (p,γ) at 1.17 Mev, sodium-21 energy levels from, (E), 19: 41838
reactions with gold-197 at 127 Mev, angular distributions from one-nucleon transfer, (T), 19: 41805(T)
NEON ISOTOPES Ne-21
energy levels from neon-21 (p,p′γ) reactions at 1.28 to 1.86 Mev, (E), 19: 41838
energy levels of, collective representation of low-lying, (T), 19: 41757
proton reactions (p,p′γ) at 1.28 to 1.86 Mev, neon-21 energy levels from, (E), 19: 41838
NEON ISOTOPES Ne-22
energy levels in, parity of 1.278 Mev resonance, (E), 19: 41837
proton reactions (p,γ) at 1.278 Mev, sodium-23 gamma decay modes from, (E), 19: 41838
proton reactions (p,γ) at 1.28 to 1.86 Mev, sodium-23 energy levels from, (E), 19: 41838
reactions with nuclei at 5 to 12 Mev, neutron spectra from, (E), 19: 41810(T)
NEON SYSTEMS
ethane–Ne, kinetic energy effects on carbon-11 reactions with, 19: 40617
H–Ne, performance in bubble chambers, 19: 40869 (CONF-650510-14)
NEPTUNIUM
separation from irradiated fuel elements, 19: 40675
solvent extraction by tributyl phosphate and di-2-amyl 2-butylphosphonate in short-residence contactors, 19: 40645 (CONF-650918-1)
NEPTUNIUM ISOTOPES Np-237
neutron fission ratios relative to uranium-235, (E), 19: 42077 (ANL-7014)
pathological effects of injected, in liver of sheep, 19: 40350 (HW-SA-3723)
NEPTUNIUM NITRIDES
decomposition pressure, 19: 40958
NERVE CELLS
neurological effects in rabbits, whole-body, 19: 40355(T) (FTD-TT-65-48, pp 111–12)
NERVOUS SYSTEM
radiation effects in human, 19: 40349 (BNL-9345)
radiation effects on, innervating mammary gland, 19: 40353(T) (FTD-TT-65-48, pp 16–17)
radiation effects on, synergistic effects of stress induced by vibration, 19: 40354(T) (FTD-TT-65-48, pp 38–9)
radiation effects on, in rabbits, 19: 40355(T) (FTD-TT-65-48, pp 111–12)
radiation effects on activity of, in dogs, 19: 40356(T) (FTD-TT-65-48, pp 469–70)
NEUTRINOS
emission effects on temperature distributions in partially degenerate helium cores in stars, (T), 19: 41237
field of negative or positive 1-spinors for, for singular-electromagnetic-field tensor, (T), 19: 41348
interactions of, supercharged particle production in high-energy, (T), 19: 41483(T)
interactions with nuclear nucleons, meson (π) production in, (T), 19: 41754
mass, (T), 19: 41482(T)
models for, description of electromagnetic, (T), 19: 41377
reactions with nuclear nucleons, meson (π) production in, (T), 19: 41754
theory for photons using, (T), 19: 41387
NEUTRON BEAMS
production in heavy water reactors, 19: 42066(P)
production of high-intensity, using cyclotron with separated orbits, 19: 41174
radiation hazards of synchrocyclotron, 19: 41171(T) (N64-33402)
scattering by matter, angular and spatial distributions of multiple, (T), 19: 41650(T)
NEUTRON CROSS SECTIONS
calculation for materials with grain structure, method for, 19: 42041 (GA-6286)
NEUTRON-DIFFRACTION ANALYSIS
collimator design for neutron powder diffractometry, (E), 19: 40492
cryostats for, design of, 19: 40852
NEUTRON DIFFRACTOMETERS
collimator design for powder, (E), 19: 40492
NEUTRON SCATTERING CROSS SECTIONS
measurement of inelastic differential, method for, 19: 42154 (KFK-261)
NEUTRON SOURCES
performance of oscillating, 19: 41641(R) (MIT-2344-3, pp 137-54)
research programs on, at Siemens-Schuckertwerke laboratories, Erlangen, Germany, 19: 42228
NEUTRON SPECTRA
measurement in poisoned heavy water and water, (E), 19: 41646
NEUTRON SPECTROMETERS
design of liquid helium-3, 19: 40928(P)
performance of chopper and rotating-crystal, 19: 42154 (KFK-261)
NEUTRON SPECTROSCOPY
use in study of atomic vibrations in crystal lattices, 19: 41996(T)
NEUTRON TOTAL CROSS SECTIONS
measurement techniques for fast, (E), 19: 41723
NEUTRONS
albedo flux from atmosphere, (E), 19: 41606
angular distribution and energy spectra from helium-4 (He-3,n) reactions at 29.8 Mev, (E), 19: 41659 (IAE-835)
angular distributions from boron-11 (d,n) reactions at 1 to 11 Mev, (E/T), 19: 41732
angular distribution from d-d reactions at 20 to 300 kev, 19: 41832
beta decay of moving longitudinally polarized free, angular distributions from, (T), 19: 41496
buckling and flux distributions in lattices of slightly enriched uranium and heavy water, (E), 19: 42049(R) (MIT-2344-3, pp 155-64)
capture by chlorine-35 and scandium-45, cross sections for, (E), 19: 41806(T)
capture by indium-115, conversion-electron from thermal, (E), 19: 41808(T)
capture in stellar nuclei, mechanisms for, (T), 19: 41235
correlation in reactors, Boltzmann equation for, 19: 42042 (JINR-P-2216)
decay constants and extrapolation length in graphite, pulsed, (E), 19: 41647
detection and measurement using boron-11 activation detector, (E), 19: 40867 (BNWL-64)
detection and measurement of, engineering drawings of ionization chamber for, 19: 40923
detection using paraffin-moderated boron trifluoride counters, (E), 19: 40890
diffusion and transport calculations in NPR tube-in-tube fuel geometry, 19: 42128(R) (BNWL-95, pp 18-23)
diffusion equation for, program system for multigroup, 19: 41649
diffusion in reactors, use of poison in direct solution of equation for, 19: 42052
diffusion in two-region assemblies of enriched uranium and heavy water, 19: 42048 (MIT-2344-3, pp 125-36)
disadvantage factor in cylindrical geometry, 19: 42063
distributions in heterogeneous reactors, method for calculating, 19: 42060
distributions of, theorems on fluctuations and fluctuation spectra in, 19: 41653
dosimetry in tissues of 60- to 400-Mev, 19: 40372
dosimetry of, 19: 40800(R) (AERE-PR/HPM-7)
dosimetry of nuclear explosion, (T), 19: 40938
dosimetry using thermoluminescent phosphors, 19: 40868 (BNWL-SA-23)
effect on pyrolysis of terphenyls, 19: 40630
effects in Tradescantia, biological, 19: 40800(R) (AERE-PR/HPM-7)
effects on base current in silicon transistors, 19: 40936 (SC-R-65-912)
effects on bromoethane, pressure and temperature effects on recoil reactions in, 19: 40626
effects on can-fuel bond in fuel elements, 19: 41089 (HW-56028)
effects on concentration of interstitials and vacancies in niobium, calculation of, 19: 41106
effects on conductivity of n-type silicon, 19: 40935 (SC-DC-65-1247)
effects on fine structure of optical absorption bands in, magnesium oxide, 19: 40632
effects on graphite, use of bromine adsorption in determining, 19: 41109(P)
effects on hardness of beryllia, 19: 41087 (AAEC/E-135)
effects on hydrolysis of uranium carbides and plutonium carbide–uranium carbide systems, 19: 40586
effects on labeled organic retentions in halohydrocarbon mixtures with bromine, 19: 40624
effects on mechanical properties of chrome nickel stainless steels, 19: 41093(T) (FTD-TT-65-125)
effects on molybdenum–uranium alloy fuel, 19: 41090 (NAA-SR-11121)
effects on n-propyl bromide, bromobenzene, 4-bromo-o-xylene, and benzyl bromide, thermal annealing of, 19: 40576
effects on phonon infrared absorption spectra in magnesium oxide, 19: 41108
effects on properties of reactor-grade graphite, 19: 40959
effects on stress-strain properties of type 304 stainless steel, 19: 40961
effects on structure of polybutadiene, 19: 40561
effects on tensile properties of Zircaloy-2 and -4, 19: 40961
effects on thermally stimulated conductivity of p-type silicon, (E), 19: 41985
effects on thermal conductivity of polyethylene at 0 to 170°C, 19: 40603
effects on 5-Mc magnetic tunnel-semiconductor logic circuits, 19: 40939

electric dipole moment of, low pass filter for determination of, 19: 41338 (ORNL-TM-1149)
emission from KIWI-TNT destruct, dose measurements of, 19: 42135 (LA-3304)
emission from plutonium-239 and uranium-233 and -235 fission fragments, (E/T), 19: 41681 (ANL-Trans-205)
emission from, of heavy ion reactions with nuclei, spectra of, (E) 19: 41810(T)
emission in deuteron stripping reactions, computer program for cross section calculations for, 19: 41677 (ORNL-TM-1151)
energy spectra in heterogeneous thermal reactors, diffusion approximation for space-dependent, (T), 19: 42056
flux at aircraft altitudes, anomalous increasis in, (E), 19: 41579
flux distribution in EBWR during power operation, (E), 19: 42076 (ANL-6751)
flux distributions in research reactor VVR-S, (E), 19: 42183
flux in fast reactor Doppler-effect calculations, resonance correction to group, (T), 19: 42057
flux in fast reactor Doppler-effect calculations, resonance correction to group, (T), 19: 42058
flux measurements in reactors, device for, 19: 42064(P)
form factors of electromagnetic, (E), 19: 41326 (HUX-2752-9)
interactions with antiprotons at 1.96 Bev/c, $\bar{N}^*$ production in, (E), 19: 41438
interactions with antiprotons, intermediate vector boson production in, (T), 19: 41484(T)
interactions with deuterons, singularities of amplitudes for elastic, (T), 19: 41504
interactions with mesons (π^+) at 1.7 Bev/c, meson (ρ) and (ω) production in, (E), 19: 41528
interactions with bound electrons, cross sections for, (E), 19: 41274
interactions with protons at 3 to 10 Bev, cross sections for elastic, (E), 19: 41347
interactions with mesons (K^-), final-state interactions in ($\Lambda\pi^-$), (T), 19: 41405
interactions with protons in nuclei, R(5) and R(8) groups in quasi-spin formalism for pairing, 19: 41839
interactions with mesons (K^-) at rest, hyperon (Σ^-) production in, (E), 19: 41494
kinetics in reflected critical assemblies, decay constants for, 19: 42040(R) (BNWL-95, pp 40-54)
mass difference with protons, (T), 19: 41511
photoproduction from lead, yields of, (E), 19: 41833
photoproduction on deuterium, laboratory observation of, 19: 41712
polarization in decay of collective states excited by meson (μ) capture, (T), 19: 41769
production in proton–vanadium-51 reactions at 1.5 to 2.3 Mev, (E), 19: 41676 (ORNL-P-1468)
production in proton-proton interactions at 2.0 Bev, (E/T), 19: 41503
reaction with natural uranium, number of fissions in, 19: 40640
reactions (n,γ) with mercury isotopes at 20 to 210 ev, spectra from (E), 19: 40896
reactions (n,γ) with vanadium, vanadium-52 energy levels from, (E), 19: 41725
reactions (n,γ) with chromium isotopes, gamma spectra from, (E), 19: 41807(T)
reactions (n,γ) with mercury-199, mercury-200 parity assignments from, 19: 41846
reactions (n,γ) with rhenium-185 in mixed crystals, chemical transformations from, 19: 40585
reactions (n,nʹγ) with bismuth-209, gold-197, and lead-206, gamma spectra from, (E), 19: 41669 (LA-DC-7096)
reactions (n,nʹγ) with yttrium-89 at 14 Mev, cross sections for, 19: 41781
reactions (n,2n) with iodine-127, search for 2.6-hr iodine-126m in, 19: 41716
reactions (n,2n) with neodymium-142, samarium-144, terbium-159, and erbium-168 at 14 Mev, production of isomeric states in, (E), 19: 41781
reactions with holmium-165 at 0 to 55 ev, resonance spins from, (E), 19: 41665 (JINR-P-2209)
reactions with niobium and rubidium to 1.3 kev, resonance parameters and radiation widths from, (E), 19: 41727
reactions with uranium-235 at 3.25 ev to 1.8 kev, capture-to-fission ratio for, (E), 19: 41749
reactions with uranium-235 at 14.9 Mev, yttrium-90, niobium-96, and lanthanum-140 yields from fission, (E), 19: 41779
reactions with ytterbium isotopes, spectra of resonance, 19: 41661 (JINR-P-2158)
reflection in elliptic systems, 19: 41645
resonance escape in heterogeneous cluster-type fuel rods, Dancoff factor and equivalence theorem for, (T), 19: 42055
scattering by copper, dispersion relations for lattice vibrations from, (E), 19: 41996(T)
scattering by elements, optical model calculations for elastic, (T), 19: 41827
scattering by lead, tantalum, thallium, and tungsten at 14 Mev, cross sections for inelastic, (E), 19: 41718
scattering by nuclei, electrodynamic effects in Coulomb, (T), 19: 41334 (JINR-P-2229)
scattering by potassium-39 at 1.49 to 3 Mev, cross sections for, (E), 19: 41737
scattering in aluminum and bismuth, excitation cross sections for, (E), 19: 41274
scattering in many-particle systems, method for differential cross sections of inelastic, 19: 42154 (KFK-261)
slowing-down and fast group constants from pulsed, 19: 41654
spectra from bismuth-209 (γ,n) reactions at 12 to 16 Mev, (E), 19: 41834
spectra from meson (μ) capture by helium-3, (T), 19: 41783
strength functions in rare earth region, target spin dependence of, 19: 41656 (BNL-9245)
thermalization of, integral, 19: 41640(R) (GA-6323)
thermalization of, temperature-dependent, (T), 19: 41652
transmission through heterogeneous multiplying and nonmultiplying media, 19: 41643 (ORNL-TM-1184)
transmission through lithium hydride slabs, Monte Carlo analysis of, 19: 41642 (NAA-SR-10853)
transport equations for, for criticality determination in two-region cells, 19: 42035 (ANL-6590)
transport equation for, approximate solution of nonlinear, (T), 19: 41651
uses of reactor, for commercial radiation chemistry, (E/T), 19: 40559

NEUTRONS, COLD
performance for radiography, (E), 19: 40722

NEUTRONS, EPITHERMAL
reactions in enriched-uranium heavy water lattices, (E), 19: 42044(R) (MIT-2344-3, pp 37-54)

NEUTRONS, FAST
correlations of, assembly for studying angular and energy, 19: 40894
effects on absorption spectra of Yakutian diamonds, 19: 41098
effects on aqueous solutions in reactors, production of chemicals by, 19: 40548 (BNWL-82)
effects on corrosion and tensile properties of hafnium-to-Zircaloy-2 welded joints, 19: 41092 (WAPD-TM-457)
effects on electric conductivity and Hall coefficients of germanium, 19: 41104(T)
effects on graphite basal plane contraction, (T), 19: 41100
effects on mechanical properties of hafnium control rods, 19: 41092 (WAPD-TM-457)
effects on modulus-of-rupture of beryllia, 19: 40959
effects on properties of cobalt–copper alloys, 19: 41095(T) (ORNL-tr-667)
effects on stored energy release in molybdenum, 19: 40961
flux distributions in enriched uranium lattices, (E), 19: 42043(R) (MIT-2344-3, pp 15-36)
radioinduced swelling in beryllia, 19: 40959
radioinduced swelling in beryllia, effects of bentonite additives on, 19: 40959
reactions (n,d) with copper-63 and -65, angular distributions from, (E/T), 19: 41755
reactions with nuclei, total cross section measurements for, (E), 19: 41723
reactions with uranium-235 and -238, fission rates for, 19: 41672(R) (MIT-2344-3, pp 5-14)

NEUTRONS, PROMPT
decay constants in solid-moderated, enriched uranium subcritical assemblies, 19: 42051 (UCRL-12013)
decay in reactors, Monte Carlo method for analysis of, 19: 42039 (BNWL-95, pp 36-9)

NEUTRONS, THERMAL
diffusion equations for, derivation of Nordheim equation from, (T), 19: 41644
diffusion in heavy water, decay constants of, (E), 19: 42045(R) (MIT-2344-3, pp 55-108)
effects on absorption spectra of Yakutian diamonds, 19: 41098
effects on alkali-halide color centers and dislocations, (E), 19: 41976
effects on purines and pyrimidines, 19: 40557
flux distribution in source-free absorbing medium, temperature effect on, (T), 19: 41652
flux distributions in heavy water lattices with single uranium rod, (E/T), 19: 42047 (MIT-2344-3, pp 115-24)
reactions (n,α) with heavy nuclei, cross sections for, (E), 19: 41809(T)
reactions (n,f) with uranium-235, gamma angular distribution in, (E), 19: 41722

reactions (n,γ) with holmium, gamma spectra from, 19: 41670 (LA-DC-7097)
reactions (n,γ) with nuclei, spectra from, 19: 40896
reactions with matter as probe of molecular motions, 19: 40455 (BNL-9297)
reactions with uranium-235 at 2200 m/sec, cross sections for fission, (E), 19: 41691
reactions with uranium-235, positron emission of fission products from, (E), 19: 41799(T)
scattering by magnetic materials, spin-wave excitation by inelastic, 19: 41987
scattering by solid solutions, one-phonon peak in, (T), 19: 41991(T)
spectra in heterogeneous lattice cells, computer program for, 19: 41648
spectra in reactor moderators, 19: 42037 (BNWL-95, pp 4-17)
spectroscopy of, in Triga Mark II thermal column, (E), 19: 42184

NEVADA TEST SITE
monitoring system for postshot drilling at, 19: 40834(R) (UCRL-14151)
radiation monitoring at, system for remote, 19: 40878 (NVO-162-5(Rev.))

NICKEL
analysis for nitrogen, isotope-dilution method for, 19: 40444
compatibility with graphite–nitrogen environment at 1000 and 1200°C, 19: 40966 (BNWL-92)
compatibility with boron carbide and uranium dioxide at 1200°C, 19: 40966 (BNWL-92)
corrosion by aluminum–silicon and water of coatings of, on uranium, 19: 40949 (ISC-640)
deposition on uranium by diffusion from molten magnesium bath, 19: 40949 (ISC-640)
deposition on zinc-coated uranium, electrolytic, 19: 40949 (ISC-640)
determination by spectrochemical methods, voltage-fluctuation patterns in, 19: 40416
determination in copper by activation, 19: 40422
effects on eutectic temperature of iron–plutonium alloys, 19: 40958
effects on phase transformation in plutonium, 19: 40958
electron and ion emission from cesiated and vacuum surfaces of, (E), 19: 41284
ion reactions with surfaces of, isotopic effect in secondary electron emission in, (E), 19: 41249
magnetic properties near Curie point, (E), 19: 41972
neutron reactions (n,γ) at 0.025 ev, spectra from, 19: 40896
nitrogen ion ranges at 0.4 and 2.5 Mev, (E), 19: 41269
thermodynamic properties at high pressures and temperatures, 19: 40459 (NP-15324)
wear characteristics of plated coatings of, for use in rotary switches, 19: 42216 (SC-DR-65-269)

NICKEL ALLOYS
analysis for niobium and tantalum, photometric method for, 19: 40442
analysis for samarium, 19: 40445
brazing alloys for René 62, properties of, 19: 40989
thermal stability study of dispersion-strengthened SLIS, 19: 41021(R) (NMI-8002.1)
Ce–Ni, phase studies, 19: 40961
Cr–Co–Fe–Mn–Mo–Ni–W, corrosion of Raonel, by coal gasification products at high temperatures, 19: 42127(R) (TID-22009)
Cr–Fe–Ni, corrosion films on, structure of oxide, 19: 40967(R) (COO-1319-27)
Cr–Fe–Ni, stress-corrosion cracking in, effects of fourth-component additions on, 19: 40967(R) (COO-1319-27)
Cr–Fe–Ni, stress-corrosion by chlorides, oxygen, and water, 19: 40967(R) (COO-1319-27)
Cr–Fe–Ni, tensile properties to 1200°F, effects of composition on, 19: 40967(R) (COO-1319-27)
Cr–Ni, diffusion in, activation energy and frequency factor for self-, 19: 40961
Cu–Ni, brazing alloy for metallized alumina-to-niobium alloy seals, 19: 40980 (LA-3302)
Cu–Ni, diffusion in, activation energy and frequency factor for self-, 19: 40961
Er–Ni, preparation for solid solubility studies, 19: 41021(R) (NMI-8002.1)
Gd–Ni, preparation for solid solubility studies, 19: 41021(R) (NMI-8002.1)
La–Ni, preparation for solid solubility studies, 19: 41021(R) (NMI-8002.1)
Mg–Ni, production of splatcooled, 19: 41021(R) (NMI-8002.1)
Ni–U, production of splatcooled, 19: 41021(R) (NMI-8002.1)
Ni–W, diffusion in, activation energy and frequency factor for self-, 19: 40961
Ni–Y, production of splatcooled, 19: 41021(R) (NMI-8002.1)

NICKEL COMPLEXES
with α, β, γ, δ-tetraphenylporphines, retentions in Szilard-Chalmers (n,γ) recoil reactions in, 19: 40612

NICKEL ISOTOPES Ni-58
alpha inelastic scattering at 43 Mev, distorted-wave calculation of, 19: 41692
decay in alpha reactions (α,xnyp) with iron-54, shell structure effects in, (T), 19: 41741

NICKEL ISOTOPES Ni-59
decay in helium-3 reactions (He-3,xnyp) with iron-56, shell structure effects in, (T), 19: 41741

NICKEL ISOTOPES Ni-60
decay in alpha reactions (α,xnyp) with iron-56, shell structure effects in, (T), 19: 41741

NICKEL ISOTOPES Ni-62
nuclear properties of, (E/T), 19: 41755

NICKEL ISOTOPES Ni-63
deposition, computer program for evaluating radiochemical data on, 19: 40636 (WAPD-TM-516)

NICKEL ISOTOPES Ni-64
nuclear properties of, (E/T), 19: 41755

NICKEL OXIDES
radiation effect on sorption of carbon monoxide and oxygen on, gamma, 19: 40578
radiation effects on catalytic oxidation of carbon monoxide on, at 25°C, 19: 40577

NICKEL STEEL
analysis for samarium, 19: 40445
Cr–Mo–Ni, properties of Super-Elso, 19: 41008 (EURAEC-1407)

NICKEL SULFATES
radiolysis of hydrated, yields in, 19: 40610

NICKEL SYSTEMS
Ni–ThO_2, compatibility of TD nickel with graphite nitrogen environment at 1000 and 1200°C, 19: 40966 (BNWL-92)

NICKELATES
electron yields from cathodes of, 19: 41124(R) (NP-15108)

NIOBIUM
analysis for nitrogen, isotope-dilution method for, 19: 40444
annealing and melting of, reactions with nitrogen, oxygen, and water vapor in, 19: 40490
corrosion by aluminum, tin, and zinc at 800 to 1100°C, 19: 40961
corrosion by lithium at 800°C, effects of oxygen on, 19: 40961
corrosion by oxygen-contaminated lithium, effects of zirconium on, 19: 40961
determination by spectrochemical methods, voltage-fluctuation patterns in, 19: 40416
determination in alloys and metals, photometric, 19: 40442
determination of, polarographic method for, 19: 40443
diffusion in, tracer studies of self-, 19: 41064
diffusion of niobium-95 and tantalum-182 in, at 874 to 2400°C, 19: 41064
effects on oxidation resistance and strength of chromium–magnesia composites, 19: 41022(R) (NP-15292)
effects on properties of tantalum, 19: 41067
interactions with oxygen, 19: 40463(R) (SRIA-425-5)
oxidation of foils of, kinetics of, 19: 40974
performance as superconductor, for inverter applications, 19: 40845(R) (N64-33676)
photoeffects in anodized electrodes of, open- and short-circuit, 19: 41080
plastic deformation of, mechanism of, 19: 40961
radiation effects on concentration of interstitials and vacancies in, calculation of, 19: 41106
reactor criticality effects per atom, (E), 19: 42077 (ANL-7014)
separation from other metal ions by ion exchange, 19: 40658
solubility in pure potassium at 1000°C, 19: 40946(R) (AI-65-93)
solvent extraction by tributyl phosphate and di-2-amyl 2-butylphosphonate in short-residence contactors, 19: 40645 (CONF-650918-1)
superconducting critical characteristic curves for, 19: 41630
thermal expansion to 2500°C, 19: 41009 (GEMP-375)

NIOBIUM ALLOYS
brazing alloys for, 19: 40989
Cu–Nb–Zr, corrosion by superheated steam, 19: 40977(P)
Fe–Nb, solubility of nitrogen in, 19: 41065
Hf–Nb, phase studies, 19: 40960
Hf–Nb–W–Y, properties of welds in C-129Y, 19: 40989
Mo–Nb, niobium-93 nuclear magnetic relaxation in, (E), 19: 41989
Mo–Nb–U, isothermal transformations of gamma-phase, 19: 40958
Mo–Nb–V–Zr, properties of welds in B-66, 19: 40989
Mo–Nb–V–Zr, stress-rupture properties of B-66, 19: 40961
Nb–Sc, phase studies of solid solution formation in, 19: 41050
Nb–Sn, phase studies, 19: 40961
Nb–Sn, superconductivity of hollow sintered cylinders of, (E), 19: 41609
Nb–Ta–V, phase diagram, 19: 41036

Nb–Ta–W–Zr, properties of welds in FS-85, 19: 40989
Nb–Ta–Y–Zr, grain size and hardness of, effects of yttrium additions on, 19: 40953 (PWAC-441)
Nb–Ta–Zr, nitrogen and oxygen contents of, effects of yttrium additions on, 19: 40953 (PWAC-441)
Nb–Ti, current density and magnetic field in cold-worked superconductors of, (E), 19: 41637
Nb–U, isothermal transformations of gamma-phase, 19: 40958
Nb–Y, phase studies of solid solution formation in, 19: 41050
Nb–Y–Zr, grain size and hardness of, effects of yttrium additions on, 19: 40953 (PWAC-441)
Nb–Zr, bonding to metallized alumina, brazing alloy for, 19: 40980 (LA-3302)
Nb–Zr, bonding to alumina–yttria, brazing alloy for, 19: 40980 (LA-3302)
Nb–Zr, critical current degradation in wide-strip superconductors of, (E), 19: 41639
Nb–Zr, current density and magnetic field in cold-worked superconductors of, 19: 41637
Nb–Zr, hardness of, effects of cooling rate and niobium content on, 19: 40961
Nb–Zr, hydridation effects on properties of, 19: 40959
Nb–Zr, mass transfer from Type 316 and 321 stainless steels to, in liquid potassium at 1400°F, 19: 40970(R) (NASA-CR-54390)
Nb–Zr, nitrogen and oxygen content of, effects of yttrium additions on, 19: 40953 (PWAC-441)
Nb–Zr, nuclear spin-lattice relaxation in type II superconductors of, (E), 19: 41611
Nb–Zr, procurement and quality evaluation of stock of, for corrosion studies, 19: 40952 (ORNL-TM-1179)
Nb–Zr, transformation kinetics in, 19: 41033

NIOBIUM CARBIDES
diffusion into zirconium at 1760°C, 19: 40412 (TIM-924)
fabrication of large parts from, 19: 40988
NbC–W, phase studies, 19: 40961

NIOBIUM ISOTOPES
Cu–Nb, oxidation at 500 to 900°C, 19: 40976

NIOBIUM ISOTOPES Nb-93
alpha reactions (α,n), (α,2n), and (α,3n) to 42 Mev, isomeric ratios from, (E), 19: 41695
alpha reactions (α,n), (α,2n), and (α,2n), statistical model for isomeric ratios in, 19: 41696
neutron reactions to 400 ev, resonance parameters and radiation widths from, (E), 19: 41727
nuclear magnetic relaxation in molybdenum–niobium alloys, 19: 41989

NIOBIUM ISOTOPES Nb-95
diffusion in niobium at 874 to 2400°C, 19: 41064
metabolism in rats, after inhalation, 19: 40314
pathological effects of injected, in rats, 19: 40384

NIOBIUM ISOTOPES Nb-96
yield in alpha fission of thorium-232 at 20 to 40 Mev, (E), 19: 41779
yield in neutron fission of uranium-235 at 14.9 Mev, (E), 19: 41779

NIOBIUM NITRIDES
crystal structure of, (E), 19: 41051
solubility products in liquid iron at 1550 to 1750°C, 19: 41065

NIOBIUM OXIDES
Al_2O_3–Nb_2O_5, phase studies, 19: 41049
Cr_2O_3–Nb_2O_5, phase studies, 19: 41049
MoO_3–Nb_2O_5, phase studies, 19: 41049
Nb_2O_5–Ta_2O_5, phase studies, 19: 41049
Nb_2O_5–TiO_2, phase studies, 19: 41049
Nb_2O_5–V_2O_5, phase studies, 19: 41049
Nb_2O_5–WO_3, phase studies, 19: 41049

NIOBIUM SYSTEMS
C–Nb–Ti, analysis for carbon, electron microprobe, 19: 40412 (TIM-924)
C–Nb–W–Zr, properties of welds in D-43, 19: 40989
C–Nb–W–Zr, stress corrosion of D-43 by boiling potassium, research program on, 19: 40970(R) (NASA-CR-54390)
C–Nb–W–Zr, stress-rupture properties of D-43, 19: 40961
Co–Nb–Si, crystal structure of compounds in, 19: 41069

NITRATE IONS
isotopic exchange equilibrium calculations, 19: 40460(R) (NYO-3462-1)

NITRATES
determination in heavy water moderator, automated, 19: 40406 (CONF-650919-2)

NITRIC ACID
isotopic exchange equilibrium calculations, 19: 40460(R) (NYO-3462-1)
production using radioinduced oxidation of atmospheric nitrogen by fission fragments, (E), 19: 40604
separation of scandium from, by solvent extraction using alkyl phosphates, 19: 40689
solvent properties for uranium spent fuel elements, 19: 41086(P)
HNO_3–$K_2Cr_2O_7$, corrosive effects on stainless steel, effects of silicon on, 19: 40947(R) (EURAEC-1403)

NITRITE IONS
isotopic exchange equilibrium calculations, 19: 40460(R) (NYO-3462-1)
yields from gamma radiolysis of nitromethane at 77°K, EPR studies of, 19: 40579

NITRITES
determination in heavy water moderator, automated, 19: 40406 (CONF-650919-2)

NITROGEN
content in niobium-based alloys, effects of yttrium additions on, 19: 40953 (PWAC-441)
determination in metals, isotope-dilution method for, 19: 40444
determination in uranium dioxide–plutonium dioxide systems, 19: 40438
determination on beryllium surface by deuteron activation methods, 19: 40453
determination, electron microprobe, 19: 40412 (TIM-924)
determination, use of beta ionization detector in chromatographic, 19: 40415(T) (CEA-tr-R-1839)
diffusion and spin relaxation of cesium in, (E), 19: 41278
diffusion in hafnium, coefficient for, 19: 40960
diffusion into urania, coefficient for, 19: 40958
electron interactions in plasma of, probability of momentum-transfer in, (E/T), 19: 41944
electron stopping in atmospheric, due to rotational excitation, (T), 19: 41600
radioinduced oxidation of atmospheric, by fission fragments, (E), 19: 40604
reactions with niobium and tantalum during annealing and melting, 19: 40490
solubility in iron alloys with niobium, tantalum, titanium, vanadium, and and zirconium, 19: 41065
solubility in stainless steel at 1000°F, effects of ammonia–hydrogen ratio on, 19: 40968(R) (EURAEC-1424)
sorption by evaporated molybdenum films, 19: 40463(R) (SRIA-426-5)
spectral line emission from plasma of, Stark broadening of, 19: 41941

NITROGEN IONS
excitation of molecular, by electron and ion impact, (E), 19: 41279
ranges in nickel and silver at 0.4 and 2.5 Mev, (E), 19: 41269
reactions with deuterium and hydrogen molecules, spectra of N_2D^+ and N_2H^+ in, (E), 19: 41252
reactions with molecular nitrogen ions at 10 to 65 kev, rotational and vibrational excitation in, (E), 19: 41279

NITROGEN ISOTOPES N-13
production in man during high-energy radiotherapy, 19: 40392 (NYO-3364-6)

NITROGEN ISOTOPES N-14
abundance in massive stars, effects of helium and hydrogen burning on, (T), 19: 41242
energy levels from proton reactions (p,γ) with carbon-13 at 0.60 to 1.8 Mev, (E), 19: 41740
exchange equilibrium calculations in oxy-nitrogen molecules, 19: 40460(R) (NYO-3462-1)
reactions with tellurium-128 and zinc-68 at 40 to 150 Mev, isomeric pair production ratios in, 19: 41674 (NYO-1930-44)

NITROGEN ISOTOPES N-15
energy levels of, from carbon-12 (t,α) reactions, (E), 19: 41706
exchange equilibrium calculations in oxy-nitrogen molecules, 19: 40460(R) (NYO-3462-1)

NITROGEN ISOTOPES N-17
production in proton reactions at 1.0 and 2.8 Bev, cross sections for, (E), 19: 41780

NITROGEN OXIDES
isotopic exchange equilibrium calculations, 19: 40460(R) (NYO-3462-1)
production using radioinduced oxidation of atmospheric nitrogen by fission fragments, (E), 19: 40604

NITROGEN SYSTEMS
C–N, spectra of diatomic, in plasma jets, (E), 19: 41287
graphite–N, effects on candidate HTLTR materials at 1000 and 1200°C, 19: 40966 (BNWL-92)
Kr–N, electron reactions at 50 kev, luminescence from, (E), 19: 41246
N–Xe, electron reactions at 50 kev, luminescence from, (E), 19: 41246

NITROSYL BROMIDES
isotopic exchange equilibrium calculations, 19: 40460(R) (NYO-3462-1)

NITROSYL CHLORIDES
isotopic exchange equilibrium calculations, 19: 40460(R) (NYO-3462-1)

NITROSYL COMPOUNDS
spectra of pentacyanonitrosylchromium(II) ion, electron spin resonance, 19: 40465 (UCRL-16175)

NITROSYL FLUORIDES

isotopic exchange equilibrium calculations, 19: 40460(R) (NYO-3462-1)
NITROUS ACID
isotopic exchange equilibrium calculations, 19: 40460(R) (NYO-3462-1)
NITRYL CHLORIDES
isotopic exchange equilibrium calculations, 19: 40460(R) (NYO-3462-1)
NITRYL FLUORIDES (NO,F)
isotopic exchange equilibrium calculations, 19: 40460(R) (NYO-3462-1)
NOISE
control of industrial, 19: 40806 (RL-SA-37)
NORLEUCINE
preparation of sulfur-35-labeled, by reactions with sulfur-35 recoil atoms, 19: 40619
NORVALINE
preparation of sulfur-35-labeled, by reactions with sulfur-35 recoil atoms, 19: 40619
NRU REACTOR
computer control of, 19: 42148 (AECL-2216)
neutron flux detectors for, self-powered, 19: 42148 (AECL-2216)
NUCLEAR BATTERIES
energy conversion in, review, 19: 41319
NUCLEAR EMULSIONS
development of, effects of additives on distortion in ultrasonic-oscillation, 19: 40884
particle track lengths in, effects of pH of impregnating solution on alpha, 19: 40597
performance and properties for dosimetry, 19: 40889
proton interactions at 9 Mev in, hyperon ($\Sigma^{\pm}$) production and decay, (E), 19: 41350
NUCLEAR ENGINEERING
research programs on, 19: 40396(R) (HMI-B-39)
NUCLEAR MAGNETIC RESONANCE
measurement in enriched tin-119 hollow cylindrical monocrystals, (E), 19: 40990
nuclear polarization effects on, (T), 19: 42001
relaxation in, linearized equations for, 19: 41751
NUCLEAR MATERIALS MANAGEMENT
criticality evaluation of packages for transport of fissile materials, 19: 40828 (SC-RR-65-98, pp 679-90)
criticality of low-assay uranium compounds in array of shipping containers, 19: 40819 (SC-RR-65-98, pp 330-56)
criticality safety procedures, 19: 40807 (RL-SEP-389(Rev.))
fuel management and inventory in EBR-II, 19: 42075 (ANL-6735)
plutonium nitrate shipping containers, design for reduced weight and cost, 19: 40825 (SC-RR-65-98, pp 609-19)
NUCLEAR MODELS
energy levels in, five-dimensional quasispin for pairing hamiltonian in J-T scheme of, 19: 41687
NUCLEAR MODELS (DROP)
fission-barrier energies and shapes in, (T), 19: 41767
NUCLEAR PHYSICS
research in high-energy, review, (E/T), 19: 41337 (NYO-2262-95)
research on, 19: 41678(R) (PR-P-65)
research programs on, 19: 40396(R) (HMI-B-39)
NUCLEAR POWER
development of, energy conversion cycles in, 19: 42121
NUCLEAR POWER PLANTS
construction of Saint-Laurent-des-Eaux, 19: 42119
design using gas-cooled heavy-water-moderated pressure-tube reactor, 19: 42112
development for water desalination and power, 19: 42124
development of, supercritical steams cycles in, 19: 42121
economics for 1000 Mw(e) pressurized water, reference, 19: 42102 (WCAP-2385(Vol.I))
feasibility of 1000 Mw(e) pressurized water, 19: 42102 (WCAP-2385 (Vol.I))
feasibility of 1000 Mw(e) pressurized water, 19: 42103 (WCAP-2385(Vol. II))
operation of, selection of personnel for, 19: 42098 (RT/PROT(65)24)
radiator design for heat rejection from, on spacecraft, (T), 19: 40731 (AD-609969)
use of dual purpose, with reverse osmosis, 19: 42120
NUCLEAR REACTIONS
analysis of cascade showers by solving inverse problem, (T), 19: 41710
angular correlations in, detector correction factors for, (T), 19: 40900
correlation effects in ground-state, (T), 19: 41814
cross section fluctuations in, finite-sample-size effects in, (T), 19: 41762
cross sections of two-nucleon knock-on and stripping, structure-factor effects on, (T), 19: 41819
cross-section measurements in, experimental-resolution effect on widths of fluctuation correlation function for, (T), 19: 41734
form factors for stripping, (T), 19: 41746
model for stripping, validity of DWBA in three-body, 19: 41777
nucleon transfer in, 19: 41795
theory for stripping, with emission of slow particles, 19: 41664 (JINR-P-2193)
wave functions in direct, overlap integrals and single-particle, (T), 19: 41728
NUCLEAR SHOWERS
production and properties of high-energy, (T), 19: 41709
NUCLEAR STRUCTURE
analysis of, conference on, 19: 41671 (LADC-6186)
book: *Structure of Matter*, 19: 41829(T)
group-theory and model-interaction methods for, in 2s-1d shell, 19: 41729
model interaction matrices for 2s-1d shell for A = 18 and 20, 19: 41730
NUCLEAR THEORY
bound states in short-range central potentials, (T), 19: 41439
meson (π)–nucleon interactions, one-particle-exchange models for, (T), 19: 41375
particle penetration of potential barriers, (T), 19: 41533
proton electromagnetic form factors in, analytic continuation of, (T), 19: 41388
scattering amplitude singularities in potential theory, (T), 19: 41550
NUCLEI
beta decay of complex, Golberger-Treiman relation for, 19: 41774
beta decay of, analysis using Geiger counters, (E), 19: 40903
charged-particle stripping reactions with, slow particle emission in, (T), 19: 41664 (JINR-P-2193)
cosmic nucleon reactions with atmospheric, showers from, (T), 19: 41300
cosmic-ray reactions with atmospheric, spectra from, (E/T), 19: 41291
coupling schemes for, surface delta interaction in, (T), 19: 41686
decay of, angular correlation measurements in, (T), 19: 40900
deuteron reactions (d,p) in Coulomb field of, spectroscopic factors for, (T), 19: 41739
deuteron reactions (d,p) with medium-weight nuclei at 28 Mev, isobaric analog states from, (E/T), 19: 41772
deuteron reactions (d,α), differential cross sections for, (T), 19: 41817
electric monopole transitions in nonspherical, (T), 19: 41812
electron capture in, K-electron emission during K, (T), 19: 41825
electron elastic scattering by magnetic moments of light, shell model for high-energy, 19: 41694
electron inelastic scattering by, radiative corrections to, (T), 19: 41752
electron scattering by, cross sections for, (T), 19: 41510
energy gaps of finite, (T), 19: 41826
energy level density in, statistical analysis of, 19: 41655 (BNL-934)
energy level spectra of, self-consistent perturbation of Hartree-Fock-Bogoliubov equations for rotational, 19: 41685
energy levels in, five-dimensional quasispin for pairing hamiltonian in J-T scheme of, 19: 41687
energy levels of spherical, variational calculation of collective, (T), 19: 41702
entropy of spin ½ system of, in magnetic fields, 19: 41713
gamma emission by, angular correlations in, (T), 19: 41698
hyperfragment scattering on heavy, Coulomb spallation in, (T), 19: 41815
ion reactions with, many-nucleon transfer in, 19: 41795
knock-on and stripping reactions, structure-factor effects on cross sections of two-nucleon, (T), 19: 41819
magnetic moments of spherical, (T), 19: 41804(T)
meson (μ^-) capture by proton pairs in, (E/T), 19: 41753
meson (μ) capture by, decay of collective states excited in, (T), 19: 41769
meson (μ) reactions with Coulomb field of, electron pair production in, (T), 19: 41486(T)
meson ($\pi^{\pm}$) scattering at low energies, double-charge-exchange, (T), 19: 41773
model interaction matrices for 2s-1d shell for A = 18 and 20, 19: 41730
neutrino reactions with nucleons in, meson (π) production in, (T), 19: 41754
neutron capture by, in stars, (T), 19: 41235
neutron scattering by, electrodynamic effects in Coulomb, (T), 19: 41334 (JINR-P-2229)
nucleon pairing in, R(5) and R(8) groups in quasi-spin formalism for, 19: 41839
nucleon pairing interactions in, superconductivity theory of, 19: 41843
nucleon reactions with, gamma spectra calculations for inelastic, 19: 41954 (NP-15338)
particle reactions at high energies, multiple meson production from, (T), 19: 41708
particle reactions at high energies, analysis of jets from, (T), 19: 41709
photon reactions in, effect of dynamical correlations on, 19: 41844
photon reactions with Coulomb field of, photon-pair production in, (E/T),

19: 41784
polarization effects on nuclear magnetic resonance and Mössbauer spectra, 19: 42001
positron scattering by, cross sections for, (T), 19: 41510
production of heavy, in thermonuclear explosions, (T), 19: 41765
proton elastic scattering at 10.5 and 14.5 Mev from, optical model potential for, (E/T), 19: 41682
proton reactions at 1.0 and 2.8 Bev, cross sections for lithium-9, carbon-16, and nitrogen-17 production in, (E), 19: 41780
proton scattering at 667 Mev, double, (E), 19: 41666 (JINR-P-2233)
reactions with complex nuclei, cluster-transfer, (T), 19: 41764
spectra of $6 \leq Z \leq 20$, in cosmic radiation, (E), 19: 41310
triton reactions (t,d) in Coulomb field of, spectroscopic factors for, (T), 19: 41739
triton reactions (t,p), differential cross sections for, (T), 19: 41817

NUCLEI (CELLS)
radiation effects on rabbit, biochemical, 19: 40375

NUCLEIC ACIDS
photochemical reactions of, in microorganisms, 19: 42212 (NYO-3424-1)
physical properties of, 19: 42212 (NYO-3424-1)

NUCLEONS
electromagnetic properties of, SU(4) symmetry for, 19: 41397
energy gap in systems of interacting, (T), 19: 41826
exchange in nuclear reactions, (T), 19: 41805(T)
interactions at 300 Bev, cross sections, (T), 19: 41358
interactions in nuclei, superconductivity theory of pairing, 19: 41843
interactions of relativistic, multiple meson production in, (T), 19: 41708
interactions with mesons (π), reciprocal bootstrap in, (T), 19: 41422
interactions with mesons (K) and mesons (π) at high energies, Regge-pole models for, (T), 19: 41426
interactions with mesons (π^+) and (π^-) at 300 to 700 Mev, amplitudes for, (E), 19: 41442
interactions with antinucleons at rest, U(12) predictions for four-meson production in annihilation, (T), 19: 41463
interactions with mesons (π) at low energies, (T), 19: 41498
interactions with mesons (K), resonance effects in, (T), 19: 41506
interactions with mesons (π) below 1 Bev, single meson (π) production in, (T), 19: 41509
interactions with hyperons, book on, 19: 41513
interactions with cosmic neutrinos, meson (μ) production in, (E), 19: 41306
interactions with photons, production of mesons (ω) and (ρ) in, 19: 41321 (AECD/TP/4)
interactions with mesons (π) at high energies, optical model for backward, (T), 19: 41332 (JINR-P-2220)
interactions with protons, polarization tensor for double, (T), 19: 41333 (JINR-P-2227)
interactions with mesons (π), one-particle-exchange models for, (T), 19: 41375
interactions with mesons (π), meson (ρ^0) and meson (ω_0) effects in, (T), 19: 41380
interactions with mesons (π), form factors from, (T), 19: 41385
interactions with mesons (π), absorptive corrections and form factors in peripheral model for ($N\rho$), 19: 41400
interactions with neutrinos, meson (π) production in, (T), 19: 41754
pairing in nuclei, R(5) and R(8) groups in quasi-spin formalism for, 19: 41839
potentials for singlet-even states, velocity-dependent, 19: 41841
production of nucleon–meson cascade by 200-Bev proton reactions with iron, (T), 19: 41955 (ORNL-TM-1121)
reactions with nuclei at high energies, analysis of jets from, (T), 19: 41709
reactions with nuclei, gamma spectra calculations for inelastic, 19: 41954 (NP-15338)
transfer in heavy ion reactions with nuclei, 19: 41795

O

OATS
strontium-90 metabolism in, effects of potassium phosphate and calcium hydroxide on, 19: 40310

OBRIGHEIM POWER REACTOR (*Germany*)
design concepts, 19: 42105
design for 1968 startup, 19: 42106

OCEANOGRAPHY
circulation near southern Berry Islands in Bahamas, dye tracer study, 19: 42201 (CU-2663-23)
instrumentation for shallow-water, testing of, 19: 42210(R) (NYO-98-8)

OILS
gas absorption by traveling drops of, on vertical wire, 19: 40398 (UCRL-16047)
radiolysis of mixtures of, with methyl methacrylate, reactions of free radicals formed in, 19: 40580

OLEIN
separation of iodide from iodine-131-labeled tri-, chromatographic, 19: 40656(T) (CEA-tr-X-609)

OPTICAL FILTERS
performance for eliminating heat absorption of casting materials, 19: 42215 (RFP-625)

OPTICAL SYSTEMS
aberrations in charged-particle beams owing to space charge, (T), 19: 41173
charged particle beam aberrations induced by electric and magnetic fringing fields, (T), 19: 41139

ORES
correlation and chronology of deposits, research program on, 19: 40778(R) (COO-689-50)

ORGANIC COMPOUNDS
proton polarization in, pulse method for determining, 19: 40473
radiation chemistry of, device for studying, 19: 40370
reactions with recoil atoms, energy transfer processes and nuclear transformations in, 19: 40620

ORGANIC COOLED REACTORS
heat transfer in power, (E), 19: 42110
status of Spanish heavy-water-moderated power, 19: 42113

ORGANIC MODERATED REACTORS
fuel element fouling in, literature survey on, 19: 40971 (RT/CHI(65)20)
heat transfer in power, (E), 19: 42110

OROTIC ACID
radiation effects on incorporation of carbon-14-labeled, in RNA in diploid yeast, 19: 40367

OSCILLATORS
design of high-stability variable-frequency, (E), 19: 40857
electron beam production for, with reduced orbital motion, (T), 19: 41134
frequency and parameter variations of wide-band, (T), 40846 (NP-15209)

OSMIUM
neutron reactions (n,α) with, cross sections for thermal, (E), 19: 41809(T)

OSMIUM ALLOYS
Mo–Os–W, phase diagrams at 1600, 2000, and 2375°C, 19: 41048
Os–Ta, crystal structure, 19: 41045

OSMIUM ISOTOPES Os-186
energy levels of, gyromagnetic ratio of 2$^+$, (E), 19: 41791
energy levels of, vibration-rotation interactions in, (T), 19: 41818

OSMIUM ISOTOPES Os-188
energy levels of, gyromagnetic ratio of 2$^+$, (E), 19: 41791
energy levels of, parity and spin of, (E), 19: 41801(T)
energy levels of, vibration-rotation interactions in, (T), 19: 41818

OSMIUM ISOTOPES Os-190
energy levels of, vibration-rotation interactions in, (T), 19: 41818

OSMIUM ISOTOPES Os-192
energy levels of, vibration-rotation interactions in, (T), 19: 41818

OXALIC ACID
preparation of actinides and lanthanides from, by solvent extraction using amines, 19: 40657

OXIDASES
radiation effects on content of ascorbic acid, in seeds of *Momordica charantia*, 19: 40371

OXIDES
determination in liquid sodium, methods for, 19: 40409(R) (MSAR-65-95)
phase equilibria of mixtures with rare earth oxides, review, 19: 40534

OXYGEN
content in niobium-based alloys, effects of yttrium additions on, 19: 40953 (PWAC-441)
corrosive effects on chromium–iron–nickel alloys, 19: 40967(R) (COO-1319-27)
determination on beryllium surface by fast neutron activation methods, 19: 40453
determination, electron microprobe, 19: 40412 (TIM-924)
determination, use of beta ionization detector in chromatographic, 19: 40415(T) (CEA-tr-R-1839)
diffusion in hafnium, coefficient for, 19: 40960
effects of content of, on properties of irradiated silicon crystals, 19: 41998(T)
effects on corrosion of type 316 stainless steel by sodium, 19: 40969(R) (MSAR-65-96)
effects on diffusion of niobium-95 and tantalum-182 in niobium, 19: 41064
effects on lithium corrosion of niobium and tantalum, 19: 40961
effects on optical properties of samarium-containing calcium fluoride

crystals, (E), 19: 41993(T)
electron stopping by atmospheric, due to rotational excitation, (T), 19: 41599
ethane-O, oxidation induced by fission fragments in, 19: 40611
ethylene--O, oxidation induced by fission fragments in, 19: 40611
interactions with niobium, 19: 40463(R) (SRIA-425-5)
ionization of, collisional excitation in auto-, (T), 19: 41244
methane-O, oxidation induced by fission fragments in, 19: 40611
O-propane, oxidation induced by fission fragments in, 19: 40611
oxidative effects on molybdenum and tungsten at high temperatures, kinetics of, 19: 40961
radiation effects on sorption of, on nickel oxide, 19: 40578
radioinduced recombination with hydrogen in presence of water vapor, gamma, 19: 40549 (COO-1032-1)
reactions with iron, effects of argon ion bombardment on, 19: 40973
reactions with niobium and tantalum during annealing and melting, 19: 40490
reactions with tungsten surfaces, electron-stimulated desorption for studying, 19: 41103(T)
separation from rare earth metals, techniques for, 19: 40948 (IS-1195)
sorption by zirconia, 19: 40961
thermal relaxation frequency of, effects of water, water-d, and water-d_2 vapors on Napier, 19: 40483

OXYGEN IONS
reactions with iron, effects of argon ion bombardment on, 19: 40973
reactions with lithium fluoride at 100 kv, effects of, (E), 19: 41256
yields of positive, from electron bombardment of light and heavy water, 19: 40581

OXYGEN ISOTOPES O-15
production in man during high-energy radiotherapy, 19: 40392 (NYO-3364-6)

OXYGEN ISOTOPES O-16
abundance in massive stars, effects of helium and hydrogen burning on, (T), 19: 41242
bremsstrahlung reactions (γ,p) at 22 to 40 Mev, branching ratios and cross sections for, (E), 19: 41790
deuteron reactions (d,α) at 15.14 Mev, isobaric spin selection rules from, (E), 19: 41720
deuteron reactions (d,p) with, DWBA and Coulomb stripping approximations for, (E), 19: 41742
deuteron reactions (d,α), differential cross sections for, (T), 19: 41817
electron inelastic scattering by, (T), 19: 41766
energy levels of, structure of even parity, (T), 19: 41816
exchange equilibrium calculations in oxy-nitrogen molecules, 19: 40460(R) (NYO-3462-1)
exchange with oxygen-18 in sodium molybdate, sodium sulfate, and sodium tungstate melts, at 700° to 900°C, 19: 40506
meson (μ) capture by, (T), 19: 41766
proton elastic scattering by, polarization from, (E), 19: 40905
reactions (O-16,O-17) with lead-208, (E), 19: 41768
scattering by lead-208, inelastic, (E), 19: 41768
triton reactions (t,p), differential cross sections for, (T), 19: 41817

OXYGEN ISOTOPES O-18
determination of abundances of, in water by activation methods, 19: 40419
energy levels of, 3.92 to 1.98 Mev transition in, (T), 19: 41797
exchange equilibrium calculations in oxy-nitrogen molecules, 19: 40460(R) (NYO-3462-1)
exchange with oxygen-16 in sodium molybdate, sodium sulfate, and sodium tungstate melts, at 700 to 955°C, 19: 40506
matrices for 2s-1d shell of, model-interaction, 19: 41730

OXYGEN ISOTOPES O-20
matrices for 2s-1d shell of, model-interaction, 19: 41730

OXYGEN SYSTEMS
O–K–Sn, phase studies, 19: 41031
O–K–Zr, phase studies, 19: 41031

P

PACKAGING
fire resistance of radioisotope containers, 19: 40831 (SC-RR-65-98, pp 723-31)
fire tests of shielded, for radioactive materials, 19: 40814 (SC-RR-65-98, pp 114-18)
of radioactive materials, international conference on, 19: 40808 (SC-RR-65-98)
of radioactive materials for transport, regulatory standards for, 19: 40811 (SC-RR-65-98, pp 45-54)
of radioactive materials, special problems in, 19: 40826 (SC-RR-65-98, pp 625-9)
standards for transport of radioactive materials, development of, 19: 40810 (SC-RR-65-98, pp 32-44)

PAINTS
use of radioactive luminous, in aircraft instruments, 19: 40940 (NP-14924)

PAIR PRODUCTION
cross section for photo-, radiative corrections to, (T), 19: 41500
detection of charged-meson-(π), in meson (ω) decay, (T), 19: 41386
meson (π)-meson (π) interaction effects on electromagnetic, (T), 19: 41505

PALLADIUM
19: 40416
determination by spectrochemical methods, voltage-fluctuation patterns in,

PALLADIUM ALLOYS
Pd–U, phase studies, 19: 40958

PALLADIUM COMPLEXES
with α, β, γ, δ-tetraphenylporphines, retentions in Szilard-Chalmers (n,γ) recoil reactions in, 19: 40612

PALLADIUM ISOTOPES Pd-106
energy levels of, vibration-rotation interactions in, (T), 19: 41818

PALLADIUM ISOTOPES Pd-108
energy levels of, vibration-rotation interactions in, (T), 19: 41818

PANCREAS
radiation effects on function and structure of, in guinea pigs and rats, 19: 40358(T) (FTD-TT-65-48, pp 577–8)

PAPER
cosmic meson (μ) interactions in layers of, gamma photons from, (E), 19: 41295

PARTICLE STATISTICS
many-body problem in, regularized explicit solution for, 19: 41530 (N64-32432)
moment distributions in, uniqueness theorem for, 19: 42204 (LA-DC-6632)

PARTICLE TRACKS
analysis of bubble-chamber, using desk computer, (E), 19: 40915
determination in xenon bubble chamber, spatial picture for, 19: 40871 (JINR-P-2179)
fission-fragment tracks on surfaces of solids, (E/T), 19: 41138
measurement in cloud chambers, semiautomatic device for, 19: 40888

PARTICLE TRAJECTORIES
variations in, induced by electric and magnetic fringing fields, (T), 19: 41139

PARTICLES
concentration in upper atmosphere, 19: 40783 (NP-15327)
dispersion and sedimentation in upper atmosphere, 19: 41112 (SC-DC-65-1312)
formation in nuclear weapon debris, theory, 19: 40782 (NP-15325)
interactions in gases, (T), 19: 41132
interactions of, algebraic structure of n-body problem, (T), 19: 41122 (N64-31207)
interactions of, collision operator for two-body, (T), 19: 41131
orbits in magnetic universe, 19: 41208 (ORNL-3827)
release in sodium fires, 19: 40803 (NAA-SR-Memo-9719)
retention of inhaled radioactive, in man, 19: 40800(R) (AERE-PR/HPM-7)
transitions of relativistic, distributions from, (T), 19: 41390

PEACH BOTTOM POWER REACTOR
experimental facilities for fuel element testing, in-pile, 19: 42089 (GA-5938)

PEBBLE BED REACTORS
development of high temperature, thorium fueled, 19: 42082 (CONF-650633-1)

PENTANES
reactions with recoil carbon-11, 19: 40550 (IS-T-27)

1-PENTENE
reactions with recoil carbon-11, 19: 40550 (IS-T-27)

PEPSIN
radiation effects on plasma pepsinogen, in rats, 19: 40363

PERCHLORIC ACID
separation of scandium from, by solvent extraction using alkyl phosphates, 19: 40689

PERIODATES
separation from iodates and iodides by paper chromatography, tracer studies of, 19: 40430

PEROXIDES
determination in heavy water moderator, automated, 19: 40406 (CONF-650919-2)

PERSONNEL
uranium content in urine of, in CNEN nuclear center, Rome, 19: 40839

PERTURBATION THEORY
method for treating ensemble averages in nonequilibrium statistical mechanics, (T), 19: 41155

spin systems in, modified Wick's theorem for, (T), 19: 41559
PHANTOMS
x-ray wide-beam dosimetry in finite thickness masonite, 19: 40881 (UR-667)
PHASE STUDIES
book: *Energetics in Metallurgical Phenomena.* Vol. I, 19: 41075
1,10-PHENANTHROLINE
3,4,7,8-tetramethyl-, effects on superconductivity enhancement in vanadium, 19: 40543
PHENANTHROLINE COMPLEXES
with rare earth chlorides, preparation and properties, 19: 40514
PHENOL
radiolysis of, ESR of radicals in, 19: 40607
2,2'-methylenebis(4-methyl-6-*t*-butyl), prevention of radioinduced odor in polyethylene using, 19: 40633(P)
PHENOL, AMINO-
radiolysis of, ESR of radicals in, 19: 40607
PHENYL ETHER
2,4-dinitrophenyl-, deuterium isotope effects in reactions with piperidine in benzene, 19: 40544
PHONONS
dispersion in crystals, computer program for analyzing, 19: 41962 (AERE-M-967)
effects on infrared absorption spectrum in neutron-irradiated magnesium oxide, 19: 41108
production in slow-neutron scattering by solid solutions, (T), 19: 41991(T)
PHOSGENE
radioinduced reactions with ethylene, yields in, 19: 40589
PHOSPHATE GLASS
radio-photoluminescence of fluoro-dosimeter, polarization of, 19: 40588
waste fixation in, study of composition range in, 19: 42192 (BNWL-80)
PHOSPHATES
determination in heavy water moderator, automated, 19: 40406 (CONF-650919-2)
determination in multispot chromatograms by neutron activation analysis, 19: 40429
radiation effects on incorporation of phosphorus-32-labeled in diploid yeast, 19: 40367
PHOSPHINE SULFIDE, TRIS(1-AZIRIDINYL)-
preparation of sulfur-35-labeled, by reactions with sulfur-35 recoil atoms, 19: 40619
PHOSPHINES
labeling with phosphorus-32 and preparation by irradiation of potassium chloride–calcium chloride crystals, 19: 40606
PHOSPHONIC ACID, BUTYL, DIBUTYL ESTER
CCl_4–dibutyl butylphosphonate, solvent properties for plutonium and thorium from fuel scrap feed, 19: 40643 (BNWL-57)
dibutyl butylphosphonate–TBP, solvent properties for thorium and uranium, 19: 40643 (BNWL-57)
PHOSPHONIC ACID, *sec*-BUTYL-, DI-2-PENTYL ESTER
effects of short-residence contactors on tributyl phosphate and di-2-amyl 2-butylphosphonate solvent extraction processes for uranium reprocessing, 19: 40645 (CONF-650918-1)
solvent properties for actinides and fission products in short-residence contactors, 19: 40645 (CONF-650918-1)
PHOSPHONIC ACID, DERIVATIVES
sorptive properties of polymers of, for iron chlorides and lanthanum, neodymium, and uranyl nitrates, 19: 40668
PHOSPHORIC ACID
radiation effects on activities of solid, in acid-catalyzed reactions, 19: 41099
PHOSPHORIC ACID, ALKYL ESTERS
solvent properties for scandium, 19: 40689
PHOSPHORIC ACID, BIS(2-ETHYLHEXYL) ESTERS
solvent properties for uranium, effects of TBP on, 19: 40678
PHOSPHORS
luminescence response of Pilot B plastic, to electrons and protons, (E), 19: 40916
properties of α-arylindenes and 2-aryl-3H-benz(e)indenes as liquid scintillation, 19: 40546
radical luminescence of crystalline, electron-hole mechanism for, 19: 40480
radioinduced luminescence of thallium-activated sodium iodide crystals, x, (E), 19: 40908(T)
PHOSPHORUS
determination in copper by activation, 19: 40422
effects of dietary, on strontium-90 metabolism in animals, 19: 40342
PHOSPHORUS COMPOUNDS
solvent properties of organo-, for rare earths, review, 19: 40693
PHOSPHORUS ISOTOPES P-30
production in man during high-energy radiotherapy, 19: 40392 (NYO-3364-6)
PHOSPHORUS ISOTOPES P-31
deuteron reactions (d,d) at 9.3 Mev, differential cross sections for, (E), 19: 41684
PHOSPHORUS ISOTOPES P-32
determination in biological material by scintillation counting of beta decay, 19: 40425
incorporation in phosphines, 19: 40606
metabolism in rats of, 19: 40319
radiation effects from injected, on nervous activity in dogs, 19: 40356(T) (FTD-TT-65-48, pp 469–70)
PHOTOCHEMISTRY
of nucleic acids, 19: 42212 (NYO-3424-1)
PHOTOCONDUCTIVITY
radioinduced in polystyrene, 19: 41091 (SC-R-65-943)
PHOTOGRAPHIC FILM
evaluation of, for radiography of steel welds, 19: 40753(R) (EURAEC-1378)
PHOTOGRAPHIC FILM DETECTORS
calibration for high energy gamma dose measurements, 19: 40909
processing of, automatic, 19: 40800(R) (AERE-PR/HPM-7)
PHOTOGRAPHY
illumination for bubble-chamber, testing Scotchlite reflective material for, (E), 19: 40917
PHOTOMULTIPLIER TUBES
performance as separating element in nanosecond coincidence circuits, 19: 40872 (JINR-P-2203)
resolution of large-area, methods for improving, (E), 19: 40895
PHOTON SHOWERS
analysis of cascade showers by solving inverse problem, (T), 19: 41710
distributions in electron-photon, in condensed media, (T), 19: 41707
distributions in, for primary energies around 1 Tev, (T), 19: 41711
electromagnetic cascade theory, angular distribution functions in, (T), 19: 41359
spectra in extensive air showers from 1000-Tev primaries, 19: 41298
x-ray spectra in, in cosmic showers at high altitudes, (E/T), 19: 41299
PHOTONS
absorption in high-density electron gas, total cross sections for, (T), 19: 41140
distribution in high-energy meson (μ) showers, 19: 41355
emission by plasma atoms, effective probability of, (E), 19: 41891(T)
emission in Cooper-pair tunneling in superconductors, (E), 19: 41631
energy in extensive air showers, (E), 19: 41309
field equations for isospin and, in rigid-sphere model of elementary particles, 19: 41473
interactions of, neutrino theory for, (T), 19: 41387
interactions with protons at .6 to 1.2 Bev, meson(π^+) production in, 19: 41323 (CALT-68-42)
interactions with electrons and mesons (μ) in meson (η) decay, (T), 19: 41457
interactions with protons, meson production amplitudes in $SU(6)_w$, (T), 19: 41462
interactions with protons in second resonance energy region, elastic Compton, (T), 19: 41465
interactions with nucleons, production of mesons (ω) and (ρ) in, 19: 41321 (AECD/TP/4)
interactions with charged particles, kinetic equations for, 19: 41940
multiplication in indium- or thallium-activated potassium and rubidium iodides, mechanism of, 19: 40495(T)
operator for scalar current of, in U-spin subgroup of SU(3) model, 19: 41341
pair production by, radiative corrections to cross section for, (T), 19: 41500
pair production in photon reactions with nuclear Coulomb field, (E/T), 19: 41784
production in electron shielding, computer program for dose rates from, 19: 41954 (NP-15338)
quantum electrodynamics of, infrared effects in, 19: 41545
reactions in condensed matter at high energies, (T), 19: 41707
reactions in nuclei, effect of dynamic correlations on, 19: 41844
reactions with colored alkali halide crystals, mechanisms for electron emission in, 19: 41979
reactions with gases, asymptotic theory for ionization in, 19: 40552 (NP-15287)
reactions with nuclear Coulomb field, photon-pair production in, (E/T), 19: 41784
scattering of intense beams of, Compton, (T), 19: 41425
spin effect with, translational inertial, (T), 19: 41440
tensor field for, from neutrino 1-spinor fields, (T), 19: 41348
transport calculations of, computer program for, 19: 41957 (UCRL-

14165)
wave-particle dualism and interference experiments of, quantum-mechanical, (T), 19: 41535
PHOTOSYNTHESIS
biochemical and physical aspects of, 19: 42212 (NYO-3424-1)
PHTHALIC ACID, DIETHYL ESTER
dielectric polarization in decalin and tetrachloroethylene, temperature dependence, 19: 40468(T) (SC-T-65-721)
PHYSICS
book: *A Collection of Problems on Mathematical Physics*, 19: 41153(T)
book: *Solid State and Low Temperature Physics in the USSR*, 19: 42004
book: *Structure of Matter*, 19: 41829(T)
molecular-beam techniques in, review, 19: 41143
PICOLINES
aniline–picoline, labeled yields in reactions with carbon-14 recoil atoms, 19: 40627
picoline–toluene, labeled yields in reactions with carbon-14 recoil atoms, 19: 40627
PIEZOELECTRIC CRYSTALS
charged-particle interactions with, equations for, 19: 41990(T)
PINCH EFFECT
plasma instabilities in low B theta, pressure dependence of, (E), 19: 41887
PIPERIDINE
reactions with 2,4-dinitrophenyl phenyl ether in benzene, kinetics of deuterium isotope effects in, 19: 40544
PIPES
couplings for respirator, locking quick-disconnects for, 19: 40834(R) (UCRL-14151)
design for transferring liquid-helium, (E), 19: 41626
system of, for liquid nitrogen cold traps in accelerator building, 19: 41165 (LA-DC-7147)
two-phase flow in, equations for, 19: 40737 (NYO-3114-6)
PIQUA POWER REACTOR
operation, June 1965, 19: 42083(R) (COO-652-16)
PLACENTA
strontium-90 transfer by, after chronic ingestion by female dogs, 19: 40327
strontium-90 transfer by, in pregnant cows, 19: 40329
strontium-90 transfer by, in pregnant cows, 19: 40330
strontium-90 transfer by, in pregnant sheep, 19: 40331
PLANARIA
radiation effects on mitosis in, dose effects on regenerating capacity in, 19: 40366
PLANETS
atmosphere structure of, errors in space vehicle acceleration measurements of, (T), 19: 41123 (NASA-TR-R-225)
perihelion precession of mercury, (T), 19: 41204 (JINR-P-2174)
precession in solar gravitational field, (T), 19: 41204 (JINR-P-2174)
spectra of, analysis of optical emission, (E), 19: 41203 (AD-600154)
PLANTS
analysis of kale for traces of gold by neutron activation methods, 19: 40437
cesium-137 content in Arctic, in Alaska, 1962 to 1965, 19: 40780 (BNWL-SA-242)
radiation dosage for lethality in dormant Guar seed, 19: 40376
radiation effects on cyanidine pigment in *Maranta leuconeura* leaves, x, (E), 19: 40362
PLASMA
acceleration in electromagnetic fields, plasmoid structure in, (E), 19: 41908
accelerator for, testing of electron-cyclotron-resonance, 19: 40761 (N64-30604)
antenna impedance in, for radio astronomy measurements, 19: 41212
book: *Ionized Gases*, 19: 41937
boundary layer between magnetic field and rarefied, structure of, (T), 19: 41905
charged-particle interactions with coronal, (T), 19: 41933
collision processes in gaseous, 19: 41850(R) (AD-617386)
conservation equations for dilute, fully ionized, (T), 19: 41889
containment by relativistic electron coils in Astron, 19: 41867 (UCRL-12455-T)
containment device for, with toroidal rotating magnetic field, 19: 41950(P)
current distribution in coaxial-gun, (E), 19: 41859 (NP-15218)
cyclotron instability of magnetized, with anisotropic ion velocity distribution function, (T), 19: 41918
cyclotron wave instabilities in, absolute, (T), 19: 41884
density fluctuations in low-β, drift wave theory for, 19: 41895
density, expansion velocity, and temperature of metallic pulse of, (E), 19: 41878
diagnostics of column of, using electric probes, (E/T), 19: 41868
diagnostics of deuterium, using tritium pulsed atomic beam, (E), 19: 41923
diagnostics of nonuniform, instrumentation design for, 19: 41855 (NP-41855)
diagnostics of rapidly compressed, method for, (E), 19: 41934
diagnostics of, low-frequency impedance characteristics of Langmuir probes for, (E/T), 19: 41949
diagnostics using pulsed relativistic electron beam, (T), 19: 41920
efficiency in microwave frequency amplifier, (E), 19: 40860
electric conductivity in, inner field fluctuation effects on, (T), 19: 41853 (LA-DC-6603)
electric discharges in, detection of centimeter waves in, 19: 41876
electric-charge separation in thermodynamic-equilibrium, in constant gravity field, (T), 19: 41919
electromagnetic properties of nonuniform, in shock tubes, 19: 41855 (NP-15142)
electromagnetic surface wave propagation in nonuniform, resonance effects on, (T), 19: 41916
electromagnetic waves in, effects on stability, (T), 19: 41849 (AD-426079)
electromagnetic-wave propagation through, in circular waveguide, (E), 19: 41903
electromagnetic-wave propagation in bounded, perpendicular to magnetic field, damping in, (T), 19: 41917
electromagnetic-wave interactions with isotropic, harmonic current and wave excitation in, (T), 19: 41927
electron and ion temperatures in helium theta-pinch, in azimuthal magnetic field, (E), 19: 41921
electron and ion temperatures in theta-pinch, in azimuthal magnetic field, (E), 19: 41860 (NP-15220)
electron compression coefficient in collisionless, (E), 19: 41892
electron density in, microwave system for measurement of low, 19: 41854 (MATT-369)
electron density measurement using ruby-laser interferometer method, 19: 41924
electron distribution and temperature in cesium, in low-voltage arc, (E), 19: 41909
electron oscillations in, (E), 19: 41907
electron oscillations in, performance of electron guns in studies of, (E), 19: 41946
electron-velocity distribution function in low-pressure cesium, in oscillation regime, (E), 19: 41877
energy states of high-density gaseous, spatially and temporally resolved, (E), 19: 41934
equations for fully ionized two-particle, methods for treating Boltzmann-Maxwell, (T), 19: 41931
flow around probes in, hypersonic rarefied, (T), 19: 41894
flow in axial magnetic field, (E), 19: 41936
heat transfer in, radiative, 19: 40750
heating of, properties of h-f, 19: 41862 (NP-15256)
hydromagnetic wave damping in magnetized, effect of transport coefficients on, (T), 19: 41869
interactions of counterstreaming, in magnetic fields, (E), 19: 41926
interactions of plasmoids with spatially modulated magnetic fields, (T), 19: 41901
ion density and temperature in strontium, spectroscopic determination of, (E), 19: 41883
ion distributions in, proton-beam techniques for measuring, (E), 19: 41899
ion lifetimes in toroidal octupole fields, (E), 19: 41896
ion oscillations in alkali-metal, in thermal equilibrium, (E), 19: 41890
ion pressure coefficient in MHD flow, (T), 19: 41156
ion-wave propagation in, collisionless, (E), 19: 41892
ionization in gas-particle, (T), 19: 41929
kinetic equations for inhomogeneous, (T), 19: 41870
light absorption coefficient of, measurement of, (E), 19: 41898
light interactions with θ-pinch, Faraday effect in He–Ne laser, 19: 41947
magnetic moment of cluster of, impinging on homogeneous axially symmetric longitudinal magnetic field, (T), 19: 41857 (NP-15206)
motion in Heliotron magnetic fields, (T), 19: 41885
motion in toroidal octupole magnetic field, (E), 19: 41896
motion of bunches of, layer mixing during field-free, (E), 19: 41856 (NP-15205)
Ohm law for partially ionized, 19: 41874
photon emission by atoms in, effective probability of, (E), 19: 41891(T)
photon interactions in, kinetic equations for, 19: 41940
pinch effect in, collision waves from inverse, (E), 19: 41904
polarization in electric fields, (T), 19: 41906
probe response to low-frequency, equations for a-c, 19: 41948

production by laser illumination of tungsten surface, (E), 19: 41943
production of electron, stability analysis of, 19: 41863 (NP-15302)
production of excited state diatomic hydrogen ions for Lorentz dissociation in DCX-1, 19: 41864 (ORNL-P-1244)
production of hot thermonuclear, by particle injection in magnetic traps, 19: 41852 (IAE-676)
properties and uses of, 19: 41900
radiation absorption in stellar, (T), 19: 41211
radiation scattering by non-equilibrium, spectral density in, (T), 19: 41930
relaxations in, formulation from Liouville equation for unified theory of, (T), 19: 41886
research programs on, at Siemens-Schuckertwerke laboratories, Erlangen, Germany, 19: 42228
shock propagation in, heating by, 19: 41861 (NP-15255)
shock propagation in, nonlinear stationary, (T), 19: 41915
shock waves in fully ionized, structure of, (T), 19: 41928
shock-wave excitation in, (E), 19: 41911
shock-wave splitting in, in accelerating tube, (E), 19: 41880
spectral line emission from nitrogen, Stark broadening of, 19: 41941
spectral line intensities in free-burning and tube arcs, (E), 19: 41873
stability in uniform magnetic field, electrostatic, (T), 19: 41897
stability of low B theta pinch, pressure dependence of, (E), 19: 41887
stability of magnetically confined, with anisotropic velocity distribution, 19: 41866 (UCRL-12052)
stability of nonideal, acoustic-wave generation and superheating, (T), 19: 41925
stability of, due to Hall effect, (T), 19: 41893
stability of, finite Larmor radius effects on gravitational, (T), 19: 41879
stability of, nonlinear mode interactions in, 19: 41865 (TID-22050)
statistical mechanics of, with type-dependent intermolecular potentials, (T), 19: 41130
striations in longitudinal magnetic field, moving, (E), 19: 41888
viscosity of partially ionized two-temperature, (T), 19: 41910
wave emission by current in layer of magnetoactive, extraordinary, (T), 19: 41882
wave excitation in confined, by modulated current, (T), 19: 41902
wave propagation along warm columns of, Dattner scattering resonances in, (T), 19: 41939
wave propagation in argon, non-quasistatic surface, (E), 19: 41942
wave resonances in hot nonuniform, spectra of, (E), 19: 41932

PLASMA JETS
design and performance for propulsion, 19: 40762 (N64-31010)
development for space propulsion, 19: 40764 (N65-27691)
development for space propulsion, 19: 40771
performance of repetitively pulsed two-stage, 19: 49763 (N64-31453)
production and properties, (E), 19: 41936
shock-wave splitting in, (E), 19: 41880
spectra from halide reactions in, emission, (E), 19: 41287
testing of continuous microwave magnetic, 19: 40761 (N64-30604)
velocity of, photographic method for measuring, 19: 41912

PLASTICS
luminescence response of Pilot B, to electrons and protons, (E), 19: 40916
temperature effects on RTV-20, 19: 42215 (RFP-625)

PLATINUM
determination by spectrochemical methods, voltage-fluctuation patterns in, 19: 40416
neutron reactions (n,a) with, cross sections for thermal, (E), 19: 41809(T)

PLATINUM COMPLEXES
with α, β, γ, δ-tetraphenylporphines, retentions in Szilard-Chalmers (n,γ) recoil reactions in, 19: 40612

PLATINUM ISOTOPES Pt-194
energy levels of, vibration-rotation interactions in, (T), 19: 41818

PLATINUM ISOTOPES Pt-196
energy levels of, vibration-rotation interactions in, (T), 19: 41818

PLATINUM SYSTEMS
H–Pt–PuO_2, reactions at 1050°C, 19: 40958

PLOWSHARE PROJECT
aggregate manufacture by nuclear explosions, 19: 40709 (PNE-5003)
base surge cloud histories of Pre-Schooner detonations in basalt, 19: 40708 (PNE-503F)
chemical applications of nuclear explosions, research program on, 19: 40706 (ORNL-TM-1191)
crater dimensions, data compilation on, 19: 40711 (SC-RR-65-220)
crater measurements in Pre-Schooner detonations, 19: 40707 (PNE-502F)
ground shock spectra from Gnome event, 19: 40713 (VUF-2401)

PLUTONIUM
criticality studies, 19: 42093 (GEAP-4912)
determination in manganese–plutonium–uranium alloys, x-ray fluorescence spectrometric, 19: 40408 (LA-3333)
diffusion in magnesium, coefficients for, 19: 40961
fracture behavior of alpha-, 19: 40958
phase transformations in, effects of cobalt, iron, or nickel on, 19: 40958
production of single-crystals of alpha-, 19: 40958
properties of recycled, in EBWR, 19: 42078 (ANL-7019)
radioinduced heating in fast reactors, (E), 19: 42114
separation from irradiated fuel elements, 19: 40675
separation from thorium and uranium by solvent extraction in processing of fuel scrap, 19: 40643 (BNWL-57)
solvent extraction by tributyl phosphate and di-2-amyl 2-butylphosphonate in short-residence contactors, 19: 40645 (CONF-650918-1)
solvent properties for tantalum at 750 to 950°C, 19: 40950 (LA-3338)
transformation temperature of, effects of thermal cycling on alpha-beta, 19: 41028 (BNWL-tr-4)
viscosity of liquid, 19: 40958

PLUTONIUM ALLOYS
Al–Pu, criticality studies, 19: 42093 (GEAP-4912)
Cd–Pu, phase studies, 19: 40958
Ce–Cu–Pu, phase studies, 19: 41054
Ce–Pu, viscosity of liquid, 19: 40958
Fe–Pu, eutectic temperature of, effects of nickel on, 19: 40958
Fe–Pu–U, oxidation and ignition behavior of, 19: 40958
fissium–Pu–U, creep at 650, 750, and 850°C, compressive, 19: 40958
fissium–Pu–U, phase transformations in, 19: 40958
fissium–Pu–U, reactions with titanium–vanadium at 600 to 750°C, 19: 40958
Ga–Pu, density of liquid, at 682 to 847°C, 19: 40958
Ga–Pu, phase transformations in delta-stabilized, effects of cobalt or iron on, 19: 40958
Mn–Pu–U, analysis for plutonium, x-ray fluorescence spectrometric, 19: 40408 (LA-3333)
Mo–Pu–U, casting procedures for, 19: 40978 (ANL-6955)
Pu–Th–U, phase studies, 19: 40958

PLUTONIUM CARBIDES
PuC–UC, performance as gas-cooled fast reactor fuel, 19: 42090 (GA-6132)
PuC–UC, radiation effects on hydrolysis of, neutron, 19: 40586

PLUTONIUM ISOTOPES
performance with uranium isotopes as fuels for power breeder reactors, (E), 19: 42081 (CONF-193-11)

PLUTONIUM ISOTOPES Pu-239
alpha decay of, conversion electron spectra from, 19: 41673 (NP-15251)
biological effects of low doses of, in rats, 19: 40338
carcinogenic effects in rats, effects of aseptic inflammation on, 19: 40381
elimination of, effects of various complexing agents in rats, 19: 40345
excretion of, effects of diethylenetriaminepentaacetic acid in rats, 19: 40346
fission fragments of, neutron emission from, (E/T), 19: 41681(T) (ANL-Trans-205)
metabolism in rats of, after repeated intravenous injection of citrate, effects of age, 19: 40326
metabolism in rats, after inhalation of citrate complex of, 19: 40316
metabolism in rats of, after intratracheal administration as acetate or nitrate salt, 19: 40317
neutron fission ratios relative to uranium-235, (E), 19: 42077 (ANL-7014)
neutron reactions (n,a) with, cross sections for thermal, (E), 19: 41809(T)
pathological effects of injected, on hematopoietic system of dogs, 19: 40379
pathological effects of inhaled, in rats, 19: 40380
pathological effects of injected, in dogs, 19: 40382
pulmonary absorption of inhaled, effects on respiration in rats, 19: 40380
reactivity per atom, 19: 42077 (ANL-7014)

PLUTONIUM ISOTOPES Pu-246
gamma spectra of, (E), 19: 41794

PLUTONIUM NITRATES
metabolism in rats, 19: 40317

PLUTONIUM(IV) NITRATES
shipping container design for reduced weight and cost, 19: 40825 (SC-RR-65-98, pp 609-19)
shipping of solutions, container tests for, 19: 40821 (SC-RR-65-98, pp 423-41)

PLUTONIUM NITRIDES
decomposition pressure, 19: 40958

PLUTONIUM OXIDES
deposition on metal substrates, electrolytic, 19: 40989
thermodynamic properties of, effects of temperature and composition on, 19: 40958

PLUTONIUM(IV) OXIDES
morphological characteristics of precipitated powders of, 19: 41024 (NUMEC-2389-5)
shipping container design, construction, and testing, 19: 40825 (SC-RR-65-98, pp 609-19)
sintered density of, effects of nitrate solution precipitating agent on, 19: 40981 (NUMEC-2389-6)
sintered density of, effects of sintering atmosphere composition on, 19: 40981 (NUMEC-2389-6)
sintered density of, effects of strontium and yttrium oxide additions on, 19: 40981 (NUMEC-2389-6)
Al_2O_3–PuO_2, phase studies, 19: 40958
BeO–PuO_2, phase studies, 19: 40958
H–Pt–PuO_2, reactions at 1050°C, 19: 40958
MgO–PuO_2, phase studies, 19: 40958
PuO_2–UO_2, analysis for nitrogen, 19: 40438
PuO_2–UO_2, electrical properties, 19: 40958
PuO_2–UO_2, morphological characteristics of coprecipitated powders of, electron microscopic study, 19: 41024 (NUMEC-2389-5)
PuO_2–UO_2, performance as gas-cooled fast reactor fuel, 19: 42090 (GA-6132)
PuO_2–UO_2, radiation effects on, 19: 41094(T) (NP-tr-1235)
PLUTONIUM POISONING
pathology of, in dogs, 19: 40379
therapeutic effects of complexing agents on, in rats, 19: 40345
PLUTONIUM RECYCLE CRITICAL FACILITY
fuel testing for EBWR experiment, 19: 42078 (ANL-7019)
PLUTONIUM RECYCLE TEST REACTOR
fuel element corrosion in crevices, simulation study, 19: 40965 (BNWL-83)
moderator analysis for boric acid, 19: 40404 (BNWL-SA-167)
PLUTONIUM SYSTEMS
BeO–Pu, neutron cross sections for dispersions of, effects of grain structure on, (T), 19: 42041 (GA-6286)
H–Pu, neutron spectra in, thermal, 19: 42037 (BNWL-95, pp 4-17)
PuO_2–polystyrene, criticality experiments on, 19: 42038(R) (BNWL-95, pp 27-35)
POISONING
by radioactive metals, drug evaluation for emergency treatment, 19: 40339
POLARISCOPES
performance and properties of proton polarimeter, (E), 19: 40905
POLISHING
sample carrying device for, 19: 40964(P)
POLONIUM
poisoning by, drug evaluation for emergency treatment, 19: 40339
POLONIUM ISOTOPES Po-210
determination in tobacco smoke, 19: 40805 (NRS-30)
neutron reactions (n,α) with, cross sections for thermal, (E), 19: 41809(T)
POLONIUM ISOTOPES Po-212
energy levels of, shell model calculation of isomeric and low-excited, 19: 41735
POLYCRYSTALS
sputtering by ions, energy dependence of, (T), 19: 41271(T)
POLYMERS
radiation chemistry of, research on, 19: 40554(T,R) (AEC-tr-6565)
radiation effects on solid-state, sensitivity thresholds for, (E), 19: 40564
radioinduced production of graft, pilot plant for, 19: 40596
POPULATIONS
biological effects of thermonuclear explosions on, of cities, 19: 40361(T) (ORNL-tr-437)
PORCELAIN ENAMELS
preparation of beta-radioactive, for fabrication into planar beta sources, 19: 40560
POROUS MATERIALS
physical properties of polystyrene foam, 19: 41000 (ACF-10)
PORPHINE
with α, β, γ, δ-tetraphenyl-, retentions in Szilard-Chalmers reactions on metal complexes of, 19: 40612
POSITRONIUM
binding energy of, nonrelativistic and relativistic theories for, 19: 41474
hyperfine splitting of, four-fermion V-A weak interactions in, (T), 19: 41410
POSITRONS
annihilation in liquid and solid metals and semiconductors, angular correlations from, (E), 19: 41285
annihilation in lithium, orthogonal plane waves in, (T), 19: 41945
annihilation in metals, many-body theory of, 19: 41159
annihilation in sodium tungsten bronze, (E/T), 19: 41158
annihilation in sodium tungsten bronze, (E/T), 19: 41158
annihilation rate in electron gas, (T), 19: 41160
emission by neutron-deficient radionuclides, use in clinical diagnosis of brain tumors, 19: 40390 (BNL-9384)
interactions with electrons in crossed beams at 1 to 250 Bev, cross sections for, (T), 19: 41493(T)
interactions with electrons, meson (π) resonance effects in, (T), 19: 41386
scattering by hydrogen at low energies, phase shifts for, (T), 19: 41267
scattering by nuclei, cross sections for, (T), 19: 41510
POTASSIUM
boiling heat transfer of, forced-flow, 19: 40741(R) (SAN-409-23)
content in man, blood analysis method for determining, 19: 40309(R) (NP-15180)
content in rocks from Indian Ocean islands, 19: 40791
corrosive effects on D-43 niobium alloy and stainless steel/niobium–zirconium alloy, research program on, 19: 40970(R) (NASA-CR-54390)
determination by spectrochemical methods, voltage-fluctuation patterns in, 19: 41416
determination in copper by activation, 19: 40422
effects of sorbed, on germanium work function, 19: 41124(R) (NP-15108)
positron annihilation in, angular correlations from, (E), 19: 41285
properties of, in plasma in thermal equilibrium, (E), 19: 41890
solvent properties for pure iron, molybdenum, and niobium at 1000°C, 19: 40946(R) (AI-65-93)
surface tension of oxygen-contaminated, 19: 40409(R) (MSAR-65-95)
POTASSIUM ALLOYS
K–Na, purification by solvent extraction using naphthalene–tetrahydrofuran, 19: 40409(R) (MSAR-65-95)
POTASSIUM BROMIDES
radiation effects on luminescence centers in silver-activated, x, 19: 41977
radiation effects on electroluminescence of activated, uv and x, 19: 41981
radiation effects on phosphorescence of, influence of F-band illumination on x, 19: 40570
radiation effects on luminescence of indium-activated, electric-field pre-exposure in x, 19: 40571
radiation effects on electroluminescence of, x, 19: 40572
reactions with praseodymium bromide, 19: 40469
POTASSIUM CHLORIDES
complexes with praseodymium, properties of, 19: 40469
lattice defects in, electron-nuclear double resonance spectra of F-center, (E), 19: 41992(T)
radiation effects on thermal de-excitation processes in thallium-activated, 19: 41101(T)
radiation effects on luminescence of europium-activated, visible and x, 19: 40567
radiation effects on phosphorescence of, influence of F-band illumination on x, 19: 40570
radiation effects on electroluminescence of, x, 19: 40572
radioinduced color centers and dislocations in, thermal-neutron, (E), 19: 41976
$CaCl_2$–KCl, radioinduced formation of phosphorus-32-labeled phosphine in, 19: 40606
KCl–rare earth chlorides, stability and volatilization, 19: 40516
KCl–SmCl–NaCl, phase studies, 19: 40517
LiCl–KCl, equilibrium between cerium and its ions in molten eutectic, 19: 40467(T) (ORNL-tr-578)
POTASSIUM CHROMATES
HNO_3–$K_2Cr_2O_7$, corrosive effects on stainless steel, effects of silicon on, 19: 40947(R) (EURAEC-1403)
POTASSIUM ERBIUM CHLORIDES
volatilization and vapor stability at 800 to 1200°C, 19: 40516
POTASSIUM FLUORIDES
KF–NaF–ScF_2, phase studies, 19: 40512
KF–ScF_3, preparation and properties of K_3ScF_6, 19: 40512
POTASSIUM FLUOTECHNETATES
preparation and properties of K_2TcF_6, 19: 40461 (ORNL-P-491)
POTASSIUM HYDROXIDES
reactions with vapor, kinetics, 19: 40462 (SC-TM-65-183)
solvent properties for aluminum casing on uranium spent fuel element, 19: 41086(P)
POTASSIUM IODIDES
iodine-127 nuclear spin echoes in, r-f excitation of, (E/T), 19: 41988
luminescence yields of, absolute gamma, 19: 40593(T)
photon multiplication in indium- or thallium-activated, mechanism of, 19: 40495(T)
radiation effects on electroluminescence of, x, 19: 40572
radiation effects on luminescence of thallium-activated, in electric field,

x, 19: 40573
POTASSIUM IONS
spectral lines in solar chromosphere, (T), 19: 41220
POTASSIUM ISOTOPES K-38
production in man during high-energy radiotherapy, 19: 40392 (NYO-3364-6)
POTASSIUM ISOTOPES K-39
neutron scattering at 1.49 to 3 Mev, cross sections for, (E), 19: 41737
POTASSIUM ISOTOPES K-40
radiation hazards of inhalation and ingestion by man of, 19: 40805 (NRS-30)
POTASSIUM ISOTOPES K-41
alpha reactions (α,n) to 42 Mev, isomeric ratios from, (E), 19: 41695
alpha reactions (α,n), statistical model for isomeric ratios in, 19: 41696
alpha reactions (α,n) with, isomeric cross section ratios for, (E), 19: 41820
POTASSIUM NITRATES
radiolysis of, electron trapping in, 19: 40609
POTASSIUM OXIDES
content in McKelveyite uranium mineral, 19: 40799
reactions of super-, with water vapor and carbon dioxide, kinetics, 19: 40462 (SC-TM-65-183)
POTASSIUM RHENIUM FLUORIDES
preparation and properties of K_2ReF_6, 19: 40461 (ORNL-P-491)
POTASSIUM SYSTEMS
O–K–Sn, phase studies, 19: 41031
O–K–Zr, phase studies, 19: 41031
POTASSIUM TARTRATES
radiation effects on single crystals of, ESR spectra of, 19: 40613
POWDERS
neutron diffractometry of, collimator design for, (E), 19: 40492
preparation of ultra-fine, by freeze-drying method, 19: 40987
POWER BREEDER REACTORS
economics of spectral-shift pressurized-water, (E), 19: 42109
reactivity and safety of sodium-cooled fast, (E), 19: 42081 (CONF-193-11)
POWER PLANTS
development of closed-cycle gas, 19: 42127(R) (TID-22009)
POWER REACTORS
design of gas-cooled heavy-water-moderated pressure-tube, 19: 42112
design of multipurpose portable, 19: 42115
design using direct coolant re-pressurizing, 19: 42125(P)
development of Dodewaard 50 Mw(e), 19: 42088(R) (EUR-2430.n)
development of heavy water, 19: 42108
energy conversion in, review, 19: 41319
fuel concepts and strategy for, in Italy, 19: 42111
heat transfer in organic-cooled and -moderated, (E), 19: 42110
heat transfer in pressurized-water, engineering data on, (T), 19: 42118
pressure vessels for, development of, 19: 42122
reactivity transients from moderator temperature variations, (T), 19: 42059
status of Spanish organic-cooled heavy-water-moderated, 19: 42113
steam cycles for, development of supercritical, 19: 42121
steam generator development for, 19: 42123
POWER SUPPLIES
design for isochronous cyclotron, 19: 41172
PRASEODYMIUM
determination by spectrochemical methods, voltage-fluctuation patterns in, 19: 40416
heat of solution in liquid tin, 19: 41044
physical and thermodynamic properties, 19: 40948 (IS-1195)
polarographic behavior in dimethylformamide and dimethylsulfoxide, 19: 40681
preparation and purification, 19: 40948 (IS-1195)
PRASEODYMIUM ALLOYS
Mg–Pr, phase studies, 19: 41011 (IS-T-15)
Nd–Pr, heat of solution in liquid tin, 19: 41044
Pr–Ru, process for improving workability of, 19: 40999(P)
PRASEODYMIUM BROMIDES
reactions with potassium and sodium bromides, 19: 40469
PRASEODYMIUM CARBIDES
eutectic temperature between carbon and dicarbide, 19: 41014 (LA-DC-6819)
lattice parameters and phase transformation temperatures in, 19: 41014 (LA-DC-6819)
microhardness, 19: 41014 (LA-DC-6819)
PRASEODYMIUM CHLORIDES
complexes with cesium, potassium, and sodium, properties of, 19: 40469
complexes with phenanthroline, preparation and properties, 19: 40514
PRASEODYMIUM COMPLEXES
with gluconic acids, stability constants, 19: 40508
PRASEODYMIUM OXIDES
content in McKelveyite uranium mineral, 19: 40799
PRASEODYMIUM PERCHLORATES
stability constants of, thermal, 19: 40509
PRASEODYMIUM SILICIDES
crystal structure, 19: 40477
crystal structure, 19: 40478
PRASEODYMIUM SULFATES
$Pr_2(SO_4)_3$–Na_2SO_4, thermal stability, 19: 40511
PRECIPITATION, ATMOSPHERIC
cesium-137 content of, in Australia and England, 1963, 19: 40805 (NRS-30)
charts of European, 1921 to 1950, 19: 41111 (EUR-2296.e)
strontium-90 content of, in Australia and England, 1963, 19: 40805 (NRS-30)
PRECIPITATION, CHEMICAL
uses for separating long- and short-lived radioisotopes in wastes, (E), 19: 42197
PRESSURE GAGES
design for measuring energy liberation in explosions, 19: 40850(T) (ORNL-tr-588)
use of differential, in system for measuring depths of cryogenic liquids, 19: 40878 (UCRL-9672(Rev.))
PRESSURE VESSELS
analysis of filament-wound sphere with polar opening, 19: 40698 (ACF-9)
design of prestressed concrete cylindrical, with detachable end cap, 19: 40728(P)
design, construction, and installation of MZFR, 19: 42163
development for power reactors, 19: 42122
fabrication for MZFR, 19: 42172
testing of, radiographic and ultrasonic methods of, 19: 42024
welds in steel, methods for automatic ultrasonic inspection of, 19: 42025
PRESSURIZED WATER REACTORS
control using boron chemical shim, 19: 42023
coolant loss-of-flow in, analysis of, 19: 42118
development of Loss of Fluid Test Reactor, (E), 19: 42134(R) (IDO-17070)
economics of spectral-shift thorium breeders power, (E), 19: 42109
feasibility of 1000 Mw(e) plant, 19: 42102 (WCAP-2385(Vol.I))
feasibility of 1000 Mw(e) plant, 19: 42103 (WCAP-2385(Vol.II))
heat transfer in, engineering data on, (T), 19: 42118
PROMETHIUM
separation from aqueous solutions of organic acids by solvent extraction using high-molecular-weight amines, 19: 40657
separation from europium and yttrium by ion exchange, effects of aqueous organic media on, 19: 40663
PROMETHIUM ISOTOPES Pm-143
energy levels from gamma-gamma correlations in decay of cerium-143, (E), 19: 41776
PROMETHIUM ISOTOPES Pm-147
biological effects in rats, after chronic low-dose oral administration, 19: 40335
pathological effects of injected, in rats, 19: 40383
processing into planar beta sources, (E), 19: 40560
PROMETHIUM ISOTOPES Pm-149
gamma transitions in, lifetime and intensities of l-forbidden M1, (E), 19: 41836
PROMETHIUM ISOTOPES Pm-151
gamma transitions in, lifetime and intensities of l-forbidden M1, (E), 19: 41836
PROPANE
O-propane, oxidation induced by fission fragments in, 19: 40611
reactions with recoil tritium, kinetic isotope effects in, 19: 40615
PROPANE, BROMO-
radiation effects on, thermal annealing of neutron, 19: 40576
PROPANE, 2,2-DIMETHYL-
reactions with recoil tritium, kinetic isotope effects in, 19: 40615
reactions with recoil tritium in presence of helium, energy loss and reactivity values of, 19: 40616
2,2-dimethylpentane–ethane, energy loss and reactivity in reactions with recoil tritium in presence of helium, 19: 40616
PROPANE, 2-METHYL-
reactions with recoil tritium, kinetic isotope effects in, 19: 40615
1,2-PROPANEDIOL, 3-(OCTADECYLOXY)-
therapeutic effects for radiation sickness in dogs, synergistic effects of blood plasma substitute, vitamin B_{12}, and antibiotic therapy, 19: 40387
1-PROPANESULFONIC ACID, 2,3-DIMERCAPTO-
effects on lipid metabolism in irradiated rats, 19: 40386(T) (FTD-TT-65-48, pp 661–2)

1-PROPANOL
effects of aqueous solutions of, on sorption of europium and yttrium by cation exchanger, 19: 40664
effects on ion exchange separation of rare earths using α-hydroxyisobutyric acid, 19: 40663
effects on ion exchange separation of europium and yttrium, 19: 40666
effects on sorption of europium and yttrium on ion exchangers, tracer studies of, 19: 40665
reactions with tritium recoil atoms, with and without benzene and cyclohexane, energy transfer in, 19: 40622
CCl_4–1–propanol, mechanism of chemical processes in reactions with chlorine-38 recoil atoms, 19: 40623

2-PROPANOL
effects of aqueous solutions of, on sorption of europium and yttrium by cation exchanger, 19: 40664
effects on ion exchange separation of rare earths using α-hydroxyisobutyric acid, 19: 40663
effects on ion exchange separation of europium and yttrium, 19: 40666
effects on sorption of europium and yttrium on ion exchangers, tracer studies of, 19: 40665
reactions with tritium recoil atoms, with and without benzene and cyclohexane, energy transfer in, 19: 40622
CCl_4–2–propanol, mechanism of chemical processes in reactions with chlorine-38 recoil atoms, 19: 40623

1-PROPANOL, 2-METHYL-
reactions with tritium recoil atoms, with and without benzene and cyclohexane, energy transfer in, 19: 40622

2-PROPANOL, 2-METHYL-
effects of aqueous solutions of, on sorption of europium and yttrium by cation exchanger, 19: 40664
effects on ion exchange separation of europium and yttrium, 19: 40666
effects on ion exchange separation of rare earths using α-hydroxyisobutyric acid, 19: 40663
effects on sorption of europium and yttrium on ion exchangers, tracer studies of, 19: 40665

PROPELLANTS
radiation effects on thermal decomposition of, gamma, 19: 40562

PROPENE
reactions with recoil tritium, kinetic isotope effects in, 19: 40615

PROPENE, 2-METHYL- POLYMERS
radiolysis of, ESR of free radicals from, 19: 40608

PROPORTIONAL DETECTORS
design for radioisotope identification, 19: 40929(P)
design of large-area gas-flow, for alpha and beta particles, 19: 40834(R) (UCRL-14151)
neutron energy response of boron trifluoride counters using paraffin moderator, (E), 19: 40890
properties of carbon dioxide-filled, for radiocarbon dating, 19: 40920

PROPULSION
book: *Fundamentals of Nuclear Flight*, 19: 42147
electric systems for space, development of, 19: 40768
ion, cesium sources for, 19: 40770
ion, development and properties of, 19: 40766
plasma accelerators for, development of cyclotron-resonance, 19: 40764 (N65-27691)
plasma, performance of two-stage, repetitively pulsed engine for, 19: 40763 (N64-31453)

PROPYLAMINE
ion, surface ionization engine for, 19: 40769

PROTACTINIUM
reactions with bromine on hafnium oxide and tantalum oxide carriers, 19: 40501
separation from thorium by ion exchange, 19: 40673

PROTACTINIUM BROMIDES
preparation, 19: 40501

PROTACTINIUM ISOTOPES Pa-233
separation from irradiated thoria by coprecipitation with manganese dioxide, 19: 40644 (BNWL-78)
separation from thorium and uranium-233 by manganese dioxide head-end step in Thorex Process, 19: 40649 (DP-982)

PROTEINS
effects of dietary, on strontium-90 metabolism in animals, 19: 40342
interactions with mesons (π^-) at 2.0 Bev/c, (E), 19: 41502
synthesis of genetic control, 19: 42212 (NYO-3424-1)

PROTON BEAMS
polarization measurements on, properties of polarimeter for, (E), 19: 40905
radiation hazards of synchrocyclotron, 19: 41171(T) (N64-33402)
uses for measuring ion density distributions in plasma, (E), 19: 41899

PROTON SHIELDING
energy deposition in, near surfaces, (T), 19: 41951 (N64-30510)
gamma ray production in, computer calculations, 19: 41954 (NP-15338)

PROTONS
acceleration and precipitation of solar wind, in magnetosphere, (T), 19: 41583
acceleration of solar, hydromagnetic-shock, (T), 19: 41230
angular correlations from lithium-6 (p,2p) reactions, cluster model wavefunctions for, (T), 19: 41842
angular distribution from d-d reactions at 20 to 300 kev, 19: 41832
attenuation in shielding, near surfaces, (T), 19: 41951 (N64-30510)
binding energy in aluminum-27, carbon-12, and sulfur-32, measurement of, 19: 41660 (ISS-65/3)
collisions with argon atoms, inelastic energy loss in, (E), 19: 41277
detection and measurement using Pilot B plastic scintillation counters, (E), 19: 40916
distributions in outer radiation belts, effect of solar flare on, (E), 19: 41312
dosimetry in tissues of 60- to 400-Mev, 19: 40372
effects on phosphorus-32-labeled phosphine formation in crystals of potassium chloride-calcium chloride, 19: 40606
electromagnetic form factors of, analytic continuation of, (T), 19: 41388
emission in deuteron stripping reactions, computer program for cross section calculations for, 19: 41677 (ORNL-TM-1151)
energy spectra variations in outer radiation belt, model for, 19: 41577
flux and rigidity spectra of solar, (T), 19: 41232
flux densities in Van Allen region, computer program for mapping, 19: 41954 (NP-15338)
form factors of, relativistic symmetry with isospin and spin for, 19: 41398
interactions of, models for angular distributions from, (T), 19: 41383
interactions of, models for angular distribution from, (T), 19: 41385
interactions with protons, data analysis system for inelastic, 19: 41322 (BNL-9231)
interactions with photons at .6 to 1.2 Bev, meson(π^+) production in, 19: 41323 (CALT-68-42)
interactions with antiprotons, annihilation at rest, (E), 19: 41325 (CU-1932-245)
interactions with mesons (π^+) at 2.35 to 2.90 Bev/c, resonance production in, (E), 19: 41418
interactions with mesons (π^+), poles and resonances in, (T), 19: 41427
interactions with mesons (K^+) at 2 Bev/c, (E), 19: 41436
interactions with mesons (π^-) at 1.5 Bev/c, dipion production in, (E), 19: 41441
interactions with meson (π) at 8 and 12 Bev/c, differential cross section for elastic, (E), 19: 41455
interactions with mesons (π) at 4 and 8 Bev/c, backward elastic, (E), 19: 41456
interactions with mesons (K^-) at 4.6 and 5.0 Bev/c, f^* (1500) production in, (E), 19: 41459
interactions with photons, $SU(6)_w$ for meson production amplitudes in, (T), 19: 41462
interactions with photons in second resonance energy region, elastic Compton, (T), 19: 41465
interactions with tritons at 1 to 3 Mev, phase-shift analysis of elastic, (T), 19: 41479(T)
interactions with protons at 1.45 Bev, differential cross section for, (E), 19: 41487(T)
interactions with mesons (π^-) at 7.5 Bev, baryon resonances and strange particle production in, (T), 19: 41488(T)
interactions with mesons (π^-) at 7.5 Bev/c, meson resonances and strange particle production in, (E), 19: 41489(T)
interactions with mesons (K^-) at rest, hyperon (Σ^-) production in, (E), 19: 41494
interactions with protons at 2.0 Bev, (E/T), 19: 41503
interactions with mesons (π^-) at 1275 Mev/c, charge exchange in, (E), 19: 41507
interactions with protons at 20 Bev, production of antiprotons, mesons and protons in, 19: 41324 (CERN-65-14)
interactions with nucleons, polarization tensor for double, (T), 19: 41333 (JINR-P-2227)
interactions with neutrons at 3 to 10 Bev, cross sections for elastic, (E), 19: 41347
interactions with emulsion nuclei at 9 Mev, hyperon ($\Sigma^\pm$) production and decay in, (E), 19: 41350
interactions with mesons (K-), range-energy relations for hyperons (Σ^-) and (Σ^+) from, (E), 19: 41369
interactions with particles at high energies, forward amplitudes for, (T), 19: 41376
interactions with mesons (K-), baryon resonances from, (T), 19: 41384
interactions with photons at 950 to 1050 Mev, hyperon (Λ^0) polarization from, (E), 19: 41367
interactions with protons at 667 Mev, double, (E), 19: 41666 (JINR-P-2233)

interactions with neutrons in nuclei, R(5) and R(8) groups in quasi-spin formalism for pairing, 19: 41839
interactions with mesons (K+), mass-spectrum κ singularity in (Kππp), (T), 19: 41417
interactions with mesons (K−) and mesons (π−), meson (η^0) production in, (T), 19: 41433
interactions with mesons (π−) at 1275 Mev/c, meson (η^0) and meson (π^0) production in, (E), 19: 41507
interactions with protons at 1.55, 2.5, and 2.9 Bev, deuteron production cross sections from, (E), 19: 41523
interactions with mesons (π−) at 905 Mev, mesons (π−) and (π^0) production in, (E), 19: 41508
mass difference with neutrons, (T), 19: 41511
meson (μ^-) capture by pairs of, in nuclei, (E/T), 19: 41753
nuclear magnetic relaxation in liquids, (T), 19: 40499
photoproduction on oxygen-16 at 22 to 40 Mev, branching ratios and cross sections for, (E), 19: 41790
polarization in compounds, pulse method for determining, 19: 40473
production in deuteron–meson (π+) interactions, partial wave dispersion relations for, 19: 41336 (NP-15335)
propagation of solar, interplanetary magnetic field effects on, (T), 19: 41228
reactions (p,α) with boron-11 at 150 and 163 kev, coincidence measurements for, (E), 19: 41699
reactions (p,αγ) with fluorine-19 at 1.4 Mev, gamma spectra from, (E), 19: 40896
reactions (p,γ) and (p,p) with boron-11 at 0.5 to 4.0 Mev, carbon-12 energy levels from, (E), 19: 41688
reactions (p,γ) with calcium-42, scandium-43 energy levels from, (E), 19: 41738
reactions (p,γ) with carbon-13 at 0.60 to 1.8 Mev, nitrogen-14 energy levels from, (E), 19: 41740
reactions (p,γ) with neon-22 at 1.278 Mev, sodium-23 gamma decay modes from, (E), 19: 41837
reactions (p,γ) with neon-20 to 1.28 to 1.86 Mev, gamma energies and yield from, (E), 19: 41838
reactions (p,γ) with neon-22 at 1.28 to 1.86 Mev, sodium-23 energy levels from, (E), 19: 41838
reactions (p,γ) with neon-21 at 1.28 to 1.86 Mev, neon-21 energy levels from, (E), 19: 41838
reactions (p,γ) with neon-20 at 1.17 Mev, sodium-21 energy levels from, (E), 19: 41838
reactions (p,He-3) with lithium-6 at 43.7 Mev, angular distributions from, (E), 19: 41786
reactions (p,n) with vanadium-51 at 1.5 to 2.3 Mev, total cross section for, (E), 19: 41676 (ORNL-P-1468)
reactions (p,p′) with samarium-147 at 4 Mev, energy levels from, (E), 19: 41778
reactions (p,pd) with carbon-12 at 155 Mev, angular correlations in, (E), 19: 41703
reactions (p′,p′γ) with cerium-140, neodymium-142, and samarium-144, 0+ states from, (E), 19: 41747
reactions (p,pn) with tellurium-128 and -130 at 40 to 150 Mev, isomeric pair production ratios in, 19: 41674 (NYO-1930-44)
reactions (p,pn) with iodine-127, search for 2.6-hr iodine-126m in, 19: 41716
reactions (p,t) with cadmium and tin even isotopes at 40 Mev, ground-state L = 0 transitions in, (E), 19: 41689
reactions (p,t) with lithium-6 at 43.7 Mev, angular distributions from, (E), 19: 41786
reactions (p,2p) with lithium-6, angular correlations from, (T), 19: 48142
reactions (p,3n) with lanthanum-139, angular momentum effects on isomeric cross section ratios in, (E), 19: 41821
reactions with beryllium and lead at 20 Bev, production of antiprotons, mesons, and protons in, 19: 41324 (CERN-65-14)
reactions with bismuth, gold, silver and thorium at 157 Mev, nucleon clustering from, (E), 19: 41831
reactions with iron at 200 Bev, nucleon–meson cascade production in, (T), 19: 41955 (ORNL-TM-1121)
reactions with mercury atoms, hydrogen and mercury spectral line excitation in, (E), 19: 41260
reactions with nuclei at 1.0 and 2.8 Bev, cross sections for lithium-9, carbon-16, and nitrogen-17 production in, (E), 19: 41780
reactions with silicon-28, silver bromide, and gold-197 at 150, 340, and 660 Mev, cascade theory for, (T), 19: 41811(T)
scattering by aluminum, copper, and polystyrene at 75 to 200 kev, multiple, (E/T), 19: 41273
scattering by aluminum-27 at 6.15 to 6.7 Mev, excitation functions for inelastic, (E), 19: 41813
scattering by carbon-12 at 156 Mev, 4.43-Mev level excitation in, (T), 19: 41675 (ORNL-P-330)
scattering by carbon-12 at 4.7 to 11.3 Mev, angular distributions and polarization in elastic, (E), 19: 41731
scattering by chromium-53 at 11 Mev, cross sections from inelastic, (E), 19: 41726
scattering by deuterium and helium-4, (T), 19: 41763
scattering by helium-4 and oxygen-16, polarization from elastic, (E), 19: 40905
scattering by magnesium-26 at 5.67 to 6.46 Mev, angular correlations and distribution in inelastic, (E/T), 19: 41693
scattering by nuclei at 10.5 and 14.5 Mev, optical model potential for elastic, (E/T), 19: 41682
scattering by nuclei at 667 Mev, double, (E), 19: 41666 (JINR-P-2233)
scattering by titanium-48 0.99-Mev state at 4.63 and 5.25 Mev, angular correlations in inelastic, (E), 19: 41690
scattering on metal surfaces, detection of deposited films by, (E), 19: 40962
stopping in matter, computer program for calculation of, 19: 41954
transmission in aluminum- and silver foils at low energies, (E), 19: 41969 (ORNL-TM-1153)
transmission through silicon single crystals at 5 Mev, direction and energy distributions from, (E), 19: 41788

PULMONARY ABSORPTION
of cerium-144, after intratracheal administration in rats, 19: 40313
of inhaled radioactive particles, 19: 40800(R) (AERE-PR/HPM-7)
of niobium-95, after inhalation by rats, 19: 40314
of plutonium-239 after inhalation, effects on respiration in rats, 19: 40380
of plutonium-239, after inhalation of citrate complex by rats, 19: 40316
of strontium-90, after intratracheal administration in rats, 19: 40312
of yttrium-91, after inhalation by rats, 19: 40314
of zirconium-95, after inhalation by rats, 19: 40314

PULSE ANALYZERS
design of multichannel, for ionization calorimeter at capacity memory cells, 19: 40853
design of multichannel, for ionization calorimeter, 19: 40854
design of stable linear pulse-adding circuits, (E), 19: 40726
distortion in, calculations of effects of pile-up on, (T), 19: 40914

PULSE GENERATORS (ELECTRONICS)
capacitors for 6-Mw 25-Mc, design of, (E), 19: 40844 (MATT-341)

PULSE MODIFIERS
design of stable linear pulse-adding circuits, (E), 19: 40726

PUMPS
design and performance for nuclear reactors, 19: 42026
fabrication of coolant, for MZFR, 19: 42174
failure of reactor coolant, consequences of, 19: 42118

PUMPS (LIQUID METAL)
bearing tests for SNAP-50/SPUR, 19: 40703 (TIM-916)
design and performance of sodium, 19: 42026
sealing system development for, 19: 40718 (TIM-909)
shaft seal tests for, dynamic, 19: 40702 (TIM-914)
testing of, gallium loop for, 19: 40727

PUREX PROCESS
diluents in, performance of normal paraffins as, 19: 40646 (CONF-650918-2)
waste fixation in phosphate glass, study of composition range in, 19: 42192 (BNWL-80)

PURINES
radiation effects on, thermal-neutron, 19: 40557

PYRIDINE
indole–pyridine, labeled yields in reactions with carbon-14 recoil atoms, 19: 40627

2,6-PYRIDINEDICARBOXLYIC ACID
use in preparation of chromatographic resins, 19: 40674

PYRIMIDINES
radiation effects on, thermal-neutron, 19: 40557

PYROCATECHOL
effects on use of chromogenic polymer for gamma dosimetry, 19: 40599

Q

QUANTUM ELECTRODYNAMICS
Feynman integrals and Feynman rules for high-spin fields, 19: 41548
gauge invariance in, 19: 41556

QUANTUM MECHANICS
book: *Lectures on Quantum Mechanics*, 19: 41567
book: *Matrix Mechanics*, 19: 41568
chemical potential calculations by summation of Fermi-Dirac functions, (T), 19: 40493
Clebsch-Gordan coefficients, methods for calculating, (T), 19: 41551
coupling constant relations in S-matrix theory, 19: 41382
decay of systems in, energy spectra from time behavior of, (T), 19: 41532

elementary particle interactions in, neutrino theory for electromagnetic and weak, (T), 19: 41387
energy levels of molecular helium hydride ion, (T), 19: 41240
energy levels of oscillator in unitary symmetry, (T), 19: 41554
fluctuations of system of anharmonic charged oscillators at negative temperature, Nyquist theorem for, 19: 41537
hypervirial theorems and sum rules derivation by differentiation, (T), 19: 41557
infrared behavior of wave function renormalization constant in, 19: 41545
many-body problem in, regularized explicit solution for, 19: 41530 (N64-32432)
momentum measurements considering effects of, accuracy of, 19: 41553
operator solutions of field-theory, N-quantum approximation for, 19: 41552
particle interactions in, three-body, 19: 41529 (N64-31206)
particle penetration of potential barriers, (T), 19: 41533
radiation beam absorption and scattering by atoms in, coherent, (T), 19: 41247
scattering of intense photon beams, Compton, (T), 19: 41425
Schroedinger equation for three-body problem, asymptotic solution of, (T), 19: 41565
transformation of classical functions to quantum-mechanical operator functions, (T), 19: 41555
transitions of relativistic particles, distributions from, (T), 19: 41390
Von Neumann's hidden variable interpretation in, 19: 41531 (SLAC-PUB-44)
wave propagation in one-dimensional random medium, stochastic equation for, 19: 41536
wave-particle dualism in, photon interference experiments and, 19: 41535

QUARTZ
shielding properties in solar cells, 19: 40931 (AD-609424)
sputtering in argon discharge, silicon oxide yields from, (E), 19: 41257

QUINALDIC ACID
polarography and reactions of 8-substituted, 19: 40545

QUINALDINE
polarography and reactions of 8-substituted, 19: 40545

R

RABBITS
lead-212 metabolism in, after intra-arterial, intravenous, or subcutaneous injection, 19: 40333
radiation effects on gonads and liver, biochemical, 19: 40375
radiation effects on mammary gland activity in, 19: 40353(T) (FTD-TT-65-48, pp 16–17)
radiation effects on nervous responses in, 19: 40355(T) (FTD-TT-65-48, pp 111–12)
radiation effects on electrical reactions of retina, 19: 40359(T) (FTD-TT-65-48, pp 590–1)
radiosensitivity of skin of, effects of 5-fluorouracil on, 19: 40394
strontium-90 metabolism in, effects of dietary constituents on, 19: 40342
strontium-90 metabolism in skeleton of, effects of dietary calcium and inflammation on, 19: 40343
toxic effects of tritium in, pathology and treatment of, 19: 40340
tritium toxicity in, 19: 40337

RADIATION
absorption and scattering by atoms, coherent, (T), 19: 41247
absorption in stellar plasma, (T), 19: 41211
biological effects, delayed, 19: 40352 (WASH-1059)
book: *Experimental Reactor Analysis and Radiation Measurements*, 19: 42014
book: *Irradiation Effects in Cladding and Structural Materials*, 19: 41107
detection of direction of incidence of, apparatus for, 19: 40927(P)
dose from radioactive luminous paints used in aircraft instruments, 19: 40940 (NP-14924)
effects on alkali-halide crystal lattices, 19: 41975
effects on current oscillations in germanium, 19: 41105(T)
effects on performance of remote measurement systems, (E), 19: 40714 (EUR-2421.d)
effects on solid-state-polymers, sensitivity thresholds for, (E), 19: 40564
effects on solids, saturation and defect structure in, 19: 41102
effects on 2-methyltetrahydrofuran, ESR spectra of trapped electron and radical yields in, 19: 40558
emission of coherent, cosmic-showers detection by, (T), 19: 41308
scattering by non-equilibrium plasma, spectral density in, (T), 19: 41930
transport of, book on, 19: 41161

RADIATION CHEMISTRY
nuclear transformations in, conference on, 19: 40614 (STI/PUB/91(Vol.I))
of fissiochemical reactions, 19: 40547(R) (AGN-8137(Vol.I))
reactor use for, (E/T), 19: 40559
research at Osaka, summary of, 19: 40555(T) (AEC-tr-6565, pp 1-7)
research on polymer, 19: 40554(T,R) (AEC-tr-6565)
research programs on, 19: 40396(R) (HMI-B-39)
research programs on, at Siemens-Schuckertwerke laboratories, Erlangen, Germany, 19: 42228

RADIATION DETECTION INSTRUMENTS
amplifier circuit designs for semiconductor, review, (E), 19: 40899
angular correlation measurements using, correction factors for, (T), 19: 40900
design and performance of neutron-activation, for in-pile flux monitoring, (E), 19: 40867 (BNWL-64)
design of scattering chamber with solid-state detectors, (E), 19: 40907
performance of double-focusing magnetic beta spectrometer, (E), 19: 40904
performance with on-line computers, (E), 19: 40918
spectrometric data processing using numerical adapted filters, (E), 19: 40906

RADIATION DETECTION INSTRUMENTS (ION CURRENT TYPE)
design, 19: 40930(P)
design for gamma dose measurements, engineering drawings of, 19: 40926
design for radiation monitoring in high-voltage laboratory, engineering drawings of, 19: 40924

RADIATION DETECTION INSTRUMENTS (PULSE TYPE)
design for radioisotope identification, 19: 40929(P)
design of multichannel, for use in nuclear medicine, 19: 40913
distortion in, calculations of effects of pile-up on, (T), 19: 40914
performance in counting events from pulsed sources, 19: 40885

RADIATION EXPOSURE CHAMBERS
design of charged-particle scattering chamber, (E), 19: 40907

RADIATION INJURIES
effects on metabolism in heart, 19: 40357(T) (FTD-TT-65-48, pp 552–3)
pathology of, from deposited cerium-144 in rat lungs, 19: 40313
pathology of, from deposited plutonium-239, in rats, 19: 40317
pathology of, in nervous system of man, 19: 40349 (BNL-9345)
pathology of, induced by injected neptunium-237, in sheep liver, 19: 40350 (HW-SA-3723)
pathology of, induced by injected promethium-147 in rats, 19: 40383
pathology of, induced by injected niobium-95 in rats, 19: 40384
protection against, effects of bone marrow transfusions in dogs, 19: 40385(T) (FTD-TT-65-48, pp 134–5)
protection against, effects of serotonin in rats, 19: 40388
protection against, effects of histamine in rats, 19: 40389
protection against, effects of tryptophan in rats, 19: 40388

RADIATION MONITORING
alarm system design factors, 19: 40804 (NP-14925)
at HNPF, April 1965, 19: 42099(R) (TID-22013)
equipment for laboratory, 19: 40924
equipment for remote, at Nevada Test Site, 19: 40878 (NVO-162-5(Rev.))
equipment for, in radioisotope packaging, 19: 40925
equipment for, satellite, 19: 40841
of Garigliano Nuclear Power Plant, 1964, 19: 42086(R) (EUR-2427.i)
system design for vent-line, 19: 40834(R) (UCRL-14151)

RADIATION PROTECTION
criteria for, in handling and shipping sealed radioisotope sources, 19: 40802 (CONF-650616-5)
procedures for, on Vostok satellites, 19: 40841
standards for fissionable materials handling, 19: 40840
technician training for, manual for, 19: 40801 (ANL-6991)

RADIATION SICKNESS
effects on lactation, 19: 40353(T) (FTD-TT-65-48, pp 16–17)
pathology and treatment of, induced by tritium in rabbits, 19: 40340
pathology of, induced by injected yttrium-91 in dogs, 19: 40377
pathology of, induced by injected strontium-90 in dogs, 19: 40378
pathology of, induced by tritium in rabbits, 19: 40337
therapy in dogs, using blood plasma substitute, butyl alcohol, vitamin B_{12}, and antibiotic, 19: 40387

RADIATION SOURCES
handling and shipping of sealed, safety criteria for, 19: 40802 (CONF-650616-5)
radiation flux distribution from cylindrical or spherical, effects of shell-shaped shields on, 19: 41960

RADIATION TARGET CANS
development for fissiochemical experiments, 19: 40547(R) (AGN-8137(Vol.I))

RADIATORS
evaluation of, for space nuclear power plants, (T), 19: 40731 (AD-609969)

RADIO WAVES

emission from moon during eclipses, lunar temperature measurements using, (E), 19: 41222
emission from type II solar outbursts, (T), 19: 41229
emission in type III solar bursts, properties of, (E), 19: 41218
emission of solar, 1953 to 1963, 19: 41217
intensity distribution from cosmic source, determination using finite-pass-band spectrometer, (T), 19: 41301
propagation in ionosphere, analysis of, 19: 41572 (NASA-CR-258)
reflection from meteor trails, polarization phenomena in, (E), 19: 41223

RADIOACTIVE CONTAMINATION
reduction in reactor effluent, by water purification, 19: 42130 (HW-68387)

RADIOACTIVE MATERIALS
activity of, geometrical and statistical errors in counting, 19: 40874 (JUL-227-CA)
analysis of mixtures of, apparatus for relative abundance, 19: 40454(P)
analysis of, substoichiometric separation in, 19: 40424
handling and shipping of sealed, safety criteria for, 19: 40802 (CONF-650616-5)
packaging and transportation of, international conference on, 19: 40808 (SC-RR-65-98)
packaging and transportation of, special problems in, 19: 40826 (SC-RR-65-98, pp 625-9)
packaging for transport of, development of standards for, 19: 40810 (SC-RR-65-98, pp 32-44)
recovery following reactor accidents, (E), 19: 42006 (IDO-10043(Vol.II) (Rev.1))
retention of inhaled, in man, 19: 40800(R) (AERE-PR/HPM-7)
shipping container design, review, 19: 40823 (SC-RR-65-98, pp 450-72)
shipping container for, development and tests of, 19: 40816 (SC-RR-65-98, pp 141-86)
shipping containers for, standardization, 19: 40822 (SC-RR-65-98, pp 442-9)
transportation of, aspects of, 19: 40812 (SC-RR-65-98, pp 74-8)
transportation of, regulatory packaging standards for, 19: 40811 (SC-RR-65-98, pp 45-54)
transportation of, review of research on, 19: 40809 (SC-RR-65-98, pp 17-31)

RADIOACTIVE WATERS
radium-226 and radon-222 content of, 19: 40805 (NRS-30)

RADIOACTIVITY
concentrations of natural, in atmosphere to 3.6 km, 19: 40790
content in stratosphere, 19: 40789
mobility spectra of small ions in air, 19: 40787
monitoring in curative waters in Lourdes Spa, San Luis Potosi, Mexico, 19: 40835
of atmosphere over Japan, 19: 40792
of sea water, data on, 19: 40792
recovery following reactor accidents, (E), 19: 42006 (IDO-10043(Vol.II) (Rev.1))

RADIOBIOLOGY
late irradiation effects, review, 19: 40352 (WASH-1059)
radioisotope distribution, effects, and excretion, 19: 40311

RADIOCHEMICAL PROCESSING PLANTS
design of, at Savannah River plant, (E), 19: 40837
economics of, for processing spent reactor fuels, (E), 19: 40661

RADIOCHEMISTRY
counting data evaluation in radioisotope deposition experiments, computer program for, 19: 40636 (WAPD-TM-516)
research programs on, 19: 40396(R) (HMI-B-39)

RADIODIAGNOSIS
of one-sided deficiency in isotope nephrogram of kidneys, design of multichannel detector for, 19: 40913

RADIOGRAPHY
equipment for detonation and shock wave studies, 19: 41118 (LA-DC-6996)
methods of, for welds in steel pressure vessels, 19: 42024
performance of cold-neutron, (E), 19: 40722
use in nondestructive materials testing, conference on, 19: 40754

RADIOISOTOPES
content in sea water, human contamination by, 19: 40309(R) (NP-15180)
determination of substoichiometric separation in, 19: 40424
disposal and processing methods for, at Hanford plant, (E), 19: 42196
distribution, effects, and excretion of, in biological systems, 19: 40311
handling and shipping of sealed, safety program of AEC for, 19: 40802 (CONF-650616-5)
packaging for shipment, engineering drawings of ion chamber for monitoring radioactivity in, 19: 40925
production and decay chains for, 19: 42008 (ORNL-NSIC-5(Vol.I and II))
production in reactors, system for study of short-lived, 19: 42017 (IS-1219)
recovery following reactor accidents, (E), 19: 42006 (IDO-10043(Vol.II) (Rev.1))
separation of long- and short-lived, in high-level waste, (E), 19: 42197
separation of remotely controlled chromatographic column for, 19: 40685

RADIOLOGICAL DEFENSE
medical planning for thermonuclear attack of cities, 19: 40361(T) (ORNL-tr-437)

RADIOLOGICAL TELEMETERING SYSTEMS
description of, for monitoring at Nevada Test Site, 19: 40876 (NVO-162-5(Rev.))

RADIOMETERS
design for measuring thermal radiation from nuclear explosions, (E), 19: 40882 (USNRDL-TR-839)

RADIOMETRIC ANALYSIS
sample preparation for liquid scintillation counting of biological materials, 19: 40436

RADIOPROTECTIVE COMPOUNDS
biochemical effects of unitol, in irradiated rats, 19: 40386(T) (FTD-TT-65-48, pp 661–2)

RADIOTHERAPY
activation of man during high-energy, 19: 40392 (NYO-3364-6)
meson (π^-) beams in, 19: 40395
of carcinomas of breast, effects of 5-fluorouracil, 19: 40394
radiation hazards from use of radium-224 for, 19: 40391 (NP-14921)

RADIUM
radiation hazards of inhalation and ingestion by man of, 19: 40805 (NRS-30)

RADIUM ISOTOPES Ra-224
excretion in rats of, effects of age, 19: 40315
metabolism in rats, after intravenous injection, 19: 40315
therapeutic use of, radiation hazards, 19: 40391 (NP-14921)

RADIUM ISOTOPES Ra-226
determination in man by analysis of teeth, 19: 40805 (NRS-30)

RADON ISOTOPES Rn-220
determination of airborne decay products from, by alpha spectroscopy, 19: 40834(R) (UCRL-14151)

RADON ISOTOPES Rn-222
determination of airborne decay products from, by alpha spectroscopy, 19: 40834(R) (UCRL-14151)
effects on incidence of lung carcinoma in miners, 19: 40805 (NRS-30)

RAIN WATER
annual precipitation for Europe, 1921 to 1950, 19: 41111 (EUR-2296.e)
fallout content of, at Fayetteville, Arkansas, 19: 40785 (TID-21224)
radioactivity in Japan, 19: 40792

RARE EARTH ALLOYS
study of CsCl-type intermediate phases in binary, with other metals, 19: 41005 (CALT-221-11)
Cd–rare earths, crystal structure of intermetallic compounds in, 19: 41040
Cu–rare earths, crystal structure of intermetallic compounds in, 19: 41040
Fe–rare earths, analysis for erbium, dysprosium, gadolinium, and scandium, 19: 40445
Hg–rare earths, crystal structure of intermetallic compounds in, 19: 41040
In–rare earths, crystal structure and thermal expansion of intermetallic compounds in, 19: 41041
Mg–rare earths, crystal structure of intermetallic compounds in, 19: 41040
Mg–rare earth, phase studies, 19: 41011 (IS-T-15)
Mg–rare earth, preparation by magnesium salt reduction of halides, 19: 40955
rare earths–Zn, crystal structure of intermetallic compounds in, 19: 41040
rare earths–Tl, crystal structure of intermetallic compounds in, 19: 41040
rare earths–Sn, crystal structure and thermal expansion of intermetallic compounds in, 19: 41041

RARE EARTH ALUMINATES
crystal chemistry of, review, 19: 40535

RARE EARTH BORIDES
book: *High-Temperature Compounds of Rare Earth Metals with Nonmetals*, 19: 41073(T)

RARE EARTH CARBIDES
book: *High-Temperature Compounds of Rare Earth Metals with Nonmetals*, 19: 41073(T)
eutectic temperatures between carbon and dicarbides of, 19: 41014 (LA-DC-6819)
lattice parameters of dicarbides of, 19: 41014 (LA-DC-6819)
microhardness of, 19: 41014 (LA-DC-6819)
phase transformation temperatures in dicarbides of, 19: 41014 (LA-DC-

6819)
RARE EARTH CHLORIDES
thermal decomposition of hydrates, 19: 40489
KCl–rare earth chlorides, stability and volatilization, 19: 40516
RARE EARTH COMPLEXES
glycolate, stability and composition, 19: 40486
properties of, review, (E), 19: 40400
review of Soviet studies on, 19: 40532
sulfosalicylate, composition and formation constants, 19: 40513
with 1,10-phenanthroline, preparation and properties of chloride, 19: 40514
with 2,2'-dipyridyl, preparation and properties of acetate, chloride, nitrate, and thiocyanate, 19: 40487
RARE EARTH COMPOUNDS
book: *High-Temperature Compounds of Rare Earth Metals with Nonmetals*, 19: 41073(T)
properties of inorganic and organic, review, (E), 19: 40400
RARE EARTH HALIDES
reduction in magnesium salt bath, 19: 40955
RARE EARTH IONS
relaxation time in crystals, spin-lattice, (T), 19: 41982
spin-lattice relaxation time of, formula for, (T), 19: 41995(T)
RARE EARTH NITRIDES
book: *High-Temperature Compounds of Rare Earth Metals with Nonmetals*, 19: 41073(T)
RARE EARTH OXIDES
analysis for neodymium and yttrium by x-ray fluorescence, 19: 40440
crystal chemistry of, review, 19: 40533
crystal chemistry of sesqui-, review, 19: 40535
phase equilibria of mixtures with other oxides, review, 19: 40534
RARE EARTH SILICATES
crystal chemistry of, review, 19: 40535
RARE EARTH SILICIDES
book: *High-Temperature Compounds of Rare Earth Metals with Nonmetals*, 19: 41073(T)
RARE EARTH SULFIDES
book: *High-Temperature Compounds of Rare Earth Metals with Nonmetals*, 19: 41073(T)
RARE EARTHS
analytical chemistry of, review, (E), 19: 40448
analytical chemistry of, review of Soviet studies on, 19: 40449
book: *Progress in the Science and Technology of the Rare Earths. Vol. 1*, 19: 40399
determination in copper by activation, 19: 40422
geochemistry of, review, 19: 40793
physical and thermodynamic properties, 19: 40948 (IS-1195)
preparation and purification, 19: 40948 (IS-1195)
reactions of, thermodynamics of electrode, 19: 40500
separation by anion exchange chromatography in magnesium nitrate solutions, 19: 40659
separation by electrophoresis in glycolic acid, 19: 40671
separation by elution chromatography, effects of glycols on, 19: 40662
separation by ion exchange, review, 19: 40691
separation by polarography, 19: 40681
separation by solvent extraction using non-phosphorus compounds, 19: 40692
separation by solvent extraction using organophosphorus compounds, review, 19: 40693
separation by solvent extraction using amines, 19: 40696(P)
separation from raw materials, review, 19: 40690
separation from thorium by ion exchange in ammonium thiocyanate–methanol–water systems, 19: 40447
separation from transplutonium elements by solvent extraction using DTPA, 19: 40676
solution chemistry of, review, 19: 40531
solvent distribution in ammonium thiocyanate–methanol–water systems, distribution coefficients for, 19: 40447
spectra of, method for obtaining atomic absorption, 19: 40526
thermal capacity of, tables of 4f electronic contributions to, 19: 40457 (IS-1156)
uses of, review, 19: 40401
RATS
antimony-124 metabolism in, after intravenous or oral administration, 19: 40318
biological effects of chronic, low-dose ingestion of strontium-90 in, 19: 40335
biological effects of chronic, low-dose ingestion of cesium-137 in, 19: 40335
biological effects of chronic, low-dose ingestion of promethium-147 in, 19: 40335
biological effects of strontium-90 in, effects of administration rate and dose on, 19: 40336
biological effects of low doses of plutonium-239 in, effects of additional biological stresses on, 19: 40338
cerium-144 excretion in, effects of complexing agents on, 19: 40347
cerium-144 metabolism in, after intratracheal administration, 19: 40313
cerium-144 metabolism in, after oral or intravenous administration, 19: 40321
effects of adrenaline and pain stimulation on blood pressure of, 19: 40360(T) (FTD-TT-65-48, pp 666)
effects of rickets on calcification of cartilage in, 19: 40351(R) (NYO-1913-1)
iodine-131-induced hypothyroidism in, 19: 40368
lead-212 metabolism in, after intra-arterial or intravenous injection, 19: 40333
metabolism of carbohydrates in liver of, tracer study, 19: 40308 (BNL-8379)
molybdenum-99 metabolism in, 19: 40319
niobium-95 metabolism in, after inhalation, 19: 40314
pathological effects of injected promethium-147 in, 19: 40383
pathological effects of injected niobium-95 in, 19: 40384
pathological effects of inhaled plutonium-239, 19: 40380
phosphorus-32 metabolism in, 19: 40319
plutonium excretion in, effects of diethylenetriaminepentaacetic acid, 19: 40346
plutonium poisoning in, therapeutic effects of complexing agents on, 19: 40345
plutonium-239 metabolism in, after inhalation of citrate complex, 19: 40316
plutonium-239 metabolism in, after intratracheal administration as acetate or nitrate salt, 19: 40317
plutonium-239 metabolism in, after repeated intravenous injection of citrate, effects of age, 19: 40326
radiation effects from injected strontium-89 and strontium-90 on pancreas of, 19: 40358(T) (FTD-TT-65-48, pp 577–8)
radiation effects on cartilage calcification in, 19: 40351(R) (NYO-1913-1)
radiation effects on blood pressure of, 19: 40360(T) (FTD-TT-65-48, pp 666)
radiation effects on pepsinogen content of blood plasma in, 19: 40363
radiation effects on urinary excretion of taurine by, gamma, 19: 40364
radiation effects on growth of progeny of male, exposed in infantile period, 19: 40365
radiation injuries in, protective effects of serotonin and tryptophan in, 19: 40388
radiation injuries in, protective effects of histamine in, 19: 40389
radiation injuries of, role of body fluids in, 19: 40369
radium-224 excretion in, effects of age, 19: 40315
radium-224 metabolism in, after intravenous injection, 19: 40315
strontium-89 metabolism in, after oral or intravenous administration, 19: 40321
strontium-89 metabolism in, effects of complexing agents, 19: 40344
strontium-90 metabolism in, after oral or intravenous administration, 19: 40321
strontium-90 metabolism in, after chronic oral administration, 19: 40323
strontium-90 metabolism in, effects of dietary constituents on, 19: 40342
strontium-90 metabolism in, 19: 40312
tellurium-127 metabolism in, after intravenous or oral administration, 19: 40318
tin-133 metabolism in, after oral or parenteral administration, 19: 40320
uranium fission products metabolism in, after oral administration of mixture, 19: 40322
uranium poisoning in, effects of thiobis(ethylenenitrilo)tetraacetic acid on, 19: 40348
yttrium-91 metabolism in, after inhalation, 19: 40314
zirconium-95 metabolism in, after inhalation, 19: 40314
REACTION MECHANISMS
chemical potentials for, calculation by summation of Fermi-Dirac functions, (T), 19: 40493
effects on asymptotic stability of detonations, (T), 19: 41117 (LA-3306)
energy transfer processes and nuclear transformations in organic compound reactions with recoil atoms, 19: 40620
REACTOR CONTROL ELEMENTS
reactivity worths of materials for, 19: 42050 (NAA-SR-11368)
REACTOR CONTROL RODS
drive mechanism for KIWI, design and performance of hydraulic, 19: 42136 (LA-DC-6941)
drive mechanism for, 19: 42033(P)
reactivity worths of, two-dimensional analysis of, (T), 19: 42034 (AAEC/E-134)
reactor criticality effects in heavy water lattices, (E), 19: 42045(R) (MIT-2344-3, pp 55-108)

REACTOR CONTROL SYSTEMS
design for graphite-moderated and water-cooled, 19: 42019(T) (ORNL-tr-669)
design of pneumatic scram system, 19: 42021
design using ball-shaped members, 19: 42029(P)
design using electrolyte injection for homogeneous reactors, 19: 42016(P)
design using moderator temperature and composition variation, 19: 42030(P)
design using moderator temperature variation, 19: 42031(P)
design using variable moderator capacity, 19: 42028(P)
performance of automatic chemical shim, 19: 42023
performance of, optimization of, 19: 42013
reliability of, methods of estimating, 19: 42022
REACTOR COOLANTS
performance of fog as, evaluation of, (E), 19: 42020
REACTOR COOLING SYSTEMS
fabrication of MZFR primary, 19: 42164
REACTOR FUEL ELEMENTS
corrosion in crevices of simulated PRTR, by boiling lithiated water, 19: 40965 (BNWL-83)
design of rod-assembly, with burnable poison, 19: 42072(P)
design of sheathed, with helical fins, 19: 40993(P)
design of sheathed, with heat transfer spacers, 19: 42074(P)
design, fabrication, and testing for MZFR, 19: 42165
development of, French industry for, 19: 42070
fabrication of aggregated clad particles with interconnected pores for coolant passage, 19: 40994(P)
fouling in organic moderated reactors, literature survey on, 19: 40971 (RT/CHI(65)20)
handling in reactors, design of mechanically operated grab for, 19: 42027(P)
heat transfer with polyzonal-spiral finning, at low gas flow rates, (E), 19: 40748
performance in test reactors, 19: 42157
processing and storing spent, regulations for, (E), 19: 40837
processing of irradiated, review of methods for, 19: 40667
processing of irradiated, sequential separation of fission products in, 19: 40675
processing spent, economics of, (E), 19: 40661
radiation effects on MZFR, 19: 42185
research programs on, at Siemens-Schuckertwerke laboratories, Erlangen, Germany, 19: 42228
spacer grid for elongated assembly of, 19: 42073(P)
testing of irradiated, for unbonded areas by ultrasonics, 19: 41089 (HW-56028)
testing of plutonium recycle, in EBWR, 19: 42078 (ANL-7019)
testing of, gamma and x-ray attenuation methods of nondestructive, 19: 42071
thermal conductance of in-pile, transient temperature method for measuring, 19: 40732(R) (CEND-3336-237)
transport container for irradiated, from power stations in United Kingdom, 19: 40829 (SC-RR-65-98, pp 711-18)
REACTOR FUEL ELEMENTS (CERAMIC)
fabrication and testing of depleted uranium dioxide, 19: 41006(R) (CEND-3107-238)
fission gas release from uranio, with central melting, 19: 41088 (GEAP-4572)
radiation effects on 304 L stainless steel clad, 19: 41094(T) (NP-tr-1235)
REACTOR FUEL ELEMENTS (DISPERSION)
neutron cross sections for plutonium in beryllium oxide matrix, effects of grain structure on, (T), 19: 42041 (GA-6286)
REACTOR FUEL PLATES
cladding of, ultrasonic detection of non-bond in, 19: 40756
fabrication of ZPR-III, 19: 40978 (ANL-6955)
REACTOR FUEL RODS
fabrication of Zircaloy-clad, for MZFR, 19: 42175
heat transfer from cylindrical, analog models for, 19: 40740 (RT/ING(64)16)
neutron buckling and flux distributions in lattices of slightly enriched uranium and heavy water, (E), 19: 42049 (MIT-2344-3, pp 155-64)
neutron flux distributions around single uranium, in heavy water, 19: 42047 (MIT-2344-3, pp 115-24)
neutron resonance escape in heterogeneous cluster-type, Dancoff factor and equivalence theorem for, (T), 19: 42055
radiation effects on 304 L stainless steel clad, 19: 41094(T) (NP-tr-1235)
REACTOR FUEL SPHERES
deposition of coatings on, rotating-drum method for, 19: 40982 (ORNL-3819)
REACTOR FUEL WIRES
fabrication of bundles of coated, 19: 40994(P)
REACTOR FUELS
analysis of irradiated power, for fission products, 19: 40411 (RT/CHI(65)2)
coating of particulate, with shock absorbing material, 19: 40992(P)
development and uses of, in Italy, 19: 42111
development of plutonium–uranium and uranium–thorium, for fast power breeders, 19: 42081 (CONF-193-11)
processing and storing spent, regulations for, (E), 19: 40837
processing spent, economics of, (E), 19: 40661
reprocessing of clad uranium dioxide, development of AIROX process for, 19: 40653 (NAA-SR-11389)
reprocessing of uranium carbide, evaluation of pyrochemical processes for, 19: 40652 (NAA-SR-11340)
shipping of slightly enriched uranium cores, tests of containers for, 19: 40820 (SC-RR-65-98, pp 357-76)
temperature measurement in BR-2, 19: 42181
REACTOR MATERIALS
book: *Irradiation Effects in Cladding and Structural Materials*, 19: 41107
environmental tests of candidate, for High Temperature Lattice Test Reactor, 19: 40966 (BNWL-92)
gamma heating of, in DFR, (E), 19: 42117
leak analysis for reactor containment, 19: 42018 (NAA-SR-10100)
research progress on, *Technical Progress Reviews*, Summer 1965, 19: 40957
REACTOR MATRICES
neutron disadvantage factor in cylindrical, 19: 42063
neutron energy spectra in, THERMOPYL program for calculating, 19: 41648
neutron migration area, multiplication factor, and reflector savings in water–uranium dioxide, 19: 42053
reactivity effect in slab, spherical, and cylindrical geometries, dynamic, (T), 19: 42061
REACTOR MODERATORS
analysis of heavy water for trace impurities, automated, 19: 40406 (CONF-650919-2)
design of fluids and movable element, 19: 42028(P)
neutron spectra in, thermal, 19: 42037 (BNWL-95, pp 4-17)
performance and replacement in HNPF, 19: 42099(R) (TID-22013)
reactivity control by variation of temperature and composition of, 19: 42030(P)
temperature of, reactivity control by variation of, 19: 42031(P)
temperature variations in, reactivity control using, 19: 42059
REACTOR OSCILLATORS
performance for measuring reactivity transfer function of LPTR, 19: 42156 (UCRL-12476)
REACTOR SAFETY
accident and incident review, 19: 42008 (ORNL-NSIC-5(Vol.I and II))
disposal of SNAP reactors after operation, methods for, 19: 42140 (NAA-SR-11353)
radioactivity recovery following accidents, review, (E), 19: 42006 (IDO-10043(Vol.II)(Rev.1))
REACTOR SAFETY EXPERIMENTS
development of Loss of Fluid Test Reactor, (E), 19: 42134(R) (IDO-17070)
performance stability in Spert IV, 19: 42152 (IDO-17088)
REACTOR THERMAL COLUMNS
neutron spectrum in, in Triga Mark II, (E), 19: 42184
REACTOR TUBES
creep buckling and collapse testing of stainless steel process, 19: 41019 (NAA-SR-11323)
REACTORS
accidents in, radioactivity recovery problems following, (E), 19: 42006 (IDO-10043(Vol.II)(Rev.1))
book: *Experimental Reactor Analysis and Radiation Measurements*, 19: 42014
containment of, leakage analysis for, 19: 42018 (NAA-SR-10100)
containment technology for U.S., 19: 42008 (ORNL-NSIC-5(Vol.I and II))
control and safety systems for, reliability of automatic, 19: 42022
control by variable moderator capacity, 19: 42028(P)
control of, lecture on, 19: 42138 (N64-33780)
control optimization for, 19: 42012
control poisons for, coating particulate, 19: 40992(P)
coolant loss accidents in, heat transfer calculations for, (T), 19: 42009 (WAPD-T-1811)
criticality of two-region, solutions of transport equation for, 19: 42035 (ANL-6590)
criticality studies, 19: 42036 (BNWL-95)
design of low-power, 19: 42067(P)
design of solid-moderated, 19: 42068(P)

kinetics of coupled-core, transport equation for, 19: 42062
loading equipment for, 19: 42032(P)
neutron correlation in, (T), 19: 42042 (JINR-P-2216)
neutron decay in, Monte Carlo analysis of prompt, 19: 42039(R) (BNWL-95, pp 36-9)
neutron diffusion equation for, use of poison in direct solution of, 19: 42052
neutron flux in, device for measurement of rate of increase of, 19: 42064(P)
neutron flux monitoring instruments for, design of boron-11-activation, (E), 19: 40867 (BNWL-64)
pump design and performance for, 19: 42026
radioisotope production in, system for study of short-lived, 19: 42017 (IS-1219)
reactivity period meter for, design of, 19: 42064(P)
reactivity worths of control rods in, two-dimensional analysis, (T), 19: 42034 (AAEC/E-134)
research programs on, at Siemens-Schuckertwerke laboratories, Erlangen, Germany, 19: 42228
scram systems for, design of pneumatic, 19: 42021
uses for chemical production, 19: 40548 (BNWL-82)
uses for commercial radiation chemistry, (E/T), 19: 40559
xenon poisoning in, (T), 19: 42010

REFLECTION
testing Scotchlite reflective material for illuminating bubble chambers, 19: 40917

REFRACTORY MATERIALS
analysis of metals for carbon, combustion furnace for, 19: 40413 (TIM-948)
book: *Irradiation Effects in Cladding and Structural Materials*, 19: 41107
book: *Thermal Radiative Properties*, 19: 41074
preparation of monocrystalline spheres of, (E), 19: 40991

RELATIVITY THEORY
book: *An Introduction to the Theory of Relativity*, 19: 41566
conservation laws in, in space-time admitting motion, (T), 19: 41542
conservation laws in, in space-times admitting general transformations, 19: 41543
generator kernel of annihilation and creation operators on static space-time, Schwartz theory for, 19: 41534
gravitation generation by axisymmetric magnetic fields, 19: 41544
gravitational radiation in canonical analysis of, (T), 19: 41561
gravitational radiation in system of two point masses, (T), 19: 41564
stability of gravitationally bound spheres of perfect fluid, (T), 19: 41563

REMOTE-CONTROL EQUIPMENT
design and use for chromatography of radioactive solutions, 19: 40685
design for hot cells, 19: 40730(P)
design of metallographic sample carrying device for polishing machine, 19: 40964(P)

RESEARCH REACTORS
auxiliary installations for MZFR, design of, 19: 42168
building construction and pressure vessel installation for MZFR, 19: 42177
construction of MZFR, 19: 42176
containment of MZFR, 19: 42167
control and data acquisition system for, digital computer feasibility as, 19: 42150 (ANL-7009)
coolant and moderator circuits of MZFK, construction of, 19: 42164
coolant pumps for MZFR, 19: 42174
description of MZFR, 19: 42160
design and fabrication principles for MZFR, 19: 42162
design for Petten research centers, Netherlands, 19: 42227
design of MZFR, for economic optimum, 19: 42161
development of L-77 Vanowen, 19: 42155 (NAA-SR-Memo-3196)
development of MZFR, 19: 42158
economics and utilization of MZFR, 19: 42159
experimental facilities for neutron spectrometry in DIORIT, 19: 42154 (KFK-261)
experimental facilities of MZFR, 19: 42179
fuel element performance, 19: 42157
fuel element testing for MZFR, in NRX, 19: 42185
fuel elements for MZFR, design, construction, and testing of, 19: 42165
fuel rod fabrication for MZFR, 19: 42175
instrumentation and controls for MZFR, 19: 42170
loading equipment for MZFR, 19: 42166
MZFR structural design of, 19: 42171
neutron irradiation facility at Munich FRM, low-temperature, 19: 42180
neutron spectrum in thermal column of Triga Mark II, (E), 19: 42184
neutron-flux distributions in VVR-S, (E), 19: 42183
pressure vessel for MZFR, design, construction, and installation of, 19: 42163
pressure vessel for MZFR, fabrication of, 19: 42172
reactivity measurements in MZFR, zero-energy, 19: 42186
reactivity of MZFR, zero-power experiment for, 19: 42178
reactivity of Triga Mark II, effects of series pulsing on, 19: 42188
safety hazards and precautions at Pegase installation, 19: 42151 (CEA-R-2518(Vol.II))
steam generator for MZFR, construction of, 19: 42173
steam power installation for MZFR, 19: 42169

RESINS
preparation and properties pyridine-2,6-dicarboxylic acid, 19: 40674

RESISTANCE FURNACES
design of remote-operated 1900°F, for combustion analysis of refractory metals, 19: 40413 (TIM-948)

RESORCINOL
effects on use of chromogenic polymer for gamma dosimetry, 19: 40599
radiolysis of, ESR of radicals in, 19: 40607
use in preparation of chromatographic resins, 19: 40674

RESORCINOL, 4-(2-PYRIDYLAZO)-
analytic use for determining niobium and tantalum, 19: 40442

RESPIRATORS
design of full-face, 19: 40834(R) (UCRL-14151)

RHENIUM
analysis for nitrogen, isotope-dilution method for, 19: 40444
coating with lanthanum hexaboride, (E), 19: 40725
stress-rupture properties, 19: 40961
thermal expansion to 2500°C, 19: 41009 (GEMP-375)
thermoelectric properties at 1000 to 2000°C, (E), 19: 40859

RHENIUM ALLOY COUPLES
Mo–Re/Re, stability of thermocouples of, (E), 19: 40859
Mo–Re/Re–W, stability of thermocouples of, (E), 19: 40859
Mo/Re–W, stability of thermocouples of, (E), 19: 40859
Re/Re–W, stability of thermocouples of, (E), 19: 40859
Re–W/Re–W, stability of thermocouples of, (E), 19: 40859

RHENIUM ALLOYS
Mo–Re, creep and stress-rupture properties at 1600°C, 19: 40961
Mo–Re, thermal expansion to 2500°C, 19: 41009 (GEMP-375)
Mo–Re, thermoelectric properties at 1000 to 2000°C, (E), 19: 40859
Mo–Re–W, properties, 19: 40961
Mo–Re–W, stress-rupture properties, 19: 40961
Re–U, structures and phase transformation kinetics of, 19: 41079
Re–W, preparation procedures, 19: 40989
Re–W, stress-rupture properties, 19: 40961
Re–W, thermal expansion to 2500°C, 19: 41009 (GEMP-375)
Re–W, thermoelectric properties at 1000 to 2000°C, (E), 19: 40859
Re–W, use of freeze-drying method for preparation of ultra-fine particles of, 19: 40987

RHENIUM COMPLEXES
preparation and structure of oxide, 19: 40525

RHENIUM COMPOUNDS
radioinduced chemical effects in, from neutron reactions (n,γ) with rhenium-185, 19: 40585

RHENIUM COUPLES
Mo–Re/Re, stability of thermocouples of, (E), 19: 40859
Re/Re–W, stability of thermocouples of, (E), 19: 40859
Re/W, stability of thermocouples of, (E), 19: 40859

RHENIUM FLUORIDE NITRIDES
preparation and properties, 19: 40461 (ORNL-P-491)

RHENIUM FLUORIDES
preparation and properties of tetra-, 19: 40461 (ORNL-P-491)

RHENIUM ISOTOPES Re-185
neutron reactions (n,γ) with, in mixed crystals, chemical transformations from, 19: 40585

RHENIUM ISOTOPES Re-186
reactions of recoil, in rhenium compounds in mixed crystals, 19: 40585

RHENIUM ISOTOPES Re-188
beta decay scheme of, (E), 19: 41801(T)

RHENIUM OXIDES
preparation and structure of ternary, 19: 40525

RHENIUM SYSTEMS
Re–ThO_2–W, thoria deformation and fracture in, (E), 19: 41058

RHODIUM
ion reactions at 5 to 12 Mev, neutron spectra from, (E), 19: 41810(T)
wear characteristics of plated coatings of, for use in rotary switches, 19: 42216 (SC-DR-65-269)

RHODIUM ISOTOPES Rh-101
half life of, from conversion electron measurements, (E), 19: 41719

RHODIUM ISOTOPES Rh-102
half life of, from conversion electron measurements, (E), 19: 41719

RHODIUM ISOTOPES Rh-103
performance as neutron flux detector, 19: 42148 (AECL-2216)

RIBONUCLEIC ACID

properties of, affecting transfer of genetic information, 19: 42212 (NYO-3424-1)
radiation effects on synthesis in diploid yeast, from carbon-14-labeled and phosphorus-32-labeled compounds, 19: 40367
RIBONUCLEIC ACID, DESOXY-
properties of, affecting transfer of genetic information, 19: 42212 (NYO-3424-1)
RIBONUCLEOTIDES
reactions of adenylic, cytidylic, and uridylic acid, with cerium, lanthanum, and lutetium, 19: 40474
RICE
calcium content of brown and polished, 19: 40781(R) (NP-15179)
strontium content of brown and polished, 19: 40781(R) (NP-15179)
RICKETS
effects on calcification of cartilage in rats, 19: 40351(R) (NYO-1913-1)
ROCKET MOTORS
development of cesium-ion, 19: 40765(R) (NP-15309)
ion, development of electron-bombardment, 19: 40760 (N64-25008)
ROCKET REACTORS
book: *Fundamentals of Nuclear Flight*, 19: 42147
control of, lecture on, 19: 42138 (N64-33780)
design and operation of, lectures on, 19: 42139 (N64-33784)
design of steam-cooled, 19: 42126(P)
development summary, 19: 42145
testing of NERVA, installation for, 19: 42144
ROCKET REACTORS (KIWI)
control rod actuators for, design and performance of hydraulic, 19: 42136 (LA-DC-6941)
fuel element testing for, non-destructive methods of, 19: 42146
gamma and neutron dose measurements from TNT destruct, 19: 42135 (LA-3304)
pump design for, liquid hydrogen, 19: 42141 (NASA-CR-54422)
thermal radiation from burning hydrogen plume in B-4E-301, 19: 42137 (LA-DC-7313)
ROCKETS
book: *High Temperatures in Aeronautics*, 19: 40767
ROCKS
age of Serra-Geral lava-flow, potassium–argon estimation of, 19: 40796
analysis for thorium and uranium using alpha scintillation counter and radioscope, 19: 40432
analysis for traces of gold by neutron activation methods, 19: 40437
correlation and chronology of volcanic, research program on, 19: 40778(R) (COO-689-50)
crushing by nuclear explosions, for manufacture of aggregate and riprap, 19: 40709 (PNE-5003)
meson (μ) energy loss in, (E/T), 19: 41345
potassium–rubidium ratios and strontium isotopic content in Indian Ocean, 19: 40791
RODS
two-phase flow and heat transfer in multirod geometries, research program on, 19: 40733(R) (GEAP-4863)
ROSE BENGAL
separation of iodide from iodine-131-labeled, chromatographic, 19: 40656(T)
ROTORS
testing of, ultrasonic methods for, 19: 41201
RUBIDIUM
content in rocks from Indian Ocean islands, 19: 40791
determination in copper by activation, 19: 40422
RUBIDIUM IODIDES
photon multiplication in indium- or thallium-activated, mechanism of, 19: 40495(T)
RUBIDIUM ISOTOPES Rb-85
neutron reactions to 1.3 kev, resonance parameters and radiation widths from, (E), 19: 41727
RUBIDIUM ISOTOPES Rb-87
alpha reactions (α,n) with, isomeric cross section ratios for, (E), 19: 41820
neutron reactions to 1.3 kev, resonance parameters and radiation widths from, (E), 19: 41727
RUBIES
radiation emission by chromium ions in, level splitting effects on, (T), 19: 40574
RUTHENIUM
effects on properties of tantalum, 19: 41067
purification of, by electron-beam zone melting, 19: 40984
separation from nitric acid solutions, 19: 40677
solvent extraction by tributyl phosphate and di-2-amyl 2-butylphosphonate in short-residence contactors, 19: 40645 (CONF-650918-1)
sorption on tungsten ferrocyanide, tracer studies of, 19: 40679
workability of, process for improvement, 19: 40999(P)
RUTHENIUM ALLOYS
workability of, process for improvement, 19: 40999(P)
RUTHENIUM, BISCYCLOPENTADIENYL-
synthesis of carrier-free ruthenium-106-labeled, 19: 40634 (BNL-8405)
RUTHENIUM CHLORIDES
reactions of ruthenium-106-, with liquid cyclopentadiene, 19: 40634 (BNL-8405)
RUTHENIUM ISOTOPES Ru-106
incorporation into ruthenocene, 19: 40634 (BNL-8405)
RUTHENIUM NITROSYL NITRATES
separation from nitric acid solutions, 19: 40677

S

SAFETY
criteria for, in handling and shipping sealed radioisotope sources, 19: 40802 (CONF-650616-5)
criticality evaluation of packages for transport of fissile materials, 19: 40828 (SC-RR-65-98, pp 679-90)
procedures for criticality control, 19: 40807 (RL-SEP-389(Rev.))
standards for fissionable materials handling, 19: 40840
technician training for, manual for, 19: 40801 (ANL-6991)
SAFETY HAZARDS
control reports on, index to UCRL quarterly, 19: 40833 (UCRL-14116)
noise control in industrial plants, 19: 40806 (RL-SA-37)
protection against, for handling and storage of spent reactor fuels, (E), 19: 40837
SALIVARY GLANDS
radium-224 content in rat, after intravenous injection, 19: 40315
SALT DEPOSITS
waste storage experiment in Lyons, Kansas, mine, 19: 42195 (ORNL-P-1479)
SAMARIUM
determination by spectrochemical methods, voltage-fluctuation patterns in, 19: 40416
determination in chromium–nickel steels and nickel based alloys, 19: 40445
effects as coactivator with cerium on emission spectra of borate phosphors, 19: 40494(T)
physical and thermodynamic properties, 19: 40948 (IS-1195)
polarographic behavior in dimethylformamide and dimethylsulfoxide, 19: 40681
preparation and purification, 19: 40948 (IS-1195)
separation from aqueous solutions of organic acids by solvent extraction using high-molecular-weight amines, 19: 40657
SAMARIUM ALLOYS
Au–Sm, phase studies of solid solutions in, 19: 41062
Co–Sm, magneto-optic properties of intermetallic compound $SmCo_5$ in, 19: 41084
Mg–Sm, thermodynamic properties, 19: 41013 (IS-T-25)
Ru–Sm, process for improving workability of, 19: 40999(P)
SAMARIUM BORIDES
thermodynamics of formation of, 19: 40524
SAMARIUM CARBIDES
eutectic temperature between carbon and dicarbide, 19: 41014 (LA-DC-6819)
lattice parameters and phase transformation temperatures in, 19: 41014 (LA-DC-6819)
microhardness, 19: 41014 (LA-DC-6819)
SAMARIUM CHLORIDES
complexes with phenanthroline, preparation and properties, 19: 40514
KCl–SmCl–NaCl, phase studies, 19: 40517
SAMARIUM COMPLEXES
with gluconic acids, stability constants, 19: 40508
SAMARIUM FLUORIDES
solubility in beryllium nitrate solutions, 19: 40670
SAMARIUM IONS
spectra in acetophenone, energy transfer in, 19: 40504
valency in calcium fluoride crystals, effects of oxygen on, 19: 41993(T)
SAMARIUM ISOTOPES
energy level structure of odd-A, (E), 19: 41778
SAMARIUM ISOTOPES Sm-143
production of isomeric states in yttrium-89 (n,n′γ) reactions at 14 Mev, cross sections for, (E), 19: 41781
SAMARIUM ISOTOPES Sm-144
deuteron reactions (d,d′γ) at 12 Mev, 0+ states from, 19: 41747
deuteron reactions (d,p) at 12 Mev, samarium-145 energy level from, (E), 19: 41778
energy levels from (p,p′γ) and (d,d′γ) reactions at 12 Mev, 0+, (E), 19: 41747
neutron reactions (n,2n) at 14 Mev, cross sections for samarium-143

isomeric states from, (E), 19: 41781
proton reactions (p,p'γ) at 12 Mev, 0+ states from, (E), 19: 41747
SAMARIUM ISOTOPES Sm-147
proton reactions (p,p') at 4 Mev, energy levels from, (E), 19: 41778
SAMARIUM ISOTOPES Sm-148
deuteron reactions (d,p) at 12 Mev, samarium-149 energy levels from, (E), 19: 41778
SAMARIUM ISOTOPES Sm-149
neutron reactions (n,α) with, cross sections for thermal, (E), 19: 41809(T)
SAMARIUM ISOTOPES Sm-150
deuteron reactions (d,p) at 12 Mev, samarium-151 energy levels from, (E), 19: 41778
energy levels of, vibration-rotation interactions in, (T), 19: 41818
SAMARIUM ISOTOPES Sm-152
deuteron reactions (d,p) at 12 Mev, samarium-153 energy levels from, (E), 19: 41778
energy levels of, vibration-rotation interactions in, (T), 19: 41818
SAMARIUM ISOTOPES Sm-154
deuteron reactions (d,p) at 12 Mev, samarium-155 energy levels from, (E), 19: 41778
SAMARIUM OXIDES
content in McKelveyite uranium mineral, 19: 40799
SAMARIUM PERCHLORATES
stability constants of, thermal, 19: 40509
SAMARIUM SILICIDES
crystal structure, 19: 40477
SAMARIUM SULFATES
$Sm_2(SO_4)_3$–Na_2SO_4, thermal stability, 19: 40511
SAMARIUM SULFIDES
magnetic susceptibility at 290 to 1300°K, 19: 41060(T)
SAMARIUM SYSTEMS
Sm–H_2O, neutron spectra in, thermal, 19: 42037 (BNWL-95, pp 4-17)
SAMPLING
method for iodine analysis in atmosphere, 19: 40402 (BMI-X-10137)
method for recovering specimens irradiated near nuclear explosion, 19: 40706 (ORNL-TM-1191)
SAP (SINTERED ALUMINUM PRODUCTS)
dissolution of, by caustic solutions in recirculation dissolver, 19: 40655 (RT/CHI(65)-1)
SARCOMAS
radioinduced by injected plutonium-239, in dogs, 19: 40382
SATELLITES
radiation monitoring on Kosmos and Vostok, 19: 40841
SAVANNAH RIVER PLANT
fuel processing and storage facilities at, (E), 19: 40837
SAVANNAH RIVER PRODUCTION REACTORS
operation control by computer, 19: 42129 (DPSPU-65-30-27)
SAXTON POWER REACTOR
fuel element thermal testing, 19: 41006(R) (CEND-3107-238)
SCANDIUM
determination in copper by activation, 19: 40422
determination in iron–rare earth alloys and medium alloyed steels, 19: 40445
preparation and purification, 19: 40948 (IS-1195)
separation from acid solutions by solvent extraction using alkyl phosphates or sorption on cellulose phosphates, 19: 40689
separation from other elements by electrophoresis in glycolic acid, 19: 40671
SCANDIUM ACETATES
preparation and crystal structure of ammoniated, 19: 40507
SCANDIUM ALLOYS
Au–Sc, phase studies of solid solutions in, 19: 41062
Cr–Sc, phase studies of solid solution formation in, 19: 41050
Mo–Sc, phase studies of solid solution formation in, 19: 41050
Nb–Sc, phase studies of solid solution formation in, 19: 41050
Sc–Ta, phase studies of solid solution formation in, 19: 41050
Sc–W, phase studies of solid solution formation in, 19: 41050
SCANDIUM CHLORIDES
solubility in hydrochloric acid at 25°C, 19: 40520
SCANDIUM FLUORIDES
KF–NaF–ScF_2, phase studies, 19: 40512
KF–ScF_3, preparation and properties of K_3ScF_6, 19: 40512
ScF_3–NaF, preparation and properties of Na_3ScF_6, 19: 40512
SCANDIUM IONS
reactions with derivatives of Arsenazo III, spectrophotometric studies of, 19: 40426
SCANDIUM ISOTOPES Sc-43
energy levels from proton reactions (p,γ) with calcium-42, (E), 19: 41738
gamma spectra and half life of isomeric, (E), 19: 41802(T)
production of isomeric, (E), 19: 41802(T)
SCANDIUM ISOTOPES Sc-44
cross section ratios from potassium-41 (α,n) reactions to 42 Mev, isomeric, (E), 19: 41695
cross-section ratios from potassium-44 (α,n) reactions, statistical model for isomeric, 19: 41696
production by potassium-41(α,n) reactions, isomeric cross section ratios for, (E), 19: 41820
yields of isomeric pair of, in deuteron reactions with scandium-45, 19: 41714
SCANDIUM ISOTOPES Sc-45
deuteron reactions (d,t) at 19 to 28.6 Mev, yields of scandium-44 isomer pairs in, 19: 41714
neutron capture cross sections and radiation widths, (E), 19: 41806(T)
SCANDIUM SILICIDES
crystal structure, 19: 40479
SCATTERING
amplitudes at high energies, behavior of real parts of forward, (T), 19: 41376
amplitudes for, construction of separable hamiltonians from, 19: 41546
amplitudes for, mass-splitting effects on symmetry relations between, (T), 19: 41430
amplitudes for, normalization integrals of Bethe-Salpeter, (T), 19: 41434
amplitudes in potential theory, singularities in, (T), 19: 41550
coupling constant relations in S-matrix theory, 19: 41382
crossing matrices, methods for evaluating, (T), 19: 41381
diagrams containing multi-particle intermediate states, method for summing, 19: 41429
dispersion relation for elastic, (T), 19: 41363
gamma resonant and nonresonant, measurement techniques for, (E), 19: 40922
matrix of, mathematical-physics methods in quantum field theory for, 19: 41540
of charged particles by shielded Coulomb potential, (T), 19: 41763
of Dirac particles by scalar potential, elastic, (T), 19: 41510
polarization change in potential, classical approximation for, (T), 19: 41501
potential, energy gap equation for soft core, 19: 41662 (JINR-P-2176)
potentials in Padé approximant for short-range, 19: 41407
theory of, radial wave equations for nonrelativistic quantum, 19: 41360
SCINTILLATION DETECTORS
amplification-channel stabilization in, reference light pulse for, 19: 40870 (IAE-695)
design of alpha, for rock analyses, 19: 40432
feasibility of cadmium-sulfide, using matched pairs of crystals, (E), 19: 40598
luminescence response of Pilot B plastic, to electrons and protons, (E), 19: 40916
performance in analysis of beta-active biological materials, 19: 40436
performance of annular-crystal, for neutron-capture gamma spectrometry, (E), 19: 40896
uses in scattering chambers, (E), 19: 40907
SEA WATER
analysis for sulfur-35, method for, 19: 40431
desalination of, development of dual-purpose nuclear power plants for, 19: 42124
desalination of, economic comparison of two evaporators for, 19: 40699 (ORNL-TM-826)
desalination of, economics of low-temperature reactors for, 19: 42097 (ORNL-TM-1152)
desalination using nuclear-powered osmosis plants, 19: 42120
radioactivity in, data on, 19: 40792
radioisotopes in, dietary contamination in Japan by, 19: 40309(R) (NP-15180)
SEALS AND GLANDS
design and performance of mechanical face-type, 19: 42026
design and testing of liquid-metal pump, 19: 40718 (TIM-909)
design for tubular elements, 19: 40705(P)
materials for liquid-metal pump, development and testing of, 19: 40718 (TIM-909)
test of NMPO blower shaft, duration, 19: 40701 (TID-22007)
tests of dynamic centrifugal shaft, for liquid metal pumps, 19: 40702 (TIM-914)
SEED
radiation dosage for lethality in dormant Guar, 19: 40376
radiation effects on content of ascorbic acid and ascorbic acid oxidase in *Momordica charantia*, 19: 40371
SEISMIC WAVES
travel times from central Pacific nuclear explosions, 19: 40779
SELENIUM
determination in copper by activation, 19: 40422

positron annihilation in, angular correlations from, (E), 19: 41285
SEMICONDUCTOR DETECTORS
amplifier circuit designs for, review, (E), 19: 40899
charge carrier trapping in lithium-drifted germanium, (E), 19: 40919
design for fissiochemical experiments, 19: 40547(R) (AGN-8137(Vol.I))
development for airborne radiation, 19: 40834(R) (UCRL-14151)
performance for internal conversion measurements, 19: 40880 (UCRL-16035)
performance in charged particle elastic scattering studies, 19: 40962
performance of lithium-drifted silicon, in thermal-vacuum environment, (E), 19: 40902
research on, 19: 41678(R) (PR-P-65)
response of surface-barrier, to fission fragments, (E), 19: 40901
use in fission-fragment detection, pulse-height defects in, 19: 40892
uses in scattering chambers, 19: 40907
SEMICONDUCTORS
radiation effects on photoconductivity in silicon, electron, 19: 40933(R) (NP-15300)
radiation effects on photoconductivity of silicon, electron, 19: 40934(R) (NP-15301)
radiation effects on germanium, neutron, 19: 40939
radiation effects on thermally stimulated conductivity of silicon, neutron, (E), 19: 41985
SENA POWER REACTOR
design and construction, 19: 42087(R) (EUR-2428.f)
SEPARATION PROCESSES
development of dry, for processing irradiated fuel elements, review of, 19: 40667
SERUMS
preparation of iodine-131-labeled sterile pyrogene-free human, 19: 40639
SHEEP
cesium-137 metabolism in adults and lambs, after oral administration, 19: 40334
liver function tests in, 19: 40350 (HW-SA-3723)
pathological effects of ingested cesium-137 in, 19: 40334
radiation injuries of liver of, induced by injected neptunium-237, 19: 40350 (HW-SA-3723)
strontium-90 metabolism in fetuses and newborn, after intravenous or oral administration to mother, 19: 40331
SHELTERS
design and costs of tunnel grid blast, 19: 40759 (ORNL-TM-1183)
ground motion effects on contents of buried, 19: 40758 (AD-426249)
SHIELDED CONTAINERS
design for shipping radioactive materials, review, 19: 40823 (SC-RR-65-98, pp 450-72)
fire resistance of lead-lined casks, analysis, 19: 40813 (SC-RR-65-98, pp 107-13)
fire resistance of lead, 19: 40831 (SC-RR-65-98, pp 723-31)
fire test of lead cask, calculations, 19: 40832 (SC-RR-65-98, pp 732-5)
fire test of 15-ton lead-lined, 19: 40827 (SC-RR-65-98, pp 631-50)
fire tests of packagings for radioactive materials, 19: 40814 (SC-RR-65-98, pp 114-18)
impact tests of casks for irradiated fuel, 19: 40818 (SC-RR-65-98, pp 261-82)
test standard for, for radioisotope sealed sources, 19: 40802 (CONF-650616-5)
SHIELDING
calculations for space vehicle, computer programs for, 19: 41954 (NP-15338)
design for low-level radiation counters, 19: 40834(R) (UCRL-14151)
properties of, for silicon solar cells, 19: 40931 (AD-609424)
radiation flux from cylindrical or spherical sources with shell-shaped, 19: 41960
SHIPPING
casks for irradiated fuel, impact tests, 19: 40818 (SC-RR-65-98, pp 261-82)
container design for radioactive materials, review, 19: 40823 (SC-RR-65-98, pp 450-72)
container design for plutonium nitrate and oxide, 19: 40825 (SC-RR-65-98, pp 609-19)
container development and tests for radioactive materials, 19: 40816 (SC-RR-65-98, pp 141-86)
container drop tests for uranium hexafluoride, 10-ton capacity, 19: 40824 (SC-RR-65-98, pp 580-608)
container fire tests, modeling of, 19: 40815 (SC-RR-65-98, pp 133-40)
container fire test, 15-ton, 19: 40827 (SC-RR-65-98, pp 631-50)
container for irradiated fuels from power stations in United Kingdom, 19: 40829 (SC-RR-65-98, pp 711-18)
container for low-assay uranium compounds, tests of, 19: 40819 (SC-RR-65-98, pp 330-56)
container response to vehicle collisions, analysis, 19: 40817 (SC-RR-65-98, pp 243-60)
container standardization for radioactive materials, 19: 40822 (SC-RR-65-98, pp 442-9)
container tests for slightly enriched uranium fuel cores, 19: 40820 (SC-RR-65-98, pp 357-76)
container tests for plutonium nitrate solutions, 19: 40821 (SC-RR-65-98, pp 423-41)
of radioactive materials, international conference on, 19: 40808 (SC-RR-65-98)
of radioactive materials, review of research on, 19: 40809 (SC-RR-65-98, pp 17-31)
of radioactive materials, aspects of, 19: 40812 (SC-RR-65-98, pp 74-8)
of radioactive materials, regulatory packaging standards for, 19: 40811 (SC-RR-65-98, pp 45-54)
of radioactive materials, special problems in, 19: 40826 (SC-RR-65-98, pp 625-9)
packages for fissile materials, criticality evaluation of, 19: 40828 (SC-RR-65-98, pp 679-90)
packaging of radioactive materials for, development of standards for, 19: 40810 (SC-RR-65-98, pp 32-44)
safety criteria for, of sealed radioisotope sources, 19: 40802 (CONF-650616-5)
safety standards for, of fissionable materials, 19: 40840
SHIPPINGPORT PRESSURIZED WATER REACTOR
development of, abstracts and indexes on, 19: 42101 (WAPD-PWR-1606 (Add.2))
SHOCK TUBES
design for plasma diagnostics, nonuniform, 19: 41855 (NP-15142)
performance of coaxial and tee types, 19: 40849 (TID-22061)
performance of double-driver, (E), 19: 41162
plasma behavior and properties in magnetically driven, (E), 19: 41936
SHOCK WAVES
effects of hydromagnetic, on solar proton events, (T), 19: 41230
excitation in plasma, (E), 19: 41911
hydrodynamic properties of, technique for observing, 19: 41118 (LA-DC-6996)
interactions of MHD supported, with magnetic fields, 19: 41120 (N64-30509)
ionization upstream from, 19: 41935
propagation in argon and xenon, properties of, 19: 41128 (UCRL-12466)
propagation in continuous media, one-dimensional, (T), 19: 41126 (SCL-DR-65-75)
propagation in double-driver shock tubes, (E), 19: 41162
propagation in plasma, heating effects from, 19: 41861 (NP-15255)
propagation in plasma in accelerating tube, splitting of, (E), 19: 41880
propagation in plasma, nonlinear stationary, (T), 19: 41915
propagation in solid explosives, 19: 42206 (LA-DC-6992)
structure in fully ionized plasma, (T), 19: 41928
structure of, book on, 19: 41161
SILICON
analysis for traces of gold by neutron activation methods, 19: 40437
corrosion by aluminum–silicon and water of coatings of, on uranium, 19: 40949 (ISC-640)
current carrier lifetimes in lithium-compensated, 19: 41964 (JINR-P-2201)
deposition on uranium by diffusion from molten magnesium bath, 19: 40949 (ISC-640)
determination by spectrochemical methods, voltage-fluctuation patterns in, 19: 40416
effects on oxidation resistance and strength of chromium–magnesia composites, 19: 41022(R) (NP-15292)
effects on stainless steel corrosion by nitric acid–potassium dichromate, 19: 40947(R) (EURAEC-1403)
nuclear resonance fluorescence in, (E), 19: 41828
performance of lithium-drifted, for radiation detection in thermal-vacuum environment, (E), 19: 40902
proton transmission at 5 Mev, direction and energy distributions from, (E), 19: 41788
radiation effects on conductivity of n-type, electron and neutron, 19: 40935 (SC-DC-65-1247)
radiation effects on diodes of, alpha, 19: 40937 (UCRL-11958)
radiation effects on efficiency of solar cells of, electron, 19: 40931 (AD-609424)
radiation effects on photoconductivity in semiconductors of, electron, 19: 40933(R) (NP-15300)
radiation effects on photoconductivity in semiconductors of, electron, 19: 40934(R) (NP-15301)
radiation effects on thermally stimulated conductivity of, neutron, (E), 19: 41985
radiation effects on ultrapure crystals of, electron, 19: 41998(T)
radioinduced base current in transistors of, neutron, 19: 40936 (SC-R-65-912)

spectra of atomic, in plasma jets, (E), 19: 41287
thermionic work function of, effects of sorbed sodium on, 19: 41124(R) (NP-15108)
SILICON FLUORIDES
spectra of diatomic, in plasma jets, (E), 19: 41287
SILICON ISOTOPES Si-28
energy levels, (E), 19: 41828
proton reactions at 150, 340, and 660 Mev, cascade theory for, (T), 19: 41811(T)
SILICON JUNCTIONS
radiation effects on defect charge state of semiconductor, 19: 41974
SILICON NITRIDES
properties and possible uses at high temperatures, 19: 41081
SILICON OXIDES
effects on oxidation resistance and strength of chromium–magnesia composites, 19: 41022(R) (NP-15292)
sorptive properties of surfaces of, for ions from aqueous solutions, 19: 42200 (COO-1354-5)
spectra of diatomic, in plasma jets, (E), 19: 41287
yield from quartz sputtering in argon discharge, (E), 19: 41257
Al_2O_3–SiO_2, radiation effects on activities in acid-catalyzed reactions, 19: 41099
Al_2O_3–SiO_2, sorptive properties of surfaces of, for ions from aqueous solutions, 19: 42200 (COO-1354-5)
Li_2O–SiO_2–ZrO_2, phase studies, 19: 41038
SILICON SYSTEMS
Al–Fe–Si–U, hot hardness and microstructure of, effects of heat treatments on, 19: 40958
Al–Fe–Si–U, properties of, effects of chromium and molybdenum on high-temperature, 19: 40958
Al–Si, corrosion by aluminum–silicon and water of coatings of, on uranium, 19: 40949 (ISC-640)
Al–Si–U, hot hardness and microstructure of, effects of heat treatments on, 19: 40958
Co–Nb–Si, crystal structure of compounds in, 19: 41069
Si–U, hot hardness and microstructure of, effects of heat treatments on, 19: 40958
Si–U, phase studies, 19: 40958
SILVER
argon ion sputtering at 160 to 200 ev, angular distributions from, 19: 41259
determination by spectrochemical methods, voltage-fluctuation patterns in, 19: 40416
determination in copper by activation, 19: 40422
effects on superconductivity of niobium–tin alloys, (E), 19: 41609
electron transmission in foils of, low-energy, 19: 41969 (ORNL-TM-1153)
helium ion scattering by, Auger electron emission from, (T), 19: 41270
nitrogen ion ranges at 0.4 and 2.5 Mev, (E), 19: 41269
proton reactions at 157 Mev, nucleon clustering from, (E), 19: 41831
proton transmission in foils of, low-energy, (E), 19: 41969 (ORNL-TM-1153)
separation from uranium by chromatography on cellulose columns, tracer studies of, 19: 40687
sorptive properties of surfaces of, for iodine in high-temperature helium loop, 19: 40397 (ORNL-TM-1134)
sublimation of monocrystalline, angular distributions from, 19: 41259
thermodynamic properties at high pressures and temperatures, 19: 40459 (NP-15324)
SILVER ALLOYS
rare earth–Ag, electric conductivity of CsCl-type phases in, 19: 41005 (CALT-221-11)
SILVER BROMIDES
proton reactions at 150, 340, and 660 Mev, cascade theory for, (T), 19: 41811(T)
SILVER COMPLEXES
with α, β, γ, δ-tetraphenylporphines, retentions in Szilard-Chalmers (n,γ) recoil reactions in, 19: 40612
SILVER IONS
angular distributions of sublimed and sputtered, from silver monocrystals, 19: 41259
SILVER ISOTOPES Ag-107
alpha reactions (α,2n) at 22 Mev, isomer production in, (E), 19: 41802(T)
meson (μ^-) capture by proton pairs in, (E/T), 19: 41753
SILVER PHOSPHATES
$Al(PO_3)_3$–$LiPO_3$–$AgPO_3$, radio-photoluminescence polarization of glasses of, 19: 40588
SINGLE CRYSTALS
preparation of spherical, refractory, (E), 19: 40991
sputtering by ions, energy dependence of, (T), 19: 41271(T)
SINTERING
process for metal oxide powder, 19: 40995(P)
SKELETON
cerium-144 content in rat, after intratracheal administration, 19: 40313
strontium-90 content in rat, after chronic oral administration, effects of age, 19: 40323
strontium-90 content of dog, after chronic ingestion, effects of age, 19: 40324
strontium-90 content in dog, after chronic ingestion, 19: 40325
strontium-90 content of dog, after chronic ingestion, 19: 40327
strontium-90 content in swine, after chronic ingestion, 19: 40328
strontium-90 content of cattle, effects of age, 19: 40330
strontium-90 content in, of sheep fetus after intravenous or oral administration to mother, 19: 40331
strontium-90 metabolism in calf, after ingestion by mother or self, effects of age, 19: 40329
strontium-90 metabolism in rabbit, effects of dietary calcium and inflammation on, 19: 40343
SKIN
radiosensitivity of rabbit, effects of 5-fluorouracil on, 19: 40394
SLUG CANS
spacer design for, 19: 42074(P)
SMOKES
polonium-210 content of tobacco, 19: 40805 (NRS-30)
SODIUM
analysis for impurities, development of methods for, 19: 40409(R) (MSAR-65-95)
analysis for oxides, by electric potential measurement, 19: 40409(R) (MSAR-65-95)
combustion of, particle and iodine release from, 19: 40803 (NAA-SR-Memo-9719)
corrosive effects on type 316 stainless steel, effects of carbon and oxygen on, 19: 40969(R) (MSAR-65-96)
determination by spectrochemical methods, voltage-fluctuation patterns in, 19: 40416
determination in copper by activation, 19: 40422
effects of sorbed, on germanium crystal electron reflection, 19: 41124(R) (NP-15108)
effects of sorbed, on germanium and silicon work function, 19: 41124(R) (NP-15108)
effects on air ionization in space vehicle hypersonic re-entry flights, 19: 41121 (N64-30658)
electron scattering at 0.003 to 25.0 ev, exchange effects and polarization in, (T), 19: 41286
impurities in, magnetic effects of, 19: 40409(R) (MSAR-65-95)
positron annihilation in, angular correlations from, (E), 19: 41285
reactions with hydrogen, light modulation in spin-exchange, (E), 19: 41262
reactor criticality effects per atom, (E), 19: 42077 (ANL-7014)
separation from magnesium cyclotron targets by solvent extraction using ethanol, 19: 40686
SODIUM ACID SULFITES
reactions with iodine compounds, 19: 40402 (BMI-X-10137)
SODIUM ALLOYS
K–Na, purification by solvent extraction using naphthalene–tetrahydrofuran, 19: 40409(R) (MSAR-65-95)
Sb–Na, electric conductivity of Na_3Sb, temperature dependence of, 19: 41124(R) (NP-15108)
SODIUM BROMIDES
radiation effects on luminescence centers in silver-activated, x, 19: 41977
radiation effects on phosphorescence of, influence of F-band illumination on x, 19: 40570
reactions with praseodymium bromide, 19: 40469
SODIUM BRONZE
Na–W, positron annihilation in, (E/T), 19: 41158
SODIUM CHLORIDES
complexes with praseodymium, properties of, 19: 40469
corrosive effects on chromium–iron–nickel alloys, 19: 40967(R) (COO-1319-27)
deformation of rock salt, at high temperature and pressure, 19: 42198
radiation effects on thermal de-excitation processes in nickel-activated, 19: 41101(T)
radiation effects on F centers and photostimulated emission in, x, (E), 19: 41980
radiation effects on luminescence of europium-activated, visible and x, 19: 40567
radiation effects on photoluminescence of, x, 19: 40569
radiation effects on phosphorescence of, influence of F-band illumination on x, 19: 40570
radiation effects on luminescence of nickel-activated, electric-field pre-exposure in x, 19: 40571

radiation effects on electroluminescence of, x, 19: 40572
radiation effects on luminescence centers in silver-activated, x, 19: 41977
radioinduced plastic flow in, x, 19: 40594
KCl–SmCl–NaCl, phase studies, 19: 40517
SODIUM FLUORIDES
KF–NaF–ScF_2, phase studies, 19: 40512
ScF_3–NaF, preparation and properties of Na_3ScF_6, 19: 40512
SODIUM GRAPHITE REACTORS
design and evaluation of 200 Mw(e) prototype, 19: 42094 (NAA-SR-11314)
tubes for, design and testing of, 19: 41019 (NAA-SR-11323)
SODIUM HYDROXIDES
solvent properties for aluminum casing on uranium spent fuel element, 19: 41086(P)
solvent properties for SAP, 19: 40655 (RT/CHI(65)-1)
SODIUM IODIDES
luminescence yields of, absolute gamma, 19: 40593(T)
radioinduced luminescence of thallium-activated crystals of, x, (E), 19: 40908(T)
radioinduced luminescence spectra of thallium-activated crystal phosphors of, thermal and x, 19: 40568
reactions with dodecane and sodium bisulfide, 19: 40402 (BMI-X-10137)
use of well-type thallium-activated crystals of, for detection of gamma radiation from uranium-235 fission products, (E/T), 19: 40891
SODIUM ISOTOPES Na-21
energy levels from neon-20 (p,γ) reactions at 1.17 Mev, (E), 19: 41838
energy levels of, collective representation of low-lying, (T), 19: 41757
SODIUM ISOTOPES Na-22
preparation by irradiation of magnesium in cyclotron, 19: 40686
separation from cyclotron targets, 19: 40637(T) (ORNL-tr-625)
SODIUM ISOTOPES Na-23
deuteron reactions (d,α) at 9.3 Mev, differential cross sections for, (E), 19: 41684
energy levels from neon-22 (p,γ) reactions at 1.28 to 1.86 Mev, (E), 19: 41838
energy levels of, collective representation of low-lying, (T), 19: 41757
gamma transitions from neon-22 (p,γ) reactions at 1.278 Mev, (E), 19: 41837
SODIUM ISOTOPES Na-24
dispersion of, caused by fire, 19: 40830 (SC-RR-65-98, pp 719-22)
leakage from radioisotope packages after fire tests, 19: 40831 (SC-RR-65-98, pp 723-31)
SODIUM MOLYBDATES
oxygen isotopic exchange in melts of, at 700 to 955°C, 19: 40506
SODIUM NITRATES
crystallization from melts, fission product uptake and separation in directional, 19: 40683
SODIUM OXIDES
content in McKelveyite uranium mineral, 19: 40799
determination in sodium by electric potential measurement, 19: 40409(R) (MSAR-65-95)
SODIUM PLUTONYL ACETATES
metabolism in rats, 19: 40317
SODIUM REACTOR EXPERIMENT
cooling system of, performance of components of primary, 19: 42096 (NAA-SR-11396)
SODIUM SILICATES
reactions with lanthanum sulfate, preparation of lanthanum silicate by, 19: 40518
SODIUM SULFATES
effects on distortion in development of nuclear emulsions, 19: 40884
oxygen isotopic exchange in melts of, at 700 to 955°C, 19: 40506
$Ce_2(SO_4)_3$–Na_2SO_4, thermal stability, 19: 40511
$Gd_2(SO_4)_3$–Na_2SO_4, thermal stability, 19: 40511
$La_2(SO_4)_3$–Na_2SO_4, thermal stability, 19: 40511
$Nd_2(SO_4)_3$–Na_2SO_4, thermal stability, 19: 40511
$Pr_2(SO_4)_3$–Na_2SO_4, thermal stability, 19: 40511
$Sm_2(SO_4)_3$–Na_2SO_4, thermal stability, 19: 40511
SODIUM TUNGSTATES
oxygen isotopic exchange in melts of, at 700 to 955°C, 19: 40506
SOILS
cosmic meson (μ) energy losses in, below 100 Tev, (T), 19: 41296
density measurements by gamma scattering, 19: 40755
strontium-90 uptake by oat plants from, effects of soil type and fertilizer program on, 19: 40310
SOLAR BATTERIES
energy conversion in, review, 19: 41319
radiation effects on efficiency of silicon, electron, 19: 40931 (AD-609424)
SOLAR FLARES
detection and measurement of, from nearby stars, (E), 19: 41203 (AD-600154)
effects on electron and proton distributions in outer radiation belts, (E), 19: 41312
effects on ionospheric sudden disturbances, 19: 41573 (RPU-S19)
gamma emission in, mechanism of, 19: 41289
photometry of eruptive phenomena in, 19: 41234
properties of, data for Sept. 1963, 19: 41603
structure of nimbus of, (T), 19: 41228
SOLAR RADIATION
acceleration of proton, by hydromagnetic shock waves, (T), 19: 41230
effects on electron production rate in ionosphere, (E/T), 19: 41598
effects on Forbush decreases, (E), 19: 41305
effects on geomagnetic storms, (E), 19: 41602
effects on ionospheric sudden disturbances, 19: 41573 (RPU-S19)
emission of r-f, from type II outburst, (T), 19: 41229
emission of X, from corona, 19: 41209(T) (N64-22932)
flux and rigidity spectra of alpha and proton, (T), 19: 41232
flux of plasma, correlations with geomagnetic distrubances, (E), 19: 41580
flux of x, (E), 19: 41231
propagation of proton, interplanetary magnetic field effects on, 19: 41228
properties of r-f, data for Sept. 1963, 19: 41603
properties of type III radio bursts in solar corona, (E), 19: 41218
radio emission from 1953 to 1963, 19: 41217
SOLENOIDS
development for high-temperature valves, 19: 40765(R) (NP-15309)
stresses in multilayer superconducting, (T), 19: 41632
use of water-cooled, in Mössbauer spectroscopy, 19: 41848
SOLID SOLUTIONS
neutron scattering by impurity atoms in, one-phonon peak in slow, (T), 19: 41991(T)
SOLIDS
book: *Solid State and Low Temperature Physics in the USSR*, 19: 42004
fission-fragment track registration on surfaces of, (E/T), 19: 41138
light scattering by density fluctuations in, (T), 19: 41971 (UCRL-7968-T)
properties of, research on, 19: 41967(R) (MIT-QPR-57)
properties of, research on, 19: 41678(R) (PR-P-65)
radiation effects on, defect structure and saturation from, 19: 41102
gas–solid, fluid mechanics and heat transfer in turbulent suspensions of, research program on, 19: 40742(R) (TID-22002)
SOLUTIONS
radiolysis of frozen, formation of solvated electrons in gamma, 19: 40551 (KFK-293)
sorption of ions by alumina, alumina–silica, and silica gel surfaces, 19: 42200 (COO-1354-5)
SOLVENT EXTRACTION PROCESSES
behavior of actinides and fission products in tributyl phosphate and di-2-amyl 2-butylphosphonate, in short-residence contactors, 19: 40645 (CONF-650918-1)
tests of flowsheets for separating plutonium, thorium, and uranium from fuel scrap, 19: 40643 (BNWL-57)
uses for separating long- and short-lived radioisotopes in wastes, (E), 19: 42197
SOLVENTS
acido-basicity of, general, 19: 40466 (UJV-1209/65)
use of paraffins as diluents in Purex Process, 19: 40646 (CONF-650918-2)
SONIC INSPECTION
methods of, for detection of non-bond in clad structures, 19: 40756
methods of, for Nimrod power plant alternator, 19: 41201
methods of, for nozzle welds in steel pressure vessels, 19: 42025
methods of, for welds in steel pressure vessels, 19: 42024
SOUND
attenuation coefficient of megacycle second, (E), 19: 41633
scattering by an impenetrable sphere, h-f, (T), 19: 41129
SOUTHWEST EXPERIMENTAL FAST OXIDE REACTOR
reactivity transients including meltdown, methods for analysis of, 19: 42100 (UNC-5092)
SPACE FLIGHT
air ionization in hypersonic re-entry, effects of cesium and sodium contaminated cone materials on, 19: 41121 (N64-30658)
propulsion systems for, development of electric, 19: 40768
SPACE POWER UNIT REACTOR
bearing tests for liquid metal pumps in, 19: 40703 (TIM-916)
SPACE VEHICLES
entry into planetary atmospheres, acceleration measurements in, (T), 19: 41123 (NASA-TR-R-225)
motion under influence of earth-moon system, 19: 41205 (N64-31725)
power plants for, analysis of radiators for nuclear, (T), 19: 40731 (AD-609969)

propulsion systems for, electric, 19: 40771
re-entry of, air ionization in hypersonic, (T), 19: 41121 (N64-30658)
shielding of, computer programs for calculations on, 19: 41954 (NP-15338)
shielding of, electromagnetic, 19: 41952(R) (N64-31552)
SPARK CHAMBERS
design and operation of neon-filled, 19: 40886
performance with avalanche and primary-ionization triggering, (E), 19: 40898
SPECIFIC HEAT
measurement in electrical conductors, pulse heating calorimetric method for, 19: 40700 (ORNL-TM-1187)
SPECTROMETERS
data processing from, using numerical adapted filters, (E), 19: 40906
SPECTROSCOPY
accuracy of, effects of standard preparation on, 19: 40434
electric arc voltage fluctuations in, 19: 40416
SPHERES
analysis of filament-wound, with polar opening, 19: 40698 (ACF-9)
fabrication of monocrystalline, from refractory materials, (E), 19: 40991
motion in fluids and ionized gases, 19: 41114 (AD-617258)
motion in smooth rotating drums, 19: 40982 (ORNL-3819)
sound wave scattering by impenetrable, h-f, (T), 19: 41129
stability of gravitationally bound of perfect fluid, (T), 19: 41563
temperature distribution in gamma-active, (T), 19: 42191 (AEET/HP/TH-20)
SPINELS
effects on oxidation resistance and strength of chromium–magnesia composites, 19: 41022(R) (NP-15292)
STAINLESS STEEL
analysis for martensite, method for, 19: 40947(R) (EURAEC-1403)
bonding to Scotchlite SPR704 reflective material, 19: 40917
corrosion by coal gasification products at high temperatures, 19: 42127(R) (TID-22009)
corrosion by nitric acid–potassium dichromate, effects of silicon on, 19: 40947(R) (EURAEC-1403)
corrosion by sodium of type 316, effects of carbon and oxygen on, 19: 40969(R) (MSAR-65-96)
corrosion products films on, composition of, 19: 40961
creep buckling and collapse properties of tubes of type 304, 19: 41019 (NAA-SR-11323)
deposition on thick steel plates, 19: 40979(R) (EURAEC-1351)
electric conductivity of 304, effects of carbon on, 19: 40409(R) (MSAR-65-95)
electron and ion emission from cesiated and vacuum surfaces of 304, (E), 19: 41284
gamma heating in DFR, (E), 19: 42117
internal friction of type 304, at 80 to 423°F, 19: 40968(R) (EURAEC-1424)
mass transfer to niobium–zirconium alloy from Type 316 and 321, in liquid potassium at 1400°F, 19: 40970(R) (NASA-CR-54390)
mechanical properties and microstructure of high purity, 19: 40947(R) (EURAEC-1403)
performance of 304, in measuring carbon in sodium, 19: 40409(R) (MSAR-65-95)
radiation effects on stress-strain properties of type 304, neutron, 19: 40961
radiation effects on mechanical properties of austenitic chrome nickel, neutron, 19: 41093(T) (FTD-TT-65-125)
solvent properties for nitrogen at 1000°F, effects of ammonia–hydrogen ratio on, 19: 40968(R) (EURAEC-1424)
sorptive properties of surfaces of, for iodine in high-temperature helium loop, 19: 40397 (ORNL-TM-1134)
stress-corrosion cracking in magnesium chloride, effects of purity on, 19: 40947(R) (EURAEC-1403)
graphite–stainless steel, heat transfer from colloidal gas suspensions of, 19: 42127(R) (TID-22009)
stainless steel–UO_2, fabrication of fuel elements of, 19: 40958
stainless steel–UO_2, radiation effects on, 19: 40958
STANDARDS
for packaging of radioactive materials for transport, 19: 40810 (SC-RR-65-98, pp 32-44)
in activation analysis, National Bureau of Standards facilities and techniques for developing, 19: 40450
STANFORD LINEAR ACCELERATOR
development, 19: 41170 (SLAC-42)
STARS
atmospheres of, effects of helium hydride ion in model, (T), 19: 41240
element formation mechanisms in, (T), 19: 41235
evolution of, computer program for solution of time dependent equations in, 19: 41210(T) (N64-25282)
flare activity of nearby, 19: 41203 (AD-600154)
gravitational radiation from binary systems of, (T), 19: 41206 (N64-33291)
isotopic abundances of carbon, nitrogen, and oxygen in, effects of helium and hydrogen burning on, (T), 19: 41242
radiation absorption in, (T), 19: 41211
radiative-acoustic waves in gaseous, 19: 41219
radio brightness contours of 3C273, (E), 19: 41226
temperature distributions in partially degenerate helium cores in, neutrino loss effects on, (T), 19: 41237
STATISTICS
analysis of effects of variables on fissiochemical reactions, 19: 40547(R) (AGN-8137(Vol.I))
error determination in one-parameter systems, 19: 42225 (UCRL-12050)
formalism for energy level density for medium and heavy nuclei, 19: 41655 (BNL-934)
formalism for particle mixtures with type-dependent intermolecular potentials, (T), 19: 41130
STEAM
corrosive effects on aluminum–chromium–iron–yttrium alloy at 500 to 1300°C, 19: 40961
steam–water, void fraction measurement by x-ray attenuation in two-phase flow of, 19: 40745
STEEL
analysis for rare earths, 19: 40445
deposition of stainless steel cladding on very thick, 19: 40979(R) (EURAEC-1351)
impact strength of thick, effects of heat treatments on, 19: 41007(R) (EURAEC-1400)
reactor criticality effects, (E), 19: 42077 (ANL-7014)
thermal conductivity of, evaluation of cut bar method for measuring, 19: 41029
welded joints in thick, effects of filler metal and flux on, 19: 41007(R) (EURAEC-1400)
welds in, methods for ultrasonic inspection of, 19: 42025
welds in, radiographic and ultrasonic methods for inspecting, 19: 42024
2,2'-STILBENEDISULFONIC ACID, 4,4'-BIS[(6-CARBOXY-2,3,4-TRIHYDROXYPHENYL)AZO]-
analytic use for zirconium determination, 19: 40441
2,2'-STILBENEDISULFONIC ACID, 4,4'-BIS[(2,3,4-TRIHYDROXY-PHENYL)AZO]-
analytic use for zirconium determination, 19: 40441
STRATOSPHERE
fallout content in, residence time of, 19: 40789
fallout in northern, 1963-64, 19: 40785 (TID-21224)
models and processes of lower, (T), 19: 41570 (CONF-765-11)
STRONTIUM
content in man, spectrographic method for determining, 19: 40309(R) (NP-15180)
content in sea water, human contamination by, 19: 40309(R) (NP-15180)
effects on strontium-90 uptake by plants from soils, 19: 40310
ion density and temperature in ionized, spectroscopic determination of, (E), 19: 41883
light resonant absorption by ionized, ion density and temperature determination from, (E), 19: 41883
separation from calcium using pyridine-2,6-dicarboxylic acid resins, chromatographic, 19: 40674
separation from uranium by chromatography on cellulose columns, tracer studies of, 19: 40687
sorption on tungsten ferrocyanide, tracer studies of, 19: 40679
STRONTIUM FLUORIDES
luminescence centers in rare-earth activated, 19: 41978
STRONTIUM ISOTOPES
content in rocks from Indian Ocean islands, 19: 40791
STRONTIUM ISOTOPES Sr-86
content in rocks from Indian Ocean islands, 19: 40791
STRONTIUM ISOTOPES Sr-87
content in rocks from Indian Ocean islands, 19: 40791
STRONTIUM ISOTOPES Sr-88
helium-3 reactions (He-3,p) with, isomeric cross section ratios for, (E), 19: 41820
STRONTIUM ISOTOPES Sr-89
beta dose from spherical particles of, calculational models for, 19: 40635 (NUS-217)
content in rain at Fayetteville, Arkansas, 19: 40785 (TID-21224)
effects on function and structure of pancreas, of injected, 19: 40358(T) (FTD-TT-65-48, pp 577–8)
metabolism in rats of, after oral or intravenous administration, 19: 40321
metabolism in rats of, after oral administration of mixed uranium fission products, 19: 40322
metabolism in rats, effects of complexing agents on, 19: 40344

STRONTIUM ISOTOPES Sr-90
biological effects in rats, after chronic low-dose oral administration, 19: 40335
biological effects in rats of, effects of administration rate and dose on, 19: 40336
content in Alaskan Arctic biota, 1959 to 1965, 19: 40780 (BNWL-SA-242)
content in food chains in Alaska, 1959 to 1965, 19: 40780 (BNWL-SA-242)
content in milk of, effects of dietary calcium consumed by cows, 19: 40341
content in northern stratosphere, 1962-63, 19: 40785 (TID-21224)
content in rain at Fayetteville, Arkansas, 19: 40785 (TID-21224)
effects on function and structure of pancreas, of injected, 19: 40358(T) (FTD-TT-65-48, pp 577–8)
metabolism by oat plants, effects of potassium phosphate and calcium hydroxide on, 19: 40310
metabolism in animals, effects of dietary constituents on, 19: 40342
metabolism in calf skeleton of, after ingestion by mother or self, effects of age, 19: 40329
metabolism in dogs of, after chronic ingestion, 19: 40324
metabolism in dogs of, after chronic ingestion, 19: 40325
metabolism in dogs and offspring of, after chronic ingestion, 19: 40327
metabolism in fetus of cattle of, after ingestion by the mother, 19: 40330
metabolism in fetus of sheep, after intravenous or oral administration to mother, 19: 40331
metabolism in milk cows of, after chronic ingestion, 19: 40332
metabolism in rats of, after oral or intravenous administration, 19: 40321
metabolism in rats of, after chronic oral administration, 19: 40323
metabolism in skeleton of, effects of dietary calcium and inflammation in rabbits, 19: 40343
metabolism in swine of, after chronic ingestion, 19: 40328
metabolisms in rats of, after intratracheal administration, 19: 40312
pathological effects in dogs of injected, 19: 40378
poisoning by, drug evaluation for emergency treatment, 19: 40339
processing into planar beta sources, (E), 19: 40560
radiation hazards of inhalation and ingestion by man of, 19: 40805 (NRS-30)
separation from fuel storage basin effluent by ion exchange, 19: 40651 (IDO-14657)
separation from milk by moving bed ion exchange columns, 19: 40697(P)
use as hydrogenation catalyst, 19: 40553(R) (NYO-2978-34)
use in beta ionization detector for chromatographic determination of permanent gases, 19: 40415(T) (CEA-tr-R-1839)

STRONTIUM MOLYBDATES
electron paramagnetic resonance of gadolinium ions in, 19: 41994(T)

STRONTIUM OXIDES
content in McKelveyite uranium mineral, 19: 40799
effects on sintered density of plutonia powders, 19: 40981 (NUMEC-2389-6)
B_2O_3–SrO, emission spectra of cerium- and samarium-activated phosphors of, 19: 40494(T)

STRONTIUM SULFIDES
luminescence properties for gamma dosimetry, infrared-stimulated, 19: 40879 (UCRL-12371)

STYRENE POLYMERS
physical properties of foam, 19: 41000 (ACF-10)
proton multiple scattering by thin films of, at 75 to 200 kev, (E/T), 19: 41273
radioinduced photoconductivity in, pulsed gamma, 19: 41091 (SC-R-65-943)
use in preparation of chromatographic resins, 19: 40674
PuO_2–polystyrene, criticality experiments on, 19: 42038(R) (BNWL-95, pp 27-35)

SULFOSALICYLATE COMPLEXES
with rare earths, composition and formation constants, 19: 40513

SULFUR
determination in copper by activation, 19: 40422
neutron reactions (n,γ) at 0.025 ev, spectra from, 19: 40896

SULFUR DIOXIDES
determination in atmosphere, use of radioactive reagent for, 19: 40410 (ORNL-P-494)
use in carbon dioxide reactor cooling streams to inhibit reaction with graphite moderator, 19: 42015(P)

SULFUR ISOTOPES S-32
proton binding energy in, measurement of, 19: 41660 (ISS-65/3)

SULFUR ISOTOPES S-35
determination in biological material by scintillation counting of beta decay, 19: 40425
determination in sea water, method for, 19: 40431
recoil reactions with biologically active compounds, yields of labeled products in, 19: 40619
recoil reactions with organic compounds, formation of polymeric products in, 19: 40628

SULFURIC ACID
separation of scandium from, by solvent extraction using alkyl phosphates, 19: 40689
H_2SO_4–H_2SO_4, solvent properties for aluminum tubes, 19: 40655 (RT/CHI(65)-1)

SUN
activity of, corpuscular streams from 19th cycle, 19: 41216
activity of, properties of 1954 to 1963 cycle of, 19: 41214
activity parameters for March 1965, 19: 41589
activity parameters for Sept. 1963, 19: 41603
charged-particle interactions with coronal plasma, 19: 41933
chromosphere of, spectral line profiles in, (T), 19: 41220
iron and oxygen autoionization in plasma of, collisional excitation in, (T), 19: 41244
magnetic field of, co-rotation of corona in model of, (T), 19: 41241
magnetic fields and motions in undisturbed photosphere of, 19: 41221
plage index spectra of, comparison with power spectra of artificial time series, 19: 41224
radio bursts in corona of, properties of type III, 19: 41218
radio emission from, 1953 to 1963, 19: 41217
spot formation, model of cyclic, 19: 41215
x radiation production and spectra of, 19: 41213
x ray emission from corona of, soft, 19: 41209(T) (N64-22932)

SUPERCONDUCTIVITY
enhancement of, chemical, 19: 40543
magnetic flux penetration in cylinders of type-II superconductors, (E/T), 19: 41612
research programs on, at Siemens-Schuckertwerke laboratories, Erlangen, Germany, 19: 42228
theory of nuclear pairing interaction, 19: 41843

SUPERCONDUCTORS
critical characteristic curves of, measurement of, 19: 41630
critical current in surface of type-II, asymmetry in, (T), 19: 41616
density of states from excitation in type II, (T), 19: 41623
electric current and magnetic field distribution in type II, 19: 41637
electron interactions in, isotropic model for coulombic, 19: 41627(T)
electron tunneling in, theoretical review for Josephson, 19: 41607 (LA-3342)
electron tunneling in, photon emission in Cooper-pair, (E), 19: 41631
energy gap of anisotropic, Ginsburg-Landau equations for, 19: 41625
energy spectrum of mixed state, with low density of vortex lines, (T), 19: 41624
magnetization of type-II, 19: 41613
microwave radiation from Josephson junctions of, (E/T), 19: 41614
order parameter in homogeneous and zero fields, perturbation range of, (T), 19: 41622
performance of magnets of, for bubble chambers, 19: 40869 (CONF-650510-14)
properties of porous niobium–tin, effects of metallic impregnants on, (E), 19: 41609
stresses in multilayer solenoid of, (T), 19: 41632
theory of, ground state in BCS, 19: 41629
transition temperature in, magnetic impurity effect on, 19: 41608(R) (MIT-QPR-57, pp 59-65)
tunneling in, theory for quasi-particle, 19: 41607 (LA-3342)
uses of hollow tubes of, for detecting Dirac magnetic monopoles, (E), 19: 41391

SUPERFLUIDITY
book: *An Introduction to the Theory of Superfluidity*, 19: 41636(T)
circulation at quantum level units in helium II, 19: 41620

SUPERHEATERS (NUCLEAR)
operating experience with central-superheat core CSH-1 in Borax-V, (E), 19: 42149 (ANL-6961)

SURFACE TENSION
measurement of alkali metal, apparatus for, 19: 40409(R) (MSAR-65-95)

SURFACES
thermal resistance of contacting, bibliography on, 19: 40744 (UCRL-14264)

SUSPENSIONS
circulation in heat exchange systems, power required for, 19: 42127(R) (TID-22009)
fluid mechanics and heat transfer in turbulent gas–solid, research program on, 19: 40742(R) (TID-22002)
heat transfer from gas-solids, 19: 42127(R) (TID-22009)

SWIMMING POOL REACTORS
cofferdam design for, 19: 42190(P)
loops for, design of trolley for displacement of, 19: 42189(P)

SWINE
strontium-90 metabolism in, after chronic ingestion, effects of dietary

calcium, 19: 40328
SWITCHES
design of multiplexers, for use with self-powered neutron flux detectors, 19: 40866 (AECL-2217)
materials of rotary, wear characteristics of plated coatings as, 19: 42216 (SC-DR-65-269)
SYNCHROCYCLOTRONS
radiation hazards in beam zones of, 19: 41171(T) (N64-33402)
SYNCHROTRONS
beams from CERN, production of antiproton and meson (K⁻), 19: 41184
magnetic screening in ITEF proton, effects on operation of, 19: 41168 (NP-15253)
site survey of 200-Bev for Berkeley, geological, 19: 41178
storage rings for CERN proton, intersecting, 19: 41176
SYSTEMS FOR NUCLEAR AUXILIARY POWER
disposal after operation, methods for, 19: 42140 (NAA-SR-11353)
SYSTEMS FOR NUCLEAR AUXILIARY POWER (SNAP-2)
safety testing of SNAPTRAN 2/10A-1 and 2/10A-3, (E), 19: 42134(R) (IDO-17070)
SYSTEMS FOR NUCLEAR AUXILIARY POWER (SNAP-50)
bearing tests for liquid metal pumps in, 19: 40703 (TIM-916)
SZILARD-CHALMERS REACTIONS
isotopic retentions in, on metal complexes with α, β, γ, δ-tetraphenylporphines, 19: 40612

T

TANTALUM
annealing and melting of, reactions with nitrogen, oxygen, and water vapor in, 19: 40490
corrosion by aluminum and aluminum–uranium alloy at 800 to 1100°C, 19: 40961
corrosion by lithium at 800°C, effects of oxygen on, 19: 40961
determination by spectrochemical methods, voltage-fluctuation patterns in, 19: 40416
determination in alloys and metals, photometric, 19: 40442
determination of traces of, spectrophotometric, 19: 40414 (UCRL-7967)
dislocation structure in, effects of cold working on, 19: 41015 (MIL-TDR-64-282)
dislocation-interstitial interactions in single crystals of, (E), 19: 42002
effects on oxidation resistance and strength of chromium–magnesia composites, 19: 41022(R) (NP-15292)
neutron inelastic scattering at 14 Mev, cross sections for, (E), 19: 41718
oxidation by plasma anodization, 19: 41124(R) (NP-15108)
oxidation of, at 300 to 1300°C, metallographic microscopic studies of, 19: 40972
oxidation of, crystal structure of products of, 19: 41047
performance of screens of, for radiography of steel welds, 19: 40753(R) (EURAEC-1378)
properties of, metallic addition effects on, 19: 41067
reactivity worths of, reactor oscillator for measurement of, 19: 42050 (NAA-SR-11368)
reactor criticality effects per atom, (E), 19: 42077 (ANL-7014)
separation from other metal ions by ion exchange, 19: 40658
separation from rare earth metals, techniques for, 19: 40948 (IS-1195)
solubility in liquid plutonium at 750 to 950°C, 19: 40950 (LA-3338)
stress-rupture properties of, 19: 40961
tantalum-181 nuclear spin resonance in, acoustic excitation of, (E), 19: 41792
tensile properties of, effects of strain-aging and quench-aging on, 19: 41042
thermal expansion to 2500°C, 19: 41009 (GEMP-375)
TANTALUM ALLOYS
Fe–Ta, solubility of nitrogen in, 19: 41065
Hf–Ta, phase studies, 19: 40960
Hf–Ta–W, properties of welds in T-111, 19: 40989
Hf–Ta–W, stress-rupture properties of T-111, 19: 40961
Mo–Ta–V, phase diagram, 19: 41036
Nb–Ta–V, phase diagram, 19: 41036
Nb–Ta–W–Zr, properties of welds in FS-85, 19: 40989
Nb–Ta–Y–Zr, grain size and hardness of, effects of yttrium additions on, 19: 40953 (PWAC-441)
Nb–Ta–Zr, nitrogen and oxygen contents of, effects of yttrium additions on, 19: 40953 (PWAC-441)
Os–Ta, crystal structure, 19: 41045
Sc–Ta, phase studies of solid solution formation in, 19: 41050
Ta–W, dislocation structure in, effects of cold working on, 19: 41015 (MIL-TDR-64-282)
Ta–W, stress-rupture properties, 19: 40961
Ta–W, thermal expansion to 2500°C, 19: 41009 (GEMP-375)
Ta–Y, phase studies of solid solution formation in, 19: 41050
TANTALUM CARBIDES
Co–TaC–TiC–WC, properties for liquid-metal pump seals, 19: 40718 (TIM-909)
TANTALUM ISOTOPES Ta-181
nuclear spin resonance of, acoustic excitation of, (E), 19: 41792
TANTALUM ISOTOPES Ta-182
beta decay of, gamma spectra from, (E), 19: 41704
diffusion in niobium at 874 to 2400°C, 19: 41064
TANTALUM NITRIDES
preparation and properties of red, 19: 40472
solubility products in liquid iron at 1550 to 1750°C, 19: 41065
TANTALUM OXIDES
crystal structure of, electron diffraction studies of, 19: 41047
reactions with ammonia to prepare red tantalum nitride, 19: 40472
Nb_2O_5–Ta_2O_5, phase studies, 19: 41049
TARTARIC ACID
preparation of actinides and lanthanides from, by solvent extraction using amines, 19: 40657
TARTARIC ACID COMPLEXES
with cerium(III) and europium(III), composition and stability, 19: 40510
with lanthanum, composition and stability, 19: 40491
TARTRATES
radiation effects on single crystals of ammonium, ESR spectra of, 19: 40613
TAURINE
radiation effects on urinary excretion of, by rats, 19: 40364
TECHNETIUM FLUORIDE NITRIDES
preparation, 19: 40461 (ORNL-P-491)
TECHNETIUM ISOTOPES Tc-94
cross section ratios from niobium-93 (α,3n) reactions to 42 Mev, isomeric, (E), 19: 41695
cross-section ratios from niobium-93 (α,3n) reactions, statistical model for isomeric, 19: 41696
TECHNETIUM ISOTOPES Tc-95
cross section ratios from niobium-93 (α,2n) reactions to 42 Mev, isomeric, (E), 19: 41695
cross-section ratios from niobium-93 (α,2n) reactions, statistical model for isomeric, 19: 41696
TECHNETIUM ISOTOPES Tc-96
cross section ratios from niobium-93 (α,n) reactions to 42 Mev, isomeric, (E), 19: 41695
cross-section ratios from niobium-93 (α,n) reactions, statistical model for isomeric, 19: 41696
TECHNICAL REPORTS
on hazards control, index to UCRL, 19: 40833 (UCRL-14116)
TEETH
analysis of, neutron activation, 19: 40435
TELEMETERING SYSTEMS
design for remote measurements in radiation environment, (E), 19: 40714 (EUR-2421.d)
TELLURIUM
determination in copper by activation, 19: 40422
positron annihilation in, angular correlations from, (E), 19: 41285
TELLURIUM ISOTOPES Te-117
decay scheme, 19: 41717
TELLURIUM ISOTOPES Te-122
alpha reactions (α,n) at 22 Mev, isomer production in, (E), 19: 41802(T)
TELLURIUM ISOTOPES Te-127
decay of, iodine-127 energy levels from, (E), 19: 41835
metabolism in rats of, after intravenous or oral administration, 19: 40318
TELLURIUM ISOTOPES Te-128
carbon-12 reactions (C-12, C-13) at 40 to 150 Mev, isomeric pair production ratios in, 19: 41674 (NYO-1930-44)
carbon-12 reactions (C-12,3n) with, angular momentum effects on isomeric cross section ratios in, (E), 19: 41821
nitrogen-14 reactions (N-14, N-13) and N-14, N-15) at 40 to 150 Mev, isomeric pair production ratios in, 19: 41674 (NYO-1930-44)
proton reactions (p,pn) at 40 to 150 Mev, isomeric pair production ratios in, 19: 41674 (NYO-1930-44)
TELLURIUM ISOTOPES Te-130
proton reactions (p,pn) at 40 to 150 Mev, isomeric pair production ratios in, 19: 41674 (NYO-1930-44)
TEMPERATURE
distribution in gamma-active spheres, (T), 19: 42191 (AEET/HP/TH-20)
effects on casting materials, 19: 42215 (RFP-625)
TERBIUM
magnetic properties at high pressures, (E), 19: 42005
magnetic transitions in, effects of hydrostatic pressure on, 19: 41077
physical and thermodynamic properties, 19: 40948 (IS-1195)
polarographic behavior in dimethylformamide and dimethylsulfoxide,

19: 40681
preparation and purification, 19: 40948 (IS-1195)
TERBIUM ALLOYS
Au–Tb, phase studies of solid solutions in, 19: 41062
Mg–Tb, thermodynamic properties, 19: 41013 (IS-T-25)
TERBIUM CARBIDES
eutectic temperature between carbon and dicarbide, 19: 41014 (LA-DC-6819)
lattice parameters and phase transformation temperatures in, 19: 41014 (LA-DC-6819)
microhardness, 19: 41014 (LA-DC-6819)
TERBIUM CHLORIDES
complexes with phenanthroline, preparation and properties, 19: 40514
TERBIUM COMPLEXES
with gluconic acids, stability constants, 19: 40508
TERBIUM IONS
electron paramagnetic resonance of trivalent in calcium fluorides, relaxation in, (E), 19: 42000(T)
spectra in acetophenone, energy transfer in, 19: 40504
TERBIUM ISOTOPES Tb-158
beta decay of, dysprosium-158 energy levels from, (E), 19: 41847
production of isomeric states in yttrium-89 (n,nγ) reactions at 14 Mev, cross sections for, (E), 19: 41781
TERBIUM ISOTOPES Tb-159
neutron reactions (n,2n) at 14 Mev, cross sections for terbium-158 isomeric states from, (E), 19: 41781
TERBIUM OXIDES
content in McKelveyite uranium mineral, 19: 40799
TERBIUM OXYSULFIDES
preparation and crystal structure, 19: 40475
TERBIUM SULFIDES
preparation and crystal structure, 19: 40475
TERPHENYL
radiation effects on photoconductivity of, electron, 19: 40601(T)
radiolysis and pyrolysis of, relation of, 19: 40630
THALLIUM
determination by spectrochemical methods, voltage-fluctuation patterns in, 19: 40416
elastic constants of single-crystal, 19: 41012 (IS-T-16)
neutron inelastic scattering at 14 Mev, cross sections for, (E), 19: 41718
optical properties of films of, in vacuum ultraviolet region, 19: 42213 (ORNL-TM-1164)
positron annihilation in, angular correlations from, (E), 19: 41285
THALLIUM ALLOYS
Pb–Tl, critical fields of superconducting, temperature dependence of, (E), 19: 41610
Pb–Tl, Debye temperature and entropy of formation of, 19: 41012 (IS-T-16)
Pb–Tl, elastic constants of single-crystal, 19: 41012 (IS-T-16)
rare earths–Tl, crystal structure of intermetallic compounds in, 19: 41040
THERMAL CONDUCTIVITY
measurement in high conductivity materials, evaluation of cut bar method for, 19: 41029
of contacting surfaces, bibliography on, 19: 40744 (UCRL-14264)
THERMAL RADIATION
book: *Thermal Radiative Properties*, 19: 41074
detection and measurement of, from nuclear explosions, (E), 19: 40882 (USNRDL-TR-839)
emission from burning hydrogen plume in Kiwi reactor run, 19: 42137 (LA-DC-7313)
radiators for reactor, materials for, 19: 42065(P)
THERMAL REACTORS
design for use at 1000 to 2000°C, 19: 42065(P)
neutron space-dependent spectra in heterogeneous, diffusion approximation for, (T), 19: 42056
THERMIONIC CELLS
conversion efficiency of, using arc mode and direct-path plasma mode, 19: 41317
energy conversion in, review, 19: 41319
radioinduced ionization of cesium vapor in, uv, 19: 40566
response of cesium diode to potential pulses, transient, (T), 19: 41318
THERMOCOUPLES
stability of refractory-metal, at 1000 to 2000°C, (E), 19: 40859
THERMODYNAMICS
effects of equation of state on asymptotic stability of detonations, (T), 19: 41117 (LA-3306)
THERMOELECTRIC CELLS
energy conversion in, review, 19: 41319
THERMOLUMINESCENT DETECTORS
performance of lithium fluoride, for gammas and neutrons, 19: 40868 (BNWL-SA-23)
performance of lithium fluoride and manganese-activated calcium sulfate for small gamma doses, 19: 40877 (RISO-101)
THERMONUCLEAR EXPLOSIONS
biological effects on populations of cities, 19: 40361(T) (ORNL-tr-437)
fallout formation and properties from ground-level, 19: 40786(T) (JPRS-30500)
production of heavy nuclei in, (T), 19: 41765
THERMONUCLEAR REACTIONS
research in Japan, 19: 41881
THERMONUCLEAR REACTORS
plasma containment by relativistic electron coils in Astron, 19: 41867 (UCRL-12455-T)
plasma production in Ogra, properties of hydrogen, 19: 41851 (IAE-635)
plasma production in Ogra, by fast particle injection, 19: 41852 (IAE-676)
THIAZOLES
4-methyl-5β-hydroxyethyl-, labeling by reactions with sulfur-35 recoil atoms, 19: 40619
THIOPHENE
radiolysis of, ESR of radicals in, 19: 40607
THOREX PROCESS
analysis of samples for thorium, automated, 19: 40405 (CONF-650919-1)
evaluation of manganese dioxide head-end step in, 19: 40649 (DP-982)
THORIUM
desorption from field-evaporated tungsten surfaces, 19: 41255
determination in copper by activation, 19: 40422
determination in rocks, using alpha scintillation counter and radioscope, 19: 40432
determination in Thorex process samples, automated, 19: 40405 (CONF-650919-1)
properties of, review, 19: 41025 (ORNL-TM-1144)
proton reactions at 157 Mev, nucleon clustering from, (E), 19: 41831
radiation hazards of inhalation and ingestion by man of, 19: 40805 (NRS-30)
reactions with 8-hydroxyquinaldinic acid, 19: 40545
separation from other elements by electrophoresis in glycolic acid, 19: 40671
separation from plutonium and uranium by solvent extraction in processing of fuel scrap, 19: 40643 (BNWL-57)
separation from protactinium by ion exchange, 19: 40673
separation from rare earths by ion exchange in ammonium thiocyanate–methanol–water systems, 19: 40447
separation from uranium leach solutions by solvent extraction, 19: 40694
separation from uranium and other elements, method for, 19: 40439
separation of protactinium-233 from, by manganese dioxide head-end step in Thorex Process, 19: 40649 (DP-982)
solvent distribution in ammonium thiocyanate–methanol–water systems, distribution coefficients for, 19: 40447
THORIUM ALLOYS
properties of, review, 19: 41025 (ORNL-TM-1144)
In–Th, hardness at 30 to 800°C, effects of indium on, 19: 40958
In–Th, tensile properties at 800°C, 19: 40958
Pu–Th–U, phase studies, 19: 40958
THORIUM CARBIDES
thermodynamic properties of nonstoichiometric, at 800 to 950°C, effects of chemical bonding on, 19: 40485
ThC_2–UC_2, phase studies, 19: 40958
THORIUM COMPOUNDS
properties of ceramic, review, 19: 41025 (ORNL-TM-1144)
THORIUM IONS
reactions with derivatives of Arsenazo III, spectrophotometric studies of, 19: 40426
THORIUM ISOTOPES
performance with uranium isotopes as fuels for power breeder reactors, (E), 19: 42081 (CONF-193-11)
THORIUM ISOTOPES Th-232
alpha fission at 20 to 40 Mev, yttrium-90, niobium-96, and lanthanum-140 yields from, (E), 19: 41779
economics as fuel in spectral-shift pressurized-water power breeders, (E), 19: 42109
neutron fission ratios relative to uranium-235, (E), 19: 42077 (ANL-7014)
reactivity per atom, 19: 42077 (ANL-7014)
THORIUM NITRATE COMPLEXES
nitryl, preparation and infrared spectra, 19: 40471
THORIUM NITRATES
enthalpy variations in solvent extraction, 19: 40669
THORIUM NITRIDES

decomposition pressure, 19: 40958
THORIUM OXIDES
deposition on metal substrates, electrolytic, 19: 40989
production of high-density spherical particles of, 19: 40963(P)
Re–ThO_2–W, thoria deformation and fracture in, (E), 19: 41058
THORIUM(IV) OXIDES
content in McKelveyite uranium mineral, 19: 40799
separation of protactinium-233 from irradiated, by coprecipitation with manganese dioxide, 19: 40644 (BNWL-78)
BeO–ThO_2, phase studies, 19: 40958
Ni–ThO_2, compatibility of TD nickel with graphite–nitrogen environment at 1000 and 1200°C, 19: 40966 (BNWL-92)
ThO_2–UO_2, gas desorption from sol-gel, 19: 41003(R) (BAW-3376-3)
ThO_2–UO_2, production of, sol-gel method for, 19: 41003(R) (BAW-3376-3)
THORIUM THIOCYANATE COMPLEXES
stability of ion configurations in, 19: 40522
THULIUM
physical and thermodynamic properties, 19: 40948 (IS-1195)
preparation and purification, 19: 40948 (IS-1195)
separation from aqueous solutions of organic acids by solvent extraction using high-molecular-weight amines, 19: 40657
spectra of, atomic, 19: 41253
THULIUM ALLOYS
Au–Tm, phase studies of solid solutions in, 19: 41062
Mg–Th, thermodynamic properties, 19: 41013 (IS-T-25)
THULIUM BORIDES
preparation of divalent, 19: 40524
THULIUM CARBIDES
eutectic temperature between carbon and dicarbide, 19: 41014 (LA-DC-6819)
lattice parameters and phase transformation temperatures in, 19: 41014 (LA-DC-6819)
microhardness, 19: 41014 (LA-DC-6819)
THULIUM CHLORIDES
complexes with phenanthroline, preparation and properties, 19: 40514
THULIUM ETHYL SULFATES
electronic shielding by closed electron shells in, use of Mössbauer effect in, 19: 40528
THULIUM FLUORIDES
electronic shielding by closed electron shells in trivalent, use of Mössbauer effect in, 19: 40528
THULIUM IONS
radioinduced charge transfer from europium ions in calcium fluoride to, x, 19: 40575
THULIUM ISOTOPES Tm-165
decay of, gamma energies and intensities from, (E), 19: 41667 (JINR-P-2239)
THULIUM ISOTOPES Tm-169
energy levels of, electron-conversion de-excitation of, (E), 19: 41705
neutron reactions (n,α) with, cross sections for thermal, (E), 19: 41809(T)
THULIUM OXIDES
content in McKelveyite uranium mineral, 19: 40799
electronic shielding by closed electron shells in trivalent, use of Mössbauer effect in, 19: 40528
THULIUM OXYSULFIDES
preparation and crystal structure, 19: 40475
THULIUM SULFIDES
preparation and crystal structure, 19: 40475
THYMIDINE
radiolysis of tritiated, at 0 to −75°C, self-, 19: 40583
THYROID GLAND
effects on heart function in rats, 19: 40368
radiation effects on physiology of, tracer study, 19: 40374
radioactivity of, from inhaled iodine-132-methyl iodide, 19: 40800(R) (AERE-PR/HPM-7)
radium-224 content in rat, after intravenous injection, 19: 40315
THYROID HORMONES
radiation effects on formation of, 19: 40374
TIMING CIRCUITS
design for accurate timing of electron and x-ray exposures, (E), 19: 41186
TIN
addition to alkali metal bath for coating of molybdenum with silicides, 19: 40998(P)
corrosive effects on Inconel, niobium, and yttrium at 800 to 1100°C, 19: 40961
determination by spectrochemical methods, voltage-fluctuation patterns in, 19: 40416
effects on superconductivity of niobium–tin alloys, (E), 19: 41609
heat of solution of neodymium, praseodymium, and neodymium–praseodymium alloys in liquid, 19: 41044
ion reactions at 5 to 12 Mev, neutron spectra from, (E), 19: 41810(T)
positron annihilation in, angular correlations from, (E), 19: 41285
preparation of single crystals of, in hollow cylindrical form, (E), 19: 40990
thermodynamic properties at high pressures and temperatures, 19: 40459 (NP-15324)
tin-119 nuclear magnetic resonance in hollow cylindrical monocrystals of, (E), 19: 40990
TIN ALLOYS
Al–Mo–Ti–Sn–Zr, mechanical properties of, effects of heat treatments on, 19: 41052
Nb–Sn, phase studies, 19: 40961
Nb–Sn, superconductivity of hollow sintered cylinders of, (E), 19: 41609
rare earths–Sn, crystal structure and thermal expansion of intermetallic compounds in, 19: 41041
TIN ISOTOPES Sn-112
reactions (p,t) at 40 Mev, ground-state L = 0 transitions in, (E), 19: 41689
TIN ISOTOPES Sn-113
metabolism in rats of, after oral or parenteral administration, 19: 40320
TIN ISOTOPES Sn-114
reactions (p,t) at 40 Mev, ground state L = 0 transitions in, (E), 19: 41689
TIN ISOTOPES Sn-116
reactions (p,t) at 40 Mev, ground-state L = 0 transitions in, (E), 19: 41689
TIN ISOTOPES Sn-118
reactions (p,t) at 40 Mev, ground-state L = 0 transitions in, (E), 19: 41689
TIN ISOTOPES Sn-119
nuclear magnetic resonance in hollow cylindrical tin monocrystals, (E), 19: 40990
TIN ISOTOPES Sn-120
reactions (p,t) at 40 Mev, ground-state L = 0 transitions in, (E), 19: 41689
TIN ISOTOPES Sn-122
reactions (p,t) at 40 Mev, ground-state L = 0 transitions in, (E), 19: 41689
TIN ISOTOPES Sn-124
reactions (p,t) at 40 Mev, ground-state L = 0 transitions in, (E), 19: 41689
TIN SYSTEMS
O–K–Sn, phase studies, 19: 41031
TISSUES
analysis for carbon-14 by liquid scintillation counting, 19: 40418
analysis of lung, for copper and zinc, neutron activation methods for, 19: 40452
dosimetry of 60- to 400-Mev nucleons in, 19: 40372
proton spectra in, near surfaces, (T), 19: 41951 (N64-30510)
TITANIUM
determination by spectrochemical methods, voltage-fluctuation patterns in, 19: 40416
effects on properties of tantalum, 19: 41067
Mo–Ti–Zr, mechanical properties of TZM, effects of forging schedule and ingot processing on, 19: 41002 (APS-5157-R)
Mo–Ti–Zr, mechanical properties of TZM, effects of carbon content on, 19: 41002 (APS-5157-R)
TITANIUM ALLOYS
analysis for niobium and tantalum, photometric method for, 19: 40442
Al–Mo–Ti–Sn–Zr, mechanical properties of, effects of heat treatments on, 19: 41052
Al–Ti–Zr, effect of zirconium on lattice parameters of epsilon phase of, 19: 41053
Be–Ti–Zr, brazing alloy for alumina-to-niobium alloy seals, 19: 40980 (LA-3302)
Cr–Ti, brazing alloy for niobium-based alloys, 19: 40989
Fe–Ti, solubility of nitrogen in, 19: 41065
Mo–Ti, coating with silicides, 19: 40998(P)
Mo–Ti, ductile-to-brittle transition temperature of sheet of, effects of recrystallization and welding on, 19: 41016 (N64-30997)
Mo–Ti–Zr, coating with silicides, 19: 40998(P)
Mo–Ti–Zr, dislocation structure in, effects of cold working on, 19: 41015 (MIL-TDR-64-282)
Nb–Ti, current density and magnetic field in cold-worked superconductors of, (E), 19: 41637
Ru–Ti, process for improving workability of, 19: 40999(P)
Ti–V, nuclear spin-lattice relaxation in type II superconductors of, (E), 19: 41611
Ti–V, reactions with fissium–plutonium–uranium at 600 to 750°C,

19: 40958
TITANIUM CARBIDES
Co–TaC–TiC–WC, properties for liquid-metal pump seals, 19: 40718 (TIM-909)
TiC–TiH, properties, 19: 40959
TITANIUM HYDRIDES
laser beam reactions with, low-voltage discharges from, (E), 19: 41133
TiC–TiH, properties, 19: 40959
TITANIUM ISOTOPES Ti-48
proton inelastic scattering at 4.63 and 5.25 Mev, angular correlations in, (E), 19: 41690
TITANIUM NITRIDES
free energy of formation at 1550 to 1750°C, 19: 41065
solubility products in liquid iron at 1550 to 1750°C, 19: 41065
TITANIUM OXIDES
Nb_2O_5–TiO_2, phase studies, 19: 41049
TITANIUM SYSTEMS
C–Nb–Ti, analysis for carbon, electron microprobe, 19: 40412 (TIM-924)
TOBACCO
polonium-210 content of smoke from, 19: 40805 (NRS-30)
TOLUENE
radiolysis of, ESR of radicals in, 19: 40607
picoline–toluene, labeled yields in reactions with carbon-14 recoil atoms, 19: 40627
TOLUENE, α-BROMO-
radiation effects on, thermal annealing of, 19: 40576
TOLUENE, CHLORO-
radiolysis of, ESR of radicals in, 19: 40607
TOLUENE, α,α,α-TRIFLUORO-
asphaltine–α,α,α–trifluorotoluene–carbon disulfide, differential dynamic polarization of fluorine and hydrogen nuclei in, (E), 19: 40497
diphenylpicrylhydrazyl–α,α,α–trifluorotoluene, differential dynamic polarization of fluorine and hydrogen nuclei in, (E), 19: 40497
TOLUENE, TRINITRO-
detonation of liquid, one-dimensional time-dependent reaction zone in, (T), 19: 42203 (LA-3297)
shock initiation of pressed, 19: 42206 (LA-DC-6992)
TRACER TECHNIQUES
atmospheric pollution evaluation by radio-release, 19: 40410 (ORNL-P-494)
TRACER TECHNIQUES (MEDICINE)
for brain tumor localization, 19: 40390 (BNL-9384)
for lipid metabolic studies, 19: 40393
TRADESCANTIA
radiation effects on neutron, 19: 40800(R) (AERE-PR/HPM-7)
TRAMEX PROCESS
analysis of samples for lithium, automated, 19: 40405 (CONF-650919-1)
TRANSDUCERS
design for remote measurements in radiation environment, (E), 19: 40714 (EUR-2421.d)
design of poswich, for use in gamma spectrometers, 19: 40921
performance of hydrostatic pressure, 19: 42210(R) (NVO-98-8)
use in neutron spectrimeters, 19: 40928(P)
TRANSISTORS
electric characteristics in saturation state, (E), 19: 40856
radioinduced base current in silicon, neutron, 19: 40936 (SC-R-65-912)
TRANSITION METALS
solubility of pure, in pure alkali metals, research program on, 19: 40946(R) (AI-65-93)
TRANSPLUTONIC ELEMENTS
separation from lanthanides by solvent extraction, 19: 40692
separation, remotely operated cells for, 19: 40720 (UCRL-7845-T)
TRAPS
design of liquid-nitrogen, (E), 19: 41626
distribution system for twenty-five liquid nitrogen, automatic, 19: 41165 (LA-DC-7147)
TRIOCTYLAMINE
solvent properties of sulfates of, for uranyl sulfates, 19: 40688
TRITIUM
binding energy of $_{\Lambda}H^{3}$, (T), 19: 41419
determination in biological material by scintillation counting of beta decay, 19: 40425
effects in recoil tritium reactions, molecule yield measurements of kinetic, 19: 40615
form factors of, d- and p-state contributions to magnetic-moment, (T), 19: 41759
form factors of, relativistic effects in, (T), 19: 41770
incorporation in compounds, 19: 40638
incorporation in ubiquinone-50, method for, 19: 40641
nuclear properties and uses, 19: 40638
production in nuclear explosion in rock, 19: 40706 (ORNL-TM-1191)
production of pulsed atomic beam of, for plasma diagnostics, (E), 19: 41923
recoil reactions in organic compounds, kinetic isotope effects in, 19: 40615
recoil reactions with alkanes and alkane mixtures, energy loss and reactivity values of, 19: 40616
recoil reactions with organic compounds, energy transfer processes and nuclear transformations in, 19: 40620
recoil reactions with alcohols and their binary mixtures with benzene and cyclohexane, energy transfer in, 19: 40622
recoil reactions with amino acids, yields in, 19: 40629
recoil reactions with liquid benzene and cyclohexane, abstraction and substitution in, 19: 40621
scattering of $^{3}H_{\Lambda}$, on heavy nuclei, Coulomb spallation in, (T), 19: 41815
toxic effects of, in rabbits, 19: 40337
toxic effects of, in rabbits, 19: 40340
TRITONS
angular distributions from cadmium and tin reactions (p,t) at 40 Mev, (E), 19: 41689
emission from proton reactions with heavy nuclei at 157 Mev, (E), 19: 41831
energy spectra from helium-3 (d,t) reactions at 20 and 25 Mev, (E), 19: 41658 (IAE-655)
interactions with protons at 1 to 3 Mev, phase-shift analysis of elastic, (T), 19: 41479(T)
photodisintegration cross sections for, (T), 19: 41824
reactions (t,α) with carbon-12 at 1.35 to 3.4 Mev, excitation curves for, (E), 19: 41706
reactions (t,d) in nuclear Coulomb field, spectroscopic factors for, (T), 19: 41739
reactions (t,p) with nuclei, differential cross sections for, 19: 41817
TRYPTOPHAN
protective effects of injected, against radiation injuries in rats, synergistic effects with serotonin, 19: 40388
TUBES
braking metallic, design of electromagnetic brake for, (E), 19: 40724
flow of hydrogen through heated, data compilation on heat transfer in turbulent, 19: 40734 (NP-15331)
flow pressure drops of air–water in, two-phase, 19: 40733(R) (GEAP-4863)
joining of, with soft metal gasket clamped between faces, 19: 40705(P)
wall thickness changes during sink drawing, factors influencing, 19: 40983(T) (ANL-Trans-189)
TUMORS
radioinduced by injected plutonium-239 in rats, effects of aseptic inflammation on incidence of, 19: 40381
radioinduced, by injected niobium-95 in rats, 19: 40384
radiotherapy using meson (π^-) beams, 19: 40395
TUNGSTEN
analysis for nitrogen, isotope-dilution method for, 19: 40444
argon-ion reactions with, Auger-electron emission in, (E), 19: 41272(T)
deformation and fracture of single crystals of, at 20 to 465°K, 19: 41046
deformation of single crystals of, by rolling at 1000°C, 19: 41066
deposition on ceramic powders by chloride and oxide processes, evaluation of, 19: 40986
desorption of thorium from field-evaporated surfaces of, 19: 41255
determination by spectrochemical methods, voltage-fluctuation patterns in, 19: 40416
determination in copper by activation, 19: 40422
dislocation-interstitial interactions in single crystals of, (E), 19: 42002
effects on properties of tantalum, 19: 41067
extrusion of tube shells of, using tungsten oxides as lubricant, 19: 40989
Fermi surface of single crystals of, (E/T), 19: 42003
gamma heating in DFR, (E), 19: 42117
ionization efficiency of electrodes of, for lithium and lithium-fluoride ion beams, (E), 19: 41141
laser beam reactions on, ion generation by, (E), 19: 41943
mercury-ion reactions with, Auger-electron injection in, (E), 19: 41272(T)
neutron inelastic scattering at 14 Mev, cross sections for, (E), 19: 41718
oxidation kinetics at 1300 to 3170°C, 19: 40961
oxygen reaction with surfaces of, electron-stimulated desorption for studying, 19: 41103(T)
properties of porous, for cesium ionization, 19: 40765(R) (NP-15309)
recrystallization of deformed microcrystals of, 19: 41061(T)
separation from other metal ions by ion exchange, 19: 40658
sintering at 1200 to 1700°C in hydrogen–bromine atmosphere, 19: 40985
sorption on tungsten ferrocyanide, tracer studies of, 19: 40679

tensile properties of powder metallurgy, effects of grain size and impurity level on, 19: 40961
thermal expansion to 2500°C, 19: 41009 (GEMP-375)
thermodynamic properties at high pressures and temperatures, 19: 40459 (NP-15324)
thermoelectric properties at 1000 to 2000°C, (E), 19: 40859
welding to tungsten, electron beam, 19: 40765(R) (NP-15309)
welding with electron-beams, 19: 40989
yield-point return in, kinetics of, 19: 40961
TUNGSTEN ALLOY COUPLES
Mo–Re/Re–W, stability of thermocouples of, (E), 19: 40859
Mo/Re–W, stability of thermocouples of, (E), 19: 40859
Re/Re–W, stability of thermocouples of, (E), 19: 40859
Re–W/Re–W, stability of thermocouples of, (E), 19: 40859
TUNGSTEN ALLOYS
analysis for niobium and tantalum, photometric method for, 19: 40442
Co–W, temper hardening properties, 19: 40961
Cr–Co–Fe–Mn–Mo–Ni–W, corrosion of Rasonel, by coal gasification products at high temperatures, 19: 42127(R) (TID-22009)
Hf–Nb–W–Y, properties of welds in C-129Y, 19: 40989
Hf–Ta–W, properties of welds in T-111, 19: 40989
Hf–Ta–W, stress-rupture properties of T-111, 19: 40961
Mo–Os–W, phase diagrams at 1600, 2000, and 2375°C, 19: 41048
Mo–Re–W, properties, 19: 40961
Mo–Re–W, stress-rupture properties, 19: 40961
Mo–W, phase studies, 19: 41035
Mo–W–Zr, phase studies, 19: 41035
Nb–Ta–W–Zr, properties of welds in FS-85, 19: 40989
Ni–W, diffusion in, activation energy and frequency factor for self-, 19: 40961
Re–W, preparation procedures, 19: 40989
Re–W, stress-rupture properties, 19: 40961
Re–W, thermal expansion to 2500°C, 19: 41009 (GEMP-375)
Re–W, thermoelectric properties at 1000 to 2000°C, (E), 19: 40859
Re–W, use of freeze-drying method for preparation of ultra-fine particles of, 19: 40987
Sc–W, phase studies of solid solution formation in, 19: 41050
Ta–W, dislocation structure in, effects of cold working on, 19: 41015 (MIL-TDR-64-282)
Ta–W, stress-rupture properties, 19: 40961
Ta–W, thermal expansion to 2500°C, 19: 41009 (GEMP-375)
W–Y, phase studies of solid solution formation in, 19: 41050
W–Zr, phase studies, 19: 41035
TUNGSTEN BRONZE
Na–W, positron annihilation in, (E/T), 19: 41158
TUNGSTEN CARBIDES
Co–TaC–TiC–WC, properties for liquid-metal pump seals, 19: 40718 (TIM-909)
Co–WC, properties for liquid-metal pump seals, 19: 40718 (TIM-909)
TUNGSTEN CHLORIDES
slip systems in single crystals of, (E), 19: 41055
TUNGSTEN COUPLES
Mo/W, stability of thermocouples of, (E), 19: 40859
Re/W, stability of thermocouples of, (E), 19: 40859
TUNGSTEN FERROCYANIDES
sorptive properties cerium, ruthenium, strontium, and tungsten, tracer studies of, 19: 40679
TUNGSTEN ISOTOPES W-182
energy levels of, gyromagnetic ratio of 2^+, (E), 19: 41791
energy levels of, vibration-rotation interactions in, (T), 19: 41818
TUNGSTEN ISOTOPES W-184
energy levels of, vibration-rotation interactions in, (T), 19: 41818
TUNGSTEN ISOTOPES W-186
energy levels of, gyromagnetic ratio of 2^+, (E), 19: 41791
energy levels of, vibration-rotation interactions in, (T), 19: 41818
TUNGSTEN OXIDES
use as lubricant for extruding tungsten tubes, 19: 40989
Nb_2O_5–WO_3, phase studies, 19: 41049
TUNGSTEN SYSTEMS
C–Nb–W–Zr, properties of welds in D-43, 19: 40989
C–Nb–W–Zr, stress corrosion of D-43 by boiling potassium, research program on, 19: 40970(R) (NASA-CR-54390)
C–Nb–W–Zr, stress-rupture properties of D-43, 19: 40961
NbC–W, phase studies, 19: 40961
Re–ThO_2–W, thoria deformation and fracture in, (E), 19: 41058
W–UN, analysis of inclusions in cermet of, electron microprobe, 19: 40412 (TIM-924)
TURBINES
development of closed-cycle gas, for power plants, 19: 42127(R) (TID-22009)

U

UBIQUINONE
preparation of carbon-14- and tritium-labeled, method for, 19: 40641
ULTRASONICS
equipment for measuring levels of boiling metals and salts, 19: 40847(R) (NYO-2910-11)
use for testing forged Inconel, 19: 41027 (WERL-0029-2)
use in nondestructive materials testing, conference on, 19: 40754
use to detect unbonded areas in irradiated fuel elements, 19: 41089 (HW-56028)
ULTRAVIOLET RADIATION
effects of polarized, on fluoro-dosimeter glass, (E), 19: 40588
effects on absorption spectra of samarium-containing calcium fluoride crystals, (E), 19: 41993(T)
effects on cesium vapor ionization in thermionic converters, (E), 19: 40566
effects on electroluminescence of activated alkali halides, 19: 41981
UNDERGROUND EXPLOSIONS
base surge cloud histories of Pre-Schooner detonations in basalt, 19: 40708 (PNE-503F)
chemical applications of nuclear, research program on, 19: 40706 (ORNL-TM-1191)
crater measurements in Pre-Schooner detonations, 19: 40707 (PNE-502F)
craters produced by, data compilation on dimensions of, 19: 40711 (SC-RR-65-220)
ground shock spectra from Gnome event, 19: 40713 (VUF-2401)
radiation monitoring of, equipment for remote, 19: 40876 (NVO-162-5 (Rev.))
rock crushing by, for manufacture of aggregate and riprap, 19: 40709 (PNE-5003)
uses of nuclear, engineering, 19: 40710 (SC-DC-65-1485)
UNDERGROUND STRUCTURES
design and costs of tunnel grid blast shelter, 19: 40759 (ORNL-TM-1183)
ground motion effects on contents of, 19: 40758 (AD-426249)
URACIL
radiation effects on incorporation of carbon-14-labeled, in RNA in diploid yeast, 19: 40367
URACIL, 5-FLUORO-
effects on radiosensitivity of, carcinomas of breast, 19: 40394
effects on radiosensitivity of rabbit skin, 19: 40394
URANIUM
coating for corrosion protection, methods for, 19: 40949 (ISC-640)
content in urine of workers of CNEN nuclear center, Rome, 19: 40839
determination in copper by activation, 19: 40422
determination in rocks, using alpha scintillation counter and radioscope, 19: 40432
determination using Arsenazo III, effects of fluoride on photocolorimetric, 19: 40428
dissolution of spent fuel elements by nitric acid, electrolytic, 19: 41086(P)
metabolism of mixed fission products of, after oral administration to rats, 19: 40322
neutron flux distributions in lattices of enriched, fast, (E), 19: 42043(R) (MIT-2344-3, pp 15-36)
neutron flux distributions around single rod of, in heavy water, (E/T), 19: 42047 (MIT-2344-3, pp 115-24)
neutron reactions with natural, number of fissions in, 19: 40640
oxidation in humid atmospheres, 19: 40958
radiation hazards of inhalation and ingestion by man of, 19: 40805 (NRS-30)
radioinduced swelling in, effects of fission gases and texture on, 19: 40958
separation by solvent extraction using 2A-hexanedione and 2-methylheptane-4,6-dione, 19: 40423
separation from hydrochloric acid solutions by solvent extraction using DEHPA, effects of TBP on, 19: 40678
separation from hydrofluoric acid-nitric acid solutions by solvent extractions using amines, 19: 40684
separation from irradiated fuel elements, 19: 40675
separation from other elements by electrophoresis in glycolic acid, 19: 40671
separation from plutonium and thorium by solvent extraction in processing of fuel scrap, 19: 40643 (BNWL-57)
separation from thorium, method for, 19: 40439
separation from traces of metals by chromatography on cellular columns, tracer studies of, 19: 40687
separation from uranium ore leach solutions by ion exchange, 19: 40694
solvent extraction by tributyl phosphate and di-2-amyl 2-butylphosphonate in short-residence contactors, 19: 40645 (CONF-650918-1)
sorption from sulfuric acid solutions by anion exchange resins, mass

transfer in, 19: 40660
tensile properties of, effects of grain size, plastic deformation, and rate loading on, 19: 40958
welding with electron-beams, 19: 40989
U–D_2O, neutron lattice parameters in two-region assemblies of, (E), 19: 42048 (MIT-2344-3, pp 125-36)
U–D_2O, neutron multiplication in poisoned lattices of, 19: 42046(R) (MIT-2344-3, pp 109-14)

URANIUM ALLOYS
analysis for niobium and tantalum, photometric method for, 19: 40442
Al–U, corrosive effects on tantalum at 800 to 1100°C, 19: 40961
Fe–Pu–U, oxidation and ignition behavior of, 19: 40958
Fe–U, phase studies, 19: 40958
fission–Pu–U, creep at 650, 750, and 850°C, compressive, 19: 40958
fission–Pu–U, phase transformations in, 19: 40958
fission–Pu–U, reactions with titanium–vanadium at 600 to 750°C, 19: 40958
Mn–Pu–U, analysis for plutonium, x-ray fluorescence spectrometric, 19: 40408 (LA-3333)
Mo–Nb–U, isothermal transformations of gamma-phase, 19: 40958
Mo–Pu–U, casting procedures for, 19: 40978 (ANL-6955)
Mo–U, elastic modulus of, effects of heat treatments on, 19: 41023 (NP-15334)
Mo–U, isothermal transformations of gamma-phase, 19: 40958
Mo–U, properties, 19: 41023 (NP-15334)
Mo–U, radiation effects on fuel elements of, 19: 41090 (NAA-SR-11121)
Mo–U–Zr, isothermal transformations of gamma-phase, effects of zirconium on, 19: 40958
Nb–U, isothermal transformations of gamma-phase, 19: 40958
Ni–U, production of splatcooled, 19: 41021(R) (NMI-8002.1)
Pd–U, phase studies, 19: 40958
Pu–Th–U, phase studies, 19: 40958
Re–U, structures and phase transformation kinetics of, 19: 41079
U–Zr, swelling of irradiated, effects of annealing temperature on, 19: 40958

URANIUM CARBIDES
fabrication, 19: 40958
phase studies, nonequilibrium, 19: 41018 (NAA-SR-10768)
preparation from carbon and uranium dioxide on pilot plant scale, 19: 40954
processing of irradiated, evaluation of pyrochemical processes for, 19: 40652 (NAA-SR-11340)
radiation effects on hydrolysis of, neutron, 19: 40586
radioinduced swelling, 19: 40958
PuC–UC, performance as gas-cooled fast reactor fuel, 19: 42090 (GA-6132)
PuC–UC, radiation effects on hydrolysis of, neutron, 19: 40586
ThC_2–UC_2, phase studies, 19: 40958

URANIUM(IV) CHLORIDES
phase transformations and melting point, 19: 40481

URANIUM COMPLEXES
malonate, stability and composition, 19: 40482

URANIUM COMPOUNDS
shipping of low-assay, tests of container for, 19: 40819 (SC-RR-65-98, pp 330-56)

URANIUM DEPOSITS (CHILE)
reconnaissance of Colimapu formation, 19: 40798 (RME-4571(Rev.))

URANIUM(IV) FLUORIDES
phase transformations and melting point, 19: 40481

URANIUM(VI) FLUORIDES
determination of, application of constriction response analyzer to continuous, 19: 40417
shipping container drop tests for, 10-ton capacity, 19: 40824 (SC-RR-65-98, pp 580-608)

URANIUM HYDRIDES
UH–ZrH, properties of, effects of destructive rapid pulse heating on, 19: 41017 (NAA-SR-10482)

URANIUM IONS
electron paramagnetic resonance of trivalent in calcium fluorides, relaxation in, (E), 19: 42000(T)
reactions with derivatives of Arsenazo III, spectrophotometric studies of, 19: 40426

URANIUM ISOTOPES
performance with plutonium and thorium isotopes as fuels for power breeder reactors, (E), 19: 42081 (CONF-193-11)

URANIUM ISOTOPES U-233
fission fragments of, neutron emission from, (E/T), 19: 41681(T) (ANL-Trans-205)
neutron fission ratios relative to uranium-235, (E), 19: 42077 (ANL-7014)
reactivity per atom, 19: 42077 (ANL-7014)
separation of protactinium-233 from, by manganese dioxide head-end step in Thorex Process, 19: 40649 (DP-982)

URANIUM ISOTOPES U-234
neutron fission ratios relative to uranium-235, (E), 19: 42077 (ANL-7014)

URANIUM ISOTOPES U-235
energy levels of, 19: 41673 (NP-15251)
fission fragments of, neutron emission from, (E/T), 19: 41681 (ANL-Trans-205)
fission product inventory for, 19: 42008 (ORNL-NSIC-5(Vol.I and II))
fission products from decay chains and nuclear properties of, 19: 42008 (ORNL-NSIC-5(Vol.I and II))
gamma radiation from fission products of, detection using thallium-activated sodium iodide crystals, (E/T), 19: 40891
neutron capture-to-fission ratio at 3.25 ev to 1.8 kev, (E), 19: 41749
neutron fission at 14.9 Mev, yttrium-90, niobium-96, and lanthanum-140 yields from, (E), 19: 41779
neutron fission in heavy water lattices, ratio of epi- and subcadmium, (E), 19: 42044(R) (MIT-2344-3, pp 37-54)
neutron fission of, ratio to uranium-238 capture, (E), 19: 42044(R) (MIT-2344-3, pp 37-54)
neutron fission of, gamma angular distribution in thermal, (E), 19: 41722
neutron fission of, positron-emitter yields from thermal, (E), 19: 41799(T)
neutron fission ratio relative to neptunium, thorium, and uranium isotopes, (E), 19: 42077 (ANL-7014)
neutron fission rates relative to uranium-238, fast, 19: 41672(R) (MIT-2344-3, pp 5-14)
neutron fission rate relative to uranium-238 in heavy water lattices, (E), 19: 42044(R) (MIT-2344-3, pp 37-54)
neutron fission reactions at 2200 m/sec, cross sections for, (E), 19: 41691
neutron reactions (n,α) with, cross sections for thermal, (E), 19: 41809(T)
reactivity per atom, 19: 42077 (ANL-7014)
shipping of low-assay, tests of container for, 19: 40819 (SC-RR-65-98, pp 330-56)

URANIUM ISOTOPES U-236
neutron fission ratios relative to uranium-235, (E), 19: 42077 (ANL-7014)

URANIUM ISOTOPES U-238
deuteron reactions (d,p) with, DWBA and Coulomb stripping approximations for, (E), 19: 41742
fission fragments from, charge distribution of, (E), 19: 41771
neutron capture by, ratio to uranium-235 fission, (E), 19: 42044(R) (MIT-2344-3, pp 37-54)
neutron capture rate in heavy water lattices, ratio of epi- and subcadmium, (E), 19: 42044(R) (MIT-2344-3, pp 37-54)
neutron fission rates relative to uranium-235, fast, 19: 41672(R) (MIT-2344-3, pp 5-14)
neutron fission rate relative to uranium-235 in heavy water lattices, (E), 19: 42044(R) (MIT-2344-3, pp 37-54)
neutron fission ratios relative to uranium-235, (E), 19: 42077 (ANL-7014)
poisoning by, drug evaluation for emergency treatment, 19: 40339
reactivity per atom, 19: 42077 (ANL-7014)

URANIUM LEACH SOLUTIONS
separation of thorium from, by solvent extraction, 19: 40694

URANIUM NITRIDES
analysis, electron microprobe, 19: 40412 (TIM-924)
decomposition pressure, 19: 40958
diffusion of carbon into, 19: 40412 (TIM-924)
fabrication, 19: 40958
W–UN, analysis of inclusions in cermet of, electron microprobe, 19: 40412 (TIM-924)

URANIUM OXIDES
deposition on metal substrates, electrolytic, 19: 40989

URANIUM(IV) OXIDES
analysis for trace impurities using radiochemical standards, accuracy of, 19: 40434
compatibility with nickel at 1200°C, 19: 40966 (BNWL-92)
content in McKelveyite uranium mineral, 19: 40799
crystal structure of, dynamics of, 19: 41032
deposition on stainless steel plates, methods for vapor, 19: 40547(R) (AGN-8137(Vol.I))
diffusion coefficient for nitrogen in, 19: 40958
diffusion from molybdenum–uranium dioxide cermets at 1700 to 2500°C, 19: 41043
fabrication, 19: 40958
fabrication of high density, by compression and sintering, 19: 40996(P)
fission fragment distribution from, (E), 19: 41748
fission gas release from, effects of temperature at 1650 to 2800°C on, 19: 41088 (GEAP-4572)

fission product release from, analysis of, 19: 42008 (ORNL-NSIC-5 (Vol.I and II))
morphological characteristics of precipitated powders of, 19: 41024 (NUMEC-2389-5)
permeability of vibratory compacted, effects of pressure and temperature on, 19: 41003(R) (BAW-3376-3)
processing irradiated, isolation box and equipment for, 19: 40715 (NAA-SR-Memo-7438)
processing of irradiated, development of AIROX process for, 19: 40653 (NAA-SR-11389)
radiation effects on melting point of, 19: 40958
sintering powders of, 19: 40995(P)
thermal conductivity of, transient temperature method for measuring, 19: 40732(R) (CEND-3336-237)
thermal conductivity to 2400°C, 19: 40958
thermal transpiration of vibratory compacted, effects of pressure on, 19: 41003(R) (BAW-3376-3)
B_4C–UO_2, thermal testing for use as fuel, 19: 41006(R) (CEND-3107-238)
Mo–UO_2, diffusion of uranium dioxide from, at 1700 to 2500°C, 19: 41043
PuO_2–UO_2, analysis for nitrogen, 19: 40438
PuO_2–UO_2, electrical properties, 19: 40958
PuO_2–UO_2, morphological characteristics of coprecipitated powers of, electron microscopic study, 19: 41024 (NUMEC-2389-5)
PuO_2–UO_2, performance as gas-cooled fast reactor fuel, 19: 42090 (GA-6132)
PuO_2–UO_2, radiation effects on, 19: 41094(T) (NP-tr-1235)
stainless steel–UO_2, fabrication of fuel elements of, 19: 40958
stainless steel–UO_2, radiation effects on, 19: 40958
ThO_2–UO_2, gas desorption from sol-gel, 19: 41003(R) (BAW-3376-3)
ThO_2–UO_2, production of, sol-gel method for, 19: 41003(R) (BAW-3376-3)
UO_2–H_2O, neutron migration, multiplication factor, and reflector savings for, 19: 42053
UO_2–ZrB_2, preparation and properties, 19: 40960

URANIUM(VI) OXIDES
enthalpy of formation of, 19: 40521
reactions with hydrofluoric acid, enthalpy of, 19: 40521

URANIUM POISONING
drug evaluation for emergency treatment, 19: 40339

URANIUM SYSTEMS
Al–Fe–Si–U, hot hardness and microstructure of, effects of heat treatments on, 19: 40958
Al–Fe–Si–U, properties of, effects of chromium and molybdenum on high-temperature, 19: 40958
Al–Si–U, hot hardness and microstructure of, effects of heat treatments on, 19: 40958
Be–C–U, phase studies, 19: 40958
C–U, analysis for carbon, electron microprobe, 19: 40412 (TIM-924)
Si–U, hot hardness and microstructure of, effects of heat treatments on, 19: 40958
Si–U, phase studies, 19: 40958
U–D_2O, neutron buckling and flux distributions in lattices of, (E), 19: 42049(R) (MIT-2344-3, pp 155-64)
U–D_2O, neutron decay constants in enriched lattices of, pulsed, 19: 42045(R) (MIT-2344-3, pp 55-108)

URANYL CHLORIDES
separation from acid solutions by solvent extraction using thenoyltrifluoroacetone in carbon tetrachloride, 19: 40682

URANYL IONS
reactions with derivatives of Arsenazo III, spectrophotometric studies of, 19: 40426
reactions with 8-hydroxyquinaldinic acid, 19: 40545

URANYL NITRATES
enthalpy variations in solvent extraction, 19: 40669
excretion by rats, effects of thiobis(ethylenenitrilo)tetraacetic acid on, 19: 40348
separation from acid solutions by solvent extraction using thenoyltrifluoroacetone in carbon tetrachloride, 19: 40682
sorption by phospho-organic resins, 19: 40668

URANYL SULFATES
criticality parameters of enriched, in L-77 Vanowen reactor, 19: 42155 (NAA-SR-Memo-3196)
separation from acid solutions by solvent extraction using thenoyltrifluoroacetone in carbon tetrachloride, 19: 40682
solubility and reactions in trioctylamine sulfates and bisulfates, 19: 40688

UREA
hydrolysis of, use as energy source for ion transfer across cellophane membrane, 19: 42199 (BNL-8397)

UREAS
use as energy source in ion transfer across cellophane membrane, 19: 42199 (BNL-8397)

URIDYLIC ACID
reactions of polyribonucleotides of, with cerium, lanthanum, and lutetium, 19: 40474

URINE
analysis for carbon-14 by liquid scintillation counting, 19: 40418
radiation effects on taurine excretion in rat, gamma, 19: 40364
uranium content in, of workers in CNEN nuclear center, Rome, 19: 40839

V

VACUUM FURNACES
design of precision, for Moessbauer measurements, (E), 19: 40858

VACUUM PUMPS
design and operation, 19: 40773

VACUUM SEALS
brazing alloys for alumina-to-niobium alloy, 19: 40980 (LA-3302)

VACUUM SYSTEMS
description of ultrahigh, 19: 40772 (ORNL-P-1465)
design and operation, 19: 40773
design of liquid-helium and liquid-nitrogen, (E), 19: 41626
design of precision cryostat for Moessbauer measurements, (E), 19: 40848
development of single-wall ultrahigh, for thin film deposition, 19: 40774

VACUUM TECHNIQUES
development and uses of, 19: 40773

VACUUM VALVES
design and operation of hydraulically actuated ultrahigh, 19: 40776
development and testing of ultrahigh, 19: 40775

VACUUM VESSELS
design of charged-particle scattering chamber, (E), 19: 40907

VALVES
design for accurate timing of electron and x-ray exposures, (E), 19: 41186
development of high-temperature solenoid-operated, 19: 40765(R) (NP-15309)

VAN ALLEN RADIATION BELTS
electron and proton distributions in outer, effect of solar flare on, (E), 19: 41312
electron and proton density distributions in, computer program for mapping, 19: 41954 (NP-15338)
electron diffusion in outer, inward radial, (E), 19: 41578
properties of, research on, 19: 41571(R) (N64-29400)
protons in outer, model for origin of, 19: 41577
structure of, effects of ionospheric electrostatic fields on, (T), 19: 41593

VAN DE GRAAFF ACCELERATORS
design of pressurized ion, 19: 41181

VANADIUM
determination by spectrochemical methods, voltage-fluctuation patterns in, 19: 40416
determination in biological material by neutron activation methods, 19: 40421
effects on properties of tantalum, 19: 41067
superconductivity enhancement of, using 3,4,7,8-tetramethyl-1, 10-phenanthroline, 19: 40543

VANADIUM ALLOYS
Fe–V, solubility of nitrogen in, 19: 41065
Mo–Nb–V–Zr, properties of welds in B-66, 19: 40989
Mo–Nb–V–Zr, stress-rupture properties of B-66, 19: 40961
Mo–Ta–V, phase diagram, 19: 41036
Nb–Ta–V, phase diagram, 19: 41036
Ti–V, nuclear spin-lattice relaxation in type II superconductors of, (E), 19: 41611
Ti–V, reactions with fissium–plutonium–uranium at 600 to 750°C, 19: 40958

VANADIUM ISOTOPES V-50
neutron reactions (n,γ), vanadium-52 energy levels from, (E), 19: 41725

VANADIUM ISOTOPES V-51
neutron reactions (n,γ), vanadium-52 energy levels from, (E), 19: 41725
proton reactions (p,n) at 1.5 to 2.3 Mev, total cross section for, (E), 19: 41676 (ORNL-P-1468)

VANADIUM ISOTOPES V-52
energy levels from vanadium (n,γ) reactions, low-lying, (E), 19: 41725

VANADIUM NITRIDES
solubility products in liquid iron at 1550 to 1750°C, 19: 41065

VANADIUM OXIDES
Nb_2O_5–V_2O_5, phase studies, 19: 41049

VEHICLES
collision of, analysis of shipping container response to, 19: 40817 (SC-RR-65-98, pp 243-60)

VELA PROJECT
ground shock spectra from Gnome event, 19: 40713 (VUF-2401)
VESSELS
description of transport container for irradiated fuels from power stations in United Kingdom, 19: 40829 (SC-RR-65-98, pp 711-18)
design for shipping plutonium nitrate and oxide, 19: 40825 (SC-RR-65-98, pp 609-19)
design for shipping spent reactor fuels, (E), 19: 40837
design of shipping containers for radioactive materials, review, 19: 40823 (SC-RR-65-98, pp 450-72)
development and tests of accident-resistant shipping, for radioactive materials, 19: 40816 (SC-RR-65-98, pp 141-86)
fire test of finned box, 19: 40827 (SC-RR-65-98, pp 631-50)
fire tests of models of shipping containers, 19: 40815 (SC-RR-65-98, pp 133-40)
standardization for shipping radioactive materials, 19: 40822 (SC-RR-65-98, pp 442-9)
tests of Class II container for shipping low-assay uranium compounds, 19: 40819 (SC-RR-65-98, pp 330-56)
tests of shipping containers for slightly enriched uranium fuel cores, 19: 40820 (SC-RR-65-98, pp 357-76)
tests of shipping containers for plutonium nitrate solutions, 19: 40821 (SC-RR-65-98, pp 423-41)
tests of 10-ton capacity shipping containers for uranium hexafluoride, drop, 19: 40824 (SC-RR-65-98, pp 580-608)
VIBRATIONS
effects of stress induced by, on radiosensitivity of rats and guinea pigs, 19: 40354(T) (FTD-TT-65-48, pp 38–9)
VIRUSES
function, properties, and structure of, 19: 42212 (NYO-3424-1)
VISCOSITY
measurement in alkali metal liquid and vapor, 19: 41001(R) (AGN-8154)

W

WASTE DISPOSAL
abstracts on management research, 19: 42194 (NP-15267)
burial, temperature distribution in gamma-active spheres, (T), 19: 42191 (AEET/HP/TH-20)
methods for separating long-lived isotopes from high-level wastes, (E), 19: 42197
methods for SNAP reactors, 19: 42140 (NAA-SR-11353)
methods used at Hanford plant, (E), 19: 42196
storage of high-level solids in salt mine, demonstration experiment on, 19: 42195 (ORNL-P-1479)
WASTE PROCESSING
abstracts on management research, 19: 42194 (NP-15267)
fixation of Purex wastes in phosphate glass, study of composition range in, 19: 42192 (BNWL-80)
methods for separating long-lived isotopes from high-level wastes, (E), 19: 42197
methods used at Hanford plant, (E), 19: 42196
solidification in underground tanks, tests of immersion heaters for, 19: 42193 (BNWL-101)
WATER
analyses of reactor coolant, 19: 42084(R) (CVNA-239)
analysis for boric acid, automated colorimetric, 19: 40404 (BNWL-SA-167)
analysis for heavy water by electrochemistry of cadmium in water–heavy systems, 19: 40427
analysis for oxygen-18, by activation methods, 19: 40419
analysis for zirconium, automated fluorescence, 19: 40403 (BNWL-SA-166)
boiling heat transfer at 300 psi, effects of electric fields on, 19: 40735(R) (NYO-2404-5)
content in McKelveyite uranium mineral, 19: 40799
corrosive effects on chromium–iron–nickel alloys, 19: 40967(R) (COO-1319-27)
cosmic meson (μ) spectra at great depths in, (E), 19: 41293
dielectric constant at 0 to 40°C, 19: 40527
effects on sorption of carbon monoxide on zinc oxide, 19: 40578
evaporation of drops of, computer program for, 19: 41110 (BNWL-74)
gamma absorption in hemispheres of, from central point source, (T), 19: 41959
gamma angular and energy distributions in, cobalt-60, (E), 19: 41953 (NP-15131)
meson (μ) energy loss in, (E/T), 19: 41345
neutron diffusion in, using oscillating source, 19: 41641(R) (MIT-2344-3, pp 137-54)
neutron spectra in poisoned, (E), 19: 41646
neutron thermalization in, integral, 19: 41640(R) (GA-6323)
purification for reactors, 5, 19: 42130 (HW-68387)
radiation effects on ammoniated and oxygenated solutions, 19: 40548 (BNWL-82)
radioinduced yields of positive oxygen ions in, electron, 19: 40581
separation of cesium-137 and strontium-90 from fuel storage basin effluent, by ion exchange, 19: 40651 (IDO-14657)
air–water, two-phase flow pressure drops in annular test section, 19: 40733(R) (GEAP-4863)
B–H_2O, neutron spectra in, thermal, 19: 42037(R) (BNWL-95, pp 4-17)
$Ce(NO_3)_3$–$LiNO_3$–H_2O, solubility ratios in, at 10, 20, and 30°C, 19: 40519
$CHCl_3$–H_2O, dissociation of 2,4-hexanedione and 6-methyl-2,4-heptanedione in, 19: 40423
Gd–H_2O, neutron spectra in, thermal, 19: 42037 (BNWL-95, pp 4-17)
NH_4SCN–methanol–H_2O, distribution coefficients of metals in, 19: 40447
Sm–H_2O, neutron spectra in, thermal, 19: 42037 (BNWL-95, pp 4-17)
steam–water, void fraction measurement by x-ray attenuation in two-phase flow of, 19: 40745
UO_2–H_2O, neutron migration, multiplication factor, and reflector savings for, 19: 42053
WATER-*d*
effects on Napier relaxation frequency of oxygen, 19: 40483
radioinduced yields of positive oxygen ions in, electron, 19: 40581
WATER-d_2
analyses of reactor coolant-moderator, 19: 42084(R) (CVNA-239)
analysis for trace impurities, automated, 19: 40406 (CONF-650919-2)
determination in light water by electrochemistry of cadmium in water–heavy water systems, 19: 40427
dielectric constant at 0 to 40°C, 19: 40527
effects on Napier relaxation frequency of oxygen, 19: 40483
isotopic exchange with fluorimide, 19: 40537
neutron diffusion parameters in, pulsed thermal, (E), 19: 42045(R) (MIT-2344-3, pp 55-108)
neutron flux distributions around single uranium fuel rod in, (E/T), 19: 42047 (MIT-2344-3, pp 115-24)
neutron spectra in poisoned, (E), 19: 41646
neutron thermalization in, integral, 19: 41640(R) (GA-6323)
production by isotopic exchange between ammonia and hydrogen, 19: 40942(P)
radioinduced yields of positive oxygen ions in, electron, 19: 40581
U–D_2O, neutron buckling and flux distributions in lattices of, (E), 19: 42049(R) (MIT-2344-3, pp 155-64)
U–D_2O, neutron decay constants in enriched lattices of, pulsed, 19: 42045(R) (MIT-2344-3, pp 55-108)
U–D_2O, neutron lattice parameters in two-region assemblies of, (E), 19: 42048 (MIT-2344-3, pp 125-36)
U–D_2O, neutron multiplication in poisoned lattices of, 19: 42046(R) (MIT-2344-3, pp 109-14)
WATER-*t*
toxic effects of, in rabbits, 19: 40337
toxic effects of, pathology and treatment in rabbits, 19: 40340
WATER COOLED REACTORS
control equipment for, 19: 42019(T) (ORNL-tr-669)
coolants for, evaluation of performance of fog as, (E), 19: 42020
economics of low-temperature, water moderated, for desalination, 19: 42097 (ORNL-TM-1152)
neutron spectrum in thermal column of Triga Mark II, (E), 19: 42184
safety hazards and precautions at Pegase installation, 19: 42151 (CEA-R-2518(Vol.II))
WATER MODERATED REACTORS
control by moderator temperature variation, 19: 42031(P)
controls by moderator temperature and composition variation, 19: 42030(P)
criticality calculations for uniform, (T), 19: 42054
economics of low-temperature, water cooled, for desalination, 19: 42097 (ORNL-TM-1152)
economics of spectral-shift pressurized-water thorium power breeders, (E), 19: 42109
fuel element assembly with burnable poison for, 19: 42072(P)
neutron spectrum in thermal column of Triga Mark II, (E), 19: 42184
safety hazards and precautions at Pegase installation, 19: 42151 (CEA-R-2518(Vol.II))
WATER SUPPLIES
production by desalination, economic comparison of two evaporators for, 19: 40699 (ORNL-TM-826)
radioactivity of, in Australia, United Kingdom, and United States, 19: 40805 (NRS-30)
WATER VAPOR
effects on Napier relaxation frequency of oxygen, 19: 40483
effects on radioinduced recombination of hydrogen with oxygen, 19: 40549 (COO-1032-1)

reactions with niobium and tantalum during annealing and melting, 19: 40490
reactions with potassium hydroxide and superoxide, kinetics, 19: 40462 (SC-TM-65-183)
WATER WAVES
ditection and measurement of Tsunami-like, 19: 42210(R) (NVO-98-8)
WEAR
of plated coatings for use in rotary switches, 19: 42216 (SC-DR-65-269)
WELDED JOINTS
design for explosive welding, 19: 40989
WELDING
development of electron-beam, 19: 40765(R) (NP-15309)
WELDS
testing of steel, evaluation of variables in radiographic, 19: 40753(R) (EURAEC-1378)
testing of, radiographic and ultrasonic methods of, 19: 42024
testing steel pressure vessel, ultrasonic methods of, 19: 42025
WELL LOGGING
equipment for neutron-gamma, modernization of, 19: 40794(T) (AEC-tr-6577)
WHISTLERS
diagnostic use for magnetospheric plasma density, (T), 19: 41596
WOOD
use in shipping container for radioactive materials, 19: 40816 (SC-RR-65-98, pp 141-86)
WYOMING (SWEETWATER CO.)
uranium occurrence in Green River Formation in, 19: 40799

X

X RADIATION
detection and measurement using matched pairs of cadmium-sulfide crystals, (E), 19: 40598
dosage of, for lethality in dormant Guar seed, 19: 40376
effect on luminescence of alkali-halide phosphors pre-exposed to electric field, 19: 40571
effects on charge transfer between ions in crystals, 19: 40575
effects on cyanidine pigment in *Maranta leuconeura* leaves, (E), 19: 40362
effects on electroluminescence of activated alkali halides, 19: 41981
effects on electroluminescence of alkali halides, 19: 40572
effects on F centers and photostimulated emission in sodium chlorides, (E), 19: 41980
effects on gonads and liver in rabbits, biochemical, 19: 40375
effects on growth of progeny of male rats exposed in infantile period, 19: 40365
effects on luminescence centers of silver-activated alkali halide phosphors, 19: 41977
effects on luminescence of europium-activated potassium- and sodium-chloride phosphors, 19: 40567
effects on luminescence spectra of thallium-activated sodium iodide crystal phosphors, 19: 40568
effects on luminescence of thallium-activated potassium iodides, in electric field, 19: 40573
effects on mitosis in Planaria, dose effects on regenerating capacity in, 19: 40366
effects on phosphorescence of alkali halide phosphors, influence of F-band illumination on, 19: 40570
effects on photoluminescence of silver-activated sodium chlorides, 19: 40569
effects on polymerization of solid acrylonitrile in presence of electric field, 19: 40582
effects on polymerization of mixtures of vinyl chloride and argon, krypton, or xenon, 19: 40584
effects on sodium chloride crystal plastic flow, 19: 40594
effects on thermal de-excitation processes in potassium and sodium chloride phosphors, 19: 41101(T)
effects on thermoluminescent reduction of chromium ions in magnesium oxide crystals, 19: 40631
emission from solar corona, soft, 19: 41209(T) (N64-22932)
emission from sun, production and spectra of, 19: 41213
exposure dose measurements in air, magnetic induction field for, 19: 40838
flux of solar, (E), 19: 41231
metabolic effects in normal and rachitic rats, 19: 40351(R) (NYO-1913-1)
pathological effects in nervous system of man, 19: 40349 (BNL-9345)
pathological effects on rabbit skin, effects of 5-fluorouracil, 19: 40394
physiological effects in guinea pigs and rats, effects of stress induced by vibration, 19: 40354(T) (FTD-TT-65-48, pp 38–9)
physiological effects in thyroid gland, 19: 40374
physiological effects on mammary gland activity, 19: 40353(T) (FTD-TT-65-48, pp 16–17)
physiological effects in rats, 19: 40360(T) (FTD-TT-65-48, pp 666)
physiological effects on body fluids in rats, 19: 40369
production of selected wavelength, method for, 19: 41163(P)
scattering of, analysis of J-phenomenon in, 19: 41357
spectra in cosmic cascade showers at high altitudes, (E/T), 19: 41299
yields from atomic L_2 and L_3 shells, approximation formulas for, (T), 19: 41245
X-RAY BEAMS
dosimetry of wide, in finite phantom thickness, 19: 40881 (UR-667)
shutter design for accurate exposure timing of, (E), 19: 41186
therapeutic use of betatron, radioactivity induced in patients by, 19: 40392 (NYO-3364-6)
X-RAY CAMERAS
design of 12-ton high-pressure, engineering drawings of, 19: 40865
X-RAY EQUIPMENT
shutter design for accurate exposure timing, (E), 19: 41186
use of x-ray tube for void fraction measurement in two-phase flow, 19: 40745
X-RAY SOURCES
spectra from K-fluorescent, 19: 40834(R) (UCRL-14151)
XANTHENONES
analytical use of phenylfluorone for determination of tantalum traces, 19: 40414 (UCRL-7967)
XENON
cesium spin relaxation in, (E), 19: 41278
radioinduced polymerization of, with vinyl chloride and, 19: 40584
reactor poisoning by, (T), 19: 42010
separation from gas mixtures, 19: 40695(P)
shock propagation in, properties of, 19: 41128 (UCRL-12466)
sorption by evaporated molybdenum films, 19: 40463(R) (SRIA-425-5)
XENON IONS
reactions with nickel surfaces, isotopic effect in secondary electron emission in, (E), 19: 41249
XENON ISOTOPES Xe-125
gamma spectra and half life of isomeric, (E), 19: 41802(T)
production of isomeric, (E), 19: 41802(T)
XENON ISOTOPES Xe-132
energy levels from decay of iodine-132 and cesium-132, (E), 19: 41745
XENON SYSTEMS
Ar–Xe, electron reactions at 50 kev, luminescence from, (E), 19: 41246
Kr–Xe, electron reactions at 50 kev, luminescence from, (E), 19: 41246
N–Xe, electron reactions at 50 kev, luminescence from, (E), 19: 41246
o-XYLENE, 4-BROMO-
radiation effects on, thermal annealing of neutron, 19: 40576

Y

YEASTS
radiation effects on incorporation of carbon-14-labeled adenino, orotic acid, and uracil in RNA in diploid, 19: 40367
YTTERBIUM
determination by spectrochemical methods, voltage-fluctuation patterns in, 19: 40416
neutron reactions (n,α) with, cross sections for thermal, (E), 19: 41809(T)
neutron resonances in, spectra of, 19: 41661 (JINR-P-2158)
physical and thermodynamic properties, 19: 40948 (IS-1195)
polarographic behavior in dimethylformamide and dimethylsulfoxide, 19: 40681
preparation and purification, 19: 40948 (IS-1195)
YTTERBIUM ALLOYS
Au–Yb, phase studies of solid solutions in, 19: 41062
Ru–Yb, process for improving workability of, 19: 40999(P)
YTTERBIUM CARBIDES
lattice parameters and phase transformation temperatures in, 19: 41014 (LA-DC-6819)
microhardness, 19: 41014 (LA-DC-6819)
YTTERBIUM CHLORIDES
complexes with phenanthroline, preparation and properties, 19: 40514
YTTERBIUM COMPLEXES
with gluconic acids, stability constants, 19: 40508
YTTERBIUM IONS
relaxation time in calcium fluoride, spin-lattice, (T), 19: 41982
spectra in synthetic lead molybdate single crystals, EPR, (E), 19: 41986(T)
spin-lattice relaxation time in calcium fluoride lattice, (T), 19: 41995(T)
YTTERBIUM ISOTOPES Yb-170
neutron strength functions for, target spin dependence of, 19: 41656 (BNL-9245)
YTTERBIUM ISOTOPES Yb-171

neutron resonances in, spectra of, 19: 41661 (JINR-P-2158)
neutron strength functions for, target spin dependence of, 19: 41656 (BNL-9245)

YTTERBIUM ISOTOPES Yb-172
neutron resonances in, spectra of, 19: 41661 (JINR-P-2158)
neutron strength functions for, target spin dependence of, 19: 41656 (BNL-9245)

YTTERBIUM ISOTOPES Yb-173
neutron resonances in, spectra of, 19: 41661 (JINR-P-2158)
neutron strength functions for, target spin dependence of, 19: 41656 (BNL-9245)

YTTERBIUM ISOTOPES Yb-174
neutron resonances in, spectra of, 19: 41661 (JINR-P-2158)

YTTERBIUM ISOTOPES Yb-176
neutron resonances in, spectra of, 19: 41661 (JINR-P-2158)

YTTERBIUM MANGANATES
Curie point determination of, 19: 41059(T)

YTTERBIUM OXIDES
content in McKelveyite uranium mineral, 19: 40799

YTTERBIUM PERCHLORATES
stability constants of, thermal, 19: 40509

YTTRIUM
corrosion by aluminum, lead, tin, and zinc at 800 to 1100°C, 19: 40961
determination by spectrochemical methods, voltage-fluctuations patterns in, 19: 40416
determination of micro amounts of, in rare earth oxides by x-ray fluorescence, 19: 40440
effects on nitrogen and oxygen content in niobium-based alloys, 19: 40953 (PWAC-441)
neutron reactions (n,γ) at 0.025 ev, spectra from, 19: 40896
physical and thermodynamic properties, 19: 40948 (IS-1195)
preparation and purification, 19: 40948 (IS-1195)
separation from aqueous solutions of organic acids by solvent extraction using high-molecular-weight amines, 19: 40657
separation from europium and promethium by ion exchange, effects of aqueous organic media on, 19: 40663
separation from europium by ion exchange, effects of alcohols on, 19: 40666
separation from europium by ion exchange using ammonium acetate eluant, 19: 40680
separation from thorium by ion exchange in ammonium thiocyanate–methanol–water systems, 19: 40447
solvent distribution in ammonium thiocyanate–methanol–water systems, distribution coefficients for, 19: 40447
sorption by strongly acidic cation exchanger, effects of aqueous solutions of alcohols on, 19: 40664
sorption on ion exchanger, effects of glycols on, 19: 40662
sorption on ion exchanger, tracer studies of effects of alcohol solutions on, 19: 50665

YTTRIUM ACETATES
preparation and crystal structure of ammoniated, 19: 40507

YTTRIUM ALLOYS
Al–Cr–Fe–Y, corrosion by steam at 500 to 1300°C, 19: 40961
Al–Cr–Fe–Y, impact properties of, 19: 40961
Al_2O_3–Y_2O_3, bonding to niobium–1 zirconium, brazing alloy for, 19: 40980 (LA-3302)
Au–Y, phase studies of solid solutions in, 19: 41062
Be–Y, vaporization of YBe_{13}, 19: 40959
Co–Y, magneto-optic properties of intermetallic compound YCo_5 in, 19: 41084
Cr–Y, phase studies of solid solution formation in, 19: 41050
Hf–Nb–W–Y, properties of welds in C-129Y, 19: 40989
Mg–Y, preparation by magnesium salt reduction of halides, 19: 40955
Mo–Y, phase studies of solid solution formation in, 19: 41050
Nb–Ta–Y–Zr, grain size and hardness of, effects of yttrium additions on, 19: 40953 (PWAC-441)
Nb–Y, phase studies of solid solution formation in, 19: 41050
Nb–Y–Zr, grain size and hardness of, effects of yttrium additions on, 19: 40953 (PWAC-441)
Ni–Y, production of splatcooled, 19: 41021(R) (NMI-8002.1)
Re–Y, process for improving workability of, 19: 40999(P)
Ta–Y, phase studies of solid solution formation in, 19: 41050
W–Y, phase studies of solid solution formation in, 19: 41050

YTTRIUM CARBIDES
eutectic temperature between carbon and dicarbide, 19: 41014 (LA-DC-6819)
lattice parameters and phase transformation temperatures in, 19: 41014 (LA-DC-6819)
microhardness, 19: 41014 (LA-DC-6819)

YTTRIUM COMPLEXES
with gluconic acids, stability constants, 19: 40508

YTTRIUM HALIDES
reduction in magnesium salt bath, 19: 40955

YTTRIUM HYDRIDES
thermodynamic properties, 19: 40959

YTTRIUM IONS
reactions with derivatives of Arsenazo III, spectrophotometric studies of, 19: 40426

YTTRIUM ISOTOPES Y-89
deuteron reactions (d,p) with, isomeric cross section ratios for, (E), 19: 41820
neutron reactions (n,n'γ) at 14 Mev, cross sections for, (E), 19: 41781
production of isomeric states in yttrium-89 (n,n'γ) reactions at 14 Mev, cross sections for, (E), 19: 41781

YTTRIUM ISOTOPES Y-90
metabolism in rats of, after oral administration of mixed uranium fission products, 19: 40322
production by rubidium-87(α,n), strontium-88(He-3,p), and yttrium-89(d,p) reactions, isomeric cross section ratios for, (E), 19: 41820
yield in alpha fission of thorium-232 at 20 to 40 Mev, (E), 19: 41779
yield in neutron fission of uranium-235 at 14.9 Mev, (E), 19: 41779

YTTRIUM ISOTOPES Y-91
metabolism in rats, after inhalation, 19: 40314
pathological effects in dogs of, after intravenous injection, 19: 40377

YTTRIUM MANGANATES
Curie point determination of, 19: 41059(T)

YTTRIUM OXIDES
content in McKelveyite uranium mineral, 19: 40799
effects on sintered density of plutonia powders, 19: 40981 (NUMEC-2389-6)
reactions with ferric oxide at 700 to 1400°C, 19: 40515

Z

ZINC
bonding to aluminum, hot-press, 19: 40949 (ISC-640)
corrosion by aluminum–silicon and water of coatings of, on uranium, 19: 40949 (ISC-640)
corrosive effects on Inconel, niobium, and yttrium at 800 to 1100°C, 19: 40961
deposition on uranium, hot dip, 19: 40949 (ISC-640)
determination in copper by activation, 19: 40422
determination in human lung tissue by neutron activation methods, 19: 40452
optical properties of films of, in vacuum ultraviolet region, 19: 42213 (ORNL-TM-1164)
positron annihilation in, angular correlations from, (E), 19: 41285
separation from aqueous solution by dithizone–cellulose acetate column, 19: 40642 (AERE-R-4969)
separation from uranium by chromatography on cellulose columns, tracer studies of, 19: 40687
solvent distribution in ammonium thiocyanate–methanol–water systems, distribution coefficients for, 19: 40447
thermodynamic properties at high pressures and temperatures, 19: 40459 (NP-15324)

ZINC ALLOYS
Al–Zn, corrosion by aluminum–silicon and water of coatings of, on uranium, 19: 40949 (ISC-640)
Al–Zn, deposition on uranium, hot dip, 19: 40949 (ISC-640)
Cu–Zr, copper-63 nuclear spin echoes in, r-f excitation of, (E/T), 19: 41988
rare earths–Zn, crystal structure of intermetallic compounds in, 19: 41040
Ru–Zn, process for improving workability of, 19: 40999(P)

ZINC COMPLEXES
with α, β, γ, δ-tetrapheaylporphines, reteations in Szilard-Chalmers (n,γ) recoil reactions in, 19: 40612

ZINC ISOTOPES Zn-68
nitrogen-14 reactions (N-14, N-13) at 40 to 150 Mev, isomeric pair production ratios in, 19: 41674 (NYO-1930-44)

ZINC OXIDES
radiation effects on catalytic oxidation of carbon monoxide on, at 270°C, 19: 40577
radiation effects on sorption of carbon monoxide on, gamma, 19: 40578

ZINC SULFATES
radiolysis of hydrated, yields in, 19: 40610

ZINC SULFIDES
compressibility of, volume, (E), 19: 41984
radiation effects on luminescence of, electron, 19: 40587

ZIRCALOY-2
corrosion and hydriding rate of, effects of heat flux on, 19: 40961
corrosion by boiling lithiated water in crevices of simulated PRTR fuel

elements, 19: 40965 (BNWL-83)
corrosion by high-temperature water, fretting, 19: 40961
crystallization of, after cold rolling and annealing, 19: 41034
deposition of copper coatings on, method of, 19: 40989
radiation effects on corrosion and tensile properties of welded joints of hafnium-to-, fast neutron, 19: 41092 (WAPD-TM-457)
radiation effects on tensile properties of, neutron, 19: 40961
welding of Inconel 600 to, joint design for explosive, 19: 40989

ZIRCALOY-4
radiation effects on tensile properties of, neutron, 19: 40961
strength of, methods for increasing, 19: 40961

ZIRCONIUM
corrosion by aluminum–silicon and water of coatings of, on uranium, 19: 40949 (ISC-640)
deposition on uranium by diffusion from molten magnesium bath, 19: 40949 (ISC-640)
determination by spectrochemical methods, voltage-fluctuation patterns in, 19: 40416
determination in copper by activation, 19: 40422
determination in water, automated fluorescence, 19: 40403 (BNWL-SA-166)
determination of, reagents for (E), 19: 40441
diffusion in stabilized, coefficients for self-, 19: 40961
diffusion into niobium carbide at 1760°C, 19: 40412 (TIM-924)
effects on properties of tantalum, 19: 41067
properties of zone refined, 19: 41030
purification by zone fusion method, 19: 41030
reactor criticality effects per atom, (E), 19: 42077 (ANL-7014)
separation from other elements by electrophoresis in glycolic acid, 19: 40671
solvent extraction by tributyl phosphate and di-2-amyl 2-butylphosphonate in short-residence contactors, 19: 40645 (CONF-650918-1)
transformation kinetics in, 19: 41033
yield point of, effects of hydrogen on, 19: 41010(R) (IITRI-578P27-10)
Mo–Ti–Zr, mechanical properties of TZM, effects of carbon content on, 19: 41002 (APS-5157-R)
Mo–Ti–Zr, mechanical properties of TZM, effects of forging schedule and ingot processing on, 19: 41002 (APS-5157-R)

ZIRCONIUM ALLOYS
analysis for niobium and tantalum, photometric method for, 19: 40442
corrosion by superheated steam, 19: 40977(P)
fabrication for fuel cladding, 19: 42175
Al–Mo–Ti–Sn–Zr, mechanical properties of, effects of heat treatments on, 19: 41052
Al–Ti–Zr, effect of zirconium on lattice parameters of epsilon phase of, 19: 41053
Be–Ti–Zr, brazing alloy for alumina-to-niobium alloy seals, 19: 40980 (LA-3302)
Be–Zr, phase studies and thermodynamics of intermetallic compounds in, 19: 41078
Ca–Nb–Zr, corrosion by superheated steam, 19: 40977(P)
Fe–Zr, solubility of nitrogen in, 19: 41065
Mo–Nb–V–Zr, properties of welds in B-66, 19: 40989
Mo–Nb–V–Zr, stress-rupture properties of B-66, 19: 40961
Mo–Ti–Zr, coating with silicides, 19: 40998(P)
Mo–Ti–Zr, dislocation structure in, effects of cold working on, 19: 41015 (MIL-TDR-64-282)
Mo–U–Zr, isothermal transformations of gamma-phase, effects of zirconium on, 19: 40958
Mo–W–Zr, phase studies, 19: 41035
Mo–Zr, phase studies, 19: 41035
Nb–Ta–W–Zr, properties of welds in FS-85, 19: 40989
Nb–Ta–Y–Zr, grain size and hardness of, effects of yttrium additions on, 19: 40953 (PWAC-441)
Nb–Ta–Zr, nitrogen and oxygen content of, effects of yttrium additions on, 19: 40953 (PWAC-441)
Nb–Y–Zr, grain size and hardness of, effects of yttrium additions on, 19: 40953 (PWAC-441)
Nb–Zr, bonding to metallized alumina, brazing alloy for, 19: 40980 (LA-3302)
Nb–Zr, bonding to alumina–yttria, brazing alloy for, 19: 40980 (LA-3302)
Nb–Zr, critical current degradation in wide-strip superconductors of, (E), 19: 41639
Nb–Zr, current density and magnetic field in cold-worked superconductors of, 19: 41637
Nb–Zr, hardness of, effects of cooling rate and niobium content on, 19: 40961
Nb–Zr, hydridation effects on properties of, 19: 40959
Nb–Zr, mass transfer from Type 316 and 321 stainless steels to, in liquid potassium at 1400°F, 19: 40970(R) (NASA-CR-54390)
Nb–Zr, nitrogen and oxygen content of, effects of yttrium additions on, 19: 40953 (PWAC-441)
Nb–Zr, nuclear spin-lattice relaxation in type II superconductors of, (E), 19: 41611
Nb–Zr, procurement and quality evaluation of stock of, for corrosion studies, 19: 40952 (ORNL-TM-1179)
Nb–Zr, transformation kinetics in, 19: 41033
U–Zr, swelling of irradiated, effects of annealing temperature on, 19: 40958
W–Zr, phase studies, 19: 41035

ZIRCONIUM BORIDES
coating with molybdenum or tungsten by chloride and oxide processes, evaluation of, 19: 40986
UO_2–ZrB_2, preparation and properties, 19: 40960

ZIRCONIUM CARBIDES
coating with molybdenum or tungsten by chloride and oxide processes, evaluation of, 19: 40986
heats of formation, 19: 40961
ZrC–ZrH, properties, 19: 40959

ZIRCONIUM HYDRIDES
neutron thermalization in, integral, 19: 41640(R) (GA-6323)
phase studies, 19: 40959
UH–ZrH, properties of, effects of destructive rapid pulse heating on, 19: 41017 (NAA-SR-10482)
ZrC–ZrH, properties, 19: 40959

ZIRCONIUM IONS
reactions with derivatives of Arsenazo III, spectrophotometric studies of, 19: 40426

ZIRCONIUM ISOTOPES
Cu–Zr, oxidation at 500 to 900°C, 19: 40976

ZIRCONIUM ISOTOPES Zr-90
deuteron reactions (d,p) with, DWBA and Coulomb stripping approximations for, (E), 19: 41742
metabolism in rats of, after oral administration of mixed uranium fission products, 19: 40322

ZIRCONIUM ISOTOPES Zr-95
metabolism in rats, after inhalation, 19: 40314

ZIRCONIUM NITRIDES
free energy of formation at 1550 to 1750°C, 19: 41065
solubility products in liquid iron at 1550 to 1750°C, 19: 41065

ZIRCONIUM OXIDES
coating with molybdenum or tungsten by chloride and oxide processes, evaluation of, 19: 40986
hydrofluorination in fluidized bed, kinetics of, 19: 40529
sorptive properties for oxygen, 19: 40961
sorptive properties for hydrogen, 19: 40484
thermal conductivity of, transient temperature method for measuring, 19: 40732(R) (CEND-3336-237)
use as a diathermanous substance in thermal reactors, 19: 42065(P)
B_2O_3–ZrO_2, preparation and sorptive properties for hydrogen, 19: 40484
Cr_2O_3–ZrO_2, formation of refractories of, 19: 40997(P)
Li_2O–SiO_2–ZrO_2, phase studies, 19: 41038
Nd_2O_3–ZrO_2, phase studies, 19: 41037

ZIRCONIUM SYSTEMS
C–Nb–W–Zr, properties of welds in D-43, 19: 40989
C–Nb–W–Zr, stress corrosion of D-43 by boiling potassium, research program on, 19: 40970(R) (NASA-CR-54390)
C–Nb–W–Zr, stress-rupture properties of D-43, 19: 40961
O–K–Zr, phase studies, 19: 41031

REPORT NUMBER INDEX

Reports, conference papers and proceedings, numbered translations, and patents abstracted during the period are included in this index. Each item is listed by report number; this is followed by the abstract number and a brief notation regarding public availability. The index entries show, when known, which reports are on file in the depository libraries, which reports have been published in open-literature journals (journal citation given), and which reports can be purchased (source and price). Whenever a report is identified by more than one number, cross references from secondary to primary report numbers are cited.

The report number codes apply to AEC reports unless designated otherwise. Non-AEC reports are identified by parenthetical notes after the report codes; e.g., (non-AEC), (British), (Canadian), (French). The note (Misc.) identifies those codes used for both USAEC and non-AEC reports. Patents are listed under the heading "PATENTS"; the country of origin is included in parentheses.

A comprehensive listing of both AEC and non-AEC report codes is contained in TID-85(3rd Rev.), *Report Number Series Used by the Division of Technical Information in Cataloging Reports*. This information is also included in the Cumulative Report Number Index (issued annually).

Public Availability of USAEC Reports

All USAEC reports abstracted in *NSA* are available to the public through one or more of the following sources:

(1) Depository libraries in the United States, in other countries, and in international agencies. A list of these depositories appears on the inside covers of each issue of *NSA*.

(2) Scientific and technical journals or other publications.

(3) Microcard Editions, Inc., in Microcard and micronegative form. Orders and inquiries should be sent to: Accounting and Shipping Department, West Salem, Wisconsin 54669.

(4) Clearinghouse for Federal Scientific and Technical Information, U. S. Department of Commerce, Springfield, Virginia 22151.

(5) Superintendent of Documents, U. S. Government Printing Office, Washington, D. C. 20402.

Public Availability of Non-AEC Reports

U. S. Reports. Many reports of U. S. Government agencies are available to the public from the Clearinghouse for Federal Scientific and Technical Information (CFSTI). This availability is given when known. Such reports should be ordered by AD number or NASA-N number. If availability is not shown, inquiries may be directed to CFSTI. In the case of NP numbers, inquiries should be by title and author.

Non-U. S. Reports. Many reports of atomic energy establishments of other countries are deposited in the libraries listed on the inside covers of each issue of *NSA*.

Additionally, the following countries have made their reports available as indicated.

AUSTRALIA

Australian Atomic Energy Commission Research Establishment. Available upon request from the Library, Australian Atomic Research Establishment, Private Mail Bag, Sutherland, New South Wales, Australia.

BELGIUM

Centre d'Étude de l'Énergie Nucléaire. Available upon request to individuals and organizations, from the Centre d'Étude de l'Énergie Nucléaire (CEN), 31, Rue Belliard, Bruxelles, Belgium.

CANADA

Atomic Energy of Canada Limited. For sale by the Technical Information Officer, Atomic Energy of Canada Limited, Chalk River, Ontario, Canada. Copies are also deposited in libraries in the United Kingdom.

National Research Council of Canada. Available from the National Research Council of Canada, Ottawa 2, Ontario, Canada.

DENMARK

Atomic Energy Commission Research Establishment, Risø. Available on exchange from the Library, Danish Atomic Energy Commission, Risø, Roskilde, Denmark. Also for sale by Jul. Gjellerup, Booksellers, 87 Sölvgade, København K., Denmark.

Danatom. Available on loan from Research Establishment, Risø, Roskilde, Denmark. Copies are available from Danatom, Aurehøjvej 2, Hellerup, Denmark.

FRANCE

Commissariat à l'Énergie Atomique. Inquiries for reports numbered 1-2199 should be addressed to Commissariat à l'Énergie Atomique, Service Central de Documentation, Centre d'Études Nucléaires de Saclay, Boite Postale No. 2, Gif-sur-Yvette (S. et O.), France. Reports numbered 2200 and above are available from La Documentation Francaise, 16 Rue Lord-Byron, Paris VIII, France.

Service Central de Protection contre les Rayonnements Ionisants. Copies are available from Ministère de la Santé Publique, Service Central de Protection contre les Rayonnements Ionisants, B. P. n° 35—LE VESINET (S. et O.), France.

GERMANY

Deutsches Elektronen-Synchrotron DESY. Copies are available from Deutsches Elektronen-Synchrotron Desy, Dokumentation, 2000 Hamburg-Gr. Flottbek 1, Notkestieg 1, Germany.

Kernforschungsanlage. Copies may be ordered from Zentralbibliothek der Kernforschungsanlage Jülich, Jülich, Bundesrepublik Deutschland.

Hahn-Meitner-Institute für Kernforschung. Available without charge from Hahn-Meitner-Institute für Kernforschung Berlin, Bibliothek, Glienicker Strasse 100, 1 Berlin 39, Germany. Copies are deposited in many national nuclear centers in the world.

Johann-Wolfgang-Goethe Universität, Frankfurt Am Main, Institut für Kernphysik, (IKF). Copies are available from Gmelin Institut, 40-42 Varrentrappstrasse, Frankfurt (Main), West Germany.

ISRAEL

Israel Atomic Energy Commission. Available without charge from Ministry of Defence/Atomic Energy Com-

mission, Soreq Research Establishment, Yavne, Israel. Copies are deposited in libraries in Israel and in other countries.

ITALY

Centro Informazioni Studi Esperienze (CISE). For sale at CISE Press Office, Casella Postale 3986, Milano, Italy. Copies are deposited in libraries in Italy.

Comitato Nazionale per l'Energia Nucleare. Copies are available from Comitato Nazionale per l'Energia Nucleare, Divisione Affari Internazionali e Studi Economici, Ufficio Pubblicazioni, Via Belisario, 15, Roma, Italy.

JAPAN

Japan Atomic Energy Research Institute (JAERI). Available from the Staff Supply Cooperative of Japan Atomic Energy Research Institute (JAERI), 1-1 Tamura-Cho, Shiba, Minato-Ku, Tokyo, Japan. Copies are deposited in depositories in Tokyo, Nagoya, and Osaka.

Nagoya University. Copies are available from Research Information Center, Institute of Plasma Physics, Nagoya University, Nagoya, Japan.

University of Tokyo. Available free of charge from Institute for Nuclear Study, University of Tokyo, Tanashi-Machi, Kitatama-gun, Tokyo, Japan.

NETHERLANDS

Reactor Centrum Nederland. For sale by Reactor Centrum Nederland, 112 Scheveningseweg, 's-Gravenhage, The Netherlands. Copies are deposited in university libraries in Holland and in many national nuclear centers in the world.

NEW ZEALAND

Institute of Nuclear Sciences. Copies are available from Librarian, Institute of Nuclear Sciences, D.S.I.R., Private Bag, Lower Hutt, New Zealand. Copies are deposited in other countries.

NORWAY

Forsvarets Forskningsinstitutt. Copies available from Norwegian Defence Research Establishment, Library, P. O. Box 25, Kjeller, Norway.

Institutt for Atomenergi. "KR" reports are available on an exchange basis from the Library, Institutt for Atomenergi, Box 40, Kjeller, Norway. Other series are not generally available to the public.

Norwegian Reactor School. Copies are available from The Library, Institutt for Atomenergi, P. O. Box 40, Kjeller, Norway.

PAKISTAN

Atomic Energy Center. Copies are available from Atomic Energy Center, P. O. Box 658, Lahore, (West Pakistan).

POLAND

Reports of the Polish nuclear institutes are published by the Nuclear Energy Information Center of the Government Commissioner for Use of Nuclear Energy. Copies are available from Ośrodek Informacji o Energii Jądrowej, Warszawa, PKiN, Poland.

SPAIN

Junta de Energia Nuclear. "JEN" reports are available without charge from Servicio de Documentation, Junta de Energia Nuclear, Ciudad Universitaria, Madrid (3), Spain.

SWEDEN

Aktiebolaget Atomenergi. "AE" reports are for sale from Aktiebolaget Atomenergi, Library Section, Box 43041, Stockholm 43, Sweden. Bibliographies and literature surveys of the VDDIT- series may be obtained from Aktiebolaget Atomenergi, Information Office, Scientific and Technical Information, Box 43041, Stockholm 43, Sweden. Other series are not generally available to the public. Organizations in the atomic energy field may obtain copies from Aktiebolaget Atomenergi. Microcopy of AE reports is available from the International Documentation Centre, Tumba, Sweden.

SWITZERLAND

CERN European Organization for Nuclear Research. Available without charge from CERN European Organization for Nuclear Research, Geneva 23, Switzerland. Copies are deposited in libraries in 13 countries.

Eidgenössisches Institut für Reaktorforschung. "EIR" reports are available from Eidgenössiches Institut für Reaktorforschung, c/o Bibliothek, Würenlingen/Ag, Switzerland.

TURKEY

Turkish Atomic Energy Commission. Copies are available free of charge from T.A.E.C., Çekmece Nuclear Research Center, P. O. Box 1, Airport, Istanbul, Turkey.

UNITED KINGDOM

United Kingdom Atomic Energy Authority. Some reports are for sale in the United States by the British Information Service (BIS), 845 Third Avenue, New York, N. Y. 10022. United Kingdom reports generally may be purchased from Her Majesty's Stationery Office, London. Copies not for sale by Her Majesty's Stationery Office may be purchased in microcopy form from Micro Methods Limited, East Ardsley, Wakefield, Yorks, England. Report copies are deposited in a large number of libraries in England.

Conferences

Published conference proceedings as well as individual unpublished papers from conferences are included in this index. A CONF number is assigned to the conference if published proceedings are received and also if only a single paper is received. The base number used is year-month-sequence. Thus, the number CONF-650101 would indicate that the conference was held in 1965, in January, and that this was the first January 1965 conference so received. This number would be assigned to complete published proceedings, or if individual papers are received, the base number would be extended to include a paper number, i.e., CONF-650101-1. As additional papers are received, they will be assigned consecutive numbers in the series, CONF-650101-1, 2, 3, 4, etc. This numbering system ensures that all papers received from a conference will be associated with that conference in this index.

If published proceedings are received after the receipt of individual papers, the complete proceedings will be abstracted and the abstract number will appear in this index with the base CONF number.

Abbreviations Used in Availability Column

AECL	For sale by Atomic Energy of Canada Ltd., Chalk River, Ontario, Canada.
BIS	For sale by British Information Service, 845 Third Avenue, New York, N. Y. 10022
CFSTI	For sale by the Clearinghouse for Federal Scientific and Technical Information, U. S. Department of Commerce, Springfield, Virginia 22151. The symbol "cy" indicates that the format of the item sold may be either a printed document or a photographic reproduction (two-thirds of original size) depending upon the availability of printed stock. The indicated price is for either format. The symbol "mn" is used to indicate

that copy is available in the form of micronegatives (microfiche). The number preceding the "mn" symbol indicates the number of micronegatives in the set. Micronegatives are available at the following prices: One micronegative, $0.50; each additional micronegative of the set, $0.25. For additional micronegative copies of the same report requested at the time of the original order, $0.25 per micronegative. Prices are reduced on micronegatives if subscription distribution is purchased.

Dep.	AEC reports: Full-size copy is on deposit in the depository libraries both inside and outside the United States. These reports are also for sale by Microcard Editions, Inc., Accounting and Shipping Department, West Salem, Wisconsin 54669. Non-AEC reports: Full-size copy on deposit in the depository libraries in the United States only.
Dep.(mn)	Same as for Dep., except copy is in micronegative (microfiche) form.
DSIR	For sale by the National Lending Library for Science and Technology (D.S.I.R.), Boston Spa, Yorkshire, England.
DTI Extension	Available from the U. S. Atomic Energy Commission, Division of Technical Information Extension, P. O. Box 62, Oak Ridge, Tennessee 37831.
EM	Blueprints and Microcopy of AEC engineering drawings are available from Clearinghouse for Federal Scientific and Technical Information, U. S. Department of Commerce, Springfield, Virginia 22151. Current prices of the CAPE- packages may be obtained from this address. TID-4100, available from the Division of Technical Information Extension, P. O. Box 62, Oak Ridge, Tennessee 37831, contains information on all the CAPE- packages for sale.
Gmelin	Available at a nominal charge and under the AED- number shown from Atomic Energy Documentation Center, Gmelin Institute, 40-42 Varrentrappstrasse, Frankfurt (Main), West Germany.
GPO	For sale by the Superintendent of Documents, Government Printing Office, Washington, D. C. 20402.
HMSO	Her Majesty's Stationery Office, London.
IAEA	Available from the International Atomic Energy Agency, Vienna, Austria, and from its sales agencies in various countries throughout the world. A list of these agencies is found in each STI/DOC and STI/PUB publication.
JCL	For sale by the Special Libraries Association Translation Center, John Crerar Library, 35 West 33rd Street, Chicago, Illinois 60616.
LC	For sale by the Library of Congress, Photoduplication Service, Washington, D. C. 20540.
NAS	National Academy of Sciences, National Research Council, Washington, D. C. 20418.
NRC	For sale by the National Research Council of Canada, Ottawa, Ontario, Canada.
ORINS	Available on interlibrary loan from the Library, Oak Ridge Institute of Nuclear Studies, Post Office Box 117, Oak Ridge, Tennessee 37831.
UKAEA, London	Available from United Kingdom Atomic Energy Authority, 11 Charles II Street, London, S. W. 1.
UN	United Nations Bookshop, United Nations Headquarters, New York, New York.
USGS	Available free of charge from the U. S. Geological Survey, Washington, D. C. 20242.

[The symbols "ph," "mf," and "fs" are used to designate that copy is available only in photostat, microfilm, or facsimile form. The symbol "mn" is used to designate that copy is available in micronegative (microfiche) form. The symbol "cy" is used to designate full size or photographically enlarged copy (two-thirds of original size).]

Report No.	Abstract No.	Availability
AAEC-E–	**(Australian)**	
134	19-42034	Dep.(mn)
135	19-41087	Dep. mn
ACF–		
9	19-40698	Dep. mn; CFSTI, $1.00 cy, $0.50 mn
10	19-41000	Dep. mn; CFSTI, $2.00 cy, $0.50 mn
412-248	19-41000	See ACF-10
ACF-SA–		
706	19-40698	See ACF-9
AD–	**(Misc.)**	
426079	19-41849	CFSTI, $13.00 cy
426145	19-41569	CFSTI, $2.60 cy
426249	19-40758	CFSTI, $3.60 cy, $0.50 mn
600154	19-41203	CFSTI, $1.00 cy
609424	19-40931	CFSTI, $3.00 cy, $0.50 mn
609969	19-40731	CFSTI, $2.00 cy, $0.50 mn
617258	19-41114	
617386	19-41850	
AEC-tr–	**(For complete listing see TID-4025)**	
6565	19-40554	Dep. mn; CFSTI, $7.00 cy, $1.50 mn
6577	19-40794	Dep. mn; CFSTI, $1.00 cy, $0.50 mn; JCL, $1.60 fs, $0.80 mf
AECD-TP–	**(Pakistani)**	
4	19-41321	Dep. mn
AECL–	**(Canadian)**	
2216	19-42148	Dep.; AECL, $1.50 cy
2217	19-40866	Dep.; AECL, $1.00 cy
2256	19-41678	See PR-P-65
2304	19-40558	Can. J. Chem., 43: 2141-7(1965)
2311	19-41032	Can. J. Phys., 43: 1397-1413(1965)
AEET-HP–	**(Indian)**	
TH-20	19-42191	Dep. mn
AERE-M–	**(British)**	
967	19-41962	Dep. mn
AERE-PR–	**(British)**	
HPM-7	19-40800	Dep.; BIS, $1.60; HMSO, 8s.
AERE-R–	**(British)**	
4741	19-41056	Phil. Mag. (8), 12: 31-9(1965)
4969	19-40642	Dep. mn; BIS, $0.30; HMSO, 1s. 9d.
4991	19-41261	Phil. Mag. (8), 12: 145-56(1965)
AFAPL-TR–	**(Non-AEC)**	
65-51	19-41002	See APS-5157-R
AFCRL–	**(Non-AEC)**	
63-380	19-41569	See AD-426145
63-550	19-41849	See AD-426079
AGC–	**(Misc.)**	
8800-5	19-42141	See NASA-CR-54422
AGN–	**(Misc.)**	
8137(Vol.I)	19-40547	Dep. mn; CFSTI, $4.00 cy, $1.00 mn
8154	19-41001	Dep. mn; CFSTI, $1.00 cy, $0.50 mn
AI–	**(Misc.)**	
65-93	19-40946	
AMP–	**(Non-AEC)**	
160	19-41863	See NP-15302
ANL–		
6590	19-42035	Dep. mn; CFSTI, $2.00 cy, $0.50 mn
6735	19-42075	Dep. mn; CFSTI, $1.00 cy, $0.50 mn
6751	19-42076	Dep. mn; CFSTI, $2.00 cy, $0.50 mn
6955	19-40978	Dep. mn; CFSTI, $2.00 cy, $0.50 mn
6961	19-42149	Dep.(mn); CFSTI, $5.00 cy, $1.00 mn
6967	19-41115	Dep. mn; CFSTI, $2.00 cy, $0.50 mn
6991	19-40801	Dep. mn; CFSTI, $5.00 cy, $1.00 mn
7009	19-42150	Dep. mn; CFSTI, $4.00 cy, $1.00 mn
7014	19-42077	Dep. mn; CFSTI, $1.00 cy, $0.50 mn
7019	19-42078	Dep. mn; CFSTI, $2.00 cy, $0.50 mn
ANL-Trans–		
189	19-40983	Dep. mn; JCL, $2.60 fs, $1.04 mf
205	19-41681	Dep. mn; CFSTI, $1.00 cy, $0.50 mn; JCL, $1.60 fs, $0.80 mf
APDA-NTS–	**(Non-AEC)**	
4	19-42079	Dep. mn; CFSTI, $2.00 cy, $0.50 mn
5	19-42080	Dep. mn; CFSTI, $3.00 cy, $0.50 mn
APS–	**(Non-AEC)**	
5157-R	19-41002	
AROD–	**(Misc.)**	
4284:3	19-41114	See AD-617258
4284:4	19-41127	See SUDAER-238
BAW–	**(Misc.)**	
3376-3	19-41003	Dep. mn; CFSTI, $3.00 cy, $0.50 mn
BMI–	**(Misc.)**	
1735	19-41004	Dep. mn; CFSTI, $1.00 cy, $0.50 mn
BMI-X–		
10137	19-40402	Dep. mn; CFSTI, $1.00 cy, $0.50 mn
BN–	**(Misc.)**	
399	19-41865	See TID-22050
BNL–		
934	19-41655	Dep. mn; CFSTI, $2.00 cy, $0.50 mn
8379	19-40308	Dep. mn; CFSTI, $1.00 cy, $0.50 mn
8397	19-42199	Dep. mn; CFSTI, $1.00 cy, $0.50 mn
8405	19-40634	Dep. mn; CFSTI, $1.00 cy, $0.50 mn
8421	19-41718	Nucl. Energy, Pts. A and B, 19: 497-500 (1965)
9046	19-41780	Phys. Rev., 139: B1513-24(1965)
9050	19-41418	Phys. Rev., 139: B1097-1102(1965)
9053	19-41408	Phys. Rev., 139: B1021-2(1965)
9079	19-41434	Phys. Rev., 139: B1401-6(1965)
9123	19-41438	Phys. Rev., 139: B1420-7(1965)
9231	19-41322	Dep. mn; CFSTI, $1.00 cy, $0.50 mn IEEE (Inst. Elec. Electron, Engrs.), Trans. Nucl. Sci., NS-12: No. 4, 231-7(1965)
9245	19-41656	Dep. mn; CFSTI, $1.00 cy, $0.50 mn
9253	19-40307	Dep. mn; CFSTI, $5.00 cy, $1.00 mn
9297	19-40455	Dep. mn; CFSTI, $2.00 cy, $0.50 mn
9311	19-41788	Phys. Rev. Letters, 15: 357-60(1965)
9317	19-41789	Phys. Rev. Letters, 15: 360-4(1965)
9329	19-41314	Dep. mn; CFSTI, $2.00 cy, $0.50 mn
9345	19-40349	Dep. mn; CFSTI, $1.00 cy, $0.50 mn
9384	19-40390	Dep. mn; CFSTI, $2.00 cy, $0.50 mn
BNWL–		
57	19-40643	Dep. mn; CFSTI, $2.00 cy, $0.50 mn
64	19-40867	Dep. mn; CFSTI, $1.00 cy, $0.50 mn
74	19-41110	Dep. mn; CFSTI, $2.00 cy, $0.50 mn
78	19-40644	Dep. mn; CFSTI, $1.00 cy, $0.50 mn
80	19-42192	Dep. mn; CFSTI, $2.00 cy, $0.50 mn
82	19-40548	Dep. mn; CFSTI, $2.00 cy, $0.50 mn
83	19-40965	Dep. mn; CFSTI, $2.00 cy, $0.50 mn
92	19-40966	Dep. mn; CFSTI, $2.00 cy, $0.50 mn
95	19-42036	Dep. mn; CFSTI, $3.00 cy, $0.50 mn
101	19-42193	Dep. mn; CFSTI, $1.00 cy, $0.50 mn
BNWL-SA–		
23	19-40868	Dep. mn; CFSTI, $1.00 cy, $0.50 mn
92	19-41723	Nucl. Instr. Methods, 36: 1-12(1965)
166	19-40403	Dep. mn; CFSTI, $1.00 cy, $0.50 mn
167	19-40404	Dep. mn; CFSTI, $1.00 cy, $0.50 mn
242	19-40780	Dep. mn; CFSTI, $1.00 cy, $0.50 mn
BNWL-tr–		
4	19-41028	Dep. mn; JCL, $2.60 fs, $0.86 mf
CALT–		
68-42	19-41323	Dep. mn; CFSTI, $1.00 cy, $0.50 mn

Report No.	Abstract No.	Availability
221-11	19-41005	Dep. mn; CFSTI, $3.00 cy, $0.75 mn
CAPE–		
1070	19-40924	
1230	19-40925	
1245	19-40865	
1246	19-40864	
1272	19-40926	
1273	19-40923	
CEA-R–	(French)	
2518(Vol.II)	19-42151	Dep.(mn)
2723	19-40932	Dep. mn
CEA-tr–	(French)	
R-1839	19-40415	Dep. mn
X-609	19-40656	Dep. mn; JCL, $1.10 fs, $0.80 mf
CEAL–		
1021	19-40843	Dep. mn; CFSTI, $1.00 cy, $0.50 mn
1022	19-41164	Dep. mn; CFSTI, $2.00 cy, $0.50 mn
CEND–	(Misc.)	
3107-238	19-41006	Dep. mn; CFSTI, $2.00 cy, $0.50 mn
3336-237	19-40732	Dep. mn; CFSTI, $1.00 cy, $0.50 mn
CERN–	(European Organization for Nuclear Research)	
65-14	19-41324	Dep.(mn)
CONF-193–	(8th Nuclear Congress, Rome, June 1963)	
11	19-42081	Dep. mn; CFSTI, $2.00 cy, $0.50 mn
CONF-276–	19-41076	(Conference on Deformation Twinning, Gainesville, Fla., Mar. 1963)
CONF-279–	(7th Annual Western Industrial Health Conference, San Francisco, Sept. 1963)	
3	19-40876	See NVO-162-5(Rev.)
CONF-366–	19-40538	(General Motors Symposium on Liquids, Structures, Properties, and Solid Interactions, Warren, Mich. Sept. 1963)
CONF-414–	(Conference on Direct Energy Conversion, Argonne, Ill., Nov. 1963)	
8	19-41320	Gmelin, AED-CONF-63-246-12
CONF-471–	(American Physical Society 5th Annual Meeting, San Diego, Calif., Nov. 1963)	
57	19-41946	Gmelin, AED-CONF-63-268-67
CONF-654–	(American Nuclear Society Meeting, San Francisco, Nov. 30–Dec. 3, 1964) Proceedings	
90	19-40630	Gmelin, AED-CONF-64-219-113
91	19-42063	Gmelin, AED-CONF-64-219-109
CONF-720–	(2nd Symposium on Protection Against Radiation Hazards in Space, Gatlinburg, Oct. 1964)	
30	19-40842	Gmelin, AED-CONF-64-190-35
CONF-758–	(American Physical Society Meeting, New York, Jan. 22–25, 1965)	
30	19-41312	Gmelin, AED-CONF-65-003-90
33	19-41313	Gmelin, AED-CONF-65-003-57
34	19-41844	Gmelin, AED-CONF-65-003-94
35	19-41838	Gmelin, AED-CONF-65-003-61
36	19-41837	Gmelin, AED-CONF-65-003-60
38	19-41526	Gmelin, AED-CONF-65-003-51
39	19-41527	Gmelin, AED-CONF-65-003-50
40	19-41939	Gmelin, AED-CONF-65-003-56
41	19-41839	Gmelin, AED-CONF-65-003-55
42	19-41525	Gmelin, AED-CONF-65-003-54
43	19-41832	Gmelin, AED-CONF-65-003-59
45	19-41637	Gmelin, AED-CONF-65-003-95
46	19-41945	Gmelin, AED-CONF-65-003-85
47	19-41286	Gmelin, AED-CONF-65-003-79
50	19-41940	Gmelin, AED-CONF-65-003-96
51	19-41941	Gmelin, AED-CONF-65-003-65
52	19-41528	Gmelin, AED-CONF-65-003-62
53	19-41524	Gmelin, AED-CONF-65-003-72
CONF-765–	(2nd Conference on Radioactive Fallout from Nuclear Weapons Tests, Germantown, Md., Nov. 3–6, 1964)	
11	19-41570	Dep. mn; CFSTI, $1.00 cy, $0.50 mn
CONF-773(Vol.I)–	19-40614	(Symposium on Chemical Effects Associated with Nuclear Reactions and Radioactive Transformation, Vienna, Dec. 1964) See STI/PUB/91(Vol.I)
CONF-794–	(Magnetism Conference, Minneapolis, Nov. 1964)	
11	19-41639	Gmelin, AED-CONF-64-204-20
CONF-812–	(Society for Applied Spectroscopy 3rd National Meeting, Cleveland, Sept. 28–Oct. 2, 1964)	
5	19-41287	Gmelin, AED-CONF-64-207-7
CONF-600701–	19-41605	(Conference on Advances in Upper Atmosphere Research, Corfu, Greece, July 1960)
CONF-620601– (Pts. 1 and 2)	19-40862	(Symposium on Electromagnetic Theory and Antennas, Copenhagen, June 25–30, 1962)
CONF-620904–	19-40767	(Symposium on High Temperatures in Aeronautics, Turin, Sept. 10–12, 1962)
CONF-620906–	19-40751	(6th Symposium on Cavitation in Real Liquids, Warren, Mich., Sept. 24–25, 1962)
CONF-620907–	19-40945	(Conference on Differential Equations and Their Applications, Prague, Sept. 5–11, 1962)
CONF-630905–	19-40754	(4th International Conference on Non-Destructive Testing, London, Sept. 9–13, 1963)
CONF-631203–	19-40352	(Late Irradiation Effects Conference, Germantown, Md., Dec. 4–6, 1963) Proceedings. See WASH-1059
CONF-640406–	(American Physical Society, Ohio Section, Spring Meeting, Cleveland, Apr. 24–25, 1964)	
4	19-40863	Gmelin, AED-CONF-64-198-6
CONF-640709–	19-41039	(2nd All-Union Symposium on Physics of Thin Ferromagnetic Films, Irkutsk, U.S.S.R., July 10–15, 1964)
CONF-641004–	(American Physical Society, Chicago, Oct. 23–24, 1964)	
14	19-41836	Gmelin, AED-CONF-64-220-42 Phys. Rev., 140: B1-8(1965)
CONF-641016–	(17th Annual Gaseous Electronics Conference, Atlantic City, Oct. 14–16, 1964)	
6	19-41944	Gmelin, AED-CONF-64-223-14
7	19-41943	Gmelin, AED-CONF-64-223-15
CONF-641108–	(American Physical Society, New York, Nov. 4–8, 1964)	
48	19-41947	Gmelin, AED-CONF-64-196-74
49	19-41942	Gmelin, AED-CONF-64-196-71
50	19-41949	Gmelin, AED-CONF-64-196-69
CONF-641114–	(American Physical Society, Southeastern Section, Chattanooga, Tenn., Nov. 1964)	
6	19-41108	Gmelin, AED-CONF-64-194-17
7	19-40632	Gmelin, AED-CONF-64-194-16
CONF-641116–	(Conference on the Role of Grain Boundaries and Surfaces in Ceramics, Raleigh, N. C., Nov. 16–18, 1964)	
8	19-40536	Gmelin, AED-CONF-64-224-11
CONF-641210–	(American Physical Society Meeting, Berkeley, Calif., Dec. 1964)	
20	19-40631	Gmelin, AED-CONF-64-236-33

Report No.	Abstract No.	Availability
21	19-41283	Gmelin, AED-CONF-64-236-36
CONF-650101–		**(Mössbauer Symposium, New York, Jan. 26, 1965)**
2	19-41848	Gmelin, AED-CONF-65-006-4
4	19-41845	Gmelin, AED-CONF-65-006-2
5	19-40922	Gmelin, AED-CONF-65-006-7
6	19-40306	Gmelin, AED-CONF-65-006-6
CONF-650103–	**19-40808**	**(International Symposium on Packaging and Transportation of Radioactive Material, Albuquerque, N. Mex., Jan. 11, 1965) See SC-RR-6598**
CONF-650106–	**19-41514**	**(Conference on Symmetry Principles at High Energy, Coral Gables, Fla., Jan. 1965)**
CONF-650115–		**(11th National Symposium on Reliability and Quality Control, Miami Beach, Fla., Jan. 12–14, 1965)**
1	19-40848	See SC-R-65-935
CONF-650203–		**(National AIME Meeting, Chicago, Feb. 14–18, 1965)**
10	19-40694	Gmelin, AED-CONF-65-005-9
CONF-650317–		**(American Physical Society Meeting, Kansas City, Mo., Mar. 25, 1965)**
2	19-40305	Gmelin, AED-CONF-65-039-22
CONF-650401–		**(American Chemical Society, Detroit, Apr. 4–9, 1965)**
7	19-41831	Gmelin, AED-CONF-65-041-24 Phys. Rev., 139: B1500-4(1965)
8	19-42120	Gmelin, AED-CONF-65-041-26
12	19-40537	Gmelin, AED-CONF-65-041-19
CONF-650403–		**(International Conference on Non-Linear Magnetics, Washington, D. C., Apr. 21–23, 1965)**
3	19-40939	Gmelin, AED-CONF-65-038-3
4	19-41084	Gmelin, AED-CONF-65-038-4
5	19-41638	Gmelin, AED-CONF-65-038-2
CONF-650405–		**(International Conference on Modern Trends in Activation Analysis, College Station, Tex., Apr. 19–22, 1965)**
7	19-40453	Gmelin, AED-CONF-65-040-16
8	19-40450	Gmelin, AED-CONF-65-040-21
9	19-40452	Gmelin, AED-CONF-65-040-20
11	19-40962	Gmelin, AED-CONF-65-040-23
14	19-40451	Gmelin, AED-CONF-65-040-12
CONF-650410–		**(American Physical Society, Washington, D. C., Apr. 26–29, 1965)**
4	19-41835	Gmelin, AED-CONF-65-073-2 Nucl. Phys., 73: 25-32(1965)
5	19-41842	Gmelin, AED-CONF-65-073-6
6	19-41833	Gmelin, AED-CONF-65-073-7
7	19-41846	Gmelin, AED-CONF-65-073-8
8	19-41840	Gmelin, AED-CONF-65-073-15
9	19-41311	Gmelin, AED-CONF-65-073-14
11	19-41841	Gmelin, AED-CONF-65-073-4
13	19-41202	Gmelin, AED-CONF-65-073-26
14	19-41604	Gmelin, AED-CONF-65-073-22
15	19-41082	Gmelin, AED-CONF-65-073-19
16	19-41083	Gmelin, AED-CONF-65-073-18
17	19-41284	Gmelin, AED-CONF-65-073-17
18	19-41310	Gmelin, AED-CONF-65-073-3
19	19-41285	Gmelin, AED-CONF-65-073-31
20	19-41847	Gmelin, AED-CONF-65-073-33
22	19-41523	Gmelin, AED-CONF-65-073-37
23	19-41843	Gmelin, AED-CONF-65-073-38
25	19-41834	Gmelin, AED-CONF-65-073-42
26	19-41948	Gmelin, AED-CONF-65-073-28
CONF-650413–		**(Symposium on Neutron Dynamics and Control, Tucson, Ariz., Apr. 5–7, 1965)**
5	19-42061	Gmelin, AED-CONF-65-042-13
6	19-41653	Gmelin, AED-CONF-65-042-12
7	19-42188	Gmelin, AED-CONF-65-042-16
9	19-42062	Gmelin, AED-CONF-65-042-4
11	19-41654	Gmelin, AED-CONF-65-042-6
CONF-650417–		**(American Nuclear Society, National Topical Meeting on Fast Reactor Technology, Detroit, Apr. 26–28, 1965)**
2	19-42090	See GA-6132
CONF-650423–		**(International Conference on Physics of Solids and High Pressures, Tucson, Apr. 19–21, 1965)**
3	19-42005	Gmelin, AED-CONF-65-058-7
CONF-650429–		**(American Power Conference, Chicago, Apr. 27–29, 1965)**
11	19-42124	ORINS
12	19-42121	ORINS
13	19-42122	ORINS
14	19-42123	ORINS
16	19-42026	ORINS
CONF-650435–		**(5th Shock Tube Symposium, Silver Spring, Md., Apr. 28–30, 1965)**
1	19-41128	See UCRL-12466
2	19-41162	Gmelin, AED-CONF-65-097-1
CONF-650510–		**(Purdue Conference on Instrumentation for High Energy Physics, Lafayette, Indiana, May 11–15, 1965)**
9	19-41322	See BNL-9231
14	19-40869	Dep. mn; CFSTI, $2.00 cy, $0.50 mn IEEE (Inst. Elec. Electron. Engrs.), Trans. Nucl. Sci., NS-12: No. 4, 138-54 (1965)
CONF-650512–		**(Symposium on Engineering Problems of Controlled Thermonuclear Research, Livermore, Calif., May 4–7, 1965)**
3	19-41864	See ORNL-P-1244
5	19-40772	See ORNL-P-1465
6	19-40844	See MATT-341
CONF-650525–		**(International Conference on the Internal Conversion Process, Nashville, Tenn., May 10–13, 1965)**
6	19-41679	See UCRL-11462(Rev.)
7	19-41680	See UCRL-16184
8	19-40880	See UCRL-16035
CONF-650539–		**(20th Annual Industrial Waste Conference, Lafayette, Ind., May 4–6, 1965)**
1	19-42195	See ORNL-P-1479
CONF-650544–		**(Symposium on Fundamental Problems in Scanning, Chicago, May 1965)**
1	19-40390	See BNL-9348
CONF-650616–		**(Health Physics Society, Annual Meeting, Los Angeles, June 14–17, 1965)**
5	19-40802	Dep. mn; CFSTI, $1.00 cy, $0.50 mn
CONF-650617–		**(Vacuum Metallurgy Conference, New York, June 21–23, 1965)**
3	19-40948	See IS-1195
CONF-650627–		**(Conference on Electromagnetic Isotope Separators and Related Ion Accelerators, and Their Applications to Physics, Aarhus, Denmark, June 14–18, 1965)**
2	19-42017	See IS-1219
CONF-650630–		**(Society of Physical Chemistry, 15th Annual Meeting, Paris, June 1–4, 1965)**
2	19-40455	See BNL-9297
CONF-650633–		**(Forum Italiano Dell'Energia Nucleare, Rome, June 18–29, 1965)**
1	19-42082	Dep. mn
CONF-650634–		**(16th Annual Mid-America Symposium on Spectroscopy, Chicago, June 14–17, 1965)**
1	19-40412	See TIM-924
CONF-650635–		**(2nd International Meeting on Accelerator Targets Designed for the Production of Neutrons, Grenoble, June 21–22, 1965)**
1	19-41676	See ORNL-P-1468
CONF-650636–		**(International Symposium on Electron and Photon Interactions at High Energies, Hamburg, June 8–12,**

Report No.	Abstract No. 1965)	Availability
1	19-41323	See CALT-68-42
2	19-41164	See CEAL-1022
CONF-650637–	**(International Conference on Luminescent Dosimetry, Palo Alto, Calif., June 21–23, 1965)**	
1	19-40868	See BNWL-SA-23
2	19-40879	See UCRL-12371
CONF-650638–	**(Physics of Quantum Electronics Conference, San Juan, Puerto Rico, June 28–30, 1965)**	
1	19-41328	See IS-1187
CONF-650640–	**(7th International Glass Congress, Brussels, June 28–July 3, 1965)**	
1	19-40464	See UCRL-11816(Rev.)
CONF-650641–	**(American Society of Mechanical Engineers, International Conference on Energetics, Gatlinburg, Tenn., June 21, 1965)**	
1	19-41314	See BNL-9329
CONF-650706–	**(International Conference on the Study of Nuclear Structure with Neutrons, Antwerp, July 19–23, 1965)**	
19	19-41670	See LA-DC-7097
20	19-41669	See LA-DC-7096
21	19-41656	See BNL-9245
CONF-650707–	**(IEEE Annual Conference on Nuclear and Space Radiation Effects, Ann Arbor, Mich., July 12–15, 1965)**	
4	19-40936	See SC-R-65-912
5	19-40935	See SC-DC-65-1247
6	19-41091	See SC-R-65-943
CONF-650711–	**(AIAA 2nd Annual Meeting and Technical Demonstration, San Francisco, July 26–29, 1965)**	
3	19-40769	ORINS
4	19-40771	ORINS
5	19-40770	ORINS
21	19-41863	See NP-15302
CONF-650712–	**(National Society of Professional Engineers, Albuquerque, N. Mex., July 2, 1965)**	
1	19-40710	See SC-DC-65-1485
CONF-650713–	**(American Veterinary Assn., 102nd Annual Meeting, Portland, Oreg., July 11–15, 1965)**	
1	19-40780	See BNWL-SA-242
CONF-650802–	**(Cryogenic Engineering Conference, Houston, Tex., Aug. 23–25, 1965)**	
5	19-41165	See LA-DC-7147
CONF-650807–	**(5th International Congress of Neuropathology, Zurich, Aug. 30–Sept. 3, 1965)**	
1	19-40349	See BNL-9345
CONF-650808–	**(American Industrial Hygiene Assn., Seattle, Aug. 6, 1965)**	
1	19-40806	See RL-SA-37
CONF-650812–	**(ASME-AIChE Heat Transfer Conference and Exhibit, Los Angeles, Aug. 8–11, 1965)**	
1	19-41119	See MIT-36-P
CONF-650902–	**(American Chemical Society, 150th National Meeting, Atlantic City, Sept. 12–17, 1965)**	
5	19-42200	See COO-1354-5
CONF-650915–	**(Systems Engineering Conference, Chicago, Sept. 20–23, 1965)**	
1	19-40704	See Y-KA-9
CONF-650917–	**(International Conference on Industrial Electronics and Control Instrumentation, Philadelphia, Sept. 8–10, 1965)**	
1	19-42129	See DPSPU-65-30-27
CONF-650918–	**(International Conference on the Chemistry of the Solvent Extraction of Metals, Harwell, Berks., England, Sept. 1965)**	
1	19-40645	Dep. mn; CFSTI, $2.00 cy, $0.50 mn
2	19-40646	Dep. mn; CFSTI, $2.00 cy, $0.50 mn
CONF-650919–	**(Technicon Analytical Symposium, New York, Sept. 8–10, 1965)**	
1	19-40405	Dep. mn; CFSTI, $2.00 cy, $0.50 mn
2	19-40406	Dep. mn; CFSTI, $1.00 cy, $0.50 mn
CONF-650920–	**(ASME–AIChE Heat Transfer Conference, Los Angeles, Sept. 1965)**	
1	19-42009	See WAPD-T-1811
CONF-651002–	**(Instrument Society of America, 20th Annual Conference, Los Angeles, Oct. 4–7, 1965)**	
4	19-42136	See LA-DC-6941
6	19-42137	See LA-DC-7313
CONF-651003–	**(4th Symposium on Detonation, Silver Spring, Md., Oct. 13–15, 1965)**	
1	19-41118	See LA-DC-6996
3	19-42206	See LA-DC-6992
5	19-42207	See LA-DC-6994
6	19-42205	See LA-DC-6990
COO–		
7-355	19-41731	Nucl. Phys., 72: 417-35(1965)
499-1	19-40647	Dep. mn; CFSTI, $1.00 cy, $0.50 mn
499-2	19-40648	Dep. mn; CFSTI, $1.00 cy, $0.50 mn
535-542	19-40904	Nucl. Instr. Methods, 36: 119-21(1965)
652-16	19-42083	Dep. mn; CFSTI, $1.00 cy, $0.50 mn
689-50	19-40778	Dep. mn; CFSTI, $5.00 cy, $1.00 mn
1032-1	19-40549	Dep. mn; CFSTI, $2.00 cy, $0.50 mn
1198-227	19-41256	J. Appl. Phys., 36: 2658-62(1965)
1319-27	19-40967	Dep. mn; CFSTI, $2.00 cy, $0.50 mn
1354-5	19-42200	Dep. mn; CFSTI, $2.00 cy, $0.50 mn
1371-15	19-41457	Phys. Rev. Letters, 15: 316-20(1965)
1420-115	19-41684	Phys. Rev., 139: B763-9(1965)
CU–	**(Misc.)**	
245	19-41325	See CU-1932-245
1932-245	19-41325	Dep. mn; CFSTI, $1.00 cy, $0.50 mn
2663-23	19-42201	Dep. mn; CFSTI, $3.00 cy, $0.50 mn
CVNA–	**(Misc.)**	
239	19-42084	Dep. mn; CFSTI, $2.00 cy, $0.50 mn
DASA–	**(Misc.)**	
1592	19-40882	See USNRDL-TR-839
DP–		
982	19-40649	Dep. mn; CFSTI, $1.00 cy, $0.50 mn
986	19-41657	Dep. mn; CFSTI, $1.00 cy, $0.50 mn
DPSPU–		
65-30-27	19-42129	Dep. mn; CFSTI, $1.00 cy, $0.50 mn
DUBNA REPORTS	**(Russian)**	
See JINR (Russian)		
EE–	**(Misc.)**	
115	19-40845	See N64-33676
EM–	**(Misc.)**	
10-5	19-40931	See AD-609424
ER–	**(Misc.)**	
6643	19-41954	See NP-15338
EUR–	**(European Atomic Energy Community)**	
2296.e	19-41111	Dep. mn
2326	19-40979	See EURAEC-1351
2339	19-40753	See EURAEC-1378
2359	19-41007	See EURAEC-1400
2362	19-40947	See EURAEC-1403
2366	19-41008	See EURAEC-1407
2421.d	19-40714	Dep.(mn)
2426.d	19-42085	Dep.(mn)
2427.i	19-42086	Dep.(mn)
2428.f	19-42087	Dep.(mn)
2430.n	19-42088	Dep. mn

Report No.	Abstract No.	Availability
EURAEC–		
1351	19-40979	Dep. mn; CFSTI, $2.00 cy, $0.50 mn
1371	19-40732	See CEND-3336-237
1378	19-40753	Dep. mn; CFSTI, $1.00 cy, $0.50 mn
1400	19-41007	Dep. mn; CFSTI, $3.00 cy, $0.75 mn
1403	19-40947	Dep. mn; CFSTI, $2.00 cy, $0.50 mn
1407	19-41008	Dep. mn; CFSTI, $2.00 cy, $0.50 mn
1414	19-40738	See NYO-3114-7
1415	19-40737	See NYO-3114-6
1424	19-40968	Dep. mn; CFSTI, $1.00 cy, $0.50 mn
1435	19-41088	See GEAP-4572
1436	19-42092	See GEAP-4909
1438	19-41006	See CEND-3107-238
1442	19-42093	See GEAP-4912
1444	19-42091	See GEAP-4852
1456	19-41010	See IITRI-578P27-10
FTD-TT–	**(Non-AEC)**	
64-1368	19-41243	CFSTI
65-43	19-40303	CFSTI
65-101	19-41574	CFSTI
65-112	19-41575	CFSTI
65-125	19-41093	CFSTI
GA–	**(Misc.)**	
5938	19-42089	Dep. mn; CFSTI, $4.00 cy, $1.00 mn
6034	19-41646	Nucl. Sci. Eng., 23: 34-44(1965)
6132	19-42090	Dep.(mn); $1.00(cy), 1(mn) CFSTI
6286	19-42041	Dep. mn; CFSTI, $1.00 cy, $0.50 mn
6323	19-41640	Dep. mn; CFSTI, $2.00 cy, $0.50 mn
GCA-TR–	**(Misc.)**	
65-4-G	19-41112	See SC-DC-65-1312
GE-TM–		
65-3-6	19-42132	Dep. mn; CFSTI, $1.00 cy, $0.50 mn
GEAP–	**(Misc.)**	
4572	19-41088	Dep. mn; CFSTI, $3.00 cy, $0.50 mn
4852	19-42091	Dep. mn; CFSTI, $3.00 cy, $0.50 mn
4863	19-40733	Dep. mn; CFSTI, $1.00 cy, $0.50 mn
4909	19-42092	Dep. mn; CFSTI, $3.00 cy, $0.75 mn
4912	19-42093	Dep. mn; CFSTI, $1.00 cy, $0.50 mn
GEMP–	**(Misc.)**	
190h	19-42138	See N64-33780
190n(Pt.B)	19-42139	See N64-33784
340	19-42133	Dep.(mn); $1.00(cy), 1(mn) CFSTI
375	19-41009	Dep. mn; CFSTI, $2.00 cy, $0.50 mn
HMI-B–	**(German)**	
39	19-40396	Dep.(mn)
HUX–		
2752-9	19-41326	Dep. mn; CFSTI, $4.00 cy, $1.00 mn
HW–		
56028	19-41089	Dep. mn; CFSTI, $1.00 cy, $0.50 mn
64483	19-42202	Dep. mn; CFSTI, $1.00 cy, $0.50 mn
68387	19-42130	Dep. mn; CFSTI, $1.00 cy, $0.50 mn
77028	19-42131	
77805	19-40650	Dep. mn; CFSTI, $1.00 cy, $0.50 mn
HW-SA–		
3723	19-40350	Dep. mn; CFSTI, $1.00 cy, $0.50 mn
I–	**(Misc.)**	
A2392-3-1	19-40736	See NYO-2512-1
IA–	**(Non-AEC)**	
1023	19-41424	Phys. Rev., 139: B1323-5(1965)
IAE–	**(Non-AEC)**	
635	19-41851	Dep. mn
655	19-41658	Dep. mn
668	19-41116	Dep. mn
676	19-41852	Dep. mn
695	19-40870	Dep. mn
713	19-40456	Dep. mn
835	19-41659	Dep. mn

Report No.	Abstract No.	Availability
IC–	**(Misc.)**	
65/33	19-41554	Phys. Rev., 139: B1433-6(1965)
65/63	19-41327	Dep. mn
IDO–		
10043(Vol.II) (Rev.1)	19-42006	Dep.(mn); $6.00(cy), 6(mn) CFSTI
14657	19-40651	Dep. mn; CFSTI, $1.00 cy, $0.50 mn
17070	19-42134	Dep. mn; CFSTI, $6.00 cy, $1.25 mn
17088	19-42152	Dep. mn; CFSTI, $3.00 cy, $0.75 mn
IITRI–	**(Misc.)**	
578P27-10	19-41010	Dep. mn; CFSTI, $2.00 cy, $0.50 mn
IS–		
1056	19-41062	Trans. Met. Soc. AIME, 233: 1488-96 (1965)
1141	19-41963	Dep. mn; CFSTI, $6.00 cy, $1.25 mn
1156	19-40457	Dep. mn; CFSTI, $2.00 cy, $0.50 mn
1187	19-41328	Dep. mn; CFSTI, $1.00 cy, $0.50 mn
1195	19-40948	Dep. mn; CFSTI, $3.00 cy, $0.50 mn
1219	19-42017	Dep. mn; CFSTI, $1.00 cy, $0.50 mn
IS-T–		
15	19-41011	Dep. mn; CFSTI, $3.00 cy, $0.50 mn
16	19-41012	Dep. mn; CFSTI, $3.00 cy, $0.75 mn
25	19-41013	Dep. mn; CFSTI, $2.00 cy, $0.50 mn
27	19-40550	Dep. mn; CFSTI, $3.00 cy, $0.75 mn
ISC–		
640	19-40949	Dep. mn; CFSTI, $2.00 cy, $0.50 mn
ISS–	**(Italian)**	
65/3	19-41660	Dep. mn
JINR–	**(Russian)**	
P-2158	19-41661	Dep.(mn)
P-2174	19-41204	Dep. mn
P-2176	19-41662	Dep. mn
P-2179	19-40871	Dep. mn
P-2184	19-41663	Dep. mn
P-2193	19-41664	Dep. mn
P-2201	19-41964	Dep. mn
P-2203	19-40872	Dep. mn
P-2208	19-41329	Dep. mn
P-2209	19-41665	Dep. mn
P-2213	19-41330	Dep. mn
P-2215	19-40873	Dep. mn
P-2216	19-42042	Dep. mn
P-2219	19-41331	Dep. mn
P-2220	19-41332	Dep. mn
P-2224	19-40458	Dep. mn
P-2227	19-41333	Dep. mn
P-2229	19-41334	Dep. mn
P-2233	19-41666	
P-2239	19-41667	Dep. mn
JPRS–	**(Non-AEC)**	
30500	19-40786	CFSTI, $1.00 cy
JüL–	**(German)**	
227-CA	19-40874	Dep.(mn)
235-RE	19-42153	Dep.(mn)
KFK–	**(German)**	
261	19-42154	Dep. mn
293	19-40551	Dep. mn
306	19-41668	Dep.(mn)
KY–		
485	19-40407	Dep. mn; CFSTI, $1.00 cy, $0.50 mn
LA–		
3297	19-42203	Dep. mn; CFSTI, $3.00 cy, $0.50 mn
3302	19-40980	Dep. mn; CFSTI, $2.00 cy, $0.50 mn
3304	19-42135	Dep. mn; CFSTI, $1.00 cy, $0.50 mn
3306	19-41117	Dep. mn; CFSTI, $4.00 cy, $1.00 mn
3309	19-41965	Dep. mn; CFSTI, $2.00 cy, $0.50 mn
3310	19-41966	Dep. mn; CFSTI, $2.00 cy, $0.50 mn
3333	19-40408	Dep. mn; CFSTI, $1.00 cy, $0.50 mn

Report No.	Abstract No.	Availability
3338	19-40950	Dep. mn; CFSTI, $1.00 cy, $0.50 mn
3342	19-41607	Dep. mn; CFSTI, $3.00 cy, $0.75 mn
LA-DC–		
6603	19-41853	Dep. mn; CFSTI, $1.00 cy, $0.50 mn
6632	19-42204	Dep. mn; CFSTI, $1.00 cy, $0.50 mn
6746	19-41761	Phys. Rev., 139: B1170-84(1965)
6799	19-41043	J. Less-Common Metals, 9: 40-7(1965)
6819	19-41014	Dep. mn; CFSTI, $1.00 cy, $0.50 mn
6941	19-42136	Dep. mn; CFSTI, $1.00 cy, $0.50 mn
6990	19-42205	Dep. mn; CFSTI, $1.00 cy, $0.50 mn
6992	19-42206	Dep. mn; CFSTI, $1.00 cy, $0.50 mn
6994	19-42207	Dep. mn; CFSTI, $1.00 cy, $0.50 mn
6996	19-41118	Dep. mn; CFSTI, $2.00 cy, $0.50 mn
7063	19-41682	Ann. Phys. (N.Y.), 34: 96-152(1965)
7093	19-41765	Phys. Rev., 139: B1207-16(1965)
7096	19-41669	Dep. mn; CFSTI, $1.00 cy, $0.50 mn
7097	19-41670	Dep. mn; CFSTI, $1.00 cy, $0.50 mn
7125	19-41767	Phys. Rev., 139: B1227-31(1965)
7128	19-41762	Phys. Rev., 139: B1185-6(1965)
7147	19-41165	Dep. mn; CFSTI, $1.00 cy, $0.50 mn
7313	19-42137	Dep. mn; CFSTI, $1.00 cy, $0.50 mn
LADC–		
6186	19-41671	Dep. mn; CFSTI, $2.00 cy, $0.50 mn
MATT–		
341	19-40844	Dep. mn; CFSTI, $2.00 cy, $0.50 mn
369	19-41854	Dep. mn; CFSTI, $1.00 cy, $0.50 mn
MIL-TDR–	**(Non-AEC)**	
64-282	19-41015	
MIT–	**(Misc.)**	
36-P	19-41119	
2344-3	19-42007	Dep.(mn); $5.00(cy), 3(mn) CFSTI
MIT-QPR–	**(Non-AEC)**	
57	19-41967	
MITNE–	**(Misc.)**	
60	19-42007	See MIT-2344-3
ML–	**(Misc.)**	
767	19-41166	Dep. mn; CFSTI, $3.00 cy, $0.75 mn
MSAR–	**(Misc.)**	
65-95	19-40409	Dep. mn; CFSTI, $2.00 cy, $0.50 mn
65-96	19-40969	Dep. mn; CFSTI, $3.00 cy, $0.75 mn
N–	**(Misc.)**	
64-21876	19-41576	CFSTI, $2.25 cy
64-22932	19-41209	CFSTI, $1.00 fs, $0.50 mn
64-25008	19-40760	CFSTI, $10.50 cy, $1.00 mn
64-25282	19-41210	
64-29400	19-41571	CFSTI, $1.60 cy
64-30509	19-41120	CFSTI, $2.00 cy, $0.50 mn
64-30510	19-41951	CFSTI, $3.00 cy, $0.75 mn
64-30518	19-41288	See NASA-CR-58203
64-30519	19-41288	See NASA-CR-58203
64-30604	19-40761	CFSTI, $4.00 cy, $0.75 mn
64-30658	19-41121	
64-30997	19-41016	CFSTI, $0.50 cy, $0.50 mn
64-31010	19-40762	CFSTI, $3.00 cy, $0.50 mn
64-31206	19-41529	CFSTI, $1.25 cy, $0.50 mn
64-31207	19-41122	CFSTI, $1.00 cy, $0.50 mn
64-31453	19-40763	CFSTI, $4.00 cy, $1.00 mn
64-31552	19-41952	CFSTI, $3.00 cy, $0.50 mn
64-31725	19-41205	CFSTI, $1.00 cy, $0.50 mn
64-32432	19-41530	CFSTI, $1.00 cy, $0.50 mn
64-33291	19-41206	CFSTI, $1.00 cy, $0.50 mn
64-33402	19-41171	CFSTI, $1.00 fs, $0.50 mn
64-33676	19-40845	CFSTI, $2.00 cy, $0.50 mn
64-33780	19-42138	$2.00(CFSTI)
64-33784	19-42139	CFSTI, $3.00 cy, $0.50 mn
65-27691	19-40764	
NAA-SR–		
4527(Pt.II)	19-42208	Dep. mn; CFSTI, $5.00 cy, $0.75 mn
10100	19-42018	Dep. mn; CFSTI, $7.53 cy, $2.25 mn
10482	19-41017	Dep. mn; CFSTI, $3.00 cy, $0.50 mn
10768	19-41018	Dep. mn; CFSTI, $2.00 cy, $0.50 mn
10853	19-41642	Dep. mn; CFSTI, $1.00 cy, $0.50 mn
11121	19-41090	Dep. mn; CFSTI, $2.00 cy, $0.50 mn
11314	19-42094	Dep. mn; CFSTI, $6.00 cy, $1.50 mn
11323	19-41019	Dep. mn; CFSTI, $3.00 cy, $0.50 mn
11340	19-40652	Dep. mn; CFSTI, $2.00 cy, $0.50 mn
11353	19-42140	Dep. mn; CFSTI, $2.00 cy, $0.50 mn
11368	19-42050	Dep. mn; CFSTI, $1.00 cy, $0.50 mn
11378(Vol.III)	19-42095	Dep. mn; CFSTI, $5.00 cy, $1.00 mn
11389	19-40653	Dep. mn; CFSTI, $3.00 cy, $0.75 mn
11396	19-42096	Dep. mn; CFSTI, $3.00 cy, $0.50 mn
NAA-SR-Memo–		
2987	19-41020	Dep. mn; CFSTI, $1.00 cy, $0.50 mn
3196	19-42155	Dep. mn; CFSTI, $2.00 cy, $0.50 mn
7438	19-40715	Dep. mn; CFSTI, $2.00 cy, $0.50 mn
9719	19-40803	Dep. mn; CFSTI, $1.00 cy, $0.50 mn
NASA-CR–	**(Misc.)**	
110	19-41529	See N64-31206
111	19-41122	See N64-31207
123	19-41530	See N64-32432
258	19-41572	CFSTI, $3.00 cy
52943	19-42138	See N64-33780
52948	19-42139	See N64-33784
54063	19-40762	See N64-31010
54064	19-40763	See N64-31453
54082	19-40760	See N64-25008
54097	19-40946	See AI-65-93
54134	19-40761	See N64-30604
54213	19-40764	See N65-27691
54390	19-40970	
54422	19-42141	
58203	19-41288	CFSTI, $3.00 cy, $0.75 mn
58669	19-41571	See N64-29400
58823	19-41120	See N64-30509
58950	19-41952	See N64-31552
59188	19-40845	See N64-33676
59249	19-41206	See N64-33291
NASA-TM–	**(Non-AEC)**	
X-53063	19-41951	See N64-30510
X-53088	19-41205	See N64-31725
NASA-TN–	**(Misc.)**	
D-1869	19-41016	See N64-30997
NASA-TR–	**(Non-AEC)**	
R-225	19-41123	CFSTI, $1.00 cy, $0.50 mn
NASA-TT–	**(Non-AEC)**	
F-202	19-41576	See N64-21876
F-8740	19-41210	See N64-25282
F-8811	19-41209	See N64-22932
F-9136	19-41171	See N64-33402
NEIC-RR–	**(Polish)**	
9	19-41207	Dep.
NEVIS–	**(Misc.)**	
139	19-41325	See CU-1932-245
NIRL-R–	**(British)**	
76	19-41167	Dep. mn; BIS, $1.40; HMSO 7s.
79	19-41442	Phys. Rev., 139: B1566-84(1965)
NMI–	**(Misc.)**	
8002.1	19-41021	
NP–	**(AEC File No. for Non-AEC Reports)**	
14921	19-40391	Dep. mn
14924	19-40940	Dep. mn
14925	19-40804	Dep. mn
15108	19-41124	
15131	19-41953	Dep. mn
15142	19-41855	
15179	19-40781	Dep. mn
15180	19-40309	Dep. mn
15205	19-41856	Dep. mn

Report No.	Abstract No.	Availability
15206	19-41857	Dep. mn
15209	19-40846	Dep. mn
15217	19-41858	Dep. mn
15218	19-41859	Dep. mn
15220	19-41860	Dep. mn
15239	19-41335	Dep. mn
15251	19-41673	Dep. mn
15253	19-41168	Dep. mn
15254	19-40875	Dep. mn
15255	19-41861	Dep. mn
15256	19-41862	Dep. mn
15267	19-42194	Dep. mn; IAEA(Free)
15280	19-40716	
15287	19-40552	CFSTI, $2.00 cy, $0.50 mn
15292	19-41022	
15300	19-40933	CFSTI
15301	19-40934	CFSTI
15302	19-41863	
15309	19-40765	
15324	19-40459	
15325	19-40782	Dep. mn
15327	19-40783	Dep. mn
15331	19-40734	
15334	19-41023	
15335	19-41336	
15338	19-41954	
15356	19-42209	Dep. mn
NP-tr-	**(AEC File No. for Non-AEC Translations)**	
1234	19-42104	Dep.(mn); $1.60(fs), $0.80(mf) JCL
1235	19-41094	Dep.(mn); $1.60(fs), $0.80(mf) JCL
NRL-	**(Misc.)**	
6290	19-40951	CFSTI, $0.50 cy, $0.50 mn
NRS-	**(Australian)**	
30	19-40805	Dep. mn
NUMEC-		
2389-5	19-41024	Dep. mn; CFSTI, $2.00 cy, $0.50 mn
2389-6	19-40981	Dep. mn; CFSTI, $1.00 cy, $0.50 mn
NUS-	**(Misc.)**	
217	19-40635	Dep. mn; CFSTI, $3.00 cy, $0.75 mn
NYO-		
98-8	19-42210	Dep. mn; CFSTI, $2.00 cy, $0.50 mn
162-5(Rev.)	19-40876	Dep. mn; CFSTI, $1.00 cy, $0.50 mn
NYO-		
1480-19	19-42211	Dep. mn; CFSTI, $3.00 cy, $0.75 mn
1913-1	19-40351	Dep. mn; CFSTI, $1.00 cy, $0.50 mn
1930-44	19-41674	Dep.(mn); $4.00(cy), 3(mn) CFSTI
1930-42	19-41696	Phys. Rev., 139: B896-904(1965)
2262-87	19-41403	Phys. Rev., 139: B973-81(1965)
2262-95	19-41337	Dep.(mn); $2.00(cy), 1(mn) CFSTI
2404-5	19-40735	Dep. mn; CFSTI, $1.00 cy, $0.50 mn
2512-1	19-40736	Dep. mn; CFSTI, $6.00 cy, $1.25 mn
2910-11	19-40847	Dep. mn; CFSTI, $1.00 cy, $0.50 mn
2978-34	19-40553	Dep. mn; CFSTI, $3.00 cy, $0.75 mn
3114-6	19-40737	Dep. mn; CFSTI, $3.00 cy, $0.75 mn
3114-7	19-40738	Dep. mn; CFSTI, $1.00 cy, $0.50 mn
3364-7	19-41169	Dep. mn; CFSTI, $1.00 cy, $0.50 mn
3364-6	19-40392	Dep. mn; CFSTI, $1.00 cy, $0.50 mn
3399-27	19-41411	Phys. Rev., 139: B1052-62(1965)
3399-31	19-41406	Phys. Rev., 139: B1006-10(1965)
3424-1	19-42212	Dep. mn; CFSTI, $2.00 cy, $0.50 mn
3462-1	19-40460	Dep. mn; CFSTI, $2.00 cy, $0.50 mn
ONR-	**(Non-AEC)**	
14-63	19-41203	See AD-600154
ORNL-		
3613	19-40654	Dep. mn; CFSTI, $1.00 cy, $0.50 mn
3819	19-40982	Dep. mn; CFSTI, $2.00 cy, $0.50 mn
3827	19-41208	Dep. mn; CFSTI, $1.00 cy, $0.50 mn
ORNL-NSIC-		
5(Vol.I&II)	19-42008	Dep. mn; CFSTI, $14.00 cy, $5.75 mn

Report No.	Abstract No.	Availability
ORNL-P-	**(Misc.)**	
330	19-41675	Dep. mn; CFSTI, $1.00 cy, $0.50 mn
491	19-40461	Dep. mn; CFSTI, $2.00 cy, $0.50 mn
494	19-40410	Dep. mn; CFSTI, $1.00 cy, $0.50 mn
917	19-40746	A.I.Ch.E. (Am. Inst. Chem. Engrs.) J., 11: 848-52(1965)
962	19-41064	Trans. Met. Soc. AIME, 233: 1533-9(1965)
964	19-40687	Talanta, 12: 823-7(1965)
1087	19-41746	Nucl. Phys., 72: 641-56(1965)
1126	19-40372	Nucl. Instr. Methods, 36: 125-40(1965)
1163	19-42198	Nature, 207: 158-9(1965)
1184	19-41610	J. Appl. Phys., 36: 2895-97(1965)
1244	19-41864	Dep.(mn); $1.00(cy), 1(mn) CFSTI
1258	19-41745	Nucl. Phys., 72: 625-40(1965)
1465	19-40772	Dep. mn; CFSTI, $1.00 cy, $0.50 mn
1468	19-41676	Dep. mn; CFSTI, $1.00 cy, $0.50 mn
1479	19-42195	Dep. mn; CFSTI, $1.00 cy, $0.50 mn
ORNL-TM-		
826	19-40699	Dep. mn; CFSTI, $1.00 cy, $0.50 mn
1041	19-41749	Nucl. Sci. Eng., 23: 45-57(1965)
1121	19-41955	Dep. mn; CFSTI, $1.00 cy, $0.50 mn
1134	19-40397	Dep. mn; CFSTI, $2.00 cy, $0.50 mn
1144	19-41025	Dep. mn; CFSTI, $2.00 cy, $0.50 mn
1149	19-41338	Dep. mn; CFSTI, $1.00 cy, $0.50 mn
1151	19-41677	Dep. mn; CFSTI, $2.00 cy, $0.50 mn
1152	19-42097	Dep. mn; CFSTI, $2.00 cy, $0.50 mn
1153	19-41969	Dep. mn; CFSTI, $4.00 cy, $0.75 mn
1164	19-42213	Dep. mn; CFSTI, $3.00 cy, $0.75 mn
1179	19-40952	Dep. mn; CFSTI, $1.00 cy, $0.50 mn
1183	19-40759	Dep. mn; CFSTI, $4.00 cy, $1.00 mn
1184	19-41643	Dep. mn; CFSTI, $4.00 cy, $0.75 mn
1185	19-41125	Dep. mn; CFSTI, $2.00 cy, $0.50 mn
1187	19-40700	Dep. mn; CFSTI, $6.00 cy, $1.25 mn
1191	19-40706	Dep. mn; CFSTI, $1.00 cy, $0.50 mn
1224	19-41970	Dep. mn; CFSTI, $1.00 cy, $0.50 mn
ORNL-tr-		
437	19-40361	Dep. mn; CFSTI, $1.00 cy, $0.50 mn; JCL, $2.60 fs, $0.86 mf
578	19-40467	Dep. mn; CFSTI, $1.00 cy, $0.50 mn; JCL, $1.60 fs, $0.80 mf
588	19-40850	Dep. mn; JCL, $1.60 fs, $0.80 mf
625	19-40637	Dep. mn; CFSTI, $1.00 cy, $0.50 mn; JCL, $1.10 fs, $0.80 mf
667	19-41095	Dep. mn; JCL, $2.60 fs, $0.89 mf
669	19-42019	Dep. mn; JCL, $1.10 fs, $0.80 mf
OTR-	**(Non-AEC)**	
112	19-40739	CFSTI, $0.50 cy, $0.50 mn
PATENTS	**(British)**	**(3s. 6d. each, U. K. Patent Office)**
997,209	19-42015	
997,292	19-41085	
997,314	19-40963	
997,328	19-40927	
997,338	19-41163	
997,387	19-42189	
997,413	19-42027	
997,765	19-40705	
997,882	19-40728	
997,925	19-42064	
997,960	19-41950	
998,117	19-40928	
998,135	19-42125	
998,153	19-41109	
998,247	19-40992	
998,301	19-40993	
998,315	19-40752	
998,387	19-40994	
998,540	19-42028	
998,624	19-42072	
998,625	19-42073	
998,771	19-40539	
998,902	19-42074	
998,933	19-42029	
998,944	19-42190	
999,005	19-42030	
999,006	19-42031	
999,274	19-42065	

Report No.	Abstract No.	Availability
999,367	19-40977	
999,434	19-40454	
999,463	19-40995	
999,618	19-40942	
999,621	19-40729	
999,699	19-42066	
999,934	19-40964	
PATENTS	**(Canadian)**	
696,293	19-40730	
696,336	19-42126	
698,037	19-42067	
703,560	19-42032	
711,364	19-40929	
711,365	19-42016	
711,366	19-42068	
712,078	19-40996	
712,250	19-42033	
712,677	19-40930	
712,678	19-42069	
713,034	19-41086	
PATENTS	**(U. S.)**	**($0.25 each, U. S. Patent Office)**
3,191,393	19-40695	
3,192,012	19-40696	
3,192,058	19-40997	
3,192,065	19-40998	
3,194,657	19-40999	
3,194,663	19-40697	
3,194,668	19-40633	
PNE–		
502F	19-40707	Dep. mn; CFSTI, $1.40 cy, $1.00 mn
503F	19-40708	Dep. mn; CFSTI, $0.45 cy, $0.50 mn
5003	19-40709	Dep. mn; CFSTI, $0.75 cy, $0.75 mn
PR-P–	**(Canadian)**	
65	19-41678	Dep.; $1.50(AECL)
PWAC–	**(Misc.)**	
441	19-40953	Dep. mn; CFSTI, $2.00 cy, $0.50 mn
R–	**(Misc.)**	
62FPD-252	19-42142	Dep. mn; CFSTI, $3.00 cy, $0.75 mn
64SD22	19-41121	See N64-30658
460	19-41023	See NP-15334
511	19-41325	See CU-1932-245
6142	19-41015	See MIL-TDR-64-282
RFP–		
397	19-42214	Dep.(mn); $1.00(cy), 1(mn) CFSTI
625	19-42215	Dep. mn; CFSTI, $1.00 cy, $0.50 mn
RISO–	**(Danish)**	
98	19-40717	Dep. mn
101	19-40877	Dep. mn
RL-SA–		
37	19-40806	Dep. mn; CFSTI, $1.00 cy, $0.50 mn
RL-SEP–		
389(Rev.)	19-40807	Dep. mn; CFSTI, $1.00 cy, $0.50 mn
RME–		
129(Rev.)	19-40784	Dep. mn; CFSTI, $2.00 cy, $0.50 mn
4571(Rev.)	19-40798	Dep. mn; CFSTI, $1.00 cy, $0.50 mn
RPU–	**(Indian)**	
S19	19-41573	Dep. mn
RT-CHI–	**(Italian)**	
(64)16	19-40540	Dep. mn
(65)1	19-40655	Dep. mn
(65)2	19-40411	Dep. mn
(65)20	19-40971	Dep. mn
RT-ING–	**(Italian)**	
(64)16	19-40740	Dep. mn
RT-PROT–	**(Italian)**	
(65)24	19-42098	Dep. mn
SAN–		
409-23	19-40741	Dep. mn; CFSTI, $1.00 cy, $0.50 mn
SB–	**(Non-AEC)**	
403(Suppl.1) (Rev.)	19-40941	CFSTI
SC-DC–		
65-1247	19-40935	Dep. mn; CFSTI, $1.00 cy, $0.50 mn
65-1312	19-41112	Dep. mn; CFSTI, $4.00 cy, $1.00 mn
65-1485	19-40710	Dep. mn; CFSTI, $2.00 cy, $0.50 mn
SC-DR–		
65-269	19-42216	Dep. mn; CFSTI, $2.00 cy, $0.50 mn
SC-R–		
65-912	19-40936	Dep. mn; CFSTI, $1.00 cy, $0.50 mn
65-933	19-41956	Dep. mn; CFSTI, $3.00 cy, $0.75 mn
65-935	19-40848	Dep. mn; CFSTI, $1.00 cy, $0.50 mn
65-943	19-41091	Dep. mn; CFSTI, $1.00 cy, $0.50 mn
SC-RR–		
65-98	19-40808	Dep. mn; CFSTI, $10.58 cy, $3.00 mn
65-98, p32-44	19-40810	Chem. Eng. Progr. 61: Symp. Ser., No. 56, 50-7(1965)
65-220	19-40711	Dep. mn; CFSTI, $5.00 cy, $1.00 mn
65-277	19-40712	Dep. mn; CFSTI, $1.00 cy, $0.50 mn
65-325	19-42217	Dep., CFSTI, $1.00 cy, $0.50 mn
SC-T–		
65-721	19-40468	Dep. mn; JCL, $1.60 fs, $0.80 mf
SC-TM–		
64-509	19-42218	CFSTI, $2.00 cy, $0.50 mn
65-183	19-40462	Dep. mn; CFSTI, $1.00 cy, $0.50 mn
SCL-DR–		
65-75	19-41126	Dep. mn; CFSTI, $2.00 cy, $0.50 mn
SLAC–		
42	19-41170	Dep. mn; CFSTI, $4.00 cy, $0.75 mn
SLAC-PUB–		
44	19-41531	Dep. mn; CFSTI, $1.00 cy, $0.50 mn
SRIA–		
425-S	19-40463	Dep. mn; CFSTI, $1.00 cy, $0.50 mn
STI-PUB–	**(International Atomic Energy Agency)**	
91(Vol.I)	19-40614	IAEA $9.00; S 189.-; £2.14.0; F.Fr. 36.-; DM 31.50 cy
STL-TR–	**(Misc.)**	
60-0000-04057	19-40931	See AD-609424
SUDAER–	**(Non-AEC)**	
238	19-41127	CFSTI
TID–		
21177	19-42219	Dep. mn; CFSTI, $1.00 cy, $0.50 mn
21224	19-40785	Dep. mn; CFSTI, $1.00 cy, $0.50 mn
21524	19-41768	Phys. Rev., 139: B1231-8(1965)
21763	19-41732	Nucl. Phys., 72: 436-48(1965)
21813	19-41448	Phys. Rev., 139: B1619-33(1965)
21821	19-41437	Phys. Rev., 139: B1415-20(1965)
21864	19-41452	Phys. Rev., 139: B1650-9(1965)
22002	19-40742	Dep.(mn); $1.00(cy), 1(mn) CFSTI
22007	19-40701	Dep. mn; CFSTI, $1.00 cy, $0.50 mn
22009	19-42127	Dep. mn; CFSTI, $2.00 cy, $0.50 mn
22013	19-42099	Dep.(mn); $3.00(cy), 1(mn) CFSTI
22023	19-42220	Dep. mn; CFSTI, $5.00 cy, $1.00 mn
22050	19-41865	Dep. mn; CFSTI, $1.00 cy, $0.50 mn
22061	19-40849	Dep. mn; CFSTI, $3.00 cy, $0.50 mn
TIM–	**(Misc.)**	
909	19-40718	Dep. mn; CFSTI, $3.00 cy, $0.75 mn

Report No.	Abstract No.	Availability
914	19-40702	Dep. mn; CFSTI, $2.00 cy, $0.50 mn
916	19-40703	Dep. mn; CFSTI, $2.00 cy, $0.50 mn
924	19-40412	Dep. mn; CFSTI, $1.00 cy, $0.50 mn
929	19-40743	Dep. mn; CFSTI, $2.00 cy, $0.50 mn
939	19-42221	Dep. mn; CFSTI, $1.00 cy, $0.50 mn
940	19-42222	Dep. mn; CFSTI, $1.00 cy, $0.50 mn
948	19-40413	Dep. mn; CFSTI, $1.00 cy, $0.50 mn
TRW-ER-	**(Misc.)**	
5805	19-40760	See N64-25008
TT-	**(Canadian)**	
65-31211	19-40786	See JPRS-30500
UCRL-		
6491(Rev.I)	19-41771	Phys. Rev., 139: B1264-71(1965)
7706	19-41984	J. Appl. Phys., 36: 2869-73(1965)
7844-T	19-40719	Dep. mn; CFSTI, $1.00 cy, $0.50 mn
7845-T	19-40720	Dep. mn; CFSTI, $2.00 cy, $0.50 mn
7967	19-40414	Dep. mn; CFSTI, $1.00 cy, $0.50 mn
7968-T	19-41971	Dep. mn; CFSTI, $1.00 cy, $0.50 mn
9672(Rev.)	19-40878	Dep. mn; CFSTI, $1.00 cy, $0.50 mn
11454	19-40721	Dep. mn; CFSTI, $1.00 cy, $0.50 mn
11462(Rev.)	19-41679	Dep. mn; CFSTI, $1.00 cy, $0.50 mn
11532	19-41883	J. Appl. Phys., 36: 2740-4(1965)
11648	19-41339	Dep. mn; CFSTI, $1.00 cy, $0.50 mn
11669	19-41436	Phys. Rev., 139: B1411-15(1965)
11816(Rev.)	19-40464	Dep. mn; CFSTI, $2.00 cy, $0.50 mn
11945	19-41735	Nucl. Phys., 72: 481-508(1965)
11958	19-40937	Dep. mn; CFSTI, $7.00 cy, $1.50 mn
12006	19-42223	Dep. mn; CFSTI, $1.00 cy, $0.50 mn
12013	19-42051	Dep. mn; CFSTI, $1.00 cy, $0.50 mn
12041-T	19-42224	Dep. mn; CFSTI, $1.00 cy, $0.50 mn
12050	19-42225	Dep. mn; CFSTI, $1.00 cy, $0.50 mn
12052	19-41866	Dep. mn; CFSTI, $1.00 cy, $0.50 mn
12117-T	19-42226	Dep. mn; CFSTI, $1.00 cy, $0.50 mn
12164	19-41180	J. Appl. Phys., 36: 2761-6(1965)
12349	19-41725	Nucl. Phys., 72: 241-53(1965)
12371	19-40879	Dep. mn; CFSTI, $1.00 cy, $0.50 mn
12455-T	19-41867	Dep. mn; CFSTI, $1.00 cy, $0.50 mn
12466	19-41128	Dep. mn; CFSTI, $1.00 cy, $0.50 mn
12476	19-42156	Dep. mn; CFSTI, $2.00 cy, $0.50 mn
12481	19-41779	Phys. Rev., 139: B1505-13(1965)
12482-T	19-41394	Phys. Rev., 139: B912-17(1965)
14106	19-41439	Phys. Rev., 139: B1428-32(1965)
14116	19-40833	Dep. mn; CFSTI, $2.00 cy, $0.50 mn
14151	19-40834	Dep. mn; CFSTI, $3.00 cy, $0.75 mn
14165	19-41957	Dep. mn; CFSTI, $1.00 cy, $0.50 mn
14264	19-40744	Dep. mn; CFSTI, $1.00 cy, $0.50 mn
16024	19-41026	Dep. mn; CFSTI, $3.00 cy, $0.75 mn
16033	19-41426	Phys. Rev., 139: B1336-47(1965)
16035	19-40880	Dep. mn; CFSTI, $1.00 cy, $0.50 mn
16047	19-40398	Dep. mn; CFSTI, $3.00 cy, $0.75 mn
16083	19-41446	Phys. Rev., 139: B1600-8(1965)
16175	19-40465	Dep. mn; CFSTI, $4.00 cy, $0.75 mn
16184	19-41680	Dep. mn; CFSTI, $1.00 cy, $0.50 mn
16220	19-41460	Phys. Rev. Letters, 15: 325-9(1965)
UJV-	**(Czechoslovakian)**	
1209/65	19-40466	Dep. mn
UNC-	**(Misc.)**	
5092	19-42100	Dep. mn; CFSTI, $4.00 cy, $0.75 mn
UR-		
667	19-40881	Dep. mn; CFSTI, $1.00 cy, $0.50 mn
875-53	19-41340	Dep. mn; CFSTI, $2.00 cy, $0.50 mn
875-80	19-41773	Phys. Rev., 139: B1372-4(1965)
875-82	19-41445	Phys. Rev., 139: B1591-9(1965)
USNRDL-TR-	**(Misc.)**	
839	19-40882	
VUF-		
2401	19-40713	Dep. mn; CFSTI, $2.00 cy, $0.50 mn
WAPD-PWR-		
1606(Add.2)	19-42101	Dep. mn; CFSTI, $3.00 cy, $0.50 mn
WAPD-T-		
1811	19-42009	Dep. mn; CFSTI, $1.00 cy, $0.50 mn
WAPD-TM-	**(Misc.)**	
457	19-41092	Dep. mn; CFSTI, $3.00 cy, $0.50 mn
516	19-40636	Dep. mn; CFSTI, $2.00 cy, $0.50 mn
WASH-		
1059	19-40352	Dep. mn; CFSTI, $7.00 cy, $1.50 mn
WCAP-	**(Misc.)**	
2385(Vol.I)	19-42102	Dep. mn; CFSTI, $7.00 cy, $1.75 mn
2385(Vol.II)	19-42103	Dep. mn; CFSTI, $4.00 cy, $1.00 mn
WERL-	**(Misc.)**	
0029-2	19-41027	
Y-KA-		
9	19-40704	Dep. mn; CFSTI, $1.00 cy, $0.50 mn

DEPOSITORIES OF USAEC REPORTS

In Countries Other than the U.S.

ARGENTINA
Buenos Aires, Comisión Nacional de Energía Atómica
AUSTRALIA
Canberra, Australian National Library
Sutherland, New South Wales, Australian Atomic Energy Commission
AUSTRIA
Vienna, Zentral Bibliothek der Physikalischen Institute der Universität
BELGIUM
Mol-Donk, Centre d'Etude de l'Energie Nucleaire
BOLIVIA
La Paz, Comisión Nacional de Energia Nuclear
BRAZIL
Rio de Janeiro, Instituto Brasileiro de Bibliografia e Documentacao
São Paulo, Instituto de Energia Atomica, Cidade Universitaria São Paulo
BURMA
Rangoon, Union of Burma Applied Research Institute, Atomic Energy Center Library
CANADA
Hamilton, McMaster University
Ottawa, National Research Council Library
Vancouver, University of British Columbia
CEYLON
Colombo, University of Ceylon
CHILE
Santiago, Instituto de Fisica y Matematicas, Universidad de Chile
CHINA
Hsinchu, Taiwan, Free China, National Tsing Hua University
COLOMBIA
Bogota, Instituto De Asuntos Nucleares
COSTA RICA
San Pedro, University of Costa Rica Library
DENMARK
Risö, Danish Atomic Energy Commission
ECUADOR
Quito, Escuela Politécnica Nacional
EL SALVADOR
San Salvador, Universidad de El Salvador, Biblioteca de Energia Nuclear
FINLAND
Helsinki, Teknillisen Korkeakoulun Kirjasto
FRANCE
Gif-sur-Yvette, Centre d'Etudes Nucléaires de Saclay
Paris, Académie des Sciences
GERMANY
Berlin, Hahn-Meitner-Institut für Kernforschun Berlin
Frankfurt/Main, Gmelin-Institut
Munich, Technische Hochschule, Bibliothek
GHANA
Accra, University College of Ghana
GREECE
Athens, Nuclear Research Center "Democritus"
GUATEMALA
Guatemala, Comisión Nacional de Energía Nuclear
HAITI
Port au Prince, University of Haiti
ICELAND
Reykjavik, University of Iceland, Atomic Energy Library
INDIA
Bombay, Department of Atomic Energy
INDONESIA
Bandung, Java, Bandung Institute of Technology
Djogjakarta, Java, Science Faculty, Gadjah Mada University
IRAN
Tehran, Tehran University Nuclear Centre
IRAQ
Baghdad, Iraqi Atomic Energy Commission
IRELAND
Dublin, University College
ISRAEL
Rehovoth, Israel Atomic Energy Commission
ITALY
Rome, Centro di Studi Nucleari della Casaccia
Rome, Comitato Nazionale per l'Energia Nucleare
JAPAN
Tokyo, National Diet Library
KOREA
Seoul, Office of Atomic Energy
LEBANON
Beirut, Lebanese National Council for Scientific Research
LUXEMBOURG
Luxembourg, Ministry of Transport and Electricity
MALAYSIA
Kuala Lumpur, University of Malaysia
MEXICO
Mexico, D.F., Comisión Nacional de Energía Nuclear
NETHERLANDS
The Hague, Reactor Centrum Nederland
NEW ZEALAND
Lower Hutt, Institute of Nuclear Sciences
NIGERIA
Ibadan, University of Ibadan
NORWAY
Lillestrom, Institutt för Atomenergi
PAKISTAN
Lahore, West Pakistan, Atomic Energy Centre
PERU
Lima, Junta de Control de Energia Atomica
PHILIPPINE REPUBLIC
Manila, Philippine Atomic Energy Commission
POLAND
Warsaw, Biura Pelnomocnika Rzadu do Spraw Wykorzystania Energii Jadrowej
PORTUGAL
Sacavem, Junta de Energía Nuclear
REPUBLIC OF SOUTH AFRICA
Pretoria, Atomic Energy Board Library
REPUBLIC OF THE CONGO
Leopoldville, Université Lovanium
SPAIN
Madrid, Junta de Energía Nuclear, Biblioteca Documentación y Publicaciones, Ciudad Universitaria
SWEDEN
Nyköping, Aktiebolaget Atomenergi
SWITZERLAND
Zürich, Eidgenössische Technische Hochschule, Bibliothek
THAILAND
Bangkok, Office of the Thai Atomic Energy Commission, Department of Science
TURKEY
Ankara, Turkish Atomic Energy Commission, Atomic Energy Library
UNITED ARAB REPUBLIC
Cairo, Atomic Energy Commission
UNITED KINGDOM
Belfast, City Library
Birmingham, Central Library
Boston Spa, National Lending Library for Science and Technology
Bristol, Central Library
Glasgow, Mitchell Library
Kingston upon Hull, Central Library
Leeds, Central Library
Liverpool, Central Library
London, Central Library, Acton
London, Science Museum Library, South Kensington
Manchester, Central Library
Newcastle upon Tyne, Central Library
Nottingham, Central Library
Sheffield, Central Library
URUGUAY
Montevideo, Comision Nacional de Energia Atomica
VENEZUELA
Caracas, Instituto Venezolano de Investigaciones Científicas
VIET-NAM
Saigon, Atomic Energy Office
YUGOSLAVIA
Belgrade, Federal Commission for Nuclear Energy

In International Agencies

AUSTRIA
Vienna, International Atomic Energy Agency
BELGIUM
Brussels, La Bibliotheque EURATOM
FRANCE
Paris, European Nuclear Energy Agency, O.E.C.D.
ITALY
Ispra, EURATOM Research Center
SWITZERLAND
Geneva, United Nations Library

UNITED STATES
GOVERNMENT PRINTING OFFICE
DIVISION OF PUBLIC DOCUMENTS
WASHINGTON, D.C. 20402

OFFICIAL BUSINESS

POSTAGE AND FEES PAID
U.S. GOVERNMENT PRINTING OFFICE

MIAMI UNIVERSITY LIBRARY